



ISSN

Period.

VOL. 552 NOS. 1 + 2 AUGUST 9

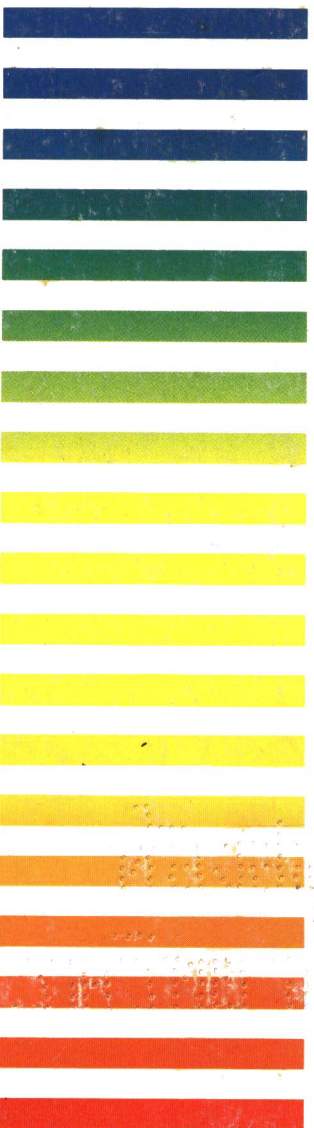
COMPLETE IN ONE ISSUE

18th Int. Symp. on Chromatography
Amsterdam, September 23-28, 1990
Part I

JOURNAL OF

CHROMATOGRAPHY

INCLUDING ELECTROPHORESIS AND OTHER SEPARATION METHODS



SYMPOSIUM VOLUMES

EDITORS

E. Heftmann (Orinda, CA)
Z. Deyl (Prague)

EDITORIAL BOARD

E. Bayer (Tübingen)
S. R. Binder (Hercules, CA)
S. C. Churms (Rondebosch)
J. C. Fetzer (Richmond, CA)
E. Gelpi (Barcelona)
K. M. Gooding (Lafayette, IN)
S. Hara (Tokyo)
P. Helboe (Brønshøj)
W. Lindner (Graz)
T. M. Phillips (Washington, DC)
S. Terabe (Hyogo)
H. F. Walton (Boulder, CO)
M. Wilchek (Rehovot)

ATTENTION

Please note that Vol. 551 (Cumulative Indexes Vols. 501-550) will appear later this year. Please do not claim; nothing is missing.

ELSEVIER

Scope. The *Journal of Chromatography* publishes papers on all aspects of chromatography, electrophoresis and related methods. Contributions consist mainly of research papers dealing with chromatographic theory, instrumental development and their applications. The section *Biomedical Applications*, which is under separate editorship, deals with the following aspects: developments in and applications of chromatographic and electrophoretic techniques related to clinical diagnosis or alterations during medical treatment; screening and profiling of body fluids or tissues with special reference to metabolic disorders; results from basic medical research with direct consequences in clinical practice; drug level monitoring and pharmacokinetic studies; clinical toxicology; analytical studies in occupational medicine.

Submission of Papers. Manuscripts (in English; four copies are required) should be submitted to: Editorial Office of *Journal of Chromatography*, P.O. Box 681, 1000 AR Amsterdam, The Netherlands, Telefax (+31-20) 5862 304, or to: The Editor of *Journal of Chromatography, Biomedical Applications*, P.O. Box 681, 1000 AR Amsterdam, The Netherlands. Review articles are invited or proposed by letter to the Editors. An outline of the proposed review should first be forwarded to the Editors for preliminary discussion prior to preparation. Submission of an article is understood to imply that the article is original and unpublished and is not being considered for publication elsewhere. For copyright regulations, see below.

Publication. The *Journal of Chromatography* (incl. *Biomedical Applications*) has 38 volumes in 1991. The subscription prices for 1991 are:

J. Chromatogr. (incl. *Cum. Indexes, Vols. 501-550*) + *Biomed. Appl.* (Vols. 535-572):
Dfl. 7220.00 plus Dfl. 1140.00 (p.p.h.) (total ca. US\$ 4519.00)

J. Chromatogr. (incl. *Cum. Indexes, Vols. 501-550*) only (Vols. 535-561):
Dfl. 5859.00 plus Dfl. 810.00 (p.p.h.) (total ca. US\$ 3604.75)

Biomed. Appl. only (Vols. 562-572):

Dfl. 2387.00 plus Dfl. 330.00 (p.p.h.) (total ca. US\$ 1468.75).

Subscription Orders. The Dutch guilder price is definitive. The US\$ price is subject to exchange-rate fluctuations and is given as a guide. Subscriptions are accepted on a prepaid basis only, unless different terms have been previously agreed upon. Subscriptions orders can be entered only by calendar year (Jan.-Dec.) and should be sent to Elsevier Science Publishers, Journal Department, P.O. Box 211, 1000 AE Amsterdam, The Netherlands, Tel. (+31-20) 5803 642, Telefax (+31-20) 5803 598, or to your usual subscription agent. Postage and handling charges include surface delivery except to the following countries where air delivery via SAL (Surface Air Lift) mail is ensured: Argentina, Australia, Brazil, Canada, Hong Kong, India, Israel, Japan*, Malaysia, Mexico, New Zealand, Pakistan, PR China, Singapore, South Africa, South Korea, Taiwan, Thailand, USA. * For Japan air delivery (SAL) requires 50% additional charge of the normal postage and handling charge. For all other countries airmail rates are available upon request. Claims for missing issues must be made within three months of our publication (mailing) date, otherwise such claims cannot be honoured free of charge. Back volumes of the *Journal of Chromatography* (Vols. 1-534) are available at Dfl. 208.00 (plus postage). Customers in the USA and Canada wishing information on this and other Elsevier journals, please contact Journal Information Center, Elsevier Science Publishing Co. Inc., 655 Avenue of the Americas, New York, NY 10010, USA, Tel. (+1-212) 633 3750, Telefax (+1-212) 633 3990.

Abstracts/Contents Lists published in Analytical Abstracts, Biochemical Abstracts, Biological Abstracts, Chemical Abstracts, Chemical Titles, Chromatography Abstracts, Clinical Chemistry Lookout, Current Contents/Life Sciences, Current Contents/Physical, Chemical & Earth Sciences, Deep-Sea Research/Part B: Oceanographic Literature Review, Excerpta Medica, Index Medicus, Mass Spectrometry Bulletin, PASCAL-CNRS, Pharmaceutical Abstracts, Referativnyi Zhurnal, Research Alert, Science Citation Index and Trends in Biotechnology.

See inside back cover for Publication Schedule, Information for Authors and information on Advertisements.

All rights reserved. No part of this publication may be reproduced, stored in a retrieval system or transmitted in any form or by any means, electronic, mechanical, photocopying, recording or otherwise, without the prior written permission of the publisher, Elsevier Science Publishers B.V., Permissions Department, P.O. Box 521, 1000 AN Amsterdam, The Netherlands.

Upon acceptance of an article by the journal, the author(s) will be asked to transfer copyright of the article to the publisher. The transfer will ensure the widest possible dissemination of information.

Submission of an article for publication entails the authors' irrevocable and exclusive authorization of the publisher to collect any sums or considerations for copying or reproduction payable by third parties (as mentioned in article 17 paragraph 2 of the Dutch Copyright Act of 1912 and the Royal Decree of June 20, 1974 (S. 351) pursuant to article 16 b of the Dutch Copyright Act of 1912) and/or to act in or out of Court in connection therewith.

Special regulations for readers in the USA. This journal has been registered with the Copyright Clearance Center, Inc. Consent is given for copying of articles for personal or internal use, or for the personal use of specific clients. This consent is given on the condition that the copier pays through the Center the per-copy fee stated in the code on the first page of each article for copying beyond that permitted by Sections 107 or 108 of the US Copyright Law. The appropriate fee should be forwarded with a copy of the first page of the article to the Copyright Clearance Center, Inc., 27 Congress Street, Salem, MA 01970, USA. If no code appears in an article, the author has not given broad consent to copy and permission to copy must be obtained directly from the author. All articles published prior to 1980 may be copied for a per-copy fee of US\$ 2.25, also payable through the Center. This consent does not extend to other kinds of copying, such as for general distribution, resale, advertising and promotion purposes, or for creating new collective works. Special written permission must be obtained from the publisher for such copying.

No responsibility is assumed by the Publisher for any injury and/or damage to persons or property as a matter of products liability, negligence or otherwise, or from any use or operation of any methods, products, instructions or ideas contained in the materials herein. Because of rapid advances in the medical sciences, the Publisher recommends that independent verification of diagnoses and drug dosages should be made.

Although all advertising material is expected to conform to ethical (medical) standards, inclusion in this publication does not constitute a guarantee or endorsement of the quality or value of such product or of the claims made of it by its manufacturer.

This issue is printed on acid-free paper.

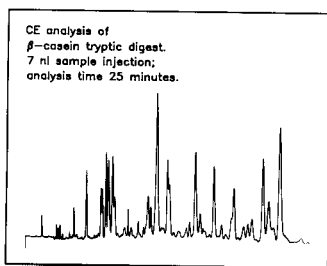
Discover new solutions



New personal CE injects simplicity and speed into your bioseparations

Capillary electrophoresis is the most significant new bioseparation tool in 20 years. Peptides, proteins, amino acid derivatives, nucleic acids, DNA fragments—even viruses and bacteria—all have been resolved by CE with unprecedented speed and efficiency. And now there's a complete, compact "personal CE" system—Isco's new Model 3850 Electropherograph™—that gives you affordable access to this powerful technology.

- An exclusive split-flow injector makes reproducible nanoliter injections as easy as HPLC.
- Dual polarity power supply delivers up to 30 kV and 300 μ A to support any CE separation method.



- Variable UV detection gives excellent sensitivity over a wide range of samples.
- Quick-change capillary holder lets you install any coated, naked, or gel-filled capillary in under two minutes.

**Contact us today
for application details.**

Isco, Inc., P.O. Box 5347
Lincoln NE 68505, U.S.A.
(800)228-4250

Isco Europe AG, Brüschr. 17
CH8708 Männedorf, Switzerland
Fax **(41-1)920 62 08**



Distributors • **Australia:** Australian Chromatography Co. • **Austria:** IN-ULA • **Belgium:** N.V. Mettler-Toledo S.A. • **Canada:** Canberra Packard Canada, Ltd. • **Denmark:** Mikrolab Aarhus • **Finland:** FTEK OY • **France:** Ets. Roucaire, S.A. • **Germany:** Colona Messtechnik GmbH • **Italy:** Analytical Control Italia S.p.A. • **Japan:** JSI Co. Ltd. • **Korea:** Sang Chong, Ltd. • **The Netherlands:** Beun-de Ronde B.V. • **Norway:** Djipl. Ing. Houm A.S. • **Spain:** CHEMICONTROL, S.L. • **Sweden:** Spectrochrom AB • **Switzerland:** IG Instrumenten-Gesellschaft AG • **U.K.:** Jones Chromatography Ltd. •

THE STANDARD TEXT ON THE SUBJECT...

Chemometrics: a textbook

D.L. Massart, *Vrije Universiteit Brussel, Belgium*,
B.G.M. Vandeginste, *Katholieke Universiteit Nijmegen, The Netherlands*,
S.N. Deming, *Dept. of Chemistry, University of Houston, TX, USA*,
Y. Michotte and L. Kaufman, *Vrije Universiteit Brussel, Belgium*

(Data Handling in Science and Technology, 2)

Most chemists, whether they are biochemists, organic, analytical, pharmaceutical or clinical chemists and many pharmacists and biologists need to perform chemical analyses. Consequently, they are not only confronted with carrying out the actual analysis, but also with problems such as method selection, experimental design, optimization, calibration, data acquisition and handling, and statistics in order to obtain maximum relevant chemical information. In other words: they are confronted with chemometrics.

This book, written by some of the leaders in the field, aims to provide a thorough, up-to-date introduction to this subject. The reader is given the opportunity to acquaint himself with the tools used in this discipline and the way in which they are applied. Some practical examples are given and the reader is shown how to select the appropriate tools in a given situation. The book thus provides the means to approach and solve analytical problems strategically and systematically, without the need for the reader to become a fully-fledged chemometrician.

Contents: Chapter 1. Chemometrics and the Analytical Process. 2. Precision and Accuracy. 3. Evaluation of Precision and Accuracy. Comparison of Two Procedures. 4. Evaluation of Sources of Variation in Data. Analysis of Variance. 5. Calibration. 6. Reliability and Drift. 7. Sensitivity and Limit of Detection. 8. Selectivity and Specificity. 9. Information. 10. Costs. 11. The Time Constant. 12. Signals and Data. 13. Regression Methods. 14. Correlation Methods. 15. Signal Processing. 16. Response Surfaces and Models. 17. Exploration of Response Surfaces. 18. Optimization of Analytical Chemical Methods. 19. Optimization of Chromatographic Methods. 20. The Multivariate Approach. 21. Principal Components and Factor Analysis. 22. Clustering Techniques. 23. Supervised Pattern Recognition. 24. Decisions in the Analytical Laboratory. 25. Operations Research. 26. Decision Making. 27. Process Control. Appendix. Subject Index.

"...it is apparent that the book is the most comprehensive available on chemometrics. Beginners and those more familiar with the field will find the book a great benefit because of that breadth, and especially because of the clarity and relative uniformity of presentation. Like its predecessor, this book will be the standard text on the subject for some time." (Trends in Analytical Chemistry)

1988 485 pages US\$ 85.25 / Dfl. 175.00 ISBN 0-444-42660-4

ELSEVIER SCIENCE PUBLISHERS

P.O. Box 211, 1000 AE Amsterdam, The Netherlands

P.O. Box 1663, Grand Central Station, New York, NY 10163, USA

7385A

JOURNAL OF CHROMATOGRAPHY

VOL. 552 (1991)

JOURNAL of CHROMATOGRAPHY

INCLUDING ELECTROPHORESIS AND OTHER SEPARATION METHODS

SYMPOSIUM VOLUMES

EDITORS

E. HEFTMANN (Orinda, CA), Z. DEYL (Prague)

EDITORIAL BOARD

E. Bayer (Tübingen), S. R. Binder (Hercules, CA), S. C. Churms (Rondebosch), J. C. Fetzer (Richmond, CA), E. Gelpí (Barcelona), K. M. Gooding (Lafayette, IN), S. Hara (Tokyo), P. Helboe (Brønshøj), W. Lindner (Graz), T. M. Phillips (Washington, DC), S. Terabe (Hyogo), H. F. Walton (Boulder, CO), M. Wilchek (Rehovot)



ELSEVIER

AMSTERDAM — LONDON — NEW YORK — TOKYO

J. Chromatogr., Vol. 552 (1991)

All rights reserved. No part of this publication may be reproduced, stored in a retrieval system or transmitted in any form or by any means, electronic, mechanical, photocopying, recording or otherwise, without the prior written permission of the publisher, Elsevier Science Publishers B.V., Permissions Department, P.O. Box 521, 1000 AN Amsterdam, The Netherlands.

Upon acceptance of an article by the journal, the author(s) will be asked to transfer copyright of the article to the publisher. The transfer will ensure the widest possible dissemination of information.

Submission of an article for publication entails the authors' irrevocable and exclusive authorization of the publisher to collect any sums or considerations for copying or reproduction payable by third parties (as mentioned in article 17 paragraph 2 of the Dutch Copyright Act of 1912 and the Royal Decree of June 20, 1974 (S. 351) pursuant to article 16 b of the Dutch Copyright Act of 1912) and/or to act in or out of Court in connection therewith.

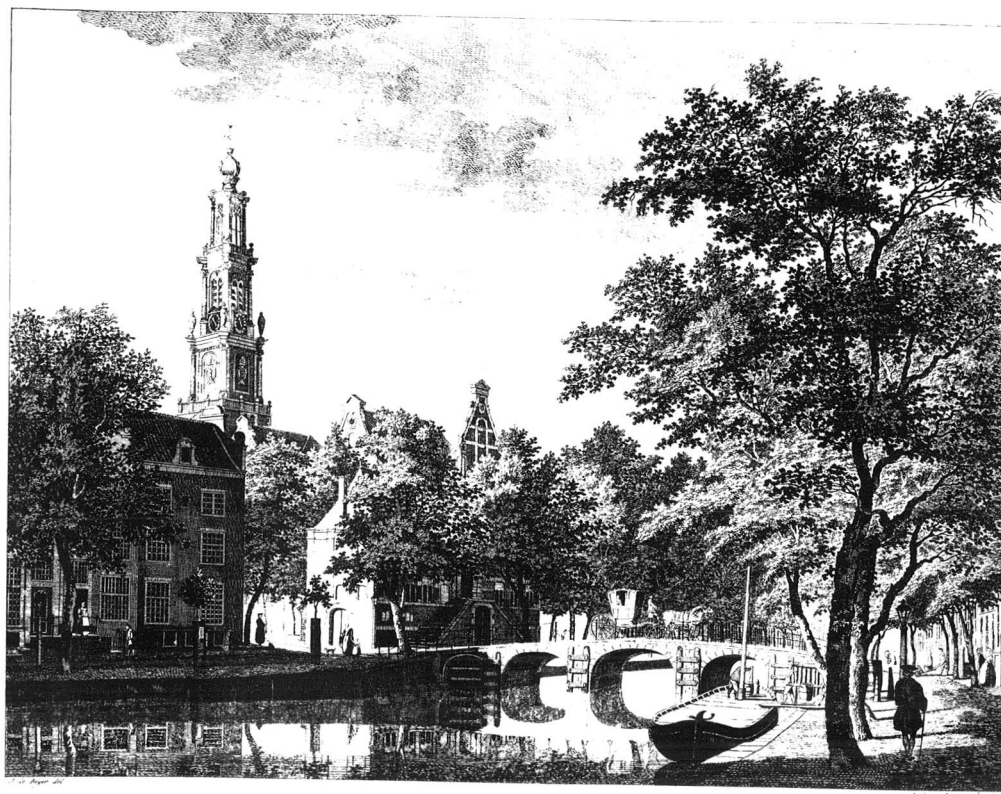
Special regulations for readers in the U.S.A. This journal has been registered with the Copyright Clearance Center, Inc. Consent is given for copying of articles for personal or internal use, or for the personal use of specific clients. This consent is given on the condition that the copier pays through the Center the per-copy fee stated in the code on the first page of each article for copying beyond that permitted by Sections 107 or 108 of the U.S. Copyright Law. The appropriate fee should be forwarded with a copy of the first page of the article to the Copyright Clearance Center, Inc., 27 Congress Street, Salem, MA 01970, U.S.A. If no code appears in an article, the author has not given broad consent to copy and permission to copy must be obtained directly from the author. All articles published prior to 1980 may be copied for a per-copy fee of US\$ 2.25, also payable through the Center. This consent does not extend to other kinds of copying, such as for general distribution, resale, advertising and promotion purposes, or for creating new collective works. Special written permission must be obtained from the publisher for such copying.

No responsibility is assumed by the Publisher for any injury and/or damage to persons or property as a matter of products liability, negligence or otherwise, or from any use or operation of any methods, products, instructions or ideas contained in the materials herein. Because of rapid advances in the medical sciences, the Publisher recommends that independent verification of diagnoses and drug dosages should be made.

Although all advertising material is expected to conform to ethical (medical) standards, inclusion in this publication does not constitute a guarantee or endorsement of the quality or value of such product or of the claims made of it by its manufacturer.

This issue is printed on acid-free paper.

SYMPOSIUM VOLUME



**18TH INTERNATIONAL SYMPOSIUM ON
CHROMATOGRAPHY**

PART I

Amsterdam, September 23–28, 1990

Guest Editors

U. A. Th. BRINKMAN
(Amsterdam)

H. POPPE
(Amsterdam)

The proceedings of the *18th International Symposium on Chromatography* are published in two consecutive volumes of the *Journal of Chromatography*: Vols. 552 and 553. The Preface to the proceedings only appears in Vol. 552; a combined Author Index to both Vols. 552 and 553 only appears in Vol. 553. The proceedings are dedicated to Professor **J. F. K. Huber**; on p. XV of Vol. 552 appears an introduction to his life and work.

CONTENTS

18TH INTERNATIONAL SYMPOSIUM ON CHROMATOGRAPHY, AMSTERDAM, SEPTEMBER 23–28, 1990, PART I

Preface

by U. A. Th. Brinkman and H. Poppe XIII

Josef F. K. Huber

by H. Poppe and U. A. Th. Brinkman XVII

THEORY

Retentions of alkyloxazoles and alkylthiazoles and their prediction based on non-linear additivity concepts in gas chromatography
by R. V. Golovnya, I. L. Zhuravleva, E. V. Yakush and V. V. Schenderjuk (Moscow, U.S.S.R.) 1

Extension of the electrostatic retention model of reversed-phase ion-pair high-performance liquid chromatography to include the effect of the eluent pH
by Á. Bartha and J. Ståhlberg (Södertälje, Sweden) and F. Szokoli (Veszprém, Hungary) 13

Adsorption and partition mode in high-performance liquid chromatography of highly polar solutes on silica
by V. D. Shatz and H. A. Kažoka (Riga, U.S.S.R.) 23

Determination of sorbent polarity and selectivity by linear regression of retention indices
by O. G. Larionov, V. V. Petrenko and N. P. Platonova (Moscow, U.S.S.R.) 31

Theoretical approach to the gas chromatographic separation of enantiomers on dissolved cyclodextrin derivatives
by M. Jung, D. Schmalzing and V. Schurig (Tübingen, Germany) 43

New aspects of quantitative structure-retention relationships in chromatography
by N. Dimov (Sofia, Bulgaria) and M. Moskovkina (Shumen, Bulgaria) 59

Comparison of various isotherm models for predicting competitive adsorption data
by J. Zhu and A. M. Katti (Knoxville, TN, U.S.A.) and G. Guiochon (Knoxville and Oak Ridge, TN, U.S.A.) 71

Calculation of retention and selectivity in reversed-phase liquid chromatography
by S. V. Galushko (Kiev, U.S.S.R.) 91

Computer-aided optimization of the experimental conditions for the isocratic reversed-phase high-performance liquid chromatographic separation of hormonal steroids
by J.-Q. Wei, J.-L. Wei and X.-T. Zhou (Jinan, China) 103

Development of a rational optimisation procedure for the automated sample clean-up with column switching in pesticide residue analysis
by E. A. Hogendoorn, R. Hoogerbrugge, C. E. Goewie and P. van Zoonen (Bilthoven, The Netherlands) and P. J. Schoenmakers (Eindhoven, The Netherlands) 113

GAS CHROMATOGRAPHY

Techniques

Production and use of capillary traps for headspace gas chromatography of airborne volatile organic compounds
by B. V. Burger, M. le Roux, Z. M. Munro and M. E. Wilken (Stellenbosch, South Africa) 137

Investigation of cross-linking chiral stationary phases within capillary columns
by X. Lou, Y. Liu and L. Zhou (Dalian, China) 153

Gas-liquid chromatography in qualitative analysis. XIX. The use of antioxidants to delay the oxidation of polyoxyethylene glycol stationary phases by A. D. Dale (Potters Bar, U.K.) and M. B. Evans (Hatfield, U.K.)	161
Gas chromatography in qualitative analysis. XX. The deactivation of diatomaceous supports by batyl alcohol by M. B. Evans, R. Bird and H. O'Sullivan (Hatfield, U.K.)	169
Gas chromatographic investigation of silica supports modified in a high-frequency low-temperature plasma by T. B. Gavrilova, Yu. S. Nikitin and E. V. Vlasenko (Moscow, U.S.S.R.) and I. Topalova, N. Petsev and Chr. Chaney (Sofia, Bulgaria)	179
Live retention database for identification in multi-step temperature-programmed capillary gas chromatography by Y. Guan and L. Zhou (Dalian, China)	187
Gas-liquid microcapillary columns precoated with graphitized carbon black by G. P. Cartoni, L. Castellani, G. Goretti, M. V. Russo and P. Zacchei (Rome, Italy)	197
Modern approach to the quantitative determination of volatiles in solid samples. Multiple headspace extraction gas chromatography for the determination of cyclohexanone residues in soil by M. R. Milana, A. Maggio, M. Denaro, R. Feliciani and L. Gramiccioni (Rome, Italy)	205
<i>Environmental Applications</i>	
Chromatographie en phase gazeuse haute résolution-spectrométrie de masse des congénères de bi-phényles polychlorés dans quelques échantillons d'origine biologique par M. R. Driss (Tunis, Tunisie), S. Sabbah (Hammam-lif, Tunisie) et M. L. Bouguerra (Tunis, Tunisie)	213
Analyse par chromatographie en phase gazeuse haute résolution-spectrométrie de masse des mélanges techniques de Phénochlor par S. Sabbah (Hammam-lif, Tunisie) et M. L. Bouguerra (Tunis, Tunisie)	223
Determination of phenoxy ester herbicides by gas and high-performance liquid chromatography by C. Sánchez-Brunete, S. Pérez and J. L. Tadeo (Madrid, Spain)	235
Solid-matrix partition for separation of organochlorine pesticide residues from fatty materials by A. di Muccio, A. Ausili, R. Dommarco, D. Attard Barbini, A. Santilio, F. Vergori, G. de Merulis and L. Sernicola (Rome, Italy)	241
Rapid method for the determination of organochlorine pesticides in milk by T. Prapamontol and D. Stevenson (Guildford, U.K.)	249
Multi-matrix-multi-pesticide method for agricultural products by L. G. M. Th. Tuinstra (Wageningen, The Netherlands), F. R. Povel (Vecnendaal, The Netherlands) and A. H. Roos (Wageningen, The Netherlands)	259
Identification by capillary gas chromatography-mass spectrometry of volatile organohalogen compounds formed during bleaching of kraft pulp by C. Rosenberg, T. Aalto, J. Tornaeus and A. Hesso (Helsinki, Finland), P. Jäppinen (Imatra, Finland) and H. Vainio (Lyon, France)	265
<i>Other Applications</i>	
Applications of capillary gas chromatography to the quality control of butter and related products by A. Antonelli and L. S. Conte (Bologna, Italy) and G. Lercker (Udine, Italy)	273
Gas chromatographic analysis of fatty acid salts by H. Rotzsche (Troisdorf, Germany)	281
Rapid derivatization and gas chromatographic determination of amino acids by P. Hušek (Prague, Czechoslovakia)	289

Analysis of multicomponent mixtures by high-resolution capillary gas chromatography and combined gas chromatography-mass spectrometry. I. Aromatics in a hydrocarbon matrix by E. Matisová, E. Juranyiová, P. Kuráň, E. Brandšteterová, A. Kočan and Š. Holotík (Bratislava, Czechoslovakia)	301
Gas chromatographic separation of unsaturated polar compounds on inorganic stationary phases containing silver nitrate by V. G. Berezkin, E. N. Viktorova and V. S. Gavrichev (Moscow, U.S.S.R.) and S. A. Range, K. R. Kuningas and A. E. Meister (Tallinn, U.S.S.R.)	313
Reaction-gas chromatography for physico-chemical investigations on aggressive gases by L. G. Berezkina, S. I. Borisova, S. V. Melnikova and V. I. Souhodolova (Moscow, U.S.S.R.)	319
Thermodesorption-gas chromatography-mass spectrometric analysis of biological materials for potential molecular precursors of the constituents of the crude oils by W. Püttmann (Aachen, Germany)	325
Simultaneous gas-liquid chromatographic determination of sugars and organic acids as trimethylsilyl derivatives in vegetables and strawberries by M. Morvai, I. Molnár-Perl and D. Knausz (Budapest, Hungary)	337
Gas chromatographic determination of N-carboxymethyl amino acids, the periodate oxidation products of Amadori compounds by R. Badoud, L. Fay and U. Richli (Lausanne, Switzerland) and P. Husek (Prague, Czechoslovakia)	345
Gas chromatographic analysis of some glycol ether analytes on a specially packed column by K. Lekova and N. Ivanova (Sofia, Bulgaria)	353
Estimation of cellulose polarity by gas chromatography by L. A. Dernovaya and Yu. A. Eltekov (Moscow, U.S.S.R.) and J. Hradil and F. Svec (Prague, Czechoslovakia)	365

COLUMN LIQUID CHROMATOGRAPHY

Sorbents

Removal of organic pollutants from aqueous solution. V. Comparative study of the extraction, recovery and chromatographic separation of some organic insecticides using unloaded polyurethane foam columns by A. B. Farag (Mansoura, Egypt) and M. S. El-Shahawi (Damietta, Egypt)	371
Preparation and evaluation of octadecyl- or phenylpropyl-treated porous glass for the high-performance liquid chromatographic analysis of bufadienolides in <i>Bufois venenum</i> by M. Okamoto (Gifu, Japan)	381
Bead cellulose derivatives as supports for immobilization and chromatographic purification of proteins by H.-F. Boeden, K. Pommerening, M. Becker, C. Rupprich and M. Holtzhauer (Berlin, Germany), F. Loth (Teltow-Seehof, Germany) and R. Müller and D. Bertram (Leipzig, Germany)	389
Chemically bonded phases for the reversed-phase high-performance liquid chromatographic separation of basic substances by B. Buszewski, J. Schmid, K. Albert and E. Bayer (Tübingen, Germany)	415
Possible role for stationary phase metal interactions in the chromatography of hydroxyamines on silica by B. Law and P. F. Chan (Macclesfield, U.K.)	429
High-performance liquid chromatography of amino acids and dipeptides on new ion exchangers of the HEMA series by K. Štulík, V. Pacáková and H. Wang (Prague, Czechoslovakia)	439

New Czechoslovak sorbent, Ekosorb by K. Chmel (Votice, Czechoslovakia) and V. Gajdůšková (Brno, Czechoslovakia)	449
Comparison of selectivity of silica and Florisil in the separation of natural pyranocoumarins by G. Głowniak (Lublin, Poland)	453
Evaluation of the application of liquid-phase titration to the examination of the adsorption activity of silica-based high-performance liquid chromatographic packings by Z. Suprynowicz, K. Pilorz and R. Lodkowski (Lublin, Poland)	463
<i>Techniques: Ion Chromatography</i>	
Optimization of ion chromatography by N. Gros and B. Gorenc (Ljubljana, Yugoslavia)	475
Carbohydrate analysis with ion chromatography using Eurokat stationary phases. Preparative separation of monosaccharides and their fluorinated derivatives by F. Oberdorfer (Heidelberg, Germany) and K. Kemper, M. Kaleja, J. Reusch and K. Gottschall (Berlin, Germany)	483
Reversed-phase liquid chromatography coupled on-line with capillary gas chromatography. I. Introduction of large volumes of aqueous mixtures through an on-column interface by E. C. Goosens, D. de Jong, J. H. M. van den Berg and G. J. de Jong (Weesp, The Netherlands) and U. A. Th. Brinkman (Amsterdam, The Netherlands)	489
<i>Techniques: Size-Exclusion Chromatography</i>	
Isolation and quantification of polymers from autoxidized fish oils by high-performance size-exclusion chromatography with an evaporative mass detector by I. C. Burkow (Tromsø, Norway) and R. J. Henderson (Stirling, U.K.)	501
Determination of chemical composition of polymers by size-exclusion chromatography with coupled density and refractive index detection. III. Polyethylene oxide and polytetrahydrofuran by B. Trathnigg (Graz, Austria)	507
Miniaturisation of size-exclusion chromatography as a powerful clean-up tool in residue analysis by J. A. van Rhijn and L. G. M. Th. Tuinstra (Wageningen, The Netherlands)	517
<i>Techniques: Supercritical Fluid Chromatography</i>	
Effects of modifiers in packed and open-tubular supercritical fluid chromatography by H.-G. Janssen, P. J. Schoenmakers and C. A. Cramers (Eindhoven, The Netherlands)	527
Combination of supercritical fluid chromatography with thin-layer chromatography on a semi-preparative scale by L. Wünsche, U. Keller and I. Flament (Geneva, Switzerland)	539
Ion-mobility spectrometry as a detection method for packed-column supercritical fluid chromatography by M. A. Morrissey and H. M. Widmer (Basle, Switzerland)	551
<i>Other Techniques</i>	
Effects of β -cyclodextrin in the mobile phase on the retention and indirect detection of non-electrolytes in reversed-phase liquid chromatography. I. Study of aliphatic alcohols by M. Gosselet and B. Sebille (Créteil, France)	563
Column switching for the high-performance liquid chromatographic analysis of polynuclear aromatic hydrocarbons in petroleum products by A. J. Packham and P. R. Fielden (Manchester, U.K.)	575
Effects of β -cyclodextrin in the mobile phase on the retention and indirect detection of non-electrolytes in reversed-phase liquid chromatography. II. Steroids by B. Agnus (Montrouge, France) and B. Sebille and M. Gosselet (Thiais, France)	583

Use of an evaporative light scattering detector in reversed-phase high-performance liquid chromatography of oligomeric surfactants
 by Y. Mengerink, H. C. J. de Man and Sj. van der Wal (Geleen, The Netherlands) 593

Selection of buffers and of an ion-pairing agent for thermospray liquid chromatographic-mass spectrometric analysis of ionic compounds
 by A. L. L. Duchateau, B. H. M. Munsters, G. T. C. Kwakkenbos and R. G. J. van Leuken (Geleen, The Netherlands) 605

On-line coupling of liquid chromatography to thin-layer chromatography for the identification of polycyclic aromatic hydrocarbons in marine sediment by fluorescence excitation and emission spectroscopy
 by R. J. van de Nesse, G. J. M. Hoogland, J. J. M. de Moel, C. Gooijer, U. A. Th. Brinkman and N. H. Velthorst (Amsterdam, The Netherlands) 613

Time-resolved luminescence detection of derivatized thiols in column liquid chromatography
 by M. Schreurs, L. Hellendoorn, C. Gooijer and N. H. Velthorst (Amsterdam, The Netherlands) 625

Spray jet assembly interface for the coupling of reversed-phase narrow-bore liquid chromatography and Fourier transform infrared spectrometry
 by G. W. Somsen, R. J. van de Nesse, C. Gooijer, U. A. Th. Brinkman and N. H. Velthorst (Amsterdam, The Netherlands) and T. Visser, P. R. Kootstra and A. P. J. M. de Jong (Bilthoven, The Netherlands) 635

 *
 * In articles with more than one author, the name of the author to whom correspondence should be addressed is indicated in the *
 * article heading by a 6-pointed asterisk (*)
 *

PREFACE

The 18th International Symposium on Chromatography (ISC) was held in Amsterdam from September 23rd to 28th, 1990. During that week, over 800 delegates met in the well known RAI Congress Centre and participated in the scientific and social events of the 18th ISC, which was organized under the auspices of the Royal Netherlands Chemical Society and the Chromatographic Society (UK). Some 70 lectures, over 350 posters and about 25 tutorials and seminars embodied the programme, which, quantitatively, was at a similar level to those of the previous two symposia in the series, Vienna (1988) and Paris (1986). Over 40 companies participated in the instrument exhibition, which was also an essential part of the programme. The social events included a reception at the "Rijksmuseum", where Rembrandt's "Nachtwacht" could be admired from a distance of only a few feet, and Thursday night's Five Continents Party with its dancing, drinking and stimulating music.

Organizing a 5-day international symposium is a major task and chairmen have to rely heavily on their colleagues and friends for scientific input, organizational help and technical assistance. We were fortunate enough to find many who contributed in one way or another, Dr. Henk Lingeman being the only one to be mentioned here in person, because of his amazing activity in the tutorial/seminar and exhibition part of the programme. The organizers were also happy and grateful to receive substantial sums of sponsoring and grant money, which allowed them to bring over a number of distinguished colleagues from the USA and Japan. It also provided them with the opportunity to support a large number of delegates from Eastern European countries and to offer a reduced fee to students, about 100 of whom were present at the symposium.

The past decade has seen tremendous growth, both scientifically and commercially, in the field of analytical separation chemistry. This was also manifest during the 18th ISC, as witnessed by lecture and session titles such as capillary chromatography, separation of biopolymers, coupled-column systems (with emphasis on liquid chromatography-gas chromatography), electrodriven separations, hyphenated techniques (especially those using mass spectrometry), immunoaffinity-based sample treatment and separations, expert systems, chemometrics and supercritical fluid chromatography. The many dedicated applications in, for example, the pharmaceutical, biomedical and environmental areas, convincingly demonstrate the practicality of the various chromatographic techniques in, often automated, routine analysis. This type of applied research was especially in the forefront during the Wednesday morning *Roland W. Frei Memorial Session*, when several of his friends and colleagues discussed topics that were near to his heart during his scientific career.

For a short time, some of us were inclined to think that the heydays of chromatography were over and that, consequently, separation scientists would meet less frequently and have less intriguing matters to discuss. We do feel, however, that the future has many more and better things in store for all of us, as the next symposia, in Aix-en-Provence (1992) and Bournemouth (1994), will no doubt prove. Please do attend these meetings in due course and, for the present, enjoy reading the papers collected in this Symposium Volume through the efforts of Dr. Erich Heftmann and Elsevier Science Publishers.

We really enjoyed having all of you with us!

Amsterdam (The Netherlands)

UDO A. Th. BRINKMAN
HANS POPPE

These proceedings volumes are dedicated to

J. F. K. HUBER



**in recognition of his contribution to the
advances of chromatography**

JOSEF F. K. HUBER

A session at the *18th International Symposium of Chromatography* was devoted to Josef Huber's 65th birthday on January 1st, 1990 (Josef likes to have things done early), and the proceedings volumes have been dedicated to him in recognition of his contribution to the field.

Josef's activities certainly have had a large impact on the development of analytical chemistry and especially chromatography during the last 30 years. His name is strongly associated by many with the inception and development of what is now known as high-performance liquid chromatography (HPLC).

Josef has been around for a long time in the field of chromatography. His Thesis, at Innsbruck University, was on a gas chromatographic method for the determination of adsorption isotherms. This subject already revealed his interest in the physico-chemical phenomena occurring in, and made accessible by, chromatography. Later, while working at Eindhoven University of Technology and University of Amsterdam, this same fundamental approach, now in the field of the dynamics of separation, allowed him to indicate very precisely the route towards more efficient separations by liquid chromatography. He was one of those early workers who realized that small particles are the essence of this work and he was prepared to work himself through the experimental difficulties that seemed to block the way to implementation.

His activities were recognized early in those days. We remember the years around 1970, when for us in Amsterdam he appeared to be more often on lecture tours than active in the laboratory. During these years he acquired a broad view and a deep insight into analytical chemistry as a whole. This allowed him, we think more than other workers of similar stature, to be not only a specialist in the chromatographic process, but also to have a great influence in other fields where he did not claim to be an expert.

Thus, during these same years he published on detectors for LC, still a central topic in modern developments; on peak capacity and information flow; on concepts from chemometrics, long before this word was known; on pre- and post-column derivatizations, also still a topic of current interest. In addition he had a clear insight into the vital importance of LC in various pharmaceutical, biomedical, environmental and industrial areas, and directed his various research groups in the right directions. Numerous workers, now well known and having their own research groups, were put on the right track, not necessarily chromatographic, by Josef.

Born a mid-European, he was aware of the cultural and scientific homogeneity of Europe. Through the days of the cold war he maintained scientific contacts with Eastern Europe. We believe we speak on behalf of the analytical chemists in that part of the world when we honour him for his activities in this respect during the course of many years.

Last but not least, his character and perhaps his roots in the old nation of Austria made him a gentleman in the best and proper sense of the word. The hectic, hard, and sometimes aggressive life in such a competitive science as analytical chemistry never corrupted his 'savoir vivre', honesty and sincerity.

Since 1990 he enjoys a pension from several universities, that owe him more

than that. Many other universities, envious of them, have recognized his merits with doctorates *honoris causa*.

We wish him a fruitful continuation of his scientific activities, but above all we wish Josef and Sepha good health and happiness for many years to come.

HANS POPPE

UDO A. Th. BRINKMAN

Retentions of alkyloxazoles and alkylthiazoles and their prediction based on non-linear additivity concepts in gas chromatography

R. V. GOLOVNYA*, I. L. ZHURAVLEVA, E. V. YAKUSH and V. V. SCHENDERJUK

A. N. Nesmeyanov Institute of Organo-Element Compounds, USSR Academy of Sciences, Vavilov st., 28, Moscow (USSR)

ABSTRACT

The gas chromatographic (GC) behaviour of 39 alkyloxazoles and alkylthiazoles was studied on three capillary columns with OV-101-KF, Triton X-305-KF and PEG-40M-KF. The regularities in the thermodynamic characteristics of sorption of azoles having O or S atoms were established. Energy contributions of methyl, ethyl and propyl groups to the partial molar free energy of sorption of alkyloxazoles and alkylthiazoles were determined. It was found that the contributions of the same alkyl group are different and dependent on the nature of the heterocycle and the position of the alkyl group with respect to the heteroatoms in the azole ring. Two methods for the prediction of retention indices on the basis of the analogy of the GC behaviour of azoles and inconstancy of the contributions of the same alkyl groups are given. The predicted retention indices are in good agreement with the experimental values.

INTRODUCTION

Computer programs using sorption-structure correlations considerably increase the number of substances that can be identified [1]. In the development of such programs for the determination of heterocyclic compounds, it is necessary to take into account the influence of the nature of the heterocyclic ring and substituents on sorption properties of substances [1-4]. It has recently been shown that one can predict retention indices of methylpyridines and methylpyrazines in capillary chromatography by taking into account various values of the energy contribution of the same molecular fragment situated in the different positions on the heterocyclic ring [5]. This approach was applied to the prediction of the retention indices of alkylthiazoles on packed columns [6].

Alkyloxazoles and alkylthiazoles with analogous molecular structure have similar physico-chemical properties [7,8]. Some alkyloxazoles and alkylthiazoles have been characterized by retention index values [6,7,9,10] but these data are not sufficient to predict the gas chromatographic (GC) behaviour of a wide range of substituted compounds.

The purpose of this work was to compare the partial molar free energies of

sorption of alkyloxazoles and alkylthiazoles analysed on capillary columns of different polarity, to determine and compare the contributions of methyl, ethyl and propyl groups to the sorption energy of azoles depending on the nature of the heterocycle and the position of the alkyl group with respect to N, O and S heteroatoms and to search for a scheme for the calculation of retention indices of alkyl-substituted oxazoles and thiazoles on the basis of the correlation established.

EXPERIMENTAL

Alkyloxazoles and alkylthiazoles were analysed using a Carlo Erba Mega 5300 gas chromatograph with a flame ionization detector at 110°C, equipped with three glass capillary columns (50 m × 0.3 mm I.D., film thickness 0.4 μm) with OV-101-KF, Triton X-305-KF and PEG-40M-KF as the stationary phases. Potassium fluoride was used to suppress the adsorption of organic bases on the surface of the column and enhance the efficiency of GC separation. It has also been found that potassium fluoride is capable of interacting with organic bases via a donor-acceptor mechanism [11]. Columns were prepared as described previously [12].

For the OV-101-KF column the coating efficiency (*CE*) calculated for *n*-tridecane at 110°C was 80%. To determine the *CE* value the equation

$$CE = \frac{n_{\text{exp}}}{n_{\text{theor}}} \cdot 100\% \quad (1)$$

was used, where n_{exp} and n_{theor} are the numbers of theoretical plates calculated from experimental data and the theory of capillary chromatography, respectively. For the Triton X-305-KF and PEG-40M-KF columns the *CE* values were 70%; calculations of *CE* were made for *n*-heptadecane at 120°C.

Substances were analysed as 1% solutions in pentane. Sample volumes were 0.1–0.2 μl. The samples were injected into the capillary column through a splitter (50:1). Helium was used as the carrier gas. The 39 compounds involved in this study were oxazole, thiazole and mono-, di- and trisubstituted oxazoles and thiazoles with methyl, ethyl and propyl groups in different positions on the heterocyclic ring. The values of retention indices [13] were calculated with respect to C₅–C₁₆ *n*-alkanes. The reproducibilities of retention indices averaged over three to ten measurements were within 2 i.u. for each of the 39 azoles.

RESULTS AND DISCUSSION

Oxazoles and thiazoles are five-membered aromatic heterocyclic molecules with two heteroatoms, *viz.*, N and O and N and S, respectively. The basic properties of these compounds arise from the presence of the N atom in the oxazole and thiazole rings. At the same time the O and S atoms produce a significant effect on the basicity and other physico-chemical properties of oxazoles and thiazoles, such as the polarizability and the dipole moment of the molecule [7,8,14]. As a result, oxazoles and thiazoles of similar structure should show different sorption thermodynamic characteristics. As the mass of a sulphur atom is twice that of oxygen, the energy of dis-

persive interaction of alkylthiazoles with stationary phases should be higher than that of corresponding alkyloxazoles.

The analogy of the GC behaviour of oxygen- and sulphur-containing aliphatic compounds such as alcohols and thiols or ethers and sulphides has been observed previously [15]. Equations to calculate retention index values of one analogous substance from the retention indices of another have been given [15]. We have studied alkyloxazoles and alkylthiazoles with analogous structures. The difference between the partial molar free sorption energies of an alkylthiazole (Tz) and an alkyloxazole (Ox) of analogous structure, $\delta\Delta G(S,O)$, can be calculated using the equation

$$\delta\Delta G(S,O) = \Delta G(Tz) - \Delta G(Ox) = -RT \ln \left[\frac{V_g(Tz)}{V_g(Ox)} \right] \quad (2)$$

where V_g is the specific retention volume of the compared compounds.

As the comparison of sorption properties was performed on the same column under the same conditions, eqn. 2 becomes

$$\delta\Delta G(S,O) = -RT \ln \left[\frac{t'(Tz)}{t'(Ox)} \right] \quad (3)$$

where t' is the adjusted retention time of compared compounds.

The $\delta\Delta G(S,O)$ values obtained are given in Table I. According to these values, the pairs of Tz and Ox analogues can be divided into two groups: di- and trisubstituted compounds with the alkyl substituent in the 2-position on the heterocycle (pairs 1–16) and compounds having no substituent in this position (pairs 17–19). Thus, for the OV-101–KF column the average value of $\delta\Delta G(S,O)$ is -3.04 kJ/mol for 2-alkyl-substituted compounds and -3.63 kJ/mol for compounds unsubstituted in the 2-position. On the polar columns the average values of $\delta\Delta G(S,O)$ for the two groups of analogues differ more sharply (see Table I).

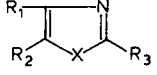
It should be noted that the 2-position in the molecules of studied compounds plays a peculiar role in thiazoles and oxazoles [7,8]. It is the preferred position in nucleophile substitution reactions because of the relatively large positive charge density on the C-2 atom [16]. Therefore, an H atom in the 2-position has relatively high acidity [8]. The $\delta\Delta G(S,O)$ values obtained (Table I) also reflect the presence of an activated H-2 atom capable of donor–acceptor interactions, including hydrogen bonding, with stationary phases. The $\delta\Delta G(S,O)$ values for compounds with a 2-H atom are always higher than those for 2-alkyl-substituted azoles.

The data on the change in sorption energy of azoles allow a linear correlation between retention index values for alkyloxazoles (I_{Ox}) and alkylthiazoles (I_{Tz}) with analogous structures. Thus, the retention indices of di- and trisubstituted alkyloxazoles having an alkyl substituent in the 2-position on the heterocycle can be calculated according to the following equations:

$$\begin{aligned} &\text{for OV-101–KF:} \\ I_{Ox} &= 1.01I_{Tz} - 163 \end{aligned} \quad (4)$$

TABLE I

DIFFERENCE IN PARTIAL MOLAR FREE ENERGIES OF THE SORPTION OF ALKYLTHIAZOLES AND ALKYL-OXAZOLES WITH ANALOGOUS STRUCTURE, $\delta\Delta G(S,O)$, ON THREE CAPILLARY COLUMNS AT 100°C

No. of pair	Compared pair ^a			$\delta\Delta G(S,O)$ (kJ/mol)		
				OV-101-KF	Triton X-305-KF	PEG-40M-KF
	R ₁	R ₂	R ₃			
1	Me	H	Me	3.13	3.50	3.53
2	H	Me	Me	3.13	3.35	3.23
3	Me	H	Et	3.02	3.47	3.42
4	Et	H	Me	3.05	3.44	3.32
5	Me	Me	Me	3.05	3.23	3.23
6	H	Me	Et	3.04	3.25	3.31
7	H	Et	Me	3.15	3.34	3.25
8	Me	H	Pr	3.02	3.47	3.40
9	Et	H	Et	2.98	3.26	3.25
10	Pr	H	Me	3.05	3.47	3.35
11	Me	Et	Me	2.96	3.43	3.34
12	Me	Me	Et	3.00	3.27	3.22
13	H	Et	Et	2.94	3.43	3.31
14	Me	Pr	Me	3.08	3.58	3.50
15	H	Et	Pr	2.96	3.47	3.33
16	Me	Pr	Et	3.01	3.55	3.44
Average				3.04	3.41	3.34
17	H	H	H	3.68	4.37	4.29
18	H	Me	H	3.66	4.22	4.11
19	Me	Me	H	3.55	4.12	4.01
Average				3.63	4.24	4.14

^a X = O for oxazoles and S for thiazoles. Me = Methyl; Et = ethyl; Pr = propyl.

for Triton X-305-KF:

$$I_{Ox} = 0.97I_{Tz} - 138 \quad (5)$$

for PEG-40M-KF:

$$I_{Ox} = 0.985I_{Tz} - 164 \quad (6)$$

The calculated and experimental values of I_{Ox} are compared in Table II. The experimental retention indices of alkylthiazoles applied for the determination of the coefficients in eqns. 4-6 are also given. The standard deviation of the calculated and experimental values of I_{Ox} (see Table II) is 2.4-5.7 i.u., depending on the polarity of the columns.

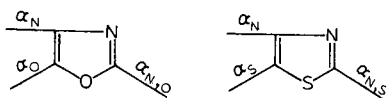
Another scheme for the prediction of the retention indices of azoles was found using the energy contributions of alkyl groups to the sorption energies of alkyl-oxazoles and alkylthiazoles. The energy contribution of an alkyl group, ΔG^{Alk} , was determined according to the following equations from the sorption energies of two compounds, one containing an alkyl group and the other not:

$$\Delta G^{\text{Alk}} = \Delta G(\text{AlkOx}) - \Delta G(\text{Ox}) = -RT \ln \left[\frac{t'(\text{AlkOx})}{t'(\text{Ox})} \right] \quad (7)$$

$$\Delta G^{\text{Alk}} = \Delta G(\text{AlkTz}) - \Delta G(\text{Tz}) = -RT \ln \left[\frac{t'(\text{AlkTz})}{t'(\text{Tz})} \right] \quad (8)$$

where t' (AlkOx) and t' (Ox) are the adjusted retention times of oxazoles containing and not containing an alkyl group, respectively, and t' (AlkTz) and t' (Tz) are corresponding values for thiazoles.

For the comparison of the ΔG^{Alk} contributions of the same alkyl group located at different positions in the oxazole and thiazole molecules, the following indications are accepted because any substituent is in an α -position with respect to one or two heteroatoms:



The values of ΔG^{Alk} for methyl, ethyl and propyl groups calculated according to eqns. 7 and 8 in Table III. When eqns. 7 and 8 could not be used because of the absence of standard substituted oxazoles and thiazoles, more complex schemes were applied (see Table III). The contributions of "independent" methyl and ethyl groups calculated from the adjusted retention times of toluene and benzene or ethylbenzene and benzene are also given in Table III.

The comparison of the alkyl group contributions in substituted oxazoles and thiazoles (see Table III) shows that maximum ΔG^{Alk} values are observed for the groups in the 5-position (α_{O} in oxazole and α_{S} in thiazole). Moreover, on the non-polar OV-101-KF column the alkyl contributions for α_{O} and α_{S} positions do not depend on the nature of the heterocycle, and are equal -2.16 and -2.10 kJ/mol for methyl groups in oxazole and thiazole, respectively. It should be noted that the ΔG^{Me} values for α_{O} - and α_{S} -positions are slightly higher than the contribution of the "independent" methyl group in toluene (see Table III).

On transferring any substituent from a α_{O} - or α_{S} -position to the α_{N} -position in an oxazole or thiazole molecule, an α -effect [17] becomes pronounced, *i.e.*, a sharp decrease in the alkyl group contribution arising from its interaction with the N heteroatom is observed. It is interesting that on non-polar and intermediate-polarity columns the ΔG^{Alk} values for the α_{N} -position of oxazoles and thiazoles are almost equal (Table III). For example, the $\Delta G^{\text{Me}}(\alpha_{\text{N}})$ values on the OV-101-KF column are -1.44 and -1.43 kJ/mol for oxazoles and thiazoles, respectively; these values are close to the contribution of methyl group in α -picoline [5]. A difference in the $\Delta G^{\text{Alk}}(\alpha_{\text{N}})$ contributions for oxazoles and thiazoles appears only on the polar PEG-40M-KF column (see Table III).

The values of the contributions of alkyl groups situated in an $\alpha_{\text{N,O}}$ - or $\alpha_{\text{N,S}}$ -position, *i.e.*, between the two heteroatoms, depend essentially on the nature of the heterocycle. This dependence manifests itself very clearly on all columns (Table III).

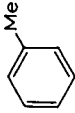
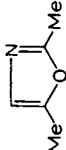
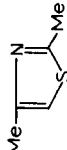
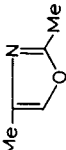
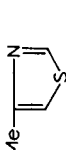
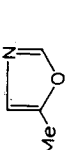

TABLE II
EXPERIMENTAL AND CALCULATED RETENTION INDICES OF ALKYL-OXAZOLES BY EQNS. 3-5 FROM RETENTION INDEX VALUES OF
ALKYLTHIAZOLES ON THREE COLUMNS AT 110°C

Compound ^a	I_{ox}			I_{Tz} (exptl.)			PEG-40M-KF	Triton X-305-KF	PEG-40M-KF	Triton X-305-KF	PEG-40M-KF		
	R ₁	R ₂	R ₃	OV-101-KF	Triton X-305-KF	PEG-40M-KF						OV-101-KF	OV-101-KF
				Exptl.	Calc.	Exptl.						Calc.	Exptl.
Me	H	Me	Me	730	1043	1050	1108	887	1225	1291			
H	Me	Me	Me	765	1092	1091	1145	922	1267	1324			
Me	H	Et	Et	818	1104	1108	1159	970	1285	1349			
Et	H	Me	Me	820	1111	1114	1171	974	1291	1356			
Me	Me	Me	Me	843	1150	1141	1200	997	1319	1380			
H	Me	Et	Et	851	1155	1147	1204	1004	1325	1388			
H	Et	Me	Pr	855	1162	1159	1222	1010	1337	1403			
Me	H	Pr	Pr	901	1175	1178	1229	1053	1357	1418			
Et	H	Et	Et	903	1172	1165	1228	1053	1343	1409			
Pr	H	Me	Me	910	1198	1201	1247	1064	1380	1428			
Me	Et	Me	Me	923	1201	1201	1252	1072	1380	1438			
Me	Me	Et	Et	926	1210	1202	1260	1077	1381	1439			
H	Et	Et	Et	940	1222	1222	1279	1090	1402	1463			
Me	Pr	Me	Me	1000	1269	1275	1319	1157	1457	1515			
H	Et	Pr	Pr	1024	1294	1293	1347	1175	1475	1534			
Me	Pr	Et	Et	1079	1327	1329	1374	1233	1512	1567			
σ^b (i.u.)				2.4	5.2	5.7							

^a General structure as in Table I.

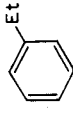

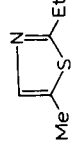
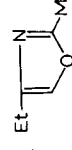
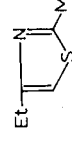
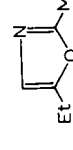
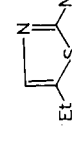
^b σ is the standard deviation of the calculated I_{ox} values.

TABLE III
 ENERGY CONTRIBUTIONS OF ALKYL GROUPS, ΔG^{alk} , TO THE SORPTION ENERGY OF ALKYLOXAZOLES AND ALKYLTHIAZOLES ON
 THREE COLUMNS AT 110°C

Starting compounds	Scheme for calculation ^a	Alkyl position ^a	$-\Delta G^{\text{alk}}$ (kJ/mol)		
			OV-101-KF	Triton X-305-KF	PEG-40M-KF
(Tol) 	(Bz) $\Delta G^{\text{Tol}} - \Delta G^{\text{Bz}}$	Me, Bz	2.06	1.92	1.75
(2) 	(1) $\Delta G^2 - \Delta G^1$	Me($\alpha_{\text{N,O}}$), Ox	1.69	1.17	0.76
(4) 	(3) $\Delta G^4 - \Delta G^3$	Me($\alpha_{\text{N,S}}$), Tz	1.11	0.29	0.05
(6) 	(5) $\Delta G^6 - \Delta G^5 - \Delta G^{\text{Me}}(\alpha_{\text{N,O}})$	Me(α_{N}), Ox	1.44	0.73	0.57
(3) 	(7) $\Delta G^3 - \Delta G^7$	Me(α_{N}), Tz	1.43	0.74	0.53
(1) 	(5) $\Delta G^1 - \Delta G^5$	Me(α_0), Ox	2.16	1.69	1.47
(8) 	(7) $\Delta G^8 - \Delta G^7$	Me(α_0), Tz	2.10	1.55	1.30

(Continued on p. 8)

TABLE III (continued)

Starting compounds	Scheme for calculation ^a	Alkyl position ^a	-ΔG ^{alk} (kJ/mol)		
			OV-101 KF	Triton X-305-KF	PEG-40M-KF
(EtBz) 	(Bz) ΔG ^{EtBz} - ΔG ^{Bz}	Et, Bz	3.94	3.59	3.27
(9) 	(1) ΔG ⁹ - ΔG ¹	Et(α _{N,O}), Ox	3.43	2.37	1.83
(10) 	(8) ΔG ¹⁰ - ΔG ⁸	Et(α _{N,S}), Tz	2.78	1.40	1.03
(11) 	(5) ΔG ¹¹ - ΔG ⁵ - ΔG ^{Me} (α _{N,O})	Et(α _N), Ox	3.27	2.05	1.95
(12) 	(7) ΔG ¹² - ΔG ⁷ - ΔG ^{Me} (α _{N,S})	Et(α _N), Tz	3.17	2.01	1.80
(13) 	(5) ΔG ¹³ - ΔG ⁵ - ΔG ^{Me} (α _{N,O})	Et(α _O), Ox	3.97	3.03	2.86
(14) 	(7) ΔG ¹⁴ - ΔG ⁷ - ΔG ^{Me} (α _{N,S})	Et(α _S), Tz	3.88	2.88	2.55

(15)		$\Delta G^{15} - \Delta G^5 - \Delta G^{Et}(\alpha_0)$	Pr($\alpha_{N,O}$), Ox	5.04	3.69	3.01
(16)		$\Delta G^{16} - \Delta G^7$	Pr($\alpha_{N,S}$), Tz	4.41	2.81	2.34
(17)		$\Delta G^{17} - \Delta G^5 - \Delta G^{Me}(\alpha_{N,O})$	Pr(α_N), Ox	5.06	3.72	3.31
(18)		$\Delta G^{18} - \Delta G^7 - \Delta G^{Me}(\alpha_{N,S})$	Pr(α_N), Tz	4.95	3.70	3.00
(19)		$\Delta G^{19} - \Delta G^6$	Pr(α_O), Ox	5.41	4.34	4.04
(20)		$\Delta G^{20} - \Delta G^4$	Pr(α_S), Tz	5.34	4.43	4.01
(21)		$\Delta G^{21} - \Delta G^5 - \Delta G^{Me}(\alpha_N) - \Delta G^{Me}(\alpha_O)$	<i>ortho</i> -Effect, Ox	0.21	0.37	0.34
(22)		$\Delta G^{22} - \Delta G^7 - \Delta G^{Me}(\alpha_N) - \Delta G^{Me}(\alpha_S)$	<i>ortho</i> -Effect, Tz	0.09	0.25	0.39
(<i>o</i> -Xyl)		$(\Delta G^{o-Xyl} - \Delta G^{Me})_2 - \Delta G^{Me}{}^b$	<i>ortho</i> -Effect, Bz	0.46	—	0.80

^a Me = Methyl; Et = ethyl; Pr = propyl; Bz = benzene; EtBz = ethylbenzene; *o*-Xyl = *o*-xylene.

^b Additional energy of Me group standing in *ortho* position to another Me-group in benzene.

TABLE IV
COMPARISON OF EXPERIMENTAL RETENTION INDICES OF ALKYLXAZOLES AND ALKYLTHIAZOLES WITH THE VALUES CALCULATED FROM THE CONTRIBUTIONS OF ALKYL GROUPS

X	Compound ^a			OV-101-KF		Triton X-305-KF		PEG-40M-KF	
	R ₁	R ₂	R ₃	I (calc.)	I (exptl.)	I (calc.)	I (exptl.)	I (calc.)	I (exptl.)
O	Me	Et	Me	927	923	1200	1201	1254	1252
O	Me	H	Pr	896	901	1174	1175	1220	1229
O	Me	Me	Me	847	843	1150	1150	1196	1200
O	Et	Me	H	843	845	1138	1145	1211	1213
O	Me	H	Et	815	818	1105	1104	1154	1159
O	H	Et	Et	942	940	1225	1222	1282	1279
O	Me	Me	Et	934	926	1212	1210	1255	1260
O	Et	H	Et	906	903	1174	1172	1231	1228
O	Me	Pr	Et	1089	1079	1332	1327	1380	1374
S	H	Me	Me	921	922	1267	1267	1334	1324
S	Me	H	Et	970	970	1283	1285	1345	1349
S	Et	H	Et	1057	1053	1349	1343	1410	1409
S	H	Et	Et	1093	1090	1395	1402	1457	1463
S	Me	Me	Et	1080	1077	1377	1381	1433	1439
S	Me	Et	Me	1081	1072	1376	1380	1432	1438
S	H	Me	Pr	1087	1089	1399	1401	1461	1463
S	Me	Me	Me	997	997	1319	1319	1379	1380
S	H	Et	Pr	1176	1175	1469	1475	1530	1534
S	Me	Pr	Et	1240	1233	1515	1512	1569	1567
Average error of calculation				4		3		4	

^a General structure as in Table I.

The contribution of any alkyl group in an $\alpha_{N,O}$ -position in oxazole is considerably greater than that of the same group in an $\alpha_{N,S}$ -position in thiazole. Thus, on the non-polar OV-101-KF column the value of $\Delta G^{Me}(\alpha_{N,O})$ is -1.69 kJ/mol but $\Delta G^{Me}(\alpha_{N,S})$ is only -1.11 kJ/mol. On polar columns the difference in the $\alpha_{N,O}$ and $\alpha_{N,S}$ contributions of the alkyl groups increases. This can probably be explained by the different dipole moments of oxazole and thiazole molecules [14].

With 4,5-dimethylthiazole and -oxazole, an *ortho*-effect of methyl groups is observed, as shown in Table III. This means that the total contribution of two vicinal methyl groups is higher than the sum of two methyl contributions in 4- and 5-methylazoles. Under the influence of the two heteroatoms the *ortho*-effect in 4,5-dimethyl-oxazole and -thiazole is less pronounced than in *o*-xylene (Table III) and in 3,4-dimethylpyridine [5].

The data in Table III, reflecting the inconstancy of the contribution of the same alkyl group because of α - and *ortho*-effects, were used to predict the retention indices of nineteen alkyl-substituted oxazoles and thiazoles other than those listed in Table III. For this purpose oxazole, thiazole and C_5 - C_{16} *n*-alkanes were analysed simultaneously under identical GC conditions. The sorption energies, $\Delta G'$, were calculated with the equation [18]

$$\Delta G' = -RT \ln t' \quad (9)$$

where t' is the adjusted retention time of the compound.

The general schemes for the calculation of the sorption energy of alkyloxazole, $\Delta G'_1$, and alkylthiazole, $\Delta G'_2$, to predict retention indices can be formulated as follows:

$$\begin{aligned} \Delta G'_1 = \Delta G'(Ox) + \Delta G^{Alk}(\alpha_O, Ox) + \Delta G^{Alk}(\alpha_N, Ox) + \\ \Delta G^{Alk}(\alpha_{N,O}, Ox) + \Delta G^{Me}(ortho\text{-effect}, Ox) \end{aligned} \quad (10)$$

$$\begin{aligned} \Delta G'_2 = \Delta G'(Tz) + \Delta G^{Alk}(\alpha_S, Tz) + \Delta G^{Alk}(\alpha_N, Tz) + \\ \Delta G^{Alk}(\alpha_{N,S}, Tz) + \Delta G^{Me}(ortho\text{-effect}, Tz) \end{aligned} \quad (11)$$

where $\Delta G'(Ox)$ and $\Delta G'(Tz)$ are sorption energies determined according to eqn. 9 for oxazole and thiazole respectively, ΔG^{Alk} are the contributions of alkyl groups in different positions of the heterocycle and $\Delta G^{Me}(ortho\text{-effect})$ are the additional sorption energies arising from the vicinal position of two methyl groups.

The $\Delta G'_1$ and $\Delta G'_2$ values obtained were converted into retention index units, using the equation given in ref. 19:

$$\Delta G'_i = -RT \left[a' + b'(I_i/100) + \frac{c'}{I_i/100 + d'} \right] \quad (12)$$

where a' , b' , c' and d' are coefficients determined from values of t' for standard *n*-alkanes, $\Delta G'_i$ is the calculated free energy of sorption of a substance i and I_i is the retention index sought.

Retention index values calculated by eqn. 12 for alkyloxazoles and alkylthiazoles are given in Table IV. The average errors of calculation are 3–4 i.u. With the polar columns the accuracy of prediction of retention indices with eqns. 10 and 11 is slightly higher than that when using the analogy of the GC behaviour of thiazoles and oxazoles (eqns. 5 and 6 and Table II).

In conclusion, the thermodynamic sorption characteristics of alkyloxazoles and alkylthiazoles on columns of different polarity were compared. The regularities established were used to confirm two methods for the prediction of retention indices based on the analogy of the GC behaviour of S- and O-containing azoles and on the unequal energy contributions of identical alkyl groups. The prediction ability of the methods was found to be accurate within 1% of the mean retention index value (see Tables II and IV). The predicted retention indices of mono-, di- and trisubstituted oxazoles and thiazoles can be used to increase the data bank for computer identification of complex mixtures of nitrogen-containing bases.

REFERENCES

- 1 D. N. Grigoryeva and R. V. Golovnya, *Zh. Anal. Khim.*, 40 (1985) 1733.
- 2 D. T. Stanton and P. C. Jurs, *Anal. Chem.*, 61 (1989) 1328.
- 3 C. T. Peng, S. F. Ding, R. L. Hua and Z. C. Yang, *J. Chromatogr.*, 436 (1988) 137.
- 4 J. E. Premecz and M. E. Ford, *J. Chromatogr.*, 388 (1987) 269.
- 5 A. L. Samusenko and R. V. Golovnya, *Chromatographia*, 25 (1988) 531.
- 6 R. V. Golovnya, I. L. Zhuravleva and E. V. Yakush, *Chromatographia*, 23 (1987) 959.
- 7 J. V. Metzger and E. J. Vincent, in J. V. Metzger (Editor), *Thiazole and Its Derivatives*, Part 1, Wiley, New York, 1979, pp. 5–164 and 360–362.
- 8 R. Lakhan and B. Ternai, *Adv. Heterocycl. Chem.*, 17 (1974) 152.
- 9 M. Petitjean, G. Vernin and J. Metzger, *Ind. Aliment. Agric.*, 98 (1981) 741.
- 10 J. T. Carlin, Q. Z. Jin, T.-C. Huang, C.-T. Ho and S. S. Chang, *J. Agric. Food Chem.*, 34 (1986) 621.
- 11 R. V. Golovnya, I. L. Zhuravleva and B. M. Polanuer, *J. Chromatogr.*, 286 (1984) 79.
- 12 R. V. Golovnya, A. L. Samusenko and E. A. Mistryukov, *J. High Resolut. Chromatogr. Chromatogr. Commun.*, 2 (1979) 609.
- 13 E. Kováts, *Helv. Chim. Acta*, 41 (1958) 1915.
- 14 S. B. Bulgarevich, V. S. Bolotnikov, V. N. Shejnkner, O. A. Osipov and A. D. Garnovskii, *Zh. Obshch. Khim.*, 45 (1975) 1821.
- 15 R. V. Golovnya and V. G. Garbuzov, *Izv. Akad. Nauk SSSR, Ser. Khim.*, (1974) 1599 and 1606.
- 16 I. J. Turchi and M. J. S. Dewar, *Chem. Rev.*, 75 (1975) 389.
- 17 D. N. Grigoryeva and R. V. Golovnya, *Zh. Anal. Khim.*, 43 (1988) 705.
- 18 R. V. Golovnya, *Chromatographia*, 12 (1979) 533.
- 19 R. V. Golovnya and D. N. Grigoryeva, *J. High Resolut. Chromatogr. Chromatogr. Commun.*, 6 (1983) 269.

Extension of the electrostatic retention model of reversed-phase ion-pair high-performance liquid chromatography to include the effect of the eluent pH

ÁKOS BARTHA* and JAN STÅHLBERG

ASTRA Pharmaceutical Production AB, Quality Control, S-151 85 Södertälje (Sweden)

and

FERENC SZOKOLI

Veszprém University, Institute for Analytical Chemistry, P.O.B. 158, H-8201 Veszprém (Hungary)

ABSTRACT

The electrostatic retention model is extended to predict the retention changes of monoprotic weak acids and bases as the eluent pH and the mobile phase concentration of the ion-pairing reagent are varied simultaneously in reversed-phase high-performance liquid chromatography. At constant ionic strength and organic modifier concentration, the magnitude of solute retention shifts can be predicted from the model equations using a very limited set of experimental data. The effect of the eluent pH on the adsorption of the sodium octylsulphonate pairing ion and the surface potential was studied. Predictions from the model were compared with experimental retention data and good agreement was found for both oppositely and similarly charged solute ion – pairing ion combinations. The advantages and limitations of applying the electrostatic retention model in the optimization of ion-pair chromatographic separations are discussed in detail.

INTRODUCTION

In reversed-phase high-performance liquid chromatography (RP-HPLC) the variation of eluent pH and/or the concentration of the organic modifier often leads to satisfactory separations of mixtures of weak organic acids and/or bases. However, when these components are accompanied by solutes of other charge type (strong acids, bases or non-ionic components) and relative hydrophobicity, one may need to add ion-pairing reagents to the eluent in order to achieve the proper separation of all components of interest.

Owing to the increased number and interdependence of mobile phase variables, the selectivity optimization of such ion-pair chromatographic (IPC) separations can become a complex task. The successful optimization of the separations precludes the correct selection of the initial value(s) and range of eluent variables (*i.e.*, the optimization parameter space) [1–4] where the search for the optimum conditions will be performed. In contrast to regular RPC systems, this is not a trivial task in ion-pair

chromatography and it often requires a large number of preliminary experiments. The number of the initial chromatographic runs could be reduced if the solute retention shifts, caused by the addition of pairing ions, could be predicted.

A number of retention models [5–8] have been suggested in RP-IPC to describe the capacity factor (k') of ionizable solutes when an ion-pairing reagent is added to the eluent at various pH values. However, in order to elucidate the retention-modifying effect of the pairing ion, the dynamic ion-exchange [5] constants, the ion-pair formation or adsorption constants [6] for each solute ion or the parameters of the assumed Freundlich-type pairing ion adsorption [7] must be determined. As a result, these models require a large amount of experimental data determined under widely varying chromatographic conditions to predict solute retention changes.

Stahlberg and co-workers developed an electrostatic theory for reversed-phase ion-pair chromatography [9–11] which has been successfully used to account for the effect of the type and concentration of the inorganic counter ions [12] and the organic modifier(s) [13]. The electrostatic retention model gives a physically consistent description of the retention processes and it allows practical equations to be derived to determine the retentions of fully ionized solutes (*i.e.*, strong acids and bases) from very few experimental data [14].

In this study, the electrostatic model was used to describe the retention of monocharged weak acids and bases as the eluent pH and the concentration of the ion-pairing reagent are varied simultaneously. A set of equations was derived to predict the direction and magnitude of retention changes for both oppositely and similarly charged solute ion-pairing ion combinations. Predictions from the theory are compared with experimental retention data and it is shown that the equations can be used to predict the solute retention shifts (assuming that the charge type of the solutes is known) from a very limited set of experimental data.

THEORY

In reversed-phase chromatography, the capacity factor of partly ionized solutes (k'_c) can be expressed as the sum of the capacity factors for the charged (k'_i) and the uncharged species (k'_0), multiplied by the corresponding equilibrium fraction (f)

$$k'_c = (1 - f)k'_0 + fk'_i \quad (1)$$

The addition of an ion-pairing reagent to the eluent will primarily influence the retention of the ionized form of the solute. The basic assumption of the electrostatic retention model of RP-IPC [9–11] is that the adsorbing pairing ions and the counter ions form an electrical double layer at the stationary phase surface and create a difference in the electrostatic potential (ψ_0) between the stationary phase and the bulk mobile phase. According to the theory, the capacity factor of the fully ionized solute (k'_i) of charge z_i is given as

$$k'_i = k'_{0i} \exp(-z_i F \psi_0 / RT) \quad (2)$$

where k'_{0i} is the capacity factor of the fully ionized form of the solute in the absence of pairing ion, F is the Faraday constant, ψ_0 is the difference in the electrostatic potential

between the surface of the stationary phase and the bulk mobile phase, R is the gas constant and T is the absolute temperature.

The fraction of ionized components (A^-) for monoprotic weak acids (HA) is defined as

$$f = (A^-)/\{(A^-) + (HA)\} \quad (3)$$

and it can be expressed using the acid dissociation constant (K_a) of the weak acid as

$$f = K_a/(K_a + [H^+]) \quad (4)$$

where $[H^+]$ is the hydrogen ion concentration. For monoprotic weak acids ($z_i = -1$), the substitution of eqns. 2 and 4 into eqn. 1 results in

$$k'_{acid} = \frac{k'_{HA} + K_a/[H^+]k'_{0A^-} \exp(F\psi_0/RT)}{1 + (K_a/[H^+])} \quad (5)$$

where k'_{HA} is the capacity factor of the non-ionized form of weak acid HA and k'_{0A^-} is the capacity factor of the ionized form in the absence of pairing ion.

Similar reasoning can be used to derive the corresponding equation for monoprotic ($z_i = +1$) weak bases (BH^+)

$$k'_{base} = \frac{k'_B + [H^+]/K_a k'_{0BH^+} \exp(-F\psi_0/RT)}{1 + ([H^+]/K_a)} \quad (6)$$

where k'_B is the capacity factor of the non-ionized form of weak base B and k'_{0BH^+} is the capacity factor of the ionized form in the absence of pairing ion.

In the absence of pairing ions, ψ_0 is defined to be zero, *i.e.*, the exponential term equals one. As a result, eqns. 5 and 6 reduce to the well known expressions developed for the regular reversed-phase chromatographic mode [15]. The above model assumes that the ion-pairing reagent is fully ionized throughout the pH range used (*i.e.*, $z_A = \pm 1$). The electrostatic potential has positive values ($\psi_0 > 0$) for positively charged and negative values ($\psi_0 < 0$) for negatively charged pairing ions. It is also assumed that the capacity factor of both the ionized (k'_{0i}) and the non-ionized form (k'_0) of the solute are constant and independent of the concentration of the pairing ion. The effect of the pairing ion on k'_0 is usually negligible compared with its influence on k'_{0i} , as a first approximation.

The organic modifier content and the ionic strength of the mobile phase influence the capacity factor and the protonation constant of the solutes, in addition to the electrostatic potential (if a pairing ion is present). To allow for a meaningful test of the model equations, the above two variables were kept constant throughout this study.

EXPERIMENTAL

All test compounds were of analytical-reagent grade and were obtained from different suppliers. Buffer components and sodium bromide were obtained from

Reanal (Budapest, Hungary) and sodium octylsulphonate from Merck (Darmstadt, Germany).

The eluents contained 10% (v/v) methanol, aqueous phosphate or citrate or acetate-malonate buffer and sodium bromide. Eluents with constant ionic strength (0.1 M) and varying pH values between 2.5 and 6.5 were prepared by titrating eluent A_i ($A_1 = 20 \text{ mM H}_3\text{PO}_4$ -80 mM NaBr; $A_2 = 20 \text{ mM citric acid}$ -80 mM NaBr; $A_3 = 10 \text{ mM acetic acid}$ -10 mM malonic acid-80 mM NaBr) with eluent B_i ($B_1 = 10 \text{ mM NaH}_2\text{PO}_4$ -10 mM Na_2HPO_4 -50 mM NaBr; $B_2 = 20 \text{ mM trisodium citrate}$ -20 mM NaBr; $B_3 = 10 \text{ mM sodium acetate}$ -10 mM malonic acid-20 mM NaOH-50 mM NaBr). When 5 mM sodium octylsulphonate was used as ion-pairing reagent, the sodium bromide concentration was decreased by the same amount in each eluent.

An LC 5600 liquid chromatograph, UV (set to 254 nm) and RI detectors (all from Varian Aerograph, Walnut Creek, CA, U.S.A.) equipped with two Model 7010 injection valves (Rheodyne, Cotati, CA, U.S.A.) were used. The analytical column was packed with 5- μm Hypersil ODS (200 mm \times 4.6 mm I.D.; Shandon, U.K.). The set-up of the equipment allowed for the simultaneous determination of solute capacity factors and pairing ion adsorption data [16]. The temperature was kept at 25°C. The eluent pH was measured with a glass electrode (Radelkis, Hungary) calibrated for aqueous standard solutions. Model calculations were performed on an IBM AT compatible computer (MS DOS 4.0, 1 MB RAM, 20 MB hard disk).

RESULTS AND DISCUSSION

Effect of eluent pH on surface potential

In order to test eqns. 5 and 6, one must determine not only solute capacity factors, but also the value of the difference in the electrical potential created by the presence of the pairing ion. In practice, eqn. 2 can be rearranged and used to calculate the actual ψ_0 values from the k' data for a fully ionized solute measured in the absence (k'_{0i}) and in the presence (k'_i) of the pairing ion of charge z_A

$$(z_i F)/(RT)\psi_0 = -\ln(k'_i/k'_{0i}) \quad (7)$$

The capacity factor data for the strong base dopamine ($z_i = +1$) were used for the calculation of ψ_0 in the pH range 2.5-6.5. The results are summarized in Table I. It can be seen that the resulting electrical potential is virtually independent of the variation of the eluent pH between 2.5 and 6.5.

The experimental adsorption data of the sodium octylsulphonate ion-pairing reagent are also included in Table I. The surface concentrations were determined from the breakthrough curves of the pairing ion, *i.e.*, from experiments independent of the capacity factor measurements used for the calculation of the ψ_0 data. The breakthrough curves were recorded at each pH value on the freshly regenerated column [16] prior to the measurements of k' data. The adsorption data show a slight decrease at higher pH values, which is just the opposite behaviour compared with the changes in k' values for the positively charged dopamine. This indicates a slightly increasing negative (repulsive) electrical charge on the surface of the silica-based stationary phase, which can be associated with dissociation of surface silanol groups. However, the relatively constant level of the pairing ion adsorption and the corresponding

TABLE I

ELUENT pH VS. CAPACITY FACTOR DATA FOR THE STRONG BASE DOPAMINE ($pK = 8.80$) IN THE ABSENCE (k'_{oi}) AND IN THE PRESENCE (k'_i) OF PAIRING ION, THE SURFACE POTENTIAL (ψ_0) CALCULATED FROM EQN. 7 AND THE ADSORPTION DATA (n_A) OF SODIUM OCTYLSULPHONATE CORRESPONDING TO 5 mM MOBILE PHASE CONCENTRATION

See Experimental for other conditions.

pH	k'_{oi}	k'_i	ψ_0 (mV)	n_A ($\mu\text{mol/g}$)
2.5	1.50	17.39	-62.8	78.6
3.5	1.56	18.45	-63.3	78.4
4.5	1.55	18.64	-63.8	78.5
5.5	1.65	19.34	-63.1	77.4
6.5	2.24	19.42	-55.4	73.1

surface potential suggests that the effect of the dissociation of the silanol groups is still negligible. At higher pH values the effect of dissociating silanol groups on the adsorption of positively charged ion-pairing reagents may become more significant [5,17,18].

The level of the surface concentration ($78 \mu\text{mol/g}$) of the sodium octylsulphonate and the resulting average surface potential (-62 mV) both fall in the region where the linearized retention equation of the electrostatic retention model (*i.e.*, eqn. 2) can be applied [19]. The capacity factor of the fully ionized dopamine increases by a factor of 11 when 5 mM pairing ion is added to the eluent. Practical chromatographic work is often performed under conditions similar to those used in this study, providing data for a realistic test of the suggested equations.

Comparison of experimental and theoretical retention behaviours of ionic solutes

The capacity factor (k') vs. eluent pH data for the positively charged ($z_i = +1$) octopamine and the negatively charged 6-hydroxynaphthalene-2-sulphonic acid ($z_i = -1$) are shown in Figs. 1 and 2. Data points measured in the absence and in the presence of 5 mM sodium octylsulphonate are represented by filled squares and circles, respectively.

The retention data of both solutes drift slightly with increasing eluent pH. However, as a first approximation the capacity factors in the absence of pairing ion (k'_{oi}) can be considered constant. Generally, with careful selection of the stationary phase and the buffer system, close to ideal retention behaviour can be obtained for strong acids and bases [3]. This idealized behaviour is represented by the dashed lines, which were placed as close as possible to the experimental points at an arbitrary level along the k' axis. For fully ionized solutes eqn. 2 is used (instead of eqn. 5 or 6) to calculate the change in capacity factors when a pairing ion is added to the eluent. The use of eqn. 2 requires a knowledge of k'_{oi} and the surface potential corresponding to the given pairing ion concentration. The results in Table I indicate that one can use an average value for ψ_0 , independent of the eluent pH.

The solid lines in Figs. 1 and 2 represent k' data which were calculated from eqn. 2, using only the k'_{oi} value of the solutes (dashed line) and an average value

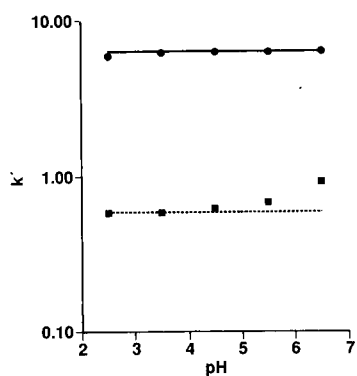


Fig. 1. k' vs. pH data for positively charged octopamine in (■) the absence and (●) the presence of sodium octylsulphonate (5 mM) pairing ion. The theoretical retention plot in the presence of the pairing ion (solid line) was calculated from eqn. 2 ($z_i = +1$, $F\psi_o/RT = -2.398$), assuming idealized retention behaviour (dashed line) in the absence of pairing ion, *i.e.*, constant $k'_{oi} = 0.59$. Column, Hypersil ODS; eluent 10% (v/v) methanol in 20 mM aqueous phosphate buffer containing sodium bromide (constant 0.1 M ionic strength); temperature, 25°C.

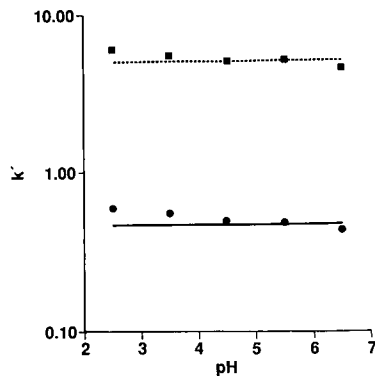


Fig. 2. k' vs. pH data for negatively charged 6-hydroxynaphthalene-2-sulphonic acid (6HN2SA) in (■) the absence and (●) the presence of sodium octylsulphonate (5 mM) pairing ion. The theoretical retention plot in the presence of the pairing ion (solid line) was calculated from eqn. 2 ($z_i = -1$, $F\psi_o/RT = -2.398$), assuming idealized retention behaviour (dashed line) in the absence of pairing ion, *i.e.*, constant $k'_{oi} = 5.2$. Other conditions as in Fig. 1.

(−62 mV) for the surface potential, determined from the k' data for dopamine (*cf.*, Table I). Compared with the size of the retention changes, remarkably good agreement is found between the experimental and calculated k' data both for increasing (Fig. 1) and decreasing (Fig. 2) solute retention.

The capacity factor vs. pH data for a weak base (adenine) and a weak acid (2,4-dihydroxybenzoic acid) are shown in Figs. 3 and 4. In the absence of a pairing ion, at pH 2.5, adenine is protonated (pK 4.12) and it has a lower retention (k'_{oi}) than its non-ionic form (k'_o) at pH 6.5. On the other hand, the retention of 2,4-dihydroxybenzoic acid is lower at high pH where the carboxyl group is fully dissociated ($pK_a = 3.21$). The experimental k' data for both solutes (filled squares) follow the S-shaped pattern well known in reversed-phase chromatography. The theoretical k' data (dotted lines) were calculated from eqns. 5 and 6 assuming a zero value for the surface potential. It is important to note that only two experimental k'_{oi} , k'_o data measured at the two limiting pH values and the literature pK values of the solutes were used in the calculations, *i.e.*, no curve fitting was applied.

When the eluent contains 5 mM sodium octylsulphonate as a pairing ion, at low pH the k' (filled circles) of the positively charged adenine increases from 2.07 (k'_{oi}) to 20.4 (k'_{base}). This value is 2.5 times higher than the retention of the uncharged form ($k'_o = 8.2$) of adenine. Owing to the increased negative surface potential in the presence of the pairing ion, the retention of 2,4-dihydroxybenzoic acid decreases dramatically and it elutes close to the column dead volume ($k'_{acid} = 0.05$) at high pH. The larger deviation between the predicted and experimental points at $k' < 0.5$ may be attributed to the error in measuring short retention times.

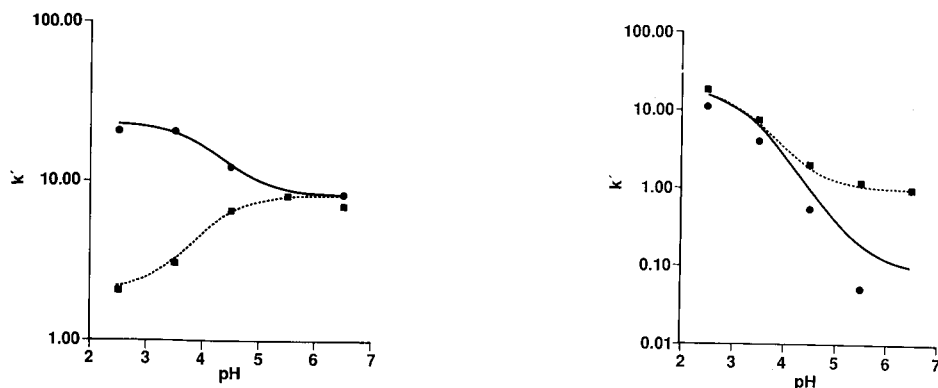


Fig. 3. k' vs. pH data for the weak base adenine ($z_i = +1$) in (■) the absence and (●) the presence of sodium octylsulphonate (5 mM) pairing ion. The theoretical retention plots in the absence (dashed line) of the pairing ion ($\psi_0 = 0$) and in the presence (solid line) of the pairing ion were calculated from eqn. 6 ($pK = 4.12$, $k'_0 = 8.2$, $k'_{0i} = 2.07$, $z_i F\psi_0/RT = -2.398$). Other conditions as in Fig. 1.

Fig. 4. k' vs. pH data for the weak acid 2,4-dihydroxybenzoic acid (2,4-DHBA) in (■) the absence and (●) the presence of sodium octylsulphonate (5 mM) pairing ion. The theoretical retention plots in the absence (dashed line) of the pairing ion ($\psi_0 = 0$) and in the presence (solid line) of the pairing ion were calculated from eqn. 5 ($z_i = -1$, $pK = 3.2$, $k'_0 = 18.5$, $k'_{0i} = 6.85$, $F\psi_0/RT = -2.398$). Other conditions as in Fig. 1.

The simultaneous effect of pairing ion addition and pH variation was calculated again from eqns. 5 and 6 (solid lines). The theoretical predictions use the pK_a , k'_0 and k'_{0i} values as described above; only the average value determined for the surface potential is introduced. None of the experimental k' data measured in the presence of the pairing ion (filled circles) were used for fitting the curves. It can be seen that the direction and magnitude of the retention changes caused by the pairing ion addition are predicted correctly by the theory.

In Fig. 5 the k' vs. pH data for *p*-aminophenol are shown in three different buffer

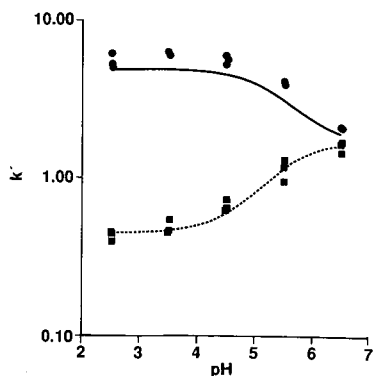


Fig. 5. k' vs. pH data for the weak base *p*-aminophenol ($z_i = +1$) in (■) the absence and (●) the presence of sodium octylsulphonate (5 mM) pairing ion. The theoretical retention plots in the absence (dashed line) of the pairing ion ($\psi_0 = 0$) and in the presence (solid line) of the pairing ion were calculated from eqn. 5 ($pK = 5.38$, $k'_0 = 1.7$, $k'_{0i} = 0.45$, $F\psi_0/RT = -2.398$). Eluent, 10% (v/v) methanol in aqueous 20 mM phosphate, citrate or acetate-malonate buffer, containing sodium bromide (constant 0.1 M ionic strength). Other conditions as in Fig. 1.

TABLE II

EXPERIMENTAL (k'_{exp}) AND THEORETICALLY PREDICTED (k'_{calc}) CAPACITY FACTORS OF FULLY IONIZED BASIC SOLUTES ($z_i = +1$) AT pH 2.5, IN THE PRESENCE OF 5 mM SODIUM OCTYLSULPHONATE ($F\psi_0/RT = -2.398$)

k'_{0i} is the capacity factor measured in the absence of pairing ion; basic pK values from ref. 21.

Solute	pK	k'_{0i}	k'_{exp}	k'_{calc}
Adenine	4.12	2.07	20.40	22.77
Cytidine	4.20	1.13	12.20	12.43
Creatinine	4.80	0.35	3.88	3.85
<i>p</i> -Aminophenol	5.38	0.45	6.14	4.95
Dopamine	8.80	1.61	17.38	17.71
Octopamine	9.60	0.58	5.89	6.49

systems (phosphate, citrate and acetate-malonate) with identical ionic strength (0.1 M). Again, theoretical k' data were calculated from eqn. 6, using the literature pK value, two experimental k'_{0i} , k'_0 data measured in the phosphate buffer system at pH 2.5 and 6.5 without pairing ion and assuming either zero (dotted line) or the average (-62 mV) value (solid line) for the electrical potential. The deviation between the predicted and the measured k' data is comparable to the relatively small differences caused by changing the type of buffer anions. This result supports the generality and practical applicability of the suggested model to other buffer systems.

The experimental and theoretically predicted k' data are compared for some other bases and acids in Tables II and III, respectively. The results are given for eluents with pH values where the compounds were ionized (see pK values) in order to test predictions for the possible largest retention changes with the addition of the pairing ion. In these calculations, only the charge type (z_i) and the capacity factor of the ionized solute (k'_{0i}) measured in the absence of a pairing ion and the average value of the surface potential were used (see eqn. 2). Again, there is generally an acceptable agreement between the experimental and the predicted k' data. When the initial (k'_{0i}) or the resulting (k'_{exp}) capacity factor values are lower than 1, the differences between the

TABLE III

EXPERIMENTAL (k'_{exp}) AND THEORETICALLY PREDICTED (k'_{calc}) CAPACITY FACTORS OF FULLY IONIZED ACIDIC SOLUTES ($z_i = -1$) AT pH 5.5, IN THE PRESENCE OF 5 mM SODIUM OCTYLSULPHONATE ($F\psi_0/RT = -2.398$)

k'_{0i} is the capacity factor measured in the absence of pairing ion; acidic pK_a values from ref. 22.

Solute	pK _a	k'_{0i}	k'_{exp}	k'_{calc}
6-Hydroxynaphthalene-2-sulphonic acid	<0.5 ^a	5.19	0.49	0.47
<i>p</i> -Toluenesulphonic acid	0.67 ^a	3.24	0.20	0.29
2,6-Dihydroxybenzoic acid	1.22	6.85	0.49	0.62
2,4-Dihydroxybenzoic acid	3.21	1.20	0.05	0.18
3,4-Dihydroxyphenylacetic acid	4.3	0.84	0.18	0.08

^a Approximate values.

experimental and calculated values are large. For k' values larger than 1, the deviations are in the range 10–20% relative.

The above results indicate that the electrostatic retention model can be advantageously used to estimate the magnitude of retention shifts for ionic solutes, when a pairing ion is added to the eluent at various pH values, from a very limited set of experimental data. In order to approximate the k' vs. pH behaviour of monocharged (monoprotic) solutes in the absence of pairing ion (*cf.*, dashed lines in Figs. 1–5), the charge type of the components, pK_a , k'_o and/or k'_{oi} values must be known. The addition of a pairing ion to the eluent often results in significantly enhanced or decreased analysis times. Therefore, the assessment of these retention shifts is of practical importance. In order to estimate the magnitude of k' changes, one must determine the value of the difference in the electrical potential. This requires only the measurement of k' of one or two fully ionized solutes in eluents of a given pH without and with ion-pairing reagent. In other words, the IPC system can be calibrated for surface potential from the retention data for a well known standard.

As a result, measurements in three eluents already provide starting point for the model to estimate the possible retention shifts. The advantage of the model is that after calibrating for the surface potential, new k' data of ionized solutes can be guessed before actually measuring the sample mixture in the presence of a pairing ion. This feature is very useful during the selection of the type and initial concentration of the pairing ions [20].

An important area of such applications is in the selection of initial mobile phase compositions prior to systematic selectivity optimization [2–4]. In this early stage of the chromatographic method development, the primary aim is to obtain chromatograms with reasonable analysis times and errors of 10–20% in predicted retention times are usually acceptable.

Retention models are often sought also in the course of the subsequent selectivity optimization. Some computer-aided procedures [8,23–26] fit multi-parameter equations through the experimental retention data points and calculate different optimization criteria as a function of the mobile phase variables. For the efficient operation of these methods the solute capacity factors must be estimated to within less than 1–2% for a broad range of experimental conditions [27]. It must be noted that neither the earlier retention models [5–8] nor the electrostatic model in its present form can comply with these requirements.

CONCLUSIONS

Based on the electrostatic theory of reversed-phase ion-pair chromatography, a set of equations have been developed to describe the retention changes of monoprotic weak acids and bases when an ion-pairing reagent is added to eluents with different pH values. According to the model, the retention of the ionized form of the solutes depends on the surface potential. Hence the surface potential can be determined from the capacity factor data for a fully ionized solute, measured in the absence and the presence of a pairing ion. Both the surface potential and the adsorption of the sodium octylsulphonate pairing ion were found to be constant when the eluent pH was varied between 2.5 and 6.5 at constant ionic strength and organic modifier concentration.

The retention equations have been tested by calculating the expected retention

behaviours of strong and weak acids and bases in the presence of a pairing ion, using only literature pK values, capacity factor data for the solutes (measured in the absence of the pairing ion) and the surface potential (determined from the retention shift of one fully ionized compound). The predictions from the model agreed well with experimental retention data for both oppositely and similarly charged solute ion-pairing ion combinations, and also for eluents with different buffer anions. The calculated and measured capacity factor data differed by 10–20% relative when the results were not affected by the experimental errors of measuring short retention times. The practical advantage of the proposed equations is that they allow one to estimate the magnitude of solute retention changes from a very limited amount of experimental data.

REFERENCES

- 1 P. J. Schoenmakers and M. Mulholland, *Chromatographia*, 25 (1988) 737.
- 2 Á. Bartha, H. A. H. Billiet and L. de Galan, *J. Chromatogr.*, 464 (1989) 225.
- 3 G. K. C. Low, Á. Bartha, H. A. H. Billiet and L. de Galan, *J. Chromatogr.*, 478 (1989) 21.
- 4 J. K. Strasters, F. Coolsaet, Á. Bartha, H. A. H. Billiet and L. de Galan, *J. Chromatogr.*, 499 (1990) 523.
- 5 J. L. M. van de Venne, J. L. H. Hendriks and R. S. Deelder, *J. Chromatogr.*, 167 (1978) 1.
- 6 A. Tilly-Melin, Y. Askemark, K.-G. Wahlund and G. Schill, *Anal. Chem.*, 51 (1979) 976.
- 7 R. C. Kong, B. Sachok and S. N. Deming, *J. Chromatogr.*, 199 (1980) 307.
- 8 A. P. Goldberg, E. Nowakowska, P. E. Antle and L. R. Snyder, *J. Chromatogr.*, 316 (1984) 241.
- 9 J. Ståhlberg, *J. Chromatogr.*, 356 (1986) 231.
- 10 J. Ståhlberg and A. Furangen, *Chromatographia*, 24 (1987) 783.
- 11 J. Ståhlberg, *Chromatographia*, 24 (1987) 820.
- 12 J. Ståhlberg and I. Hagglund, *Anal. Chem.*, 60 (1988) 1958.
- 13 Á. Bartha, Gy. Vigh and J. Ståhlberg, *J. Chromatogr.*, 506 (1990) 85.
- 14 Á. Bartha and J. Ståhlberg, *J. Chromatogr.*, 535 (1990) 181.
- 15 Cs. Horváth, W. Melander and I. Molnar, *Anal. Chem.*, 49 (1977) 142.
- 16 Á. Bartha and Gy. Vigh, *J. Chromatogr.*, 260 (1983) 337.
- 17 R. H. A. Sorel, A. Hulshoff and S. Wiersema, *J. Liq. Chromatogr.*, 4 (1981) 1961.
- 18 O. A. G. J. van der Houwen, R. H. Sorel, A. Hulshoff, J. Teeuwssen and A. W. M. Indemans, *J. Chromatogr.*, 393 (1981) 209.
- 19 J. Ståhlberg and Á. Bartha, *J. Chromatogr.*, 456 (1988) 253.
- 20 Á. Bartha, Gy. Vigh and Z. Varga-Puchony, *J. Chromatogr.*, 499 (1990) 423.
- 21 D. D. Perrin, *Dissociation Constants of Organic Bases in Aqueous Solutions*, Butterworth, London, 1965.
- 22 G. Kortum, W. Vogel and K. Andrussov, *Dissociation Constants of Organic Acids in Aqueous Solution*, Butterworth, London, 1961.
- 23 B. Sachok, R. C. Kong and S. N. Deming, *J. Chromatogr.*, 199 (1980) 317.
- 24 P. M. J. Coenegracht, N. V. Tuyen, H. J. Metting and P. M. J. Coenegracht-Lamers, *J. Chromatogr.*, 389 (1987) 351.
- 25 P. Wester, J. Gottfries, K. Johansson, F. Klinteback and B. Winblad, *J. Chromatogr.*, 415 (1987) 261.
- 26 F. Szokoli, Zs. Nemeth and J. Inczedy, *Chromatographia*, 29 (1990) 265.
- 27 P. J. Schoenmakers and T. Blaffert, *J. Chromatogr.*, 384 (1987) 117.

CHROMSYMP. 2335

Adsorption and partition mode in high-performance liquid chromatography of highly polar solutes on silica

V. D. SHATZ* and H. A. KAŽOKA

Institute of Organic Synthesis, Latvian Academy of Sciences, Riga, Latvia (U.S.S.R.)

ABSTRACT

The investigation of chromatographic systems with silica and mobile phases consisting of ethyl acetate and weakly soluble polar components ethylene glycol, triethylene glycol and formamide has shown that mixed mechanism of sorption is possible. When the solubility of the polar component is good, as in case of methanol, the retentions observed are typical of adsorption chromatography. When ethylene glycol, which has limited solubility, is used as the mobile phase component, a liquid stationary phase consisting mainly of polar solvent is formed in the pores of silica. This leads to a mixed mechanism of retention, selectivity changes and improvement of the peak shape. The formation of a liquid stationary phase both from saturated and unsaturated solutions is observed.

INTRODUCTION

Reversed-phase chromatography has become the most popular method of separation and analysis of organic substances belonging to different classes and widely differing in their properties. Nevertheless, the reversed-phase mode is not always the best or only choice for a given analytical task. This decision is very often based simply on tradition or use in similar experiments. Therefore it is our opinion that the analytical potential of high-performance liquid chromatography (HPLC) on unmodified silica is often underestimated. One of the potential advantages of unmodified silica is its higher selectivity in terms of the structural differences of the chromatographed solutes. The use of normal-phase separations in combination with reversed-phase ones can offer additional possibilities in thorough process and quality control.

Very polar organic substances, many of them biologically important, require eluents of high polarity in order to be eluted from unmodified silica. The lower aliphatic alcohols from methanol to propanol are most frequently used for this purpose as mobile phase components. Ethylene glycol (EG) and some other highly polar mono- and bifunctional additives have been mentioned as possible eluent constituents [1], some of them having even higher elution strength than methanol. It has been shown [2–9] that mobile phases saturated with polar solvents, *e.g.*, water [2,6,8,9], EG [2], dimethyl sulphoxide [3], triethylene glycol (TEG) [4], formamide [5] or ethanol [7], generate a liquid stationary phase in pores of unmodified silica. The

obtained liquid-liquid partition chromatographic systems have been shown to be useful in analytical chromatography. Nevertheless, solvents of this kind have not been used widely until now. For example, no EG-containing eluents are cited in a review of 700 drug analyses [10].

The high viscosity of many highly polar solvents is a distinct disadvantage. However, if their high elution strength is taken into account, relatively low

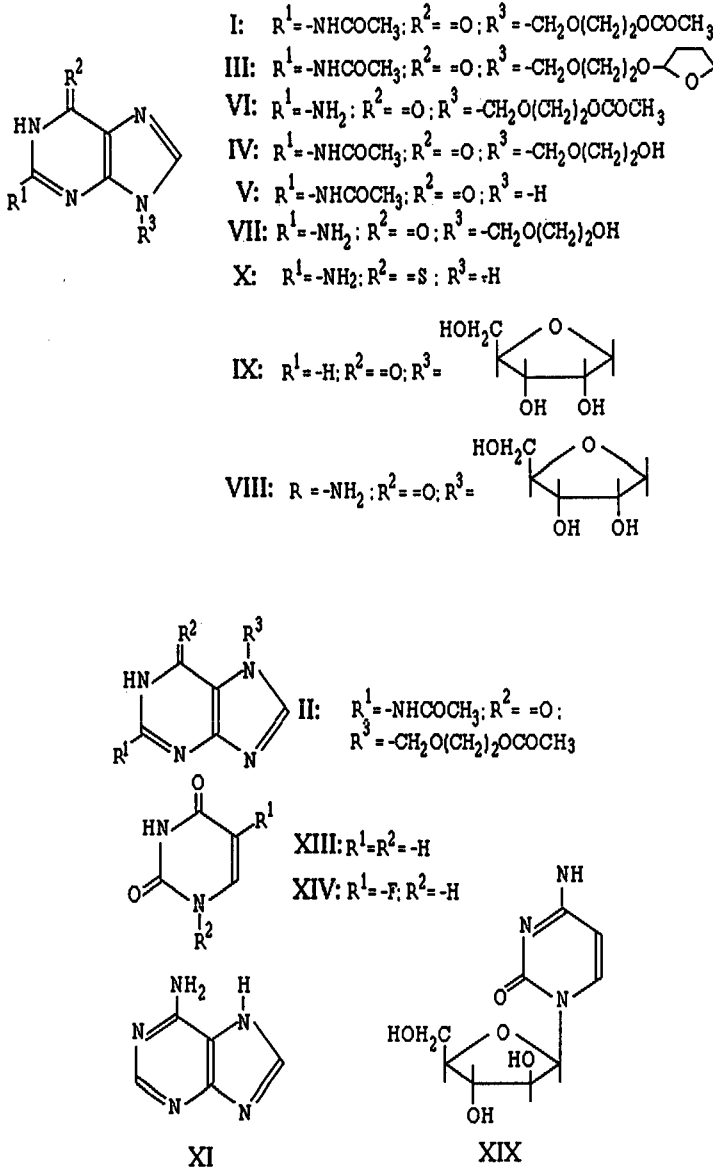


Fig. 1. Solutes under study.

concentrations of such solvent should be sufficient to obtain reasonable capacity factors. Bifunctional solvents, being adsorbed onto silica, may generate a surface layer with polar groups in contact with both the mobile and stationary phases. This may lead to additional selectivity effects compared with monofunctional solvents.

The goal of this work was to investigate the sorption behaviour of polar solutes in normal-phase chromatography on silica with mobile phases containing ethyl acetate and several highly polar additives and to discuss the applicability of this approach in analytical chromatography.

EXPERIMENTAL

The substances under study were the derivatives of purine and pyrimidine shown in Fig. 1.

A DuPont Model 8800 HPLC system with spectrophotometric detector ($\lambda = 254$ nm) was used for retention measurements. A 250×4.6 mm I.D. column from DuPont was packed with Zorbax SIL. Samples ($10\text{--}25 \mu\text{l}$ of $0.05\text{--}1$ mg/ml solution in the mobile phase) were injected via a Rheodyne 7125 loop injector. The eluents consisted of ethyl acetate as the less polar solvent, and EG, TEG, formamide and methanol as polar modifiers. All solvents were of "pure" grade and were supplied by Fluka. Column temperature was 25°C .

Capacity factors were calculated according to a standard formula:

$$k' = \frac{t_R - t_0}{t_0} \quad (1)$$

where t_R and t_0 are retention times of solute under study and benzene, respectively.

RESULTS AND DISCUSSION

Most of the substances under study are only slightly soluble in the hydrocarbons

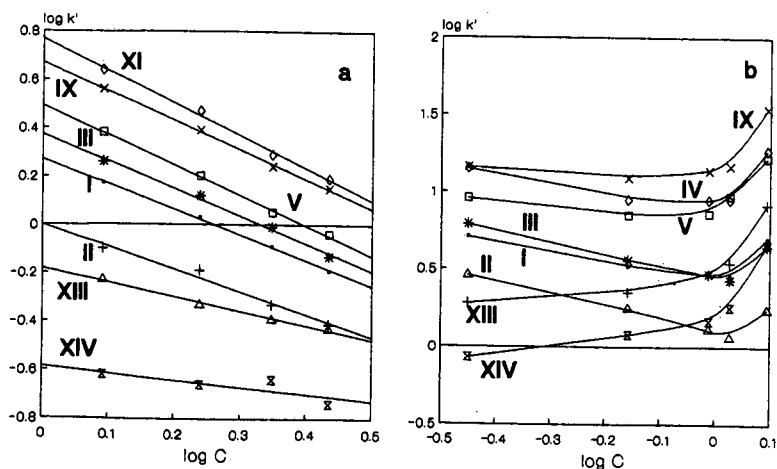


Fig. 2. Relationship between the concentration of methanol (a) or ethylene glycol (b) and capacity factors.

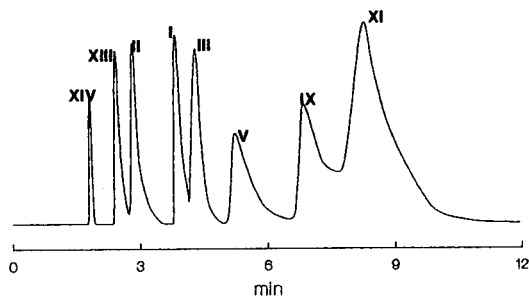


Fig. 3. Chromatogram of test solutes in the mobile phase, containing 5% methanol in ethyl acetate.

and chloroform that are generally used in normal-phase HPLC as less polar components of mobile phases. These solvents are immiscible with EG, and therefore ethyl acetate was chosen as a relatively non-polar solvent. It is completely miscible with methanol and dissolves up to 6.5% of EG at room temperature.

The relationship between capacity factors and molar concentrations of EG and methanol in ethyl acetate is shown in Fig. 2. It is seen that ethyl acetate-methanol eluents have sufficient elution strength for most of the compounds. At the same time peak tailing is typical (Fig. 3), especially for strongly retained solutes. Solute behaviour, represented in Fig. 2a, is typical for normal-phase adsorption chromatography. The relationship between $\log k'$ and the logarithm of molar concentration of methanol is almost linear. The system selectivity does not change very markedly with increase of polar solvent concentration. This relationship can be expressed by the linear equation:

$$\log k' = b - p \log C \quad (2)$$

where C is the molar concentration of polar solvent in the mobile phase. It is known that the silica surface in equilibrium with eluent may be covered by a layer of the most polar solvent (in this case, methanol). The displacement of these molecules by the solute molecule can occur in the act of sorption. The average number of released methanol molecules per solute molecule is equal to parameter p of eqn. 2. It may be concluded from Fig. 2a that p values in this data set lie between 0.5 and 1.3. These are typical values for normal-phase adsorption chromatography on silica [11]. It follows then that, notwithstanding the high polarity of the studied compounds, a one-point sorption scheme is prevailing, on average about one molecule of methanol being displaced from the surface upon the sorption of one solute molecule.

This is not the case when EG-containing mobile phases are used (Fig. 2b). The relationship between $\log k'$ and $\log C$ is not linear. When the concentration of EG is increased in the range 2–4%, only a slight decrease of retention is observed for most of the solutes. The slope is unusually low for adsorption chromatography on silica. A further increase of C leads to an increase in retention of some of the solutes. A similar relationship between the concentration of stronger eluent component and retention was described previously [7,8,12]. The observed effect results in selectivity changes and inversion of elution order for some pairs of solutes. Consequently, this parameter can

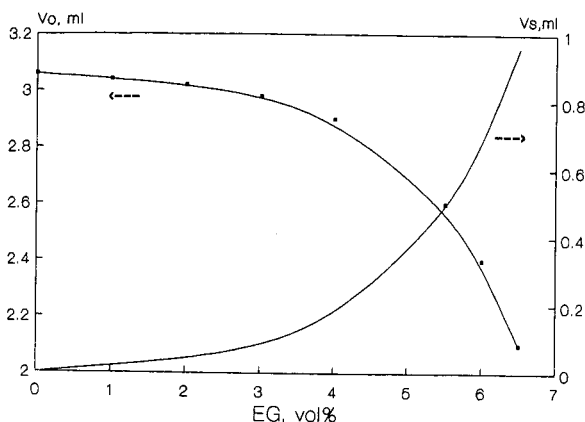


Fig. 4. Dependence of measured column dead volume (V_0) and calculated volume of liquid stationary phase (V_s) on the concentration of ethylene glycol (EG) in the mobile phase.

be used as an efficient tool for selectivity variation. If the amount of EG used for mobile phase preparation exceeded the limit of miscibility C_1 (6.5%, v/v; $\log C = 0.062$), a two-phase system was formed, and an ethyl acetate layer saturated with EG was used as eluent. Retention values observed with saturated eluents did not depend on the ratio of solvent volumes and were close to k' measured at C_1 .

It is seen that a sharp increase in retention of all solutes takes place when the amount of EG approaches its limit of solubility. The increase of EG concentration in the mobile phase leads to a decrease in t_0 values. It is most pronounced near C_1 (Fig. 4) but undoubtedly takes place over the whole range of C . The observed effects can be explained by deposition of EG-rich bulk liquid in the pores of silica. It acts as additional amount of stationary phase. The obtained results show that formation of a liquid stationary phase does not necessarily require saturation of the mobile phase, but is possible with unsaturated solutions as well. Probably the deposition of bulk liquid is stimulated by the adsorption forces in the pores of silica. The volume of the stationary phase formed may be estimated from the decrease of t_0 . The data in Fig. 4 show its dependence on EG concentration. It follows that retention with a mixed mechanism takes place over a wide range of EG concentrations. The phase ratio for the system with a saturated mobile phase is estimated to be about 0.5. The role of the partition process depends on the concentration of polar solvent and on the chemical structure of the solutes. It is most important at high C and for relatively less polar solutes. It is probably dominant for substances XIII and XIV that were only slightly retained by adsorption even at low EG concentration.

A correlation was found between k' and partition coefficients measured by the shake-flask method. It is further evidence of a partition mechanism of separation. It was concluded from comparison of the partition coefficients and capacity factors that the phase ratio of the system is about 0.6. This value is in a good agreement with the value obtained from decrease of t_0 .

The elution strength of binary ethyl acetate-EG systems is not sufficient for some of the most polar solutes. Therefore a series of ternary ethyl acetate-EG-

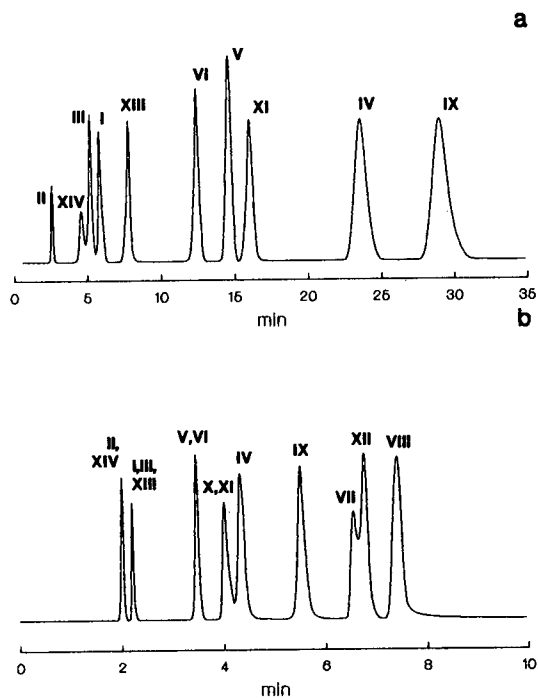


Fig. 5. Chromatograms of test solutes in (a) ethylene glycol-saturated mobile phase and (b) ternary solvent consisting of methanol-ethylene glycol-ethyl acetate (6:10:84).

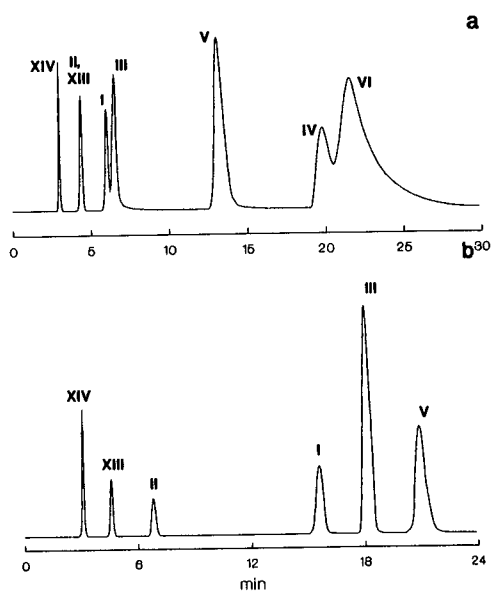


Fig. 6. Chromatograms of test solutes in the mobile phases consisting of ethyl acetate with addition of 4% triethylene glycol (a) and 1% formamide (b).

methanol mixtures was tested. Fig. 5b shows one of the chromatograms thus obtained. All the solutes under study are eluted at reasonable k' values. The experiments show that, in order to maintain the good peak symmetry typical of the partition mode, the proportion of EG in the mobile phase should exceed the proportion of methanol.

Similar results were obtained with TEG and formamide as mobile phase constituents (Fig. 6). It should be emphasized here that in these cases the concentration of the polar solvents was far from saturation. Therefore the properties of such systems should differ from those of partition systems reported earlier [13].

The chromatograms in Figs. 5 and 6 show that peak shape is much better in the systems with a mixed or partition mechanism than in adsorption system ethyl acetate–methanol (Fig. 3). Each of the solvents produced systems with different selectivity of separation.

REFERENCES

- 1 L. R. Snyder and J. J. Kirkland, *Introduction to Modern Liquid Chromatography*, Wiley-Interscience, New York, 1979, pp. 248–250.
- 2 J. P. Crombeen, S. Heemstra and J. C. Kraak, *J. Chromatogr.*, 282 (1983) 95.
- 3 J. P. Crombeen, S. Heemstra and J. C. Kraak, *Chromatographia*, 19 (1984) 219.
- 4 J. J. Kirkland and C. H. Dilks, *Anal. Chem.*, 45 (1973) 1778.
- 5 H. Poetter, M. Hulm and S. Schumann, *J. Chromatogr.*, 391 (1985) 440.
- 6 N. A. Parris, *J. Chromatogr. Sci.*, 12 (1974) 753.
- 7 J. F. K. Huber, M. Pawlowska and P. Markl, *Chromatographia*, 17 (1983) 653.
- 8 J. F. K. Huber, V. Pawlowska and P. Markl, *Chromatographia*, 19 (1984) 19.
- 9 J. H. M. Van den Berg, J. Milley and R. S. Deelder, *J. Chromatogr.*, 132 (1977) 421.
- 10 V. D. Shatz and O. V. Sahartova, *High Performance Liquid Chromatography, Basic Theory, Methodology, Application in Drug Chemistry*, Zinatne, Riga, 1988, pp. 303–346.
- 11 V. D. Shatz and O. V. Sahartova, *High Performance Liquid Chromatography, Basic Theory, Methodology, Application in Drug Chemistry*, Zinatne, Riga, 1988, p. 142.
- 12 K.-G. Wahlund and J. Beijersten, *Anal. Chem.*, 54 (1982) 128.
- 13 H. Musso and H. Beecken, *Chem. Ber.*, 90 (1957) 1808.

Determination of sorbent polarity and selectivity by linear regression of retention indices

OLEG G. LARIONOV*, VICTOR V. PETRENKO and NATALIA P. PLATONOVA

Institute of Physical Chemistry, U.S.S.R. Academy of Sciences, Leninskii Prospekt 31, 117915 Moscow (U.S.S.R.)

ABSTRACT

A regression equation for the description of retention indices through molecular parameters of sorbates is proposed. Electron polarizability, dipole moment, molar volume, the molecular connectivity indices of first order and electron-acceptor and electron-donor energetic constants were chosen as descriptors. The regression coefficients obtained relate to the ability of a surface to effect some sorbate-sorbent interactions. The validity of the expression was shown for a wide range of sorbent polarity. A high significance of the steric factor $G = \chi/V_m$ was revealed. A set of test sorbates was specified for routine determinations of sorbent polarity.

INTRODUCTION

Sorbate-sorbent interactions (SSI) play an important role in sorbate retention in gas chromatography and define both the total polarity and the selectivity of a sorbent. Some recent studies were devoted to the elucidation of the influence of different SSIs on substance retention in gas-liquid chromatography (GLC) [1–5]. As the ability to effect all SSIs relates to the molecular structure of a sorbate and its physico-chemical characteristics, attempts have been made to express the retention of a sorbate through its molecular parameters [6–12]. Also, the determination of stationary phase selectivity by its ability to enter into SSIs was carried out [13,14].

In previous work [15], we demonstrated the scope of the determination of sorbent abilities to undergo some SSIs by multiple linear regression for adsorption energies. This paper deals with the same method applied to retention indices.

The following expression was advanced for the adsorption energy of a sorbate, and includes dispersion, orientation, electron-acceptor and electron-donor terms:

$$-\Delta U = K_1\alpha G + K_2(2\mu^2/3kT + \alpha G) + K_3W_a + K_4W_d + K_5 \quad (1)$$

where α is the polarizability of the sorbate molecule, μ its dipole moment and W_a and W_d its electron-acceptor and electron-donor constants [16]. The coefficients K_1 – K_4 are proportional to the physico-chemical adsorbent characteristics involved in the expressions for each type of SSI. Accordingly, knowing the values of these coefficients

would allow us to estimate an adsorbent's ability to effect certain SSI quantitatively. The applicability of eqn. 1 was tested with a set of 30 sorbates for three adsorbents of different polarity. However, Kováts retention indices are a more convenient and a more readily available source of information on chromatographic properties of adsorbents than adsorption energies. Thus our final aim was the adoption of retention indices as original data for evaluating an adsorbent's ability for different intermolecular interactions.

From the well known thermodynamic expressions [17]

$$\Delta F_{\text{ads.}} = \Delta U_{\text{ads.}} - T\Delta S_{\text{ads.}} \quad (2)$$

$$\Delta F_{\text{ads.}} = -RT(\ln V_s - 1) \quad (3)$$

and the expression for retention indices (*RI*):

$$RI = (100/b)(\ln V_s - a) \quad (4)$$

where *a* and *b* are the intercept and the slope for the retention equation for *n*-alkanes, one may obtain the following expression:

$$RI = D(-\Delta U_{\text{ads.}}) + DT(\Delta S_{\text{ads.}}) + DRT(1 - a) \quad (5)$$

where $D = 100/bRT$.

Eqn. 1 may be used as an expression for $-\Delta U_{\text{ads.}}$ in eqn. 5 but the expression for $\Delta S_{\text{ads.}}$ through molecular parameters is a more complex problem. However, if there is a correlation between $\Delta U_{\text{ads.}}$ and $\Delta S_{\text{ads.}}$ on an adsorbent (as is the case for many adsorbents), it becomes possible to neglect the second, high correlating term, in regression analysis, in which event the expression for *RI* will have the following form:

$$RI = K_1 D\alpha G + K_2 D(2\mu^2/3kT + \alpha G) + K_3 DW_a + K_4 DW_d + K_5 \quad (6)$$

Eqn. 6 is applicable for multiple linear regression also, in which event desired values of the coefficients K_i for a sorbent may be obtained by using the molecular parameters for the sorbates and their retention indices on the sorbent. The non-equivalence of *RI* units for various adsorbents is accounted for by the constant *D*. For two adsorbents with similar values of *RI* and different values of *b* the coefficients K_i will differ.

EXPERIMENTAL

Generation of descriptors

The physico-chemical and topological parameters for the sorbate molecules were obtained in the following way. Polarizability, α , was calculated from the Lorentz-Lorenz equation:

$$\alpha = \frac{3}{4\pi L} \cdot V_m \cdot \frac{(n^2 - 1)}{(n^2 + 2)} \quad (7)$$

where V_m is the molar volume and n is the refractive index. Dipole moments were taken from ref. 18. The constants W_d and W_a for the gas phase were calculated from the data presented in ref. 16. For molecules with two electron-donor atoms (dioxane, nitroalkanes), W_d values were multiplied by 2. Thermodynamic W_d values for alcohols and ethers are very close. However, the accessibility of the oxygen atom in dialkyl ethers is much lower than in the corresponding alcohols, so the W_d values for ethers were divided by 2.

To take steric effects into account, some topological descriptors [19] were also involved. The molecular connectivity indices (MCI) of the first order were calculated from the expression:

$${}^1\chi = \sum^n (\delta_i \delta_j)^{-1/2} \quad (8)$$

where n is the number of valence bonds in a molecule and δ_i and δ_j are the atom number of valences directed to the adjoining non-hydrogen (*e.g.*, C, O, N) atoms. For cyclic molecules an allowance for a ring equal to 0.5 was subtracted from the values of ${}^1\chi$. For example, for the calculation of ${}^1\chi$ value for acetone:

$${}^1\chi = (1 \times 4)^{-1/2} + (4 \times 2)^{-1/2} + (4 \times 2)^{-1/2} + (4 \times 1)^{-1/2} = 1.707$$

The steric factor G was calculated as the ratio ${}^1\chi/V_m$ and was then normalized to the maximum magnitude, so the G factor ranges in value from 0.63 (CCl_4) to 1.00 (CH_3NO_2). This factor seems to reflect the degree of engagement of a molecule with a surface. Hence we may assume that the product αG has the meaning of the "effective polarizability" of a molecule for adsorption on a surface. Fig. 1 illustrates this phenomenon for adsorption of non-polar alkanes on completely non-polar hydrogen treated thermally graphitized carbon black (HT GTCB) when eqn. 6 reduces to

$$RI = K_1 D \alpha G + K_5 \quad (9)$$

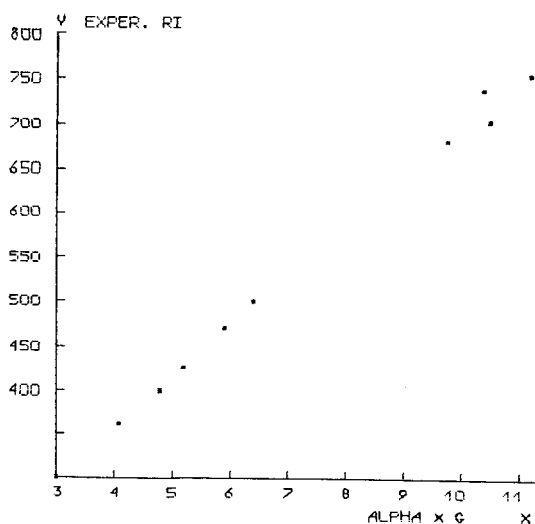


Fig. 1. Experimental RI values vs. αG on HT GTCB at 150°C .

The RI values of linear and branched butanes, pentanes and octanes [20] show a good linear dependence on their αG values, while alkanes with the same α values (or number of carbon atoms) have different retention indices.

Twenty sorbates with various structure and their molecular descriptors are listed in Table I. The descriptors of other molecules are available as supplementary material.

TABLE I
VALUES OF CHOSEN DESCRIPTORS FOR 20 SUBSTANCES

No. Sorbate	α (\AA^3)	μ^2 (D^2)	W_a (kJ/mol) ^{1/2}	W_d (kJ/mol) ^{1/2}	G
1 Hexane	11.85	0	0	0	0.67
2 Heptane	13.7	0	0	0	0.70
3 Octane	15.53	0	0	0	0.73
4 Nonane	17.38	0	0	0	0.75
5 Benzene	10.38	0	0	4.5	0.85
6 Ethanol	5.09	2.8	0.933	11.7	0.74
7 <i>n</i> -Propanol	6.95	2.8	0.923	11.8	0.77
8 <i>n</i> -Butanol	8.78	2.7	0.922	11.8	0.80
9 Isobutanol	8.81	2.6	0.907	11.9	0.74
10 <i>tert.</i> -Butanol	8.93	2.4	0.859	12.1	0.64
11 Methyl ethyl ketone	8.20	7.7	0	10.4	0.76
12 Acetone	6.35	8.0	0	10.6	0.70
13 Nitromethane	4.94	12.0	0	12.2	1.00
14 Nitroethane	6.74	12.8	0	12.8	0.97
15 2-Nitropropane	8.55	13.9	0	13.4	0.90
16 1-Nitropropane	8.57	13.7	0	12.8	0.95
17 Ethyl acetate	8.80	3.1	0	9.2	0.86
18 Acetonitrile	4.38	15.5	0	9.4	0.79
19 Dioxane	8.60	0.2	0	22.7	0.89
20 Pyridine	9.53	4.8	0	20.7	0.94

The data set

RI values for the following sorbents were taken as initial data for regression analyses: commercial Porapaks and Chromosorb Century Series, Polysorb N and its three modifications, copolymers of divinylbenzene (DVB) and glycidyl methacrylate (GMA) together with its three modifications, barium sulphate and graphitized thermal carbon black (GTCB). The structures of the sorbents and literature references are given in Table II. Also, a copolymer of epithiopropyl methacrylate (ETPMA) and ethylene dimethacrylate (EDMA) modified by ethylenediamine (EDA) (GS-EDA) [21] was studied. Further, this sorbent was modified by adsorption of Ni(II) ions on its surface. RI values for these two sorbents were measured at 150°C. A Tswett 530 chromatograph equipped with a flame ionization detector and with helium as carrier gas was used.

Ref. 22 was used as a mathematical basis for the multiple linear regression method. A BASIC program with matrix statements was written for an Iskra 226 personal computer. The correlation coefficient R was used in order to ascertain the validity of the regression expression.

TABLE II
SORBENTS INVESTIGATED

Name	Polymer matrix	Modification agent (or functional groups)	R/ ref.
GTCB			
Porapak Q	DVB-EVB		23
Porapak QS	DVB-EVB		24
Porapak S	DVB-EVB		24
Porapak P	DVB-EVB	Vinylpyridine	25
Porapak R	DVB-EVB	Styrene	25
Porapak N	DVB-EVB	Vinylpyrrolidone	25
Porapak T	DVB-EVB	Vinylpyrrolidone	25
Chromosorb 102	DVB-styrene	Ethylene dimethacrylate	25
Chromosorb 101	DVB-styrene		26
Chromosorb 105	DVB-styrene		26
Chromosorb 104	DVB-acrylonitrile		26
DVB-GMA	DVB-GMA		26
DVB-GMA '1	DVB-GMA		27
DVB-GMA '2	DVB-GMA	-CH(OH)CH ₂ OH	27
DVB-GMA '3	DVB-GMA	-CH(OH)CH ₂ N ⁺ (CH ₂ CH ₂ OH) ₃ OH ⁻	27
Polysorb N	DVB-2,5-methylvinylpyridine	-CH(OH)CH ₂ NHC(CH ₂ OH) ₃	27
Polysorb N '1	As above	-CH ₃	27
Polysorb N '2	As above	-CH ₂ OH	27
Polysorb N '3	As above	-COOH	27
GS-EDA	EDMA-ETPMA	-CH ₃ ; N _{pyr} =O	27
GS-EDA-Ni	EDMA-ETPMA	-CH(SH)CH ₂ NH(CH ₂) ₂ NH ₂	
BaSO ₄		As above + Ni ²⁺	28

RESULTS AND DISCUSSION

To verify the validity of eqn. 6 the set of 20 sorbates (Table I) was processed using slightly polar Porapak P, Porapak T (medium polarity) and GS-EDA as a polar sorbent with electron-acceptor groups. The structures of the sorbates in the data set differ significantly, so the descriptors of eqn. 6 were uncorrelated. The correlation matrix is shown in Table III.

The scatter plots for moderately polar and polar sorbents are given in Figs. 2 and 3. The regression coefficients with standard deviations, their Student *t*-values and *R* values for the three sorbents are given in Table IV. For each sorbent the correlations

TABLE III
CORRELATION MATRIX FOR DESCRIPTORS USED IN EQN. 6 (*N* = 20)

	αG	μ^2	W_a	W_d
αG	1.00	-0.476	-0.386	-0.444
μ^2		1.000	-0.277	0.284
W_a			1.000	0.214
W_d				1.000

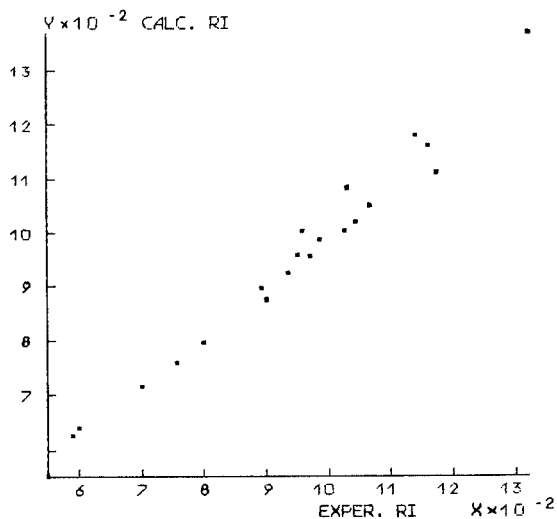


Fig. 2. Calculated vs. experimental RI values on Porapak P at 175°C.

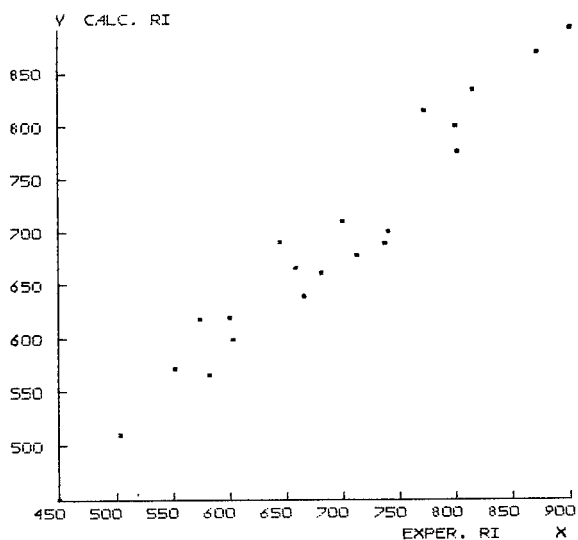


Fig. 3. Calculated vs. experimental RI values on GS-EDA sorbent at 150°C.

between regression coefficients show the same behaviour and the term K_5 is highly correlated with K_1 . The correlation matrix for GS-EDA is shown in Table V.

Taking the wide range of RI values (about 500 i.u.), the simplicity of eqn. 6 and the different structures of the sorbates into account, one may consider the R values as fairly high and the deviations from experimental RI values as fairly small. It should be noted that exclusion of the steric factor G from eqn. 6 decreases R for the three sorbents

TABLE IV

REGRESSION COEFFICIENTS K_i WITH THEIR STANDARD ERROR AND STUDENT'S t -VALUES ON THREE SORBENTS

Parameter	Porapak P		Porapak T		GS-EDA	
	K_i	t	K_i	t	K_i	t
K_1	120 ± 9	13.0	132 ± 9	14.9	109 ± 9	11.4
K_2	16 ± 4	4.5	28 ± 3	8.3	37 ± 4	9.0
K_3	3 ± 6	0.5	25 ± 6	4.3	39 ± 7	5.7
K_4	17 ± 3	6.3	17 ± 3	6.6	66 ± 4	16.3
K_5	181 ± 42	4.1	208 ± 35	5.7	259 ± 38	6.3
s (i.u.)	29.9 (3.8%)		24.5 (3.4%)		34.4 (3.6%)	
R	0.970		0.972		0.985	

to 0.891, 0.890 and 0.973, respectively. Hence the presence of G significantly increases the validity of eqn. 6 with an unchanged number of regression coefficients.

Comparing K values from Table IV it can be seen that the polar Porapak T, as compared with Porapak P, relates to increasing the ability to effect orientation SSI (K_2 increases from 16 to 28) and electron-donor ability of the sorbent surface (K_3 increases from 3 to 25), whereas the electron-acceptor ability (K_4) remains the same. This is in accordance with expectations given the presence of $-C(O)O-$ groups on the more polar polymer surface due to modification by ethylene dimethacrylate. For the GS-EDA sorbent low values of K_1 and abrupt increases for K_2 – K_4 values were observed. This is in accord with the presence on the surface of hardly polarizable amino groups with appreciable dipole moments and electron-donor properties and with electron-acceptor properties of the $-SH$ group. Hence apparently the K values are in agreement with the sorbent's expected abilities to effect SSI.

The following conclusions were made after subsequent analyses for various sorbents with a changed sorbate set, number of sorbates in a set and alternate descriptors (Balaban indices, $^2\chi$, donor number). Small variations of the sorbate set have no appreciable effect on K values except when substances with high descriptor magnitudes (pyridine, W_d ; alcohols, W_a ; nitroalkanes, and nitriles, μ^2) are excluded. Perceptible regression standard deviations and standard errors in coefficients the K_i are obviously connected with two sources: a rough approximation of the real SSI by

TABLE V

CORRELATION BETWEEN THE REGRESSION COEFFICIENTS FOR GS-EDA SORBENT

	K_1	K_2	K_3	K_4	K_5
K_1	1.00	0.454	0.499	0.201	-0.939
K_2		1.000	0.567	-0.395	-0.472
K_3			1.000	-0.320	-0.494
K_4				1.000	-0.383
K_5					1.000

eqn. 6 and with the inadequacy of the chosen descriptors to characterize the behaviour of some sorbate molecules. The latter is concerned especially with μ , W_d and ${}^1\chi$. We have used the dipole moments which characterize the whole molecule whereas for adsorption obviously the dipole moments of individual bonds ($=C=O$, $-C\equiv N$) are more important. Equilibrium thermodynamic values of W_d from ref. 16 do not include differences in the spatial accessibility of donor atoms in various molecules (compare alcohols with dialkyl ethers) and different degrees of availability of the same functional group with carbon chains of various length (compare methanol with butanol). Some allowances for W_d were made from the start of the study (see Experimental). In general, the steric factor G describes the degree of engagement of a molecule with a surface fairly well. For example, G values for molecules with different structures are as follows: *n*-butanol 0.80, isobutanol 0.74, *tert.*-butanol 0.64, planar pyridine 0.94 and *n*-hexane 0.67. For molecules with similar structures the G values are as follows: di-*n*-butyl ether 0.79, *n*-nonane 0.75, *tert.*-butanol 0.64 and carbon tetrachloride 0.63. Some problems arise because of the cyclic structure of molecules, or the presence of triple bonds or heteroatoms from atoms of higher atomic number (Cl, Br, I, S) in a molecule. The wide confidence interval for K_3 relates to the narrow ranges of the values of W_a used.

For many of sorbents studied, aryl compounds (benzene, toluene) show high deviations, both positive and negative, from experimental RI values. This, perhaps, relates to the inadequate description of the molecules by the factor G and to disregarded interactions of the aromatic electron ring with sorbent polymer chains. For all sorbents very low predicted RI values were obtained for small molecules of chloro-substituted alkanes, especially for chloroform and methylene chloride. This clearly relates to the incorrect description of the molecules by the factor G .

In spite of the difficulties discussed for most sorbates, a satisfactory prediction of RI values was observed. The K_i values obtained conformed with the physico-chemical nature of the surface functional groups.

For practical application of the method to comparisons of sorbent surface properties, it is necessary to fulfil the following conditions. For every sorbent the test set of sorbates must be the same. The requirements for the sorbates included in test set are as follows: (1) all kinds of SSI included in eqn. 6 must be represented; (2) the magnitude of the descriptors should have as wide a range as possible; (3) the descriptors must be uncorrelated; (4) the chromatographic behaviour of the sorbates should be adequately described by all of the chosen molecular parameters; (5) a small number set is more convenient for routine analysis and collection of reference RI values; and (6) all the substances should be commonly used in chromatographic practice.

Nine sorbates conforming to these conditions were selected: hexane, nonane, ethanol, *n*-propanol, *n*-butanol, acetone, methyl ethyl ketone, nitromethane and pyridine. Their descriptor correlation matrix is shown in Table VI. The test set RI values were processed for 23 sorbents. The results are given in Table VII. It should be noted that for barium sulphate the K values were evaluated approximately because of the low R value arising from the extremely high polarity of this ionic sorbent. Calculated contributions of each term in eqn. 6 for Parapak QS, Chromosorb 104 and the GS-EDA sorbent are given in Table VIII. Examination of the various types of SSI contributions shows that they are comparable. Hence it is a very rough approximation to apply their RI values as representative of one kind of SSI.

TABLE VI
CORRELATION MATRIX FOR DESCRIPTORS USED IN EQN. 6 ($N = 9$)

	αG	μ^2	W_a	W_d
αG	1.00	-0.544	-0.393	-0.438
μ^2		1.000	-0.325	0.505
W_a			1.000	0.220
W_d				1.000

For evaluation of the overall sorbent polarity, summarizing of "specific" coefficients K_2 - K_4 normalized to their maximum values was carried out:

$$P = (K_2/95 + K_3/122 + K_4/92) \cdot 100 \quad (10)$$

Calculated P values are given in Table VII. It is worth remarking that the overall polarity masks the variations of individual K values and correlates with Rohr-schneider's polarity calculated through the sum of five net RI values (see Table IX).

For non-polar GTCB all "specific" K values are equal to zero. Porapaks show

TABLE VII

THE COEFFICIENTS K_i AND R VALUES FOR REGRESSION ANALYSES WITH TEST SET OF SORBATES ($N = 9$)

Sorbent	K_1	K_2	K_3	K_4	K_5	R	P
GTCB	108	0	0	0	67	0.991	0
Porapak Q	130	16	14	-1	154	0.995	29
Porapak QS	158	19	14	0	120	0.999	32
Porapak S	182	29	33	-1	111	0.997	58
Porapak P	138	29	16	16	89	0.999	61
Porapak R	175	30	38	-1	120	0.999	63
Porapak N	180	40	35	3	127	0.999	74
Porapak T	156	52	42	11	102	0.999	101
Chromosorb 102	144	17	11	1	146	0.999	28
Chromosorb 101	125	26	14	13	104	0.999	53
Chromosorb 105	177	27	27	3	98	0.999	53
Chromosorb 104	132	69	43	21	94	0.999	131
DVB-GMA	118	56	50	14	139	0.998	115
DVB-GMA '1	110	43	48	24	119	0.999	111
DVB-GMA '2	105	48	55	33	128	0.997	131
DVB-GMA '3	117	46	56	35	126	0.998	132
Polysorb N	104	18	36	40	1	0.986	93
Polysorb N '1	112	30	43	44	41	0.988	115
Polysorb N '2	83	54	63	32	160	0.997	144
Polysorb N '3	117	95	122	38	38	0.993	240
GS-EDA	132	59	68	58	150	0.996	181
GS-EDA-Ni	145	36	52	92	138	0.999	181
BaSO ₄	83	147	203	102	443	0.960	432

TABLE VIII

CONTRIBUTIONS OF EACH TERM OF EQN. 6 FOR THREE SORBENTS: (A) PORAPAK QS, (B) CHROMOSORB 104 AND (C) GS-EDA

Sorbate	Sorbent	<i>RI</i>		Contribution of term number				
		Exptl.	Predicted	1	2	3	4	5
Hexane	A	600	602	482	0	0	0	120
	B	600	594	499	0	0	0	94
	C	600	603	465	0	0	0	138
Ethanol	A	400	409	226	21	40	2	120
	B	690	698	234	97	154	118	94
	C	1007	996	218	47	161	432	138
Methyl ethyl ketone	A	565	557	378	56	0	2	120
	B	850	856	392	265	0	105	94
	C	990	1015	365	128	0	384	138
Nitromethane	A	495	506	297	87	0	2	120
	B	935	932	308	408	0	122	94
	C	1079	1069	286	198	0	447	138
Pyridine	A	695	698	540	35	0	3	120
	B	1025	1024	560	163	0	207	94
	C	1500	1497	521	79	0	759	138

TABLE IX

COMPARISON OF POLARITIES CALCULATED FOR CHROMOSORB AND PORAPAKS BY EQN. 10 AND ROHRSCHEIDER'S POLARITY [29]

Method	Chromosorb				Porapak				
	102	105	101	104	Q	P	R	N	T
By eqn. 10	28	53	53	131	29	61	63	74	101
Rohrschneider	197	347	555	1831	68	708	331	499	1240

increasing K_2 and K_3 values as the original polymer matrix is modified by vinylpyrrolidone, vinylpyridine and ethylene dimethacrylate. It should be noted that the K values depend both on the type of functional group and on its concentration on the surface, because the "average" molecular characteristics of a surface change with variation in the polymer composition.

For the Chromosorb Century Series, Chromosorb 104 is the most polar sorbent. Its K_3 and especially K_2 values are very high owing to the presence of electron-donor cyano groups [$\mu(\text{CH}_3\text{CN}) = 3.94 \text{ D}$]. Some electron-acceptor ability of the surface may be accounted for by partial positive charges on the carbon atom in the cyano group.

Modified copolymers of DVB and GMA show decreasing K_2 values after destruction of the epoxy ring [$\mu(\text{C}_2\text{H}_2\text{O}) = 1.9 \text{ D}$ and $\mu(\text{C}_2\text{H}_5\text{OH}) = 1.7 \text{ D}$] and

gradually increasing K_4 values as the concentration of OH groups on the surfaces is increased.

Increasing K_2 , K_3 and K_4 values after introducing OH groups onto the original Polysorb N surface were observed. Subsequent conversion of this group into COOH increases K_2 and K_3 significantly but the decrease in K_4 (electron acceptor) may be accounted for by the formation of intermolecular bonds such as $-\text{COOH} \cdots \text{N}$ (pyridine ring). Extremely high values of K_2 and K_3 for the third modification of Polysorb N relate to the high dipole moment and strong electron-donor ability of the $=\text{N}=\text{O}$ bond conjugated with the pyridine ring.

Very high values of K_4 were found for the GS-EDA sorbent with SH and NH groups. Adsorption of Ni(II) ions on this surface leads to an abrupt increase in K_4 owing to the electron-acceptor properties of the ion and to a decrease in K_2 and K_3 owing to the formation of a chelate complex of ethylenediamine with the Ni(II) ion.

REFERENCES

- 1 J. R. Smith, A. H. Tameesh and D. J. Waddington, *J. Chromatogr.*, 151 (1978) 27.
- 2 R. V. Golovnya and T. A. Misharina, *J. Chromatogr.*, 190 (1980) 1.
- 3 Th. Kleinert and W. Ecknig, *J. Chromatogr.*, 315 (1984) 75 and 85.
- 4 S. Dong, M. Brendle and B. J. Donnet, *Chromatographia*, 28 (1989) 469.
- 5 T. Takagi, Ya. Shindo, H. Fujiwara and Yo. Sasaki, *Chem. Pharm. Bull.*, 37 (1989) 1556.
- 6 H. Lamparczyk and A. Radecky, *Chromatographia*, 18 (1984) 715.
- 7 F. Patte, M. Etcheto and P. Laffort, *Anal. Chem.*, 54 (1982) 2239.
- 8 J. Hradil, F. Svec, N. M. Gogitidze and T. T. Andronikashvili, *J. Chromatogr.*, 324 (1985) 277.
- 9 M. Gassion-Matas and G. Firro-Pamies, *J. Chromatogr.*, 187 (1980) 1.
- 10 K. Osmialowski, J. Halkiewicz and R. Kaliszan, *J. Chromatogr.*, 361 (1986) 63.
- 11 J. Bermejo and M. D. Guillen, *Anal. Chem.*, 59 (1987) 94.
- 12 M. N. Hasan and P. C. Jurs, *Anal. Chem.*, 60 (1988) 978.
- 13 M. S. Klee, M. A. Kaiser and K. B. Laughlin, *J. Chromatogr.*, 279 (1983) 681.
- 14 T. J. Betts, *J. Chromatogr.*, 354 (1986) 1.
- 15 O. G. Larionov, V. V. Petrenko and N. P. Platonova, *J. Chromatogr.*, 537 (1991) 295.
- 16 V. A. Terentyev, *Termodinamika Donorno-Akseptornoj Svyazi*, Saratov University Publishing House, Saratov, 1981, p. 36.
- 17 A. V. Kiselev, *Mezhmolekulyarnye Vzaimodeystviya v Adsorbtsii i Kromatografii*, Vysshaya Shkola, Moscow, 1986, p. 153.
- 18 O. A. Osipov, V. I. Minkin and A. D. Garnovski, *Spravochnik po Dipol'nym Momentam*, Vysshaya Shkola, Moscow, 1976, p. 54.
- 19 L. B. Kier and L. H. Hall, *Molecular Connectivity in Chemistry and Drug Research*, Academic Press, New York, 1976, p. 54.
- 20 N. N. Avgul, A. V. Kiselev and D. P. Poshkus, *Adsorbtsiya Gazov i Parov na Odnorodnykh Poverkhnostyakh*, Khimiya, Moscow, 1975, p. 380.
- 21 V. Marousek, M. Bleha, E. Votavova and J. Kalal, *Sci. Pap. Prague Inst. Chem. Tech.*, 3 (1980) 269.
- 22 N. Draper and G. Smith, *Applied Regression Analysis*, Wiley, New York, 1981, p. 340.
- 23 A. V. Kiselev and Ya. Yashin, *Gazo-adsorbtsionnaya Khromatografiya*, Khimiya, Moscow, 1979, p. 22.
- 24 S. B. Dave, *J. Chromatogr. Sci.*, 7 (1969) 389.
- 25 W. R. Supina and L. P. Rose, *J. Chromatogr. Sci.*, 7 (1969) 192.
- 26 W. R. Supina, *The Packed Column in Gas Chromatography*, Supelco, Bellefonte, PA, 1974, p. 70.
- 27 Z. A. Reznikova, *Dissertation*, Institute of Reagents and Pure Substances, Moscow, 1985, pp. 59 and 73.
- 28 L. D. Belyakova, O. G. Larionov and L. M. Strokina, *Izv. Akad. Nauk SSSR, Ser. Khim.*, (1988) 1491 and 2454.
- 29 G. Gastello and G. D'Amato, *J. Chromatogr.*, 254 (1983) 69.

Theoretical approach to the gas chromatographic separation of enantiomers on dissolved cyclodextrin derivatives

M. JUNG, D. SCHMALZING and V. SCHURIG*

Institut für Organische Chemie, Universität Tübingen, Auf der Morgenstelle 18, D-7400 Tübingen (Germany)

ABSTRACT

The theoretical concept described previously for enantiomer separation by complexation gas chromatography was extended to polysiloxane stationary phases containing dissolved cyclodextrin derivatives. A relationship between the chiral separation factor α and the cyclodextrin molality was derived. The theory was verified by comparing the predicted and measured dependence of α on the cyclodextrin molality for various racemates. Retention increases R' were determined as a measure of the enantiomer–cyclodextrin interactions and of the contribution of these interactions to the total retention time. By measuring R' at different temperatures, Gibbs-Helmholtz parameters ($\Delta_{R,S}\Delta G$, $\Delta_{R,S}\Delta H$ and $\Delta_{R,S}\Delta S$) of enantiomer discrimination were obtained from the $\ln(R'_R/R'_S)$ vs. $1/T$ plots. Because of the difficulty of finding a truly inert reference standard, these data are affected by a systematic error which restricts the interpretation of the observed enantioselectivities to a qualitative manner.

INTRODUCTION

Enantiomer separation by gas chromatography on chiral stationary phases is based on the different stabilities of diastereomeric 1:1 associates formed rapidly and reversibly. In complexation gas–liquid chromatography (GLC) employing stationary phases containing dissolved transition metal β -diketonates, extensive studies on the thermodynamics of molecular association including enantioselectivity have been performed [1–7]. For derivatized cyclodextrin stationary phases, which have become increasingly important for enantiomer separation by GLC in the last few years [8–13], there are still only a few theoretical investigations available [14,15]. It was therefore of interest to investigate systematically whether the model developed for complexation GLC can also be applied to dissolved cyclodextrin stationary phases.

The consideration of retention increases R' (or retention increments, a quantitative measure of the interactions between solute and cyclodextrin) and the relationship between the chiral separation factor α and the cyclodextrin molality m allows a better understanding of enantioselectivity and it may guide the optimization of enantiomer separations.

EXPERIMENTAL

Instrumentation

A Carlo Erba Fractovap 2101 instrument equipped with a flame ionization detector was used. Retention times were determined using a Shimadzu C-R 3A integrator.

Column preparation and gas chromatographic procedure

Cyclodextrin derivatives and capillary columns were prepared and used as described previously [9]. Fused-silica columns (25 m × 0.25 mm I.D.) with a film thickness of 0.2 μm (permethylated β-cyclodextrin dissolved in OV-1701) were employed. The inlet pressure was 1.0 bar hydrogen.

Determination of net retention times and retention increases, R'

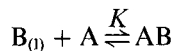
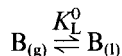
Retention increases were determined as described for complexation GLC [6]; all measurements were performed at least three times. Net retention times t' were measured from the methane peak. The relative net retention r_0 of a solute with respect to a reference standard was calculated from the ratio $t'_0(\text{solute})/t'_0^*(\text{standard})$ obtained on an achiral reference column (eqn. 10). The relative net retention r of a solute with respect to a reference standard was calculated from the ratio $t'(\text{solute})/t'^*(\text{standard})$ obtained on the chiral, cyclodextrin-containing column (eqn. 9). The retention increase R' was calculated according to $R' = (r/r_0) - 1$ (eqn. 8).

In order to study systematically the influence of the choice of the standard, all relative retention data were determined with respect to four different commercial *n*-alkanes (hereafter abbreviated C₇, C₈, etc.) as standards ($k' \approx 0.4$ – 0.8 for the smallest).

THEORETICAL

Consider a volatile solute B eluting through a column containing a dilute solution of a cyclodextrin derivative A (e.g., permethylated β-cyclodextrin) in an (achiral) solvent S (e.g., a polysiloxane such as OV-1701).

In analogy with the theory advanced for complexation GLC [1–4], the present derivation is based on two equilibria:



The partition coefficient K_L^0 of B between the gaseous and pure liquid phase is

$$K_L^0 = \frac{a_{B(l)}}{a_{B(g)}} \quad (1)$$

and the thermodynamic stability constant K of AB in the given solvent S is

$$K = \frac{a_{AB}}{a_A a_{B_0}} \quad (2)$$

As the total amount of solute present in the liquid phase is $a_{B_0} + a_{AB}$, the apparent partition coefficient is

$$K_L = \frac{a_{B_0} + a_{AB}}{a_{B(g)}} \quad (3)$$

Using eqns. 1 and 2, this can be rewritten as [1,2]

$$K_L = K_L^0(1 + Ka_A) \quad (4)$$

Employing the fundamental equation of chromatography

$$t' = \frac{K_L}{\beta} \cdot t'_m \quad (5)$$

where t'_m = dead time, t' = net retention time, K_L = partition coefficient between mobile and stationary phases and β = phase ratio, an analogous equation can be written for the net retention time:

$$t' = t'_0 \left(\underset{\text{physical}}{1} + \underset{\text{chemical contribution}}{Ka_A} \right) \quad (6)$$

where t_0 is the (experimentally not available) net retention time on a totally identical reference column devoid of the cyclodextrin derivative A.

In eqn. 6, the retention increase (or retention increment) R' is defined as [4]

$$R' = Ka_A \quad (7)$$

R' is a quantitative measure of the increase in the retention of B caused by the addition of the cyclodextrin derivative A to the achiral solvent S. Hence the determination of R' allows one to quantify the "physical" (K_L^0) and "chemical" (K) contributions to the total retention.

As it is experimentally impossible to determine t' and t'_0 with strictly identical column parameters such as column length, diameter, film thickness or flow-rate, it is useful, according to Schurig *et al.* [4], to rewrite eqn. 6 in terms of *relative retention data* in order to obtain an equation that is independent of these parameters:

$$r = r_0(1 + R')$$

or

$$R' = \frac{r}{r_0} - 1 \quad (8)$$

where r is the relative net retention of solute B with respect to an inert reference standard B* (e.g., a small n -alkane):

$$r = \frac{t'}{t'^*} \quad [\text{chiral column (A in S)}] \quad (9)$$

$$r_0 = \frac{t'_0}{t'^*_0} \quad [\text{achiral reference column (only S)}] \quad (10)$$

The chiral separation factor α

Suppose solute B is a racemic mixture of the enantiomers B_R and B_S. Since $K_{LR}^0 = K_{LS}^0$, enantiomer separation of B_R and B_S must be due to different values of K_R and K_S . The chiral separation factor is given by^a

$$\alpha = \frac{K_{LR}}{K_{LS}} = \frac{t'_R}{t'_S} = \frac{r_R}{r_S} \quad (11)$$

Using eqns. 4 and 7, a very useful relationship is obtained:

$$\alpha = \frac{K_R a_A + 1}{K_S a_A + 1} = \frac{R'_R + 1}{R'_S + 1} \quad (12)$$

Enantiomer separation ($\alpha > 1$) requires retention increases R' of the two enantiomers being $R'_R, R'_S > 0$ and $R'_R \neq R'_S$.

Thermodynamic data

Applying the thermodynamic relationship

$$\Delta G = -RT \ln K \quad (13)$$

the ratio of the thermodynamic stability constants

$$\frac{K_R}{K_S} = \frac{R'_R}{R'_S} = \frac{r_R - r_0}{r_S - r_0} \quad (14)$$

yields the difference in the free enthalpies of formation of the diastereomeric associates^{b,c}:

$$\Delta \Delta G = \Delta G_R - \Delta G_S = -RT \ln \frac{R'_R}{R'_S} \quad (15)$$

^a Where R arbitrarily represents the enantiomer eluted later so that $\alpha \geq 1$.

^b Where R arbitrarily represents the chemically more strongly bonded enantiomer (more negative ΔH).

^c Note that only for large R' values does R'_R/R'_S approach $(R'_R + 1)/(R'_S + 1) = \alpha$ (cf., eqn. 12 and eqn. 15 becomes $\Delta \Delta G = -RT \ln \alpha$. The latter equation is sometimes used instead of eqn. 15 as a measure of the chiral recognition $\Delta \Delta G$.

The ratio R'_R/R'_S and thus $\Delta\Delta G$ are independent of the cyclodextrin activity a_A in the solvent S.

It is further possible [16,17] to determine enthalpic and entropic contributions to $\Delta\Delta G$, *i.e.*, $\Delta\Delta H$ and $\Delta\Delta S$, from the Gibbs–Helmholtz relationship (Van 't Hoff plot):

$$\frac{\Delta\Delta G}{T} = f\left(\frac{1}{T}\right) = \Delta\Delta H \cdot \frac{1}{T} - \Delta\Delta S \quad (16)$$

RESULTS AND DISCUSSION

n-Alkanes and the reference standard problem

n-Alkanes (hereafter abbreviated C₇, C₈, etc.) have been used in complexation GLC as inert reference standards for the determination of relative retention data (r values, see eqns. 8–10) as they are not capable of coordinating with transition metal ions. For cyclodextrins, unfortunately, we cannot find any reference standard that would be totally inert toward molecular association.

In order to test the suitability of *n*-alkanes as “inert” reference standards employing cyclodextrin derivatives, $\log t'$ versus n (number of carbon atoms) curves were recorded and compared with those obtained on a reference column containing the pure polysiloxane without cyclodextrin (see Fig. 1). There are still straight lines for permethylated β -cyclodextrin and for heptakis(3-trifluoroacetyl-2,6-dimethyl)- β -cyclodextrin, but the slopes are slightly steeper than on the achiral reference column. As the slope is independent of the experimental parameters (flow-rate, column length, etc., only affect the intercept at $n = 0$ in the logarithmic diagram), this means that there is some interaction between alkane and cyclodextrin, increasing with the carbon number n , *i.e.*, *n*-alkanes do not represent totally inert reference standards for cyclodextrin phases. However, the best results should be obtained if a small *n*-alkane ($k' \approx 0.4$ – 0.8) is used as a standard. The retention increases R' of all solutes were calculated with respect to four different *n*-alkane standards, and indeed the smallest standard always yielded the largest R' value (which is still considered to be too small, *cf.*, Table I; note that between the use of the standards C₉ and C₁₂ an error in R' of *ca.* 10% is introduced).

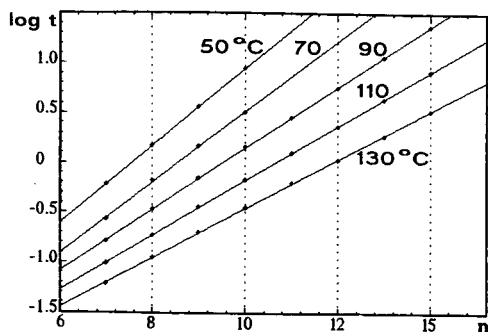


Fig. 1. $\log t'$ vs. n (number of C atoms) for the homologous series of *n*-alkanes on permethylated β -cyclodextrin in OV-1701 at different temperatures.

TABLE I

INFLUENCE OF THE CHOICE OF THE *n*-ALKANE STANDARD, DEMONSTRATED FOR A TYPICAL EXAMPLE: SOLUTE I FROM TABLE II, $T = 100^\circ\text{C}$, MOLALITY OF PERMETHYLATED β -CYCLODEXTRIN $m_A = 0.065$.

Enantiomer	Standard	k'	r^a	r_0^a	R^b	$\Delta\Delta G$ (J/mol) ^c
First eluted	C ₉		19.51	12.74	0.531	1006 1020
	C ₁₀	12.87	10.04	6.62	0.518	
	C ₁₁		5.19	3.48	0.491	
	C ₁₂		2.70	1.84	0.464	
Second eluted	C ₉			22.10	12.74	0.734
	C ₁₀	14.58	11.37	6.62	0.719	
	C ₁₁		5.88	3.48	0.689	
	C ₁₂		3.05	1.84	0.658	

^a $\pm 1\%$.

^b $\pm 2\%$.

^c ± 10 .

Suppose the standard itself had a small retention increase R'_0 (with respect to a hypothetical ideal standard). A relationship between the measured $R' = (r/r_0) - 1$ values and the ideal, true $R'_{\text{true}} = (r_{\text{true}}/r_0) - 1$ values can be derived; the r values (but not r_0) must be corrected in analogy with eqn. 8:

$$r_{\text{true}} = (1 + R'_0)r$$

$$R'_{\text{true}} = \frac{r_{\text{true}}}{r_0} - 1 = (1 + R'_0)\frac{r}{r_0} - (1 + R'_0) + R'_0 \quad (17)$$

$$= (1 + R'_0)R' + R'_0$$

R'_0 is not an inaccessible quantity. The comparison of calculated and measured α vs. molality curves (see below) allows R'_0 to be estimated.

It may be noted that, in contrast to *n*-alkanes, the homologous series of γ -lactones do not yield a straight $\log t'$ vs. n line (see Fig. 2, top).

Dependence of the chiral separation factor α on the cyclodextrin molality m_A

Eqn. 7 allows the calculation of the retention increase R' at a molality m_A^a , i.e., $R'(m_A)$, if R' at a molality m_A^0 , i.e., $R'(m_A^0)$, is known:

$$\frac{R'(m_A)}{m_A} = \frac{R'(m_A^0)}{m_A^0} \quad (18)$$

^a Eqn. (7) can also be written in the form

$$R' = K_{(m)}m_A \quad (7a)$$

Here, the molality concentration scale m_A is used instead of the unknown activity a_A because m_A is independent of temperature and the weight rather than the volume is determined for practical reasons when preparing GLC columns.

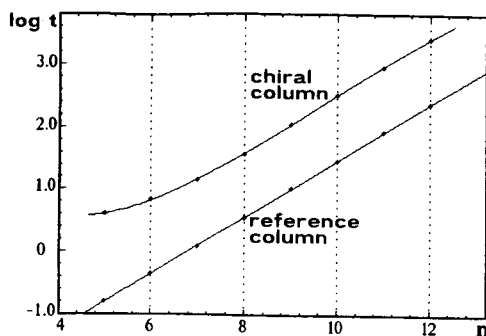


Fig. 2. $\log t'$ vs. n (number of C atoms) for the homologous series of γ -lactones (enantiomer eluted later) on heptakis(3-trifluoroacetyl-2,6-dimethyl)- β -cyclodextrin in OV-1701 (top) and on pure OV-1701 (bottom) at 170°C .

Thus a complete α vs. m_A curve can be calculated, using eqns. 12 and 18, if the $R'_R(m_A^0)$ and $R'_S(m_A^0)$ values at a single molality m_A^0 are provided:

$$\alpha(m_A) = \frac{m_A R'_R(m_A^0) + m_A^0}{m_A R'_S(m_A^0) + m_A^0} \quad (19)$$

Eqn. 19 shows that the α vs. m_A curve levels off as m_A increases, and Fig. 3 clearly shows how this is influenced by the retention increase R'_R (R'_S being calculated from eqn. 19).

Figs. 4 and 5 show some measured α vs. m_A curves (all data are listed in Table II). In Figs. 6-9 the measured α values (independent of any standard!) are compared with the calculated curves for some racemates.

There is good agreement between the calculated and measured curves, which is a clear support for the validity of our approach. Further, it can be seen that the finite retention increase R'_0 of the standard should in no case be above 0.1 (according to eqn. 17, this would lead, for example, to an error of 0.2 for a measured R' value of 1.0).

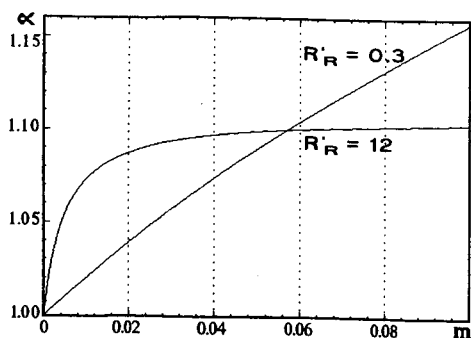
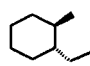
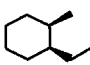

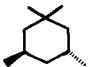
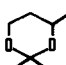
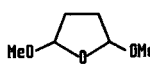
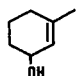
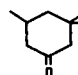
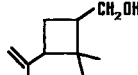
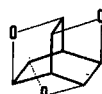
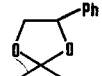
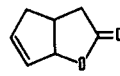





Fig. 3. Simulated α vs. m_A curves, assuming $\alpha = 1.10$ for $m_A^0 = 0.057$ and retention increases $R'_R(m_A^0)$ of 0.3 and 12, respectively.

TABLE II

RETENTION INCREASES R'_R AND R'_S ($\pm 2\%$), SEPARATION FACTORS α AND $\Delta\Delta G$ (IN J/mol, ± 10) FOR TWELVE CHIRAL SOLUTES ON OV-1701 CONTAINING DIFFERENT MOLALITIES OF PERMETHYLATED β -CYCLODEXTRIN

Me = Methyl; Ph = phenyl.

Solute	Temperature and standard	Parameter	Cyclodextrin molality, m_A					
			0.027	0.042	0.057	0.065	0.088	0.096
A 	40°C, C ₇	R'	0.195	0.334	0.413	0.530	0.637	0.655
		α	0.221	0.388	0.480	0.609	0.725	0.757
		$\Delta\Delta G$	1.022	1.041	1.047	1.051	1.054	1.061
B 	40°C, C ₇	R'	0.263	0.464	0.578	0.729	0.889	0.918
		α	0.294	0.523	0.650	0.815	0.998	1.038
		$\Delta\Delta G$	1.025	1.040	1.045	1.050	1.057	1.063
C 	40°C, C ₇	R'	0.427	0.773	0.971	1.227	1.505	1.556
		α	0.509	0.931	1.164	1.462	1.796	1.857
		$\Delta\Delta G$	1.057	1.089	1.098	1.105	1.116	1.118
D 	50°C, C ₇	R'	0.450	0.480	0.470	0.460	0.460	0.460
		α	0.102	0.326	0.320	0.338	0.485	0.527
		$\Delta\Delta G$	0.165	0.434	0.469	0.500	0.719	0.765
E 	50°C, C ₇	R'	1.058	1.082	1.113	1.122	1.158	1.158
		α	1310	770	1030	1060	1060	1010
		$\Delta\Delta G$	0.187	0.382	0.513	0.551	0.790	0.804
F 	75°C, C ₈	R'	1.037	1.058	1.066	1.070	1.088	1.087
		α	560	510	480	480	490	480
		$\Delta\Delta G$	-0.002	0.041	0.007	0.001	0.003	0.030
G 	75°C, C ₈	R'	0.056	0.125	0.113	0.115	0.162	0.193
		α	1.058	1.080	1.105	1.113	1.159	1.159
		$\Delta\Delta G$	-	-	-	-	-	-
H 	75°C, C ₈	R'	0.542	0.843	1.005	1.048	1.530	1.685
		α	0.764	1.172	1.422	1.492	2.202	2.383
		$\Delta\Delta G$	1.144	1.178	1.208	1.217	1.266	1.260
I 	100°C, C ₉	R'	1000	950	1010	1020	1050	1000
		α	0.167	0.265	0.319	0.323	0.445	0.484
		$\Delta\Delta G$	0.236	0.353	0.433	0.442	0.588	0.636
K 	115°C, C ₉	R'	1.059	1.069	1.087	1.090	1.099	1.102
		α	1010	830	890	910	810	790
		$\Delta\Delta G$	0.199	0.410	0.502	0.531	0.784	0.826
L 	115°C, C ₉	R'	0.290	0.560	0.689	0.734	1.083	1.137
		α	1.077	1.106	1.124	1.113	1.168	1.171
		$\Delta\Delta G$	1180	970	980	1010	1000	990
M 	115°C, C ₉	R'	0.763	1.061	1.381	1.510	2.211	2.261
		α	0.851	1.185	1.551	1.702	2.484	2.539
		$\Delta\Delta G$	1.050	1.060	1.071	1.077	1.085	1.085
N 	115°C, C ₉	R'	350	360	370	390	380	380
		α	0.091	0.081	0.141	0.152	0.204	0.166
		$\Delta\Delta G$	0.132	0.138	0.219	0.239	0.328	0.291
O 	115°C, C ₉	R'	1.038	1.053	1.069	1.075	1.103	1.107
		α	1220	1720	1430	1450	1530	1810
		$\Delta\Delta G$	0.219	0.292	0.362	0.392	0.506	0.506
P 	115°C, C ₉	R'	1.053	1.063	1.081	1.085	1.102	1.105
		α	840	790	860	850	860	880
		$\Delta\Delta G$	840	790	860	850	860	880

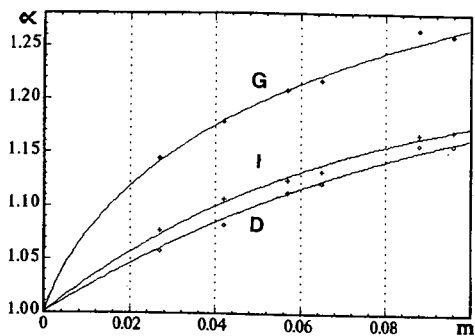


Fig. 4. Measured α vs. molality m_A curves for solutes G, I and D (data from Table II).

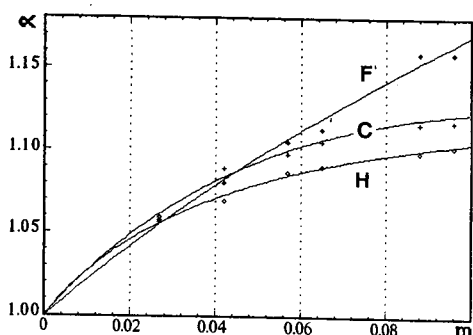


Fig. 5. Measured α vs. molality m_A curves for solutes F, C and H (data from Table II).

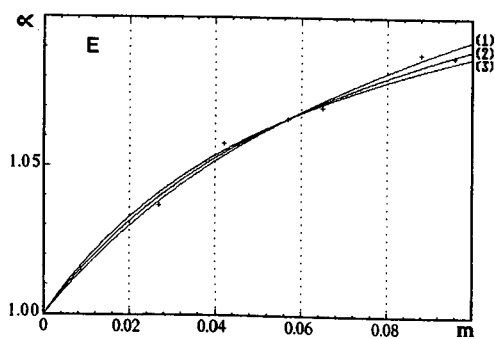


Fig. 6. Comparison of measured α values and calculated α vs. m_A curves for the typical solute E from Table II. The calculations are based on the R' values for $m_A^0 = 0.057$: (1) measured R' values; (2) and (3) measured R' values correlated for the retention increase R'_0 of the standard according to eqn. 17, assuming (2) $R'_0 = 0.1$ and (3) $R'_0 = 0.2$ for $m_A^0 = 0.057$.

A practical aspect of these investigations is that for most solutes (except those with very small R' values) it is not useful to increase the cyclodextrin molality m_A above 0.1. The retention increase R' and analysis time would also increase without much improvement in α .

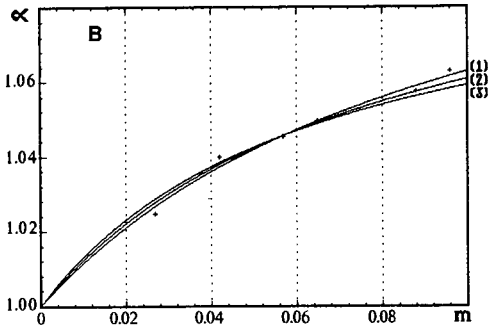


Fig. 7. Comparison of measured α values and calculated α vs. m_A curves for the typical solute B from Table II. The calculations are based on the R' values for $m_A^0 = 0.057$: (1) measured R' values; (2) and (3) measured R' values corrected for the retention increase R'_0 of the standard according to eqn. 17, assuming (2) $R'_0 = 0.1$ and (3) $R'_0 = 0.2$ for $m_A^0 = 0.057$.

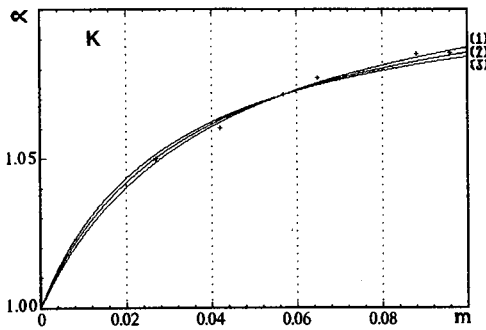


Fig. 8. Comparison of measured α values and calculated α vs. m_A curves for the typical solute K from Table II. The calculations are based on the R' values for $m_A^0 = 0.057$: (1) measured R' values; (2) and (3) measured R' values corrected for the retention increase R'_0 of the standard according to eqn. 17, assuming (2) $R'_0 = 0.1$ and (3) $R'_0 = 0.2$ for $m_A^0 = 0.057$.

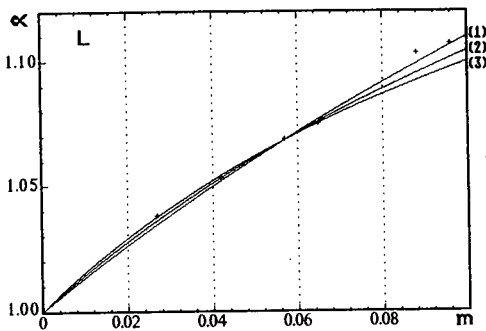


Fig. 9. Comparison of measured α values and calculated α vs. m_A curves for the typical solute L from Table II. The calculations are based on the R' values for $m_A^0 = 0.057$: (1) measured R' values; (2) and (3) measured R' values corrected for the retention increase R'_0 of the standard according to eqn. 17, assuming (2) $R'_0 = 0.1$ and (3) $R'_0 = 0.2$ for $m_A^0 = 0.057$.

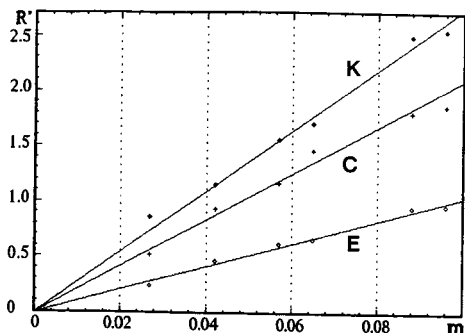


Fig. 10. Measured retention increase R'_R vs. cyclodextrin molality m_A curves for solutes K, C and E from Table II.

Retention increase R'

Some R'_R vs. m curves (data from Table II) are shown in Figs. 10 and 11. The slight deviation from the expected straight lines (*cf.*, eqn. 7 and the footnote with eqn. 7a) can be explained by the systematic error caused by the finite retention increase R'_0 of the standard itself (*cf.*, eqn. 17; note that also R'_0 itself depends on m_A ; the deviation is more obvious for weakly complexing solutes, *e.g.*, solute H in Fig. 11).

The R' values rarely exceed 1.5 (the same was found for 3-perfluoroacylated 2,6-dimethyl- β -cyclodextrins), whereas in complexation GLC [17–19] often values around or above 20 are observed. This demonstrates how weak the solute–cyclodextrin interactions are (*cf.*, racemate F) and that the contribution of these interactions to the total retention time (*cf.*, eqn. 6) is not dominant.

Measurements of R' values on heptakis(3-heptafluorobutanoyl-2,6-dimethyl)- β -cyclodextrin in OV-1701 [14] indicate that in case of failure of enantiomer separation the R' values are relatively small or intermediate and equal for both enantiomers.

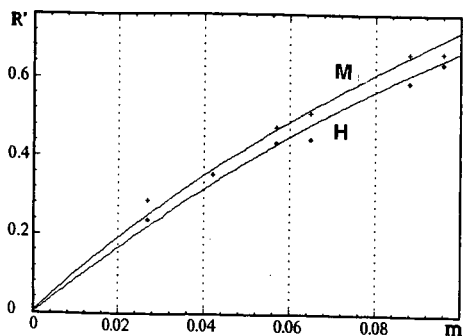


Fig. 11. Measured retention increase R'_R vs. cyclodextrin molality m_A curves for solutes M and H from Table II.

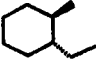
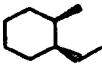

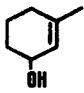
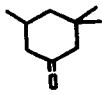
Thermodynamic data: $\Delta\Delta G$, $\Delta\Delta H$ and $\Delta\Delta S$

For some racemates, $\Delta\Delta H$ and $\Delta\Delta S$ were determined in addition to $\Delta\Delta G$ by temperature-dependent studies according to eqn. 16, still using four different *n*-alkanes as reference standards. The results are listed in Table III and shown in Figs. 12–17. It should be noted that, because of the reference standard problem described above, the figures are affected by a systematic error restricting the interpretation of the observed enantioselectivities to a qualitative manner. However, they clearly show that a temperature-dependent reversal of the elution order due to an isoenantioselective temperature ($T_{\text{iso}} = \Delta\Delta H/\Delta\Delta S$) [16,17] will not be observed within the temperature range of the experiment. By extrapolation of the straight lines in Figs. 12–17, T_{iso} was calculated to be above 450°C, and in the case of the racemate C (*cis*-pinane) it was even found to be outside the range of positive absolute temperatures. Ln α vs. $1/T$ plots for several racemates on heptakis(3-trifluoroacetyl-2,6-dimethyl)- β -cyclodextrin indicate that lower isoenantioselective temperatures are also possible (e.g., for 1-phenyl-2,6-dimethyloxirane at 150°C, for isomenthol at 180°C and for a series of γ -penta- to γ -decalactones at 210–230°C), the temperatures being still too high to be verified experimentally. These results are in contrast to complexation GLC, where isoenantioselective temperatures between 15 and 100°C have often been observed [17–19].

There is no direct relationship between $\Delta\Delta G$ on the one hand and favourable values of the chiral separation factor α or the peak resolution on the other. According to eqns. 12 and 15, a certain $\Delta\Delta G$ value can result either from a large α and small R' values or *vice versa*.

TABLE III

GIBBS–HELMHOLTZ PARAMETERS CALCULATED BY LINEAR REGRESSION ACCORDING TO EQN. 16 FOR THE STRAIGHT LINES OF VAN 'T HOFF PLOTS IN FIGS. 12–17

Solute	Cyclodextrin molality, m_A	Standard	$\Delta\Delta H$ (J/mol) ^a	$\Delta\Delta S$ (J/K · mol) ^b
A 	0.065	C ₇	-390	-0.11
	0.057	C ₇	-420	-0.15
	0.042	C ₇	-410	-0.11
B 	0.065	C ₇	-330	-0.13
		C ₈	-380	-0.22
		C ₉	-420	-0.29
C 	0.065	C ₁₀	-410	-0.20
		C ₇	-320	0.44
		C ₈	-350	0.39
		C ₉	-360	0.40
G 	0.065	C ₁₀	-330	0.55
		C ₈	-4570	-10.22
		C ₉	-4530	-10.05
		C ₁₀	-4560	-10.09
H 	0.065	C ₁₁	-4650	-10.26
		C ₈	-3350	-7.22
		C ₉	-3150	-6.51
		C ₁₀	-3100	-6.22
		C ₁₁	-3180	-6.20

^a ±40.

^b ±0.3.

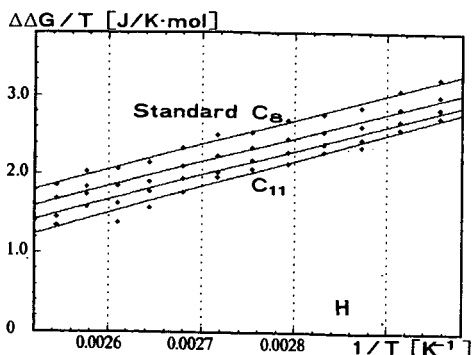


Fig. 12. Van 't Hoff plots for solute H (*cf.*, Tables II and III) (calculations of $\Delta\Delta G$ with respect to four different *n*-alkanes as reference standards), obtained on OV-1701 containing 0.065 *m* permethylated β -cyclodextrin.

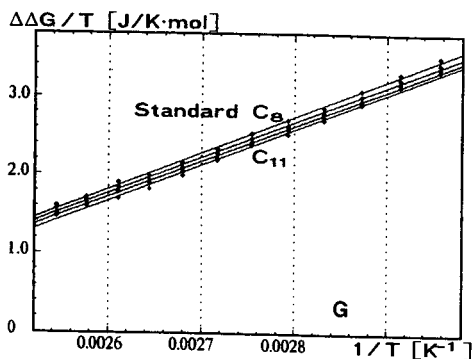


Fig. 13. Van 't Hoff plots for solute G (*cf.*, Tables II and III) (calculations of $\Delta\Delta G$ with respect to four different *n*-alkanes as reference standards), obtained on OV-1701 containing 0.065 *m* permethylated β -cyclodextrin.

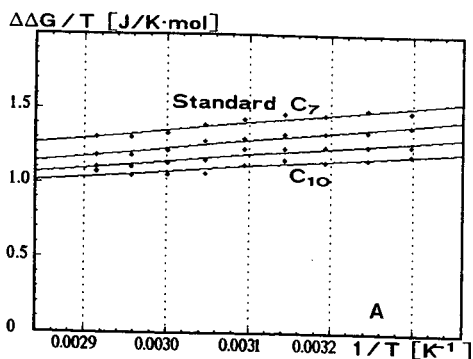


Fig. 14. Van 't Hoff plots for solute A (*cf.*, Tables II and III) (calculations of $\Delta\Delta G$ with respect to four different *n*-alkanes as reference standards), obtained on OV-1701 containing 0.065 *m* permethylated β -cyclodextrin.

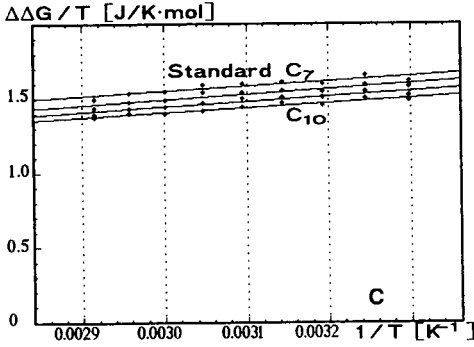


Fig. 15. Van 't Hoff plots for solute C (*cf.*, Tables II and III) (calculations of $\Delta\Delta G$ with respect to four different *n*-alkanes as reference standards), obtained on OV-1701 containing 0.065 *m* permethylated β -cyclodextrin.

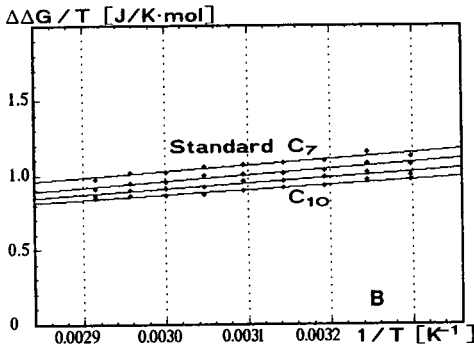


Fig. 16. Van 't Hoff plots for solute B (*cf.*, Tables II and III) (calculations of $\Delta\Delta G$ with respect to four different *n*-alkanes as reference standards), obtained on OV-1701 containing 0.065 *m* permethylated β -cyclodextrin.

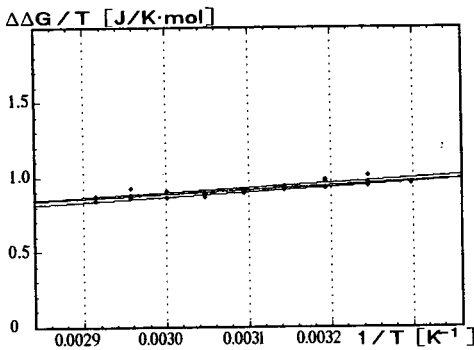


Fig. 17. Van 't Hoff plots for solute B, obtained on OV-1701 containing different molalities (0.042, 0.057 or 0.065 *m*) of permethylated β -cyclodextrin (standard: C_7). $\Delta\Delta G$ does not depend on the cyclodextrin molality m_A .

In contrast to α , $\Delta\Delta G$ is independent of the cyclodextrin molality m_A (*cf.*, Fig. 17 and eqn. 15).

Further observations

Changing the polysiloxane solvent might result in different K_L^0 (or K) and thus in different α values (owing to polarity or solvation effects). However, the replacement of OV-1701 with PS-086, a polysiloxane solvent of similar polarity, did not affect α or R' appreciably. Also, the replacement of all methyl protons with deuterium in permethylated β -cyclodextrin did not have a significant effect on the values of α , R' or $\Delta\Delta G$.

CONCLUSION

It could be shown that the theoretical treatment of enantioselectivity advanced in complexation GLC can also be applied to dissolved cyclodextrin stationary phases. However, there is no totally inert reference standard available for the determination of relative retention data, and therefore a small systematic error is introduced into the calculation of the retention increase R' . Yet, the good agreement of calculated and measured α vs. molality m_A curves supports the validity of our approach. The slight deviation from the expected linearity of the R' vs. m_A relationship is due to the systematic error mentioned above. The molecular association between the racemates and the cyclodextrin derivative is relatively weak, which results in small values of R' . Hence its contribution to the total retention time is not dominant. In contrast to complexation GLC, temperature-dependent reversals of the elution order (isoelectroselective temperatures) were extrapolated to occur only at temperatures too high to be measured or to be non-existent.

REFERENCES

- 1 E. Gil-Av and J. Herling, *J. Phys. Chem.*, 66 (1962) 1208.
- 2 M. A. Muhs and F. T. Weiss, *J. Am. Chem. Soc.*, 84 (1962) 4697.
- 3 J. H. Purnell, in A. B. Littlewood (Editor), *Gas Chromatography 1966*, Institute of Petroleum, London, 1967, p. 3.
- 4 V. Schurig, R. C. Chang, A. Zlatkis and B. Feibush, *J. Chromatogr.*, 99 (1974) 147.
- 5 V. Schurig and W. Bürkle, *J. Am. Chem. Soc.*, 104 (1982) 7573.
- 6 V. Schurig, *Inorg. Chem.*, 25 (1986) 945.
- 7 V. Schurig, W. Bürkle, K. Hintzer and R. Weber, *J. Chromatogr.*, 475 (1989) 23.
- 8 V. Schurig and H.-P. Nowotny, *J. Chromatogr.*, 441 (1988) 155.
- 9 H.-P. Nowotny, D. Schmalzing, D. Wistuba and V. Schurig, *J. High Resolut. Chromatogr.*, 12 (1989) 383.
- 10 V. Schurig, H.-P. Nowotny and D. Schmalzing, *Angew. Chem.*, 101 (1989) 785.
- 11 W. A. König, S. Lutz, P. Mischnick-Lübbecke, B. Brassat and G. Wenz, *J. Chromatogr.*, 447 (1988) 193.
- 12 V. Schurig, *Angew. Chem. Int. Ed. Engl.*, 29 (1990) 939.
- 13 D. W. Armstrong, W. Li, C.-D. Chang and J. Pitha, *Anal. Chem.*, 62 (1990) 914.
- 14 V. Schurig and M. Jung, in D. Stevenson and I. D. Wilson (Editors), *Proceedings of the International Meeting on Chromatography, University of Surrey, Guildford, September 12-15, 1989*, Plenum Press, New York, in press.
- 15 D. W. Armstrong, W. Li and J. Pitha, *Anal. Chem.*, 62 (1990) 217.
- 16 K. Watabe, R. Charles and E. Gil-Av, *Angew. Chem., Int. Ed. Engl.*, 28 (1989) 192.
- 17 V. Schurig, J. Ossig and R. Link, *Angew. Chem., Int. Ed. Engl.*, 28 (1989) 194.
- 18 R. Link, *Doctoral Thesis*, University of Tübingen, Tübingen, 1987.
- 19 H. Laderer, *Doctoral Thesis*, University of Tübingen, Tübingen, 1990.

CHROMSYMP. 2103

New aspects of quantitative structure–retention relationships in chromatography

N. DIMOV*

Chemical Pharmaceutical Institute, 1156 Sofia (Bulgaria)

and

M. MOSKOVKINA

High Pedagogical Institute, 9700 Shumen (Bulgaria)

ABSTRACT

The usual task of quantitative structure–retention relationships (QSRR) in chromatography is to predict retentions, whereas in spectroscopy the resulting spectra are used for structure elucidation. It is shown that if an equation with a good correlation is found, QSRR can also be used for a similar purpose, with consideration of exceptions from the rule. Equations for the dependence of the retention in gas, high-performance liquid and thin-layer chromatography on molecular mass and selected structural fragments of eighteen benzodiazepines are proposed. Any deviation from the rule is connected with a given influence of a neighbour on the corresponding structural fragment atoms. A new quantity given to fragment evaluation is used for considering the intramolecular group influences.

INTRODUCTION

One of the challenges in quantitative structure–property relationship (QSPR) investigations is to predict the properties of a substance when the structure is known. There is also another possibility, namely to predict the structure from the properties. To use system and solute properties for precalculation of retention is the usual task of quantitative structure–retention relationships (QSRR) in chromatography, whereas in the spectroscopy the resulting spectra are used for structure elucidation. In this paper we show that QSRR can be also used for a similar purpose. We assume that the chromatographic retention on a given stationary phase is influenced both by extensive (molecular mass, number of atoms, etc.) and intensive (structural features) solute properties. Such a differentiation is similar to that in spectroscopy. The absorption band in IR spectroscopy, for example, of a ketone C=O group is at about 1720 cm^{-1} . This value is due to the vibration of the bond between two atoms with corresponding mass (extensive property). This band moves down to 1670 cm^{-1} or up to 1820 cm^{-1} depending on the neighbouring atoms and/or functional groups. Hence a band anywhere between 1670 to 1820 cm^{-1} could be connected with the presence of a C=O group. Its exact location serves for structural elucidation. If a valid rule (equation) about the dependence of chromatographic retention on some general properties of

a series of compounds can be defined, any deviation from this rule can also be connected with a given influence of corresponding functional groups and, as a next step, the influence of neighbouring atoms on the functional group in question. Therefore, if QSRR is exact enough it can serve for reliable considerations on the structure of compounds the retention of which differs from the rule.

The present status of QSRR studies shows the following problems in modelling: (i) lack of reproducibility of the experimental retention data for substances of interest, (ii) correct representation of the corresponding substance structure and (iii) adequate mathematical data handling.

Analytical results in biological, pharmacological, clinical studies, etc., show poor reproducibility. This situation, does not apply, however, with chromatographic determinations. Modern experimental methods based on high-resolution gas (GC), high-performance liquid (HPLC) and thin-layer chromatography (TLC) give very repeatable results for retention, which can be used in QSRR investigations. There are also a great variety of topological, geometric, quantum chemical, etc., indices [1,2], which make the second problem also less difficult. Mathematical data handling on a purely theoretical base is not yet possible. There are however, many empirical and semi-empirical equations [3–30] connecting the retention with the solute properties. The accuracy achieved can be considered satisfactory for identification purposes in limited cases only, *e.g.*, with one chromatographic technique used for similar compounds. No general mathematical approach for the adequate solution of the third problem in all chromatographic modes is available.

We advocate the use of a linear model, given elsewhere [30], for retention data handling. This model has been used for the derivation of equations describing chromatographic retention in different modes. It has been already applied with success for hydrocarbons and halogenated hydrocarbons [31–33]. These compounds however, cannot be analysed by TLC or HPLC and therefore it is not possible to compare the significant parameters and their estimates in different chromatographic modes. This study deals with the retention data of eighteen benzodiazepines, obtained in adsorption (thin-layer and liquid) and partition (gas and liquid) chromatographic modes.

THEORY

It is well known that the general physico-chemical equation connecting the absolute retention with the enthalpy of solution, ΔH_s , and the entropy of solution, ΔS_s , is

$$RT \ln V_g = \Delta H_s - T\Delta S_s \quad (1)$$

where V_g is the specific retention volume, T is the absolute temperature and R is a constant. Rearranging eqn. 1 to

$$RT \ln r_{1,2} = \Delta(\Delta H_s)_{1,2} - T\Delta(\Delta S_s)_{1,2} \quad (2)$$

where $r_{1,2}$ is the relative retention of solutes 1 and 2, it can be seen that the relative retention depends on the relative changes in ΔH_s and ΔS_s . If the solute molecules differ

significantly in their ΔH_s values (*e.g.*, homologous neighbours separated by GC on a non-polar stationary phase), their retention is governed mostly by $\Delta(\Delta H_s)_{1,2}$. When the difference in $\Delta(\Delta H_s)_{1,2}$ is negligible (*e.g.*, closely related structures and equal molecular masses), then the retention still depends on ΔH_s , but separation can be achieved if the stationary phase provides a greater difference in the solution entropy (*e.g.*, use of liquid crystals). The experimentally obtained numerical values show that $\Delta(\Delta S_s)_{1,2}$ usually plays a modifying role for retention [34,35].

Different solution theories based on quantum-chemical calculations lead to a general equation analogous in its form and meaning [36]:

$$\Delta E = \varepsilon_1 + \Sigma \varepsilon_r \quad (3)$$

where ΔE is the change in the system energy after non-destructive interactions (*e.g.*, solutions), ε_1 is the magnitude of dispersive forces and ε_r are different other forces. Again there is a basic contributor ε_1 and modifying contributors $\Sigma \varepsilon_r$.

We have tested the validity of analogous equations reported in a series of papers [30–33,37–42] and we have proposed a biparametric model based on the additivity principle as a general model for QSRR studies in GC [30]:

$$R = b_0 + \sum_{i=1}^n b_i B_i + \sum_{j=n+1}^{n+k} b_j T_j \quad (4)$$

where R represents the corresponding retention (usually the retention index in GC and R_F in TLC or the capacity factor (k') in HPLC in this work. B_i are basic and T_j are tuning contributors to retention. The constants $b_0 - b_j$ are regressor (parameter) estimates. It was accepted [30] that the B term in eqn. 4 includes solute properties, allowing the calculation of a value for $R_{\text{calc.}}$, which does not differ from $R_{\text{exp.}}$ by more than ± 10 –15%. Every solute property answering the above demands and even linear or non-linear [28,29,43] equations including the corresponding property can be used as the B term.

The T term includes also solute properties, which can correlate insignificantly with retention and do not correlate with the properties included in the B term. They have to possess a high discrimination power and be able to approximate the roughly calculated $R_{\text{calc.}}$ to the value of $R_{\text{exp.}}$.

RESULTS AND DISCUSSION

The retention data used in this investigation were taken from the literature [44,45]. The molecular mass, Mm , is a general solute property that can be used in all of the studied chromatographic modes and it was tested as a B contributor. The molecular fragments (see Fig. 1) C=O, -OH, -F, -NO₂, N-R₂ and flat rings (phenyl and cyclopropane) were tested as T contributors. We assumed that the presence of a given fragment is counted as 1 and its absence as 0. The parameter -F for halazepam was taken to be 3, because there are three -F atoms (see Fig. 1). The parameter C=O for camazepam was taken as 2 for a similar reason, assuming no difference in their retention contributions. Correspondingly, prazepam has three flat rings, whereas tetrazepam has only one.

TABLE I

RETENTION DATA (R_F FOR TLC, k' FOR HPLC AND RETENTION INDEX I FOR GC) FOR 15 BENZODIAZEPINES, THEIR MOLECULAR MASS (Mm) AND PARAMETRIC VALUES

No.	Compound	R_F^a	R_F^b	k^c	k' (RP) ^d	I^e	Mm^f	C=R ₃ (N-CO)	R ₄ (-OH)	R _{2,5} (-F)	R ₁ (-NO ₂)	Flat ring	N=R ₂
1	Medazepam	40	74	3.66	—	2272	270	0	0	0	0	2	1
2	Przepam	36	74	1.49	—	2652	324	1	0	0	0	3	1
3	Tetrazepam	34	76	2.03	21.44	2437	288	1	0	0	0	1	1
4	Pinazepam	31	79	1.32	10.96	2529	308	1	0	0	0	2	1
5	Flurazepam	30	48	6.10	—	2771	387	1	0	1	0	2	1
6	Halazepam	18	76	1.05	16.46	2292	352	1	0	3	0	2	1
7	Camazepam	13	79	0.08	13.61	2930	371	2	0	0	0	2	1
8	Nimetazepam	12	77	1.12	3.62	2662	295	1	0	0	1	2	1
9	Flunitrazepam	10	72	0.34	3.1	2600	313	1	0	1	1	2	1
10	Temazepam	8	59	0.42	5.76	2589	300	1	1	0	0	2	1
11	Lormetazepam	6	67	0.10	6.39	2674	334	1	1	0	0	2	1
12	Nordazepam	4	55	1.36	8	2493	270	1	0	0	0	2	0
13	Lorazepam	1	36	0.11	4.6	2423	320	1	1	0	0	2	0
14	Nitrazepam	0	36	0.99	3	2720	281	1	0	0	1	2	0
15	Oxazepam	0	40	0.47	4.62	2350	286	1	1	0	0	2	0

Mm	0.5	0.1	0.5	0.2	0.4
N-CO		0	0	0	0
-OH			0.2	0.3	0.3
-F				0	0.2
-NO ₂					0.1
Flat ring					0

Intercorrelation coefficients

^a $R_F \times 100$ on silica gel 60 F₂₅₄ with cyclohexane-toluene-diethylamine (75:15:10) [44,45] (basic mobile phase).

^b $R_F \times 100$ on silica gel 60 F₂₅₄ with chloroform-methanol (90:10) [44,45] (neutral mobile phase).

^c k' on Spherisorb SSW with 100 μ l of perchloric acid in 1000 cm³ of methanol [44] (adsorption HPLC).

^d RP: ODS-Hypersil, methanol-water-0.1 M phosphate buffer (55:25:20) [44] (reversed-phase HPLC).

^e I on DB1 (SE-30) wide-bore capillary column (modern GC) at 250°C [44].

^f Mm is taken in all calculations as $Mm \times 10^{-2}$.

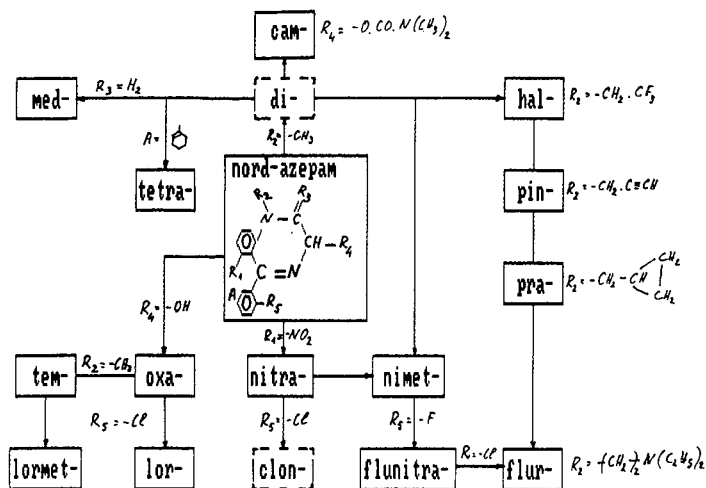


Fig. 1. Molecular fragments tested.

The corresponding retention data, the values of the molecular mass (*Mm*) and the values of selected parameters (fragments) are summarized in Table I.

The intercorrelation between the selected parameters was calculated and was found to be negligible (Table I). Therefore, we correlated first the retention with all seven selected factors in all chromatographic modes. Because of the high probability of chance correlations [46] we checked the validity of the parametric estimates in two ways: applying the leave-one test and reducing the number of factors with the requirement that the variances remain statistically equal. Surprisingly, the parametric estimates remain with a constant sign and within a limited range of values. The maximum and minimum quantities obtained in the leave-one test are given in Table II. For comparison of both full and reduced equations, see eqns. 5–9a.

The studies show that in GC just the parameter molecular mass satisfies the requirements of the *B* term in eqn. 4. In TLC such a parameter is the N–R₂ group. In the other chromatographic modes neither parameter as a basic contributor covers the experimental retention value by more than 85%. Nevertheless, there is always a leading contributor. Taking into account the negligible intercorrelation between the parameters (see Table I) and both the leave-one test and reducing parameters, we consider the sign and quantity of the estimate of a given parameter to represent a real quantitative evaluation of its influence on retention under the given chromatographic conditions.

The two types of equations can be given as follows for the various chromatographic modes:
for GC:

$$I = 1219 + 353.6Mm + 150.4(N-CO) - 50(-OH) - 143(-F) + 183(-NO_2) + 29(\text{flat}) + 43(N-R_2) \tag{5}$$

$$I = 992 + 502.7Mm - 161.2(-F) + 232.7(-NO_2) \tag{5a}$$

TABLE II

MAXIMUM AND MINIMUM VALUES (ACCORDING TO THE LEAVE-ONE TEST) OF PARAMETER ESTIMATES b_1 - b_7 IN ALL CHROMATOGRAPHIC MODES

Mode	b_1 (Mm)	b_2 (N-CO)	b_3 (-OH)	b_4 (-F)	b_5 (-NO ₂)	b_6 (flat ring)	b_7 (N-R ₂)
GC	324	176	-54	-117	171	32	13
	360	119	-67	-154	226	81	38
RP-HPLC	1.9	2.9	-4	-1.3	-6.1	-10	0.6
	3.1	1.6	-6	1.3	-8	-11.8	1.2
HPLC (SiO ₂)	4	-4	-1.3	-0.5	-0.9	1	-1.0
	5	-5	-2	0.7	0.4	1	-1.6
TLC (neutral)	-29	18	-8	-4	-14	-0.2	10
	-33	20	-11	4.5	-9	4	35
TLC (basic)	6	-16	-16	-4	-14	-0.2	10
	9	-19	-19	-5	-15	0.3	13

with statistically equal variances;
for reversed-phase HPLC:

$$k' = 1.25 + 2.26Mm + 1.54(N-CO) - 4.90(-OH) + 1.41(-F) - 7.32(-NO_2) - 11(\text{flat}) + 0.88(N-R_2) \quad (6)$$

$$k' = -6.53 + 5.777Mm - 6.03(-OH) - 7.35(-NO_2) - 11.33(\text{flat}) \quad (6a)$$

with statistically equal variances;
for adsorption-mode HPLC:

$$k' = -7.6 + 4.74Mm - 4.22(N-CO) - 2.12(-OH) + 0.57(-F) - 0.82(-NO_2) + 1.15(\text{flat}) - 1.06(N-R_2) \quad (7)$$

$$k' = -3.43 + 2.65Mm - 3.13(N-CO) - 1.38(-OH) \quad (7a)$$

with statistically equal variances;
for TLC with chloroform-methanol (neutral phase):

$$R_F = 110.3 - 31Mm + 18.1(N-CO) - 8.4(-OH) + 3.59(-F) - 8.4(-NO_2) + 4.57(\text{flat}) + 34.5(N-R_2) \quad (8)$$

$$R_F = 46.21 - 8.91(-OH) + 26.41(N-R_2) \quad (8a)$$

with statistically equal variances.
for TLC with diethylamine as modifier (basic phase):

$$R_F = 10.4 - 7.53Mm - 17.3(\text{N-CO}) - 18.6(-\text{OH}) - 4.7(-\text{F}) \\ - 14.6(-\text{NO}_2) - 0.3(\text{flat}) + 13.1(\text{N-R}_2) \quad (9)$$

$$R_F = 27 - 13.5(\text{N-CO}) - 16.7(-\text{OH}) - 15.5(-\text{NO}_2) + 14(\text{N-R}_2) \quad (9a)$$

with statistically equal variances.

If the parametric estimations from eqns. 5-9a are compared with the corresponding values in Table II, several conclusions can be drawn:

(1) The values of regressor (parametric) estimates coincide with quantity and sign in most instances, which confirms the lack of chance correlation.

(2) The greater difference between the estimates of Mm in Table II or eqn. 5 and in eqn. 5a for GC can be explained if the assumption regarding the additivity of the contributions of the different parameters is correct: the sum of estimates of Mm and N-CO- from Table II (353.6 + 150.4) is equal to the estimate of Mm in eqn. 5 (502.7). Hence the N-CO- group does not make a specific individual contribution to the retention and its estimation is incorporated in the Mm parameter estimate of eqn. 5.

The role of Mm in TLC with a neutral mobile phase (eqn. 8) is also clear: the greater the molecular mass, the greater is the retention and the lower the R_F value. This well known qualitative observation is now quantified.

(3) According to eqn. 8a (neutral mobile phase), the retention depends mostly on the N-R₂ fragment, whereas Table II and eqn. 8 give two significant parameters: N-CO and Mm . If the additivity of the parameter contributions is again valid, then the sum of the estimates b_1 , b_2 and b_7 (Table II or eqn. 8) should be equal to the estimate of the N-R₂ parameter in eqn. 8a, which is indeed the case.

(4) The case described by eqns. 8, 8a and 13 shows that if the azepine N atom is substituted (the parameter N-R₂ = 1), the solute is retained more weakly than the pattern nordazepam (Tables I and III). The only drastic exception when the reduced equation 8a is used is flurazepam (Table III). However, its structure (Fig. 1) contains an additional N atom is observed in its -R₂ substituent, and it can be assumed that this N atom compensates for the decrease in retention due to the substitution of the azepine N atom. It is known that the interaction between a basic N atom and a silica surface with neutral mobile phases is of the greatest importance for the retention, and this was quantified in this study.

(5) Considering the case described by eqn. 9 (basic mobile phase), the influence of N-R₂, as can be expected, decreases, the influence of the other fragments also becomes significant and the discrimination is better.

(6) The hydroxyl group is an important parameter in all chromatographic modes. An -OH group in the solute molecule increases the retention in chromatographic modes with liquid mobile phases, because of silanophilic interactions. Again, a behaviour known in chromatographic practice was quantified. The insignificant role of the -OH group in the GC of benzodiazepines is probably due to the high temperature of analysis.

(7) Considering the influence of the -NO₂ group, we observed that its presence increases the molecular polarity and its GC and TLC retentions increase. The retention in reversed-phase HPLC decreases, probably because of a decrease in the solubility of the solute in the non-polar C₁₈ stationary phase.

TABLE III

COMPARISON OF EXPERIMENTAL AND CALCULATED R_F VALUES ACCORDING TO EQNS. 8a AND 13

No.	Compound	R_F		
		Exp.	Calc. (eqn. 8a)	Calc. (eqn. 13)
1	Medazepam	74	73	76
2	Prazepam	74	73	76
3	Tetraepam	76	73	76
4	Pinazepam	79	73	76
5	Flurazepam	48	73	48
6	Halazepam	76	73	76
7	Camazepam	79	73	76
8	Nimetazepam	77	73	76
9	Flunitrazepam	72	73	76
10	Temazepam	59	64	60
11	Lormetazepam	67	64	65
12	Nordazepam	55	46	54
13	Lorazepam	36	37	36
14	Nitrazepam	36	46	35
15	Oxazepam	40	37	41

Taking into account that in GC and reversed-phase HPLC the retention is mostly due to solubilization, whereas in adsorption-mode HPLC and TLC both solubilization and adsorption take place, some more general conclusions may be drawn. Solubilization is a bulk process, in which a solute molecule interacts with the whole surface, whereas in the adsorption mode only a few atoms can interact with the stationary phase surface. The results show that probably the influence of solubilization in the mobile phase predominates over adsorption in adsorption HPLC. This can explain why the molecular mass and the $-\text{NO}_2$ and $-\text{OH}$ groups act in the observed manner. In TLC probably adsorption on the surface predominates and the retention is mostly due to the presence of an active fragment, in this instance $\text{N}-\text{R}_2$. The decrease in k' in HPLC modes could be explained on a similar basis: the solubility in the mobile phase predominates over adsorption on the silica surface.

Eqns. 5a-9a can serve for considering the influence of different parameters (fragments) on the retention, and also for the selection of compounds for which the calculated retention differs from the rule. The differences obtained between $R_{\text{exp.}}$ and $R_{\text{calc.}}$ may be connected with unequal contributions of equal chromatophores, owing to specific structural features (*e.g.*, intramolecular interactions such as $\text{H} \cdots \text{O}$ bonding or shielding). In other words, the contribution of the fragments, called chromatophores, might be tuned by the influence of specific neighbouring atoms, groups or other structural peculiarities. This tuning effect cannot be evaluated in advance but if, in the cases of greater discrepancies between $R_{\text{calc.}}$ and $R_{\text{exp.}}$, we exchange the arbitrary value of 1.0 given to the fragments in question, we can decrease this discrepancy. The new fragment evaluation is accepted as a quantification of this

influence. In other words, we expect to evaluate the difference between equal functional groups due to different adjacent atoms. A new series of equations can now be formulated, allowing a better description of the retention of the studied compounds in the interpolation region.

The evaluations of N-CO- and -OH fragments in GC have to be corrected:

$$I = 1116.7 + 429.67Mm + 123.4(\text{CO-N})^{\text{cor.}} - 77.9(-\text{OH})^{\text{cor.}} - 151.2(-\text{F}) + 164.8(-\text{NO}_2) \quad (10)$$

with almost the same parametric estimates as in Table II, eqn. 10 has a higher correlation coefficient, $r = 0.993$, maximum discrepancy, $\Delta_{\text{max}} = 40$ i.u., and only two incorrect arrangements, those of the peaks of temazepam and lormetazepam.

The new equation for reversed phase HPLC is

$$k' = -8.98 + 6.544Mm - 5.45(-\text{OH})^{\text{cor.}} - 8.28(-\text{NO}_2)^{\text{cor.}} - 11.58(\text{flat}) \quad (11)$$

again with the same values and signs as in Table II, but with higher $r = 0.987$, $\Delta_{\text{max}} = 2.4$ and only two incorrect arrangements, halazepam and lorazepam.

For adsorption-mode HPLC, the new equation is

$$k' = -0.927 + 1.949Mm - 2.77(\text{CO-N})^{\text{cor.}} - 1.34(-\text{OH})^{\text{cor.}} + 0.62(\text{flat}) - 0.65(\text{N-R}_2)^{\text{cor.}} \quad (12)$$

with $r = 0.999$, $\Delta_{\text{max}} = 0.3$ and only one incorrect arranged compound (nordazepam).

For TLC with a neutral mobile phase, we have

$$R_F = 35.66 - 10.4(-\text{OH})^{\text{cor.}} + 40.2(\text{N-R}_2)^{\text{cor.}} \quad (13)$$

with $r = 0.99$, $\Delta_{\text{max}} = 3.8$ and a 100% correct arrangement of the R_F values of the spots.

For TLC with a basic mobile phase, the equation becomes

$$R_F = 28.28 - 13.49(\text{CO-N})^{\text{cor.}} - 14.85(-\text{OH}) - 14.49(-\text{NO}_2) + 11.73(\text{N-R}_2)^{\text{cor.}} \quad (14)$$

with $r = 0.998$, $\Delta_{\text{max}} = 1.6$ and a 100% correct arrangement of the R_F values of the spots.

The superscript cor. means that the value for the presence of a given fragment differs from 1. For example, in reversed-phase HPLC the presence of an -OH group in the compounds lorazepam and lorazepam is evaluated as 1.2 units instead of 1.0, in order to minimize the discrepancy between $k'_{\text{exp.}}$ and $k'_{\text{calc.}}$. We assume that this change in fragment evaluation is necessary in order to compensate for the influence of the -Cl atom in the adjacent phenyl ring. In adsorption-mode HPLC the necessary change is even greater, 1.7 units instead of 1. Similar corrections are necessary in TLC with a

neutral mobile phase; the presence of an -OH group in temazepam and lormetazepam has a greater influence on the retention than in lorazepam and oxazepam.

The fragment evaluations are found on a chemical logic basis. They are not constants; their values depend rather on the kind of chromatographic conditions used. They are meaningful only for the interpolation region. They could be used, however, for considering the intramolecular group influences on intermolecular interactions, and we see in this a new aspect of QSRR application.

The kind of substituent -R₂ in the N-R₂ group is also very important, and this has already been shown in TLC with a neutral mobile phase.

The results presented illustrate that comparable equations for all the studied chromatographic modes describing quantitatively the corresponding chromatographic retentions can be created on a single model. There are fragments selected from the solute molecule which are responsible for the retention in chromatography and these can be called chromatophores. Their contributions are additive, but in some instances the fragment evaluations differ from 1.0, depending on the neighbouring atoms. Therefore, after obtaining preliminary results, the fragment evaluation can be tuned so that more accurate interpolation equations can be obtained (eqns. 10-14). The evaluations from both the first and second groups of equations allow quantitative considerations of the contributions of different solute fragments, while the difference of a given fragment evaluation from 1.0 could be used for considering intramolecular interactions. The equations could also be used for formulating preliminary assumptions about the retention mechanism in particular chromatographic techniques.

REFERENCES

- 1 D. Bonchev, *Information Theoretic Indices for Characterization of Chemical Structures*, Research Studies Press, Chichester, 1983.
- 2 R. Kaliszan, *CRC Crit. Rev. Anal. Chem.*, 16 (1986) 323.
- 3 H. Tenney, *Anal. Chem.*, 30 (1958) 2.
- 4 V. G. Berezkin, *Neftekhimiya*, 1 (1961) 169.
- 5 G. Schomburg, *J. Chromatogr.*, 14 (1964) 157.
- 6 J. Bonastre and P. Grenier, *Bull. Soc. Chim. Fr.*, (1967) 1395.
- 7 K. Altenburg, in H. Struppe (Editor), *Gas Chromatographie 1968*, Akademie Verlag, Berlin, 1968, p. 1.
- 8 N. Dimov and D. Shopov, *J. Chromatogr.*, 44 (1969) 170.
- 9 J. Takacs, C. Szita and G. Tarjan, *J. Chromatogr.*, 56 (1971) 1.
- 10 P. Weiner and D. Howery, *Can. J. Chem.*, 50 (1972) 448.
- 11 M. Chastrette and G. Lenfant, *J. Chromatogr.*, 77 (1973) 255.
- 12 M. Chastrette and G. Lenfant, *J. Chromatogr.*, 84 (1973) 275.
- 13 J. Dubois and J. Chretien, *J. Chromatogr. Sci.*, 12 (1974) 811.
- 14 A. N. Korol, *Chromatographia*, 8 (1975) 385.
- 15 A. N. Korol, *Chromatographia*, 8 (1975) 811.
- 16 A. N. Korol, *J. Chromatogr.*, 126 (1976) 171.
- 17 M. Randić, *J. Chromatogr.*, 161 (1978) 1.
- 18 A. N. Korol and L. Lysyuk, *Theor. Eksp. Khim.*, 16 (1980) 792.
- 19 F. Calixto and A. Raso, *Chromatographia*, 14 (1981) 596.
- 20 F. Calixto and A. Raso, *Chromatographia*, 15 (1982) 521.
- 21 F. Calixto and A. Raso, *J. Chromatogr.*, 322 (1985) 35.
- 22 L. Buydens and D. Massart, *Anal. Chem.*, 53 (1981) 1990.
- 23 L. Buydens and D. Massart, *Anal. Chem.*, 55 (1983) 738.
- 24 P. Buryan and J. Macak, *J. Chromatogr.*, 237 (1982) 381.
- 25 H. Lamparczyk, *Chromatographia*, 16 (1983) 664.

- 26 J. Bermejo and M. Guillen, *J. High Resolut. Chromatogr. Chromatogr. Commun.*, 7 (1984) 191.
- 27 J. Premecz and M. Ford, *J. Chromatogr.*, 388 (1987) 23.
- 28 K. Heberger, *Chromatographia*, 25 (1988) 725.
- 29 K. Heberger, *Anal. Chim. Acta*, in press.
- 30 N. Dimov, *Anal. Chim. Acta*, 201 (1987) 217.
- 31 N. Dimov and Ov. Mekenyan, *Anal. Chim. Acta*, 212 (1988) 317.
- 32 N. Dimov and R. Milina, *J. Chromatogr.*, 463 (1989) 159.
- 33 N. Dimov and Ov. Mekenyan, *J. Chromatogr.*, 471 (1989) 227.
- 34 H. Poppe, *Chromatographia*, 14 (1981) 89.
- 35 T. Sugiyama, *J. Chromatogr.*, 295 (1984) 387.
- 36 B. Pullman (Editor), *Intermolecular Interactions: from Diatomic to Biomolecules*, Wiley, Chichester, 1978.
- 37 N. Dimov, *J. Chromatogr.*, 119 (1976) 109.
- 38 N. Dimov and D. Papazova, *Chromatographia*, 12 (1979) 443.
- 39 N. Dimov and S. Boneva, *J. Chromatogr.*, 206 (1981) 549.
- 40 N. Dimov and S. Boneva, *Chromatographia*, 22 (1986) 271.
- 41 D. Papazova, R. Milina and N. Dimov, *Chromatographia*, 25 (1988) 177.
- 42 N. Dimov, Ov. Mekenyan and Iv. Bangov, *Pharmazie*, 44 (1989) 771.
- 43 R. Golovnja and O. Grigoreva, *Zh. Anal. Khim.*, 40 (1985) 316.
- 44 M. Japp, K. Garthwaite, A. Geeson and M. Osselton, *J. Chromatogr.*, 439 (1988) 317.
- 45 A. H. Stead, R. Gill, T. Wright, J. P. Gibbs and A. C. Moffat, *Analyst (London)*, 107 (1982) 1106.
- 46 J. G. Topliss and R. P. Edwards, *J. Med. Chem.*, 22 (1979) 1238.

Comparison of various isotherm models for predicting competitive adsorption data

JIE ZHU

Department of Chemistry, University of Tennessee, Knoxville, TN 37996-1600 (U.S.A.)

A. M. KATTI^a

Department of Chemical Engineering, University of Tennessee, Knoxville, TN 37996-1600 (U.S.A.)
and

GEORGES GUIOCHON*

Department of Chemistry, University of Tennessee, Knoxville, TN 37996-1600 and Division of Analytical Chemistry, Oak Ridge National Laboratory, Oak Ridge, TN (U.S.A.)

ABSTRACT

Competitive adsorption isotherms were determined for 2-phenylethanol and 3-phenylpropanol on ODS-silica with methanol-water as the mobile phase. The experimental data were fitted to the Langmuir competitive isotherm, the second-order ideal adsorbed solution isotherm of LeVan and Vermeulen, the seven-parameter quadratic isotherm (ratio of two second-degree polynomials) and the competitive Fowler isotherm. The best results were obtained by adjusting the five parameters of the competitive Fowler isotherm by a non-linear regression. Unfortunately, this isotherm gives the mobile phase concentration as a function of the surface coverage and the equation cannot be inverted in closed form.

INTRODUCTION

Determination of competitive equilibrium isotherms is important in theoretical and experimental studies in order to evaluate the separation process. The isotherm is the fundamental thermodynamic property which has to be measured in order to permit the accurate prediction of the individual band profiles in non-linear chromatography [1]. Once the adsorption data have been obtained, however, they are put in a functional form by fitting to a model for use in the calculation of individual component profiles [2,3].

For single-component systems, several dynamic methods have been developed to measure adsorption isotherms accurately while avoiding the use of batch techniques, which are time consuming and require the use of large amounts of chemicals. The methods of elution by characteristic point (ECP) and frontal analysis (FA) are the most popular. ECP is based on using the rear boundary of a non-linear elution profile to measure the isotherm [1,4]. The main disadvantage of this

^a Present address: Ciba Geigy, CH-4002 Basle, Switzerland.

method is that the experimental profile recorded deviates from the ideal profile because of the band broadening due to the finite efficiency of real columns. Thus an error is made in the calculation of the amount adsorbed. This deviation causes an error in the measured isotherm. However, with the modern, high-efficiency columns used in high-performance liquid chromatography (HPLC), this error remains acceptable. Another drawback is that separate detector calibration is required.

On the other hand, FA is based on making a series of step changes in the concentration of the mobile phase at the column inlet and writing an integral mass balance [5,6]. Compared with ECP, FA has the advantages that it does not require detector calibration and that the nature of the front (which is self-sharpening) makes the measurement independent of the column efficiency, as long as this efficiency exceeds about 100 theoretical plates. FA has the inconvenience of requiring a much larger amount of product than ECP. It has been shown that for high-efficiency columns ECP and FA give the same experimental isotherm [7].

Other methods have been proposed for the measurement of single-component isotherms, based on recording high-concentration band profiles and calculating the best-fit parameters to a known isotherm model [8–10]. Lastly, there are methods in which the isotherm is determined by the retention time of a small sample pulse injected on a concentration plateau [11].

For the measurement of binary and multi-component isotherms, several of these chromatographic methods can be applied. Frontal analysis has been extended and employed in the determination of two component competitive isotherms [12–14]. Step and pulse techniques have been suggested, using labelled compounds [11,15]. They are impractical for most organic compounds, for which labelled molecules are difficult and expensive to synthesize. Recently, a method based on analyzing the individual band profiles for a series of large-volume rectangular injections of binary mixtures has been proposed [16].

In the analysis of single-component isotherm data, several models can be used which accurately fit experimental isotherm data and provide a convenient means of obtaining an accurate prediction of the band profiles [17–19]. The Langmuir isotherm is the most common. The bi-Langmuir, Freundlich and Fowler isotherms [20,21] have also been used.

For the binary and multi-component cases, the competitive Langmuir isotherm model is often used, owing to its simplicity. However, this model, which does not satisfy the Gibbs–Duhem equation, lacks thermodynamic rigor. Further, the use of the Langmuir single-component parameters in the competitive model does not give an accurate prediction of overloaded elution profiles [16,22] and does not account well for the experimental competitive adsorption data [23]. A thermodynamically consistent competitive isotherm has been derived by LeVan and Vermeulen [24], who used the ideal adsorption solution (IAS) theory and introduced into the Langmuir equation an additional term accounting for the difference in column saturation capacities of the two components.

The Fowler isotherm can also be extended to binary mixtures and take into account the competitive behavior of the two components [20]. Statistical thermodynamic models have shown that the competitive isotherm should be the ratio of two polynomials of the same degree [25,26]. The Langmuir isotherm is the ratio of two first-degree polynomials. A better result is predicted with the use of the ratio of two

second-degree polynomials. Finally, a binary isotherm model based on ion-exchange formalism has been proposed by Velayudhan and Horváth [27]. None of these models has been used yet to account for competitive adsorption data and to calculate individual band profiles in non-linear chromatography.

In this paper, experimental adsorption data determined by two-component frontal analysis [12,14] are reported and a comparison is made between four of the competitive isotherm models listed above, the competitive Langmuir model, the quadratic isotherm model, the LeVan and Vermeulen IAS model and the competitive Fowler isotherm.

THEORY

The classical equations of two-component frontal analysis [12,13,18] were used to derive the amount of the component adsorbed at equilibrium from the breakthrough curves recorded as the column response to step changes in the concentration.

Four isotherm models have been used to account for the measured experimental data. The simplest model is the competitive Langmuir isotherm model [28]:

$$q_1 = \frac{a_1 C_1}{1 + b_1 C_1 + b_2 C_2} \quad (1)$$

$$q_2 = \frac{a_2 C_2}{1 + b_1 C_1 + b_2 C_2} \quad (2)$$

where q_1 and C_i are the concentrations of the i th component at equilibrium in the stationary and the mobile phase, respectively, and a_i and b_i are numerical coefficients, characteristic of the components and of the chromatographic system. The column saturation capacity is $q_{i,s} = V_{sp} a_i / b_i$, where V_{sp} is the volume of stationary phase contained in the column.

The Langmuir model has been corrected for its thermodynamic inconsistency by LeVan and Vermeulen [24], using the IAS theory. The first-order approximation of their equation is the Langmuir isotherm if the column saturation capacity is the same for the two components. If the column saturation capacity is different for the two components, the LeVan and Vermeulen isotherm is represented by a series which converges very rapidly and can be limited in most practical cases to its first two terms. The second-order approximation of their isotherm can be written as

$$q_1 = \frac{a_1 C_1 + a_2 C_2 b_1 C_1}{b_1 C_1 + b_2 C_2} + \left(\frac{a_1}{b_1} - \frac{a_2}{b_2} \right) \frac{b_1 b_2 C_1 C_2}{(b_1 C_1 + b_2 C_2)^2} \ln(1 + b_1 C_1 + b_2 C_2) \quad (3)$$

$$q_2 = \frac{a_1 C_1 + a_2 C_2 b_2 C_2}{b_1 C_1 + b_2 C_2} + \left(\frac{a_2}{b_2} - \frac{a_1}{b_1} \right) \frac{b_1 b_2 C_1 C_2}{(b_1 C_1 + b_2 C_2)^2} \ln(1 + b_1 C_1 + b_2 C_2) \quad (4)$$

Eqns. 1 and 2 (or 3 and 4) must be valid for any combination of mobile phase

concentrations of the two components (C_1, C_2). Obviously, they must also be valid when one of these concentrations is zero. Thus, eqn. 1 (or 3) gives the Langmuir single-component isotherm for the first component when $C_2 = 0$. The coefficients a_i and b_i in eqns. 1–4 are the coefficients of the single-component Langmuir isotherms.

The third isotherm we used is the quadratic isotherm, suggested by statistical thermodynamics and for which different derivations have been discussed [23,25]:

$$q_1 = \frac{a_1 C_1 + a_{12} C_1 C_2}{1 + b_1 C_1 + b_2 C_2 + b_{12} C_1 C_2} \quad (5)$$

$$q_2 = \frac{a_2 C_2 + a_{21} C_1 C_2}{1 + b_1 C_1 + b_2 C_2 + b_{21} C_1 C_2} \quad (6)$$

where $b_{12} = b_{21}$. In eqns. 5 and 6, the coefficients a_i and b_i are the same as in the single-component isotherm of the i th component. The coefficients a_{ij} and b_{ij} have to be determined for the binary mixture.

The last isotherm we used is the competitive Fowler isotherm [20]:

$$\frac{1}{C_1} \cdot \frac{\theta_1}{1 - (\theta_1 + \theta_2)} = b_0 e^{-\chi_1(\theta_1 + \theta_2)} \quad (7)$$

$$\frac{1}{C_2} \cdot \frac{\theta_2}{1 - (\theta_1 + \theta_2)} = b_0 e^{-\chi_2(\theta_1 + \theta_2)} \quad (8)$$

where θ_i is the ratio $q_i/q_{s,i}$ of the stationary phase concentration of the i th component to its column saturation capacity and χ_i is a numerical coefficient. For a binary mixture, this isotherm has five parameters ($q_{s,1}, q_{s,2}, \chi_1, \chi_2$ and b_0).

Each isotherm model was tested (i) by using the single-component parameters of the corresponding model (Langmuir or Fowler) in a mixing model and by adjusting the other parameters, when needed (*i.e.*, with the quadratic isotherm model) using a non-linear least-squares fitting method and (ii) by empirically fitting the corresponding equations to the isotherm data and determining the best values of the parameters, using a non-linear least-squares fitting method.

The non-linear least-squares fit was accomplished using the SAS library and the SYSNLIN procedure, so that the parameters calculated give the least error for both components. Success with this method depends considerably on the choice of a suitable initial solution. We have found that searching empirically for an acceptable set of solutions using “what if” calculations carried out with the 123 spreadsheet (Lotus Development, Cambridge, MA, U.S.A.) and its graphics module permits the rapid selection of a satisfactory initial solution for the SAS program.

The absolute error between the data points and the best parameter isotherm given by each model was calculated by

$$E_i = \sum_{j=1}^n (q_{\text{exp},j} - q_{t,j})^2 \quad (9)$$

where i is the component number and j stands for the rank of the data point. This error was calculated for each model and the results were compared.

EXPERIMENTAL

Equipment

Frontal analysis was performed by pumping the mobile phase with a Gilson (Middleton, WI, U.S.A.) Model 302 pump through a ten-port Valco (Houston, TX, U.S.A.) pneumatically actuated valve fitted with two 2-ml sample loops, a column and a detector. The column was immersed in a Haake (Saddlebrook, NJ, U.S.A.) water-bath. Step changes in the solute concentration were made by switching the Valco valve after filling the proper loop with a solution of the sample in the mobile phase at the required concentration. The effluent composition was monitored by a Spectroflow 757 variable-wavelength UV detector (Applied Biosystems, Ramsey, NJ, U.S.A.) at 272 nm. The effluent was sampled using a four-port electrically actuated Valco valve with an internal 2- μ l loop.

The quantitative composition at each plateau was determined by an on-line HPLC unit consisting of a Beckman (Berkeley, CA, U.S.A.) Model 110B pump, the Valco four-port valve, a YMC (Morris Plains, NJ, U.S.A.) cartridge column and a Spectroflow Model 757 UV detector set at 254 nm. Both UV analog signals were digitized through a Gilson Model 621 system interface box and monitored using the 714 controller software on an IBM (Armonk, NY, U.S.A.) Model 50Z PS/2 computer.

Columns and chemicals

The adsorption column was packed in-house at 7000 p.s.i. with 10- μ m Spherical ODS-silica from Vydac (Hesperia, CA, U.S.A.) in a 250 \times 2.1 mm I.D. column. A 3- μ m YMS 5 \times 0.46 cm I.D. cartridge column was used for on-line analysis.

2-Phenylethanol and 3-phenylpropanol were purchased from Fluka (Ronkonkoma, NY, U.S.A.). Methanol and water were purchased from Burdick and Jackson (Muskegon, MI, U.S.A.). All these products were used without further purification. The mobile phase was methanol-water (50:50). Concentrations are reported in mg/ml; a concentration of 1 mg/ml is 8.2 mM for 2-phenylethanol and 7.4 mM for 3-phenylpropanol.

Procedures

Step changes in the solute concentrations were made in the mobile phase stream at the column inlet. The composition of the column effluent was monitored. Fig. 1 illustrates two typical frontal steps from which the amount adsorbed was calculated. The trace obtained from monitoring the effluents exhibits a primary plateau and a sub-plateau for each step. The concentration of the primary plateaux is known and the composition of the effluent at each sub-plateau was determined by on-line analysis. Samples were taken on-line, at the point where the arrow is drawn, on both the primary plateau and the sub-plateaux.

The chromatograms are shown in the upper part of Fig. 1. Note that the concentration of the 2-phenylethanol, the first component, at each sub-plateau is greater than that at the primary plateau. This is due to the displacement effect of the second component on the first. However, the concentration of 3-phenylpropanol, the second component, at the sub-plateaux is lower than that on the primary plateau.

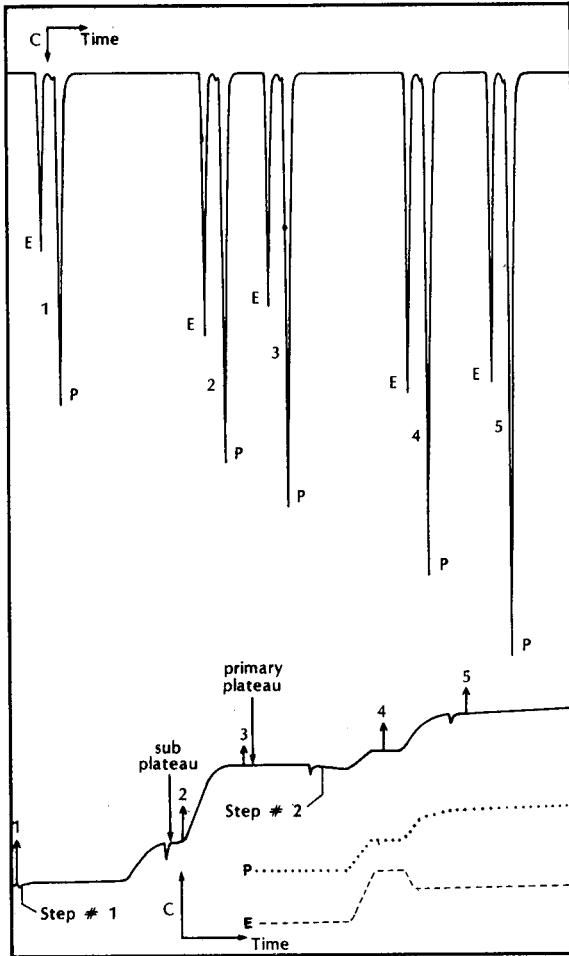


Fig. 1. Frontal profiles and effluent chromatograms. Bottom traces: frontal analysis. Solid line, detector profile in frontal analysis; dotted line, reconstructed profile for 3-phenylpropanol; dashed line, reconstructed profile for 2-phenylethanol. The arrows 1-5 indicate the times when an eluate sample was collected and analyzed. Top trace: analysis of the eluate samples taken during frontal analysis.

RESULTS AND DISCUSSION

The pure component adsorption isotherms of 2-phenylethanol and 3-phenylpropanol were measured as described above. The two series of data are plotted in Fig. 2 (symbols). A non-linear least-squares analysis of these experimental data to the Langmuir Isotherm shows an excellent fit to the pure component data over the whole concentration range (Fig. 2, solid lines).

Competitive isotherm data were obtained under conditions of increasing total sample concentration, but at a constant ratio of the concentrations of the two components. The ratios of the 2-phenylethanol (PE) to 3-phenylpropanol (PP)

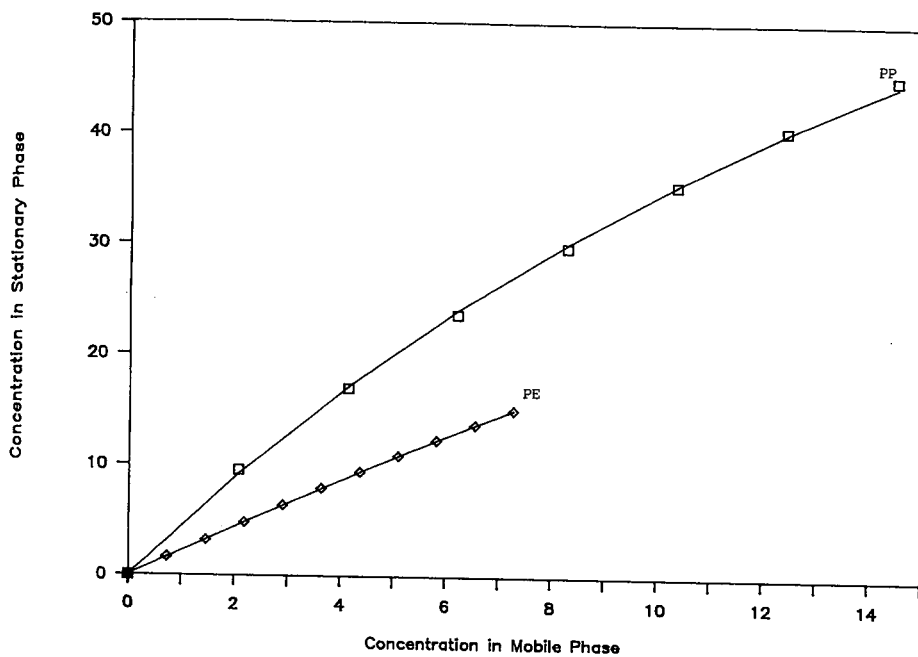


Fig. 2. Experimental single-component data for \diamond = 2-phenylethanol and \square = 3-phenylpropanol, fitted to single-component Langmuir model (solid lines). All concentrations in mg/ml. Experimental conditions: 250×2.1 mm I.D. column packed with $10\text{-}\mu\text{m}$ Vydac ODS-silica; mobile phase, methanol-water (50:50); flow-rate 0.25 ml/min.

TABLE I
SUMMARY OF ISOTHERM PARAMETERS

Isotherm	Parameters		
Competitive Langmuir (single-component)	$a_1 = 2.3$ $b_1 = 0.015$	$a_2 = 4.82$ $b_2 = 0.039$	
Competitive Langmuir (best-fit parameters)	$a_1 = 2.4$ $b_1 = 0.022$	$a_2 = 3.83$ $b_2 = 0.01913$	
Quadratic isotherm (three floating parameters)	$a_1 = 2.30$ $a_{1,2} = 0.030$ $b_1 = 0.015$	$a_2 = 4.82$ $a_{2,1} = -0.20$ $b_2 = 0.039$	$b_{1,2} = 0.0$
Quadratic isotherm (seven floating parameters)	$a_1 = 2.3$ $a_{1,2} = 0.020$ $b_1 = 0.021$	$a_2 = 3.85$ $a_{2,1} = -0.075$ $b_2 = 0.022$	$b_{1,2} = 0.0$
Fowler isotherm (single-component, six parameters)	$q_{s,1} = 154$ $\chi_1 = 0.0048$ $b_1 = 0.0149$	$q_{s,2} = 138$ $\chi_2 = 0.029$ $b_2 = 0.0335$	
Fowler isotherm (single-component, five parameters)	$q_{s,1} = 104$ $\chi_1 = 0.366$ $b_1 = 0.0242$	$q_{s,2} = 187$ $\chi_2 = 0.378$ $b_2 = 0.0242$	
Fowler isotherm (best-fit parameters)	$q_{s,1} = 105$ $\chi_1 = 0.338$	$q_{s,2} = 160$ $\chi_2 = 0.366$	$b = 0.0242$

concentration investigated were 1:1, 1:3 and 3:1. The experimental data are shown as symbols in Figs. 3–10, where they are compared with the predictions of the various isotherms studied (solid lines). In each figure, (a) shows the isotherms of 2-phenylethanol and (b) those of 3-phenylpropanol.

The competitive Langmuir model (eqns. 1 and 2) was used first to account for the competitive adsorption data. The parameters a_1 , a_2 , b_1 and b_2 were obtained by regression to the single-component data (Fig. 2). They are reported in Table I. The comparison between the prediction of this competitive isotherm and the experimental data is shown in Fig. 3. For 2-phenylethanol (Fig. 3a), very good agreement is observed with the experimental data, except for the 1:3 mixture at high concentrations. However, for 3-phenylpropanol (Fig. 3b), strong deviations are observed. The adsorbed amount of 3-phenylpropanol determined experimentally is 20–30% less than that predicted by the competitive Langmuir model.

As the column saturation capacities are not equal for the two components (153 and 124 mg/ml for PE and PP, respectively), the LeVan and Vermeulen model [24] was tried. However, in the region for which data were taken, this model gives results (not shown) that were virtually the same as the competitive Langmuir isotherm. This is explained by the relatively small difference in column saturation capacities between the two components (20%) and the small curvature of the isotherm in the concentration range investigated, although measurements were made in nearly the whole accessible range, which is limited by the solubility of 3-phenylpropanol.

In order to try to improve the isotherm prediction, the competitive Langmuir model was used empirically. The values of the coefficients a_i and b_i in eqns. 1 and 2 that give the least error for the entire set of adsorption data (*i.e.*, the two-single component isotherms and the six mixed isotherms) were determined from a non-linear fit. As summarized in Table I, a_1 does not change, a_2 decreases by 20%, b_1 increases by 50% and b_2 decreases by 50%. Fig. 4a shows that there is hardly any change in the already very good fit for 2-phenylethanol (*cf.*, Fig. 3a), except for a substantial improvement of the fit in the high concentration range of the 1:3 mixture data. On the other hand, Fig. 4b shows a marked improvement in the fit for 3-phenylpropanol. The sum of errors reported in Table II has decreased from 287 to 47 (mg/ml)². Still, the experimental data for the 1:3 and the 1:1 PE–PP mixtures are 8–10% lower than predicted by the model (Fig. 4b). Further, this improvement has been achieved at the cost of a less satisfactory fit of the single-component adsorption data by the competitive isotherm (see Fig. 7, dashed line).

The experimental data were then fitted to the quadratic competitive isotherm, given by eqns. 5 and 6 (Fig. 5). Keeping with the rigor of this isotherm, the coefficients a_1 , a_2 , b_1 and b_2 derived from the single-component adsorption data were used and the coefficients a_{12} , a_{21} and b_{12} were determined by minimizing the error between the experimental and theoretical data. Surprisingly, although this model has seven parameters instead of four, the results are not much better than those of the competitive Langmuir model. For 2-phenylethanol (Fig. 5a) the model predicts nearly the same amount of component adsorbed at equilibrium as the competitive Langmuir isotherm derived from the single-component adsorption data (compare Figs. 3a and 5a) for the 3:1 and the 1:1 mixtures. The results are slightly better for the 1:3 mixture. For 3-phenylpropanol, the results are slightly better for the 1:3 mixture and somewhat better for the 1:1 mixture. The improvement is significant for the 3:1 mixture (compare

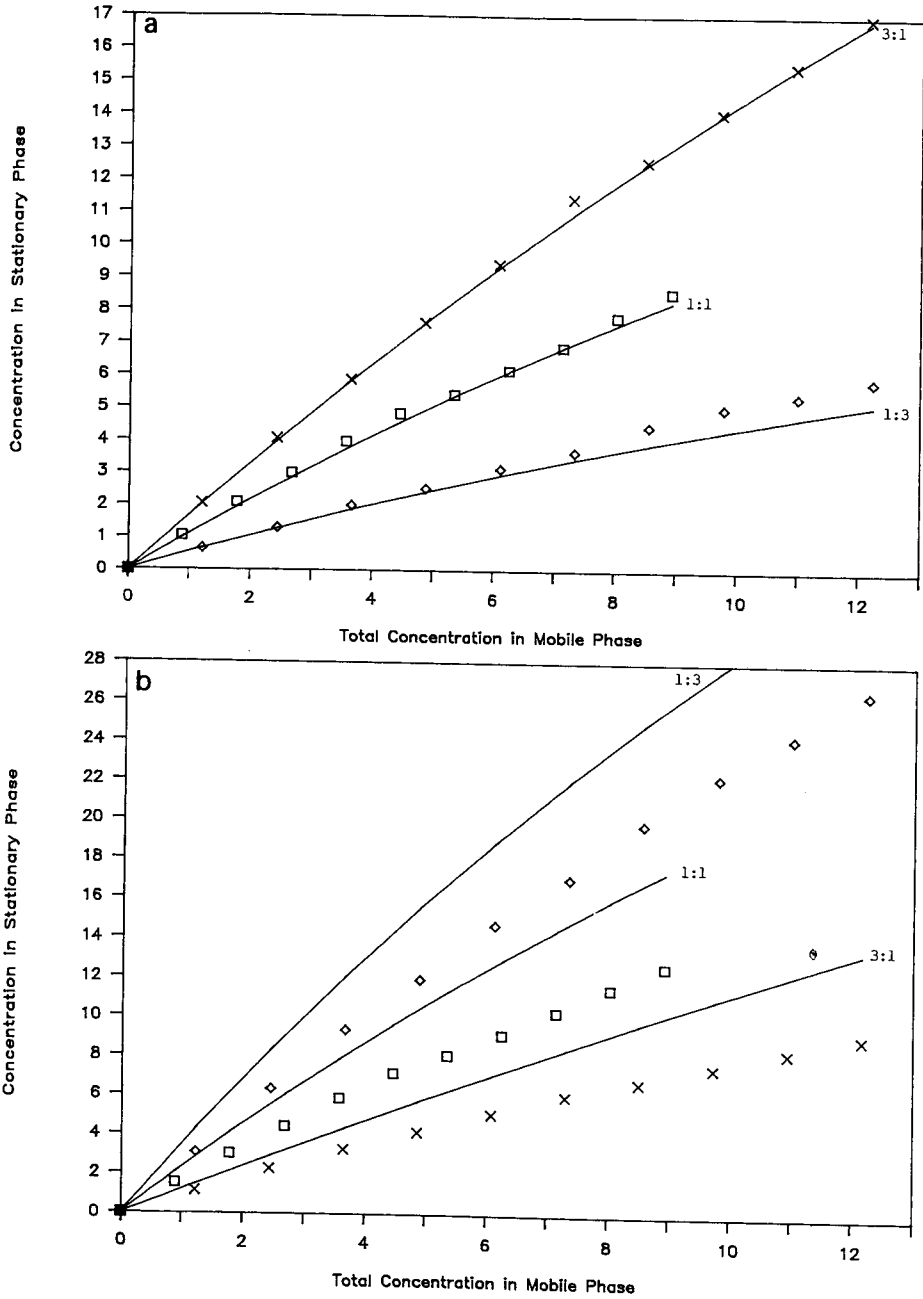


Fig. 3. Comparison of competitive isotherm experimental data and the competitive Langmuir isotherm with single-component parameters. All concentrations in mg/ml. Experimental conditions: see text and Fig. 2. Competitive adsorption data for $\diamond = 1:3$, $\square = 1:1$ and $\times = 3:1$ mixtures. (a) 2-phenylethanol; (b) 3-phenylpropanol.

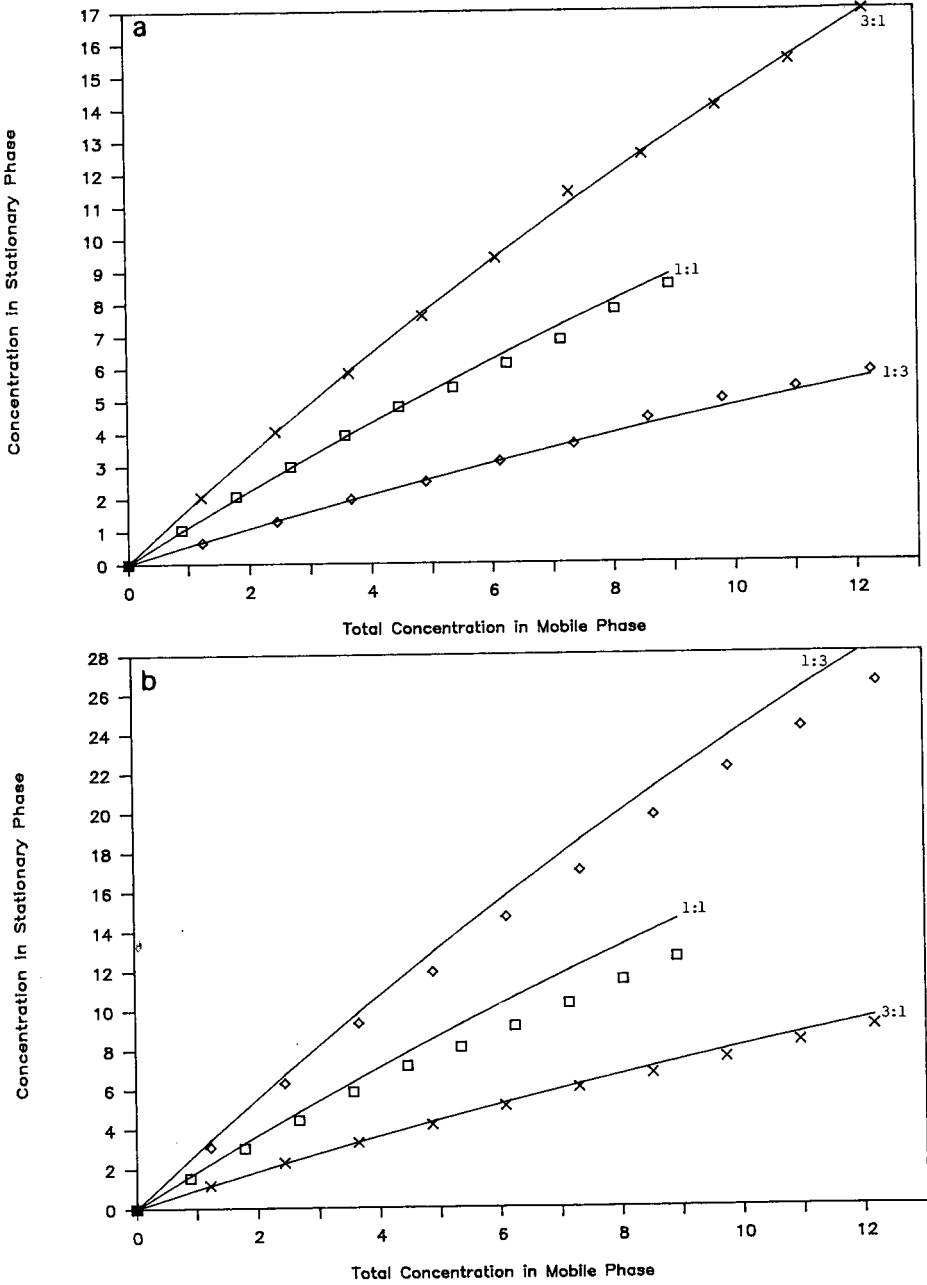


Fig. 4. Comparison of competitive isotherm experimental data and the competitive Langmuir isotherm with the best-fit Parameters. All concentrations in mg/ml. Experimental conditions: see text and Fig. 2. Same experimental data (symbols) as in Fig. 3. (a) 2-phenylethanol, (b) 3-phenylpropanol.

TABLE II
SUMMARY OF ERRORS (mg/ml)²

The error is given as the sum of the squares of the differences between the calculated and the experimental concentrations (eqn. 9). The values in parentheses were derived using only the six competitive isotherms. For the other values, the summation is extended to the two single-component isotherms.

Isotherm	2-Phenylethanol	3-Phenylpropanol
Competitive Langmuir (single-component)	2.4	287
Competitive Langmuir (best-fit parameters)	1.98 (1.78)	47 (16.4)
Quadratic isotherm (three floating parameters)	1.26	75.8
Quadratic isotherm (seven floating parameters)	1.15 (0.93)	56.9 (8.3)
Fowler isotherm (single-component)	0.7 (0.5)	12.9 (12.6)
Fowler isotherm (best-fit parameters)	0.7 (0.56)	34.1 (0.77)

Figs. 3b and 5b). Overall, the fits are better (see Table II) but still not completely satisfactory. As seen in Fig. 4b, the Langmuir isotherm does not account accurately for the decrease in the slope of the 3-phenylpropanol competitive isotherm with increasing 2-phenylethanol concentration. A correction to that slope is supplied by the quadratic isotherm, using a best value of a_{21} which is negative, but the correction is insufficient.

We then used the quadratic isotherm as an empirical model. A non-linear regression was used to calculate the set of coefficients which minimize the sum of the errors (eqn. 9). Fig. 6 gives the best results in terms of the isotherms predicted. The agreement is excellent for 2-phenylethanol, with a slightly better fit than with the Langmuir models (Fig. 6a and Table II). For the 3-phenylpropanol data also the agreement is very good (Fig. 6b), much better than when the data are fitted to the competitive Langmuir isotherm equation (Table II). This situation was to be expected as the new isotherm has seven parameters instead of four.

We compare in Fig. 7 the single-component isotherms predicted by the competitive isotherm eqns. 1, 2 and 5, 6 ($C_1 = 0$ or $C_2 = 0$) with the experimental data with empirically optimized coefficients. The fit with the experimental data is now less good than with the single-component Langmuir isotherms (Fig. 2). The advantage of the competitive Langmuir isotherm and the quadratic isotherm with single-component Langmuir isotherm coefficients is that these isotherms fit very well the experimental data obtained for the single-component equilibrium isotherms. As in all curve-fitting processes, however, we lose some and gain some in fitting the whole set of data on the competitive isotherm equations and optimizing the coefficients. The fit of the competitive equilibrium data is greatly improved at the expense of the fit of the single-component equilibrium data. Nevertheless, the fit of single-component equilibrium data with either the Langmuir competitive isotherm or the quadratic isotherm is still very good for 2-phenylethanol (Fig. 7). For 3-phenylpropanol, the quality of the fit is still acceptable, especially at high concentrations for the Langmuir isotherm. At low

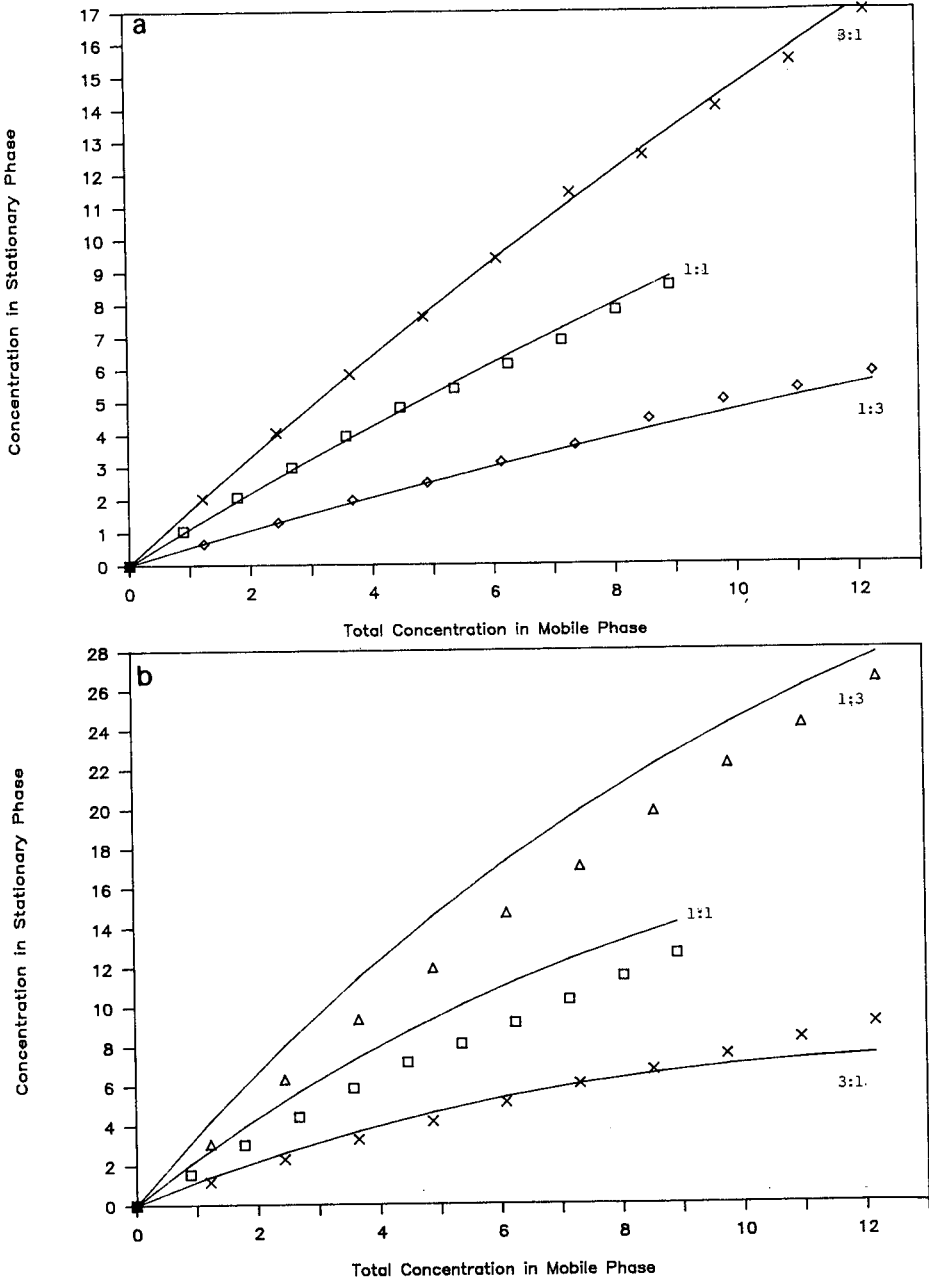


Fig. 5. Comparison of competitive isotherm experimental data and the prediction of the quadratic isotherm with three floating parameters. All concentrations in mg/ml. Experimental conditions: see text and Fig. 2. Same experimental data (symbols) as in Fig. 3. Δ = 1:3 mixture. (a) 2-phenylethanol; (b) 3-phenylpropanol.

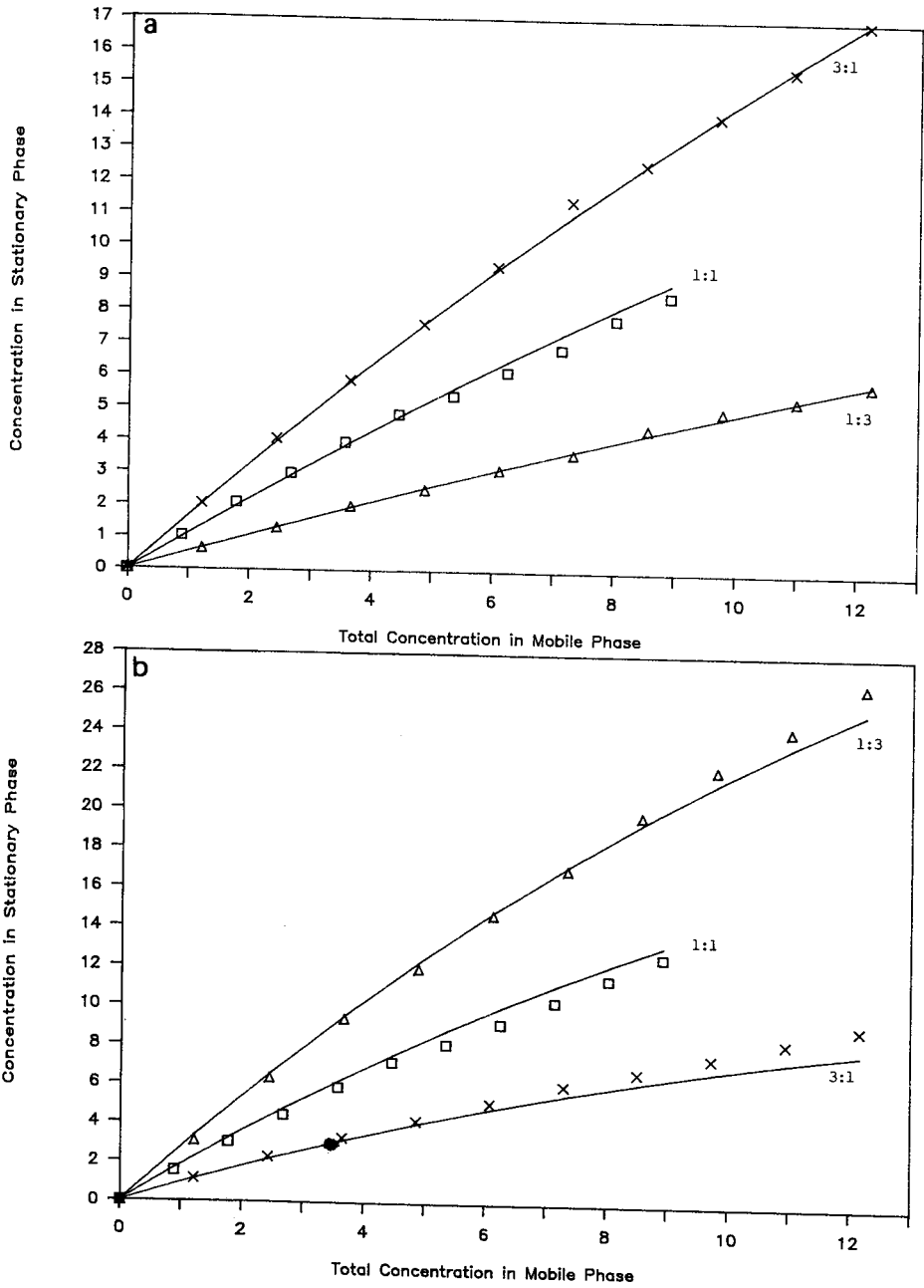


Fig. 6. Comparison of competitive isotherm experimental data and the prediction of the quadratic isotherm with seven floating parameters. All concentrations in mg/ml. Experimental conditions: see text and Fig. 2. Same experimental data (symbols) as in Fig. 3. Δ = 1:3 mixture. (a) 2-phenylethanol; (b) 3-phenylpropanol.

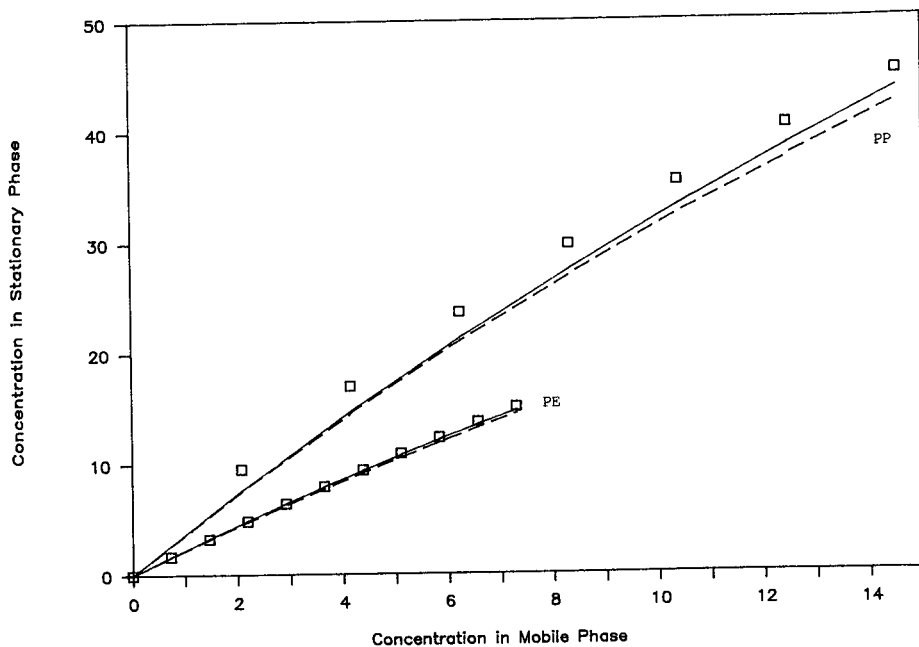


Fig. 7. Comparison of single-component experimental data with the best-fit competitive Langmuir model (solid line) and the quadratic seven floating parameters (dashed line) isotherm. All concentrations in mg/ml. Experimental conditions: see text and Fig. 2. Same experimental data as in Fig. 2.

concentrations for the Langmuir isotherm and over the whole concentration range for the quadratic isotherm, the amount of 3-phenylpropanol adsorbed at equilibrium is significantly higher than that predicted by the "best" isotherm.

Finally, the data were fitted to the Fowler isotherm (eqns. 7 and 8). For single-component isotherms, the agreement is excellent, as good as with the Langmuir isotherm (*cf.*, Figs. 2 and 8). In the case of competitive isotherms, however, the coefficient b must be the same for both components. Therefore, if we want to use the single-component Fowler isotherm parameters in a competitive Fowler isotherm, we must introduce this condition ($b_1 = b_2$) in the fitting calculation of the single-component data. We then obtain different numerical values for the coefficients, but the fit remains very good. Only these latter isotherms are shown in Fig. 8, for the sake of clarity. The two sets of isotherms would be almost impossible to distinguish. In Fig. 8, and in subsequent figures dealing with the competitive equilibrium data, we have plotted the concentration in the mobile phase *versus* that in the stationary phase at equilibrium, following the form of eqns. 7 and 8, and to illustrate the practical drawback of the Fowler isotherm, *i.e.*, the impossibility of inverting its equation in closed form.

In Fig. 9a and b we show the competitive isotherms obtained by introducing in eqns. 7 and 8 the best values of the "single-component" Fowler isotherm coefficients just obtained. The results are satisfactory, as shown by the error reported in Table II. The fit achieved is as good as with the quadratic seven floating parameter or with the

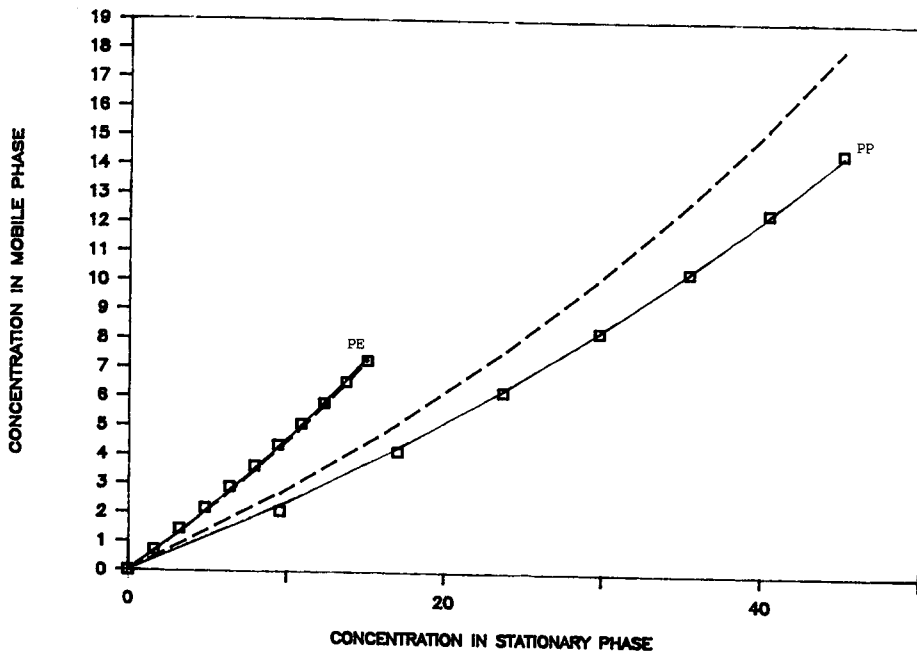


Fig. 8. Comparison of single-component data with five-parameter best-fit single-component Fowler model (solid lines) and best-fit competitive Fowler model (dashed lines). All concentrations in mg/ml. Experimental conditions: see text and Fig. 2. Same experimental data as in Fig. 2.

competitive Langmuir isotherms for 2-phenylethanol. For 3-phenylpropanol, the fit is nearly as good as for 2-phenylethanol, a considerable improvement over the results provided by the other isotherms using single-component isotherm coefficients (*cf.*, Figs. 3b, 5b and 9b).

Last, we show in Fig. 10a and b the competitive isotherms obtained by fitting the experimental data to the competitive Fowler isotherm. The agreement is excellent for both components, except for the high concentration points in the 1:1 mixture data. The single-component isotherm predicted by the competitive Fowler isotherm now obtained (*i.e.*, by making C_1 or C_2 equal to zero in eqn. 7 or 8, respectively, with the numerical coefficients in the last line of Table I) agrees well with experimental data for 2-phenylethanol (Fig. 8, dashed line). For 3-phenylpropanol, substantial disagreement is again observed. The amount adsorbed at equilibrium predicted by this isotherm is about 15% less than measured (Fig. 8).

CONCLUSIONS

The problem of finding a good model to predict the competitive adsorption behavior of the components of a mixture based on the use of single-component data is a major one in multi-component non-linear chromatography. It is important because the individual band profiles in chromatography are very sensitive to small deviations of the isotherms from linear behavior [2], so we need a very good model. The problem is

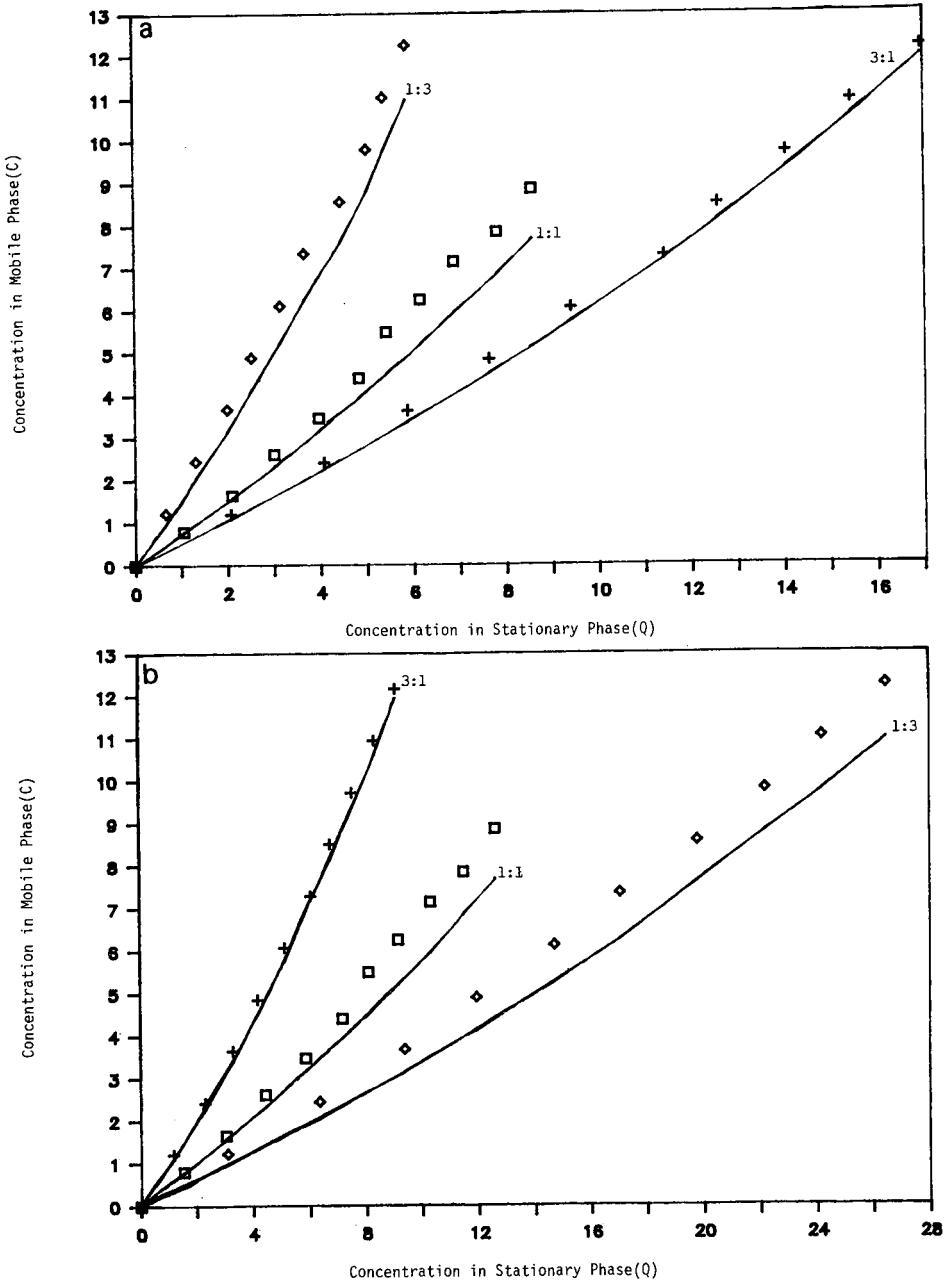


Fig. 9. Comparison of the competitive isotherm experimental data and the prediction of the competitive Fowler isotherm with the single-component parameters (five parameters). All concentrations in mg/ml. Experimental conditions: see text and Fig. 2. Same experimental data as in Fig. 3. (a) 2-phenylethanol; (b) 3-phenylpropanol.

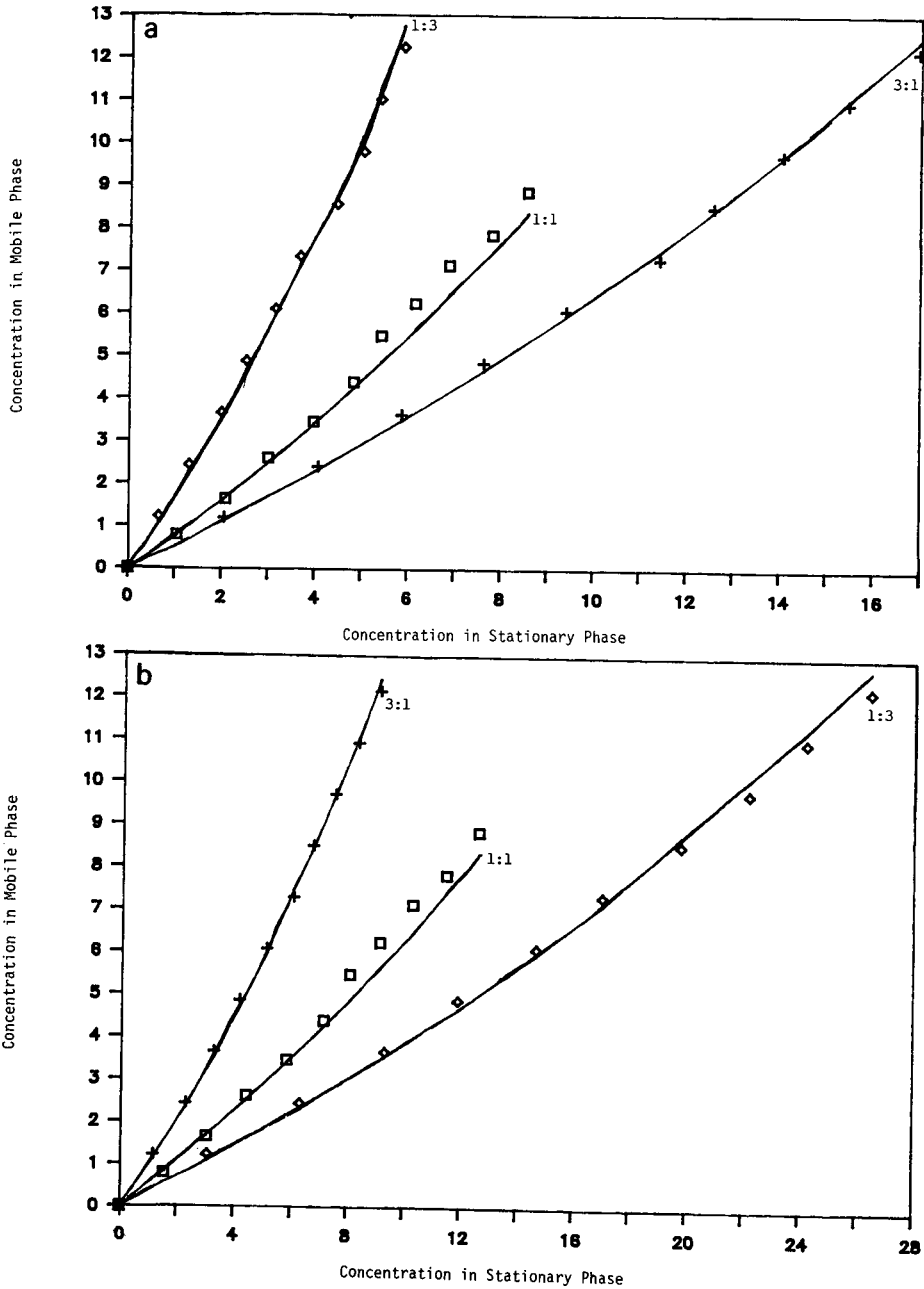


Fig. 10. Comparison of the competitive isotherm experimental data and the prediction of the competitive Fowler isotherm with the best-fit parameters. All concentrations in mg/ml. Experimental conditions: see text and Fig. 2. Same experimental data as in Fig. 3. (a) 2-phenylethanol; (b) 3-phenylpropanol.

important also from the practical point of view, because it is much easier and faster to collect single-component data than competitive adsorption data.

The solution of this problem in a particular case was the main aim of this work and it remains unsolved. None of the isotherms available gives results which are completely satisfactory. The second aim, in case the first could not be achieved, as has happened, was to find an isotherm model which could be fitted to a whole set of experimental data and account for them empirically.

The results presented here and our conclusions are restricted to one specific case. They can reasonably be expected to apply to many pairs of monofunctional homologues in reversed-phase liquid chromatography, but not far beyond. This is but a small fraction of the separation problems encountered in preparative chromatography.

The IAS model, although thermodynamically more sound than the Langmuir competitive isotherm, does not give significantly better results than the empirical Langmuir model in this case, essentially because the difference in column saturation capacities is small and the range of coverage (*i.e.*, concentrations reported to the saturation capacity) investigated remains low. In spite of its soundness and increased complexity, the quadratic isotherm did not give much improved results.

Our experiments showed that the apparent a parameter of the isotherms (*i.e.*, the slope of the competitive isotherm at the origin) decreases in the presence of an increasing amount of the other component. As it is more significant for 3-phenylpropanol than for 2-phenylethanol, it was more difficult to obtain a good fit for the former. This explains why the quadratic isotherm with seven floating parameters gives much better results than that with three floating parameters. In the latter instance, the only way to adjust the slopes of the competitive isotherms would be by choosing a negative value of $a_{1,2}$, but if the full correction to the slope were made, the fit would degrade rapidly with increasing concentrations. The addition of three new parameters to the model does not improve the number of degrees of freedom much. In the former instance, the selection of a value of a_2 lower than that given by the single-component Langmuir isotherm permits a much better overall fit of the data.

Although the quadratic isotherm with seven floating parameters gives a good fit of the experimental data, there is significant doubt regarding the theoretical meaning of this result. As the pure component data are well accounted for by a Langmuir isotherm, adsorbate-adsorbate interactions are low between the molecules of the pure components. As the two components are homologues, there is no reason to think that adsorbate-adsorbate interactions between a molecule of 2-phenylethanol and a molecule of 3-phenylpropanol are any stronger than these interactions between two molecules of either 2-phenylethanol or 3-phenylpropanol. This would mean that the origin of the deviation from competitive Langmuir behavior lies in the non-ideal behavior of the mobile phase solution rather than in adsorbate-adsorbate interactions.

Of all the models investigated here, only the competitive Fowler isotherm accounts accurately enough for this effect. With optimized values of the five parameters, it accounts very well for the whole set of experimental data. This is especially noteworthy in the case of 3-phenylpropanol (Table II). Model error is observed, however, at high concentrations of 3-phenylpropanol and a systematic error of about 15% in the single-component isotherm of this compound is observed. The five

coefficients of the competitive Fowler isotherm are much easier to determine in practice than the seven parameters of the quadratic isotherm. The adjustment of the parameter b is the most critical, while changes in χ_1 and χ_2 have much less importance.

The excellent results obtained with the Fowler isotherm are only mildly satisfying. Eqns. 7 and 8 cannot be inverted and solved for q_1 and q_2 . The programs calculating band profiles in non-linear chromatography, however, need the local values of these stationary phase concentrations [2,29]. Their calculation as a function of C_1 and C_2 by numerical inversion of the two isotherm equations in each loop of the program, or even their search in a precalculated table, would increase markedly the CPU time required.

ACKNOWLEDGEMENTS

We thank YMC for the gift of the cartridge column used for the on-line analysis of the adsorption column effluent and Vydac for the gift of the adsorbent used.

This work was supported in part by grant CHE-8901382 from the National Science Foundation and by the cooperative agreement between the University of Tennessee and the Oak Ridge National Laboratory. We acknowledge support of our computational effort by the University of Tennessee Computing Center.

REFERENCES

- 1 E. Glueckauf, *Trans. Faraday Soc.*, A186 (1946) 35.
- 2 G. Guiochon, S. Golshan-Shirazi and A. Jaulmes, *Anal. Chem.*, 60 (1988) 1856.
- 3 G. Guiochon and S. Ghodbane, *J. Phys. Chem.*, 92 (1988) 3682.
- 4 E. Cremer and J. F. K. Huber, *Angew. Chem.*, 73 (1961) 461.
- 5 D. H. James and C. S. G. Phillips, *J. Chem. Soc.*, (1954) 1066.
- 6 G. Schay and G. Szekely, *Acta Chim. Hung.*, 5 (1954) 167.
- 7 J. M. Jacobson, J. P. Frenz and Cs. Horváth, *J. Chromatogr.*, 316 (1984) 53.
- 8 J. A. Jonsson and P. Lovkvist, *J. Chromatogr.*, 408 (1987) 1.
- 9 S. Golshan-Shirazi and G. Guiochon, *Anal. Chem.*, 60 (1988) 2364.
- 10 E. Dose, S. Jacobson and G. Guiochon, *Anal. Chem.*, in press.
- 11 F. Helfferich and D. L. Peterson, *Science (Washington, D.C.)*, 142 (1963) 661.
- 12 J. M. Jacobson, J. P. Frenz and Cs. Horváth, *Ind. Eng. Chem. Res.*, 26 (1987) 43.
- 13 J. M. Jacobson and J. P. Frenz, *J. Chromatogr.*, 499 (1990) 5.
- 14 J.-X. Huang and G. Guiochon, *J. Colloid Interface Sci.*, 128 (1989) 577.
- 15 S. H. Hyun and R. P. Danner, *AIChE J.*, 9 (1963) 121.
- 16 Z. Ma, A. M. Katti and G. Guiochon, *J. Phys. Chem.*, 94 (1990) 6911.
- 17 J. Frenz and Cs. Horváth, *AIChE J.*, 21 (1985) 400.
- 18 S. Golshan-Shirazi, S. Ghodbane and G. Guiochon, *Anal. Chem.*, 60 (1988) 2630.
- 19 S. Golshan-Shirazi and G. Guiochon, *Anal. Chem.*, 60 (1988) 2634.
- 20 R. H. Fowler and E. A. Guggenheim, *Statistical Thermodynamics*, Cambridge University Press, Cambridge, 1939.
- 21 S. Golshan-Shirazi and G. Guiochon, *J. Phys. Chem.*, 94 (1990) 495.
- 22 A. M. Katti and G. Guiochon, *J. Chromatogr.*, 499 (1990) 21.
- 23 A. M. Katti, Z. Ma and G. Guiochon, *AIChE J.*, 36 (1990) 1722.
- 24 M. D. LeVan and T. Vermeulen, *J. Phys. Chem.*, 85 (1981) 3247.
- 25 B. C. Lin, S. Golshan-Shirazi, Z. Ma and G. Guiochon, *J. Chromatogr.*, 475 (1989) 1.
- 26 M. Moreau, P. Valentin, C. Vidal-Madjar, B. C. Lin and G. Guiochon, *J. Colloid Interface Sci.*, 141 (1991) 127.
- 27 A. Velayudhan and Cs. Horváth, *J. Chromatogr.*, 443 (1988) 13.
- 28 G. M. Schwab, *Ergebnisse der exacten Naturwissenschaften*, Vol. 7, Springer, Berlin, 1928, p. 276.
- 29 M. Czok and G. Guiochon, *Anal. Chem.*, 62 (1990) 189.

Calculation of retention and selectivity in reversed-phase liquid chromatography

S. V. GALUSHKO

Institute of Bioorganic Chemistry and Oil Chemistry, Academy of Sciences of the Ukrainian SSR, 253660 Kiev, 94 (USSR)

ABSTRACT

A method has been developed to calculate retention in reversed-phase high-performance liquid chromatography based on the molecular structure of the analyte and characteristics of the sorbents and mobile phases. A simple approach based on solvophobic theory is used.

INTRODUCTION

One of the main problems in chromatography is to predict the retention of compounds by studying their structure and physicochemical properties. It is now impossible to predict retentions by precisely describing the chromatographic process and calculating intermolecular interactions in a chromatographic system. Methods using the correlation between different properties of analyte compounds and their retentions are now in widespread use. To calculate retention, use has been made of solubility parameters [1], retention indices [2–4], solvent interactions indices [5,6], the correlation between retention and hydrophobicity constants [7,8] distribution constants, molecular areas [7,9,10–19], Van der Waals volumes, dipole moments and the number of carbon atoms in the molecule [14,15], molecular connectivity [16–18], etc. Some of the approaches [19] use the relationship between the activity coefficients of a substance in a certain chromatographic system and retention. A calculation method has been proposed that involves two contributions to selectivity, a polar and a non-polar one [20,21]. A series of alkylbenzenes are used to standardize the retention scale, which can then be employed to calculate the retention and selectivity of the compounds investigated for different mobile phase compositions. A method has recently been developed to predict the retention of compounds in reversed-phase high-performance liquid chromatography (RP-HPLC) based on the molecular structure of the analyte [22]. The retentions are calculated as retention indices on the alkyl aryl ketone scale. The increments for substitutions on aromatic and aliphatic carbons have been obtained [22,23], and a program for calculating retention indices has been developed [24]. A number of other studies have been reviewed [22].

Empirical correlation approaches are normally not associated with specific re-

tion theories, so that their applications are limited. To use these approaches one must have experimental results from studying the physico-chemical and chromatographic properties of compounds and also reference data (often unavailable) on new or rare compounds. At present there are several retention theories in RP-LC [25–38]. Without going into the details of each of these theories, it can be noted that they do not provide adequate means of calculating the retentions of compounds. The solvophobic theory [32–35] now seems to give the most suitable approach to calculating retention and selectivity; however, to determine the energy contributions to retention we must know such characteristics as the area of the hydrophobic contact with the sorbent surface, the acentric factor and dipole moments. Normally a full set of characteristics is not available and it is very difficult to derive them. The same is true of molecular statistical approaches [36–38] that require a preliminary determination or a complicated calculation of the activity coefficients for compounds in a chromatographic system.

The aim of this work was to study the possibility of developing of a simple method for calculating the retention and selectivity in RP-LC on octadecyl sorbents that would produce satisfactory results without preliminary wide-scale experiments.

THEORY

To develop a method for calculating retention and selectivity it is necessary to employ some model concepts of the retention mechanism, the surface layer structure and the character of interactions of retained substances with mobile and stationary phases (SP). Much theoretical and experimental evidence has recently been produced to show that a bonded hydrocarbon layer seems to have a structure intermediate between brush and liquid and the eluent molecules are able to penetrate this layer, producing a considerable effect on its properties [36,39,40]. The penetration increases with increasing solvent hydrophobicity [36,39]. It has also been shown that the chromatographic process simultaneously involves both the distribution and competitive adsorption in RP-LC. The distribution processes are dominant and the surface layer exhibits quasi-liquid properties [36,41–43]. To calculate approximately the retention and selectivity we propose to use a simple two-layer continuum model of a chromatographic system: (1) the surface of a modifier sorbent in RP-LC has a surface layer (SL) that involves octadecyl radicals and some of the components of a mobile phase (MP); (2) the SL is assumed to be a quasi-liquid that has its own characteristics, *i.e.*, surface tension (γ_s) and dielectric constant (ϵ_s), and the SL characteristics vary with varying MP composition and sorbent properties; and (3) the molecules of a retained substances penetrate into the SL. The retention is determined by the difference in molecule solvation energies in the MP and SL.

We emphasize that the SL is regarded not as a layer of a liquid hydrocarbon but as a specific layer containing surface-fixed alkyl radicals and some amount of MP components. It is obvious that this layer should have characteristics different from those of a hydrocarbon.

By assuming a surface layer that has certain average characteristics and the possibility of a substance penetrating this layer, we can apply a simple procedure for calculating the retention in this case. The general expression for the retention is

$$\ln k' = \frac{-\Delta G}{RT} + \phi \quad (1)$$

where ϕ is the phase ratio. The retention is determined by the differences in the solvation energies in the distribution system [32]:

$$\Delta G = \Delta G_{\text{solv.s.}} - \Delta G_{\text{solv.m.}} \quad (2)$$

According to refs. 32, 35 and 44,

$$\Delta G_{\text{solv.}} \approx \Delta G_c \times \Delta G_{\text{int.}} \quad (3)$$

$$\Delta G = \Delta G_{\text{c.s.}} - \Delta G_{\text{c.m.}} + \Delta G_{\text{int.s.}} - \Delta G_{\text{int.m.}} \quad (4)$$

where $\Delta G_{\text{c.s.}}$ and $\Delta G_{\text{c.m.}}$ are the energies required to generate a cavity of molecular size in the SL and MP, respectively; $\Delta G_{\text{int.s.}}$ and $\Delta G_{\text{int.m.}}$ are the energies of the interaction of the molecules with the surrounding medium in the SL and MP, respectively.

The simplest version is [34]

$$\Delta G_c = NA\gamma + NA_1\gamma(k_1^e - 1) \quad (5)$$

where N is Avogadro's number, A is the cavity surface area in the liquid, γ is the surface tension (for water $\gamma = 72.6 \cdot 10^{-3} \text{ N m}^{-1}$), A_1 is the solvent molecule area and k_1^e is the characteristic constant for every liquid (for water $k^e = 1.277$ [35,44]). To calculate the approximate value of A , the Van der Waals radius of a molecule is normally used with the molecule regarded as spherical [35,44]. In this instance an approximate value of the molecular area is derived whereas the value of the area of a cavity generated in the solvent appears to be more correct [35]. The simplest and the most exact way to determine the cavity area in a solvent is to use the experimental values of partial molar volumes of different compounds in this solvent. The modern methods of measurement make it possible to obtain values of partial molar volumes with an error of less than $0.1 \text{ cm}^3 \text{ mol}^{-1}$ [45]. The literature reports numerous data on partial molar volumes of different classes of compounds such as alcohols, hydrocarbons, ethers and amino acids. The values of partial molar volumes for several hundred substances have been collected [45]. Experimental data for many compounds have shown that the additivity of the action of separate molecular fragments is a good approximation for calculating molar volumes [45]. Thus, considering the cavity shape to be spherical, we can assume

$$A = N^{-2/3} \cdot 4.836 \left(\sum_i V_i \right)^{2/3} \quad (6)$$

where V_i are the increments of partial molar of volumes of fragments. A large set of experimental values of partial molar volumes for different compounds [45] enables us to find the values of $\sum V_i$ for almost any structure. In addition simple equations have been proposed to calculate the values of V_i with great accuracy [45-47]. Thus the values of ΔG_c can be calculated as follows:

$$\Delta G_c = N^{1/3} \gamma \cdot 4.836 \left[\left(\sum_i V_i \right)^{2/3} + v_m^{2/3} (k_m^e - 1) \right] \quad (7)$$

where v_m is molar volume of MP.

Note that to simplify the calculations we use only the partial molar volumes obtained in water, assuming the cavity parameters in an SL and MP to be similar [45]. An important point is a correct choice of the form of the potential of the interaction of the solute with surrounding medium, ΔG_{int} . Solvophobic theory uses the sum of Van der Waals and electrostatic interactions [32–35,44]:

$$\Delta G_{\text{int}} \approx \Delta G_{\text{vdw}} + \Delta G_{\text{e.s.}}$$

Here Onsager's continuum model of a reactive field is used to calculate $\Delta G_{\text{e.s.}}$ [44,48] and a complicated expression derived by Haligoglu and Sinanoglu [32,44] is used to calculate the Van der Waals interaction energy. As mentioned above, to calculate this term, it is necessary to know the characteristics of a substance, which are unknown and difficult to obtain. It should be noted that almost all approaches for calculating the Van der Waals interaction energy are approximate and need either a great number of sophisticated characteristics of substances or a number of empirical parameters [49,50]. At present the continuum theories involving only electrostatic interactions are applied for an approximate calculation of the solvation energy [50–53]. We suggest that the molecule of a substance be considered as consisting of dipoles, each of which separately interacts with the surrounding continuum. In this case,

$$\Delta G_{\text{int}} \approx \Delta G_{\text{e.s.}} = -\frac{1}{2} \cdot \frac{2(\varepsilon - 1)}{(2\varepsilon + 1)} \cdot \sum_j \frac{\mu_j^2}{a_j^3} \quad (8)$$

where μ_j are the bond dipole moments, a_j the effective radius of an imaginary sphere in which the dipole is located and ε the dielectric permittivity of the surrounding continuum.

Such an approach does not need quantum chemical methods to calculate the atom charges. The bond dipole moments are determined for almost all bonds and, in many instances, vary insignificantly for various compounds [54,55]. More strictly, each dipole is not surrounded by a totally closed sphere of solvent molecules; it is more correct to speak about ball segments. The approach proposed is based on the assumption that in different compounds the parameters of a ball segment in which the same dipole is located vary in a small range, so that to calculate the electrostatic energy this parameter can be approximated by the effective radius of the sphere (a_j). By substituting eqns. 7 and 8 in eqn. 4 we obtain

$$-\Delta G = N^{1/3} \cdot 4.836 [(\gamma_m - \gamma_s)(\sum_i V_i)^{2/3} + v_m^{2/3}(k_m^e - 1)\gamma_m - v_s^{2/3}(k_s^e - 1)\gamma_s] + [f(\varepsilon_s) - f(\varepsilon_m)] \sum_j \frac{\mu_j^2}{a_j^3} \quad (9)$$

where $f(\varepsilon) = (\varepsilon - 1)/(2\varepsilon + 1)$.

The expression obtained involves several unknown parameters of SL: k_s^e , $f(\varepsilon_s)$, γ_s and v_s . To determine the parameters of the SL for a given sorbent and column, we

can use any standard substance, *e.g.*, benzene, and calculate the values for SL relative to this standard. Then:

$$\ln k'_x = \frac{1}{RT} \left\{ N^{1/3} \cdot 4.836 (\gamma_m - \gamma_s) \left[\left(\sum_i V_i \right)^{2/3} - (V_{st})^{2/3} \right] + \right. \\ \left. [f(\varepsilon_s) - f(\varepsilon_m)] \left(\sum_j \frac{\mu_j^2}{a_j^3} - \sum_j \frac{\mu_{j,st}^2}{a_{j,st}^3} \right) \right\} + \ln k'_{st}. \quad (10)$$

Thus, when a standard substance is used it is not necessary to determine the values of σ , v_s and k_s^e , which simplifies further calculations. Eqn. 10 can be reduced to a more useful form:

$$\ln k'_x = \ln k'_{st} + 16.48 (\gamma_m - \gamma_s) \left[\left(\sum_i V_i \right)^{2/3} - (V_{st})^{2/3} \right] +$$

where $\Delta G_{e.s.,jH_2O}$ and $\Delta G_{e.s.,st.H_2O}$ are the increments of the contribution $\Delta G_{e.s.}$ for dipole j of molecule x and the contribution of $(\Delta G)_{e.s.}$ for the standard substance in water, respectively. Here ΔG is expressed in kJ mol^{-1} , γ in N m^{-1} and V in $\text{cm}^3 \text{mol}^{-1}$. The values of γ_s and $f(\varepsilon_s)$ can easily be found by using, in addition to a standard, two or more reference substances. The simplest way is to solve eqn. 11 graphically for these reference substances, assuming $\ln k'_x$ (calculated) = $\ln k'_x$ (experimental) ($\ln k'_{\text{exp}}$). Thus, eqn. 11 can be expressed in the form

$$0.8234 [f(\varepsilon_m) - f(\varepsilon_s)] \left(\sum_j \Delta G_{e.s.,jH_2O} - \Delta G_{e.s.,st.H_2O} \right) \quad (11)$$

$$f(\varepsilon_s) = -b\gamma_s + \beta \quad (12)$$

where

$$\beta = \frac{\gamma_m b - f(\varepsilon_m) c + \ln k'_{st} - \ln k'_x}{c}$$

$$b = 16.48 \left[\left(\sum_i V_i \right)^{2/3} - V_{st}^{2/3} \right]$$

$$c = 0.8234 \left(\sum_j \Delta G_{e.s.,jH_2O} - \Delta G_{e.s.,st.H_2O} \right)$$

Taking two arbitrary values of γ_s and using eqn. 12, one can calculate two values of $f(\varepsilon)_s$ for each reference compound and construct plots of γ_s vs. $f(\varepsilon)_s$ for these compounds. The coordinates of intersection point determine the values of SL parameters [γ_s and $f(\varepsilon)_s$]. Naturally, to determine the values of γ_s and $f(\varepsilon)_s$ more precisely, it is necessary to employ compounds that have a large difference in ΔG_c and $\Delta G_{e.s.}$, *i.e.*, differing in size and polarity (*e.g.*, ethylbenzene, benzophenone, *o*-cresol and phenol).

As the number of reference substances rises the error in determining $f(\epsilon_s)$ and γ_s decreases.

RESULTS AND DISCUSSION

To test the applicability of the above approach, we used the retention data for various aromatic compounds in refs. 56 and 57.

The basic equation for calculating the retention was eqn. 10 or 11. To determine the increments V_i we used the values of partial molar volumes given for many compounds in ref. 45. The basic fragments of organic compounds are given in Table I.

TABLE I
INCREMENTS OF PARTIAL MOLAR VOLUMES FOR SOME FRAGMENTS

Fragment ^a	V_i (cm ³ mol ⁻¹)	Fragment ^a	V_i (cm ³ mol ⁻¹)	Fragment	V_i (cm ³ mol ⁻¹)
H(ar.)	6.8	-OH	11.7	-C-NH ₂	29.0
-CH ₂ -	16.0	-CH ₂ OH	28.2	 O	
		-COOH	25.9	-CH-COOH	33.4
-CH ₃	26.4	-COOH(ar.)	23.5	 NH ₂	
-CH ₃ (ar.)	22.5	-C-	13.0	-N(CH ₃) ₂	49.2
		 O		-Cl	20-22 ^b
=CH-	13.5	O		O	
-C ₆ H ₅	74.5	 -C-O-	20.0	-S-	16.1
-C ₆ H ₄ -	65.3	O		-NH-	7.0
		 -C-H	22.3	-C≡N	20.5
-C ₆ H ₄ N	71.2	-O-CH ₃	31.5	-NO ₂	21.6
-C ₆ H ₃ N	64.9	-O-	5.2	-NH ₂	14.7

^a ar. = Aryl.

^b No data concerning the partial molar volumes of Cl-containing compounds have been elucidated in the literature. The V_i value is derived from increments of the volume in molecular crystals [49].

Eqn. 8 involves an empirical parameter, the effective radius. This parameter may be derived either experimentally or using some physical considerations. We used the simple relationship $a_j = 1/2 (r_1 + r_2) g$, where r_1 and r_2 are the Van der Waals radii of the atoms contained in the dipole and g is a correlation parameter. The initial condition is $g = 1$, *i.e.*, the radius of a sphere is half the sum of the Van der Waals atomic radii. Using this value and choosing benzene as a standard substance ($V_{st.} = 81.3$ cm³ mol⁻¹ [45] and $\Delta G_{e.s.st.H_2O} = -26.16$ kJ mol⁻¹ ($6C_{sp^2} - H$)) we resolved graphically eqn. 12 for phenol, ethylbenzene, *o*-cresol and benzophenone (Fig. 1). The $\sum_i V_i$ and $\sum_i \Delta G_{e.s.jH_2O}$ values for these compounds were calculated by using the increments from Tables I and II. Fig. 1 shows that the straight lines intersect in a very

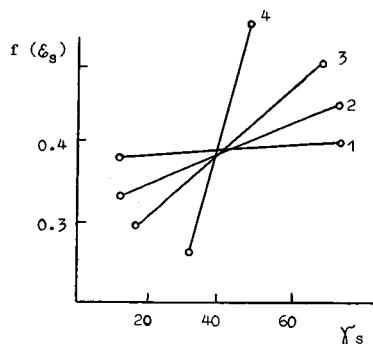


Fig. 1. Determination of SL parameters of Merck RP-18 sorbent [56]. For calculation of the two data points for each compound eqn. 12 was used. Compounds: 1 = phenol; 2 = *o*-cresol; 3 = benzophenone; 4 = ethylbenzene.

limited region, defining the limits $f(\epsilon_s) = 0.38-0.40$ ($\epsilon_s = 5.5 + 7.0$) and $\gamma_s = 36.10^{-3}-43 \cdot 10^{-3} \text{ N m}^{-1}$. These values seem to be reasonable for the parameter of a surface layer. It should be mentioned that the surface layer of a modified sorbent was characterized in ref. 33 by a quantity such as dielectric permittivity, and the value of ϵ_s reported [33] was 35. A different value of ϵ_s of 22 was derived in ref. 58 using another method of calculation and a different octadecyl sorbent. We used average values of the SL parameters γ_s and ϵ_s to calculate the capacity factors for all 35 compounds.

TABLE II

INCREMENTS OF $\Delta G_{e.s.,H_2O}$ FOR SOME DIPOLES

Dipole ^a	$a_j \times 10^{10} \text{ (m)}^b$	g	μ_j (D) [54]	$-\Delta G_{e.s.,H_2O}^c$ (kJ mol ⁻¹)
C _{sp} 2-H	1.49	1.00	0.7	4.36
C _{sp} 3-H	1.49	1.00	0.4	1.42
C _{sp} 2-C _{sp} 3	1.80	1.00	0.68	2.33
C _{sp} 2-C _{sp}	1.80	1.00	1.15	6.68
C _{sp} 3-C _{sp}	1.80	1.00	1.48	11.06
C-O	1.66	1.00	0.7	3.15
C=O	1.74	1.05	2.4	32.20
C-N	1.69	1.00	0.45	1.24
C≡N	2.37	1.40	3.1	21.25
O-H(ar. acid)	1.35	1.00	1.51	27.28
O-H	1.20	0.89	1.51	38.80
N-H	1.38	1.00	1.31	19.20
N-O	1.55	1.00	0.3 [55]	0.71
N=O	2.20	1.42	2.0 [55]	11.04
C-Cl	2.34	1.30	1.59	5.80
C-S	1.8	1.00	0.9	4.09

^a ar. = aryl

^b For calculation of $a_j = (r_1 + r_2)/2$, the Van der Waals radii (r) from ref. 49 were used: C = 0.18; H = 0.117; O = 0.152; N = 0.15; Cl = 0.18 nm.

^c For calculation of $\Delta G_{e.s.,H_2O}$, eqn. 8 was used.

The calculated results show that the simplest approach to define the value of a_j as half the sum of Van der Waals atomic radii generally results in good agreement between the calculated values of $\ln k'$ and those of given in ref. 56.

By analysing deviations in calculating the retentions of benzyl alcohol, benzonitrile, nitrobenzene and chlorobenzene we found the values of a_j for O-H, C=N, N=O and C-Cl dipoles that enabled us to obtain more exact results. Of course, the values of a_j can be further refined by analysing systematic errors in calculating the retentions of series of compounds that belong to the same class.

The results of calculating $\Delta G_{e.s.}$ and the parameters for calculating these values are given in Table II, and show that the value of g for the many dipoles is only slightly different from 1, except for the dipoles C \equiv N, N=O and C-Cl. Hence it is possible in many instances to apply the simplest approach to determine the value of a_j . The present method for calculating ΔG_{int} does not allow us to take into account the

TABLE III
COMPARISON OF CALCULATED AND EXPERIMENTAL VALUES OF $\ln k'$
Sorbent: Merck RP-18 [56].

Compound	$\ln k'_{calc}$	$\ln k'_{exp}$	Difference
Aniline	2.63	2.94	0.31
Dimethyl <i>o</i> -phthalate	4.84	5.09	-0.25
Phenol	3.10	3.13	0.03
2,4-Dimethylphenol	5.13	5.22	0.09
Benzyl alcohol	3.26	3.26	-
Quinoline	5.13	5.58	-0.45
Benzaldehyde	3.80	3.72	-0.08
Anisole	6.20	5.77	0.43
<i>o</i> -Nitroaniline	2.34	3.81	-1.47
N,N-Dimethylaniline	7.38	6.26	1.12
<i>m</i> -Nitrophenol	2.74	3.89	-1.15
Toluene	5.86	6.27	-0.41
2-Phenylethanol	4.22	3.89	0.33
Chlorobenzene	6.08	6.44	-0.36
<i>m</i> -Dinitrobenzene	4.14	3.99	0.15
Diethyl <i>o</i> -phthalate	6.40	6.46	-0.06
Benzonitrile	4.00	4.00	-
Benzophenone	6.57	6.96	-0.39
1-Phenylethanol	3.91	4.04	-0.13
Ethylbenzene	7.12	7.38	-0.26
<i>n</i> -Nitroacetophenone	4.01	4.18	-0.17
Anethole	8.60	8.13	0.47
<i>o</i> -Cresol	4.30	4.23	0.07
Diphenyl ether	8.18	8.58	-0.40
Acetophenone	4.47	4.34	0.13
Biphenyl	8.34	8.91	-0.57
Nitrobenzene	4.45	4.42	-
Naphthalene	7.17	11.81	-4.64
3-Phenylpropanol	4.85	4.94	-0.09
Anthracene	9.22	12.84	-3.62
N-Methylaniline	5.08	5.01	0.07
Benzene	4.95	4.95	-

decrease in the interaction of a molecule of a substance with water produced by an intermolecular hydrogen bond (*e.g.*, *o*-nitroaniline). We can introduce some correlations to calculate this effect. The value of 2–4 kJ mol⁻¹ (average hydrogen bond) seems to be a reasonable correction. To derive more adequate values of the corrections we must do additional research.

The results given in Table III show good agreement between the calculated values and those given in ref. 56. It is necessary to explain the difference between $\ln k'_{\text{calc}}$ and $\ln k'_{\text{exp}}$ for naphthalene and anthracene. The values of $\ln k'$ in H₂O for these compounds were derived by linearly extrapolating the values of $\ln k'$ measured at high concentrations of methanol in MP [56]. It was shown later on that for naphthalene the dependence of $\ln k'$ on methanol concentration passes through a maximum at low methanol concentration under RP-LC conditions [57]. Such an effect probably occurs with anthracene also. As a result, the values of $\ln k'_{\text{exp}}$ derived by extrapolation would be overestimated in comparison with the real values. To test the method proposed once more, we analysed the retention data of various compounds on another column as used in ref. 57. In that case all the values of $\ln k'$ were derived experimentally. It is known that when one changes from one sorbent to another (even of the same type), the retention of the same compounds varies, sometimes quite appreciably. Fig. 2 shows the plot of the correlation of the retention of the same substances obtained on two different columns with octadecyl sorbents. It is seen that there is virtually no correlation. Various surface structures of the stationary phases or the possible presence of unreacted silanol groups and consequently various contents of the mobile phase in SL can be reasons for such phenomena. From the proposed approach this implies that the surface tensions and dielectric permittivities of these sorbent SLs are very different. Therefore, to calculate the retention of compounds on a certain column we must first determine the characteristics of the SL. Taking, as in the former instance, benzene as a standard substance, we solved eqn. 12 graphically for three compounds. The intersection point determined the necessary parameters of

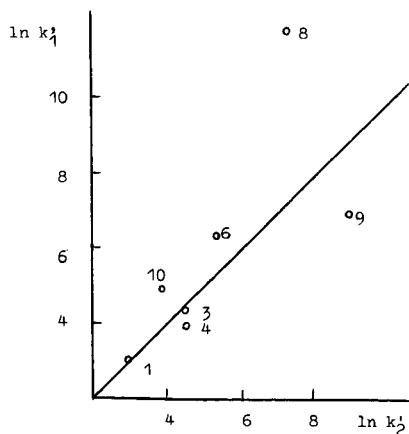


Fig. 2. Comparison of values of $\ln k'$ in water on Merck RP-18 [56] and ODS-Hypersil [57]. Compounds: 1 = phenol; 3 = nitrobenzene; 4 = *m*-dinitrobenzene; 6 = chlorobenzene; 8 = naphthalene; 9 = benzophenone; 10 = benzene.

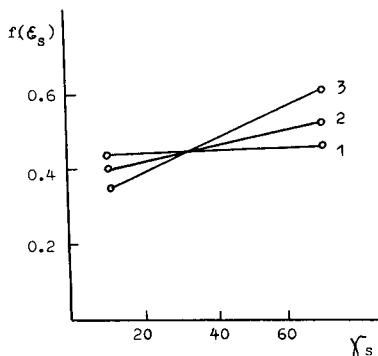


Fig. 3. Determination of SL parameters. Sorbent: ODS-Hypersil [57]. Compounds: 1 = phenol; 2 = nitrobenzene; 3 = benzophenone.

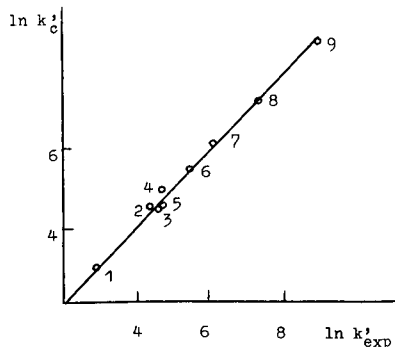


Fig. 4. Comparison of experimental [57] and calculated in $\ln k'$ values. MP H_2O ; $\gamma_s = 32 \cdot 10^{-3} \text{ N m}^{-1}$, $f(\epsilon_s) = 0.435$ ($\epsilon_s = 11.0$). Compounds: 2 = *p*-cresol; 5 = *p*-chlorophenol; 7 = 2,4-dichlorophenol; others as in Fig. 2.

the SL (Fig. 3). It is seen that the straight lines intersect in very limited range of values. Using these parameters of the SL, we calculated the retentions of all compounds. The results given in Fig. 4 and Table IV show good agreement between the theoretical and the experimental values, including those for naphthalene. It should be noted that for both columns the calculated ϕ values are very close to the typical value of 2.8 for RP columns [59].

It seems promising to extend the present approach to calculate the retentions of compounds belonging to different classes, and also to the case when eluents containing organic solvents are used. This research is in progress.

TABLE IV

COMPARISON OF CALCULATED AND EXPERIMENTAL VALUES OF $\ln k'$

Sorbent: ODS Hypersil [57].

Compound	$\ln k'_{\text{exp}}$	$\ln k'_{\text{calc}}$	Difference
Phenol	3.12	3.05	0.07
<i>p</i> -Cresol	4.32	4.51	-0.19
Nitrobenzene	4.49	4.37	0.12
<i>m</i> -Dinitrobenzene	4.58	4.96	-0.38
<i>p</i> -Chlorophenol	4.62	4.49	0.13
Chlorobenzene	5.40	5.45	-0.05
2,4-Dichlorophenol	6.00	6.14	-0.14
Naphthalene	7.22	7.23	-0.01
Benzophenone	8.99	8.75	0.24

REFERENCES

- 1 R. Tisser, H. Billet and P. J. Schoenmakers, *J. Chromatogr.*, 22 (1976) 185.
- 2 J. T. Baker, *Anal. Chem.*, 51 (1979) 1693.
- 3 R. N. Smith, *J. Chromatogr.*, 236 (1982) 313.
- 4 R. N. Smith, *Anal. Chem.*, 56 (1984) 256.
- 5 P. Jandera, H. Colin and G. Guiochon, *Anal. Chem.*, 54 (1982) 435.
- 6 H. Colin, G. Guiochon and P. Jandera, *Anal. Chem.*, 55 (1983) 442.
- 7 K. Jinno, *Chromatographia*, 17 (1983) 367.
- 8 V. D. Grygorjev, V. D. Shatz, L. A. Brovkalis and G. I. Chipens, *Bioorg. Khim.*, 9 (1983) 869.
- 9 K. Jinno and K. Kawasaki, *J. Chromatogr.*, 316 (1984) 1.
- 10 R. Koopmans and R. Rekker, *J. Chromatogr.*, 285 (1984) 267.
- 11 R. N. Smith, *J. Chromatogr.*, 209 (1981) 1.
- 12 J. Thus and J. Kraak, *J. Chromatogr.*, 320 (1985) 271.
- 13 Cs. Horváth and W. Melander, *J. Chromatogr. Sci.*, 15 (1977) 393.
- 14 A. B. Kiselev, D. I. Poshkus and Ya. I. Yashin, *Molekularnaya Osnovy Khromatografii*, Khimiya, Moscow, 1986, p. 272.
- 15 A. Tchara, H. Colin and G. Guiochon, *Anal. Chem.*, 56 (1984) 621.
- 16 B. Karger, J. Gant, A. Nartkopf and P. Weiner, *J. Chromatogr.*, 122 (1976) 185.
- 17 B. Karger, J. Gant, A. Nartkopf and P. Weiner, *J. Chromatogr.*, 128 (1976) 65.
- 18 P. Lehtonen, *J. Chromatogr.*, 267 (1983) 277.
- 19 S. Petrvic, S. Logic and J. Refer, *J. Chromatogr.*, 348 (1985) 49.
- 20 P. Jandera, *J. Chromatogr.*, 352 (1986) 112.
- 21 P. Jandera, *J. Chromatogr.*, 352 (1986) 91.
- 22 R. M. Smith and C. M. Burr, *J. Chromatogr.*, 465 (1989) 75.
- 23 R. M. Smith and C. M. Burr, *J. Chromatogr.*, 481 (1989) 85.
- 24 R. M. Smith and C. M. Burr, *J. Chromatogr.*, 485 (1989) 325.
- 25 H. Colin and G. Guiochon, *J. Chromatogr.*, 141 (1977) 289.
- 26 V. Renak and E. Smolkova, *Chromatographia*, 9 (1976) 219.
- 27 V. Renak and E. Smolkova, *J. Chromatogr.*, 191 (1980) 71.
- 28 L. R. Snyder and J. J. Kirkland, *Introduction to Modern Liquid Chromatography*, Wiley, New York, 1979, p. 863.
- 29 J. Knox and A. Pryde, *J. Chromatogr.*, 112 (1975) 171.
- 30 H. Colin and G. Guiochon, *J. Chromatogr.*, 158 (1978) 183.
- 31 F. Murakami, *J. Chromatogr.*, 178 (1979) 393.
- 32 Cs. Horváth, W. Melander and I. Molnár, *J. Chromatogr.*, 125 (1976) 129.
- 33 Cs. Horváth, W. Melander and I. Molnár, *Anal. Chem.*, 49 (1977) 142.
- 34 Cs. Horváth and W. Melander, *J. Chromatogr. Sci.*, 15 (1977) 393.
- 35 O. Sinanoglu, in *Molecular Interactions*, Vol. 3, Wiley, New York, 1982, p. 284.
- 36 D. Martire and R. Boehl, *J. Phys. Chem.*, 87 (1983) 1045.
- 37 M. Jaromis and D. Martire, *J. Chromatogr.*, 351 (1986) 1.
- 38 M. Jaromis and D. Martire, *J. Chromatogr.*, 387 (1987) 55.
- 39 G. V. Lisichkin, G. V. Kudryavtsev, A. A. Serdan, C. M. Staroverov and A. D. Yuffa, *Modifitsirovannue Kremnezemy v Sorbstsii, Katalyze i Khromatografii*, Khimiya, Moscow, 1986, p. 248.
- 40 R. Giplin, M. Gangoda and A. Krishen, *J. Chromatogr. Sci.*, 20 (1982) 345.
- 41 C. Lochmuller and D. Wilder, *J. Chromatogr. Sci.*, 17 (1976) 233.
- 42 H. Colin and G. Guiochon, *J. Chromatogr.*, 141 (1977) 289.
- 43 J. Knox and A. Pryde, *J. Chromatogr.*, 112 (1975) 171.
- 44 T. Haligoglu and O. Sinanoglu, *Ann. N.Y. Acad. Sci.*, 158 (1969) 310.
- 45 V. P. Belousov, *Termodinamika Vodnyh Rastvorov Neelektrolitov*, Khimiya, Leningrad, 1983, p. 264.
- 46 J. Edward, P. Farrel and T. Shahidi, *J. Chem. Soc., Faraday Trans. 1*, 73 (1977) 858.
- 47 S. Teresawa, H. Itsuki and S. Arakawa, *J. Phys. Chem.*, 79 (1975) 2345.
- 48 R. Rein, V. Renugopalakrishnan, S. Nir and T. Swisler, *Int. J. Quantum Chem. Quantum Biol. Symp.*, 2 (1975) 99.
- 49 A. I. Kitaygorodskii, *Molekulyarnaya Kristally*, Nauka, Moscow, 1971, p. 424.
- 50 L. Salem, *Elektrony v Khimicheskikh Reaktsiyakh*, Mir, Moscow, 1985, p. 283.
- 51 G. Klopman, *Chem. Phys. Lett.*, (1967) 200.

- 52 R. Constansiel, *Theoret. Chem. Acta Bul.*, 54 (1980) 123.
- 53 J. Rivail and D. Rinaldi, *Chem. Phys.*, 18 (1976) 233.
- 54 V. I. Minkin, O. D. Osipov and Yu. A. Zhdanov, *Dipolnyye Momenty v Organicheskoi Khimii*, Khimiya, Leningrad, 1963, p. 248.
- 55 O. Exner, *Dipole Moments in Organic Chemistry*, Georg Thieme, Stuttgart, 1975, p. 33.
- 56 P. J. Schoenmakers, H. Billet and L. de Galan, *J. Chromatogr.*, 185 (1979) 179.
- 57 P. J. Schoenmakers, H. Billet and L. de Galan, *J. Chromatogr.*, 282 (1983) 107.
- 58 S. Weber and J. Orr, *J. Chromatogr.*, 322 (1985) 433.
- 59 H. Colin, M. Krstulovic, F. Gionnard, G. Guiochon, Z. Yun and P. Jandera, *Chromatographia*, 17 (1983) 9.

CHROMSYMP. 2158

Computer-aided optimization of the experimental conditions for the isocratic reversed-phase high-performance liquid chromatographic separation of hormonal steroids

JI-QING WEI*, JI-LU WEI and XIAN-TENG ZHOU

Department of Internal Medicine, Affiliated Hospital of Shandong Medical University, 68 Huaiyin Street, Jinan 250022 (China)

ABSTRACT

A computer-aided optimization is described for selecting the optimum conditions for the isocratic reversed-phase high-performance liquid chromatographic (RP-HPLC) separation of twenty hormonal steroids. With factorial design and computer simulation, an isocratic RP-HPLC system that separated the twenty steroids simultaneously within 30 min was developed.

INTRODUCTION

Reversed-phase high-performance liquid chromatography (RP-HPLC) is a popular technique for hormonal steroid analysis and a wide range of experimental conditions have been used. Reviews of HPLC as applied to steroid analysis have been published by Heftmann and Hunter [1], Kautsky [2] and Robards and Towers [3]. For a complex biological sample containing many hormones, the use of a ternary mobile phase permitted high selectivity [4–6]. However, the selection of the optimum mobile phase composition and other conditions is difficult and complex for multi-component separations by isocratic RP-HPLC. A few optimization procedures have been described, such as solvent triangle [7], window diagram [8,9] and factorial design techniques [10–12] and a multi-criteria decision-making method [13]. In this paper, optimization of an isocratic RP-HPLC system for the separation of twenty steroid hormones by means of factorial design and computer simulation, which has been used to separate fourteen steroids perfectly [14], is described.

EXPERIMENTAL

Chemicals

Methanol was of general-reagent grade. Tetrahydrofuran was analytical-reagent grade and was redistilled before use. The serial numbers, trivial names and abbreviations of the steroid standards used are listed in Table I. Of these samples, 11-hydroxyandrostenedione (11-OHA), 11-hydroxytestosterone (11-OHT), 11-hydroxy-

TABLE I
SERIAL NUMBERS, TRIVIAL NAMES AND ABBREVIATIONS OF STEROIDS

No.	Trivial name	Abbreviation	No.	Trivial name	Abbreviation
1	Cortisone	E	11	Androstenedione	A
2	Cortisol	F	12	Methandienone	MeA
3	11-Hydroxyandrostenedione	11-OHA	13	11-Deoxycorticosterone	DOC
4	16-Hydroxyprogesterone	16-OHP	14	Testosterone	T
5	11-Hydroxytestosterone	11-OHT	15	11-Hydroxyprogesterone	11-OHP
6	Corticosterone	B	16	17-Methyltestosterone	MeT
7	19-Norandrostenedione	19-NA	17	17-Hydroxyprogesterone	17-OHP
8	11-Deoxycortisol	S	18	Estriol	E ₃
9	21-Deoxycortisol	21-DOF	19	Estradiol	E ₂
10	19-Nortestosterone	19-NT	20	Estrone	E ₁

progesterone (11-OHP), 16-hydroxyprogesterone (16-OHP), 19-norandrostenedione (19-NA) and 21-deoxycortisol (21-DOF) were kindly donated by Dr. Louis Dehennin (Fresnes, France), 19-nortestosterone (19-NT), methandienone and 17-methyltestosterone by Professor Tong-hui Zhou (Beijing, China) and some others by Professor Cheng-yu Ma (Beijing, China) and Professor Xie-liang Su (Tianjin, China).

HPLC

A Model LC-6A liquid chromatograph (Shimadzu, Kyoto, Japan) was used, consisting of an LC-6A pump, a Shim-pack CLC-ODS/H column (25 cm × 4.6 mm I.D.) mounted in a CTO-6A column oven, a Model 7125 injector (Rheodyne, Cotati, CA, U.S.A.) with a 20- μ l loop, an SPD-6AV UV-VIS spectrophotometric detector, an RF-535 fluorescence monitor and a Shimadzu C-R4A data processor. The effluent from the analytical column was first monitored at 254 nm by the UV detector and then by the fluorescence detector linked in series, with excitation and emission wavelength of 285 and 310 nm, respectively.

OPTIMIZATION METHOD

The optimization procedure was focused on selecting the optimum mobile phase composition and column temperature. First, the variables were studied in detail by means of a complete two-level factorial design. Then, a computer program was used to simulate chromatograms of these steroids under various experimental conditions. Finally, the theoretically optimum experimental conditions were tested on the HPLC system.

Factorial design

The mobile phase was a ternary system containing tetrahydrofuran, methanol and water. The fractions of tetrahydrofuran and methanol in the solvent were chosen as variables X_1 and X_2 , respectively, and the column temperature was chosen as variable X_3 in the factorial design (Table II). The ranges of these variables were set on the basis of prior knowledge from the literature and personal experience. The upper and the lower limits are denoted by 1 and -1 , respectively. The retention times (t_R) of

TABLE II
EXPERIMENTAL PRESENTATION AT A COMPLETE TWO-LEVEL FACTORIAL DESIGN

Variable	Experiment No.							
	1	2	3	4	5	6	7	8
X_1	1	1	1	1	-1	-1	-1	-1
X_2	1	1	-1	-1	1	1	-1	-1
X_3	-1	1	-1	1	-1	1	-1	1
X_1 = Tetrahydrofuran:				+1 = 21% (v/v)			-1 = 15% (v/v)	
X_2 = Methanol:				+1 = 33% (v/v)			-1 = 27% (v/v)	
X_3 = Column temperature:				+1 = 49°C			-1 = 41°C	

the seventeen steroids with UV absorption were measured by the UV detector in the factorial design experiments, and were then used to estimate the coefficients $\alpha_0, \alpha_1, \alpha_2, \alpha_3, \alpha_4, \alpha_5, \alpha_6$ and α_7 by Yates' algorithm [15]. The dead time was measured as the first peak resulting from the injection of methanol-water (60:40, v/v).

Computer simulation

A computer program was written in BASIC and run on the C-R4A data processor for simulation of chromatograms while the three variables X_1, X_2 and X_3 changed systematically within certain ranges. The minimum R_s was chosen as a measure of separation and the maximum t_R as a measure of analysis time. The predicted t_R was calculated using the following equation:

$$t_R = \alpha_0 + \alpha_1 X_1 + \alpha_2 X_2 + \alpha_3 X_3 + \alpha_4 X_1 X_2 + \alpha_5 X_1 X_3 + \alpha_6 X_2 X_3 + \alpha_7 X_1 X_2 X_3 \quad (1)$$

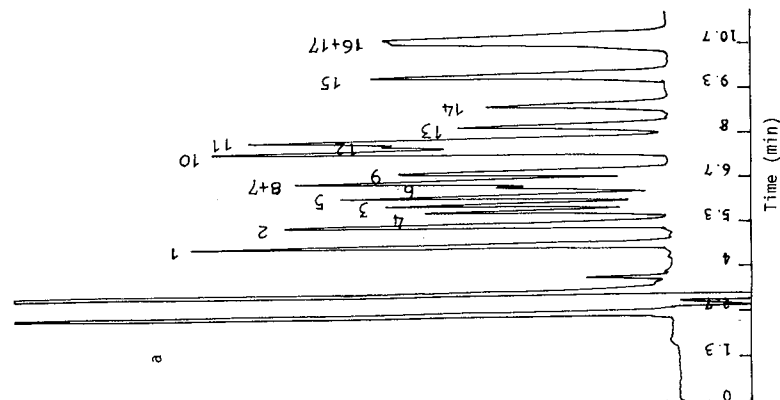
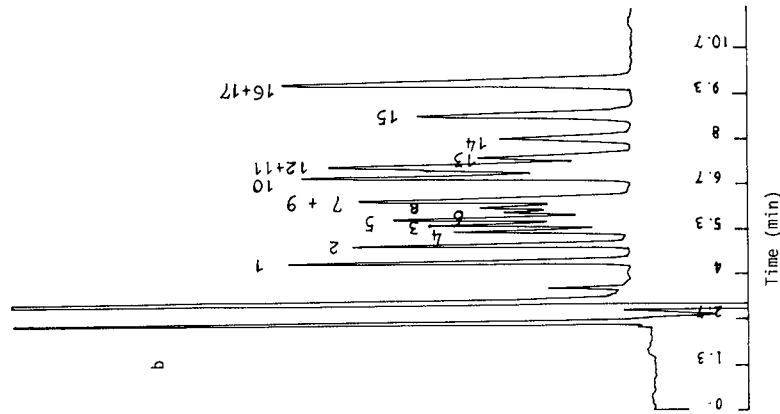
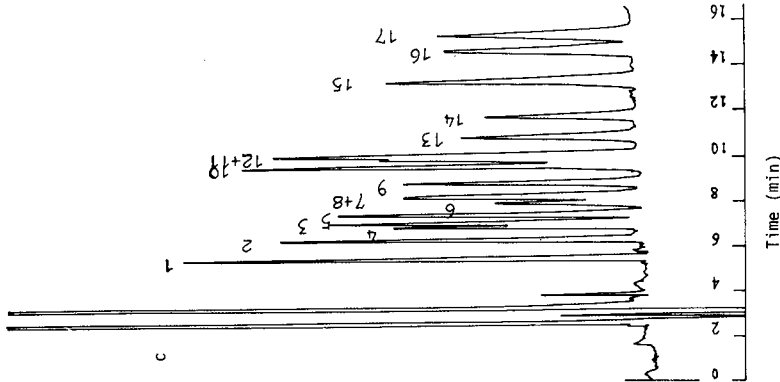
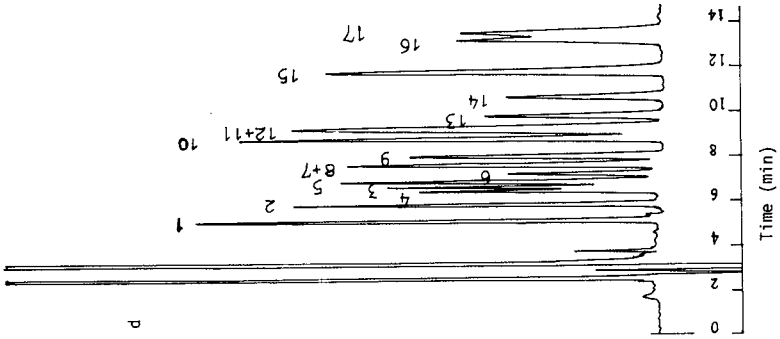
where t_R is the retention time in minutes of an individual steroid under a given set of conditions and X_1, X_2 and X_3 are values of the three variables as indicated above. The predicted t_R values were used to predict R_s by the following equation:

$$R_s = \frac{(t_{R_{i+1}} - t_{R_i})}{A/H_{i+1} + A/H_i} \quad (2)$$

where A/H , provided by the C-R4A automatically, is the area/height ratio of a peak, representing approximately the width at half-height ($W_{\frac{1}{2}}$) of an isosceles triangle ($W_{\frac{1}{2}} = 0.9394A/H$). A linear function describing the relationship between A/H and t_R was obtained on the basis of A/H and t_R values from eight experiments of factorial design. F is a correct coefficient of R_s calculated by A/H instead of peak width (W) by the classical equation

$$R_s = 2(t_{R_{i+1}} - t_{R_i})/(W_{i+1} + W_i) \quad (3)$$

A/H was easier to obtain than W .



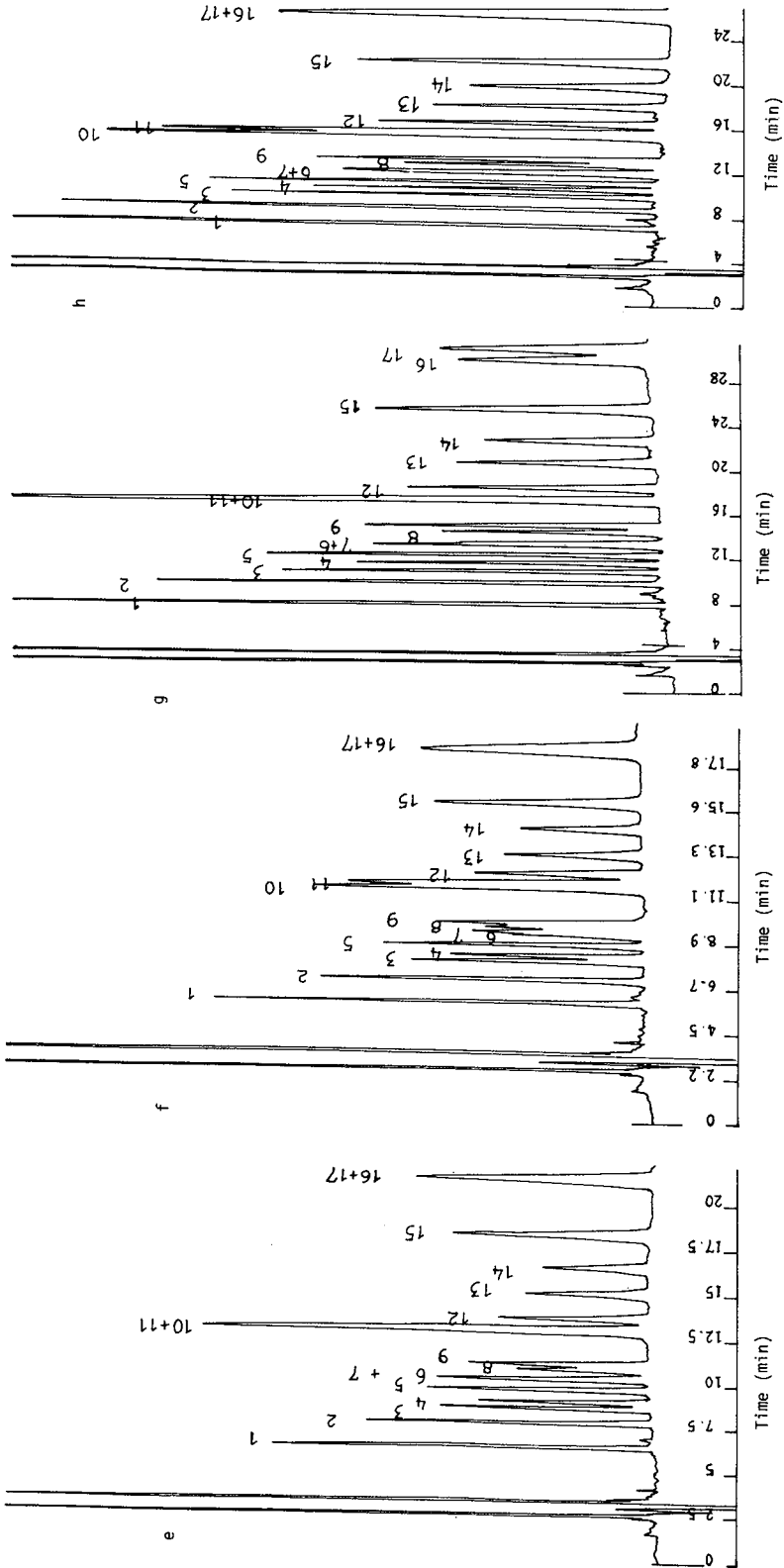


Fig. 1. Chromatograms of a mixture of twenty steroids. Mobile phase composition and column temperature in (a)–(d) as in Table II, Expt. Nos. 1–8, respectively; column, Shim-pack ODS (25 cm x 4.6 mm I.D.); detector, UV (254 nm). Peak numbers represent steroid numbers as in Table I.

TABLE III

RETENTION TIMES (min) OF SEVENTEEN STEROIDS ON CHANGING THE VARIABLES ACCORDING TO TABLE II

Steroid No. ^a	Experiment No.							
	1	2	3	4	5	6	7	8
1	4.67	4.43	5.53	5.16	6.49	5.98	7.91	7.18
2	5.28	4.94	6.39	5.87	7.88	7.11	9.82	8.73
3	5.87	5.55	7.16	6.68	8.73	8.02	10.84	9.85
4	5.65	5.34	6.97	6.48	9.10	8.32	11.62	10.42
5	6.11	5.72	7.51	6.92	9.80	8.83	12.35	10.99
6	6.40	5.92	8.02	7.28	10.46 ^b	9.32	13.48 ^b	11.81 ^b
7	6.59 ^b	6.22 ^b	8.27 ^b	7.71 ^b	10.35 ^b	9.51	13.24 ^b	12.01 ^b
8	6.54 ^b	6.07	8.40 ^b	7.63 ^b	10.93	9.75	14.44	12.65
9	6.84	6.28 ^b	8.92	8.06	11.25	9.96	15.02	13.07
10	7.47	6.93	9.66	8.85	13.03 ^b	11.67	17.24 ^b	15.22
11	7.80 ^b	7.30 ^b	10.16 ^b	9.35 ^b	13.16 ^b	11.94	17.41 ^b	15.59
12	7.65 ^b	7.15 ^b	9.96 ^b	9.18 ^b	13.76	12.47	18.34	16.34
13	8.20	7.54	10.95	9.86	15.13	13.36	20.69	17.95
14	8.81	8.11	11.82	10.69	16.55	14.64	22.64	19.73
15	9.74	8.82	13.37	11.87	18.40	15.97	25.55	21.83
16	10.68 ^b	9.74 ^b	14.77	13.27	21.36 ^b	18.90 ^b	29.98	25.94 ^b
17	10.88 ^b	9.78 ^b	15.47	13.60	21.54 ^b	18.56 ^b	30.95	26.22 ^b

^a Steroid numbers as in Table I.^b The peak of the steroid overlapped the peak of another steroid.

TABLE IV

CALCULATED MEAN EFFECTS (α VALUES) ON THE RETENTION TIMES OF SEVENTEEN STEROIDS ON CHANGING THE VARIABLES ACCORDING TO TABLE II

Steroid No. ^a	α_0	α_1	α_2	α_3	α_4	α_5	α_6	α_7
1	5.92	-0.97	-0.53	-0.23	0.13	0.08	0.04	-0.01
2	7.00	-1.38	-0.70	-0.34	0.19	0.13	0.06	-0.02
3	7.84	-1.52	-0.79	-0.31	0.19	0.11	0.05	-0.01
4	7.99	-1.88	-0.88	-0.35	0.27	0.15	0.08	-0.03
5	8.53	-1.96	-0.91	-0.41	0.26	0.17	0.07	-0.02
6	9.09	-2.18	-1.06	-0.50	0.32	0.20	0.10	-0.03
7	9.24	-2.04	-1.07	-0.38	0.28	0.14	0.07	-0.03
8	9.55	-2.39	-1.23	-0.53	0.37	0.22	0.11	-0.04
9	9.92	-2.40	-1.34	-0.58	0.38	0.23	0.12	-0.04
10	11.26	-3.03	-1.48	-0.59	0.46	0.25	0.12	-0.05
11	11.86	-3.37	-1.60	-0.57	0.51	0.25	0.12	-0.05
12	11.59	-2.94	-1.54	-0.54	0.44	0.22	0.11	-0.04
13	12.96	-3.82	-1.90	-0.78	0.63	0.34	0.18	-0.07
14	14.12	-4.27	-2.10	-0.83	0.70	0.37	0.18	-0.07
15	15.69	-4.74	-2.46	-1.07	0.79	0.47	0.23	-0.09
16	18.08	-5.96	-2.91	-1.12	1.01	0.51	0.27	-0.13
17	18.37	-5.94	-3.18	-1.33	1.08	0.59	0.32	-0.12

^a Steroid numbers as in Table I.

RESULTS AND DISCUSSION

The seventeen steroids with UV absorption were not separated simultaneously in the eight factorial design experiments (Fig. 1, Table III). The elution order of some steroids varied with the experimental conditions, such as 16-OHP and 11-OHA, and S and 19-NA, which made the separation complex.

The individual effects and interaction effects of variables X_1 , X_2 and X_3 on the t_R of an individual steroid are indicated by α_1 , α_2 , α_3 , α_4 , α_5 , α_6 and α_7 (Table IV). Negative α_1 , α_2 and α_3 indicated that there was a negative relationship between variables X_1 , X_2 and X_4 and t_R . The α_0 values are average retention times of individual steroids, including the dead time. In eight experiments, the dead time was 2.62 ± 0.02 min (mean \pm S.D.) with a relative standard deviation of 0.7%.

With the computer program, no satisfactory HPLC conditions were found between -1 and $+1$, so the domain of variables searched was extended to -3 and $+3$. Optimum theoretical HPLC conditions were found where X_1 , X_2 and X_3 were -0.333 , -2 and $+1$, respectively, representing the mobile phase composition tetrahydrofuran-methanol-water (17:24:59, v/v/v) and a column temperature of 49°C . When the optimum theoretical HPLC conditions were tested with the HPLC system, a satisfactory separation was obtained. The actual t_R and R_s values corresponded closely to the predicted values (Table V, Fig. 2). The twenty hormonal steroids, including three natural fluorescent materials, E_1 , E_2 and E_3 , were simultaneously separated within 30 min and progesterone could be eluted within 45 min. The results suggested that the optimization procedure for isocratic RP-HPLC conditions is simple, accurate and rapid.

TABLE V

COMPARISON BETWEEN ACTUAL AND PREDICTED RETENTION TIMES (t_R)

Mobile phase, tetrahydrofuran-methanol-water (17:24:59, v/v/v); flow-rate, 1 ml/min; column, Shim-pack ODS (25 cm \times 4.6 mm I.D.); column temperature, 49°C .

Steroid No. ^a	Actual t_R (min)	Predicted t_R (min)	Steroid No. ^a	Actual t_R (min)	Predicted t_R (min)
1	7.05	7.04	2	8.45	8.46
3	9.66	9.59	4	9.98	9.97
5	10.50	10.55	6	11.27	11.35
7	11.75	11.65	8	12.20	12.19
9	12.85	12.72	10	14.61	14.58
11	15.18	15.07	12	15.63	15.58
13	17.04	17.14	14	18.81	18.83
15	20.96	20.95	16	24.66	24.62
17	25.23	25.26			

^a Steroid numbers as in Table I.

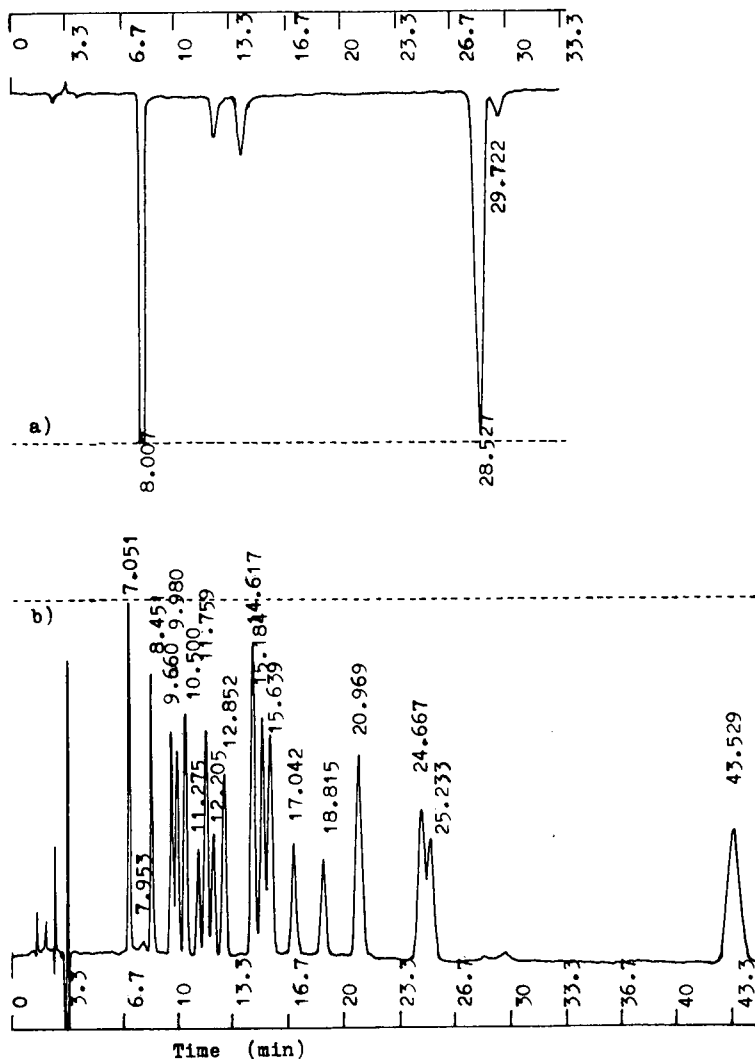


Fig. 2. Optimized isocratic separation of steroid mixture. Column, Shim-pack ODS (25 cm \times 4.6 mm I.D.); column temperature, 49°C; mobile phase, tetrahydrofuran–methanol–water (17:24:59, v/v/v); flow-rate, 1 ml/min; detector, (a) fluorescence (λ_{ex} , 285 nm, λ_{em} , 310 nm); (b) UV (254 nm). Peaks: (a) 8.007 = estriol; 28.527 = estradiol; 29.722 = estrone; (b) 7.051 = E; 7.953 = estriol; 8.451 = F; 9.66 = 11-OHA; 9.98 = 16-OHP; 10.50 = 11-OHT; 11.275 = B; 11.759 = 19-NA; 12.205 = S; 12.852 = 21-DOF; 14.617 = 19-NT; 15.184 = A; 15.639 = MeA; 17.042 = DOC; 18.815 = T; 20.969 = 11-OHP; 24.667 = MeT; 25.233 = 17-OHP; 43.529 = progesterone.

ACKNOWLEDGEMENTS

We are indebted to Dr. L. Dehennin, Professor T. H. Zhou, Professor C. Y. Ma and Professor X. L. Su for kindly donating steroid standards, and Dr. Win-yu Dai, Dr. Shan Li and Dr. Hou-de Zhang for their kind help.

REFERENCES

- 1 E. Heftmann and I. R. Hunter, *J. Chromatogr.*, 165 (1979) 283.
- 2 M. P. Kautsky (Editor), *Steroid Analysis by HPLC: Recent Applications*, Marcel Dekker, New York, 1981.
- 3 K. Robards and P. Towers, *Biomed. Chromatogr.*, 4 (1990) 1.
- 4 K. J. Darney, B. L. Wing and L. L. Ewing, *J. Chromatogr.*, 257 (1983) 81.
- 5 E. S. Halperin-Walega and F. E. Greene *J. Liq. Chromatogr.*, 8 (1985) 1677.
- 6 J. Q. Wei, X. T. Zhou and J. L. Wei, *Clin. Chem.*, 33 (1987) 1354.
- 7 L. R. Snyder, *J. Chromatogr. Sci.*, 16 (1978) 223.
- 8 S. N. Deming and M. L. H. Turnoff, *Anal. Chem.*, 50 (1978) 546.
- 9 M. Otto and W. Wegscheider, *J. Liq. Chromatogr.*, 6 (1983) 685.
- 10 W. Lindberg, E. Johansson and K. Johansson, *J. Chromatogr.*, 211 (1981) 201.
- 11 P. Wester, J. Gotteries and K. Johansson, *J. Chromatogr.*, 415 (1987) 261.
- 12 J. W. Weyland, C. H. P. Bruins and D. A. Doornbos, *J. Chromatogr. Sci.*, 22 (1984) 31.
- 13 A. K. Smilde, C. H. P. Bruins and D. A. Doornbos, *J. Chromatogr.*, 410 (1987) 1.
- 14 J. Q. Wei, J. L. Wei and X. T. Zhou, *Biomed. Chromatogr.*, 4 (1990) 34.
- 15 G. E. P. Box, W. G. Hunter and J. S. Hunter, *Statistics for Experiments. An Introduction to Design, Data Analysis and Model Building*, Wiley, New York, 1978.

CHROMSYMP. 2211

Development of a rational optimisation procedure for the automated sample clean-up with column switching in pesticide residue analysis

E. A. HOGENDOORN*, R. HOOGERBRUGGE, C. E. GOEWIE^a and P. VAN ZONEN
National Institute of Public Health and Environmental Protection (RIVM), P.O. Box 1, 3720 BA Bilthoven (The Netherlands)

and

P. J. SCHOENMAKERS

Philips Research Laboratories, P.O. Box 80 000, 5600 JA Eindhoven (The Netherlands)

ABSTRACT

Column-switching procedures usually involve at least one step gradient elution over the first column. In order to find optimal conditions for column switching in a rational way a computer program has been developed which calculates retention times and peak volumes for elution under step gradient conditions. Based on experimentally determined relations for retention *versus* mobile phase composition, the program calculates iteratively the displacement of analytes and sample interferences on the first column. Corrections for the distortion of solvent front and peak position of the solutes during step-gradient elution are included. The prediction of the peak volume is based on a diffusion model. The performance of the simulation procedure is evaluated with the application of a practical residue analytical method, the simultaneous determination of procymidone and iprodione in fennel. In this case, the program was shown to accurately predict retention times and peak volumes of a major fennel interference and the compounds of interest eluted under stepwise gradient conditions. Optimal conditions for reversed-phase liquid chromatography column switching are more rapidly found by the present procedure in comparison to trial and error optimisation.

INTRODUCTION

For several years, reversed-phase liquid chromatography (RPLC) with column switching has been applied routinely for the automated clean-up of crop extracts for pesticide residue analysis [1-3]. Besides automation, the most important advantages of this approach are improvement of the sensitivity by introduction of larger sample volumes under controlled band-broadening conditions and improvement of the

^a Present address: DHV Raadgevend Ingenieursbureau B.V., P.O. Box 85, 3800 AB Amersfoort, The Netherlands.

selectivity by transferring accurate volumes containing only the analytes of interest to the second column.

The principal events occurring in column switching are schematically shown in Fig. 1. After the injection of an aliquot of uncleaned sample extract (event I) on the first column (C-1), a clean-up (event II) is performed with a certain volume of M-1, the mobile phase of C-1. During this event (II) the more polar sample interferences (S1), usually abundant in concentrated extracts, are removed largely from C-1. Clean-up takes place until the first analyte starts to elute from C-1. After this, in event III of Fig. 1, C-1 is switched temporarily on-line with the second separation column (C-2). With a certain volume of M-2 the analytes (A) are transferred from C-1 to C-2. Finally the analytes (A1 and A2) are separated on C-2 (event IV) and simultaneously (event V) C-1 will be washed with a strong eluent for the removal of the apolar sample interferences (S2) and reconditioned with a volume M-1 prior to the next injection.

Most crucial in the development of column-switching procedures is the choice of the eluotropic strength of the clean-up solvent (M-1). A low eluotropic strength allows the injection of a large volume of sample without significant band-broadening and provides a high potential for the removal of early eluting interferences. However, a higher eluotropic strength will speed up the clean-up process and, more important,

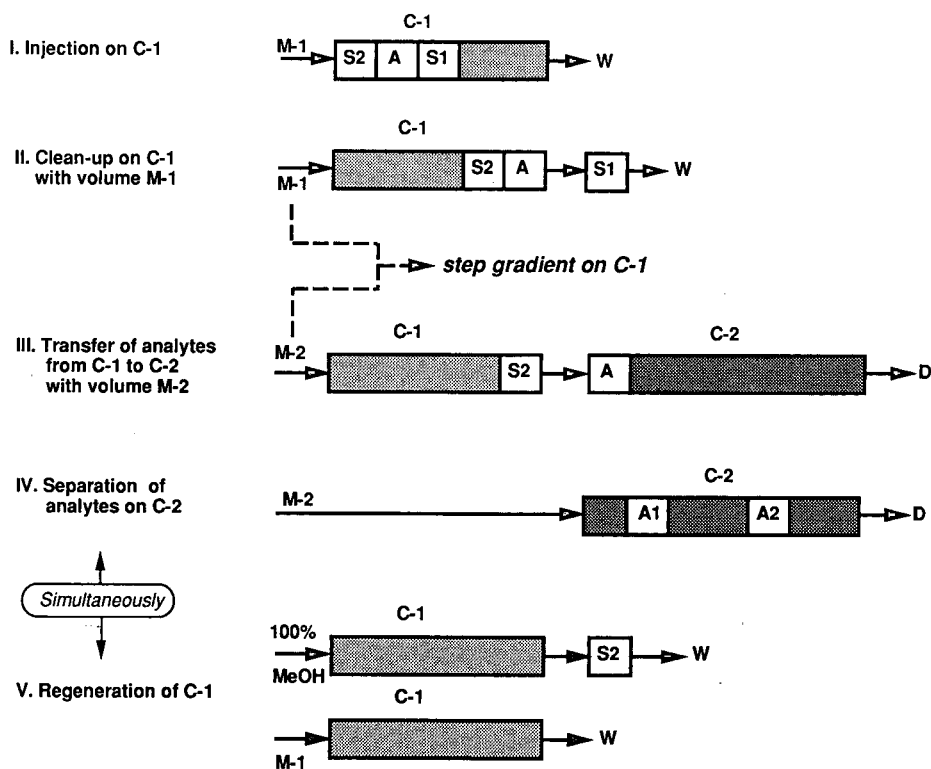


Fig. 1. Principal events in an on-line clean-up with RPLC column switching. C-1 = first C_{18} separation column; C-2 = second C_{18} separation column; M-1 = clean-up eluent of C-1; M-2 = mobile phase of C-2; S1 and S2 = sample interferences; A = analytes; W = waste; D = detection (for further explanation see Introduction).

will decrease the peak volumes of the analytes which is favourable for the transfer of small fractions to the second separation column (C-2). The separation of analytes will mainly take place on C-2 (see Fig. 1), which means that the mobile phase composition M-2 in a column-switching procedure is usually fixed in order to obtain a good separation.

So far, in our applications [1–3] a clean-up solvent (M-1), containing 5–20% of organic modifier, was found by “trial-and-error” to yield a sufficient clean-up performance between the analytes (A) and the early-eluting sample interferences (S1). However, similar to an off-line procedure [4], the residue determination of some fungicides in fennel [5] required more clean-up steps. After considerable trial-and-error effort an optimal clean-up was found using a three-step gradient elution on the first column (C-1). This application illustrates the complexity of finding appropriate on-line clean-up conditions to be used in RPLC column switching. In order to simplify this procedure we investigated the chromatographic processes involved in column switching. This type of elution can be regarded as a step-gradient elution, in which the mobile phase composition on C-1 is changed discontinuously in such a way that the elutropic strength of each subsequent step increases.

Mathematical equations based on the observed retention volume (V_r) of a solute in an isocratic elution have been described [6–9] for the calculation of the optimal composition and volume of the mobile phases used in step-gradient elution LC. On the basis of a linear relationship between the isocratic capacity factor of a solute and the volume fraction of the stronger eluent component, general equations were derived predicting the retention for step-gradient elution in thin-layer chromatography (TLC) [10–12]. Using TLC as a pilot technique, a simple graphical model was developed for the optimisation of step-gradient elution in high-performance liquid chromatography (HPLC) [13,14]. This model was then further evaluated, providing equations which allow the search for an optimum gradient program by means of calculation [15] or by simulation [16] with a computer program.

This paper describes the development of a computer program which accurately predicts retention times and peak volumes of analytes eluting under step-gradient conditions as applied in RPLC column-switching procedures. The determination of procymidone and iprodione residues in fennel extracts was used as a model system for the development of the proposed procedure.

METHOD DEVELOPMENT

General strategy

An important problem in developing an accurate model for the prediction of solute retention under step-gradient conditions is caused by the practical execution of this type of gradient as illustrated in Fig. 2. Compared to the profile (A) of an ideal step gradient, two noticeable deviations always occur in the resulting elution profile (B) obtained from a solvent-delivery system. When executing a step gradient, it takes some time before the first change in solvent composition reaches the top of the column. This first deviation is called the delay time (t_d) of the gradient and is caused by the connective tubing. The second deviation is the time needed to accomplish a new mobile phase composition at the head of the column. This effect is caused by the volume of the mixing chamber and is related to the time constant (τ) of the mixing process. Both t_d

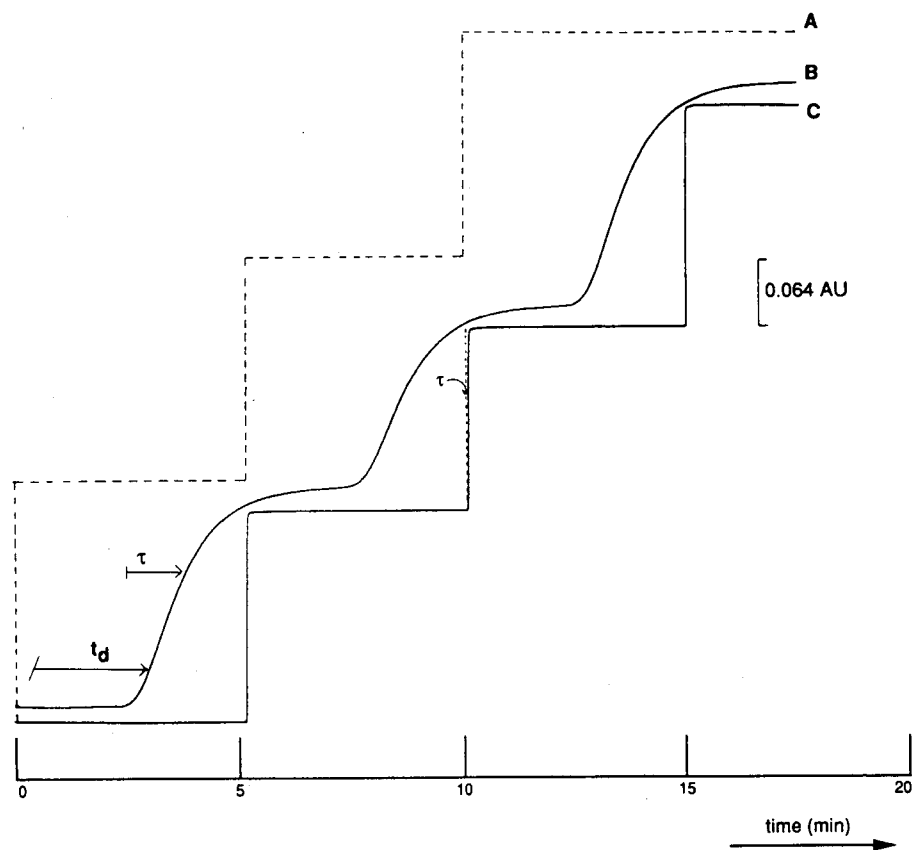


Fig. 2. Different gradient profiles of the same three-step-gradient-elution program, for which each step, executed at time intervals of 0, 5 and 10 min, corresponds with an increase of 20% solvent A (0.1% acetone in water) in solvent B (pure water). A = ideal step-gradient profile; B = step-gradient profile with a binary gradient pump system; C = profile with the gradient pump in combination with a valve-switching system (see Fig. 3) and a stop-flow time of 5 min. B and C are recorded without a column and with UV detection at 254 nm.

and τ of a step gradient obtained from a binary pump system are indicated in Fig. 2.

As was outlined in several studies [17–19], the most important deviation factors for retention prediction in gradient elution are the mixing effect and the delay time of the gradient. For linear gradient elution these effects are negligible if the steepness of the gradient is kept small [17–19].

In a column-switching procedure (see Fig. 1), however, the steepness of the gradient on C-1 during a step gradient elution is almost maximal (see Fig. 2) and therefore the effects of mixing and gradient delay will play a dominant role in the chromatographic process. The resulting disagreements between practical and simulated values for retention in step-gradient elution have been ascribed to these effects [16].

The development of our model will be explained in the next three sections.

Firstly, the theory of step-gradient elution in relation to the transport of a solute under column-switching conditions will be discussed. The following section will explain the principles of the proposed model of chromatogram simulation to be used for the prediction of retention times and peak volumes of analytes eluting under step-gradient conditions. Finally, the different steps of the simulation procedure are summarized in the last section.

Prediction of retention in step-gradient elution

Isocratic retention data. A first step in predicting retention times for solutes eluting under gradient conditions is to describe the capacity factor, k , for each solute as a function of the mobile phase composition. A simple linear relation often used for the description of retention in RPLC [20,21] is:

$$\log k = \log k_w - S\varphi \quad (1)$$

where k_w is the (extrapolated) capacity factor in pure water, φ is the volume fraction of the organic modifier and S is a constant depending on the organic modifier used. This linear equation appeared often not valid in the extreme regions of φ [21], normally used in column-switching procedures, and therefore a quadratic $\ln k$ vs. φ relationship was preferred according to ref. 21:

$$\ln k = a\varphi^2 + b\varphi + c \quad (2)$$

where the coefficients a , b and c are experimentally determined constants.

An important parameter in the prediction of the retention times in column-switching experiments is the length, L , of the first column (C-1). Separation on C-1 of A from S1 (see Fig. 1) must be completed by the time the compounds have travelled the length of the column. Based on the general equations used in RPLC [22] for the description of the retention time of a solute (t_r) and the unretained compound (t_0), an equation can easily be derived which describes in isocratic elution the distance (ΔL in mm) travelled by a solute during a time Δt as:

$$\Delta L = [L/(1 + k)]\Delta t/t_0 \quad (3)$$

Using eqns. 2 and 3, the retention time of a solute occurring under ideal stepwise gradient elution conditions (see Fig. 2) can be calculated. The solute elutes when the sum of the different travelled distances ($\Sigma\Delta L$), obtained with different isocratic elutions, equals the total length (L) of the first column (C-1).

Correction terms for retention prediction. For an accurate prediction of retention in step-gradient elution two corrections must be made to eqn. 3. Correction for the most obvious deviation, the delay time (t_d), is simply carried out by measuring its value and subtracting it from the time used in the step gradient.

Due to the delay of the next solvent front, a correction must also be made for the position of the solute in the column. Normally in column switching, using two pumps and a high-pressure switching valve, a one-step-gradient elution with two eluents (M-1 and M-2) on C-1 is applied, yielding a profile of the solvent front which corresponds closely to the ideal profile. This is also illustrated in Fig. 2, showing the profile (C) of

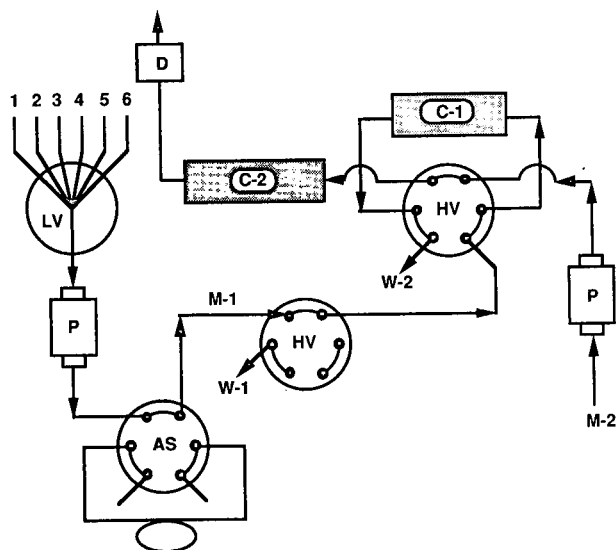


Fig. 3. LC system for the execution of step-gradient elution and column switching. AS = autosampler; LV = six-way low-pressure valve for the selection of different clean-up eluents. HV-1 and HV-2 = six port high-pressure valves; C-1 = first C_{18} separation column; C-2 = second C_{18} separation column; W-1 = waste during a stop-flow on C-1 for the performance of an abrupt solvent change; W-2 = waste during elution (clean-up) on C-1; P = LC-pump; D = UV detector; all flows are set at 1 ml/min (for further details: see Theory, Experimental and Results and Discussion).

a three-step gradient obtained with the LC column-switching system presented in Fig. 3. In this figure, the combined use of a solvent-selection valve (LV) and a high-pressure valve (HV-1) regulates an abrupt change in solvent composition by means of a temporarily "stopped flow" on the first column (C-1).

Assuming unretained migration of the solvent front without distortion, two equations were derived (see Appendix I) for more accurate prediction of retention in column-switching experiments. For a one-step-gradient elution the retention is given by the equation:

$$t_r = t_0(1 + k_2) + (t_d + t_1)[(k_1 - k_2)/k_1] \quad (4)$$

and the equation for the retention obtained with a two-step gradient corresponds to

$$t_r = t_0(1 + k_3) + t_d[(k_1 - k_3)/k_1] + [t_1(k_1 - k_2)k_3]/k_1k_2 + t_2[(k_2 - k_3)/k_2] \quad (5)$$

In these equations, k_1 , k_2 and k_3 are the capacity factors of the solute at the three different mobile phase compositions.

Design of the model for the prediction of retention and peak volume

Our model, developed for the prediction of retention and peak volume, is based on the diffusion occurring during the transport of a solute in tubing and column. In this model, schematically presented in Fig. 4, the migration of a solute is proposed to

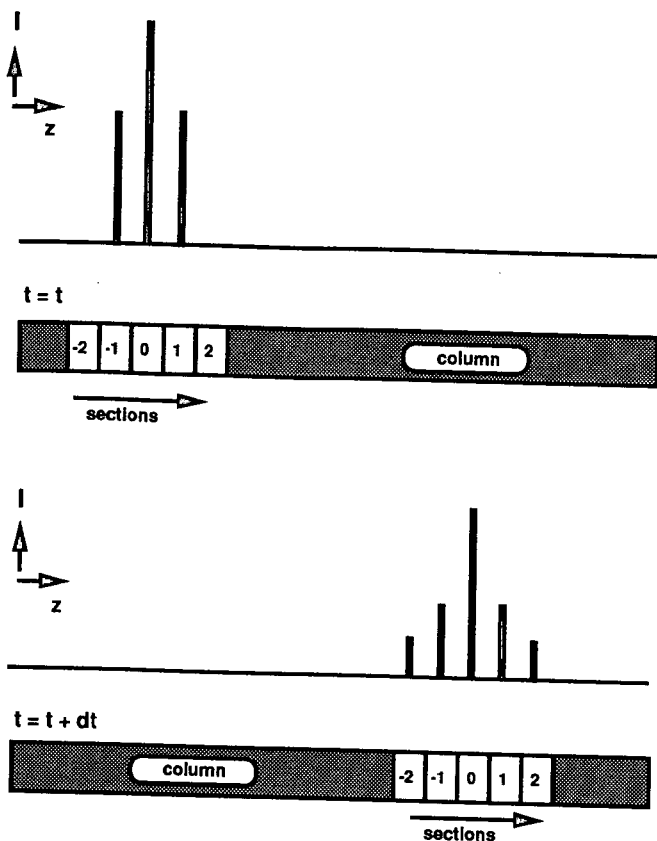


Fig. 4. Schematic representation of the migration (z) of a solute with an intensity I in a number (n) of sections migrating through a column or tubing by means of a diffusion process. For further explanation, see text.

be arranged by means of a number (n) of small interconnected sections (s) moving through the chromatographic system. The position ($n = 0$) of the central section (s_0) as a function of time corresponds with the actual place of the solute in the column (or tubing); the intensity in s_0 and the surrounding sections is determined by diffusion. The schematic presentation of Fig. 4 shows the position of section n , $z_n(t)$, and the intensity in section n , $I_n(t)$, of a solute during migration in five sections at the time intervals t and $t + \Delta t$. The cumulative displacement of a solute in the sections during a certain time interval, Δt , is given by its current place (z_n) plus the travelled distance (Δz) during Δt , which can be expressed by the relation

$$z_n(t + \Delta t) = z_n(t) + \Delta z \tag{6}$$

In this equation a distance (Δz) travelled in the tubing corresponds to

$$\Delta z = u_{\text{tub}} \Delta t \tag{7}$$

and a distance (Δz) travelled in the column is equal to

$$\Delta z = u_{\text{col}} \Delta t / (1 + k) \quad (8)$$

in which u_{tub} and u_{col} stand for the linear velocity of the unretained compound in tubing or column, respectively.

At the start of an elution, a solute will have a maximum intensity (concentration) in section s_0 . After a time (Δt), the new intensity $I_n(t + \Delta t)$, of the solute will be divided over a number of sections at both sides of the maximum intensity in section zero (see Fig. 4). Due to the open connection between the sections the new intensity of a solute in each section is not only determined by the transport of solute *to* the two adjacent sections but also by the transport *from* the adjacent sections. The change in intensity of a solute in a section during the migration can be seen as a diffusion process described for each step (Δt) by the equation

$$I_n(t + \Delta t) = I_n(t) + D\{[I_{n+1}(t) + I_{n-1}(t) - 2I_n(t)]\Delta t / dp_n^2\} \quad (9)$$

in which D is a diffusion coefficient and dp the average distance between two sections corresponding to

$$dp_n = [z_{n+1}(t) - z_{n-1}(t)]/2 \quad (10)$$

Using the general relationship between H , the height of one theoretical plate of a column, and the diffusion coefficient D derived by Giddings [23] as

$$H = 2D/Lv \quad (11)$$

in which v is the migration velocity (mm/s) of a solute, the diffusion coefficient (D) of eqn. 9 can be expressed as

$$D = Hu_{\text{col}}/[2(1 + k)] \quad (12)$$

Applying (step-) gradient elution, the exact mobile phase composition (φ) during elution must be known in order to predict accurate chromatographic values. The calculation of φ as a function of z and t , including (i) a correction for solvent front distortion (mixing effect), (ii) the position of the solute in the column and (iii) the delay time (t_d) can be described by the equation

$$\varphi(t, z) = \varphi_0 + \Delta\varphi\{1 - \exp[-(t - [t_s + t_d + z/u_{\text{col}}])/\tau]\} \quad (13)$$

in which φ_0 represents the value of φ at the start of the step gradient, $\Delta\varphi$ the size (increase of φ) of a step and t_s the time of solvent change (switching time).

The value of the time constant, τ , can be determined graphically from the step gradient profile as illustrated in profile B of Fig. 2. Knowing the relation between k and φ (eqn. 2) the changing k value during step gradient elution can be calculated.

Final computer-simulation procedure

For the prediction of retention times and peak volumes of solutes eluting under step-gradient conditions a computer program has been written in Lightspeed Pascal. This program performs an iterative calculation, using eqn. 3 for transport, eqns. 9 and 12 for diffusion and eqn. 13 for the distortion of the solvent front.

Before the calculation takes place, the H value of the column, the delay time (t_d) and the time constant (τ) of the gradient, and the coefficients a , b and c (eqn. 2) of the solutes are introduced in the program by means of an input file. The latter parameters must be determined experimentally from a minimum of three isocratic experiments.

A visual simulated chromatogram is obtained by transferring the data to a graphic computer program which prints the peak intensities (I) against the elution times.

In order to speed up the procedure, two selection criteria are added to the computer program. The first one is the application of eqns. 4 and 5. These equations rapidly provide the retention times of the compounds eluting under a selected one- or two-step gradient. If the retention difference between adjacent peaks (Δt_r) is promising, the simulation is started to provide complete chromatographic information.

The second time-saving criterion is the simultaneous calculation of the resolution, $R_s = \Delta t_r / [2(\sigma_1 + \sigma_2)]$, between successive peak pairs in the simulated chromatogram. Depending on the desired resolution, a decision can be made on whether a graphical output of the chromatogram is made. The scheme of the final rational optimisation procedure is given in Fig. 5.

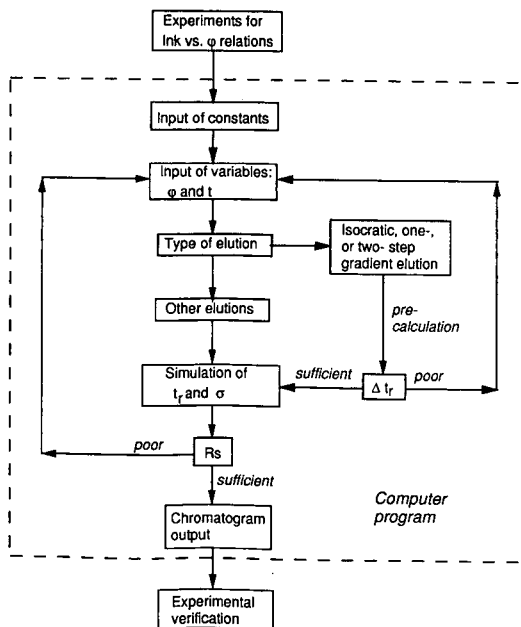


Fig. 5. Scheme of the rational optimisation procedure.

EXPERIMENTAL

Reagents

The fungicides iprodione, 1-isopropylcarbamoyl-3-(3',5'-dichlorophenyl)hydantoin, and procymidone, N-(3',5'-dichlorophenyl)1,2-dimethylcyclopropane dicarboximide), both with a purity > 99%, were obtained from Dr. S. Ehrenstorfer (Promochem, Wesel, Germany). Analytical-grade dichloromethane was bought from Merck (Darmstadt, Germany) and methanol and acetonitrile, both HPLC grade, were purchased from Baker (Deventer, The Netherlands). Potassium bromide (KBr) and anhydrous sodium sulphate (Na₂SO₄) were bought from Merck. Demineralised water was purified in a Milli-Q (Millipore, Bedford, MA, U.S.A.) system to obtain LC-grade water for use in eluents and standard solutions. The solvent compositions (v/v) of the isocratic mobile phases were prepared by accurately weighing the necessary volumes of water and organic modifier. Stock standard solutions of the fungicides were prepared in acetonitrile and for the LC analyses dilutions were made in the mobile phase. RPLC test mixtures, containing uracil and fluoranthene for the measurement of the retention of an unretained compound and the efficiency (*N*) of a column, respectively, were obtained from Chrompack (Middelburg, The Netherlands).

Equipment

The LC instrumentation consisted of the following components: an ASPI 232-401 autosampler (Gilson, Villiers-le-Bel, France) equipped with three programmable high-pressure valves (Type 7010, Rheodyne, Cotati, CA, U.S.A.) and one programmable six-way solvent-selection valve (Type 5011, Rheodyne); two isocratic pumps: one Model 9208 from Kipp Analytica (Delft, The Netherlands) and one Model 400 from Kratos (Ramsey, NJ, U.S.A.); one binary gradient pump Model 250 from Perkin-Elmer (Norwalk, CT, U.S.A.) with a helium degassing system from Perkin-Elmer equipped with air tight bottle connections from Omnifit (Cambridge, U.K.) for delivering mobile phases to the pumps under light pressure (60 p.s.i.).

The flow valve scheme for executing a stepwise gradient elution with a solvent-selection valve in combination with column switching is depicted in Fig. 3. All flow-rates were set at 1 ml/min.

A 50 × 3 mm I.D. column, packed with ChromSpher C₁₈, 5 μm-particles, from Chrompack, was used as a first column (C-1) in combination with a 10 × 2 mm I.D. guard column packed with 40-μm pellicular C₁₈ material. A 100 × 4.6 mm I.D. column, packed with MicroSpher C₁₈, 3-μm particles, from Chrompack, was used as a second separation column (C-2). Detection (UV at 229 nm) was performed with a LC-95 UV detector (Perkin-Elmer) equipped with a Kipp recorder.

A Macintosh McII (Apple, Cupertino, CA, U.S.A.) personal computer was used for calculation and simulation.

Preparation of fennel extracts

A 50-g aliquot of an homogenised blank fennel sample was weighed into a cup of a Warring blender, together with 200 ml of dichloromethane and 100 g of sodium sulphate. After blending for 3 min the mixture was transferred into a tube and centrifuged for 5 min at 7000 g. A 100-ml volume of the dichloromethane phase was dried over sodium sulphate and concentrated to 5 ml in a Kuderna Danish apparatus.

For experiments 200 μl of extract, corresponding with 1 g of fennel, were pipetted into a calibrated tube and made to dryness with a gentle stream of nitrogen. Prior to the LC analysis, the residue was dissolved in 100 μl of acetonitrile and brought to a volume of 1 ml with water (blank fennel extract) or with a suitable standard solution of procymidon and iprodione in water (spiked fennel solution).

RESULTS AND DISCUSSION

Application of the computer-simulation program

The application of the optimisation procedure is schematically presented in Fig. 5. The program does not (yet) find optimal separation conditions automatically. At this stage it should be applied by an analyst with a basic knowledge of RPLC. The optimal separation conditions must be found step by step with the application of different elution programs in a rational way. An important tool in selecting suitable gradient-elution programs is the graphical interpretation of the resulting $\ln k$ vs. ϕ plots. The first step is to enter, by means of an input file, into the computer program the values of the parameters which will serve as constants for a particular application. These are the a , b and c coefficients of the quadratic $\ln k$ vs. ϕ relations of the compounds to be separated and the constants of the LC system. The relevant parameters are the injection volume, the gradient delay time (t_d), the time constant (τ) for the distortion of the solvent front, the flow and the efficiency of the column (H).

The second step is to enter the variables for an elution program. The program asks for the number of steps and the length (min) and fraction of modifier (ϕ) of each step.

After introducing the variables and constants, the program calculates first rapidly the retention times of the solutes. Based on the resulting differences in retention (Δt_r) the analyst must decide to proceed with a simulation or to introduce new step-gradient elution conditions (ϕ and t values).

After the simulation, the analyst must decide again, based on the calculated resolutions (R_s), whether other elution conditions must be tried out to improve the separation. This decision depends mainly on the type of application and the concentration of the interferences (S1 or S2, see Fig. 1). In pesticides residue analysis an obtained partial pre-separation on a short first column (C-1) is normally sufficient for the final separation on the highly efficient second separation column (C-2).

If the resolution seems appropriate, the data of the calculated intensities and peak volumes are converted into a chromatogram rendering the exact volumes for clean-up and transfer to be used in column-switching procedure (see Fig. 1).

The simulation time is mainly determined by the number of compounds and by the step size of the iterative calculation procedure. Using an iteration step of 0.004 min, the simulated chromatograms of the three compounds used in this application were calculated within 2 min. The graphical display of a chromatogram containing three solutes takes about 5 min.

Retention behaviour of iprodione, procymidone and fennel

The earlier described automated clean-up procedure of fennel extracts for the determination of iprodione and procymidone [5] was performed with a three-step gradient elution on a 15×3.2 mm I.D. C₁₈ precolumn. However, in this study, it

appeared that the efficiency (N) of this precolumn and of other small columns tested with a variety of C_{18} materials decreased very rapidly on injection of fennel extracts. Therefore this type of columns were not suitable for the purpose of this study. Acceptable results in terms of stability were obtained with 50×3 mm I.D. C_{18} columns, in combination with small disposable guard columns directly connected to the separation column (see Experimental). When replacing the low-cost guard column every 2 days while analysing fennel extracts, the efficiency (N of the column) remained constant (1750 ± 250) for more than 7 days.

The first step of the proposed procedure was the determination of the retention behaviour of the compounds by establishing their $\ln k$ vs. ϕ relations. In the fennel extract, one major interference was found to elute closely to the two fungicides. The retention of this fennel interference, denoted as "fennel", and the retention of the two fungicides iprodione and procymidone was measured in five different mobile phases providing the $\ln k$ vs. ϕ plots presented in Fig. 6. The crossing of the $\ln k$ vs. ϕ lines illustrates that this is an interesting clean-up (separation) problem. As explained in the introduction (see Fig. 1), clean-up in an on-line column-switching procedure is normally focussed on the removal of the first eluting sample interferences (S1). However, in this application the situation is reversed. The clean-up eluent (M-1) must prevent the elution of the fennel interference (S2 in Fig. 1) from C-1 during the transfer of the analytes to the second column (C-2). In the next sections the computer program will be applied to establish optimal clean-up conditions for this problem.

Prediction of retention and peak volume under isocratic conditions

The plots of Fig. 6 suggest that the clean-up can be performed with the use of only one clean-up eluent (M-1) consisting of a high percentage of methanol (> 60%). This solvent is also appropriate for the mobile phase (M-2) of the second column. To confirm this, the performance of the computer program was first tested for isocratic elutions. In order to compare the simulated chromatograms with experimental ones, fennel extracts were spiked with approximately 50 ppm of iprodione and procymidone,

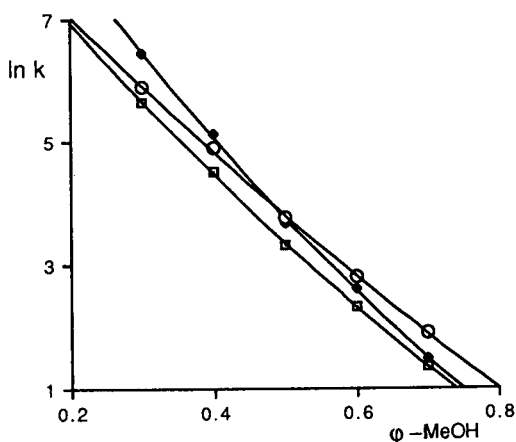


Fig. 6. Plots of $\ln k$ vs. volume fraction of organic modifier (ϕ) in water for procymidone (\square), iprodione (\blacklozenge) and fennel (\circ) on a 50×3 mm I.D. C_{18} column (C-1). MeOH = Methanol.

rendering an equal UV response at 229 nm for the compounds involved.

The chromatographic results for simulated and experimental isocratic elutions on a 50 × 3 mm I.D. column (C-1) are listed in Table I. It must be mentioned that in this study still the same column is used for the comparison between experiment and prediction meaning that the calculated values are based on the input of the measured values for retention.

The separations between procymidone and iprodione and between iprodione and fennel, mentioned in Table I, are characterised by the resolution (R_s). The obtained resolutions at 40% methanol are deceptive due to the elution of fennel between procymidone and iprodione at this mobile phase composition. The results of Table I show that sufficient resolution ($R_s = 2$) between fungicides and fennel can be obtained at $\phi = 0.6$ and also that the resolution increases with increasing eluotropic strength. This is also demonstrated in Fig. 7, which shows the simulated and corresponding experimental chromatograms of two different isocratic elutions with ϕ values of 0.65 (A) and 0.60 (B), respectively.

The good agreement between the simulated and experimental chromatograms emphasises the usefulness of an accurate chromatogram simulation in selecting clean-up conditions. For example, Fig. 7 illustrates that with a transfer fraction of 2.6 ml of 60% methanol or 1.6 ml of 65% methanol from the first column (C-1) to the second column (C-2), only the fungicides will be transported to C-2 and the fennel (S2) will be retained on C-1. Of course, the first 1 ml of 65% or the 1.5 ml of 60% methanol of the chromatogram, containing the early-eluting interferences (S1), will be sent to waste in a column-switching procedure. Based on these results it can be concluded that an appropriate separation can be achieved with an isocratic heart-cutting procedure, using a mobile phase in the range of 60 to 70% methanol.

TABLE I

COMPARISON OF SIMULATED (sim.) AND EXPERIMENTAL (exp.) VALUES FOR DIFFERENT ISOCRATIC ELUTIONS ON C-1

σ = Peak volume at 0.6 of the peak height.

ϕ (Methanol)		Procymidone		Iprodione		Fennel		R_s	
		t_r (min)	σ (min)	t_r (min)	σ (min)	t_r (min)	σ (min)	Procymidone/ iprodione	Iprodione/ fennel
0.4	exp.	14.9	0.36	27.4	0.65	22.1	0.43	4.6	2.5
	sim.	14.9	0.38	26.5	0.69	22.1	0.57	3.8	1.8
0.5	exp.	4.51	0.11	6.81	0.17	6.85	0.16	4.1	0.1
	sim.	4.59	0.12	6.84	0.17	7.06	0.18	3.9	0.3
0.6	exp.	1.85	0.045	2.32	0.062	2.85	0.063	2.2	2.1
	sim.	1.82	0.045	2.28	0.057	2.79	0.069	2.2	2.0
0.7	exp.	0.94	0.031	1.02	0.031	1.38	0.035	0.7	2.7
	sim.	0.94	0.025	1.02	0.026	1.39	0.035	0.7	3.1

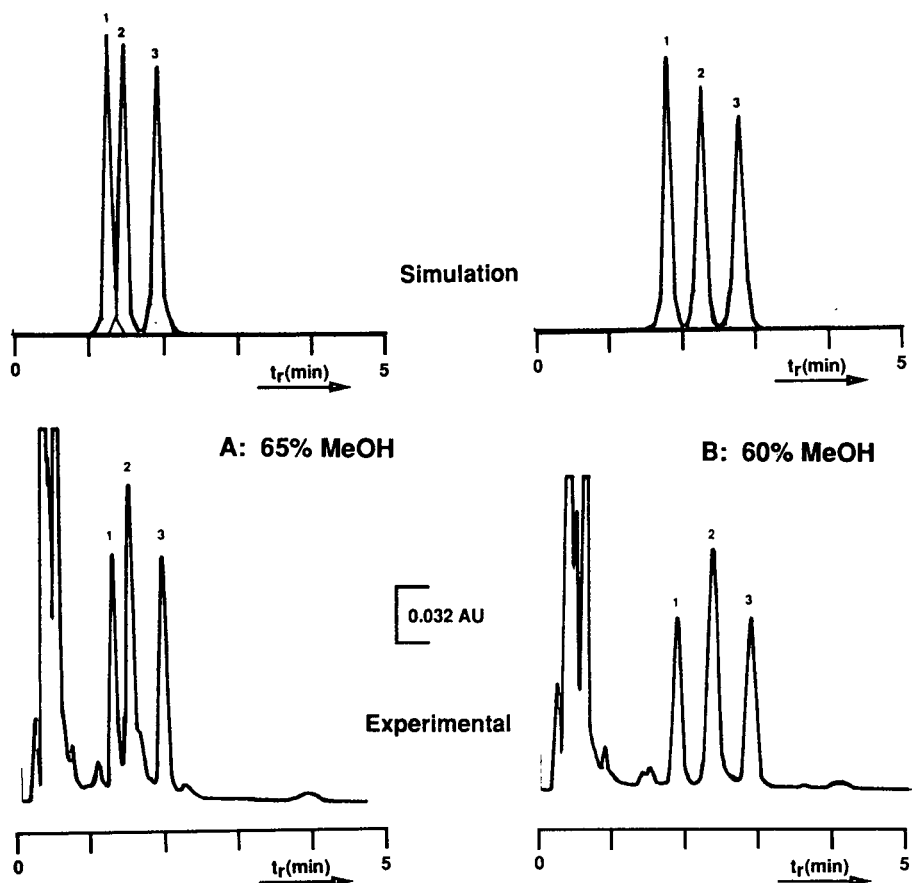


Fig. 7. Comparison of simulated and experimental isocratic chromatograms on C-1: A, 65% methanol and B, 60% methanol as the mobile phase. Injection of a 50- μ l fennel extract (0.1 g/ml) containing 50 ppm procymidone (1), 65 ppm iprodione (2) and a fennel interference (3); UV detection at 229 nm; flow-rate, 1 ml/min.

Prediction of retention and peak volume in step-gradient elution

The computer program used to simulate step-gradient conditions was first tested for a number of different one-step gradient elutions. The experimental values were obtained under column-switching conditions with the gradient profile C of Fig. 2, which has a delay time (t_d) of 0.18 min and time constant (τ) of 0.03 min.

The results of nine different one-step gradient elutions are listed in Table II. These data show a good agreement between prediction and experiment of chromatographic values for the various one-step gradient elutions. The deviations of the retention times are less than 2% and the deviations of the peak volumes are generally below 10%. Only in the last two gradients ($\Delta\phi > 0.35$), three deviations of approximately 25% in peak volume were observed.

Two examples, illustrating the good match of simulated and experimental

TABLE II

COMPARISON OF SIMULATED AND EXPERIMENTAL VALUES FOR ONE-STEP-GRADIENT ELUTION

exp. = Experimental with switching valves (Fig. 3); sim. = computer simulation with profile C of Fig. 2; calc. = calculated with eqn. 4.

Elution programme		Procymidone		Iprodione		Fennel		
Time (min)	ϕ (Methanol)		t_r (min)	σ (min)	t_r (min)	σ (min)	t_r (min)	σ (min)
4	0.50	exp.	4.49	0.042	5.19	0.055	5.38	0.065
∞	0.60	sim.	4.41	0.047	5.12	0.057	5.37	0.070
		calc.	4.46	—	5.14	—	5.38	—
1.5	0.60	exp.	1.89	0.038	2.19	0.036	2.51	0.047
∞	0.65	sim.	1.81	0.036	2.11	0.035	2.47	0.047
		calc.	1.81	—	2.09	—	2.44	—
5	0.40	exp.	6.05	0.032	6.39	0.040	6.68	0.045
∞	0.65	sim.	6.07	0.031	6.41	0.036	6.71	0.048
		calc.	6.08	—	6.4	—	6.69	—
2	0.40	exp.	3.25	0.033	3.58	0.042	3.88	0.038
∞	0.65	sim.	3.31	0.031	3.57	0.036	3.95	0.048
		calc.	3.29	—	3.54	—	3.92	—
5	0.40	exp.	6.38	0.045	7.01	0.055	7.28	0.065
∞	0.60	sim.	6.43	0.045	7.07	0.057	7.37	0.070
		calc.	6.43	—	7.05	—	7.36	—
3	0.40	exp.	4.58	0.045	5.15	0.062	5.54	0.061
∞	0.60	sim.	4.66	0.046	5.23	0.057	5.61	0.070
		calc.	4.65	—	5.2	—	5.59	—
2	0.40	exp.	3.77	0.048	4.38	0.058	4.85	0.062
∞	0.60	sim.	3.78	0.045	4.31	0.057	4.74	0.069
		calc.	3.75	—	4.28	—	4.71	—
5	0.30	exp.	6.31	0.028	6.56	0.042	6.95	0.038
∞	0.65	sim.	6.39	0.028	6.64	0.036	7.02	0.048
		calc.	6.36	—	6.59	—	6.98	—
5	0.30	exp.	6.01	0.021	6.12	0.032	6.42	0.032
∞	0.70	sim.	6.09	0.023	6.21	0.024	6.53	0.034
		calc.	6.06	—	6.16	—	6.49	—

chromatograms, are presented in Fig. 8. The chromatograms in this figure clarify that with the use of a one-step gradient the separation between fungicides and fennel is poor when using clean-up eluents of 50 or 60% methanol (Fig. 8A). Applying a one-step-gradient elution, baseline resolution between fungicides and fennel can be achieved with 30% methanol (for the removal of S1) and 70% methanol (to retain fennel as S2 on C-1) as clean-up solvents (Fig. 8B).

Finally, some two- and three-step-gradient elutions were investigated. As in a column-switching procedure, the instantaneous solvent change was achieved by stopping the flow on the column until the next solvent composition had reached the top

A - 4 ml 50% MeOH
- elution with 60% MeOH

B - 5 ml 30% MeOH
- elution with 70% MeOH

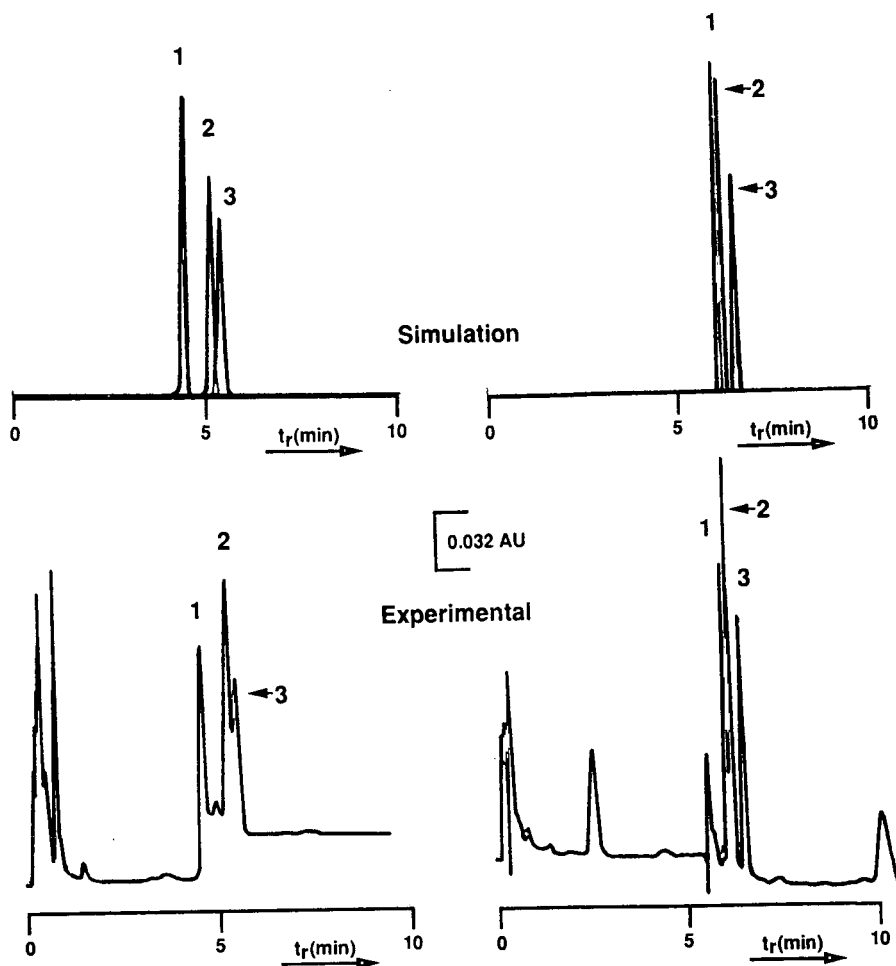


Fig. 8. Comparison of simulated and experimental one-step-gradient-elution chromatograms; conditions as in Fig. 7. For discussion, see text.

(entrance) of the column (see Fig. 3). In order to predict peak volumes under this type of multi-step gradient elution, the contribution to the peak volume (σ) during a "stop-flow" period must be known. For stop-flow experiments with time intervals of 1 to 5 min, using mobile phases of 40, 50 and 60% methanol, no significant contribution to the peak volume ($< 1\%$) of the solutes was measured on the 50×3 mm I.D. C_{18} column. This interesting result implies that the increase in peak volume during a stop-flow is small. A diffusion coefficient of $0.001 \text{ mm}^2/\text{min}$ for each compound was used in the computer program to account for this effect.

The obtained simulated and experimental results of one two-step- and two

different three-step-gradients are summarised in Table III. The similarity between predicted and experimental retention is again satisfactory. The predicted peak volumes are somewhat smaller than the experimental values with deviations in the range 10–30%. The performance of the simulation program is illustrated in Fig. 9, showing a good resemblance between a simulated and an experimental three-step-gradient elution chromatogram.

The data on the last two lines of Tables III include the results of the three-step-

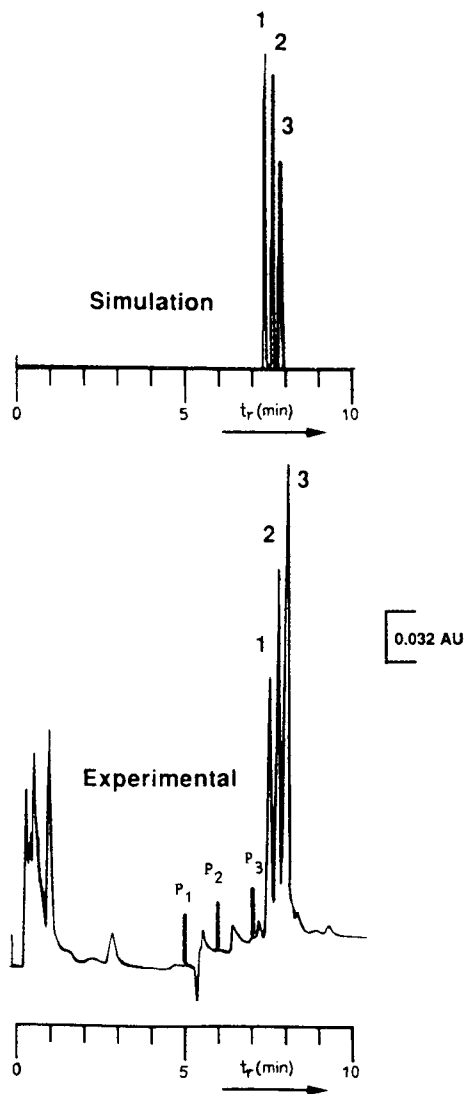


Fig. 9. Comparison of a simulated and experimental three-step-gradient-elution chromatogram: 5 min 30% methanol; 1 min 50% methanol; 1 min 60% methanol; elution with 70% methanol. P₁–P₃: stop-flow points of 2.5 min to obtain the right mobile phase composition (see Fig. 3); further conditions as in Fig. 6. Peaks: 1 = procymidone; 2 = iprodione; 3 = fennel.

TABLE III

COMPARISON OF SIMULATED AND EXPERIMENTAL VALUES FOR TWO- AND THREE-STEP-GRADIENT ELUTIONS

exp. = Experimental with switching valves (Fig. 3); sim. = computer simulation with profile C of Fig. 2; calc. = calculated with eqn. 5; exp.* = experimental with a binary pump system; sim.* = computer simulation with profile B of Fig. 2.

Elution programme			Procymidone		Iprodione		Fennel	
Time (min)	ϕ (Methanol)		t_r (min)	σ (min)	t_r (min)	σ (min)	t_r (min)	σ (min)
5	0.3	exp.	6.91	0.028	7.15	0.031	7.37	0.029
1.5	0.6	sim.	6.84	0.024	7.06	0.024	7.31	0.034
∞	0.7	calc.	6.9	—	7.09	—	7.32	—
2	0.4	exp.	4.47	0.047	4.71	0.041	4.92	0.047
1	0.5	sim.	4.34	0.024	4.59	0.024	4.81	0.034
1	0.6							
∞	0.7							
5	0.3	exp.	7.51	0.035	7.72	0.038	7.93	0.041
1	0.5	sim.	7.41	0.022	7.63	0.024	7.85	0.034
1	0.6							
∞	0.7	exp.*	8.48	0.045	8.95	0.051	9.15	0.051
		sim.*	8.64	0.035	9.04	0.035	9.28	0.044

gradient, but now executed with a binary pump possessing a gradient profile B as shown in Fig. 2. It is remarkable that also in this situation with a delay time of 2.5 min and a time constant of 1.3 min for the distortion of the solvent front, the predicted values for retention and peak volume correspond very well with the experimental values. Tables II and III also contain the results of the retention predicted with eqns. 4 and 5. The calculated values for the step-gradient elutions are in good agreement with the experimental and simulated values. Using these equations, the retention of solutes for one- and two-step-gradient programs performed with column switching can be determined very quickly.

Determination of procymidone and iprodione in fennel extracts

With the developed computer program two different clean-up procedures with either isocratic elution (heart-cutting) or a step-gradient elution were found to be suitable for the determination of procymidone and iprodione in fennel extracts. To verify the predicted optimal clean-up conditions experimentally, realistic additions of procymidone and iprodione at the 1-ppm level to fennel extracts were made and the spiked samples were analysed with an RPLC column-switching system as described in Fig. 3. In this set-up, a 100×4.6 mm I.D. column packed with MicroSpher C_{18} , $3 \mu\text{m}$, was used as the second separation column (C-2). In a first experiment the two separation columns, C-1 and C-2, were coupled on-line and a sample ($50 \mu\text{l}$) of a spiked fennel extract (1 g/ml) was analysed without clean-up using a mobile phase of 70% methanol in water (1 ml/min). The resulting chromatogram, shown in Fig. 10A, seems to illustrate that a clean-up procedure with column switching is not necessary. However, it is not advisable to inject fennel extracts without clean-up onto analytical columns.

Chromatogram B of Fig. 10 demonstrates the result of a selected two-step-gradient elution (result of Fig. 8B), using a clean-up on C-1 with 5 ml of 30% methanol and 0.9 ml of 70% methanol, followed by a transfer of the fungicides containing fraction from C-1 to C-2 with 0.3 ml of 70% methanol.

The last chromatogram (Fig. 10C) shows the predicted isocratic heart-cutting clean-up on C-1 using 70% methanol for M-1 and M-2 (see Table I). An even more "clean" chromatogram is obtained with this eluent using 0.85 ml for the clean-up on C-1 and 0.3 ml for the transfer of the fungicides from C-1 to C-2.

So far, the solvent strength in our column-switching procedures was only varied using one organic modifier. The good separation result with the proposed procedure is in agreement with earlier studies [24,25], indicating that an accurate variation of the solvent strength can result in useful changes in elution order favourable for the separation of compounds with a similar molecular size and chemical nature. It is well known that solvent optimization using different solvents (usually methanol, acetonitrile and tetrahydrofuran) can be very successful for influencing the elution order for maximum resolution of the sample compounds [21,26,27]. In future research we will examine if this powerful option can be built into the prediction program. However, in this study, the same retention behaviour of the involved compounds was observed (similar to Fig. 6) using acetonitrile instead of methanol which made the application of a second modifier not attractive for this study.

No clean-up: C-1 on-line C-2.

Clean-up: - 5.0 ml 30% MeOH
- 0.9 ml 70% MeOH.
Transfer: - 0.3 ml 70% MeOH.

Clean-up: 0.85 ml 70% MeOH.
Transfer : 0.30 ml 70% MeOH.

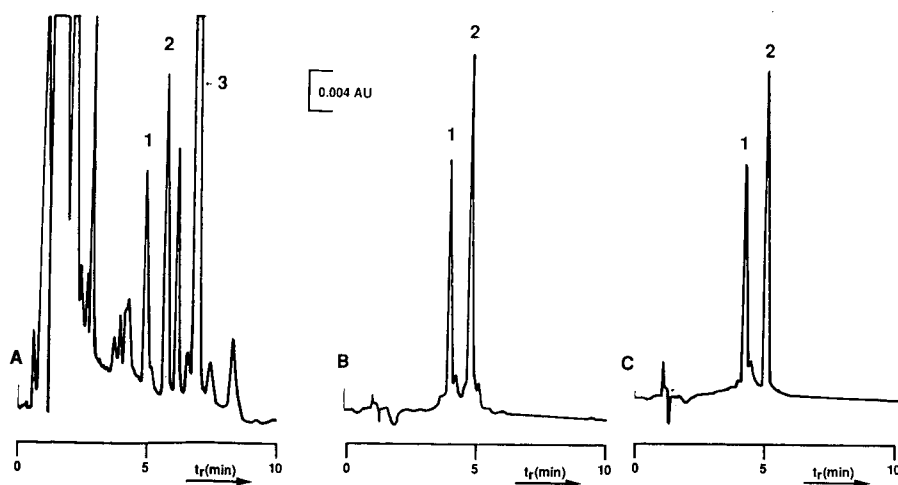


Fig. 10. Final results of the clean-up performance of a fennel (3) extract (1 g/ml) spiked with 1 ppm procymidone (1) and 1.3 ppm iprodione (2). Injection: 50 μ l on C-1; UV detection at 229 nm. For further explanation, see text.

CONCLUSIONS

A new approach for the prediction of retention and peak volume of compounds, occurring under step-gradient RPLC conditions has been described. From the $\ln k$ vs. φ relations of the involved compounds and the plate number (N) of the column, accurate chromatograms are rapidly simulated with a computer program. Compared to trial-and-error optimisation of column-switching procedures this approach yields a significant time saving in finding optimal clean-up conditions with beneficial aspects, such as reduced solvent consumption and extension of the column life.

Good performance of the simulation program has been demonstrated for the residue analysis of procymidone and iprodione in fennel extracts.

The developed procedure, tested in this paper on column switching, is not restricted by the dimensions of the column. Consequently, the computer program is amendable for the optimisation of a separation problem on a high-efficiency column applying step-gradient elution. Using sensitive UV detection, step-gradient elution will provide more stable baselines in comparison to linear gradient elution [28]. This aspect makes this type of elution very suitable for trace-level determination of pesticides which we will examine in future research.

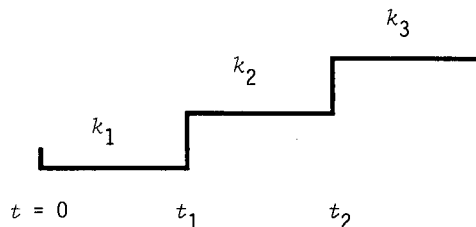
ACKNOWLEDGEMENTS

The technical assistance of Mrs. M. de Lange and Mr. J. Smits is greatly acknowledged.

APPENDIX 1

Derivation of equations for the prediction of the retention time of a solute, i , under one- and two-gradient-elution conditions with correction for the place in a column

To derive an equation correcting the position of a solute for the changing solvent fronts used in step-gradient elution, we consider an ideal one- or two-step gradient with solvent fronts migrating through the column without deformation. Schematically the involved steps are as follows:



In this diagram t_1 and t_2 are the switching-time intervals after the start of the elution program at $t = 0$ and k_1 , k_2 and k_3 are the corresponding capacity factors of the solute at three different mobile phase compositions. During the first elution with a time t_1 , the solute will travel a distance, ΔL , which equals

$$\Delta L = ut_1/(1 + k_1) \quad (\text{A1})$$

where u is the velocity of the unretained compound.

After the first change in composition the solute migrates with k_1 until it is taken over by the next front. The passing takes place at time t_{p1} , when the position of the solute corresponds to that of the front, according to the equation

$$ut_{p1}/(1 + k_1) = u(t_{p1} - t_1 - t_d) \quad (\text{A2})$$

in which t_d is delay time of the step gradient for reaching the top of the column. Rearranging eqn. A2 gives

$$t_{p1} = \{(1 + k_1)/k_1\} (t_1 + t_d) \quad (\text{A3})$$

The travelled distance during the first step with correction for solvent delay is equal to

$$\Delta L_1 = ut_{p1}/(1 + k_1) = (u/k_1)(t_1 + t_d) \quad (\text{A4})$$

For a one-step gradient the solute will elute from the column with the second solvent. The distance to be travelled during this final step corresponds to

$$\Delta L_2 = L - \Delta L_1 \quad (\text{A5})$$

With $L = ut_0$ (t_0 is the retention time of the unretained compound), the retention time of the second step, t_{p2} , is obtained by dividing ΔL_2 by the migration factor $u/(1 + k_2)$ which results in

$$t_{p2} = u[t_0 - (t_1 + t_d)/k_1](1 + k_2)/u \quad (\text{A6})$$

Eqn. A6 can be rearranged into

$$t_{p2} = t_0(1 + k_2) - [(t_1 + t_d)(1 + k_2)/k_1] \quad (\text{A7})$$

The final retention time, t_r , is obtained by adding the two retentions ($t_{p1} + t_{p2}$) which results in

$$t_r = t_0(1 + k_2) + (t_d + t_1)[(k_1 - k_2)/k_1] \quad (\text{A8})$$

This equation describes the retention time of a solute for one-step gradient elution.

For the prediction of the retention time occurring in a two-step gradient elution, the process continues at eqn. A4, the travelled distance during the first elution with correction for solvent delay. After the executing of the second switch, at time t_2 , the second solvent front will pass the solute at time t_{p2} according to the equation

$$(u/k_1)(t_1 + t_d) + u/(1 + k_2) \{t_{p2} - [(1 + k_1)/k_1](t_1 + t_d)\} = u(t_{p2} - t_2 - t_d) \quad (\text{A9})$$

Reorganising eqn. A9 renders

$$t_{p2} = [(t_1 + t_d)(k_2 - k_1)]/k_2k_1 + [(t_2 + t_d)(1 + k_2)]/k_2 \quad (\text{A10})$$

The travelled distance of the solute during time t_{p2} is then

$$\Delta L_2 = \{u(t_{p2} - t_{p1})\}/(1 + k_2) \quad (\text{A11})$$

Substitution of eqns. A3 and A10 in eqn. A11 gives

$$\Delta L_2 = [u/(1 + k_2)] \{[(t_1 + t_d)(k_2 - k_1)]/k_2k_1 + [(t_2 + t_d)(1 + k_2)]/k_2 - [(1 + k_1)/k_1](t_1 + t_d)\} \quad (\text{A12})$$

Rearranging eqn. A12 gives

$$\Delta L_2 = (u/k_2)(t_2 - t_1) \quad (\text{A13})$$

which is the travelled distance during the second elution with correction for the delay of the solvent front.

The sum of the travelled distance is obtained by the addition of eqns. A4 and A13 rendering

$$\Sigma \Delta L = u[t_d/k_1 + t_1(k_2 - k_1)/k_2k_1 + t_2/k_2] \quad (\text{A14})$$

After the two elution steps the solute will be eluted from the column with the third and final elution solvent. The distance to be travelled during this last step corresponds with

$$\Delta L_3 = L - \Sigma \Delta L \quad (\text{A15})$$

With $L = ut_0$, the retention time of the third step, t_{p3} , is found by dividing ΔL_3 by the migration factor $u/(1 + k_3)$ which gives

$$t_{p3} = u[t_0 - t_d/k_1 - t_1(k_2 - k_1)/k_2k_1 - t_2/k_2](1 + k_3)/u \quad (\text{A16})$$

For the final elution time, t_r , the retention time of the first two steps (t_{p2} , eqn. A10) must be added to the retention time of last step (t_{p3} , eqn. A16)

$$t_r = [(t_1 + t_d)(k_2 - k_1)]/k_2k_1 + [(t_2 + t_d)(1 + k_2)]/k_2 + t_0(1 + k_3) - [t_d(1 + k_3)/k_1] - t_1[(k_2 - k_1)(1 + k_3)]/k_2k_1 - t_2(1 + k_3)/k_2 \quad (\text{A17})$$

Reorganising eqn. A17 gives

$$t_r = t_0(1 + k_3) + t_d[(k_1 - k_3)/k_1] + [t_1(k_1 - k_2)k_3]/k_1k_2 + t_2[(k_2 - k_3)/k_2] \quad (\text{A18})$$

which is the predicted retention time of a solute in a two-step-gradient elution.

REFERENCES

- 1 C. E. Goewie and E. A. Hogendoorn, *J. Chromatogr.*, 404 (1987) 352.
- 2 C. E. Goewie and E. A. Hogendoorn, *J. Chromatogr.*, 410 (1987) 211.

- 3 E. A. Hogendoorn and C. E. Goewie, *J. Chromatogr.*, 475 (1989) 432.
- 4 E. A. Hogendoorn, C. E. Goewie, H. H. van den Broek and P. A. Greve, *Meded. Fac. Landbouwwet., Rijksuniv. Gent*, 49 (1984) 1219.
- 5 P. A. Greve (Editor), *Analytical methods for Residues of Pesticides in Foodstuffs*, SDU Publishers, The Hague, 5th ed., 1988.
- 6 P. Jandera and J. Churáček, *J. Chromatogr.*, 170 (1979) 1.
- 7 P. Jandera and J. Churáček, *J. Chromatogr.*, 91 (1974) 223.
- 8 M. Borówko, M. Jaroniec, J. Narkiewicz, A. Patrykiewicz and W. Rudzinski, *J. Chromatogr.*, 153 (1978) 309.
- 9 M. Borówko, M. Jaroniec, J. Narkiewicz and A. Patrykiewicz, *J. Chromatogr.*, 153 (1978) 321.
- 10 W. Golkiewicz and M. Jaroniec, *J. High Resolut. Chromatogr. Chromatogr. Commun.*, 1 (1978) 245.
- 11 E. Soczewinski and W. Markowski, *J. Chromatogr.*, 370 (1986) 63.
- 12 W. Markowski, *J. Chromatogr.*, 485 (1989) 517.
- 13 W. Golkiewicz, *Chromatographia*, 14 (1981) 411.
- 14 W. Golkiewicz, *Chromatographia*, 14 (1981) 629.
- 15 W. Golkiewicz, *Chromatographia*, 21 (1986) 259.
- 16 W. Markowski and W. Golkiewicz, *Chromatographia*, 25 (1988) 339.
- 17 B. F. D. Ghrist, B. S. Cooperman and L. R. Snyder, *J. Chromatogr.*, 459 (1988) 1.
- 18 B. F. D. Ghrist and L. R. Snyder, *J. Chromatogr.*, 459 (1988) 25.
- 19 B. F. D. Ghrist and L. R. Snyder, *J. Chromatogr.*, 459 (1988) 43.
- 20 J. W. Dolan, J. R. Grant and L. R. Snyder, *J. Chromatogr.*, 165 (1979) 31.
- 21 P. J. Schoenmakers, H. A. H. Billiet, R. Tijssen and L. de Galan, *J. Chromatogr.*, 149 (1978) 519.
- 22 L. R. Snyder and J. J. Kirkland, *Introduction to Modern Liquid Chromatography*, Wiley, New York, 2nd ed., 1979.
- 23 J. C. Giddings, *J. Chem. Phys.*, 31 (1959) 1462.
- 24 M. A. Quarry, R. L. Grob, L. R. Snyder, W. Dolan and M. P. Rigney, *J. Chromatogr.*, 384 (1987) 163.
- 25 L. R. Snyder, M. A. Quarry and J. L. Glajch, *Chromatographia*, 24 (1987) 33.
- 26 S. Sekulic, P. R. Haddad and C. J. Lambertson, *J. Chromatogr.*, 363 (1986) 125.
- 27 P. J. Schoenmakers and M. Mulholland, *Chromatographia*, 25 (1988) 737.
- 28 E. A. Hogendoorn and P. van Zoonen, *Meded. Fac. Landbouwwet., Rijksuniv. Gent*, 55 (1990) 1275.

CHROMSYMP. 2145

Production and use of capillary traps for headspace gas chromatography of airborne volatile organic compounds

B. V. BURGER*, M. LE ROUX, Z. M. MUNRO and M. E. WILKEN

Laboratory for Ecological Chemistry, University of Stellenbosch, Stellenbosch 7600 (South Africa)

ABSTRACT

The production of adsorption traps with activated charcoal particles embedded on the inside surface of glass capillary tubes and of capillary traps containing thick (10-15 μm) and ultra-thick (145 μm) films of an apolar stationary phase is described. The application of these traps to the headspace detection of organic volatiles in various gas samples and in air and the problems involved in the use of these traps are discussed.

INTRODUCTION

Strictly, the determination of airborne volatiles released into the atmosphere by, for example, living organisms or industrial processes is not a headspace analytical problem. With certain adaptations the basic principles can, however, be applied equally effectively to the determination of airborne volatiles in a gas that is not in equilibrium with a liquid or a solid. This field of analytical work has been reviewed by Núñez *et al.* [1] and several books and monographs have appeared on the subject [2,3].

Automated systems for the routine determination of headspace volatiles are commercially available. These systems perform fairly well in normal headspace analyses, but the volumes of headspace gas that can be sampled are often relatively small. The increasing awareness of the deleterious effects of some airborne volatiles on the environment, and the threat to human health from even small concentrations of hazardous chemicals in the atmosphere, have created the need for more sensitive methods of detection in which volatiles can be concentrated from large volumes of air. The trapping of volatiles on various adsorbents in packed traps has therefore become popular. The trapped volatiles are normally desorbed thermally, swept from the trap and transferred to the analytical column by the carrier gas. However, desorption with a solvent, followed by conventional analysis of a sample of the extract, can also be done. Concentrating the volatiles on a trap in an off-line manner has the advantage that samples can be taken at any time at short notice and can be stored for subsequent analysis.

Packed traps, however, have serious disadvantages. One of these is that in many applications such large amounts of adsorbent are used that the formation of artefacts by decomposition during thermal desorption or by concentration from slightly impure solvents cannot be avoided. As pointed out by Grob and Habich [4], packed traps were developed for use in packed-column gas chromatography (GC) and, when applied to

capillary analysis, have given unsatisfactory results, the most serious problem being incomplete transfer of the sample from the trap to the capillary column. This is due to the difference between the flow-rate required for complete and rapid desorption from, for example, a packed 3 mm I.D. concentration trap and the flow-rate through a capillary column. Grob and Habich approached this problem by using capillary traps with approximately the same diameter as the capillary column, whereby the linear flow-rate through the trap is increased to facilitate rapid and complete sample desorption. Two trap types, a charcoal-coated open-tubular trap (COT) and a trap coated with a thick layer of immobilized PS-255 (FT), were used with promising results.

Unfortunately, Professor Kurt Grob died before he could complete his pioneering work on these capillary traps. However, his enthusiasm for this work prompted others to continue with the further development of the technique. Activated charcoal traps were made by Burger *et al.* [5] and used for the GC-mass spectrometric (MS) determination of plant volatiles. Conditions under which thermally labile compounds could be desorbed from activated charcoal traps [6] and a method for the desorption of such compounds with a suitable solvent [7] were developed, and techniques for the introduction of the traps into the injector of the gas chromatograph for the desorption of the volatiles were elaborated [8].

These traps, although suitable for the qualitative detection of organic volatiles in air samples, have relatively low capacities for highly volatile substances. One way to increase the capacity of a capillary trap is to increase its length. A device for the desorption of volatiles from such a long (1 m) capillary trap was developed by Burger and Munro [6], and the capacities of capillary traps coated with a stationary phase and with a combination of stationary phase and several different adsorbents were determined. Such long capillary traps were also used by Bicchi *et al.* [9] for the determination of plant volatiles. Blomberg and Roeraade [10] succeeded in increasing the capacity of these traps considerably by increasing the thickness of the stationary phase film to about 100 μm by immobilizing a thick prepolymer film formed on the column wall during dynamic coating.

Despite a considerable volume of research having been done on both the short and long capillary traps, their application has been limited to use by a few groups with the expertise and instrumentation for their production and use. This is an unfortunate situation, because these traps lend themselves to the trapping of airborne volatiles in emergency situations with which any analytical laboratory might be faced at any time. It is the aim of this paper to give detailed descriptions of the production of various trap types and the techniques for the trapping, desorption and analysis of volatiles from a variety of gas samples.

EXPERIMENTAL

Instrumental

GC analyses were carried out with Carlo Erba Model 4160 and 5300 and Siemens Sichomat 2 gas chromatographs equipped with flame ionization detectors, using helium as carrier gas. All glass and fused-silica capillaries used for analytical separations were coated by the Laboratory for Ecological Chemistry. Column specifications and analytical conditions are given in Figs. 3-8. GC-MS analyses were performed with a Carlo Erba QMD 1000 system.

Production of activated charcoal capillary traps (COTs)

Capillary traps coated with a layer of activated charcoal particles were produced by a method adapted from that used by Grob [11]. Activated charcoal (SCII; Chemviron, Brussels, Belgium) was ground in a TS 250 swingmill (Dickie and Stockler, Johannesburg, South Africa) for 1 min and elutriated through a series of screens. The 25–38- μm fraction was washed with 6 *M* nitric acid to remove heavy metal ions and basic material, whereafter it was washed free from acid on a sintered-glass filter. It was then stirred with distilled water for several days and finally filtered off, dried in an oven at 120°C and stored in an air-tight bottle.

A glass-wool plug with a length of about 3 mm was inserted into a length of glass capillary tubing (20 cm \times 1.16 mm O.D. \times 0.45 mm I.D.) followed by a thin glass rod (7 cm \times 0.35 mm). The rod was used to push the glass-wool plug into the capillary and was inserted into the capillary so that its tail-end was about 3 mm inside the tip of the capillary, which was just sufficiently constricted in a flame to prevent the rod from falling out. The tail-end of the glass rod had an uneven surface to prevent it from forming a gas-tight seal with the constricted tip of the capillary.

Activated charcoal was filled into the capillary, which was dropped down a 3-m length of glass tubing onto a hard surface to compact the charcoal until a column of 8 cm of activated charcoal had been obtained. A glass-wool plug followed by a thin glass rod was then inserted from the upper end of the capillary and the capillary was carefully bent at an angle of 90° about 5 cm above the glass-wool plug. This prevented the glass rod from being moved upwards by gas expelled from the activated charcoal when heated. The capillary was fastened along the aligned edges of a U-shaped aluminium support (1.5 mm thickness) with bands of aluminium foil, which were in turn firmly stretched over the capillary with the help of elastic insulating tape as shown in Fig. 1. Vacuum (0.01 Torr) was applied to both ends of the glass capillary and the activated charcoal was heated carefully with the flame from a small Bunsen burner, starting from the top of the column of activated charcoal particles and moving downwards. After this step had been repeated two or three times, the packed section of the capillary was finally heated to red heat, again slowly moving downwards along the capillary with the tip of the flame. The capillary was left to cool under vacuum and was then removed from the U-shaped support and trimmed to the required length (*ca.* 7 cm). Activated charcoal particles not in contact with the glass were blown from the capillary with a jet of nitrogen from a length of fused-silica tubing (0.1 mm I.D. \times 0.17 mm O.D.). In some instances it was necessary to loosen particles by gently turning the fused-silica tube. The sharp edges of the finished capillary were finally rounded with a small diamond file.

Production of thick-film capillary traps (FTs)

Thick-film capillary traps were produced by coating borosilicate-glass or fused-silica capillary tubing (*ca.* 0.3–0.35 mm I.D.) with a thick film of cross-linked, apolar stationary phase. Traps with a 15- μm film of cross-linked polydimethylsiloxane, for example, were made by using a solution of 2.82 g of PS 255 (vinyl-modified polydimethylsiloxane; Petrarch Systems, Bristol, PA, U.S.A.) and 85 mg of dicumyl peroxide (DCUP) in 15 ml of pentane. Stationary phases such as SE-30 and SE-54 dissolve very slowly and the mixture of stationary phase, DCUP and solvent was therefore left to stand in the dark for at least 1 day.

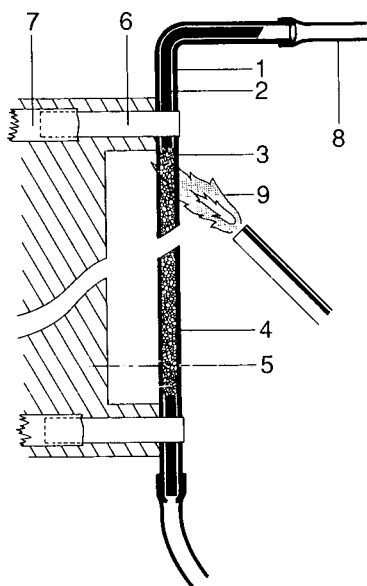


Fig. 1. Production of an activated charcoal open-tubular trap (COT). 1 = Borosilicate capillary tubing; 2 = thin glass rod; 3 = fine glass-wool plug; 4 = activated charcoal particles; 5 = aluminium plate; 6 = aluminium foil strip; 7 = elastic insulating tape; 8 = polyethylene connections to vacuum pump; 9 = flame from small Bunsen burner.

Lengths of fused-silica capillary tubing (*ca.* 2–3 m \times 0.32 mm I.D.) were coated with the stationary phase by the static coating technique. To do this, one end of a capillary had to be sealed before the vacuum was applied to the other end to evaporate the solvent from the solution in the capillary. There are several methods to seal off glass and fused-silica capillaries, one of which is to use a plug of hardened waterglass. It must be taken into consideration, however, that waterglass will not adhere to the fused silica in the presence of a highly concentrated solution of the stationary phase. An intermediate plug of a solvent is therefore required. Capillaries were therefore coated as follows: a plug of about 5 cm of pentane was carefully pushed into a capillary using a conventional capillary filling vessel. The pressure was released and the other end of the capillary was closed by inserting in into a piece of silicone-rubber such as a septum in order to prevent the solvent from flowing back out of the capillary. The end of the capillary containing the solvent was then lowered into the stationary phase solution, using another capillary filling vessel. Care was taken not to introduce an air bubble into the capillary between the pentane and coating solution. The stationary phase solution was pushed into the capillary, care being taken not to exceed the maximum allowable pressure in the glass vessel. It is also good practice to use a safety shield during this operation. As soon as the solvent had reached the other end of the capillary the latter was stoppered with the rubber septum. The inlet end of the capillary was removed from the coating solution, wiped clean and also stoppered with a septum. The first septum was removed, the tip of the capillary dipped into a waterglass solution and the longest possible section of the capillary warmed with the

hand or with the help of a piece of cloth soaked in water at 35–40°C. This forced a small volume of pentane out of the capillary. As soon as a few droplets of pentane had left the capillary, the heat source was removed and a short plug of waterglass was sucked into the capillary. The capillary was removed from the waterglass and laid down horizontally in a draught-free location. Extreme care was taken to avoid temperature fluctuations, for example by touching the capillary, to avoid the waterglass being forced out of the capillary by the expanding liquid. The stopper at the other end was removed and the capillary was left for 12–24 h to allow the waterglass to harden. To avoid breakthrough due to the presence of microscopic bubbles in the coating solution or solvent, the liquid in the capillary was pressurized with nitrogen at 1–2 kg/cm² for a few hours. This normally does not remove tiny bubbles in the waterglass and it is therefore advisable to use waterglass that has not recently been shaken or poured into a smaller vessel, but rather to fill a convenient vessel with the waterglass a day or more in advance.

Vacuum (*ca.* 20 Torr) was then applied to the open end of the capillary. This can be done with the capillary in a water-bath, but care has to be taken to avoid any moisture coming into contact with the waterglass, as it will soften and cause breakthrough. We prefer to carry out the removal of the solvent with the capillary in a horizontal position on the laboratory bench where it had been left for the waterglass to dry. After all the solvent had been evaporated from the capillary, it was opened at the other end and purged for several hours with nitrogen. Both ends were sealed with septa, then the capillary was coiled and heated in a GC oven from 160 to 200°C at 0.3°C/min, whereafter it was opened, connected to the injector of a gas chromatograph and conditioned at 270°C for several days. It was used as a long capillary trap or divided into short (5–7-cm) traps.

Production of ultra-thick-film traps (UFTs)

Traps having linings of a cross-linked polysiloxane rubber with a thickness of *ca.* 145 μm were prepared by stretching a polysiloxane–rubber tube (0.65 mm O.D. × 0.30 mm I.D., Silastic, medical grade tubing; Dow Corning, Midlands, MI, U.S.A.) freezing it in liquid nitrogen and inserting it into a fused-silica capillary tube (0.53 mm I.D.). On removal of the capillary from the liquid nitrogen, the rubber tube regained its elasticity and expanded to fit tightly into the capillary, giving a capillary trap with a 145-μm lining and an I.D. of 240 μm. The finished product was conditioned at 270°C for several days with a carrier gas flow of *ca.* 5 ml/min and used as a long (1-m) capillary trap or divided into short traps. A detailed description of the production of UFTs has appeared elsewhere [12].

Loading the traps

The headspace gas was drawn through the trap at a suitable flow-rate (see figure legends), which was regulated by using a length of glass or fused-silica tubing as a restriction. For applications requiring very long sampling times, such as the detection of organic volatiles in the atmosphere or the trapping of semiochemicals in the field, a portable vacuum bottle was made from a 14-l light petroleum gas container fitted with, *inter alia*, a vacuum meter and a needle valve. A T-piece was used for applications requiring sampling in parallel with two traps or trap types. All connections downstream from the traps were made with polyethylene tubing (1.2 mm O.D. × 0.9 mm

I.D.). In applications requiring the headspace gas to be forced through the traps, nitrogen that had been purified by passing it through a column of activated charcoal was used. In these analyses the traps were inserted into the headspace through screw-caps fitted with PTFE-lined silicone-rubber septa. Determinations of the organic volatiles in human breath were done by either drawing a sample of the breath from an inflated PTFE gas sampling bag (BGI, Waltham, MA, U.S.A.) or, preferably, by sampling the breath flowing through a glass breathing tube (2 cm I.D.) at atmospheric pressure. The glass tube was fitted with a simple diaphragm type non-return valve and the breath was withdrawn from the breathing tube through a small hole just downstream from the non-return valve, about 15 cm from the person's mouth.

Owing to the strong adsorption of many compounds on glass and other surfaces, the use of syringes to handle headspace gas samples was avoided except in basic studies in which, for example, gas samples containing highly volatile compounds were used to study the capacity of traps for different compounds.

Desorption of the trapped volatiles

Volatiles were desorbed from short traps in the injector of a gas chromatograph as described by Grob and Habich [4], by inserting the trap into the injector from below (Fig. 2). The column was fitted with a ferrule and the other hardware normally used for its installation. The trap was connected to the column with a short length of shrinkable PTFE tubing. In order to avoid thermal decomposition of the stationary phase in the trap and possibly also in the column, the connection was pre-shrunk on glass capillaries with the same outside diameter as the trap and column.

If a fused-silica capillary column is used, it is possible that the available PTFE tubing will not shrink to the required diameter. It is then advisable to fit the column with one half of a press-fit connector which is connected to the capillary trap with the PTFE tubing as shown in Fig. 2.

In some gas chromatographs the injector has a very small hole which cannot be widened to allow easy passage of the shrinkable PTFE connection between trap and column. In some of these instruments it is possible to remove the septum cap, push the capillary column upwards until it protrudes from the top of the injector, whereafter the trap can be connected to the column. The trap can then be lowered into the injector, the septum cap replaced and the ferrule-retaining nut tightened. If the carrier gas is left turned on during this operation and the split valve is open, the introduction of air into the capillary column is restricted to some extent. However, if the trap has to be introduced into the injector from the top, the method recently described by Grob *et al.* [8] will produce more reliable results.

The desorption of volatiles from a long trap can be done by installing it in a stainless-steel tube which can be ohmically heated [6]. The analyses in this study, however, were carried out using a Siemens Sichromat 2 gas chromatograph. The trap was installed in the first oven with the analytical column in the second. The live switching device of the instrument was not used. The trap was connected to the analytical column with a re-useable butt connector [13] or, in the case of a long ultra-thick-film trap, by using a short length of thinner fused silica, one end of which was permanently connected to the column with a press-fit connector and the other end simply inserted into the trap, the silicone-rubber lining of the trap providing a gas-tight

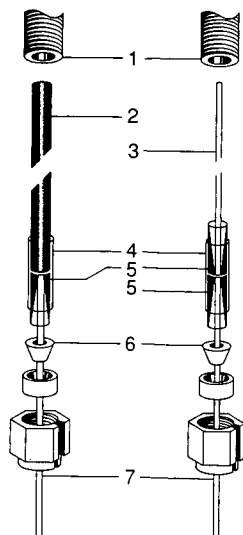


Fig. 2. Connection of capillary traps to a fused-silica capillary column for desorption of trapped volatiles in the injector of a gas chromatograph. 1 = Injector; 2 = borosilicate glass with activated charcoal particles embedded on its inside surface (COT); 3 = fused-silica capillary coated with a thick film of stationary phase (FT); 4 = shrinkable PTFE tubing; 5 = one half of a press-fit connector; 6 = ferrule; 7 = fused-silica column.

connection. All connections were positioned in the first oven to reduce the effect of any possible cold spots and dead volumes in the connections between trap and column. The volatiles desorbed from the trap in the first oven were cryotrapped on the analytical column by selecting an appropriately low temperature in the second oven, or by using solid carbon dioxide.

RESULTS AND DISCUSSION

The production of activated charcoal open-tubular traps (COTs) was demonstrated by Professor Kurt Grob during a course at the University of Stellenbosch in 1986. In principle the method consists in fusing activated charcoal particles into the inside surface of a borosilicate glass capillary tube. This is done by packing the capillary with the charcoal particles, applying vacuum to the open end of the capillary tube and heating the capillary with a small Bunsen burner in order to force the charcoal particles into the soft glass. The charcoal that has not been in contact with the glass is subsequently blown out of the charcoal-coated capillary with a thin fused-silica capillary tube. We have used the same method, but it was found that traps of about 6 cm could be produced only with difficulty as a sudden release of gas from the activated charcoal towards the end of the process often caused the expansion of the traps, which then had to be discarded. Another problem encountered at a later stage was that the charcoal particles did not adhere properly to the glass surface and could easily be blown out to leave an almost empty capillary with a rough inside surface.

These two problems were solved by removing all traces of fine activated charcoal dust from the material to be used in the traps, because restriction of the flow of gas through the capillary was apparently responsible for the sudden expansion of capillaries during the heating process. Fine dust particles sticking to the larger activated charcoal particles apparently also prevented proper contact between these particles and the glass surface. The only way to remove all the fine dust particles was to wash the activated charcoal through a series of sieves with water. It was found that one of the resulting fractions produced by this procedure and having a particle size of 25–38 μm gave perfectly stable COTs. As a further precaution against the expansion of the glass during heating, vacuum was applied to both ends of the capillary tube as shown in Fig. 1.

Activated charcoal traps, although preferred for trapping the more volatile compounds, have certain disadvantages. The first is the high catalytic activity of the material, which often results in decomposition of thermally labile compounds, resulting in the production of artefacts. This is illustrated by a comparison of the results obtained with an FT (d_f 10 μm) and a COT (particle size 25–38 μm) in the headspace analyses of a white wine (Fig. 3). The COT clearly has a very high capacity and even very volatile compounds such as ethanol (eluting at *ca.* 10 min) are retained on the trap. However, with the exception of a few of the constituents normally present in wine, all of the components eluting before ethanol (compare the expanded trace in Fig. 3B) appear to be artefacts. These compounds are not present in the analysis carried out with the FT (Fig. 3C) but, on the other hand, only relatively small amounts of the other highly volatile headspace constituents of the wine were retained on this trap. From a comparison of the gas chromatograms shown in Fig. 3 it appears that, even allowing for a longer sampling time, the later eluting peaks produced by the FT are larger than those produced by the COT. This may be due to irreversible adsorption and/or decomposition on the COT, or otherwise to the preferential adsorption of moisture by the activated charcoal which, consequently, gradually loses its ability to retain the larger molecules. Organic volatiles are retained on the FT by dissolution in the apolar phase layer, which is highly hydrophobic. The water therefore does not have any appreciable influence on the retention of the organic volatiles on the FT. Apparently neither of these traps is ideal for this specific analysis. However, if certain highly volatile and thermally stable compounds have to be trapped, the COT may still be the best trap for the purpose. The FT, again, may be ideal for the determination of thermally labile heavy constituents in a headspace gas. As mentioned earlier, the thermal decomposition of labile compounds can be avoided to a certain extent by temperature-programmed desorption [6], or even more effectively by desorption with solvent, followed by direct transfer of the solvent plus the volatiles to the capillary column for analysis [7].

In some analyses of gas samples with a high moisture content, it was found that the colour of the activated charcoal changed from a dull grey to shiny black, presumably owing to the adsorption or condensation of moisture in the trap. Again only limited amounts of highly volatile compounds were retained when this happened. This is illustrated by an analysis with a COT and an FT in parallel of the air in a chemical factory (Fig. 4).

In view of the often unpredictable behaviour of COTs, we prefer to use FTs in the exploratory stages of an investigation. In principle, pieces of a thick-film fused-silica or

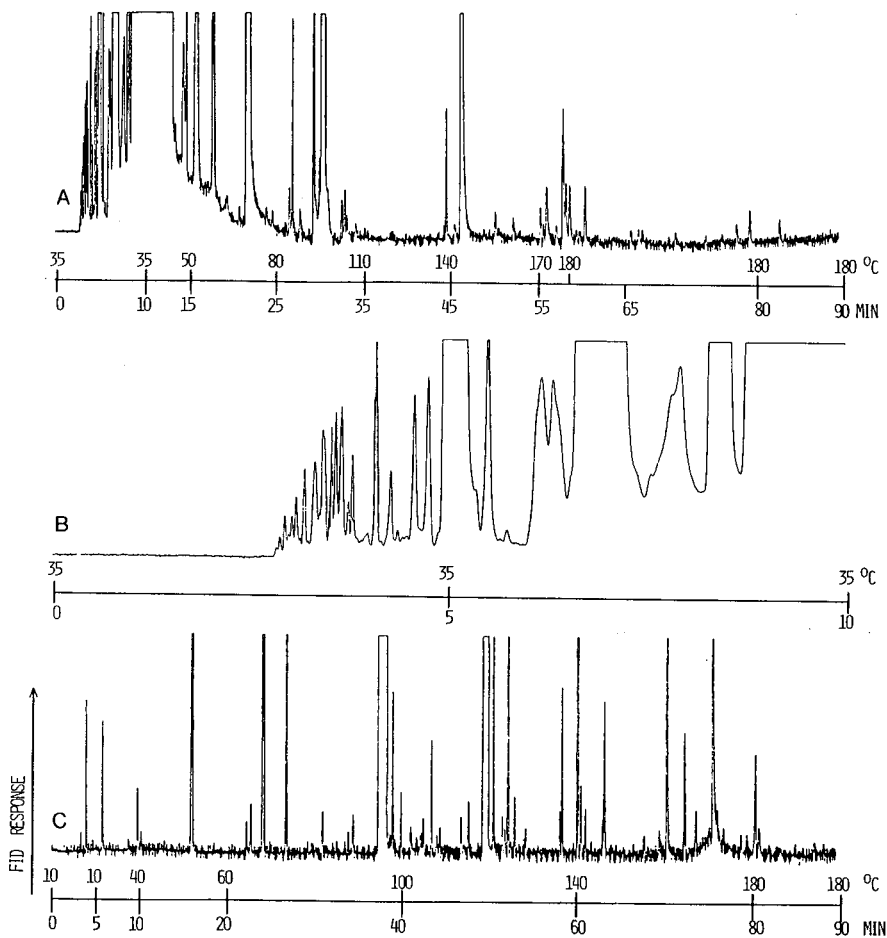


Fig. 3. Chromatograms from the headspace gas of a white wine (Chenin blanc). Column, 30 m \times 0.32 mm I.D. fused silica, 0.25- μ m cross-linked Carbowax 20M; helium as carrier gas at 25 cm/s. (A) Volatiles trapped from 11 ml of headspace gas drawn through a COT (particle size 25–38 μ m) at 3.4 ml/min, desorbed by temperature programming the injector from 100 to 300°C at *ca.* 20°C/min and cryotrapped on the column with solid CO₂; column held at 35°C for 10 min and then programmed from 35 to 180°C at 3°C/min. (B) Expanded section of (A). (C) Volatiles trapped from 34 ml of headspace gas drawn through an FT (film thickness 10 μ m) at 3.4 ml/min; desorbed in the injector of the gas chromatograph at 180°C for 5 min and cryotrapped on the column with solid CO₂; column held at 10°C for 5 min and then programmed from 30 to 180°C at 2°C/min. Data acquisition was started after completion of the desorption step. FID = Flame ionization detection.

glass column can be used as short film traps. However, most applications require traps having much thicker stationary phase films than those used in commercially available columns and prospective users of this technique therefore have to be able to produce traps in the laboratory. The problems involved in obtaining straight lengths of glass capillary tubing with the correct dimensions, coating the tubing and coupling the trap to the capillary column, are probably responsible for the apparent lack of interest in

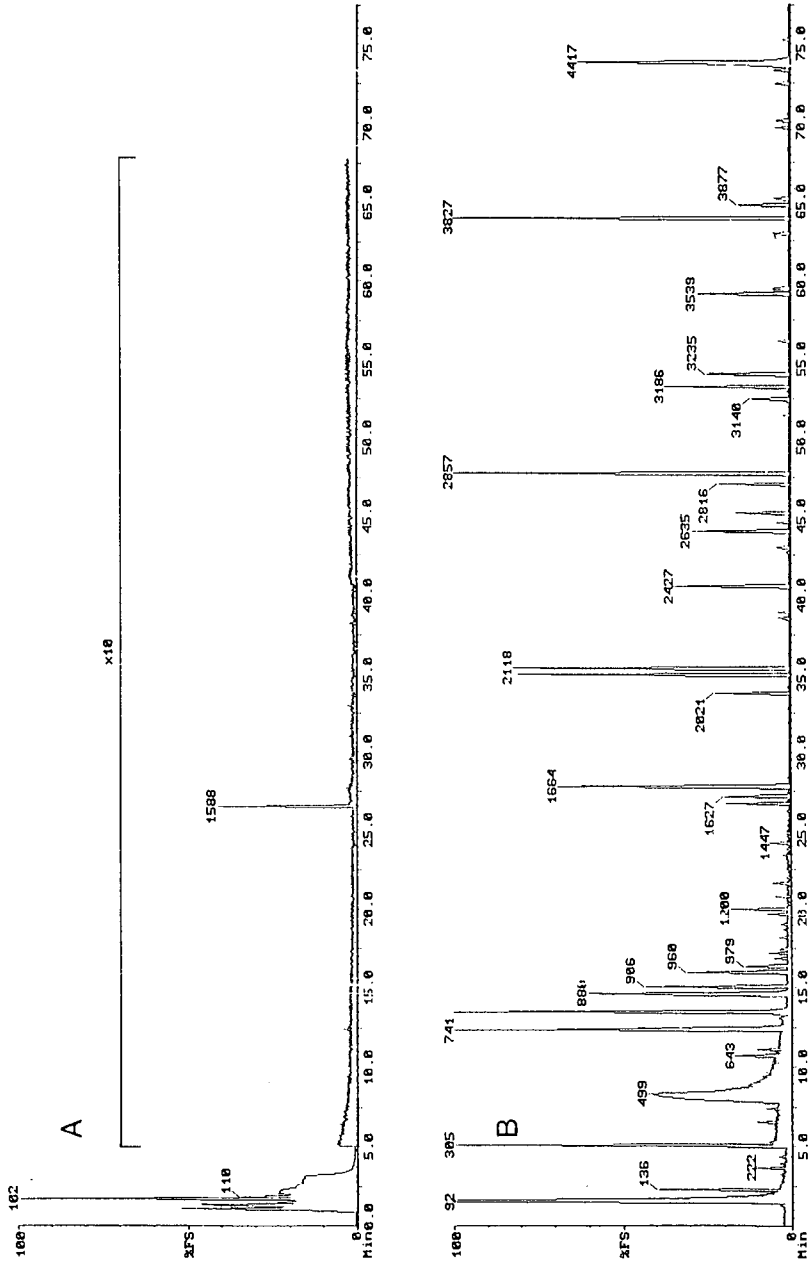


Fig. 4. GC-MS analysis of airborne organic volatiles in a chemical plant. Column, 40 m \times 0.3 mm I.D. glass, 0.6- μ m PS 089-OH; helium as carrier gas at 28.6 cm/s; temperature programme, 40–250°C at 2°C/min; 450 ml of air sampled at 30 ml/min. Activated charcoal and film traps used in parallel. (A) Volatiles trapped on a COI (particles size 25–38 μ m) and desorbed by temperature programming the injector from 120 to 220°C at *ca* 20°C/min; the volatiles were cryotrapped on the column with solid CO₂. (B) Volatiles trapped on an FT (film thickness 10 μ m), desorbed at 200°C and cryotrapped on the column with solid CO₂. Data acquisition started after completion of the desorption step.

capillary trapping techniques. We prefer to prepare short capillary traps from straight lengths of glass capillary tubing, as it is possible to seal off a filled glass capillary with a tiny flame and to remove the small gas bubble that is formed during the process within less than 1 min. In this paper the production of short traps from fused-silica tubing is described, as this material is readily available. It is possible, however, that shrinkable PTFE tubing that will shrink tightly onto fused silica with O.D. 0.45 mm may not be available. This problem can be solved by increasing the diameter of the column by making use of a press-fit connector cut in half. One half of the connector is permanently connected to the column and the other half to the fused-silica trap, whereafter the trap and column can be connected to each other with shrinkable PTFE tubing in the usual manner (Fig. 2). It is advisable, however, to pre-shrink the connecting PTFE tubing on the two sections of the press-fit connector before they are fitted to the column and trap, to avoid damaging their stationary phase layers.

The limited capacity of short film traps was a serious problem until Blomberg and Roeraade [10,14,15] developed short and long capillary traps with film thicknesses of up to 100 μm . These traps therefore have stationary phase layers that are about six times as thick as those obtainable with static coating procedures. They used an

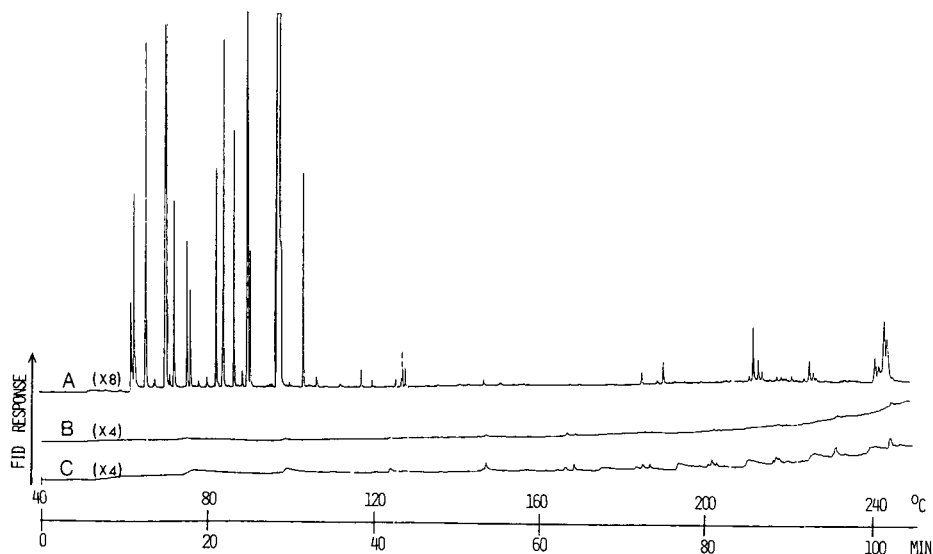


Fig. 5. Quantitative analysis of the headspace gas from 20 g of the pulp of a yellow monkey orange (*Strychnos madagascariensis*). Column, 40 m \times 0.3 mm I.D. glass, 0.4- μm OV-1701-OH; helium as carrier gas at 28.6 cm/s; temperature programme, 40–250°C at 2°C/min. (A) Headspace gas (1 ml) was pushed through two short (7-cm) ultra-thick-film traps (film thickness 145 μm) connected in series to the 1-l flask containing the fruit at 0.5 ml/min; trapped volatiles desorbed at 220°C. Constituents determined: 1 = 1-butanol (0.7 μg); 2 = methyl butanoate (1.5 μg); 3 = ethyl 2-methylpropanoate (2.6 μg); 4 = ethyl butanoate (29.8 μg); 5 = butyl acetate (1.4 μg); 6 = ethyl 2-methylbutanoate (1.1 μg); 7 = propyl butanoate (1.6 μg); 8 = butyl propanoate (2.6 μg); 9 = methyl hexanoate (1.9 μg); 10 = butyl 2-methylpropanoate (16.2 μg); 11 = butyl butanoate (45.1 μg). Quantification was done by on-column injection of a mixture of the synthetic compounds as external standards. The desorbed volatiles were not cryotrapped, and the analysis was started directly after the traps had been installed in the injector. (B) Gas chromatogram of volatiles desorbed from the second trap; desorption at 220°C. (C) Blank analysis; desorption at 250°C.

ingenious technique to produce these traps, but it is unlikely that the expertise required for the production of the traps will be available in many analytical laboratories. We therefore devised a simple method of inserting a polysiloxane-rubber lining into fused-silica capillaries in order to produce traps with a film thickness of 145 μm and a final I.D. of 240 μm . These traps were expected to have a high background owing to the thermal decomposition of the very thick rubber lining. It was found, however, that background peaks that could be expected to interfere with the detection of minor constituents in a headspace gas, appeared only when the desorption was done at 250°C. In Fig. 5 a quantitative GC analysis is shown of the headspace gas of the fleshy parts of the fruit of the tree *Strychnos madagascariensis* (yellow monkey orange tree). The fruit has a flavour similar to that of the mango and is particularly rich in the esters of butanoic acid. The flavour constituents were trapped under conditions that gave no breakthrough to a second trap, connected in series to the first, and the analysis thus gives an indication of the capacity of an ultra-thick-film trap. Despite the high capacity of the trap, desorption of the esters at an injector temperature of 220°C was rapid enough to give acceptable peak shapes even for the early-eluting constituents, without having to resort to cryotrapping of the desorbed volatiles.

In initial experiments with long ultra-thick-film traps a desorption temperature of 100°C was used in order to avoid the possible generation of background peaks. As expected, the long desorption time of 25 min resulted in peak broadening of the more

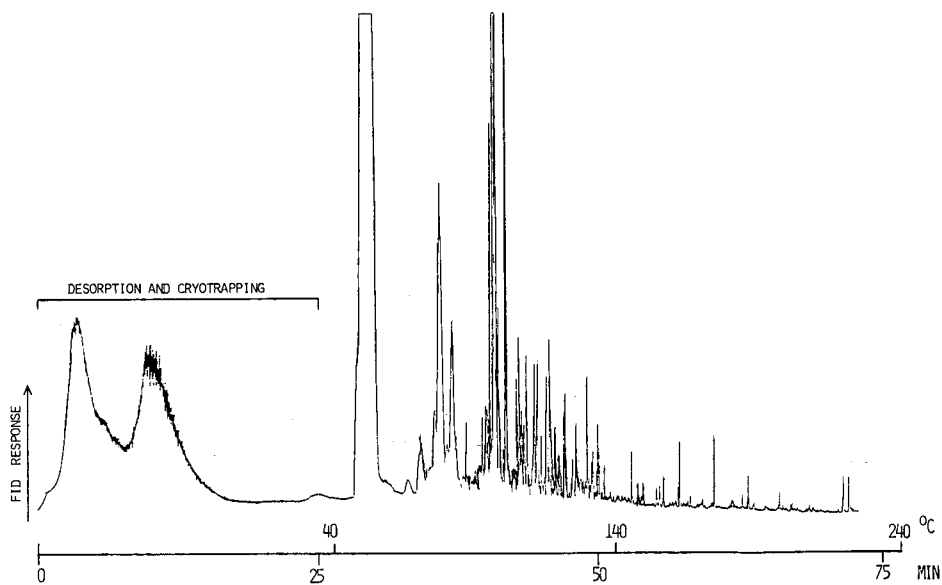


Fig. 6. Chromatogram of the organic volatiles trapped from the air in a synthetic organic chemistry laboratory. Column, 25 m \times 0.32 mm I.D. fused silica, 0.75- μm cross-linked PS 255; helium as carrier gas at 28.6 cm/s; temperature programme, 40–250°C at 4°C/min. The volatiles were trapped from 1.2 l of air on a 1-m ultra-thick-film trap (film thickness 145 μm) at a flow-rate of 13 ml/min, desorbed at 100°C for 25 min and cryotrapped at 0°C.

volatile constituents. This is illustrated by a chromatogram of the volatiles from the air in a chemical laboratory shown in Fig. 6. In Fig. 7 two analyses of air sampled from a street in Stellenbosch are shown, illustrating the improved peak shapes of the more volatile compounds obtained by cryotrapping at a lower temperature. Cryotrapping with solid carbon dioxide gave perfect peak shapes in the GC separation of the organic volatiles in human breath shown in Fig. 8.

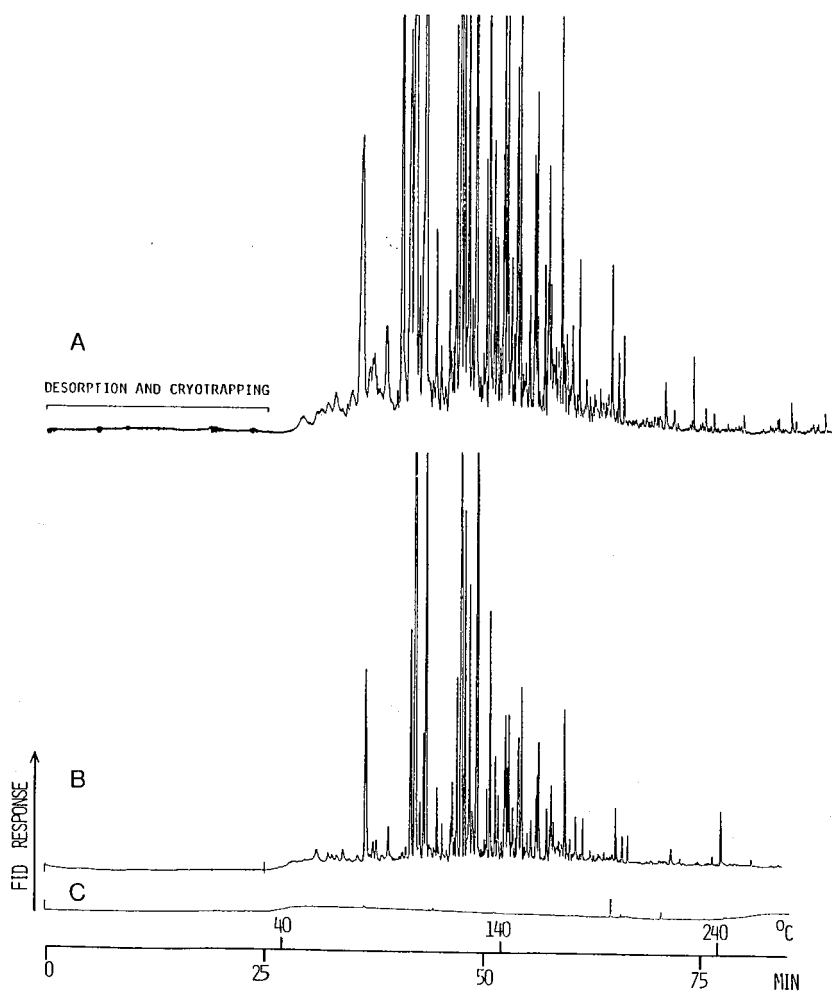


Fig. 7. Chromatograms of the organic volatiles trapped at different times of the day from air on a street in Stellenbosch. The volatiles were trapped from 1.3 l of air on a 1-m ultra-thick-film trap (film thickness 145 μm) at a flow-rate through the trap of 13 ml/min. Gas chromatographic conditions as in Fig. 6. (A) Volatiles desorbed at 100°C for 25 min and cryotrapped at 0°C. (B) Volatiles desorbed at 100°C for 25 min and cryotrapped at -17°C. (C) Blank analysis: desorption at 100°C for 25 min; cryotrapping with solid CO_2 .

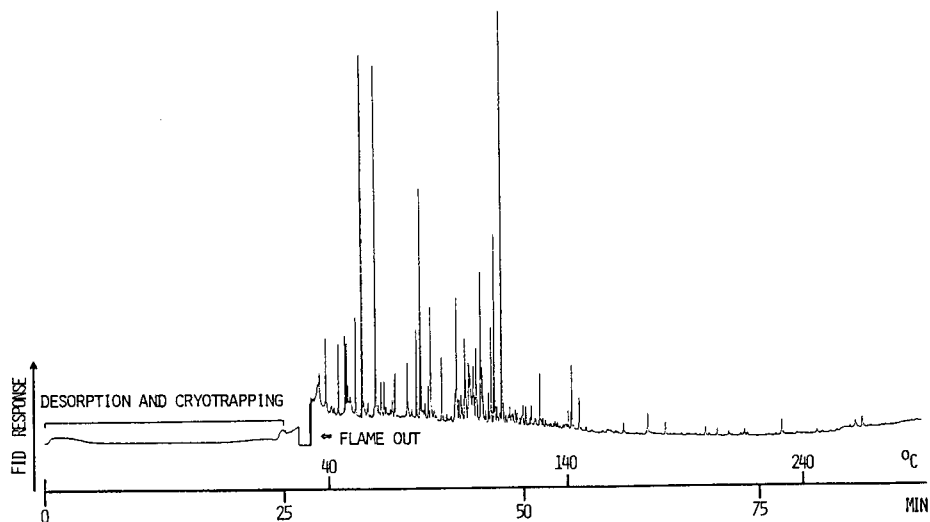


Fig. 8. Chromatogram of organic volatiles trapped from 1.3 l of human breath on a 1-m ultra-thick-film trap (film thickness 145 μm) at a flow-rate through the trap of 13 ml/min. The breath was drawn from a breathing pipe fitted with a non-return valve. The volatiles were desorbed at 100°C for 25 min and were cryotrapped on the column with solid CO_2 . Chromatographic conditions as in Fig. 6.

CONCLUSIONS

COTs have a high capacity, and even highly volatile compounds can be effectively trapped on them. However, they behave unpredictably when volatiles are trapped from gas with a high moisture content or when long sampling times have to be employed. Decomposition of thermally labile compounds during the desorption from a COT is a problem. FTs are to be preferred in the exploratory stages of a headspace analytical investigation. Highly volatile compounds are, however, not effectively retained and may be present in the resulting gas chromatogram only in low proportions. Work on the application of UFTs to headspace analytical problems is still in an early stage. The capacity of these traps is expected to be about ten times that of the FTs, but more research has to be done to determine their capacity for specific compounds and compound types, and to establish optimum conditions for their desorption. Fortunately they have a remarkably low bleed in spite of the thickness of the polysiloxane-rubber lining. Except when the headspace contains highly volatile or relatively involatile constituents, it should be possible to analyse almost any headspace gas with these traps.

ACKNOWLEDGEMENTS

The support of this work by the Foundation for Research Development (Pretoria, South Africa) and the University of Stellenbosch is gratefully acknowledged.

REFERENCES

- 1 A. J. Núñez, L. F. González and J. Janák, *J. Chromatogr.*, 300 (1984) 127.
- 2 G. Charalambous (Editor), *Analysis of Food and Beverages, Headspace Techniques*, Academic Press, New York, 1978.
- 3 B. Kolb (Editor), *Applied Headspace Gas Chromatography*, Heyden, London, 1980.
- 4 K. Grob and A. Habich, *J. Chromatogr.*, 321 (1985) 45.
- 5 B. V. Burger, Z. M. Munro and J. H. Visser, *J. High Resolut. Chromatogr. Chromatogr. Commun.*, 11 (1988) 496.
- 6 B. V. Burger and Z. Munro, *J. Chromatogr.*, 370 (1986) 449.
- 7 B. V. Burger and Z. Munro, *J. Chromatogr.*, 402 (1987) 95.
- 8 K. Grob, A. Artho, Ch. Frauenfelder and I. Roth, *J. High Resolut. Chromatogr.*, 13 (1990) 257.
- 9 C. Bicchi, A. D'Amato, F. David and P. Sandra, *J. High Resolut. Chromatogr.*, 12 (1989) 316.
- 10 S. Blomberg and J. Roeraade, *J. High Resolut. Chromatogr. Chromatogr. Commun.*, 11 (1988) 457.
- 11 K. Grob, *Second Kurt Grob Course on Capillary Chromatography*, University of Stellenbosch, 1986.
- 12 B. V. Burger, M. le Roux and W. J. G. Burger, *J. High Resolut. Chromatogr.*, 13 (1990) 777.
- 13 B. V. Burger, unpublished work.
- 14 J. Roeraade and S. Blomberg, *J. High Resolut. Chromatogr.*, 12 (1989) 138.
- 15 S. Blomberg and J. Roeraade, *J. High Resolut. Chromatogr.*, 13 (1990) 509.

CHROMSYMP. 2093

Investigation of cross-linking chiral stationary phases within capillary columns

XIANWEN LOU, YOUQIN LIU and LIANGMO ZHOU*

Dalian Institute of Chemical Physics, Chinese Academy of Sciences, Dalian 116012 (China)

ABSTRACT

Four diamide chiral stationary phases (CSPs), undecenoyl-L-valine-(*S*)- α -phenylethylamide (CSP-1), OV-225-L-valine-*tert*-butylamide (CSP-2), XE-60-L-valine-*tert*-butylamide (CSP-3) and poly-cyanoethyl vinyl siloxane 25% cyanoethyl-L-valine-*tert*-butylamide, were cross-linked within both glass and fused-silica capillary columns with dibenzoyl peroxide (DBP) as the cross-linking reagent. The effects of the CSP skeleton on the degree of cross-linking and racemization (decrease in enantiomeric excess) of the stationary phase during cross-linking were investigated. The performance of the cross-linked columns in terms of enantioselectivity, thermal stability, acid-base characteristics and column efficiency were determined and compared. The results show that the CSP skeleton may have considerable effects on both cross-linking and racemization.

INTRODUCTION

Since the first paper on the direct separation of amino acid enantiomers by gas chromatography (GC) [1], the development of novel chiral stationary phases has attracted wide attention. In GC, the direct separation of enantiomers is more efficient, sensitive, accurate and faster than indirect separation. The performance of direct GC separation depends to a large extent on the performance of the CSPs or the chiral columns used. Usually cross-linked capillary columns have more stable films and can even be used in supercritical fluid chromatography (SFC) [2,3]. Great efforts have been made in preparing cross-linked chiral capillary columns in recent years. Several methods for the immobilization of CSPs within capillary columns have been suggested [4-7], but in the cross-linking of diamide CSPs racemization effects have been observed [6].

It was the purpose of this work to investigate the effects of CSP skeletons and cross-linking conditions on the performance of cross-linked chiral capillary columns in terms of the degree of cross-linking, decrease in enantiomeric excess (e.e.), etc.

EXPERIMENTAL

Chemicals and materials

CSP-1 was synthesized in our laboratory [8]. CSP-2, CSP-3 and CSP-4 were

synthesized according to Frank *et al.* [9] and Saeed *et al.* [10] with some modifications [11]. OV-225, XE-60 and SE-54 were obtained from Chrompack, PEG 20M from Fluka, amino acids from Sigma, polycyanoethyl vinyl siloxane from Jiling Chemical Industry Co. and blank fused-silica capillary columns from Yongnian Optical Fibre Manufacturer.

Preparation of columns

Unless stated otherwise, the columns were statically coated with a 1% (w/v) dichloromethane solution of the stationary phase and a 6% (w/w, based on the stationary phase) solution of DBP. After static coating, the columns were conditioned under a carrier gas flow. Cross-linking was carried out with temperature programming from 40 to 190°C, the final temperature being maintained at 190°C for 2 h. The columns were then rinsed successively with pentane, dichloromethane and water. All the columns were tested in a GC RIA gas chromatograph equipped with a split injector and a flame ionization detector, before and after rinsing.

Determination of racemization

In order to determine the racemization of the stationary phase during cross-linking, the cross-linked columns were filled with 6 M hydrochloric acid, both ends were sealed and the stationary phases in the columns were hydrolysed at 110°C for 20 h [6]. After cooling the hydrolysates were collected, dried, derivatized and then analysed on a cross-linked CSP-4 column. Racemization was expressed as the decrease in e.e.:

$$\begin{aligned} D(\text{e.e.}) &= 1 - [A(\text{L}) - A(\text{D})]/[A(\text{L}) + A(\text{D})] \\ &= [2 A(\text{D})]/[A(\text{L}) + A(\text{D})] \end{aligned} \quad (1)$$

where $D(\text{e.e.})$ is the decrease in the enantiomeric excess and $A(\text{L})$ and $A(\text{D})$ are the peak areas of L- and D-Val, respectively, in the hydrolysates.

Derivatization

Amino acids were derivatized as N(O,S)-trifluoroacetyl isopropyl esters according to McKenzie and Tenaschuk [12].

RESULTS AND DISCUSSION

The structures and basic performances of the CSPs are listed in Table I.

TABLE I
STRUCTURES AND BASIC PERFORMANCES OF THE CHIRAL STATIONARY PHASES

CSP	Structure	M.p. (°C)	$[\alpha]_{\text{D}}^{20}$ in CH_2Cl_2	Maximum temperature limit (°C)
CSP-1	Undecenoyl-L-Val-(S)- α -NHCH(CH ₃)C ₆ H ₅	101-103	-36.0	180
CSP-2	OV-225-L-Val-NHC(CH ₃) ₃		-7.3	190
CSP-3	XE-60-L-Val-NHC(CH ₃) ₃		-10.7	180
CSP-4	Polycyanoethyl vinyl siloxane-L-Val-NHC(CH ₃) ₃		-8.8	180

TABLE II
EFFECTS OF DBP/CSP RATIO ON CROSS-LINKING AND RACEMIZATION

CSP	DBP (%)		2		6		12		20		100	
	<i>d</i> (%) ^a	<i>e</i> (%) ^b	<i>d</i> (%)	<i>e</i> (%)	<i>d</i> (%)	<i>e</i> (%)	<i>d</i> (%)	<i>e</i> (%)	<i>d</i> (%)	<i>e</i> (%)	<i>d</i> (%)	<i>e</i> (%)
CSP-2			40	20	65	26			62	30	60	38
CSP-3									12	3	23	7
CSP-4	39	2	43	2	68	2	60	4			55	10

^a Degree of cross-linking (%).

^b Decrease in e.e. (%) of the stationary phase.

CSP-1 is a stationary phase with vinyl groups, but its molecular weight is low (386) and it can only be co-cross-linked with polymeric molecules such as PEG 20M or SE-54 to obtain sufficient cross-linking. However, after adding polymeric molecules, the enantioselectivity of the CSP was decreased and the polarity changed [13].

The effects of the DBP/CSP ratio on the degree of cross-linking (%) and racemization of CSP-2, CSP-3 and CSP-4 are listed in Table II.

CSP-2 is a stationary phase with a polycyanopropyl siloxane skeleton (OV-225). A degree of cross-linking of 65% can be obtained, but with pronounced racemization (decrease in e.e. = 26%) (Table II).

CSP-3 and CSP-4 are stationary phases with a polycyanoethyl skeleton. Although the degree of cross-linking of CSP-3 is not satisfactory, the decrease in e.e. is only 7% even with 100% (w/w based on CSP-3) of DBP. CSP-4 also contains

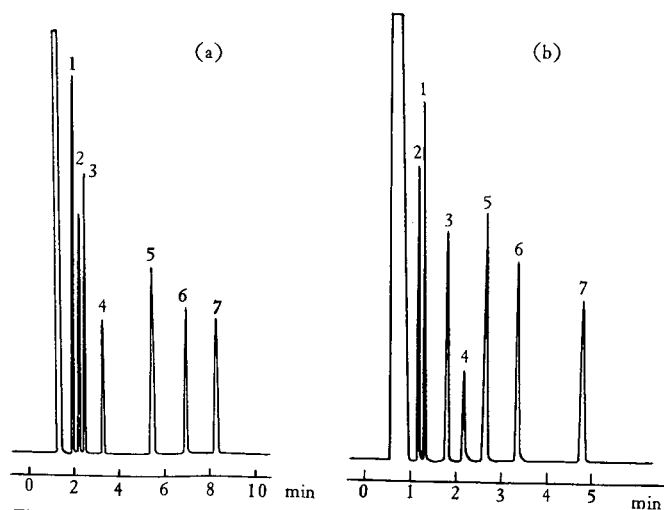


Fig. 1. Chromatograms of the test mixture in cross-linked columns. Columns (20 m × 0.25 mm I.D.): (a) cross-linked CSP-2 fused silica; (b) cross-linked CSP-4 fused silica. Temperature, 130°C; carrier gas, hydrogen. Peaks: 1 = dodecane; 2 = 2-octanone; 3 = tridecane; 4 = 1-octanol; 5 = naphthalene; 6 = 2,6-dimethylaniline; 7 = 2,6-dimethylphenol.

TABLE III
BASIC PERFORMANCE OF THE CROSS-LINKED COLUMNS

Stationary phase	<i>d</i> (%) ^a	<i>e</i> (%) ^b	<i>CE</i> (%) ^c	Acid/base ^d	Maximum temperature limit (°C)
CSP-1 + PEG 20M	50		75	1.02	190
CSP-1 + SE-54	50		75	1.04	190
CSP-2	65	26	80	1.02	210
CSP-3	12	3	55	1.01	
CSP-4	68	2	85	1.02	210

^a Degree of cross-linking (%).

^b Decrease in e.e. (%) of the stationary phase.

^c Coating efficiency; sample, alanine; temperature, 120°C.

^d Ratio of peak area per unit weight of 2,6-dimethylphenol to 2,6-dimethylaniline at 140°C.

vinylgroups, and gives good results with respect to both degree of cross-linking (68%) and racemization (decrease in e.e. = 2%) in comparison with the other CSPs studied. For CSP-2 and CSP-4, 6% DBP is optimum in preparing the cross-linked columns; a higher proportion did not increase the cross-linking but increased the racemization (Table II).

Fig. 1 shows the chromatograms of a mixture of apolar, polar, acidic and basic compounds with known composition by the cross-linked columns. The peaks in the chromatograms are almost symmetric.

TABLE IV
 α -VALUES OF AMINO ACID ENANTIOMERS ON THE CROSS-LINKED COLUMNS

Amino acid	CSP-1 + PEG 20M		CSP-2		CSP-4	
	α	<i>T</i> (°C)	α	<i>T</i> (°C)	α	<i>T</i> (°C)
Ala	1.030	100	1.089	100	1.133	100
Val	1.042	100	1.069	100	1.096	100
Thr	1.026	100	1.048	110	1.088	100
a-Ile	1.046	100	1.053	120	1.114	100
Ile	1.044	100	1.047	120	1.100	100
Leu	1.050	100	1.107	100	1.187	100
Pro					1.013	100
Ser	1.020	100	1.034	130	1.062	120
Asp	1.009	130	1.026	130	1.034	130
Met	1.031	130	1.039	150	1.079	140
Phe	1.030	130	1.033	150	1.067	140
Glu	1.023	130	1.034	150	1.069	140
Orn			1.029	190	1.037	190
Tyr			1.023	190	1.028	190
Lys			1.026	190	1.033	190
Trp			1.021	190	1.028	190
<i>n</i> -Val	1.038	110	1.078	120	1.148	100
<i>n</i> -Leu	1.038	110	1.066	120	1.154	100

TABLE V
THERMAL STABILITY OF WALL-COATED AND CROSS-LINKED CSP-4 COLUMNS

Sample: alanine. Test temperature: 130°C.

Wall-coated			Cross-linked		
Temperature (°C)	Time (h)	α	Temperature (°C)	Time (h)	α
190	4	1.087	190	2	1.085
190	14	1.087	200	12	1.083
190	24	1.086	200	22	1.081
190	44	1.082	200	42	1.080

The basic performances of the cross-linked capillary columns are listed in Table III. It can be seen that CSP-4 gives the best results with respect to both degree of cross-linking and racemization among the four CSPs studied.

The separation factors (α -values) of amino acid enantiomers on the cross-linked columns are listed in Table IV. Table V shows the thermal stability of both wall-coated and cross-linked CSP-4 columns. The cross-linked column can be used up to at least 200°C without noticeable bleeding and racemization.

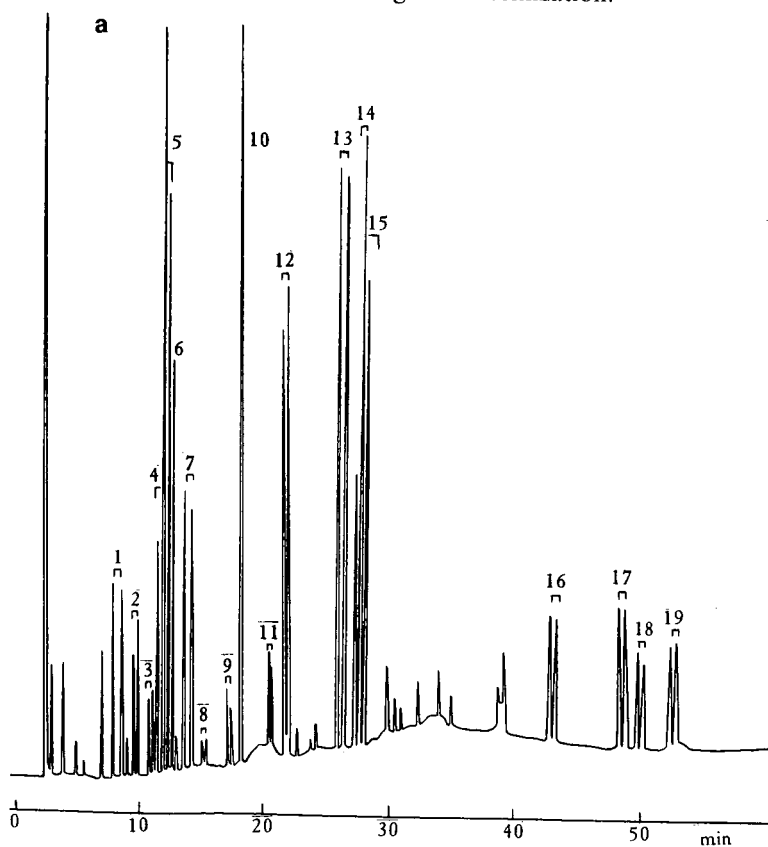


Fig. 2.

(Continued on p. 158)

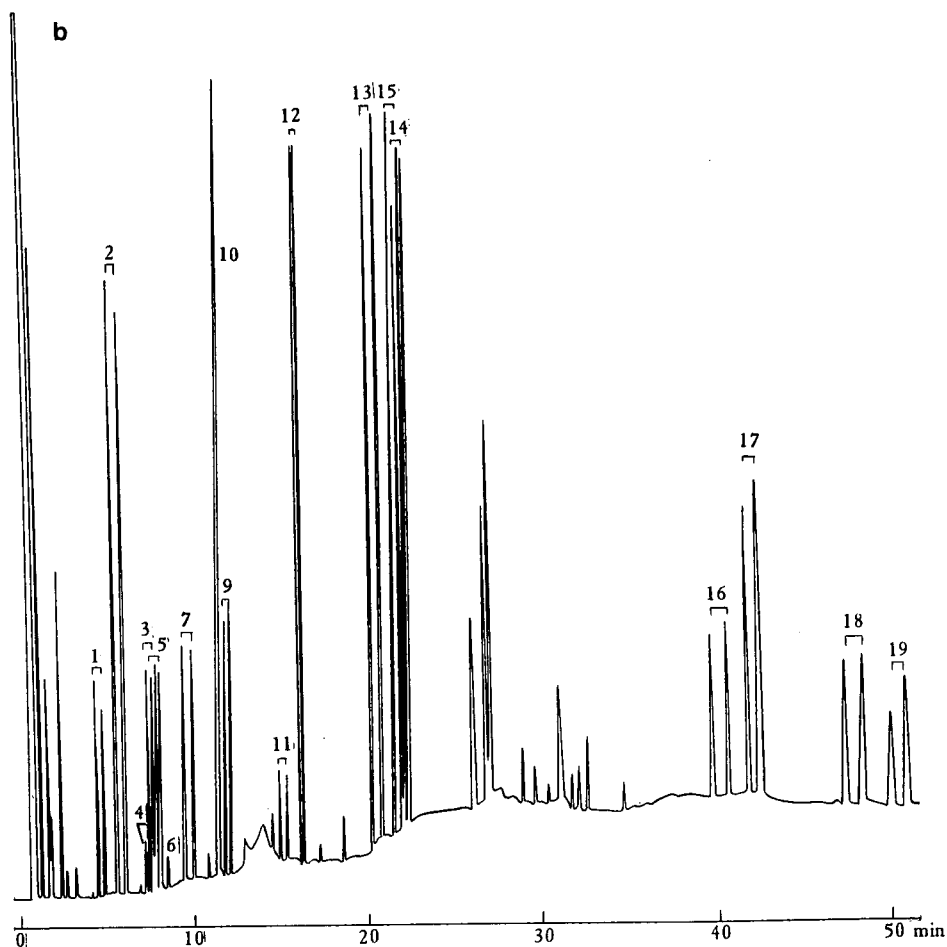


Fig. 2. Enantiomeric separation of amino acids by GC in cross-linked columns. Columns (20 m \times 0.25 mm I.D.): (a) cross-linked CSP-2 fused silica; (b) cross-linked CSP-4 fused silica. Temperature, 100°C (6 min), programmed at 4°C/min to 190°C; carrier gas, hydrogen. Peaks: 1 = Ala; 2 = Val; 3 = Thr; 4 = *a*-Ile; 5 = Ile; 6 = Gly; 7 = Leu; 8 = *n*-Leu; 9 = Ser; 10 = Pro; 11 = Cys; 12 = Asp; 13 = Met; 14 = Glu; 15 = Phe; 16 = Orn; 17 = Tyr; 18 = Lys; 19 = Trp (*D*-enantiomers eluted first).

TABLE VI
REPRODUCIBILITY OF CROSS-LINKED CSP-4 COLUMNS

Column	α^a	$k'(L)^a$	d (%)	e (%)	CE (%) ^a	Acid/base ^b
1	1.133	4.59	68	2	85	1.02
2	1.134	4.64	69	2	87	1.02
3	1.133	4.65	69	2	82	1.02
4	1.133	4.79	71	2	80	1.03

^a α , $k'(L)$ (capacity factor of L-alanine) and CE were tested at 100°C. Sample: alanine.

^b See Table III.

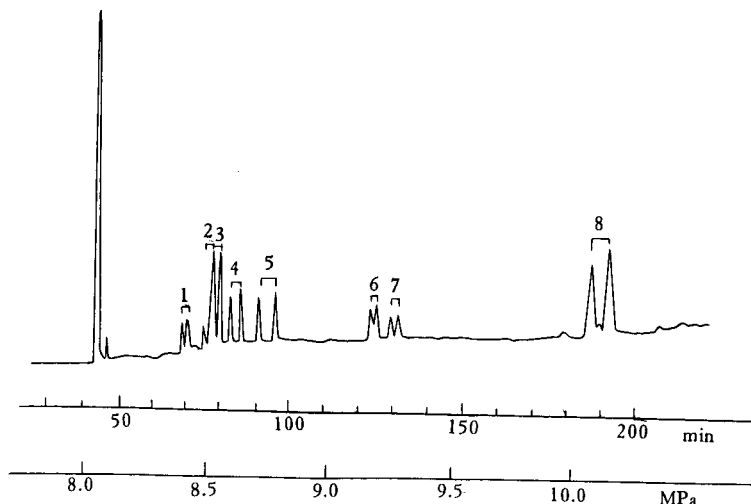


Fig. 3. Enantiomeric separation of amino acids by SFC in a cross-linked CSP-2 column. Column, 20 m \times 0.10 mm I.D., glass; mobile phase, carbon dioxide, 8.0 MPa (60 min) increased at 0.05 MPa/min; column temperature, 60°C; detector, flame ionization (250°C). Peaks: 1 = Val; 2 = *a*-Ile; 3 = Ile; 4 = *n*-Val; 5 = Leu; 6 = Ser; 7 = Asp; 8 = Met (*D*-enantiomers eluted first).

Good reproducibility of the preparation of the cross-linked chiral capillary columns was obtained. Table VI gives the data for four cross-linked CSP-4 columns with 6% DBP.

Fig. 2 shows chromatograms for the separation of amino acid enantiomers with the cross-linked columns. Fig. 3 shows the chromatogram of some amino acid enantiomers obtained with a cross-linked CSP-2 column using SFC.

CONCLUSION

The CSP skeleton may have a large effect on both the degree of cross-linking and racemization with DBP as the cross-linking reagent. CSP-4 has both a polycyanoethyl siloxane skeleton and vinyl groups and gives the best results in terms of degree of cross-linking and enantioselectivity (α -values) among the four CSPs studied.

ACKNOWLEDGEMENTS

We thank Professors Qinghai Wang, Daoqien Zhu and Yafong Guang and Mr. Yufong Sheng for technical help and valuable discussions. This work was supported by the National Natural Science Foundation of China.

REFERENCES

- 1 E. Gil-Av, B. Feibush and R. Charles-Sigler, *Tetrahedron Lett.*, (1966) 1009.
- 2 K. Grob and G. Grob, *J. Chromatogr.*, 213 (1981) 211.
- 3 J. Bradshaw, S. K. Aggarwal, C. A. Rouse, B. J. Tarbet, K. E. Markides and M. L. Lee, *J. Chromatogr.*, 405 (1987) 169.

- 4 W. Roder, F.-J. Ruffing, G. Schomburg and W. H. Pirkle, *J. High Resolut. Chromatogr. Chromatogr. Commun.*, 10 (1987) 655.
- 5 P. Macaudière, M. Caude, R. Rosset and A. Tambuté, *J. Chromatogr. Sci.*, 27 (1989) 383.
- 6 G. Lai, G. Nicholson and E. Bayer, *Chromatographia*, 26 (1988) 229.
- 7 G. Schomburg, I. Benecke and G. Severin, *J. High Resolut. Chromatogr. Chromatogr. Commun.*, 8 (1985) 391.
- 8 L. Zhou, Z. Zhang and X. Lou, in *Proceedings of the 3rd China-Japan Joint Symposium on Analytical Chemistry, Hefei, China, 1988*, Academia Sinica and the Japan Society for Analytical Chemistry, p. 231.
- 9 H. Frank, G. J. Nicholson and E. Bayer, *J. Chromatogr. Sci.*, 15 (1977) 174.
- 10 T. Saeed, P. Sandra and M. Verzele, *J. Chromatogr.*, 186 (1979) 611.
- 11 S. Zhang, G. Wang, T. Zhang and L. Zhou, *Huaxie Sheji*, 7 (1985) 197.
- 12 S. L. McKenzie and D. Tenaschuk, *J. Chromatogr.*, 173 (1979) 53.
- 13 X. Lou and L. Zhou, in *Proceedings of the 3rd Chinese National Symposium on Capillary Chromatography, Lanzhou, China, 1988*, Chinese Chemical Society, p. 42.

Gas-liquid chromatography in qualitative analysis

XIX. The use of antioxidants to delay the oxidation of polyoxyethylene glycol stationary phases

A. D. DALE

Biokinetix Ltd., Potters Bar, Hertfordshire (UK)

and

M. B. EVANS*

Department of Chemistry, Hatfield Polytechnic, Hatfield, Hertfordshire (UK)

ABSTRACT

The sensitivity that polyoxyethylene glycols (PEG) show towards oxidative degradation at elevated temperatures is well known. Experiments have been conducted to investigate the possible use of antioxidants as stationary phase additives to prevent this oxidation. It has been shown that significant differences in antioxidant efficiency exist, depending on whether the activity is determined under static or dynamic conditions. This difference has been shown to be due to the volatility of the antioxidants in the carrier gas stream.

In view of the above findings, a novel antioxidant based on the PEG 400 molecule has been synthesized and evaluated. This compound is markedly less volatile than the conventional antioxidants and inhibits significantly the oxidation of PEG phases.

INTRODUCTION

The polyoxyethylene glycols (PEGs) are a ubiquitous group of compounds which, among other uses, have been employed for many years as polar stationary phases in gas-liquid chromatography [1]. Applications of these phases are legion and include the separation of alcohols [2], aldehydes [3], ketones [4] and fatty acids [5]. PEGs are extremely sensitive to aerial oxidation, especially at elevated temperatures and this can lead to serious difficulties in analysis, due to stationary phase degradation.

The oxidation of polyoxyethylene glycols has been studied by various workers who have identified several compounds as degradation products, which include formic acid [6], formaldehyde [7] and acetaldehyde [8]. In contrast, little work is published of the non-volatile products arising from aerial oxidation. However, it is known that when PEGs are oxidised as thick films or blocks, shorter chain PEGs are formed as non-volatile products [9]. Previous studies have also suggested that the degradation proceeds, at least in part, by a free radical mechanism [10].

Free-radical scavengers are commonly used to protect foodstuffs [11], rubbers and plastics [12] from the deleterious effects of aerial oxidation. Accordingly, it was decided to test the efficiency of such compounds as oxidation inhibitors in PEG stationary phases. The results of this work are now reported.

MATERIALS AND METHODS

Instrumentation

The gas chromatograph used was a Pye Model 104 (Pye-Unicam, Cambridge, UK), equipped with glass columns (6 ft. \times 0.25 in. I.D.) and flame ionisation detection.

The column packing comprised of 10% PEG 400 or PEG 20M supported on 60–80 mesh Chromosorb W AW prepared and packed in the conventional manner [13].

The output of the gas chromatograph was interfaced with a Spectra-Physics (Hemel Hempstead, UK) System 4 integrator to yield retention data.

Sylvester apparatus

The apparatus was constructed in-house and is shown in Fig. 1. The compound under test (0.1 g) was dissolved in the appropriate stationary phase, generally PEG 400 (10 ml). The mixture was transferred to a 100-ml conical flask fitted with a B14 ground glass joint and the adaptor tube fitted. The assembly was filled with pure oxygen gas and the rubber tube connection to the manometer quickly fitted to the adaptor. The completed apparatus was placed, as indicated in Fig. 1, in an oil bath which was maintained at 100°C. The oxygen uptake was measured by the movement of the float.

A typical trace of oxygen uptake *versus* time is shown in Fig. 2. Generally, an induction period is observed, even for pure materials, followed by a rapid exponential increase. Eventually, an upper limit is approached, at which the rate of uptake decreases to zero.

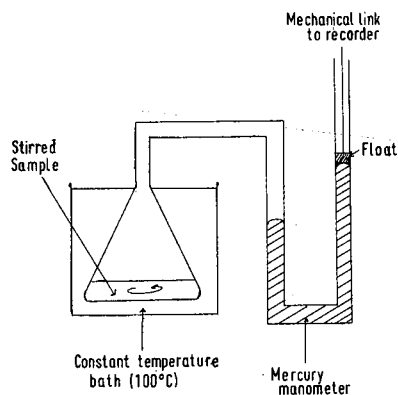


Fig. 1. Sylvester apparatus used in oxygen uptake experiments.

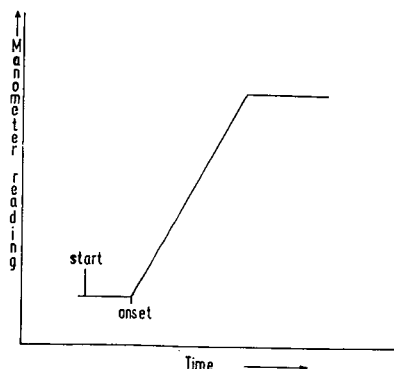


Fig. 2. Typical trace from Sylvester apparatus.

Materials

The support and stationary phase materials used were supplied by Greyhound Chemicals (Liverpool, UK). All other chemicals were purchased from BDH (Poole, UK) except the Ionex 220, which was obtained from Shell Industries (Sittingbourne, UK). All chemicals were analytical grade (A.R.) or the purest available, and all were used without further purification.

Hydrogen and oxygen-free nitrogen were supplied by British Oxygen (London, UK) and the helium by Air Products (London, UK). The compressed air was supplied from an in-house compressor, freed from oil droplets by a simple trap and passed through a carbon filter before use.

The following compounds were used to determine the Kováts indices of the stationary phases: iodobutane, dioxane, 1-butanol, pyridine, toluene, octan-2-yne, chlorobenzene, hexan-2-one and 2,4-dimethylpentan-3-ol.

Preparation of the novel antioxidant based on PEG 400

3,5-Di-*tert.*-butyl-4-hydroxybenzoic acid (1 g, 0.004 mol) was heated under reflux with thionyl chloride (5 ml, 0.005 mol) using an oil bath for 1 h at 120°C. After this time, the reaction had moderated and the excess thionyl chloride was distilled to waste.

The crude acid chloride was an orange oil at the temperature of the oil bath; no attempt was made to characterise the product. Polyoxyethylene glycol 400 (5 ml, 0.08 mol) was then added to the hot acid chloride via the reflux condenser. Initially, two layers were formed but there followed a rapid evolution of acidic gases and the contents of the flask became homogeneous.

The solution was heated at 120°C for a further 30 min, then allowed to cool. Chloroform (30 ml) was added to the flask and the resultant extracted with saturated sodium hydrogen carbonate solution (3 × 20 ml) and then washed with water (3 × 20 ml). The organic phase was separated, dried over anhydrous sodium sulphate and the chloroform removed by evaporation under nitrogen to yield 2.0 g of PEG 3,5-di-*tert.*-4-hydroxybenzoate. Details of the purification and characterisation of the product are given elsewhere [14].

RESULTS AND DISCUSSION

A range of conventional antioxidants, listed in Table I, was investigated for their ability to delay the oxidation of PEGs under static conditions, using the Sylvester apparatus and PEG 400 as the test compound. A concentration of 1% was chosen and, as the results, shown as Table I, indicate, all the compounds were effective in delaying the uptake of oxygen, and hence the onset of oxidation, for at least 2 h, whilst the control sample of PEG 400 started to degrade after about 30 min and that of the PEG 20M within 1 h.

The experiment was then repeated under dynamic conditions, by incorporating each antioxidant at a 1% concentration into a series of 10% PEG 400, Chromosorb W AW column packings. Air was used as the carrier gas at 150°C at a flow-rate of 50 ml/min and the oxidation monitored by the periodic chromatography of the test compounds. Appropriate hydrocarbons were included in the calibration solutions to enable the Kováts retention indices of the test compounds to be determined as a test of phase polarity [15,16]. The results, a representative example of which is shown as Fig. 3, indicate that little or no protection against aerial oxidation was afforded by any of the antioxidants under the conditions investigated.

As may be seen from Fig. 3, the k' values showed a rapid decrease, indicating that the mass of the stationary phase within the column was decreasing. There was, however, no concomitant change in the retention index (I) values for the test compounds, as shown in Table II, suggesting that the chemical structure of the remaining stationary phase was little changed during oxidation, in agreement with evidence based on high-performance liquid chromatographic studies [14]. A similar result was found when PEG 20M was substituted for PEG 400, but, as might be expected, the rate of degradation was somewhat slower.

During these experiments, it was noticed that the antioxidant ethoxyquin has a

TABLE I

THE EFFECTIVENESS OF CERTAIN ANTIOXIDANTS, INCLUDING A NOVEL PEG BASED ANTIOXIDANT, IN DELAYING THE ONSET OF OXIDATION OF PEG 400 AND PEG 20M, UNDER STATIC CONDITIONS

Antioxidant	Time before onset of oxidation (h)	
	PEG 400	PEG 20M
Control	0.5	1.0
BHT ^a	2.0	2.0
BHA ^b	2.5	2.8
Ionex 220 ^c	10.0	10.5
4-Hydroxy-3,5-di- <i>tert.</i> -butylphenol	18.0	20.0
4-Hydroxy-3,5-di- <i>tert.</i> -benzoic acid	5.5	6.0
Ethoxyquin ^d	11.0	12.5
PEG based antioxidant	> 26.0	> 26.0

^a BHT = butylated hydroxytoluene or 4-methyl-2,6-di-*tert.*-butylphenol.

^b BHA = butylated hydroxyanisole or 4-methoxy-2-*tert.*-butylphenol.

^c Ionex 220 = 4,4'-methylene-bis-di-*tert.*-butylphenol.

^d Ethoxyquin = 6-ethoxy-1,2-dihydro-2,2,4-trimethylquinoline.

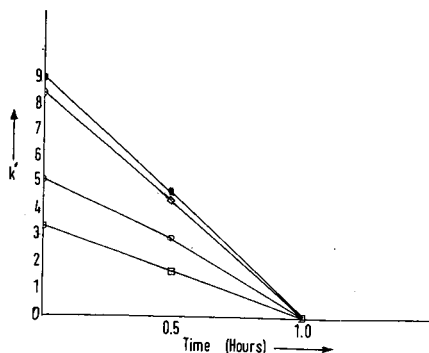


Fig. 3. The effect of oxidation upon a column packed with 10% PEG 400 with 1% BHA coated on Chromosorb W AW. The plot shows the variation of capacity factor (k') with time. Carrier gas: air at 150°C at a flow-rate of 50 ml/min. \square = Octan-2-yne; \circ = dioxane; \diamond = 1-butanol; \blacksquare = chlorobenzene.

native fluorophore when illuminated with radiation at 380 nm. By examining a column packed with PEG 400 and ethoxyquin on Chromosorb W AW under such conditions at various times during the oxidation, it was found that the fluorescence was rapidly lost from the column, with the loss starting at the injector end and moving steadily through the column. This observation strongly supports the hypothesis that the antioxidants investigated were rapidly lost from the column under dynamic conditions, thereby explaining their apparent lack of protection. A similar observation also has been reported by Evans and Newton [17] during an investigation of hindered phenols as antioxidants by inverse chromatography with squalene as the stationary phase.

These findings suggest that the conventional antioxidants investigated were of little practical value under dynamic conditions due to their volatility. Attempts were therefore made to prepare an antioxidant compatible with PEGs that might be expected to be less volatile than the materials so far examined. After a consideration of a number of possibilities, it was decided to use PEG 400 as the base material and to introduce antioxidant groups by esterification of the terminal hydroxyls by a hindered phenol, namely 3,5-di-*tert*-4-hydroxybenzoic acid.

The PEG 400 ester antioxidant proved to be relatively simple to prepare, as

TABLE II

THE EFFECT OF OXIDATION UPON A COLUMN PACKED WITH 10% PEG 400, INCORPORATING 1% BHA COATED ON CHROMOSORB W AW

Variation in retention index measurements. Air as carrier gas 150°C and a flow-rate of 50 ml/min.

Compound	Time (h)		
	0	0.5	1.0
Octan-2-yne	1062	1058	1057
Dioxane	1140	1138	1145
1-Butanol	1234	1236	1238

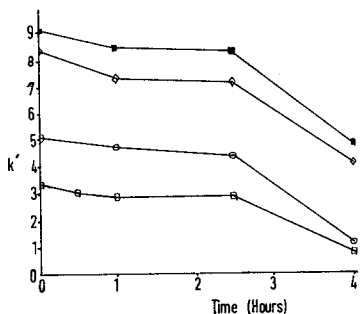


Fig. 4. The effect of oxidation upon a column packed with 10% PEG 400 and 1% PEG based antioxidant on Chromosorb W AW. The plot shows the variation of capacity factor with time. Carrier gas: air at 150°C at a flow-rate of 50 ml/min. \square = Octan-2-yne; \circ = dioxane; \diamond = 1-butanol; \blacksquare = chlorobenzene.

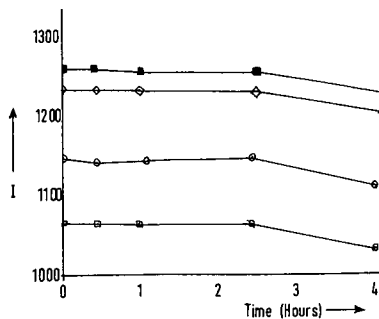


Fig. 5. The effect of oxidation upon a column packed with 10% PEG 400 and 1% PEG based antioxidant on Chromosorb W AW. The plot shows the variation of retention index with time. Conditions and symbols as in Fig. 4.

described earlier. In addition to structural characterisation, the novel compound was subjected to a COSHH hazard assessment, which included an Ames test for potential mutagenicity [18]. This revealed the material to be a very weak mutagen and reasonably safe.

The PEG 400 antioxidant was evaluated under static conditions using the Sylvester apparatus and found to be very efficient in delaying the onset of oxidation of PEG 400 and PEG 20M, the results being shown in Table I. These results show the compound to be as efficient as the other antioxidants investigated.

The evaluation under the dynamic conditions showed it to be extremely good at delaying the oxidation of PEG 400 at 150°C, again with air as the carrier gas with a flow-rate of 50 ml/min, as demonstrated by the data shown in the oxidation curves in Figs. 4 and 5.

The k' and I values were found to be fairly constant for about 150 min, compared with the BHT control, where the k' values showed a decrease after 30 min. After the delay period, the rate of degradation, as indicated by the change in the k' values, was similar for both the PEG antioxidant and the control columns.

When the experiment was repeated at 175°C, the novel antioxidant delayed the onset of oxidation for PEG 400 for about 10 min. These results should be compared with the other antioxidants, where no protection was observed and degradation started immediately. Similar results were obtained when PEG 20M was used as the stationary phase, suggesting that the antioxidant was not affected by the molecular weight of the stationary phase.

CONCLUSIONS

The potential use of antioxidants to prevent, or at least delay, the onset of oxidation of PEG stationary phases has been investigated. It has been shown that, under static conditions, the antioxidants investigated do delay the onset of oxidation but this effect is not found under the dynamic conditions of gas chromatography. The

difference between static and dynamic systems has been shown to be related to the volatility of the antioxidant in the carrier gas stream.

In view of this finding, a novel antioxidant based on the PEG 400 molecule has been synthesised and the compound tested. The results of static and dynamic tests show that this novel antioxidant delays the oxidation of PEG stationary phases for significant periods of time and offers a significant advantage over conventional antioxidants at moderate operating temperatures. Further work is in progress designed to yield PEG based antioxidants with improved thermal stability.

REFERENCES

- 1 C. Horváth, in L. S. Ettre and A. Zlatkis (Editors), *The Practice of Gas Chromatography*, Interscience, New York, 1st ed., 1967, p. 177.
- 2 H. Takei, K. Nakashima, O. Adachi, E. Shinagawa and A. Ameyama, *Clin. Chem.*, 31 (1985) 1985.
- 3 S. T. Raupp, *Z. Anal. Chem.*, 164 (1958) 135.
- 4 E. R. Adlard, in D. H. Desty (Editor), *Vapour Phase Chromatography*, Butterworths, London, 1957, p. 103.
- 5 D. V. McCalley, C. V. Thomas, A. J. Floyd and L. C. Loveson, *Chromatographia*, 20 (1985) 664.
- 6 C. Weurman and J. Dhout, *Nature (London)*, 184 (1959) 1480.
- 7 M. Kieser and D. J. Sissons, *Nature (London)*, 185 (1960) 529.
- 8 J. R. Condor, N. A. Fruitwalla and M. K. Shingari, *J. Chromatogr.*, 269 (1983) 171.
- 9 L. Dulong, *Farbe Lack.*, 73 (1967) 11.
- 10 W. G. Lloyd, *J. Polymer Sci.*, 1A (1963) 2551.
- 11 H. A. Boekenoogen, in H. A. Boekenoogen (Editor), *Oils, Fats and Fat Products*, Vol. 2, Interscience, London, 1968, p. 631.
- 12 F. Jacobs, *Caoutchouc Gutta-Percha*, 30 (1933) 16548.
- 13 M. B. Evans, *Chromatographia*, 4 (1971) 441.
- 14 A. D. Dale, *Ph.D. Thesis*, Hatfield Polytechnic CNA, Hatfield, 1989.
- 15 M. B. Evans and J. F. Smith, *J. Chromatogr.*, 36 (1968) 4899.
- 16 M. B. Evans, J. J. Dowling and J. K. Haken, *J. Chromatogr.*, 500 (1990) 355.
- 17 M. B. Evans and R. Newton, *Chromatographia*, 12 (1979) 83.
- 18 B. N. Ames, J. McCann and Y. Yamasaki, *Mutat. Res.*, 31 (1975) 347.

CHROMSYMP. 2201

Gas chromatography in qualitative analysis

XX. The deactivation of diatomaceous supports by batyl alcohol

MICHAEL B. EVANS*, ROY BIRD and HELEN O'SULLIVAN

Division of Chemical Sciences, Hatfield Polytechnic, College Lane, Hatfield, Hertfordshire AL10 9AB (U.K.)

ABSTRACT

Treatment of diatomaceous supports by the naturally occurring 1,2-diol batyl alcohol is shown to prevent problems due to the adsorption of polar analytes, at the liquid–solid interface, in packed column gas–liquid chromatography. The addition of small quantities of batyl alcohol is found to deactivate diatomaceous supports effectively, as judged by peak symmetry measurements and a study of the dehydration of tertiary aliphatic alcohols by stop-flow chromatography. The protection provided by batyl alcohol is shown to be equivalent to that afforded by diglycerol, although not as efficient at elevated temperatures. Batyl alcohol is found to be more effective as a deactivator than the equivalent *n*-alkanol behenyl alcohol. The relative merits of *n*-alkanols, alkane-1,2-diols and polyoxyethylene glycols are considered and the deactivation process discussed.

INTRODUCTION

In gas–liquid chromatography the adsorption of solute molecules at the liquid–solid interface can lead to shifts of retention [1], with concomitant peak asymmetry, and in extreme cases solute isomerism or decomposition [2]. The detrimental effects of this phenomenon upon the reliability of analytical results has long been appreciated and a number of methods have been developed for the deactivation of diatomaceous support materials, including: (i) acid [3] or base [4] washing; (ii) coating with carbon [5], a noble metal [6] or an inert polymer [7]; (iii) partial sintering at elevated temperatures [8]; (iv) chemical deactivation of the active sites by conversion to apolar silyl ethers [9]; (v) saturation of the surface adsorptivity by a surfactant [10]; and (vi) deposition of a non-extractable film of Carbowax 20M [11].

When carried out under carefully controlled conditions each of these methods is capable of preventing solute adsorption. However, on a routine laboratory scale it has been our experience that the use of surfactants is capable of reliable results more consistently than the other methods. In particular, outstanding results have been achieved with the use of polyols, such as diglycerol [12].

Batyl alcohol, DL-3-octadecyloxy-1,2-propanediol, is a contaminant of naturally occurring squalene, which is the precursor of the commonly used apolar phase squalane. During the hydrogenation of squalene, and the subsequent cleanup of the product, the batyl alcohol is completely removed [13]. Batyl alcohol is structurally related to diglycerol, thus it would seem that a potential tail-reducer provided by nature is inadvertently lost. In order to test this hypothesis the work, now to be described, was performed.

EXPERIMENTAL

Equipment

Gas chromatography was performed using a Series 204 gas chromatograph equipped with glass columns and flame-ionization detection (Philips Analytical, Cambridge, U.K.). The columns (2 m × 4 mm I.D.) were packed with 20% (w/w) mixtures of stationary phase (for details see text) and non-acid-washed 60–80 BS mesh Chromosorb P (Phase Separations, Deeside, Clwyd, U.K.). The packings were prepared by a two-stage slurry technique [12] and purged at 20°C with nitrogen prior to use. The following operating conditions were employed: column temperature, 100°C (except where stated); injection temperature, 120°C; detector temperature, 150°C; and carrier gas nitrogen, at a flow-rate of 40 ml/min. Mixtures of test solutes and *n*-alkane standards, dissolved in an inert solvent, were introduced by means of SGE microsyringes (Scientific Glass Engineering, Milton Keynes, UK).

Stop-flow chromatography

In order to monitor the dehydration of *tert*-alkanols the chromatograph was modified by the introduction of a simple Hoke toggle valve into the carrier gas pipework, between the nitrogen cylinder regulator and the pressure control module. Mixtures of *tert*-alkanols and *n*-alkane standards were introduced into the chromatograph and the carrier gas flow stopped, by closure of the toggle valve, once the solutes were judged to be half-way down the column.

After a predetermined time the flow of nitrogen was resumed and chromatograms were recorded in the normal way. Generally it was found to be necessary to re-ignite the hydrogen flame of the detector on resumption of the carrier gas flow.

Materials

The stationary phases used were obtained from Jones Chromatography (Hengoed, U.K.). The test solutes and *n*-alkanes were obtained from BDH (Poole, U.K.) or Aldrich Chemicals (Gillingham, U.K.) and were used as supplied. The batyl and benenyl alcohols, used as deactivators, were obtained from Aldrich Chemicals, neither were further purified before use.

RESULTS AND DISCUSSION

Previously it has been suggested that the deactivator molecule should be capable of directing polar functional groups towards the active sites on the support surface whilst presenting an apolar surface towards the liquid phase [12], as illustrated in Fig. 1.

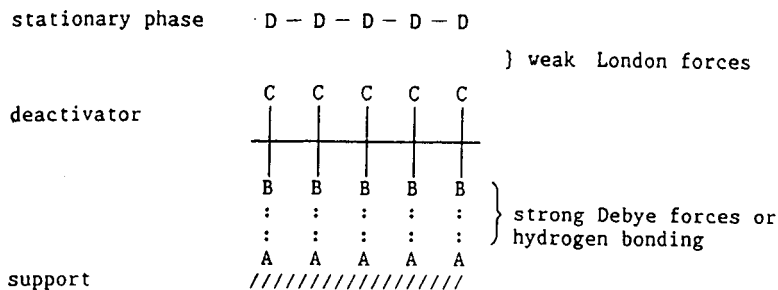


Fig. 1. Direction of polar functional groups. A = Silanol, SiOH, active sites on the surface of diatomaceous supports; B = pendant polar groups (amino, carboxyl, hydroxyl, nitrile, nitro) strongly bonded to active sites; and C = apolar groups (methyl, methylene, phenyl), weak association with stationary phase (D).

n-Alkanols and alkane-1,2-diols would be expected to yield protective films due to strong hydrogen bonding between the hydroxyl groups and the acidic silanol groups on the support surface (Fig. 2).

Diglycerol has been found to be particularly effective as a support deactivator, however, excess diol can cause significant shifts of retention, particularly for hydroxylic analytes. Batyl alcohol, which possesses a terminal 1,2-diol group together with a long alkyl chain, might be expected to be as effective as diglycerol as a deactivator but with less effect upon the overall selectivity of the column.

In order to assess the tail-reducing properties of batyl alcohol a series of experiments were performed as follows: (i) measurement of peak asymmetry values for

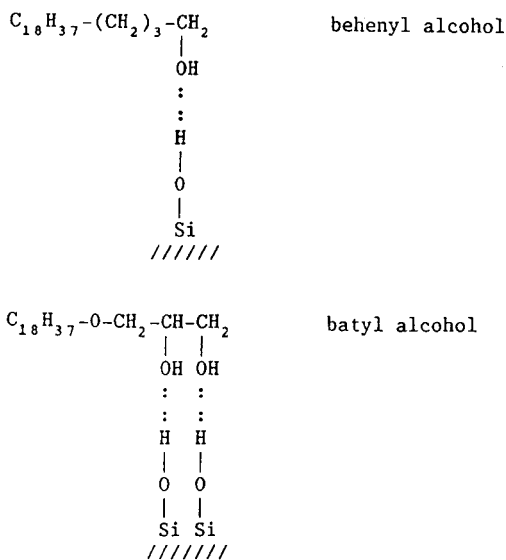


Fig. 2. Hydrogen bonding between hydroxyl groups of behenyl and batyl alcohol, respectively, and silanol groups of the solid support.

a range of polar solutes as a test of support adsorptivity; (ii) determination of the degree of decomposition of compounds, which readily undergo acid-catalysed elimination reactions, by stop-flow chromatography; (iii) study of the thermal stability of the protective film; and (iv) investigation of the retention characteristics of the deactivated columns, in particular variations of retention with changes of deactivator concentration.

Study of peak symmetry

The adsorption of solute molecules at the liquid–solid interface results in the distortion of the normally symmetrical peaks typical of linear non-ideal chromatography. When the liquid–solid adsorption is characterised by a convex isotherm, as is normally the case, a distinctive tailing peak is observed. The degree of peak distortion may be defined quantitatively by the peak asymmetry factor [14], *viz.*,

$$P_{\text{asym.}} = \frac{W_1 - W_2}{W_1 + W_2}$$

where W_1 and W_2 are the component peak widths at base (in order of increasing retention) measured either side of a perpendicular through the peak maximum. Thus a $P_{\text{asym.}}$ value of zero corresponds to a symmetrical peak, a positive value to a leading peak and a negative value to a tailing peak. Furthermore, the greater the numerical value the more severe is the peak distortion.

Of the commonly available diatomaceous supports the firebrick type are the most adsorptive [15]. Accordingly, squalane columns were prepared using Chromosorb P, deactivated by pretreatment with either batyl alcohol or behenyl alcohol, and $P_{\text{asym.}}$ values measured for solutes possessing a range of polar functional groups. In order to achieve a meaningful comparison of the adsorptivity of the various columns, steps were taken to ensure the introduction of the test solutes at a constant on-column sample size.

As expected the column prepared using untreated Chromosorb P gave highly distorted peaks for all solutes with the exception of *n*-alkanes. On the other hand, that treated with batyl alcohol gave substantially symmetrical peaks, in all cases, indicating that the surface silanols had been effectively deactivated. In contrast the more polar solutes gave rise to tailing peaks with the equivalent behenyl alcohol column, as illustrated by the peak asymmetry data in Table I. As can be seen, even when the concentration of behenyl alcohol was increased to give the equivalent hydroxyl content to that of the batyl alcohol treated column the peak tailing persisted. At first sight the results for 2-methylpentan-2-ol appear to be inconsistent. This we believe could be associated with partial on-column decomposition occurring on the behenyl alcohol column leading to perturbation of the $P_{\text{asym.}}$ values.

On the evidence of the peak symmetry experiments it would seem that batyl alcohol is a more efficient deactivator than behenyl alcohol. Presumably because it is able to cope more effectively with vicinal silanol groups.

Study of on-column reactions

The adsorption of solute molecules upon the support surface can lead to solute isomerisation or decomposition. This phenomenon has been used to compare the

TABLE I

PEAK ASYMMETRY VALUES FOR BATYL ALCOHOL AND BEHENYL ALCOHOL TREATED SQUALANE-CHROMOSORB P COLUMNS

Columns: I = 20% squalane, 1% batyl alcohol, Chromosorb P; II = 20% squalane, 1% behenyl alcohol, Chromosorb P; III = 20% squalane, 2% behenyl alcohol, Chromosorb P.

Solute	$P_{\text{asym.}}$		
	I	II	III
Anisole	0.00	-0.05	0.00
<i>n</i> -Butyl acetate	-0.07	-0.44	-0.11
<i>n</i> -Butyl cyanide	0.00	-0.67	-0.30
Hexane-2-one	0.00	-0.55	-0.08
Isopropylbenzene	0.00	-0.07	-0.03
2-Methylpentan-2-ol	+0.09	-0.18	-0.23
Pentan-1-ol	-0.08	-0.48	-0.09

adsorptivity of support materials, and the effectiveness of deactivation procedures through: (i) detection of additional peaks due to volatile decomposition products together with measurements of peak distortion [16]; (ii) measurements of changes of peak areas, relative to those of *n*-alkanes, with elevation of column temperature [15]; (iii) monitoring the on-column decomposition of compounds, susceptible to acid-catalysed reactions, by stop-flow chromatography; and (iv) spectroscopic analysis of the solute before and after chromatography [2].

In our experience the third of these methods is the most reliable and is applicable equally well to gas chromatography, normal-phase liquid chromatography and packed-column supercritical fluid chromatography [17]. Accordingly the respective efficiency of batyl alcohol and behenyl alcohol deactivation was tested by a study of the acid-catalysed dehydration of 2-methylpentan-2-ol and 3-methylpentan-3-ol, which proceeds via an initial protonation followed by the elimination of water to yield alkene mixtures [18].

Test mixtures of the tertiary alcohols and *n*-octane as internal standard were chromatographed and relative peak areas measured for a range of column residence times. With the untreated squalane, Chromosorb P column the alcohol peaks disappeared rapidly with residence time, due to on-column reaction. In contrast the *tert.*-alkanols remained unchanged on the batyl alcohol column for residence times up to 60 min, as shown by the results in Table II. With the behenyl alcohol column evidence of on-column decomposition was discernible after only 10 min, even with the 2% loading.

As expected peak widths increased with column residence time as indicated by the relative plate values shown in Table III. Whereas with open-tubular columns peak dispersion during stop-flow chromatography can be a problem [19], in the case of packed-columns the peak dispersion is much less than might have been expected for a gaseous mobile phase. For this reason packed-column gas chromatography would appear to be an ideal vehicle for the study of a wide range of chemical reactions by the stop-flow technique.

TABLE II

 INVESTIGATION OF THE EFFICIENCY OF BATYL ALCOHOL AND BEHENYL ALCOHOL PROTECTIVE FILMS BY THE STOP-FLOW CHROMATOGRAPHY OF *tert.*-ALKANOLS

Columns: I = 20% squalane, 1% batyl alcohol, Chromosorb P; II = 20% squalane, 1% behenyl alcohol, Chromosorb P; III = 20% squalane, 2% behenyl alcohol, Chromosorb P.

Solute	Residence time ^a (min)	Peak area ratio ^b		
		I	II	III
2-Methylpentan-2-ol	0	1.00	1.00	1.00
	10	1.00	0.60	0.94
	20	1.01	0.40	0.84
	30	1.02	0.24	0.77
	40	1.01	0.19	0.66
	50	1.01	—	0.61
	60	1.00	—	0.52
3-Methylpentan-3-ol	0	1.00	1.00	1.00
	10	1.02	0.53	0.89
	20	0.99	0.38	0.80
	30	1.00	0.17	0.76
	40	1.00	0.12	0.68
	50	1.00	—	0.61
	60	1.01	—	0.57

^a Residence time correspond to the period of time during which the carrier gas flow was stopped.

^b *n*-Octane used is internal standard. Peak area ratios expressed relative to the value for zero residence time.

TABLE III

DEPENDENCE OF COLUMN PLATE VALUE UPON RESIDENCE TIME IN STOP-FLOW GAS CHROMATOGRAPHY

Columns: I = 20% squalane, 1% batyl alcohol, Chromosorb P; II = 20% squalane, 2% behenyl alcohol, Chromosorb P.

Solute	Residence time ^a (min)	Relative plate number ^b	
		I	II
<i>n</i> -Octane	0	1.00	1.00
	10	0.81	0.79
	20	0.75	0.76
	30	0.67	0.70
	40	0.59	0.61
	50	0.52	0.54
	60	0.43	0.48

^a Residence time corresponds to the period of time during which the carrier gas flow was stopped.

^b Relative plate numbers expressed relative to the value for zero residence time — initial plate numbers 1971 and 1652, respectively.

Thermal stability of the protective film

The thermal stability of a gas chromatographic liquid phase may be determined by thermogravimetry [20], measurement of detector standing current [21] or relative retention measurements [22]. Each of the methods was used to determine the stability of diglycerol deactivated supports [12] and it was concluded that the third was the most appropriate. Accordingly the respective stabilities of the batyl alcohol and behenyl alcohol protective films were determined by retention index measurements [22], using a thermally stable silicone fluid as stationary phase.

As described previously [12], the columns were cycled daily between 100 and 200°C and the retention characteristics monitored by recording chromatograms of appropriate calibration mixtures at 100°C. In contrast to diglycerol deactivated columns, both the batyl alcohol and behenyl alcohol treated columns displayed shifts of retention indicative of the loss of the protective film.

At 150°C, however, the batyl alcohol deactivated column gave satisfactorily stable columns, as illustrated by the data in Table IV. The thermal stability of the behenyl alcohol protected column was somewhat inferior. With the hydroxylic solutes the values for retention index were found to decrease, pass through a minimum value and then increase. Since these increases of retention index were accompanied by peak tailing it would seem that the loss of behenyl alcohol was sufficient to give analyte molecules access to surface silanols.

TABLE IV

INVESTIGATION OF THE THERMAL STABILITY OF BATYL ALCOHOL AND BEHENYL ALCOHOL SURFACE COATINGS

Temperature: 150°C. Columns: I = 17% OV-17, 3% batyl alcohol, Chromosorb P; II = 17% OV-17, 3% behenyl alcohol, Chromosorb P.

Solute	Column	Retention index ^a						
		0 h	5 h	10 h	15 h	20 h	25 h	30 h
Isopropyl acetate	I	721	721	721	720	720	720	721
2-Methylpropan-1-ol	I	721	725	725	724	725	724	722
3-Methylbutan-2-one	I	748	747	746	746	746	746	745
Butan-1-ol	I	771	772	769	770	771	766	770
Pentan-1-ol	I	882	882	882	884	885	885	884
<i>n</i> -Butyl cyanide	I	906	906	906	905	905	905	904
Isopropyl acetate	II	721	720	719	722	723	723	725
2-Methylpropan-1-ol	II	714	712	711	714	717	720	724
3-Methylbutan-2-one	II	748	745	745	746	748	748	749
Butan-1-ol	II	763	759	762	768	776	783	792
Pentan-1-ol	II	872	867	869	874	884	889	898
<i>n</i> -Butyl cyanide	II	901	900	900	902	904	906	909

^a Retention index calculated using the expression:

$$I = 100 N + 100 n \cdot \frac{\log R_x - \log R_N}{\log R_{N+n} - \log R_N}$$

where R_x , R_N and R_{N+n} are the adjusted retentions, obtained using methane as void volume marker [23], of the analyte and *n*-alkane standards containing *N* and *N* + *n* carbon atoms, respectively.

TABLE V

THE EFFECT OF BATYL ALCOHOL DEACTIVATOR CONCENTRATION UPON THE RETENTION BEHAVIOUR OF SQUALANE COLUMNS

Columns: I = 18% squalane, 2% batyl alcohol, Chromosorb P; II = 16% squalane, 4% batyl alcohol, Chromosorb P.

Solute	Retention index			
	I	II	δI^a	$\delta I'^b$
Toluene	763	769	6	1
4-Methylpent-3-en-2-one	765	784	19	4
1,2-Dibromethane	800	811	11	3
Chlorobenzene	837	846	9	1
3-Bromopropan-1-ol	900	954	54	54
Benzonitrile	927	951	24	10
Phenetole	963	974	11	1

^a $\delta I = I_{4\%} - I_{2\%}$.

^b $\delta I'$ = change in retention index for equivalent diglycerol columns.

The differences between the thermal stability of the diglycerol, batyl alcohol and behenyl alcohol protected columns may be explained in terms of the potential points of attachment between deactivator and support. With diglycerol both diol groups may act as ligands, so that to remove the protective film up to four hydrogen bonds need to be broken, whereas with batyl alcohol and behenyl alcohol only two hydrogen bonds and a single hydrogen bond, respectively, need to be cleaved.

Effect of batyl alcohol pretreatment upon the retention behaviour of apolar columns

On the evidence of previous work [1] batyl alcohol pretreatment might be expected to affect the retention behaviour of apolar columns in either of two ways, depending upon the activity of the support and the deactivator concentration, firstly, by preventing the adsorption of solute molecules and secondly by contributing to the partition process.

In order to determine the magnitude of the latter effect, which from an analytical standpoint is the more important, squalane columns were prepared using batches of Chromosorb P coated with 2 and 4% (w/w), respectively, of batyl alcohol. After careful conditioning the retention behaviour of each column was determined by measuring the values for the retention index of a range of solutes. The results obtained, which are shown in Table V, indicate that the addition of batyl alcohol has little effect upon phase selectivity, except towards hydroxylic solutes. In general the shifts of retention are slightly greater than those observed with diglycerol but less than those for amine antioxidant deactivated columns [24]. These observations suggest that batyl alcohol approaches the behaviour of the ideal deactivator by providing a compact polar layer on the support surface with an apolar overlayer in contact with the stationary phase.

CONCLUSIONS

Pretreatment of diatomaceous supports with hydroxylic compounds has been found to lead to apolar columns equally suitable for the analysis of both apolar and polar solutes. In general alkane-1,2-diols, such as batyl alcohol, appear to be more effective than monohydroxyl compounds, presumably because the former are able to chelate more effectively the surface silanols. On this evidence it is interesting to speculate about the apparent efficiency of polyoxyethylene glycols [25] as support deactivators. Because of their low hydroxyl content, interactions in addition to those involving the terminal hydroxyl groups need to be invoked. One possibility is the interaction between segments of the polyoxyethylene chain, oriented in the form of a crown ether, and alkali metal ions held electrostatically on the support surface. Work is in progress to test this hypothesis and the results will be presented in a later communication.

ACKNOWLEDGEMENT

The secretarial assistance of Miss Jane Fordham is gratefully acknowledged.

REFERENCES

- 1 M. B. Evans and J. F. Smith, *J. Chromatogr.*, 28 (1967) 277.
- 2 M. B. Evans, *Chromatographia*, 3 (1970) 337.
- 3 M. M. Daniewski and W. A. Aue, *J. Chromatogr.*, 150 (1978) 506.
- 4 D. M. Ottenstein, *J. Chromatogr. Sci.*, 11 (1973) 136.
- 5 K. Grob, *Helv. Chim. Acta*, 48 (1965) 1362.
- 6 E. C. Omerod and R. P. W. Scott, *J. Chromatogr.*, 2 (1959) 65.
- 7 T. Onaka and T. Okamoto, *Chem. Pharm. Bull.*, 10 (1962) 757.
- 8 J. F. K. Huber and A. I. M. Keulemans, *Informal Symposium of the Gas Chromatography Discussion Group, Chelsea College, London, April, 1963*.
- 9 E. C. Horning, E. A. Moscatelli and C. C. Sweeley, *Chem. Ind. (London)*, (1959) 751.
- 10 W. Averill, in N. Brenner, J. E. Callen and M. D. Weiss (Editors), *Gas Chromatography*, Academic Press, New York, 1958, p. 31.
- 11 S. Kapila, W. A. Aue and J. M. Augl, *J. Chromatogr.*, 87 (1973) 35.
- 12 M. B. Evans, *Chromatographia*, 4 (1971) 441.
- 13 L. S. Ettre, *Chromatographia*, 7 (1974) 261.
- 14 M. B. Evans and J. F. Smith, *J. Chromatogr.*, 36 (1968) 489.
- 15 D. M. Ottenstein, *Adv. Chromatogr.*, 3 (1966) 137.
- 16 H. L. McDonell and D. L. Eaton, *Anal. Chem.*, 40 (1968) 1453.
- 17 M. B. Evans, M. S. Smith and J. M. Oxford, *J. Chromatogr.*, 479 (1989) 170.
- 18 F. Carey and R. Sunbury, *Advanced Organic Chemistry*, Plenum, London, 2nd ed., 1984.
- 19 M. B. Evans, Hatfield Polytechnic, Hatfield, unpublished results, 1987.
- 20 C. Horvath, in L. S. Ettre and A. Zlatkis (Editors), *The Practice of Gas Chromatography*, Wiley, New York, 1967, p. 175.
- 21 S. J. Hawkes and J. C. Giddings, *Anal. Chem.*, 36 (1964) 2229.
- 22 E. Kovats, *Helv. Chim. Acta*, 41 (1958) 1915.
- 23 R. Feinland, A. J. Andreatch and D. T. Cotrupe, *Anal. Chem.*, 33 (1961) 991.
- 24 M. B. Evans, R. Newton and J. D. Carmi, *J. Chromatogr.*, 166 (1978) 101.
- 25 W. A. Aue, C. R. Hastings and S. Kapila, *Anal. Chem.*, 45 (1973) 725.

CHROMSYMP. 2326

Gas chromatographic investigation of silica supports modified in a high-frequency low-temperature plasma

T. B. GAVRILOVA, Yu. S. NIKITIN and E. V. VLASENKO

Department of Chemistry, Lomonosov State University of Moscow, 119899 Moscow (U.S.S.R.)
and

I. TOPALOVA, N. PETSEV* and Chr. CHANEV

Faculty of Chemistry, University of Sofia, 1 Anton Ivanov Avenue, Sofia 1126 (Bulgaria)

ABSTRACT

The modification of gas chromatography (GC) supports and adsorbents by glow discharge is of practical interest as it is a method of producing changes in particular surface properties. The adsorption properties of the surface of Silochrom CX-1 modified in a high-frequency low-temperature plasma with argon and benzene vapours were investigated using GC. The thermodynamic characteristics of series of aliphatic and aromatic hydrocarbons and oxygen-containing compounds were measured. The modified silica adsorbents were used for the separation of structural isomers and other mixtures of organic compounds. The modifications of silica described here improve the uniformity of the adsorbent surface and hence the separation properties, increasing the selectivity of the silica supports. This will expand the field of application of silica adsorbents.

INTRODUCTION

Silica adsorbents are often subjected to geometrical and chemical modification [1]. A very promising approach is to treat the sorbents in a high-frequency low-temperature plasma (HFLTP). This method, in an argon medium, has been used successfully to improve the gas chromatographic (GC) properties of several supports, including diatomite covered with a liquid phase [2–4], glass balls and capillary columns [5], adsorbents covered with monolayers of different compounds [6–8] and polymers [4].

The use of a HFLTP in polymer formation [9] offers the possibility of combining thermal treatment and the following co-polymerization with the formation of thin films on the sorbent surface which are resistant to aggressive media.

This paper reports a study of the application of chemical treatment in an HFLTP as a method of modifying silica adsorbents for use in GC.

EXPERIMENTAL

The silica adsorbent Silochrom CX-1 (specific surface area 32 m²/g by nitrogen and 28 m²/g by krypton absorption; pore volume 1.24 cm³/g) was studied as a column packing before and after plasma treatment. It was found that after 1 and 3 min of plasma action the specific surface area measured by the adsorption of nitrogen was 33 and 35 m²/g, respectively.

Before being modified, the Silochrom CX-1 was washed with concentrated hydrochloric acid to remove iron impurities and with distilled water to remove chloride ions.

The treatment in the HFLTP was carried out in an argon atmosphere as described previously [10,11]. The Silochrom CX-1 was impregnated with benzene as a modifying agent and then subjected to the action of the HFLTP in a benzene vapour medium.

The GC analyses were carried out on a Tswett gas chromatograph equipped with flame ionization detection and glass columns (25–100 cm × 3 mm I.D.); nitrogen was used as the carrier gas.

The retention volumes (V_g) (per gram of adsorbent) and the relative retention volume (V_{rel}) were calculated. The initial differential heats of adsorption (q_1) at low surface coverings were determined from the slope of the linear relationship $\log(V_g) = f(1/T)$, where T is the column temperature. The measurements of V_g were carried out within a temperature range in which the compounds gave symmetrical chromatographic peaks and the retention times did not depend on the amount of sample used.

RESULTS AND DISCUSSION

It is well known that adsorption on silica depends on the geometrical structure of the surface [12]. For this reason the influence of the argon plasma on the properties of the Silochrom CX-1 surface was studied.

Some chromatographic characteristics of Silochrom CX-1 treated for different periods of time in the argon HFLTP are given in Table I. These values were derived from chromatograms of compounds of different polarities, V_{rel} values (related to V_g of *n*-nonane) and coefficients of symmetry K_{as} (measured at one tenth of the height of

TABLE I
CHROMATOGRAPHIC CHARACTERISTICS OF SILOCHROM CX-1 TREATED FOR VARIOUS TIMES IN THE ARGON HFLTP

Adsorbate	T_c (°C)	Untreated		HFLTP treated			
		V_{rel}	K_{as}	1 min		3 min	
				V_{rel}	K_{as}	V_{rel}	K_{as}
<i>n</i> -Heptane	60	0.19	1.0	0.19	1.0	0.19	1.0
Benzene	60	0.89	1.0	0.89	1.0	0.93	1.0
Toluene	60	2.98	1.6	2.98	1.3	3.08	1.3
Diethyl ether	100	19.65	1.7	18.76	1.3	20.03	1.3

TABLE II

THERMODYNAMIC CHARACTERISTICS OF ADSORPTION ON TREATED SILOCHROM CX-1 IN ARGON HFLTP

Column temperature $T_c = 100^\circ\text{C}$.

Adsorbate	Untreated			Treated in HFLTP for 1 min		
	V_g (cm^3/g)	V_{rel}	q (kJ/mol)	V_g (cm^3/g)	V_{rel}	q (kJ/mol)
<i>n</i> Heptane	2.2	0.29	38	3.8	0.29	—
<i>n</i> -Octane	4.0	0.54	42	7.2	0.54	43
<i>n</i> -Nonane	7.4	1.00	46	13.2	1.00	45
Ethylbenzene	28.8	3.90	53	44.2	3.35	55
1,3,5-Trimethylbenzene	84.7	11.40	64	127.4	9.65	65
Toluene ^a	—	7.30	—	—	6.20	—
Ethylbenzene ^b	—	7.20	—	—	6.10	—

^a Relative retention with respect to *n*-heptane.^b Relative retention with respect to *n*-octane.

the chromatographic peak) [13]. As seen from Table I, the results were optimal when the samples were treated in the HFLTP for 1 min. The lowest values of V_{rel} and K_{as} for polar toluene and diethyl ether show that in these instances the modified surface is less specific and more uniform. It is suggested that after a 3-min plasma treatment an erosion effect increases the silichrom surface and its geometrical ununiformity and V_{rel} increase too.

The differential heats of adsorption of *n*-aliphatic and aromatic hydrocarbons

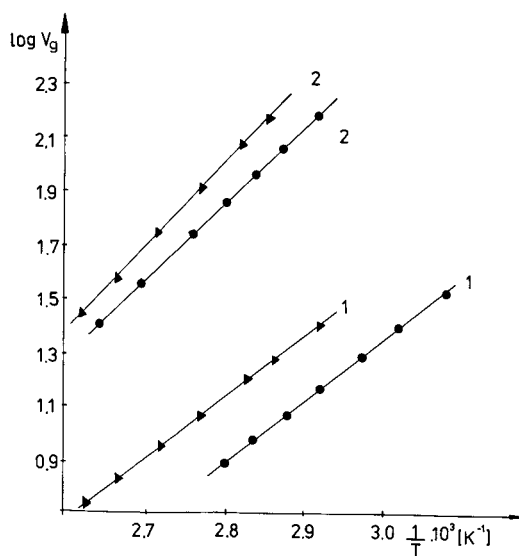


Fig. 1. Plot of $\log V_g$ versus $1/T$. 1 = *n*-Octane; 2 = ethylbenzene; (●) = untreated Silochrom CX-1; (▲) = Silochrom CX-1 treated in argon HFLTP. Column, 70×0.25 cm; particle size, 0.160–0.250 mm.

TABLE III

RETENTION VOLUMES V_g ON UNMODIFIED AND ON BENZENE-MODIFIED SILOCHROM CX-1 TREATED IN THE HFLTP

Adsorbate	T_c (°C)	Untreated		Treated in HFLTP with benzene	
		V_g (cm ³ /g)	K_{as}	V_g (cm ³ /g)	K_{as}
<i>n</i> -Hexane	60	6.4	1.0	7.9	1.0
<i>n</i> -Heptane	60	15.0	1.0	18.3	1.0
Benzene	60	69.4	1.0	48.9	1.0
Toluene	60	231.0	1.6	98.0	1.0
Diethyl ether	80	381.3	1.7	109.4	1.0
Acetone	80	746.4	1.8	211.5	1.1

(Fig. 1 and Table II) were determined from the retention volumes Silochrom CX-1. Treatment in the argon HFLTP leads to an increased specific retention of the hydrocarbons compared to retention on untreated Silochrom CX-1. The decrease in the relative retention volumes of the aromatic hydrocarbons on treated adsorbents shows decrease in the amount of adsorption due to specific interactions (according to the classification of Kiselev [14]). This could also be explained by the removal of hydroxy groups from the adsorbent surface as a result of the action of plasma (Table II). The values of the heats of adsorption of the hydrocarbons on untreated and treated Silochrom CX-1 do not significantly change.

The modification in the HFLTP was carried out in various organic vapours to achieve changes in the chemistry of the silica adsorbent surface. In this investigation benzene was chosen as a modifying agent as it polymerizes under the action of the plasma and covers the surface with a hydrocarbon film [9]. Using a gravimetric method it was found that after impregnation with benzene and treatment in the HFLTP with benzene vapour, the Silochrom CX-1 sample contains 1.2% of a carbon product.

A comparison of the values of K_{as} and V_g (Table III) of compounds with various polarities shows that the modification leads to changes in the surface properties. There is a significant improvement in the symmetry of the chromatographic peaks and a decrease in the values of V_g of the compounds under investigation. This indicates that the surface homogeneity was also improved.

The surface of an adsorbent is sensitive to the structural differences of isomeric aromatic hydrocarbons (Fig. 2). Polymethylbenzenes are always retained to a greater degree on modified Silochrom CX-1 than the corresponding isomeric alkylbenzenes. Similar differences in the retention of alkylbenzenes have been observed on adsorbents of different polarities and on Silochrom C-120 [15].

The modification of the surface leads to an increase in the retention of *n*-alkanes, the adsorption of which is based on dispersion forces. Aromatic hydrocarbons are retained on the surface of the HFLTP-modified Silochrom CX-1 less than on the unmodified surface. In this instance it can be assumed that most of the silanol groups are removed by the plasma action or are covered by a modifying layer. The

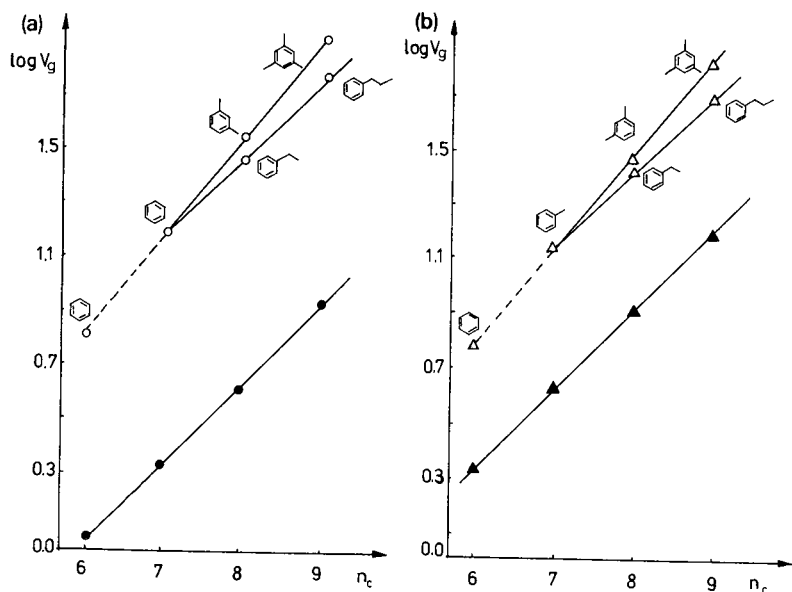


Fig. 2. Relationship between $\log V_g$ and the number of carbon atoms at 100°C. (a) Unmodified Silochrom CX-1; (b) modified Silochrom CX-1. (●, ▲) = *n*-alkanes; (○, △) = alkylbenzenes. Column as in Fig. 1.

specific interaction between silanols and the π -electrons of the aromatic ring will decrease as well as the retention volumes.

The relative retentions and heats of adsorption of *n*-alkanes (C_5 – C_{10}), aromatic

TABLE IV

RETENTION VOLUMES V_g AT 120°C AND INITIAL DIFFERENTIAL ADSORPTION HEATS q ON SILOCHROM CX-1

Adsorbate	V_g (cm^3/g)	Untreated			Modified in HFLTP with benzene			
		V_{rel}^a	q (kJ/mol)	q_{sp}	V_g (cm^3/g)	V_{rel}	q (kJ/mol)	q_{sp}
<i>n</i> -Octane	2.1	0.58	42	—	4.0	0.56	41	—
<i>n</i> -Nonane	3.6	1.00	46	—	7.1	1.00	45	—
<i>n</i> -Decane	6.8	1.90	51	—	12.6	1.80	50	—
Ethylbenzene	13.5	3.70	53	11	10.5	1.50	49	8
<i>n</i> -Propylbenzene	21.4	5.90	59	13	20.2	2.80	51	6
<i>n</i> -Butylbenzene	39.4	10.90	64	13	37.6	5.30	54	4
Diethyl ether	39.4	10.90	61	33	15.8	2.20	57	29
Di- <i>n</i> -propyl ether	81.2	22.50	66	28	38.9	5.50	62	25
Di- <i>n</i> -butyl ether	226.0	62.8	71	24	117.5	16.50	67	22
Ethyl acetate	107.0	29.70	62	29	42.0	5.90	59	26
<i>n</i> -Propyl acetate	186.0	51.7	65	27	79.9	11.10	62	25
<i>n</i> -Butyl acetate	489.0	135.8	67	25	149.0	21.00	65	24

^a Relative retention time with respect to *n*-nonane.

hydrocarbons (C_8 – C_{10}), some ethers and esters on benzene- modified and unmodified Silochrom CX-1 were determined (Table IV).

The retention of those adsorbate molecules which interact specifically with the surface, is decreased on the modified Silochrom CX-1 whereas the retention of *n*-alkanes increases as they are not adsorbed specifically on the surface. A similar effect was observed when a pyrocarbon film covered the Silochrom CX-1 surface [16]. A comparison of the values of V_{rel} of modified and unmodified Silochrom CX-1 confirms this statement.

In contrast to the retention data the heats of adsorption of the *n*-alkanes do not change significantly when Silochrom CX-1 is modified with benzene in the HFLTP. However, the modification leads to a decrease in the heats of adsorption of hydrocarbons and oxygen-containing compounds and to a decrease in the percentage contribution of specific interactions (Table IV) in the total adsorption energy [14]. This effect is more predominant when alkylbenzenes are adsorbed onto the modified Silochrom CX-1.

The adsorption energy of alkylbenzenes increases with the carbon chain length of the molecule. This is due to an increase in dispersion interactions, which means that the share of q_{sp} (calculated as the difference between an alkane and an alkylbenzene with an equal number of carbon atoms) on unmodified Silochrom CX-1 is insignificant for alkylbenzenes (11–13 kJ/mol). Their adsorption on the modified

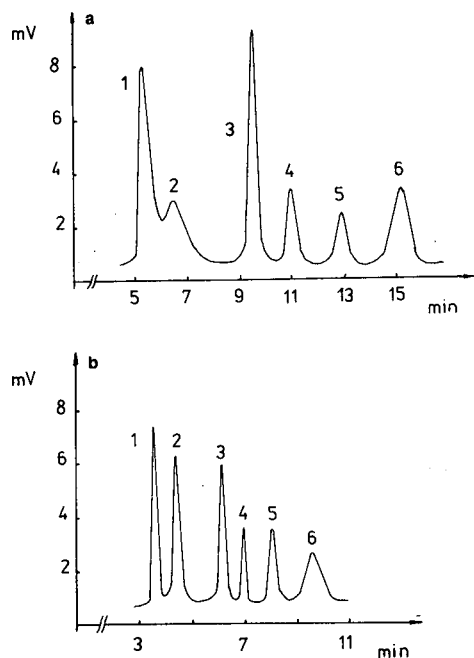


Fig. 3. Separation of dialkyl ethers. Peaks: (1) = diisopropyl ether; (2) = dipropyl ether; (3) = diisobutyl ether; (4) = dibutyl ether; (5) = diisopropyl ether; (6) = dipentyl ether. (a) Unmodified Silochrom CX-1; (b) modified Silochrom CX-1. Column as in Fig. 1; column temperature, 120–150°C.

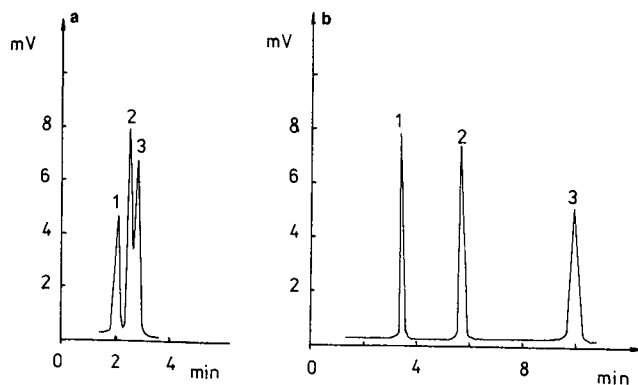


Fig. 4. Chromatogram of a mixture of: (1) 2,2,4-trimethylpentane, (2) *trans*-1,2-dimethylcyclohexane and (3) *cis*-1,2-dimethylcyclohexane. (a) Unmodified Silochrom CX-1; (b) Silochrom CX-1 modified with benzene vapour in HFLTP. Column as in Fig. 1; column temperature 50°C.

Silochrom CX-1 surface is characterized by a decrease of q_{sp} with an increase in the number of methylene groups (from 4 to 8 kJ/mol).

It is likely that during the modification of the Silochrom CX-1 with benzene in the HFLTP a hydrocarbon film is formed which has a shielding effect on the active adsorption centres on the surface.

CONCLUSIONS

It can be concluded that this modification leads to an increase in the surface uniformity of Silochrom CX-1 and significantly changes the energy of specific interactions between the adsorbent and adsorbate (compared to the adsorption of unmodified Silochrom CX-1). As a result of this, the selectivity of the Silochrom CX-1 surface towards isomeric compounds increases. Chromatograms of the two different test mixtures on unmodified and modified Silochrom CX-1 are shown in Figs. 3 and 4.

The results of the experiments show the possibility of changing the surface properties of Silochrom CX-1 by treatment with an HFLTP in the presence of benzene. This will expand the field of applications of silica adsorbents.

REFERENCES

1. A. V. Kiselev, *Mezhmolekulyarnye vzaimodeistvia v adsorpsii i khromatografii (Intermolecular Interactions in Adsorption and Chromatography)*, Vysshaya Shkola, Moscow, 1986.
2. Y. Yamamoto, S. Oka and K. Hayashi, *Bull. Chem. Soc. Jpn.*, 55 (1982) 441.
3. S. Oka, Y. Yamamoto and K. Hayashi, *Bull. Chem. Soc. Jpn.*, 55 (1982) 3496.
4. S. A. Volkov, K. I. Sakodynskii, A. B. Gilman, V. M. Kolotyркиn, N. F. Zelenkova, T. K. Zakharova and V. K. Potapov, *J. Chromatogr.*, 242 (1982) 166.
5. S. R. Springston and D. A. Dezero, *J. Chromatogr.*, 454 (1989) 80.
6. N. D. Petsev, T. B. Gavrilova, I. Topalova, Chr. Dimitrov, G. Pavlova-Veriovkina and St. Ivanov, *Izv. Khim. Inst. Bulg. Akad. Nauk.*, 15 (1982) 123.
7. T. B. Gavrilova, T. M. Roshchina, E. V. Vlasenko, Chr. Dimitrov, St. Ivanov, N. Petsev and I. Topalova, *J. Chromatogr.*, 364 (1986) 439.

- 8 T. B. Gavrilova, I. V. Parshina, Chr. Dimitrov, St. Ivanov, N. Petsev and I. Topalova, *J. Chromatogr.*, 402 (1987) 87.
- 9 H. Yasuda, *Plasma Polymerisation*, Academic Press, Orlando, FL, San Diego, CA, Tokyo, 1985.
- 10 Chr. Dimitrov, N. D. Petsev, M. Gigova and St. I. Ivanov, *C.R. Acad. Bulg. Sci.*, 31 (1978) 1429.
- 11 N. Petsev, I. Topalova, St. I. Ivanov, Chr. Dimitrov, T. B. Gavrilova and E. V. Vlasenko, *J. Chromatogr.*, 286 (1984) 57.
- 12 N. K. Bebris, E. Ya. Gienko, G. E. Zaytseva, A. V. Kiselev, G. L. Kustova, B. A. Lipkind, Yu. S. Nikitin and Ya. I. Yashin, *Neftokhimiya*, 10 (1970) 773.
- 13 M. S. Vigdergauz and R. I. Izmailov, *Primenenije gazovoy khromatografii dlya opredeleniya fiziko-khimicheskikh svoystv veshchestv (Application of Gas Chromatography for Identification of Physico-chemical Properties of Substances)*, Nauka, Moscow, 1967.
- 14 A. V. Kiselev, *Zur. Fiz. Khim.*, 41 (1967) 2470.
- 15 Yu. S. Nikitin, Ron Tak Ro and N. K. Shonia, *J. Chromatogr.*, 446 (1988) 55.
- 16 N. K. Bebris, Yu. S. Nikitin, A. A. Pyatygin and N. K. Shonia, *J. Chromatogr.*, 364 (1986) 409.

CHROMSYMP. 2104

Live retention database for identification in multi-step temperature-programmed capillary gas chromatography

YAFENG GUAN* and LIANGMO ZHOU

Laboratory of Analytical Chemistry, Dalian Institute of Chemical Physics, Chinese Academy of Sciences, P.O. Box 100, Dalian 116012 (China)

ABSTRACT

A calculation procedure for multi-step temperature programmed gas chromatographic retention times and that was investigated over diverse temperature programme conditions is described. Thermodynamic parameters of components, calculated from their Kováts retention indices and the isothermal retention times of *n*-alkanes, are utilized in the procedure. The influence of column dead time and variations of Kováts retention indices is examined. The calculation accuracies are better than 1% in most instances. A live retention time database for multi-step temperature programming was constructed using this procedure.

INTRODUCTION

Calculation of temperature-programmed retention times or indices from isothermal data has been reported in the past using different approaches [1–9]. The correct way for such a conversion is through thermodynamic theory [1–4]. The ultimate goal of the calculation is to replace standard samples in qualitative analysis using capillary gas chromatography. It is therefore critical that the calculation accuracy is compatible with the overall accuracy of the gas chromatograph. It is also vitally important that the isothermal retention data used for the calculation are easy to measure and to document, and to be transferrable between laboratories.

The type of isothermal retention data and their accuracy will undoubtedly affect the calculation accuracy. The thermodynamic quantities ΔS and ΔH of a component on a given stationary phase have been proposed as basic data for intercolumn data transfer [1,3]. It was found, unfortunately, that ΔS and ΔH are dependent on the stationary phase film thickness, phase ratio (β) and column temperature [1,4], although the agreement between Kováts retention indices on the columns tested is better than ± 0.5 index unit.

Calculation of linear temperature-programmed retention indices with high accuracy had been described in a previous paper [4]. As most of the temperature-programmed analyses involve initial and final hold times, or even several programming steps, the calculation of retention time in multi-step temperature programming is more demanding.

In this work, Kováts retention indices at two temperature were chosen as the basic data. Retention times of *n*-alkanes at two temperatures were used to characterize the column and carrier gas flow. They were also used to calculate, in combination with Kováts retention indices, the thermodynamic parameters of components. The calculation accuracies for different classes of compounds under diverse temperature-programmed conditions were demonstrated.

CALCULATION

The entropy and enthalpy terms of each component on a column are determined by

$$-\frac{\Delta H}{R} = [\ln k(i, T_1) - \ln k(i, T_2)] \left(\frac{T_1 T_2}{T_2 - T_1} \right) \quad (1)$$

$$\frac{\alpha}{\beta} = \exp \left[\ln k(i, T) - \frac{\Delta H}{RT} \right] \quad (2)$$

where $\alpha = \exp(\Delta S/R)$.

The deduction of eqns. 1 and 2 is the same as described previously [4], the film thickness or phase ratio dependence of the thermodynamic parameters being corrected automatically without the need to know them.

The calculation of the multi-step temperature-programmed retention time of each component is achieved by solving the following numerical integration equation:

$$\int_0^{t_i} \frac{dt}{T(t) \left[1 + \frac{\alpha}{\beta} \exp \left(\frac{-\Delta H}{RT(t)} \right) \right]} = 1 \quad (3)$$

where $T(t) = T_0 + \sum r(i)t(i)$; $i = 0, 1, 2, \dots$

The $r(i)$ value can be positive, negative or zero, corresponding to upward temperature programming, downward programming and a plateau, respectively. There is no limitation to the number of steps or the function type of the programming rate. To ensure calculation accuracy, the time interval of the integration should be $\leq 0.005t_0(T)$.

When a series of *n*-alkanes can be mixed into the sample, a temperature-programmed retention index, as defined by Van den Dool and Kratz [10], can provide better accuracy for compound identification, as it tolerates instability of the gas chromatograph to a greater extent.

EXPERIMENTAL

A Model GC-R1A gas chromatograph (Shimadzu, Kyoto, Japan) was used for all experiments. An external thermometer was used to calibrate the oven temperature under isothermal conditions. Four cross-linked fused-silica columns coated with

TABLE I
COLUMN SPECIFICATIONS

Column No.	Stationary phase	Length (m)	I.D. (mm)	Film thickness (μm)	Manufacturer
1	OV-1	50	0.31	0.52	Hewlett-Packard
2	SE-54	25	0.25	0.3	Dalian Institute of Chemical Physics
3	PEG-20M	25	0.25	0.2	Dalian Institute of Chemical Physics
4	FFAP	30	0.20	0.32	Lanzhou Institute of Chemical Physics

different stationary phases from different manufacturers were randomly selected for the test. Their specifications are listed in Table I.

Samples containing hydrocarbon, phenols, alcohols, esters, ketones, aromatic hydrocarbons and amines were used in the experiments. Hydrogen was used as the carrier gas. The splitting ratio of the injection was 1:50. The temperatures of the injection port and detector block were 250°C. An IBM AT-class microcomputer with math coprocessor was used for computation. Software was written in Quick-Basic V.4.0 (Micro-Soft). The typical calculation time for a 22-component sample with a 35-min chromatogram was 13–20 s.

RESULTS AND DISCUSSION

The calculation accuracy of the retention time, according to eqn. 3, is affected by the errors of thermodynamic parameters, column dead time and temperature. We use $\Delta S/R - \ln \beta$ as one term (entropy term) instead of ΔS . For columns with the same stationary phase and reproducible Kováts retention indices but different film thicknesses and dimensions, their entropy and enthalpy terms $\Delta H/R$ are different [1,4]. One way to obtain accurate values of these terms is to measure all the components on the column used [1–3,5]. It is a tedious task and often impossible to carry out. Another procedure, as we propose, is to use the Kováts retention indices, either measured or published, to calculate the isothermal terms. The only additional experimental data needed in the calculation are the retention times of *n*-alkanes measured at two temperatures on the column to be used.

The calculated and experimental results are given in Table II for an OV-1 column. There is excellent agreement for even multi-step temperature programming. The chromatographic conditions are listed in Table III. Tabulated Kováts retention indices, most of them from published data [11], were used in the calculation as this column was well defined.

Tables IV, VI and VIII further demonstrate the fitness of the calculation and observed results for three columns with different polarities and under diverse temperature programming conditions. The differences between the calculated and measured retention times is less than 1%, regardless of the steps of temperature programming and the properties of the stationary phases.

For polar phase columns from different manufacturers, the reproducibility of the Kováts retention indices if poor and published data can hardly be used at the

TABLE II
RETENTION TIME CALCULATION FOR COLUMN 1

Component	Programme A		Programme B		Programme C		Programme D	
	Calc.	Meas.	Calc.	Meas.	Calc.	Meas.	Calc.	Meas.
Decane	5.78	5.73	8.57	8.55	6.11	6.13	5.98	5.96
<i>o</i> -Cresol	6.29	6.26	9.17	9.21	6.75	6.80	6.50	6.50
<i>p</i> -Cresol	6.71	6.68	9.68	9.68	7.33	7.30	6.94	6.94
2,6-Xylenol	7.55	7.51	10.48	10.41	8.51	8.53	7.84	7.82
Undecane	7.95	7.92	10.90	10.82	9.19	9.21	8.30	8.28
2,4-Xylenol	8.44	8.40	11.32	11.26	10.02	10.03	8.87	8.86
2,5-Xylenol	8.48	8.45	11.36	11.30	10.10	10.12	8.93	8.92
3,5-Xylenol	8.90	8.87	11.72	11.66	10.87	10.89	9.45	9.44
2,3-Xylenol	9.13	9.10	11.91	11.84	11.26	11.26	9.75	9.74
3,4-Xylenol	9.48	9.45	12.19	12.12	11.89	11.90	10.21	10.20
Dodecane	10.35	10.34	12.87	12.79	13.51	13.48	11.46	11.45
<i>o</i> - <i>tert.</i> -Butylphenol	11.45	11.45	13.70	13.65	15.56	15.47	13.07	13.05
1-Decanol	11.67	11.66	13.87	13.80	16.11	16.04	13.40	13.37
2,3,5-Trimethylphenol	11.95	11.97	14.09	14.06	16.64	16.55	13.76	13.75
Tridecane	12.76	12.79	14.77	14.75	18.20	18.14	14.84	14.83
2- <i>tert.</i> -Butyl-4-cresol	13.43	13.46	15.35	15.38	19.31	19.26	15.69	15.69
6- <i>tert.</i> -Butyl-3-cresol	13.70	13.74	15.59	15.64	19.70	19.67	16.01	16.03
Tetradecane	15.53	15.53	17.18	17.27	22.24	22.22	17.94	18.01
Pentadecane	10.43	19.35	20.55	20.87	—	—	21.05	21.25

TABLE III
TEMPERATURE PROGRAMMING CONDITIONS FOR COLUMN 1

Condition	Step No.	Temperature (°C)	Hold time (min)	Programming rate (°C/min)
A	1	97.5	3.0	6.0
	2	155.0	Hold	
B	1	77.0	5.0	10.0
	2	158.0	Hold	
C	1	97.5	2.0	2.0
	2	109.0	2.0	4.0
	3	125.0	2.0	6.3
	4	150.0	2.0	8.0
	5	220.0	Hold	
D	1	77.5	0.0	10.0
	2	98.0	0.0	4.0
	3	118.0	0.0	2.0
	4	128.0	0.0	8.0
	5	144.0	0.0	4.0
	6	164.0	0.0	2.0
	7	170.0	0.0	3.0
	8	200.0	Hold	

TABLE IV
RETENTION TIME CALCULATION FOR COLUMN 2

For temperature programming conditions see Table V.

Component	Programme A		Programme B		Programme C		Programme D	
	Calc.	Meas.	Calc.	Meas.	Calc.	Meas.	Calc.	Meas.
Decane	2.32	2.35	—	—	1.88	1.90	2.60	2.63
<i>o</i> -Cresol	3.57	3.50	3.53	3.50	2.68	2.62	4.04	4.05
<i>p</i> -Cresol	4.10	4.04	3.95	3.94	3.01	2.94 ^a	4.60	4.62
Undecane	3.91	3.92	3.81	3.81	2.91	2.94 ^a	4.39	4.39
Dodecane	6.59	6.60	5.54	5.55	4.88	4.88	7.33	7.34
1-Decanol	8.55	8.53	6.85	6.84	7.12	7.13	10.57	10.56
Tridecane	9.07	9.09	7.22	7.22	7.84	7.90	11.48	11.49
Tetradecane	11.21	11.20	8.76	8.76	11.15	11.21	15.82	15.82
Methyl undecanoate	11.76	11.75	9.15	9.15	12.06	12.09	16.75	16.73
Pentadecane	13.53	13.52	10.17	10.17	14.74	14.79	18.72	18.72
Methyl dodecanoate	14.31	14.29	10.55	10.57	15.97	15.99	19.33	19.34
Hexadecane	16.98	16.94	11.78	11.81	20.23	20.22	20.80	20.84

^a Peaks overlap.

present stage. In view of this difficulty, measured Kováts retention indices were used in the calculations for columns 3 and 4. The data in Tables VI and VIII demonstrate the accuracy of the procedure for polar phase columns. Their temperature programming conditions are listed in Tables VII and IX, respectively.

For apolar stationary phases, columns with highly reproducible Kováts retention indices are commercially available. It is feasible to use published standard Kováts retention indices for the calculations. However, for each individual column, its Kováts retention indices will certainly show some deviation from the standard values. To simulate the real situation, the Kováts retention indices of some arbitrarily selected compounds were varied deliberately by ± 0.5 index unit and were used for the

TABLE V
TEMPERATURE PROGRAMMING CONDITIONS FOR COLUMN 2

Condition	Step No.	Temperature (°C)	Hold time (min)	Programming rate (°C/min)
A	1	87.0	5.0	8.0
	2	137.0	Hold	
B	1	87.0	3.0	10.0
	2	157.0	Hold	
C	1	97.5	5.0	4.0
	2	127.5	Hold	
D	1	82.5	2.0	2.0
	2	90.0	2.0	4.2
	3	107.0	2.0	8.0
	4	200.0	Hold	

TABLE VI
RETENTION TIME CALCULATION FOR COLUMN 3

Component	Programme A		Programme B		Programme C		Programme D	
	Calc.	Meas.	Calc.	Meas.	Calc.	Meas.	Calc.	Meas.
Decane	1.33	1.34	1.39	1.40	1.29	1.29	1.29	1.17
Ethylbenzene	1.53	1.53	1.62	1.62	1.50	1.50	1.36	1.33
Undecane	1.67	1.69	1.82	1.83	1.68	1.69	1.47	1.45
Dodecane	2.24	2.25	2.61	2.60	2.41	2.44	1.98	1.97
2-Octanone	2.33	2.34	2.70	2.71	2.50	2.52	2.08	2.04
Tridecane	3.11	3.29	3.81	3.77	3.58	3.57	2.85	2.81
Octyl acetate	4.21	4.20	5.35	5.33	5.01	5.00	3.97	3.90
Tetradecane	4.29	4.24	5.52	5.47	5.17	5.15	4.06	4.03
1-Octanol	5.37	5.31	7.22	7.20	6.74	6.69	5.20	5.13
Pentadecane	5.73	5.66	7.70	7.66	7.20	7.18	5.59	5.62
1-Pentadecene	6.50	6.42	8.65	8.62	8.08	8.03	6.47	6.45
1-Nonanol	7.00	6.92	9.35	9.32	8.65	8.57	7.01	6.97
Hexanecane	7.33	7.27	9.87	9.84	9.05	9.03	7.38	7.45
1-Decanol	8.70	8.64	12.04	12.04	10.79	10.72	8.76	8.74
Heptadecane	8.99	9.06	12.52	12.53	11.18	11.19	9.03	9.10
2,6-Xylidine	10.22	10.22	14.60	14.68	12.70	12.67	10.10	10.07
Octadecane	10.62	10.66	15.80	15.91	13.34	13.40	10.46	10.51

TABLE VII
TEMPERATURE PROGRAMMING CONDITIONS FOR COLUMN 3

Condition	Step No.	Temperature (°C)	Hold time (min)	Programming rate (°C/min)
A	1	85.0	0.0	6.0
	2	220.0	Hold	
B	1	81.5	2.0	6.5
	2	94.5	2.0	9.5
	3	113.5	2.0	4.0
	4	122.0	2.0	1.5
	5	125.0	2.0	5.0
	6	200.0	Hold	
C	1	82.0	2.0	6.0
	2	94.0	0.0	2.0
	3	98.0	0.0	9.5
	4	117.0	0.0	2.0
	5	121.0	0.0	4.0
	6	129.0	0.0	6.0
	7	200.0	Hold	
D	1	91.0	2.0	6.5
	2	104.0	0.0	4.0
	3	112.0	0.0	7.0
	4	126.0	0.0	9.0
	5	143.0	0.0	7.0
	6	200.0	Hold	

TABLE VIII
RETENTION TIME CALCULATION FOR COLUMN 4

Component	Programme A		Programme B		Programme C	
	Calc.	Meas.	Calc.	Meas.	Calc.	Meas.
Decane	1.11	1.12	1.06	1.06	1.08	1.07
Ethylbenzene	1.34	1.33	1.28	1.25	1.31	1.27
Dodecane	2.01	2.03	1.91	1.91	1.96	1.94
Tridecane	2.97	2.96	2.78	2.75	2.84	2.80
Octyl acetate	4.30	4.24	3.77	3.74	3.85	3.79
Tetradecane	4.58	4.61	3.96	3.96	4.03	4.03
1-Octanol	5.99	6.00	4.89	4.89	5.01	4.98
Pentadecane	6.87	6.90	5.61	5.60	5.81	5.80
1-Pentadecene	7.79	7.82	6.52	6.53	6.80	6.80
1-Nonanol	8.16	8.17	6.94	6.94	7.19	7.18
Hexadecene	8.92	8.94	7.92	7.86	8.01	8.02
1-Decanol	10.05	10.08	9.58	9.59	9.44	9.44
Heptadecane	10.68	10.72	10.59	10.56	10.47	10.46
2-Ethylhexanoic acid	11.39	11.42	11.64	11.64	11.66	11.60
Octadecane	12.23	12.30	13.20	13.18	13.70	13.66
2,6-Xylidine	12.96	13.00	14.30	14.30	15.52	15.42

TABLE IX
TEMPERATURE PROGRAMMING CONDITIONS FOR COLUMN 4

Condition	Step No.	Temperature (°C)	Hold time (min)	Programming rate (°C/min)
A	1	99.5	5.0	7.9
	2	200.0	Hold	
B	1	99.5	2.0	6.0
	2	111.5	0.0	1.9
	3	119.0	0.0	4.0
	4	137.0	0.0	7.5
	5	152.0	0.0	3.0
	6	158.0	0.0	8.5
	7	175.0	0.0	5.0
	8	200.0	Hold	
C	1	99.5	2.0	6.0
	2	111.5	2.0	7.8
	3	127.0	2.0	2.0
	4	131.0	2.0	4.5
	5	140.0	2.0	6.0
	6	200.0	Hold	

TABLE X

EFFECT OF VARIATION OF KOVÁTS RETENTION INDEX ON CALCULATED RESULTS

Calculated on column 1 with temperature programme C.

Component	Increment of all Kováts retention indices					
	0 i.u.		-0.5 i.u.		+0.5 i.u.	
	Meas.	Calc.	Calc.	Calc.	Calc.	
<i>o</i> -Cresol	6.80	6.75	6.72	6.77		
<i>p</i> -Cresol	7.30	7.33	7.30	7.34		
2,6-Xylenol	8.53	8.51	8.48	8.53		
2,4-Xylenol	10.03	10.02	9.98	10.04		
2,5-Xylenol	10.12	10.10	10.06	10.13		
3,5-Xylenol	10.89	10.87	10.83	10.90		
2,3-Xylenol	11.26	11.26	11.22	11.29		
3,4-Xylenol	11.90	11.89	11.85	11.92		
<i>o</i> - <i>tert.</i> -Butylphenol	15.47	15.56	15.51	15.59		
1-Decanol	16.04	16.11	16.06	16.13		
2,3,5-Trimethylphenol	16.64	16.55	16.59	16.66		
2- <i>tert.</i> -Butyl-4-cresol	19.26	19.31	19.27	19.33		
6- <i>tert.</i> -Butyl-3-cresol	19.67	19.70	19.66	19.72		

calculation of retention time. A comparison between the calculated values using the standard and varied Kováts retention indices and the measured values is shown in Table X. The results show that the relative deviations of the calculated retention times and the Kováts retention indices are of the same order of magnitude.

In the measurement of *n*-alkane retention times at two isothermal states, the retention times of methane are used as the column dead time [$t_0(T)$], which always has the highest relative deviation. The error in the $t_0(T)$ determination will influence the

TABLE XI

CALCULATION USING DIFFERENT t_0 VALUES ON COLUMN 2

Component	Programme C		Programme D	
	Measured t_0	Extrapolated t_0	Measured t_0	Extrapolated t_0
Decane	1.88	1.79	2.60	2.16
<i>o</i> -Cresol	2.68	2.55	4.04	3.41
<i>p</i> -Cresol	3.01	2.87	4.60	3.94
Undecane	2.91	2.78	4.39	3.76
Dodecane	4.85	4.65	7.33	6.63
1-Decanol	7.12	6.96	10.57	10.03
Tridecane	7.84	7.70	11.48	11.03
Tetradecane	11.15	11.12	15.82	15.67
Methyl undecanoate	12.06	12.05	16.75	16.65
Pentadecane	14.74	14.76	18.72	18.68
Methyl dodecanoate	15.97	16.01	19.33	19.30
Hexadecane	20.23	20.30	20.80	20.73

calculated results, particularly the earlier eluting components. Table XI gives the calculated results on column 2 using measured and extrapolated [12] column dead times. The influence is dependent on the programming conditions.

The above procedure leads to an easy and reliable database for identification in multi-step temperature-programmed capillary gas chromatography. Isothermal runs and linear temperature programming are the simplest forms or a step unit in multi-step programming, and are included in the procedure and the database.

ACKNOWLEDGEMENTS

This work was supported by the Chinese National Natural Science Funds, contract No. 0289019, and the Youth Scientific Funds of the Chinese Academy of Sciences and Dalian Institute of Chemical Physics, contract No. QJ-002.

REFERENCES

- 1 J. Curvers, J. Rijks and C. Cramers, *J. High Resolut. Chromatogr. Chromatogr. Commun.*, 8 (1985) 607.
- 2 E. E. Akporhonor, S. Le Vent and D. R. Taylor, *J. Chromatogr.*, 405 (1987) 67.
- 3 E. V. Dose, *Anal. Chem.*, 59 (1987) 2414.
- 4 Y. Guan, J. Kiraly and J. Rijks, *J. Chromatogr.*, 472 (1989) 129.
- 5 P.-C. Lu, B.-C. Lin, X.-H. Chu, C.-R. Luo, G.-D. Lai and H.-C. Li, *J. High Resolut. Chromatogr. Chromatogr. Commun.*, 9 (1986) 702.
- 6 R. V. Golovnya and V. P. Utaletz, *J. Chromatogr.*, 36 (1968) 276.
- 7 E. B. Moinár, P. Moritz and J. Takács, *J. Chromatogr.*, 66 (1972) 205.
- 8 J. Krupcik, P. Cellar, D. Repka, J. Garaj and G. Guiochon, *J. Chromatogr.*, 351 (1986) 111.
- 9 M. Maek, A. Y. Badjah Jadj Ahmed, A. Touabet and B. Y. Meklati, *Chromatographia*, 22 (1986) 245.
- 10 H. van den Dool and P. D. Kratz, *J. Chromatogr.*, 11 (1963) 463.
- 11 *The Sadtler Standard Gas Chromatography Retention Index Library*, Sadtler Research Laboratories, Division of Bio-Rad Laboratories, Philadelphia, PA, 1986.
- 12 M. L. Peterson and J. Hirsch, *J. Lipid Res.*, 1 (1959) 132.

CHROMSYMP. 2332

Gas-liquid microcapillary columns precoated with graphitized carbon black

G. P. CARTONI*, L. CASTELLANI, G. GORETTI, M. V. RUSSO and P. ZACCHEI

Department of Chemistry, University of Rome "La Sapienza", Piazzale Aldo Moro 5, 00185 Rome (Italy)

ABSTRACT

Glass and fused-silica capillary columns (100 μm I.D.) were precoated with a very thin layer of graphitized carbon black and then coated with polar liquid phases. The layer of carbon black in the inner walls increased the wettability of the capillary columns and, consequently, a very uniform coating was obtained. The polymeric polar liquid phases were also more strongly retained on the carbon black, and these microcapillary columns showed a much higher temperature stability. Columns coated with free fatty acid phase, Carbowax 20M, 40M and 600M were prepared. The columns were tested with a mixture of polar compounds.

INTRODUCTION

Capillary columns with internal walls modified by a thin layer of graphitized carbon black (GCB) have been used in gas chromatography (GC) for a long time. They have been the object of many studies since they present very high efficiencies, are simple to prepare and because it is possible to change their selectivity by varying the stationary phase charge, thus allowing operations in both gas-liquid chromatographic and gas-solid-liquid chromatographic contexts [1–13].

Until now research has been carried out mainly with graphitized columns with an I.D. of 200–500 μm , although promising results have been obtained with columns of 150–160 μm I.D. [6,7]. Microcapillary columns (I.D. < 200 μm) are, as has recently been shown, characterized by a large number of theoretical plates (N) per metre and per second. Moreover, they present mass transfer resistance values (C) such as to allow analytical separation even at high linear velocity values. The main constraint on their use has been the insufficient rate of response of detectors and recorders, which may by now be largely regarded as outdated by modern equipment standards. At present, the only hindrance to their use is the sampling rate. In fact, when such high values per second for theoretical plates are reached ($N/s = 10^4$), with columns of 50 μm I.D. the sampling rate becomes a strongly limiting factor, especially for the separation of substances having low retention time [14–28].

This study describes the technique for preparing microcapillary columns precoated with Carbowax A, of 100 μm I.D., and then coated with polar stationary phases, reaching high efficiency. Some complex-mixture separations are reported.

Moreover, particular attention has been devoted to the possibility of using these microcapillary columns for aromatic and aliphatic amines, given the promising results obtained on classical capillary columns precoated with GCB [29].

EXPERIMENTAL

Equipment

Two DANI gas chromatographs were used, Model 3900 and Model 6500 (Monza, Italy), equipped with a flame ionization detector and split injector with 1:500 split ratio, and connected to a Shimadzu CR3A integrator-recorder.

Preparation of microcapillaries

Glass capillaries with 100 μm I.D. were obtained from Duran glass tubes cleaned with a solution of sulphuric acid (96%)–0.1 *M* potassium dichromate for 48 h, washed extensively in water and acetone and then dried. After this treatment, the tubes were drawn using a Carlo Erba GCDM 60 drawing machine. The 100 μm I.D. glass capillaries thus obtained were washed in dichloromethane and dried under nitrogen flow. The fused-silica capillaries were supplied by SGE (Australia).

The columns were precoated with a solid support, Carbowax A (Supelco, Bellefonte, PA, U.S.A.), a GCB having a surface area of around 12 m^2/g . The dynamically deposited support increased the surface area with respect to the smooth capillary, increasing stationary phase wettability. This allowed a uniform deposit of the stationary phase to be obtained. Support depositing was carried out with a GCB suspension prepared with 50 mg GCB, 25 ml carbon tetrachloride, 25 ml dichloromethane and then exposing to ultrasonic waves for about 30 min. Approximately 2 ml of this suspension were made to flow at high speed (*ca.* 60 cm/s) through the capillary for four times in succession, each time reversing flow direction and waiting for solvent evaporation. The support layer of GCB obtained inside the capillary was then thermally treated with Carbowax 20M (C 20M). This pretreatment was carried out by statically depositing C 20M from a 0.2% solution in dichloromethane. After conditioning in a flow of hydrogen for about 10 min at a temperature of 240°C, the column was put into the oven at a temperature of 280°C for one night, after having sealed both ends under a flame. The column was cooled to room temperature and then washed with dichloromethane. Pretreatment with C 20M probably increases the wettability of capillary internal surface for polar stationary phases, deactivates the walls and makes the GCB surface uniform.

After undergoing this treatment, the column is statically coated with the stationary phase. Using a concentrated solution enabled the desired film thickness to be obtained. The columns were conditioned by programming the temperature to increase by 3°C min from 50°C to 240°C and keeping the column at the latter temperature for 90 min under hydrogen flow. Microcapillary columns were prepared using different stationary phases: C 20M, C 40M, C 600M and free fatty acid phase (FFAP). Assessment of GC parameters of the columns was carried out by GC of a mixture of *n*-octanol, 2,6-dimethylphenol (DMF) and 2,6-dimethylaniline (DMA) at 90°C. In the reported analysis hydrogen, as carrier gas, is used with a linear gas velocity of the values given in Table I.

TABLE I

COLUMN CHARACTERISTICS (I.D. 100 μm)

C = Carbowax; FFAP = free fatty acid phase; DMA = 2,6-dimethylaniline, DMF = 2,6-dimethylphenol.

Column No.	Phase	Length (m)	D_f (μm)	k'	U_{opt} (cm/s)	H_{min} (mm)	N/s	UTE (%)	Test substance
1	C 20M	5.7	0.10	52.2	52.6	0.109	4830	87	DMA
2	C 20M	16.0	0.07	51.1	54.2	0.091	5960	100	DMA
3	C 40M	5.5	0.10	57.9	50.2	0.116	4330	82	DMA
4	C 40M	5.5	0.20	87.0	55.0	0.110	5050	87	DMA
5	C 40M	4.6	0.10	85.2	54.0	0.116	4660	81	DMF
6	C 40M	7.2	0.10	45.1	51.1	0.087	5870	100	DMA
7	C 600M	6.0	0.07	49.3	57.3	0.103	5560	93	DMA
8 ^a	C 600M	15.0	0.07	49.3	56.6	0.094	6020	100	DMA
9 ^a	C 600M	10.0	0.07	61.9	54.3	0.088	6130	100	DMA
10	FFAP	8.5	0.07	58.9	60.7	0.115	5280	82	DMF

^a Fused silica.

RESULTS AND DISCUSSION

Fig. 1A and B shows the effects due to pretreatment with C 20M. The gas chromatograms were obtained at 90°C by injecting the mixture of DMF, DMA and *n*-octanol on two glass columns with stationary phase C 40M. The chromatogram in Fig. 1A was obtained on a column not pretreated with C 20M, while the one in Fig. 1B was obtained on a column pretreated with C 20M. As may be observed in Fig. 1A,

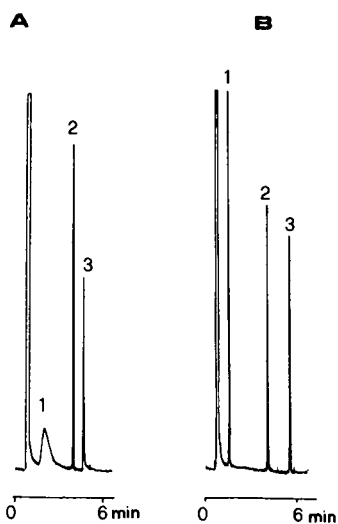


Fig. 1. Gas chromatograms of polar compounds on two columns: (A) not pretreated by C 20M; (B) pretreated by C 20M at 90°C. Peaks: 1 = *n*-octanol; 2 = DMA; 3 = DMF.

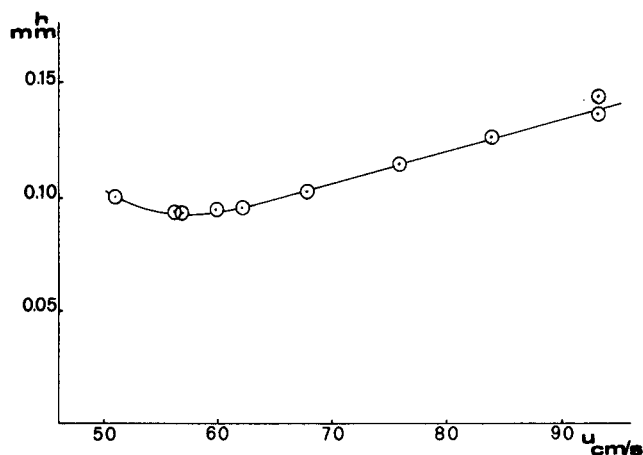


Fig. 2. Van Deemter plot of DMA at 90°C. Column 7 of Table I.

the octanol peak is considerably deformed and the DMF peak shows a slight tail. In Fig. 1B, all the peaks are symmetrical.

Table I shows the GC characteristics of some columns that were pretreated and coated with a polar stationary phase. Theoretical plate height (H_{min}), capacity ratio (k'), liquid film thickness (D_f), optimum linear velocity (U_{opt}), utilized theoretical efficiency (UTE%) and number of plates per second (N/s) are reported for each column. From the results in the table, all the columns show UTE values that lie between 82 and 100%, H_{min} values ranging from 0.08 to 0.116 mm, with optimum linear velocities between 50 and 60 cm/s and N/s values between 4400 and 6000.

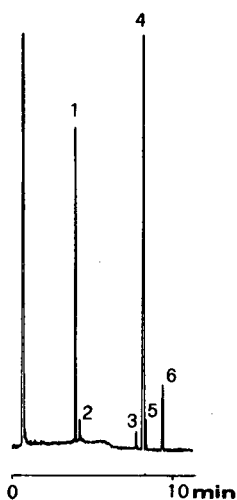


Fig. 3. Olive oil analysis on column 3 of Table I (C 20M), fatty acid methyl esters. Peaks: 1 = palmitic; 2 = palmitoleic; 3 = stearic; 4 = oleic; 5 = elaidinic; 6 = linoleic acid. Temperature 180°C.

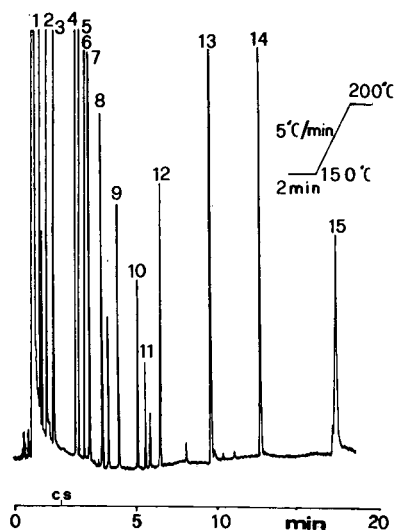


Fig. 4. Gas chromatogram of free fatty acid mixture. Column 9 of Table I. (FFAP) Peaks: 1 = acetic; 2 = propionic; 3 = butyric; 4 = valeric; 5 = caproic; 6 = heptanoic; 7 = caprylic; 8 = pelargonic; 9 = capric; 10 = undecenoic; 11 = undecylenic; 12 = lauric; 13 = myristic; 14 = palmitic; 15 = stearic acid.

Fig. 2 shows the Van Deemter curve obtained on column, 7 of Table I at a temperature of 90°C. Note that, even if linear velocity is considerably increased, efficiency still remains high. In fact, the mass transfer term (C) of this column is $15 \cdot 10^{-5}$ s. The temperature stability of these columns is higher than that of the columns coated with the same phases without GCB precoating and is similar to that obtained with the same bonded phases [30].

Some examples of complex mixture analysis carried out on these microcapillary

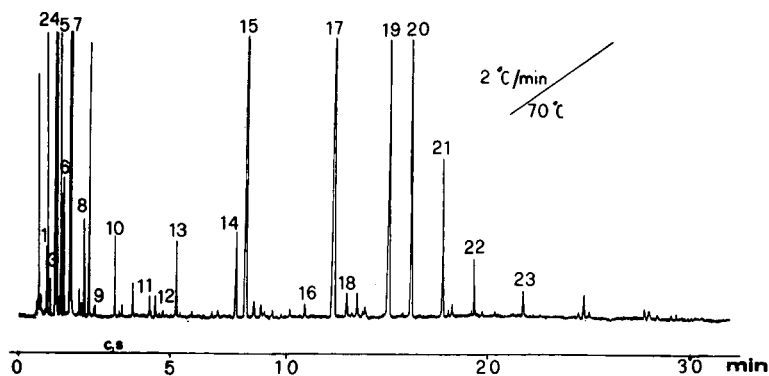


Fig. 5. Lemon petit grain oil, column 7 of Table I (C 600M). Peaks 1 = α -thujene; 2 = α -pinene; 3 = camphene; 4 = β -pinene; 5 = sabinene; 6 = myrcene; 7 = limonene; 8 = γ -terpinene; 9 = *p*-cymene; 10 = methyleptanone; 11 = nonanal; 12 = 3-octanol; 13 = citronellal; 14 = linalool; 15 = β -caryophyllene; 16 = humulene; 17 = neral; 18 = α -terpineol; 19 = geranial; 20 = neryl acetate; 21 = geranyl acetate; 22 = nerol; 23 = geraniol.

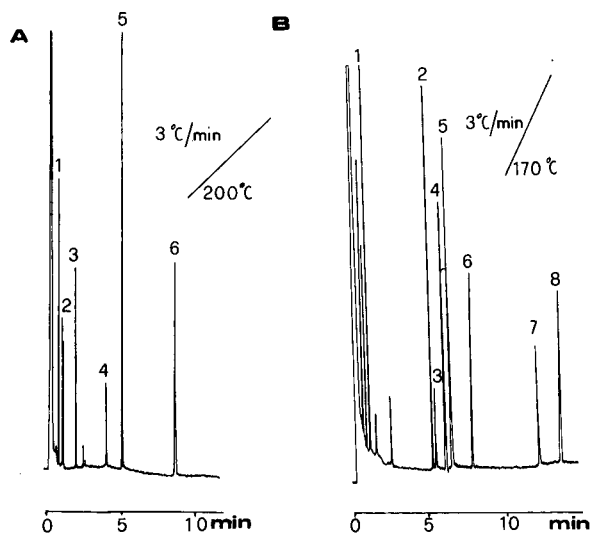


Fig. 6. Gas chromatograms of high-boiling amines on column 3 of Table I. Peaks: (A) 1 = *o*-phenylenediamine; 2 = *p*-phenylenediamine; 3 = *o*-nitroaniline; 4 = *m*-nitroaniline; 5 = 4-biphenylamine; 6 = *p*-nitroaniline; (B) 1 = 4-metroxyphenyl-1,2-ethylaminopropane; 2 = *N,N*-dimethyl-1,2-diphenylmethoxyethylamine; 3 = *N*-methyl-3,3-diphenylpropylamine; 4 = ketocaine; 5 = *N*-methyl-1,2-diphenylmethoxyethylamine; 6 = cyclizine; 7 = 2-diphenylmethoxyethylamine, 8 = adiphenine.

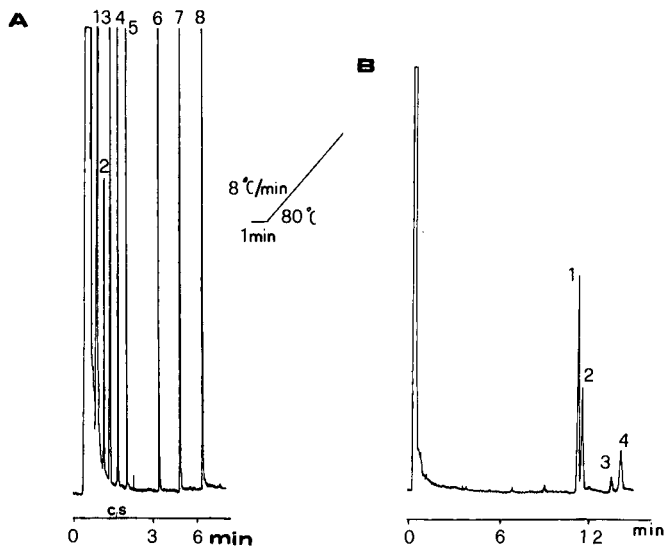


Fig. 7. Gas chromatogram of aliphatic amines on column of Table I. Peaks: (A) 1 = dipropylamine; 2 = pentylamine; 3 = dibutylamine; 4 = heptylamine; 5 = octylamine; 6 = decylamine; 7 = undecylamine; 8 = dodecylamine; (B) 1 = ephedrine; 2 = ψ -ephedrine; 3 = norephedrine; 4 = ψ -norephedrine. Temperature 125°C.

columns are reported. Fig. 3 shows the chromatogram obtained by analysing a mixture of fatty acid methyl esters, prepared by transesterification of an olive oil. Analysis was carried out with a C 20M column (column 2 in Table I) and with analysis time under 10 min. Fig. 4 shows the results obtained using a column of FFAP (Table I, column 10) in analysing a mixture of free acids ranging from acetic acid to stearic acid. In particular, it is possible to observe the separation (saturated-unsaturated) of undecenoic acid from undecylenic acid. Fig. 5 shows a typical example of essential oil analysis. The chromatogram was obtained by analysing an essential oil of lemon petit grain on column 7 (Table I).

Fig. 6 and 7 show four examples of amine analysis carried out on two C 40M columns: column 3 with $D_f = 0.1 \mu\text{m}$ and column 4 with $D_f = 0.2 \mu\text{m}$. Both columns may be used to analyse amines, but the lower phase charge of column 3 allows a reduction in the analysis times of high-boiling amines, while the greater phase charge makes column 4 more suitable for analysing low-boiling amines. Fig. 6 shows two analyses of high-boiling amines carried out on column 3, the first aromatic (A) and the second (B) of aliphatic type. In contrast, Fig. 7 shows two analyses of amines carried out on column 4. Fig. 7A is a mixture of aliphatic amines from pentyl to dodecylamine. Fig. 7B is a separation of ephedrine carried out isothermally at 125°C.

From the above, it is possible to note that all the columns present good efficiency with symmetrical peaks. Thus, it can be concluded that, even with reduced-diameter columns, GCB pre-coating does not reduce the typical characteristics of these microcapillary columns, namely high efficiency, low analysis times and lower operating temperatures, compared with classical capillary columns.

REFERENCES

- 1 C. Vidal Madjar, S. Bekany, M. F. Gonnard and G. Guichon, in R. Stock (Editor), *Gas Chromatography 1970*, Institute of Petroleum, London, 1971, p. 20.
- 2 G. Nota, G. Goretti, M. Armenante and G. Marino, *J. Chromatogr.*, 95 (1974) 229.
- 3 G. Goretti, A. Liberti and G. Nota, *Chromatographia*, 8 (1975) 486.
- 4 C. Vidal Madjar, S. Bekany, M. F. Gonnard, P. Arpino and G. Guichon, *Anal. Chem.*, 49 (1977) 768.
- 5 G. Goretti, A. Liberti and M. Ciardi, *Essenze Deriv. Agrum.*, 47 (1977) 269.
- 6 M. V. Russo, G. Goretti, A. Liberti, J. Laencina Sanchez and J. Flores Lorenzo, *Essenze Deriv. Agrum.*, 54 (1984) 13.
- 7 G. Goretti, A. Liberti and G. Pili, *J. High Resolut. Chromatogr. Chromatogr. Commun.*, 1 (1978) 143.
- 8 G. Goretti and A. Liberti, *J. Chromatogr.*, 161 (1978) 89.
- 9 A. Bacaloni, G. Goretti, A. Laganà and B. M. Petronio, *J. Chromatogr.*, 175 (1979) 169.
- 10 A. Liberti, G. Goretti and M. V. Russo, *J. Chromatogr.*, 279 (1983) 1.
- 11 M. V. Russo, G. Goretti and A. Liberti, *J. High Resolut. Chromatogr. Chromatogr. Commun.*, 8 (1985) 536.
- 12 F. Bruner, G. Crescentini, F. Mangani and M. Xiang, *Ann. Chim.*, 77 (1987) 745.
- 13 F. Bruner, G. Crescentini, F. Mangani, P. Palma and M. Xiang, *J. Chromatogr.*, 399 (1987) 87.
- 14 R. C. Kong and M. L. Lee, *J. High Resolut. Chromatogr. Chromatogr. Commun.*, 6 (1983) 319.
- 15 R. C. Kong, S. M. Fields, W. P. Jackson and M. L. Lee, *J. Chromatogr.*, 289 (1984) 105.
- 16 C. L. Wolley, K. E. Markides, M. L. Lee and K. D. Bartle, *J. High Resolut. Chromatogr. Chromatogr. Commun.*, 9 (1986) 506.
- 17 A. Farbrot, S. Folestad and M. Lanson, *J. High Resolut. Chromatogr. Chromatogr. Commun.*, 9 (1986) 117.
- 18 C. P. M. Schutjes, E. A. Vermeer, G. J. Scherpenzeel, R. W. Bally and C. A. Cramers, *J. Chromatogr.*, 289 (1984) 157.
- 19 M. Proot, D. P. Sandra and M. Verzele, *J. High Resolut. Chromatogr. Chromatogr. Commun.*, 8 (1985) 426.

- 20 A. Aerts, J. Rijks, A. Bergard and L. Blombey, *J. High Resolut. Chromatogr. Chromatogr. Commun.*, 9 (1986) 49.
- 21 M. Proot and P. Sandra, *J. High Resolut. Chromatogr. Chromatogr. Commun.*, 9 (1986) 618.
- 22 C. A. Cramers, *J. High Resolut. Chromatogr. Chromatogr. Commun.*, 9 (1986) 676.
- 23 K. J. Hyver, *J. High Resolut. Chromatogr. Chromatogr. Commun.*, 11 (1988) 69.
- 24 F. Lancas, F. David and P. Sandra, *J. High Resolut. Chromatogr. Chromatogr. Commun.*, 11 (1988) 73.
- 25 L. Wolley, B. J. Tarlet, K. D. Bartle, K. E. Markides, J. S. Brandshaw and M. L. Lee, *J. High Resolut. Chromatogr. Chromatogr. Commun.*, 11 (1988) 113.
- 26 K. Janak, V. Kahle, M. Horka and K. Tesakik, *J. High Resolut. Chromatogr. Chromatogr. Commun.*, 11 (1988) 63.
- 27 A. Van Es, C. Cramers and J. Rijks, *J. High Resolut. Chromatogr. Chromatogr. Commun.*, 12 (1989) 303.
- 28 G. P. Cartoni, G. Goretti, B. Neri and M. V. Russo, *J. Chromatogr.*, 475 (1989) 145.
- 29 G. Goretti, M. Ciardi and C. Di Palo, *J. High Resolut. Chromatogr. Chromatogr. Commun.*, 3 (1980) 523.
- 30 P. Sandra, M. Van Roelenbosch, I. Temmerman and M. Verzele, *Chromatographia*, 16 (1982) 63.

CHROMSYMP. 2285

Modern approach to the quantitative determination of volatiles in solid samples

Multiple headspace extraction gas chromatography for the determination of cyclohexanone residues in soil

M. R. MILANA*, A. MAGGIO, M. DENARO, R. FELICIANI and L. GRAMICCIONI

Laboratorio Tossicologia Applicata, Istituto Superiore di Sanita, Viale Regina Elena 299, 00161 Rome (Italy)

ABSTRACT

The application of multiple headspace extraction gas chromatography to the quantitative determination of volatiles in soil samples has been studied by means of a simulated system represented by cyclohexanone absorbed on a soil. An example of fast and accurate determination is reported. It has been experimentally demonstrated that this technique may overcome the problems linked to the handling of a solid matrix contaminated by volatiles, because it is not required to reproduce the solid matrix to perform a quantitative determination, it being sufficient to obtain complete vaporization of the calibration standard.

INTRODUCTION

The importance of environmental monitoring with respect to ubiquitous contaminants, has long been recognized, and this has led to the availability of standardized monitoring methods and reference materials [1].

A different situation pertains in the field of the accidental contamination of the environment caused by unforeseeable events, such as spillages, illegal waste, or accidents in chemical plants, ships, tanktrucks etc. In almost all such cases, besides the environmental "first aid" measures, it is necessary to perform quantitative determinations of the substances accidentally present in the environmental matrices. It is quite common to deal with volatile organic substances; their analysis is not too difficult in air, by means of absorbent tubes [2], and in aqueous samples, by means of static or dynamic headspace techniques [3–5]. When the polluted matrix is the soil, however, many difficulties arise. It is very difficult to carry out accurately liquid–solid extractions when the substances are volatile. Also, headspace techniques, calibrated by the usual methods, such as standard additions, internal standard or external calibration, rarely produce accurate results. This inadequacy is due to the practical impossibility

of overcoming matrix effects that dramatically influence partitioning of the volatile between the soil and the headspace [6], leading to highly inaccurate results [7].

A modern solution to these problems is an improvement of the automated headspace gaschromatographic analysis, a discontinuous gas extraction technique, called multiple headspace extraction (MHE-GC).

This technique is a repeated withdrawal of headspace in equilibrium with a solid sample, followed by a GC separation of the components in the headspace. If repeated extraction steps are performed the resulting chromatogram shows a series of peaks decreasing in their areas according to a logarithmic law. Theoretically extraction could be carried out until all the volatiles had been removed. However, after few steps (from six to nine) a mathematical extrapolation may be applied, to obtain the total amount of the compound to be determined. In fact, as extensively described by Kolb [8], it can be assumed that the chromatographic peak area is proportional to the concentration:

$$A_n = A_1 e^{(1-n)k^*} \quad (1)$$

where A_n is the peak area of the n^{th} step, and k^* is a constant including both chemical and instrumental parameters.

Eqn. 1 can be treated as a geometrical progression:

$$\Sigma A_n = A_1(1 + e^{-k^*} + e^{-2k^*} + e^{-3k^*} \dots) \quad (2)$$

and calculated according to:

$$\Sigma A_n = A_1 / (1 - e^{-k^*}) \quad (3)$$

Therefore, the total amount of a volatile in a vial is obtained from Eqn. 3, where A_1 is the experimental value of the peak area of the first MHE step. The value of k^* can be experimentally obtained by plotting the natural logarithms of the area values *versus* the number n of extraction steps (injections); in fact, at equilibrium, a straight regression line is obtained and the regression coefficient of this straight line corresponds to k^* .

To perform an accurate quantitative determination, calibration is carried out by submitting a vial containing only few microlitres of the volatile to the MHE procedure under the same instrumental conditions adopted for the solid matrix. By multiplying the response factor obtained from the standard by the total area value of the analyte peaks in the sample, the amount of the volatile in the sample can be easily obtained.

The suitability of this procedure for the fast quantitative determination of residual volatiles in contaminated soils has been experimentally studied by means of a simulated system of contamination. This system consists of a soil contaminated by a known amount of a volatile substance. Cyclohexanone was chosen as the volatile substance, and garden soil as representative of a common soil.

EXPERIMENTAL

Contaminated soil sample

A 30-g sample of the soil was accurately weighed and placed in a glass flask with a ground glass stopper. Then, 30 μl of an aqueous cyclohexanone standard solution (9420 mg/l) were added by means of a microsyringe, and the flask was slowly shaken mechanically, to allow the cyclohexanone to be absorbed homogeneously by the soil. The sample was shaken for 2 h at room temperature. The concentration of cyclohexanone in the soil was 9.42 $\mu\text{g/g}$.

Analytical samples

A 1-g sample of the contaminated soil was placed in a 20-ml headspace vial, 100 μl distilled water were added, and the vial was sealed with an open-centre aluminum cap and PTFE-faced butyl rubber septum. A small amount of water was added to promote the release of the volatile. This addition will be further discussed later. Six replicate soil samples were prepared. A blank sample was prepared by placing 1 g of uncontaminated soil and 100 μl of distilled water in a headspace vial.

Calibration standard

A 1- μl volume of the aqueous cyclohexanone standard was placed in an empty headspace vial, through the septum of an already sealed vial, by means of a 1- μl microsyringe. This calibration vial contained 9.42 μg of cyclohexanone in 1 μl of water. Three replicate calibration standards were prepared.

Instrumentation

The GC system consisted of a Perkin-Elmer 8500 gas chromatograph, equipped with a Perkin-Elmer HS101 automatic headspace sampler and a flame ionization detector. Data collection and handling were performed with an Epson PCAX2 and Perkin-Elmer Nelson 2600 chromatography software.

Operating conditions

The fused-silica column (10 m \times 0.53 mm I.D.) was CP-Sil-19 CB, with film thickness, 2 μm (Chrompack, the Netherlands). The GC operating conditions were as follows: oven temperature, 60°C (isothermal); injector temperature, 160°C; detector temperature, 220°C; carrier gas, nitrogen; headpressure, 40 kPa; run time, 6 min. The MHE operating conditions were as follows: thermostat temperature, 100°C; needle temperature, 110°C; transfer line temperature, 120°C; injections per vial, 9; thermostating time, 45 min (soil samples), 15 min (standards); pressurization time, 1 min; injection time, 0.10 min; withdrawal time, 0.20 min; number of vents, 1. It must be stressed that thermostating times are different between samples and standards. In fact, to perform an accurate MHE determination, it is of fundamental importance to evaporate the calibration standard totally. Therefore, some preliminary tests were carried out by analysing identical standards after increasing thermostating times; it was observed that 15 min were sufficient, at the selected temperature, to ensure the complete vaporization of cyclohexanone standard.

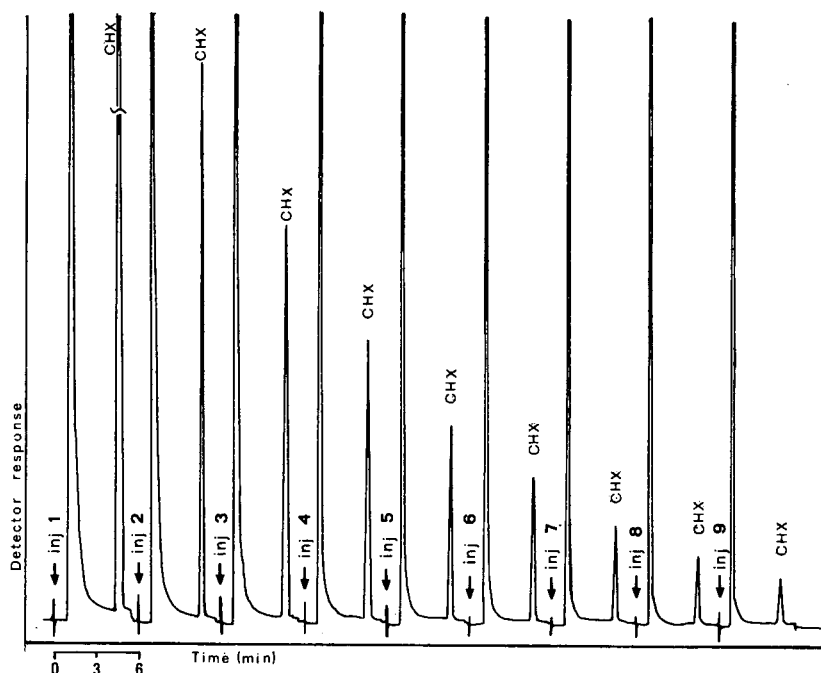


Fig. 1. Chromatograms from a nine-step MHE determination of cyclohexanone in a contaminated soil sample.

MHE-GC determination

Analytical samples, calibration standard and blank samples were submitted to the nine-step MHE-GC determination of cyclohexanone in contaminated soil, under the above described conditions. The chromatograms obtained from a contaminated soil sample are shown in Fig. 1.

RESULTS

Computing of the results

By plotting the natural logarithms of the peak area *versus* the number of the injection, straight regression lines were obtained for both the standards and the samples. Fig. 2 shows the plot of two straight regression lines obtained from the averaged standards and from one of the six replicate soil samples.

The straight regression line calculated from the standards was:

$$\ln \text{ area} = -0.35 (\text{number of injection}) + 7.79$$

with a linear correlation coefficient $r_{xy} = 0.9999$.

The value of k^* (0.35) obtained for the standard was inserted into eqn. 3,

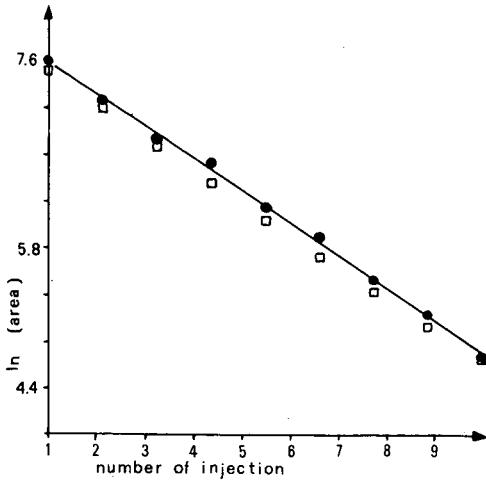


Fig. 2. Straight regression lines from MHE determinations of cyclohexanone in standards (\square) and in a contaminated soil sample (\bullet).

together with the experimental A_1 value (1777.2), and the total area value for cyclohexanone standard was computed:

$$\Sigma A_n = 1777.2/1 - e^{-0.35} = 6078.7$$

The total area value corresponding to 9.42 μg of cyclohexanone yields a response factor of amount per unit peak area, *i.e.*:

$$9.42 \mu\text{g}/6078.7 \text{ area unit} = 0.0015$$

TABLE I

RECOVERY OF CYCLOHEXANONE FROM CONTAMINATED SOIL SAMPLES BY MHE-GC

Cyclohexanone added to soil, 282.6 μg per 30 g; soil aliquot submitted to MHE determination, 1 g; cyclohexanone theoretically present in 1-g soil aliquot 9.42 μg ; number of replicate determinations, 6.

Sample	Cyclohexanone		Recovery (%)	Total area
	Theoretical (μg)	Experimental (μg)		
1	9.42	10.08	107.0	6505.9
2	9.42	8.98	95.3	5794.8
3	9.42	9.76	103.6	6298.1
4	9.42	8.74	92.8	5639.9
5	9.42	9.83	104.4	6343.3
6	9.42	8.76	93.0	5652.8
Mean values	9.42	9.36	99.4	6039.1
S.D.		0.6	6.4	386.2
R.S.D. (%)		6.4	6.4	6.4

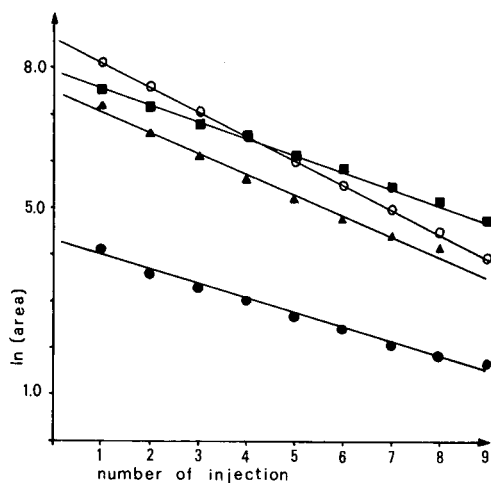


Fig. 3. Effect of increasing addition of water on the recovery of cyclohexanone from contaminated soil: (●) no addition, 4% recovery; (▲) 0.005% (v/w) addition, 48% recovery; (■) 0.01% (v/w) addition, 99.4% recovery; (○) standard, theoretical amount of cyclohexanone.

The same procedure was followed for the samples, and the total area values were computed. By multiplying these values by the above-reported response factor, the amount of cyclohexanone in the samples was easily obtained. The results from the six replicate samples, the corresponding recovery percentages, and the total area values are shown in Table I.

DISCUSSION

As described in Experimental, small amounts of water were added to the sample, to promote the release of cyclohexanone from the soil. This system is typical of a medium-polar compound absorbed on a strongly polar matrix. In these cases, small amounts of another polar compound, with a greater affinity for the matrix than the analyte, will facilitate the release of the absorbed compound, and also enhance the analytical recovery from the sample.

In this study, it was experimentally observed that the addition of increasing amounts of water to the soil samples led to the optimization of the recovery of cyclohexanone. This effect is illustrated in Fig. 3, which shows four straight regression lines corresponding to the addition of increasing amounts of water: 0%, 0.005%, and 0.01% v/w. The fourth line is that of the reference standard. It can be seen that the addition of 0.01% water led to quantitative recovery of cyclohexanone, and the corresponding regression line is superimposed on that of the standard. Therefore, the addition of 0.01% water was deemed essential to carry out the determination.

The analytical procedure was applied to six replicate soil samples; in all the tested samples, the recovery of cyclohexanone was practically quantitative. The amount of cyclohexanone theoretically present in the 1-g soil aliquots submitted to the MHE-GC determination was 9.42 μg ; the amount found was 9.36 μg (mean value from six determinations; range, 8.74–10.03 μg).

The repeatability of the developed method, expressed as percentage relative standard deviation (R.S.D.) was 6.4%. This relatively high value may be explained taking into account the inhomogeneity of cyclohexanone in the soil and the intrinsic variability due to handling of volatiles. However, this situation reflects what may actually happen in authentic samples of a contaminated soil. On the other hand, the study was aimed at solving analytical problems linked to the handling to contaminated soils.

The addition of a small amount of water may be reasonably proposed as a systematic step in the determination of volatiles in a contaminated soil sample, when the determination is extremely urgent, as in the case of accidents, spillages, etc. In fact, if the contaminating compounds have a good affinity for soil (*i.e.* with polar groups in their structure, and not too high a volatility), they will be better released to the headspace by the action of water. In contrast, if the compounds have poor affinity for soil (*i.e.* non-polar structures, high volatility) they will not remain strongly absorbed by the soil and are likely to escape to the atmosphere. Therefore, there is a low probability of finding large amounts of this type of compound in soil. In any case, a small amount of water is very unlikely to interfere with the determination of non-absorbed compounds; on the other hand, if the time available for the determination is not too short (*i.e.* soil-monitoring programs, routine procedures, *etc.*) it is advisable to evaluate the water content of the soil samples before defining the correct amount of water to add.

CONCLUSIONS

The developed procedure may be considered as a validated example of a rapid and simple quantitative determination of volatiles in a contaminated soil sample. By and large, MHE-GC appears to be the most convenient technique to use when a solid sample has to be tested; it requires minimal sample handling, minimal consumption of materials and, most important of all, it is unnecessary to reproduce the matrix to perform accurate determination of volatiles. It is sufficient to ensure the complete vaporization of the calibration standard.

REFERENCES

- 1 R. L. Grob (Editor), *Chromatographic Analysis of the Environment*, 2nd edn., Marcel Dekker, New York, 1983.
- 2 B. Kolb and P. Pospisil, *Chromatogr. Newsletter*, 8 (1980) 35.
- 3 S. L. Friant and I. H. Suffet, *Anal. Chem.*, 51 (1979) 2167.
- 4 M. H. Gordon, *Int. Analyst*, 2 (1987) 16.
- 5 J. Drozd and J. Novak, *J. Chromatogr.*, 165 (1979) 141.
- 6 W. Closta, H. Klemm, P. Pospisil, R. Riegger, G. Siess and B. Kolb, *Chromatogr. Newsletter*, 11 (1983) 13.
- 7 B. Kolb, *Chromatographia*, 15 (1982) 587.
- 8 B. Kolb, P. Pospisil and M. Auer, *Chromatographia*, 19 (1984) 113.

CHROMSYMP. 2275

Chromatographie en phase gazeuse haute résolution– spectrométrie de masse des congénères de biphényles polychlorés dans quelques échantillons d'origine biologique

M. R. DRISS

Département de Chimie, Faculté des Sciences, Campus Universitaire le Belvédère, 1060, Tunis (Tunisie)

S. SABBAB

Institut National de Recherche Scientifique et Technique, 2050, Hammam-lif (Tunisie)

et

M. L. BOUGUERRA*

Département de Chimie, Faculté des Sciences, Campus Universitaire le Belvédère, 1060, Tunis (Tunisie)

ABSTRACT

High-resolution gas chromatography–mass spectrometry of polychlorinated biphenyl congeners in biological samples

A study is performed on polychlorinated biphenyl (PCB) congener residues in samples of human blood and milk as well as in falcon and pigeon eggs.

Most of the PCB congeners found in these biological samples were quantified by high-resolution gas chromatography (HRGC). A PCB technical mixture —namely, DP6 (Phenochlor)— was used for the calibration as its composition was previously determined by HRGC–mass spectrometry.

The usefulness of such a congener analysis is outlined.

It is the first time to the best of our knowledge that a Phenochlor mixture is used for standardization.

INTRODUCTION

L'analyse des résidus de biphényles polychlorés (PCBs) débute par leur extraction de la matrice originelle; l'extrait ainsi obtenu est soumis, après purification, à la chromatographie en phase gazeuse (CPG) avec détection à capture d'électrons (ECD).

L'utilisation des colonnes capillaires dans le domaine de l'analyse des PCBs a permis l'obtention d'une information qualitative détaillée de la composition des PCB [1–5]. Le pouvoir de séparation et la haute résolution de ces colonnes de chromatographie ont révélé que les PCBs, dans les mélanges techniques, étaient représentés par près d'une centaine de composés [6] et que dans les produits environnementaux, l'empreinte des PCBs pouvait varier d'une matrice à l'autre.

L'incertitude sur la mesure, exprimée en équivalent de mélange technique, est d'autant plus importante que le profil des PCBs diffère de celui des produits de référence. Ce fait est particulièrement frappant dans le cas de matériel biologique

provenant d'organismes supérieurs (oiseaux, mammifères) [7–9] pour lesquels les composés fortement chlorés sont amplifiés, ce qui conduit à une surestimation de la quantification en termes d'équivalent de mélanges techniques.

Les limites de ce mode de quantification apparaissent ainsi doublement. D'une part, la réduction des nombreuses données contenues dans un chromatogramme à une seule grandeur qui est l'expression de la concentration en PCBs totaux, fait perdre l'information qualitative sur la contamination [10,11]. D'autre part, l'expression de la mesure en équivalent de mélange technique ne permet pas une appréciation satisfaisante des processus discriminants vis-à-vis des différents chlorobiphényles.

Ces méthodes quantitatives utilisées dans la détermination des PCBs ont été critiquées dès 1975 [11].

Dans ce contexte, la quantification par congénère trouve toute sa justification, elle permet une meilleure approche du comportement des PCBs et de leurs effets sur l'environnement. En effet, il est important, notamment sur le plan de la toxicité, de préciser quels sont les composés retenus par la matière vivante et quels sont les processus intervenant dans cette sélection [12,13].

La méthode de quantification par congénère est plus précise car elle s'adresse effectivement à la concentration réelle du composé présent dans l'extrait étudié. Souvent, le problème à résoudre concerne la disponibilité des congénères purs nécessaires à la réalisation des solutions étalons et la sélection des composés à prendre en considération pour le dosage résiduel des PCBs. Or, la plupart des congénères ne sont pas disponibles commercialement et lorsqu'ils existent, leur coût rend difficile l'acquisition des 209 composés.

Pour pallier à ces difficultés, nous proposons dans le présent travail une méthode de quantification des congénères de PCB basée sur l'utilisation d'un mélange technique de Phénochlor (DP6) dont la composition est préalablement déterminée par CPG haute résolution (CPG-HR)–spectrométrie de masse (SM) [14]. Les facteurs de réponse des congénères sont déterminés par CPG–ECD. Dans ces conditions, la quantification se fait de la façon classique, composé par composé.

Diverses études ont utilisé l'Aroclor [15] et le Clophen [16] comme référence pour la quantification des congénères de PCB mais c'est la première fois, à notre connaissance, que le Phénochlor DP6 est pris comme étalon pour ce type de dosage.

Les échantillons étudiés, sont: le lait maternel, le sang d'adulte et les oeufs de faucon et de pigeon.

PARTIE EXPÉRIMENTALE

Matériels et conditions opératoires

Les échantillons d'oeufs de Faucon et de Pigeon proviennent d'un lot qui a fait l'objet d'une étude précédente quant à la concentration globale en PCBs [17–19].

Quant aux échantillons de lait maternel et de sang d'adulte, ils proviennent d'un lot d'une centaine de donneurs qui a fait lui aussi, de son côté, l'objet d'un travail précédent [20].

Les échantillons objet de la présente étude ont été choisis pour représenter une grande variété de concentrations en PCBs.

La CPG sur colonne capillaire a été menée sur un chromatographe Varian 3700 équipé d'un détecteur à capture d'électrons (Ni 63). Une colonne capillaire en silice

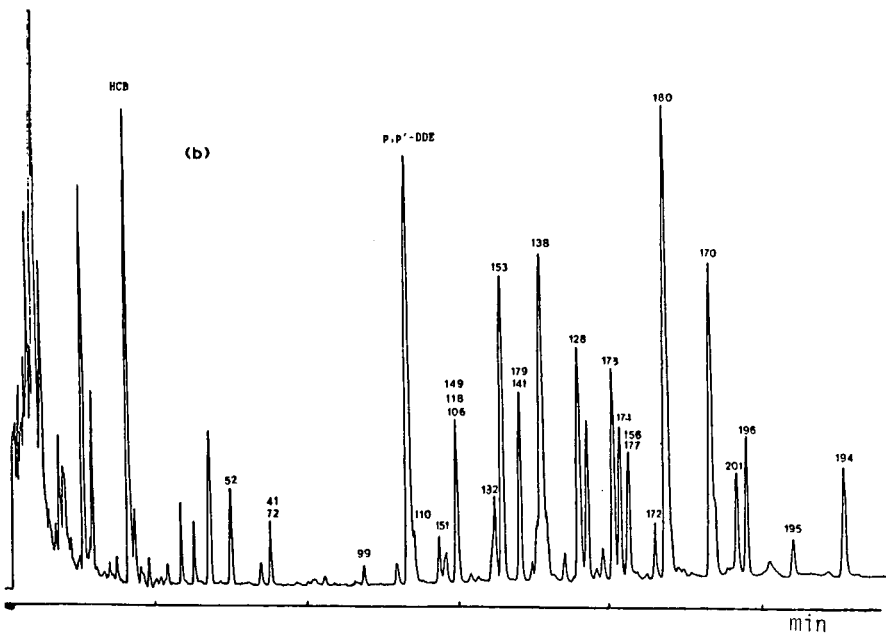
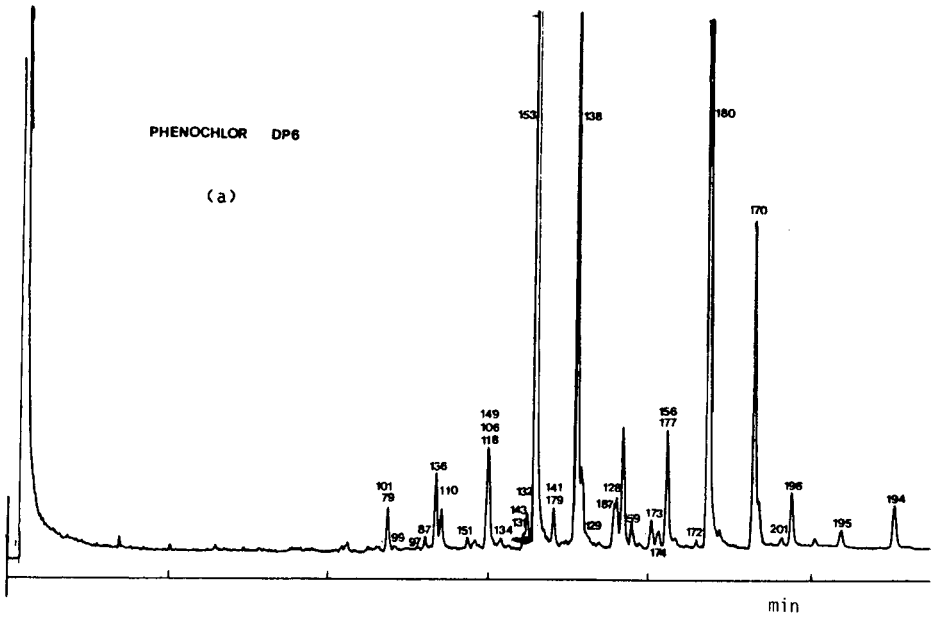


Fig. 1

(Continué sur la p. 216)

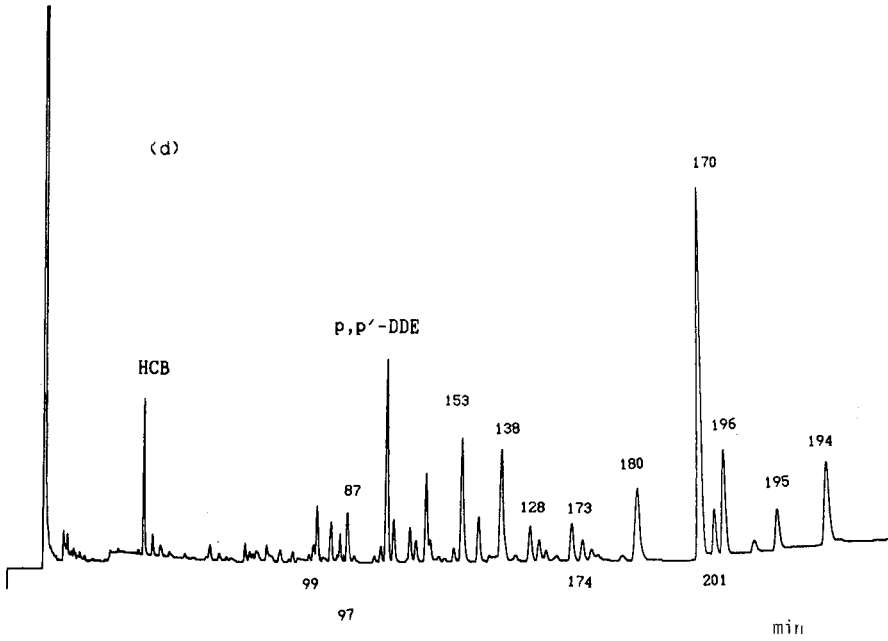
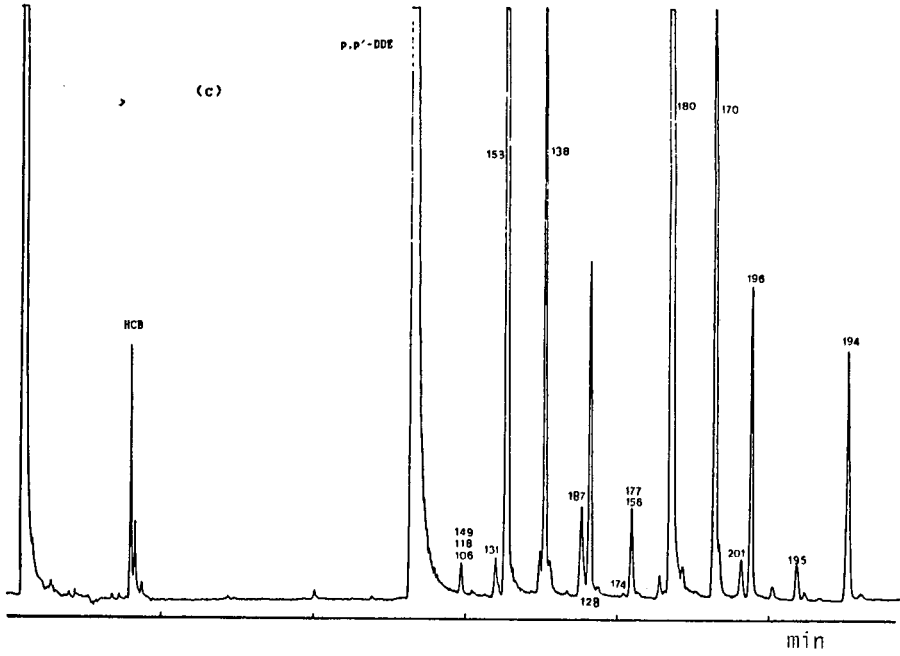


Fig. 1.

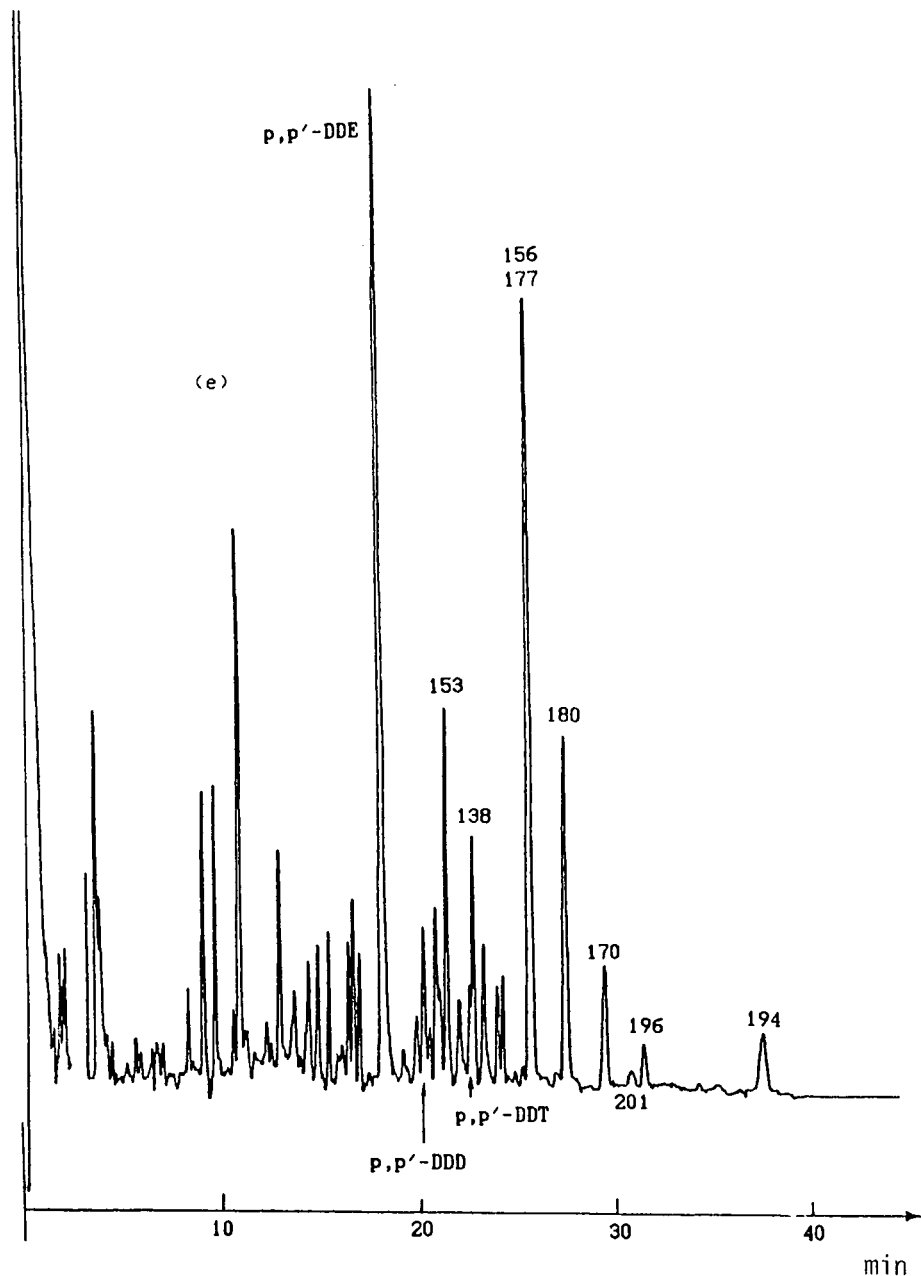


Fig. 1. (a) Chromatogramme du mélange technique DP6; (b) chromatogramme d'un échantillon de lait maternel; (c) chromatogramme d'un échantillon d'oeuf de faucon; (d) chromatogramme d'un échantillon de sang d'adulte; (e) chromatogramme d'un échantillon d'oeuf de pigeon. Appareil: Varian 3700 équipé d'un détecteur à capture d'électrons (Ni 63). Colonne: capillaire (WCOT), en silice fondue, 25 m × 0,32 mm D.I., paroi interne recouverte d'un film (0,12 μ m) de CP-Sil 5. Conditions chromatographiques: voir texte.

fondue, de 25 m de long et de 0,32 mm de D.I., de paroi interne recouverte de la phase CP-Sil 5 dont l'épaisseur du film est de 0,12 μm , est utilisée dans ce travail.

Pour l'analyse chromatographique des échantillons de lait maternel, d'oeuf de faucon et de sang d'adulte, la température du four est programmée à la vitesse de 3°C/min de 150 à 200°C avec un palier de 4 min à la température initiale. Quant à l'analyse de l'extrait d'oeuf de pigeon, la température de la colonne est programmée de 130 à 200°C à la vitesse de 3°C/min. D'autre part, les températures du détecteur et de l'injecteur sont respectivement 300 et 260°C. Le volume injecté est de 1 μl (injection directe). La pression du gaz vecteur, l'hydrogène, est fixée à 17 p.s.i. Le débit du gaz additionnel (azote U) est de 30 ml/min. Les temps de rétention, les aires des pics et le calcul des concentrations sont fournis par un calculateur intégrateur CDS 111.

La CPGHR-SM utilisée pour la détermination de la composition du mélange DP6 a été menée sur un chromatographe de type Girdel série 32, équipé de la colonne capillaire CP-Sil 5 précédemment décrite, et couplé à un spectromètre de masse Nermag 10-10C muni d'un système de traitement des données Spectral 30. Les spectres de masse ont été enregistrés en mode impact électronique (IE) avec une énergie d'ionisation de 70 eV et une température de source de 200°C.

Méthode de quantification

L'injection du DP6 sur la colonne capillaire CP-Sil 5 (détection par capture d'électrons) donne un chromatogramme révélant 27 pics (Fig. 1a). Pour les composés majoritaires, à chaque pic du chromatogramme correspond un composé. Cependant, quelques groupements —paires voire triplets— de composés demeurent non résolus; on obtient au total 17 pics correspondant à des chlorobiphényles identifiés avec une confortable marge de confiance et que l'on peut, en outre, quantifier. Ces congénères représentent 84% en masse du DP6. Ils ont été identifiés au moyen des indices de rétention mesurés par rapport aux *n*-alkyltrichloroacétates et de plus, déduits par le calcul selon la règle de Sisson et Welti [21] qui veut que l'indice de rétention d'un PCB soit égal à la somme des demi-indices de rétention de chacune de ses demi-structures. Les indices de rétention mesurés sont donnés par l'expression:

$$I_x = 100(TR_x - TR_z)/(TR_{z+1} - TR_z) + 100_z$$

dans laquelle I_x est l'indice du congénère x , TR_z est le temps de rétention du *n*-alkyltrichloroacétate dont le pic émerge immédiatement avant celui du soluté x et dont le nombre d'atomes de carbone du radical *n*-alkyle est z . TR_{z+1} est le temps de rétention du *n*-alkyltrichloroacétate, immédiatement élué après le soluté x , dont le nombre d'atomes de carbone du radical *n*-alkyle est $z + 1$.

Quant à la fraction massique x_i , du congénère i , dans le DP6, elle est déduite de l'analyse par CPGHR-SM. Ainsi la valeur x_i et la masse spécifique m_i du congénère i sont liées à la masse (m_t) du DP6 injecté par la relation:

$$m_i = m_t x_i / 100$$

(m_t est généralement exprimée en ng).

Par détection en capture d'électrons, le facteur de réponse E_i d'un congénère i nécessaire pour le dosage résiduel est alors exprimé par la relation:

$$E_i = A_i / m_i$$

TABLEAU I

POURCENTAGE MASSIQUE ET FACTEURS DE RÉPONSE DES CONGÉNÈRES DE PCB DANS LE DP6

No. IUPAC	% massique	F.R.R. (ECD) ^a	No. IUPAC	% massique	F.R.R. (ECD) ^a
52	0,48	N.E. ^{b,f}	134	N.D. ^c	N.E. ^d
49+47	0,26	N.E. ^c	131+143	0,38	N.E. ^c
42+44	0,15	N.E. ^c	132	N.D.	N.E. ^b
37	0,02	N.E. ^b	153	18,65	0,497
41+72	0,10	N.E. ^c	141+179	1,67	N.E. ^c
70	0,15	N.E. ^b	138	16,79	0,642
66+95	0,45	N.E. ^c	129	0,12	0,987
80+89	0,12	N.E. ^c	187	1,21	1,132
92+84	0,30	N.E. ^c	128	4,38	1,174
79+101	2,20	N.E. ^c	159	N.D.	N.E. ^d
99	0,29	0,532	173	0,83	2,122
97	0,39	0,590	174	0,59	0,346
87	0,84	0,980	156+177	2,90	N.E. ^c
136+85	0,55	N.E. ^c	180	14,50	1,177
110	2,21	0,755	170	18,40	0,842
151	0,53	0,532	201	1,50	0,953
106+			196	0,85	1,142
118+149	6,10	N.E. ^c	195	0,67	0,542

^a F.R.R.: facteur de réponse par rapport à l'aldrine (F.R.R. = 1 pour un ng d'aldrine).

^b Non détecté en ECD.

^c Coélués sur CP-Sil 5.

^d Non détecté en SM.

^e N.D. = non décelé.

^f N.E. = non évalué.

dans laquelle A_i représente l'aire du pic du congénère i .

Afin d'établir la courbe de calibration pour chaque congénère à doser, des solutions étalons de DP6 de différentes concentrations ont été injectées. Ainsi a été déterminée la gamme de concentration pour laquelle le plus grand nombre de congénères détectés par SM présentent une réponse linéaire en détection par capture d'électrons (Tableau I). Il apparaît sur ce tableau, à la concentration optimale de travail, que certains congénères quantifiés par SM ne sont pas décelés en ECD. Par ailleurs, comme à chaque congénère de PCB correspond un facteur de réponse en ECD, en cas de coélution des composés, cette grandeur ne peut plus être évaluée. D'ailleurs, une nette disparité des valeurs du facteur de réponse E_i pour les congénères isomères heptachlorés et hexachlorés a été mise en évidence (Tableau I). Ce résultat a été, du reste, déjà signalé par Mullin *et al.* [22].

RÉSULTATS ET DISCUSSIONS

Sur le Tableau II figurent les teneurs résiduelles des PCBs détectés dans les échantillons de lait maternel, de sang et d'oeufs de faucon et de pigeon. Pour tous ces échantillons, l'empreinte des PCBs en CPG diffère de celle du mélange technique DP6 (Fig. 1b, c, d et e). Ce résultat montre bien que, lors de l'évaluation des teneurs en PCBs

TABLEAU II
TENEUR DES CONGÉNÈRES DE PCB DANS LES ÉCHANTILLONS D'OEUF DE FAUCON ET DE PIGEON, DE LAIT MATERNEL ET DE SANG D'ADULTE

No. IUPAC	Structure	Oeuf de faucon			Oeuf de pigeon			Lait maternel			Sang d'adulte		
		OF1 (%)	OF2 (%)	OF3 (%)	OP1 (%)	OP2 (%)	OP3 (%)	LM1 (%)	LM2 (%)	LM3 (%)	SA1 (%)	SA2 (%)	SA3 (%)
99	2,2',4,4',5	N.D.	N.D.	N.D.	N.D.	N.D.	N.D.	1,15	1,02	1,08	1,27	2,6	0,76
97	2,2',3,6,6'	N.D.	N.D.	N.D.	N.D.	N.D.	N.D.	N.D.	N.D.	N.D.	2,5	5,3	2,27
87	2,2',3,4,5	N.D.	N.D.	N.D.	N.D.	N.D.	N.D.	N.D.	N.D.	N.D.	2,29	7,07	4,93
110	2,3,3',4,6	N.D.	N.D.	N.D.	N.D.	N.D.	N.D.	N.D.	N.D.	N.D.	N.D.	N.D.	N.D.
151	2,2',3,5,5',6	N.D.	N.D.	N.D.	N.D.	N.D.	N.D.	0,17	0,10	N.D.	N.D.	N.D.	N.D.
153	2,2',4,4',5,5'	13,97	15,36	13,82	26,35	10,59	30,5	10,52	5,30	6,30	16,4	12,9	20,6
138	2,2',3,4,4',5'	11,72	13,56	7,04	16,35	51,81	20,08	23,72	11,20	13,45	13,31	8,6	7,54
187	2,2',3,4',5,5',6	4,24	3,80	5,02	N.D.	N.D.	N.D.	N.D.	0,70	8,12	1,4	1,56	2,07
128	2,2',3,3',4,4'	0,86	0,63	2,39	N.D.	N.D.	N.D.	N.D.	12,21	N.D.	3,86	6,89	8,28
173	2,2',3,3',4,5,6	N.D.	N.D.	N.D.	N.D.	N.D.	N.D.	3,00	5,17	N.D.	2,2	2,05	2,22
174	2,2',3,3',4,5,6'	0,3	1,68	0,98	N.D.	N.D.	N.D.	2,23	3,04	2,25	1,27	2,02	2,34
180	2,2',3,4,4',5,5'	14,83	18,23	3,67	20,63	8,08	25,4	12,03	9,23	12,75	10,03	9,89	6,73
170	2,2',3,3',4,4',5	23,83	17,3	35,95	18,52	6,59	12	20,40	22,50	30,50	18,32	18,8	17,77
201	2,2',3,3',4',5,5',6	4,99	6,93	N.D.	5,17	0,84	0,13	6,05	10,23	11,32	8,2	4,3	3,74
196	2,2',3,3',4,4',5',6	12,72	11,6	15,06	4,5	14,7	7,2	10,35	9,02	7,12	8,47	12,98	10,30
195	2,2',3,3',4,4',5,6	4,24	3,8	6,12	N.D.	N.D.	N.D.	3,45	4,47	2,37	2,15	1,09	1,52
194	2,2',3,3',4,4',5,5',6	8,48	7,73	10,04	8,5	7,3	5,3	6,90	5,80	4,75	8,31	4,02	8,91
Total (ppm)		127,2	115,9	20,33	1,533	3,217	0,62	0,834	1,815	0,195	7,84	5,66	5,27

totaux, l'utilisation d'un mélange technique de référence pourrait conduire à des résultats discutables.

Les types d'échantillons sélectionnés (lait, sang et oeufs) permettent d'apprécier des niveaux de présence des PCBs dans des proportions bien différentes. En effet la présence de contaminants dans la matière vivante est la résultante d'un ensemble de processus, différents d'une espèce à l'autre; processus d'absorption (régime alimentaire), de redistribution intracorporelle (rôle des lipides), de transfert et d'élimination de polluants (métabolisme),... Les facteurs environnementaux et biologiques influent sur ces processus [23,24] et il semble à première vue normal que des différences de concentration apparaissent pour ces congénères dans les types d'échantillons étudiés.

La contamination du lait, du sang et des oeufs de faucon et de pigeon est marquée par la prédominance des chlorobiphényles: 153, 138, 180 et 170. Donc, ces congénères apparaissent comme peu métabolisables par les organismes étudiés et par là, accumulables dans leurs tissus. Une propriété commune de ces molécules est que les deux groupements phényles de chaque congénère comporte l'un des détails de structures suivants: trichloro-2,4,5-phényle, trichloro-2,3,4-phényle et tétrachloro-2,3,4,5-phényle.

Quant aux congénères 194, 195, 196 et le 201 octachloré, qui se rencontrent à une teneur appréciable dans nos échantillons, leur présence pourrait de plus s'expliquer par leur degré de chloration élevé qui les rend réfractaires à l'élimination [25].

Certains congénères présents dans le DP6 ne se rencontrent que: dans le sang uniquement pour les congénères 87 et 97; dans le lait uniquement pour les congénères 151; et dans ces deux fluides d'origine humaine: 99.

Tous ces composés ont l'un des groupements phényles substitués en position 2,5 ou 2,3,6.

Les congénères qui ont été décelés dans cette étude dans le lait et le sang humains ont été aussi récemment rapportés dans le tissu adipeux à l'exception du congénère 201 [26].

CONCLUSION

La détermination des résidus de congénères de PCB peut être menée par CPGHR en utilisant des solutions standards issues des mélanges techniques de Phénochlor dont les compositions ont été préalablement déterminées. Ainsi une solution étalon de DP6 se révèle convenable pour la quantification de la plupart des congénères de PCB détectés dans les fluides biologiques et les oeufs. La méthode proposée, comparativement aux analyses classiques de dosage des PCBs, pourrait, à notre avis, permettre une meilleure compréhension des mécanismes de bioaccumulation et de persistance de ces composés dans la biosphère et l'environnement.

RÉSUMÉ

La plupart des résidus de congénères de PCB présents dans des échantillons de lait maternel, de sang d'adulte, d'oeufs de faucon et de pigeon ont été quantifiés par chromatographie en CPGHR. Pour la calibration, on a utilisé un mélange technique de PCBs, le Phénochlor DP6, dont la composition a été déterminée au préalable par CPGHR-SM. L'intérêt de l'analyse des PCBs par congénère est par ailleurs discuté.

BIBLIOGRAPHIE

- 1 D. E. Wells, M. J. Gillespie et A. E. A. Porter, *J. High Resolut. Chromatogr. Chromatogr. Commun.*, 8 (1985) 443.
- 2 P. W. Albro, J. T. Corbett et J. L. Schroeder, *J. Chromatogr.*, 205 (1981) 103.
- 3 J. C. Duinker et M. T. Hillbrand, *Environ. Sci. Technol.*, 17 (1983) 449.
- 4 L. Tuinstra et A. Traag, *J. Assoc. Off. Anal. Chem.*, 66 (1983) 708.
- 5 K. Ballschmiter et M. Zell, *Fresenius' Z. Anal. Chem.*, 302 (1980) 20.
- 6 P. R. Shwartz, R. D. Campbell, D. L. Stalling, R. J. Little, J. D. Petty, J. M. Hogan et E. M. Kaiser, *Anal. Chem.*, 56 (1984) 1303.
- 7 E. Schulte et R. Malisch, *Fresenius' Z. Anal. Chem.*, 319 (1984) 54.
- 8 A. Abarnou, D. Robineau et P. Michel, *Oceanol. Acta.*, 9 (1986) 19.
- 9 S. Safe, L. Safe et M. Mullin, *J. Agric. Food Chem.*, 33 (1985) 24.
- 10 S. Tanabe, F. Gondaira et A. Subramanian, *J. Agric. Food Chem.*, 38 (1990) 899.
- 11 A. S. Y. Chau et R. C. J. Sampson, *Environ. Lett.*, 8 (1975) 89.
- 12 G. Y. Leon, E. A. Emmett et E. D. Pellizzari, *Toxicol. Appl. Pharmacol.*, 87 (1987) 48.
- 13 S. Tanabe, *Marine Pollut. Bull.*, 20 (1989) 247.
- 14 S. Sabbah et M. L. Bouguerra, *J. Chromatogr.*, 552 (1991) 223.
- 15 L. Tuinstra et A. Traag, *J. Assoc. Off. Anal. Chem.*, 66 (1983) 708.
- 16 E. Schulte et R. Malisch, *Fresenius' Z. Anal. Chem.*, 314 (1983) 545.
- 17 M. R. Driss et M. L. Bouguerra, *Analisis*, 8 (1987) 361.
- 18 M. R. Driss, L. Mahmoud, L. Bahri et M. L. Bouguerra, *Bull. Ecol.*, 19 (1988) 43.
- 19 M. R. Driss, M. L. Bouguerra et S. Sabbah, dans A. A. Orio (Rédacteur), *Environmental Contamination, Third Internal Conference Acts, Venice, 26-29 September 1988*, UNEP-WHO, Venice, 1988.
- 20 S. Sabbah, Z. Jemaa et M. L. Bouguerra, *Analisis*, 15 (1987) 399.
- 21 D. Sisson et D. Welti, *J. Chromatogr.*, 60 (1971) 15.
- 22 M. D. Mullin, C. M. Pochini, S. McCrindle, M. Romkes, S. Safe et L. Safe, *Environ. Sci. Technol.*, 18 (1984) 468.
- 23 S. Safe, A. Parkinson, M. A. Denomme et T. Fujita, *Environ. Health Perspect.*, 60 (1985) 47.
- 24 L. B. Willet, T. T. Y. Liu et G. F. Fries, *J. Dairy Sci.*, 73 (1990) 2136.
- 25 P. de Voogt, D. E. Wells, L. Reutergrårdh et U. A. Th. Brinkman, *Int. J. Environ. Anal. Chem.*, 40 (1990) 1.
- 26 D. T. Williams et G. L. Lebel, *Chemosphere*, 20 (1990) 33.

CHROMSYMP. 2172

Analyse par chromatographie en phase gazeuse haute résolution–spectrométrie de masse des mélanges techniques de Phénochlor

S. SABBAH

Institut National de Recherche Scientifique et Technique, 2050 Hammam-lif (Tunisie)

et

M. L. BOUGUERRA*

Département de Chimie, Faculté des Sciences, Campus Universitaire le Belvédère, 1060 Tunis (Tunisie)

ABSTRACT

Analysis of Phenochlor technical mixtures by high-resolution gas chromatography–mass spectrometry

The composition of polychlorinated biphenyl (PCB) congeners in Phenochlor technical mixtures, viz., DP3, DP4, DP5 and DP6, was determined by high-resolution gas chromatography (HRGC). The analysis was performed on two capillary columns, OV-101 and CP-Sil 5. Around 50 congeners were identified by means of their retention indices and quantified by both flame ionization detection and HRGC–mass spectrometry. The response factors of the PCB congeners at various chlorination levels were obtained by electron impact mass spectrometry.

INTRODUCTION

Les biphényles polychlorés (PCBs) sont produits par chloration du biphényle. Cette réaction conduit à un mélange technique dont le degré de chloration conditionne les propriétés physico-chimiques. En théorie, on peut aboutir ainsi à la formation de 209 composés distincts communément appelés congénères. Pour les désigner, on a recours à la nomenclature de Ballschmiter et Zell [1].

Les PCBs sont caractérisés par une grande stabilité chimique et thermique, une ininflammabilité, une résistivité et une constante diélectrique élevées.

Commercialement, il existe diverses marques déposées pour les mélanges de PCBs: Aroclor (États Unis), Phénochlor (France), Clophen (R.F.A.), Kanéchlor (Japon), Sovol (U.S.S.R.) et Fenchlor (Italie).

Jusqu'à un très récent passé, beaucoup de travaux ne rapportaient que la teneur globale des PCBs (pourcentage des PCBs totaux d'un échantillon).

Compte tenu des performances de la chromatographie sur colonne capillaire pour la résolution des PCBs, on peut à l'heure actuelle dans la plupart des cas, surtout pour les composés majoritaires, admettre qu'à chaque pic du chromatogramme

correspond un composé; il n'en demeure pas moins cependant quelques groupements, paires ou triplets de composés, non résolus. Dans ces conditions, la quantification se fait de la manière classique en ayant recours à des solutions d'étalonnage. Dans son principe, cette méthode est plus précise, comparativement à celle permettant d'atteindre la teneur globale en PCBs, car il s'agit effectivement de concentrations de composés présents dans l'extrait étudié. Le problème à résoudre concerne la disponibilité à l'état pur des congénères nécessaires à la réalisation des solutions étalons et le choix des composés à prendre en compte pour exprimer la contamination par les PCBs.

Divers travaux rapportent une évaluation des PCBs dans l'environnement en terme d'indice de similitude par rapport à un mélange technique de PCBs pris comme étalon. De manière évidente, l'incertitude sur l'expression globale des PCBs augmente avec les écarts de composition des extraits étudiés par rapport à ceux des mélanges techniques. Le séjour des PCBs dans l'environnement entraîne une évolution de leur composition d'où la prédominance des composés les plus persistants. Un écart notable par rapport à la composition généralement observée constituerait une information sur la bioaccumulation et la biotransformation sélective des PCBs [2].

Cependant si la chromatographie en phase gazeuse (CPG) sur colonnes capillaires permet la résolution de la plupart des congénères de PCBs, elle n'en pose pas moins le problème de leur quantification.

La quantification des PCBs au moyen de la détection à capture d'électrons (ECD), spécifique des composés organohalogénés, nécessite impérativement une calibration au moyen de solutions étalons du fait de l'absence de relation entre la réponse de ce détecteur et la structure chimique d'un congénère de PCBs donné. En outre, pour le détecteur à ionisation de flamme, les facteurs de réponse, de chaque composé de degré de chloration donné, sont directement proportionnels à la masse molaire du congénère de PCBs considéré. Cette proportionnalité a été notamment vérifiée par Albro *et al.* [3,4]. Ainsi, la composition des mélanges techniques de PCBs peut être exprimée par les pourcentages molaires; ils seront donc utilisés comme standards secondaires pour la calibration en capture d'électrons [5].

La contamination de l'environnement en Tunisie par les PCBs est patente du fait des résidus détectés dans des matrices aussi diverses que les moules, les oeufs de Faucon, le sang et le lait maternel comme le montre les travaux de notre laboratoire [6-8].

Il était dès lors intéressant d'étudier dans le détail la composition de ces PCBs d'autant que, si dans la littérature, on relève de telles études pour l'Aroclor [9,10] et le Clophen [11-13] il n'en est pas de même, à notre connaissance, pour ce qui est des Phénochlors.

Dans le présent travail, nous proposons une méthode d'analyse par congénère de PCBs pour les mélanges techniques de Phénochlor type DP3, DP4, DP5 et DP6. Cette méthode, basée sur la séparation par CPG sur colonnes capillaires CP-Sil 5 et OV-101, utilise d'une part les indices de rétention pour l'identification et d'autre part la détection à ionisation de flamme (FID) et la spectrométrie de masse (SM) pour la quantification.

Sur un total de 82 pics apparaissant sur le chromatogramme des PCBs, une cinquantaine ont été identifiés et quantifiés.

La distribution des groupes d'isomères élucidés, par les deux modes de quantification, concerne environ 80% en masse pour chaque mélange.

PARTIE EXPÉRIMENTALE

Les solutions de mélanges techniques de Phénochlor analysées, DP3, DP4, DP5 et DP6 (Rhône Poulenc, France) ont été préparées dans l'hexane (qualité pour analyse, Merck). Elles ont été utilisées, pour l'analyse CPG haute résolution (CPGHR), à une concentration de 1 $\mu\text{g}/\mu\text{l}$ en FID et de 10 $\text{ng}/\mu\text{l}$ en ECD. Quant à la concentration utilisée pour l'analyse CPGHR-SM, elle est de 50 $\text{ng}/\mu\text{l}$.

Pour la quantification des PCBs par SM nous avons utilisé le naphthalène deutérié (C_8D_8 , Supelco) comme étalon interne. Les facteurs de réponse des PCBs de divers niveaux de chloration, par rapport à l'étalon interne, ont été déterminés sur une solution de 10 congénères de PCBs (Supelco) (Tableau I). La réponse de l'étalon interne a été calibrée sur une gamme de concentration de 10 à 50 $\text{ng}/\mu\text{l}$.

Les *n*-alkyltrichloroacétates caractérisés par leur grande stabilité thermique et leur limite de détection en capture d'électron de l'ordre du picogramme, ont été utilisés comme référence pour la détermination des indices de rétention des PCBs. Nous les avons préparés par estérification des *n*-alcools correspondants C_9 à C_{16} , (Fluka) avec l'acide trichloroacétique (Merck) en milieu benzénique (Prolabo), l'acide sulfurique (Merck) étant le catalyseur [14].

La chromatographie sur colonne capillaire a été réalisée sur un chromatographe Varian 3700 équipé d'un détecteur à capture d'électrons (Ni 63) et à ionisation de flamme. Les temps de rétention, les aires des pics et le calcul des concentrations sont fournis par un calculateur intégrateur CDS 111 associé au chromatographe. Deux colonnes capillaires de type WCOT ont été utilisées dans cette étude, l'une en silice fondue, de 25 m de long et de 0,32 mm de diamètre intérieur; l'épaisseur du film de la phase CP-Sil 5 (Chrompack, Pays-Bas) recouvrant sa paroi interne est de 0,12 μm . L'autre colonne est en verre; elle mesure 25 m de long et 0,25 mm de diamètre intérieur, sa paroi interne est recouverte d'un film de la phase OV-101 (Varian, France) dont l'épaisseur est de 0,20 μm . La température de la colonne CP-Sil 5 est programmée à la vitesse de 3°C/min de 150 à 200°C avec un palier de 4 min à la température initiale. La colonne OV-101 est utilisée en mode isotherme à 200°C. D'autre part, les températures

TABLEAU I

FACTEURS DE RÉPONSE (*FR*), RELATIF À C_8D_8 , DES CONGÉNÈRES DE PCBs, À DIVERS NIVEAUX DE CHLORATION, DÉTERMINÉS PAR SM

Structure	IUPAC No.	<i>FR</i>
C_8D_8		1,000
Cl_1 -2	1	1,281
Cl_2 -3,3'	11	1,023
Cl_3 -2,4,5	29	0,956
Cl_4 -2,2',4,4'	47	0,765
Cl_5 -2,3',4,5',6	121	0,670
Cl_6 -2,2',3,3',6,6'	136	0,621
Cl_7 -2,2',3,4,5,5',6	185	0,478
Cl_8 -2,2',3,3',4,4',5,5'	194	0,334
Cl_9 -2,2',3,3',4,4',5,5',6	206	0,312
Cl_{10} -2,2',3,3',4,4',5,5',6,6'	209	0,280

du détecteur et de l'injecteur sont respectivement 300 et 260°C. La pression de l'hydrogène (gaz vecteur) en ECD est fixée à 17 p.s.i. et le débit du gaz additionnel (azote U) est de 30 ml/min. Le gaz vecteur en FID est l'hélium à la pression de 20 p.s.i. Le volume injecté est de 1 μ l (rapport de division: 1:10).

L'analyse CPGHR-SM a été réalisée sur un spectromètre de masse quadripolaire Nermag R10-10C couplé à un chromatographe Girdel 32C équipé de la colonne capillaire CP-Sil 5 précédemment décrite. La CPGHR-SM est munie d'un système de traitement des données Spectral 30. Les spectres de masse ont été enregistrés en mode impact électronique (IE) avec une énergie d'ionisation de 70 eV et une température de source de 200°C. La gamme de balayage des spectres est de m/z 100 à m/z 500 et couvre ainsi tous les degrés de chloration des congénères de PCBs.

MÉTHODE ANALYTIQUE

Analyse qualitative

Pour identifier les PCBs apparaissant sur les chromatogrammes des mélanges de Phénochlor (Fig. 1), nous avons déterminé les temps de rétention des congénères de

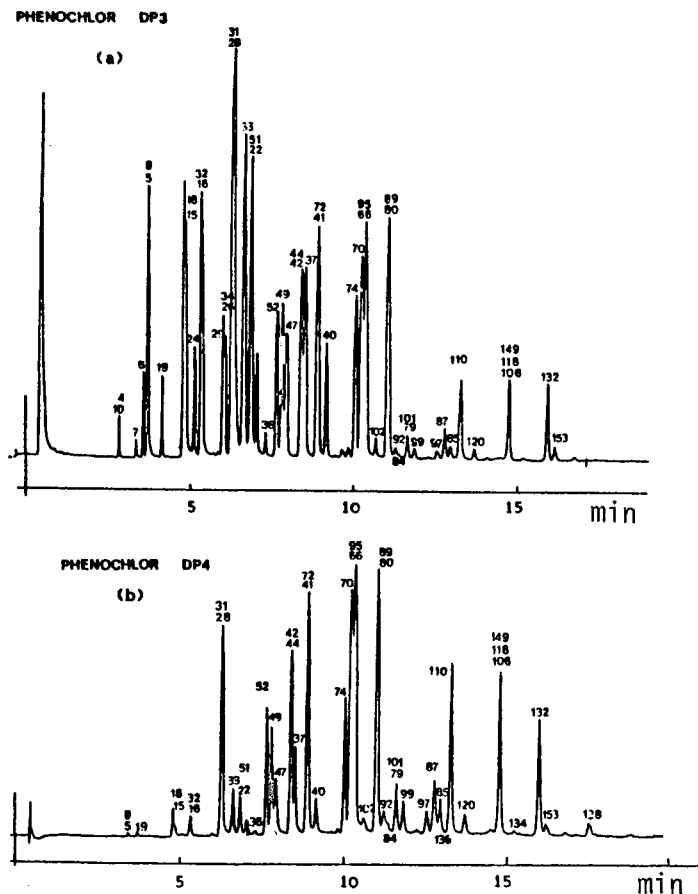


Fig. 1.

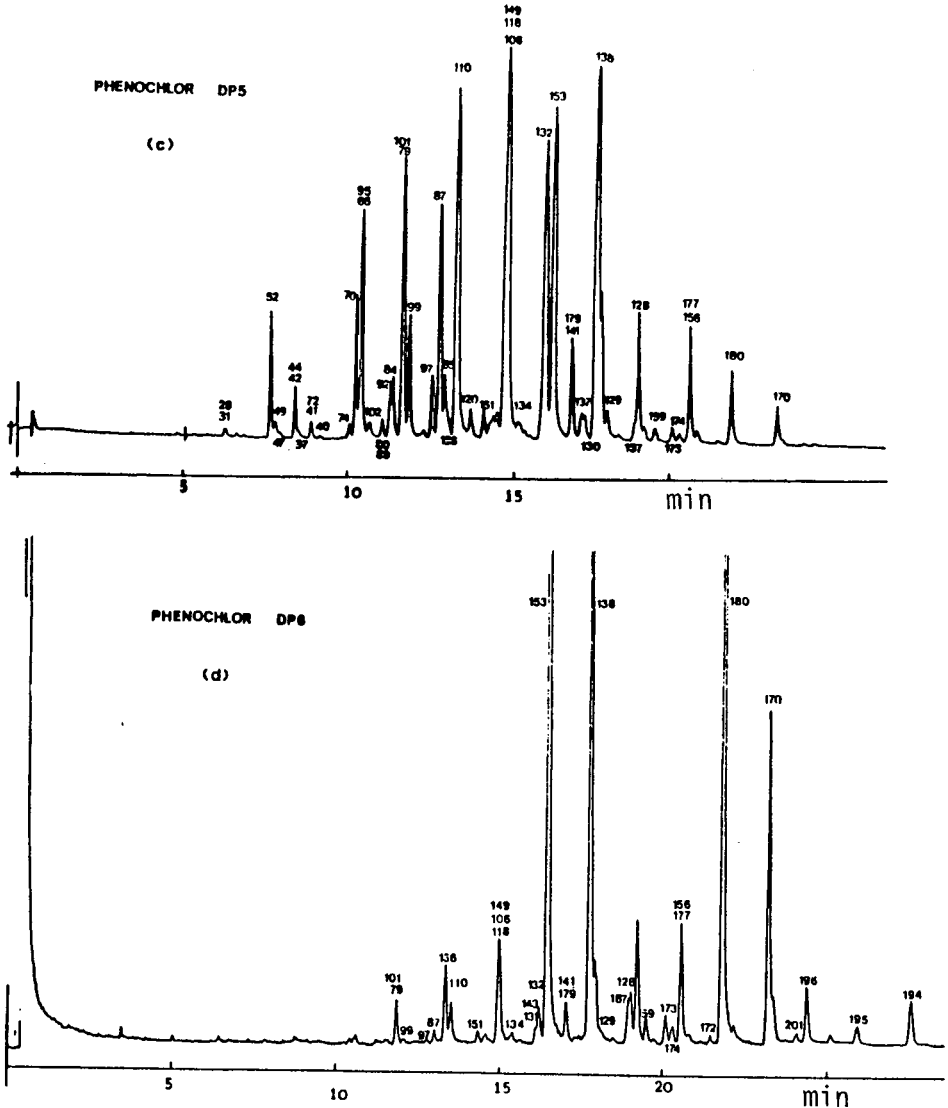


Fig. 1. Chromatogrammes des mélanges techniques de Phénochlor; (a) DP3; (b) DP4; (c) DP5; et (d) DP6. Appareil: Varian 3700 équipé d'un détecteur à capture d'électrons (Ni 63). Colonne: capillaire (WCOT), en silice fondue, 25 m \times 0,32 mm, paroi interne recouverte d'un film (0,12 μ m) de CP-Sil 5. Gaz: gaz vecteur hydrogène U ($P = 17$ p.s.i.); gaz additionnel azote U (30 ml/min). Conditions de température: Injecteur, 260°C; détecteur, 300°C; colonne: programmée de 150 à 200°C à la vitesse de 3°C/min avec un palier de 4 min à la température initiale.

PCBs présents dans l'Aroclor 1242, 1254 et 1016 en nous basant sur les caractéristiques chromatographiques des PCBs données par littérature.

Pour l'Aroclor 1242, nous avons exploité les résultats de Krupcik *et al.* [15] sur la colonne OV-101. Pour ce qui est de l'Aroclor 1016 et 1254, nos chromatogrammes sur

CP-Sil 5 sont comparés à ceux de Tuinstra et Traag [9] et Ballschmiter et Zell [1].

En vue de la confirmation des congénères de PCBs identifiés, nous avons déterminé leurs indices de rétention (I_x) par rapport aux n -alkyltrichloroacétates, en ECD, sur les colonnes OV-101 (en isotherme, $I_{x(i)}$) et CP-Sil 5 (en programmation de température, $I_{x(p)}$) selon les expressions suivantes [16]:

$$I_{x(i)} = 100 \frac{\log(TR_{(x)}/TR_{(z)})}{\log(TR_{(z+1)}/TR_{(z)})} + 100z$$

$$I_{x(p)} = 100 \frac{TR_{(x)} - TR_{(z)}}{TR_{(z+1)} - TR_{(z)}} + 100z$$

dans lesquelles I_x est l'indice du congénère x , $TR_{(z)}$ est le temps de rétention du n -alkyltrichloroacétate dont le pic émerge immédiatement avant celui du soluté x et dont le nombre d'atomes de carbone du radical n -alkyle est z . $TR_{(z+1)}$ est le temps de rétention du n -alkyltrichloroacétate, immédiatement élué après le soluté x , dont le nombre d'atomes de carbone du radical n -alkyle est $z+1$.

Quant aux degrés de chloration des différents congénères de PCBs, ils ont été élucidés à partir de nos résultats obtenus par la SM.

Méthode de calcul

La lecture des chromatogrammes des mélanges commerciaux de Phénochlor, en FID, a permis de déterminer leur composition massique. En fait le pourcentage molaire des congénères identifiés dans un mélange de PCBs est calculé à partir des aires des pics correspondants. Quant à la fraction massique x_i de chaque PCB, elle est donnée par l'expression suivante:

$$x_i = \frac{A_i M_i}{\sum_i A_i M_i}$$

Pour un congénère i , A_i et M_i représentent respectivement l'aire du pic et la masse molaire. En cas de coélution, le facteur x_i a deux significations:

(a) Pour des congénères isomères, x_i donne une valeur unique relative à la fraction massique des deux congénères à la fois.

(b) Pour des congénères non-isomères, la composition relative n'étant pas connue, x_i donne une valeur estimée.

L'analyse des mélanges techniques de PCBs par SM nécessite impérativement la calibration des PCBs de différents niveaux de chloration [17–19]. De ce fait, un des isomères de chaque degré de chloration est utilisé pour représenter tous les isomères d'un groupe donné. Ainsi une solution standard renfermant les dix PCBs sélectionnés et un étalon interne (naphtalène deutérié) est alors analysée afin de déterminer le facteur de réponse de chaque congénère. Ce facteur est alors obtenu pour chaque PCB de calibration puis utilisé dans la quantification des mélanges techniques.

Pour chaque degré de chloration, les facteurs de réponse, par rapport à l'étalon interne, sont reportés sur le Tableau I.

Le facteur de réponse FR_i d'un congénère i , relatif à l'étalon interne E_i , est donné par l'expression:

$$FR_i = \frac{(A_i C_{E_i})}{(A_{E_i} C_i)}$$

dans laquelle A_i et A_{E_i} sont respectivement les aires des pics du congénère i et de l'étalon interne E_i , C_i et C_{E_i} les concentrations du congénère i et de l'étalon interne E_i .

RÉSULTATS ET DISCUSSION

Sur le Tableau II figurent les pourcentages massiques déterminés par FID (séparation effectuée sur OV-101) et SM et les indices de rétention relatifs à la séparation sur la colonne CP-Sil 5, des congénères identifiés dans le DP3, DP4, DP5 et le DP6.

Pour les pics résolus, la différence des valeurs des indices mesurés (par rapport aux *n*-alkyltrichloroacétates) et calculés (par addition des indices de rétention des demi-structures) est située dans une marge de ± 2 unités, marge analogue à celle d'autres auteurs [1,3].

Les PCBs dont la séparation n'est pas satisfaisante sont, de ce fait, entachés d'ambiguïté. D'ailleurs, plusieurs auteurs, disposant d'un certain nombre de congénères et utilisant le couplage CPGHR-SM signalent la difficulté qu'il y a à distinguer deux isomères de PCB coélués [9,15]. Dans notre cas, nous avons obtenu avec la colonne CP-Sil 5 des interférences pour huit paires d'isomères, huit paires de congénères non-isomères et une paire d'isomères avec un congénère non-isomère. Lorsqu'on travaille avec la colonne OV-101, l'ordre d'élution est légèrement différent: les congénères 28 et 31 sont séparés, ainsi que le 85 et le 136 qui coélueraient pourtant sur la phase précédente. Quant aux congénères 15 et 17, ils sont dans ce cas coélués. Des interférences analogues ont été signalées pour diverses colonnes dans la littérature [4].

La distribution des groupes d'isomères de PCB pour les quatre mélanges de Phénochlor est donnée sur le Tableau III. Chaque mélange renferme plus de quatre groupes d'isomères à l'exception du DP3 où il y a essentiellement trois groupes. Le groupe majoritaire dans le DP3 est celui des biphényles trichlorés, pour le DP4 c'est celui des tétrachlorés, alors que les biphényles hexachlorés prédominent dans le cas du DP6. Le mélange technique DP5 renferme quant à lui trois groupes d'isomères assez disparates: tétra-, penta- et hexachlorés.

Nos résultats pour ces deux modes de quantification, FID et SM, sont en accord quant à la composition des Phénochlors, toutefois la distribution en pourcentage massique des groupes d'isomères élucidés pour chaque mélange est plus importante par la spectrométrie de masse. Ces écarts pourraient bien évidemment trouver leur origine dans les caractéristiques différentes des deux techniques et des possibles causes d'erreur susceptibles de les entacher (pour la FID: réponse faible pour les congénères les plus chlorés; pour la SM: vitesse de balayage, nombre de mesure sous chaque pic).

CONCLUSION

Ce travail a permis pour la première fois, à notre connaissance, d'élucider en

40	2,2',3,3'	1172,6	0,82	1,81	0,02	—	0,80	1,70	0,02	—
74	2,4',4',5	1204,9	1,44	4,05	0,46	—	1,40	4,00	0,44	—
70	2,3',4',5	1212,7	3,33	7,42	3,20	0,25	3,20	7,10	3,50	0,15
{ 66	2,3',4,4'	1218,2	(3,57)	(8,50)	(7,44)	(0,75)	(3,62)	(7,80)	(6,98)	(0,45)
{ 95	2,2',3,5',6	1218,2	—	—	—	—	—	—	—	—
102	2,2',4,5,6'	1233,1	—	1,46	0,75	—	—	1,32	0,55	—
{ 80	3,3',5,5'	1248,8	—	(6,43)	(0,41)	(0,08)	—	(6,23)	(0,40)	(0,12)
{ 89	2,2',3,4,6'	1248,8	—	—	—	—	—	—	—	—
{ 92	2,2',3,5,5'	1258,8	—	(2,40)	(4,05)	(0,31)	—	(2,34)	(4,00)	(0,30)
{ 84	2,2',3,3',6	1263,1	—	(2,99)	(8,57)	(1,68)	—	(3,20)	(8,70)	(2,20)
{ 79	3,3',4,5'	1274,1	—	—	—	—	—	—	—	—
{ 101	2,2',4,5,5'	1274,1	—	—	—	—	—	—	—	—
{ 99	2,2',4,4',5	1282,7	—	2,41	3,40	0,36	—	2,12	3,20	0,29
119	2,3',4,4',6	1300,1	—	0,24	0,37	—	—	0,16	0,28	—
97	2,2',3,6,6'	1311,7	—	1,58	2,62	0,29	—	1,80	2,82	0,39
87	2,2',3,4,5'	1322,7	—	2,17	5,03	0,69	—	1,95	4,93	0,84
85	2,2',3,4,4'	1330,7	—	tr	tr	0,37	—	tr	tr	0,32
136	2,2',3,3',6,6'	1330,7	—	1,51	0,79	0,18	—	1,27	0,85	0,23
110	2,3,3',4',6	1345,5	—	3,93	8,65	1,81	—	3,64	8,60	2,21
120	2,3',4,5,5'	1364,3	—	0,93	0,83	—	—	0,90	0,86	—
151	2,2',3,5,5',6	1381,6	—	—	0,68	0,28	—	—	0,76	0,53
{ 106	2,3,3',4,5	1409,9	—	(3,01)	(13,20)	(5,35)	—	(3,41)	(14,10)	(6,10)
{ 118	2,3',4,4',5	1409,9	—	—	—	—	—	—	—	—
{ 149	2,2',3,4',5',6	1409,9	—	tr	0,46	—	—	tr	0,51	—
134	2,2',3,3',5,6	1423,7	—	—	0,13	—	—	—	0,14	—
133	2,2',3,3',5,5'	1431,5	—	—	(0,79)	(0,43)	—	—	(0,53)	(0,38)
{ 131	2,2',3,3',4,6	1437,4	—	—	—	—	—	—	—	—
{ 143	2,2',3,4,5,6'	1437,4	—	—	—	—	—	—	—	—
132	2,2',3,3',4,6'	1453,1	—	2,98	5,50	tr	—	2,28	4,88	tr
153	2,2',4,4',5,5'	1463,9	—	0,64	6,42	19,95	—	0,86	7,02	18,65
{ 141	2,2',3,4,5,5'	1485,1	—	—	(1,25)	(1,05)	—	—	(1,25)	(1,67)
{ 179	2,2',3,3',5,6,6'	1485,1	—	—	—	—	—	—	—	—
137	2,2',3,4,4',5	1492,5	—	—	0,39	tr	—	—	0,43	0,09
130	2,2',3,3',4,5	1496,4	—	—	0,55	tr	—	—	0,59	0,07
138	2,2',3,4,4',5'	1508,5	—	—	9,71	17,54	—	—	8,96	16,79
129	2,2',3,3',4,5	1518,7	—	—	0,63	tr	—	—	0,74	0,12
187	2,2',3,4',5,5',6	1535,3	—	—	tr	0,95	—	—	0,25	1,21

(Continué sur la p. 232)

TABLEAU II (continué)

IUPAC No.	Structure	Indices de rétention ^a	Pourcentage massique ^b déterminé par FID			Pourcentage massique ^b déterminé par SM				
			DP3	DP4	DP5	DP6	DP3	DP4	DP5	DP6
128	2,2',3,3',4,4'	1547,9	—	—	1,93	4,86	—	—	2,16	4,38
159	2,3,3',4,5,5'	1563,8	—	—	tr	—	—	—	tr	—
173	2,2',3,3',4,5,6	1581,3	—	—	tr	0,85	—	—	tr	0,83
174	2,2',3,3',4,5,6'	1587,9	—	—	tr	0,56	—	—	tr	0,59
{ 156	2,3,3',4,4',5	1595,3	—	—	(1,26)	(2,40)	—	—	(1,48)	(2,90)
{ 177	2,2',3,3',4',5,6	1595,3	—	—	—	—	—	—	—	—
180	2,2',3,4,4',5,5'	1629,4	—	—	0,95	14,97	—	—	0,94	14,50
170	2,2',3,3',4,4',5	1665,4	—	—	tr	21,48	—	—	0,18	18,40
201	2,2',3,3',4',5,5'	1686,4	—	—	—	1,46	—	—	—	1,50
196	2,2',3,3',4,4',5',6	1693,7	—	—	—	tr	—	—	—	0,85
195	2,2',3,3',4,4',5,6	1728,4	—	—	—	tr	—	—	—	0,67
194	2,2',3,3',4,4',5,5'	1763,8	—	—	—	tr	—	—	—	0,72

^a Les indices de rétention des congénères de PCBs, dans les Phénoclors, ont été calculés par rapport aux *n*-alkyltrichloroacétates en CPG sur colonne capillaire CP-Sil 5 et par détection à capture d'électrons.

^b Les congénères unis par une accolade () sont coélus sur les deux colonnes de chromatographie. Les congénères unis par un crochet () sont coélus sur la colonne OV-101 seulement. Les chiffres entre parenthèses représentent le pourcentage massique *x*; global pour les congénères coélus. tr = Trace; — = non décelé.

TABLEAU III
DISTRIBUTION DES GROUPES D'ISOMÈRES DE PCB DANS LES MÉLANGES TECHNIQUES DE PHÉNOCHLOR

Phénochlor	Groupe d'isomères (FID)								Groupe d'isomères (SM)							
	Cl ₂	Cl ₃	Cl ₄	Cl ₅	Cl ₆	Cl ₇	Cl ₈		Cl ₂	Cl ₃	Cl ₄	Cl ₅	Cl ₆	Cl ₇	Cl ₈	
DP3	9,7	55,06	20,75	—	—	—	—	—	11	60,51	19,66	—	—	—	—	
Nombre d'isomères	4	10	8	—	—	—	—	—	4	12	8	—	—	—	—	
DP4	0,12	16,06	44,41	16,16	5,13	—	—	—	0,30	17,71	42,00	14,01	4,41	—	—	
Nombre d'isomères	1	9	10	7	3	—	—	—	1	9	10	7	3	—	—	
DP5	—	tr	21,82	17,05	27,98	0,95	—	—	—	tr	22,02	28,54	27,12	1,80	—	
Nombre d'isomères	—	—	8	7	12	1	—	—	—	—	8	7	12	4	—	
DP6	—	0,03	3,5	1,66	43,25	38,81	1,46	—	—	0,02	3,35	8,24	41,12	37,12	2,33	
Nombre d'isomères	—	1	7	4	6	5	1	—	—	1	7	6	6	5	3	

grande partie la composition des mélanges techniques de Phénochlors. Partant de ce résultat, il devient maintenant possible d'obtenir à partir d'une information qualitative des résultats quantitatifs fiables. L'utilisation des indices de rétention, la linéarité entre la réponse en FID et la masse molaire d'un PCB en vue de l'analyse des composés présents dans les Phénochlors DP3, DP4, DP5 et DP6 permettent l'attribution, dans la majeure partie des cas, d'un pic à un congénère déterminé ainsi que sa quantification. Ces mélanges peuvent alors être utilisés comme standards secondaires lors de l'analyse des résidus de congénères de PCBs dans les échantillons les plus divers.

REMERCIÉMENTS

L'étude en SM a été conduite au Laboratoire de Chimie Organique Structurale (Université Pierre et Marie Curie, Paris VI, France). Nous remercions vivement M. J. P. Morizur et Mlle C. Lange pour leur assistance.

BIBLIOGRAPHIE

- 1 K. Ballschmiter et M. Zell, *Fresenius' Z. Anal. Chem.*, 302 (1980) 20.
- 2 J. S. Christopher, J. L. Zajicek et P. H. Peterman, *Arch. Environ. Contam. Toxicol.*, 19 (1990) 748.
- 3 P. W. Albro et L. Fishbein, *J. Chromatogr.*, 69 (1972) 273.
- 4 P. W. Albro, J. W. Corbett et J. L. Schroeder, *J. Chromatogr.*, 205 (1981) 103.
- 5 T. R. Schwartz, R. D. Campbell, D. L. Stalling, R. L. Little, J. D. Petty, J. W. Hogan et E. M. Kaiser, *Anal. Chem.*, 56 (1984) 1303.
- 6 M. R. Driss et M. L. Bouguerra, *Analisis*, 15 (1987) 361.
- 7 M. R. Driss, L. Mahmoud, L. Bahri et M. L. Bouguerra, *Bull. Ecol.*, 19 (1988) 43.
- 8 S. Sabbah, Z. Jemaa et M. L. Bouguerra, *Analisis*, 15 (1987) 399.
- 9 L. Tuinstra et A. Traag, *J. Assoc. Off. Anal. Chem.*, 66 (1983) 708.
- 10 R. H. Liu, S. Ramesh, J. Y. Liu et S. Kim, *Anal. Chem.*, 56 (1984) 1808.
- 11 S. Jensen et G. Sundstrom, *Ambio*, 3 (1974) 70.
- 12 E. Shulte et L. Acker, *Fresenius' Z. Anal. Chem.*, 268 (1974) 260.
- 13 J. C. Duinker, D. E. Schultz et G. Petrick, *Anal. Chem.*, 60 (1988) 47.
- 14 W. J. Hickinbottom, *Reactions of Organic Compounds*, Longman, London, 1959, p. 122.
- 15 J. Krupcik, J. Kriz, D. Prusova, P. Suchanek et Z. Cervenka, *J. Chromatogr.*, 142 (1977) 797.
- 16 J. Tranchant, *Manuel Pratique de Chromatographie en Phase Gazeuse*, Masson, Paris, 1982, p. 197.
- 17 A. N. Alford-Stevens, T. A. Bellar, J. W. Eichelberger et W. L. Buddle, *Anal. Chem.*, 58 (1986) 2014.
- 18 J. E. Gebhart, T. L. Hayes, A. L. Alford-Stevens et W. L. Buddle, *Anal. Chem.*, 57 (1985) 2458.
- 19 M. D. Erickson, J. S. Stanley, J. K. Turman, J. E. Going, D. Redford et D. T. Heggem, *Environ. Sci. Technol.*, 22 (1988) 71.

Determination of phenoxy ester herbicides by gas and high-performance liquid chromatography

C. SÁNCHEZ-BRUNETE, S. PÉREZ and J. L. TADEO*

Departamento de Protección Vegetal, CIT-INIA, Aptdo. 8111, 28080 Madrid (Spain)

ABSTRACT

The determination of phenoxy ester herbicides was carried out by high-performance liquid (HPLC) and gas chromatography (GC) and their identification by GC–MS spectrometry. Standards of herbicide esters were obtained from the appropriate acid and a suitable alcohol, mainly 2-butoxyethyl, isooctyl or isobutyl alcohol, using acetyl chloride as a catalyst. The mixture was heated at 100°C for 1 h, after cooling 2 ml of acetate buffer (pH 4.6) were added and then the mixture was diluted to volume with methanol. Good ester conversion (>95%) was achieved. The phenoxy esters were analysed by reversed-phase HPLC on a Spherisorb ODS-2 (5- μ m) column with acetonitrile–water (85:15) as mobile phase at a flow-rate of 1 ml/min and UV detection at 280 nm. GC was performed on a BP-5 capillary column with helium as carrier gas (10 ml/min) and flame ionization detection. Esters were identified by GC–ion trap detection on a BP-1 capillary column. Several mixtures of phenoxy ester herbicides in formulations were analysed using the proposed methods and good agreement between the HPLC and GC results was obtained.

INTRODUCTION

Phenoxy acids are an important group of selective herbicides usually formulated in the form of salt or alkyl esters. Analysis of phenoxy ester formulations is based on hydrolysis to the corresponding acid, which is determined by high-performance liquid chromatography (HPLC) [1,2] or gas chromatography (GC) after methylation [3]. Therefore, the acid equivalent and not the ester concentration is determined.

Esterification of phenoxy acids has been reviewed by Cochrane [4] and several workers have carried out derivatization with diazomethane [5], boron trifluoride–methanol [5,6] or fuming sulphuric acid–ethanol [7]. Noble [8] proposed the use of acetyl chloride and the appropriate alcohol to obtain standards of the different phenoxy esters used in commercial formulations. These standards can be used to determine phenoxy esters in pesticide formulations by direct GC analysis.

The aim of this work was to study the determination of phenoxy ester herbicides in formulations by HPLC and GC and their identification by GC–ion trap detection (ITD). The results are compared with those obtained by HPLC determination of the corresponding acids, based on the AOAC method [1].

EXPERIMENTAL

Instrumentation

The liquid chromatograph was a Beckman Model 421A equipped with a 20- μ l loop injector, a Model 160A fixed-wavelength UV detector, a Spectra-Physics SP4290 integrator and a Spherisorb ODS-2 (C₁₈) column (250 \times 4.6 mm I.D.).

A Perkin-Elmer Model 8500 gas chromatograph with a flame ionization detector, an ion trap detector (Finnigan) and a split/splitless injector was employed.

HPLC

Phenoxy esters. Acetonitrile–water (85:15) was used as the eluent at a flow-rate of 1 ml/min. The detection wavelength was fixed at 280 nm. The herbicide concentration was calculated by comparing the peak areas obtained for samples with those obtained for standards.

Phenoxy acids. Acetonitrile–0.2% acetic acid (40:60) was used at a flow-rate of 1.5 ml/min. The detection wavelength was fixed at 280 nm. The equivalent concentration of esters was calculated by comparing the peak areas obtained for hydrolysed samples with those obtained for the acid standards and then corrected by multiplying by the ratio $MW_{\text{ester}}/MW_{\text{acid}}$.

GC

A BP-5 fused-silica column (12 m \times 0.53 mm I.D.) with a film thickness of 1 μ m was used with helium as the carrier gas at a flow-rate of 10 ml/min and flame ionization detection. The temperature programme was 180°C, held for 5 min, increased at 25°C/min to 250°C, held for 10 min. A 1- μ l volume of sample was injected and the herbicide concentration was calculated by comparing the peak areas obtained for samples with those obtained for the ester standards.

Identification was carried out by GC–ITD with a BP-1 capillary column (12 m \times 0.22 mm I.D.) and helium as carrier gas at a flow-rate of 10 ml/min. The temperature programme was 85°C, held for 5 min, increased 20°C/min to 250°C, held for 5 min. A 2- μ l volume was injected with the split closed for 1 min.

Mass spectrometric acquisition parameters

The following conditions were used: transfer line temperature, 250°C; mass range, 40–350 dalton; scan rate, 0.5 s per scan, 2- μ scans; r.f. voltage, 1.1 MHz and 0–7.5 kV; automatic gain control from 78 μ s to 25 ms; solvent delay, 3 min.

Materials

Phenoxy acids were obtained as test substances from several manufacturers: 2,4-D [(2,4-dichlorophenoxy)acetic acid] from Condor (Middlesex, U.K.); 2,4-DP [(2,4-dichlorophenoxy)propionic acid] from BASF (Ludwigshafen, Germany); MCPA [(4-chloro-2-methylphenoxy)acetic acid] and MCPP [(4-chloro-2-methylphenoxy)propionic acid] from Azko (Rotterdam, The Netherlands).

Preparation of standard solutions

Esters. A mixture (1:5) of acetyl chloride and a suitable alcohol was prepared, previously cooling the alcohol in an ice-bath. A 2-ml volume of the mixture was added

to 50 mg of the phenoxy acid and the resulting mixture was then heated at 100°C in a sand-bath for 1 h. After cooling to room temperature, 2 ml of acetate buffer (pH 4.6) were added and the solution was transferred to a 100-ml volumetric flask with methanol.

Acids. A 50-mg amount of the phenoxy acid was dissolved in 100 ml of methanol.

Ester hydrolysis. A 100-mg amount of the corresponding phenoxy ester, or the equivalent amount of the formulated herbicide, was dissolved in 50 ml of methanol and 20 ml of 5 M potassium hydroxide solution. After reaction for 1 h, the mixture was acidified to pH 6 with 10 M acetic acid (*ca.* 0.8 ml) and diluted to the final volume (100 ml) with methanol.

RESULTS AND DISCUSSION

The different esters of the phenoxy acids were obtained by the procedure described above. The ester conversion was >95% in all instances, which is in agreement with the results obtained by Noble [8].

The determination of phenoxy esters was accomplished by HPLC and GC under the conditions given above and their retention times are shown in Table I. Direct GC analysis of phenoxy esters in formulations has been carried out previously by other workers [8–10]. However, the determination of these compounds by HPLC has usually been done after hydrolysis to the acids, using different alkyl-silica columns and buffered mobile phases [1,2,11,12]. In this work, an alternative HPLC method for the determination of these herbicides as esters was developed. Although UV detection at 220 nm showed a sensitivity about five times higher, the response at 280 nm produced a cleaner baseline and was selected for the determination. Under these conditions, the detection limit was about 20 ng for each phenoxy ester. These compounds were also determined by HPLC after hydrolysis to the free acids (Table II). The sensitivity obtained with this procedure, which is based on the AOAC method [1], was about 50% lower than that achieved with the proposed HPLC method for the esters. Some representative chromatograms are shown in Fig. 1.

Individual phenoxy esters have been identified previously by capillary GC on the basis of their retention times [8]. In this work, the identification of the phenoxy esters

TABLE I

RETENTION TIMES OF PHENOXY ESTERS DETERMINED BY HPLC AND GC

HPLC: column, Spherisorb ODS-2 (C₁₈) (250 × 4.6 mm I.D.); mobile phase, acetonitrile–water (85:15); flow-rate, 1 ml/min. GC: column, BP-5 (12 m × 0.53 mm I.D.); carrier gas, helium at a flow-rate of 10 ml/min.

Ester	Retention time (min)	
	HPLC	GC
2,4-D 2-butoxyethyl	5.12	7.37
2,4-D isobutyl	5.15	3.75
2,4-DP 2-butoxyethyl	6.28	7.08
MCPA 2-butoxyethyl	5.26	6.89
MCPD 2-ethylhexyl	14.10	6.73

TABLE II
RETENTION TIMES OF PHENOXY ACIDS DETERMINED BY HPLC

Column, Spherisorb ODS-2 (C₁₈) (250 × 4.6 mm I.D.); mobile phase, acetonitrile-0.2% acetic acid (40:60); flow-rate, 1.5 ml/min.

Acid	Retention time (min)
2,4-D	7.50
2,4-DP	11.27
MCPA	7.73
MCPP	12.00

was carried out by GC-ITD. The mass spectra of these compounds show a molecular ion with high relative abundance in all instances [13,14], which for MCPA and MCPP esters represents the base peak of the spectrum. For the 2-butoxyethyl esters a remarkable peak is observed at m/z $M - 73$ caused by the loss of the $-O(CH_2)_3CH_3$ fragment. The spectra of 2,4-D esters show the base peak at m/z 57 (C₄H₉⁺) or m/z 41 (C₃H₅⁺), which correspond to the alcohol portion of the ester; these ions are also present in the spectra of MCPA and MCPP esters. All the phenoxy esters (RCOOR') show the R⁺ ion. Fig. 2 shows the mass spectra of some 2,4-D esters.

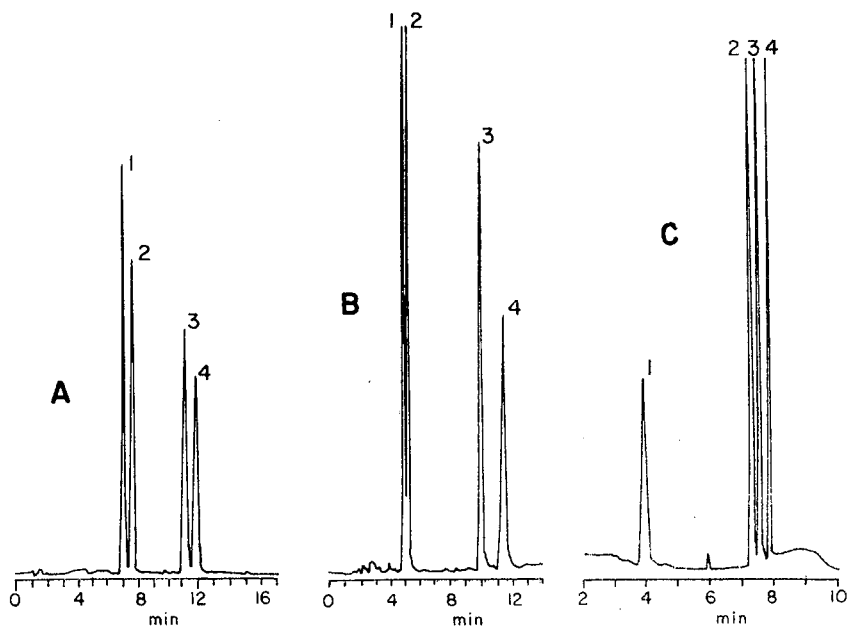


Fig. 1. (A and B) HPLC of phenoxy acids and phenoxy esters. (A) 1 = 2,4-D; 2 = MCPA; 3 = 2,4-DP; 4 = MCPP. (B) 1 = 2,4-D 2-butoxyethyl ester; 2 = MCPA 2-butoxyethyl ester; 3 = 2,4-D 2-ethylhexyl ester; 4 = MCPA 2-ethylhexyl ester. (C) GC of phenoxy esters. 1 = 2,4-D isobutyl ester; 2 = MCPA 2-butoxyethyl ester; 3 = 2,4-DP 2-butoxyethyl ester; 4 = 2,4-D 2-butoxyethyl ester.

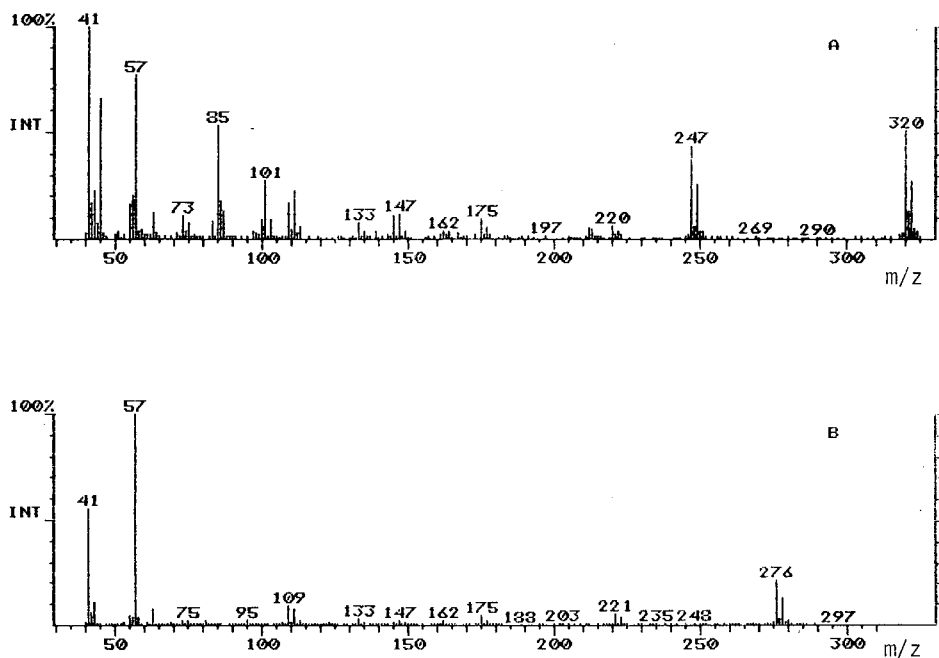


Fig. 2. Mass spectra of (A) 2,4-D 2-butoxyethyl ester and (B) 2,4-D isobutyl ester.

Several phenoxy esters were determined in technical materials and commercial formulations following the described procedures. Table III shows the results of the determination of these compounds as esters by HPLC and GC and after conversion to acids by HPLC. Good agreement between the HPLC and GC results was obtained in the ester determination. The equivalent values obtained by HPLC of the acids, based on the AOAC method [1], were also very close to those of the ester determination.

TABLE III

DETERMINATION OF PHENOXY ESTERS IN TECHNICAL MATERIALS AND COMMERCIAL FORMULATIONS

Sample		Active ingredient found \pm S.D. (%) ^a		
Acid	Ester	HPLC		GC: ester
		Acid	Ester	
2,4-D	2-Butoxyethyl	31.14 \pm 1.50	30.40 \pm 0.83	29.20 \pm 0.47
2,4-D	Isobutyl	96.40 \pm 1.30	97.30 \pm 0.56	97.00 \pm 0.48
2,4-D	Isobutyl	37.00 \pm 1.15	37.30 \pm 0.85	37.70 \pm 0.30
2,4-DP	2-Butoxyethyl	92.20 \pm 2.74	92.00 \pm 2.20	91.90 \pm 1.30
2,4-DP	2-Butoxyethyl	31.00 \pm 1.30	30.60 \pm 1.06	29.80 \pm 0.54
MCPA	2-Butoxyethyl	23.20 \pm 0.70	22.80 \pm 0.50	22.60 \pm 0.70
MCPP	2-Ethylhexyl	93.30 \pm 2.35	91.90 \pm 1.45	91.90 \pm 1.45

^a Values are the means of five determinations \pm standard deviation.

Nevertheless, the proposed methods determine the specific ester concentration instead of the acid equivalent concentration obtained with the AOAC method.

CONCLUSION

The HPLC and GC methods proposed for the determination of phenoxy esters in formulations are simple, fast and reproducible. They allow the specific determination of esters with reliability and the results are in agreement with those obtained by the official method based on conversion to acids.

The HPLC method has the advantage that the phenoxy acids and the phenoxy esters can be analysed with the same column. On the other hand, the GC-ITD method allows the identification of the phenoxy esters from their mass spectra.

ACKNOWLEDGEMENTS

The authors acknowledge the receipt of a grant from the Comisión Interministerial de Ciencia y Tecnología.

REFERENCES

- 1 K. Helrich (Editor), *Official Methods of Analysis of the Association of Official Analytical Chemists*, Arlington, VA, 1990, p. 184.
- 2 T. S Stevens, *Adv. Chromatogr.*, 19 (1981) 91.
- 3 J. Henriët, A. Martijn and H. H. Porlsen (Editors), *CIPAC Handbook*, CIPAC, Harpenden, 1985, p. 2069.
- 4 W. P. Cochrane, *J. Chromatogr. Sci.*, 17 (1979) 124.
- 5 E. A. Woolson and C. I. Harris, *Weeds*, 15 (1967) 168.
- 6 C. R. Sell and J. C. Maitlen, *J. Agric. Food Chem.*, 31 (1983) 572.
- 7 H. Siltanen and R. Mutanen, *Chromatographia*, 20 (1985) 685.
- 8 A. Noble, *Pestic. Sci.*, 23 (1988) 259.
- 9 J. P. Barrete and R. Payfer, *J. Assoc. Off. Agric. Chem.*, 47 (1964) 259.
- 10 A. Noble and D. J. Hamilton, *Pestic. Sci.*, 28 (1990) 203.
- 11 P. Jandera, L. Svoboda, J. Kubat, J. Schvantner and J. Churacek, *J. Chromatogr.*, 292 (1984) 71.
- 12 S. H. Hoke, E. E. Brueggemann, L. J. Baxter and T. Trybus, *J. Chromatogr.*, 357 (1986) 429.
- 13 C. H. Van Peteghem and A. M. Heyndrickx, *J. Agric. Food Chem.*, 24 (1976) 635.
- 14 C. S. Feung, R. H. Hamilton and R. O. Mumma, *J. Agric. Food Chem.*, 24 (1976) 1013.

CHROMSYMP. 2299

Solid-matrix partition for separation of organochlorine pesticide residues from fatty materials

A. DI MUCCIO*, A. AUSILI, R. DOMMARCO, D. ATTARD BARBINI, A. SANTILIO, F. VERGORI, G. DE MERULIS and L. SERNICOLA

Laboratorio di Tossicologia Applicata, Istituto Superiore Di Sanità, Viale Regina Elena 299, 00161 Rome (Italy)

ABSTRACT

A fast, single-step and efficient partition between *n*-hexane and acetonitrile on ready-to-use, disposable cartridges of Kieselghur-type material has been developed for the separation of organochlorine (OC) pesticide residues from oils and fats. The extract is cleaned up with Florisil minicolumn chromatography, followed by a solid-matrix sulphuric acid treatment. Carry-over of lipid material through the partition step is lower compared to conventional, separatory-funnel partition. Recovery of eighteen OC pesticides from 1.0 g olive oil was between 72% and 104% at spiking levels between 0.01 and 0.15 mg/kg for the different compounds.

INTRODUCTION

One of the major problems the analyst faces in the determination of organochlorine (OC) pesticide residues in fats and oils is the isolation of pesticide residues from the bulk of lipidic material.

To this end, several techniques are in use including separatory-funnel partition between immiscible solvents [1,2], size-exclusion chromatography [3–6] or sweep co-distillation [7–11]. Adsorption column chromatography on Florisil [12–14], alumina [15] or silica gel [16] has been used as a final clean up step before determination by gas chromatography (GC) with electron-capture detection (ECD).

All the above-mentioned procedures for the isolation of OC pesticide residues from fatty materials involve time-consuming operations, reusable glassware, large amounts of solvents and reagents, maintenance of costly apparatus and skilled operators.

In previous papers [17,18] we have reported that the traditional partition between *n*-hexane and acetonitrile can be carried out advantageously on disposable, ready-to-use Extrelut columns (filled with macroporous diatomaceous earth) for the isolation of organophosphate (OP) pesticide from several vegetable oils.

The purpose of the present paper is to describe the ability of the solid-matrix partition step to isolate several OC pesticide residues from different fatty materials.

EXPERIMENTAL

Reagents and materials

Analytical-reagent-grade chemicals were used. Light petroleum (40–60°C), *n*-hexane, iso octane, benzene, ethyl acetate, acetonitrile (saturated with *n*-hexane) and methanol were redistilled from an all-glass apparatus. Sulphuric acid (95%, density 1.824 g/ml) was used. Florisil PR, 60–100 mesh (Supelco, Bellefonte, PA, USA), was activated at 130°C overnight. Extrelut-3® and Extrelut-1® columns (E. Merck, Darmstadt, Germany, Cat. Nos. 15372 and 15371, respectively) were used with a disposable needle (E. Merck, Cat. No. 15373) at the column end as a flow restrictor. OC reference standards were from the collection in this laboratory.

Apparatus

The analyses were carried out on a DANI 6800 gas chromatograph equipped with an electron-capture detector. A glass column (1.8 m × 4 mm I.D.) was packed with OV-17 plus QF-1 (1.5% and 1.95%, respectively) on Chromosorb W HP, 100–120 mesh. The temperatures were as follows: oven, 210°C; inlet block, 230°C; outlet block, 250 °C; detector, 250°C. The carrier gas was nitrogen at a flow-rate of 55 ml/min. A rotary evaporator (bath temperature, 40°C; reduced pressure) was used to concentrate solutions.

Procedure

Between 2 and 3 g of lipidic material were placed in a 5-ml volumetric flask, dissolved and diluted to volume with *n*-hexane. Then, 3 ml of the solution was transferred to an Extrelut-3 column which was left to equilibrate for 10 min. The column was then eluted under gravity alone with three 5-ml portions of acetonitrile saturated with *n*-hexane. Eluates were collected in a 50-ml Erlenmeyer flask, 4 ml of methanol added, and the solution was carefully concentrated to dryness by means of rotary evaporator. Any traces of solvent were removed with a gentle stream of nitrogen.

The residue was dissolved in 1 ml *n*-hexane and quantitatively transferred with *n*-hexane washings to a Florisil column [19] (2.5 g in a 300 mm × 10 mm I.D. glass column with PTFE stopcock). The column was then eluted with 50 ml of *n*-hexane–benzene–ethyl acetate (180:19:1) at a flow-rate of 2–3 ml/min. The eluate was carefully concentrated to dryness, dissolved in 2 ml of isooctane and analysed by GC–ECD for the determination of heptachlor epoxide, dieldrin, endrin and metoxychlor, which otherwise would be destroyed by the successive sulphuric acid clean-up, and, if possible, of other compounds. To remove interfering peaks that prevent the determination of some compounds, the extract was quantitatively transferred with light petroleum washings onto an Extrelut-1 column previously loaded with 1 ml concentrated sulphuric acid [20].

The Extrelut-1 column was eluted with four 5-ml portions of light petroleum. All the solvent eluates from the column since the transfer of the sample solution were collected, carefully concentrated to dryness and dissolved in 2 ml isooctane.

The final samples were analysed by GC–ECD. For recovery experiments the oil or fat samples were weighed and dissolved, and diluted with the solution of standard compounds.

RESULTS AND DISCUSSION

Extrelut-3 columns are ready-to-use, disposable glass cartridges filled with a macroporous diatomaceous earth with a nominal volume of 3 ml. In this procedure, the cartridges were used as a solid support to carry out the liquid-liquid partition to separate OC pesticide residues from the bulk of lipidic material.

The performance of the solid-matrix partition system has been studied with respect to its ability to remove lipidic material and to recover a number of the most commonly sought OC pesticide residues.

In Table I are presented data that show the removal of lipidic material through liquid-liquid partition on Extrelut-3 and Florisil column chromatography.

Five different vegetable oils and one animal fat were used to test the performance of the solid-matrix partition step. The oils were commercial samples from the retail market; the animal fat was extracted from "speck" (a ham typical of a north-eastern region of Italy) with *n*-hexane-acetone (1:1).

Data in Table I indicate that with up to 1.8 g of olive oil, peanut oil and corn oil a fair removal of the bulk of lipid could be obtained with the Extrelut-3 column partition alone. With soya bean oil, mixed seed oil and pork fat, a slightly worse performance was observed. However, even in the worst cases the difference can be explained primarily by the differences in the composition of lipids tested. Also, the fact that the tests were carried out at different times, with different batches of Extrelut-3 columns and acetonitrile could have contributed. The reduced carry-over of lipidic material through the partition step allows the use of a minicolumn of Florisil for clean-up, with substantial saving of solvents and time, compared to classical separatory-funnel partition [1,2].

Under the conditions adopted, the amount of lipids released into the acetonitrile eluate did not vary greatly with the amount applied to the Extrelut-3 column. As to the maximum amount of lipid that can be loaded on the Extrelut-3 columns, it

TABLE I
REMOVAL OF THE LIPIDIC MATERIAL THROUGH THE STEPS OF THE DESCRIBED PROCEDURE

Lipid type	Amount applied to Extrelut-3 column (g)	Amount in the eluate after Extrelut-3 partition \pm S.D. (mg)	Amount in the eluate after Florisil chromatography \pm S.D. (mg)
Olive oil	1.0	18.9 \pm 1.53 (<i>n</i> =7)	2.5 \pm 0.93 (<i>n</i> =7)
	1.8	31.4 \pm 3.60 (<i>n</i> =6)	— ^a
Peanut oil	1.0	52.8 \pm 9.01 (<i>n</i> =5)	10.6 \pm 6.2 (<i>n</i> =3)
	1.8	26.1 \pm 1.03 (<i>n</i> =6)	— ^a
Corn oil	1.5	37.8 (<i>n</i> =1)	7.3 (<i>n</i> =1)
		53.9 (<i>n</i> =1)	3.5 (<i>n</i> =1)
	1.8	34.8 \pm 5.76 (<i>n</i> =6)	— ^a
Soya bean oil	1.8	210.9 \pm 9.80 (<i>n</i> =6)	— ^a
Mixed seed oil	1.8	126.4 \pm 9.80 (<i>n</i> =6)	— ^a
Pork fat extracted from speck	0.4-0.9 (<i>n</i> =9)	77.5 \pm 28.43 (<i>n</i> =9)	6.3 \pm 10.9 (<i>n</i> =9)

^a Not determined.

should be noted that a substantial portion of the nominal volume of 3 ml should be left to the *n*-hexane in order that a true *n*-hexane-acetonitrile partition takes place. With applied amounts higher than those in Table I, the sample becomes too viscous and is not readily sorbed into the Extrelut particles. So, a true partition between immiscible solvents does not occur and a tendency for the sample to be mechanically displaced into the acetonitrile eluate was observed.

The extraction *p* values (the fraction of solute partitioning into the non-polar phase of an equivolume two-phase system [21,22]) of the compounds studied can be used as a criterion to estimate the range of applicability of the partition step. As can be seen from the extraction *p* values given in Table II, pesticides having *p* values between *n*-hexane and acetonitrile lower than 0.91 were satisfactorily recovered from 1.0 g of olive oil, indicating a good performance of the method also with respect to highly lipophilic compounds such as mirex (*p* = 0.91). The 15-ml volume of acetonitrile, chosen on the basis of our previous works [17,18], proved to be sufficient to recover the studied compounds. So, no further refinement was deemed necessary.

The sample extracts were cleaned up by Florisil column chromatography as reported by Suzuki *et al.* [19]. This clean-up without any modification proved to be

TABLE II

MEAN RECOVERY VALUES OF EIGHTEEN ORGANOCHLORINE PESTICIDES FROM 1.0 g OF OLIVE OIL THROUGH THE DESCRIBED PROCEDURE

Pesticides ^f	Recovery (mean ± S.D., <i>n</i> = 6) (%)	Spiking level (mg/kg)	<i>p</i> Value ^a	
			This laboratory ^b	Others ^c
HCB	72.4 ± 9.78	0.01	0.89	—
α-HCH	99.5 ± 9.81	0.01	0.03	—
τ-HCH	98.7 ± 9.87	0.01	0.11	—
β-HCH	91.6 ± 8.53	0.02	0.05	—
δ-HCH	104.5 ± 9.13	0.01	0.10	—
Aldrin ^d	86.2 ± 8.91	0.01	0.64	0.73
Heptachlor epoxide ^d	82.9 ± 7.99	0.01	0.24	0.29
τ-Chlordane	89.8 ± 7.45	0.03	0.34	0.40
α-Chlordane	89.4 ± 9.55	0.03	0.31	—
<i>p,p'</i> -DDE	89.7 ± 9.39	0.03	0.52	0.56
Dieldrin ^d	95.3 ± 7.23	0.05	0.30	0.33
<i>o,p'</i> -TDE	93.1 ± 8.41	0.05	0.21	—
Endrin ^d	101.2 ± 8.51	0.05	0.34	0.35
<i>o,p'</i> -DDT	94.8 ± 8.51	0.05	0.47	0.47
<i>p,p'</i> -TDE	91.4 ± 7.59	0.05	0.18	0.17
<i>p,p'</i> -DDT	96.9 ± 9.49	0.05	0.34	0.38
Endosulphan sulphate ^e	—	0.06	<0.01	—
Mirex	85.4 ± 9.04	0.11	0.76	0.91
Methoxychlor ^d	101.3 ± 8.72	0.15	0.04	0.07

^a *p* values between *n*-hexane and acetonitrile.

^b *p* values by GC-ECD after single distribution between equal volumes of *n*-hexane and acetonitrile.

^c *p* values from refs. 21 and 22.

^d Compounds which have been determined after the Florisil clean-up alone.

^e Not recovered through the Florisil clean-up.

^f All abbreviations used are according to ref. 23.

generally effective with a lipid load up to about 100 mg. After Florisil column chromatography the amount of lipid left in the eluate is below 10 mg (see Table I). When necessary (for example, soya bean oil and mixed seed oil) the Florisil column chromatography can be conveniently scaled up.

Recovery experiments were carried out by spiking olive oil, chosen as a model lipid, with nineteen OC pesticides at levels ranging, for the different compounds, between 0.01 and 0.15 mg/kg. The compounds selected for the tests include the most commonly sought OC pesticides. In Table II are presented the results of the recovery experiments, which show satisfactory values for the compounds studied, with the exception of endodulfan sulphate. This compound proved to be retained on the Florisil column. However, on the basis of its *p* value, it is reasonable to assume that it can be recovered through the solid-matrix partition step. Some of the compounds (namely, heptachlor epoxide, dieldrin, endrin and metoxychlor) were determined after Florisil column chromatography and the others after sulphuric acid treatment. Indeed, with certain samples after Florisil chromatography large tailing after the injection and some negative peaks prevented or made it difficult to allocate a good baseline for the determination of some compounds. In these cases an additional clean-up by solid-matrix sulphuric acid treatment [20] was sufficient to remove the interference and to give a clean GC baseline, almost resembling that obtained by injection of the standard mixture. In Fig. 1 are shown typical gas chromatogram obtained by in-

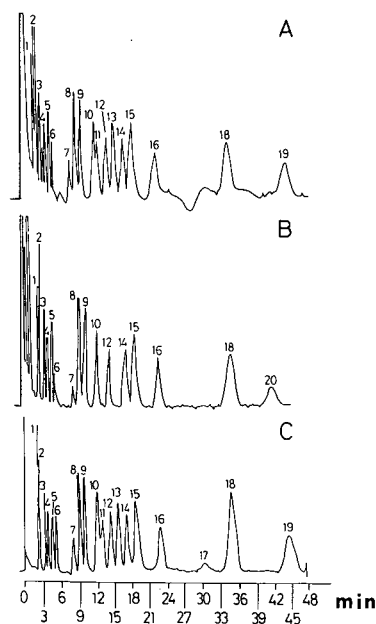


Fig. 1. Typical gas chromatograms of an extract of 1 g olive oil spiked with nineteen OC pesticides at levels shown in Table II after Florisil clean-up (A), the same sample after the additional sulphuric acid treatment (B), and the standard solution of nineteen OC pesticides (C), each of which at concentrations equivalent to the spiking levels. Peaks: 1 = HCB; 2 = α -HCH; 3 = τ -HCH; 4 = β -HCH; 5 = δ -HCH; 6 = aldrin; 7 = heptachlor epoxide; 8 = τ -chlordane; 9 = α -chlordane; 10 = *p,p'*-DDE; 11 = dieldrin; 12 = *o,p'*-TDE; 13 = endrin; 14 = *o,p'*-DDT; 15 = *p,p'*-TDE; 16 = *p,p'*-DDT; 17 = endosulfan sulphate; 18 = mirex; 19 = methoxychlor; 20 = δ -keto-Endrin. (For conditions see text.) The abbreviations used are according to ref. 23.

jecting an extract of spiked olive oil after Florisil clean-up (A) and the same sample after the additional clean-up by sulphuric acid (B) in comparison with the gas chromatograms of the standard mixture (C).

The behaviour of the studied compounds during the sulphuric acid treatment on Extrelut-1 has already been reported by us [20]. In particular, endrin and methoxychlor are almost completely lost through sulphuric acid clean-up, while dieldrin is recovered as endrin ketone, which appears as a peak with a retention time longer than that of the parent compound. Although aldrin and heptachlor epoxide were well recovered as pure compounds through sulphuric acid clean-up in our previous work [20], in this procedure they are better determined after Florisil clean-up as they appear to be somewhat retained by the additional sulphuric acid clean-up step. This effect is probably due to the presence of the small amount of charred material that forms on the top of the solid-matrix column loaded with sulphuric acid. Of course, the amount of the charred material depends on the amount of lipid left in the eluate after Florisil and this, in its turn, on the type of fatty material analysed (see Table I).

Thus, to overcome a possible influence of variable amounts of charred material on the recovery of the other compounds also studied, we decided to elute the solid-matrix sulphuric acid column with a total of 20 ml of light petroleum, instead of 10 ml as reported in our previous paper [20]. Indeed, recovery experiments with lipids other than olive oil gave values consistent with those shown in Table II.

After sulphuric acid clean-up, the final eluate contains very low amounts (in the order of 1–2 mg) of lipidic material and for this reason is amenable to both packed and capillary on-column injection systems. The gas chromatograms after sulphuric acid treatment are free from interfering peaks and are almost indistinguishable from those obtained with the standard solution of pure pesticides (see Fig. 1).

Finally, it is reasonable to assume that other chlorinated compounds, such as polychlorinated biphenyls (PCBs) can be recovered through the described procedure. However, the samples used for recovery experiments were "blanks" under the conditions adopted. So, the determination of organochlorine pesticide should not have been impaired by the presence of PCBs, which normally occur at levels well below those used for recovery experiments. Indeed, the main scope of the present work was to demonstrate that a rapid, simple solid-matrix partition can be a substitute for the conventional techniques used for the separation of organochlorine pesticides from the bulk of lipidic material, *i.e.*, separatory-funnel partition between immiscible solvents [1,2], size-exclusion chromatography [3–6] or sweep co-distillation [7–11].

CONCLUSIONS

The described procedure consists of a solid-matrix partition step followed by two clean-up steps, the sulphuric acid treatment step being optional, depending on the compounds being determined and/or on the sample matrix. It offers a simple, rapid way to determine OC pesticides residues in oils and fats. The solid-matrix partition step offers significant savings of glassware, solvents, reagents and time compared to conventional techniques used. Furthermore, the clean-up is based on simple operations which require a minimum of reagents and glassware and do not require skilled operators or costly apparatus.

REFERENCES

- 1 S. Williams (Editor), *Official Methods of Analysis*, Association of Official Analytical Chemists, Arlington, VA, 14th ed., 1984, sec. 29.014.
- 2 M. J. de Faubert Maunder, H. Egan, E. W. Godly, E. W. Hammond, J. Roburn and J. Thomson, *Analyst (London)*, 89 (1964) 168.
- 3 S. Williams (Editor), *Official Methods of Analysis*, Association Official Analytical Chemists, Arlington, VA, 14th ed., 1984, sec. 29.037.
- 4 L. D. Johnson, R. H. Waltz, J. P. Ussary and F. E. Kaiser, *J. Assoc. Off. Anal. Chem.*, 59 (1976) 174.
- 5 M. P. Seymour, T. M. Jefferies and L. J. Notarianni, *Analyst (London)*, 111 (1986) 1203.
- 6 A. H. Roos, A. J. Van Munsteren, P. M. Nab and L. G. M. Th. Tuinstra, *Anal. Chim. Acta*, 196 (1987) 95.
- 7 R. W. Storherr and R. R. Watts, *J. Assoc. Off. Anal. Chem.*, 48 (1965) 1154.
- 8 J. Pflugmacher and W. Ebing, *Z. Anal. Chem.*, 263 (1973) 120.
- 9 M. Eichner, *Z. Lebensm.-Unters.-Forsch.*, 167 (1978) 245.
- 10 B. Luke and J. C. Richards, *J. Assoc. Off. Anal. Chem.*, 67 (1984) 295.
- 11 S. L. Head and V. W. Burse, *Bull. Environ. Contam. Toxicol.*, 39 (1987) 848.
- 12 S. Williams (Editor), *Official Methods of Analysis*, Association of Official Analytical Chemists, Arlington, VA, 14th ed., 1984, sec. 29.015.
- 13 B. McMahon and J. A. Burke, *J. Assoc. Off. Anal. Chem.*, 61 (1978) 640.
- 14 T. Stijve and E. Cardinale, *Mitt. Gebiete Lebensm. Hyg.*, 65 (1974) 131.
- 15 A. V. Holden and K. Marsden, *J. Chromatogr.*, 44 (1969) 481.
- 16 H. Steinwandter and H. Schluter, *Z. Anal. Chem.*, 286 (1977) 90.
- 17 A. Di Muccio, A. M. Cicero, I. Camoni, D. Pontecorvo and R. Dommarco, *J. Assoc. Off. Anal. Chem.*, 70 (1987) 106.
- 18 A. Di Muccio, A. Ausili, L. Vergori, I. Camoni, R. Dommarco, L. Gambetti, A. Santillio and F. Vergori, *Analyst (London)*, 115 (1990) 1167.
- 19 T. Suzuki, K. Ishikawa, N. Sato and K.-I. Sakai, *J. Assoc. Off. Anal. Chem.*, 62 (1979) 681.
- 20 A. Di Muccio, A. Santillio, R. Dommarco, M. Rizzica, L. Gambetti, A. Ausili and F. Vergori, *J. Chromatogr.*, 513 (1990) 333.
- 21 M. C. Bowman and M. Beroza, *J. Assoc. Off. Anal. Chem.*, 48 (1965) 943.
- 22 M. Beroza, M. N. Inscoc and M. C. Bowman, *Residue Rev.*, 30 (1969) 1.
- 23 C. R. Worthing (Editor), *The Pesticide Manual*, The British Protection Council, Thornton Heath, 8th ed., 1987.

CHROMSYMP. 2355

Rapid method for the determination of organochlorine pesticides in milk

TIPPAWAN PRAPAMONTOL and DEREK STEVENSON*

Robens Institute, University of Surrey, Guildford, Surrey GU2 5XH (UK)

ABSTRACT

This method involved one step solvent extraction of milk with ethyl acetate–acetone–methanol by ultrasonication. The supernatants were further cleaned-up and enriched by solid-phase extraction using octadecyl (C₁₈)-bonded silica cartridges, then assayed by capillary gas–liquid chromatography with electron capture detection. The recoveries of eleven organochlorine pesticides (OCPs) from raw milks were quantitative, ranging from 90–110% at 10 times the limit of detection (LOD). The LOD ranged from 0.5 µg/l whole milk for α -hexachlorocyclohexane to 2.5 µg/l whole milk for 1,1,1-trichloro-2,2-bis(*p*-chlorophenyl)ethane. The day-to-day variation of the method was evaluated over 7 days using 3 different pools of spiked cow milks (at the LOD, 5 and 10 times the LOD). The coefficient of variations (C.V.s) were 16 ± 6, 10 ± 2 and 9 ± 3% (mean S.D.), respectively.

The method showed no emulsion problems common with conventional non-polar solvent extraction, and the use of solid-phase extraction considerably reduced the sample clean-up process compared with the existing methods. The method also showed that OCPs in milk could be extracted quantitatively without extraction of total fat, and that OCPs spiked into cows milk could be used to construct calibration curves for human milk determinations.

INTRODUCTION

Organochlorine pesticide (OCP) pollutants in human milk have been of interest since residues were detected in ethnic American mothers in 1951 [1]. Since then methodology for studying pesticide residues in milk has been subject to some controversy because of the results from inter-laboratory comparisons [2]. Conventional methods to extract fat soluble compounds from fatty matrices often involve complete extraction of fat from the matrices, followed by extensive clean-up before chromatographic or other analysis. These methods are often lengthy, labour intensive and costly. The fat content and composition in milk is influenced by several physiological factors [2–4], for instance there are differences in fat content both between individuals and with milk from one individual before and after feeds. These factors have made collection of single samples of human milk for exposure studies unrepresentative [5]. However, increasing understanding of human lactation and milk composition has paralleled both the improvement of the analytical techniques, and greater awareness of the need to monitor occupational and environmental exposure to chemicals.

Several approaches to extraction and clean-up of milk have been reported. A

typical procedure for milk samples would involve treatment with concentrated sulphuric acid, extraction with non-polar solvents such as petroleum ether or *n*-hexane followed by clean-up of extracts using column adsorption chromatography [6–8]. High-performance gel permeation chromatography has been reported as showing some advantages over conventional adsorption chromatography, for the separation of large molecular components of fat from OCPs and polychlorinated biphenyls (PCBs) [9]. The extraction of milk fat with a mixture of *n*-hexane–acetone (1:1) is common as this allows total fat determination using gravimetric methods. Following this initial extraction, the fats were then redissolved in *n*-hexane before further clean-up, with concentrated sulphuric acid [10,11], or by adsorption chromatography [12,13]. However, solvent extraction of OCPs and other organochlorine compounds from milk using more polar solvent mixtures has been reported [14,15]. This work showed low fat content in these extracts compared with the other approaches. Suzuki *et al.* [14] used a mixture of hexane–acetonitrile–ethanol (20:5:1) to extract a 10-ml milk sample followed by Florisil minicolumn chromatography for clean-up. There have been reports that the fat in high fat containing raw milk is more readily extracted than lower fat milks. Muccio *et al.* [15] modified Suzuki's method by using Chem Elut cartridges to extract OCPs from a mixture of milk–acetonitrile–ethanol by eluting with light petroleum (b.p. 40–60°C)–acetonitrile–ethanol (100:25:5). The eluates were concentrated and further cleaned-up using a Florisil minicolumn.

Ultrasonication has proved useful in milk fat homogenisation [16], since fat soluble compounds in milk could possibly be trapped or bound in milk fat globules, thereby affecting the reproducibility of recovery. This problem is overcome if milk fat globules are completely broken down during the extraction process using for example ultrasonication.

The objective of the present study was to develop a rapid and simple method to determine OCPs in milk such that studies in humans could be undertaken. Ideally, all method development and calibration would be carried out using uncontaminated human milk, but this is very difficult to obtain [17,18]. Consequently, dairy milk was considered suitable for much of the programme.

EXPERIMENTAL

Standards and reagents

Hexachlorocyclohexane (HCH) isomers: α -HCH, β -HCH, γ -HCH (lindane); 1,1,1-trichloro-2,2-bis(*p*-chlorophenyl)ethane (*p,p'*-DDT); 1,1-dichloro-2,2-bis(*p*-chlorophenyl)ethylene (*p,p'*-DDE); 1,1-dichloro-2,2-bis(*p*-chlorophenyl)ethane (*p,p'*-DDD); endrin; dieldrin; aldrin and heptachlor were from Polyscience (USA). Heptachlor epoxide and 1,1-dichloro-2-(*o*-chlorophenyl)-2-(*p*-chlorophenyl)ethylene (*o,p'*-DDE) were products of Promochem (Germany). Octadecyl (C₁₈) bonded silica cartridges (500 mg/2.8 ml) were products of Analytichem (USA). Organic solvents (pesticide residue grade), acetonitrile, acetone, methanol, *n*-hexane and ethyl acetate were obtained from BDH (Poole, UK); 2,2,4-trimethylpentane (isooctane) was obtained from J. T. Baker (Hayes, UK).

Standard pesticide mixture: a stock standard solution (approximately 0.5 mg/ml) of each pesticide was prepared separately in isooctane, except β -HCH which was prepared in *n*-hexane–toluene (1:1). Spiking solutions of all OCPs were prepared in

TABLE I
CONCENTRATION OF SPIKING STANDARD MIXTURES

OCPs	Spiking concentrations ($\mu\text{g/ml}$)						
	I	II	III	IV	V	VI	VII
α -HCH	0.1	0.2	0.3	0.4	0.5	0.7	1.0
β -HCH	0.2	0.4	0.6	0.8	1.0	1.4	2.0
γ -HCH	0.1	0.2	0.3	0.4	0.5	0.7	1.0
Heptachlor	0.2	0.4	0.6	0.8	1.0	1.4	2.0
Aldrin	—	—	—	—	—	—	—
Heptachlor epoxide	0.2	0.4	0.6	0.8	1.0	1.4	2.0
<i>o,p'</i> -DDE	—	—	—	—	—	—	—
<i>p,p'</i> -DDE	0.3	0.6	0.9	1.2	1.5	2.1	3.0
Dieldrin	0.3	0.6	0.9	1.2	1.5	2.1	3.0
Endrin	0.4	0.8	1.2	1.6	2.0	2.8	4.0
<i>p,p'</i> -DDD	0.3	0.6	0.9	1.2	1.5	2.1	3.0
<i>p,p'</i> -DDT	0.5	1.0	1.5	2.0	2.5	3.5	5.0

ethyl acetate. The concentrations of these are shown in Table I. Aldrin (5 ng/ml milk) and *o,p'*-DDE (10 ng/ml milk) were used as internal standards. Working pesticide mixture solutions were prepared in isoctane the concentration of these are shown in Table II.

Apparatus and materials

The capillary gas chromatograph with ^{63}Ni electron capture detector (ECD), was Hewlett-Packard Model 5890A with an automatic injector, Hewlett-Packard

TABLE II
CONCENTRATION OF WORKING STANDARD MIXTURES

OCPs	Working concentrations (ng/ml)						
	1	2	3	4	5	6	7
α -HCH	1	2	3	4	5	7	10
β -HCH	2	4	6	8	10	14	20
γ -HCH	1	2	3	4	5	7	10
Heptachlor	2	4	6	8	10	14	20
Aldrin	10	10	10	10	10	10	10
Heptachlor epoxide	2	4	6	8	10	14	20
<i>o,p'</i> -DDE	20	20	20	20	20	20	20
<i>p,p'</i> -DDE	3	6	9	12	15	21	30
Dieldrin	3	6	9	12	15	21	30
Endrin	4	8	12	16	20	28	40
<i>p,p'</i> -DDD	3	6	9	12	15	21	30
<i>p,p'</i> -DDT	5	10	15	20	25	35	50

(Wokingham, UK). Capillary fused-silica column (10 m \times 0.32 mm I.D.) 1- μ m SE 52/4 phase was from SAC Chromatography (Cambridge, UK). The ultrasonicator was from Radleys (Saffron Walden, UK). Pyrex test tubes with PTFE-lined screw caps, size 100 \times 16 mm and 120 \times 16 mm were from FSA (Loughborough, UK).

PROCEDURE

Spiked cows milk

Both pooled pasteurised and raw cows milk were stirred in warm water (at 37°C) for half an hour then 250 μ l of spiking solutions were added to 50 ml of well-mixed milk. This was stirred in warm water for another half an hour. Spiked milk (2 ml) was aliquoted into glass tubes and stored at -20°C in a freezer. These spiked cows milk were used for calibration purposes when determining OCP levels in human milk.

Solvent extraction

All 2-ml milk samples were thawed and mixed well in warm water before processing. Internal standard mixture (50 μ l of aldrin 0.2 ng/ μ l, and *o,p'*-DDE 0.4 ng/ μ l) were added to human milk samples, spiked and unspiked cows milk. All milk samples (2 ml each) were extracted with 10 ml ethyl acetate-methanol-acetone (2:4:4) and vortexed for 1 min. All sample tubes were then placed in an ultrasonic bath for 20 min. The tubes were centrifuged at 2000 rpm, for 15 min at 20°C and the total supernatant aspirated into 500-ml conical flasks. The average volume of supernatant was 11.5 ml.

Solid phase extraction

After the initial solvent extraction, solid-phase extraction cartridges were used to further clean up and concentrate samples. C₁₈-cartridges (500 mg) were pre-conditioned with 2 \times 1 ml iso-octane, 2 \times 1 ml ethyl acetate, 2 \times 1 ml methanol and 2 \times 1 ml distilled water. The vacuum was turned off, and care was taken to keep the cartridges wet. An aliquot of 13 ml of distilled water was added to the supernatants. The diluted supernatants were then passed through the cartridges at a flow-rate of 6-8 ml/min. The conical flask was rinsed with 2 \times 1 ml distilled water. The cartridges were washed with 2 \times 1 ml 25% acetonitrile-water and dried by pulling air through the cartridges for 3 min. The OCPs were eluted from the cartridges with 2 \times 0.5 ml iso-octane.

Capillary gas-liquid chromatography

Operating conditions were: injection port 200°C; detector oven (ECD) 320°C; column oven, initial temperature 80°C for 1 min, increased by 10°C/min to 250°C and held for 10 min; inlet pressure 4.3 p.s.i. which was 40 cm/s gas velocity; splitless injection with purge off for 1 minute, injection volume was 1 μ l.

Quantitation

Every series of determinations contained one blank sample of unspiked pasteurised cows milk, pasteurised cows milk spiked at seven known concentrations, eight human milk samples (for OCP determination), three spiked raw cows milk (for

quality control) and one human milk for control. Peak area ratios of each pesticide were calculated. The calibration curve for extracted OCPs was obtained from linear regression analysis. The OCPs in human milk samples, human milk control and spiked raw cows milk controls were calculated from the calibrations obtained with the extracted OCPs.

Total milk fat content determination

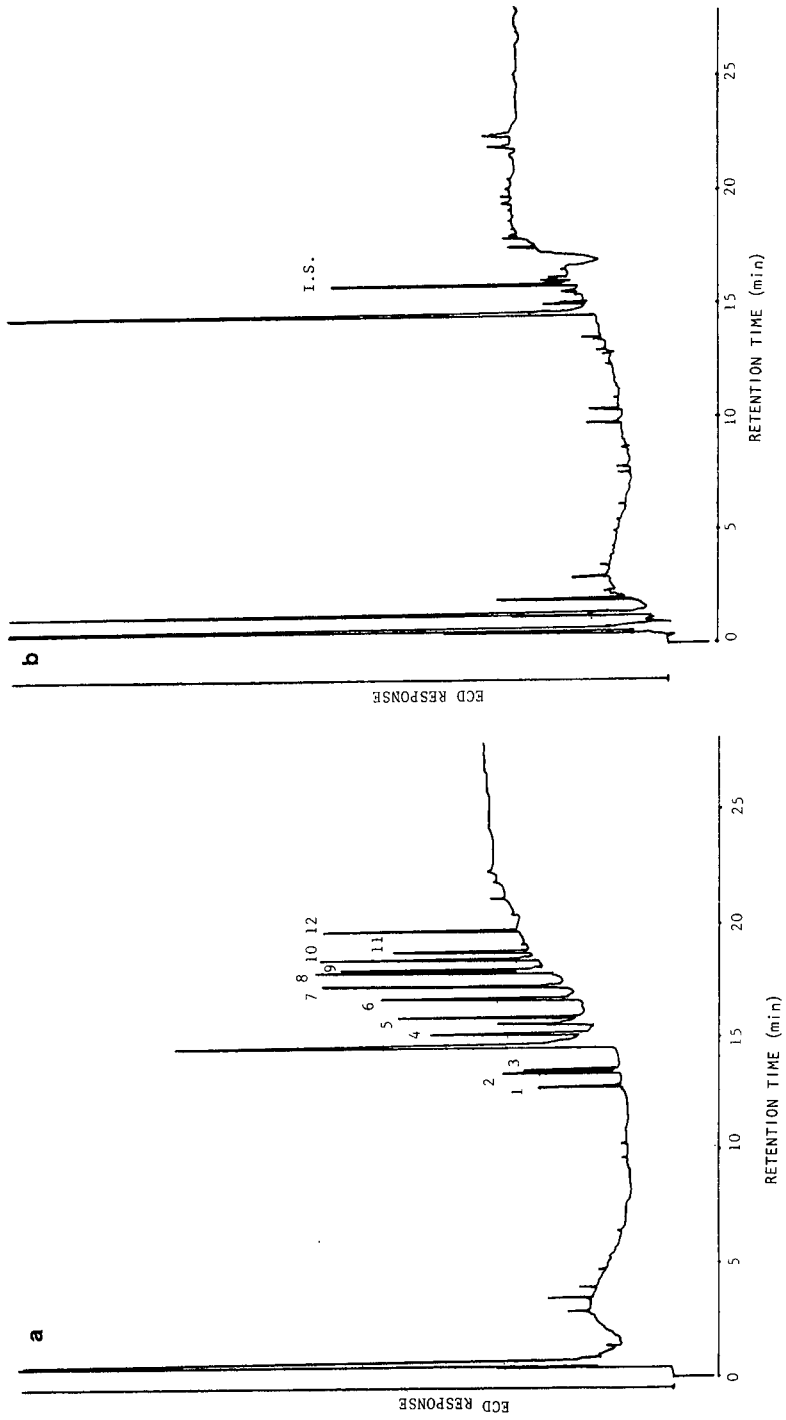
Milk samples (2 ml) were extracted with 8 ml of *n*-hexane-acetone (1:1), by vortexing for 1 minute and ultrasonification for 20 min [10,11]. After centrifugation at ca. 1000 g, for 15 min at 20°C, the supernatants were aspirated into the pre-weighed glass tubes. The solvent extraction was repeated and the supernatants combined. The supernatants were then dried under nitrogen at 40°C to constant weight and weighed. The total fat content was obtained by difference.

RESULTS AND DISCUSSION

The novel sample preparation procedure described for pasteurized and raw cows milk and human milk showed no problems with emulsions or viscous supernatants which might clog the solid-phase extraction. The fat content of pasteurized and raw cows milk was about 0.74% using the present method, and about 4.1% using the microscale (total fat extraction) method. The fat content in human milk extracts from the present method was 0.60% and from the microscale total fat extraction method was 1.78%. Thus the fat content in solvent extracts from both types of cows milk was around 18% of total fat. It was not necessary to extract total fat to get quantitative recovery of OCPs. Chromatograms of pure OCP standards, unspiked and spiked cows milk, and human milk are shown in Fig. 1. Aldrin (5 ng/ml whole milk) and *o,p'*-DDE (10 ng/ml whole milk) were evaluated as internal standards in this method. Both were suitable, *i.e.* they were well separated from the other OCPs

TABLE III
RECOVERY OF OCPs FROM SPIKED COWS MILK

Compound	Low		Medium		High	
	Concentration (ng/ml)	Recovery (%)	Concentration (ng/ml)	Recovery (%)	Concentration (ng/ml)	Recovery (%)
α -HCH	0.5	83	2.5	105	5	103
β -HCH	1	119	5	91	10	97
γ -HCH	0.5	80	2.5	86	5	96
Heptachlor	1	82	5	88	10	91
Aldrin	5	(100)	5	(100)	5	(100)
Heptachlor epoxide	1	100	5	88	10	95
<i>p,p'</i> -DDE	1.5	93	7.5	92	15	90
Dieldrin	1.5	96	7.5	95	15	97
Endrin	2	116	10	108	20	110
<i>p,p'</i> -DDD	1.5	132	7.5	111	15	104
<i>p,p'</i> -DDT	2.5	101	12.5	112	25	97



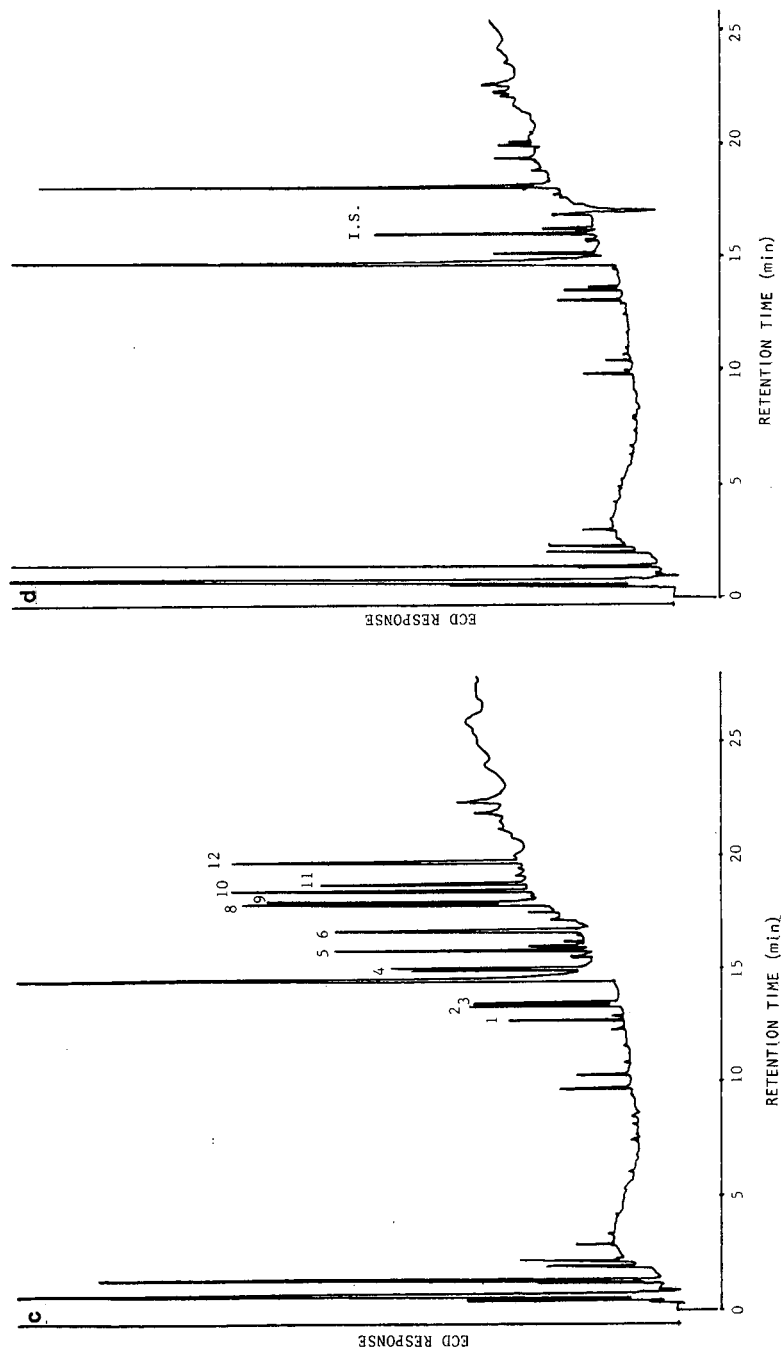


Fig. 1. Specimen chromatograms of (a) OCP standards, (b) unspiked cows milk, (c) spiked cows milk, (d) human milk sample. Peak identification: 1 = α HCH; 2 = β -HCH; 3 = γ -HCH; 4 = Heptachlor; 5 = Aldrin; 6 = Heptachlor epoxide; 7 = *o,p'*-DDE; 8 = *p,p'*-DDE; 9 = *p,p'*-DDD; 10 = Endrin; 11 = *p,p'*-DDD; 12 = *p,p'*-DDT. Chromatographic conditions: Column: 10 m \times 0.3 mm I.D., 1- μ m SE52/4; detector: ECD; temperature: 80°C for 1 min then rise 10°C per min to 250°C for 10 min; injector: 200°C; detector: 320°C.

TABLE IV
LINEARITY OF CALIBRATION LINES

Compound	Pure OCP standard		Extracted OCP standard		% Recovery OCP
	Slope	<i>r</i>	Slope	<i>r</i>	
α -HCH	0.0929	0.9984	0.0731	0.9866	79
β -HCH	0.0579	0.9984	0.0546	0.9964	94
γ -HCH	0.1052	0.9992	0.0945	0.9919	89
Heptachlor	0.0881	0.9935	0.0595	0.9983	68
Aldrin	as internal standard				
Heptachlor epoxide	0.0954	0.9970	0.0885	0.9801	93
<i>p,p'</i> -DDE	0.0716	0.9971	0.0709	0.9964	99
Dieldrin	0.0774	0.9914	0.0721	0.9954	93
Endrin	0.0541	0.9981	0.0635	0.9978	117
<i>p,p'</i> -DDD	0.0526	0.9986	0.0511	0.9961	97
<i>p,p'</i> -DDT	0.0389	0.9944	0.0538	0.9957	136

and eluted in the middle of the chromatograms among those OCPs of interest. There was often some interference in human milk samples at the retention time corresponding to *o,p'*-DDE, but not at that of aldrin. Hence, aldrin has been used as internal standard for most of this work. So far, using this method for human milk there has been no interference at the retention time of aldrin. Aldrin is rapidly metabolised to dieldrin by a wide range of organisms, including man [19] so this could explain why no aldrin residues occur. A large peak appeared at a retention time of 14.5 min, this was a "ghost" peak from the GC system and did not interfere with the assay. The gas chromatographic (GC) conditions chosen including the temperature programme rate were optimised. No peaks were seen in human milk other than DDE and DDT.

TABLE V
LIMIT OF DETECTION AND REPRODUCIBILITY OF OCPs IN COWS MILK

Compound	LOD (ng/ml milk)	Low		Medium		High	
		ng/ml milk	% C.V. ^a (<i>n</i> = 7)	ng/ml milk	% C.V. (<i>n</i> = 7)	ng/ml milk	% C.V. (<i>n</i> = 7)
α -HCH	0.5	0.5	9	2.5	8	5	2
β -HCH	1	1	14	5	8	10	7
γ -HCH	0.5	0.5	25	2.5	9	5	8
Heptachlor	1	1	23	5	14	10	14
Aldrin	I.S. ^b	5	—	5	—	5	—
Heptachlor epoxide	1	1	18	5	7	10	9
<i>p,p'</i> -DDE	1.5	1.5	13	7.5	9	15	8
Dieldrin	1.5	1.5	12	7.5	12	15	8
Endrin	2	2	25	20	10	20	10
<i>p,p'</i> -DDD	1.5	1.5	11	7.5	11	15	11
<i>p,p'</i> -DDT	2.5	2.5	13	25	11	25	12

^a C.V. = Coefficient of variation.

^b I.S. = Internal standard.

The recovery of eleven OCPs from spiked cow milks is shown in Table III. Recoveries of 80% or greater were achieved for all OCPs. The limit of detection (LOD) of this method for 11 OCPs (shown in Table III as the low value) ranged from 0.5–2.5 ng/ml with only 2 ml of milk sample required. This is favourable when compared with the existing methods which employed a larger milk volume [2]. The linearity of calibration curves of eleven OCPs in pure and processed standards were greater than 0.99 (Table IV) except for α -HCH (0.9866) and heptachlor epoxide (0.9801) which sometimes showed chromatographic interferences. The recovery of OCPs calculated from the slopes of the two calibration curves is also shown in Table IV. The day-to-day variations (for 7 days) of three different pools of spiked cows milk (0.5–2.5; 2.5–12.5 and 5–25 ng/ml whole milk) are shown in Table V.

CONCLUSIONS

This method allows the assay of 40 samples per week, with 2 h for sample preparation and only 1–2 ml human milk samples. It is simpler than current published methods and will allow a survey of OCP exposure to infants via mothers milk to be carried out.

ACKNOWLEDGEMENTS

T. P. is grateful to the British Council for her scholarship, to Dr. D. Jackson of Bristol University for providing British mothers' milk, and to Professor K. Amatayakul, Dr. P. Cheovanit and the Research Institute for Health Sciences' staff of Chiang Mai University, Thailand, for collecting Northern Thai mothers' milk.

REFERENCES

- 1 E. P. Laug, T. M. Kunze and C. S. Prickett, *Arch. Industr. Hyg.*, 3 (1951) 245.
- 2 S. A. Slorach and P. Vaz, *Assessment of Human Exposure to Selected Organochlorine Compounds Through Biological Monitoring*, Swedish National Food Administration, Uppsala, 1983.
- 3 K. Norén, *Arch. Environ. Contam. Toxicol.*, 12 (1983) 277.
- 4 D. A. Jackson, S. M. Imong, A. Silprasert, S. Ruckphaopunt, M. W. Wooldridge, J. D. Baum and K. Amatayakul, *Br. J. Nutr.*, 59 (1988) 349.
- 5 A. M. Ferris, R. M. Clark, M. Ezrin and R. G. Jensen, *J. Am. Diet. Assoc.*, 88 (1988) 694.
- 6 D. Veierov and N. Aharonson, *J. Assoc. Off. Anal. Chem.*, 63 (1980) 532.
- 7 A. E. Karakaya, S. Burgaz and I. Kenzik, *Bull. Environ. Contam. Toxicol.*, 39 (1987) 506.
- 8 C. Fookan and W. Butte, *Chemosphere*, 16 (1987) 1301.
- 9 M. P. Seymour, T. M. Jeffries and L. J. Notarianni, *Analyst (London)*, 111 (1980) 1203.
- 10 R. Vaz and G. Blomkvist, *Chemosphere*, 14 (1985) 223.
- 11 R. Vaz, Swedish National Food Administration, personal communication.
- 12 N. F. Wood, *Analyst (London)*, 94 (1969) 399.
- 13 J. D. Tessani and E. P. Savage, *J. Assoc. Off. Anal. Chem.*, 63 (1980) 736.
- 14 T. Suzuki, K. Ishikawa, N. Sato and K. Sakai, *J. Assoc. Off. Anal. Chem.*, 62 (1979) 681.
- 15 A. D. Muccio, M. Rizzica, A. Ausili, I. Camoni, R. Dommarco and F. Vergori, *J. Chromatogr.*, 456 (1988) 143.
- 16 F. E. Martinez, I. D. Desai, A. G. F. Davidson and A. Radcliffe, *J. Pediat. Gastroenterol. Nutr.*, 6 (1987) 593.
- 17 J. Bailey, V. Knauf, W. Mueller and W. Hobson, *Environ. Res.*, 21 (1980) 190.
- 18 M. K. J. Siddigui, M. C. Saxeno, A. K. Bnorgaua, T. D. Seth, C. R. K. Marti and D. Kuty, *Environ. Res.*, 24 (1981) 24.
- 19 W. J. Hayes, Jr., *Pesticides studied in man*, Williams and Wilkins, Baltimore, MD, 1982, pp. 23.

CHROMSYMP. 2313

Multi-matrix–multi-pesticide method for agricultural products

LOUIS G. M. Th. TUINSTRA*

State Institute for Quality Control of Agricultural Products, Bornsesteeg 45, 6708 PD Wageningen (The Netherlands)

FRANK R. POVEL

Finnigan MAT Benelux, Landjuweel 7, 3905 PE Veenendaal (The Netherlands)

and

ARIE H. ROOS

State Institute for Quality Control of Agricultural Products, Bornsesteeg 45, 6708 PD Wageningen (The Netherlands)

ABSTRACT

In an initial experiment 21 pesticides were used as test compounds to develop a method of analysis in different types of matrices for pesticides which can be analysed by gas chromatography. An attempt was made to combine a generally applicable clean-up method with a universal detection system, *i.e.* the ion trap detector. Experiments showed that potentially it should be possible to develop a quantitative method for at least 17 compounds in different matrices.

INTRODUCTION

In the Netherlands 400 pesticides are allowed for certain applications. Thirteen multi-methods exist [1] for the determination of about 220 pesticides in various food-stuffs. The presence of other pesticides may be determined by special methods, generally applicable to only one pesticide. It is impossible for controlling authorities to have all these methods available and ready for immediate analysis. Recently, due to environmental concern, the Dutch government has mandated that the quantity of pesticides used should be decreased by at least 50% in the coming years.

There is an urgent need for a universally applicable method with a high throughput of samples. In the literature several methods based on gas chromatographic analysis are available [2,3] but the different extracts obtained need to be analysed with several specific detectors, *e.g.*, the electron-capture and nitrogen–phosphorus detector. In recent years the use of small mass spectrometers has increased rapidly.

Here we report initial results obtained with an ion trap detector for a group of pesticides generally not included in multimethods. As clean-up, gel permeation chro-

matography (GPC) was used. The approach and applicability of a procedure using a slightly modified Luke extraction procedure and also using an ion trap detector has been tested recently with good results by Mattern *et al.* [41].

EXPERIMENTAL

Matrices

Tomato, cucumber, cauliflower, endive, chicory, capsicum, apple, wheat, potatoes and lettuce were analysed alone and with pesticide spikes.

Pesticides

Alachlor, biphenox, bromacil, crufomate, diallate, dinobuton, fenarimol, flua-zifop-butyl, imazalil, lenacil, metamitron, metribuzin, nitrofen, nitrothal-isopropyl, pendimethalin, pirimicarb were analysed individually and benodanil, chlorpropham, triadimefon, triallate and trifluralin were analysed using existing multi-methods.

Gel permeation chromatography

A Bio-Beads SX3 column (45 × 1 cm), eluted with acetone-cyclohexane (1:1) at a flow-rate of 1 ml/min was used. Injection volume, 1 ml; pump, Waters M45; fraction collector, Gilson 202; fraction volume, 13.5 ml; fractionating starting 16.5 min after injection; total time of analysis, 30 min [5].

Gas chromatography-mass spectrometry (GC-MS)

A Varian 3400 gas chromatograph in combination with a Finnigan MAT ITS 40 ion trap detector was used. The gas chromatograph was equipped with a septum programmable injector and with a 30 m × 0.25 mm I.D. J&W DB-5 capillary column, film thickness 0.25 μm. Helium flow-rate 1.5 ml/min; injection volume, 1 μl. Injection temperature, 60°C for 1 min, then at a rate of 300°C/min heated to 325°C. Column temperature started isothermally at 92°C. After 1 min the column was heated up to 325°C at a rate of 20°C/min. The ITS was operated in the electron-impact mode. Each second a spectrum from mass 49 to 449 was recorded.

Extraction and clean-up

After homogenisation of the sample, 100 g were macerated with 200 ml of acetone for 3 min, filtered over glasswool and after addition of 60 ml of saturated sodium chloride solution extracted with 150 ml of hexane for 1 min. After separation the organic phase was washed twice with water, dried over sodium sulphate, concentrated to 5.0 ml, and diluted to 10.0 ml with acetone-cyclohexane (1:1). For clean-up 1.0 ml was injected into the GPC system. The appropriate fraction was collected, the internal standard PCB 153 (2,4,5,2',4',5'-hexachlorobiphenyl) added and the fraction concentrated to 500 μl; 1 μl of this solution was injected into the GC-MS system.

RESULTS AND DISCUSSION

In the literature, much information is available on GC behaviour of pesticides and their mass spectra. The use of GC-MS in combination with a widely applicable

TABLE I
IDENTIFICATION NUMBER OF PESTICIDES USED IN EXPERIMENTS

Number	Compound	Number	Compound
1	Chlorpropham	12	Imazalil
2	Trifluralin	13	Benodanil
3	Triallate	14	Biphenox
4	Nitrothal-isopropyl	15	Diallate
5	Crufomate	16	Metribuzin
6	Fluazifopbutyl	17	Bromacil
7	Nitrofen	18	Triadimefon
8	Fenarimol	19	Dinobuton
9	Pirimicarb	20	Metamitron
10	Alachlor	21	Lenacil
11	Pendimethalin		

extraction and clean-up technique for pesticides in all kind of matrices is rare. Though these techniques do exist [2,3] they are used mostly in combination with several other detection and/or separation techniques. We chose 21 pesticides to test a single method. Until now only five of these 21 pesticides have been incorporated in a multi-method, the other 16 are determined in individual methods [1].

The behaviour of these compounds, *e.g.* extraction with acetone from vegetable

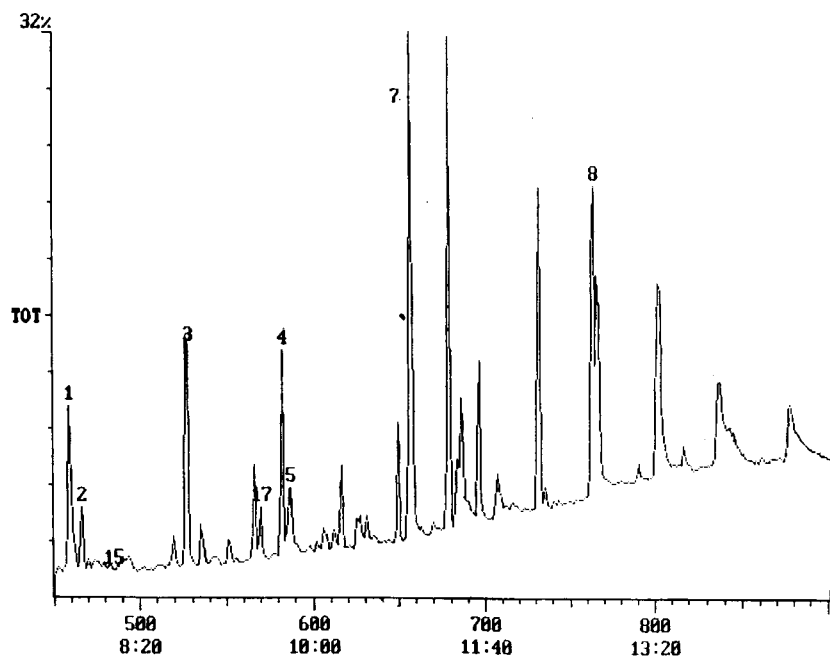


Fig. 1. Reconstructed ion chromatogram of a tomato extract spiked with a selected number of pesticides (full-scan mode). For identification see Table I. x-Axis: scan No. and time in mins.

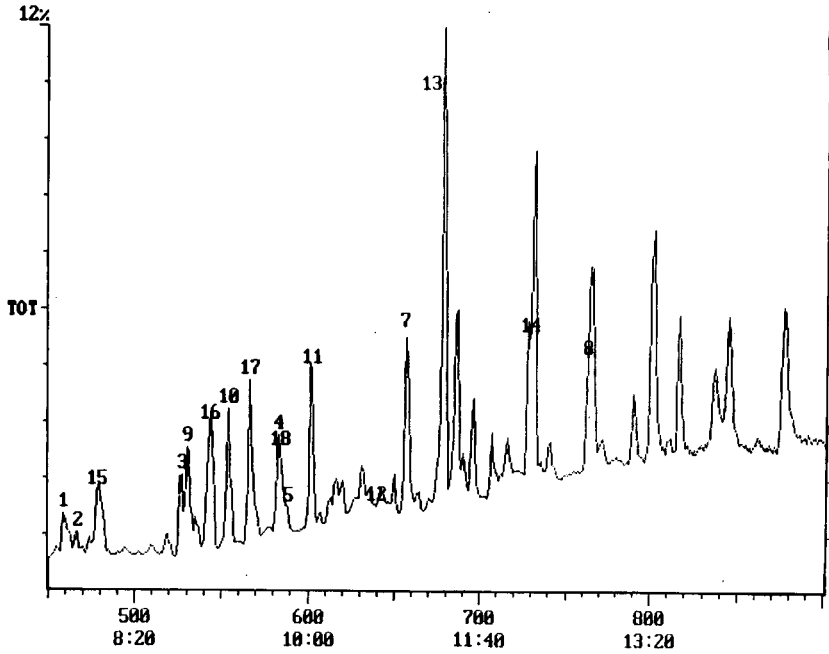


Fig. 2. Reconstructed ion chromatogram of a combined cucumber, capsicum and chicory extract spiked with pesticides (full-scan mode). For identification see Table I. x-Axis: scan No. and time in min:s.

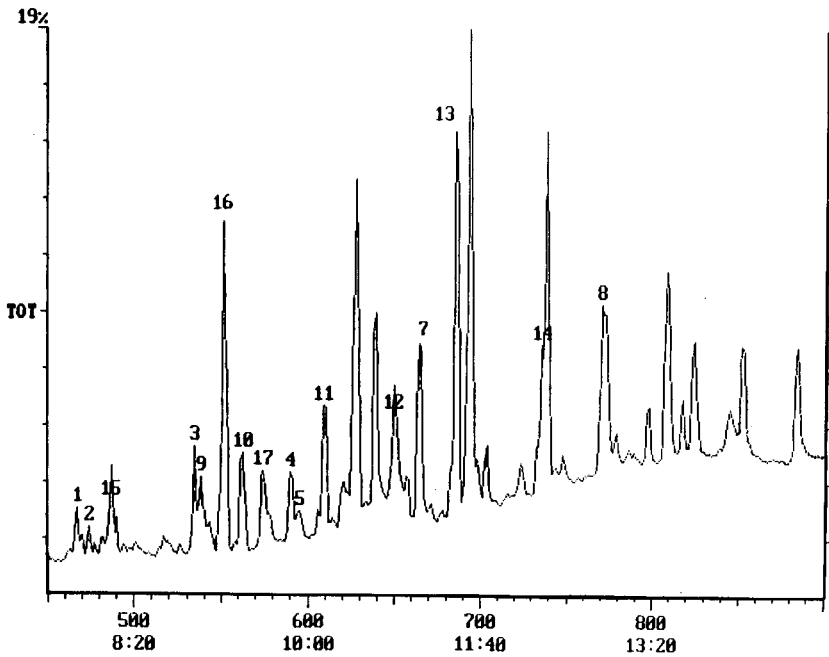


Fig. 3. Reconstructed ion chromatogram of a combined endive, cucumber and cauliflower extract spiked with pesticides (full-scan mode). For identification see Table I. x-Axis: scan No. and time in min:s.

matrices and clean-up by GPC is described by Specht and Tillkes [3]. They describe the behaviour of about 400 pesticides and industrial organic contaminants, as well as their recoveries. Recently Steinwandter [6] described a less time-consuming acetone extraction in combination with GPC using acetone. Good recovery data were obtained.

Since compatibility of extraction solvent with eluent is advantageous, acetone was used in our experiment as extraction solvent and acetone-cyclohexane as eluent for GPC. Initially the method was checked only with standards. Recoveries better than 75% were obtained. The above-mentioned matrices were spiked at 0.25 mg/kg pesticide and analysed both on a Hewlett-Packard mass-selective detector (HP MSD) [7] and a Finnigan MAT ITS 40.

This paper reports data obtained with the ITS 40 mass spectrometer. The sensitivity of the ion trap detector allows full-scan mass spectra to be obtained without having to resort to monitoring a few selected ions. Thus it should be possible to identify each compound on the basis of their total spectrum rather than on basis of a few selected ions. The identification procedure followed implied that in a certain retention window the chromatogram was searched for a spectrum similar to that of the compound of interest. In each case where the similarity was above a certain threshold the compound was regarded as being identified, after which quantification followed.

In Table I the identification numbers of the tested pesticides are given and in Fig. 1 the result for a tomato extract is shown. This matrix was spiked with a pesticide mixture containing eight pesticides. The data system numbers the chromatographic peaks automatically when they are identified following the above-mentioned procedure.

All the compounds except fluazifopbutyl (compound 6) could be detected. Furthermore, diallate (compound 15), present as a contaminant in the standard of triallate, was also detected, as was bromacil (compound 17). Interference of a phthalate was observed at retention time 12 min 10 s. In order to test the method for all 21 pesticides simultaneously, we combined several matrices spiked with different groups of pesticides. These combined extracts contained all pesticides mentioned in Table I. Figs. 2 and 3 are examples of the chromatograms obtained.

In addition to fluazifopbutyl (compound 6), dinobuton, metamitron and lenacil (compounds 19, 20 and 21) were also not recovered. In general, the recovery of all compounds in the matrices was lower than obtained with standards (0–80% and < 75% respectively). We suspect that during the evaporation step losses occurred whereas with standards, with no evaporation step, no exceptional losses occurred. Nevertheless, of the 21 pesticides used, 17 pesticides were detectable. Of these 17 pesticides, in the past 12 had to be analysed with individual methods [1]. Therefore, according to our findings, it should be possible to develop multi-methods for the determination of pesticides in many different matrices.

ACKNOWLEDGEMENT

Arrienne Matser is acknowledged for her analytical assistance in the development of the method.

REFERENCES

- 1 P. A. Greve, *Analytical Methods for Residues of Pesticides*, SDU Publishers, The Hague, 5th ed., 1988.
- 2 M. A. Luke, J. E. Froberg, G. M. Doose and H. Masumoto, *J. Assoc. Off. Agric. Chem.*, 64 (1981) 1187-1195.
- 3 W. Specht and M. Tillkes, *Fresenius Z. Anal. Chem.*, 322 (1985) 433-445.
- 4 G. C. Mattern, G. M. Singer, J. Louis, M. Robson and J. D. Rosen, *J. Agric. Food Chem.*, 38 (1990) 402-407.
- 5 A. H. Roos, A. J. van Munsteren, F. M. Nab and L. G. M. Th. Tuinstra, *Anal. Chim. Acta*, 196 (1987) 95-102.
- 6 H. Steinwandter, *Fresenius Z. Anal. Chem.*, 331 (1988) 449-502.
- 7 L. G. M. Th. Tuinstra, A. H. Roos, A. M. Matser, W. A. Traag and J. A. van Rhijn, *Fresenius Z. Anal. Chem.*, 339 (1991) 384-386.

Identification by capillary gas chromatography–mass spectrometry of volatile organohalogen compounds formed during bleaching of kraft pulp

CHRISTINA ROSENBERG*, TIINA AALTO, JARKKO TORNAEUS and ANTTI HESSO

Institute of Occupational Health, Topeliuksenkatu 41 aA, SF-00250 Helsinki (Finland)

PAAVO JÄPPINEN

Enso-Gutzeit Oy, SF-55800 Imatra (Finland)

and

HARRI VAINIO

International Agency for Research on Cancer, F-69372 Lyon (France)

ABSTRACT

The occurrence of volatile halogenated compounds in spent liquors from kraft softwood and hardwood pulp bleaching processes was studied. The identity of the low-molecular-mass constituents was verified by capillary gas chromatography–mass spectrometry using an NBS/Wiley reference database and mass spectra of reference compounds. The purgeable fraction of the first chlorination stage of the softwood pulp contained numerically most of the organohalogen compounds detected. The ratio of chlorine to chlorine dioxide applied at this stage greatly affected the formation of the compounds. Identity was confirmed for fourteen components, of which two, dichloroacetonitrile and trichloromethanesulphonyl chloride, have not been previously identified in, *e.g.*, bleach kraft effluents. The most abundant volatile compounds were chloroform, 1,1,1-trichloropropanone, trichloromethanesulphonyl chloride, 1,1,2,3,3-pentachloro-1-propene and pentachloropropanone. Several of these volatile compounds are known mutagens or suspected carcinogens.

INTRODUCTION

Organochlorine compounds found in effluents from kraft mill bleaching processes are derived from the use of chlorine-containing bleaching agents. The chemical composition of these chlorinated compounds has been extensively studied since the 1970s [1]. It has been established that most of the chlorine is bound to high-molecular-mass material, and that only *ca.* 30% occurs in the low-molecular-mass ($M < 1000$) fraction in the spent liquor of the first chlorination step and only 5% in the first alkaline extraction liquor of softwood kraft pulp [1].

Research in this field has concentrated especially on environmental effects of the effluents. The chlorinated compounds found in effluents are often resistant to chemical and biological degradation. Many of these compounds are toxic to aquatic organisms and several of them are genotoxic. The identified compounds include

chlorinated acids [2], phenolics [3,4], and neutral compounds such as chlorinated acetones and aldehydes [5,6] and furanones [7,8]. The lipophilic properties of some chlorinated compounds have received special attention because of the possibility of bioaccumulation in aquatic systems [9–11]. Suntio *et al.* [12] reviewed the properties of *ca.* 250 chemicals identified in bleached pulp mill effluents.

However, scant data are available on volatile organochlorine compounds formed during the bleaching operation. Chloroform has been reported to be the most abundant halogenated compound in the volatile fraction of bleached kraft mill effluents [13,14]. Further investigation is required concerning the nature and occurrence of volatile organohalogens formed and potentially released into the work environment during the bleaching process.

This paper describes the identification of low-molecular-mass purgeable organohalogen compounds in spent liquors from different bleaching stages of softwood and hardwood kraft pulp.

EXPERIMENTAL

The bleaching process and sample collection

Single samples of spent liquors were taken at a kraft pulp mill from one softwood and one hardwood line with production capacities of about 300 and 1100 t/d, respectively. The bleaching was accomplished by multi-stage treatment with chlorine (C), alkali (E) and chlorine dioxide (D). The liquors were sampled at the wash filters after each bleaching stage.

The reagent in the first bleaching stage of the softwood kraft process consisted of a mixture of chlorine and chlorine dioxide (either 90:10 or 50:50). The complete bleaching sequence was C₉₀/D₁₀ (or C₅₀/D₅₀)–E₁–D₁–E₂–D₂. The E₁ stage was combined with hypochlorite treatment. The total charge of chlorine compounds was 50 kg/t of pulp in the first chlorination stage, expressed as active chlorine. The kappa number of the unbleached pulp was *ca.* 25.

The hardwood kraft process utilized chlorine dioxide alone in the first chlorination stage (D₀). The first alkaline extraction stage consisted of hypochlorite treatment followed by alkaline plus oxygen treatment (E/O). The complete bleaching sequence was thus D₀–E₁–E/O–D₁–E₂–D₂. The hardwood pulp had a kappa number of *ca.* 20, and the consumption of bleaching agent, expressed as active chlorine, in the D₀ step was 36 kg/t of pulp.

Isolation of volatile compounds

About 1.5 l of spent liquor was purged with nitrogen at a rate of 50 ml/min for 1 h and concurrently heated at the process temperature, *i.e.*, 45–55°C. The reaction vessel was equipped with a magnetic stirrer and any volatilized compounds were trapped in a glass coil, immersed in a mixture of ethanol and dry-ice, or in an activated charcoal tube connected in series with the coil. The temperature of the cold-trap was about –70°C. The purged liquor was then discarded and replaced with a new 1.5-l sample of liquor, and the collection of volatile compounds was continued using the same trapping equipment. This procedure was repeated a third time. The coil and the charcoal tube were then eluted with ethyl acetate and *n*-pentane, respectively. The ethyl acetate eluate was concentrated to one twentieth of its original volume prior to analysis.

Gas chromatography-mass spectrometry

All eluates were analysed by capillary gas chromatography with mass spectrometric detection (GC-MS). The mass spectrometric system consisted of a Hewlett-Packard quadrupole mass spectrometer (HP 5990A) operating in the electron impact (EI) mode (70 eV) and equipped with a merged NBS/Wiley database (HP 59983K). The mass spectra were confirmed using a Finnigan MAT 8200 mass spectrometer with an on-line computer system and an NBS database (MAT INCOS 5.6E). The system was operated in the EI mode at 70 eV at a resolution of 3000.

The EI mass spectra were recorded in the range m/z 35–550. A fused-silica column (50 m \times 0.3 mm I.D.) coated (0.17 μm) with 95% dimethyl–5% diphenylpolysiloxane (Hewlett-Packard) was used, coupled directly to the ion source.

The temperature of the transfer line was 250°C in both mass spectrometers. The ion source temperature and emission current were 180° and 0.3 mA, respectively, in the Hewlett-Packard system and 150°C and 1 mA, respectively, in the Finnigan MAT 8200 system. Helium was used as carrier gas (24 cm/s at 100°C) and samples of 1 μl were injected using an on-column technique at 35°C. Chloroform was analysed using split injection in a Grob-type split-splitless injector operating at 220°C and with a 1:10 splitting ratio. The column temperature program was as follows: 6 min at 35°C, increased from 35 to 100°C at 5°C/min and from 100 to 250°C at 10°C/min, and held for 15 min at 250°C.

RESULTS AND DISCUSSION

The purgeable organohalogen compounds identified in the spent bleaching liquors included chlorinated and brominated alkanes, alkenes, esters, ketones, benzenes and some chlorinated sulphur compounds (Tables I and II).

A reconstructed ion chromatogram of the cold-trap eluate from the C₉₀/D₁₀ first chlorination stage spent liquor is given in Fig. 1. Emphasis was placed on peaks with isotopic cluster patterns typical of chlorine and bromine compounds. Some of the compounds were identified using mass spectral interpretation confirmed by comparison with the mass spectrum of a reference compound (technique A). Others were identified by mass spectral interpretation and comparison with reference spectra from the NBS and Wiley databases (technique B).

In the C₉₀/D₁₀ first chlorination stage sample fourteen volatile organohalogen compounds were encountered, eleven of which were identified using technique A and three using technique B (Table I). In addition, six peaks with a typical chlorine isotope cluster pattern were registered, but their identity was not solved accurately enough (Fig. 1, peaks I–VI). Of the eleven category A compounds, two have not been reported previously to be present in spent bleach effluents, *viz.*, dichloroacetonitrile [Chemical Abstracts Service (CAS) No. 3018-12-0] (Fig. 2a) and trichloromethanesulphonyl chloride (CAS No. 2547-61-7) (Fig. 2b) [5,12].

Dichloroacetonitrile has been reported as a component formed in the chlorination of humic acid, a precursor of halogenated compounds formed during chlorination of drinking water [15].

In this study, the source of trichloromethanesulphonyl chloride remained obscure. Chlorinated dimethylsulphones have been reported in biologically treated bleached kraft effluents [16]. The latter compounds were suggested to be derived from dimethyl thioether residues from the cooking process prior to bleaching [1].

TABLE I

PURGEABLE ORGANOHALOGEN COMPOUNDS IDENTIFIED IN THE SPENT LIQUOR FROM THE FIRST CHLORINATION (C_{90}/D_{10}) STAGE OF SOFTWOOD PULP

Peak No. ^a	Compound identified	Retention time (min) ^b	C_{90}/D_{10}	
			Identification technique	Peak area
—	Chloroform ^c	—	A ^d	—
1	Trichloroethene	6.95	A	*** ^e
2	Bromodichloromethane	7.09	A	*
3	Dichloroacetonitrile	7.38	A	**
4	Tetrachloroethene	10.25	A	*
5	1,1,1-Trichloropropanone	11.61	B ^f	****
6	Methyl 2,2-dichloropropanoate	12.65	B	*
7	Pentachloroethane	16.89	A	*
8	1,4-Dichlorobenzene	18.28	A	*
9	Trichloromethanesulphonyl chloride	18.88	A	***
10	1,2-Dichlorobenzene	19.12	A	*
11	1,1,2,2-Tetrachloropropane	19.48	B	**
12	1,1,2,3,3-pentachloro-1-propene	20.79	A	****
13	Pentachloropropanone	21.02	A	****

^a Peak number refer to Fig. 1 (reconstructed ion chromatogram from the C_{90}/D_{10} stage cold-trap eluate in ethyl acetate).

^b The retention times are reported in minutes as absolute retention time. The relative standard deviation for the retention times was 0.01 within the elution range ($n = 12$).

^c Chloroform was analysed in the *n*-pentane eluate from the activated charcoal tube connected in series with the cold trap and is therefore not recorded in Fig. 1.

^d A = identification based on mass spectral interpretation and comparison with the spectrum of a reference substance.

^e * → **** = Increasing peak area.

^f B = identification based on mass spectral interpretation and comparison with a reference spectrum from the library database.

TABLE II

PURGEABLE ORGANOHALOGEN COMPOUNDS IDENTIFIED IN THE SPENT LIQUORS FROM THE FIRST (C_{50}/D_{50}) AND SECOND (D_1) CHLORINATION STAGES OF SOFTWOOD PULP AND THE FIRST CHLORINATION STAGE (D_0) OF HARDWOOD PULP

Compound identified	C_{50}/D_{50} (softwood)	D_1 ^a (softwood)	D_0 (hardwood)
Chloroform	A	A	A ^b
Dichloroacetonitrile	— ^c	—	A
Methyl chloroacetate	B ^d	—	—
1,1,1-Trichloropropanone	B	B	B
Tribromomethane	A	A	—
2,5-Dichlorothiophene	—	—	A
Trichloromethanesulphonyl chloride	A	—	—
Pentachloropropanone	A	A	—
Tetrachlorothiophene	A	A	—

^a Belongs to the bleaching sequence beginning with the C_{90}/D_{10} stage.

^b A = identification based on mass spectral interpretation and comparison with the spectrum from a reference substance.

^c Not present.

^d B = identification based on mass spectral interpretation and comparison with a reference spectrum from the library database.

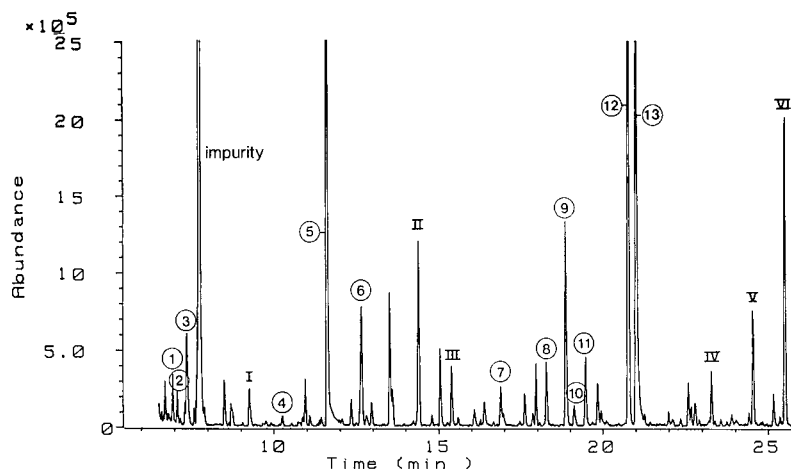


Fig. 1. A reconstructed ion chromatogram of the cold-trap eluate in ethyl acetate from the C_{90}/D_{10} first chlorination stage of softwood. Peaks 1–13 are listed in Table I. Compounds I–VI exhibited a chlorine isotope cluster pattern, but their identification was not unequivocal.

The category B compounds have also been found in bleached kraft effluents as such (peak 5), as a precursor (peak 6) or as a related compound (peak 11) [6, 17, 18].

Chloroform was found and confirmed with complete identification (category A) in the *n*-pentane eluates from the activated charcoal tubes connected in series with the cold trap. Traces of tetrachloroethene, 1,1,1-trichloroethane and carbon tetrachloride were also detected. The identity of the latter was verified by the selected ion monitoring technique with the Hewlett-Packard quadrupole mass spectrometer. The ions monitored were m/z 164, 166, 97, 99 and 117, 119 with intensities of 75/100%, 100/66% and 100/99%, respectively.

Quantification of the peaks was not done. However, on comparing the relative abundances of the GC-MS peaks, it was evident that the five most abundant compounds were chloroform, 1,1,1-trichloropropanone, trichloromethanesulphonyl chloride, 1,1,2,3,3-pentachloro-1-propene and pentachloropropanone. Chloroform accounted for about 80% of the relative abundance of the aforementioned compounds. The high proportion of chloroform in the volatile fraction is consistent with effluent studies [14,19].

The purgeable fraction from the softwood C_{90}/D_{10} first bleaching stage contained most of the organohalogen compounds identified. Considerably fewer compounds were detected in the cold-trap eluate when chlorine-chlorine dioxide (50:50) was used (C_{50}/D_{50}) in the softwood bleaching process. This was to be expected, as previous studies had showed that the formation of organohalogen compounds decreases with decreasing chlorine consumption [20,21]. Only seven compounds were detected (Table II, C_{50}/D_{50} column), five of which were identified by technique A and two by technique B. The overall pattern was similar to that for the C_{90}/D_{10} sample, in that chloroform, pentachloropropanone and trichloromethanesulphonyl chloride were the most abundant compounds. Even fewer volatile organohalogen compounds were detected in the spent liquor of the D_1 second chlorination stage (preceded by the

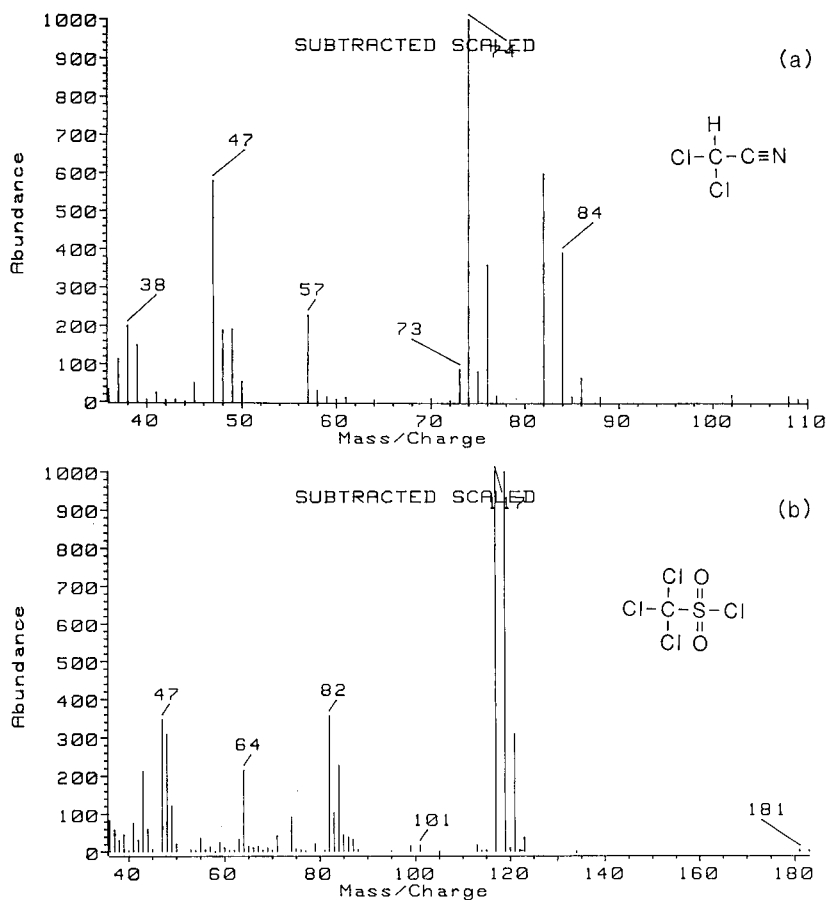


Fig. 2. Electron impact mass spectra obtained from peaks 3 and 9 in Fig. 1 (C_{90}/D_{10} first chlorination stage of softwood). (a) Dichloroacetone nitrile; (b) trichloromethanesulphonyl chloride.

C_{90}/D_{10} stage). Of the total of five compounds classified (Table II, D_1 column), four belonged to the identification category A and one to category B. Trichloromethanesulphonyl chloride was not detected at this stage; instead, another chlorinated sulphur compound, tetrachlorothiophene, was encountered. This compound has also been previously identified in spent pulp bleach liquors [11].

Bleaching of hardwood usually produces less organohalogen compounds [22], which was also evident in this study for volatile compounds. In the first chlorination stage of hardwood pulp (D_0), only three compounds were identified by technique A and one by technique B (Table II, D_0 column). On the other hand, the use of chlorine dioxide alone in this stage may account for the small number of compounds identified.

Virtually no volatile organohalogen compounds were detected in the cold-trap eluates from the softwood or hardwood third chlorination stage (D_2) or the alkali stages. However, chloroform and traces of 1,1,1-trichloroethane were found in the activated charcoal eluates from every stage of the two bleaching processes. Similarly,

traces of tetrachloroethene, carbon tetrachloride and bromodichloromethane were found in all but the alkaline stages of the hardwood bleaching process. It is noteworthy that whereas the relative abundance of chloroform and carbon tetrachloride decreased with decreasing chlorine use, that of 1,1,1-trichloroethane and bromodichloromethane remained more or less constant. This seems to indicate that they are present as impurities rather than as bleaching-derived compounds. The concentration of chloroform in the second chlorination stage of softwood (D_1) was about one quarter of that detected in the first chlorination stages (C_{90}/D_{10} and C_{50}/D_{50}). The corresponding figure was one fifteenth in the first chlorination stage with hardwood (D_0). The enhancement of chloroform formation by hypochlorite treatment [1,22] was evident in the E/O stage of the hardwood process. In this stage, which followed the first alkaline extraction stage combined with hypochlorite, the relative abundance of chloroform approached that found in the C_{90}/D_{10} stage of the softwood process.

CONCLUSIONS

The laboratory analysis of liquors from different bleaching stages of softwood and hardwood kraft pulp revealed numerous volatile low-molecular-mass organohalogen compounds. Most of the compounds were derived from the first bleaching stage. It is probable that these volatile compounds may be released into the workplace air during the process. Of the fourteen halogenated purgeable compounds identified, two have not been found previously in bleach kraft effluents, *viz.*, dichloroacetonitrile and trichloromethanesulphonyl chloride. Some of the most abundant compounds identified are known mutagens, *e.g.*, 1,1,2,3,3-pentachloro-1-propene and pentachloropropanone [23], or suspected carcinogens, *e.g.*, chloroform and carbon tetrachloride [24]. Further investigation is required to estimate the exposure of workers to these potentially harmful organohalogen compounds formed during bleaching of kraft pulp with chlorine-containing agents.

ACKNOWLEDGEMENTS

We thank Mrs. Ritva Wirmoila for skilful technical assistance. The work was partially financed by the Finnish Work Environment Fund, which is gratefully acknowledged.

REFERENCES

- 1 K. P. Kringstad and K. Lindström, *Environ. Sci. Technol.*, 18 (1984) 236A.
- 2 K. Lindström and F. Österberg, *Environ. Sci. Technol.*, 20 (1986) 133.
- 3 J. Paasivirta, J. Knuutinen, J. Tarhanen, T. Kuokkanen, K. Surma-Aho, R. Pauku, H. Kääriäinen, M. Lahtiperä and A. Veijanen, *Water Sci. Technol.*, 15 (1983) 97.
- 4 K. Lindström and J. Nordin, *J. Chromatogr.*, 128 (1976) 13.
- 5 K. P. Kringstad and K. Lindström, *Proceedings of 1982 Research and Development Division Conference, TAPPI, Ascherville, NC, August 29–September 1, 1982*.
- 6 E. Talka and M. Priha, *Pap. Puu — Papp. Trä*, 69 (1987) 221.
- 7 B. Holmbom, R. V. Voss, R. D. Mortimer and A. Wong, *Environ. Sci. Technol.*, 18 (1984) 333.
- 8 L. Kronberg, B. Holmbom, M. Reunanen and L. Tikkanen, *Environ. Sci. Technol.*, 22 (1988) 1097.
- 9 K. P. Kringstad, F. de Sousa and L. M. Strömberg, *Environ. Sci. Technol.*, 18 (1984) 59.
- 10 A. B. McKague, M.-C. Kolar and K. P. Kringstad, *Environ. Sci. Technol.*, 22 (1988), 523.

- 11 A. B. McKague, M.-C. Kolar and K. P. Kringstad, *Environ. Sci. Technol.*, 23 (1989), 1126.
- 12 L. R. Suntio, W. Ying Shiu and D. Mackay, *Chemosphere*, 17 (1988) 1249.
- 13 E. Talka, *Pap. Puu — Papp. Trä*, 68 (1986) 670.
- 14 C. Lauenberger, W. Giger, R. Coney, J. W. Graydon and E. Molnar-Kubica, *Water Res.*, 19 (1985) 885.
- 15 M. P. Italia and P. C. Uden, *J. Chromatogr.*, 449 (1988) 326.
- 16 R. H. Voss, *Environ. Sci. Technol.*, 17 (1983) 530.
- 17 K. P. Kringstad, P. O. Ljungquist, F. de Sousa and L. M. Strömberg, *Environ. Sci. Technol.*, 15 (1981) 562.
- 18 G. E. Carlberg, H. Drangsholt and N. Gjoes, *Sci. Total Environ.*, 48 (1986) 157.
- 19 M. Gregov, M. Priha, E. Talka, O. Valtila, A. Kangas and K. Kukkonen, *Tappi*, 71 (1988) 175.
- 20 P. Axegård, *Tappi*, 6 (1986) 54.
- 21 W. H. Rapson and C. B. Anderson, *Pulp Pap. Mag. Can.*, Jan. (1966) T-47.
- 22 P. Axegård, *Nord. Cellulosa*, No. 7 (1988) 31.
- 23 G. R. Douglas, E. R. Nestman, A. B. McKague, O. P. Kamara, E.-G. Lee, J. A. Ellenton, R. Bell, D. Kowbel, V. Liu and J. Pooley, in M. D. Waters, S.S. Sandhu, J. Lewtas, L. Claxton, N. Chernof and S. Nesnow (Editors), *Short-Term Bioassays in the Analysis of Complex Environmental Mixtures III*, Plenum Press, New York, 1983, pp. 431.
- 24 IARC, *Overall Evaluation of Carcinogenicity: an Updating of IARC Monographs*, Vols. 1-42, Suppl. 7, International Agency for Research on Cancer, Lyon, 1987.

CHROMSYMPO. 2343

Applications of capillary gas chromatography to the quality control of butter and related products

A. ANTONELLI*

Istituto di Industrie Agrarie, Università degli Studi, Via S. Giacomo 7, 40126 Bologna (Italy)

L. S. CONTE

MAF, Ispettorato Repressione Frodi, Ufficio di Bologna, Via S. Giacomo 7, 40126 Bologna (Italy)

and

G. LERCKER

Istituto di Tecnologie Alimentari, Università di Udine, Via Marangoni 97, 33100 Udine (Italy)

ABSTRACT

Analyses performed to establish the quality of butter are essentially based on the packed column gas chromatographic determination of fatty acid composition. One of the main problems is the determination of the short-chain fatty acids, particularly butyric acid. In previous work, comparing results obtained by on column injection with those obtained by split injection, with and without silanized glass-wool in the liner, at two different pre-set splitting ratios, it was found that a packed injector at the highest splitting ratio gives results equivalent to those obtained with on-column injection. When small amounts of butyric acid must be detected, less volatile esters are more suitable than those obtained by rapid transesterification with sodium butoxide. In this paper results obtained for the determination of the amount of butter in bakery products are reported. Results for both real samples and model systems gave highly significant values for the correlation coefficient for split and on-column injection on the basis of fatty acid butyl esters. Triglycerides were also determined in order to measure the amount of butter by means of trienanthine.

INTRODUCTION

James and Martin [1] first determined the fatty acid composition of milk by packed column gas chromatography in 1956, and subsequently capillary GC [2–15] was also used for this purpose. The main problem concerning butter analysis is the determination of the short-chain fatty acids (C_4 – C_8), and this is increased when split injection is used even if simple devices can sometimes help in obtaining results close to those given by on-column injection [15].

The use of less volatile esters (*e.g.*, butyl or benzyl esters) might provide an interesting solution of the problem [11,12,16–21]. The rapid method proposed by Christopherson and Glass [22] can be used with sodium butoxide instead of sodium methoxide [16,17].

In recent years, a particular kind of butter has been produced in the European

Economic Community (EEC) namely "concentrated butter". This butter is employed only for bakery and confectionery products and to distinguish this product [23–25] some denaturants are added, *i.e.*, stigmasterol (stigmasta-5,22-dien-3 β -ol), trienanthine (glycerol triheptanoate) and vanillin (4-methoxy-3-hydroxybenzaldehyde).

In this paper the calibration and application of a simple method for butter analysis and its determination in bakery products is described. For the latter purpose both butyric and enanthic acid were used. The level of the former was assumed to be 3.75% (average of 90 values in the literature [17]) and that of, the latter 1.1% as stated by the EEC [25].

We have already used packed column GC for the determination of butter fatty acids such as butyl esters [17]. Good results with packed columns were obtained when butyric acid was used as a measure of the amount of butter in bakery products, whereas less reliable results were obtained when enanthic acid was used for this purpose.

The application of capillary GC was studied with the following aims: (a) to improve the determination of enanthic acid; (b) to reduce the time of analysis; (c) to separate possible *trans* isomers in order to detect the presence of hydrogenated fats; and (d) determination of trienanthine.

EXPERIMENTAL

Standard solutions

Standard solutions of pure triglycerides in *n*-hexane and in olive oil were prepared with glycerol tributanoate at concentrations of 0.69, 13.2, 18.6 and 28.1 mg/ml for butyric acid determination, and glycerol triheptanoate (trienanthine) (K&K Rare and Fine Chemicals, Plainview, NY, U.S.A.) and glycerol trioctanoate (Fluka, Buchs, Switzerland) at a concentration of 1 mg/ml as internal standard (I.S.) for triglyceride determination.

Sodium butoxide

A 1 *M* solution of sodium butoxide in butanol was prepared following the method used by Zaugg [26] for the preparation of sodium ethoxide.

Fatty acid composition

A Carlo Erba Mega Series 5300 gas chromatograph, equipped with split-splitless and on-column injectors with a 30 m \times 0.32 mm I.D. fused-silica capillary column, coated with RTX-2330 cyanopropylsilicone phase (0.25 μ m) (Restek, U.S.A.), was used. The carrier gas (hydrogen) flow-rate was 3.0 ml/min, the splitting ratio (when applied) 1:80, the oven temperature was programmed from 50 to 200°C at 5°C/min and the flame ionization detector and injector (for split injection only) temperature were 210°C. The chromatogram were recorded and the relative peak areas calculated with Spectra-Physics Model 4290 integrators working at 1 V full-scale.

Triglyceride determination

A Carlo Erba Fractovap 4200 gas chromatograph, equipped with a split-splitless injector a flame ionization detector with a 10 m \times 0.32 mm I.D. fused-silica capillary column, coated with RTX-1 (0.15 μ m) (Restek), was used. The carrier gas

(helium) flow-rate was 2.2 ml/min, the splitting ratio 1:60, the oven temperature was programmed from 200 to 340°C at 8°C/min and the flame ionization detector and injector temperature were 340°C. The chromatograms were recorded and the relative peak areas calculated with Spectra-Physics Model 4290 integrators working at 1 V full-scale.

Sample preparation

For fatty acid determination, 0.5 g of butter or lipid extract from bakery products [17] were weighed in a screw-capped tube, then 0.75 ml of sodium butoxide solution and 5 ml of *n*-hexane were added. After vigorous vortex shaking for 30 s, the sample was centrifuged at 2200 *g* for 10 min and washed three times with 2 ml of distilled water. Finally, 1 μ l of the organic layer was injected into the gas chromatograph. The reaction yield (85%) was reported in a previous paper [17]. Triglyceride determination was performed by dissolving 30 mg of fat in 0.5 ml of toluene; 25 μ l of this solution were added to the same volume of I.S. (glycerol trioctanoate) solution. Finally, 1 μ l of organic layer was injected into the gas chromatograph.

RESULTS AND DISCUSSION

In previous work [15] we studied the chromatographic behaviour of butter fatty acids as methyl esters obtained according to Christopherson and Glass [22]. The outcome of split (silanized glass-wool packed or not) and on-column injections were compared on the basis of their relative standard deviations (R.S.D.s) as a function of the numbers of carbon atoms. Further, two different pre-set splitting ratios and several reaction times were investigated.

From this previous study, the on-column and split injection mode with the packed liner appeared to be a more accurate method for the determination of short-chain fatty acids than the split mode without a packing in the liner. In fact the R.S.D.s for on-column and split injection with a packed liner were <10% when higher splitting ratios were used [15]. The transmethylation reaction seemed not to be influenced by reaction times between 20 and 300 s.

Even though these results suggested that split injection was advantageous, problems connected with dirt in the liner packing necessitated frequent changes of the liner. The use of less volatile esters as described here gives similar results without a liner packing. Further, it is possible to limit the losses of the most volatile fatty acids, eluting as butyl esters, by means of capillary columns coated with relatively thermostable stationary phases without an appreciable reduction in resolution.

To evaluate the quantitative chromatographic behaviour of butyl esters of short-chain fatty acids, mainly butyric and enanthic acid, standard solutions of glycerol tributanoate as described under Experimental were analysed with the same column and different injection techniques (split and on-column). Each sample was analysed three times for both injection techniques. The analysis of variance (ANOVA) on the R.S.D. showed no significant differences, *i.e.*, the accuracies of the two methods of sample introduction were identical.

Regression analysis (split *versus* on-column injection) was applied to verify the agreement of these data. The results showed a highly significant correlation ($r = 1.00$) and also that the relative equation fully explains their relationship ($F = 5.817 \cdot 10^{-5}$).

TABLE I
RESULTS OF DETERMINATION OF BUTTER CONTENT IN REAL SAMPLES

The determinations were performed with butyric (C_4) and enanthic acid (C_7) in both split and on-column modes.

Sample No.	Declared butter (%)	Split injection ^a		On-column injection					
		Butter (%) (C_4)	R.S.D. (%)	Butter (%) (C_7)	R.S.D. (%)	Butter (%) (C_4)	R.S.D. (%)	Butter (%) (C_7)	R.S.D. (%)
1	7.5	8.59 ± 0.15	1.75	9.16 ± 0.00	0.00	7.25 ± 0.15	2.07	8.24 ± 0.47	5.70
2	6.0	5.59 ± 0.33	5.90	8.80 ± 0.13	1.48	6.04 ± 0.04	0.66	6.72 ± 0.22	3.27
3	13.0	16.17 ± 0.46	2.84	15.42 ± 0.38	2.46	13.12 ± 1.01	7.70	13.82 ± 0.75	5.43
4	2.00	2.35 ± 0.11	4.68	2.75 ± 0.16	5.82	1.80 ± 0.14	7.78	2.25 ± 0.14	6.22

^a Results are means ± S.D. ($n=3$).

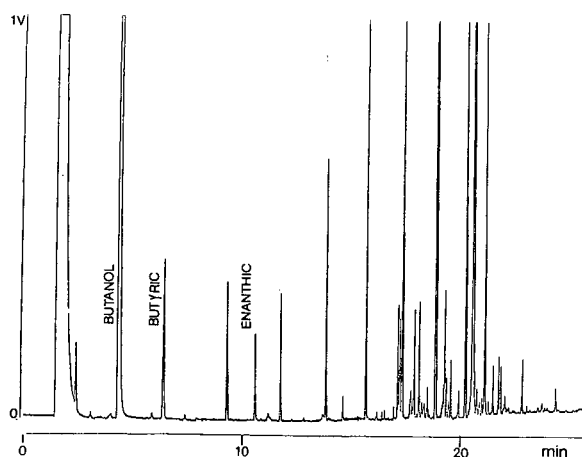


Fig. 1. Fatty acid composition as butyl esters of a lipid extract of a biscuit on carbon chain.

It is also evident that split injection tends to give slightly increased results as the value of the slope is 1.12.

When the method was applied to real samples this behaviour was confirmed. Butter contents reported on the label, together with our results, are given in Table I. Regression analysis (split *versus* on-column injection) of the results showed that when calculations were performed with enanthic acid, the two injection modes were equivalent, confirmed by the correlation coefficient ($r = 0.891$), whereas when butyric acid was used for the same purpose, on-column injection gave more accurate results (Table I). Otherwise the regression parameters were very high in both instances. It might be that the two determinations can be considered to be complementary, because the natural variation of butyric acid may be balanced by the technical addition of enanthic acid, and *vice versa*.

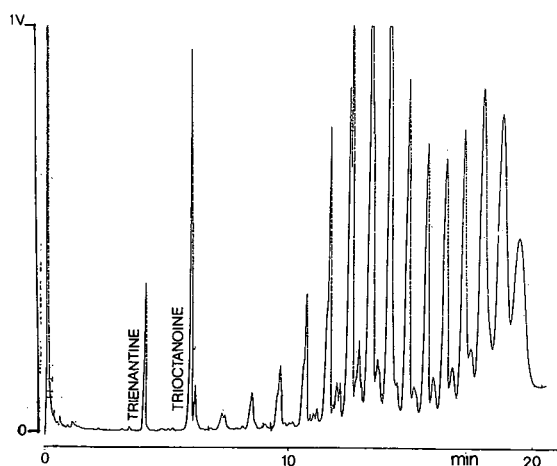


Fig. 2. Triglyceride analysis of a lipid extract of a biscuit.

TABLE II
RESULTS OF DETERMINATION OF BUTTER CONTENT IN REAL SAMPLES

The determinations were performed with trienanthine in the split mode.

Sample No.	Butter content (%)		
	Declared	Found ^a	R.S.D.
1	7.5	7.37 ± 0.14	1.90
2	6.0	7.40 ± 0.65	8.78
3	13.0	13.57 ± 0.32	2.36
4	2.00	2.53 ± 0.13	5.14

^a Mean ± S.D. (n=3).

An example of fatty acid composition as butyl esters is shown in Fig. 1. The use of a cyanopropyl-bonded stationary phase allows the evaluation of the possible presence of *trans* isomers of unsaturated fatty acids. No significant amounts were detected in the samples examined.

As trienanthine is added to concentrated butter as the pure triglyceride, its direct determination (Fig. 2) can be a rapid and useful means of establishing the amount of EEC concentrated butter in bakery products.

Results obtained in this way (Table II) show low R.S.D.s close to those obtained by fatty acid determinations. Further, the absolute data are in good agreement with the others.

The methods reported in this paper are similar in precision and accuracy, with no effect of differences in sample preparation or chromatographic conditions.

REFERENCES

- 1 A. T. James and A. J. P. Marin, *Biochem. J.*, 63 (1956) 144.
- 2 P. W. Parodi, *J. Dairy Sci.*, 60 (1977) 1550.
- 3 V. Antila and V. Kankare, *Milchwissenschaft*, 38 (1983) 478.
- 4 H. T. Badings and C. De Jong, in J. Rijks (Editor), *Proceedings of the 5th International Symposium on Capillary Chromatography, Riva del Garda, April 26-28, 1983*, Elsevier, Amsterdam, 1983, p. 543.
- 5 W. Butte, *Chromatographia*, 261 (1983) 142.
- 6 G. Lercker, C. Zullo and A. Tortorelli, *Riv. Ital. Sostanze Grasse*, 64 (1987) 321.
- 7 L. Matter, *Lebensm. Gerichtl. Chem.*, 42 (1988) 26.
- 8 P. Kalo, P. Elo and M. Antila, *Milchwissenschaft*, 43 (1988) 416.
- 9 P. Lund, *Milchwissenschaft*, 43 (1988) 159.
- 10 M. J. Prager, *J. Assoc. Off. Anal. Chem.*, 72 (1988) 418.
- 11 D. P. Casper, D. J. Schingoethe, R. P. Middaugh and R. J. Baer, *J. Dairy Sci.*, 71 (1988) 1267.
- 12 R. P. Middaugh, R. J. Baer, D. P. Casper, D. J. Schingoethe and S. W. Seas, *J. Dairy Sci.*, 71 (1988) 3179.
- 13 R. J. Bear, K. M. Tieszen, D. J. Schingoethe, D. P. Casper, W. A. Eisenbeitz, R. D. Sharer and R. M. Clark, *J. Dairy Sci.*, 72 (1989) 1424.
- 14 L. Matter, D. Schrenker, H. Husmann and G. Schomburg, *Chromatographia*, 27 (1989) 31.
- 15 L. S. Conte, R. Zironi and G. Lercker, in P. Sandra and G. Redant (Editors), *Proceedings of the 10th International Symposium on Capillary Chromatography, Riva del Garda, May 22-25, 1989*, Hüthig, Heidelberg, 1989, p. 889.
- 16 J. L. Iverson and A. J. Sheppard, *J. Assoc. Off. Anal. Chem.*, 60 (1977) 284.
- 17 L. S. Conte, A. Antonelli and A. Minguzzi, *Boll. Chim. Igien.*, 41 (1990) 347.

- 18 E. P. Jones and V. L. Davidson, *J. Am. Oil Chem. Soc.*, 42 (1965) 121.
- 19 P. O. Bethge and K. Lindström, *Analyst (London)*, 99 (1974) 137.
- 20 P. W. Jones and J. Kay, *J. Sci. Food Agric.*, 27 (1976) 1005.
- 21 A. T. G. Steverink, *Analyst (London)*, 109 (1984) 170.
- 22 S. W. Christopherson and R. L. Glass, *J. Dairy Sci.*, 52 (1969) 1289.
- 23 EEC Regulation No. 232/75, EEC Official Journal 31.1.75, N.L. 24/45, Luxembourg.
- 24 EEC Regulation No. 1932/81, EEC Official Journal 14.7.81, N.L. 181/6, Luxembourg.
- 25 EEC Regulation No. 3143/85, EEC Official Journal 12.11.85, N.L. 298/9, Luxembourg.
- 26 H. E. Zaugg, in F. Fieser and M. Fieser (Editors), *Reagents for Organic Synthesis*, J. Wiley, New York, London, Sydney, 1st ed., 1967.

CHROMSYMP. 2110

Gas chromatographic analysis of fatty acid salts

H. ROTZSCHE

Hüls Aktiengesellschaft, FE-Zentrale, Analytik Werk Troisdorf, D-5210 Troisdorf (Germany)

ABSTRACT

Generally, the analysis of fatty acid salts is based on their treatment with a strong acid to remove the cation, extraction of the liberated fatty acids and their methylation with an appropriate reagent for the gas chromatographic (GC) analysis of the fatty acid methyl esters. Surprisingly, it was found that fatty acid salts can be reacted directly with a methylating agent, *e.g.*, boron trifluoride (BF_3)–methanol complex or dimethylformamide–dimethylacetal, without prior acidification and extraction. With BF_3 –methanol, the fatty acid salt or salt mixture is reacted in a septum vial with excess of methanol and BF_3 –methanol complex at 70°C for 30 min. After cooling, the reaction mixture can be injected directly into the gas chromatograph without any further preparation. By calibration, the contents of bonded and free fatty acids and the distribution of the individual fatty acids in the salt or salt mixture can be determined. The GC separation of the fatty acid methyl esters is carried out on a surface-bonded, cross-linked stationary phase (FS column) as usual. The analysis of metal stearate stabilizers and lubricants takes only 70 min and both the total and the distribution of the fatty acids, from lauric to behenic acid, can be calculated from a single analysis. For instance, the relative standard deviation was 2.66% for the content of free and bonded fatty acids in calcium stearate and 1.21% for the content of stearic acid.

INTRODUCTION

Metal salts of fatty acids (C_8 – C_{18}) are widely used both as stabilizers and as lubricants for plastics. As commercially available batches vary in their chemical and physical characteristics and hence in their lubricant and stabilizer performance, it is necessary to characterize such technical-grade products chemically. Usually, the analysis of fatty acid salts is based on their reaction with a strong acid to liberate the fatty acids, which for their part are esterified, *e.g.*, with methanol in the presence of potassium hydroxide [1], perchloric acid [2], a cation-exchange resin [3] or boron trifluoride [4] and then analysed as their methyl esters by gas chromatography (GC). We have found that the liberation of the fatty acids from their salts and the subsequent extraction can be omitted as the fatty acid salts themselves can be reacted directly with strong methylating agents such as dimethylformamide dimethyl acetal or boron trifluoride–methanol complex to form the methyl esters. This reaction permits the salts to be converted directly to the methyl esters and these can be analysed to determine the content and the distribution of the individual fatty acid salts by injecting the reaction mixture into a gas chromatograph.

EXPERIMENTAL

Chemicals

Analytical-reagent grade chemicals were used unless indicated otherwise.

Methanol was obtained from Merck (Darmstadt, Germany). Boron trifluoride-methanol complex [14% (w/w) BF_3 dissolved in methanol] (Merck-Schuchardt) was of synthetic grade and the metal salts of fatty acids (zinc stearate, calcium stearate, magnesium stearate) were of technical grade from P. Greven Fettchemie (Bad Münstereifel, Germany). Fatty acids (myristic, palmitic and stearic acid) were of synthetic grade (>98%). N-Methyl-N-trimethylsilyltrifluoroacetamide (MSTFA) was obtained from Macherey, Nagel & Co. (Düren, Germany), toluene and light petroleum (b.p. 40–60°C) [Deutsches Arzneibuch No. 7 (DAB 7)] from Merck, diethyl ether (stabilized with ionone) (DAB 7) from Asid Bons (Böblingen, Germany) and sodium carbonate from Merck.

Materials

Crimp-seal vials N 20-5 (5 ml), septa (Teflon/silicone-rubber and aluminium crimp-on caps were purchased from Macherey, Nagel & Co. Syringes (5 μl) with removable needles (85 RN) were obtained from Hamilton (Bonaduz, Switzerland).

Chromatography

A Model 8500 gas chromatograph (DANI Analysentechnik, Mainz-Kastel, Germany) was equipped with a flame ionization detector, a temperature-programmed vaporizer and a Shimadzu Model C-R3A computing integrator. A 25 m \times 0.32 mm I.D. fused-silica column coated with 0.2- μm DB-1 crosslinked and chemically bonded poly(dimethylsiloxane) (J & W Scientific, Folsom, CA, U.S.A.) was used with helium 4.6 [$\geq 99.996\%$ (v/v) purity] (Linde, Höllriegelskreuth, Germany) as carrier gas at 0.5 bar pressure, corresponding to a column flow-rate of *ca.* 0.7 ml/min at 50°C. The temperature of the flame ionization detector was 280°C and the splitting ratio was 1:20. The injector (temperature-programmed vaporizer) was programmed from 60 to 280°C within a few seconds and the column temperature was raised from 80 to 300°C at a rate of 10°C/min.

A second column [30 m \times 0.25 mm I.D., fused-silica, coated with 0.50- μm Stabilwax DA chemically bonded poly(ethylene oxide)] from Restek (Bellefonte, PA, U.S.A.) was used with helium 4.6 as carrier gas at 0.7 bar pressure. The temperature of the flame ionization detector was 270°C and the splitting ratio was 1:15. The temperature-programmed vaporizer was programmed from 80 to 270°C within a few seconds and the column temperature was raised from 90 to 260°C at 10°C/min.

The third column was 25 m \times 0.32 mm I.D. F.S., coated with 0.30- μm FFAP-CBDA (chemically bonded, for the determination of acids), from Chrompack (Middelburg, The Netherlands). The carrier gas was helium 4.6 at a pressure of 0.5 bar, the temperature of the flame ionization detector was 280°C and the splitting ratio was 1:20. The temperature-programmed vaporizer was programmed from 80 to 280°C and the column temperature was increased from 80 to 270°C at 8°C/min.

Procedures

A sample of *ca.* 100 mg of the fatty acid salt mixture was introduced into the

vial and weighed. After the addition of 2 ml of methanol and 1 ml of the boron trifluoride-methanol complex, the vial was sealed and heated for 30 min at 70°C. After cooling, the vial was unsealed, 200 mg of sodium carbonate were cautiously added (whilst wearing goggles) and the vial was resealed. Samples (1 μ l) were withdrawn through the septum and injected into the GC apparatus. The separation was effected on both column 1 (Fig. 1) and column 2 (Fig. 2).

For quantification, the external standard method was applied. A synthetic mixture of myristic, palmitic and stearic acid, its composition corresponding approximately to the distribution of the fatty acids in the investigated metal salts, was reacted with boron trifluoride-methanol in the same way as above, and the counts per milligram of the respective fatty acid were used for the calculation of the content of the fatty acid in the metal salt.

Instead of the external standard method, an internal standard could also be used. However, when investigating various fatty acid salts, there is the risk of a general standard compound being coeluted with an impurity contained in a technical product.

It is well known that free fatty acids react with boron trifluoride-methanol. Therefore, in the course of the new direct reaction with the metal salts, not only the bonded but also the residual free fatty acids present as contaminants in the salts can react, and the total (bonded plus free) fatty acids will be found. However, the (low) content of free fatty acids can easily be determined separately as follows and subtracted from the total.

A 100 mg-sample of the metal salt of the fatty acid was extracted with toluene by ultrasonic treatment (30 min) and centrifuged. A 1- μ l volume of the solution was injected into a gas chromatograph equipped with the FFAP-CBDA column, which was specially developed for the analysis of free fatty acids.

For comparison purposes, a conventional method for the investigation of metal salts of fatty acids was applied to the analysis of all three technical-grade stearates (calcium, magnesium and zinc stearate). A 10-20-g sample of the stearate was extracted with 250 ml of light petroleum, the solution containing free fatty acids and further soluble organic compounds was evaporated to dryness and the residual solid matter was vacuum dried and weighed. This solid residue was either methylated with boron trifluoride-methanol as already described or silylated as follows. A 0.1-mg sample was dissolved in 1 ml of toluene, silylated with MSTFA for 30 min at 70°C in a sealed vial to form the trimethylsilyl derivatives of the fatty acids and analysed under the same conditions as described under *Chromatography* to give the free fatty acid content and distribution.

The residue from the extraction, *i.e.*, the main constituent being insoluble in light petroleum, contained the fatty acid salts, free of fatty acids and other soluble organic compounds. A sample of 1-1.5 g was refluxed for 2 h with 5 *M* hydrochloric acid and after cooling, it was filtered, washed free from chloride, air dried and extracted with diethyl ether in a Soxhlet apparatus for 6 h. Finally, the solution was evaporated to dryness and the residue was weighed to yield the weight of bonded fatty acids. In order to obtain the proportion of each individual fatty acid (*i.e.*, the bonded fatty acid distribution), a sample of 0.1 g was dissolved in 1 ml of toluene and derivatized with MSTFA or methylated with boron trifluoride-methanol, then analysed as described above.

RESULTS AND DISCUSSION

From each of the technical-grade stearates (calcium, magnesium and zinc stearate) three samples were reacted with boron trifluoride-methanol and, after being allowed to cool, each reaction mixture was analysed seven times. Figs. 1 and 2 show typical chromatograms.

Tables I-III give the mean values of the contents of the individual C_{14} - C_{20} saturated fatty acids (bonded + free) found with the proposed method. The standard deviation and the relative standard deviation of the determinations are given, and also the contents of the free fatty acids determined by injection of the toluene extracts of the salts without derivatization.

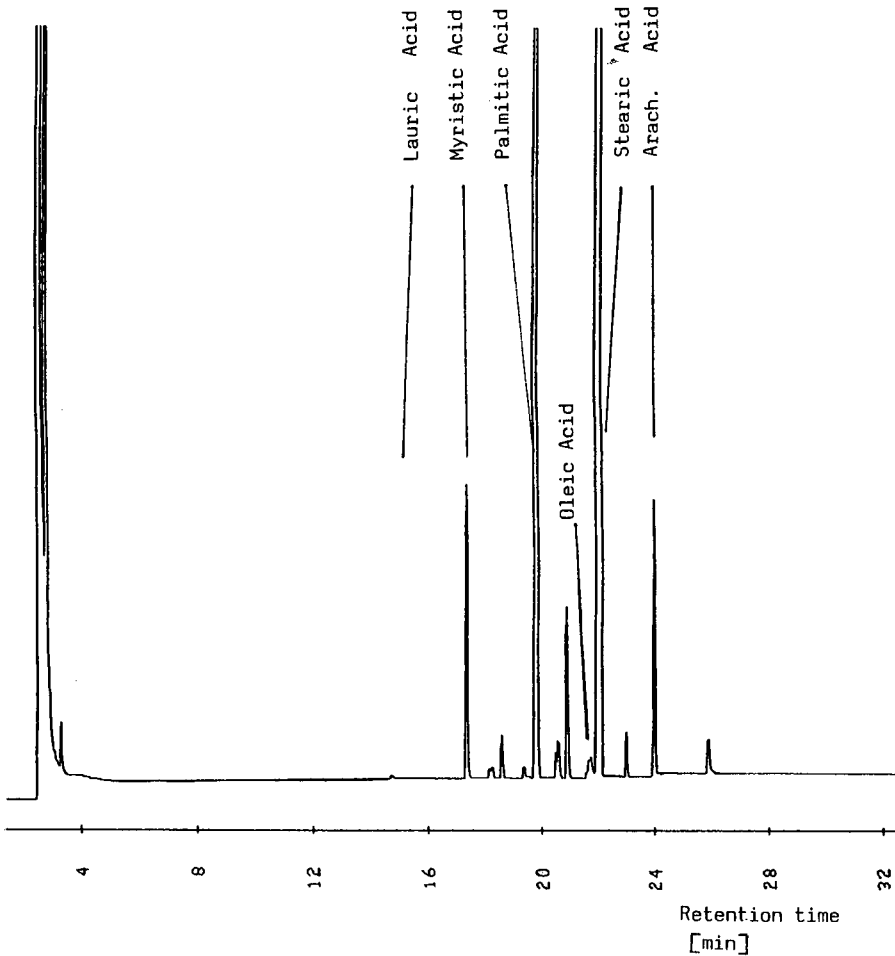


Fig. 1. Gas chromatogram of the methyl esters of fatty acids formed by the reaction of magnesium stearate with $\text{BF}_3\text{-CH}_3\text{OH}$ (non-polar liquid phase): Conditions: fused-silica column (25 m \times 0.32 mm I.D.) coated with DB-1, film thickness 0.20 μm . Temperature programmed from 80 to 300°C at 10°C/min. Arach. = Arachidic.

TABLE I

DETERMINATION OF THE DISTRIBUTION OF FATTY ACIDS IN TECHNICAL-GRADE MAGNESIUM STEARATE

Parameter	Myristic acid	Pentadecanoic acid	Palmitic acid	Heptadecanoic acid	Stearic acid	Arachidic acid
\bar{x} (%) ^a	1.69	0.74	30.97	1.82	63.73	1.38
s (%) ^b	0.18	0.14	0.72	0.21	0.65	0.24
$(s/\bar{x}) \cdot 100$ (%) ^c	10.65	18.92	2.32	11.54	1.02	17.39
Free fatty acid content (direct injection of the toluene extract) (%)	0.05	—	0.24	—	0.26	—
Content of bonded fatty acids (found by conventional method) (%)	1.8	0.5	29.6	1.4	65.4	1.1
Content of free fatty acids (found by conventional method) (%)	0.03	—	0.14	—	0.22	—

^a Mean value of 21 determinations^b Standard deviation^c Relative standard deviation

For comparison, the values obtained with the described conventional determination of bonded and free fatty acids are presented. Acids at levels <0.1% are not reported.

The results in Tables I–III show that the direct derivatization of fatty acid salts with boron trifluoride–methanol proceeds completely with all C₁₄–C₂₀ fatty acids

TABLE II

DETERMINATION OF THE DISTRIBUTION OF FATTY ACIDS IN TECHNICAL-GRADE CALCIUM STEARATE

Parameter defined as in Table I.

Parameter	Myristic acid	Pentadecanoic acid	Palmitic acid	Heptadecanoic acid	Stearic acid	Arachidic acid
\bar{x} (%)	1.84	0.59	31.30	1.86	63.58	1.19
s (%)	0.07	0.06	0.61	0.17	0.77	0.06
$(s/\bar{x}) \cdot 100$ (%)	3.80	10.17	1.95	9.14	1.21	5.04
Free fatty acid content (direct injection of the toluene extract) (%)	0.09	—	0.36	—	0.59	—
Content of bonded fatty acids (found by conventional method) (%)	2.2	0.5	31.0	1.5	63.5	1.0
Content of free fatty acids (found by conventional method) (%)	0.03	0.07	0.08	—	0.12	—

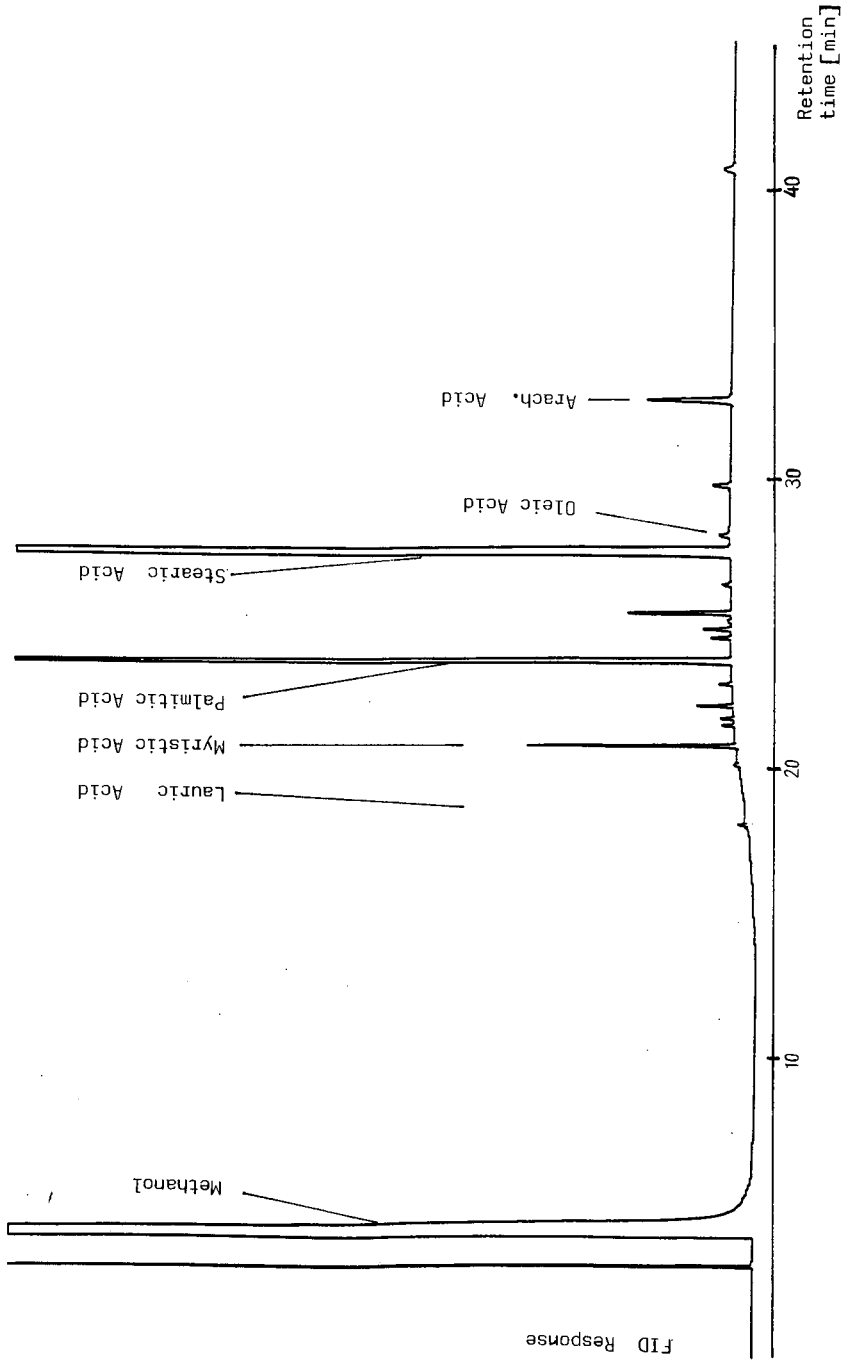


Fig. 2. Gas chromatogram of the methyl esters of fatty acids formed by the reaction of magnesium stearate with $\text{BF}_3\text{-CH}_3\text{OH}$ (polar liquid phase). Conditions: fused-silica column (30 m \times 0.25 mm I.D.) coated with Stabilwax DA, film thickness 0.50 μm . Temperature programmed from 90 to 260°C at 10°C/min. Arach. = Arachidic.

TABLE III
 DETERMINATION OF THE DISTRIBUTION OF FATTY ACIDS IN TECHNICAL-GRADE
 ZINC STEARATE^a Parameters defined as in Table I.

Parameter	Myristic acid	Pentadecanoic acid	Palmitic acid	Heptadecanoic acid	Stearic acid	Arachidic acid
\bar{x} (%)	2.03	0.55	30.97	1.82	62.96	1.77
s (%)	0.05	0.05	0.60	0.06	0.62	0.19
$(s/\bar{x}) \cdot 100$ (%)	2.46	9.09	1.94	3.30	0.98	10.73
Free fatty acid content (direct injection of the toluene extract) (%)	0.12	—	0.33	—	0.68	—
Content of bonded fatty acids (found by conventional method) (%)	2.1	0.4	29.6	1.2	64.8	1.4
Content of free fatty acids (found by conventional method) (%)	0.01	—	0.11	—	0.12	—

salts from magnesium to zinc, and that the standard deviation is very good, considering that technical-grade salts were reacted. With two exceptions, the coincidence with conventionally obtained values was fairly good. One exception, the difference between the content of stearic acid in magnesium stearate and zinc stearate found with both methods, may be explained by the errors of both methods, and the other discrepancy, the distinctly lower values of free acids (*e.g.*, 0.01, 0.11 and 0.12% for zinc stearate) found with the conventional method compared with the direct underivatized determination (0.12, 0.33, and 0.68%) could be a result of the tedious and multi-stage sample preparation in the conventional method.

As the usual gravimetric determination of the total content of bonded fatty acids (extraction of a 1–2-g sample to remove all organic compounds except bonded fatty acids, boiling of the extraction residue with hydrochloric acid, washing of the liberated fatty acids, extraction, evaporation to dryness and weighing) is very tedious and error prone, we tried to quantify the boron trifluoride–methanol reaction with respect to the determination of the total content of fatty acids by applying an external standard method (a sample of weighed pure fatty acids was reacted in the same way as the fatty acid salt and the respective peak areas were related to the corresponding peak area obtained with the true, weighed sample). In Table IV, the values obtained with the boron trifluoride–methanol reaction are compared with those given by the gravimetric method. The results are considered to be satisfactory, especially with regard to the fact that in the derivatization method fatty acid at levels <0.1% were not taken into consideration and that with the gravimetric method the values for the free fatty acids must be too high because the extraction includes not only fatty acids but also fatty alcohols and hydrocarbons. Nevertheless, more thorough investigations are planned to confirm the applicability of the direct derivatization of metal salts of fatty acids.

TABLE IV
DETERMINATION OF THE TOTAL CONTENT OF FATTY ACIDS IN METAL STEARATES

Parameter	Magnesium stearate	Calcium stearate	Zinc stearate
\bar{x}^a	89.93	90.17	89.46
s (%) ^b	0.37	2.40	1.62
$(s/\bar{x}) \cdot 100$ (%) ^c	0.41	2.66	1.81
Free fatty acids (GC) (%)	0.55	1.04	1.13
Bonded fatty acids (gravimetric) (%)	91.41	91.40	90.03
Free fatty acids (gravimetric) (%)	0.74	1.15	1.58

^a Mean value of two reactions with $\text{BF}_3\text{-CH}_3\text{OH}$ and four injections each (free + bonded fatty acids).

^{b,c} See Table I.

Regarding the residue within the injection port, caused by the metal content and the boron trifluoride reaction products of the injected sample, as a guide the number of injections into the gas chromatograph should be limited to twenty, then the injector should be purified (replacement of the glasswool or glass/quartz liner).

REFERENCES

- 1 S. Tau, T. Tatsuno and T. Okada, *J. Chromatogr.*, **447** (1988) 198.
- 2 J. V. Wisniewski, *Facts Methods*, **8** (1967) 9.
- 3 B. Staucher, L. Cecon and C. Calzolari, *Riv. Ital. Sostanze Grasse*, **59** (1982) 619.
- 4 T. A. Miller and P. York, *Int. J. Pharm.*, **23** (1985) 55.

Rapid derivatization and gas chromatographic determination of amino acids

PETR HUŠEK

Institute of Endocrinology, Národní třída 8, 116 94 Prague 1 (Czechoslovakia)

ABSTRACT

Reaction conditions for the derivatization of amino acids with chloroformates were established. In an aqueous reaction medium the reagents are able to esterify not only the side-chain reactive groups but even the carboxylic group. Suitable derivatives for the determination of amino acids by capillary gas chromatography were found to be the N(O,S)-ethoxycarbonyl ethyl esters, which are formed in a few seconds. Six stationary phases were tested with a mixture of derivatized protein amino acids. A moderately polar stationary phase of the OV-1701 type permits the determination of amino acids with good resolution in less than 5 min.

INTRODUCTION

Determinations of amino acids can nowadays be achieved at levels down to 10^{-18} mol using fluorimetric [1–4] or voltametric detection [5–7], combined with high-performance liquid chromatography (HPLC) or capillary electrophoresis [3,4]. However, although one-purpose amino acid analysers are no longer essential, routine automated measurements of amino acids with modern, flexible HPLC instruments are hardly possible with relatively inexpensive systems [7]. Therefore, gas chromatography (GC), with its capillary flexibility, resolving power and speed of analysis and with the instrumental costs being one third of those of HPLC, is worth re-examination. The main problem is the need for derivatization, commonly involving laborious and multi-step procedures taking 1 h or more [8,9], thereby losing the advantage of the speed of GC itself. However, some derivatization procedures require only 15 min [10,11]. Considering both the time of sample preparation and the overall duration of analysis, two procedures can be considered as the most rapid, one based on HPLC (condensation with phenyl isothiocyanate [12]) and the other on GC (condensation with dichlorotetrafluoroacetone [10]). Both permit the determination of a wide range of amino acids within 30 min. An alternative rapid procedure based on treatment of amino acids with fluorenylmethyl chloroformate and HPLC analysis was published recently [13,14].

In this paper a procedure is described that is uniquely rapid. The derivatives can be prepared in a few seconds and the subsequent capillary GC analysis can be performed in a few minutes. The total time of sample preparation and the analysis can

be as short as 5 min. Other advantages are simple sample handling, the ability to effect derivatization in aqueous solutions and the use of inexpensive reagents.

The derivatization is based on the treatment of amino acids with chloroformates and is an extension of a recent study of chloroformate-induced esterification of carboxylic groups [15].

EXPERIMENTAL

Chemicals

Methyl and ethyl chloroformate (MCF, ECF), pyridine, chloroform, methanol and ethanol were obtained from Fluka (Buchs, Switzerland). An equimolar solution of seventeen protein amino acids in 0.1 *M* hydrochloric acid (AA-S-18) was purchased from Sigma (St. Louis, MO, U.S.A.) and used together with a complementary solution of the following amino acids in 0.1 *M* hydrochloric acid: asparagine, glutamine, tryptophan, cysteine, ornithine, hydroxyproline and *p*-chlorophenylalanine (internal standard). The concentration of cystine in the AA-S-18 solution was adjusted to equimolarity.

Procedures

Amino acids in residues (not more than 100 μg in total) are treated with 100 μl of water-ethanol-pyridine (60:32:8) and 5 μl of ECF are added and mixed by briefly shaking the tube (3–5 s). Gas evolution (carbon dioxide) usually occurs. Then, 100 μl of chloroform (containing 1% ECF) are added and the derivatives are extracted into the organic phase by striking the tube against a pad for about 5 s. The chloroform layer clears during this process and the aqueous phase turns opaque. An aliquot of the organic phase is injected into the capillary column.

Alternatively, 15 μl of the amino acid solution in 0.1 *M* hydrochloric acid are diluted to 60 μl with water and 40 μl of ethanol-pyridine (4:1) are added. The procedure is then continued as above.

If treatment with MCF is preferred, the solvent used is water (or 20–25 *mM* hydrochloric acid)-methanol-acetonitrile-pyridine (60:16:16:8). Addition of the reagent (5 μl) is followed by addition of 100 μl of chloroform containing 1% of MCF.

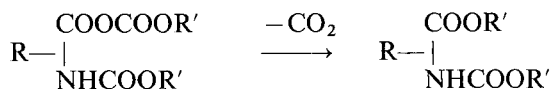
Instruments

A Model 5890 gas chromatograph (Hewlett-Packard) with a flame ionization detector and a Model 3392A integrator was employed throughout with temperature ranges as given in the figure legends. The injector and detector temperatures were 200–250 and 250–300°C, respectively (the lower setting was used with columns coated with the most polar phases). Hydrogen was used as the carrier gas. Six different columns with increasing stationary phase polarity, *i.e.*, from methyl- through phenyl- to cyanopropylsilicones, were tested with the derivatized amino acids; the lengths and inside diameters were as follows: (A) 25 m \times 0.32 mm CP-Sil 5 CB [100% dimethylpolysiloxane (DMS), 0.11 μm film thickness] from Chrompack (Middelburg, The Netherlands); (B) 25 m \times 0.20 mm HP-5 (5% diphenyl-95% DMS, 0.33 μm) from Hewlett-Packard (Palo Alto, CA, U.S.A.); (C) 15 m \times 0.25 mm DB-17 (50% diphenyl-DMS, 0.25 μm) from J & W Scientific (Folsom, CA, U.S.A.); (D) 10 m \times 0.25 mm CP-Sil 19 CB (7% phenyl-7% cyanopropyl-DMS, 0.2 μm) from

Chrompack; (E) 15 m × 0.25 mm DB-225 (25% phenyl-25% cyanopropyl-DMS, 0.25 μm); and (F) 30 m × 0.25 mm DB-23 (50% cyanopropyl-DMS, 0.25 μm), both from J & W Scientific. The hydrogen head pressure corresponding to each column is given in the legends to the figures.

RESULTS AND DISCUSSION

Chloroformates have been used previously, but the treated groups involved only alcoholic and amino groups [11,13,14,16,17], with the exception of the formation of mixed anhydrides as chemical intermediates [18–20]. A process of instantaneous decarboxylation of the intermediate alkoxy-carbonyl esters (mixed anhydrides) was applied only with keto acids [21] and even on the macroscale of organic chemistry instantaneous decarboxylation of prepared mixed anhydrides was not observed [22,23]. A surprising finding was that pyridine as a catalyst (and only pyridine among many organic bases tested) is responsible for the instantaneous decarboxylation. The resulting N(O,S)-alkoxy-carbonyl alkyl esters are formed by the decarboxylation of the intermediate alkoxy-carbonyl esters:



The process of decarboxylation is induced by pyridine provided that the base is present in a molar excess with respect to the reagent, and this is fulfilled under the given conditions. It should be noted that even the reagent starts to decompose when added to the medium. The evolution of carbon dioxide, being accompanied by foaming of the solvent, can also be observed with a blank sample and has nothing to do with decarboxylation of the minute amount of the solute, when present. The decomposition products are thus carbon dioxide, alcohol and hydrogen chloride, which blocks the catalytic activity of pyridine; this is the reason why the pyridine should be present in a molar excess.

The yield of derivatives did not prove to be related to the decarboxylation of the reagent. The phenomenon of reagent decomposition followed by gas evolution does not have to proceed at all, as it does not occur in the instance of an increased ethanol concentration in the medium up to 40% (Fig. 1). Under such condition even higher yields with the hydroxyl-containing aliphatic amino acids and cysteine were observed; the basic amino acids, however, respond in the opposite way. The opposite behaviour takes place when the ethanol concentration is lowered to 20%. From Fig. 1, it is therefore apparent that an ethanol concentration in the middle of the tested range affords optimum results for the various amino acids.

The yield of amino acids from Fig. 1 and also that of H and Q can be partially influenced even by addition of water (100 μl) as a counter phase to the chloroform extraction. The yield of basic amino acids improves (by about 10–15%, the highest with H) and that of the hydroxy amino acids decreases by about 5–10%. However, the response of Q declined by over 30% on addition of water and extraction without an extra water is therefore to be preferred.

Not all the reactive groups in amino acid side-chains are altered by the action of

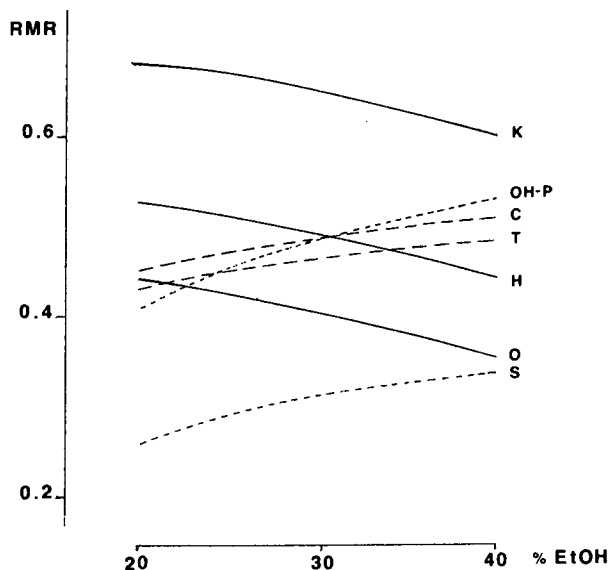


Fig. 1. Influence of changes in water-ethanol (EtOH) volume ratio in the reaction medium on the molar responses of amino acids.

the reagent. The imino group of arginine remains untouched, which is the reason for absorption of this amino acid derivative in the columns tested. The free imino group of indole in the molecule of W and free β -hydroxy groups in T, S and that in OH-P do not prevent the compounds from being eluted from the columns. The sulphhydryl group of C, the phenolic group of Y and the imino group of the imidazole ring of H are derivatized. A marked difference in the retention times of the amides N and Q indicates that a dissimilar derivative formation takes place; a GC-mass spectrometric (MS) study is in progress [24]. However, the responses of N, D and C were markedly improved when 1% ECF was added to the chloroform.

Double-derivative formation with E and Q was observed by GC and confirmed

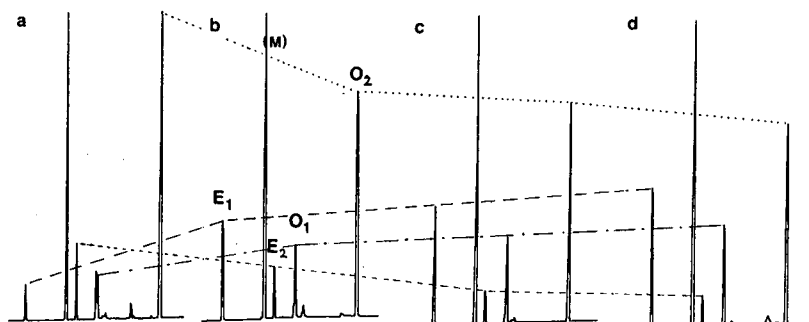


Fig. 2. Influence of acidification or alkalization of the aqueous reaction medium on the double-derivative formation with E and O. M was added as internal standard. Water as component of the reaction medium (b) was replaced with (a) 100 mM ammonia solution, and (c) 20 mM and (d) 100 mM hydrochloric acid.

TABLE I
REPRODUCIBILITY OF THE PROCEDURE

Mean molar responses (relative to internal standard) (RMR) and relative standard deviations (R.S.D.) were obtained by preparing ten individual samples analysed on the OV-1701 capillary column. Amino acids are sequenced according to elution order on this column.

Amino acid	Abbreviation	RMR	R.S.D. (%)
Alanine	A	0.441	3.7
Glycine	G	0.388	2.5
Valine	V	0.671	3.3
Leucine	L	0.718	2.5
Isoleucine	I	0.666	2.9
Threonine	T	0.465	3.6
Serine	S	0.312	3.1
Glutamic acid	E	0.298	8.3
Proline	P	0.713	2.7
Asparagine	N	0.428	2.2
Aspartic acid	D	0.361	4.2
Methionine	M	0.663	2.3
Hydroxyproline	OH-P	0.483	4.0
Phenylalanine	F	1.066	2.3
Cysteine	C	0.493	4.6
Glutamine	Q	0.305	5.3
Ornithine	O	0.407	3.4
Lysine	K	0.658	2.7
Histidine	H	0.486	5.8
Tyrosine	Y	1.061	2.6
Tryptophan	W	0.992	3.4
Cystine	C-C	0.554	3.5

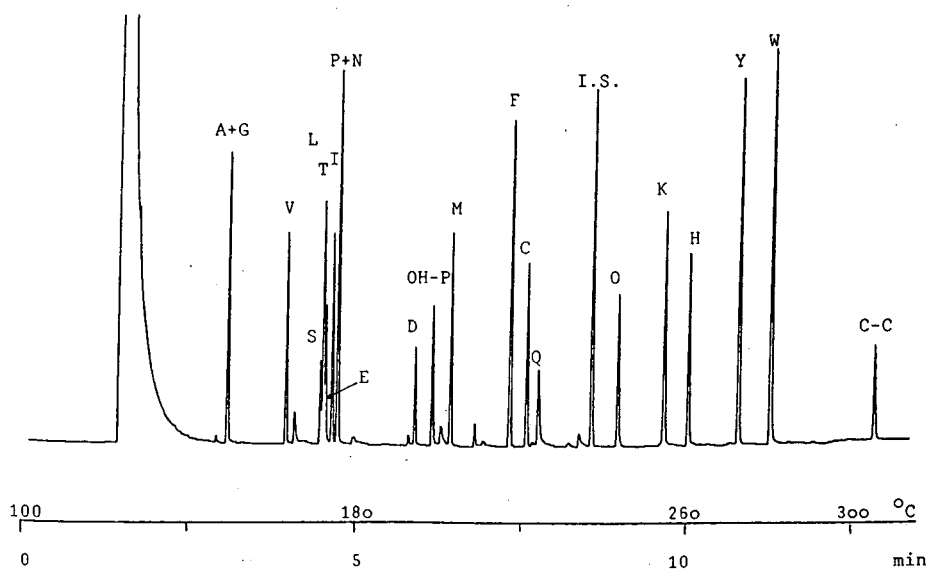


Fig. 3. EOC amino acid ethyl esters separated on a phase of OV-1 type (column A). Hydrogen head pressure, 100 kPa; temperature, increased at 16°C/min.

by MS. The compounds with lower retention are products of an internal cyclization resulting in the formation of pyroglutamic acid (assigned to E) and alkylated 3-aminopiperidinone in the case of O [eluted following F in Figs. 5 and 6 (not assigned)]. The main peak, assigned to O, has the expected structure of the N^α, N^ω -di-EOC ethyl ester. The process of internal cyclization of both can be influenced by acidification or alkalization of the reaction medium, as shown in Fig. 2. By means acidification with dilute hydrochloric acid the cyclization is promoted, especially with E, so that the ratio of pyroglutamic to glutamic acid diethyl ester changes from 2:1 in water to 3:1 in 20–25 mM hydrochloric acid, which is desirable. The decline in O due to the cyclization to the piperidinone is low. In contrast, the use of ammonia is a means of suppressing the cyclization of O; with E, however, both peaks are low and the responses of other amino acids are slightly altered. The use of dilute hydrochloric acid is superior as with E the peak of interest is augmented and the molar responses of other amino acids do not deteriorate. When amino acids were treated with MCF the cyclization was promoted more by a partial replacement of methanol with

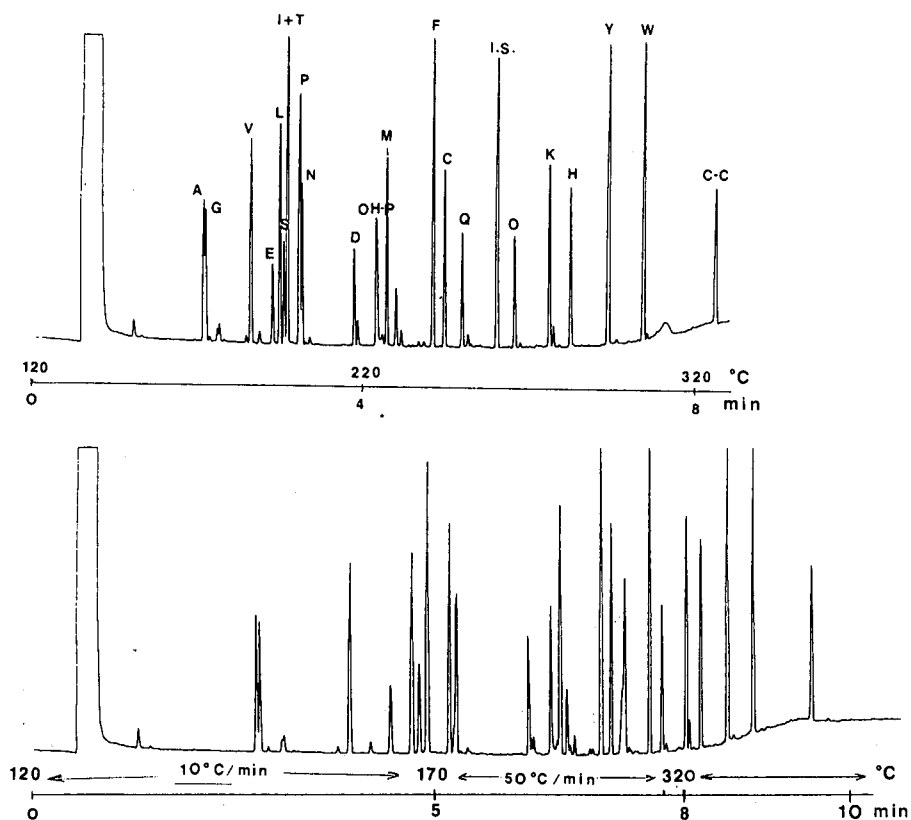


Fig. 4. EOC amino acid ethyl esters separated on a phase of SE-54 type (column B) with linear (25°C/min, top) and multi-linear (10 and 50°C/min, bottom) temperature programming. Hydrogen head pressure, 150 kPa.

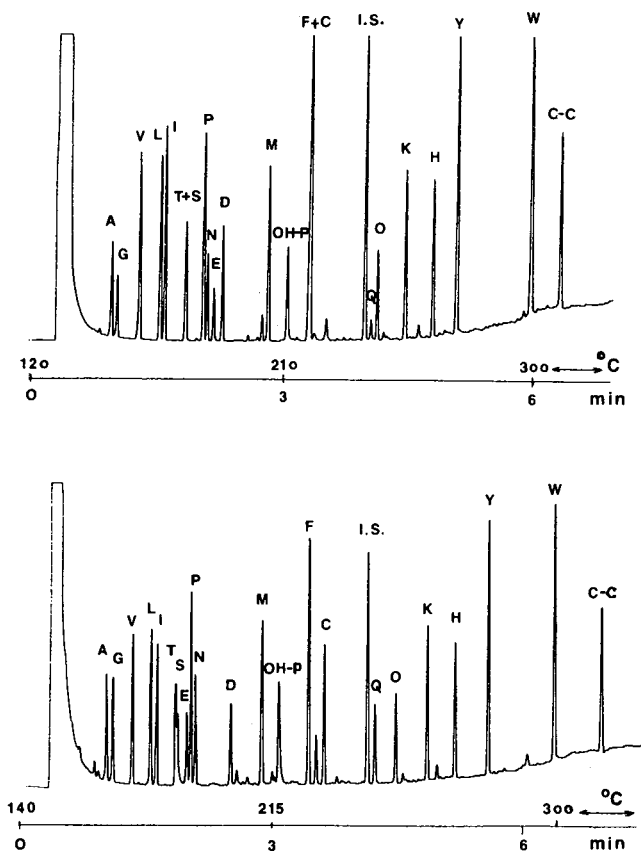


Fig. 5. Amino acids as MOC methyl (top) and EOC ethyl esters (bottom) analysed on a phase of OV-17 type (column C) under conditions optimum for their separation. Temperature, increased at 30 and 25°C/min; hydrogen head pressure, 70 and 60 kPa, respectively.

acetonitrile, as indicated under Experimental. In this way even the yields of T and S were slightly improved.

The reproducibility of derivative formation with ECF under the optimum reaction conditions with dilute (20 mM) hydrochloric acid in the medium is given in Table I. The relative standard deviations were lower than 5% on average; higher values were observed with three amino acids, E, Q and H. The values were obtained with the Chrompack CP-Sil 19 CB capillary column.

The subsequent examination of various stationary phases was aimed at obtaining optimum resolution in the fastest possible analysis. First choice the thermally most stable least polar phases OV-1 and SE-54 were tested, followed by the moderately polar phases OV-17 and OV-1701 and finally the most polar, least stable phases with a high abundance of cyanopropyl groups. The results of this study are given in Figs. 3-7.

The chromatograms show clearly that the polarity of the stationary phase markedly influences the resolution of some pairs or groups of amino acids, *e.g.*, the resolution of the pairs A-G, L-I and T-S. With increasing phase polarity the

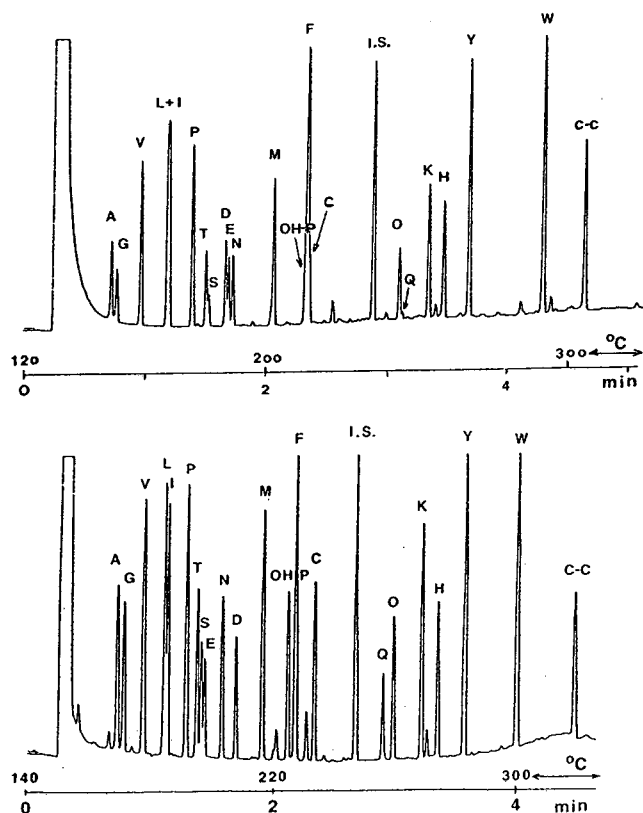


Fig. 6. Amino acids as MOC methyl (top) and EOC ethyl esters (bottom) analysed on a phase of OV-1701 type (column D) under conditions optimum for their separation. Temperature, increased at 40°C/min; hydrogen head pressure, 50 kPa.

resolution A–G continuously improves, from no resolution at all with OV-1, through a good resolution with the moderately polar phases to such a marked shift of G to a higher retention that it moves even behind V (Fig. 7). The opposite occurred with the pair L–I, the best resolution being achieved with the methylsilicone phase (Fig. 3), poorer with the moderately polar phases and failing completely with the most polar phases. This is of course a substantial shortcoming of the use of the polar phases in the analysis of amino acids as their EOC ethyl esters. The retention times of T–S (S–T sequence with the least polar phases) undergo a reversal of elution order with an increase in phase polarity, and a marked shift of both these amino acids with free hydroxy groups to nearly doubled retention times, compared with the L–I pair, can be observed. With the moderately polar OV-17, which otherwise is one of the most powerful, the reversal of the elution order of S–T to T–S only just occurs, so that the resolution of these amino acids fails or is very poor (Fig. 5). Incorporation of a small amount of cyanopropyl groups into the structure of this phase would not be helpful, as even such a low proportion as 7% (Fig. 6) alters the elution order of T–S vs. E and P completely.

It is a fortunate combination of phenyl, cyanopropyl and methyl groups in the

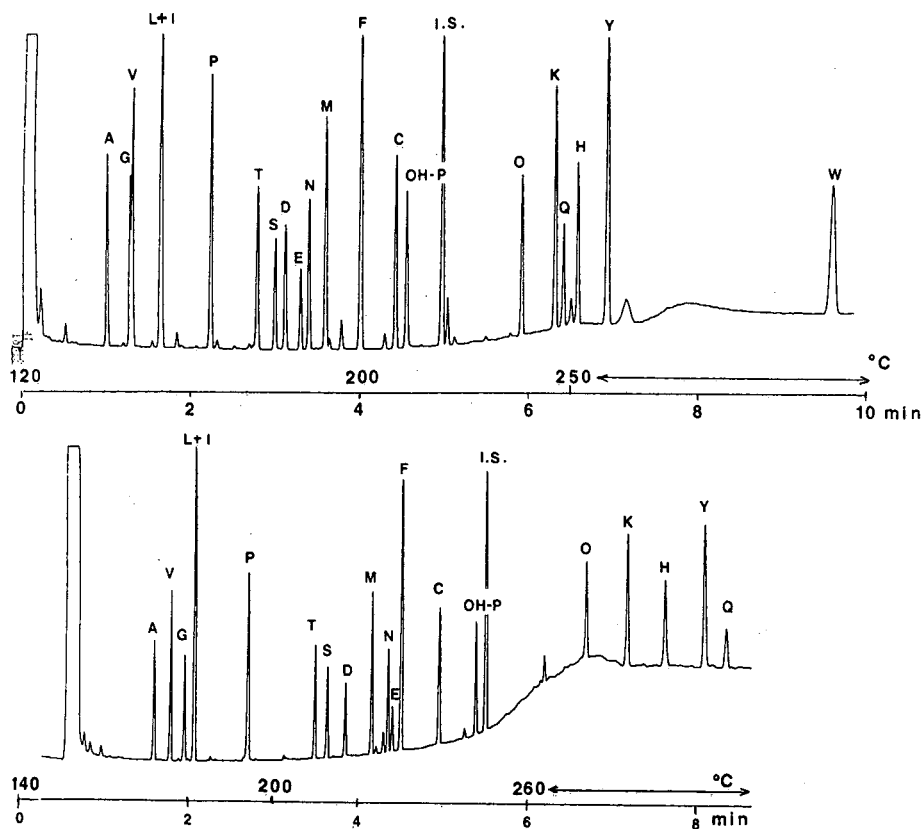


Fig. 7. EOC amino acid ethyl esters analysed on cyanopropyl phases of OV-225 (top) and OV-275 (bottom) type, corresponding to columns E and F. Temperature, increased at $20^{\circ}\text{C}/\text{min}$ (both columns); hydrogen head pressure, 150 (top) and 175 kPa (bottom).

composition of the OV-1701 phase that results in good resolution, even when the separation of the L-I pair starts to deteriorate owing to the presence of cyanopropyl groups in the phase structure, as already mentioned.

The chosen temperature gradient of $40^{\circ}\text{C}/\text{min}$, permitting a high speed of analysis, is both necessary and optimum, because any change (or starting at a lower temperature) would be at the cost of separating the S-E pair, although the resolution of the L-I pair would be improved.

Other amino acids, *e.g.*, OH-P, N and Q similarly undergo a considerable increase in retention times. OH-P moves from a position between D and M on the least polar phase to between C and I.S., as shown in Fig. 7. In the same direction, N changes from elution with or behind P to elution behind M, and Q changes position from behind C to behind Y (DB-23 column). The influence of phase polarity on the retention behaviour of some amino acids is, therefore, remarkable.

With MOC amino acid methyl esters, which are prepared equally as smoothly as the ethyl esters, no satisfactory resolution on the columns tested could be achieved. The results with OV-1701 (Fig. 6) were clearly inferior to those obtained with the EOC

ethyl esters. The use of OV-17 seems to be promising provided that a column with a higher resolving power is used. However, the response of S is low, because of the lower extraction into the organic layer, and the response of Q is nearly zero, pointing further to the necessity to elucidate the structure of the compound by MS. These limitations are inherent in the procedure and must be taken in account. The inability to elute arginine with the underivatized imino group of its guanidine moiety persists and it is the major obstacle to the general adoption of this approach of amino acid determination via chloroformate treatment.

The stability of the EOC amino acid ethyl esters is good; Q starts to decline first. If storage is intended, it is recommended to separate chloroform from the counter phase and to keep the layer in refrigerator. No changes were observed after storage for 1 week.

Split injection was used for amino acid analyses throughout this study. If a splitless technique is preferred, it would be necessary to take up the chloroform layer, evaporate it to nearly dryness (remaining drop of pyridine) at room temperature and dissolve the residue in a polar solvent with a higher boiling point, perhaps dimethylformamide. This suggestion has not been investigated.

In conclusion, the method presented is unique in the rapidity of sample preparation and speed of GC analysis. Its drawback is the inability to determine arginine, the only protein amino acid which would require another procedure or additional reaction step.

ACKNOWLEDGEMENTS

Part of this study was done at Michigan State University (East Lansing, MI, U.S.A.) using facilities in the Department of Biochemistry, directed by Professor C. C. Sweeley. The cooperation and contributions of the departmental staff are gratefully acknowledged. Thanks are also due to J&W Scientific for donating some of the capillary columns employed.

REFERENCES

- 1 D. T. Blankenship, M. A. Krivanek, B. L. Ackerman and A. D. Cardin, *Anal. Biochem.*, 178 (1989) 227.
- 2 S. C. Beale, J. C. Savage, D. Wiesler, S. M. Wietstoc and M. Novotny, *Anal. Chem.*, 60 (1988) 1765.
- 3 M. Yu and N. J. Dovichi, *Anal. Chem.*, 61 (1988) 37.
- 4 Y. F. Cheng and N. J. Dovichi, *Science*, 242 (1988) 562.
- 5 S. M. Lunte, T. Mohabbat, O. S. Wong and T. Kuwana, *Anal. Biochem.*, 178 (1989) 202.
- 6 M. D. Oates, B. R. Cooper and J. W. Jorgenson, *Anal. Chem.*, 62 (1990) 1573.
- 7 R. A. Sherwood, A. C. Titheradge and D. A. Richards, *J. Chromatogr.*, 528 (1990) 293.
- 8 C. W. Gehrke, R. W. Zumwalt and K. C. Kuo (Editors), *Amino Acid Analysis by Gas Chromatography*, CRC Press, Boca Raton, FL, 1987.
- 9 S. L. MacKenzie, D. Tenaschuk and G. Fortier, *J. Chromatogr.*, 387 (1987) 241.
- 10 P. Hušek, V. Felt and M. Matucha, *J. Chromatogr.*, 252 (1982) 217.
- 11 M. Makita, S. Yamamoto and S. Kiyama, *J. Chromatogr.*, 237 (1982) 279.
- 12 S. A. Cohen, B. A. Bindlingmeyer and T. L. Tarvin, *Nature (London)*, 320 (1986) 769.
- 13 E. J. Miller, A. J. Narkates and M. A. Niemann, *Anal. Biochem.*, 190 (1990) 92.
- 14 B. Gustavsson and I. Betnér, *J. Chromatogr.*, 507 (1990) 67.
- 15 P. Hušek, J. A. Rijks, P. A. Leclercq and C. A. Cramers, *J. High Resolut. Chromatogr.*, 13 (1990) 633.
- 16 N.-O. Ahnfelt and P. Hartvig, *Acta Pharm. Suec.*, 19 (1982) 367.
- 17 M. Ahnoff, S. Chen, A. Green and I. Grundevik, *J. Chromatogr.*, 506 (1990) 593.

- 18 S. Björkman, *J. Chromatogr.*, 339 (1985) 339.
- 19 S. Björkman, *J. Chromatogr.*, 414 (1987) 465.
- 20 A. Carlson and O. Gyllenhaal, *J. Chromatogr.*, 508 (1990) 333.
- 21 J. M. Domagala, *Tetrahedron Lett.*, 21 (1980) 4997.
- 22 T. B. Windholz, *J. Org. Chem.*, 23 (1958) 2044.
- 23 S. Kim, Y. C. Kim and J. I. Lee, *Tetrahedron Lett.*, 24 (1983) 3365.
- 24 P. Hušek, Z. H. Huang and C. C. Sweeley, in preparation.

Analysis of multicomponent mixtures by high-resolution capillary gas chromatography and combined gas chromatography–mass spectrometry

I. Aromatics in a hydrocarbon matrix

E. MATISOVÁ*, E. JURANYIOVÁ, P. KURÁŇ and E. BRANDŠTETEROVÁ

Department of Analytical Chemistry, Faculty of Chemical Technology, Slovak Technical University, Radlinského 9, 812 37 Bratislava (Czechoslovakia)

A. KOČAN

Institute of Preventive Medicine, Limbova 14, 833 01 Bratislava (Czechoslovakia)

and

Š. HOLOTÍK

Central Laboratory of Mass Spectrometry, Faculty of Chemical Technology, Slovak Technical University, Radlinského 9, 812 37 Bratislava (Czechoslovakia)

ABSTRACT

Achievements and problems of qualitative analysis of multicomponent mixtures are demonstrated on a complex hydrocarbon sample. Emphasis is given to the analysis of aromatics with the broader range of boiling points in a complex hydrocarbon matrix. In the petroleum fraction (150–350°C) used as the raw material for the analysis of *n*-alkanes by gas chromatography–mass spectrometry with electron-impact ionization using paraffins, olefins, naphthenes and aromatics (PONA) columns under optimized temperature-programmed conditions, it was found out that the sample consists of a multicomponent mixture of hydrocarbons belonging to various hydrocarbon groups at about the same concentration level: alkanes, naphthenes and aromatics. As the sample was very complex, the detailed analysis of aromatic hydrocarbons was performed in aromatic concentrate from liquid chromatography fraction. Identification was based on combination of isothermal retention data (on OV-101) and mass spectral data measured under temperature-programmed conditions using PONA columns. Higher-boiling-point aromatics were characterized using only mass spectral data. The 256 aromatics were characterized as to group (alkylbenzenes, indanes, tetralins, indenes, naphthalenes or acenaphthenes) and further with carbon atom number or the type of substituents. The precise structure with assignment of position of substituents was determined for 51 aromatics.

INTRODUCTION

The definition and criteria of complex organic systems were given by Schomburg [1]. The first categories of these systems represent multicomponent samples and constituents with very similar physical and/or chemical properties (as optical

enantiomers and structural isomers). Natural and synthetic hydrocarbon samples are real multicomponent mixtures (the component number depending on group-type composition and on the range and distribution of boiling points of the components present in the mixture) with a large number of position isomers and enantiomers, numbers of which rapidly increase with increasing carbon atom number.

High-resolution capillary gas chromatography (HRCGC) is the most generally useful method for the analysis of complex hydrocarbon mixtures with the ultimate aim of complete component analysis, thus providing a true paraffins, olefins, naphthenes and aromatics (PONA) analysis. The disadvantage of this method is that every peak must be identified or at least classified according to the chemical group to which it belongs. Peak identification in a chromatogram is carried out on the basis of retention data and gas chromatography–mass spectrometry (GC–MS) [2,3]. MS has gained wide acceptance in petroleum chemistry as a means of providing structural data on the constituents of hydrocarbon mixtures. Its success is based on the principle that any given hydrocarbon type can be recognized by a set of specific spectral peaks [4–6].

Aromatics represent an important group of hydrocarbons in various petroleum products. Detailed information on their composition in feed materials, intermediates and commercial products is required for process development and quality control programs. The other important area of component identification is the environment used. Generally, aromatic hydrocarbons may be analysed directly in various hydrocarbon samples by HRCGC on a single column with non-polar, medium-polarity and polar stationary phases under isothermal and temperature-programmed GC conditions, using multidimensional GC (switching system with two or more columns) or in aromatic concentrates from liquid chromatography fractions using a column with various polarities of the stationary phase. Surveys of their application were published by Kumar *et al.* [7] and Matisová [8]. The individual aromatics were separated, identified and/or quantified, mostly with carbon atom numbers up to 10.

Single-column capillary GC [7,9,10] and multidimensional GC systems [11–16] (with packed and capillary columns) usually employ a very polar (*e.g.* Carbowax 1540, TCEP, SP-2340, OV-275) column to separate the aromatic from the saturated/olefinic hydrocarbons. However, in the case of very complex hydrocarbon mixtures with carbon atom numbers over 12 these systems fail to separate aromatics from compounds of other hydrocarbon groups. Therefore, for the analysis of higher-boiling-point fractions it is necessary to use off-line or on-line combination of liquid chromatography (LC) with capillary GC.

The aim of this paper was to show the possibilities of using single column capillary GC (with commercially available, chemically bonded, non-polar silicone capillary columns) for the detailed analysis of aromatic hydrocarbons in a petroleum fraction with boiling range 150–350°C, with the stress on identification of aromatics with boiling range 150–270°C in the concentrate from a liquid chromatography (LC) fraction using combined retention and mass spectral data. In this study the concentration of aromatics was approximately equal to the constituents of other hydrocarbon groups. The analysis of multicomponent mixture of trace aromatics in a hydrocarbon matrix will be the subject of Part II.

EXPERIMENTAL

GC measurements were performed on an HP Model 5890A gas chromatograph equipped with a split-splitless injection system, a flame ionization detection (FID) system and an HP Model 3396A integrator (Hewlett-Packard, Avondale, PA, U.S.A.). The analysis was carried out on a PONA fused-silica capillary column (Hewlett-Packard) which is a special-purpose cross-linked methyl silicone column with 0.5 μm film thickness for the separation of paraffins, olefins, naphthenes and aromatics (50 m \times 0.2 mm I.D.) and on glass capillary column (52 m \times 0.25 mm I.D.) with statically coated OV-101 dimethylsilicone phase [17] having a film thickness of 0.38 μm . Hydrogen was used as a carrier gas at a linear velocity of 40 cm for the isothermal measurements (80–160°C) and TPG conditions adjusted to the initial temperature of the temperature programme (70 to 160°C at 1.5°C/min, then to 280°C at 15°C/min, and then held for 15 min). The other instrumental conditions were: injector temperatures, 250°C and 300°C, respectively; detector temperature, 300°C; split ratio, 1:70.

GC-MS measurements with electron-impact (EI) ionization (70 eV ionization energy) were performed on an HP Model 5890A gas chromatograph equipped with a split-splitless injection system and a Model 5970 mass-selective detector (Hewlett Packard) with the direct interface. All experimental work was done on a PONA column of the given temperature programmed conditions with helium as carrier gas at a linear gas velocity of 38 cm/s at the initial temperature of the programme run. The other instrumental conditions were: injector and detector temperatures, 300°C and 275°C respectively; split ratio, 1:70.

The raw material for analysis of *n*-alkanes (fraction of crude oil imported from the U.S.S.R. with boiling range 150–350°C) was the sample used for the analysis of aromatic hydrocarbons. From this multicomponent hydrocarbon mixture (0.6–0.7 ml) the aromatic fraction was isolated by column LC on silica gel (50 \times 1.2 cm; particle size 70–100 μm) according to the modified [18] ASTM method D 2549-68 [19], with *n*-pentane (80 ml) for the elution of paraffinic and naphthenic fraction; the aromatic fraction was eluted with 80 ml of dichloromethane or methanol with a flow-rate of 1 ml/min. The aromatic fraction was evaporated using a Model RVO-64 rotary evaporator (Mikrotechna, Prague, Czechoslovakia) to a final volume of 0.5 ml.

The raw material sample (0.5 μl) was injected with a 1- μl Hamilton syringe; isolated aromatic fractions (1.5–2.0 μl) were injected with a 10- μl Hamilton syringe. For measurements of retention data *n*-alkanes were injected together with the isolated aromatic fraction. Methane was used for the determination of the gas hold-up time.

RESULTS

Analysis of multicomponent hydrocarbon mixture

In recent years *n*-alkanes have been extensively used in the manufacture of detergents, fatty acids, alcohols, petroproteins and various speciality chemicals. The technology of *n*-alkanes C₉–C₂₂ is based on their selective adsorption on molecular sieves from the petroleum fraction (a multicomponent mixture of hydrocarbons consisting of *n*-alkanes, branched alkanes, naphthenes and aromatics) and the following extraction. During the adsorption process of *n*-alkanes from the raw material small

amounts of aromatic hydrocarbons are also retained on molecular sieves. The presence of aromatics in the final product, the light fraction of *n*-alkanes C₉-C₁₅, was confirmed by UV spectrometry and their concentration was found to be in the range 10²-10³ ppm. As aromatics are potential carcinogens, it is very important to know their composition in *n*-alkanes. Therefore, it was necessary to perform qualitative analysis of aromatics in the raw material (petroleum fraction) and to determine their distribution in the technological process and mainly in the final product. The trace analysis of individual aromatics in an *n*-alkane matrix will be the subject of Part II.

Hewlett-Packard PONA fused-silica capillary columns, which are special-purpose cross-linked methyl silicone phase columns tailored for hydrocarbon (paraffins, olefins, naphthenes and aromatics) analysis, were chosen for capillary GC and combined GC-MS analysis. Due to the large number of components present in the raw material and their broad range of boiling points (150-350°C) experimental conditions of capillary GC under temperature-programmed conditions with hydrogen as carrier gas were optimized in such a way that a considerably large number of peaks was resolved in a brief period of analysis. From capillary GC profiles it was evident that it would be problematic to perform qualitative analysis of aromatics using retention data measurements as a consequence of a very high probability of co-elution of components of the multicomponent hydrocarbon mixture. Much information on the composition of the raw material was received from the combined GC-MS technique with EI ionization under similar chromatographic conditions. By monitoring selective ions characteristic for certain hydrocarbon groups such as paraffins, naphthenes and aromatics from the acquired mass spectra, mass chromatograms were obtained. From the results it was clear that the co-elution of many components of various hydrocarbons groups is taking place and in most cases GC-MS measurements produced complex mixed spectra which are fairly difficult to interpret. Therefore the qualitative analysis of aromatic hydrocarbons was performed in the aromatic fraction of the raw material.

Analysis of multicomponent mixture of aromatic hydrocarbons

Aromatic hydrocarbons were isolated by off-line adsorption column liquid chromatography on silica gel using a modification of the American Society for Testing and Materials (ASTM) method D2549-68 [19]. The reason for choosing this modified method [18] was its good reproducibility and the production of stock solution of aromatics suitable for repeat GC and GC-MS analyses.

For qualitative capillary GC analysis it is necessary to use a capillary column with the defined stationary phase which gives the opportunity of measurements of reliable retention data with good interlaboratory reproducibility and with good selectivity towards analysed compounds. There is little information available on standards for aromatic hydrocarbons (especially for carbon atom numbers over 9, where is the large number of possible isomers), so for identification purposes the only possibility is to use published retention data on non-polar silicone stationary phases. With regard to these requirements we first decided to use a PONA column with chemically bonded dimethyl silicone phase for its good temperature stability and other column qualities.

Due to the fact in the literature there are certain data on the dependence of retention characteristics on the cross-linking method and film thickness of bonded non-polar phase, and to the small number of published isothermal retention data for

aromatic hydrocarbons on PONA columns [20] and generally on bonded dimethylsilicones, we have verified the agreement of retention indices of a sample of alkylbenzenes with known composition with those on OV-101 columns [21], as alkylbenzenes represent the major part of the monoaromatic fraction of natural and synthetic hydrocarbon mixtures. The four PONA columns tested [22] showed reproducible chromatographic properties, capacity ratios and high efficiencies. The standard deviation of the retention indices measured on a single column ($n=4$) was 0.03 i.u., with confidence interval, $L_{1,2}(I) \pm 0.05$ i.u. ($\alpha = 0.05$), and the differences among the columns were found to be up to 0.3 i.u. Indices determined on conventionally coated dimethylsilicone columns are slightly but significantly lower, the difference being in most cases about 1 i.u. As most published retention indices of aromatics are on conventional non-polar silicone capillary columns [21-27], measurements were performed on an OV-101 glass capillary column. The chromatogram of aromatics isolated from the raw material and *n*-alkanes C_7-C_{13} at 100°C is given in Fig. 1.

Isothermal measurements were also performed at temperatures in the range 80-160°C. In our laboratory we optimized experimental conditions (isothermal temperature in the range 80-130°C) for the analysis of multicomponent mixture of alkylbenzenes on an OV-101 glass capillary column and the only optimum was found to be at 100°C [28]. Analysing aromatics of the raw material (the fraction with carbon atom numbers over 9 with boiling points in the range 150-350°C) at higher temperatures there was co-elution of many peaks. Peak numbering at various temperatures and the assignment of peak numbers both for isothermal GC and temperature programmed GC-MS for positive peak identification was difficult. Therefore, for the qualitative analysis of higher-boiling-point compounds the stress was on GC-MS measurements. The measured retention indices of aromatics at 100°C and their temperature coefficients are given in Table I. Compound characterization was based on the comparison of the measured data with those in the literature [21,25,27].

Qualitative analysis by combination of GC-MS with EI ionization was the next step in the identification of aromatics in the aromatic fraction of the multicomponent hydrocarbon mixture studied. The total ion current (TIC) chromatogram is given in Fig. 2. Identification using the combined technique was based on information obtained from interpretation of the acquired mass spectra; mass chromatograms of selective ions of characteristic aromatics groups found in the mixture (alkylbenzenes, indanes/tetralins, indenenes, naphthalenes and acenaphthenes/biphenyls), examples for indanes/tetralins and naphthalenes are given in Figs. 3 and 4 and mass chromatograms of molecular ions of alkylbenzenes, the most frequently occurring compounds in the aromatic fraction of the raw material (Fig. 5). The acquired mass spectra and mass chromatograms of molecular ions of some types of compounds made possible the determination of molecular weights and carbon atom numbers of the individual components and/or the type and number of substituents. In many cases mixed mass spectra were obtained and from mass chromatograms of selective ions it was possible to confirm the number or the type of compounds eluted in one peak.

More detailed structure with the assigned position of substituents was determined using the combined retention and mass spectral data (Table I). It has to be pointed out that in the case of mixed spectra interpretation was not possible for a compound with low content. Further, the assignment of a corresponding peak number under temperature-programmed GC-MS and isothermal GC conditions was not

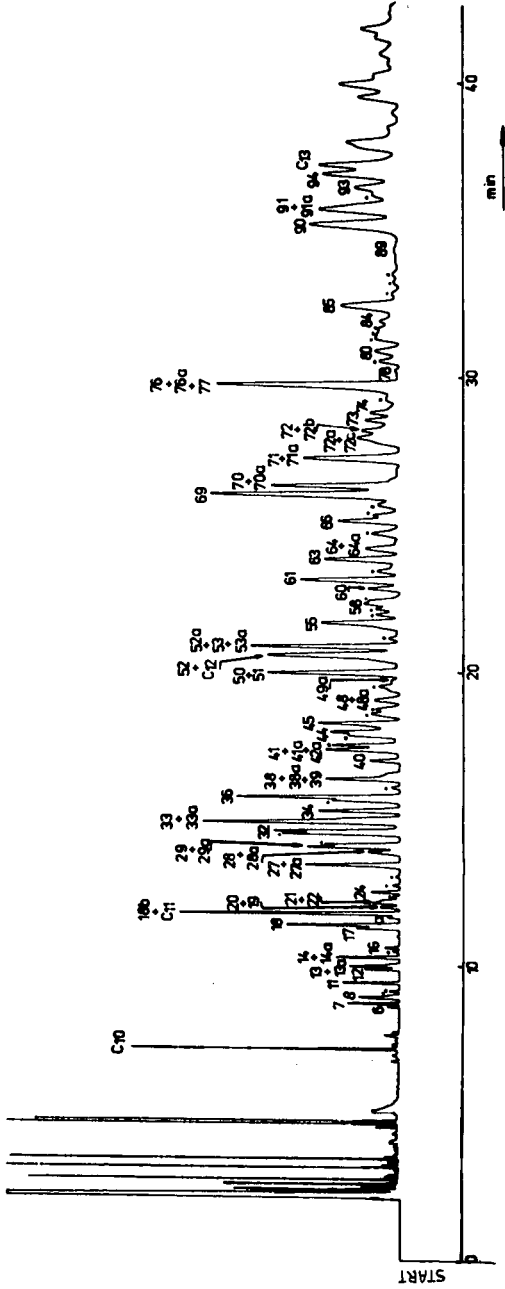


Fig. 1. Chromatogram of aromatics in aromatic fraction of the raw material isolated by LC on silica gel eluted between *n*-alkanes C_{10} - C_{13} at 100°C on OV-101 capillary column with as carrier gas hydrogen at a linear velocity of 40 cm/sec.

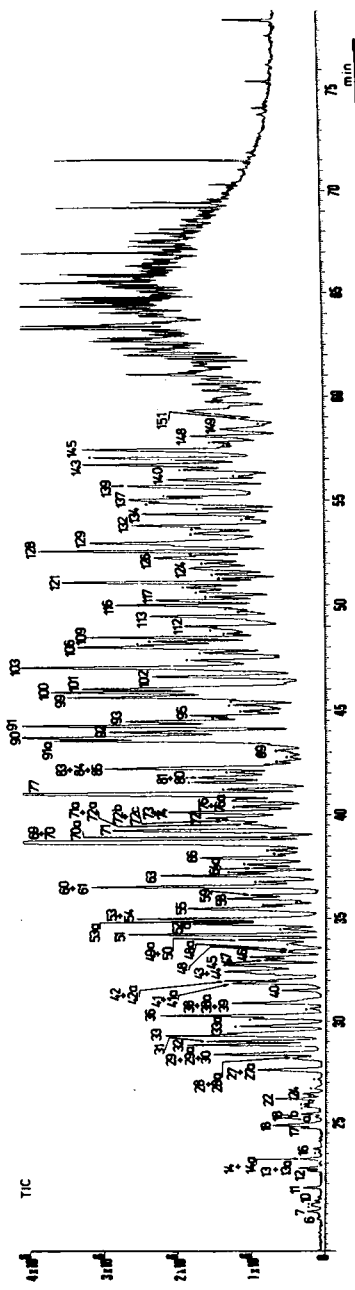


Fig. 2. Total ion current (TIC) chromatogram by GC-MS analysis of aromatic fraction of the raw material isolated by LC on silica gel; measurements were performed on a PONA column under the temperature-programmed conditions: $t_1 = 70^\circ\text{C}$; $G_1 = 1.5^\circ\text{C}/\text{min}$; $t_2 = 160^\circ\text{C}$; $G_2 = 15^\circ\text{C}/\text{min}$; $t_3 = 280^\circ\text{C}$; 15 min isothermal; carrier gas, helium at 38 cm/s.

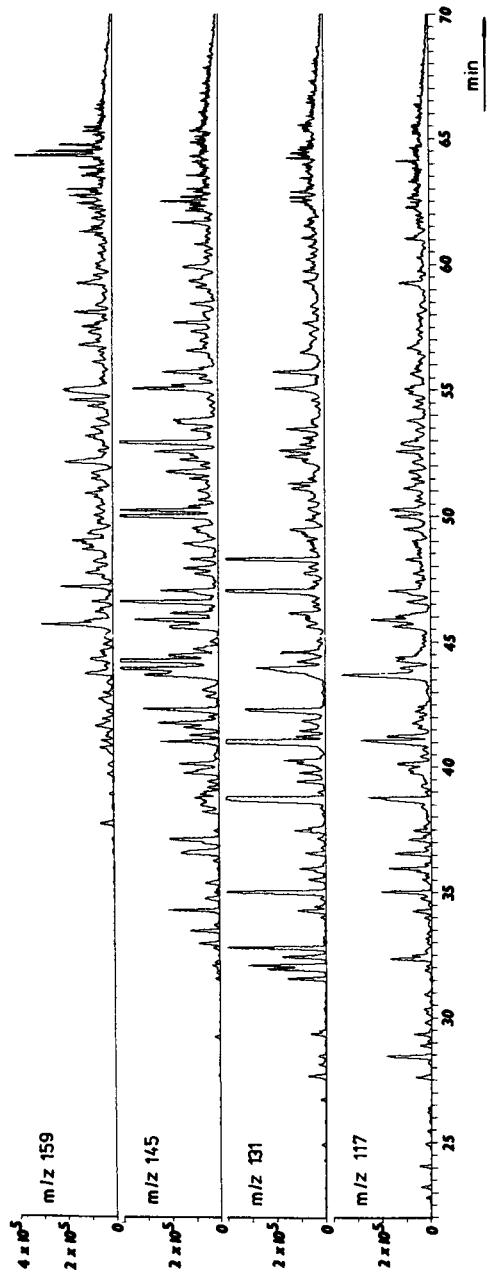


Fig. 3. Mass chromatogram of selective ions of indanes/tetralins in aromatic fraction of the raw material; experimental conditions as in Fig. 2.

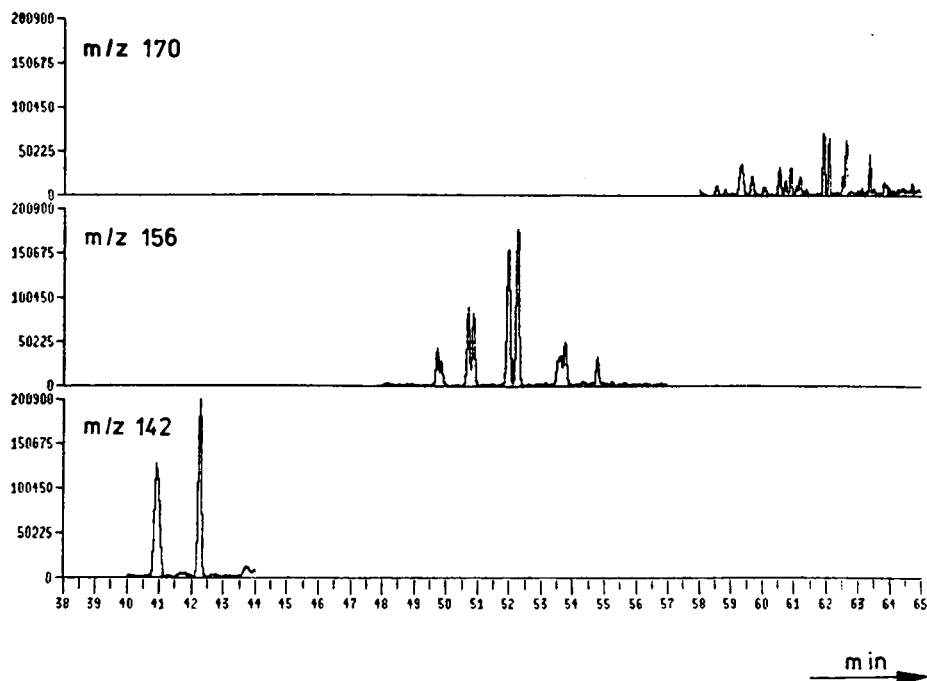


Fig. 4. Mass chromatogram of selective ions of naphthalenes in aromatic fraction of the raw material; experimental conditions as in Fig. 2.

TABLE I

RETENTION INDICES (I) OF AROMATIC HYDROCARBONS DETERMINED IN AROMATIC FRACTION OF THE RAW MATERIAL OF THE TECHNOLOGY OF *n*-ALKANES ON OV-101 STATIONARY PHASE AT 100°C AND THEIR TEMPERATURE COEFFICIENTS (dI/dT)

Peak No.	Compound ^a	I	dI/dT	Peak No.	Compound ^a	I	dI/dT
6	1,3-DiEtB	1039.2	0.265	15	Unidentified	1078.2	0.270
7	1-Me-3-nPrB	1041.8	0.265	16	1,3-DiMe-2-EtB	1080.4	0.365
8	1,4-DiEtB + 1-Me-4-nPrB	1046.6	0.295	17	Me-iBuB or 2-Ph-3-MeButane	1091.9	0.290
9	nBuB	1048.0	0.225	18	1-Me-3-sBuB + 1,2-DiMe-3-EtB	1093.7	0.315
10	1,2-DiEtB	1051.3	0.325	18a	1-Et-2-iPrB + Me-iBuB		
11	1-Me-2-nPrB	1057.2	0.335		or 2-MePhButane	1098.0	0.305
12	1,4-DiMe-2-EtB	1066.7	0.290	18b	1-Me-4-sBuB	1100.0	0.305
13	1,3-DiMe-4-EtB	1068.6	0.310	19	1-Et-4-iPrB	1103.4	0.285
13a	Indane C ₁₀	1069.7	0.445	20	Indane C ₁₀	1103.4	—
14	1,2-DiMe-4-EtB	1074.4	0.300	21	2-Me-2-PhButane	1105.6	0.380
14a	Indane C ₁₀	1074.4	0.460	22	1,2,4,5-TetraMeB + AB C ₁₁	1106.4	0.380

TABLE I (continued)

Peak No.	Compound ^a	<i>I</i>	<i>dI/dT</i>	Peak No.	Compound ^a	<i>I</i>	<i>dI/dT</i>
23	1,2,3,5-TetraMeB	1108.7	0.440	57	Indane C ₁₁	1212.4	0.450
24	iPeB	1111.1	0.320	58	Indane C ₁₁ + AB C ₁₂	1213.4	0.385
25	Indane C ₁₁	1114.4	0.440	59	1,2,4-TriMe-3-EtB	1214.5	0.475
26	1,4-DiMe-2-iPrB	1118.7	0.225	60	Indane C ₁₂	1217.7	0.665
27	1-Et-3-nPrB	1124.4	0.265	61	1,4-Di-nPrB	1220.0	0.320
27a	5-MeIndane	1124.4	0.455	62	AB C ₁₂	1222.2	0.325
28	1,2-DiMe-4-iPrB	1130.3	0.315	63	AB C ₁₂ + Indane C ₁₂	1225.2	0.375
28a	1,3-DiEt-5-MeB	1130.3	—	64	AB C ₁₂	1227.7	0.325
29	1,3-DiMe-5-nPrB	1132.4	0.345	64a	Indane C ₁₂	1227.7	0.630
29a	AB C ₁₁	1132.4	0.210	65	AB C ₁₂	1231.7	0.360
30	Indane C ₁₀	1133.5	0.560	66	1-Me-3-nPeB	1234.1	0.310
31	1-Me-3-nBuB	1139.4	0.265	67	AB C ₁₂	1235.3	0.355
32	1,2,3,4-TetraMeB	1138.3	0.440	68	AB C ₁₂	1237.7	0.340
33	Tetralin C ₁₀ + 1,4-DiEt-2-MeB (traces)	1143.2	0.550	69	Indane C ₁₁ + AB C ₁₂	1240.2	0.585
33a	nPeB	1143.2	0.335	70	HeB (branched)	1242.0	0.335
34	1,4-DiMe-2-nPrB	1147.7	0.325	70a	Indane C ₁₂ + Indene C ₁₁ + AB C ₁₂	1242.0	0.660
35	1,3-DiMe-4-nPrB	1152.0	0.330	71	1-Me-2-nPeB	1247.8	0.370
36	1-Me-2-nBuB	1153.0	0.335	71a	Indane-unidentified	1247.8	0.555
37	1,3-DiEt-2-MeB	1156.8	0.390	72a	AB C ₁₂ + AB C ₁₃	1251.9	0.350
38	1,3-DiMe-2-nPrB	1160.1	0.330	72b	AB C ₁₂ + AB C ₁₃	1253.4	0.275
38a	AB C ₁₁	1160.1	0.330	72c	Indane C ₁₂	1251.9	0.630
39	Indene-unidentified + Naph(traces)	1161.7	0.550	72	AB C ₁₂	1253.4	0.440
40	MeIndane C ₁₁	1666.6	0.465	73	Indane C ₁₂	1255.5	0.325
41	Indane C ₁₁	1170.4	0.465	74	AB C ₁₂	1257.0	0.375
41a	1,2-DiEt-3-MeB + Indane C ₁₁ + 1-Et-3-sBuB	1170.4	0.275	75	AB C ₁₃ + Indane C ₁₂ (traces)	1259.7	0.315
42	Indane C ₁₁ + AB C ₁₂ (traces)	1171.9	0.480	76	AB C ₁₂	1262.7	0.350
42a	AB C ₁₁	1170.4	0.365	76a	AB C ₁₂	1262.7	0.410
43	1-iPr-3-nPrB + Indane C ₁₁	1175.3	0.545	77	Indane C ₁₁ + 2-MeNaph	1262.7	0.660
44	1,2-DiMe-3-nPrB	1176.3	0.505	78	AB C ₁₃ + Indane C ₁₂	1265.1	0.625
45	MeIndane C ₁₁ + AB C ₁₂	1179.3	0.510	79	Indane C ₁₂ + AB C ₁₂	1267.0	0.670
46	1,3,5-TriMe-2-EtB + AB C ₁₂	1182.3	0.355	80	Indane C ₁₂	1268.9	0.710
47	1,2,5-TriMe-3-EtB + AB C ₁₂	1183.5	0.295	81	AB C ₁₂ + AB C ₁₃	1271.2	0.595
48	1-Et-4-sBuB	1186.4	0.310	82	AB C ₁₂ + Indane C ₁₂ (traces)	1272.0	0.655
48a	Indane C ₁₂ + AB C ₁₂	1186.4	0.560	83	1-MeNaph	1273.0	0.825
49	1,4-DiMe-2-sBuB	1190.6	0.265	84	AB C ₁₂	1274.3	0.710
49a	AB C ₁₂	1191.7	0.210	85	Indane C ₁₂	1277.1	0.545
50	1,2,3-TriMe-5-EtB	1194.7	0.265	86	AB C ₁₃	1279.0	—
51	MeTetralin + AB C ₁₂	1194.7	0.570	87	AB C ₁₃ + Indane C ₁₂	1281.0	—
52	1,3-DiMe-4-sBuB + AB C ₁₂	1198.1	0.305	88	Indane C ₁₂ + AB C ₁₃	1282.3	—
52a	AB C ₁₁ + Indane C ₁₂ (traces)	1202.2	0.335	89	AB C ₁₃	1286.3	—
53	Indane C ₁₁	1202.2	0.590	90	AB C ₁₃ + Indane C ₁₂	1290.7	0.650
53a	MePeB	1202.2	0.277	91	Indane C ₁₂ + AB C ₁₃	1293.1	0.810
54	AB-unidentified	1204.4	0.225	91a	MeHeB + Indane C ₁₂	1293.1	0.345
55	1,3-Di-nPrB	1208.7	0.355	92	Indane C ₁₂	1295.5	0.540
56	nPrMeEtB	1210.9	0.245	93	Indane C ₁₂ + AB C ₁₃	1296.5	0.560
				94	AB C ₁₂ + Indane C ₁₂	1298.5	0.735

^a Abbreviations: Me = methyl; Et = ethyl; Pr = propyl; Bu = butyl; Pe = pentyl; He = hexyl; B = benzene; AB = alkylbenzene; Ph = phenyl; Naph = naphthalene.

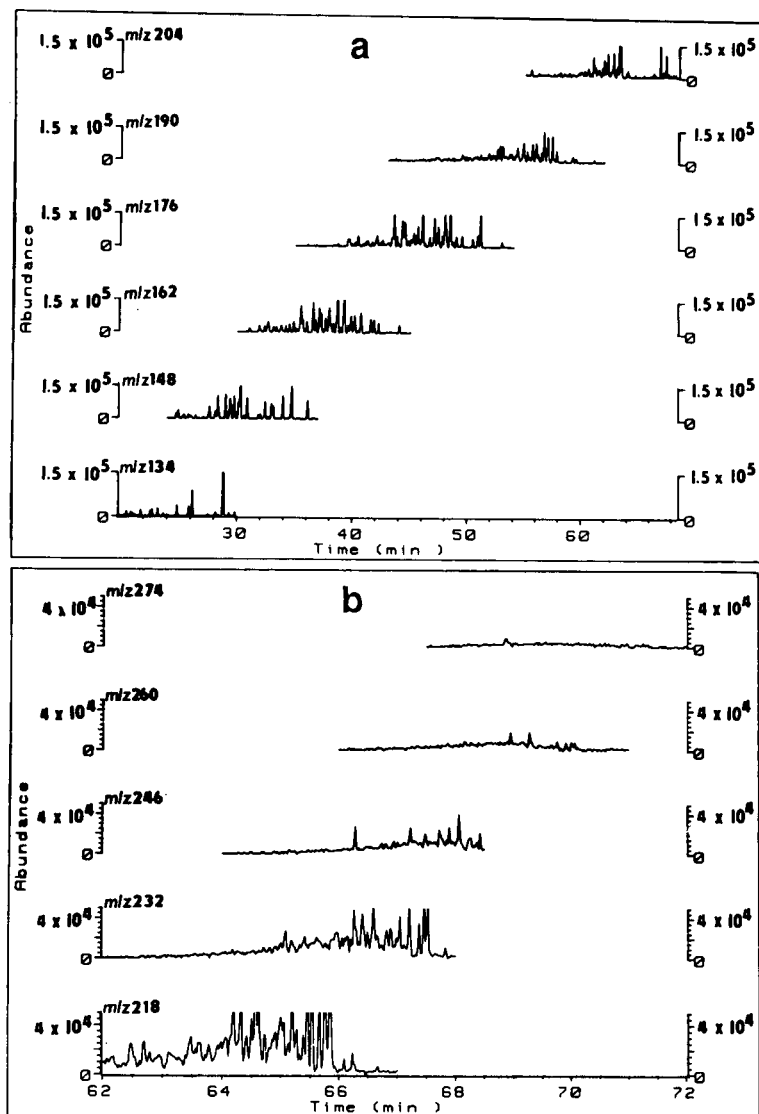


Fig. 5 (a) Alkylbenzene map C_nH_{2n-6} , where $n = 10-14$, of the aromatic fraction of the raw material; experimental conditions as in Fig. 2 (b). Alkylbenzene map C_nH_{2n-6} , where $n = 15-20$, of the aromatic fraction of the raw material; experimental conditions as in Fig. 2.

always possible. In these cases, using mass spectra and mass chromatograms, only the type of compound was determined. This comprises mainly the aromatics eluting in the upper part of the fraction with boiling points up to 270°C . In this region there is also a lack of published retention data (Table II).

As in the light fraction of the *n*-alkanes C_9-C_{15} (boiling points range $151-270^\circ\text{C}$) higher-boiling-point aromatics of the petroleum fraction do not occur, de-

TABLE II

CHARACTERIZATION OF AROMATIC HYDROCARBONS BY GC-MS

Peak No.	Compound ^a	Peak No.	Compound ^a
95	Indene C ₁₂ + AB C ₁₃	124	Indane C ₁₃ + AB C ₁₄
96	AB C ₁₃ + Indane C ₁₃	125	Naph C ₁₂ + Indane C ₁₃
97	AB C ₁₃ + Indene C ₁₃ (traces)	126	Naph C ₁₂ + Indane C ₁₄
98	AB C ₁₃ + Indane C ₁₂	127	Indane C ₁₄ + Indene C ₁₃ + AB C ₁₄
99	AB C ₁₃ + Indane C ₁₃	128	Indane C ₁₃ + AB C ₁₄ + Acen C ₁₄
100	Indane C ₁₃	129	Indane C ₁₄ + AB C ₁₄
101	AB C ₁₃	130	Indane C ₁₃
102	Indane C ₁₃ + AB C ₁₃	131	Indane C ₁₄ + AB C ₁₄ + Naph C ₁₂
103	Indane C _{12,13} + AB C ₁₃	132	Indane C ₁₃ + AB C ₁₄ + Naph C ₁₂
104	AB C ₁₃	133	Indane C ₁₄ + AB C ₁₄
105	AB C ₁₃ + Indane C ₁₃	134	AB C ₁₄ + Indane C ₁₃ + Indene C ₁₃
106	AB C ₁₃	135	Indane C ₁₃ + Naph C ₁₂
107	Biphenyl + AB C ₁₃	136	AB C ₁₄ + Indane C ₁₃
108	Indane C ₁₂	137	Indane C ₁₃
109	AB C ₁₃	138	Indane C ₁₃ + AB C ₁₄
110	Indane C ₁₃ + AB C ₁₄	139	Indane C ₁₃
111	Indane C ₁₃ + AB C ₁₃	140	Long chain AB C ₁₄
112	Indane C ₁₃ + AB C ₁₃	141	Long chain AB C ₁₄
113	Indane C ₁₃ + AB C ₁₃	142	AB C ₁₄ + Indane C ₁₃ (traces)
114	Indene C ₁₃ + Naph C ₁₂	143	AB C ₁₄
115	Naph C ₁₂ + Indane C ₁₃ + AB C ₁₄	144	Long chain AB C ₁₄
116	Indane C ₁₂ + Acen C ₁₃	145	Acen C ₁₃ + AB C ₁₄
117	Indane C ₁₂	146	Indane C ₁₃
118	AB C ₁₃ + Indane C ₁₄	147	AB C ₁₄
119	Indane C ₁₃ + AB C ₁₄ + Naph C ₁₂	148	Indane C ₁₄ + Acen C ₁₃ (traces)
120	AB C ₁₃ + Naph C ₁₂	149	Indane C ₁₄ + AB C ₁₅ (traces)
121	AB C ₁₃ + Indane C ₁₃ (traces)	150	AB C ₁₅ + Indene C ₁₄ + Indane C ₁₄ + Acen C ₁₄ + Naph C ₁₃
122	Indane C ₁₄ + AB C ₁₄ + Indene C ₁₃		
123	Indane C ₁₃		

^a Abbreviations: AB = alkylbenzene; Naph = naphthalene; Acen = acenaphthene.

tailed analysis of compounds eluted at the rapidly increasing portion of the temperature program (15°C/min) was not performed.

CONCLUSIONS

In the analysis of multicomponent samples the choice of separating system is very important, mainly in the case of single-column analysis. Though PONA columns are specially tailored for hydrocarbon analysis and offer high quality with respect to efficiency and thermal stability, they are insufficient to resolve complex hydrocarbon mixtures with a broader range of boiling points under optimized experimental conditions. The combination of GC-MS with EI ionization (mass fragmentography, selected-ion monitoring) is of great help in distinguishing various groups of compounds eluting in one peak (as alkanes, naphthenes or aromatics). For the detailed identification of aromatic hydrocarbons it is necessary to separate different groups of com-

pounds to collect retention and mass spectral data which can be easily and unambiguously interpreted. In the petroleum fraction studied aromatic hydrocarbons were analysed in concentrate from the LC fraction. From measured isothermal retention data (I , dI/dT) and mass spectral data (mass spectra, mass chromatograms) the following compounds of several aromatics groups were identified: 51 alkylbenzenes with carbon atom number C_9 – C_{12} , one indane, three naphthalenes and one biphenyl with the assignment of exact structure. The other components were characterized by carbon atom number and/or type of substituents but without assignment of final structures: 93 C_{11} – C_{15} alkylbenzenes, 82 C_{10} – C_{14} indanes/tetralins, nine C_{10} – C_{13} indenes, ten C_{11} – C_{13} naphthalenes and six C_{12} – C_{14} acenaphthenes/biphenyls.

ACKNOWLEDGEMENTS

The authors would like to acknowledge the assistance of Hewlett-Packard Analytical Instrumentation (Vienna, Austria) and Dr. H. P. Schiefer and Dr. F. Lorber for providing the GC instrumentation used and presenting the PONA column to support this and other scientific projects.

REFERENCES

- 1 G. Schomburg, *LC · GC*, 5 (1987) 304.
- 2 I. M. Whittmore, in K. H. Altgelt and T. H. Gouw (Editors), *Chromatography in Petroleum Analysis*, Marcel Dekker, New York, 1979, pp. 50–70.
- 3 E. M. Steward and E. W. Pitzer, *J. Chromatogr. Sci.*, 26 (1988) 218.
- 4 M. E. Fitzgerald, V. A. Cirillo and F. J. Galbraith, *Anal. Chem.*, 34 (1962) 1276.
- 5 E. J. Gallegos, J. W. Green, L. P. Lindeman, R. L. Le Turneau and R. M. Teeter, *Anal. Chem.*, 39 (1967) 1833.
- 6 S. Zadro, J. K. Haken and W. V. Pinczewski, *J. Chromatogr.*, 323 (1985) 305.
- 7 B. Kumar, R. K. Kuchhal, P. Kumar and P. L. Gupta, *J. Chromatogr. Sci.*, 24 (1986) 99.
- 8 E. Matisová, *J. Chromatogr.*, 438 (1988) 131.
- 9 C. L. Stuckey, *J. Chromatogr. Sci.*, 7 (1969) 177.
- 10 E. Matisová, J. Krupčík, P. Čellár and A. Kočan, *J. Chromatogr.*, 346 (1985) 17.
- 11 M. G. Block, R. B. Callen and J. H. Stockinger, *J. Chromatogr. Sci.*, 15 (1977) 504.
- 12 P. van Arkel, J. Beens, H. Spaans, D. Grutterink and R. Verbeek, *J. Chromatogr. Sci.*, 26 (1987) 141.
- 13 F. P. Di Sanzo, J. L. Lane and R. E. Yoder, *J. Chromatogr. Sci.*, 26 (1988) 206.
- 14 F. P. Di Sanzo and V. J. Giarrocco, *J. Chromatogr. Sci.*, 26 (1988) 258.
- 15 J. Curvers and P. van der Sluys, *J. Chromatogr. Sci.*, 26 (1988) 267.
- 16 J. Curvers and P. van der Engel, *J. Chromatogr. Sci.*, 26 (1988) 271.
- 17 E. Matisová, M. Rukgrilová, J. Krupčík, E. Kovačičová and Š. Holotik, *J. Chromatogr.*, 455 (1988) 301.
- 18 P. Kuráň, *Thesis*, Faculty of Chemical Technology, Slovak Technical University, Bratislava, 1989.
- 19 *Annual Book of ASTM Standards*, Part 24, American Society for Testing and Material, Philadelphia, PA, 1975, method D2549-68.
- 20 J. A. Lubeck and D. L. Sutton, *J. High Resolut. Chromatogr. Chromatogr. Commun.*, 6 (1983) 328.
- 21 E. Matisová, E. Kovačičová, P. T. Ha, E. Kolek and W. Engewald, *J. Chromatogr.*, 475 (1989) 113.
- 22 E. Matisová and P. Kuráň, *Chromatographia*, 30 (1990) 328.
- 23 A. F. Sljachov, B. I. Anvaer, O. V. Zolotareva, N. N. Romina, N. N. Novikova and R. I. Koreskova, *Zh. Anal. Chim.*, 30 (1975) 788.
- 24 W. Engewald, L. Wennrich and E. Ritter, *J. Chromatogr.* 174 (1979) 315.
- 25 V. A. Gerasimenko, A. V. Kirilenko and V. M. Nabivach, *J. Chromatogr.*, 208 (1981) 9.
- 26 V. A. Gerasimenko and V. M. Nabivach, *Zh. Anal. Khim.*, 37 (1982) 110.
- 27 T. Tóth, *J. Chromatogr.*, 279 (1983) 157.
- 28 E. Matisová, E. Kovačičová, J. Garaj and G. Kraus, *Chromatographia*, 27 (1989) 494.

CHROMSYMP. 2202

Gas chromatographic separation of unsaturated polar compounds on inorganic stationary phases containing silver nitrate

V. G. BEREZKIN*, E. N. VIKTOROVA and V. S. GAVRICHEV^a

A. V. Topchiev Institute of Petrochemical Synthesis, USSR Academy of Sciences, Leninsky Prospect 29, Moscow B-71 (U.S.S.R.)

and

S. A. RANG, K. R. KUNINGAS and A. E. MEISTER

Institute of Chemistry, Academia Teë 15, Tallinn, Estonia (U.S.S.R.)

ABSTRACT

The separation of unsaturated compounds using gas chromatographic packed columns with inorganic liquid stationary phases was studied. Steam of steam–nitrogen was used as the mobile phase. Comparison of the retention characteristic for olefinic hydrocarbons and polar unsaturated compounds with AgNO_3 and LiNO_3 as stationary phases was carried out. Examples of separations on other nitrates are presented.

INTRODUCTION

Glycol solution containing silver salts (usually silver nitrate) is one of the most selective liquid phases used to separate complex mixtures of olefinic hydrocarbon isomers. However, the use of this type of phase is limited by the poor stability at high temperatures [1,2]. Previously, we have shown [3] that the simultaneous application of steam as a carrier gas and some inorganic salts coated on a solid support as a liquid stationary phase led to the formation of salt solutions with unique chromatographic properties. Phases of this type were found to be characterized by very high selectivity with respect to oxy compounds (*e.g.*, alcohols) and unsaturated compounds if use is made of silver salts. The thermal stability of inorganic silver-containing phases permits stereoisomers of olefinic hydrocarbons up to C_{16} to be separate.

The aims of this work were as follows: (1) to study the selective separations obtained with inert gas containing steam at concentrations corresponding to water vapour saturation at 60 and 25°C as the carrier gas; (2) further evaluation of the chromatographic characteristics of mixed phases containing AgNO_3 and another nitrate in chromatography with steam as the carrier gas; and (3) investigation of the possibility of using stationary phases with AgNO_3 for the separation of both olefins and other classes of polar saturated and unsaturated compounds.

^a Author deceased.

EXPERIMENTAL

Separations of C_1 – C_5 aliphatic alcohols, C_{10} – C_{16} unsaturated hydrocarbons, some unsaturated alcohols and ethers was studied. Water–salt phases formed in the interaction steam of with either pure salt or salt mixtures were used as stationary phases. In the latter instance $AgNO_3$ was used as one of the components of the mixture.

The gas chromatographic system, described in detail previously [4], consists of a gas chromatograph equipped with a stem generator. The sorbent is prepared by deposition of an inorganic salt or salt mixture from an aqueous solution in amount of 5 or 10% (w/w) on Chromaton N AW (Lachema, Brno, Czechoslovakia) or 20% (w/w) on Celite C-22 (Ferak, Berlin, Germany). The column dimensions were 2 m \times 3 mm I.D. When pure steam was used as the carrier gas, the column temperature was 108°C and the inlet vapour pressure 1.2–1.3 atm. The linear velocity of the carrier gas (nitrogen) was 4 cm/s. To saturate the inert gas while working with steam an inert gas mixture bubbler was used. The saturation temperature was 25 or 60°C. According to reference data, the water saturation pressure at these temperature is 23.7 and 150 Torr, respectively. The temperature of the column packed with $AgNO_3$ on Celite C-22 (nitrogen–steam mixed mobile phase) was 80°C. To ascertain whether a homogeneous liquid phase (aqueous salt solution) was formed with the salt mixture direct visual observation of the physical state of the salt was carried out in a test-tube at temperatures typical of chromatography with steam and steam–nitrogen mixtures.

RESULTS AND DISCUSSION

Retention data for some organic compounds are given in Tables I–IV. It is interesting that even $LiNO_3$ can be used to separate olefinic isomers although it is inferior to $AgNO_3$ in this respect. An increase in the salt content leads to an increase in retention and improves the separation. It should be mentioned that the elution trends are the same as with $AgNO_3$, *i.e.* the *trans* isomer is eluted before the *cis* isomer (Table I).

The molecular mass, ester structure and polar group position affect the retention of unsaturated esters on $LiNO_3$ (Table II). Thus allyl formate (b.p. 83.6°C) elutes last although its boiling point is close to that of ethyl acrylate (80.3°C), which elutes earlier (relative retentions 1.5 and 0.56, respectively). The following retention *vs.* polarity dependence is observed: on $AgNO_3$ ethyl acrylate elutes first whereas on $LiNO_3$ allylethyl ether (b.p. 67.6°C) elutes first.

An extremely strong retention of unsaturated alcohols compared with that of aliphatic alcohols is typical for both $LiNO_3$ and $AgNO_3$, although the nature of the retention differs considerably. An increase in lithium salt content leads to a sharper increase in the retention of cinnamyl alcohol compared with allyl alcohol. In the presence of $AgNO_3$, the elution of allyl alcohol is retarded compared with cinnamyl alcohol.

With aliphatic alcohols, the retention is stronger with $LiNO_3$, but $AgNO_3$ shows the ability to separate aliphatic alcohols with respect to its polarity and not molecular mass.

The fact that lithium salts show a stronger retention with respect to unsaturated

TABLE I

CAPACITY FACTORS (k') AND RELATIVE RETENTION TIMES (t_{rel})^a FOR UNSATURATED HYDROCARBONS WITH LiNO₃ and AgNO₃

Carrier gas, steam; temperature, 108°C; column 200 × 3 mm I.D.

Compounds	Dry salt on solid support											
	LiNO ₃				AgNO ₃				LiNO ₃ + AgNO ₃			
	5%		10%		5%		10%		2% + 2%		5% + 5%	
	k'	t_{rel}	k'	t_{rel}	k'	t_{rel}	k'	t_{rel}	k'	t_{rel}	k'	t_{rel}
<i>trans</i> -5-Decene	0.28	0.22	0.28	0.13	0.60	0.18	0.59	0.16	0.76	0.33	0.60	0.17
1-Decene	0.37	0.22	0.37	0.17	0.71	0.22	0.71	0.19	0.78	0.34	0.72	0.21
<i>cis</i> -5-Decene	0.35	0.27	0.51	0.24	0.83	0.26	0.84	0.23	0.82	0.36	0.85	0.25
<i>trans</i> -6-Dodecene	0.45	0.35	0.66	0.31	0.95	0.29	0.99	0.27	0.86	0.38	0.96	0.28
1-Dodecene	0.55	0.42	0.86	0.40	1.05	0.32	1.26	0.34	0.91	0.40	1.12	0.33
<i>cis</i> -6-Dodecene	0.66	0.51	1.14	0.53	1.22	0.38	1.45	0.40	0.97	0.43	1.32	0.38
<i>trans</i> -5-Tridecene	0.80	0.62	1.42	0.66	1.50	0.46	1.66	0.45	1.09	0.48	1.67	0.48
<i>cis</i> -5-Tridecene	1.02	0.78	1.73	0.80	1.85	0.57	2.09	0.57	1.26	0.55	1.93	0.56
1-Tetradecene	1.30	1.00	2.16	1.00	3.25	1.00	3.66	1.00	2.28	1.00	3.45	1.00
1-Cetene	2:18	1.68	4.59	2.125	6.75	2.08	9.66	2.64	3.50	1.54	6.78	1.97

^a Internal standard, ethyl vinylacetate.

polar compounds than to aliphatic compounds was used to develop a procedure for the analysis of impurities (ethyl acetate and butyl acetate) in vinyl acetate. Ethyl acetate impurity elutes before the major peak of vinyl acetate.

TABLE II

CAPACITY FACTORS (k') AND RELATIVE RETENTION TIMES (t_{rel})^a FOR SOME UNSATURATED ESTERS

Carrier gas, steam; temperature, 108°C; column 200 × 3 mm I.D.

Compounds	Dry salt on solid support											
	LiNO ₃				AgNO ₃				LiNO ₃ + AgNO ₃			
	5%		10%		5%		10%		2% + 2%		5% + 5%	
	k'	t_{rel}	k'	t_{rel}	k'	t_{rel}	k'	t_{rel}	k'	t_{rel}	k'	t_{rel}
Ethyl acrylate	0.73	0.73	0.95	0.56	0.5	0.19	0.5	0.17	1.56	0.40	2.10	0.51
Allyl ethyl ether	0.6	0.6	0.79	0.46	0.58	0.22	0.75	0.25	1.72	0.44	2.10	0.51
Allyl methacrylate	0.72	0.72	1.43	0.84	1.08	0.42	1.66	0.55	2.11	0.54	3.36	0.82
Ethyl vinylacetate	1.0	1.0	1.71	1.0	2.58	1.0	3.0	1.0	3.89	1.0	4.08	1.0
Allyl formate	1.55	1.55	2.57	1.50	2.75	1.07	3.17	1.06	4.78	1.23	4.36	1.07

^a Internal standard, ethyl vinylacetate.

TABLE III

CAPACITY FACTORS (k') AND RELATIVE RETENTION TIMES (t_{rel})^a FOR SATURATED AND ALIPHATIC ALCOHOLS

Compounds	Dry salt on solid support											
	LiNO ₃				AgNO ₃				LiNO ₃ + AgNO ₃			
	5%		10%		5%		10%		2% + 2%		5% + 5%	
	k'	t_{rel}	k'	t_{rel}	k'	t_{rel}	k'	t_{rel}	k'	t_{rel}	k'	t_{rel}
Methanol	7.5	1.74	13.2	1.51	5.4	1.64	8.33	1.79	8.47	1.72	12.08	1.55
Ethanol	4.3	1.0	8.77	1.0	3.3	1.0	4.66	1.0	4.93	1.0	7.79	1.0
Propanol	3.5	0.81	4.7	0.54	1.8	0.55	3.11	0.67	4.93	1.0	5.2	0.67
Butanol	2.8	0.65	3.6	0.41	1.4	0.42	2.33	0.5	1.33	0.27	4.3	0.55
Amyl alcohol	0.45	0.1	2.23	0.25	0.4	0.12	1.77	0.38	0.93	0.19	0.95	0.12
Allyl alcohol	3.5	0.81	4.42	0.50	59	17.88	262.4	56.31	4.72	0.96	70.7	9.08
Cinnamyl alcohol	16.3	3.79	173.8	19.82	41.4	12.55	146	31.33	13.4	13.4	2.72	-

^a Internal standard, ethyl vinylacetate.

TABLE IV

RELATIVE RETENTION TIMES FOR SOME ORGANIC COMPOUNDS

Carrier gas, steam-nitrogen mixture; temperature, 80°C.

Compound	Dry salt on solid support			
	5% LiNO ₃ + 5% AgNO ₃		10% LiNO ₃ + 10% AgNO ₃	
	H ₂ O pressure ^a (Torr)	H ₂ O pressure ^b (Torr)	H ₂ O pressure ^a (Torr)	H ₂ O pressure ^b (Torr)
Undecane	0.0888	0.0832	0.0921	1.129
Dodecane	0.215	0.207	0.211	0.242
Tridecane	0.471	0.455	0.457	0.492
Tetradecane	1.000	1.000	1.000	1.000
1-Decene	0.371	0.135	0.0679	
<i>trans</i> -2-Decene	0.168	0.079		
<i>cis</i> -2-Decene	0.364	0.193		
<i>trans</i> -3-Decene	0.210	0.073		
<i>cis</i> -3-Decene	0.484	0.146		
<i>trans</i> -4-Decene	0.234	0.066		
<i>cis</i> -4-Decene	0.503	0.123		
<i>trans</i> -5-Decene	0.028	0.058		
<i>cis</i> -5-Decene	0.320	0.093		
Ethanol	0.285	1.0	0.281	0.735
Methanol	0.327	2.029	0.311	1.426

^a Nitrogen was saturated by passing it through the bubbler at 25°C.^b Nitrogen was saturated by passing it through the bubbler at 60°C.

Mixed phases containing $\text{Al}(\text{NO}_3)_3 \cdot 9\text{H}_2\text{O}$ or $\text{Zn}(\text{NO}_3)_2 \cdot 6\text{H}_2\text{O}$ in addition to silver salts were tested as possible stationary phases for separating both polar and non-polar compounds. Preliminary tests with the use of individual stationary phases for separating *cis* and *trans* isomers of 3-hexene were carried out. Steam–nitrogen was used as the mobile phase. When $\text{Zn}(\text{NO}_3)_2 \cdot 6\text{H}_2\text{O}$ was used as the stationary phase, the capacity factors, k' , for *cis*-3-hexene and *trans*-3-hexene were 3.67 and 1.33, respectively (temperature 35°C). With $\text{Al}(\text{NO}_3)_3 \cdot 9\text{H}_2\text{O}$ as the stationary phase the capacity factors for *cis*- and *trans*-3-hexene were 1.18 and 0.82, respectively (at 78°C).

The separation of unsaturated hydrocarbons on $\text{Al}(\text{NO}_3)_3 \cdot 9\text{H}_2\text{O}$ was studied with pure steam as the carrier gas at 120°C. A good separation of *cis* and *trans* isomers was achieved. The capacity factors for *cis*-3-hexene, *cis*-2-octene, *trans*-5-decene and *cis*-5-decene were 0.79, 2.72, 4.36 and 5.11, respectively. Both phases were highly selective with respect to *cis* and *trans* isomers of unsaturated compounds. Note, however, that with LiNO_3 alone a clear separation of olefinic hydrocarbons was unobtainable when steam–nitrogen was used as the mobile phase. Both *cis* and *trans* isomers and double-bond positional isomers were successfully separated with a mixed LiNO_3 – AgNO_3 stationary phase (Table IV).

When using a sorbent containing 20% AgNO_3 on Celite C-22 the best efficiency was found for alkenes [height equivalent to a theoretical plate (HETP) of *cis*-5-tridecene – 0.42 mm] and for unsaturated esters (HETP for allyl methacrylate – 0.63 mm). For the alcohols the efficiency was poorer (HETP for ethanol = 1.2 mm). This can be explained by the especially strong interaction of alcohols with water–salt solutions.

In Fig. 1 the chromatogram of dissolved C_{10} – C_{13} alkenes is shown. Almost all the peaks are symmetrical. The stationary phases investigated are highly selective

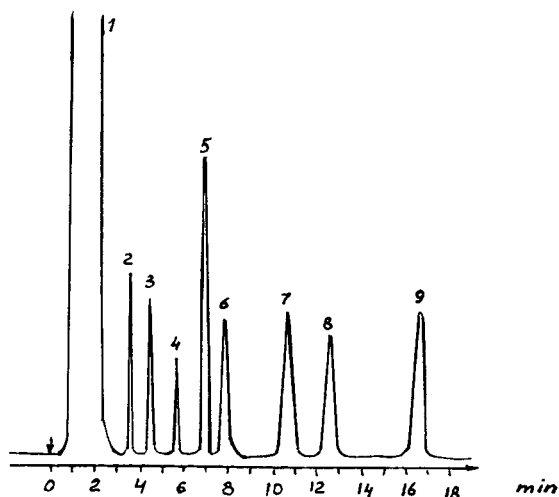


Fig. 1. Separation of C_{10} – C_{13} olefins on AgNO_3 using steam as the mobile phase at 108°C. Experimental conditions: stationary phase, 20% AgNO_3 on Celite C-22; stainless-steel column (2 m \times 3 mm I.D.). Peaks: 1 = hexane; 2 = *trans*-5-decene; 3 = 1-decene; 4 = *cis*-5-decene; 5 = *trans*-6-dodecene; 6 = 1-dodecene; 7 = *cis*-6-dodecene; 8 = *trans*-5-tridecene; 9 = *cis*-5-tridecene.

towards alkenes. The difference in the retention indices for decene isomers, $\Delta I = I_{\text{cis-5-decene}} - I_{\text{trans-5-decene}}$, is 76 units, *i.e.* the selectivity towards these isomers is essentially higher than that with known polar and non-polar stationary phases. For example, with squalane this difference is 3 units [5], with Apiezon L 2 units [6] and with dibutyl tetrachlorophthalate 6 units [7].

CONCLUSIONS

Pure and mixed inorganic salts impregnated on a solid support with steam as the mobile phase can be used to obtain highly effective packed columns.

The simultaneous use of nitrate solutions (*e.g.*, lithium, aluminium and zinc nitrates) as stationary phase and steam as the mobile phase at 105–110°C permits good separations of *cis* and *trans* isomers of unsaturated hydrocarbons, especially high-boiling C₁₃–C₁₄ compounds, to be obtained.

Good separations of polar unsaturated compounds (alcohols and esters) are obtained with steam as the mobile phase and stationary phases containing both pure LiNO₃, and a salt mixture (AgNO₃ + LiNO₃).

The selectivity of the inorganic salt phase deteriorates when the water content in mixed mobile phase decreases, in addition to the temperature of nitrogen saturation with water vapour.

REFERENCES

- 1 A. Zlatkis and J. M. R. de Andrade, *Chromatographia*, 2 (1969), 38.
- 2 S. P. Wasik and R. L. Brown, *Anal. Chem.*, 48 (1976) 2218.
- 3 E. N. Viktorova, V. G. Berezkin and V. S. Gavrichev, *J. Chromatogr.*, 398 (1987) 317.
- 4 V. G. Berezkin, E. N. Viktorova and V. S. Gavrichev, *J. Chromatogr.*, 456 (1988) 351.
- 5 L. Sojak, J. Hrivnak and P. Major, *Anal. Chem.*, 45 (1973) 293.
- 6 A. Wherli and E. Kovats, *Helv. Chim. Acta*, 42 (1959) 2709.
- 7 M. Ryba, *Chromatographia*, 5 (1972) 23.

CHROMSYMP. 2250

Reaction-gas chromatography for physico-chemical investigations on aggressive gases

L. G. BEREZKINA*, S. I. BORISOVA, S. V. MELNIKOVA and V. I. SOUHODOLOVA

Research Institute for Fertilizers, Insecticides and Fungicides, Leninsky Prospect 55, Moscow 117333 (U.S.S.R.)

ABSTRACT

Reaction-gas chromatographic methods for determining aggressive gases such as HClO_4 , HF and NH_3 were developed. The methods were used for examining thermal decomposition processes of $\text{Be}(\text{ClO}_4)_2 \cdot 4\text{H}_2\text{O}$, $\text{AlF}_3 \cdot 3\text{H}_2\text{O}$ and $\text{NH}_4\text{H}_2\text{PO}_4$. The additional requirements arising when using reaction conversions in physico-chemical investigations were examined.

INTRODUCTION

Chromatography is widely used for physico-chemical investigations [1,2]. In previous papers [3–5] we have proposed a number chromatographic methods for studying the kinetics and equilibrium of heterogeneous chemical processes that proceed with gaseous components present. The methods are based on direct insertion of a chemical reactor into the gas line of a chromatograph. The conditions of the application of gas chromatography to studies of the kinetics and equilibria of heterogeneous reactions in gas-condensed phase systems have been substantiated. It was shown [3] that with thermal conductivity detection (TCD) the signal height is directly proportional to the rate of gas evolution in the process being studied. By increasing the amount of condensed phase in the reactor, a maximum constant concentration, *viz.*, partial equilibrium pressure, of volatile product in the carrier gas was attained [4].

With a multi-component composition of gaseous products, it is proposed to use schemes with the flow being split after the reactor and two detectors, and to use selective absorption (removal) of some components from the gas stream.

In the chromatographic analysis of gases, the determination of aggressive and hardly detectable species is a real and often difficult problem. In the chromatographic methods described above, it is proposed to use reaction conversion of such gases into other gases that easily detected by TCD. For this purpose, into the gas line of the chromatograph after the main reactor where the process being studied takes place is introduced an additional reactor for reaction conversion of aggressive component.

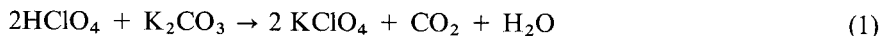
In order to apply reaction-gas chromatography to kinetic studies, it is necessary

to establish the following specific conditions. In kinetic experiments, conversion of a reaction component should proceed faster than its rate of formation in the process being studied. Quantitative conversion of a component should be provided over a wide range of concentrations in accordance with minimum and maximum rates of its formation in the main process. The reactor volume for analytical conversion (and amounts of chemical reagents) should be sufficiently small that the broadening in the additional volume does not distort the shape of the evolving product zone. The volume of the reactor is selected in preliminary tests.

In this paper, reaction-gas chromatographic methods for determining the aggressive gaseous compounds HClO_4 , HF and NH_3 are described. The peculiarities of the application of the methods to physico-chemical investigations are considered using the following examples: (i) thermal decomposition of $\text{Be}(\text{ClO}_4)_2 \cdot 4\text{H}_2\text{O}$; (ii) kinetics and equilibrium of the $\text{AlF}_3 \cdot 3\text{H}_2\text{O}$ dehydration process; and (iii) equilibrium of ammonium phosphate decomposition.

EXPERIMENTAL

The thermal decomposition of $\text{Be}(\text{ClO}_4)_2 \cdot 4\text{H}_2\text{O}$ proceeds with the evolution of water and highly aggressive, thermally labile HClO_4 . Thermolysis of this salt was studied at 130–350°C in a carrier gas (helium) flow. For the detection of HClO_4 evolved during thermolysis of the perchlorate, an exchange reaction method (eqn. 1) involving the formation and subsequent detection of CO_2 was employed:



A schematic diagram of the apparatus used for this purpose is presented in Fig. 1. A mixture of anhydrous potassium carbonate (granular) and quartz particles (diameter between 0.25 and 0.5 mm) was placed on a glass porous partition (Schott No. 1 standard filter) in the hot zone of reactor 1 above the weighed perchlorate sample 9. The reactor was placed in a preliminary heated (to a given temperature) oil-bath.

To establish the accuracy and precision of the procedure, the following aspects were established.

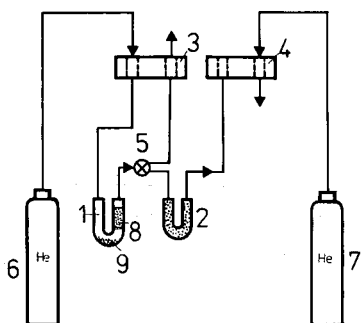


Fig. 1. Schematic diagram of apparatus for reaction exchange and detection of HClO_4 : 1 = reactor; 2 = absorber for water; 3, 4 = katharometers; 5 = flow-dividing valve; 6, 7 = carrier gas tanks; 8 = potassium carbonate; 9 = perchlorate sample.

(1) The perchloric acid evolved does not decompose until it comes into contact with the potassium carbonate. No acid decomposition products (oxygen, chlorine or chlorine oxides) were apparently formed. This conclusion was made based on the following special experiments. After the reactor for K_2CO_3 , H_2O and CO_2 from the gaseous phase were absorbed (in the cartridge containing granular KOH); with TCD recording no gas evolution at all was observed. Moreover, the absence of chlorine and chlorine oxides in the off-gases was confirmed by a chemical iodimetric method.

(2) The primary potassium carbonate and potassium perchlorate formed are thermally resistant under the test conditions. This was confirmed by the absence of gas evolution in the primary potassium carbonate and perchlorate formed (in the absence of an exchange reaction) at $350^\circ C$.

(3) The quantitative aspects of the exchange reaction in eqn. 1 were controlled on the basis of the stoichiometry, proceeding from the known ClO_4^- ion content in the perchlorate sample of known weight. The exchange reaction proceeds quantitatively over the entire range of concentrations corresponding to the initial perchlorate decomposition rate of $0.05\%/min$ and a maximum rate of $8\%/min$.

(4) The exchange reaction is not rate limiting, and the determination of carbon dioxide evolution rate reflects the perchlorate decomposition kinetics. To establish this, tests were conducted in a special reactor, in which in the process of perchlorate decomposition a carrier gas flow was fed below the net partition by switching a valve; delivery of $HClO_4$ to carbonate was stopped and no CO_2 was registered by the detector. Therefore, perchloric acid in the potassium carbonate layer is not accumulated, *i.e.*, the exchange reaction proceeds faster than the decomposition being studied.

In the process of $Be(ClO_4)_2 \cdot 4H_2O$ decomposition, water is evolved together with perchloric acid; moreover, 1 mol of water per mole of compound is evolved as a result of the exchange reaction.

To record the kinetics of CO_2 and H_2O evolution simultaneously, an installation (Fig. 1) with two thermal conductivity detectors was used, the flow after the reactor being split into two streams. In one stream, water vapour was absorbed in the cartridge containing anhydrous magnesium perchlorate (2), and detector 4 recorded the concentration of CO_2 formed in the exchange reaction (see Fig. 3, curve a); in the other stream, detector 3 measured combined H_2O and CO_2 evolution. The rate and amount of water evolved were determined by the differences in heights and areas on the basis of H_2O and CO_2 detector calibrations, each made separately (differences with stoichiometric quantities for CO_2 and H_2O did not exceed 3 and 4%, respectively).

To detect HF evolved from the thermolysis of $AlF_3 \cdot 3H_2O$, reaction of the former with $CaCO_3$, leading to the formation of CO_2 , was used.

Analytical validation of the above procedure was accomplished in the following way: HF equilibrium partial pressures above hydrofluoric acid solutions of known concentration were measured and the values obtained were compared with literature data [6]. Details of the procedure are as follows: The hydrofluoric acid solution was coated on to the quartz layer in the reactor and a carrier gas (helium) flow, saturated with water vapours and HF , was passed through the $CaCO_3$ layer. Water vapour was absorbed in the cartridge containing anhydrous magnesium perchlorate and the CO_2 concentration in this flow was detected. In Fig. 2 the data obtained are presented in

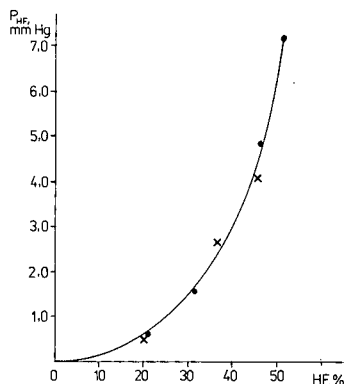


Fig. 2. Partial pressure of HF vapour (P_{HF}) versus HF concentration in solution at 25°C. ●, Literature data; ×, experimental data.

comparison with the literature data. The maximum deviation does not exceed 10% relative.

To control ammonia and water evolution in the initial stages of ammonium dihydrogenphosphate decomposition, the data on which are contradictory, a method was used based on ammonia oxidation with potassium hyperbromite solution in accordance with the reaction



The characteristics of the method have been presented previously [7].

It was shown, however, that the reaction conversion proceeds slowly owing to diffusive retardation in the solution, and is rate-limiting with regard to the kinetics of ammonium dihydrogenphosphate decomposition. Consequently, the dynamic (flow) modification of the method described was used only to study equilibrium of ammonium dihydrogenphosphate decomposition at low temperature.

RESULTS AND DISCUSSION

In Fig. 3, kinetic curves for gaseous product evolution under conditions of heating at a constant rate of $\text{Be}(\text{ClO}_4)_2 \cdot 4\text{H}_2\text{O}$ are presented as examples. The de-

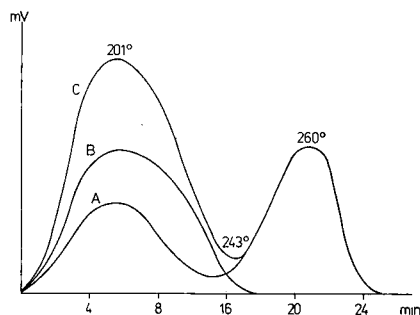
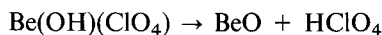


Fig. 3. Kinetic curves of $\text{Be}(\text{ClO}_4)_2 \cdot 4\text{H}_2\text{O}$ decomposition: (a) $\text{HClO}_4(\text{CO}_2)$ evolution; (b) H_2O evolution; (c) $\text{HClO}_4(\text{CO}_2) + \text{H}_2\text{O}$ evolution.

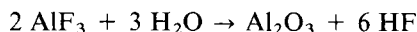
composition starts at 140°C and proceeds with splitting of the process into two macrostages. Perchloric acid (as CO₂) and water appear in the gaseous phase simultaneously, *i.e.*, evolution of the water of hydration does not occur as a preliminary process. In the first stage 3 mol of water are removed, 1 mol of which takes part in the pyrohydrolysis with the formation of HClO₄. The perchloric acid (CO₂) is evolved in two stages; the degree of decomposition in the minimum of the kinetic curve a in Fig. 3 is 50%.

On the basis of kinetic data for the reaction mixture formed in the minimum of the kinetic curve, the decomposition scheme of perchlorate is considered to be



The formation of the intermediate product was ascertained by NMR and X-ray diffraction analysis.

It was found that the dehydration of AlF₃ · 3H₂O occurs in one macrostage, the main amount of water being evolved at 100–160°C; however, 0.2–0.25 mol of water per mole of salt is held in the aluminium fluoride lattice; the removal of residual water occurs on further heating to 400–450°C and is accompanied by a pyrohydrolysis process:



The respective kinetic curves are presented in Fig. 4.

The carrier gas flow was saturated with water when passing through the AlF₃ · 3H₂O layer and equilibrium water vapour pressures were determined (1.7, 4.3, 12.1, 57.1, 160.7 and 598.8 mmHg at 89.6, 100.4, 113.8, 127.5, 134.5 and 150.7°C, respectively).

Fig. 5 represents the dependence of P_{NH_3} on the temperature of the ammonium

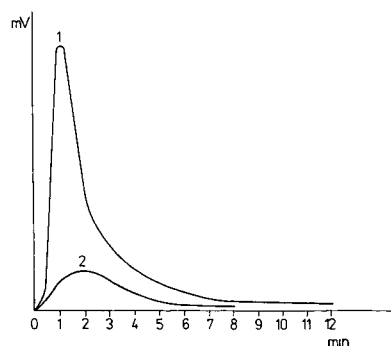


Fig. 4. Evolution kinetic curves: HF: curve 1, $n = 1$, maximum detection for sensitivity. H₂O: curve 2, $n = 10$, detector response attenuated by a factor of 10.

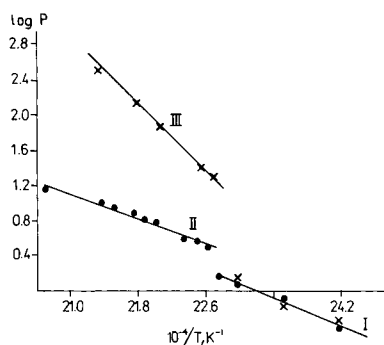


Fig. 5. Vapour pressure (P) of (●) NH₃ and (×) H₂O versus temperature (T) in the thermal decomposition of ammonium dihydrogenphosphate. I, solid phase decomposition; II and III decomposition in the melt.

dihydrogenphosphate thermal decomposition process obtained by the above-mentioned procedure involving ammonia oxidation to elemental nitrogen.

In conclusion, the examples presented demonstrate the use of reaction gas chromatographic methods for detecting the reactive gases HClO_4 , HF and NH_3 in physico-chemical investigations. Similar methods may be suitable for other reactive gases.

REFERENCES

- 1 S.Z. Roginsky, M. I. Yanovsky and A. D. Berman, *Osnovnie Primeneniya Khromatografii v Katalize*, Nauka, Moscow, 1972.
- 2 A. V. Kiselev and Ya. I. Yashin, *Gas und Flüssigkeits Adsorptionchromatographie*, Hüthig, Heidelberg, 1985.
- 3 L. G. Berzkina, S. I. Borisova and N. Tamm, *J. Chromatogr.*, 69 (1972) 31–36.
- 4 L. G. Berezkina, S. I. Borisova and S. V. Melnikova, *J. Chromatogr.*, 365 (1986) 423–428.
- 5 L. G. Berezkina and V. I. Souhodolova, *J. Chromatogr.*, 457 (1988) 159–164.
- 6 G. Ryss, *Khimiya Ftora i ego Neorganicheskikh Soedinenii*, Gozkimizdat, Moscow, 1956, pp. 83–86.
- 7 L. G. Berezkina, S. V. Melnikova and V. I. Souhodolova, *Zh. Anal. Khim.*, 28 (1973) 177–179.

CHROMSYMP. 2294

Thermodesorption–gas chromatography–mass spectrometric analysis of biological materials for potential molecular precursors of the constituents of the crude oils

WILHELM PÜTTMANN

Lehrstuhl für Geologie, Geochemie und Lagerstätten des Erdöls und der Kohle, RWTH Aachen, Lochnerstrasse 4-20, W-5100 Aachen (Germany)

ABSTRACT

Thermodesorption technique coupled on-line with gas chromatography (GC) and mass spectrometry (MS) has been developed for the determination of hydrocarbons trapped in coal and rock samples. The method can also be applied to the determination of volatile constituents present in biological materials. The desorption step is carried out in the pre-heated injector of a gas chromatograph. The mobilized compounds are transferred without splitting to the initial part of a cold GC column. After 10 min of desorption the GC–MS analysis is started. The identification of individual compounds is achieved by GC–MS analysis of related molecular ions or significant fragment ions. When micro-samples (0.25–2.0 mg) of dried plant material are heated to 300°C in a helium stream, compounds such as long-chain fatty acids, carboxylic acid esters, aldehydes and ketones as well as steroids and tocopherols are desorbed from the biological matrix without decomposition. In addition, the thermally labile chlorophylls decompose to yield phytadienes as pyrolysis products of the phytol moiety. The phytadienes can be used to estimate the original amount of chlorophyll present in the sample and to determine the chlorophyll:tocopherol ratio in different algae and terrestrial plant materials. This ratio partly reflects the pristane:phytane concentration ratio determined in extracts of mature sediments rich in related fossilized biological materials. The analysis also provides chemotaxonomic information about the sterol composition of plants.

INTRODUCTION

The isoprenoid alkanes pristane (C₁₉H₄₀) and phytane (C₂₀H₄₂) are common constituents of ancient rocks, coals and crude oils. Both compounds have been suggested to originate from chlorophyll as the major precursor molecule [1]. Oxidation during the earliest stages of chlorophyll decomposition generates phytanic acid, the precursor of pristane. Under anaerobic conditions the phytol side-chain of chlorophyll is reduced to phytane after hydrolysis. Low pristane:phytane concentration ratios in crude oils were once thought to indicate a primary marine plant input, whereas land plant material was thought to produce the high pristane:phytane ratios commonly observed in coals [1]. However, organic geochemical research has shown that a wide variety of potential precursor molecules for both compounds exist in nature, including tocopherols [2] and archaeobacterial diphytanyl ethers [3,4]. The significance of the pristane:phytane ratio as a palaeo-environmental indicator [5] has

been questioned based on these findings and by considering the geological constraints of a large set of crude oils and rocks which have been investigated [6]. However, it remains to be clarified whether the pristane:phytane ratio in fossil materials is primarily controlled by palaeo-environmental conditions during sedimentation or by the type of organic matter input. This is unclear largely as a result of insufficient knowledge about the abundance and relative amounts of potential precursor molecules for pristane and phytane in recent plant material.

In this study, thermodesorption (TD) coupled on-line to gas chromatography (GC) and mass spectrometry (MS) is used for the analysis of plant material for pristane and phytane precursors and also for sterols as precursor molecules of steranes in crude oils and coals.

Volatile compounds emitted from plants have recently been analysed using head-space analytical techniques [7,8], overcoming the difficulties in isolating these volatiles by conventional solvent extraction and separation methods [7]. The advantage of the application of head-space techniques is the avoidance of contamination during the extraction and treatment of extracts. Plant constituents which are volatile at higher temperatures can be recovered in a similar way by the thermal treatment of samples in an inert gas atmosphere. However, this can cause not only desorption of the molecules present in the plant, but also the generation of fragments from high-molecular-weight compounds and biopolymers. A useful method to study the nature of biopolymers is pyrolysis combined with GC and MS [9–11]. An alternative approach is the application of pyrolysis combined with field ionization MS. The application of this method to spruce needles provided information about the chemical structure of pyrolysis products generated from macromolecules and at the same time information about the content of thermally stable constituents such as α -tocopherol and β -sitosterol in plants [12,13].

This study focusses on the qualitative analysis of thermally stable plant constituents of molecular mass less than 500. The compounds are thermally extracted from plant material in a helium gas flow using a desorption temperature of 300°C. As the recovery rates for individual compounds have not yet been determined, the method cannot provide quantitative data at this stage. The method has previously been used to study the hydrocarbon content of coals and rock samples [14,15] and the uptake of atmospheric pollution by plant waxes [16].

EXPERIMENTAL

Samples

The sample material analysed and amount of sample used for the analysis are listed in Table I. The *Chlorococcales* algae were cultured in the laboratory; algae samples 4–8 originate from the North Sea. The spruce and pine needles were taken from trees in a remote area of the Eifel mountains of western Germany.

The samples were stored in a deep freezer and then dried under a nitrogen atmosphere before carrying out the analysis. The amount of sample required for the analysis depended on the lipid content of each sample and on the sensitivity of the mass spectrometer.

TABLE I
SAMPLES ANALYSED USING TD-GC-MS

Sample no.	Sample	Amount analysed (mg)
1	<i>Tetraedron minimum</i> (Chlorococcales)	0.830
2	<i>Chlorella fusca</i> (Chlorococcales)	0.638
3	<i>Pediastrum duplex</i> (Chlorococcales)	0.250
4	<i>Scenedesmus obliquus</i> (Chlorococcales)	0.322
5	<i>Fucus</i> sp. (Phaeophyceae)	0.830
6	<i>Halidrys</i> sp. (Phaeophyceae)	0.670
7	<i>Cladophora</i> (Chlorophyceae)	0.520
8	<i>Plocamium</i> (Rhodophyceae)	0.984
9	Spruce needles	1.851
10	Pine needles	1.815

Thermodesorption

Crushed sample material is placed in small glass tubes (10 × ca. 1 mm I.D.) with one end sealed. The glass tubes are pre-heated in a gas flame to remove contamination before the sample is introduced. The exact sample weight is determined using a micro-scale autobalance (Perkin-Elmer).

Thermodesorption is carried out with an autosampler commonly used with elemental analysers (Carlo Erba), which is mounted on top of a split-splitless injection system for GC (Varian). The autosampler drops the glass tubes into the liner of the heated injection port under a helium atmosphere. Helium is also used as the carrier gas for GC. The injection port is operated at a temperature of 300°C in the splitless mode. Volatile compounds present in the sample are transferred to the inlet end of the GC column where they are trapped. Test measurements revealed that a desorption time of 10 min is sufficient for a complete release of the desorbable compounds. The glass tubes are removed from the GC liner after each run.

Gas chromatography

Trapping of the desorbed compounds is achieved by maintaining the oven temperature of the gas chromatograph at 40°C during thermodesorption. The GC separation is carried out using a Varian 3700 gas chromatograph equipped with a 25 m × 0.25 mm I.D. fused-silica column coated with chemically bonded SE-54 silicone as the stationary phase (film thickness 0.25 μm). After the completion of desorption the oven temperature is increased from 40 to 300°C at a rate of 4°C/min and held at the final temperature for 20 min.

Mass spectrometry

The GC capillary column is directly routed into the ion source of a Finnigan MAT 8200 mass spectrometer, which is operated with an electron energy of 70 eV, an emission current of 1.0 mA and an ion source temperature of 240°C. The mass spectra are recorded from 50 to 700 mass units with a scan time of 1.1 s. The data are processed with an INCOS data system. Mass chromatography is used for the selective registration of individual ions.

Determination of the relative intensities has been carried out by comparing the peak integration data of phytadienes (for chlorophyll) and of α -tocopherol and the steroids using the reconstructed ion chromatogram (RIC) intensities. When superimposition with other compounds occurred, the data were obtained from mass chromatograms of fragments or molecular ions using a correction factor determined by comparing the peak intensity in the mass chromatogram and the RIC of a sample where superimposition of the compound is not visible.

RESULTS AND DISCUSSION

Lipids with long carbon chains

The RIC in the scan range 1200–4100 obtained from the GC–MS analysis of *Tetraedron minimum* (sample 1) is shown in Fig. 1. Constituents with lower boiling points ($<200^{\circ}\text{C}$) were not detected in this sample. Two major compounds are the n - C_{16} fatty acid (3) and the n - C_{18} monounsaturated fatty acid (5). The dominance of the C_{18} unsaturated fatty acid over the C_{16} fatty acid has been reported previously [17] to be a typical feature of green algae. Owing to their high polarity, both compounds elute from the SE-54 column as broadened peaks. This is unavoidable because the total lipid content of the algae, which ranges from non-polar to highly polar compounds, is transferred to the column. Except for fatty acids, other types of compounds are sufficiently resolved by the SE-54 capillary column. n -Alkanes are minor constituents of the desorbed material with the exception of n -heptadecane (1) and n -tricosane (6). The dominance of these two n -alkanes is very rare in plant materials

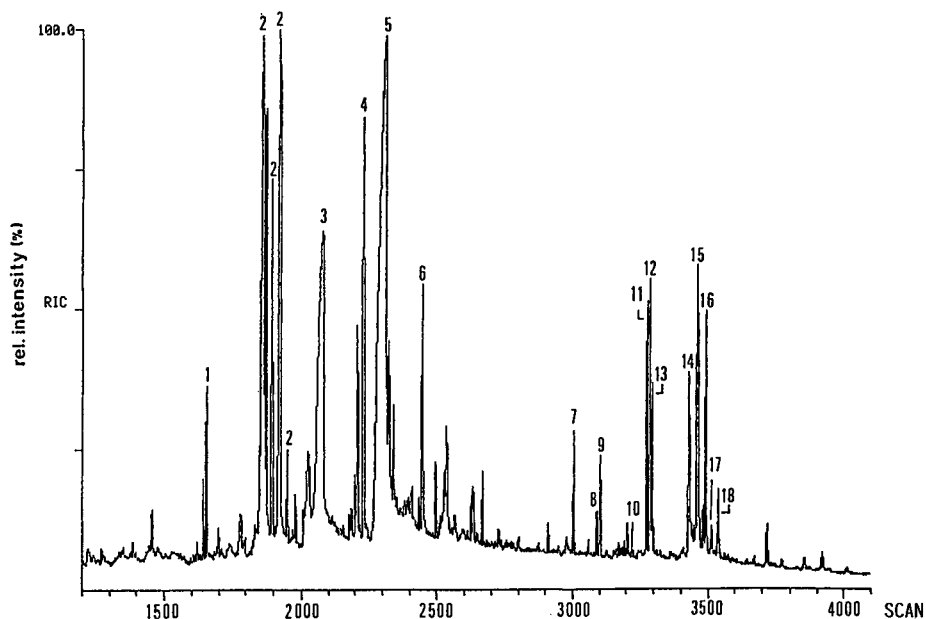


Fig. 1. RIC in the scan range 1200–4100 obtained by GC–MS analysis of the volatile material thermally desorbed from the algae *Tetraedron minimum* at 300°C . For identification of compounds see Table II.

and in sedimentary extracts. Twenty years ago the predominance of $n\text{-C}_{17}$ and $n\text{-C}_{23}$ within the n -alkane pattern of the Eocene Green River oil shale was ascribed to the abundance of *Tetraedron* sp. in this shale [18]. Recently, combined morphological and organic geochemical investigations have shown this abundance to also exist in the Eocene Messel lake sediment deposits near Darmstadt, Germany. *Tetraedron* algae, identified by scanning electron microscopy as *Tetraedron minimum*, make up the major part of the organic matter in the sediment [10,19].

In the lower boiling point range of the thermal extract of *Tetraedron minimum* phytadienes [2] are present at a relatively high abundance, in addition to fatty acids and n -alkanes. The elution order of the five possible isomers has been partly clarified [20]. It has been proposed that phytadienes are short-lived geochemical intermediates which are easily incorporated into the macromolecular network in sediments [20]. Nevertheless, phytadienes have been detected in the paraffinic fractions of extracts of green and brown leaves recently deposited on soil [21]. Attempts to find the compounds in the solvent extracts of the samples analysed in this study failed. Their absence in fresh biological materials indicates that the formation of phytadienes in living plants is not an important process.

Two isomeric phytadienes are generated as main products of pyrolysis of authentic chlorophyll [22]. Thus, under these TD conditions phytadienes can be expected to be the degradation products of chlorophyll present in algae and spruce and pine needles. The amount of phytadienes in the thermal extracts allows the calculation of the amount of chlorophyll in the samples analysed, assuming that complete decomposition of the chlorophyll occurs. Phytol (compound 4 in Table II) survives the thermal

TABLE II

COMPOUNDS IDENTIFIED BY GC-MS ANALYSIS OF THE THERMAL EXTRACT OF *TETRAEDRON MINIMUM*

Compound No.	Compound name	Molecular weight
1	<i>n</i> -Heptadecane	240
2	Phytadienes	278
3	<i>n</i> -Hexadecanoic acid	256
4	Phytol	296
5	<i>n</i> -Octadecenoic acid	282
6	<i>n</i> -Tricosane	324
7	Squalene	410
8	2-Heptacosanone	394
9	<i>n</i> -Hexacosanoic acid methyl ester	410
10	γ -Tocopherol	416
11	2-Nonacosanone	422
12	<i>n</i> -Octacosanoic acid methyl ester	438
13	α -Tocopherol	430
14	Ergost-7-en-3-ol	400
15	Stigmast-7,22-dien-3-ol	412
16	Octacosadienal	404
17	Stigmast-7-en-3-ol	414
18	α -Tocopherolquinol	448

treatment at 300°C as it is present in most of the thermal extracts investigated. Consequently, the phytadienes must originate primarily from chlorophyll which has not yet been hydrolysed.

In the higher boiling point range of the thermal extracts, apart from the olefinic hydrocarbon squalene (7), a set of polar compounds can be detected (Fig. 1 and Table II). These compounds are methyl ketones (8,11), methyl esters of long-chain carboxylic acids (9,12), an unsaturated aldehyde (16) and alcohols such as tocopherols (10, 13, 18) and sterols (14, 15, 17). Despite the polar nature of the compounds they appear as relatively sharp peaks, which indicates that the method allows a simultaneous recognition of volatile plant constituents over a wide polarity range.

Tocopherols

Tocopherols have recently attracted the interest of organic geochemists. α -Tocopherol has been reported to be present in soil extracts [21] and in a wide variety of sedimentary extract [23]. The thermal degradation of α -tocopherol at 350°C yields duroquinone and degradation products of pristene [24]. Tocopherols are remarkably stable under thermal treatment, although the compounds are known to be highly reactive chemically. Under flash pyrolysis conditions at 610°C tocopherol partly survives [2]. During the thermal treatment used in this study, degradation products of tocopherols such as prist-1-ene have not been detected. Thus TD at 300°C appears to be a suitable method for the mobilization of tocopherols from a biological matrix without decomposition.

Fig. 2 shows the presence of tocopherols in the thermal extract of the algae *Tetraedron minimum* using mass chromatography of the base peak ions. γ -Tocopherol is recognized in the mass chromatogram of m/z 151 (Fig. 2a) and α -tocopherol using m/z 165 (Fig. 2b) The base peak integration data show that γ -tocopherol contributes only approximately 5% to the total tocopherol content. An additional compound tentatively identified from mass spectral data is α -tocopherolquinol (18), the hydrolysis product of α -tocopherol. This compound has previously been reported to occur mainly in microorganisms [25]. The other *Chlorococcales* algae investigated here differ from *Tetraedron minimum* in so far as the α -tocopherolquinol was only detected in *Tetraedron minimum*. The role of tocopherols in nature is not fully understood. It has been postulated that the compounds are intermediates in the electron transport associated with both photosynthesis and respiration [26]. The ratio of chlorophyll to tocopherols has therefore been examined in leaves and subcellular fractions from leaves. Chlorophyll:tocopherol concentration ratios ranging from 8.3 to 100 have been determined in various plant materials [27]. The chlorophyll:tocopherol content has been calculated in the samples analysed based on the assumption that the amount of phytadienes generated during thermal extraction reflects the original chlorophyll content of the biological material investigated. Only the peak integration data of α -tocopherol have been used for the calculation. Table III shows that this ratio varies in the algae from 8.4 to 127, which is in a similar range to that described by Bucke *et al.* [27]. Remarkably, the spruce and pine needles have much lower ratios, with values of 3.0 and 1.9, respectively. On average, the *Chlorococcales* algae tend to have higher chlorophyll:tocopherol ratios than the various marine algae.

Based on these findings, higher pristane:phytane concentration ratios should be predicted in fossil material derived from higher plants than in material derived from

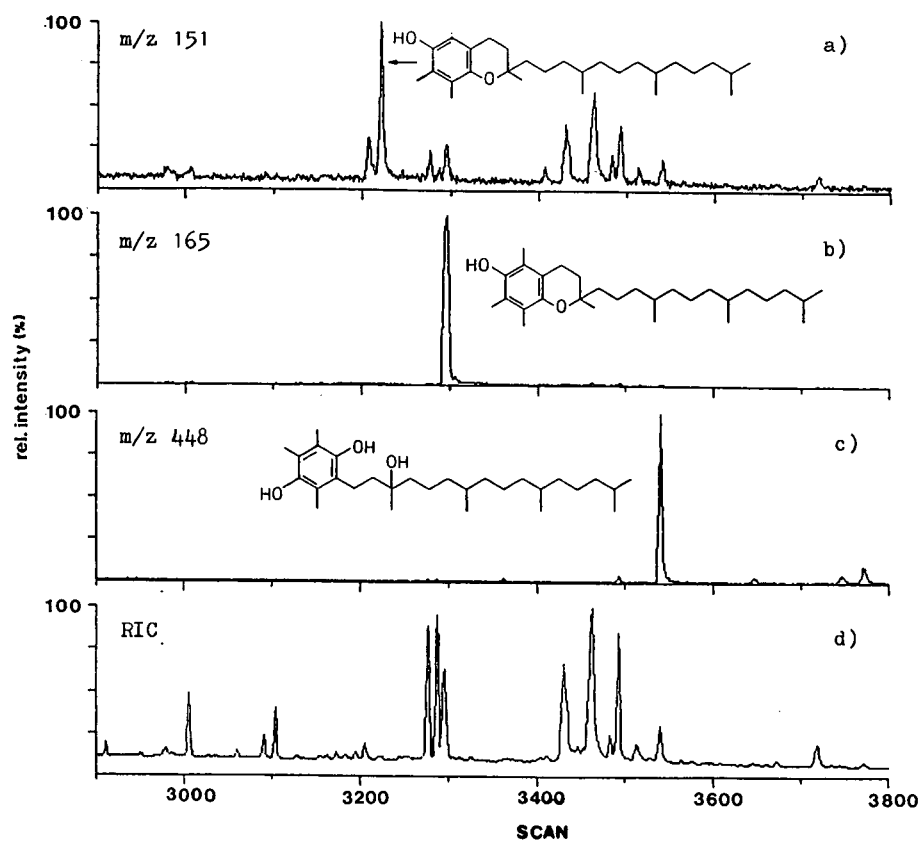


Fig. 2. Identification of tocopherol compounds within the desorbed material of the algae *Tetraedron minimum* (sample 1, in Table I) using GC-MS analysis. Within the scan range 2900-3800 γ -tocopherol is recognized by mass chromatography of m/z 151 (a), α -tocopherol by mass chromatography of m/z 165 (b) and α -tocopherolquinol by mass chromatography of m/z 448 (c). In addition to the mass chromatograms, the RIC is shown in (d).

TABLE III

RELATIVE INTENSITIES OF CHLOROPHYLL *VERSUS* α -TOCOPHEROL AND OF CHLOROPHYLL *VERSUS* THE SUM OF DETECTABLE STEROIDS IN THE ANALYSED SAMPLES

Chlorophyll content estimated from peak integration data of phytadienes in GC-MS analysis.

Sample material	Chlorophyll: α -Tocopherol	Chlorophyll: Steroids
<i>Tetraedron minimum</i>	28.8	3.8
<i>Chlorella fusca</i>	46.3	4.3
<i>Pediastrum duplex</i>	12.7	8.0
<i>Scenedesmus obliquus</i>	37.6	10.7
<i>Fucus</i> sp.	16.0	2.6
<i>Halidrys</i> sp.	8.4	2.1
<i>Cladophora</i>	40.9	4.1
<i>Plocamium</i>	18.6	11.4
Spruce needles	3.0	1.9
Pine needles	1.9	0.8

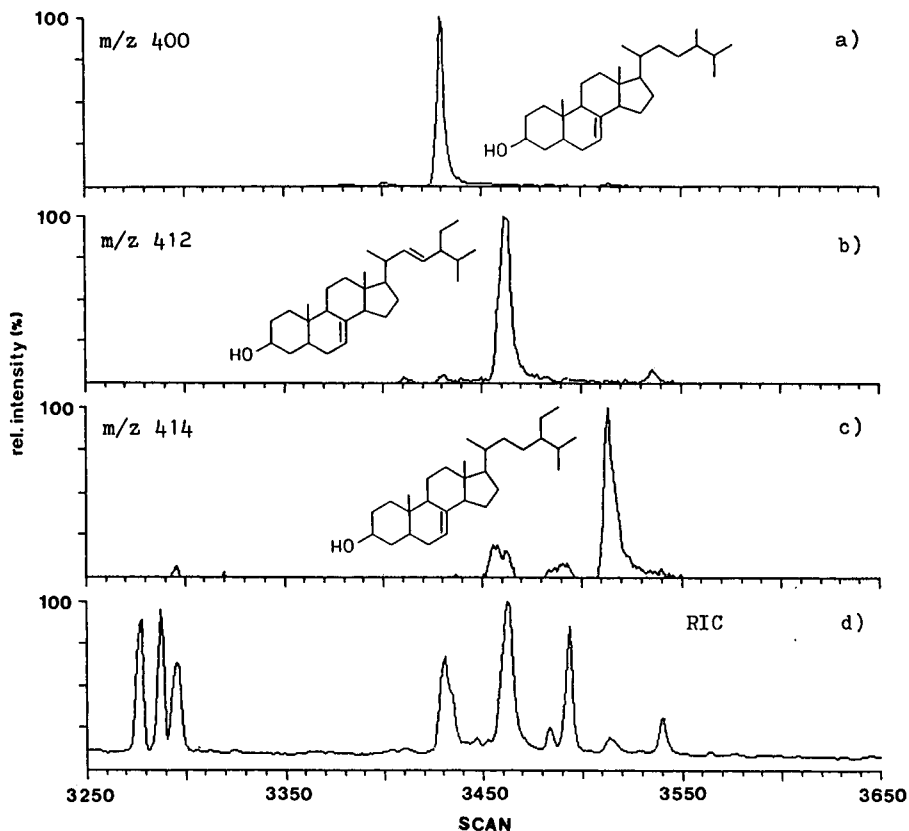


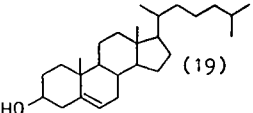
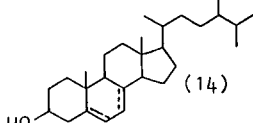
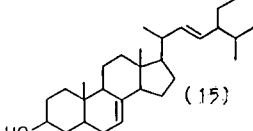
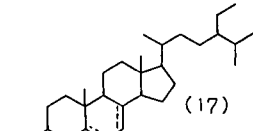
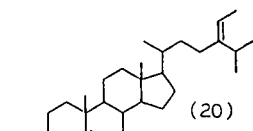
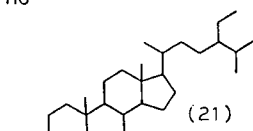
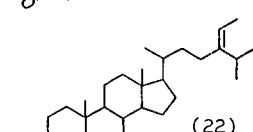
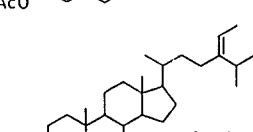
Fig. 3. GC-MS analysis of sterols present in the desorbed material of the algae *Tetraedron minimum* (sample I in Table I). Mass chromatography is used for the identification of three individual sterols: (a) m/z 400 for ergost-7-en-3-ol; (b) m/z 412 for stigmast-7,22-dien-3-ol; and (c) m/z 414 for stigmast-7-en-3-ol. The RIC in the scan range 3200–3650 is shown in trace (d). The estimated relative intensities of the sterols are given in Table IV.

algae, assuming that the phytol generated by the hydrolysis of chlorophyll is completely converted to phytane and that the tocopherol is degraded to pristane after burial and heating of the biological material in sediments. In fact, high-volatile bituminous A coals are known to provide extracts with very high pristane:phytane ratios of up to fifteen [28,29], whereas in crude oils generated in hypersaline environments the pristane:phytane ratios are often less than 0.5 [5]. Thus the tendency observed in the biological material investigated here is partly reflected by what is already known from fossil material. However, there are many other potential precursor molecules present in nature. For example, in coals, which are in general deposited and coalified under oxidizing conditions, the proposed pathway [1,5] of pristane generation from phytol via oxidation to phytanic acid and the subsequent decarboxylation may enhance the pristane:phytane ratios.

TABLE IV

DISTRIBUTION OF STEROLS AND STEROIDAL KETONES ANALYSED IN THE MATERIAL DESORBED FROM EIGHT ALGAE AND TWO NEEDLES FROM HIGHER PLANTS

The sample numbers reflect the analysed specimen listed in Table I. Abundance: X = low, XX = moderate and XXX = high. Ac = Acetyl.

Structures of Compounds	Sample numbers									
	1	2	3	4	5	6	7	8	9	10
 (19)	-	-	-	-	-	-	-	XX	-	-
 (14)	Δ^7 XX	Δ^7 XX	Δ^7 XX	Δ^7 XX	-	-	Δ^5 X	-	Δ^5 XX	-
 (15)	Δ^7 XXX	Δ^7 XXX	Δ^7 XXX	Δ^7 XXX	-	-	-	-	-	-
 (17)	Δ^7 X	Δ^7 X	Δ^7 X	Δ^7 X	-	-	Δ^5 XXX	-	Δ^5 XX	Δ^5 XX
 (20)	-	-	-	-	XXX	X	-	-	-	-
 (21)	-	-	-	-	-	-	X	-	XX	X
 (22)	-	-	-	-	-	X	-	-	-	-
 (23)	-	-	-	-	-	XX	-	-	-	-

Steroids

More than 70 years ago it was recognized that sterols can be converted into petroleum-like substances by thermal or chemical treatment [30]. A major interest in organic geochemical research is to reconstruct the reaction pathways of steroids found in the sedimentary record back to their precursor biological material. This requires a knowledge of the steroid composition of recent and ancient biological input materials and the possible transformation processes which affect the sterols in sediments. A summary of the current state of knowledge of the biological occurrence of steroids with different side-chains and their geological fate has been presented by Mackenzie *et al.* [31]. The lack of information concerning the steroid composition of biological materials is mainly due to time-consuming preparative procedures, including the derivatization of sterols prior to GC analysis. This work shows that sterols survive thermal desorption in an atmosphere of inert gas. The compounds are recovered by on-line GC-MS analysis as relatively sharp peaks, which provide rapid information about the steroid composition of biological material without any pretreatment of the samples except for drying.

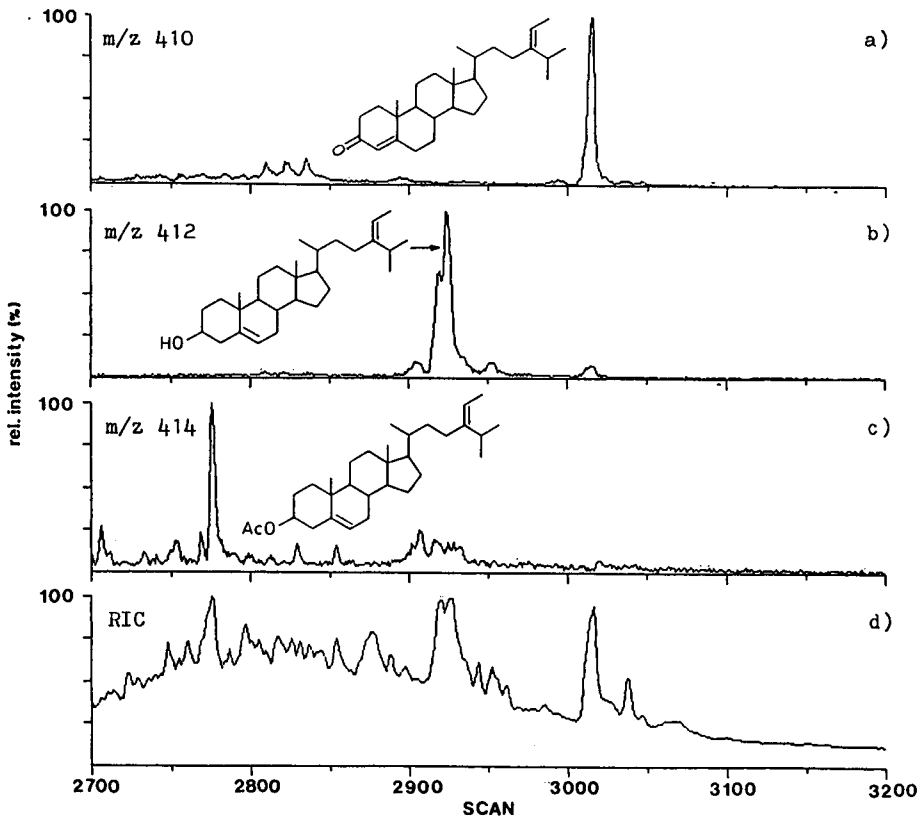


Fig. 4. GC-MS analysis of sterols present in the desorbed material of the algae *Halidrys* sp. (sample 6 in Table I). Mass chromatography of m/z 410 (a), 412 (b) and 414 (c) is used to recognize the three individual sterols. The RIC is shown in (d).

In the material desorbed from *Tetraedron minimum* three sterols are present at relatively high abundances, as shown by mass chromatography of the molecular ions of individual sterols. The compounds are identified based on published mass spectral data [32]. Ergost-7-en-3-ol (14) is recovered by mass chromatography of m/z 400 (Fig. 3a). The mass chromatogram of m/z 412 (Fig. 3b) shows one major peak which represents stigmast-7,22-dien-3-ol (15) as the highest intensity sterol. Stigmast-7-en-3-ol (17) contributes with only minor intensity, as seen by a comparison of the m/z 414 trace (Fig. 3c) and the RIC (Fig. 3d). All the *Chlorococcales* algae investigated here provided a similar sterol distribution, with the Δ^7 -components as the dominant constituents. It is remarkable that the related Δ^5 -sterols, which are usually dominant in biological materials, cannot be detected in the *Chlorococcales* algae.

Table IV lists the sterols and steroid ketones identified in the ten samples analysed, with an indication of their relative abundance. The list shows that in the analysed samples the occurrence of Δ^7 -sterols is restricted to the *Chlorococcales* algae. *Cladophora* and spruce and pine needles contain the related Δ^5 - C_{28} and C_{29} sterols (14,17), accompanied by stigmast-4-en-3-one (21 in Table IV). The other marine algae, *Fucus* sp., *Halidrys* sp. and *Plocamium* each have very specific steroid compositions. *Plocamium* shows a complete lack of C_{28} and C_{29} steroids (Table IV). The only steroid detected in high abundance in this alga is Δ^5 -cholestenol (19). Similarly, the steroid composition of *Fucus* sp. is strongly dominated by only one compound, which has been identified as stigmast-5,24(28)-dien-3-ol (20). This is confirmed by the analysis of the algae *Halidrys*, sp. the steroid composition of which is also dominated by $\Delta^{24(28)}$ -steroids. As shown by GC-MS analysis of the thermal extract of these algae, the steroids are dominated by stigmast-4,24(28)-dien-3-one (Fig. 4a). In addition, the stigmast-5,24(28)-dien-3-ol (Fig. 4b) and the related acetate (Fig. 4c) are recovered by mass chromatography of m/z 412 and m/z 414, respectively. The compounds are shown in Table IV as compounds 20, 22 and 23.

Peak integration data have been compared to assess the amount of steroids in relation to the chlorophyll content of the samples analysed. The results (Table III) show that the ratio of chlorophyll to the sum of steroids varies between 0.8 and 11.4. Like the chlorophyll:tocopherol ratio, the lowest values are observed in the terrestrial plant material. In the algae the ratio varies significantly without any dominance in the algae from the North Sea or the *Chlorococcales* algae.

These results indicate that the well known problems of the correlation of the sterols detected in sediments with those in potential biological precursors could probably be partly solved by the use of the type of analysis described in this paper. This requires a microscopic analysis of well defined micro-samples in combination with micro-TD and GC-MS analysis of the lipid content.

ACKNOWLEDGEMENTS

Samples of algae from the North Sea were kindly provided by Dr. G. Gassmann of the Biologische Anstalt Helgoland. Dr. K. Goth (Forschungsinstitut Senckenberg, Frankfurt) is thanked for providing the samples of chlorococcales algae.

REFERENCES

- 1 J. D. Brooks, K. Gould and J. W. Smith, *Nature (London)*, 222 (1969) 257.
- 2 H. Goossens, J. W. de Leeuw, P. A. Schenck and S. C. Brassell, *Nature (London)*, 312 (1984) 440.
- 3 M. Kates, L. S. Yengoyan and P. S. Sastry, *Biochim. Biophys. Acta*, 98 (1965) 252.
- 4 B. Chappe, P. Albrecht and W. Michaelis, *Science (Washington, D.C.)*, 217 (1982) 65.
- 5 B. M. Didyk, B. R. T. Simoneit, S. C. Brassell and G. Eglinton, *Nature (London)*, 272 (1978) 216.
- 6 H. L. ten Haven, J. W. de Leeuw, J. Rullkötter and J. S. Sinninghe Damsté, *Nature (London)*, 330 (1987) 641.
- 7 B. V. Burger, Z. M. Munro and J. H. Visser, *High Resolut. Chromatogr. Chromatogr. Commun.*, 11 (1988) 496.
- 8 J. H. Loughrin, T. R. Hamilton-Kemp, R. A. Andersen and D. F. Hildebrand, *Phytochemistry*, 29 (1990) 2473.
- 9 M. Nip, E. W. Tegelaar, J. W. de Leeuw, P. A. Schenck and P. J. Holloway, in D. Leythaeuser and J. Rullkötter (Editors), *Advances in Organic Geochemistry 1985; Org. Geochem.*, 10 (1986) 769.
- 10 K. Goth, J. W. de Leeuw, W. Püttmann and E. W. Tegelaar, *Nature (London)*, 336 (1988) 759.
- 11 E. W. Tegelaar, J. W. de Leeuw, C. Largeau, S. Derenne, H.-R. Schulten, R. Müller, J. J. Boon, M. Nip and J. C. M. Sprenkels, *J. Anal. Appl. Pyrol.*, 15 (1989) 29.
- 12 H.-R. Schulten, N. Simmleit and H. H. Rump, *Int. J. Environ. Anal. Chem.*, 27 (1986) 412.
- 13 H.-R. Schulten, N. Simmleit and R. Müller, *Anal. Chem.*, 61 (1989) 221.
- 14 R. G. Schaefer and W. Püttmann, *J. Chromatogr.*, 395 (1987) 203.
- 15 W. Püttmann, C. B. Eckardt and R. G. Schaefer, *Chromatographia*, 25 (1988) 279.
- 16 W. Püttmann, *Chromatographia*, 26 (1988) 171.
- 17 H. Schneider, E. Gelpi, E. O. Bennett and J. Oró, *Phytochemistry*, 9 (1970) 613.
- 18 E. Gelpi, H. Schneider, J. Mann and J. Oró, *Phytochemistry*, 9 (1970) 603.
- 19 W. Püttmann and K. Goth, *Cour. Forsch.-Inst. Senckenberg*, 107 (1988) 105.
- 20 J. W. de Leeuw, B. R. T. Simoneit, J. J. Boon, I. C. Rijpstra, F. de Lange, J. C. W. v.d. Leeden, V. A. Correia, A. Burlingame and P. A. Schenck, in R. Campos and J. Goni (Editors), *Advances in Organic Geochemistry 1975, ENADIMSA, Madrid, 1977*, p. 61.
- 21 A. Hollerbach, *Naturwissenschaften*, 65 (1978) 202.
- 22 D. van de Meent, J. W. de Leeuw and P. A. Schenck, in A. G. Douglas and J. R. Maxwell (Editors), *Advances in Organic Geochemistry 1979*, Pergamon Press, Oxford, 1980, p. 469.
- 23 S. C. Brassell, G. Eglinton and J. R. Maxwell, *Biochem. Soc. Trans.*, 11 (1983) 575.
- 24 E. Fernholz, *J. Am. Chem. Soc.*, 59 (1937) 1154.
- 25 P. E. Hughes and S. B. Tove, *J. Bacteriol.*, 151 (1982) 1397.
- 26 C. Martius, *Ciba Foundation Symposium Quinones and Electron Transport 1960*, Churchill Livingstone, London, 1961, p. 312.
- 27 C. Bucke, R. M. Leech, M. Hallaway and R. A. Morton, *Biochim. Biophys. Acta*, 112 (1966) 19.
- 28 M. Radke, R. G. Schaefer, D. Leythaeuser and M. Teichmüller, *Geochim. Cosmochim. Acta*, 44 (1980) 1787.
- 29 W. Püttmann, M. Wolf and E. Wolff-Fischer, in D. Leythaeuser and J. Rullkötter (Editors), *Advances in Organic Geochemistry 1985; Org. Geochem.*, 10 (1986) 625.
- 30 W. Steinkopf, H. Winterwitz, W. Roederer and A. Wolynski, *J. Prakt. Chem.*, 100 (1919) 65.
- 31 A. S. Mackenzie, S. C. Brassell, G. Eglinton and J. R. Maxwell, *Science, (Washington, D.C.)*, 217 (1982) 491.
- 32 Z. V. Zaretski, *Mass Spectrometry of Steroids*, Wiley, New York, 1976.

CHROMSYMP. 2233

Simultaneous gas–liquid chromatographic determination of sugars and organic acids as trimethylsilyl derivatives in vegetables and strawberries

MAGDOLNA MORVAI and IBOLYA MOLNÁR-PERL*

Institute of Inorganic and Analytical Chemistry, L. Eötvös University, P.O. Box 123, H-1443 Budapest (Hungary)

and

DEZSÓ KNAUSZ

Institute of General and Inorganic Chemistry, L. Eötvös University, P.O. Box 32, H-1518 Budapest 112 (Hungary)

ABSTRACT

The simultaneous determination of organic acids (succinic, malic, pimelic, tartaric, shikimic, citric, quinic, caffeic and chlorogenic acids), sorbitol and sugars (arabinose, rhamnose, fructose, galactose, glucose, sucrose, maltose and raffinose) as trimethylsilyl (TMS)-oxime and TMS derivatives in a single solution has been developed. The optimum conditions for the simultaneous derivatization and the rapid quantitative evaluation of the nineteen compounds by capillary gas–liquid chromatography are reported in this paper. Reproducibility data reveal that $\geq 0.02 \mu\text{g}$ of acids in the presence of $\leq 12 \mu\text{g}$ of sugars can be determined with a relative standard error (R.S.E.) of $\leq 11.2\%$, whereas the main constituents are determined with an R.S.E. of $\leq 3.6\%$.

INTRODUCTION

It is important to be able to determine, both qualitatively and quantitatively, the composition of organic acids and sugars present in plant foods. The concentrations of these compounds in vegetables or fruits are characteristic, and are influenced by factors such as maturity, ripeness and storage conditions. The recommended analytical methods for the determination of sugars and organic acids are often used in parallel, rather than simultaneously. However, some methods have recently been published which can be used to determine sugars and organic acids simultaneously. These methods include high-performance liquid chromatography (HPLC) of apple juice [1] and in cucumber fermentation [2], and gas–liquid chromatography (GLC) in grape musts [3], propolis [4], birch sap [5] and apple samples [6].

The goal of the work reported here was to extend earlier work [6–10] on the simultaneous determination of sugars and organic acids in carrots, potatoes, cucumbers and strawberries. These compounds are present in very different concentra-

tions. A second goal was to complete the recently [6] developed technique for a simple and rapid capillary GLC procedure.

EXPERIMENTAL

All materials and reagents were of analytical-reagent grade from Reanal (Budapest, Hungary), Fluka (Buchs, Switzerland) and Serva (Heidelberg, Germany).

Carrots, cucumbers and potatoes were purchased from the local market. Strawberries of known varieties were obtained from the Research Farm of the University of Horticulture and Food Industry, Horticulture Faculty (Kecskemét, Hungary). The varieties used were as follows: (1) Induka; (2) Korona; (3) Kortés; (4) Primella; (5) Pocahontas; (6) Tufts; (7) Aiko; (8) Aliso; (9) Elvira; (10) Favorit; (11) Fertődi; and (12) Gorella.

Preparation of the samples for gas-liquid chromatographic analysis

Peeled carrot, cucumber and potato were grated and 2, 5, 10 or 20 g of the homogenised samples were either extracted at 25°C or by refluxing with 80% aqueous methanol or ethanol for 20 min. The insoluble material was then collected on a glass filter (6 cm I.D.) and washed several times with 80% aqueous methanol or ethanol. The combined filtrates and washings were concentrated to 100 cm³ (stock solution) on a rotary evaporator at 50–60°C.

The strawberries were homogenised in a food mixer and the sieved pulp (free of stones) was used for derivatization.

Preparation of trimethylsilyl (TMS) oxime and TMS derivatives

Various amounts of organic acids, arabinose, rhamnose, sorbitol, maltose or raffinose ($1.25 \cdot 10^{-4}$ – $1 \cdot 10^{-3}$ g) and the same amount of sugars ($2.5 \cdot 10^{-3}$ – $2 \cdot 10^{-2}$ g of fructose, glucose and sucrose) in model solutions (weighed with analytical precision) or the stock solutions of vegetables or strawberry pulps, (containing sugars and acids corresponding to the amount applied in standards) were evaporated to dryness in a rotary evaporator at 50–60°C. The dehydrated residues were treated with 1.0 cm³ of pyridine (containing 1.25 g of hydroxylamine hydrochloride per 100 cm³) and were heated for 30 min at 75°C. The cooled samples were then trimethylsilylated with a mixture of 1.8 cm³ of hexamethyldisilane (HMDS) and 0.2 cm³ of trifluoroacetic anhydride (TFAA) in 4-cm³ reactivials for 60 min at 100°C. The filtered solutions were then evaporated to 0.5 cm³ in a rotary evaporator at 50–60°C. The residues were transferred quantitatively to 1-cm³ reactivials with a solution of HMDS–TFAA (9:1) and diluted to a volume of 1 cm³.

Separation of TMS-oxime or TMS derivatives

The gas chromatograph used was a Chrompack CP 900 instrument (Chrompack International, Middelburg, The Netherlands) equipped with a flame ionisation detector and a wall-coated open tubular fused-silica column (10 m × 0.25 mm I.D.), coated with CP-Sil-5CB, DF 0.12 (Chrompack, Cat. No. 7700, column No. 225660).

The temperatures of both the injection and detector ports were 300°C. Using a temperature programme of 120–160°C at 10°C/min and a hold-time at 160°C of 3 min, followed by 160–280°C at 10°C/min and a hold-time at 280°C of 6 min, 30 min were required to elute the TMS-oxime and TMS derivatives of the organic acids and sugars. The nitrogen pressure was 30 kPa with a split ratio of 100:1.

RESULTS AND DISCUSSION

Extraction, derivatization and gas-liquid chromatographic conditions

Extraction. A quantitative extraction procedure is the first step in obtaining accurate acid and sugar determinations by GLC analysis. A study has been carried out to determine the optimum extraction conditions (Fig. 1a-d: extraction yield of carrot), as the available literature data [11-14] were contradictory in two respects. These are: (1) the low ratio of the extracting agent to the sample [11-14] *e.g.* applying 10 [12], 14 [14], 20 [13] or 50 g [11] of sample to 100 cm³ of 60 [11], 75 [13] or 80% [12,14] aqueous ethanol; and (2) the time and temperature conditions of extractions: *e.g.* performing the extractions for 5 [11] or 10 min [13] at room temperature, or overnight at 0°C [14], or by boiling for 15 min [12].

The extractions carried out, which were followed by measuring the main acid and sugar components of carrots, potatoes and cucumbers as TMS-oxime and TMS derivatives, showed that quantitative extraction yields can be achieved using 2 or 5 g of sample per 100 cm³ of 80% aqueous methanol or ethanol at 25°C, or by refluxing with

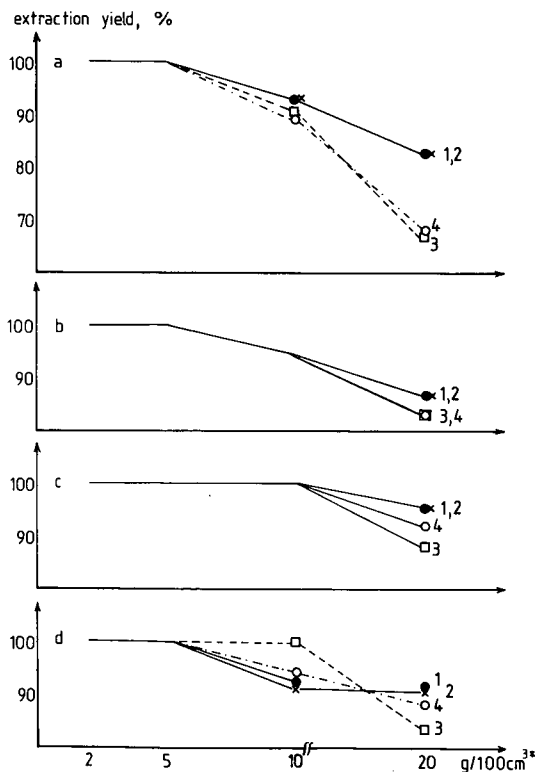


Fig. 1. Extraction yields of the main components of carrot, obtained under various conditions. (a) Malic acid; (b) fructose; (c) glucose; (d) sucrose. Conditions: addition of (1) 2; (2) 5; (3) 10; and (4) 20 g of fresh grated carrot to 100 cm³ of 80% aqueous methanol (1,2) or 80% aqueous ethanol (3,4) with continuous stirring for 20 min. (1,3) Values obtained with extractions at 25°C; (2, 4) heated under refluxing. Results expressed as g per 100 cm³* relative to the weight of fresh carrot.

stirring for 20 min. This was achieved for all four components (Fig. 1a–d, malic acid, fructose, glucose and sucrose extraction yields of carrot). A shorter extraction time (10 min) or lower ratio of sample to extracting agent (10 or 20 g per 100 cm³) was unsatisfactory. The same trend of extractions were observed for potatoes and cucumbers.

Derivatization and gas-liquid chromatographic conditions. To obtain a simultaneous quantitative derivatization, without any side-reactions, of the organic acids and sugars, a detailed study was required based on earlier studies [6,15] with packed columns (15% Dexsil 300 GC, 3 m × 4 mm I.D.).

In this work the basic investigations of derivatization were repeated. The data obtained (by measuring the products on the capillary column) have proved that using this derivatization procedure and a method with about a five-fold increase of sensitivity, and comparing the results to those obtained using a packed column, no side-reactions could be detected.

To determine the optimum GLC conditions, and taking into account the literature data [16], the 10-, 20- and 30-m columns and several temperature programmes were tested. A 10-m capillary column and the temperature programme detailed under experimental was determined to be the optimum for this purpose.

TABLE I

REPRODUCIBILITY OF THE SIMULTANEOUS DETERMINATION OF VARIOUS AMOUNTS OF ORGANIC ACIDS AND SUGARS AS TMS-OXIME OR TMS DERIVATIVES BY CAPILLARY GLC

The letters a–d define the amounts of components injected: (a) 0.125, (b) 0.25, (c) 0.60 and (d) 1.0 µg of organic acids or arabinose, rhamnose, maltose or raffinose, and (a) 0.25, (b) 5, (c) 10 and (d) 20 µg of fructose, glucose or sucrose.

Acid/sugar	Integral units equivalent to 1 µg of substance					Standard error	Relative standard error (%)
	a ^a	b ^a	c ^a	d ^a	Mean ^b		
Succinic acid	(1944)	1385	1318	1396	1366	68.7	5.0
Malic acid	(2338)	1784	1848	1796	1809	34.0	1.9
Pimelic acid	(1975)	1542	1548	1500	1530	26.1	1.7
Tartaric acid	2451	2423	2638	2482	2499	96.1	3.8
Arabinose	3347	3390	3180	3249	3304	96.0	2.9
Shikimic acid	2632	2694	2716	2708	2688	38.1	1.4
Citric acid	1997	1995	1957	1942	1973	27.0	1.4
Rhamnose	2389	2400	2376	2503	2417	58.2	2.4
Quinic acid	2924	2980	2944	2955	2958	23.4	0.79
Sorbitol	3967	4205	4172	3913	4064	145.8	3.6
Fructose	3383	3370	3302	3246	3325	63.7	1.9
Glucose	3606	3672	3535	3664	3619	63.4	1.8
Caffeic acid	2444	2525	2501	2448	2480	39.9	1.6
Sucrose	3184	3109	3188	3160	3160	36.3	1.2
Maltose	3073	3078	3107	2987	3061	51.7	1.2
Chlorogenic acid	3711	3814	3837	3727	3772	62.5	1.7
Raffinose	2884	2972	3160	2967	2996	116.7	3.9

^a Mean of at least three parallel tests.

^b Mean of a–d values.

TABLE II
 REDUCIBILITY OF SUGAR AND ORGANIC ACID COMPONENTS OF CARROTS, POTATOES AND CUCUMBERS OBTAINED AFTER
 QUANTITATIVE EXTRACTION (TESTS a-d) AND OF STRAWBERRIES, MEASURED AS TMS-OXIME OR TMS DERIVATIVES

Acid/sugar	Composition ^a (% w/w)								
	Carrots				Strawberries				
	a	b	c	d	Mean ± S.D.	R.S.D. (%)	Potatoes (test a)	Cucumbers (test a)	Strawberries
Succinic acid	0.078	0.093	0.085	0.091	0.087 ± 0.007	7.8	0.0135	0.0035	0.0070
Malic acid	0.59	0.59	0.58	0.58	0.58 ± 0.008	1.3	0.068	0.17	0.036
Prmelic acid	0.028	0.031	0.031	0.028	0.029 ± 0.002	6.3	0.044	—	—
Tartaric acid	0.0067	0.0068	0.0054	0.0070	0.065 ± 0.00072	11.2	0.017	0.011	—
Pentose	— ^b	—	—	—	—	—	—	—	0.038
Citric acid	0.071	0.073	0.066	0.066	0.069 ± 0.0036	5.2	0.045	—	0.438
Quinic acid	0.10	0.10	0.10	0.10	0.10	—	—	—	0.0066
Sorbitol	0.015	—	—	—	—	—	—	—	—
Fructose	0.89	0.89	0.88	0.93	0.89 ± 0.024	2.7	0.67	0.99	1.98
Glucose	1.09	1.01	1.09	1.08	1.07 ± 0.039	3.6	0.53	0.99	1.74
Caffeic acid	0.067	0.069	0.074	0.070	0.070 ± 0.0029	4.2	0.035	0.043	0.049
Sucrose	1.67	1.77	1.75	1.74	1.76 ± 0.014	0.8	0.55	0.023	0.75
Maltose	—	—	—	—	—	—	0.0033	—	0.0030
Chlorogenic acid	0.0030	—	—	—	—	—	—	—	—
Raffinose	0.019	0.021	0.020	0.024	0.021 ± 0.0021	1.0	—	—	0.0085

^a Calculated as the percentage of the fresh weight of samples a-d carried out in parallel. The mean values obtained after eight quantitative extractions, i.e. 2 or 5 g of vegetable, using 100 cm³ of 80% aqueous methanol (tests a and b) or 100 cm³ of aqueous ethanol (tests c and d). a and c were extracted at 25°C; b and d were extracted using reflux condenser.

^b No data available, i.e. values below detection limit.

Reproducibility study

The reproducibility and usefulness of the proposed method were shown by the results with model solutions (Table I, Fig. 2a) and by the composition of carrots (Table II, Fig. 2b). The reproducibility measurements showed a relative standard error (R.S.E.) of 0.8–11.1% (depending on the amount used and the detection limit of the minor constituents). For the major components such as malic acid, fructose, glucose and sucrose, an R.S.E. \leq 3.6% was obtained.

TABLE III

DISTRIBUTION OF THE MAIN CHARACTERISTIC COMPONENTS OF STRAWBERRIES (VARIETIES 1–12) AS A FUNCTION OF RIPENESS

Gathered on 16 May 1990 (a), on 24 May 1990 (b) and on 31 May 1990 (c).

Varieties	Time of gathering	Distribution (% w/w)				
		Malic acid	Citric acid	Fructose	Glucose	Sucrose
Induka	a	0.213	0.492	1.73	1.54	0.323
	b	0.098	0.506	1.77	1.58	0.220
	c	0.027	0.327	2.88	2.58	0.144
Korona	a	—	0.054	2.05	1.72	0.302
	b	0.013	0.505	2.05	1.82	0.458
	c	0.018	0.358	3.43	3.02	0.421
Kortes	a	0.018	0.660	1.81	1.67	0.545
	b	0.017	0.573	2.09	1.88	0.387
	c	0.034	0.290	2.70	2.38	0.400
Primella	a	0.021	0.682	2.35	2.22	0.035
	b	0.045	0.598	2.35	1.98	0.15
	c	0.067	0.278	2.61	2.39	0.246
Pocahontas	a	0.076	0.559	1.96	1.66	0.180
	b	0.016	0.393	2.58	2.25	0.028
	c	0.016	0.389	1.84	1.72	—
Tufts	a	0.045	0.321	1.65	1.46	0.132
	b	0.049	0.343	2.47	2.19	0.111
	c	0.016	0.335	3.01	2.56	0.022
Aiko	a	0.044	0.458	1.73	1.42	0.479
	b	0.045	0.495	1.74	1.55	0.592
	c	0.036	0.438	1.98	1.74	0.75
Aliso	a	0.050	0.837	1.71	1.51	0.36
	b	0.028	0.371	2.04	1.91	0.093
	c	0.0025	0.321	3.08	2.81	—
Elvira	a	0.068	0.913	2.10	1.95	0.265
	b	0.064	0.888	2.50	2.21	0.029
	c	—	0.042	2.50	2.31	0.013
Favorit	a	0.092	0.726	1.50	1.47	0.34
	b	0.054	0.477	2.07	1.81	0.089
	c	0.0015	0.010	2.79	2.62	—
Fertődi	a	0.189	0.156	1.48	1.30	0.016
	b	0.111	0.332	1.81	1.51	—
	c	0.096	0.215	2.15	1.72	—
Gorella	a	0.029	0.387	1.74	1.54	0.031
	b	0.034	0.487	2.64	2.38	0.010
	c	0.012	0.422	2.02	1.77	—

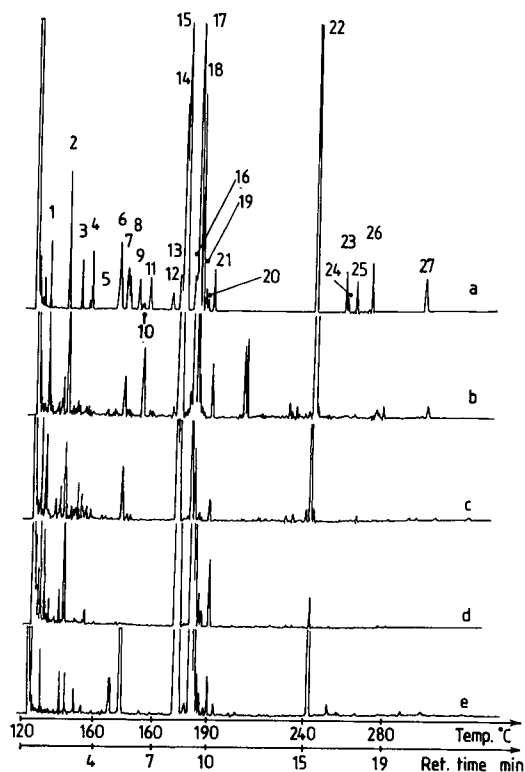


Fig. 2. Chromatograms of TMS and TMS-oxime derivatives of acids and sugars obtained with (a) model solutions, (b) extracts of carrot, (c) potato, (d) cucumber and (e) strawberry pulp (variety 1). Peaks: 1 = succinic acid; 2 = malic acid; 3 = pimelic acid; 4 = tartaric acid; 5 = xylose; 6 = arabinose; 7 = shikimic acid; 8 = citric acid; 9 = rhamnose₁; 10 = rhamnose₂; 11 = quinic acid; 12 = fructose₁; 13 = sorbitol; 14 = fructose₂; 15 = fructose₃; 16 = galactose; 17 = glucose₁; 18 = glucose₂; 19 = glucose₃; 20 = glucose₄; 21 = caffeic acid; 22 = sucrose; 23 = maltose₁; 24 = maltose₂; 25 = chlorogenic acid₁; 26 = chlorogenic acid₂; 27 = raffinose. Note: the elimination of peaks 12, 19 and 20, probably originating from incomplete oximation, needs further study.

Composition of vegetables and strawberries

The sugar and organic acid contents of carrots, potatoes, cucumbers and strawberries were measured as TMS-oxime and TMS derivatives (Tables II and III and Fig. 2b-e). No literature data could be found for the GLC analysis of these components from a single injection using the same varieties of strawberries. The evaluation of this extraction and GLC procedure was therefore restricted. However, it was shown to serve as a general application both for vegetables extracted prior to derivatization and for directly derivatizable pulps, such as strawberries.

The data showed that constituents from $3 \cdot 10^{-3}\%$ (Table II, 0.003% chlorogenic acid) to about 1.8% (Table II, 1.76% sucrose) could be determined with an acceptable reproducibility.

The usefulness of the method can be characterised by the determination of the

small changes in both the organic acid and the sugar composition of the different varieties of strawberries obtained as a function of maturity (Table III).

The comparison of these results with previously published values is limited by: (1) the basis of reference, which is not uniformly accepted; (2) the fact that comprehensive studies cannot be found in the literature for the optimum (quantitative) extraction and analytical conditions for the simultaneous determination of organic acids and sugars from any matrices; and (3) the compilation [17] which relates to the sugar contents of various berries from 1969 to 1979 is the only basis of comparison for strawberries. In order of listing, the fructose (1.02–3.20 g per 100 g), glucose (1.48–3.40 g per 100 g) and sucrose (0.20–1.56 g per 100 g) contents of eight varieties [originating from the U.S.A. (five), Switzerland (one), the U.K. (one) and India (one), all calculated as g per 100 g fresh weight], were in good agreement with the results obtained here for the twelve varieties grown in Hungary (Table III).

Further extension of this method to prove its use in the analysis of other natural matrices containing additional organic acid and sugar components is in progress.

ACKNOWLEDGEMENTS

The authors thank P. Sass and K. Bujdosó-Megyeri for the valuable strawberry samples. The financial support of MÉM (Project G/8) is gratefully acknowledged.

REFERENCES

- 1 D. B. Gomis, M. D. G. Alvarez, J. J. M. Alonso and A. N. Vallina, *Chromatographia*, 25 (1988) 701.
- 2 M. J. Lazaro, E. Carbonell, M. C. Aristoy, J. Safon and M. Rodrigo, *J. Assoc. Off. Anal. Chem.*, 72 (1989) 52.
- 3 J. E. Marcy and D. E. Carroll, *Am. J. Enol. Vitic.*, 33 (1982) 176.
- 4 W. Maciejewicz, M. Daniewski and Z. Mielniczuk, *Chem. Anal. (Warsaw)*, 29 (1984) 421.
- 5 H. Kallio, S. Ahtonear, J. Paulo and R. R. Linko, *J. Food Sci.*, 50 (1985) 266.
- 6 M. Morvai and I. Molnár-Perl, *J. Chromatogr.*, 520 (1990) 201.
- 7 I. Molnár-Perl and M. Pintér-Szakács, *J. Chromatogr.*, 216 (1981) 219.
- 8 I. Molnár-Perl and M. Pintér-Szakács, *J. Chromatogr.*, 365 (1986) 171.
- 9 M. Morvai, M. Pintér-Szakács and I. Molnár-Perl, *J. Chromatogr.*, 446 (1988) 237.
- 10 I. Molnár-Perl and M. Pintér-Szakács, *Carbohydr. Res.*, 138 (1985) 83.
- 11 R. J. Bushway, J. L. Bureau and D. F. McGann, *J. Food Sci.*, 49 (1984) 75.
- 12 D. H. Picha, *J. Agric. Food Chem.*, 33 (1985) 743.
- 13 G. W. Chapman, Jr., and R. J. Horvat, *J. Agric. Food Chem.*, 37 (1989) 947.
- 14 M. Horbowicz, J. Czapski and J. Bakowski, *Acta Aliment. Pol.*, 6 (1980) 227.
- 15 M. Morvai and I. Molnár-Perl, *Proceedings of the Euro Food Chem. V., Versailles, 1989*, Vol. 2, INRA, Paris, 1989, p. 497.
- 16 S. Noro, N. Kudo and T. Kitsuwu, *J. Jpn. Soc. Hortic. Sci.*, 58 (1989) 17.
- 17 R. E. Wrolstad and R. S. Shallenberger, *J. Assoc. Off. Anal. Chem.*, 64 (1981) 91.

CHROMSYMP. 2085

Gas chromatographic determination of N-carboxymethyl amino acids, the periodate oxidation products of Amadori compounds

RAPHAËL BADOUD*, LAURENT FAY and URS RICHLI

Nestec Ltd, Research Centre, Vers-chez-les-Blanc, P.O. Box 44, CH-1000 Lausanne 26 (Switzerland)
and

PETR HUŠEK

Research Institute of Endocrinology, Národní trída 8, CS 11694 Prague 1 (Czechoslovakia)

ABSTRACT

Periodate oxidation of Amadori compounds (1-amino-1-deoxy-2-ketoses), formed by the glycosylation of primary amino groups of free amino acids or N-terminal and ϵ -lysyl amino groups in peptides and proteins with aldoses, leads to the formation of N-carboxymethyl amino acids. The latter are then analysed by gas chromatography as their ethyl ester N-ethoxycarbonyl derivatives, after a straightforward derivatization reaction with ethyl chloroformate in a mixture of ethanol, pyridine and water. The amounts of N-carboxymethylated amino acids directly reflect the extent of glycosylation of the various amino sites. Application of this approach to food products is discussed.

INTRODUCTION

Free amino acids and ϵ -amino groups of lysine residues in peptides and proteins readily react with reducing sugars, particularly aldoses, to form 1-amino-1-deoxy-2-ketoses upon Amadori rearrangement of an intermediate glycosylamine [1]. This glycosylation reaction occurs during food processing and storage. It represents the first step in a series of complex transformations which eventually lead to the generation of brown pigments and numerous desirable or undesirable flavour compounds. This process is known as the Maillard reaction or non-enzymatic browning [2–5].

In food products, the blockage of the ϵ -amino group of lysine residues can be initiated under very mild conditions: a milk powder stored at room temperature leads to the progressive loss of this essential amino acid and eventually to the development of a brown colour. Under physiological conditions, enzymes, proteins and DNA can also be modified by glycosylation [3–5]. This process is of special concern in, *e.g.*, diabetic subjects, where physiological and immunological functions may be impaired.

Recently, we proposed a new approach to the measurement of both protein-bound and free Amadori products [6], consisting in determining the N-carboxymethylamino acid derivatives (CM-AAs) arising from the periodate oxidation of the corre-

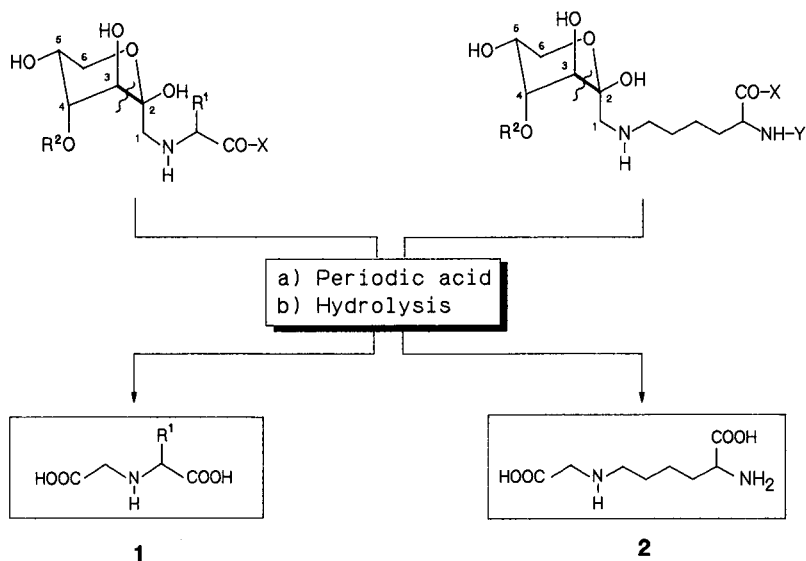


Fig. 1. Reaction pathway for the periodate oxidation of Amadori compounds derived from α -amino acids and ϵ -lysine residues with glucose ($R^2 = H$) or lactose ($R^2 = \text{galactosyl}$). Formation of N-carboxymethyl amino acids (CM-AAs, **1**) and N $^{\epsilon}$ -carboxymethyllysine (ϵ -CM-Lys, **2**).

sponding N-glycosylated species (Fig. 1). In this paper, we report a simple analytical method for the determination of various CM-AAs by gas chromatography (GC) after a straightforward derivatization reaction with ethyl chloroformate.

EXPERIMENTAL

Materials

N-Carboxymethyl derivatives of alanine (CM-Ala), valine (CM-Val), leucine (CM-Leu), isoleucine (CM-Ile), phenylalanine (CM-Phe) and the mono and bis derivatives of lysine (α -CM-Lys, ϵ -CM-Lys and bis-CM-Lys) were synthesized by reaction of the corresponding amino acids with glyoxylic acid according to Kihlberg *et al.* [7]. All compounds were fully characterized by NMR and mass spectrometry and gave satisfactory elemental analyses. The N-carboxymethyl derivative of glycine (CM-Gly, iminodiacetic acid), O-benzyl-L-serine and periodic acid were purchased from Fluka (Buchs, Switzerland). Ethyl chloroformate was obtained from Aldrich (Steinheim, Germany).

Apparatus

A Hewlett-Packard HP-5890 gas chromatograph with an HP-7673A autosampler and an HP-3392A integrator was used; data were acquired and treated using an HP-3350 laboratory automation system. Hydrolyses were performed using a Thermoreactor TR 105 dry-block heater (E. Merck, Darmstadt, Germany).

Separation conditions

The conditions were as follows: DB-5 fused-silica capillary column (30 m \times

0.32 mm I.D.) (J&W Scientific); carrier gas (helium) pressure, 10 p.s.i.; splitless injector temperature, 250°C; oven temperature programme 50°C (1 min), 30°C/min to 200°C, 5°C/min to 300 (5 min); flame ionization detector temperature, 300°C.

Samples

Dehydrated tomato powder was obtained from a food product development centre (Francereco, Beauvais, France). Model milk powder samples, the water activity of which were adjusted using saturated aqueous magnesium chloride, were heated for various periods of time at 40–50°C to induce glycosylation.

Sample treatment

Approximately 150 mg (exactly weighed) of sample were homogenized in 10 ml of water in a 260 × 40 mm I.D. Pyrex tube with a 29/32 ground joint. A 10-ml volume of a 100 mM aqueous periodic acid solution was added and the mixture was left in the dark for 2 h at room temperature with occasional shaking. Excess of periodic acid was decomposed with 2 ml of 2 M sodium thiosulphate, then water and concentrated hydrochloric acid were added to make a final volume of 150 ml in 6 M HCl. The tube was fitted with a reflux condenser and the mixture was heated at 110°C for 24 h for the milk powders and 2 h for the tomato samples. The hydrolysate was diluted with water and filtered. An aliquot was evaporated to dryness under a stream of nitrogen and reconstituted in 1 ml of 0.1 M HCl. O-Benzylserine (internal standard, 25.6 nmol) was added and the mixture was applied to a small column (20 × 4 mm I.D.) of Dowex 50W-X4. After the resin had been rinsed with 10 ml of water, the compounds of interest were eluted with 2 ml of 3 M ammonia solution and the solvent was removed under a stream of nitrogen.

Derivatization

The eluate from the cation-exchange resin was dissolved in 100 µl of water-ethanol-pyridine (60:32:8, v/v/v) and 5 µl of ethyl chloroformate were added. After 2 min at room temperature the mixture was diluted with 0.5 ml of saturated aqueous sodium hydrogencarbonate and the derivatives were extracted with 2 ml of dichloromethane. The organic phase was dried (sodium sulphate) and the solvent removed *in vacuo*. The residue was reconstituted in 100 µl of dichloromethane containing hydrocarbons (C₁₆, C₂₀, C₂₄, C₂₈) before injection.

RESULTS

On treatment with periodic acid, Amadori compounds gave rise to the formation of CM-AAs by selective cleavage of the C-2–C-3 bond (Fig. 1). These uncommon amino acids were derivatized with ethyl chloroformate in ethanol-pyridine-water according to the reaction scheme in Fig. 2 and analysed by capillary GC.

Fig. 3 shows the separation of a standard mixture of CM-AAs as their ethyl ester N-ethoxycarbonyl derivatives, including N-carboxymethylglycine (CM-Gly), -alanine (CM-Ala), -valine (CM-val), -leucine (CM-Leu), -isoleucine (CM-Ile), -phenylalanine (CM-Phe) and the mono and bis derivatives of lysine (α -CM-Lys, ϵ -CM-Lys and bis-CM-Lys). By the use of this type of derivatization it was possible to separate α -CM-Lys and ϵ -CM-Lys on a apolar stationary phase (SE-54). In con-

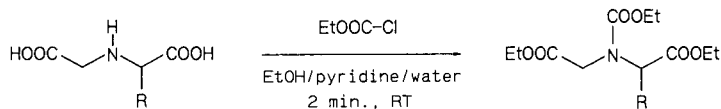


Fig. 2. Formation of ethyl ester N-ethoxycarbonyl derivatives of CM-AAs by reaction with ethyl chloroformate. Et = Ethyl.

trast, using the classical derivatization procedure including esterification with isobutyl alcohol and acylation with pentafluoropropionic acid, these two compounds could only be resolved on a medium-polar phase (OV-1701). The CM-AA derivatives were less volatile than the corresponding amino acids but the elution orders of these two series of compounds were identical. The ethyl ester N-ethoxycarbonyl derivatives were stable for at least 2 weeks at room temperature (variation of response factors below 0.5% for all the CM-AAs studied).

Calibration graphs were linear in the range 2–15 $\mu\text{g/ml}$ (correlation coefficients 0.981–0.991) for all the compounds investigated. This narrow range was chosen because of the low concentrations expected in the actual samples.

The reliability of the determination of the α -, ϵ - and bis-CM-Lys was tested. Blank samples (non-oxidised milk hydrolysates) were spiked at three different levels, then passed through the cation-exchange resin. The recoveries were better than 80% for all the CM-AAs investigated. The spiked samples were then derivatized and analysed in several replicates. The results are reported in Table I.

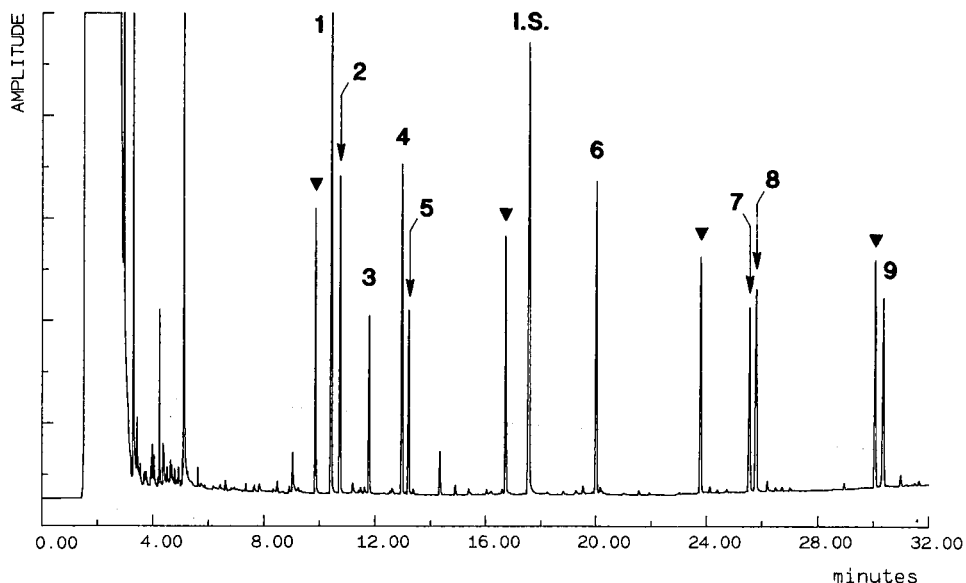


Fig. 3. Separation of a standard mixture of CM-AAs after derivatization with ethyl chloroformate. Peaks: 1 = CM-Gly; 2 = CM-Ala; 3 = CM-Val; 4 = CM-Leu; 5 = CM-Ile; 6 = CM-Phe; 7 = α -CM-Lys; 8 = ϵ -CM-Lys; 9 = bis-CM-Lys; I.S. = O-benzyl-L-serine; ▼ = added hydrocarbons (C_{16} , C_{20} , C_{24} , C_{28}).

TABLE I

PRECISION AND ACCURACY OF THE DETERMINATION OF THE VARIOUS CM-LYS DERIVATIVES IN SPIKED MILK HYDROLYSATES

The amount of standards were added to 1 ml of hydrolysate containing 0.5 mg of sample.

Derivative	Amount added (μg)	Amount measured (μg)	R.S.D. ^a (%)	<i>n</i> ^a
α -CM-Lys	1	0.8	10.5	3
	6	6.4	8.8	6
	10	9.8	8.3	5
ϵ -CM-Lys	1	0.7	6.7	3
	6	6.6	5.1	4
	10	9.7	10.3	4
Bis-CM-Lys	1	1.3	6.8	2
	6	6.4	4.9	4
	10	10.3	6.9	5

^a R.S.D. = relative standard deviation; *n* = number of replicates.

Two food samples were chosen to test the method: a tomato powder for its relatively high content of free amino acids and reducing sugars, and a milk powder for evaluating the extent of blockage of the ϵ -lysine residues. Both samples were oxidized with periodic acid then hydrolysed. After clean-up through a strong cation-exchange resin, the hydrolysates were derivatized as described above and analysed by GC.

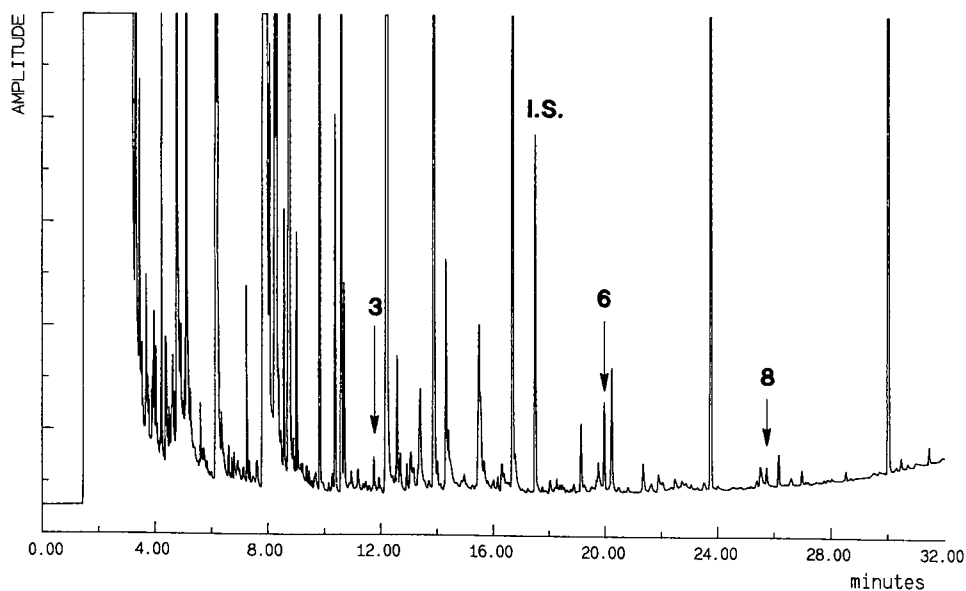


Fig. 4. Chromatogram of a tomato powder after periodate oxidation and ethyl chloroformate derivatization. Peaks as in Fig. 3.

Several CM-AAs were detected in the tomato sample, as shown in Fig. 4. These were CM-Val (2 $\mu\text{mol/g}$), CM-Phe (18 $\mu\text{mol/g}$) and ϵ -CM-Lys (<2 $\mu\text{mol/g}$), the identities of which were confirmed by mass spectrometry. Other derivatives could not be identified owing to interferences with common protein-hydrolysate amino acids. In a deliberately heat-damaged milk powder, only ϵ -CM-Lys was found (80 $\mu\text{mol/g}$).

DISCUSSION

In the past, free Amadori products have been determined by GC [8] or ion-exchange high-performance liquid chromatography [9] while protein-bound Amadori compounds derived from the glycosylation of ϵ -lysine groups with glucose or lactose have been determined by measuring the furosine which is released on acid hydrolysis [10]. As mentioned earlier, a new approach has been proposed recently to establish the extent of glycosylation which consists in the determination of the CM-AAs that are released by oxidative degradation of Amadori compounds.

The determination of amino acids by GC is usually performed after esterification of the carboxylic acid group and perfluoroacylation of the remaining functional groups (NH_2 , OH, SH). We used this two-step procedure for the determination of CM-AAs in milk samples [6]. However, this derivatization method is time consuming, and high temperatures and anhydrous conditions are needed to obtain high and reproducible yields. In this study, CM-AAs were analysed by GC as their ethyl ester N-ethoxycarbonyl derivatives after reaction with ethyl chloroformate (Fig. 4). This new procedure was developed recently by Husek [11] for the determination of various amino acids and carboxylic acids. Applied to the different CM-AAs, quantitative derivatizations were obtained using very mild reaction conditions (2 min at room temperature).

Not all theoretically expected CM-AAs were investigated because of a lack of reference compounds. Moreover, several derivatives may not be formed at all during the periodate treatment owing to the presence of oxidizable functional groups (*e.g.*, in methionine or tyrosine). In products containing proteins or large peptides, ϵ -CM-Lys (CML) is expected to be present in much larger amounts than the other CM-AAs as the ϵ -lysine groups largely predominate. This is verified in milk samples wherein only CML was detected as a result of the oxidative cleavage of the lactose-lysine Amadori compound. On the other hand, other CM-AAs can be formed in systems containing relatively large amounts of free or N-terminal amino acids. In dry tomato powder, the presence of noticeable amounts of Amadori products was first shown by Reutter and Eichner [9]; other CM-AAs were detected as shown in Fig. 2.

It should be mentioned that CML is not only formed by periodate oxidation. It has also been detected in food and in biological systems and was shown to be the consequence of the breakdown by oxygen of fructose-lysine Amadori compound [4]. Up to now, however, no other CM-AAs which could have been generated under similar conditions have been identified.

CONCLUSION

It has been shown that CM-AAs produced by periodate oxidation of Amadori products can be readily derivatized with ethyl chloroformate under very mild condi-

tions. The determination of these uncommon amino acids by GC as their ethyl ester N-ethoxycarbonyl derivatives can be used to evaluate the sites and the extent of glycosylation of the various primary amino groups in amino acids, peptides and proteins. This approach provides a new tool for investigating the glycosylation reaction both in food products and in biological materials.

ACKNOWLEDGEMENTS

We are grateful to F. Hunston for skilful technical assistance and to G. Philippoussian for revising the manuscript.

REFERENCES

- 1 J. E. Hodge, *J. Agric. Food Chem.*, 1 (1953) 928–947.
- 2 L. C. Maillard, *C. R. Acad. Sci.*, 154 (1912) 66–68.
- 3 J. W. Baynes and V. Monnier, *The Maillard Reaction in Aging, Diabetes, and Nutrition*, Alan R. Liss, New York, 1989.
- 4 P. A. Finot, H. U. Aeschbacher, R. F. Hurrel and R. Liardon, *The Maillard Reaction in Food Processing, Human Nutrition and Physiology*, Birkhäuser, Basle, 1990.
- 5 F. Ledl and E. Schleicher, *Angew. Chem., Int. Ed. Engl.*, 29 (1990) 565–594.
- 6 R. Badoud, F. Hunston, L. Fay and G. Pratz, in P. A. Finot, H. V. Aeschbacher, R. F. Hurrel and R. Liardon (Editors), *The Maillard Reaction in Food Processing, Human Nutrition and Physiology*, Birkhäuser, Basle, 1990, pp. 79–84.
- 7 J. Kihlberg, R. Bergman and B. Wickberg, *Acta Chem. Scand., Ser. B*, 37 (1983) 911–916.
- 8 R. Wittmann, *Thesis*, University of Münster, 1986.
- 9 R. Reutter and K. Eichner, *Z. Lebensm.-Unters.-Forsch.*, 188 (1989) 28–35.
- 10 G. H. Chiang, *J. Agric. Food Chem.*, 31 (1983) 1373–1374.
- 11 P. Hušek, *J. Chromatogr.*, 552 (1991) 289–299.

CHROMSYMP. 2084

Gas chromatographic analysis of some glycol ether analytes on a specially packed column

K. LEKOVA*

Institute of Chemical Industry, Sofia 1592 (Bulgaria)

and

N. IVANOVA

Institute of Special Chemicals, Vladaja, Sofia 1741 (Bulgaria)

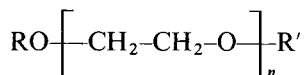
ABSTRACT

The retention behaviour and analysis of some glycol ethers on a specially packed column are reported. A column (0.45 m × 2.0 mm I.D.) packed with a deep acid-washed pink diatomite Chromosorb P, deactivated by a layer of poly(ethylene glycol succinate) additionally coated with a higher content of the same polyester phase was used. Transmission electron microscopic observation of the support surface after the polyester deactivation and the additional coating was carried out. The performance of the proposed short column was compared with that of a wide-bore capillary column (10.0 m × 0.53 mm I.D., 1.2 μm film thickness) and the parameters obtained are given. The glycol ether retentions under linear temperature programming conditions were expressed in terms of relative retention temperatures and retention indices; *n*-alkanols were selected as fixed points on the retention index scale of glycol ethers. The performance of the proposed column with some isomeric oxygen-containing analytes such as xylenols, phenols and ketones is reported. Special attention was given to the main product 2-methoxyethanol and capillary gas chromatography–mass spectrometry with selective detection was employed.

INTRODUCTION

Glycol ethers (GE) have found widespread applications as solvents, emulsifiers and intermediates in various organic syntheses. Hence there is a need for the development of an analytical method for their rapid and reliable determination and gas chromatography (GC) is still the method of choice [1–4].

The glycol ethers considered in this work (Table I) have the general formula



where R is an alkyl group with values 1, 2 or 4, R' is hydrogen, hydroxy or *n*-alkyl and *n* = 1 or 2.

The polar character of glycol ethers gives rise to problems in their analysis on conventional GC packed columns. Even when using a relatively inert support such as silanized diatomites, coated with polar polyglycol phase, severe peak tailing and loss of

sample owing to adsorptive effects is still evident [4]. The use of a porous polymer support, *e.g.*, Porapak Q, improves the GE peak shapes but the retention is significant [2].

In the last 15 years, support deactivation with polymers [5–8] has become an effective and indispensable method for obtaining reliable retention data and quantitative results for various polar analytes on packed columns. Using the procedure given in previous papers [6,8], a polyester type instead of a polyglycol type of phase for support deactivation was investigated.

The aim of this work was to develop a specially packed column for the analyses of some glycol ethers as an alternative to a wide-bore (WB) capillary column.

The optimum combination of column dimensions, phase loading, carrier gas, flow-rate and some other aspects, related to polyester deactivated Chromosorb P, contributed to the retention and separation of C₃–C₁₈ *n*-alkanols and glycol ethers.

EXPERIMENTAL

Preparation of GC column packing

The iron content of Chromosorb P was reduced to 0.015% by thorough acid washing in a modified Soxhlet apparatus of our design [5,6,9]. The next step in the deactivation of the support was carried out with poly(ethylene glycol succinate) (PEGS) as follows: Chromosorb P was coated with 5.0% (w/w) PEGS, treated at 300°C for 24 h with argon at a flow-rate of 5 ml/min and subjected to methanol extraction as described in detail elsewhere [6–8]. This deactivated support coated with 15% (w/w) PEGS was used for column packing; empty glass columns were deactivated with dimethyldichlorosilane (DMDCS) in advance [5,6]. The packed column was conditioned at 210°C for 24 h with argon at a flow-rate of 20 ml/min.

GC apparatus

The GC measurements were carried out with a Model PU 304 chromatograph (Philips, Cambridge, U.K.), equipped with a dual flame ionization detector and a Model PU 4800 microcomputer with a built-in integrator. Glass packed (0.45 m × 2.0 mm I.D.) and fused-silica (FS) WB capillary (10.0 m × 0.53 mm I.D.) columns were used and their performances were compared. Hydrogen was used as the carrier gas. The samples were introduced with a Hamilton 1.0- μ l microsyringe. For the WB column direct injection was used. For the determination of 2-methoxyethanol the internal standard (I.S.) method was used with diethylene dioxide as a standard.

GC measurements were performed with linear temperature programming (LTP). The retention behaviour of GEs under LTP conditions was expressed as relative retention temperature (*RRT*) and retention index (*I*) according to following equations:

$$RRT_{LTP} = T_{R(i)}/T_{R(S)}$$

where $T_{R(i)}$ is the retention temperature of the analyte i (°C) and the $T_{R(S)}$ is the retention of the standard and

$$I_{LTP} = 100 \left[\frac{T_{R(i)} - T_{R(n)}}{T_{R(n+1)} - T_{R(n)}} + n \right]$$

where $T_{R(n)}$ and $T_{R(n+1)}$ are the retention temperatures of the n -alkanols as fixed points and n is the carbon number of the fixed points, as described [9].

The peak asymmetry factor, f_{as} , was determined using the peak width at 10% of the peak height, $W_{0.1}$ [8]; 1-butanol and 1-octanol were used as test asymmetry substances.

Electron microscopy (EM)

For observation of the changes on the diatomite surface during the various treatments, transmission electron microscopy (TEM) was used. The micrographs were obtained with a Model EM 400 instrument (Philips, Eindhoven, The Netherlands). Support samples were prepared by the carbon-platinum (C-Pt) replica technique as described elsewhere [8,9]. A Model 306 vacuum evaporator (Edwards, Crowley, U.K.) was used.

Gas chromatographic-mass spectrometric (GC-MS) apparatus and measurements

GC-MS for identifying impurities in 2-methoxyethanol was carried out on a Hewlett-Packard GC-MS system consisting of an HP 5890 gas chromatograph, an HP 5970 B-UNIX mass-selective detector and an HP 9000 computer. The column was FS HP-1 (cross-linked dimethylsilicone), 0.33 μm film thickness (25.0 m \times 0.2 mm I.D.). The carrier gas was helium at a total flow-rate of 35 ml/min. The temperature programme and other conditions are given in the figure captions. Typical MS conditions were electron impact (EI) ionization, ionization energy 70 eV, vacuum $3 \cdot 10^{-8}$ – $8 \cdot 10^{-8}$ bar and ion source temperature 220°C.

Chemicals, reagents and materials

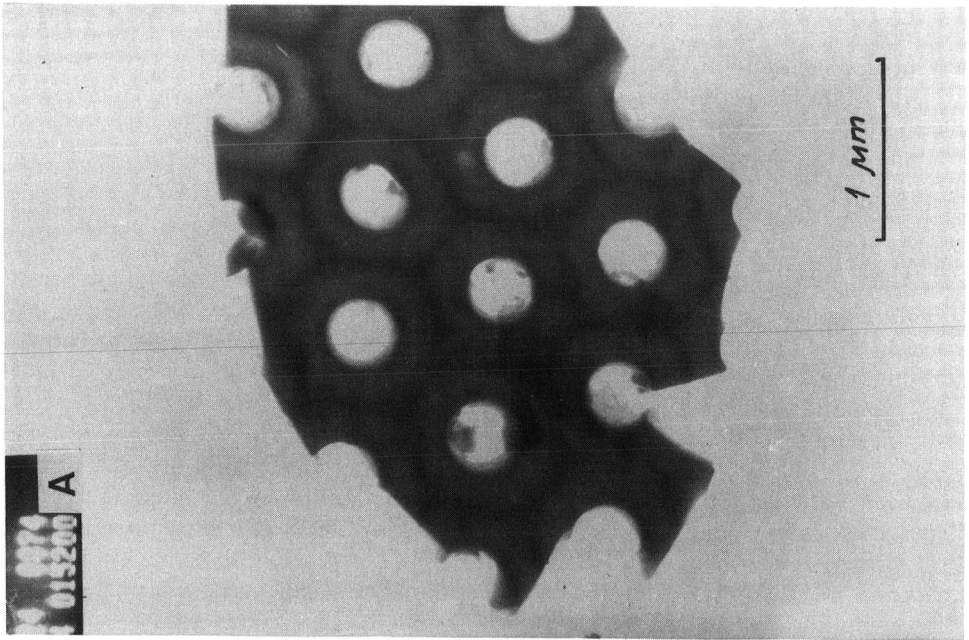
All analytes, solvents and reagents were of analytical or GC quality. The ketones, alkanols, xlenols and phenols were supplied by PolyScience (Evanston, IL, U.S.A.), Supelco (Gland, Switzerland) and Fluka (Buchs, Switzerland). Chromosorb P was supplied by Johns-Menville (Denver, CO, U.S.A.) and PEGS and DMDCS by E. Merck (Darmstadt, Germany). Glycol ethers were supplied by Hoechst (Frankfurt, Germany). The main product 2-methoxyethanol was produced in the Organic Chemistry Department of the Institute of Chemical Industry (Sofia, Bulgaria).

RESULTS AND DISCUSSION

The polar character of the glycol ethers shown in Table I necessitates special attention to the support activity. Most column packings employed for the analysis consist of white diatomites, deactivated with silanes and polyglycols, as liquid stationary phases [1–4].

Some advantages of pink supports deactivated with polymers, and of polyester-type phases, *e.g.*, PEGS, in comparison with white supports and polyglycol-type phases, particularly of poly(ethylene glycol) 20M, were reported recently [6–8]. It has also been pointed out that a polymer used as a deactivator improves the compatibility between the support siliceous surface and the polymer used as a separation liquid [7].

The polyester phase PEGS has been found to be a reasonable choice for analysing polar, closely boiling and/or isomeric analytes [6,8]; it is not only a good tail reducer but also increases selectivity.



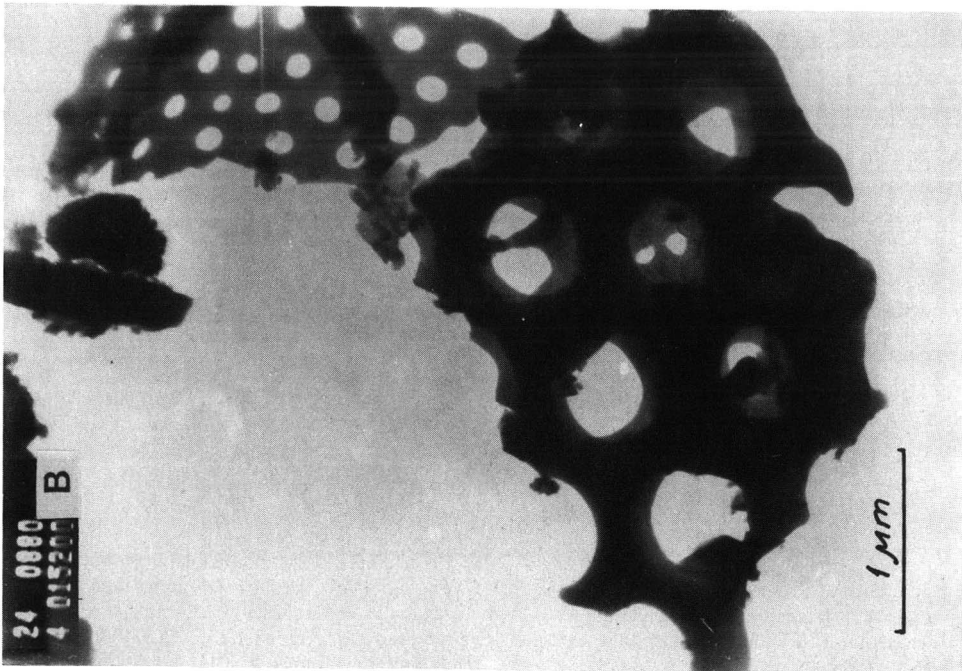
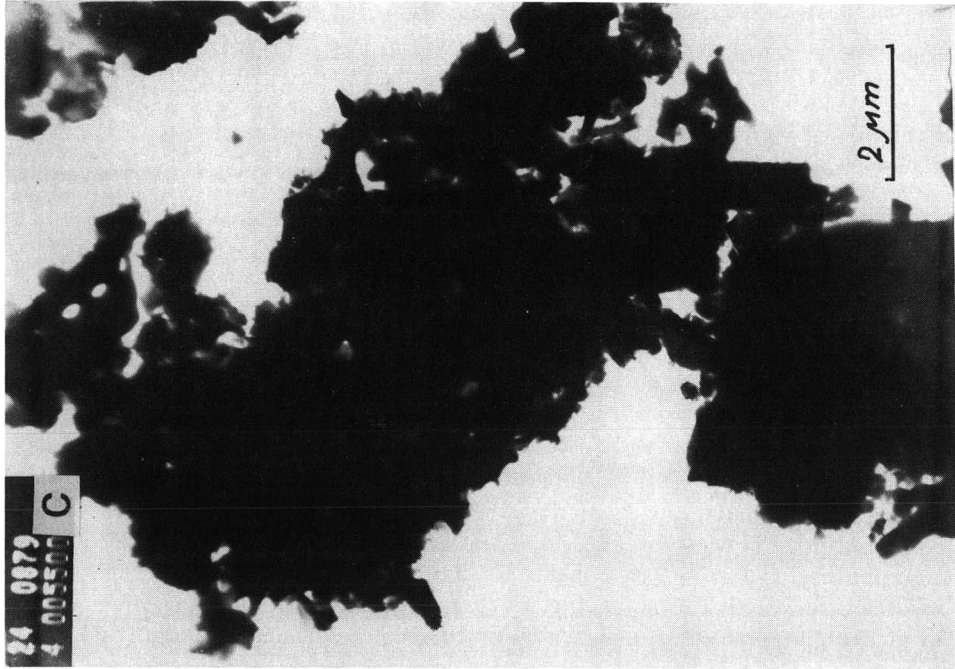


Fig. 1. Electron micrographs of (A) Chromosorb P AW (0.015% iron content) surface deactivated by polymer (PEGs), treated at 300°C and solvent extracted, magnification $\times 15\ 200$, and (B and C) Chromosorb P AW, polyester deactivated and coated with the same polymer at higher content (15%, w/w), (B) $\times 15\ 200$ and (C) $\times 5500$.

TABLE I

BOILING POINTS (T_b) AND RETENTION TEMPERATURES (T_R), RELATIVE RETENTION TEMPERATURES (RRT) AND RETENTION INDICES (I) UNDER LTP CONDITIONS OF GLYCOL ETHERS

Compound ^a	Formula	T_b (°C)	T_R (°C)	RRT_{LTP}	I_{LTP} (i.u.)
2-Methoxyethanol (2)	CH ₃ OCH ₂ CH ₂ OH	124.3	61	1.17	477.8
2-Ethoxyethanol (3)	C ₂ H ₅ OCH ₂ CH ₂ OH	135.1	65	1.25	516.7
2-Butoxyethanol (4)	C ₄ H ₉ OCH ₂ CH ₂ OH	171.2	84	1.61	690.0
2-(2-Methoxyethoxy)ethanol (7)	CH ₃ O(CH ₂ CH ₂ O) ₂ H	193.2	125	2.40	995.5
1-Methoxy-2-(2-ethoxyethoxy)methane (5)	CH ₃ O(CH ₂ CH ₂ O) ₂ CH ₃	161.0	87	1.67	713.3
1-Ethoxy-2-(2-ethoxyethoxy)ethane (6)	C ₂ H ₅ O(CH ₂ CH ₂ O) ₂ C ₂ H ₅	188.0	96	1.85	773.3
1-Butoxy-2-(2-ethoxyethoxy)butane (8)	C ₄ H ₉ O(CH ₂ CH ₂ O) ₂ C ₄ H ₉	256.0	136	2.61	1090.9
Diethylene dioxide (I.S.) (1)	OCH ₂ CH ₂ OCH ₂ CH ₂	101.3	52	1.00	384.6

^a Elution peak numbers as shown in Fig. 3 are given in parentheses.

In previous studies it was shown that when observing the changes on the siliceous diatomite surface, TEM is preferable to the scanning mode [7–9]. The electron micrographs (Fig. 1) illustrate the polymer spreading on the surface; the coverage with PEGS used as a deactivator is insufficient (Fig. 1A), while additional coating with PEGS at a higher concentration ensures much greater surface coverage (Fig. 1B and C).

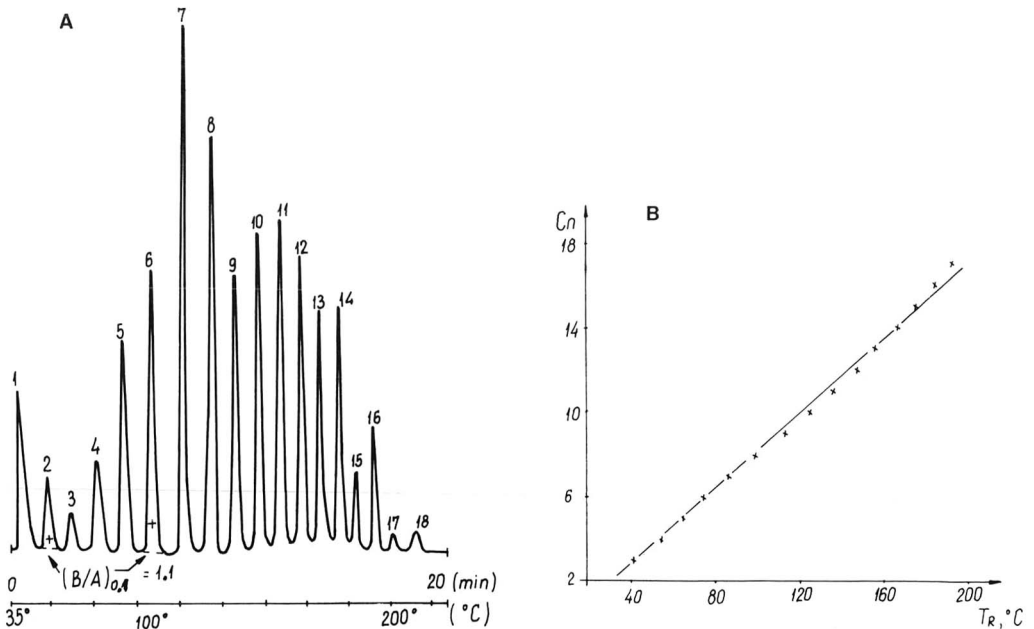


Fig. 2. (A) Chromatogram of a test mixture of C₃–C₁₈ *n*-alkanols: 1 = propanol; 2 = butanol; 3 = pentanol; 4 = hexanol; 5 = heptanol; 6 = octanol; 7 = nonanol; 8 = decanol; 9 = undecanol; 10 = dodecanol; 11 = tridecanol; 12 = tetradecanol; 13 = pentadecanol; 14 = hexadecanol; 15 = heptadecanol; 16 = octadecanol; 17 = nonadecanol; 18 = eicosanol. GC conditions as specified in Fig. 3. (B) Plot of the number of carbon atoms (C_n) for *n*-alkanols versus the retention temperatures, T_R (°C).

TABLE II

COMPARISON OF THE PROPOSED SHORT PACKED (A) AND THE WIDE-BORE CAPILLARY (B) COLUMNS

Parameter ^a	Column	
	A (0.45 m × 2 mm I.D.)	B (10.0 m × 0.53 mm I.D., 1.2 μm)
K_2	3.5	4.8
$\alpha_{1,2}$	2.0	2.0
$R_{1,2}$	2.75	6.54
$TZ_{1,2}$	1.33	4.5
$N_{\text{eff}(2)}/m$	760	986
$H_{\text{eff}(2)}$	0.13	0.10
$(B/A)_{0.1(3)}^b$	1.08	1.15

^a K = Capacity (or partition ratio); α = selectivity; R = resolution; TZ = separation number; N_{eff} = number of effective plates; H_{eff} = height equivalent to a theoretical plate. Subscripts: 1 = *n*-heptane; 2 = *n*-octane; 3 = *n*-octanol.

^b Measured with a micrometric magnifying glass (± 0.1 mm).

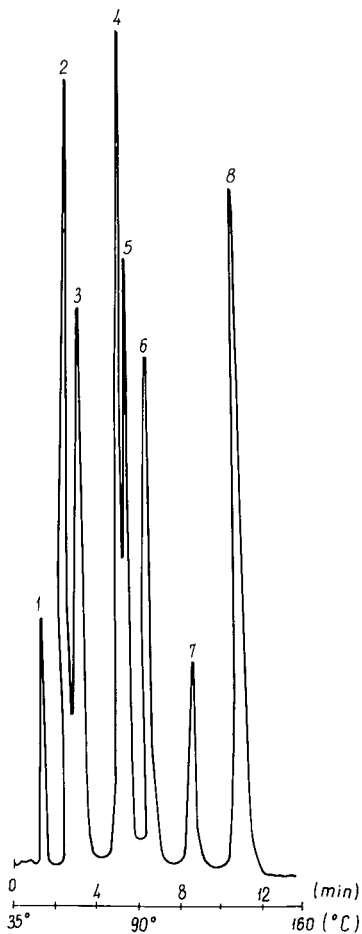


Fig. 3. Chromatogram of glycol ethers: peak numbers as shown in Table I. Conditions: glass column (45.0 cm × 2.0 mm I.D.) packed with Chromosorb P AW (0.015% iron) deactivated with PEGS film and additionally coated with 15% (w/w) PEGS; column temperature, programmed from 35°C to 160°C at 9.5°C/min; injector temperature, 250°C; hydrogen flow-rate, 13.5 ml/min; diethylene dioxide as an internal standard (I.S.); sample volume injected, 0.2–0.3 μl.

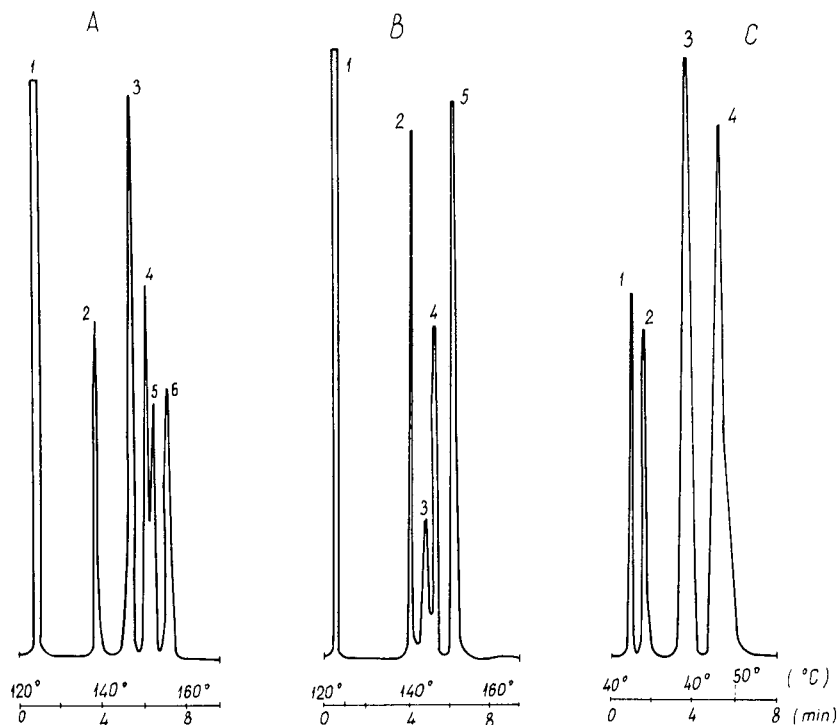


Fig. 4. Chromatograms of oxygen-containing analyte mixtures. (A) Xylenols: 2 = 2,6-, 3 = 2,5-, 4 = 2,3-, 5 = 2,5- and 6 = 3,4-xenol in benzene (=1). Column temperature, programmed from 120°C (1 min) to 160°C at 6°C/min; hydrogen flow-rate, 16 ml/min; other conditions as in Fig. 3. (B) Phenols: 2 = phenol, 3 = *m*-cresol, 4 = *o*-ethylphenol and 5 = *p*-ethylphenol in benzene (=1). (C) Ketones: 1 = 3-pentanone, 2 = 2-methylpentanone, 3 = 4-heptanone and 4 = 2-heptanone. Column temperature, programmed from 40°C (4 min) to 70°C at 6.5°C/min; hydrogen flow-rate, 13.1 ml/min; other conditions as in Fig. 3.

TABLE III

REPEATABILITY OF RETENTION OF GLYCOL ETHERS UNDER LTP CONDITIONS IN TERMS OF RELATIVE RETENTION TEMPERATURES (RRT) AND RETENTION INDICES (I)

\bar{x} = Average value ($n = 6$); S.D. = standard deviation; R.S.D. = relative standard deviation.

Glycol ether ^a	RRT_{LTP}			I_{LTP}^b		
	\bar{x}	S.D.	R.S.D. (%)	\bar{x}	S.D.	R.S.D. (%)
2	1.17	0.05	4.28	477.8	0.51	0.11
3	1.25	0.06	4.38	516.7	0.45	0.09
4	1.61	0.03	1.64	690.0	0.58	0.08
7	2.40	0.06	2.55	995.5	0.51	0.05
5	1.67	0.05	3.06	713.3	0.37	0.05
6	1.85	0.05	2.59	773.3	0.39	0.05
8	2.61	0.05	2.00	1090.9	0.31	0.03
1	1.00	—	—	384.6	0.46	0.12

^a Numbers as shown in Table I and Fig. 3.

^b C_3-C_{11} *n*-alkanols as fixed points (Fig. 2B).

A miniaturized column packed with polyester deactivated Chromosorb P and additionally coated with a higher content of PEGS under LTP conditions give an effective separation of various polar mixtures, as shown in Figs. 2-4. Compounds are eluted with symmetrical peak shapes, relatively low column temperatures and shorter

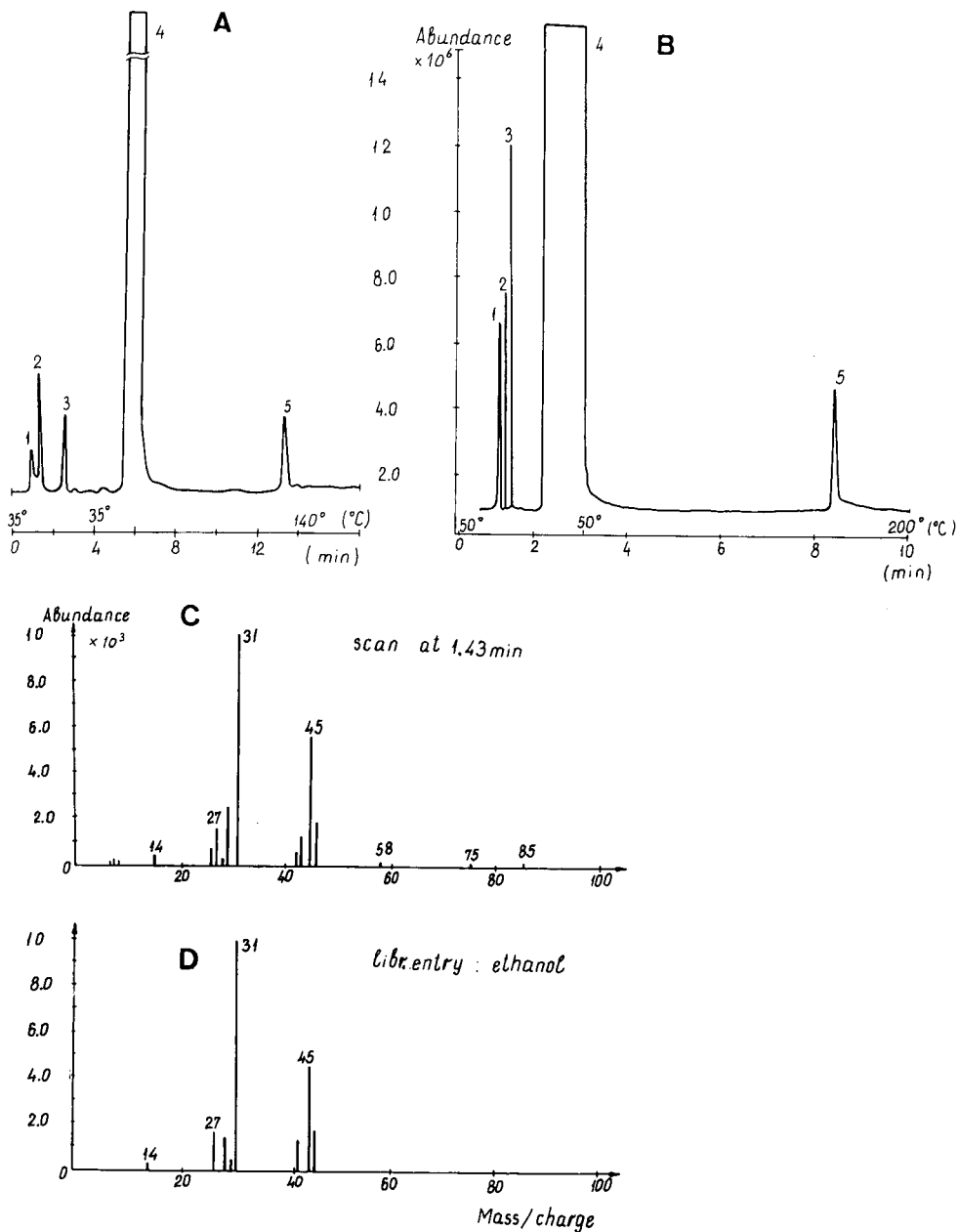


Fig. 5.

(Continued on p. 362)

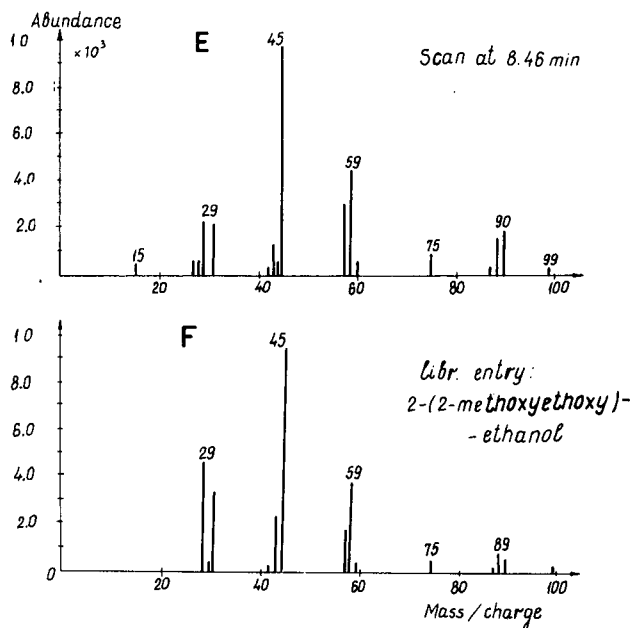


Fig. 5. Chromatograms of 2-methoxyethanol and its impurities (A) on the proposed packed column and (B) on a capillary column. (A) Flame ionization detection. Peaks: 1 = unidentified; 2 = ethanol; 3 = diethylene dioxide (I.S.); 4 = main peak; 5 = 2-(2-methoxyethoxy)ethanol. Column temperature, programmed from 35°C (4 min) to 150°C at 9.5°C/min; hydrogen flow-rate, 13.5 ml/min; other conditions as in Fig. 3. (B) Mass-selective detection total ion chromatogram. Peaks: 1 = air; 2 = water; 3 = ethanol; 4 = main peak; 5 = 2-(2-methoxyethoxy)ethanol. Column, 25.0 m \times 0.2 mm I.D., 0.33 μ m, HP-1 fused silica; column temperature, programmed from 50°C (3 min) to 200°C (5 min) at 8°C/min; injector temperature, 250°C; detector temperature, 250°C; MS scan, 10–150 u. (C–F) Mass spectra of impurities: C = ethanol, E = 2-(2-methoxyethoxy)ethanol found in 2-methoxyethanol, and D and F = library spectra for comparison.

analysis times. For this miniaturized column only 1.5 cm³ of packing material is required.

The column performance was evaluated preliminarily with a test mixture of C₃–C₁₈ *n*-alkanols. The chromatogram in Fig. 2 illustrates an analysis without baseline noise and with low adsorption activity; the peak asymmetry factor, f_{as} , for 1-butanol and 1-octanol (Fig. 2, Table II) is *ca.* 1.0. Good experimental results and a comparison between the proposed and a wide-bore capillary column (Table II) show that the former could be an alternative to the WB capillary column.

The retention of the glycol ethers (Fig. 3) expressed as retention temperatures, T_R , relative retention temperatures, RRT , and retention indices, I , under LTP conditions are given in Table III. It is demonstrated that the retention of *n*-alkanols used as fixed points on the retention index scale of the glycol ethers increases linearly with increase in the number of carbon numbers, C_n (Fig. 2B). The retention of the GEs under investigation corresponds better to *n*-alkanols than to *n*-alkanes [9]; the retention of 1-ethoxy-2-(2-ethoxyethoxy)ethane (C₈) is just between those of C₇ and C₉ alkanols, but between C₅ and C₆ *n*-alkanes. The results from the statistical

evaluation of retention data (Table III) indicate that the retention indices, I , are to be preferred to RRT s and that the S.D. for I is 0.31–0.58 index units.

Special attention was paid to the analysis of the main product, 2-methoxyethanol (Fig. 5). Despite the different types columns used, their separation efficiencies are very similar. The identification of impurities with the proposed PEGS column was carried out with standards with confirmation by mass-selective detection data (Fig. 5C–F).

CONCLUSIONS

A miniaturized packed PEGS column was evaluated by analysing selected polar glycol ethers and some other oxygen-containing compounds such as alkanols, phenols, xylenols and ketones.

The effects and benefits of the polyester as a deactivator and a separation phase have been pointed out. The polar compounds are eluted with highly reproducible retention values, symmetrical peak shapes, relatively low column temperatures and shorter analysis time.

A comparison of the performances of the proposed and wide-bore capillary columns showed that the former column is comparable to the latter. Hence a packed PEGS column could be an alternative to wide-bore capillary columns with respect to separation power, resolution, etc.

ACKNOWLEDGEMENTS

The authors are grateful to Dr. E. Kaschieva of the Higher Institute of Chemical Technology, Sofia, for the TEM observations. They thank Hewlett-Packard (Vienna, Austria) for the GC–MS analysis of the 2-methoxyethanol product, and Dipl. Eng. R. Dojkova of the Institute of Chemical Industry, Sofia, for its synthesis.

REFERENCES

- 1 O. Schupp and J. Lewis (Editors), *GC Compilation*, ASTM Special Technical Publication DS-25 A, American Society for Testing and Materials, Philadelphia, 1967.
- 2 J. Palframan and E. Walker, *Analyst (London)*, 92 (1967) 535.
- 3 J. Haken and V. Khemangkorn, *J. Chromatogr. Sci.*, 10 (1972) 41.
- 4 O. Diment, K. Kazanski and A. Miroshnikov, *Glycols and Other Derivatives of Ethylene and Propylene Oxides*, Khimiya, Moscow, 1976.
- 5 K. Lekova, L. Kardjieva, N. Hlebarova and V. Natan, *J. Chromatogr.*, 212 (1981) 85.
- 6 K. Lekova, N. Popova, S. Ivanichkova, S. Takeva and K. Kodjuharova, *J. Chromatogr.*, 292 (1984) 129.
- 7 K. Lekova, *Commun. Dept. Chem., Bulg. Acad. Sci.*, 19 (1986) 503.
- 8 K. Lekova, M. Bursukova, S. Ivanichkova, N. Bojkova and R. Petkova, *J. Chromatogr.*, 446 (1988) 31.
- 9 K. Lekova, M. Radulova, M. Bursukova and E. Rasheva, *J. Chromatogr.*, 446 (1988) 23.

Estimation of cellulose polarity by gas chromatography

L. A. DERNOVAYA and Yu. A. ELTEKOV*

Institute of Physical Chemistry, Academy of Sciences of the U.S.S.R., 117071 Moscow (U.S.S.R.)
and

J. HRADIL and F. SVEC

Institute of Macromolecular Chemistry, Czechoslovak Academy of Sciences, 16206 Prague (Czechoslovakia)

ABSTRACT

The interaction between bead cellulose and methanol, ethanol, acetonitrile, nitromethane, acetone, 2-butanone, chlorobenzene and tetrahydrofuran during gas chromatography has been studied. From the specific retention volumes, initial differential heats of adsorption and the contributions of the specific interaction energies of molecules adsorbed to the cellulose surface to the total adsorption energy have been estimated. The calculated Kováts' indices and Rohrschneider's equation constants have been employed for comparison of the polarity and selectivity of the cellulose surface with various polymer sorbents.

INTRODUCTION

The number of stationary phases has increased considerably in recent times. The important role in these is that of the polymeric sorbents. The most important advantage provided by these phases is the surface reactivity, allowing numerous changes in surface properties and porosity, and thus polymer sorbents are the most universally used. Up to now, there has been no comprehensive study which deals with intermolecular interactions between organic molecules and the polymer, and with the thermodynamics of these reactions.

This study is concerned with the adsorption of low-molecular-weight compounds on bead cellulose at different temperatures and compares many known polymer sorbents.

EXPERIMENTAL

Macroporous cellulose beads were synthesized by a procedure described elsewhere [1–4]. The sorbent particle size was 0.25–0.50 mm, the specific surface area in the dry state 110 m²/g as determined with an Areatrone analyser (Strolein, Germany), mean pore size 50 nm and pore volume 1.18 ml/g.

Retention time was measured with a set of organic compounds within the temperature range 60–100°C by means of a Tswet 102 chromatograph with a flame

ionization detector. The cellulose sorbent was heated for 2 h at 100°C in a flow of helium (30 ml/min) prior to chromatographic measurements. The dead retention volume was determined by methane.

From the experimental retention times the corrected retention volumes, V_R , were calculated. The differential heat of adsorption, $-\Delta U$, was determined from the temperature dependence of retention volume [5]. Kováts' indices were used as relative retention parameters [6]. The classification of Rohrschneider [7,8], in a modified version by Supina [9], was used for polarity estimation of bead cellulose and some other polymer sorbents.

RESULTS AND DISCUSSION

Our results permit comparison of adsorption interactions of different molecules with polymer adsorbents and cellulose. Recently the linear dependence of logarithm of retention volume on the number of carbon atoms and molecular polarizability α was revealed for homologous series of *n*-alkanes and aromatic compounds. The molecular non-specific interaction energy is approximately proportional to α/r^6 , where r is the distance between interacting molecules. The contribution of specific interactions to the total adsorption energy is then estimated as the difference between retention data (Kováts' indices) of *n*-alkanes and organic compounds bearing functional groups. Kováts' indices, I , calculated from retention volumes of polar compounds, are summarized in Table I. Fig. 1 illustrates the relation of Kováts' indices to molecular polarizability, and the actual values are given in Table I. The highest difference is observed with alcohols, nitromethane and acetonitrile. The retention of alcohols is determined by the ability to form hydrogen bonds with the surface hydroxyl groups of the cellulose. High retention of the strongly polarized acetonitrile ($\mu = 3.96$ D) and nitromethane ($\mu = 3.44$ D) occurs owing to the specific dipole-dipole interaction with

TABLE I

RETENTION DATA OF ORGANIC COMPOUNDS ON CELLULOSE SORBENT AT COLUMN TEMPERATURE 100°C

Adsorbate	$\alpha(\text{\AA}^3)^a$	$\mu(\text{D})^b$	$\log V_R^c$	I^d	I^e
Methanol	3.23	1.65	2.15	935	700
Acetonitrile	4.4	3.96	2.09	919	700
Ethanol	5.06	1.7	2.10	921	670
Acetone	6.32	2.73	1.72	819	520
1-Propanol	6.89	1.66	2.35	984	640
Nitromethane	7.2	3.44	2.11	924	570
2-Butanone	8.2	2.8	1.96	885	500
Tetrahydrofuran	10.0	1.63	1.83	747	240
Benzene	10.3	0	1.28	671	170
Chlorobenzene	12.3	1.72	1.86	861	240

^a Polarizability.

^b Dipole moment.

^c Retention volume.

^d Kováts' index.

^e Kováts' index differences between sorbate and alkane.

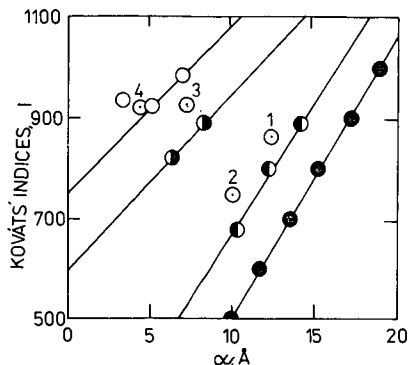


Fig. 1. Effect of polarizability, α (\AA^3), on Kovats' indices, I . ● = Alkanes; ◐ = aromatic hydrocarbons; ◑ = ketones; ○ = alcohols; 1 = chlorobenzene; 2 = tetrahydrofuran; 3 = nitromethane; 4 = acetonitrile.

the polar cellulose surface. The retention data of polar compounds indicates extensive specific interactions and suggests that the cellulose may be classified as polar sorbent of the second type according to the sorbent classification of Kiselev and Yashin [5].

For polarity relations of various adsorbents and stationary phases the chromatographic polarity scale developed by Rohrschneider [7,8] is traditionally used. Comparison of retention indices, I , of polar compounds on different sorbents facilitates calculation of the relative polarity of cellulose. If squalane is considered to be the most non-polar stationary phase, with polarity defined as $P = 0\%$ then the opposite extreme is β, β' -dicyandiethylene, $P = 100\%$. Thus the polarity of cellulose with respect to benzene is 5%. This approach provides a tool to compare various sorbents using Kovats' scale relating retention indices for 2-butanone. As a base, the index for retention of 2-butanone on Chromosorb 106 was defined as $I = 0$. The upper limit of the scale was chosen as the index achieved on the copolymer methyl methacrylate-acrylonitrile with the highest retention value and was defined as 100%. All other sorbents fit into this scale very well (Fig. 2).

Any sorbent may be described by its retention of selected compounds of different polarity. The original Rohrschneider approach uses Kovats' indices and relates them to squalane [9]. Table II lists the data acquired for cellulose and some other sorbents. From Table II it can be seen that the cellulose sorbent exhibits strong specific adsorption due to the donor-acceptor intermolecular interaction with molecules such as alcohols, nitromethane or ketones. The polarity of the cellulose surface is high even in comparison with commercial sorbents with attached polar groups, e.g. Chromosorb 104 with nitril groups or Polysorb N with a free electron pair on nitrogen in the pyridine ring.

The mechanism of retention of various compounds in polymeric sorbents is not clearly understood. It is expected that, due to the dependence of retention on the temperature and chemical nature of the sorbent surface, the interaction proceeds between solvent and adsorbent or between free solvent and fixed solvent [11]. We studied the relation between retention of polar compounds at low concentrations and low temperatures (60–100°C) and the thermodynamic characteristics for the cellulose. The data for differential internal energy ($-\Delta U$) determined from the retention

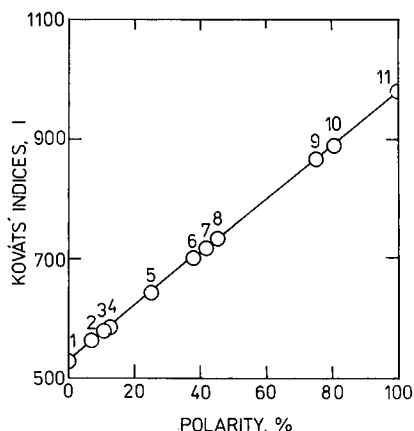


Fig. 2. Scale of polarity of adsorbents calculated on 2-butanone at 100°C. 1 = Chromosorb; 2 = Porapak QS; 3 = Chromosorb 102; 4 = Chromosorb 105, Porapak Q and Porapak S; 5 = Chromosorb 101 and Chromosorb 107; 6 = copolymer methyl methacrylate (MMA)-ethylene dimethacrylate (EDMA) (10:90); 7 = Porapak T; 8 = copolymer MMA-methyl methacrylate with 2-hydroxyethyl methacrylate (HEMA)-EDMA (8:32:60); 9 = Chromosorb 104; 10 = Cellulose; 11 = copolymer HEMA-acrylonitrile (AN)-EDMA (55:6:39).

diagram of ketones and alcohols sorbed on cellulose indicate a high polarity for the cellulose surface.

Table III lists values of $-\Delta U$ obtained for the temperature range 60–100°C and the values, $\Delta(-\Delta U)$, of the contribution of the specific interaction to the total adsorption energy—calculated as a difference between heat of adsorption of polar molecules and *n*-alkanes interpolated to equal polarizability.

Table III shows that cellulose is the most selective sorbent when it interacts with alcohols accompanied by the formation of hydrogen bonds between the hydroxyl of

TABLE II
RETENTION ROHRSCHEIDER INDICES FOR DIFFERENT POLYMERIC SORBENTS

Adsorbent	Functional group	Temperature (°C)	Rohrschneider index				Ref.
			Benzene	Ethanol	Methyl ethyl ketone	Nitro-methane	
Cellulose	OH	100	0.22	5.37	3.54	4.67	—
Chromosorb 104	CN	100	1.67	1.66	2.62	4.32	12
Polysorb N	Pyridine	100	1.24	3.44	2.14	3.53	12
Spheron S 90F	OH	150	0.26	1.29	0.82	1.96	12
Synachrome E5	Phenyl	150	0.40	0.21	0.36	0.38	12
<i>Copolymers:</i>							
GMA-EDMA (60:40)	Epoxy	150	0.18	2.33	1.89	2.81	15
MMA-HEMA-EDMA (8:32:60)	OH	150	1.40	2.80	2.24	3.54	14
HEMA-AN-EDMA (55:6:39)	OH, CN	150	3.58	5.05	4.38	4.24	14
Porapak Q	Phenyl	150	0.52	1.15	0.93	1.37	12
Porapak T	EDMA	150	1.30	2.60	2.21	3.34	12

TABLE III
DIFFERENTIAL INTERNAL ENERGIES OF ADSORBENTS (kJ/mol)

Adsorbate	Cellulose		Chromosorb	Chromosorb	Chromosorb
	$-\Delta U$	$\Delta(-\Delta U)$	101 [13], $-\Delta U$	102 [13], $-\Delta U$	104 [13], $-\Delta U$
Methanol	61.9	44	35.9	38.1	47.8
Ethanol	62	40	42.3	44.7	54.2
1-Propanol	73.3	42	48.7	51.3	60.6
Acetone	54.0	32	41.2	35.3	52.8
2-Butanone	57.2	27	47.6	41.9	59.2
Hexane	37.1	—	50.1	51.3	50.4

alcohol and hydroxyl located at the cellulose surface. The mean energy is -42 ± 2 kJ/mol for alcohols and -29 ± 3 kJ/mol for ketones. The extent of $\Delta(-\Delta U)$ for aromatic hydrocarbons is insignificant and results from weak specific intermolecular interactions with the non-specific interaction energy are 4–13 kJ/mol [10]. Fig. 3 depicts the polarity scale of various sorbents compared using the $-\Delta U$ data for ethanol and 2-butanone. Zero is defined as $-\Delta U$ for ethanol on the polar polymeric sorbent Chromosorb 101, with 100% being ethanol on cellulose. The selectivity of other sorbents toward ethanol is located within these limits. For 2-butanone the relation is partly distorted. The highest energy belongs to the interaction with Chromosorb 104, the smallest to Chromosorb 102. The extent of $-\Delta U$ of 2-butanone for cellulose is lower than for ethanol. This consideration results in the data given in Table IV where the conventional chromatographic polarity of cellulose is compared with some other polymer sorbents using Kovats' indices at 100°C or differential internal energies calculated according to method applied in Fig. 1.

The suggested polarity scale, as well as Rohrschneider's scale, allows estimation of quantitative data on specific interactions with polar molecules. The advantages of

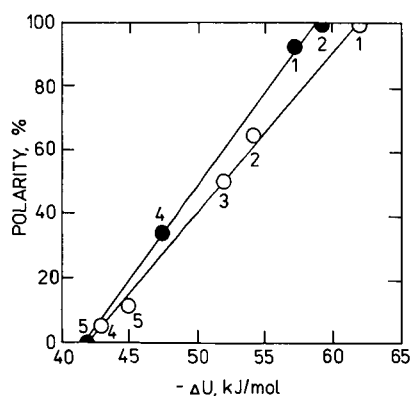


Fig. 3. Scale of polarity according to differential internal energy ($-\Delta U$) of ethanol (○) and 2-butanone (●) adsorption. 1 = Cellulose; 2 = Chromosorb 104; 3 = Porapak T; 4 = Porapak Q; 5 = Chromosorb 102.

TABLE IV

RELATIVE POLARITY (P) OF ADSORBENTS ACCORDING TO KOVATS' INDICES (I) AND DIFFERENTIAL ENERGY ($-\Delta U$)

Adsorbent	$P(\%)$		
	I (2-butanone)	$-\Delta U$ (kJ/mol)	
		Ethanol	2-Butanone
Cellulose	100	100	90
Chromosorb 104	95	65	100
Porapak Q	15	35	5
Chromosorb 102	10	—	10
Chromosorb 106	0	—	—
Chromosorb 101	—	0	0

the proposed conventional scale which uses $-\Delta U$ are the comparison of energy values and the insignificant effect of temperature.

REFERENCES

- 1 J. Peska, J. Stamberg and Z. Blace, *Czech. Pat.*, 172 640 (1976).
- 2 J. Peska, J. Stamberg, J. Hradil and M. Ilavsky, *J. Chromatogr.*, 125 (1976) 455.
- 3 J. Baldrian, J. Plestil and J. Stamberg, *Collect. Czechosl. Chem. Commun.*, 76 (1976) 3555.
- 4 J. Peska, J. Stamberg and J. Hradil, *Makromol. Chem.*, 53 (1976) 73.
- 5 A. V. Kiselev and Ya. I. Yashin, *Adsorptionsnaya Gazovaya i Zhidkostnaya Khromatographia*, Khimia, Moscow, 1979.
- 6 A. Werli and E. Kovats, *Helv. Chim. Acta*, 42 (1959) 2709.
- 7 L. Rohrschneider, *J. Chromatogr.*, 17 (1965) 1.
- 8 L. Rohrschneider, *Advances in Chromatography*, Marcel Dekker, New York, 1967.
- 9 N. Supina, *Nasadochnie Kolonki v Gazovoi Khromatographii*, Mir, Moscow, 1977, p. 107.
- 10 L. I. Dernovaya and Yu. A. Eltekov, *J. Chromatogr.*, 455 (1988) 263.
- 11 K. I. Sakodinskii and L. I. Panina, *Polymernye Sorbenty Dlya Molekulyarnoi Khromatographiii*, Nauka, Moscow, 1977, p. 51.
- 12 J. Hradil, M. Krivakova, P. Stary and J. Coupek, *J. Chromatogr.*, 79 (1973) 99.
- 13 A. V. Kiselev, D. P. Poshkus and Ya. I. Yashin, *Molekularnie Osnovy Khromatographii*, Nauka, Moscow, 1986, p. 155.
- 14 J. Hradil and J. Lukas, *J. Chromatogr.*, 172 (1979) 85.
- 15 J. Lukas, F. Svec and J. Kalal, *J. Chromatogr.*, 153 (1978) 15.

CHROMSYMP. 2322

Removal of organic pollutants from aqueous solution

V. Comparative study of the extraction, recovery and chromatographic separation of some organic insecticides using unloaded polyurethane foam columns

A. B. FARAG

Chemistry Department, Faculty of Science, Mansoura University, Mansoura (Egypt)

and

M. S. EL-SHAHAWI*

Chemistry Department, Faculty of Science at Damietta, Mansoura University, Damietta (Egypt)

ABSTRACT

The concentration of dissolved insecticides in aqueous media was determined by chromatographic separation on polyurethane foam columns. The results of preliminary screening tests on the removal of insecticides by the unloaded polyurethane foam indicated that a reasonable percentage of the insecticides was retained on the foam. Therefore attempts were made to extract these compounds from aqueous media using foam columns. Various parameters affecting the retention and separation of these compounds were studied, including temperature, flow-rate, pH, insecticide concentration, shaking time, sample volume and eluting solvent. The complete separation and quantitative recovery of these compounds from the foam with acetone in a Soxhlet extractor were achieved. The method can be used to preconcentrate insecticides in tap water and modified to determine dissolved insecticides in industrial and natural waters. Polyurethane foam has a good capacity for use when large volume samples need to be handled and is an inexpensive sorbent compared to other known solid sorbents.

INTRODUCTION

Insecticides can enter water systems from various sources. Edward [1,2] has reported sources of insecticides to include run-off from agricultural land, direct entry from crop spraying, industrial and sewage effluent, cattle spraying, dust and rainfall. The presence of insecticides in the aquatic environment has been known to cause severe health problems to animals, birds and humans [3]. The removal or reduction of these organic pollutants to an acceptable concentration by extraction with steam distillation, solvent extraction, oxidation, or adsorption on carbon or other solid supports has been investigated [4-7]. Such preconcentration techniques are often slow or cumbersome and too expensive for routine use where many large volume samples are concentrated on-site prior to quantitative analysis [7].

Polyurethane foam has recently been used as an inexpensive solid extractor and effective sorbent for the removal of water pollutants [8–13]. The solid foam concentrates various species in solution by a phase distribution mechanism rather than by adsorption [12,13].

This paper reports the effect of various parameters on the extraction of some organic insecticides from aqueous solution by polyurethane foam and attempts to establish the mechanism of extraction by the unloaded foam.

EXPERIMENTAL

Reagents and materials

All chemicals used were of analytical-reagent grade. Polyurethane foam, an open cell polyether (bulk density 30 kg m^{-3}) was supplied by K.G., Schaum (Stoffwerk, Kremsmunster, Austria). The foam was cut and washed as previously described [9]. Foam loaded with tributyl phosphate (TBP) was prepared by mixing the dried foam cubes with 5% TBP in benzene ($5 \text{ cm}^3 \text{ g}^{-1}$ dry foam) with stirring for 10 min. The reagent foams were then dried [9].

The insecticides studied were: Dimethoate, O,O-dimethyl-SCN (methyl carbamoyl methyl) phosphorodithioate (I); Azodrine (Nuvacron), 3-hydroxy-*N*-methyl-*cis*-crotonamide dimethyl phosphate (II); and Lannate (methomyl), 5-methyl-*N*-(methyl carbamoyl) oxythioacetamide (III). Stock solutions ($100 \mu\text{g cm}^{-3}$) of each compound were prepared in a 100-cm^3 measuring flask by dissolving the exact weight of the insecticide in 5 cm^3 of acetone and diluting with distilled water. A series of standard solutions of these compounds was prepared by diluting their stock solutions with water; the solutions were stored in polyethylene bottles.

Apparatus

A Varian 634 S double-beam UV–visible spectrophotometer with 1-cm quartz cells was used for the absorbance measurements. An Orion pH meter and glass columns, $12 \text{ cm} \times 10 \text{ mm I.D.}$, were also used.

General procedures

Batch experiments. To investigate the effect of shaking time on the uptake of the compounds on polyurethane foam, the foam cubes (0.3 g) were equilibrated with a 100-cm^3 solution of each compound ($60 \mu\text{g cm}^{-3}$) in separate polyethylene bottles and shaken for various time intervals up to 30 min. The foam cubes were then separated by decantation and the amount of the compound remaining in solution was measured spectrophotometrically at the wavelength of maximum absorption. The amount of compound retained on the foam was then calculated by difference. Following these procedures, the effect of pH, extraction media and temperature were determined. An extraction isotherm was determined for each compound ($20\text{--}100 \mu\text{g cm}^{-3}$).

Flow experiments. In the flow experiments, 1 g of dry foam was packed into the column using the vacuum method of foam column packing [14]. Tap or distilled water ($0.5\text{--}3 \text{ dm}^3$) samples containing 0.3 mg of each compound were passed through the foam column at $5\text{--}10 \text{ cm}^3 \text{ min}^{-1}$. All the compounds were retained quantitatively. After squeezing water from the foam, the compound was then recovered from the foam

in a Soxhlet extractor with 50 cm³ of acetone. The analyte was determined by measuring the absorbance of the solution.

The mixture containing Dimethoate (0.1 mg) and Lannate (0.1 mg) was passed through the foam column at 2–3 cm³ min⁻¹. Dimethoate was washed out first with 100 cm³ of acetone and Lannate was then recovered with 50 cm³ of 0.3 M sodium chloride at pH 5.

RESULTS AND DISCUSSION

Preliminary experiments have shown that the extraction of the investigated compounds (I, II and III, Fig. 1) by the unloaded and the TBP-loaded polyurethane foam using batch experiments is rapid and equilibrium is reached in less than 30 min, followed by a plateau. The results obtained are summarized in Fig. 2. A better percentage extraction was obtained with the TBP-loaded foam and a shaking time of 30 min was used in subsequent work.

Extraction isotherm

The uptake of the investigated insecticides from aqueous solution by the unloaded and TBP-loaded foam was dependent on their initial concentrations. Therefore, the extraction isotherms were determined over a wide range of equilibrium concentrations (20–100 μg cm⁻³) for each compound. The results are presented in Fig. 3. The extraction isotherms of the insecticides tested exhibited a first-order behaviour at low concentrations. The adsorption of the different species by the unloaded foam increases in the order: Azodrine > Dimethoate > Lannate. Similar trends were obtained with the TBP-loaded foams. Solvent extraction is therefore the most probable mechanism for the adsorption of these compounds by the unloaded foams. The acidity of the absorbate (pK_a) and the molecular weight obviously play an important role in determining the adsorption efficiency in the TBP-loaded foam; this is also the case with the unloaded foam. The effect of temperature on the extraction efficiency of the unloaded foam was determined at 35 and 45°C. The percentage adsorption increases slightly with increasing temperature.

The effect of pH on the total insecticide removal was carried out over the pH range 3–9. The adsorption profiles of the investigated compounds are given in Fig. 4. It can be seen that the extraction of compounds I and II increases with increasing pH and reaches a plateau at about pH 6. In contrast, compound III displays a minimum removal at pH 5 by the unloaded foam and the percentage removal increases markedly at higher pH.

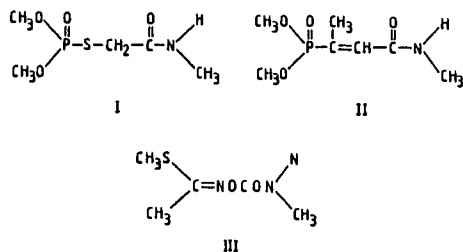


Fig. 1. Structures of I, II and III.

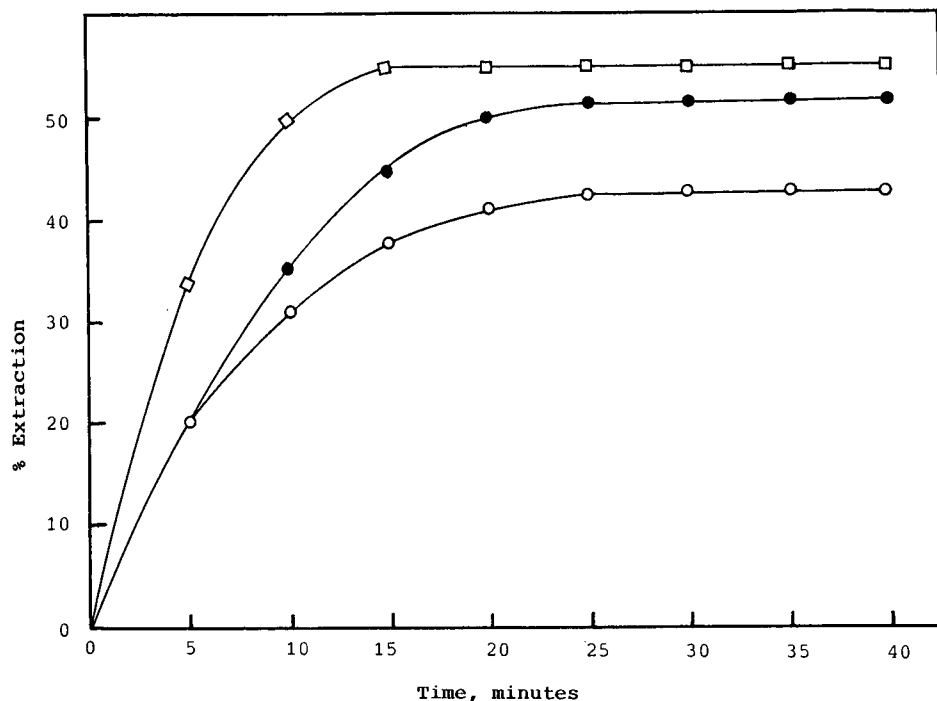


Fig. 2. Effect of shaking time on the extraction of the insecticides by unloaded foam. (□) Azodrine; (●) Dimethoate; and (○) Lannate.

The efficiency and rate of extraction of Lannate by the unloaded foam was generally decreased by the addition of ethanol (0–10%) to the aqueous solution. This is probably due to the formation of inactive species (liophilic association) which are not adsorbed from the aqueous solution [15]. The results are summarized in Fig. 5. The amount of Lannate adsorbed at equilibrium for each ethanol concentration is in the order 0% > 5% > 10% ethanol content. This order agrees with the suggestion of Kirkwood [16] that the smaller the dielectric constant, the larger the amount extracted. Thus, the nature of the media has a marked effect on the adsorption characteristics.

Dynamic experiments

On the basis of the batch experiments, the quantitative retention and recovery of these compounds were investigated using the foam column mode. Distilled or tap water samples (0.5–3 dm³) containing 0.3 mg of each compound were percolated through separate foam columns at a flow-rate of 5–10 cm³ min⁻¹. Complete retention of the compounds was achieved. The insecticides were then recovered from the foam columns with 50 cm³ of acetone in a Soxhlet extractor and determined spectrophotometrically at the maximum absorption wavelength for each species. The results are summarized in Table I. The dependence of recovery on flow-rate through the foam column was investigated by percolating Lannate (0.1 mg) through the column at

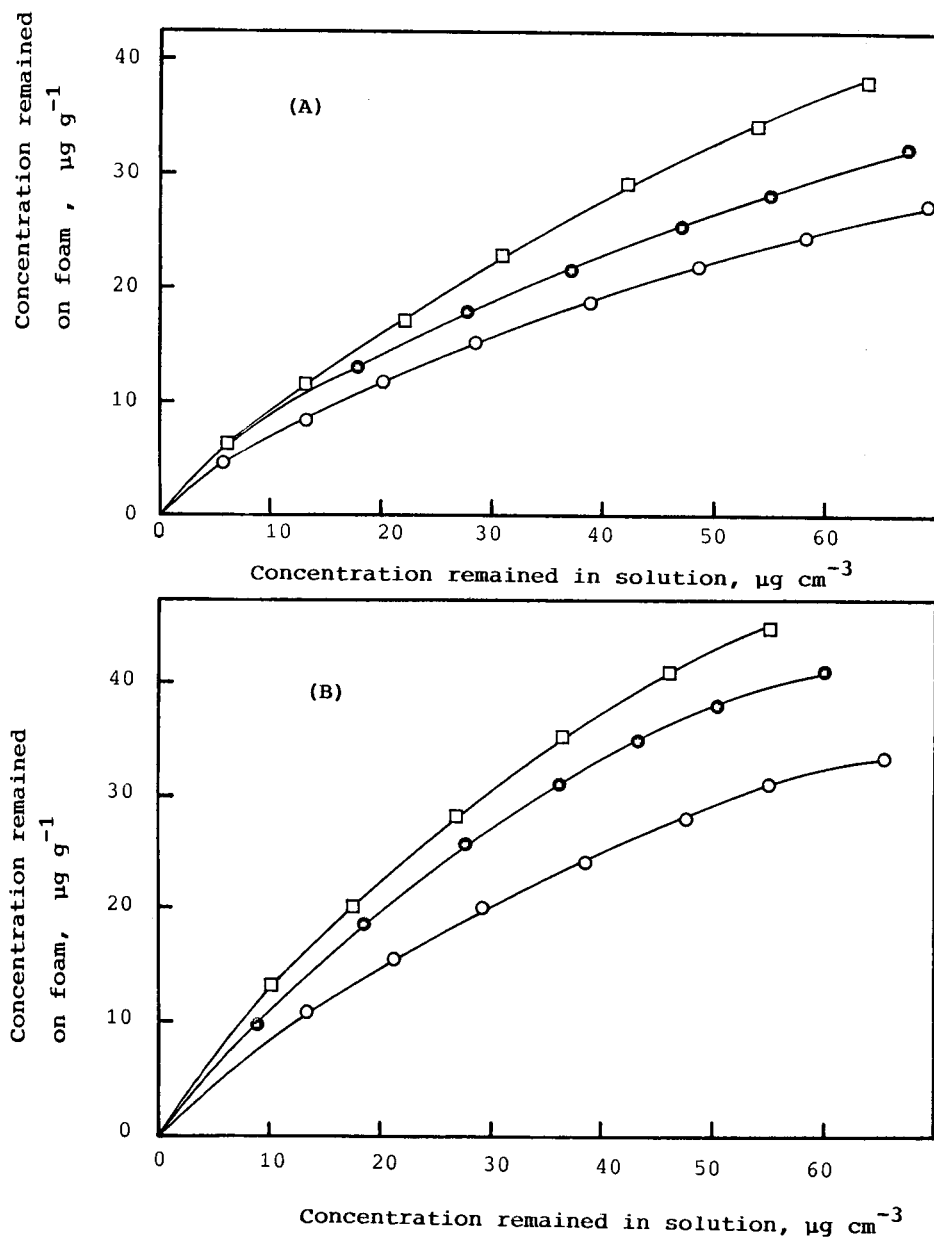


Fig. 3. Extraction isotherms of the insecticides with (A) unloaded foam and (B) TBP-loaded foam. (\square) Azodrine; (\bullet) Dimethoate; and (\circ) Lannate.

various flow-rates. Complete retention of Lannate was obtained up to $10 \text{ cm}^3 \text{ min}^{-1}$ and the efficiency of extraction decreased significantly to 64% at $15 \text{ cm}^3 \text{ min}^{-1}$.

The quantitative retention and elution of Dimethoate was determined. Fig. 6 shows the chromatograms for eluting Dimethoate at flow-rates of 1–3, 5 and 8–10 $\text{cm}^3 \text{ min}^{-1}$.

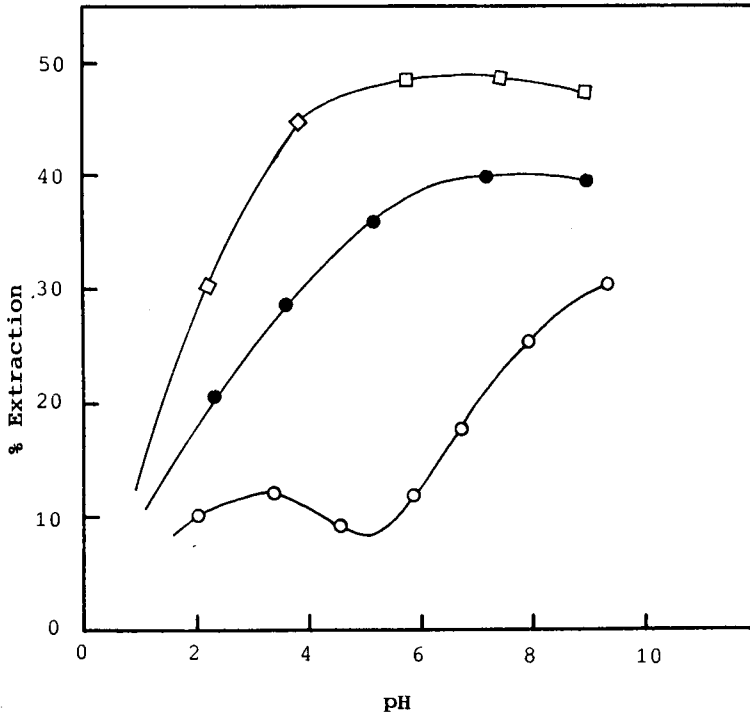


Fig. 4. Effect of pH on the extraction of the insecticides tested with unloaded foam. (□) Azodrine; (●) Dimethoate; and (○) Lannate.

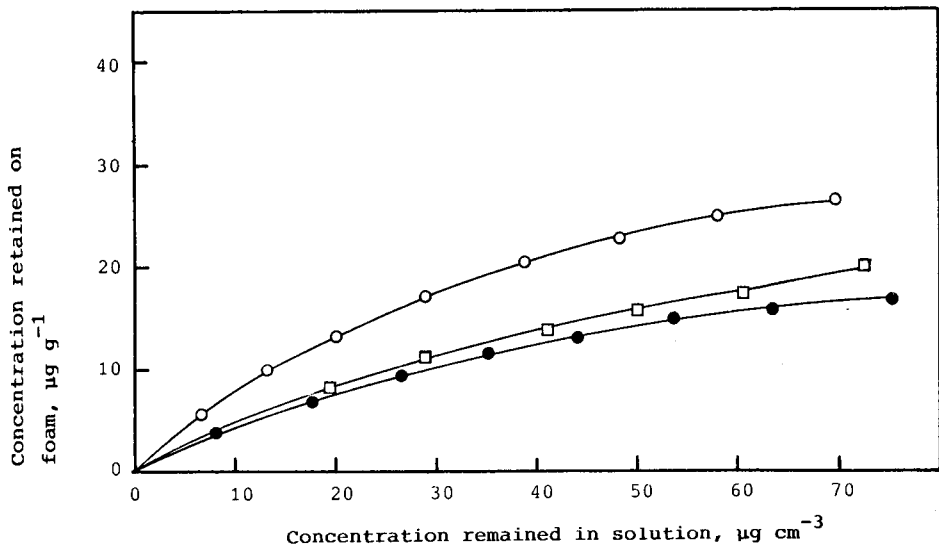


Fig. 5. Effect of ethanol percentage on the extraction of Lannate. (○) 0%; (□) 5%; and (●) 10% ethanol.

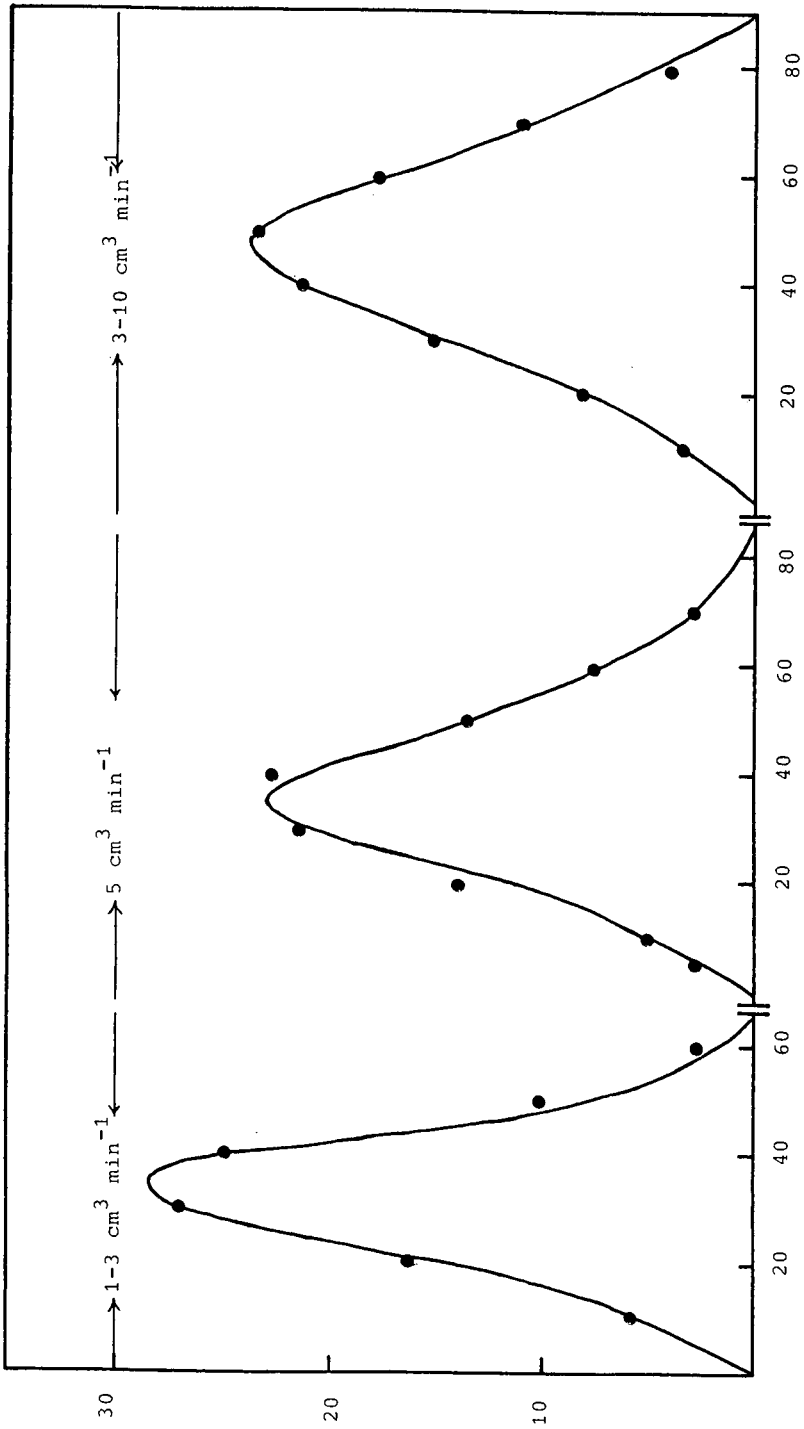


Fig. 6. Effect of flow-rate on the elution of Dimethoate (0.1 mg) with acetone.

TABLE I
EXTRACTION AND RECOVERY OF THE INSECTICIDES

A 0.3-mg mass was extracted from 2 dm³ of aqueous solution by the unloaded foam columns at 3–5 cm³ min⁻¹. (a) Average of duplicate determinations from distilled water; (b) average of duplicate determinations from tap water.

Insecticide	Recovery (%)		Wavelength (nm)
	a	b	
Dimethoate	97	94	320
Azodrine	95	98	306
Lannate	93	90	570

min⁻¹. The height equivalent to a theoretical plate (HETP) was calculated from the elution curves using the equation [17]

$$N = 8 \left(\frac{V_{\max}^2}{W^2} \right) = \left(\frac{L}{\text{HETP}} \right)$$

where N = number of plates, V_{\max} = volume of eluate at peak maximum, W = width of the peak at 1/e the maximum solute concentration and L = length of the foam bed. The HETP values were 2.1, 2.4 and 2.6 mm at flow-rates of 1–3, 5 and 8–10 cm³ min⁻¹, respectively. The value of HETP was also calculated from the break-through capacity curve using the equation [11]

$$N = \left(\frac{\bar{V} \cdot V'}{(\bar{V} - V')^2} \right) = \left(\frac{L}{\text{HETP}} \right)$$

where \bar{V} is the volume of effluent at the centre of the S-shaped break-through curve where the concentration is one half the initial concentration, and V' is the volume at which the effluent has a concentration of 0.1578 of the initial concentration. The value of HETP obtained by this method was 2.3 mm, confirming the values obtained from the elution curves. The proposed column method has been tested for the separation of Dimethoate and Lannate. Dimethoate was eluted first with acetone and Lannate was then recovered with 0.3 M sodium chloride at pH 5 at a flow-rate of 1–2 cm³ min⁻¹.

REFERENCES

- 1 C. A. Edward, *Persistent Pesticides in the Environment*, CRC Press, Boca Raton, FL, 2nd ed., 1973.
- 2 C. A. Edward, *Environmental Pollution by Pesticides*, Plenum Press, New York, p. 409.
- 3 L. T. Kurkland, S. Shibko, A. Kolbye and R. Shapiro, *Haz. Mercury Environ. Res.*, 4 (1971) 9.
- 4 A. H. Romano and R. S. Safferman, *J. Am. Water Works Assoc.*, 55 (1963) 169.
- 5 H. Oda, M. Kishida and C. Yokokawa, *Carbon*, 19 (1981) 243.
- 6 H. Oda and C. Yokokawa, *Carbon*, 21 (1983) 485.
- 7 J. F. Uthe, J. Reinke and H. D. Gesser, *Environ. Lett.*, 3 (1972) 117.
- 8 A. B. Farag, A. M. El-Wakil, M. S. El-Shahawi and M. Mashaly, *Anal. Sci.*, 5 (1989) 415.
- 9 A. B. Farag, A. M. El-Wakil and M. S. El-Shahawi, *Fresenius Z. Anal. Chem.*, 324 (1986) 59.

- 10 G. J. Moody and J. D. R. Thomas, *Chromatographic Separation and Extraction with Foamed Plastics and Rubbers*, Marcel Dekker, New York, 1982.
- 11 T. Braun, J. D. Naveratil and A. B. Farag, *Polyurethane Foam Sorbents in Separation Science*, CRC Press, Boca Raton, FL, 1985.
- 12 H. J. Bowen, *J. Chem. Soc. A*, (1970) 1082.
- 13 K. M. Gough and H. D. Gesser, *J. Chromatogr.*, 115 (1975) 383.
- 14 T. Braun and A. B. Farag, *Anal. Chim. Acta*, 62 (1972) 476.
- 15 T. Hayashita and M. Takagi, *Talanta*, 32 (1985) 399.
- 16 K. G. Kirkwood, *J. Chem. Phys.*, 2 (1934) 351.
- 17 E. Glueckauf, *Trans. Faraday Soc.*, 51 (1955) 34.

CHROMSYMP. 2097

Preparation and evaluation of octadecyl- or phenylpropyl-treated porous glass for the high-performance liquid chromatographic analysis of bufadienolides in *Bufo venenum*

MITSUYOSHI OKAMOTO

Gifu Prefectural Tajimi Hospital, 5-161, Maehata cho, Tajimi, Gifu 507 (Japan)

ABSTRACT

The retention and selectivity of bufadienolides (cinobufagin, resibufogenin, bufalin) in *Bufo venenum* were studied using high-performance liquid chromatography on octadecyl- or phenylpropyl-treated porous glass. From elemental analysis data for carbon, the maximum number of bonded octadecyl or phenylpropyl surface groups per 100 Å² of glass (mean pore diameter 157 Å, specific surface area 213 m²/g) in octadecyl or phenylpropyl gel was calculated to be 2.15 and 1.97, respectively. Using acetonitrile–water mixtures as the eluent, bufadienolides were separated on octadecyl or phenylpropyl gels, but with different degrees of resolution.

INTRODUCTION

At present, chemically bonded stationary phases are used most widely as column-packing materials for reversed-phase high-performance liquid chromatography (HPLC). These materials consist of organic functional groups, such as octadecyl, octyl, ethyl and phenyl groups, bonded to silicas. In previous papers [1–4], I have suggested that the features of silicas, which are important in determining the number of accessible alkylamino or phenyl groups per 100 Å² are the pore diameter and the specific surface area. The identification of drugs and determination of their concentration, especially in oriental formulations and for forensic science purposes, require several types of column gels for HPLC and several types of column gels for gas chromatography. This paper therefore considers how the chromatographic properties of octadecyl- or phenylpropyl-modified glass gels make them, like chemically modified silica gels, important HPLC or micro-HPLC columns gels. However, there have been few reports of HPLC analyses on octadecyl- or phenylpropyl-treated glass columns in physical and chemical research [5–9]. Therefore, the analysis of bufadienolides in *Bufo venenum* (toad cake) using HPLC was compared with previous high-performance thin-layer chromatographic (HPTLC) analysis [10].

EXPERIMENTAL

Reagents

Octadecyldimethylchlorosilane (ODS) and phenylpropyldimethylchlorosilane (PHP) were obtained from Petrach Systems (Bristol, PA, U.S.A.). Uracil, benzene, naphthalene, diphenyl and anthracene were obtained from Wako (Osaka, Japan). Porous glass and porous silicas differing in their mean particle size, mean pore diameter, specific surface area and pore volume (Table I) were purchased from Fuji-Davison (Nagoya, Aichi, Japan). Cinobufagin, resibufogenin and bufalin were provided by Kampo Labs., Kanebo Co. (Osaka, Japan). The other reagents and organic solvents were of analytical reagent grade.

Apparatus

The HPLC measurements were carried out on a Twinkle instrument (Jasco, Tokyo, Japan), equipped with a Uvidec-100IV variable-wavelength detector (Jasco, Tokyo, Japan) and a column of 150 × 4.6 mm I.D., packed with ODS- or PHP-treated glass (or silica).

Stationary phase and elemental analysis

As described previously [1-4], 7-g samples of dried glass were added to 70 ml of a 3.4% solution of ODS (or PHP) in dry toluene containing 3 ml of triethylamine. The glass or silica suspension was refluxed for 5 h, filtered through a glass filter (1 μm), washed several times with toluene, chloroform, methanol and acetone, and then dried *in vacuo* at 70°C for 2 days. The final products are listed in Table II as glass-

TABLE I
CHARACTERISTICS OF ORIGINAL GLASSES AND SILICAS

Sample ^a	Means particle size (μm)	Mean pore diameter (Å)	Specific surface area (m ² /g)	Pore volume (ml/g)
Glasses	5.2	157	213	1.48
Silicas	5.5	131	330	1.08

^a These names were assigned for convenience and are not commercial names.

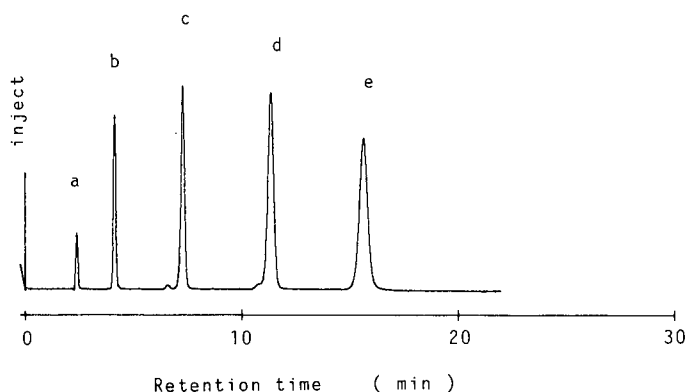
TABLE II
CHARACTERISTICS OF TREATED GLASSES AND SILICAS

Treated gel	Specific surface area (m ² /g)	Carbon content (%)	Average pore diameter (Å)	Pore volume (ml/g)	Number of surface groups per gram (× 10 ²¹)	Number of surface groups per 100 Å ²
Glass-ODS	133	13.8	152	0.97	0.457	2.15
Glass-PHP	164	8.2	155	1.16	0.419	1.97
Silica-ODS	228	19.7	122	0.70	0.456	2.00
Silica-PHP	244	12.5	120	0.73	0.505	2.07

ODS, glass-PHP, silica-ODS and silica-PHP. The characteristics of these materials are also given in Table II. The carbon contents of the treated glass or silicas were determined by elemental analysis using an MT-3 CHN elemental analyser (Yanagimoto, Kyoto, Japan). The specific surface areas, mean pore diameters and pore volumes of the column glass and column silicas were determined with an MOD-220 porosimeter (Carlo Erba, Milan, Italy) and SA-1000 surface-area, pore-volume analyser (Shibata, Tokyo, Japan), and the data are shown in Table II.

A

Glass-PHP



B

Silica-PHP

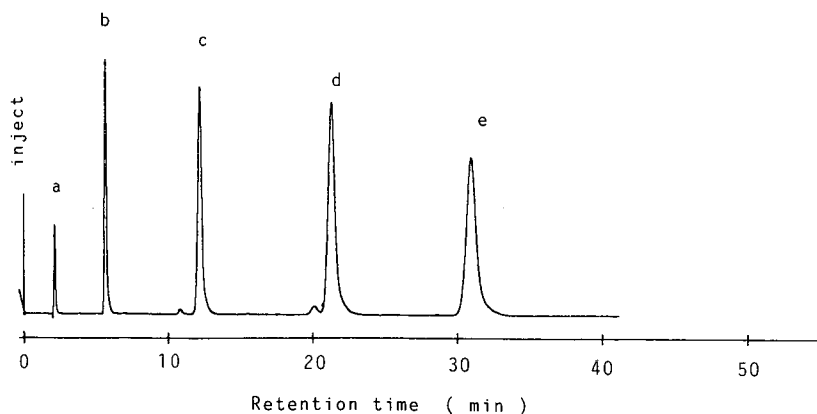


Fig. 1. Typical liquid chromatograms obtained with some aromatic hydrocarbons on glass-PHP or silica-PHP. (A) Glass-PHP: phenylpropyl-treated porous glass. (B) Silica-PHP: phenylpropyl-treated porous silica. Mobile phase: methanol-distilled water (60:40). Flow-rate: 1 ml/min. Detection: 254 nm UV. Peaks: a = uracil; b = benzene; c = naphthalene, d = diphenyl, e = anthracene.

Column preparation

The column glass or column silicas were packed into the stainless-steel column (150 × 4.6 I.D.) using the slurry technique.

Sample preparation

As previously described [10], 100 mg of *Bufo venenum* were extracted four times with 10 ml of acetonitrile–distilled water (1:1). The mixture was warmed in a hot water bath at 50°C for 15 min, and was mixed ultrasonically (45 W, 38 kHz, 10 min). After centrifugation (1500 g, 5 min), the upper phase was filtered through a membrane filter (0.22 μm). The upper phase was made up to volume with acetonitrile–distilled water (1:1) in a 50-ml volumetric flask, then an aliquot of the upper phase was injected onto the HPLC system.

RESULTS AND DISCUSSION

From the elemental analysis of the treated glass, the number of accessible ODS or PHP surface groups per 100 Å² of glass can be calculated as previously described [1–4]. The results are given in Table II. Fig. 1 shows typical liquid chromatograms obtained with some aromatic hydrocarbons on glass-PHP or silica-PHP.

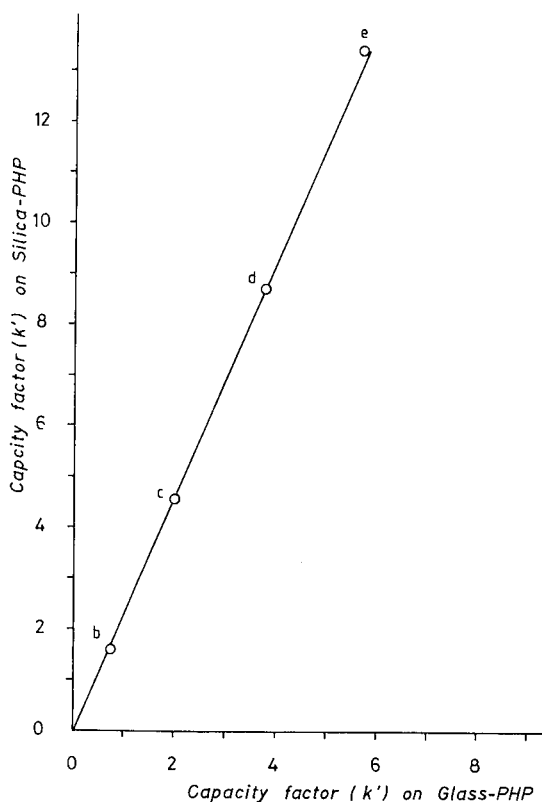


Fig. 2. Correlations between the capacity factors (k') of some aromatic hydrocarbons on glass-PHP versus silica-PHP. Chromatographic conditions as in Fig. 1. Points: b = benzene; c = naphthalene; d = diphenyl, e = anthracene.

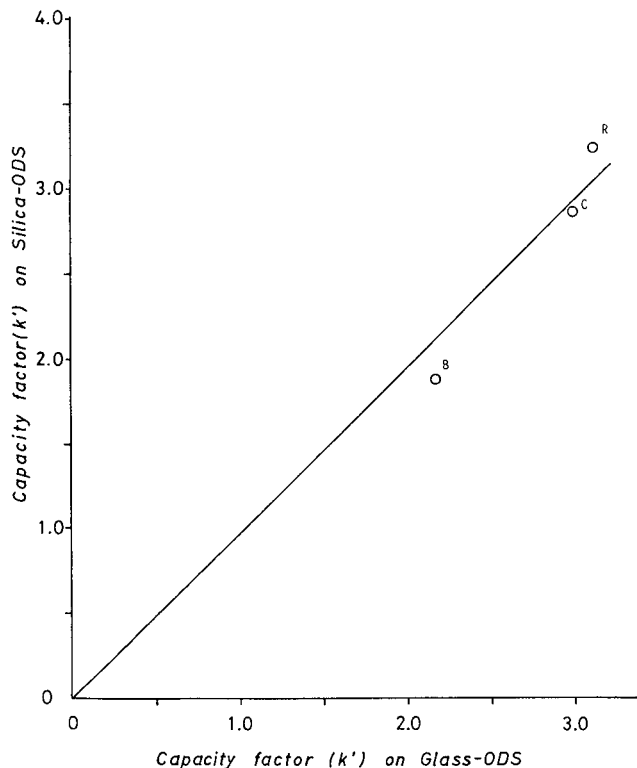


Fig. 3. Correlations between the capacity factors (k') of bufadienolides on glass-ODS versus silica-ODS. Mobile phase: acetonitrile-distilled water (50:50). Detection: 300 nm UV. Flow-rate: 1 ml/min. Points: B = bufalin; C = cinobufagin; R = resibufogenin.

Fig. 2. shows the correlations between the capacity factors (k') of some aromatic hydrocarbons on glass-PHP versus silica-PHP.

Figs. 3–5 show the correlations between the capacity factors (k') of bufadienolides of glass-ODS versus silica-ODS, glass-ODS versus glass-PHP and glass-PHP versus silica-PHP. The curves of capacity factors (k') obtained with the glass-ODS, glass-PHP series provide similar resolution and retention in Figs. 3–5.

Typical calibration graphs of peak area versus amount of bufalin, resibufogenin and cinobufagin are linear in the range 0.10–0.60 μg , 0.10–1.10 μg and 0.14–1.40 μg respectively. The extraction of bufalin, resibufogenin and cinobufagin from commercial *Bufonis venenum* was substantially complete within the 5–30, 5–55 and 7–70 $\mu\text{g}/\text{ml}$ ranges, and the reproducibility of the assays was good down to a concentration of 5 $\mu\text{g}/\text{ml}$ bufalin, 5 $\mu\text{g}/\text{ml}$ resibufogenin and 7 $\mu\text{g}/\text{ml}$ cinobufagin. The mean recovery from five samples containing 5–30 μg of bufalin, 5–55 μg of resibufogenin and 7–70 μg of cinobufagin per ml were 96.4, 97.4 and 98.3% [coefficients of variation (C.V.) 3.37, 3.57 and 1.87%], respectively.

Figs. 6 and 7 show typical liquid chromatograms obtained with bufadienolides from commercial *Bufonis venenum* on glass-ODS or silica-ODS. The resolution value

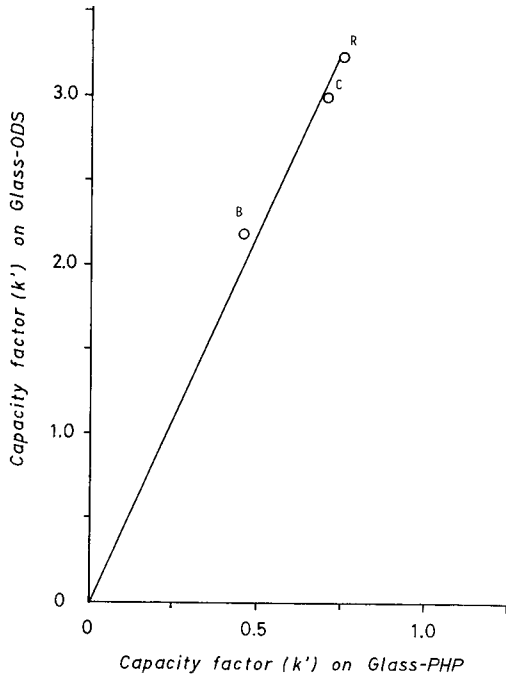


Fig. 4. Correlations between the capacity factors (k') of bufadienolides on glass-ODS versus glass-PHP. Conditions as in Fig. 3.

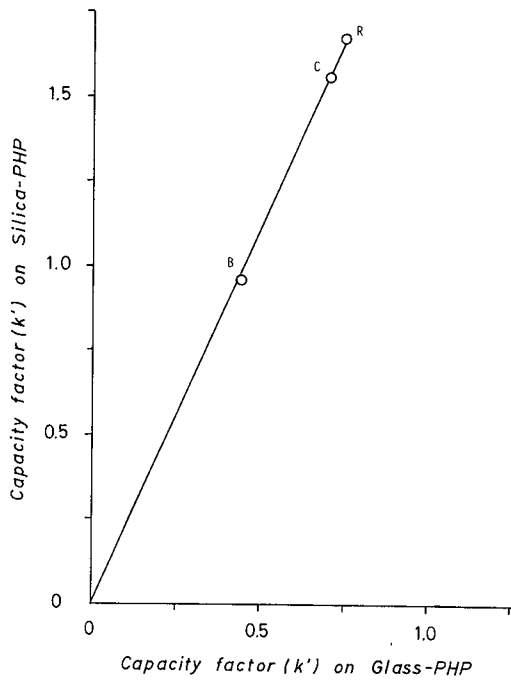


Fig. 5. Correlations between the capacity factors (k') of bufadienolides on glass-PHP versus silica-PHP. Conditions as in Fig. 3.

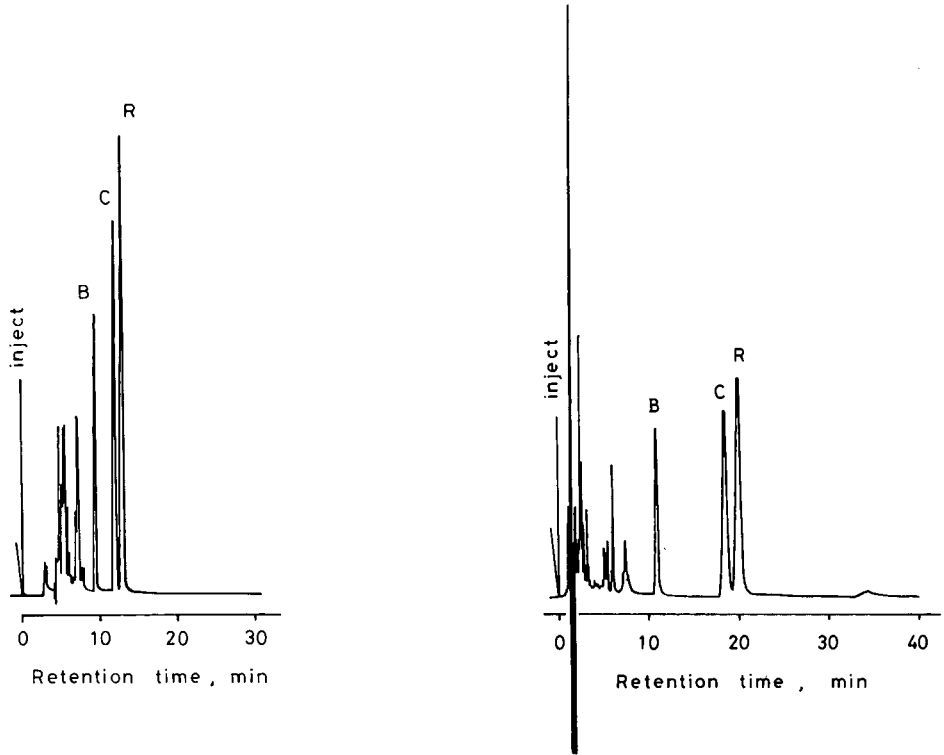


Fig. 6. Typical liquid chromatogram obtained with bufadienolides in commercial *Bufo venenum* on glass-ODS. Column: 400 × 4.6 mm I.D. Peaks: B = bufalin; C = cinobufagin; R = resibufogenin. Other chromatographic conditions as in Fig. 3.

Fig. 7. Typical liquid chromatogram obtained with bufadienolides in commercial *Bufo venenum* on silica-ODS. Column: 150 × 4.6 mm I.D. Other chromatographic conditions and peaks as in Fig. 6.

(R_s) of resibufogenin versus cinobufagin on glass-ODS and silica-ODS was 1.38 and 1.33 with the HPLC conditions in Figs. 6 and 7. Table III shows the bufalin, resibufogenin and cinobufagin contents in commercial *Bufo venenum*.

TABLE III

BUFADIENOLIDES CONTENTS IN COMMERCIAL *BUFO VENENUM*

$n = 7$.

Sample	Bufadienolides (%)			Recovery (%)	C.V. (%)
	Bufalin	Cinobufagin	Resibufogenin		
Sample 1	2.08	5.20	6.52	96.1–98.3	2.05
Sample 2	1.84	4.51	3.02	94.7–98.7	2.33
Sample 3	1.06	1.83	2.85	93.5–97.3	2.34
Sample 4	2.30	5.80	2.78	95.3–98.6	2.16
Sample 5	1.51	2.80	4.80	96.5–98.8	2.07

These results also show that bufadienolides and some aromatic hydrocarbons can be separated on column glass treated with ODS or PHP groups using either an acetonitrile–distilled water or a methanol–distilled water mixture as the eluent.

It is concluded from the present investigation that it is not sufficient to evaluate column gels solely on the basis of the carbon content of chemically bonded reversed-phase materials. The pore size distribution of the glass supports, the bulkiness of the ligands bonded to the glass and the molecular size of the solute must also be considered.

On the other hand, in the analysis of bufadienolides from *Bufo venenum*, the sensitivity of this HPLC method was three times that of previous HPTLC method [10].

REFERENCES

- 1 M. Okamoto, *J. Chromatogr.*, 202 (1980) 55.
- 2 M. Okamoto and H. Kishimoto, *J. Chromatogr.*, 212 (1981) 251.
- 3 M. Okamoto and F. Yamada, *J. Chromatogr.*, 247 (1982) 167.
- 4 M. Okamoto and F. Yamada, *J. Chromatogr.*, 283 (1984) 61.
- 5 J. Rayss, A. Dawidowicz, Z. Suprynowicz and B. Buszewski, *Chromatographia*, 17 (1983) 437.
- 6 Z. Suprynowicz, J. Rayss, A. L. Dawidowicz and R. Lodknowski, *Chromatographia*, 20 (1985) 677.
- 7 M. Okamoto and K. Jinno, *Chromatographia*, 21 (1986) 467.
- 8 M. Okamoto and K. Jinno, *J. Chromatogr.*, 395 (1987) 171.
- 9 M. Okamoto, K. Jinno, M. Yamagami, K. Nobuhara and K. Fukushima, *J. Chromatogr.*, 396 (1987) 345.
- 10 M. Okamoto, *Chromatographia*, 26 (1988) 145.

CHROMOSYMP. 2096

Bead cellulose derivatives as supports for immobilization and chromatographic purification of proteins

H.-F. BOEDEN*, K. POMMERENING, M. BECKER, C. RUPPRICH and M. HOLTZHAUER
Central Institute of Molecular Biology, Robert-Rössle-Strasse 10, O-1115 Berlin (Germany)

F. LOTH

Institute of Polymer Chemistry, O-1530 Teltow-Seehof (Germany)

and

R. MÜLLER and D. BERTRAM

Leipziger Arzneimittelwerk GmbH, O-7050 Leipzig (Germany)

ABSTRACT

Characteristic data are presented for Divicell, a macroporous bead cellulose with excellent flow parameters. The preparation of Divicell derivatives and their properties are described with respect to their application as chromatographic supports. The ion exchangers Divicell DEAE and Divicell CM were manufactured in two types with different exclusion limits and an available capacity for proteins of up to 100 mg/ml gel. Divicell Blue is a bead cellulose with covalently bound Cibacron Blue F3G-A and was found to be a very suitable adsorbent for the selective separation and purification of human serum albumin. Activation of Divicell with sodium periodate, epichlorohydrin and 5-norbornene-2,3-dicarboximido carbonochloridate provided activated supports used for immobilization of ligands in organic solvents and in aqueous solutions. Coupling of amines, diamines, amino acids, carbohydrates and proteins is described. The immobilized ligands retained their biological activity as determined by their specific adsorption of proteins. Divicell alkyl derivatives were tested in hydrophobic interaction chromatography with bovine serum albumin as a model. Examples are presented of the application of Divicell derivatives to the purification of biomacromolecules such as immunoglobulins and lectins by affinity chromatography. The results were comparable to those obtained using the corresponding Sepharose-derived adsorbents.

INTRODUCTION

Hydrophilic polymers, especially cross-linked agarose and dextran, play a dominant role as supports for chromatographic procedures in biosciences and biotechnology. During the last 10 years, cellulose has achieved increasing importance in the form of highly porous beads owing to its mechanical and chemical stability. Various techniques have been described for the preparation of macroporous cellulose beads [1–4]. Bead cellulose has been tested as a packing material in gel chromatography [3,5]. The hydroxyl groups of bead cellulose can be converted by the usual chemical reactions applied to other hydrophilic matrices, *e.g.*, fibrous cellulose and agarose. The preparation of ion-exchange derivatives of bead cellulose partly cross-linked and their use in chromatographic separation and purification processes was described by

Štamberg *et al.* [1,2], Motozato and Hirayama [6] and Gemeiner *et al.* [7]. A further application of bead cellulose was investigated in dye–ligand chromatography for the purification of proteins [7–9].

Different methods have been used for the introduction of active groups and ligands into bead cellulose. First, Turková *et al.* [10] described the immobilization of trypsin to dialdehyde bead cellulose. The activation of cellulose beads with chloroformates was reported by Drobnik *et al.* [11]. Several other activation methods with cross-linked bead cellulose for the purification of immunoglobulins were evaluated by Peng *et al.* [12]. Recently, a novel carbonochloridate (chloroformate) for the activation of hydrophilic supports, especially of bead cellulose was described by Büttner *et al.* [13]. Various methods have been employed for immobilization of biospecific ligands to bead cellulose used in the chromatographic purification of proteins and in biotransformation processes [14–19].

In this work, Divicell, a macroporous bead cellulose produced by Leipziger Arzneimittelwerk (Leipzig, Germany), was investigated with respect to its characterization and use as a chromatographic support, especially for immobilization of ligands and purification of biopolymers. The aim of this work was the preparation of various Divicell derivatives with regard to different activation methods and the development of biospecific sorbents possessing high efficiencies for adsorption and desorption of proteins. The suitability of Divicell sorbents as chromatographic supports was tested using several model systems of protein chromatography based on hydrophobic interaction and affinity of proteins to coupled biospecific ligands.

EXPERIMENTAL

Materials

Bead cellulose Divicell (particle size 80–200 μm) was obtained from Leipziger Arzneimittelwerk, Sepharose 2B, 4B, 6B, and CL-6B, CNBr–Sepharose 4B, Con A–Sepharose and Blue Dextran 2000 from Pharmacia (Uppsala, Sweden), 5-norbornene-2,3-dicarboximido carbonochloridate (Cl-CO-ONB) from the Institute for Drug Research (Berlin, Germany), immunoglobulins and antisera from the State Institute for Immunopreparations and Nutrient Media (Berlin, Germany), Cibacron Blue F3G-A, lysozyme and human γ -globulin from Serva (Heidelberg, Germany), trypsin from Boehringer (Mannheim, Germany), human and bovine serum albumin (HSA and BSA, respectively) from the Institute of Vaccines (Dessau, Germany) and porcine insulin from Berlin-Chemie (Berlin, Germany). Penicillin acylase was a gift from Dr. B. Rockstroh (Research Centre of Biotechnology, Berlin, Germany). The following proteins were prepared by standard methods: human immunoglobulin G (human IgG) [20], crude hen egg ovalbumin [21], human methaemoglobin (MetHb) [22], concanavalin A (Con A) [23], crude wheat germ (WGA) [18], soybean (SBA) [24] and peanut (PNA) [25] agglutinins. All other reagents were of analytical-reagent grade.

Determination of exclusion limit

The exclusion limit of Divicell was determined with Blue Dextran 2000. A 50-ml volume of Divicell was equilibrated in a column (25 \times 1.6 cm I.D.) with 0.1 *M* phosphate buffer (pH 7). Blue Dextran (5 mg in 0.5 ml of phosphate buffer) was

loaded on the column and chromatographed at a flow-rate of 6–8 ml/h. Blue Dextran splits off into two fractions, one excluded and the other non-excluded. The exclusion limit was determined by means of a calibration graph (ratio of the excluded to non-excluded amounts of Blue Dextran from Sepharose 2B, 4B and 6B *versus* their exclusion limits of $4 \cdot 10^6$, $20 \cdot 10^6$ and $40 \cdot 10^6$ dalton, respectively).

Determination of porosity

Pore-size distribution was measured with a Type 2000 mercury porosimeter (Carlo Erba, Milan, Italy). Samples of Divicell were dehydrated by stepwise transfer into water–ethanol mixtures, followed by ethanol and finally diethyl ether. The diethyl ether was removed at room temperature.

Electron microscopy

Transmission electron micrographs were obtained with a BS 500 electron microscope (Tesla, Prague, Czechoslovakia). Dried samples of Divicell were embedded in methyl polymethacrylate. After dissolving the polyester, ultra-thin sections were contrasted with Pt/Ir–C at an angle of 45°C.

Preparation of Divicell DEAE and Divicell CM ion exchangers

The ion exchangers were prepared by conversion of Divicell with 2-chloroethyl-diethylamine and chloroacetic acid [26], respectively and were characterized as described previously [27].

Divicell DEAE-H. Wet Divicell (205 g, cellulose content 40.5 g) was mixed with 20 g of 2-chloroethyl-diethylamine hydrochloride dissolved in 100 ml of water for 30 min at room temperature. The mixture was dried under vacuum (water-jet pump) at 60°C until the weight was constant. After cooling to room temperature, 12 g of sodium hydroxide in 100 ml of water were added dropwise with stirring. The mixture was then heated at 90°C for 30 min followed by acidification with 0.5 M hydrochloric acid at room temperature and washing with water.

Divicell DEAE-L. The same procedure was applied with 40 g of 2-chloroethyl-diethylamine hydrochloride, 20 g of sodium hydroxide and 2.3 g of epichlorohydrin in 100 ml of water.

Divicell CM-H. Divicell (205 g wet weight) was converted into the CM derivative with 20.2 g of sodium monochloroacetate in 100 ml of water at room temperature for 30 min. After drying, 8 g of sodium hydroxide in 73 ml of water were added as described above. The mixture was then heated at 70°C for 2 h. After cooling to room temperature, the support was washed with water.

Divicell CM-L. The procedure was carried out with 30.3 g of sodium chloroacetate, 12 g of sodium hydroxide and 2.3 g of epichlorohydrin in 100 ml of water as described for the H-derivative.

Preparation of Divicell Blue

A 20-g amount of wet Divicell was suspended in 36 ml of water and the mixture was heated in a 500-ml flask at 60°C with stirring. A solution of 0.32 g of Cibacron Blue F3G-A (C.I. 61211) in 12.8 ml of water was added dropwise. Stirring was continued at 60°C for 1 h, then 16 g of sodium chloride were added. After a further 1 h the temperature was increased to 90°C and 1.28 g of sodium carbonate were added to the

stirred suspension. Two hours later the mixture was allowed to cool to room temperature, then the unbound dye was removed by washing with water and determined spectrophotometrically ($\epsilon_{615} = 1.3 \cdot 10^5 \text{ l mol}^{-1} \text{ cm}^{-1}$). The content of covalently fixed dye was 6–8 mg/ml gel.

Conversion of Divicell with sodium periodate into Divicell Dialdehyde

A 100-ml volume of settled Divicell was transferred into a 500-ml vessel and 120 ml of 0.05 or 0.1 *M* sodium periodate were added. The suspension was stirred at room temperature for 2, 4 or 6 h. After addition of 30 ml of ethylene glycol the mixture was stirred for 1 h and then filtered. The support was washed with 2 l of distilled water and stored in a refrigerator in the presence of 0.02–0.04% sodium azide. The dialdehyde content (see Table III) was determined via stoichimetric consumption of hydroxyl ions under definite conditions as a consequence of the Cannizzaro reaction of dialdehyde groups [28,29].

Activation of Divicell with epichlorohydrin to Divicell Epoxy

Divicell Epoxy was prepared by a modified procedure according to Matsumoto *et al.* [30]. Briefly, a mixture of 40% (v/v) wet Divicell and 12% (v/v) epichlorohydrin in 1 *M* sodium hydroxide solution (final concentration) was agitated at 50°C for 30 min. After cooling to room temperature, the support was washed exhaustively with water on a sintered-glass funnel. The support was transferred into acetone or isopropanol and stored at 4–8°C.

The content of epoxy groups was determined as described by Sundberg and Porath [31]. Divicell Epoxy contained 20–25 μmol of active groups per millilitre sedimented gel. An additional run through the above activation procedure increased the content of epoxy groups of this gel to 40–50 $\mu\text{mol/ml}$.

Activation of Divicell with Cl-CO-ONB to Divicell ONB-Carbonate

This Divicell derivative was prepared as described recently [13]. A 100-ml volume of Divicell sedimented in water was transferred into acetone and washed thoroughly with acetone (water content *ca.* 0.3%). Approximately 2 g of Cl-CO-ONB dissolved in 100 ml of acetone were added to the slurry. The suspension was gently agitated at room temperature for 16–20 h. The solvent was sucked off and the support was washed with a tenfold volume of acetone.

The content of active ONB-carbonate groups determined spectrophotometrically at 270 nm [13] was 25 $\mu\text{mol/ml}$ gel. For the preparation of low- and high-activated supports the amount of Cl-CO-ONB was reduced and increased, respectively. Divicell ONB-Carbonate was stored at room temperature in acetone in the absence of humidity.

Coupling of proteins to Divicell Dialdehyde

A 1-ml volume of activated gel sedimented in water was equilibrated with 0.1 *M* phosphate buffer (pH 7). After removing the supernatant, 1 ml of protein solution (8–10 mg/ml in the above buffer) was added and the suspension was stirred at room temperature for 6 h. The unbound protein was washed out using the coupling buffer.

For inactivation of remaining aldehyde groups, the Divicell derivative was equilibrated with 0.1 *M* phosphate buffer (pH 8) and 1 ml of ethanolamine adjusted

to pH 8 was added. After stirring for 24 h at 2°C or room temperature, the support was thoroughly washed with buffer and finally with water.

To convert the initially formed carbinolamine or the corresponding Schiff's base into the more stable amine, the gel was equilibrated with 0.1 M borate buffer (pH 9). Then 5 mg of sodium borohydride in 1 ml of buffer were added and the suspension was stirred for 30 min at room temperature. An additional 5 mg of sodium borohydride were added and stirring was continued for 30 min.

Finally, the support was washed exhaustively with 0.1 M phosphate buffer (pH 7) or suitable application buffer.

Immobilization of ligands to Divicell Epoxy

Divicell Epoxy was transferred from acetone or isopropanol to water. The suction-dried gel was added to the coupling solution in a 1:1 to 1:2 (v/v) ratio. This suspension was gently agitated at an appropriate temperature for 1–3 days. After washing out the unbound material with coupling buffer or water (at least ten bed volumes), unreacted epoxy groups were deactivated by incubation with 1 M ethanolamine (pH 8–11) for 24 h at room temperature. Finally, the gel was thoroughly washed with water, 0.1 M borate buffer (pH 8.0) and again with water. The ligand-containing gel should be stored at 4–8°C in the presence of 0.02–0.04% sodium azide.

The immobilization of N-acetyl-D-glucosamine (GlcNAc) and N-acetyl-D-galactosamine (GalNAc) was carried out according to Uy and Wold [32].

For coupling of heparin, the polysaccharide was precipitated with isopropanol from a commercial solution. The precipitate was dissolved in water (80 mg/ml) and adjusted for coupling to pH 11 with sodium hydroxide.

Coupling of iminodiacetic acid (IDA) was performed as described by Porath and Olin [33].

Divicell IDA–Cu²⁺ and IDA–Zn²⁺ were prepared by loading of solutions of copper (II) chloride and zinc acetate (5 mg/ml) on Divicell IDA as described previously [34]. The contents of Cu²⁺ and Zn²⁺ bound to the support were calculated from differences between the amounts of ions added and unbound. The determination of Cu²⁺ was carried out after treatment of the Cu²⁺ solutions with concentrated ammonia by measurement of the absorbance at 620 nm. Zn²⁺ was determined by titration with 0.01 M EDTA in the presence of Eriochrome Black T.

Immobilization of ligands to Divicell ONB-Carbonate

Coupling of ligands was carried out by the same procedure as described for the immobilization to Divicell Epoxy; however, the immobilization to Divicell ONB-Carbonate was complete after 1–20 h at 4°C or room temperature.

Residual ONB-carbonate was deactivated by hydrolysis in 0.1 M borate buffer (pH 8) (room temperature, 16 h) or by blocking with 0.5–1 M Tris, glycine and ethanolamine, respectively, at pH 7–9 (4°C or room temperature, 16 or 2 h).

For immobilization of low-molecular-mass ligands, the molar ratio of offered ligand to active groups was 1.1:1 to 20:1 (see Table V). The amounts of proteins applied for immobilization varied from 1 to 25 mg per millilitre of coupling solution and millilitre of activated gel (see Table VI).

Determination of immobilized ligands

The amount of immobilized protein was most often calculated from the spectrophotometrically determined unbound protein prior to and after immobilization. To suppress the absorption at 270 nm of released HONB, the protein solutions were acidified to pH 2–3. Fixed protein was also determined after treatment of the support with 1 M sodium hydroxide solution at room temperature for 16 h in the alkaline supernatant according to Lowry *et al.* [35].

The activity of immobilized trypsin and penicillin acylase was determined according to Hummel [36] with tosyl-L-arginine methyl ester (TAME) and according to Balasingham *et al.* [37] with benzylpenicillin as substrates, respectively.

The determination of coupled heparin was performed by the method of Smith *et al.* [38].

Immobilized GlcNAc, GalNAc or GalN were determined after hydrolysis of the support with 6 M hydrochloric acid at 100°C for 6–8 h by the modified Morgan–Elson method [39].

The amount of aminohexyl residues was calculated from the determination of NH₂ groups according to Schmitt and Walker [40] or by acidimetric titration using an AT 3 autotitrator (MLW, Dresden, Germany).

Coupled amino acids or alkyl- and arylamines were determined using the Kjeldahl method [41].

Chromatographic purification of proteins

All chromatographic separations were performed with glass columns at low pressure and at 4°C or room temperature using a Microperpex peristaltic pump, a Uvicord S UV monitor and a Redirac fraction collector from LKB (Bromma, Sweden). Proteins were loaded on the respective support in the appropriate equilibration/binding buffer if not stated otherwise. Unbound protein was washed off with the same buffer (at least a fivefold column volume).

Generally, flow-rates were *ca.* 1–2 column volumes per hour. The UV profiles were recorded using the absorption at 280 nm. The purification was checked by sodium dodecyl sulphate polyacrylamide gel electrophoresis (SDS-PAGE) or in an SDS-free system (PAGE) and by specific analysis of the isolated proteins.

Determination of binding capacity for proteins on Dvicell sorbents

A 0.5–10-ml volume of the Dvicell sorbent was equilibrated in a column with an appropriate buffer. A defined protein solution was applied until the absorbance at 280 nm of the effluent was the same as that of the sample. Then the column was washed with the equilibration buffer until the absorption of the eluate was <0.01. All protein-containing fractions were pooled. The capacity was calculated from the difference between applied and unbound protein amounts. This value was compared with the amount of protein that was eluted specifically (see Table VII).

Hydrophobic interaction chromatography (HIC) of BSA

For example, Dvicell Pentyl was prepared by coupling of *n*-pentylamine to Dvicell ONB-Carbonate (34 μmol active groups/ml gel) with a molar ratio of 1.1 mol of amine per mole of ONB-carbonate in acetone for 1 h at room temperature. The coupling was quantitative with respect to the active groups.

Columns (25 × 1 cm I.D.) with the respective HIC support were equilibrated with 0.05 M phosphate buffer (pH 7.4) containing 2 M ammonium sulphate. A 2-ml volume of BSA in equilibration buffer (50 mg/ml) was loaded and subsequently eluted with 5 ml of equilibration buffer, 10 ml of 0.05 M phosphate buffer (pH 7.4), 10 ml of 6 M urea in water and 10 ml of 0.05 M phosphate buffer (pH 7.4) containing 2 M potassium thiocyanate (flow-rate 15.3 cm/h). Protein elution was monitored by UV absorption 280 nm. BSA was determined in the urea-containing fractions. The capacity of support was 23.0 mg protein/ml gel and the recovery was ≥95%.

Examples of other HIC supports derived from Divicell ONB-Carbonate are given in Table VIII. The binding capacities for lysozyme were comparable to those for BSA, but elution was effected with less chaotropic eluents as for BSA (data not shown).

The process operating with Divicell Pentyl was simulated by two series of ten adsorption–elution cycles of BSA (elution with 6 M urea). Each series was followed by a cycle with ten gel volumes of 1 M sodium hydroxide solution at room temperature (“cleaning-in-place”).

Isolation of HSA from human serum using Divicell Blue

A 10-ml volume of Divicell Blue was equilibrated in a column (15 × 1.1 cm I.D.) with 0.05 M Tris–HCl buffer (pH 8) containing 0.5 M sodium chloride. A 2-ml volume of human serum was added and the non-adsorbed serum proteins were removed with equilibration buffer. Then the adsorbed HSA was eluted with 0.05 M Tris–HCl buffer (pH 8) containing 1 M potassium thiocyanate. The amount of HSA was calculated from its absorbance at 279 nm ($A_{1\%}^{1\text{cm}} = 0.531$).

Fractions of washed-out proteins and eluted HSA were pooled, dialysed against 0.01 M phosphate buffer (pH 7) and concentrated by ultrafiltration (UM 10 membrane; Amicon, The Netherlands).

Removal of HSA was monitored by cellulose acetate foil (CAF) electrophoresis of the starting material and the pooled and concentrated washings (see Fig. 6).

Purification of anti-human IgG from rabbit antiserum

The affinity support was prepared by coupling of 10 mg of human IgG to 2 ml of Divicell ONB-Carbonate (55 μmol active groups/ml gel); 4.8 mg of human IgG were immobilized per millilitre of gel. A 1.5-ml volume of the support was packed into a column (7 × 0.6 cm I.D.) and washed with twenty column volumes each of 0.1 M glycine–HCl (elution buffer), water and phosphate-buffered saline (PBS, binding buffer).

After equilibration with PBS, 1 or 2 ml of rabbit anti-human IgG serum was diluted with an equal volume of PBS containing 0.05% Tween 20 and loaded onto the column at 4°C. The flow-rate was 2 and 4 ml/h, respectively. The rabbit anti-human IgG was eluted first with 0.1 M glycine–HCl buffer (pH 2.8), followed by the same buffer (pH 2.2). The flow-rate in all steps was about 2–3 ml/h. Fractions of 1 ml were collected and adjusted to pH 7 with 0.5 M K₂HPO₄. Antibody-containing fractions were pooled and used for analysis.

Purification of human IgG from human serum

The immobilization of goat anti-human IgG to Divicell using Divicell ONB-

Carbonate (4.3 and 42.3 μmol active groups/ml gel, respectively) resulted in supports with 2.7 mg goat IgG/ml gel in each instance. Affinity chromatography was performed as described for purification of rabbit anti-human IgG. A 1-ml volume of human serum was loaded onto 2 ml of gel. Human IgG was eluted with glycine-HCl buffer (pH 2.5).

Isolation of wheat germ agglutinin (WGA) on Divicell GlcNAc

For preparation of WGA, Divicell GlcNAc (7 μmol GlcNAc/ml gel) was synthesized starting from Divicell Epoxy. A 1000-ml volume of a wheat germ extract dialysed against PBS containing 5 g of total protein were loaded onto a Divicell GlcNAc column (20 \times 1.5 cm I.D.) at room temperature. WGA was eluted with 0.5 M formic acid at a flow-rate of 30 ml/h. Breakthrough fractions and washings were rechromatographed. Pooled fractions containing WGA were dialysed against distilled water and lyophilized. The purity of WGA was tested by SDS-PAGE and its biological activity by haemagglutination.

Purification of hen egg ovalbumin on Divicell Con A

Divicell Con A (8.8 mg concanavalin A/ml gel) was packed into a column (9 \times 1.5 cm I.D.) and equilibrated with 0.1 M sodium acetate (pH 6.5) containing 0.2 M sodium chloride, 1 mM calcium chloride and 1 mM manganese(II) chloride. A 10-ml portion of crude ovalbumin (10 mg/ml equilibration buffer) was loaded on the column at room temperature. The specific elution was performed with equilibration buffer complemented with 0.2 M D-glucose (flow-rate 12 cm/h). Fractions containing ovalbumin were combined, dialysed against distilled water and lyophilized. The purity of ovalbumin was checked by SDS-PAGE. It was found that 66% of the applied protein could be recovered as electrophoretically pure ovalbumin.

Testing of purified proteins

All purified proteins were subjected to PAGE (non-denaturing system No. 1 according to Maurer [42], T = 7.5%) and 7.5–15% T gradient SDS-PAGE according to Laemmli [43], staining with Coomassie Brilliant Blue G-250.

Isolated antibodies were tested by single (SRID) [44] and double radial immunodiffusion (DRID) [45]. Titres of purified IgGs were determined by an enzyme-linked immunosorbent assay (ELISA) using 1:10 to 1:10⁶ serial dilutions of the starting and purified material. The second antibody was conjugated with alkaline phosphatase. The substrate for the indicator reaction was *p*-nitrophenyl phosphate. The conditions used for ELISA were as described by Peng *et al.* [12].

A haemagglutination assay for WGA was performed in two-fold serial dilutions with trypsinized human type A erythrocytes according to Osawa and Matsumoto [46].

RESULTS AND DISCUSSION

Characteristic properties of Divicell

Divicell swollen in water or organic solvents represents a support of regular formed beads with a cellulose content of 70–90 mg/ml. After removal of solvents and careful drying at room temperature, the beads showed distinct shrinkage. However,

TABLE I
CHARACTERISTIC PARAMETERS OF DIVICELL

Parameter	Value
Particle diameter	80–200 μm
Swelling volume	10–15 ml/g cellulose
Porosity	70–90%
Exclusion limit	$5 \cdot 10^6$ – $20 \cdot 10^6$ dalton
Flow-rate at 0.2 MPa	≥ 1000 cm/h

reswelling in solvents yielded beads with about 80% of the original swelling volume. Divicell accomplishes the essential parameters of a matrix for chromatographic purposes (see Table I). Depending on the preparation conditions for Divicell, the swelling volume, porosity and exclusion limit can be varied in the limits given in Table I.

The pore-size distribution was determined by mercury porosimetry and is demonstrated in Fig. 1. Although the samples of bead cellulose were dried, the results indicate the macroporosity of the matrix. From the differential curves (not shown), the mean pore diameter was calculated and was *ca.* 30 and 100 nm for the samples with exclusion limits of $5 \cdot 10^6$ and $20 \cdot 10^6$ dalton, respectively. The highly porous structure of Divicell is also evident from the electron micrograph (Fig. 2) of a sample with an exclusion limit of $5 \cdot 10^6$ dalton for the water-swollen beads. Pores with diameters up to 1 μm can be seen.

The mechanical stability and rigidity of Divicell are remarkable for a bead-formed biopolymer without cross-linking, as is demonstrated by the dependence of flow-rate on the operating pressure (Fig. 3). The flow-rate of Divicell (curve A) considerably exceeds that of cross-linked agarose (Sephacrose CL-6B, curve D). A higher flow-rate, suggesting increased stability, was observed after activation and coupling of ligands (curves B and C). A reason could be a cross-linking of the matrix after activation with epichlorohydrin or by multi-point attachment of ligands. Generally, a

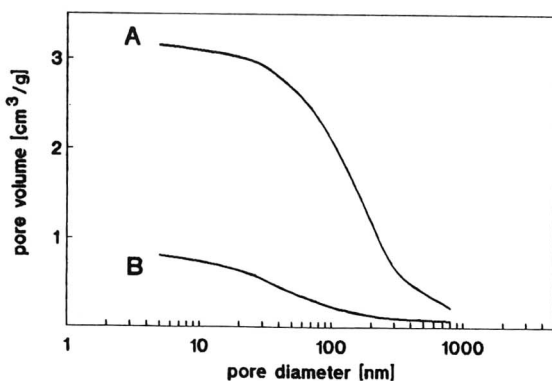


Fig. 1. Pore-size distribution for Divicell (integral curves) determined by mercury porosimetry of dried samples. Exclusion limit of Divicell swollen in water was (A) $20 \cdot 10^6$ dalton and (B) $5 \cdot 10^6$ dalton.

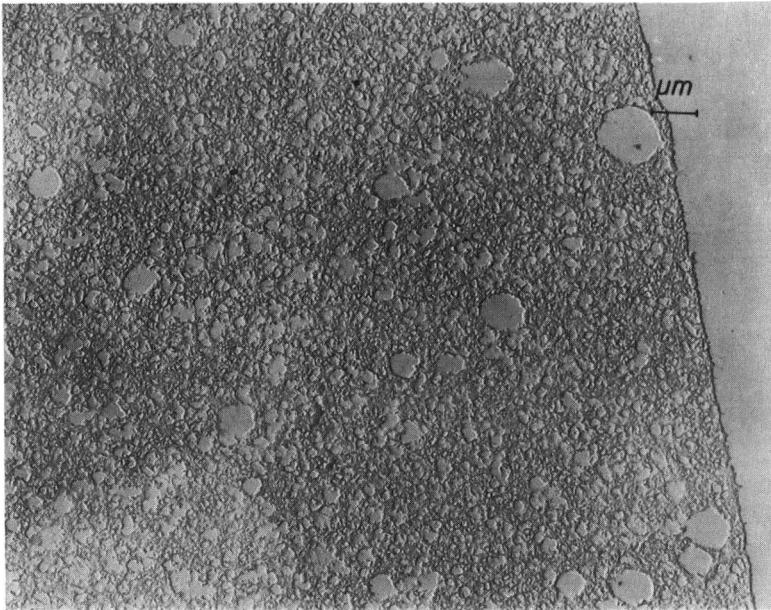


Fig. 2. Transmission electron micrograph of Divicell (ultra-thin section) showing the pore structure of the cellulose matrix.

linear increase in flow-rate was observed up to 0.2 MPa. The curves have smaller slopes for flow-rates at pressures > 0.2 MPa, but, the gel bed did not collapse even at 2.0 MPa. With smaller Divicell beads ($50\text{--}80\ \mu\text{m}$ diameter), the linear range extended to 0.8 MPa. In addition, Divicell beads remain stable during stirred batch processes for at least 1000 h if sodium azide is added as a preservative. This high mechanical

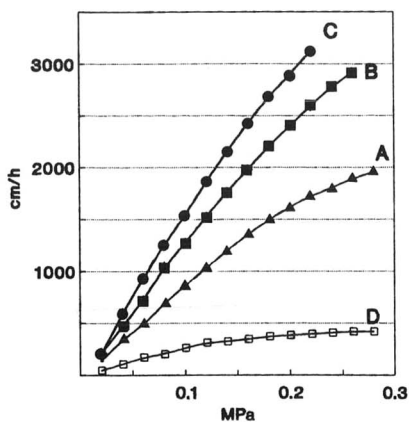


Fig. 3. Flow characteristics of Divicell supports in comparison with Sepharose CL-6B. The flow-rates were determined on a column (32×0.8 cm I.D.) with distilled water as mobile phase. Supports: (A) Divicell; (B) Divicell GlcNAc; (C) Divicell Con A; (D) Sepharose CL-6B.

stability recommends the application of bead cellulose supports in large-scale processes, *e.g.*, in biotechnology.

Like fibrous cellulose, Divicell shows a high resistance to many chemicals (data not shown). For instance, it is stable in 0.1 *M* hydrochloric acid or 0.1 *M* sodium hydroxide solution for 1 week at room temperature. No changes in bead size, bead shape or flow-rate could be observed after treatment of unmodified Divicell with 1 *M* sodium hydroxide solution at least 6 h at room temperature. Also, the use of concentrated salt solutions or chaotropic substances, *e.g.*, 3 *M* sodium chloride, 3 *M* potassium thiocyanate, 8 *M* urea or 6 *M* guanidinium hydrochloride, or detergents such as sodium dodecyl sulphate or Triton X-100 did not alter these parameters. The thermal stability allows autoclaving at 120°C.

Irreversible interactions could not be detected between unmodified cellulose beads and proteins. When 2 ml of human serum per millilitre of gel were loaded in buffers (ionic strength >0.1, pH >4), all proteins could be recovered in the flow-through within the detection limit of UV monitoring or the Lowry protein assay.

All these advantageous properties suggest that Divicell should be suitable for the preparation of derivatives for chromatography, *e.g.*, ion-exchange, dye-ligand or activated supports for immobilization of ligands.

Divicell DEAE, CM and Blue

Partial etherifications of hydroxyl groups of bead cellulose were performed with reactive chlorocompounds, *e.g.*, chloroethyldiethylamine, chloroacetic acid or the triazine dye Cibacron Blue F3G-A, in the presence of bases. The resulting supports were the anion exchanger Divicell diethylaminoethyl (Divicell DEAE), the cation exchanger Divicell carboxymethyl (Divicell CM) and the dye matrix Divicell Blue. They were characterized by their swelling volumes, contents of charged or dye groups and binding capacities for selected proteins such as HSA, insulin, methaemoglobin (MetHb) and lysozyme (Table II). For ion-exchange chromatography (IEC), in each instance two types (H and L) were prepared by cross-linking of the matrix with epichlorohydrin. As a consequence of the smaller exclusion limit of L-types, these supports should be used preferably for purification of peptides and proteins with molecular masses up to 30 000. H-types can be applied for purification of large proteins (MW > 30 000). The ion-exchange capacity was 1–2 mequiv./g dry cellulose (0.07–0.3 mequiv./ml gel). The binding capacities for proteins were 75–200 mg/ml sedimented gel, depending on the applied support or the protein. In chromatographic columns the operating pressure can be raised to 0.1 and 0.3 MPa for the H- and L-derivatives, respectively. In stirred reactors with suspended paddles, Divicell DEAE and CM were stable over a period of 500 h at 300 r.p.m.

Divicell Blue was prepared by modifying the usual procedure [47] (see Experimental). By varying the experimental conditions the amount of coupled dye could be stretched over a wide range (2–15 mg dye/ml gel). The covalent linkage between dye and cellulose is more stable than that in other polysaccharides, *e.g.*, dextran or agarose. Acid hydrolysis of Divicell Blue produces no quantitative cleavage of the dye-cellulose bond under conditions described for other polysaccharides [9,48].

Immobilized Cibacron Blue F3G-A possesses an affinity to nucleotide cofactor-dependent enzymes and blood proteins [8]. For instance, Travis and co-workers [49,50] purified albumin both on Blue dextran-Sepharose and on a material where the

TABLE II
SELECTED DATA FOR DIVICELL DEAE, CM AND BLUE

The swelling volume was calculated from the content of cellulose per millilitre of sedimented gel (drying at 105–110°C for 24 h). The capacity of ion exchangers was determined by titration. For determination of the binding capacity for proteins the following buffers were used for binding/elution: (1) 0.05 M Tris–HCl (pH 8)/the same buffer containing 1 M NaCl; (2) 0.05 M Tris–HCl with 50% (v/v) isopropanol (pH 8)/the same buffer containing 1 M NaCl; (3) and (4) 0.05 M acetate (pH 6)/the same buffer containing 2 M NaCl; (5) 0.01 M phosphate (pH 5)/the same buffer containing 1 M KSCN.

No.	Divicell derivative	Swelling volume (ml/g cellulose)	Ion-exchange capacity (mequiv./g cellulose)	Binding capacity (mg protein/ml gel)
1	DEAE-H ^a	12–14	1.2	HSA 100
2	DEAE-L ^b	6– 8	2.0	Insulin 75
3	CM-H ^a	12–14	1.0	MetHb 100
4	CM-L ^b	7– 9	1.4	Lysozyme 200
5	Blue	10–15	5·10 ^c	HSA 50

^a Exclusion limit 1·10⁶ dalton.

^b Exclusion limit 3·10⁴ dalton.

^c mg dye/ml gel.

dye was bound directly to agarose (Blue Sepharose). When the dye was coupled to fibrous cellulose, albumin was not separated from other proteins [51,52]. With Divicell Blue, however, it was possible to adsorb HSA selectively [8]. The binding capacity for a support with 3.6 mg of dye was *ca.* 45 mg/ml gel if HSA was diluted in 0.01 M phosphate buffer (pH 5). The amount of adsorbed HSA was lower using 0.05 M Tris–HCl (pH 8). An example of the application of Divicell Blue for the isolation of HSA from human serum is shown later in Fig. 6.

Activation of Divicell with sodium periodate and immobilization of proteins to Divicell Dialdehyde

By treatment of Divicell with sodium periodate, the vicinal hydroxyl groups in positions 2 and 3 of the glucose unit are oxidized to aldehyde groups with splitting of the C–C bond (Fig. 4). The activation procedure is very simple and can be stopped by addition of ethylene glycol. The degree of oxidation can be adjusted over a broad range by variation of the reaction time or temperature and the concentration of sodium periodate. Divicell Dialdehyde could be stored over a period of 2 years as an aqueous suspension in the presence of 0.02–0.04% sodium azide at 4°C. During that time no decrease in the degree of activation or coupling capacity for proteins was observed [28]. The mechanical stability of the activated gel expressed as pressure–flow behaviour was not diminished in comparison with the unmodified material (Fig. 3, curve A). This finding was surprising, as it had been expected that the support would lose its excellent flow properties because of cleavage of glucose rings [10,53].

The immobilization of proteins to Divicell Dialdehyde was carried out under mild conditions (6 h at room temperature). Using constant protein concentrations for coupling, not only the amount of immobilized protein but also the coupling yield increased proportionally to the degree of activation (Table III). Of course, the cou-

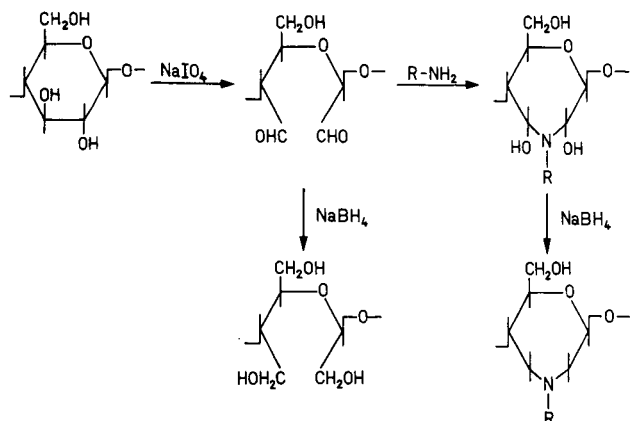


Fig. 4. Reaction scheme for periodate oxidation of glucose units of cellulose and subsequent covalent binding of ligand (RNH_2), completed by reduction with NaBH_4 .

pling yield also depends on the kind of protein. Applying the same conditions, the yield for immobilization of MetHb was double that for human γ -globulin. The maximum yield was up to 82% of the offered MetHb. After coupling of proteins, the unreacted aldehyde groups can be blocked with ethanolamine. A reduction with sodium borohydride (see Fig. 4) is recommended to stabilize the covalent bond between ligand and matrix by conversion of the carbinolamines or Schiff's bases formed into stable C-N bonds. Immobilized MetHb was able to bind oxygen reversibly and showed a pseudo-peroxidatic activity as measured by oxidation of aniline to 4-aminophenol.

Activation of Divicell with epichlorohydrin and immobilization of ligands to Divicell Epoxy

The activation of supports with epoxy compounds, e.g., epichlorohydrin or 1,4-butanediol diglycidyl ether, has been described previously [30-33, 54]. The reac-

TABLE III

IMMOBILIZATION OF PROTEINS TO DIVICELL DIALDEHYDE AS A FUNCTION OF CONCENTRATION OF ACTIVE GROUPS

Standard conditions were used as described under Experimental.

Preparation of Divicell Dialdehyde			Protein	Immobilized amount (mg/ml gel)	Coupling yield (%)
Amount of NaIO_4 (mg/ml gel)	Reaction time (h)	Amount of active groups ($\mu\text{mol/ml gel}$)			
13	2	21	MetHb	3.9	48
13	6	40	MetHb	4.9	60
26	4	71	MetHb	6.7	82
13	6	48	Human γ -globulin	2.8	28

tivity of epoxy groups is relatively low. Therefore, for coupling of ligands strong alkaline conditions, elevated temperatures, high concentrations of ligands and long reaction times were used. Advantages of epoxy-activated gels are the increased stability by cross-linking of the matrix during activation, the ability to couple compounds containing hydroxyl groups and the high stability of the ether or C–N bond between the support and attached ligands (minimized leakage). The degree of activation of Divicell Epoxy could be varied from 20 to about 50 $\mu\text{mol/ml}$ gel (Table IV). The epoxy support could be stored in isopropanol or acetone at 4°C for 1 and 2 years, respectively, without a substantial decrease in activity.

The hydrolysis of active groups was investigated at pH 9.5 and 11.0 at 40°C and compared with that of epoxy-activated Sepharose 6B [55]. It was found that the rate of hydrolysis of epoxy groups for the bead cellulose derivative was significantly lower. After 24 h the percentage of epoxy groups remaining on the Divicell support was 80% (pH 9.5) and 40% (pH 11) and on the corresponding Sepharose support 50% and 14%, respectively. Complete deactivation of Divicell Epoxy was achieved in 0.1 *M* sodium hydroxide solution at room temperature after 7 days or by reaction with 1 *M* ethanolamine (pH 9) for 24 h at room temperature.

Similar flow properties were obtained for Divicell Epoxy and Divicell GlcNAc prepared by coupling of N-acetyl-D-glucosamine (GlcNAc) to the epoxy support (Fig. 3, curve B).

A large excess of ligands was necessary for immobilization to Divicell Epoxy (Table IV). Using low-molecular-mass ligands, such as 4-nitroaniline, 1,6-diaminohexane (1,6-DAH), IDA, GalNAc and GlcNAc, up to a fifteenfold molar excess with respect to the active groups was added. High immobilization rates of coupled ligands

TABLE IV
IMMOBILIZATION OF LIGANDS TO DIVICELL EPOXY

Coupling medium: (1) ethanol; (2) 0.1 *M* borate (pH 8.3); (3) 2 *M* Na₂CO₃; (4) and (5) 0.1 *M* NaOH; (6) 1 *M* potassium phosphate (pH 8); (7) water adjusted to pH 11 with 0.1 *M* NaOH; (8) 1 *M* potassium phosphate (pH 7.5). For abbreviations, see text.

No.	Amount of epoxy groups ($\mu\text{mol/ml}$ gel)	Ligand	Added amount of ligand ($\mu\text{mol/ml}$ gel)	Temperature (°C) ^a	Time (h)	Immobilized ligand ($\mu\text{mol/ml}$ gel)	Coupling yield relative to active groups (%)
1	20	4-Nitroaniline	72	r.t.	48	20	100
2	20	1,6-DAH	200	r.t.	72	7.6	38
3	46	IDA	680	65	24	35	76
4	40	GlcNAc	600	37	24	7	18
5	46	GalNAc	300	37	24	9	20
6	21	Human γ -globulin	50 ^b	r.t.	65	6.9 ^b	14 ^c
7	40	Heparin	80 ^b	r.t.	72	0.8 ^b	1 ^c
8	35	Penicillin acylase	115 ^d	r.t.	48	46 ^d	40 ^c

^a r.t. = Room temperature.

^b mg/ml gel.

^c With respect to amount of ligand added.

^d Units/ml gel.

depended on the degree of activation. With GlcNAc, 2, 4 and 6 μmol were bound on supports with 10, 20 and 30 μmol epoxy groups/ml gel, respectively. The fixation of GlcNAc or GalNAc to highly activated gels yielded supports that were comparable to the corresponding Sepharose-derived supports [32,56]. The Divicell derivatives obtained were used successfully for the purification of lectins (see Table IX).

The maximum yield of coupled proteins was 40%. The enzyme activity of immobilized penicillin acylase was 530 units/g cellulose, which is about half of that found by Burg *et al.* [57] after coupling to an epichlorohydrin-activated synthetic polymer.

Activation of Divicell with Cl-CO-ONB and immobilization of ligands to Divicell ONB-Carbonate

The activation of supports with Cl-CO-ONB was described recently by Büttner *et al.* [13]. The activation was performed in anhydrous organic solvents and, in general, highly activated gels were used for coupling of ligands. However, in our investigations the activated supports were always prepared by conversion of Divicell with Cl-CO-ONB in non-dried solvents, especially acetone. The resulting Divicell ONB-Carbonate (Fig. 5) was stored in acetone containing *ca.* 0.3% of water. Only a small decrease (maximum 5–10%) in active groups was observed over a period of 2 years. The amount of ONB-carbonate groups could be reproducibly adjusted in the range of 4–80 $\mu\text{mol}/\text{ml}$ gel.

Covalent binding of ligands was carried out both in organic solvents and in aqueous solutions (Tables V and VI). Owing to the higher reactivity of ONB-carbonate groups compared with epoxy groups, the immobilization of ligands takes place under milder conditions (lower temperature and pH, shorter coupling times). The attachment of compounds with only hydroxyl groups failed. Immobilization of ligands bearing amino groups resulted in high coupling yields. In most instances, for immobilization of small molecules an excess of ligands was applied in up to twenty times the amount of active groups (Table V). Coupling of 1,6-DAH gave higher yields in isopropanol than in an aqueous medium.

Data obtained by testing the flow characteristics led to the assumption that the Divicell matrix was cross-linked by 1,6-DAH. The flow-rate was similar to that found for Divicell Con A (Fig. 3, curve C), whereas when ethanolamine was coupled the flow-rates were identical with those for the unmodified Divicell (Fig. 3, curve A).

Results for immobilization of proteins are given in Table VI. The coupling conditions were tested over the pH range 5.0–8.5 in different buffers for between 1 and 16 h. The coupling yield was 70–90% in most instances. Only for coupling of human γ -globulin at pH 5.0 and of BSA and protein A using low-activated supports

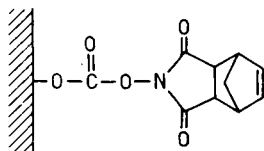


Fig. 5. Structure of active groups on Divicell ONB-Carbonate (NB = 5-norbornene-2,3-dicarboximidyl residue).

TABLE V

IMMOBILIZATION OF LIGANDS TO DIVICELL ONB-CARBONATE

Coupling medium: (1) acetone; (2) dioxane; (3) 0.1 M NaHCO₃ (pH 9); (4) isopropanol; (5) 0.1 M borate (pH 8.5); (6) 0.1 M borate (pH 8.3); (7) 0.1 M NaHCO₃ (pH 9); (8) 0.1 M borate (pH 8.9).

No.	Amount of active groups ($\mu\text{mol/ml gel}$)	Ligand	Added amount of ligand ($\mu\text{mol/ml gel}$)	Temperature ($^{\circ}\text{C}$) ^a	Time (h)	Immobilized ligand ($\mu\text{mol/ml gel}$)	Coupling yield relative to active groups (%)
1	34	<i>n</i> -Pentylamine	38	r.t.	1	34	100
2	34	Benzylamine	38	r.t.	1	27	78
3	80	1,6-DAH	800	4	20	16	20
4	26	1,6-DAH	520	r.t.	2	17	65
5	44	GalN ^b	150	4	18	27	61
6	60	Glycine	180	r.t.	16	60	100
7	30	ϵ -ACS ^c	600	r.t.	18	30	100
8	39	L-Lysine	390	r.t.	2	23	60

^a r.t. = Room temperature.

^b D-Galactosamine.

^c ϵ -Aminocaproic acid.

TABLE VI

IMMOBILIZATION OF PROTEINS TO DIVICELL ONB-CARBONATE

Coupling buffer: (1) PBS; (2) and (3) 0.1 M borate (pH 8.3); (4) 3 mM phosphate (pH 7.0); (5) 0.1 M acetate (pH 5.0); (6) and (7) 0.07 M phosphate (pH 7.4) containing 0.15 M NaCl; (8) and (9) 0.1 M borate (pH 8.3); (10) 0.1 M acetate (pH 6) containing 0.2 M NaCl; (11) 0.1 M phosphate (pH 7.5); (12) 0.1 M phosphate (pH 8.0); (13) 0.1 M borate (pH 8.5) containing 10 mM CaCl₂

No.	Amount of active groups ($\mu\text{mol/ml gel}$)	Protein	Added amount of protein (mg/ml gel)	Temperature ($^{\circ}\text{C}$) ^a	pH	Time (h)	Immobilized protein (mg/ml gel)	Coupling yield (%)
1	4.3	Goat anti-human IgG	3.6	4	7.3	16	2.7	75
2	8.8	Human IgG	5.0	4	8.3	16	4.6	92
3	51	Human IgG	5.0	4	8.3	16	4.8	96
4	6.7	Human IgG	1.1	r.t.	7.0	2	1.0	91
5	30	Human γ -globulin	12.0	r.t.	5.0	2	7.2	60
6	4.4	BSA	1.0	4	7.4	2	0.4	40
7	30	BSA	10.0	4	7.4	2	8.7	87
8	26	Con A	10.0	r.t.	8.3	1	7.1	71
9	65	Con A	25.0	r.t.	8.3	16	17.5	70
10	26	Con A	10.7	4	6.0	2	8.8	88
11	7.5	Protein A	3.0	r.t.	7.5	3	1.5	50
12	26	Protein A	2.0	r.t.	8.0	16	1.8	90
13	80	Trypsin	350 ^b	r.t.	8.5	6	300 ^b	86

^a r.t. = Room temperature.

^b Units/ml gel.

(4.4 and 7.5 μmol of active groups/ml gel, respectively) was the yield diminished to 40–60%. The amounts of covalently bound proteins ranged from 0.4 up to 17.5 mg/ml gel.

After coupling of proteins, the supports also possess improved flow properties, as shown for immobilized Con A in Fig. 3 (curve C). The biological activities of immobilized proteins were retained at all times (see Tables VII and IX). An application of sorbents in affinity chromatography is demonstrated for coupled IgG, Con A and protein A. Immobilized enzymes proved to be highly effective biocatalysts. The maximum activities of bound trypsin and penicillin acylase were 3300 and 1900 units/g cellulose, respectively. The specific activities are significantly higher than those reported for trypsin–agarose from Sigma, trypsin coupled to sodium periodate-activated bead cellulose [10] and for penicillin acylase immobilized to a synthetic polymer [57], and corroborate the successful application of Divicell supports for biotransformation processes. Trypsin–bead cellulose was used for the catalytic conversion of porcine insulin into human insulin ethyl ester [15,16] and coupled penicillin acylase for the manufacture of 6-aminopenicillanic acid from culture broths [19]. No loss of activity was found for either support after multiple reuse over a period of 500 h. These results correspond to the finding that the stability of immobilized trypsin was much higher than that of the soluble enzyme, as described by Guisan and Blanco [58].

Sorbents containing ligands coupled via ONB-carbonate groups can also be used with advantage because of the minimum leakage due to the stable urethane linkage formed between ligand and matrix [13]. Splitting off of [^{14}C]glycine immobilized to Divicell ONB-Carbonate was similar as for Divicell Epoxy under acidic (pH 4) or alkaline (pH 8.3) conditions (<1% after 1200 h at room temperature). In comparison, a leakage of 1% of [^{14}C]glycine was observed after 40 h (pH 8.3) and 220 h (pH 4), respectively, with a support prepared by coupling to cyanogen bromide-activated Sepharose [59].

Binding capacity for proteins on Divicell sorbents

The binding capacity of Divicell derivatives was tested by both static and dynamic methods. The amounts of bound proteins were determined by application either of a single protein (Table VII) or by isolation of proteins from crude products, such as seed protein extracts or sera (see Table IX). The binding capacities ranged from 1 to 30 mg/ml gel, depending on the sorbent and the applied protein.

The capacities of Divicell sorbents were compared with those for commercially available Sepharose supports. For instance, Lysine–Sepharose 4B (4–5 μmol lysine/ml gel) binds about 0.6 mg plasminogen/ml gel (Pharmacia data sheet). The higher capacity for Divicell Lysine as indicated in Table VII can be attributed to the greater amount of immobilized lysine.

Protein A–Sepharose CL-4B (2 mg protein A/ml gel) adsorbs about 20 mg human IgG/ml gel (Pharmacia data sheet). Probably the lower binding of human IgG to Divicell Protein A (example 7, Table VII) is due to possible steric hindrance during the formation of the protein A–human IgG complex. By decreasing the immobilized amount of protein A to bead cellulose to 0.5 mg/ml gel, the reversible adsorption of human IgG is also diminished (example 8, Table VII), but calculated with respect to 1 mg of attached protein A this is of the same order of magnitude as for Sepharose supports.

TABLE VII
BINDING CAPACITY OF DIVICELL SORBENTS FOR PROTEINS

The following buffers were used for binding/elution of proteins: (1) 0.05 M phosphate (pH 7.4) containing 2 M (NH₄)₂SO₄/6 M urea; (2) and (3) PBS/0.5 M formic acid; (4) 0.1 M phosphate (pH 7.5)/the same buffer containing 0.015 M ϵ -ACS; (5) 0.05 M phosphate (pH 7.0)/ 50 mM glycine; (6) 0.1 M acetate (pH 6.0)/50 mM EDTA; (7) and (8) 0.1 M phosphate (pH 7.2) containing 0.15 M NaCl/0.1 M glycine-HCl (pH 2.2); (9) 0.1 M acetate (pH 6.0) containing 0.15 M NaCl, 1 mM CaCl₂ and 1 mM MnCl₂/the same buffer containing 0.2 M methyl- α -D-glucoside.

No.	Divicell derivative	Immobilized ligand per ml gel	Bound protein	Binding capacity (mg/ml gel)
1	Pentyl	34 ^a	BSA	23.0
2	GalN	37 ^a	SBA	2.4
3	Ovalbumin	6.0 ^b	WGA	2.0
4	Lysine	23 ^a	Plasminogen	1.5
5	IDA-Cu ²⁺	36 ^c	Con A	24
6	IDA-Zn ²⁺	35 ^c	Plasminogen	14
7	Protein A	1.5 ^b	Human IgG	9.4
8	Protein A	0.5 ^b	Human IgG	4.7
9	Con A	6.6 ^b	Ovalbumin	3.1

^a μ mol.

^b mg.

^c μ g-atoms.

The following results were obtained by comparison of the respective concanavalin A derivatives: Divicell Con A adsorbs 3.1 mg ovalbumin/ml gel (see Table VII) and Con A-Sepharose (13 mg Con A/ml gel) has a capacity of 2.8 mg, although its content of immobilized Con A is about twice as high as for the corresponding Divicell derivative.

Cu²⁺ and Zn²⁺ chelates have frequently been used in immobilized metal ion chromatography for the purification and separation of human serum proteins, enzymes and lectins [33,34,60–63]. Therefore, Divicell IDA-Cu²⁺ and -Zn²⁺ were prepared by loading of IDA-bead cellulose with Cu²⁺ and Zn²⁺ salts. By testing their reversible adsorption of proteins, Con A and plasminogen were selected for the Cu²⁺ and Zn²⁺ chelates, respectively. In either instance the binding capacity was found to be the highest compared with the other Divicell affinity supports.

Hydrophobic interaction chromatography (HIC) on Divicell alkyl supports

HIC is a useful tool in the separation of proteins [64]. We tested the suitability of hydrophobic Divicell supports prepared from Divicell ONB-Carbonate for adsorption and desorption in a model system using BSA (Table VIII). The density of ligands was 27–34 μ mol/ml gel. The binding capacity of BSA to sorbents containing short-chain alkyl residues was 21–23 mg/ml gel. It increased to 29 (octyl derivative) and 47 mg/ml gel (decyl or dodecyl support).

In accordance with other workers [65] who described an increase in interaction forces between an HIC support and proteins with increasing alkyl chain length, in our system the elution conditions for supports with longer alkyl residues had to be much

TABLE VIII

BINDING CAPACITIES AND RECOVERY FOR BOVINE SERUM ALBUMIN

Preparation of supports was carried out according to the pentyl derivative (see Table V). The coupling yield was 90–100% except for Divicell Benzyl. In each instance 100 mg of BSA were loaded on a column (2.5×1 cm I.D.) at room temperature. The binding buffer was 0.05 M phosphate (pH 7.4) containing 2 M $(\text{NH}_4)_2\text{SO}_4$.

Divicell derivative	Immobilized ligand ($\mu\text{mol/ml}$ gel)	Capacity for BSA (mg bound/ml gel)	Recovery (%)	Elution medium
Propyl	32.3	23.5	99	0.05 M phosphate (pH 7.4)
Butyl	30.6	22.4	99	0.05 M phosphate (pH 7.4)
Pentyl	34.0	23.0	95	6 M urea
Hexyl	34.0	21.3	95	50% acetonitrile ^a
Octyl	34.0	28.7	85	50% acetonitrile ^a
Decyl	27.1	47.0	90	80% methanol ^a
Dodecyl	27.1	47.2	90	80% methanol ^a
Benzyl	26.7	29.7	90	6 M urea

^a Mixture with water (v/v).

more drastic, whereas variation of the ligand density over a certain range (10–55 $\mu\text{mol/ml}$ gel) had no substantial effect.

Reuse of Divicell Pentyl was tested with a series of 22 loading–elution cycles. The support was regenerated with 1 M sodium hydroxide solution after ten cycles each time. For each loading–elution cycle the recovery of BSA was $93.0 \pm 1.5\%$ ($n = 20$, determined by UV absorbance). Only traces of protein were eluted during regeneration (simulation of cleaning-in-place). No significant changes in binding capacity, recovery or flow-rate could be observed during these experiments.

Application of Divicell sorbents in affinity chromatography

Purification of proteins. Selected examples of the application of Divicell sorbents are presented in Table IX. Sorbents derived from activated supports were prepared by coupling of ligands to Divicell ONB-Carbonate (Nos. 2–6) and to Divicell Epoxy (Nos. 7–9). Each purified protein was checked by electrophoresis (CAF, PAGE and SDS-PAGE) and fulfilled the purification criteria.

Starting from biological material, the amount of bound protein per millilitre of sorbent was lower than expected from the binding capacity determined using a defined protein solution (Table VII). For instance, to the lysine support 1.5 mg (Table VII) and 0.8 mg (Table IX) of plasminogen were bound by application of a plasminogen solution and human serum, respectively, and to the protein A support 4.7 mg (Table VII) or 4.2 mg (Table IX) of human IgG were adsorbed when a human IgG solution or human serum was used.

Generally, the binding capacities were sufficient for the isolation of 10–500-mg amounts of the proteins listed in Table IX using small columns.

Dye–ligand affinity chromatography on Divicell Blue. The application of Divicell Blue for purification of HSA from human serum is demonstrated in Fig. 6. Under the conditions used only HSA was specifically adsorbed on the support. The other serum proteins could be washed out with equilibration buffer (first peak). This was proved

TABLE IX

DIVICELL SORBENTS FOR CHROMATOGRAPHIC PURIFICATION OF PROTEINS

The following buffers were used for binding/elution of proteins: (1) 0.05 M Tris-HCl (pH 8.0) containing 0.5 M NaCl/the same buffer containing 1 M KSCN; (2) PBS containing 0.05% Tween 20/0.1 M glycine-HCl (pH 2.8 and 2.2); (3) PBS containing 0.05% Tween 20/0.1 M glycine-HCl (pH 2.5); (4) 0.1 M phosphate (pH 7.2) containing 0.15 M NaCl/0.1 M glycine-HCl (pH 2.3); (5) 0.1 M acetate (pH 6.5) containing 0.2 M NaCl, 1 mM CaCl₂ and 1 mM MnCl₂/the same buffer containing 0.2 M D-glucose; (6) 0.1 M phosphate (pH 7.5)/the same buffer containing 0.015 M *ε*-ACS; (7)-(9) PBS/0.5 M formic acid.

No.	Divicell sorbent	Immobilized ligand (mg/ml gel)	Applied material ^a per ml gel	Purified protein	Bound protein (mg/ml gel)
1	Blue	6-8	0.2 ml human serum	HSA	10-15
2	Human IgG	4.8	2 ml rabbit antiserum	Rabbit anti-human IgG	2.5
3	Goat anti-human IgG	2.7	1 ml human serum	Human IgG	1.5
4	Protein A	0.5	0.5 ml human serum	Human IgG	4.2
5	Con A	8.8	6.7 mg crude ovalbumin	Ovalbumin	4.4
6	Lysine	23 ^b	15 ml human serum	Plasminogen	0.8
7	GlcNAc	7 ^b	125 mg total protein ^c	WGA	7.2
8	GalNAc	9 ^b	75 mg total protein ^c	SBA	2.6
9	GalNAc	9 ^b	150 mg total protein ^c	PNA	10.0

^a Dissolved in binding buffer.

^b μ mol/ml gel.

^c From plant seed extract.

by CAF electrophoresis (see insets in Fig. 6). More than 95% of the HSA was removed from human serum with only low non-specific adsorption of other proteins. The recovery for HSA was about 80%.

Immunoaffinity chromatography. The model system human IgG-anti-human IgG was chosen. First, human IgG was immobilized (4.8 mg/ml gel) to purify the corresponding antibodies from antiserum. The chromatographic profile is shown in Fig. 7. The total amount of purified rabbit anti-human IgG was 2.5 mg/ml gel.

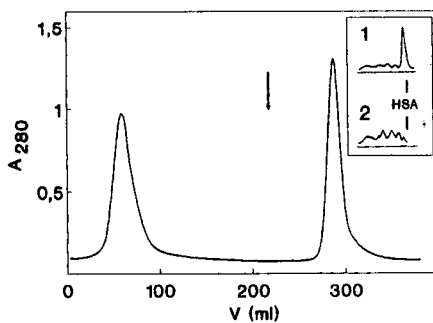


Fig. 6. Isolation of HSA from human serum using Divicell Blue (see Experimental). The arrow indicates the elution of HSA with Tris-HCl buffer containing 1 M KSCN. In the insets the densitogram for cellulose acetate foil (CAF) electrophoresis of human serum is shown (1) before and (2) after affinity chromatography.

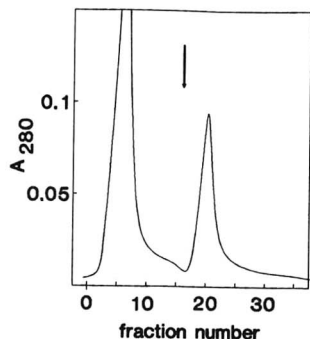


Fig. 7. Purification of rabbit anti-human IgG by affinity chromatography on a column of human IgG immobilized to Dvicell (see Experimental). A 2-ml volume of rabbit antiserum were applied. After washing the antibodies were eluted with 0.1 M glycine-HCl buffer (pH 2.8) (arrow).

Approximately 90% of the antibodies were eluted at pH 2.8 and 10% by subsequent elution at pH 2.2. The purity of the antibodies was tested by PAGE (Fig. 8).

Electrophoresis suggests that pure IgG was eluted. For comparison with an agarose support, human IgG-Sephrose was prepared from CNBr-Sephrose 4B. The immobilized amount was 5 mg human IgG/ml gel and the yield of antibodies was 2.8 mg. Also, no contamination was detectable by PAGE (Fig. 8, gel No. 5).

The amounts of IgG eluted were also determined by SRID with sheep anti-rabbit IgG and rabbit IgG as standard. The activity of antibodies was checked by

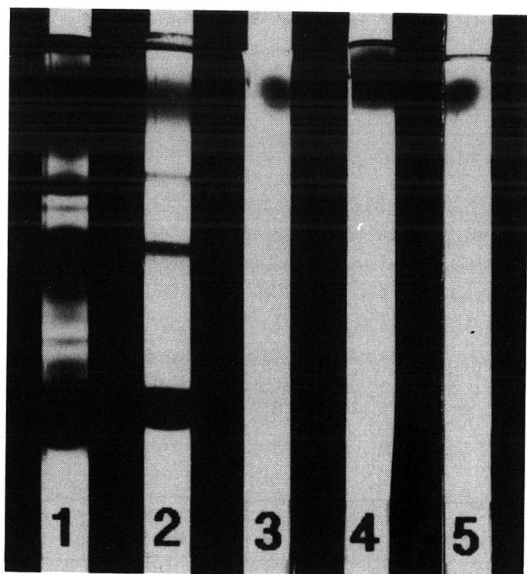


Fig. 8. PAGE of (1) rabbit anti-human IgG serum, (2) PBS-washing fraction, (3) 15 μ g and (4) 100 μ g of rabbit anti-human IgG eluted from a Dvicell column at pH 2.8 and (5) 15 μ g of rabbit anti-human IgG eluted from a human IgG-Sephrose column at pH 2.8.

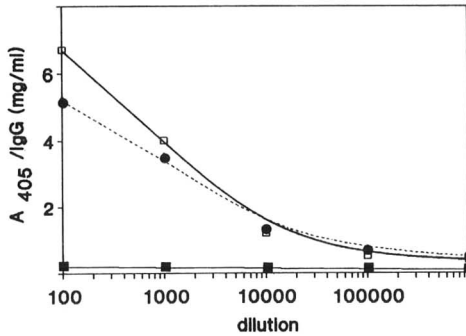


Fig. 9. Determination of the activity of rabbit anti-human IgG eluted at pH 2.8 by an ELISA. Serial dilutions were made from (□) antibodies (360 $\mu\text{g}/\text{ml}$) eluted from a Divicell column, and (●) antibodies (400 $\mu\text{g}/\text{ml}$) eluted from a Sepharose column and (■) from the starting rabbit anti-human IgG serum. First human IgG was bound on microtitre plates, then diluted samples were added to the wells. After binding of antibodies, goat anti-rabbit IgG conjugated with alkaline phosphatase was used as the second antibody. The substrate was 4-nitrophenylphosphate. Amounts of 4-nitrophenolate formed were measured spectrophotometrically at 405 nm.

DRID and ELISA. The results of ELISA are demonstrated in Fig. 9. The graphical representation shows that the antibodies eluted from the Divicell column gave higher titres per milligram of IgG than those eluted from the Sepharose sorbent. A similar relationship was obtained by comparison of the eluates at pH 2.2. However, the specific affinity of antibodies against human IgG was about 50% higher in the pH 2.2 eluates for both Divicell and Sepharose adsorbents, showing that the antibodies with the highest affinity were desorbed under stronger elution conditions.

For the opposite example, goat anti-human IgG was coupled to Divicell to isolate human IgG from human serum. The amount of IgG eluted was 1.5 mg/ml gel when the activation level of Divicell ONB-Carbonate was low (4.3 μmol active groups/ml gel) and decreased to 0.35 mg/ml when a high-activated support (42.3 $\mu\text{mol}/\text{ml}$ gel) was used for immobilization of antibodies.

Our results conflict with those of Peng *et al.* [12], who found that high binding efficiencies were only achieved when the concentration of goat anti-human IgG immobilized to a cross-linked bead cellulose was less than 0.2 mg/ml gel. A reduction in the efficiency from 55 to 5% was reported when the concentration of the antibody was increased to more than 2.0 mg/ml gel. In this attempt the efficiency of 100% was fixed at a 1:1 ratio of immobilized antibody to adsorbed human IgG. In our experiments we determined an efficiency of 55% for 2.7 mg of immobilized goat anti-human IgG. We assume that this apparent contradiction is due to the higher macroporosity of Divicell, which diminished steric effects caused by the matrix, or to the lower activation level of the support, preventing multi-point attachment of immobilized antibody, which may decrease its efficiency.

Purification of lectins. The affinity of many proteins to carbohydrates can be used for the chromatographic separation and purification of lectins [66]. For this purpose GlcNAc and GalNAc immobilized to Divicell Epoxy were utilized for purification of WGA, SBA and PNA from the corresponding plant seed extracts (see Table IX). For instance, the elution profile of WGA is shown in Fig. 10. The isolated

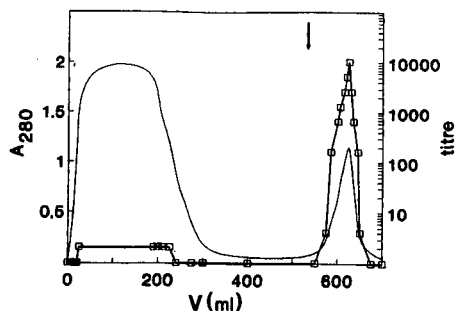


Fig. 10. Purification of WGA from a crude wheat germ extract on Dvicell GlcNAc (see Experimental). Chromatography was monitored by measuring absorbance at 280 nm for determination of protein and by a haemagglutination assay presented as a titre. The arrow indicates elution with 0.5 M formic acid.

amount of WGA was 420 mg from 5 g of total protein in the crude extract obtained from 1 kg of wheat germs. The binding capacity of WGA is comparable to that described for Sepharose affinity sorbents [32,56]. The eluted WGA was electrophoretically pure (SDS-PAGE) and showed a high biological activity. The titre in the haemagglutination assay was about 2000 in dilution series starting with 10 mg WGA/ml.

With reuse of Dvicell GlcNAc, the amount of WGA eluted decreased after 8 cycles to 0.2 mg/ml gel. Probably deacetylation of bound GlcNAc by formic acid was partly responsible for the diminished efficiency, because after reacetylation and further use of the sorbent the WGA eluted increased to 2.4 mg/ml gel.

The purification of SBA and PNA on Dvicell GalNAc was carried out under similar conditions to those described for WGA (see Table IX). When Dvicell GalN prepared from Dvicell ONB-Carbonate was applied, a binding capacity for SBA of 2.4 mg/ml gel was obtained.

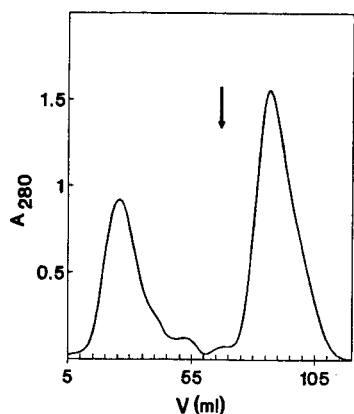


Fig. 11. Affinity chromatographic purification of ovalbumin on Dvicell Con A (see Experimental). Ovalbumin was eluted with equilibration buffer complemented with 0.2 M D-glucose (arrow).

Purification of ovalbumin. The high biological activity of Con A attached to Divicell ONB-Carbonate could be demonstrated (see above). Therefore, this sorbent is suitable for the purification of glycopeptides or glycoproteins containing oligosaccharides with glucose and mannose residues [67]. We used Divicell Con A in the chromatography of ovalbumin from hen eggs as a model (see Fig. 11). Elution of adsorbed protein with buffer containing D-glucose led to electrophoretically pure ovalbumin (recovery 66%) and was similar to results that were obtained using Con A-Sephrose.

CONCLUSIONS

The bead cellulose Divicell has been demonstrated to be a support with advantageous properties. Further modifications of the matrix were possible with respect to the preparation of many different supports and for use of these Divicell derivatives in ion-exchange, hydrophobic interaction and affinity chromatography or related techniques. Chemical modifications by activation and coupling of ligands did not change the macroporosity and the advantageous chromatographic properties. Because of the very good mechanical and chemical stability, the high biological activity of immobilized ligands and the high yields of purified proteins, Divicell supports are especially suitable for the use in large-scale protein separations.

ACKNOWLEDGEMENTS

The authors thank Dr. A. Wergin and Mr. A. Schnauss (Central Institute of Molecular Biology) for experiments on the purification of lectins, Dr. W. Schössler (Klinikum Berlin-Buch) for help with the immunochemical techniques and Mrs. D. Büttner, Mrs. H. Boske, Mrs. H. Scheer and Mr. D. Jobsky (Central Institute of Molecular Biology) for excellent technical assistance.

REFERENCES

- 1 J. Štamberg, J. Peška, H. Dautzenberg and B. Philipp, in T.C. J. Gribnau, J. Visser and R. J. F. Nivard (Editors), *Affinity Chromatography and Related Techniques*, Elsevier, Amsterdam, 1982, pp. 131–141.
- 2 J. Štamberg, *Sep. Purif. Methods*, 17 (1988) 155.
- 3 S. Kuga, *J. Chromatogr.*, 195 (1980) 221.
- 4 J. Štamberg, J. Peška, D. Paul and B. Philipp, *Acta Polym.*, 30 (1979) 734.
- 5 J. Peška, J. Štamberg, J. Hradil and M. Ilavský, *J. Chromatogr.*, 125 (1976) 455.
- 6 Y. Motozato and C. Hirayama, *J. Chromatogr.*, 288 (1984) 499.
- 7 P. Gemeiner, M. J. Beneš and J. Štamberg, *Chem. Pap.*, 43 (1989) 805.
- 8 P. Mohr and K. Pommerening, *Affinity Chromatography — Practical and Theoretical Aspects*, Marcel Dekker, New York, Basle, 1985, pp. 196–201.
- 9 M. Naumann, R. Reuter, P. Metz and G. Kopperschläger, *J. Chromatogr.*, 466 (1989) 319.
- 10 J. Turková, J. Vajčner, D. Vančurová and J. Štamberg, *Collect. Czech. Chem. Commun.*, 44 (1979) 3411.
- 11 J. Drobňák, J. Labský, H. Kudlvasrová, V. Saudek and F. Švec, *Biotechnol. Bioeng.*, 24 (1982) 487.
- 12 L. Peng, G. J. Calton and J. W. Burnett, *J. Biotechnol.*, 5 (1987) 255.
- 13 W. Büttner, M. Becker, C. Rupprich, H.-F. Boeden, P. Henklein, F. Loth and H. Dautzenberg, *Biotechnol. Bioeng.*, 33 (1989) 26.
- 14 P. Gemeiner, C. Polák, A. Breier and L. Petruš, *Enzyme Microb. Technol.*, 8 (1986) 109.
- 15 A. Könnecke, C. Schönfels, M. Hänslér and H.-D. Jakubke, *Tetrahedron Lett.*, 31 (1990) 989.

- 16 C. Rupprich, M. Becker, W. Büttner, H.-F. Boeden, K.-L. Schröder, A. Hänicke and A. Könnecke, *Biomater. Artif. Cells Artif. Organs*, 18 (1990) in press.
- 17 J. Turková, L. Petkov, J. Sajdok, J. Káš and M. Beneš, *J. Chromatogr.*, 500 (1990) 585.
- 18 A. Wergin, H.-F. Boeden, C. Rupprich, A. Schnauss and M. Holtzhauer, in A. Kallikorm and T. C. Bøg-Hansen (Editors), *Lectins—Biology, Biochemistry, Clinical Biochemistry*, Vol. 8, Sigma, St. Louis, MO, in press.
- 19 B. Rockstroh, personal communication.
- 20 M. Steinbuch and R. Audran, *Arch. Biochem. Biophys.*, 134 (1969) 279.
- 21 R. C. Warner, in H. Neurath and K. Bailey (Editors), *The Proteins*, Vol. IIA, Academic Press, New York, 1954, p. 440.
- 22 K. Pommerening, M. Kühn, W. Jung, K. Buttgerit, P. Mohr, J. Štamberg and M. Beneš, *J. Int. Biol. Macromol.*, 1 (1979) 79.
- 23 B. B. L. Agrawal and I. J. Goldstein, *Biochim. Biophys. Acta*, 147 (1967) 262.
- 24 N. Nishikata, *J. Biochem.*, 95 (1984) 1169.
- 25 T. Terao, T. Irimura and T. Osawa, *Hoppe Seyler's Z. Physiol. Chem.*, 356 (1975) 1682.
- 26 D. Bertram, H. Dautzenberg, E. Krause, F. Loth, K. Pommerening and E.-M. Sobek, *E. Ger. Pat. Appl.* 255.738, A1 (1988).
- 27 M. Rybák, Z. Brada and I. M. Hais, *Säulenchromatographie an Cellulose-Ionenaustauschern*, Gustav-Fischer, Jena, 1966, pp. 80–101.
- 28 K. Pommerening and H. Rein, in preparation.
- 29 B. T. Hofreiter, B. H. Alexander and J. A. Wolf, *Anal. Chem.*, 27 (1955) 1930.
- 30 I. Matsumoto, Y. Mizuno and N. Seno, *J. Biochem.*, 85 (1979) 1091.
- 31 L. Sundberg and J. Porath, *J. Chromatogr.*, 90 (1974) 87.
- 32 R. Uy and F. Wold, *Anal. Biochem.*, 81 (1977) 98.
- 33 J. Porath and B. Olin, *Biochemistry*, 22 (1983) 1621.
- 34 Z. El Rassi, Y. Truei, Y.-F. Maa and Cs. Horváth, *Anal. Biochem.*, 169 (1988) 172.
- 35 O. H. Lowry, N. J. Rosebrough, A. L. Farr and R. J. Randall, *J. Biol. Chem.*, 193 (1951) 265.
- 36 B. C. N. Hummel, *Can. J. Biochem. Biophysiol.*, 37 (1959) 1393.
- 37 K. Balasingham, D. Warburton, P. Dunnill and M. D. Lilly, *Biochim. Biophys. Acta*, 276 (1972) 250.
- 38 P. K. Smith, A. K. Mallia and G. T. Hermanson, *Anal. Biochem.*, 109 (1980) 466.
- 39 E. A. Davidson, *Methods Enzymol.*, 8 (1966) 52.
- 40 H. N. Schmitt and J. E. Walker, *FEBS Lett.*, 81 (1977) 403.
- 41 S. Jacob, *Methods Biochem. Anal.*, 33 (1965) 241.
- 42 H. R. Maurer, *Disc Electrophoresis*, Walter de Gruyter, Berlin, 1971, p. 44.
- 43 U. K. Laemmli, *Nature (London)*, 227 (1970) 680.
- 44 G. Mancini, J.-P. Vaerman, A. O. Carbonara and J. F. Heremans, *Protides Biol. Fluids, Proc. Colloq.*, 11 (1964) 370.
- 45 O. Ouchterlony, *Acta Pathol. Microbiol. Scand.*, 25 (1948) 186.
- 46 T. Osawa and I. Matsumoto, *Methods Enzymol.*, 28 (1972) 323.
- 47 H.-J. Böhme, G. Kopperschlager, J. Schulz and E. Hofmann, *J. Chromatogr.*, 69 (1972) 209.
- 48 C. R. Lowe and J. C. Pearson, *Methods Enzymol.*, 104 (1984) 97.
- 49 J. Travis and R. Pannel, *Clin. Chim. Acta*, 49 (1973) 49.
- 50 J. Travis, J. Bowen, D. Tewksbury, D. Johnson and R. Pannel, *Biochem. J.*, 157 (1976) 301.
- 51 S. Angal and P. D. G. Dean, *Biochem. J.*, 167 (1977) 301.
- 52 G. Birkenmeyer, *Ph.D. Thesis*, Section of Medicine, University of Leipzig, Leipzig, 1981.
- 53 L. Petruš, P. Gemeiner and T. Némethy, *Collect. Czech. Chem. Commun.*, 49 (1984) 821.
- 54 J. Porath and N. Fornstedt, *J. Chromatogr.*, 51 (1970) 479.
- 55 Pharmacia Fine Chemicals *Affinity Chromatography—Principles and Methods*, Ljungföretagen, Örebro, 1983, p. 31.
- 56 P. Vretblad, *Biochim. Biophys. Acta*, 434 (1976) 169.
- 57 K. Burg, O. Mauz, S. Noetzel and K. Sauber, *Angew. Makromol. Chem.*, 157 (1988) 105.
- 58 J. M. Guisan and R. M. Blanco, *Ann. N.Y. Acad. Sci.*, 501 (1987) 67.
- 59 M. Baeseler, H.F. Boeden, R. Koelsch and J. Lasch, in preparation.
- 60 J. Porath, J. Carlsson, J. Olsson and G. Belfrage, *Nature (London)*, 258 (1975) 598.
- 61 L. Andersson, *ISI Atlas Sci.*, (1988) 318.
- 62 J. Porath, *Trends Anal. Chem.*, 7 (1988) 254.
- 63 S. A. Margolis, A. J. Fatiadi, L. Alexander and J. J. Edwards, *Anal. Biochem.*, 183 (1989) 108.

- 64 S. Pahlman, in O. Hoffmann-Ostenhof, M. Breitenbach, F. Koller, D. Kraft and O. Scheiner (Editors), *Affinity Chromatography*, Pergamon Press, Oxford, 1978, pp. 161–173.
- 65 M. N. Schmuck, M. P. Nowlan and K. M. Gooding, *J. Chromatogr.*, 371 (1986) 55.
- 66 I. E. Liener, N. Sharon and I. J. Goldstein (Editors), *The Lectins — Properties, Functions and Applications in Biology and Medicine*, Academic Press, New York, 1986.
- 67 R. K. Merkle and R. D. Cummings, *Methods Enzymol.*, 138 (1987) 232.

CHROMSYMP. 2105

Chemically bonded phases for the reversed-phase high-performance liquid chromatographic separation of basic substances

BOGUSŁAW BUSZEWSKI^a, JUTTA SCHMID, KLAUS ALBERT and ERNST BAYER*

Institut für Organische Chemie der Universität Tübingen, Auf der Morgenstelle 18, D-7400 Tübingen (Germany)

ABSTRACT

A chemically bonded phase with a peptide group (PB) for reversed-phase high-performance liquid chromatography (HPLC) is described. This packing was prepared by a two-stage modification of the surface of silica gel with mono- and trifunctional 3-aminopropylsilane and then with an appropriate derivative of a fatty acid. Packings prepared in this way were compared with standard C₁₈ materials used in HPLC. Surface characteristics of the packings before and after chemical modification were determined by different physico-chemical methods, *e.g.*, porosimetry, elemental analysis, ¹³C and ²⁹Si cross-polarization magic angle spinning NMR and HPLC. Chromatographic properties of these packings were evaluated by comparison between log *k'* of one phase and log *k'* of a second phase for substances with different chemical natures. The PB packing was found to be especially useful for the separation of basic substances.

INTRODUCTION

The reversed-phase high-performance liquid chromatographic (RP-HPLC) separation of polar organic substances, especially those with strongly basic character, using conventional chemically bonded phases (CBP) poses many problems, connected with the strong interactions between the chromatographed substance, the mobile phase and the modified packing surface [1,2]. Hence modification of the composition of the mobile phase (careful adjustment of pH and/or addition of ionic substances) is necessary [3,4]. Improved separation selectivity can also be obtained by tailoring the properties of the column packing material [5,6].

Hydrophobic packing materials with different lengths of the alkyl chains, *e.g.*, C₂, C₈ and C₁₈, are available for RP-HPLC [6-10]. In addition, many HPLC applications require packings containing polar functional groups (NO₂, NH₂, CN or/and OH) bonded to short alkyl chains (C₃, C₄) [7-9]. Various specific packing

^a Permanent address: Department of Chemical Physics, Faculty of Chemistry, Maria Curie Skłodowska University, Pl-20 031 Lublin, Poland.

materials, *e.g.*, donor-acceptor, chiral and chelate CBPs, have also been elaborated [9,11-13].

In order to increase the separation selectivity and to widen the analytical capabilities of RP-HPLC techniques, increased attention has centred on the preparation of packing materials suitable for the selective determination of compounds belonging to a group of substances with similar physical and/or chemical properties, *e.g.*, amino acids, peptides, pharmaceuticals. In only a few papers, however, is information given concerning the preparation procedure, surface characterization and the determination of physico-chemical properties of these packing materials [14,15]. This information is very important, however, particularly when the retention mechanism during the chromatographic process is to be studied [16]. Hence for this purpose various relationships between the capacity factor (k') and mobile phase composition or/and different properties of separated compounds, *eg.*, polarity, molecular building or molecular weight, have been used [5,9,16,17]. All of these factors have an influence on the reproducibility of the retention data, particularly during routine analysis.

In this paper, a new chemically bonded phase carrying a peptide group (PB) suitable for the RP-HPLC separation of various polar substances is described. On the basis of the physico-chemical surface characteristics of the prepared phases, the chromatographic properties were compared with those of standard C_{18} packing materials. In addition, the PB phases were applied to the separation of some basic drugs ($pK_a = 9.8-11.6$) and a paracelsin-peptide mixture.

EXPERIMENTAL

Materials and reagents

LiChrospher Select B (E. Merck, Darmstadt, Germany) was used as the support for the preparation of CBPs. The physico-chemical characteristics of this unmodified silica gel are listed in Table I.

For chemical modification, 3-aminopropyldimethylmethoxysilane (MNH_2), 3-aminopropyltriethoxysilane (TNH_2) (Fluka, Buchs, Switzerland), octadecyldimethylchlorosilane (MC_{18}) (Wacker, Munich, Germany), stearic acid (Aldrich-Chemie,

TABLE I
PHYSICAL CHARACTERISTICS OF BARE LICHROSPHER SELECT B

Characteristic	Abbreviation	Value
Particle size (μm)	d_p	5.0
Specific surface area (m^2/g)	S_{BET}	570
Mean pore diameter (nm)	D	5.76
Pore volume (cm^3/g)	V_p	0.96
Concentration of surface accessible silanol groups ^a ($\mu mol/m^2$)	α_{SiOH}	5.18
pH, 5% aqueous suspension ^b		5.01

^a According to ref. 18.

^b According to ref. 19.

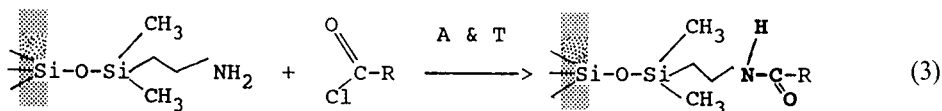
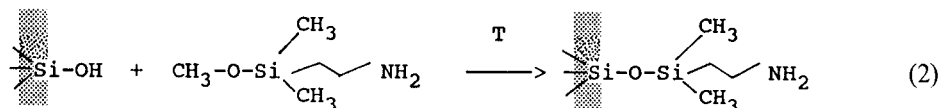
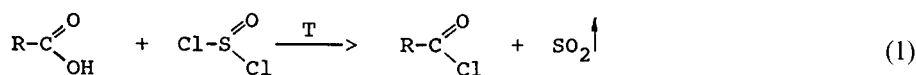
Steinheim, Germany) and specially prepared dry morpholine [19] (Riedel de Haën, Seelze, Germany) were used. Methanol, toluene and *n*-hexane (E. Merck) were used. All reagents were of analytical-reagent grade.

The prepared phases were packed into 125 × 4.6 mm I.D. and 60 × 4.6 mm I.D. stainless-steel tubes purchased from Bischoff (Leonberg, Germany).

Methanol, acetonitrile, water for HPLC (E. Merck) and phosphate buffer (pH 2.3) were used to prepare mobile phases for the chromatographic investigations.

Preparation of CBPs

The phases with a peptide group (PB) were prepared in a two-stage reaction. The silica gel was first treated with monofunctional (^MNH₂) or trifunctional (^TNH₂) aminopropylsilane modifiers, followed by reaction of the amino groups with stearyl chloride. This derivative was prepared in our laboratory according to ref. 20 (eqn. 1). In general, the reactions of PB phases can be illustrated by eqns. 1–3, where R is C₁₈H₃₇, T is heating and A is reaction activator (morpholine).



Silica gel (5 g) was dried at 180°C under vacuum (10⁻³ Pa) in a glass reactor for 12 h. Portions of 3 g of silica gel were reacted with 0.3 M 3-aminopropyltrimethoxysilane or 0.1 M 3-aminopropyltriethoxysilane and heated to 110 ± 5°C for 8 h (eqn. 2). The product was filtered off and washed with dry toluene, methanol and *n*-hexane and dried at room temperature.

This intermediate product was heated at 120°C under vacuum (10⁻³ Pa) for 12 h and then allowed to react at 110 ± 5°C for 8 h with a 1:1 molar ratio of stearyl chloride in dry morpholine as an activator [19,21] (eqn. 3). The final product was filtered off, washed with dry toluene, methanol and *n*-hexane and dried at room temperature.

The packing with standard ^MC₁₈ phase was prepared using octadecyldimethylchlorosilane according to the procedure described previously [19,21].

The characteristics of the prepared packings are listed in Table II.

Apparatus

The porosity parameters characterizing the starting material were determined by the BET method on the basis of the low-temperature adsorption-desorption of

nitrogen using a Model 1800 automatic sorption apparatus (Carlo Erba, Milan, Italy).

The concentration of surface silanol groups (α_{SiOH}) of bare LiChrospher SB was determined using the method proposed by Nondek and Vydroš [18].

The pH of an aqueous suspension of the bare packing material was determined with a Model E-512 pH meter (Metrohm, Herisau, Switzerland).

The density of coverage (α_{RP} and/or $n\alpha_{\text{RP}}$) of the CBPs was calculated from the percentage of carbon (P_c) and nitrogen (P_N) as determined with a Model 1104 elemental analyser (Carlo Erba).

Solid-state NMR measurements were performed on a Bruker (Karlsruhe, Germany) MSL 200 spectrometer with 200–300-mg samples in double-bearing rotors of zirconia. Magic angle spinning (MAS) was carried out at a spinning rate of 4 kHz. ^{29}Si cross-polarization (CP) MAS NMR spectra were recorded with a pulse repetition time of 2 s. In the case of ^{13}C CP-MAS NMR spectra a contact time of 12 ms was applied. All NMR spectra were externally referenced to liquid tetramethylsilane and the chemical shifts are given in parts per million.

Chromatographic measurements were made with a Model LC-31 liquid chromatograph (Bruker) with a Model 7121 sampling valve (Rheodyne, Berkeley, CA, U.S.A.) and Model 3380A computing integrator (Hewlett-Packard, Karlsruhe, Germany). Chromatograms were recorded at 206, 220 and 254 nm using also a Model 655 A UV-VIS spectrophotometer (Hitachi-Merck, Darmstadt, Germany).

Column packing procedure

PB phases were shaken in an ultrasonic bath for 5 min with 38 ml of tetrachloroethylene-1-propanol (2:1, v/v) (for $^{\text{M}}\text{C}_{18}$ phase the slurry composition was 1 g of prepared packing in 35 ml of isopropanol). The slurry was then filled in the columns using 150 ml of methanol as a packing solvent. All columns were packed using a Shandon packing pump (Shandon, Frankfurt, Germany) under a pressure of 50 MPa according to procedures described previously [22].

RESULTS AND DISCUSSION

Surface characterization of CBP

Table II gives the elemental analysis data for the various packings obtained by chemical modification of bare silica gel (the most important surface characteristics of the bare support are listed in Table I). Table II also gives the coverage densities (α_{RP} and $n\alpha_{\text{RP}}$), which were calculated using equations presented previously [23]. Fig. 1 shows the ^{29}Si CP-MAS NMR spectra of unmodified and modified material packings.

From the data in Table II it can be seen that a *ca.* 20% higher density of coverage is obtained with mono functional ($^{\text{M}}\text{NH}_2$; packing No. 1) than trifunctional aminosilanes ($^{\text{T}}\text{NH}_2$; packing No. 2; eqn. 2). These observations were confirmed by ^{29}Si CP-MAS NMR measurements. On the basis of the ^{29}Si CP-MAS NMR investigations, it is possible to define the undersurface structure of chemically bonded films (Fig. 1A-b and B-b). From analysis of the spectra presented in Fig. 1A and B, it can be concluded that the first stage of chemical modification with aminosilanes reduces the silanol contribution. Almost total blocking of the geminal silanol groups takes place (Q_2 ; $\delta = -91$ ppm). The contribution of the free silanol groups (Q_3 ; $\delta = -100$ ppm) decreases and the M ($\delta = +13$ ppm), T_2 ($\delta = -56$ ppm), T_3

TABLE II
CHARACTERISTICS OF MODIFIED PACKINGS

CBP = chemically bonded phase; P_C = percentage of carbon; P_N = percentage of nitrogen; α_{RP} = concentration of chemically bonded groups ($\mu\text{mol}/\text{m}^2$); $n\alpha_{RP}$ = number of alkylsilyl ligands per unit surface area (nm^{-1}); M = monofunctional silane; T = trifunctional silane; NH_2 = amino phase; PB = peptide bond.

No. of packing	Type of packing	Type of CBP	Coverage			
			P_C	P_N	α_{RP}	$n\alpha_{RP}$
1	LiChrospher $^{\text{M}}\text{NH}_2$	Monomer	6.74	1.58	2.89	1.74
2	LiChrospher $^{\text{T}}\text{NH}_2$	Polymer	5.82	1.19	2.38	1.43
3	LiChrospher $^{\text{M}}\text{PB}$	Monomer	19.75	1.64	2.33	1.33
4	LiChrospher $^{\text{T}}\text{PB}$	Polymer	14.29	1.22	1.82	1.06
5	LiChrospher $^{\text{M}}\text{C}_{18}$	Monomer	23.21	—	2.42	1.46

($\delta = -60$ ppm) and T_4 ($\delta = -66$ ppm) peaks appear in the spectrum. These peaks correspond to the bonded alkylsilyl ligands. Peak M corresponds to the monofunctional structure of CBP whereas peaks T_2 , T_3 and T_4 correspond to the net polymer structure formed [23–26].

Reaction of the amino groups with chloro derivatives of a fatty acid (see eqn. 3) causes a significant increase in the surface carbon content (P_C): 65% for the monofunctional structure of the packing (packing No. 3) and 60% for the net polymer (packing No. 4, see Table II). The α_{RP} values also indicate that a higher coverage

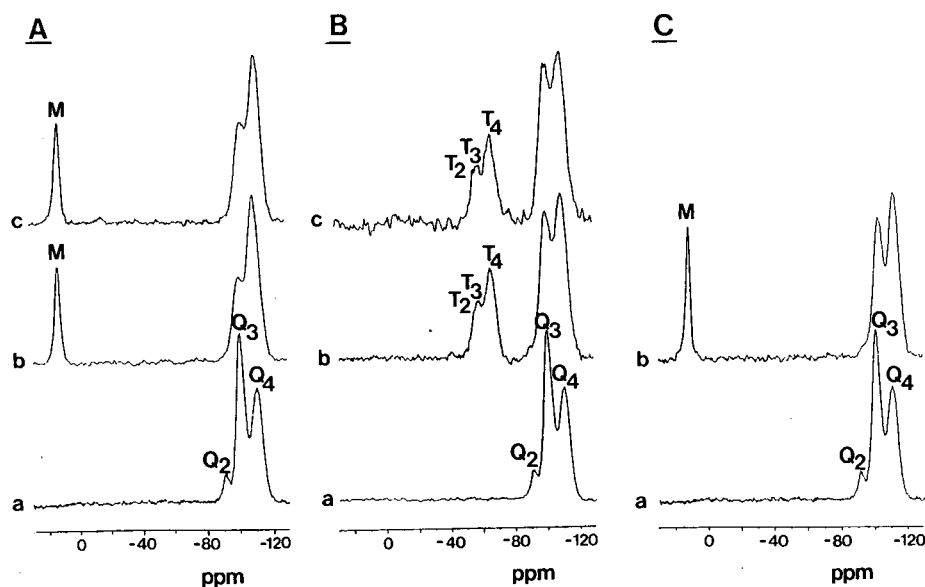


Fig. 1. ^{29}Si CP-MAS NMR spectra of bare silica gel (A, B, C-a) with (A-b) $^{\text{M}}\text{NH}_2$ phase, (A-c) $^{\text{M}}\text{PB}$ phase, (B-b) $^{\text{T}}\text{NH}_2$ phase, (B-c) $^{\text{T}}\text{PB}$ phase and (C-b) $^{\text{M}}\text{C}_{18}$ phase.

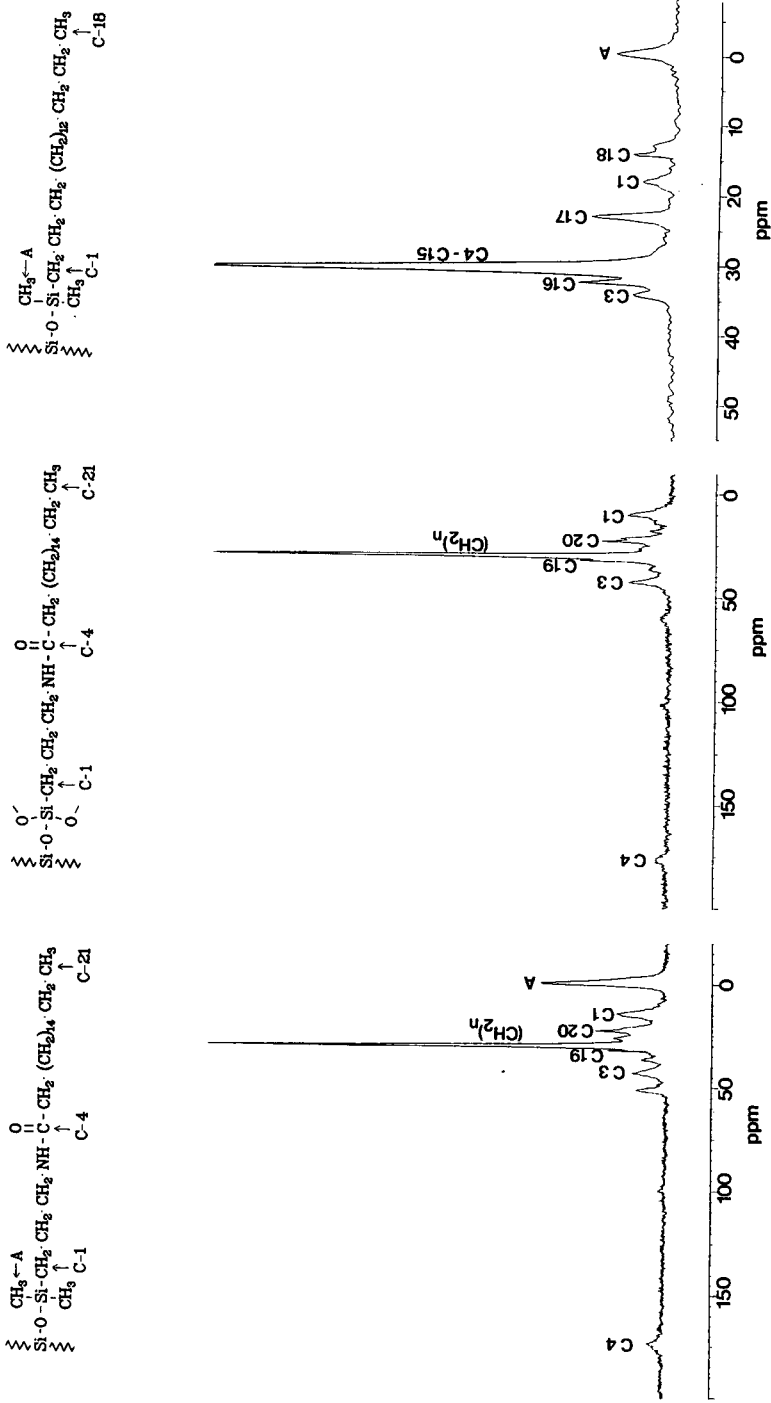


Fig. 2. ¹³C CP-MAS NMR spectra of modified silica gel with (a) ^mTPB phase, (b) ^mTPB phase and (c) ^mC₁₈ phase.

density was obtained with the C_{18} packing (No. 5), but the alkylsilyl chains bonded with the support surface are shorter (by three methylene groups) than bonded PB ligands. However, this difference is not large (*ca.* 5% for monofunctional packings 3 and 5). Therefore, evaluation and comparison of the physico-chemical properties of both monofunctional phases were of interest. In order to obtain information on the difference between ${}^M C_{18}$ and ${}^M PB$ phases, these were investigated by ${}^{13}C$ CP-MAS NMR spectroscopy. The spectra obtained are presented in Fig. 2.

From Fig. 2a–c, it is apparent that after the reaction of amino groups with chloro derivatives of a fatty acid (packings 1 and 2; see eqn. 3), almost all accessible NH_2 groups are blocked and peptide bonds formed [27]. In Fig. 2a and b the C_4 peak ($\delta = +174$ ppm) is observed. With the monofunctional reagent, a single siloxane bond [$\equiv Si-O-Si(CH_3)_2-$] is formed ($\delta = -2.5$ ppm) [24,25]. When the surface is modified with a trifunctional ethoxysilane, the ethanol liberated is adsorbed on the residual silanol groups via hydrogen bonding. This is reflected in a small peak ($\delta = +61.8$ ppm) in the spectrum (Fig. 2b). This effect has been described previously by Bayer *et al.* [25] for the adsorption of methanol during surface modification with methoxysilanes. The signal corresponding to the alkylsilyl part of bonded ligands for all three packings is localized between $\delta = +10$ and $+40$ ppm [24,25].

Chromatographic properties

The chromatographic behaviour of the prepared packings was evaluated with two chemically different classes of substances, alkylbenzenes and anilines. In Fig. 3, the relationship between the logarithm of the capacity factors (k') and the number of methylene groups in the alkyl chain (n_c) of alkylbenzene homologues is shown. The similarity of the plots indicates that the hydrophobic properties of the ${}^M PB$ and ${}^M C_{18}$ phases (packings 3 and 5, Table II) are almost identical (Fig. 3). However, the difference in the slopes of the lines for ${}^M C_{18}$ and ${}^M PB$ packings may be caused by stronger interactions between C_{18} chains and chains originating from alkylbenzenes.

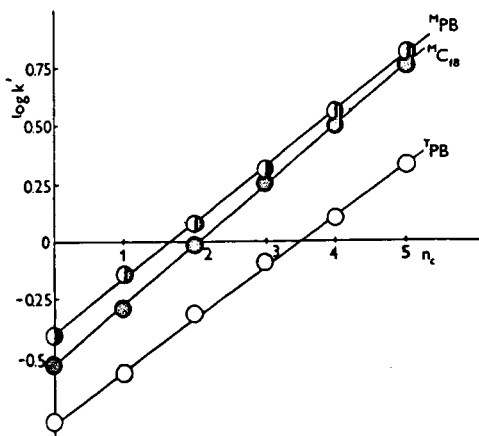


Fig. 3. Dependence of $\log k'$ on the number of methylene groups (n_c) in the homologous series of alkylbenzenes (benzene, toluene, ethylbenzene, propylbenzene and butylbenzene) for packings ${}^M PB$, $T^M PB$ and ${}^M C_{18}$ (see Table II).

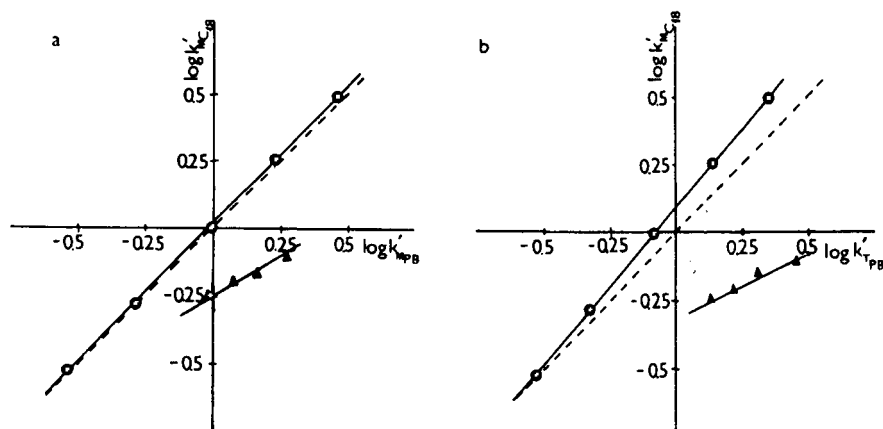


Fig. 4. Relationships between (a) $\log k'$ for $^{\text{M}}\text{C}_{18}$ and $\log k'$ for $^{\text{M}}\text{PB}$ and (b) $\log k'$ for $^{\text{M}}\text{C}_{18}$ and $\log k'$ for $^{\text{T}}\text{PB}$ phases for (●) alkylbenzenes (see Fig. 3) and (▲) anilines (aniline, methylaniline, dimethylaniline and diethylaniline).

This effect appears particularly with an increase in the alkyl chain length in the solute molecule (n_c values). The weaker hydrophobic interactions observed with the $^{\text{M}}\text{PB}$ phase are probably caused by a strong charge localized in the peptide group. This conclusion was also confirmed by the plot obtained for the $^{\text{T}}\text{PB}$ phase (packing No. 4; Fig. 3), which was also a straight line with a slope similar to that of the $^{\text{M}}\text{PB}$ packing. The vertical displacement of the plot of the $^{\text{T}}\text{PB}$ phase in relation to the $^{\text{M}}\text{PB}$ phase can be attributed to the lower coverage density of the net polymer structure of CBP on the silica gel surface. This influences the degree of shielding of the residual silanol groups, which also participate in the RP-HPLC elution process. This effect is clearly seen in Fig. 4, where $\log k'$ of the test substances on one phase is plotted against the corresponding $\log k'$ values on a reference phase ($^{\text{M}}\text{C}_{18}$).

According to hydrophobic theory [1–5,16,17], when using the $\log k' - \log k'$ relationship for comparison of two packings with similar surface properties compensation of the interactions between the separated solutes the mobile phase and the surface of the material packing should be expected. In this connection, the slopes of the straight line plotted for both packings should be equal to unity (dashed lines in Fig. 4a and b). Different effects taking place during RP-HPLC elution in chromatographic columns cause the deviations of real straight lines from the theoretical lines.

Considering the $\log k' vs. \log k'$ relationship for both monofunctional phases (packings 3 and 5; Fig. 4a), it can be stated that the experimental result of this relationship for alkylbenzenes is virtually identical with the theoretical assumption. Small differences in the slopes of straight lines may result from different α_{RP} values (Table II). In both instances the hydrophobic character of the packings can be observed (chain–chain interactions). An effect of the peptide group on the elution of aniline is also observed. However, the residual silanol groups can also participate in the elution mechanism. This effect manifests itself in the correlation of $\log k' vs. \log k'$ for $^{\text{T}}\text{PB}$ and C_{18} phases (Fig. 4b). In this instance the slopes of the straight lines for both test mixtures (alkylbenzenes and anilines) were significantly greater, as shown by the

deviations from unity. The differences in α_{RP} values were also higher (Table II). Moreover, the silanophobic interactions also influence this effect [1-6,9,16,17]. As a consequence, for the ^TPB packing, greater mobility of the bonded chains can be expected owing to the nitrogen atom (in the peptide group) which has a strong tendency for interaction [26-28]. Hence the influence of these effects is better represented as in Fig. 5.

On the basis of Fig. 5, a comparison of both phases containing the peptide group and a different undersurface structure of CBP was made. The linear dependences of alkylbenzenes and anilines indicate that (i) the hydrophobic interactions are preferentially found for the packings with a monofunctional structure of PB, (ii) the influence of silanols is more significant for packings obtained using a trifunctional silane, (iii) the straight line shift for alkylbenzenes is due to differences in α_{RP} values and (iv) the peptide group does not play an important role in the retention mechanism of non-polar solutes as is the case with polar solutes.

The comparison of the separation of the mixture of basic substances ($pK_a = 8.98-11.74$) presented in Fig. 6 is interesting especially from the viewpoint of selectivity. Daldrup and Kardel [29] proposed three of these four substances (peaks 1, 3 and 4) as sensitive indicators of the quality of test packings. We added melperone [4'-fluoro-4-(4-methylpiperidino)butyrophenone, $pK_a = 9.2$] to the test mixture. In Table III the most important retention parameters (k' and $\alpha_{i,j}$) and asymmetry factors (f_{As}) are listed.

On comparing the chromatograms in Fig. 6a-c, it can be seen that the separation of all four substances was only been obtained on the packings containing the peptide group. In both instances the peaks are symmetrical and sharp and the retention time is relatively short (Table III). However, improved resolution and separation selectivities between peaks 1 and 2 and between 3 and 4 were obtained on the packing with a monofunctional structure of the PB phase. Although the retention time was about half of that for a conventional C_{18} HPLC packing (Fig. 6c), peaks 1 and 2 could not be resolved (Table III). The C_{18} phase also has a tendency to produce tailing, particularly

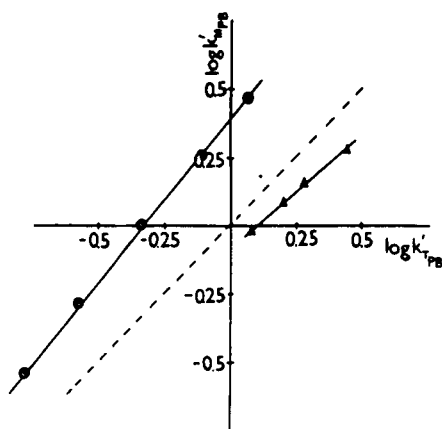


Fig. 5. Relationship between $\log k'$ for ^MPB and $\log k'$ for ^TPB phases obtained by injection of alkylbenzenes and anilines (abbreviations as in Fig. 4).

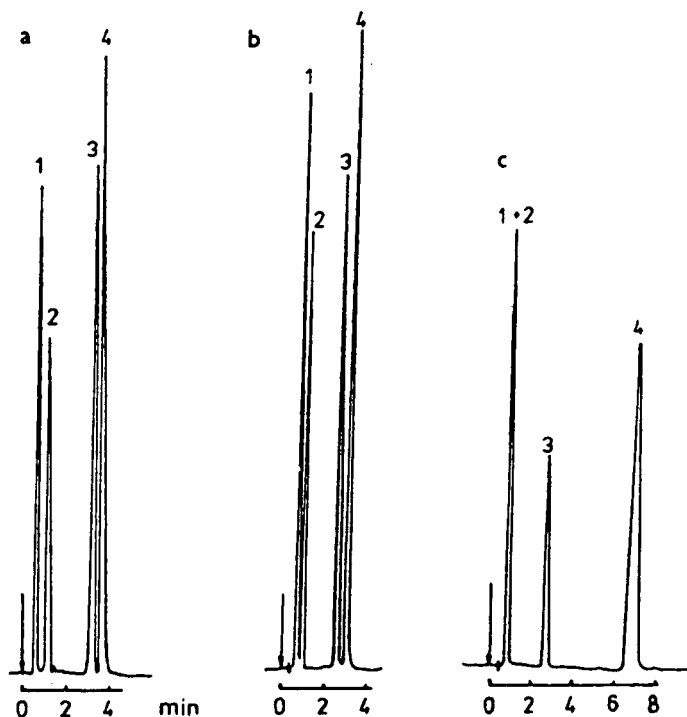


Fig. 6. Chromatograms of the test mixture obtained on columns packed with (a) ^MPB phase, (b) ^TPB phase and (c) ^MC₁₈ phase. Peaks: 1 = DPHA; 2 = MELP; 3 = MPPH; 4 = DZPM. For abbreviations and separation conditions, see Table III.

TABLE III

COMPARISON OF k' , α_{ij} AND f_{As} VALUES FOR TEST MIXTURE OF SUBSTANCES WITH BASIC CHARACTER, OBTAINED ON COLUMNS 1, 4 AND 5

Mobile phase: 156 ml acetonitrile + 340 ml phosphate buffer, pH 2.3 (6.66 g of KH_2PO_4 + 4.8 g of 85% H_3PO_4 in 1 l of water for HPLC). DPHA = diphenylhydramine hydrochloride; MLPN = melperone; MPPH = 5-(*p*-methylphenyl)-5-phenylhydantoin; DZPM = diazepam.

No. of peak	Compound	No. of column								
		3			4			5		
		k'	α_{ij}	f_{As}	k'	α_{ij}	f_{As}	k'	α_{ij}	f_{As}
1	DPHA	0.61		1.09	0.74		1.25	0.78		1.20
2	MLPN	1.22		1.10	1.15		1.25	—		—
			6.05			2.84			6.14	
3	MPPH	7.20		1.12	3.27		1.30	4.73		1.35
4	DZPM		1.16			1.24			2.91	
		8.60		1.13	4.05		1.50	13.75		1.50

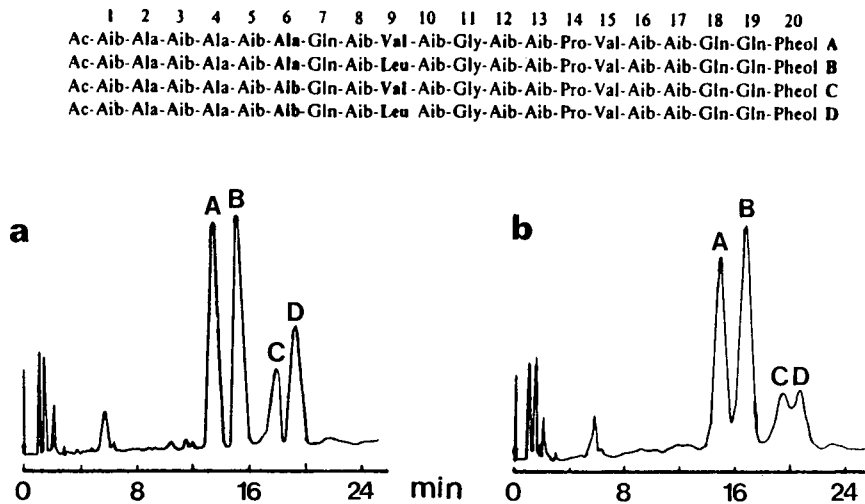


Fig. 7. Amino acid sequence of four peptides of paracelsine (A–D) and RP-HPLC separations of this protein obtained on columns packed with (a) $M^{18}PB$ and (b) $M^{18}C_{18}$ phases. Separation conditions: column, 125×4.6 mm I.D.; mobile phase, acetonitrile–methanol–water (34:33:33, v/v/v); flow-rate, 1 ml/min; detection, UV at 206 nm.

for peak 4 (diazepam, Fig. 6c). This can be seen in Table III, where the capacity factors increase with increasing pK_a values. The smallest f_{As} values (1.09–1.13) are found on the packing with a monofunctional PB phase.

HPLC applications

The hydrophobic properties and the specific selectivity of the packings with $M^{18}PB$ phase toward basic substances may be utilized to advantage in the separation of four peptides contained in the protein mixture paracelsine [30]. This natural product, which is particularly important for haemolysis of erythrocytes, contains four peptides with slightly different primary structures of the amino acids in positions 6 and 9 (see Fig. 7). All chiral components of paracelsine (A–D) are of L configuration. In Fig. 7 the chromatograms obtained from the RP-HPLC separation of this substance with (a) $M^{18}PB$ and (b) C_{18} phases (packings 3 and 5, Table II) are shown.

This improved selectivity of the $M^{18}PB$ phase toward this class of substances is apparent, full resolution of peptide pairs A, B, C and D being obtained. In spite of the higher α_{RP} values, the C_{18} phase (Table II) does not allow optimum resolution of the peptides, although the retention times are similar for both phases. This is probably due to specific interactions between the separated proteins and hydrophobic alkylsilyl ligands containing peptide groups.

CONCLUSIONS

The chemical modification of the LiChrospher Select B surface using $M^{18}NH_2$ silane yielded a higher coverage density (about 20%) than modifying it with $T^{18}NH_2$ silane. This difference in the coverage density was found to be independent of the PB

structures and of the structure of CBP resulting from the first modifying stage with 3-aminopropyl silanes.

CP-MAS NMR investigations not only confirmed the elemental analysis but also gave information about the structure of the CBP formed and detailed insight into the contributions of the different silanol groups (Q_2 , Q_3 and Q_4) before and after chemical modification.

RP-HPLC measurements indicated that the hydrophobic interactions between the packing surfaces, solute and mobile phase are preferentially found for packings with a dense film of the monomeric structure of CBP and therefore the mass transfer of the separated substances is better.

For the separation of polar substances (particularly with a basic character), better selectivity and resolution were found for packings involving the peptide group than for conventional C_{18} packings. In addition, the material containing a PB group was successfully applied to the separation of peptides and proteins.

ACKNOWLEDGEMENTS

B.B. is grateful to the Alexander von Humboldt Foundation for a grant.

REFERENCES

- 1 Cs. Horváth, *LC Mag.*, 1 (1983) 552.
- 2 R. K. Gilpin and A. Squires, *J. Chromatogr. Sci.*, 19 (1981) 195.
- 3 K. G. Wahlund and A. Sokolowski, *J. Chromatogr.*, 151 (1978) 299.
- 4 B. A. Person and B. L. Karger, in H. Engelhardt (Editor), *Practice of High Performance Liquid Chromatography*, Springer, Heidelberg, 1986, pp. 201–214.
- 5 B. Buszewski, Z. Suprynowicz, P. Staszczuk, K. Albert, B. Pfeleiderer and E. Bayer, *J. Chromatogr.*, 449 (1990) 305.
- 6 L. Sander and S. A. Wise, *LC·GC Int.*, 3 No. 6 (1990) 24.
- 7 R. E. Majors, *J. Chromatogr. Sci.*, 18 (1980) 489.
- 8 R. E. Majors, *LC·GC Int.*, 3, No. 4 (1990) 12.
- 9 L. Sander and S. A. Wise, *CRC Crit. Rev. Anal. Chem.*, 18 (1987) 299.
- 10 B. Buszewski, *Chem. Stosow.*, 32 (1988) 203.
- 11 L. Nondek, *J. Chromatogr.*, 373 (1986) 61.
- 12 A. M. Krstulović (Editor), *Chiral Separations by HPLC*, Ellis Horwood, Chichester, 1989, Ch. III, pp. 175–537.
- 13 W. Szczepaniak, J. Nawrocki and W. Wasiak, *Chromatographia*, 12 (1979) 484 and 559.
- 14 C. Pidgeon and U. V. Venkataram, *Anal. Biochem.*, 176 (1989) 36.
- 15 K. A. Dill, J. Naghizadeh and A. Marqusee, *Annu. Rev. Phys. Chem.*, 39 (1988) 234.
- 16 J. G. Dorsey and K. A. Dill, *Chem. Rev.*, 89 (1989) 331.
- 17 R. Kaliszan, in P. R. Brown and R. A. Hartwick (Editors), *High Performance Liquid Chromatography*, Wiley, New York, 1989, Ch. 14, pp. 563–600.
- 18 L. Nondek and V. Vyskočil, *J. Chromatogr.*, 206 (1981) 581.
- 19 B. Buszewski, *Ph.D. Thesis*, Slovak Technical University, Bratislava, 1986.
- 20 E. Ott, *Org. Synth.*, Coll. Vol. II (1943) 528.
- 21 B. Buszewski, A. Jurášek, J. Garaj, L. Nondek, I. Novák and D. Berek, *J. Liq. Chromatogr.*, 10 (1987) 2325.
- 22 B. Buszewski, D. Berek, I. Novák and J. Garaj, *Chem. Listy*, 81 (1987) 552.
- 23 B. Buszewski, *Chromatographia*, 29 (1990) 233.
- 24 K. Albert, B. Pfeleiderer and E. Bayer, in D. E. Leyden and W. T. Collins (Editors), *Modified Surfaces in Science and Industry*, Gordon and Breach, New York, 1988, pp. 287–303.
- 25 E. Bayer, K. Albert, J. Reiners, M. Nieder and D. Müller, *J. Chromatogr.*, 264 (1983) 197.

- 26 M. G. Voronkov, V. P. Miliyeshkiewich and Y. A. Juzeliewskij, *Sililoksanovaja Swjaz*, Nauka, Novosibirsk, 1976.
- 27 K. Albert, B. Buszewski, J. Schmid and E. Bayer, in preparation.
- 28 W. H. Pirkle, D. W. Hause and J. M. Finn, *J. Chromatogr.*, 192 (1980) 339.
- 29 T. Daldrup and B. Kardel, *Chromatographia*, 18 (1984) 81.
- 30 B. Pfleiderer, K. Albert, K. D. Lork, K. K. Unger, H. Brückner and E. Bayer, *Angew. Chem. Int. Ed. Engl.*, 28 (1989) 327.

CHROMSYMP. 2080

Possible role for stationary phase metal interactions in the chromatography of hydroxyamines on silica

BRIAN LAW* and PAN F. CHAN

Drug Kinetics Group, ICI Pharmaceuticals Plc, Safety of Medicines Department, Mereside, Alderley Park, Macclesfield SK10 4TG (U.K.)

ABSTRACT

Problems associated with the non-elution or peak tailing of dihydroxyamines on silica with methanol–aqueous buffer mobile phases have been investigated. The problem is confined to molecules where the hydroxy groups are phenolic in nature and ortho to one another. Study of a controlled set of compounds shows that non-elution/elution with poor peak shape is a function of the distance between the dihydroxy and amine moieties. In terms of the stationary phase, the problem appears to be related to the metal content of the silica. Demineralisation of the silica by acid washing was ineffective, however, flushing the column with EDTA resulted in elution of all dihydroxyamines with improved peak shape.

INTRODUCTION

The chromatography of basic compounds on silica with buffered aqueous methanol eluents is usually associated with good efficiency and peak symmetry [1,2]. In a previous study [3] investigating the chromatographic characteristics of phenethylamine analogues, problems were encountered with certain compounds which gave asymmetric peaks (*e.g.*, adrenaline) or failed to elute (*e.g.*, noradrenaline). With a single exception these compounds possessed an *ortho* dihydroxy function in the aromatic ring. Such compounds are important biochemically, *e.g.*, catechol amines, and as drug metabolites.

The purpose of this present work was the elucidation of the mechanism of the secondary interaction responsible for the non-elution or poor symmetry. In so doing, it was hoped that the poor chromatographic characteristics of these compounds could be improved, thus further extending the applicability of this approach in drug analysis.

EXPERIMENTAL

Chromatography was carried out using a Water 6000A high-performance liquid chromatography (HPLC) pump which was used to deliver eluent at 1 ml/min to various columns (see below). Injections were made with a Rheodyne 7125 injection valve fitted with a 20- μ l sample loop. Detection was carried out at 254 nm using an LDC III fixed-wavelength (254 nm) detector.

The eluent consisted of methanol–aqueous ammonium acetate buffer (9:1, v/v), pH 9.1, prepared as previously described [2]. This was also used with the addition of pentane-2,4-dione (Aldrich) (1% v/v) or ethylenediaminetetraacetic acid (EDTA, BDH) (2 to 10 mM).

Test compounds were obtained from a variety of commercial sources or from the ICI chemical collection. These were prepared in methanol at *ca.* 2 mg/ml, and 1–5 μ l injected. The dead volume was determined with diphenylamine.

Columns were stainless-steel, 100 \times 4.6 mm I.D., slurry packed in-house with different batches of Spherisorb S5W silica (5 μ m). Similar columns, packed with Kromasil (100 A-SIL) 5- μ m silica and YMC (A-001, 120A) 5- μ m silica were obtained from Hichrom (Reading, U.K.). A glass-lined column (100 \times 3 mm I.D.) with metal free frits was packed by Scientific Glass Engineering.

RESULTS AND DISCUSSION

The origin of secondary interactions

Initially, a wide range of non-phenethylamine compound types were examined. These compounds which possess significant structural dissimilarity to the dopamine type compounds studied previously [3], are shown in Fig. 1. As well as containing an amine function, the compounds contained a mixture of alcoholic, phenolic and alkoxy functions *ortho* to one another in a ring system.

Of this group, only one compound, 3,4-dihydroxyphenylpropylamine (A) was not eluted and a further two, apomorphine (C) and 3,4-dihydroxytamoxifen (D) were eluted with poor peak shape, asymmetry ($A_s > 8$). The remainder were eluted with high efficiency and good peak symmetry ($A_s < 1.2$). From these data, it would appear that elution problems only occur when the two oxygen atoms are phenolic in nature. The presence of *ortho*-dialcohols, *ortho*-dialkoxy or mixed *ortho*-phenolic alkoxy compounds, had no deleterious effect on chromatographic performance.

ortho-Diphenols are well known metal chelators [4], and these results suggest some form of secondary interaction with metals in the chromatographic system.

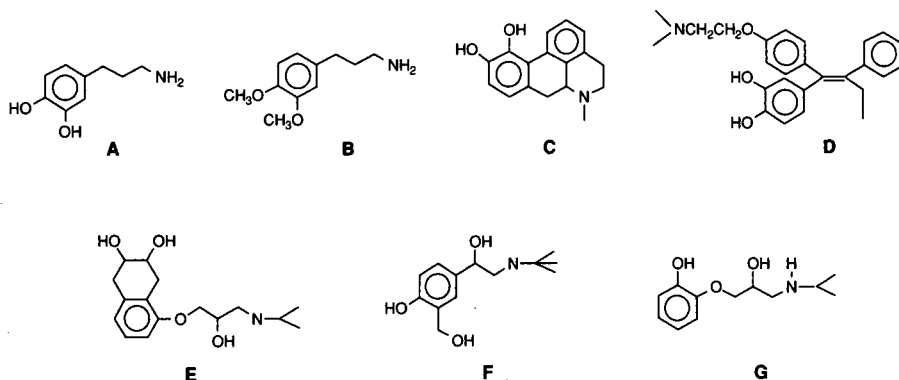


Fig. 1. Structures of various solutes studied, A = 3,4-dihydroxyphenylpropylamine, B = 3,4-dimethoxyphenylpropylamine, C = apomorphine, D = 3,4-dihydroxytamoxifen, E = nadalol, F = salbutamol and G = ICI 46040.

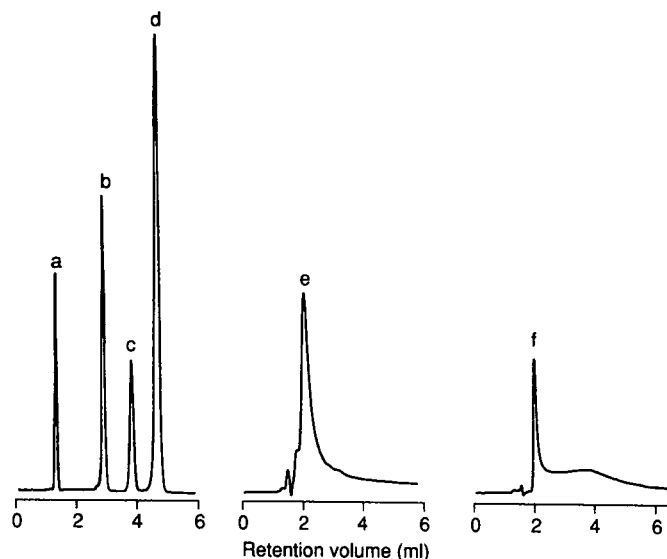


Fig. 2. Chromatograms showing simple alkylamines. a = Diphenylamine, b = benzylamine, c = phenethylamine, d = phenylpropylamine, e = ICI 83378 and f = 6-hydroxydopamine.

However, they do not explain the reason why some compounds elute easily, albeit with poor peak shape (*e.g.*, apomorphine), but other compounds (*e.g.*, 3,4-dihydroxyphenylpropylamine) do not elute at all.

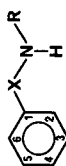
To address this problem, further analysis was carried out using a more controlled set of test compounds, where the length of the amine side chain and the number and position of the ring hydroxyls was systematically varied. The structure and retention characteristics of these compounds are shown in Table I and some typical chromatograms for simple solutes and ring hydroxylated amines which exhibit poor peak shape are shown in Fig. 2.

As expected, the compounds with the *ortho* ring hydroxyls failed to elute, or eluted with poor symmetry. The compound with the tailing peak also showed variable retention, k' increasing with decreasing mass injected and also a non-linear peak height response with mass injected. These phenomena, which were also observed with the compounds mentioned earlier, are common where more than one retention mechanism operates.

Analysis of this data indicated that the compounds which failed to elute completely (**2**, **5**, **6**, **9** and **12**) could be distinguished through having a small chain (three atoms or less) between the phenyl ring and the amino function. The only 3,4-dihydroxy compound which did elute, although with poor peak shape, was compound **14** which had a longer side chain with four atoms between the ring and the amine function. It is unlikely that the N-isopropyl or the side chain hydroxyl functions in this compound played any role, as both these groups were present in compound **9**, and the N-isopropyl group was also present in compound **6**, both of which did not elute. It would appear therefore that it is the close proximity of the amine and dihydroxy function which is responsible for the non-elution of compounds **2**, **5**, **6**, **9** and **12**, as well those such as adrenaline in the previous study [3].

TABLE I
STRUCTURES AND RETENTION DATA FOR VARIOUS RING SUBSTITUTED PHENYLALKYLAMINES

Column: 100 × 4.6 mm I.D. Spherisorb S5W silica batch F5387; eluent: methanol–ammonium acetate buffer (9:1).



No.	Compound	k' ^a	3	4	5	6	X	R
1	Benzylamine	0.96	H	H	H	H	CH ₂	H
2	3,4-Dihydroxybenzylamine	NE ^b	OH	OH	H	H	CH ₂	H
3	Phenethylamine	1.61	H	H	H	H	CH ₂ CH ₂	H
4	4-Hydroxyphenethylamine (tyramine)	1.74	H	OH	H	H	CH ₂ CH ₂	H
5	3,4-Dihydroxyphenethylamine (dopamine)	NE	OH	OH	H	H	CH ₂ CH ₂	H
6	3,4-Dihydroxynorephedrine	NE	OH	OH	H	H	CH(OH)CH(CH ₃)	H
7	5-Hydroxydopamine	3.9 ^c	OH	OH	OH	H	CH ₂ CH ₂	H
8	6-Hydroxydopamine	1.4 ^c	OH	OH	H	OH	CH ₂ CH ₂	H
9	ICI 46399	NE	OH	OH	H	H	CH(OH) CH ₂	CH(CH ₃) ₂
10	Phenylpropylamine	2.19	H	H	H	H	CH ₂ CH ₂ CH ₂	H
11	3,4-Dimethoxyphenylpropylamine	3.52	OCH ₃	OCH ₃	H	H	CH ₂ CH ₂ CH ₂	H
12	3,4-Dihydroxyphenylpropylamine	NE	OH	OH	H	H	CH ₂ CH ₂ CH ₂	H
13	ICI 45849	0.91	H	H	H	H	OCH ₂ CH(OH)CH ₂	CH(CH ₃) ₂
14	ICI 83378	0.42 ^d	OH	OH	H	H	OCH ₂ CH(OH)CH ₂	CH(CH ₃) ₂
15	ICI 101812	0.84	OH	H	OH	H	OCH ₂ CH(OH)CH ₂	CH(CH ₃) ₂

^a k' = Capacity factor.

^b NE = not eluted.

^c Approximate value due to poorly defined tailing peak.

^d Poor peak shape.

It is possible to rationalise these data through postulation of a two-point interaction between the dihydroxyamine and the silica surface. Given that ion-exchange is the major mechanism of retention [5], then the ionised amine function will undergo a charge-charge interaction with the ionised silanol groups on the silica surface. The distance between the amine and the ring hydroxyls then controls the degree of the secondary interaction. When the side chain is short (≤ 3 atoms) it can be envisaged that the dihydroxy group is brought into close proximity to the silica surface leading to a relatively strong secondary interaction and hence infinite retention. When the side chain is long, however (> 3 atoms), the ring hydroxyls are less likely to come into close contact with the surface. In these latter circumstances, the strength of the secondary interaction is reduced and manifested only in poor peak symmetry.

This discrimination between compounds which failed to elute and those which eluted asymmetrically would also explain the characteristics of apomorphine and 3,4-dihydroxytamoxifen discussed earlier, where the rigid structure results in a greater distance between the amine and dihydroxy group than that seen in the simpler compounds.

It is also interesting to note (Table I), the influence of the addition of a third ring hydroxyl. Thus, 5- and 6-hydroxydopamine (trihydroxyphenethylamines) both eluted but gave very distorted peaks, whereas dopamine (3,4-dihydroxyphenethylamine) failed to elute. It would appear, therefore, that the presence of an additional third phenolic hydroxyl can turn a non-eluting compound into one which elutes, albeit with poor peak shape. Since the phenolic groups are acidic, the addition of a third such group to the molecule will increase the overall negative charge of the molecule in the alkaline eluent (pH 9.1). This will therefore increase the electrostatic repulsion between the hydroxy amine and the ionised silanols resulting in shortened retention compared with the dihydroxy compound.

In an attempt to rationalise the elution/non-elution characteristics of the compounds studied, the Functional Group Contribution (FGC) approach was applied. In a previous study [5], using a similar HPLC system, it was shown that retention increments for various substituents (N-alkylation, ring hydroxylation, etc.) on phenylalkylamines are additive. In the same study, the non-basic solute phenol was also shown to have minimal retention ($k' \approx 0.02$). In order to account for the non-elution of the short chain dihydroxyamines, it would be predicted, on the basis of the additivity rules, that catechol (1,2-dihydroxybenzene) despite its non-basisity would have significant retention in this cation-exchange system.

Catechol and other simple hydroxybenzenes were analysed and the results are shown in Table II. As expected, most of the compounds had relatively short retention eluting at or near the void volume. Catechol and pyrogallol, however, the two compounds having *ortho*-dihydroxy groups, showed somewhat greater retention and poor peak shape, with asymmetry values of around 7.

Although catechol has only slightly greater retention than phenol, the effect of the second hydroxyl group is very significant when considered in FGC terms. The FGC value (τ) for the second hydroxyl group is defined as:

$$\tau = \log \left(\frac{k'_s}{k'_p} \right)$$

TABLE II
RETENTION CHARACTERISTICS FOR HYDROXYBENZENE DERIVATIVES

Column: 100 × 4.6 mm I.D. Spherisorb S5W silica batch F5387; eluent: methanol–ammonium acetate buffer (9:1).

Compound	k'	Peak symmetry
Phenol	0.00	good
Catechol (1,2-dihydroxybenzene)	0.11 ^a	poor
Resorcinol (1,3-dihydroxybenzene)	0.00	good
Pyrogallol (1,2,3-trihydroxybenzene)	0.75 ^a	poor
Phlorglucinol (1,3,5-trihydroxybenzene)	0.00	good

^a Approximate value.

where k'_s and k'_p refer to the capacity factors for the substituted and parent compounds, respectively, catechol and phenol in this instance. As k' for phenol is zero, the τ value for a second *ortho*-hydroxyl is infinite. Thus, the FGC approach explains the observed effect in that addition of a second hydroxyl to a monohydroxy compound (*e.g.*, tyramine) would increase retention from k' 1.74 (Table I) to infinity as observed for dopamine.

The results for pyrogallol and phlorglucinol, the two trihydroxybenzenes, however, cannot be rationalised in the same manner.

Elimination of secondary interactions

Trace metal impurities in silica are believed to be the cause of problems in the chromatography of a number of substance such as hop acids [6], and they are apparently the cause of the problem in the case of the catecholamines studied here. Metals in silica can exert their influence either directly, or indirectly through their effects on silanols, which can be made highly acidic and hence very reactive [7]. In the case of the catecholamines a direct interaction is more likely suggesting that the offending metals are situated on the silica surface and hence easily removed.

Various treatment processes have been proposed for the removal of trace impurities, such as acid washing [8,9] or washing with specific metal complexing agents

TABLE III
METAL CONTENT OF SILICA BATCHES USED IN THIS STUDY

All samples Spherisorb S5W from Phase Separations. Results obtained following digestion in HF and analysis by inductively coupled plasma atomic emission spectroscopy.

Batch No.	Element concentration (ppm)							
	Fe	Al	Ca	Ti	Zr	Na	K	Mg
F5387	551	304	117	283	104	6008	<25	37
5068	175	241	57	88	25	5880	<25	30
Acid washed	65	176	23	44	11	318	<25	<10

[6,10]. Initially we investigated acid washing which has been previously shown to reduce the metal content of silica significantly. An acid-washed silica with relatively low metal content (Table III) was obtained from Phase Separations. This material was packed into a glass lined column complete with metal free frits. To further minimise possible interactions with metals other than those in the column, as observed by Trumbore *et al.* [11], PTFE tubing was used for the injection loop, column to valve and column to detector connections. Analysis using this "metal free" system failed to give any improvement in the chromatography of the dihydroxy compounds. These results confirm the view that the offending metals are present in the silica and not in the column tubing or frits as indicated previously [11], and that acid washing, at least in this instance, is ineffective.

An interesting solution to the problem of metal interactions applied by Roberts *et al.* [12], involved inclusion of the analyte or an analyte analogue in the mobile phase to block the active metal sites. It was not possible to use this approach in the present study due to the unstable nature of catechol compounds which undergo rapid oxidation in the basic eluent (pH 9.1). An alternative approach involving EDTA, a well known metal-complexing agent which has also been used very effectively in the demineralisation of silica [10] was evaluated. This compound (in the free acid form) was introduced into the eluent up to a concentration of 10 mM, and 500 ml passed through a column packed with the acid-washed material. The column was tested before, and after washing with the EDTA. The post-wash test was carried out with EDTA in the eluent. The test compounds were those listed in Tables I and II. In this instance there was a dramatic effect, with EDTA washing resulting in an improvement

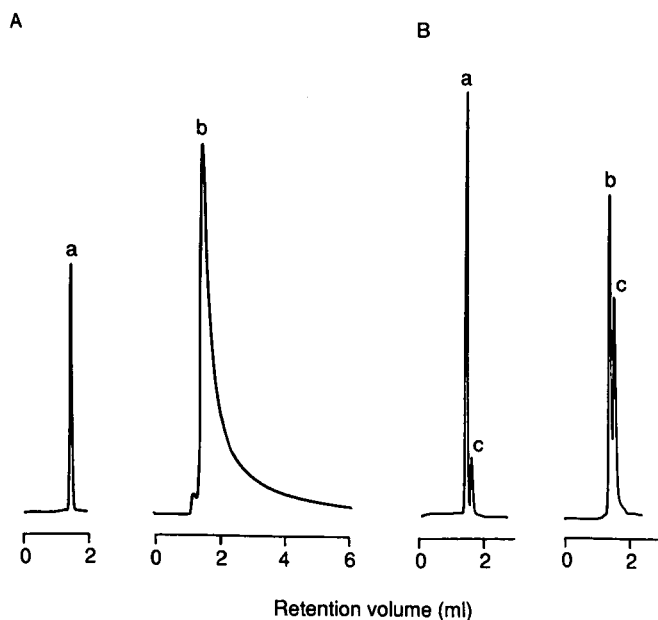


Fig. 3. Chromatograms showing a = phenol, and b = catechol chromatographed on silica (batch F5387) (A) before and (B) after washing with EDTA. Peak c is a system peak due to the inclusion of EDTA in the eluent.

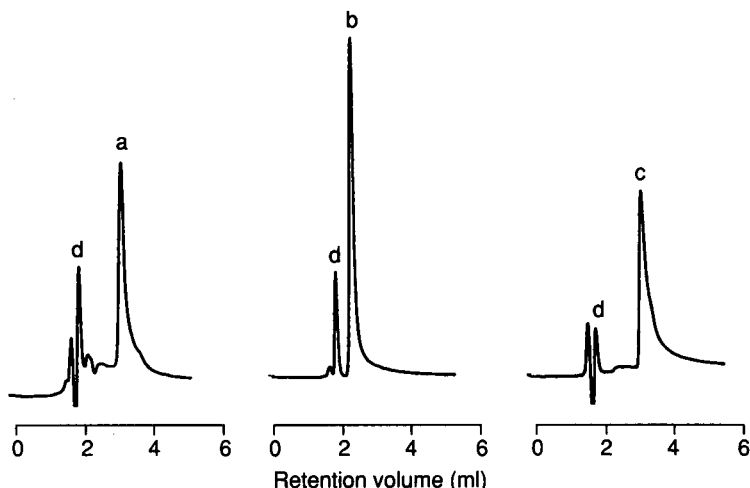


Fig. 4. Chromatograms showing a = ICI 83378, b = 6-hydroxydopamine and c = 3,4-dihydroxybenzylamine on silica (batch F5378) after washing with EDTA. Peak d is a system peak due to the presence of EDTA in the eluent.

in peak shape (Figs. 3 and 4) and elution of all the dihydroxy compounds but with poor symmetry. One side effect of chromatographing with EDTA in the eluent was the reduction in the retention of all the compounds eluted. This reduction increased with k' ranging from 5% for benzylamine (k' ca. 0.9) to 56% for 5-hydroxydopamine (k' ca. 3.9).

Removal of EDTA from the eluent not only corrected the decrease in retention but the dihydroxy compounds were still eluted or gave the improved peak symmetry seen with EDTA in the eluent.

EDTA is a charged polar species and its observed effect may have been due to factors other than washing of metals from the stationary phase, *i.e.*, ion-pairing with the protonated amine or modification of the silica surface. A second less polar metal chelating agent, namely pentane-2,4-dione used at a concentration of 1% was therefore evaluated. However, because of its high UV absorbance, its effect could only be evaluated after washing of the column unlike EDTA which was actually included in the eluent during chromatography. On a mol-per-mass basis the dione seemed much less efficient in demineralisation of the silica. Typically, chromatographic performance was improved by passing approximately 6 mmol of EDTA or 60 mmol pentane-2,4-dione/1.5 g silica through the column. As expected, there appeared to be a relationship between the total metal content and the mass of chelating agent producing an effect. On the acid-washed silica (Table III), elution of the hydroxyamines such as 3,4-dihydroxybenzylamine was brought about with a total wash of only 1.1 mmol EDTA/1.5 g silica. The more heavily metal loaded silica, *i.e.*, batch F5387 required considerably more EDTA, typically 6 mmol EDTA/1.5 g silica.

It is unclear which of the metal impurities in the silica are responsible for the tailing or non-elution of these dihydroxyamines. Verzele *et al.* [8], determined 19 metals in silica in the ppm range, although it is unlikely that all of these are capable of forming organic complexes. Of those that do, Al and Fe figure highly as impurities in

many chromatographic silicas, and both are capable of forming complexes with EDTA, diketones and *ortho*-diphenols [4].

To further understand this problem, two silicas from different manufacturers were examined; these were Kromasil and YMC silica. The Kromasil silica is claimed to have typical levels of Al and Fe of 20 ppm. The data for YMC silica indicates Al levels to range from 16.8 to 5.4 ppm and Fe levels 18 to 0.5 ppm (data from five batches).

Both Kromasil and YMC silica showed similar selectivity and retention properties to the Spherisorb material, although both columns without any pretreatment eluted all the dihydroxyamines mentioned previously. The YMC column, however, with the lowest metal content, showed peak shape and symmetry comparable to the Spherisorb silica after EDTA washing.

Differentiating between the effects of Al and Fe is difficult since most silicas contain similar quantities (within a factor of 2) of these two elements. Furthermore, acid or EDTA washing appears effective at removing them to the same degree (Table III and refs. 9 and 10).

CONCLUSIONS

These data show that the non-elution or poor peak shape seen with aromatic dihydroxyamines on silica is due to an interaction of the diphenol and metal atoms in the silica matrix. The distance between the amine function and the diphenol appears to control the chromatographic characteristics. A short distance gives non-elution, whilst a large distance results in elution with poor peak shape.

In terms of the stationary phase, the problem appears to be related to the metal content of the silica. Acid washing of the silica although reducing the metal content, was ineffective in improving chromatographic performance. Washing the column with specific metal-chelating agents, *i.e.*, EDTA or pentane-2,4-dione, especially the former, was very effective.

It is unclear which of the metals are causing the secondary interaction, although Al and Fe with their well-known chelation properties, are the likely candidates. From the data generated here, it would appear that chromatographic silicas need to be very pure with much less than 20 ppm of the aforementioned elements in order to give good chromatography with the catechol amines.

ACKNOWLEDGEMENTS

We wish to thank Peter Myers of Phase Separations for the gift of the acid-washed silica and the elemental analysis, and Jane Durham for expert typing.

REFERENCES

- 1 I. Jane, *J. Chromatogr.*, 111 (1975) 227.
- 2 B. Law, *Trends Anal. Chem.*, 9 (1990) 31.
- 3 B. Law, R. Gill and A. C. Moffat, *J. Chromatogr.*, 301 (1984) 165.
- 4 F. A. Cotton and G. Wilkinson, *Advanced Inorganic Chemistry*, Interscience Publishers, London, 3rd ed., 1972.
- 5 B. Law, *J. Chromatogr.*, 407 (1987) 1.
- 6 M. Verzele and C. Dewaele, *J. Chromatogr.*, 217 (1981) 399.

- 7 P. C. Sadek, C. J. Koester and L. D. Bowers, *J. Chromatogr. Sci.*, 25 (1987) 489.
- 8 M. Verzele, M. De Potter and J. Ghysels, *J. High Resolut. Chromatogr. Chromatogr. Commun.*, 2 (1979) 151.
- 9 J. Nawrocki, D. L. Moir and W. Szczepaniak, *Chromatographia*, 28 (1989) 143.
- 10 J. Kohler, D. B. Chase, R. D. Farlee, A. J. Vega and J. J. Kirkland, *J. Chromatogr.*, 352 (1986) 275.
- 11 C. N. Trumbore, R. D. Tremblay, J. T. Penrose, M. Mercer and F. M. Kelleher, *J. Chromatogr.*, 280 (1983) 43.
- 12 D. W. Roberts, R. J. Ruane and I. D. Wilson, *J. Chromatogr.*, 471 (1989) 437.

High-performance liquid chromatography of amino acids and dipeptides on new ion exchangers of the HEMA series

KAREL ŠTULÍK*, VĚRA PACÁKOVÁ and HEPING WANG^a

Department of Analytical Chemistry, Charles University, Albertov 2030, 128 40 Prague 2 (Czechoslovakia)

ABSTRACT

The separation of a number of essential amino acids and dipeptides was studied in ion-exchange systems based on poly(hydroxyethyl methacrylate) stationary phases modified with various ionizing groups (carboxymethyl, a weak cation exchanger; sulphobutyl, a strong cation exchanger; diethylaminoethyl, a weak anion exchanger) and on an ethylene dimethacrylate-based hydrophobic column. The ion-exchange materials also exhibited hydrophobic properties, caused by the poly(hydroxyethyl methacrylate) matrix. The dependence of the capacity factors on the mobile phase pH, the ionic strength, the type and concentration of the displacer salt and the content of the organic modifier (methanol) was investigated. The best separations of amino acids and dipeptides, with baseline resolution for many test compounds, was attained with cation exchangers, HEMA Bio 1000 CM and SB. The analytes were detected either by measurement of the absorbance at 210 nm or amperometrically at a copper electrode, at a potential of +0.15 V (Ag/AgCl) (for separations at pH > 6).

INTRODUCTION

High-performance liquid chromatography (HPLC) has proved to be a highly efficient method for separation of amino acids and peptides [1,2]. A great variety of separation modes have been investigated, primarily reversed-phase, ion-exchange and size-exclusion systems, reversed-phase chromatography being the most common. It has been shown [3] that C₈ columns are more efficient than C₁₈ columns for the separation of peptides. Ion-exchange columns have the advantages of large loading capacities and high resolving power [4,5], but long-chain peptides are difficult to separate because they are strongly bound to the stationary phase matrix [6]. Size-exclusion separations are applicable to peptides in a wide molecular-weight range of *ca.* 100–5 · 10⁶ dalton [7,8]; the analytes are often resolved better than in reversed-phase systems, but their behaviour is far from the theoretical assumptions [8], which complicates the prediction and optimization of the experimental conditions.

The retention of amino acids and especially peptides is primarily affected by the mobile phase pH because of the well known, complex acid–base properties of these

^a On leave from the Department of Chemistry, CISR Institute, Beijing, China.

compounds and because of the obvious effect of the pH in the ion-exchange systems. The ionic strength of the mobile phase and the content of an organic modifier exert a smaller effect through variation of the mobile phase polarity and solubility of the analytes. The type of displacer salt and its concentration affect the ion-exchange separations.

The reversed-phase mechanism is most complex. The retention of peptides usually increases with increasing pH (*e.g.* with peptide-bonded phases [9]): at low pH values, amino acids and peptides have a net positive charge owing to protonation of the amino groups, which suppresses the analyte solubility in the mobile phase but also decreases their affinity for the non-polar stationary phase. The presence of an organic modifier usually causes a decrease in the retention time [10], owing to improved solubility of the analytes in the mobile phase, but $\log k'$ (capacity factor) *versus* modifier content dependences exhibiting a minimum have also been reported [11].

Ion-pairing agents have been used extensively in reversed-phase separations and, for example, the retention of positively charged amino acids and peptides increased with increasing concentration of trifluoroacetate or phosphate used as ion-pairing agents [12–14]. It is also possible to predict the retention times for a particular ion-pairing agent [12]. The effect of the counter-ion depends on its hydrophobicity [12].

A number of authors [15–21] have derived empirical rules for prediction of the retention of peptides in reversed-phase systems. Retention coefficients have been defined to describe the effect of the individual amino acid residues [15]: it has been found that an individual set of the retention coefficients is necessary for each position of an amino acid within the peptide [22]. Reversed-phase separations are usually more efficient and faster than ion-exchange separations, except for hydrophilic amino acids and peptides that are not retained [23]. Non-ionic polyethylene alcohol surfactants can be used to control the retention of polypeptides in reversed-phase systems through variation of the mobile phase surface tension [24].

Amino acids and peptides are difficult to detect. Either the analytes are derivatized, or very low wavelengths must be used (200–220 nm) for UV photometry, except for the substances containing aromatic systems, which absorb around 280 nm. The terminal amino groups and aromatic systems can be electrochemically oxidized [25]. Detection based on chelate formation at a passivated copper electrode [13,14,26–28] is a very convenient, selective and sensitive technique for amino acids and short peptides.

The present paper deals with a critical comparison of separations of amino acids and peptides on a newly produced [28] series of ion exchangers, based on a poly-(hydroxyethyl methacrylate) matrix, modified with various ionizable groups and on an ethylene dimethacrylate hydrophobic column. The ion-exchange materials also exhibit hydrophobic and size-exclusion properties, so that there is a possibility of combination of the advantages of various separation modes, as briefly discussed in our previous paper [29].

EXPERIMENTAL

Apparatus

The liquid chromatograph used consisted of an LC-XPD pump and an LC-UV variable-wavelength detector (Pye-Unicam, Cambridge, U.K.), a Rheodyne 7125

injection valve with a 20- μ l loop (Rheodyne, Cotati, CA, U.S.A.), an ADLC 2 electrochemical detector with a tubular copper electrode [13], an aqueous saturated Ag/AgCl reference and a stainless-steel counter-electrode and a TZ 4620 chart recorder (Laboratorní Přístroje, Prague, Czechoslovakia), and the following stainless-steel columns: HEMA Bio 1000 CM, 7 μ m, 80 \times 8 mm I.D.; HEMA Bio 1000 SB, 10 μ m, 80 \times 8 mm I.D.; HEMA Bio 1000 DEAE, 10 μ m, 80 \times 8 mm I.D.; EDMA, 10 μ m, 80 \times 8 mm I.D. (all from Tessek, Prague, Czechoslovakia) and Partisil SCX, 10 μ m, 250 \times 4.6 mm I.D. (Pye Unicam).

The HEMA Bio 1000 columns are based on a hydrophilized hydroxyethyl methacrylate matrix and have an exclusion limit of 800 000–2 \cdot 10⁶ dalton. The CM column is a weak cation exchanger with the carboxymethyl ion-exchange group and an exchange capacity of 0.9–1.1 mequiv./g. The SB column is a strong cation exchanger containing the sulphobutyl groups and has an exchange capacity of 1.4–1.8 mequiv./g. The DEAE column is a weakly basic anion exchanger with the diethylaminoethyl group and a capacity of 1.2–1.5 mequiv./g. The EDMA column is hydrophobic, based on an ethylene dimethacrylate matrix. The unmodified HEMA materials exhibit weak hydrophobic interactions.

Chemicals

The standard substances of the amino acids and peptides studied (Gly, Ala, Val, Leu, Ile, Ser, Asp, Glu, Lys, Asn, Cys, Met, Phe, Tyr, His, Trp, Pro, Gly-NH₂, Gly-Gly, Glu-Ala, Gly-Val, Gly-Leu, Gly-Phe, Gly-Tyr, Gly-Asp, Gly-Glu, Gly-His, Gly-Asn and Leu-Gly) were of analytical-grade purity, supplied by Sigma (St. Louis, MO, U.S.A.). The substances were used as received. Stock solutions with a concentration of 0.1 mg/ml were obtained by dissolving the substances in a particular mobile phase and were stored in a refrigerator. The working solutions were prepared immediately prior to measurements by diluting the stock solutions with the mobile phase used.

The mobile phase consisted of an aqueous phosphate buffer (orthophosphoric acid–potassium dihydrogenphosphate) at various concentrations (from 0.001 to 0.020 *M*), at various pH values (from pH 3 to 7, adjusted by additions of orthophosphoric acid and potassium hydroxide solutions), containing varying amount of methanol (between 0 and 20%, v/v) and varying concentrations (from 0.02 to 0.2 *M*) of displacer salts (lithium chloride, sodium chloride, potassium chloride or magnesium chloride). When working with the EDMA column, trifluoroacetic acid was used at various concentrations (from 0.05 to 0.5%) instead of the phosphate buffer.

All the other chemicals used were analytical-reagent grade, obtained from Lachema (Brno, Czechoslovakia) and were not further purified.

Procedure

All the experiments were carried out at a mobile phase flow-rate of 0.5 ml/min and at room temperature (22 \pm 2°C). The mobile phases were deaerated by passage of helium. The UV photometric detection was carried out at 210 nm. The amperometric detection at a copper tubular electrode was performed at a potential of +0.15 V (Ag/AgCl, aqueous, saturated), after working electrode activation at –0.3 V (for details see refs. 13 and 27).

The retention data were expressed in terms of the capacity factors, $k' = (t_R - t_M)/t_M$, where t_R and t_M are the retention and dead times, respectively; the dead time was obtained as the solvent peak retention time.

RESULTS AND DISCUSSION

Separation of amino acids

Selected values of the capacity factors on the studied stationary phases are listed in Table I.

The dependence of the capacity factors on the pH (see Fig. 1 for the HEMA Bio 1000 CM column) is similar for the HEMA Bio 1000 CM and SB, *i.e.* the retention decreases with increasing pH. The retention of the amino acids containing negatively charged functional groups (*e.g.* Glu and Asp) is more influenced by the mobile phase pH. The zwitterions formed at higher pH values are generally less retained than the corresponding, positively charged, amino acids at low pH values. It is evident that the amino acid retention on these columns is controlled not only by ion exchange, but also by hydrophobic interactions, as demonstrated in Fig. 1 by the significantly greater retention of Tyr and Phe containing the hydrophobic chains $-\text{CH}_2\text{C}_6\text{H}_4\text{OH}$ and $-\text{CH}_2\text{C}_6\text{H}_5$, respectively. For this reason, the retention of the test amino acids on the Partisil SCX column, which is a sole strong cation exchanger, is generally similar and lower than on the HEMA Bio 1000 SB column (see Table I). As expected, the retention of the amino acids on the EDMA column, which exhibits purely hydrophobic interactions, is virtually independent of the mobile phase pH. The retention on the HEMA Bio 1000 DEAE column, a weak anion exchanger, is generally very low, even

TABLE I
CAPACITY FACTORS OF AMINO ACIDS ON THE CATION EXCHANGER STUDIED

Mobile phase: 0.002 M potassium dihydrogen phosphate, pH 5.3.

Amino acid	Capacity factor			
	HEMA Bio 1000 CM	HEMA Bio 1000 SB	Partisil SCX	EDMA ^a
Asp	0.11	0.13	0.14	0.25
Asn	0.11	0.14	0.16	0.09
Glu	0.25	0.25	0.16	0.38
Cys	0.51	—	0.84	0.125
Pro	0.53	0.81	1.20	0.25
Ser	0.56	1.19	0.80	0.125
Gly	0.58	1.00	0.44	0.125
Ala	0.58	1.06	0.80	0.156
Val	0.58	1.25	0.84	0.38
Met	0.67	1.88	1.20	1.80
Ile	0.70	1.69	1.10	1.88
Leu	0.70	1.94	0.80	2.06
Phe	1.02	4.12	1.48	7.12
Tyr	1.19	6.00	0.80	6.06
Trp	3.90	27.0	—	> 15
His	14.50	> 30	—	—

^a 0.2% trifluoroacetic acid, pH 1.6.

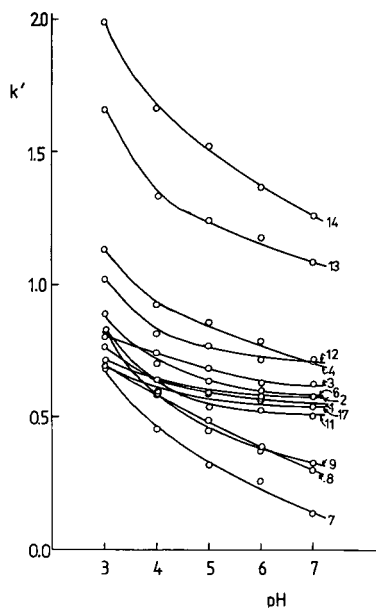


Fig. 1. Dependence of the amino acid capacity factors on the mobile phase pH. HEMA Bio 1000 CM column; mobile phase, $1.5 \cdot 10^{-3}$ M aqueous phosphate buffer. 1 = Gly; 2 = Ala; 3 = Val; 4 = Leu; 6 = Ser; 7 = Asp; 8 = Glu; 9 = Lys; 11 = Cys; 12 = Met; 13 = Phe; 14 = Tyr; 17 = Pro.

at high pH values (≥ 9); this column seems to be unsuitable for separation of compounds of this type and thus was not further studied.

The concentration of phosphate in the mobile phase, *i.e.* the ionic strength, little affects the amino acid retention on the hydrophobic EDMA column (the retention slightly decreases with increasing phosphate concentration, as increasing ionic strength causes a decrease in the mobile phase polarity). The retention on the Partisil SCX column also somewhat decreases with increasing phosphate concentration, as expected for the ion-exchange mechanism. The greatest effect can be seen with the HEMA Bio 1000 CM and SB columns (see Fig. 2 for the CM column). The retention of the positively charged amino acids and those containing hydrophobic groups decreases with increasing phosphate concentration: on the other hand, the retention of negatively charged solute molecules increases with increasing phosphate concentration up to a value of *ca.* $7 \cdot 10^{-3}$ M. This effect again stems from the dual character of the HEMA materials, *i.e.* that of an ion exchanger and a hydrophobic phase. The amino acids are separated into three groups by ion exchange, namely positively charged, negatively charged and uncharged molecules. Within these groups, the elution order is primarily determined by the hydrophobicity and size of the amino acid functional groups, *e.g.* Gly < Ala < Leu < Phe < Tyr ($-H < -CH_3 < -CH_2CH-(CH_3) < -CH_2C_6H_5 < -CH_2C_6H_4OH$).

The content of the organic modifier, methanol, in the mobile phase has little effect on the amino acid retention on the ion-exchange columns HEMA Bio 1000 CM, SB and Partisil SCX. The only exceptions are His and Trp: the retention of the former

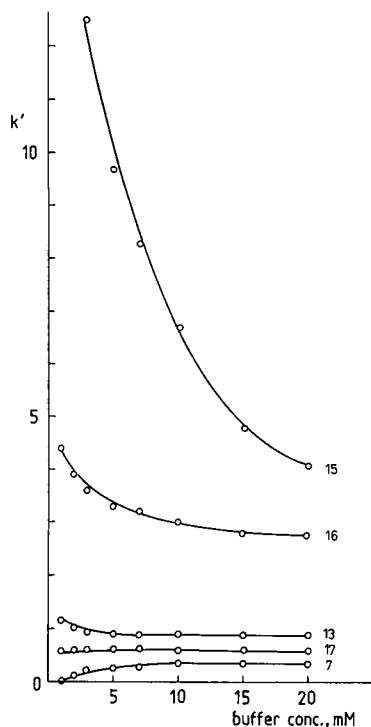


Fig. 2. Dependence of the capacity factors for selected amino acids on the phosphate buffer concentration in the mobile phase. HEMA Bio 1000 CM column; mobile phase, aqueous phosphate buffer, pH 5.3. 7 = Asp; 13 = Phe; 15 = His; 16 = Trp; 17 = Pro; k' values for the other amino acids are generally less than 1.

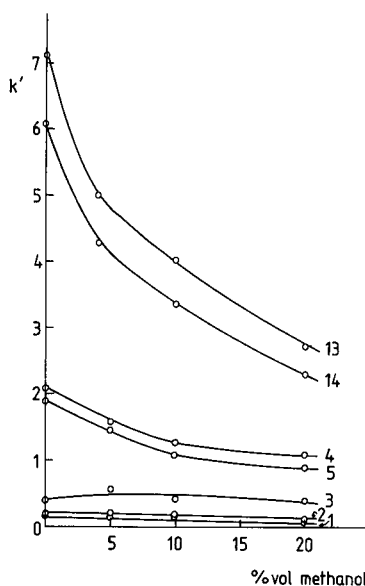


Fig. 3. Dependence of the capacity factors for selected amino acids on the methanol content in the mobile phase. EDMA column; mobile phase, 0.2% trifluoroacetic acid, pH 1.6. 5 = Ile; other amino acids as in Fig. 1.

increases with increasing methanol content (the k' value on the 1000 CM column changes from 7.1 to 9.1 on an increase in the methanol content from 0 to 15%, v/v), while that of the latter very slightly decreases (the change in k' being from 6.6 to 6.2). On the other hand, the retention on the EDMA hydrophobic column is strongly affected by the methanol content (Fig. 3, Table II). The retention decreases with increasing methanol content, and the effect is more pronounced for more hydrophobic amino acids. It can be seen from Fig. 4 that there exists a linear relationship between $\log k'$ and the carbon number in the amino acid functional group, which also confirms the hydrophobic nature of the interactions involved. It is evident that hydrophobic columns represent a promising alternative to ion-exchange and chemically bonded columns in amino acid separations.

Separation of dipeptides

The separation of dipeptides is very similar to that of the amino acids. The

TABLE II

DEPENDENCE OF THE CAPACITY FACTORS OF AMINO ACIDS ON THE METHANOL CONTENT

EDMA column; mobile phase, 0.2% trifluoroacetic acid, pH 1.6.

Amino acid	Capacity factor		
	5% Methanol	10% Methanol	20% Methanol
Asp	0.16	0.19	0.22
Asn	0.16	0.16	0.06
Glu	0.34	0.31	0.28
Cys	0.12	0.12	0.12
Pro	0.25	0.22	0.125
Ser	0.16	0.125	0.09
Gly	0.16	0.125	0.03
Ala	0.28	0.16	0.38
Val	0.66	0.40	0.38
Met	1.44	1.19	0.98
Ile	1.44	1.06	0.88
Leu	1.53	1.25	0.91
Phe	5.00	4.01	2.75
Tyr	4.30	3.38	2.30
Trp	> 15	> 15	12.4

retention data on the HEMA Bio 1000 CM, SB and Partisil SCX columns are given in Table III. In general, the HEMA Bio 1000 CM and SB columns separate dipeptides better than the Partisil SCX column, for which the capacity ratios are too low. However, with increasing length of the peptides, the capacity factors increase and then

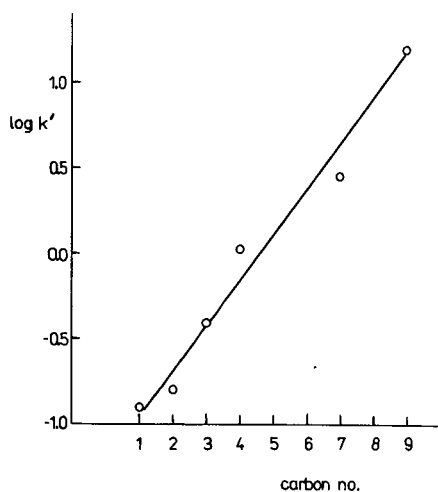


Fig. 4. Dependence of $\log k'$ on the carbon number in the amino acid functional groups. Conditions as in Fig. 3.

TABLE III
CAPACITY FACTORS OF DIPEPTIDES ON THE CATION EXCHANGERS STUDIED

Mobile phase, 0.002 M potassium dihydrogenphosphate, pH 5.3.

Dipeptide	Capacity factor		
	HEMA Bio 1000 CM	HEMA Bio 1000 SB	Partisil SCX
Gly-Asp	1.09	0.57	0.20
Gly-Glu	1.40	0.86	0.30
Gly-Gly	2.17	2.86	1.00
Gly-Ala	2.20	2.86	1.17
Gly-Val	2.61	4.00	1.60
Gly-Leu	3.28	6.79	2.04
Gly-Phe	4.80	14.4	1.70
Gly-Tyr	5.91	21.86	1.10
Gly-Met	2.52	6.21	1.65

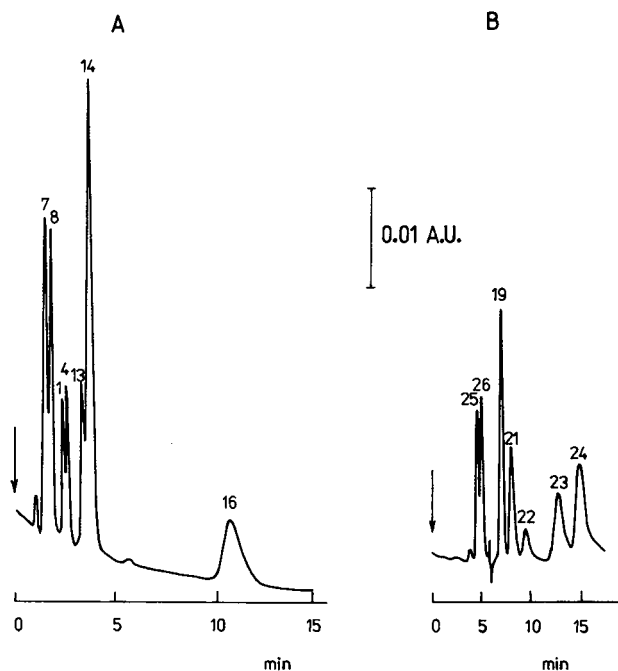


Fig. 5. Chromatogram of selected amino acids (A) and dipeptides (B). HEMA Bio 1000 CM column; mobile phase, 10^{-3} M phosphate buffer with 5% (v/v) methanol; UV photometric detection at 210 nm. Peaks: 1 = Gly; 4 = Leu; 7 = Asp; 8 = Glu; 13 = Phe; 14 = Tyr; 16 = Trp; 19 = Gly-Gly; 21 = Gly-Val; 22 = Gly-Leu; 23 = Gly-Phe; 24 = Gly-Tyr; 25 = Gly-Asp; 26 = Gly-Glu.

the HEMA columns cease to be useful and the Partisil column becomes optimal, as demonstrated by Fig. 5 in our previous paper [30].

The effect of the type of the displacer salt cation was studied in detail for the Partisil SCX column in our previous paper [30]. It has been shown that the plots of the $\log k'$ values against the ratio of the hydrated ion radius r and its charge number z are linear:

$$\log k' = a(r/z) + b$$

where slope a and intercept b are constants characteristic of the system, and verify the validity of the ion-exchange mechanism. The same dependences were obtained for the HEMA Bio 1000 CM and SB columns in this paper (see also Fig. 3 and Table II in ref. 30).

An example of a separation of amino acids and of dipeptides containing the same amino acid residues is given in Fig. 5. As the UV photometric and amperometric detection was studied in detail in our previous papers [13,14,29,30], it is not discussed here.

It can be concluded that the HEMA phases that combine the ion-exchange, hydrophobic and size-exclusion mechanism widen the possibilities of separation of amino acids and dipeptides. For longer peptides it is preferable to use columns with pure ion-exchange properties.

REFERENCES

- 1 W. Voelter, *High Performance Chromatography in Protein and Peptide Chemistry*, Walter de Gruyter, Berlin, 1981.
- 2 S. A. Borman, *Anal. Chem.*, 54 (1982) 21A.
- 3 A. J. Banes, G. W. Link and L. R. Snyder, *J. Chromatogr.*, 326 (1985) 419.
- 4 F. E. Regniér and K. M. Gooding, *Anal. Biochem.*, 103 (1980) 1.
- 5 M. Dizdaroğlu, *J. Chromatogr.*, 334 (1985) 49.
- 6 A. N. Radhakrishnan, S. Stein, A. Licht, K. A. Gruber and S. Udenfriend, *J. Chromatogr.*, 132 (1977) 552.
- 7 G. W. Welling, K. Slopsema and S. W. Wester, *J. Chromatogr.*, 359 (1986) 307.
- 8 A. K. Taneja, S. Y. M. Lau and R. S. Hodges, *J. Chromatogr.*, 317 (1984) 1.
- 9 G. W.-K. Fong and E. Grushka, *Anal. Chem.*, 50 (1978) 1154.
- 10 S.-N. Lin, L. A. Smith and R. M. Caprioli, *J. Chromatogr.*, 197 (1980) 31.
- 11 B. Grego and M. T. W. Hearn, *Chromatographia*, 14 (1981) 589.
- 12 D. Guo, C. T. Mant and R. S. Hodges, *J. Chromatogr.*, 386 (1987) 205.
- 13 K. Štulík, V. Pacáková, M. Weingart and M. Podolák, *J. Chromatogr.*, 367 (1986) 311.
- 14 K. Štulík, V. Pacáková and G. Jokuszies, *J. Chromatogr.*, 436 (1988) 334.
- 15 D. Guo, C. T. Mant, A. K. Taneja, J. M. R. Parker and R. S. Hodges, *J. Chromatogr.*, 359 (1986) 499.
- 16 D. Guo, C. T. Mant, A. K. Taneja and R. S. Hodges, *J. Chromatogr.*, 359 (1986) 519.
- 17 J. L. Meek, *Proc. Natl. Acad. Sci. U.S.A.*, 77 (1980) 1632.
- 18 M. J. O'Hare and E. C. Nice, *J. Chromatogr.*, 171 (1979) 209.
- 19 T. Sasagawa, T. Okuyama and D. C. Teller, *J. Chromatogr.*, 240 (1982) 329.
- 20 H. Gaertner and A. Puigserver, *J. Chromatogr.*, 350 (1985) 279.
- 21 J. L. Meek and Z. L. Rossetti, *J. Chromatogr.*, 211 (1981) 15.
- 22 R. A. Houghten and S. T. DeGraw, *J. Chromatogr.*, 386 (1987) 223.
- 23 I. Molnár and Cs. Horváth, *J. Chromatogr.*, 142 (1977) 623.
- 24 M. T. W. Hearn and B. Grego, *J. Chromatogr.*, 296 (1984) 309.
- 25 M. W. White, *J. Chromatogr.*, 262 (1983) 420.

- 26 W. Th. Kok, H. B. Hanekamp, P. Bos and R. W. Frei, *Anal. Chim. Acta*, 142 (1982) 31.
- 27 K. Štulík, V. Pacáková, Kang Le and B. Hennissen, *Talanta*, 35 (1988) 455.
- 28 *Catalogue*, Tessek, Prague, 1990.
- 29 Heping Wang, V. Pacáková and K. Štulík, *J. Chromatogr.*, 509 (1990) 245.
- 30 Heping Wang, V. Pacáková, K. Štulík and T. Barth, *J. Chromatogr.*, 519 (1990) 244.

CHROMSYMP. 2271

New Czechoslovak sorbent, Ekosorb

KAREL CHMEL

Glass-works Kavalier, 239 39 Votice (Czechoslovakia)

and

VĚRA GAJDŮŠKOVÁ*

Veterinary Research Institute, Hudcova 70, 621 32 Brno (Czechoslovakia)

ABSTRACT

A new sorbent, Ekosorb, has been developed and tested. It is prepared on the basis of a modified silica gel and warrants perfect purification of food extracts from fats and other co-extract substances. The pure eluate is suitable for trace analysis of polychlorinated aromatic compounds (polychlorinated biphenyls, hexachlorobenzene), chlorinated pesticides etc. Recovery of residues of chlorinated compounds is higher than 96%, allowing a quantitative determination and detection by gas chromatography. Ekosorb is an equivalent to Florisil.

INTRODUCTION

Polychlorinated aromatic compounds [polychlorinated biphenyls (PCBs), benzenes and other derivatives] and chlorinated pesticides are hazardous, persistent chemicals which have been detected in all environmental compartment including the food chain. These chemicals are more soluble in fat than in aqueous systems. Levels of these compounds must be monitored periodically so that trends and levels of exposures can be assessed.

Quantitative determination of chemical residues in biological samples requires use of accurate and reliable methods. Sample extraction and clean-up are two of the most important steps for ensuring the reliability of the procedure [1]. Florisil is an effective sorbent used for the clean-up of animal fats and biological sample extracts for the analysis of pesticides, PCBs and other non-polar contaminants [1-3].

A new sorbent, Ekosorb, has been developed and tested in Czechoslovakia [4]. This paper presents a comparison of results obtained using Florisil and Ekosorb.

EXPERIMENTAL

Solvents and chemicals

All solvents used were glass-distilled and free from interfering residues as tested by gas chromatography (GC). Anhydrous Na₂SO₄ and glass wool were pre-washed with hexane and petroleum ether.

The standards used were 1,1-dichloro-2,2-bis(4-chlorophenyl)ethene (*p,p'*-DDE) and hexachlorobenzene (HCB) from Supelco (U.S.A.) and PCBs (as Delor 106, an equivalent to Aroclor 1260) from Chemko. (Strážské, Czechoslovakia). All standards were dissolved in hexane.

Florisil (60–100 mesh), PR grade, was obtained from Serva (U.S.A.).

Ekosorb (60–120 mesh) was prepared from silica gel by modifying its surface with a thin layer of magnesium silicate (Czechoslovak patent application [4]).

Fat preparation and fortification

Raw chick fat was homogenized with hexane. The hexane layer was filtered through anhydrous N_2SO_4 and evaporated to dryness under vacuum on a water-bath at 30°C. Dried fat was free from *p,p'*-DDE, HCB and PCBs at the limit of detection (0.010 mg/kg) as tested by GC. This fat was dissolved in hexane and fortified by addition of an appropriate volume of the respective standard solution. The fortification levels are shown in Table I. The hexane phase was evaporated to dryness under vacuum on a water-bath at 30°C.

Clean-up recovery

Clean-up of all fortified fat samples was carried out in six parallel determinations by the following procedure: 14 g of activated Florisil or Ekosorb (see Table I) in glass columns was pre-washed with 20 ml petroleum ether. Then, 0.1 g of fat was dissolved in a small volume of petroleum ether and added to the column. The residues were eluted with 75 ml of 6% ethyl ether in petroleum ether. The eluate was evaporated to dryness under vacuum on a water-bath at 30°C. The residues were dissolved in hexane for GC analysis.

Gas chromatography

A Varian Vista 6000 gas chromatograph equipped with a ^{63}Ni electron-capture detector was used.

Packed column. A glass column, 250 cm \times 2 mm I.D., packed with Chromosorb W HP (80–100 mesh) coated with 5% OV-101, was used. The GC conditions were as follows: nitrogen carrier gas flow-rate, 30 ml/min; injector temperature, 235°C; oven temperature, 21°C; detector temperature, 300°C. On-column injection was used; the sample size injected was 2 μ l.

Capillary column. A 12 m \times 0.32 mm I.D. silica capillary column coated with SE-30 (0.5 μ m film) was used. The GC conditions were as follows: hydrogen carrier gas flow-rate, 2.5 ml/min; nitrogen make-up gas flow-rate, 30 ml/min; temperature programme, 100°C for 2 min, then to 210°C at 20°C/min and then held for 12.5 min; injector temperature, 220°C, detector temperature, 300°C. The sample size injected was 1 μ l; the injection was splitless for 75 s.

RESULTS AND DISCUSSION

Table I shows the comparison of recoveries of the chlorinated compounds under study after clean-up of the fortified fat on Ekosorb and Florisil. Conditions conforming with those given in official analytical methods [1–3] were used for the activation of the sorbents, *i.e.*, 24 h at 130°C, 4 h at 400°C and 4 h at 650°C. HCB was

TABLE I

RECOVERIES OF PCBs, HCB AND *p,p'*-DDE FROM FAT USING EKOSORB AND FLORISOL

Activated	Added (mg/kg)	Recovery (mean \pm S.D., $n=6$) (%)	
		Florisol	Ekosorb
PCBs			
130°C, 24 h	0.860	98.8 \pm 2.6	99.6 \pm 2.6
400°C, 4 h	0.860	95.4 \pm 3.2	98.9 \pm 2.8
650°C, 4 h	0.860	82.8 \pm 4.8	96.3 \pm 3.1
HCB			
130°C, 24 h	0.260	95.2 \pm 3.8	96.8 \pm 3.6
400°C, 4 h	0.260	87.4 \pm 5.7	92.6 \pm 4.0
<i>p,p'</i>-DDE			
130°C, 24 h	0.600	96.8 \pm 2.2	97.2 \pm 2.3
400°C, 4 h	0.600	94.6 \pm 2.9	96.3 \pm 2.7

included among the compounds under study, because it shows greater retention with Florisol than with other chlorinated aromatic compounds. As demonstrated in Table I, recoveries of all test compounds are higher on Ekosorb than Florisol. The differences became more pronounced when the activation temperatures were increased.

The purity of eluates from Ekosorb and Florisol is shown on chromatograms of PCBs separated from the fortified fat samples (Fig. 1). Ekosorb warrants perfect purification of food extracts from fat and other co-extract substances, which are

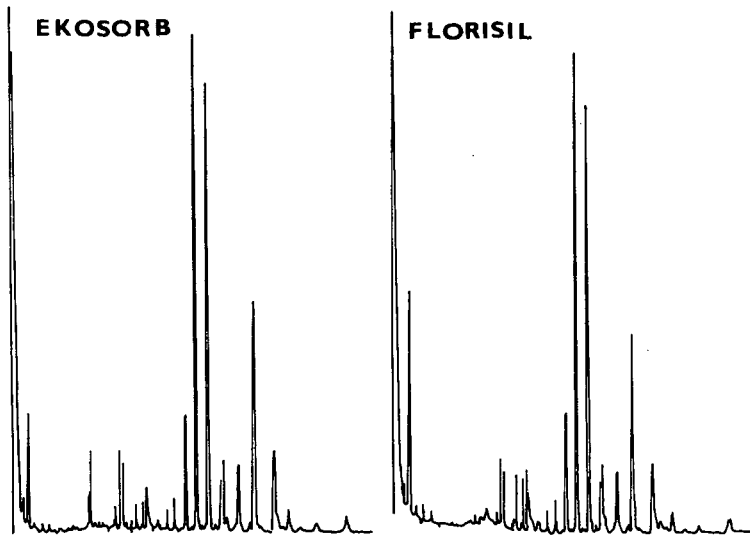


Fig. 1. Electron-capture chromatograms of Ekosorb and Florisol eluates of PCB-fortified fat on the SE-30 silica capillary column.

quantitatively retained on the sorbent column. The pure extract is suitable for trace analysis of polychlorinated aromatic compounds (PCBs, benzenes), chlorinated pesticides, etc.

Ekosorb can be used repeatedly after washing out the retained co-extract substances with acetone and water, drying and combustion of organic impurities at 650°C.

Twelve batches of Ekosorb, prepared under laboratory conditions, and three batches from pilot production were tested. Commercial production has already been launched by Glass-works Kavalier (Votice, Czechoslovakia). Constant-quality, reproducible recoveries of all test compounds and high purity of eluates were confirmed in all batches checked.

Compared with Florisil, Ekosorb possesses further advantages. Ekosorb is a synthetic sorbent, its preparation is quick, simple and inexpensive. It is prepared from silica gel for column chromatography (60–120 mesh) by modifying its surface with a thin layer of magnesium silicate. The composition of the batches tested was 97.0% SiO₂ and 2.7% MgO. The activity and sorption capacity of Ekosorb can be changed to comply with the composition of the compound under study and the character of the sample.

Confirmatory examinations of the use of Ekosorb for the determination of pesticides and hazardous industrial polychlorinated aromatic compounds in food, feedstuffs and other biological materials and environmental compartments are ongoing.

ACKNOWLEDGEMENT

We thank Mrs. M. Zukalová for her technical assistance.

REFERENCES

- 1 J. D. McKinney, L. Moore, A. Prokopetz and D. B. Walters, *J. Assoc. Offic. Anal. Chem.*, 67 (1984) 122–129.
- 2 W. Liao, W. D. Smith, T. C. Chiang and L. R. Williams, *J. Assoc. Offic. Anal. Chem.*, 71 (1988) 742–747.
- 3 S. Williams (Editor), *Official Methods of Analysis*, Association of Official Analytical Chemists, Arlington, VA, 13th ed., 1984, sec. 16.059.
- 4 K. Chmel and V. Gajdušková, *Czechoslovak Patent Application PV 210-90 'Sorbent'*, 1990.

Comparison of selectivity of silica and Florisil in the separation of natural pyranocoumarins

KAZIMIERZ GŁOWNIAK

Department of Pharmacognosy and Technological Laboratory, Medical Academy, Pstrowskiego 12, 20-007 Lublin (Poland)

ABSTRACT

Natural pyranocoumarin standards were separated using thin layers of Florisil (magnesium silicate) or silica and a sandwich chamber. Binary and ternary solvents containing a polar modifier (diisopropyl ether, ethyl acetate, acetonitrile or 2-propanol) as a mobile phase were used. Based on the relationship between R_M values and the concentration of polar modifier in the eluent, the optimum conditions were chosen for the separation of the isomers (samidin and isosamidin or *cis*- and *trans*-khellactone) and pyranocoumarin components of plant extracts from the fruits of *Libanotis* species. The correlation of retention parameters for silica and Florisil showed individual differences in selectivity.

INTRODUCTION

A large number of plant species containing coumarins, furanocoumarins and pyranocoumarins have been investigated using thin-layer chromatography [1,2] and over-pressurized thin-layer chromatography (TLC) [3,4]. The TLC method is useful for chemotaxonomic studies [5,6], analyses of coumarins and their metabolites [7-10], optimization of high-performance liquid chromatographic systems [11,12] and preparative separations by thin-layer, column [9,13] or medium-pressure liquid chromatography [14]. Interesting results for the optimization of the chromatographic system for the separation of furanocoumarins using silica gel and Florisil (magnesium silicate) adsorbents [15] stimulated a comparison of the selectivities of these two adsorbents in the separation of natural pyranocoumarins. The choice of silica and Florisil was due to the different surface structures and characteristics of the adsorption sites, leading to different selectivity characteristics. Systematic studies of the selectivity of the investigated systems (adsorbent-binary or ternary eluent) allows the selection of the optimum conditions for the separation of pyranocoumarin standards and for the chemotaxonomic study of medicinal plant species containing pyranocoumarins and their identification in plant extracts by TLC.

EXPERIMENTAL

The extraction of powdered ripe fruits from *Libanotis transcaucasica* Schischkin, *Libanotis delichostylos* Schischkin and *Seseli libanotis* (*Libanotis intermedia* Rupr.) was carried out with methanol in a Soxhlet-type extractor at room temperature. Analytical (and micropreparative) TLC was carried out on 100 × 200 mm or 200 × 200 mm glass plates covered with 0.25- or 0.5-mm layers of silica gel Si-60H (E. Merck, Darmstadt, Germany) or Florisil (Fluka, Buchs, Switzerland).

The separation was performed in sandwich-type glass chambers [16] with a glass distributor (Polish Reagents, Poland); 2- μ l samples of the standard solutes (1.0 mg/cm³ in dichloromethane) were applied in the form of spots or short bands and eluted with appropriate eluents over a distance of 15 cm. The spots were localized under UV light at 254 nm.

Materials

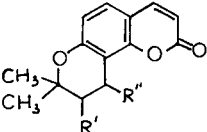
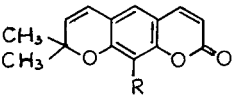
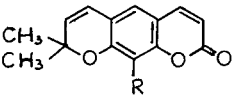
The pyranocoumarin standards (Table I) were obtained from the Department of Chemistry, Royal Danish School of Pharmacy, Copenhagen, Denmark. Organic solvents of analytical-reagent grade were purchased from E. Merck. The plant material was collected in the Pharmacognostic Garden, Medical Academy of Lublin, in 1989.

RESULTS AND CONCLUSIONS

The results of the optimization of the adsorbent–eluent systems for separation of ten pyranocoumarin standards with binary eluent mixtures are shown in Figs. 1 and 2 as plots of R_M vs. concentration of acetonitrile in dichloromethane. (% , v/v).

Pyranocoumarins with two hydroxy groups in the molecule such as *cis*- (**9**) and *trans*-khellactone (**10**) were strongly adsorbed, giving measurable R_M values only at higher concentrations of the modifiers (polar solvents added to dichloromethane or *n*-heptane) for both adsorbents examined.

TABLE I
STRUCTURES OF THE COMPOUNDS INVESTIGATED

Structure	Name	R	R'	R''	No. ^a
	Samidin		OCOH = C(CH ₃) ₂	OCOCH ₃	1
	Isosamidin		OCOCH ₃	OCOH = C(CH ₃) ₂	2
	Visnadin		OCOCH(CH ₃)		
	Dihydroseselin		H	OCOCH ₃	3
	Pterixin		H	H	4
	Disenecieryl- <i>cis</i> -khellactone		OCOCH = C(CH ₃) ₂	OCOC(CH ₃) = CHCH ₃	6
	<i>cis</i> -Khellactone		OCOCH = C(CH ₃) ₂	OCOCH = C(CH ₃) ₂	8
	<i>trans</i> -Khellactone		OH	OH	9
	Xanthyletin	H	OH	OH	10
	Luvangetin	OCH ₃			7

^a Numbering corresponds to typical sequence and analogy of molecular structure and polarity.

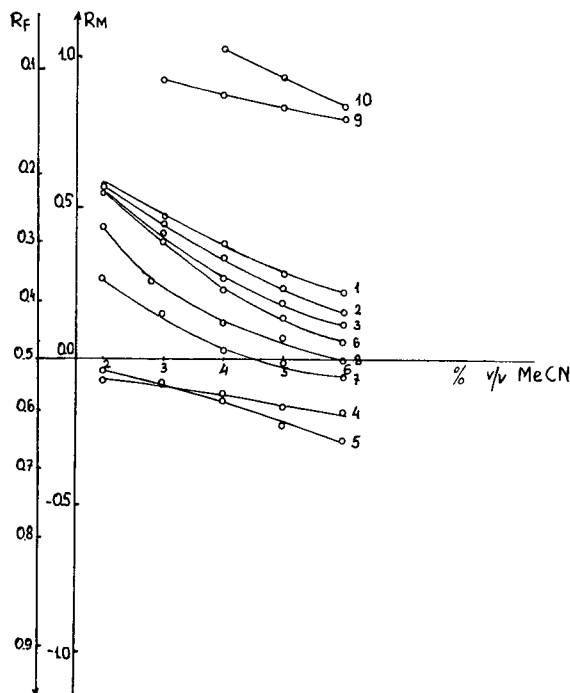


Fig. 1. R_M values of pyranocoumarins vs. concentration of acetonitrile (MeCN) in dichloromethane as the eluent and silica as the adsorbent. Numbering of solutes as in Table I.

An increase in selectivity at higher acetonitrile concentrations for silica and a decrease for Florisil were observed for both adsorbents: the separation of isomers *cis*-**(9)** and *trans*-khellactone **(10)** or samidin (**(1)** and isosamidin **(2)**) is possible, but they have the weakest retention on silica.

The selectivity of the system used is also illustrated by R_M vs. R_M correlation plots obtained for silica and Florisil with a few mobile phases chosen in optimization investigations; 6% (v/v) acetonitrile in dichloromethane (Fig. 3), 6% (v/v) ethyl acetate in dichloromethane (Fig. 4), 10% (v/v) diisopropyl ether in dichloromethane (Fig. 5) and 5% (v/v) 2-propanol mixture in *n*-heptane-dichloromethane (1:1) (Fig. 6). The spread of points in the R_M vs. R_M correlation plots shows the different selectivities of the two adsorbents. Points lying close to a vertical line (e.g., Fig. 6, **(3)** and **(7)**; **(1)** and **(2)**) correspond to solutes well separated on Florisil but which have similar R_F (R_M) values on silica.

The selectivity also depends on the eluent used. One can compare of solutes **(1)** and **(2)** in Fig. 6 (no separation on either adsorbents) and in Figs. 4 and 5 (good separation on Florisil). For some eluents the spread of points is minimal (Fig. 3), which shows that both adsorbents have similar selectivities.

The less polar pyranocoumarins, such as xantyletin (**(5)**) and dihydroseselin (**(4)**) were easily separated in all the systems examined.

Pyranocoumarins possessing the same polar radicals in the molecule, such as samidin (**(1)**), isosamidin (**(2)**) and pterixin (**(6)**) can be better separated on Florisil than on silica.

TABLE II
 R_M AND ΔR_M VALUES OF PYRANOCUMARINS
 Selectivities for solutes No. 1-4 and 6-10 are relative to xanthyletin (No. 5).

Com- pound ^a	10% (v/v) diisopropyl ether in dichloromethane			5% (v/v) 2-propanol in dichloromethane-heptane (1:1)			6% (v/v) acetonitrile in dichloromethane			6% (v/v) ethyl acetate in dichloromethane				
	Silica R_M	Florisol R_M	ΔR_M	Silica R_M	Florisol R_M	ΔR_M	Silica R_M	Florisol R_M	ΔR_M	Silica R_M	Florisol R_M	ΔR_M		
1	0.30	0.53	0.18	0.25	0.25	-0.33	0.04	0.64	0.26	0.54	0.38	0.80	0.52	0.67
2	0.28	0.51	0.37	0.44	-0.11	-0.33	-0.06	0.54	0.18	0.46	0.38	0.80	0.68	0.83
3	0.25	0.48	0.31	0.38	-0.10	0.26	0.01	0.61	0.15	0.43	-0.30	0.12	0.49	0.64
4	-0.18	0.05	-0.23	-0.16	-0.25	0.11	-0.50	0.10	-0.18	0.10	-0.36	0.06	-0.30	-0.15
5	-0.23	0.00	-0.07	0.00	-0.36	0.00	-0.60	0.00	-0.28	0.00	-0.42	0.00	-0.15	0.00
6	0.21	0.44	0.35	0.42	-0.20	0.16	-0.15	0.45	0.08	0.36	-0.20	0.22	0.43	0.58
7	-0.08	0.15	-0.13	-0.06	-0.15	0.21	-0.38	0.22	-0.07	0.21	-0.18	0.24	0.28	0.43
8	0.14	0.37	0.22	0.29	-0.30	0.06	-0.26	0.34	-0.01	0.27	-0.19	0.23	0.35	0.50
9	1.08	1.31	1.06	1.13	0.17	0.53	1.02	1.62	0.81	1.09	1.04	1.46	0.96	1.11
10	1.26	1.49	1.12	1.19	0.30	0.66	1.12	1.72	0.86	1.14	1.20	1.62	1.07	1.22

^a See Table I.

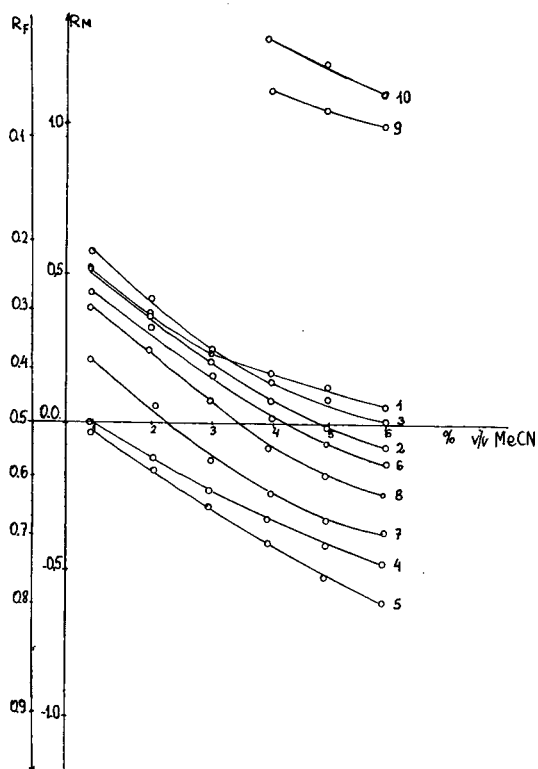


Fig. 2. R_M values of pyranocoumarins vs. concentration of acetonitrile (MeCN) in dichloromethane as the eluent and Florisil as the adsorbent.

A ternary eluent containing 5% (v/v) 2-propanol in *n*-heptane-dichloromethane (1:1) shows the greatest eluent strength for polar pyranocoumarins *e.g.*, *cis*-**(9)** and *trans*-khellactone **(10)** on silica, but with weaker selectivity for other compounds.

Table II summarizes the R_M and ΔR_M values obtained for the same eluent and both adsorbents, where the ΔR_M values are a measure of the selectivity $\{\Delta R_M = \log \alpha$, where α = separation factor; $R_M = \log[(1 - R_F)/R_F] = \log k'\}$.

The 6% (v/v) acetonitrile (modifier) shows a similar selectivity on silica and Florisil for almost all the compounds studied. Comparison of pyranocoumarins possessing similar large polar radicals such as samidin **(1)** isosamidin **(2)** visnadin **(3)**, pterixin **(6)** and disenecieryl-*cis*-khellactone **(8)** shows that 6% ethyl acetate in dichloromethane as a mobile phase and Florisil is the most selective system for their separation. Different selectivities of silica and Florisil with 5% 2-propanol in heptane-dichloromethane (1:1) as eluent for the separation of stereoisomers [*cis*- **(9)** and *trans*-khellactone **(10)**] was established.

The results illustrated above can be utilized in the preparative chromatography of the natural pyranocoumarins in plant material extracts with both adsorbents and 5% diisopropyl ether in dichloromethane as the mobile phase. Fig. 7 shows the separation of coumarin extracts from *Libanotis* species fruits in comparison with

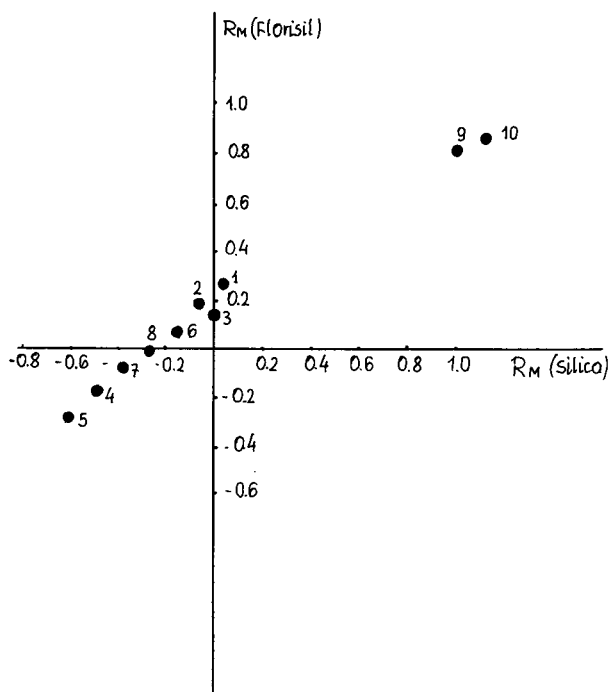


Fig. 3. Correlation of R_M values obtained on silica and Florisil with 6% (v/v) acetonitrile in dichloromethane.

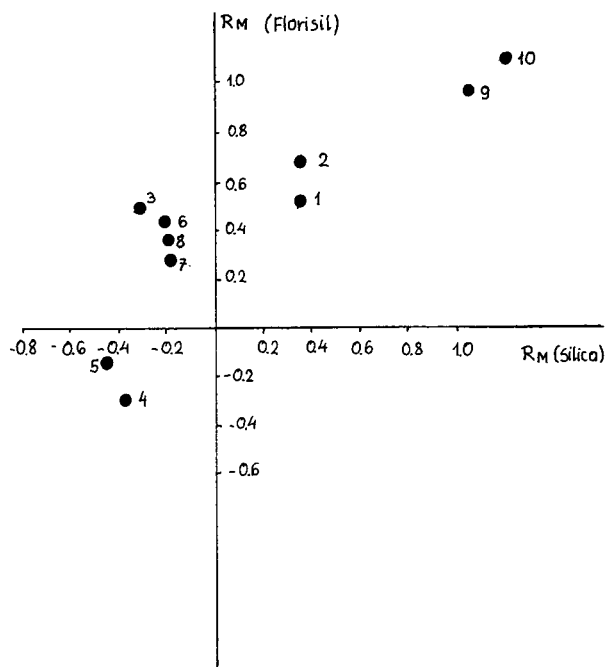


Fig. 4. Correlation of R_M values obtained on silica and Florisil with 6% (v/v) ethyl acetate in dichloromethane.

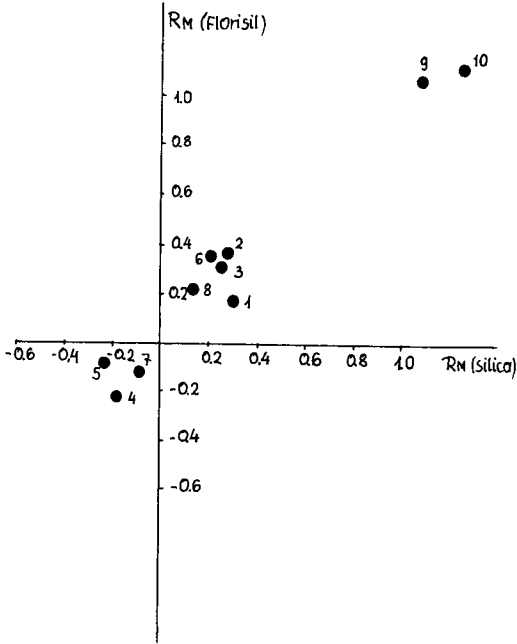


Fig. 5. Correlation of R_M values obtained on silica and Florisil with 10% (v/v) diisopropyl ether in dichloromethane.

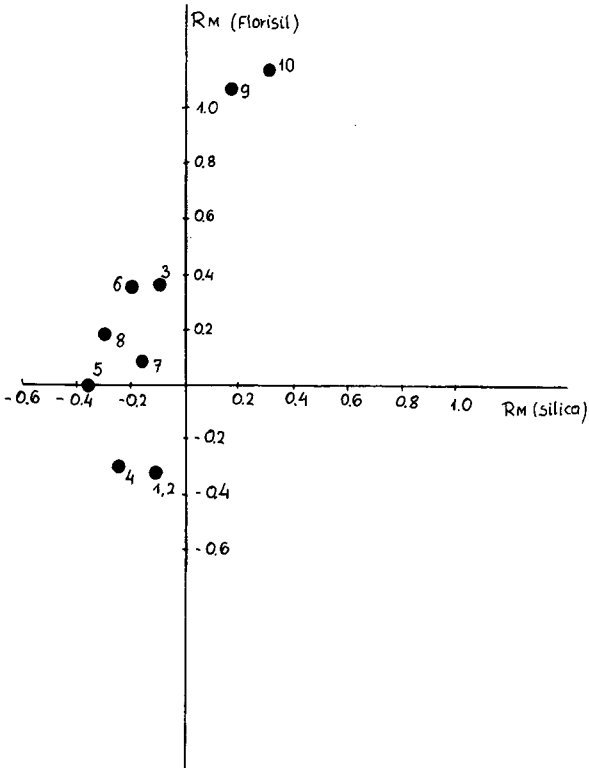


Fig. 6. Correlation of R_M values obtained on silica and Florisil with 5% (v/v) 2-propanol in *n*-heptane-dichloromethane (1:6).

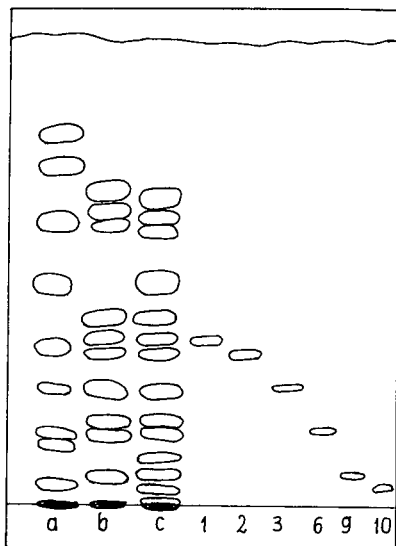


Fig. 7. Separation of extracts from *Libanotis* species fruits. Eluent, 5% (v/v) diisopropyl ether in dichloromethane; adsorbent, silica (a) *Libanotis transcaucausica* Schischkin; (b) *Libanotis delichostylos* Schischkin; (c) *Libanotis intermedia* Rupr. (*Seseli libanotis*).

pyranocoumarin standards. Some of them (samidin, pterixin, *cis*-khellactone) have been reported in the plants examined and others are characteristic of *Libanotis* and *Seseli* species [17]. The good separation of standard and all the coumarin components of the extracts examined revealed the different coumarin compositions.

Chromatography on Florisil and silica layers is useful for chemotaxonomic studies of *Umbelliferous*, *Seseli* and *Libanotis* species plants containing pyranocoumarins and can provide information on the presence of the compounds investigated by rechromatography with standards, and can be applied in screening studies of medicinal plants containing pyranocoumarins.

REFERENCES

- 1 K. Wierzchowska-Renke, *Acta Pol. Pharm.*, 31 (1974) 225.
- 2 B. Kamiński, K. Głowniak, A. Majewska, J. Petkowicz and D. Szaniawska-Dekundy, *Farm.Pol.*, 34 (1978) 25.
- 3 Dz. Nyiredy, S. Y. Meszaros, K. Dallenbach-Tölke, K. Nyiredy-Mikita and O. Sticher, *J. Planar Chromatogr.*, 1 (1988) 54.
- 4 Sz. Nyiredy, C. A. J. Erdelmeier and O. Sticher, in R. E. Kaiser (Editor), *Planar Chromatography*, Vol. 1, Hüthig, Heidelberg, Basle, New York, 1986, p. 128.
- 5 H. E. Nordly and S. Nagy, *J. Chromatogr.*, 207 (1981) 21.
- 6 R. V. Tamma, C. C. Miller and R. Everett, *J. Chromatogr.*, 332 (1985) 236.
- 7 M. Kowalska and J. Skrzypczakowa, *Diss. Pharm. Cracow*, 26 (1964) 225.
- 8 J. Karlsen, L. E. J. Boomsma and A. Baerheim Svendsen, *J. Chromatogr.*, 42 (1969) 550.
- 9 J. Mendez and J. Rubido, *Planta Med.*, 36 (1979) 219.
- 10 E. H. Dertly, R. C. Beier, G. W. Ivie and L. D. Rowe, *Photochemistry*, 23 (1984) 439.
- 11 K. Głowniak and M. Bieganowska, *J. Liq. Chromatogr.*, 8(1985) 2927.

- 12 K. Głowniak and M. Bieganowska, *J. Chromatogr.*, 370 (1986) 281.
- 13 T. M. Swager and J. H. Vardellina, II, *Phytochemistry*, 24 (1985) 805.
- 14 G. C. Zoog, Sz. Nyiredy and O. Sticher, *Chromatographia*, 27 (1989) 591.
- 15 T. Wawrzynowicz, M. Waksmundzka-Hajnos and M. Bieganowska, *Chromatographia*, 28 (1989) 161.
- 16 E. Soczewiński, in R. E. Kaiser (Editor), *Planar Chromatography*, Vol. 1, Hüthig, Heidelberg, Basle, New York, 1986, pp. 79–117.
- 17 R. D. H. Murray, J. Mendez and S. A. Brown, *The Natural Coumarins*, Wiley, Chichester, 1982.

CHROMSYMP. 2300

Evaluation of the application of liquid-phase titration to the examination of the adsorption activity of silica-based high-performance liquid chromatographic packings

Z. SUPRYNOWICZ, K. PILORZ* and R. LODKOWSKI

Department of Chemical Physics, Faculty of Chemistry, Maria Curie-Skłodowska University, Lublin (Poland)

ABSTRACT

The theoretical basis of the chromatographic titration method was investigated and the correctness of the determination of the strong silanol fraction was confirmed. Application of liquid-phase titration to the comparison of reversed-phase high-performance liquid chromatographic packings is described and the possibility of sorbent evaluation is discussed.

INTRODUCTION

The variety of silica surface chemistry, caused by the structure of amorphous silica, *e.g.*, by variation in the distances of hydrogen-bonded silanols [1,2], is reflected in the broad range of pK_a and pH values of commercially available silicas and can influence the properties and quality of alkyl-bonded phases for high-performance liquid chromatography (HPLC). Because the strength of hydrogen bonds depends on the acidity of the silanols [3], the concept of the existence of acidic reactive silanols on the silica surface has been formulated and confirmed experimentally [2,4–7], supporting the previous concept of reactive silanols by Snyder and Ward [8]. Blockage of the acidic reactive silanols appeared unexpectedly to have a large effect on the packing efficiency [5], undesirable adsorption of basic compounds and hydrolytic stability of alkyl-bonded phases formed on silicas containing such groups [9,10]. Attention has also been paid to the influence of metal oxide impurities in chromatographic-grade silica gels on the chromatographic process [11]. Sadek *et al.* [12] and Nawrocki [13] have shown that the metal atoms can create “structural Lewis sites” and influence the silica surface atoms and their hydroxyl groups. This was confirmed by acid washing results [14–16]. A review by Nawrocki and Buszewski [17] summarizes work on reactive silanols on silica gel surfaces.

In a series of papers by Nawrocki and co-workers [18–24], the application of the gas-phase titration method to the examination of the adsorption activity of chromatographic packings was proposed. It was suggested that at least two types of adsorption centres differing significantly in adsorption energy exist on the surface of

silica-based chromatographic packings. The method proposed by Nawrocki and co-workers should permit the determination of the number of strong adsorption centres on the sorbent (so-called acidic silanols), usually interfering with the chromatographic determination, causing peak tailing and even irreversible adsorption of sample substances. This method can be potentially useful for the evaluation of chromatographic packings and for their standardization.

This paper considers the evaluation of the effectiveness and correctness of the method of chromatographic titration on the basis of a simple theoretical description of the processes occurring on chromatographic columns. The assumed model permits the description of systems including either a gas or non-polar liquid as the mobile phase.

THEORETICAL

Chromatographic titration consists in the injection of a strongly adsorbed substance (so-called "blocker") followed by injections of small portions of a relatively weakly adsorbed substance ("marker"). The retention time of the "marker" changes during the elution of the "blocker", finally attaining the minimum value at the moment the "blocker" peak appears at the end of the column. A graphical dependence of the minimum retention time of the "marker" on the amount of "blocker" injected should be in the form of a broken line and its vertex should correspond to the number of strong adsorption centres.

The main assumptions of the chromatographic titration method can be defined as follows: (1) at the moment of "marker" elution (for the injection giving the minimum value of the retention time), the "blocker" molecules are uniformly distributed along the column, and (2) the "blocker" molecules adsorb only on the centres of high adsorption energy and "marker" molecules adsorb on the remaining centres.

Let us consider the latter assumption. According to Riedo and Kováts [25], we accept the following definition of the capacity factor k' :

$$k' = (V_R - V_0)/V_0 = \frac{A}{V_0} \cdot \frac{d\Gamma}{dc} \quad (1)$$

where V_R = retention volume (dm^3), V_0 = total mobile phase volume in the column (dm^3), A = total adsorbent surface area in the column (m^2), Γ = excess Gibbs isotherm (the dividing plane is placed at the solid-liquid interface) (mol/m^2) and c = concentration of the chromatographed substance (mol/dm^3). An isotherm that can be utilized for the description of the considered system should possess one characteristic feature, *viz.*, it must be limited. We shall utilize the Langmuir isotherm (Li) and the isotherm which can be called the "limited Henry's isotherm" (LHi):

$$\Theta = \frac{Kc}{1 + Kc} \quad (\text{Li})$$

$$\Theta = \begin{cases} Kc & c \leq 1/K \\ 1 & c > 1/K \end{cases} \quad (\text{LHi}) \quad (2)$$

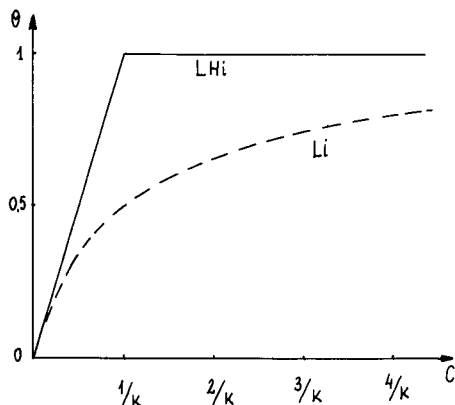


Fig. 1. The Langmuir isotherm (dashed line) and limited Henry's isotherm (solid line).

where Θ = the degree of surface coverage and K = Henry's constant (dm^3/mol).

The shapes of both isotherms are presented in Fig. 1. In order to simplify our model we shall consider only two types of adsorption centres, *viz.*, strong and weak, neglecting also the competitive adsorption of the mobile phase molecules. Owing to such a simplification, the results obtained can be related directly to gas chromatography. According to Langmuir [26], we use the above isotherms as local ones whereas a global isotherm is calculated from the following equation:

$$\Theta = \frac{\Theta_1 N_1 + \Theta_2 N_2}{N_1 + N_2} \tag{3}$$

where N_1 and N_2 are the number of strong and weak adsorption centres, respectively. From eqns. 3 and 2 we obtain the particular global isotherms:

$$\Theta = \frac{c}{N_1 + N_2} \left(\frac{K_1 N_1}{1 + K_1 c} + \frac{K_2 N_2}{1 + K_2 c} \right) \tag{Li}$$

$$\Theta = \begin{cases} c \cdot \frac{K_1 N_1 + K_2 N_2}{N_1 + N_2} & c \leq 1/K_1 \\ \frac{N_1 + K_2 N_2 c}{N_1 + N_2} & 1/K_1 < c \leq 1/K_2 \\ 1 & c > 1/K_2 \end{cases} \tag{LHi}$$

where the subscripts 1 and 2 relate to strong and weak adsorption centres, respectively. Isotherms 4 describe the adsorption of the "blocker". Because the "marker" concentration is significantly lower than that of the "blocker" (theoretically infinitely low), it can be assumed that its molecules adsorb only on the free centres and do not

compete with the "blocker" molecules. Therefore, the global isotherm of the "marker" can be presented in the following form:

$$\Theta_M = \frac{(1 - \Theta_{B1})N_1\Theta_{M1} + (1 - \Theta_{B2})N_2\Theta_{M2}}{N_1 + N_2} \quad (5)$$

where the subscripts M and B relate to the "marker" and "blocker", respectively.

$$\Theta_M = \frac{c_M}{N_1 + N_2} \left(\frac{N_1 K_{M1}}{1 + K_{B1}c_B} + \frac{N_2 K_{M2}}{1 + K_{B2}c_B} \right) \quad (\text{Li})$$

$$\Theta_M = \begin{cases} K_{M1}c_M \cdot \frac{N_1(1 - K_{B1}c_B)}{N_1 + N_2} + K_{M2}c_M \cdot \frac{N_2(1 - K_{B2}c_B)}{N_1 + N_2} & c_B \leq 1/K_{B1} \quad (6) \\ K_{M2}c_M \cdot \frac{N_2(1 - K_{B2}c_B)}{N_1 + N_2} & 1/K_{B1} < c_B \leq 1/K_{B2} \quad (\text{LHi}) \\ 0 & c_B > 1/K_{B2} \end{cases}$$

During derivation of the above equations the assumption of infinite dilution of the "marker" was made and thus the Henry's isotherm was used as the local isotherm of the "marker".

According to the definition mentioned above, the surface excess of the "marker" can be expressed as follows:

$$\Gamma_M = \frac{(N_1 + N_2)\Theta_M - V_{\text{mono}}c_M}{A} \quad (7)$$

where V_{mono} denotes the monolayer volume (dm^3).

From eqns. 1, 7 and 6 we can obtain finally the dependence of the "marker" capacity coefficient on the "blocker" concentration:

$$k'_M(c_B) = \frac{1}{V_0} \left(\frac{N_1 K_{M1}}{1 + K_{B1}c_B} + \frac{N_2 K_{M2}}{1 + K_{B2}c_B} \right) \quad (\text{Li})$$

$$k'_M(c_B) = \begin{cases} K_{M1} \cdot \frac{N_1(1 - K_{B1}c_B)}{V_0} + K_{M2} \cdot \frac{N_2(1 - K_{B2}c_B)}{V_0} & c_B \leq 1/K_{B1} \quad (8) \\ K_{M2} \cdot \frac{N_2(1 - K_{B2}c_B)}{V_0} & 1/K_{B1} < c_B \leq 1/K_{B2} \quad (\text{LHi}) \\ 0 & c_B > 1/K_{B2} \end{cases}$$

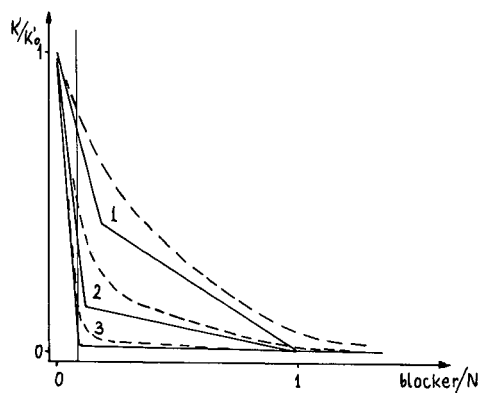


Fig. 2. Theoretical dependence of the capacity coefficient of a "marker" on the amount of "blocker" in the column. A constant "blocker" concentration in the mobile phase was assumed. Lines as in Fig. 1. The vertical line indicates the strong silanol fraction ($f = 0.1$). Parameter s values: (1) 10; (2) 50; (3) 500. Other parameters: $K_{B2} = 100$; $r = 1$.

In order to simplify matters, we have neglected in the above equations the term related to monolayer volume. In the case of strong positive adsorption taking place in the range of low concentrations, this term does not play a significant role. One should remember, however, that only the presence of this term permits negative values of the capacity coefficient, *e.g.*, for a substance whose molecules are excluded from the surface layer. It is worth noting that for typical adsorbents characterized by a specific surface area of *ca.* 100 m²/g and porosity of the order of 1 ml/g monolayer volume ranges from several tens to hundreds of microlitres per gram of the adsorbent, depending on the molecular size of the adsorbate. In further considerations this term will be neglected.

Fig. 2 shows the dependence of the "marker" k' value on the amount of the "blocker" contained in the column (calculated from eqns. 4 and 6–8). A capacity coefficient is presented in the form of the fraction of the "marker" k' value on the "blocker"-free column and the unit of the amount of "blocker" is monolayer capacity ($N_1 + N_2$). Solid lines correspond to LHi and dashed lines to Li assuming the following parameter values:

$$f = N_1/(N_1 + N_2) = 0.1; \quad r = V_0/(N_1 + N_2) = 1; \quad K_{B2} = 100;$$

$$s = K_{B1}/K_{B2} = \begin{cases} 10 & \text{for 1} \\ 50 & \text{for 2} \\ 500 & \text{for 3} \end{cases}$$

We have also assumed that $K_{M1}/K_{M2} = K_{B1}/K_{B2}$. The vertical line in Fig. 2 shows the fraction of the strong adsorption centres.

As one would expect, the line corresponding to the Langmuir isotherm is smooth. The higher the ratio of adsorption constants s , the closer this line is to the broken line obtained for the limited Henry's isotherm. The position of the vertex is obtained from the expression $f + r/K_{B1} + (1 - f)/s$. The vertex is always shifted to

the right so the strong centre fraction established on the basis of its position must be overestimated.

The ratio of the slopes of the two broken line sections can be calculated in a simple manner. We obtained the following expression:

$$\frac{1-f+r/K_{B2}}{1-f} \cdot \frac{s^2f+1-f}{sf+1-f+r/K_{B2}} \approx s$$

Such an approximation is the better the greater is the product sf . The slope ratio values for broken lines presented in Fig. 2 are 5.8, 42.9 and 496.5 for $s = 10, 50$ and 500 , respectively. The practical determination of the s value (*i.e.*, the difference in adsorption energy for centres 1 and 2 equal to $RT \ln s$) is limited by the too low accuracy of the slope determination for the second section of the broken line, especially for high s values. On the other hand, the evaluation of s at low levels is significantly underestimated.

Let us now consider the first assumption of chromatographic titration. It is well known that the "blocker" does not distribute uniformly along the column but forms a band in which the "blocker" concentration depends on the elution time and the distance from the column inlet. For the Langmuir isotherm the shape of such a band cannot be predicted in a simple manner, but it is possible for the limited Henry's

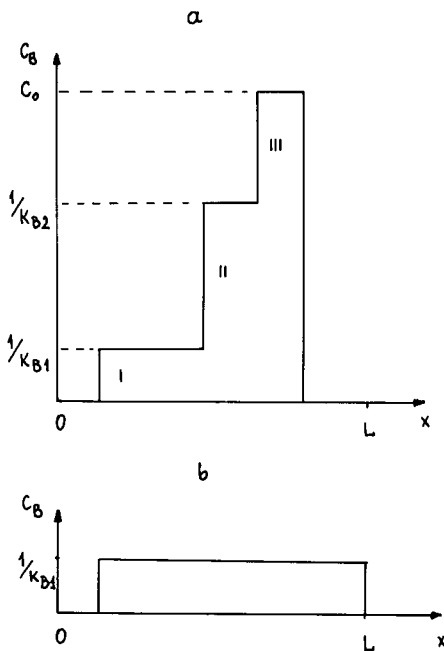


Fig. 3. Theoretical "blocker" band shape in a column of length L , (a) some time after injection and (b) at the moment of maximum strong centre blockage. c_0 denotes the "blocker" concentration of the injected solution.

isotherm. Neglecting the "diffusion" band broadening, we obtain a step band as presented in Fig. 3a, where c_0 denotes the "blocker" concentration of the injected solution.

According to Giddings [27], the migration rate of the band back edges can be expressed in the following form:

$$\begin{aligned}
 v_I &= v_0 \left\{ 1 + \frac{N}{V_0} \left[K_{B1}f + K_{B2}(1 - f) \right] \right\} \\
 v_{II} &= v_0 \left[1 + \frac{N}{V_0} \cdot K_{B2}(1 - f) \right] \\
 v_{III} &= v_0
 \end{aligned}
 \tag{9}$$

where v_0 denotes the linear velocity of an unretained substance band.

Let us consider the moment at which the "blocker" distribution in the column is the most uniform. This takes place when step II (Fig. 3a) vanishes at the moment of the appearance of the "blocker" band front at the column outlet. Such a situation is presented in Fig. 3b. The retention time of the "blocker" band front t_R is equal to L/v_{II} , and the length of this part of the column where the "blocker" concentration is constant is equal to $L - v_I t_R$. We can now calculate the amount of "blocker" corresponding to the inflection point in Fig. 2 covering the correction for the band shape. Taking monolayer capacity as a unit, we obtain:

$$[f + r/K_{B1} + (1 - f)/s][1 - (v_I/v_{II})] = [f + r/K_{B1} + (1 - f)/s] \left(\frac{sf}{r/K_{B2} + sf + 1 - f} \right) = f$$

Thus, the fact of taking into account the "blocker" band shape causes the inflection point abscissa to be equal to the actual strong adsorption centre fraction (within the developed model). We can also calculate the ratio of the slopes of the two sections of the broken line:

$$[0.5s + (1 - f)/2sf] / \left\{ 1 + (1 - 2f)/2sf - [0.5 + (1 - f)/2sf](1 - 1/s) \frac{K_{M2}}{K_{B2}} \right\}$$

For typical parameters the value of this ratio is close to 0.5s, which is surprising and suggests a strong dependence of this ratio on the "blocker" band shape. The above expression contains a new parameter, K_{M2}/K_{B2} , which introduces the "marker" properties. Fixing its value at 0.01 we obtain slope ratios equal to 3.9, 23.4 and 249.3 for $s = 10, 50$ and 500 , respectively. A characteristic feature of the above expression is a lack of parameter r connected with chromatographic column properties.

The most striking feature of chromatographic titration curves is the decrease in subsequent section slopes. Slope values for the first and second sections can be calculated from the following expressions:

$$\frac{K_{M1}}{r} \cdot \frac{1 + (1-f)/fs^2}{1 + (1-f)/sf[1 - (1-1/s)K_{M2}/K_{B2}]}$$

$$\frac{K_{M2}}{r} \cdot \frac{2 + (1-2f)/sf - [sf + (1-f)/sf](1-1/s)K_{M2}/K_{B2}}{1 + (1-f)/sf[1 - (1-1/s)K_{M2}/K_{B2}]}$$

We obtained 5.8, 42.6 and 491.3 for the first section and 1.47, 1.82 and 1.97 for the second ($s = 10, 50$ and 500 , respectively). For the chosen set of parameters $K_{M1} = s$ and $K_{M2} = 1$. In practice, the accurate determination of the acidic silanol adsorption energy (on the basis of K_{M1}) is not possible because we cannot determine the total number of accessible silanols. Hence we cannot determine the parameter r and cannot express the injected "blocker" amount as the monolayer capacity fraction. On the other hand, it seems reasonable that if we can assume similar r values and similar silanol access for different sorbents, we can compare the slopes of corresponding sections and draw a conclusion concerning silanol adsorption energies of different packings.

In liquid-phase titration, the problem of the presence of water and other polar contaminants in the liquid mobile phase arises. Water can influence the "marker" retention in a very complicated manner, especially in the case of injection of a large amount of amine, which is believed to be able to displace all other adsorbates. In front of the amine band the water content on the column increases and after the band a region of decreased water content may be expected. Water evidently partially deactivates the packing surface and decrease the "marker" retention time, but it is not clear if it affects the slope of the LPT curve. Moreover, because an amine is much more strongly adsorbed than water, the position of the inflection point should not be affected by its presence.

In gas chromatography the experiment is performed at much higher temperatures and the low water content in the mobile phase may be easily maintained, so under proper experimental conditions the influence of water can be neglected.

From the above theoretical considerations we can draw the following conclusions:

(1) The position of the inflection point for the chromatographic titration curve should determine the actual strong adsorption centre fraction.

(2) The slope ratio of subsequent sections is a measure of the adsorption energy difference for two types of centres. In practice, we can say that this difference is high (above *ca.* 11 kJ/mol, which corresponds to $s = 100$ at room temperature) when the second section is horizontal (the slope is of order of $0.01 \mu\text{mol}^{-1}$) or low when the second section slope can be determined with reasonable accuracy (it is of order of $0.1 \mu\text{mol}^{-1}$).

(3) The slope of the section corresponding to strong silanols is a measure of their adsorption energy, but in practice it can only be used to compare sorbents.

EXPERIMENTAL

An attempt to apply the LPT method to a system with a liquid mobile phase (LiChrosorb C₁₈ + hexane) was also made.

Apparatus and materials

Chromatographic measurements were performed using a chromatograph consisting of an HPP-4001 syringe pump, LC-2563 UV detector (Laboratorní Přístroje, Prague, Czechoslovakia) and Rheodyne Model 7120 injection valve. LiChrosorb Si-100 C₁₈ packings^a were synthesized in our laboratory using monochlorodimethyloctadecylsilane in the presence of the activator, morpholine dissolved in dry toluene (1:1) [28,29], and a high coverage density, $\alpha_{RP} = 3.5\text{--}3.55 \mu\text{mol}/\text{m}^2$, was obtained. The specific surface area of the bare silica (measured by a sorptomatic method) was *ca.* 300 m²/g. In order to reveal potential differences in the adsorption activities of the tested packings, two types of LiChrosorb Si-100 (with mean particle diameter 10 μm), *i.e.*, untreated and hydrochloric acid washed, were used. The hydrochloric acid (1:1) washing was performed at its boiling temperature in Soxhlet apparatus (a thin layer of adsorbent) for 1 week. Then the packing samples were washed with distilled water (two portions of fresh water per day) until the pH of the water did not change. This procedure required a long time of operation (*ca.* 3 weeks).

Columns of 100 \times 4 mm I.D. contained the same amount of packing.

Liquid-phase titration procedure

The investigated columns were flushed with acetone and hexane (*ca.* 50-ml portions) at 320 K, then thermostated (water-jacket) at 306 K. Hexane containing 20 ppm of water was used as the mobile phase at a flow-rate of 1 ml/min. The UV detector was operated at 254 nm and its sensitivity was 0.01 a.u.f.s.

When a stable baseline was obtained, pure butylamine was injected. During the elution of the amine from the column, 10- μl portions of 0.5% ethyl methyl ketone in hexane were injected. For each amine injection the shortest ketone retention time was found. Dead volumes were determined by means of butylbenzene and values of 1.03 and 1.04 ml were obtained for packings based on untreated and acid-washed silica, respectively.

RESULTS AND DISCUSSION

The chromatographic titration curves for both packings are presented in Fig. 4. The inflection points correspond to 0.04 and 0.06 $\mu\text{mol}/\text{m}^2$ and the slope ratios obtained for packings based on untreated and washed silica are 10 and 70, respectively. The shape of the titration curve for untreated silica gel and the low slope ratio seem to indicate the existence of two types of strong adsorption centre differing slightly in adsorption energy. Another inflection point may be expected which is connected with blocking of all strong adsorption centres. We can estimate its position at *ca.* 0.15 $\mu\text{mol}/\text{m}^2$ of amine. This value cannot be obtained from the data presented here but on the basis of other results we can expect the value of k'/S_{BET} to be close to 0.025 m⁻² starting from an amount of injected amine equivalent to all strong adsorption sites. In such a case acid washing of the silica gel would reduce the number of strong

^a The commercial trade name of the RP packing material produced by Merck is LiChrosorb RP-18. We have synthesized our packing material on the basis of commercially available LiChrosorb Si-100 using monochlorodimethyloctadecyl silane, without endcapping. It differs from LiChrosorb RP-18 but we use a similar (not the same) name to express its origin and properties.

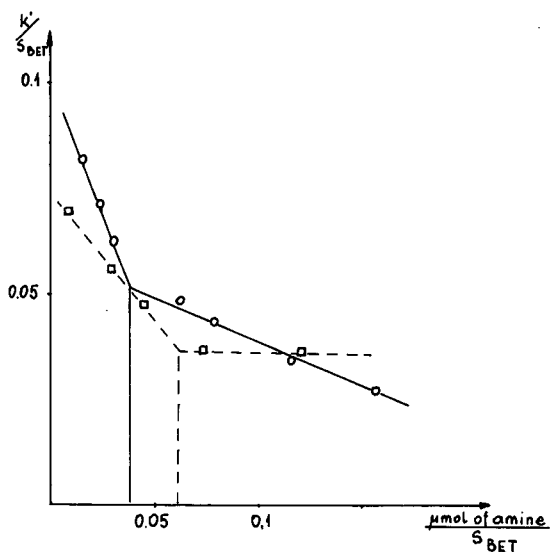


Fig. 4. Experimental LPT curves for (□) acid-washed and (○) untreated LiChrosorb C_{18} .

silanols by a factor of 2.5. This estimation is confirmed by the amine peak shapes presented in Fig. 5 and the way in which pyridine was eluted from the column. Additionally, 1 μ l of pure pyridine was injected onto each column. For the acid-washed silica 110 ml of hexane were sufficient for its complete elution from the column. The peak descent to the baseline was clearly seen at a sensitivity of 0.01 a.u.f.s. With the untreated silica 200 ml of hexane could not elute pyridine completely and a clear descent of the peak to the baseline was not observed.

The density of coverage of the two packings and their surface areas per column are almost the same, so its is difficult to explain why the curves in Fig. 4 intersect. For

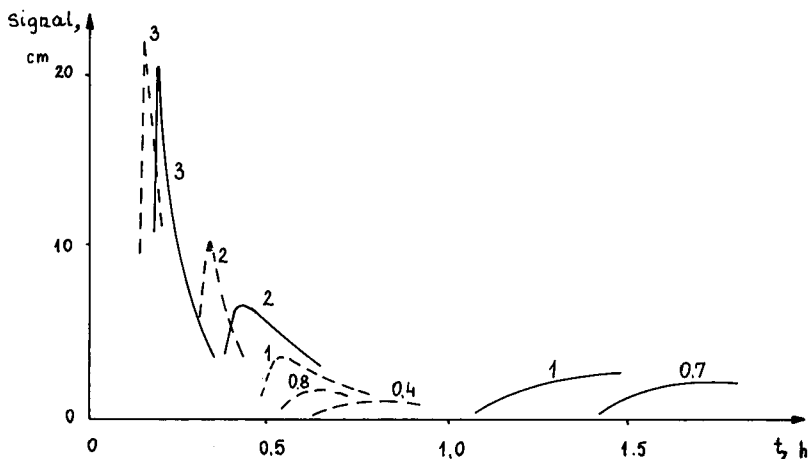


Fig. 5. *n*-Butylamine peak shapes for (dashed line) acid-washed and (solid line) untreated LiChrosorb C_{18} . Numbers indicate injected amine volumes (μ l). 0.01 a.u. = 20 cm.

large amounts of injected amine the two curves should have horizontal parts at the same level. If there are no errors in the surface and coverage density determinations, this result seems to indicate an increase in the degree of surface hydroxylation after acid washing. This supposition, of course, needs further experimental evidence for confirmation.

CONCLUSIONS

The description of chromatographic titration presented here, in spite of its simplification, permits a quantitative evaluation of the main assumptions in the method. The position of the inflection point for the LPT curve should give precisely the strong adsorption centre fraction, but the slope of a particular section of the curve allows us only to distinguish between strong and weak centres.

Although LPT is time consuming and requires a large amount of hexane, it seems to be promising for the evaluation of HPLC packings. In comparison with gas-phase titration new problems appear: (1) the water adsorbed on the sorbent (we used hexane in equilibrium with atmospheric water vapour) partially deactivates the column and hinders the measurement of the effect of the injection of a small amount of a "blocker"; (2) the lower detection sensitivity and thus the necessity for the injection of a larger amount of "marker"; and (3) in some instances the "marker" tail is eluted too slowly and can deactivate the column.

REFERENCES

- 1 M. I. Hair and W. Hertl, *J. Phys. Chem.*, 70 (1969) 4269.
- 2 M. L. Mueller, R. W. Linton, G. E. Maciel and B. L. Hawkins, *J. Chromatogr.*, 319 (1983) 9.
- 3 M. I. Hair and W. Hertl, *J. Phys. Chem.*, 74 (1970) 91.
- 4 D. W. Sindort and G. E. Maciel, *J. Phys. Chem.*, 86 (1982) 5208.
- 5 D. B. Marshall, K. A. Stutter and C. G. Lochmueller, *J. Chromatogr. Sci.*, 22 (1984) 217.
- 6 D. B. Marshall, C. L. Cole and D. E. Conolly, *J. Chromatogr.*, 361 (1986) 71.
- 7 D. B. Marshall, C. L. Cole and D. A. Norman, *J. Chromatogr. Sci.*, 25 (1987) 262.
- 8 L. R. Snyder and J. W. Ward, *J. Phys. Chem.*, 70 (1966) 3941.
- 9 J. Koehler and J. J. Kirkland, *J. Chromatogr.*, 385 (1987) 125.
- 10 J. Koehler, D. B. Chase, R. D. Farlee, A. J. Vega and J. J. Kirkland, *J. Chromatogr.*, 352 (1986) 275.
- 11 M. Verzele and C. Dewaele, *J. Chromatogr.*, 217 (1981) 399.
- 12 P. C. Sadek, C. J. Koester and D. L. Bowers, *J. Chromatogr. Sci.*, 25 (1987) 489.
- 13 J. Nawrocki, *J. Chromatogr.*, 407 (1987) 171.
- 14 M. Verzele, M. DePotter and J. Ghyzels, *J. High Resolut. Chromatogr. Chromatogr. Commun.*, 2 (1979) 151.
- 15 M. Verzele, *LC Mag.*, 1 (1983) 217.
- 16 M. Verzele and C. Dewaele, *J. Chromatogr.*, 217 (1981) 399.
- 17 J. Nawrocki and B. Buszewski *J. Chromatogr.*, 449 (1988) 1.
- 18 J. Nawrocki, *J. Chromatogr.*, 391 (1987) 266.
- 19 J. Nawrocki, *J. Chromatogr.*, 407 (1987) 171.
- 20 J. Nawrocki, *Chromatographia*, 23 (1987) 722.
- 21 J. Nawrocki and B. Buszewski, *J. Chromatogr.*, 449 (1988) 1.
- 22 J. Nawrocki, *Chromatographia*, 23 (1987) 722.
- 23 J. Nawrocki, D. L. Moir and W. Szczepaniak, *Chromatographia*, 28 (1989) 139.
- 24 J. Nawrocki, D. L. Moir and W. Szczepaniak, *J. Chromatogr.*, 467 (1989) 31.
- 25 F. Riedo and E. Kováts, *J. Chromatogr.*, 239 (1982) 1.
- 26 I. Langmuir, *J. Am. Chem. Soc.*, 38 (1916) 2221; 40 (1918) 1361.
- 27 J. C. Giddings, *Dynamics of Chromatography. Part. I*, Marcel Dekker, New York, 1965.
- 28 B. Buszewski, A. Jurasek, J. Garaj, L. Nondek, J. Novak and D. Berek, *J. Liq. Chromatogr.*, 10 (1987) 2325.
- 29 Z. Suprynowicz, R. Lodkowski, B. Buszewski and K. Pilorz, presented at the 13th Symposium on Column Liquid Chromatography, Stockholm, June 25-30, 1989, poster M/TU-P-008.

CHROMSYMP. 2152

Optimization of ion chromatography

N. GROS and B. GORENC*

Department of Chemistry and Chemical Technology, University of Ljubljana, 61000 Ljubljana (Yugoslavia)

ABSTRACT

The strategy for planning ion chromatographic separations on a Dionex AS4A column was developed on the basis of the examination of the effect of NaHCO_3 , $\text{NaHCO}_3 + \text{Na}_2\text{CO}_3$ and Na_2CO_3 eluents on the retention times of chloride, bromide, sulphate, nitrite, nitrate and hydrogenphosphate. The suppressor limitations of increasing the eluent concentration, the upper eluent concentration limits of conductivity background stabilities, the upper concentration limits above which the anions are no longer well separated and the lower limits at which peaks become too wide or asymmetric were determined. On these bases the separation of other combination of anions can also be optimized.

INTRODUCTION

There are two specific characteristics of the Dionex 4000i ion chromatography system, a column and an anion micromembrane suppressor, both protected by a patent.

The first consequence of these characteristics is that one does not fill the columns with commercially available anion-exchange resins, but buys the column on the basis of the manufacturer's information about anions that can be separated on it and a description of the analytical problems that can be solved. For example, for so-called hydrophilic anions four Dionex columns, AS1, AS2, AS3 and AS4, are available [1], but for anions such as chloride, bromide, sulphate, nitrite, nitrate and hydrogenphosphate present in similar concentration ranges the AS4 column offers the best selectivity [2].

For work on such a column, the manufacturer provides not only a list of suitable eluents [3], but also a specific eluent composition ($[\text{NaHCO}_3 + \text{Na}_2\text{CO}_3] = 1.7 + 1.8 \text{ mmol/l}$) as being the best for the AS4A column. This eluent composition is probably an acceptable solution for many applications, but it is impossible for it to be the best for all of them. There is no doubt that the separation of all six of the mentioned anions is very good under these conditions. However, if the sample contains only three of them, *e.g.*, nitrite, nitrate and sulphate, the situation is different. These anions have very different retention times and there is no reason for the time of analysis to be so long, while the anions are not only well separated at shorter retention times but also their peaks are sharper, better defined and therefore more suitable for quantitative analysis.

Applications of the AS4A column using other eluent compositions have been reported [4–20], but they are of little practical value when we want to optimize the separation of a combination of anions that is not the same as any of those published. From particular applications we can only get an idea of trying another eluent and the only thing we know after each experimental step is the necessity to try another stronger or weaker eluent in the next one. However, solving an analytical problem by trial and error in this way can be very time consuming and there is no progress in problem solving from one combination of anions to another; the starting position remains the same all the time.

The aim of this work was to build up a background for planning the separations of different combinations of anions by establishing the effect of the concentrations of three eluents (NaHCO_3 , $\text{NaHCO}_3 + \text{Na}_2\text{CO}_3$ and Na_2CO_3) of increasing eluting strength on the retention behaviour of chloride, bromide, sulphate, nitrite, nitrate and hydrogenphosphate, which are common constituents of many different aqueous samples, and therefore to make it possible to solve different analytical problems more easily and effectively.

However, in our system not only the column but also the suppressor determines the limits of our examinations. The manufacturer suggests the operating conditions for this also. It is certain that the suppressor cannot compensate for the background conductivity of any eluent composition. The upper eluent concentration limits at which the instabilities of the background conductivity are still of such a magnitude that the chromatographic peaks can be recognized were determined for all three eluents used. From the methodological point of view this offers the possibility of making a decision about the suitability of the AS4A column for the determination of a component not previously examined after only one experimental step under extreme eluting conditions.

EXPERIMENTAL

Apparatus and experimental conditions

The Dionex 4000i ion chromatographic apparatus consisted of an AG4A guard column, an AS4A separation column, an anion micromembrane suppressor, and a conductimetric detector, with an injection volume of 50 μl , eluent flow-rate 2.0 ml/min, regenerant sulphuric acid concentration 12.5 mmol/l and regenerant flow-rate 2.8 ml/min. A Spectra-Physics SP 4290 integrator was used.

Reagents and procedures

All solutions and eluents were prepared from analytical-reagent grade chemicals using deionized water obtained from a Milli-Q water purification system (Millipore, Bedford, MA, U.S.A.). All salts were in the sodium form to avoid any effect of different cations.

Six stock solutions, each with an anion concentration of 1 g/l, were used and all the working solutions listed in Table I were prepared from them.

A comparison was made between the retention times of all six anions obtained with solutions prepared from only one salt and a solution with a mixture of all six anions. No significant differences were found so all subsequent experiments were performed with a mixture of all six anions.

TABLE I
WORKING SOLUTIONS

Solution	Cl ⁻ (mg/l)	Br ⁻ (mg/l)	SO ₄ ²⁻ (mg/l)	NO ₂ ⁻ (mg/l)	NO ₃ ⁻ (mg/l)	HPO ₄ ²⁻ (mg/l)
A	2.5	—	—	—	—	—
B	—	7	—	—	—	—
C	—	—	7	—	—	—
D	—	—	—	4.5	—	—
E	—	—	—	—	6	—
F	—	—	—	—	—	15
G	2.5	7	7	4.5	6	15

Two stock eluent solutions, 100 mmol/l NaHCO₃ and 100 mmol/l Na₂CO₃ were used. All other eluent compositions were prepared in the chromatographic system by mixing these two solutions with deionized water obeying the microprocessor program.

RESULTS AND DISCUSSION

The results of examination of the effects of NaHCO₃, NaHCO₃ + Na₂CO₃ and Na₂CO₃ eluent concentrations on the retention times of chloride, bromide, sulphate, nitrite, nitrate and hydrogenphosphate are presented in Figs. 1–3. It is evident that the retention behaviour of anions is much more alike when Na₂CO₃ or NaHCO₃ + Na₂CO₃ is used, than with NaHCO₃ as the eluent. With the first two eluents the retention times of all six anions are very similar and relatively short after a small increase of eluent concentration, whereas with NaHCO₃ the anions remain well separated at all concentrations. Hence already from the graphical presentation of the results it can be concluded that the usable eluent concentration range is the widest when using NaHCO₃ as eluent, but on the basis of the chromatograms and integrator

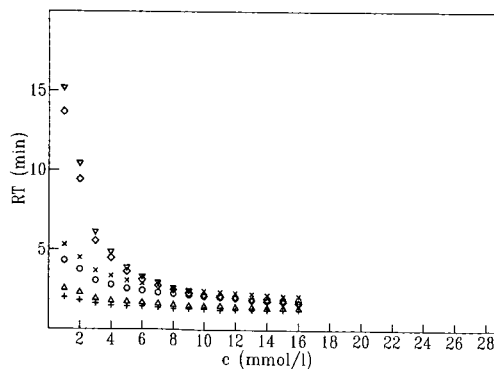


Fig. 1. Effect of Na₂CO₃ eluent concentration on the retention times (RT) of anions. + = Cl⁻; Δ = NO₂⁻; ○ = Br⁻; × = NO₃⁻; ∇ = HPO₄²⁻; ◇ = SO₄²⁻.

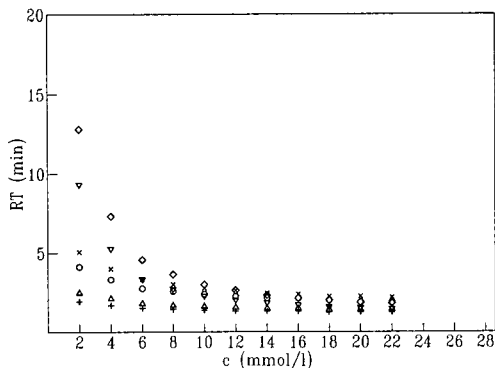


Fig. 2. Effect of $\text{NaHCO}_3 + \text{Na}_2\text{CO}_3$ eluent on the retention times of anions. The concentrations represent the total concentration of the two constituents, which were always present in equal amounts. Symbols as in Fig. 1.

baseline codes fairly specific concentration limits for all three eluents can be determined.

Eluent concentration limits for the separation and determination of all six anions

In the Introduction it was mentioned that the suppressor determines the limit of increase in eluent concentration while above this limit the background conductivity becomes completely unstable, the chromatograms become unrepeatable and peaks can no longer be recognized. However, the concentration limit under which an eluent can be used is also eluent dependent. From Fig. 4, which shows the effect of eluent concentration on the background conductivity, the upper limits of usable concentration ranges for all three eluents can be determined as 16 mmol/l for Na_2CO_3 , 22 mmol/l for $\text{NaHCO}_3 + \text{Na}_2\text{CO}_3$ and 28 mmol/l for NaHCO_3 .

The background conductivity also becomes unstable below these concentrations, but it has no effect on peak recognition; however, it is important because it impedes the accurate determination of anion concentrations. These eluent concentra-

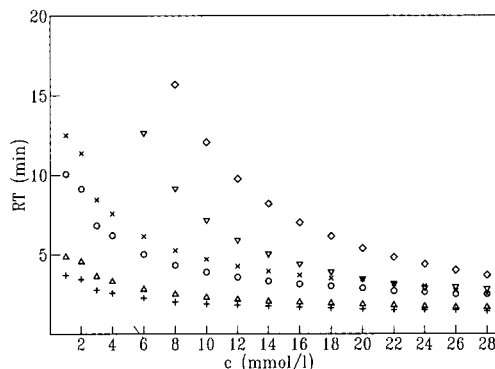


Fig. 3. Effect of NaHCO_3 eluent concentration on the retention times of anions. Symbols as in Fig. 1.

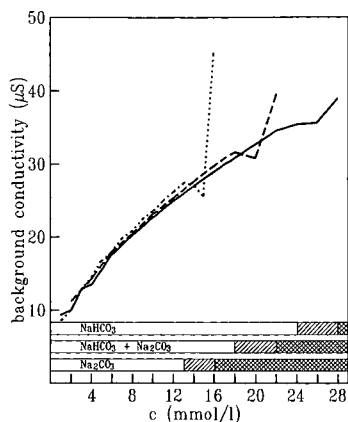


Fig. 4. Dependence of the background conductivity on the concentrations of the three eluents. The bands are divided into three parts. From left to right there is a range of stable background conductivity, a range of small instability and a range of completely unstable background conductivity. Solid line, NaHCO_3 , dotted line, Na_2CO_3 ; dashed line, $\text{NaHCO}_3 + \text{Na}_2\text{CO}_3$.

tion limits of unstability of the background conductivity which can be seen from Fig. 4 are 13 mmol/l for Na_2CO_3 , 18 mmol/l for $\text{NaHCO}_3 + \text{Na}_2\text{CO}_3$ and 24 mmol/l for NaHCO_3 .

However, for the successful separation of the six anions two eluent concentration limits already mentioned are not very important, because at such high eluent concentrations the anions are no longer well separated. Hence the limit which has to be considered now is not the limit of the available eluent concentration range but the limit of the suitable eluent concentration range. From this point of view it can be seen that Na_2CO_3 is unsuitable for the separation of this mixture as sulphate and hydrogenphosphate are unseparated over the whole eluent concentration range. In contrast, all the anions can be successfully separated using $\text{NaHCO}_3 + \text{Na}_2\text{CO}_3$ below 6 mmol/l and NaHCO_3 below 18 mmol/l.

There is also a lower limit to the eluent concentration because the peaks become too wide or very asymmetric and their determination becomes unreliable. The lower limits of eluent concentrations for different anions and also previously mentioned upper limits of usable eluent concentration ranges are shown in Fig. 5. The results offer the possibility of planning a successful separation and determination of all six anions in mixtures under different conditions.

Possibilities for planning the separations of other combinations of anions

There are generally two cases of other combinations of anions, one when the mixture contains only some of above-mentioned anions and the other when the mixture contains not only some of these anions but also other anions that have not been examined. Before describing the methodology for solving these two types of analytical problems, two approaches that were developed for this purpose should be described. Fig. 6 offers the possibility, for a combination of anions, of answering the question of whether they are separated under selected eluting conditions. Further, on

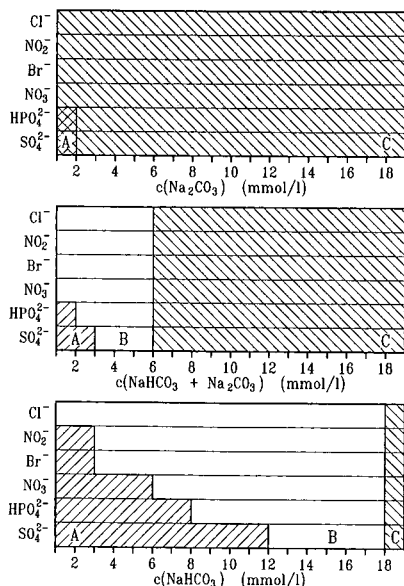


Fig. 5. Usable concentration ranges for the separation of all six anions (B). A, Peaks are too wide or asymmetric; C, not all of the six peaks are separated.

the basis of Fig. 7, the elution sequence of anions under these conditions can be predicted.

On these bases, the separation of any combination of examined anions can easily be optimized and the separation conditions can be simply predicted. Na_2CO_3 will probably be more suitable for the elution of anions with very long or very different retention times. On the other hand, NaHCO_3 will probably offer the best possibilities for the elution of anions with very short or very similar retention times. Because

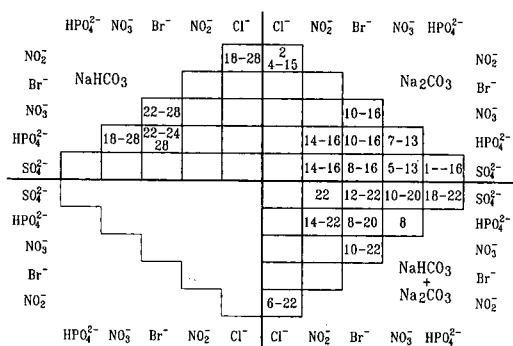


Fig. 6. Eluent concentrations at which the combinations of anions are not separated. Empty boxes represent anions that are well separated over the whole eluent concentration range. Numbers in boxes represent eluent concentrations (mmol/l) at which two ions are not separated. The basis for the decision as to whether ions were separated and not separated were the integrator's baseline codes (BC) present in each chromatographic report (BC : 01 - separated).

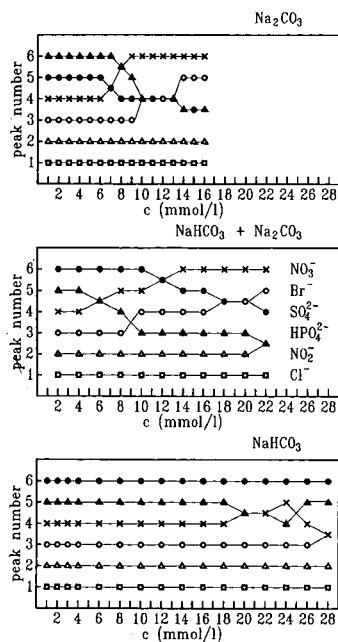


Fig. 7. Effect of eluent concentration on the elution sequence of anions.

of its very wide usable concentration range, it could also be the most suitable for planning gradient elution separations.

The results can also be helpful for the optimization of a mixture that also contains other anions, but some additional experiments would be necessary. First the usability of the AS4A column for the determination of an anion has to be established, suitable eluting conditions for this anion have to be determined and then combined with the optimum separating conditions for other anions.

REFERENCES

- 1 J. Weiss, *Handbook of Ion Chromatography*, Dionex, Sunnyvale, CA, 1986, p. 35.
- 2 J. Weiss, *Handbook of Ion Chromatography*, Dionex, Sunnyvale, CA, 1986, p. 25.
- 3 J. Weiss, *Handbook of Ion Chromatography*, Dionex, Sunnyvale, CA, 1986, p. 28.
- 4 J. Weiss, *Handbook of Ion Chromatography*, Dionex, Sunnyvale, CA, 1986, p. 58.
- 5 J. Weiss, *Handbook of Ion Chromatography*, Dionex, Sunnyvale, CA, 1986, p. 59.
- 6 J. Weiss, *Handbook of Ion Chromatography*, Dionex, Sunnyvale, CA, 1986, p. 60.
- 7 J. Weiss, *Handbook of Ion Chromatography*, Dionex, Sunnyvale, CA, 1986, p. 64.
- 8 J. Weiss, *Handbook of Ion Chromatography*, Dionex, Sunnyvale, CA, 1986, p. 65.
- 9 J. Weiss, *Handbook of Ion Chromatography*, Dionex, Sunnyvale, CA, 1986, p. 191.
- 10 J. Weiss, *Handbook of Ion Chromatography*, Dionex, Sunnyvale, CA, 1986, p. 192.
- 11 J. Weiss, *Handbook of Ion Chromatography*, Dionex, Sunnyvale, CA, 1986, p. 204.
- 12 J. Weiss, *Handbook of Ion Chromatography*, Dionex, Sunnyvale, CA, 1986, p. 206.
- 13 *Dionex Application Note, An 49*, Dionex, Sunnyvale, CA, 1983.
- 14 *Dionex Application Note, An 50*, Dionex, Sunnyvale, CA, 1983.
- 15 *Dionex Application Update, Au 102*, Dionex, Sunnyvale, CA, 1987.
- 16 *Dionex Application Note, An 24*, Dionex, Sunnyvale, CA, 1988.
- 17 *Dionex Application Update, Au 113*, Dionex, Sunnyvale, CA, 1989.
- 18 J.-F. Jen, K. E. Daugherty and J. G. Tarter, *J. Chromatogr. Sci.*, 27 (1989) 504.
- 19 A. Clossen, W.-D. Miersch and A. Hesse, *J. Clin. Chem. Clin. Biochem.*, 28 (1990) 91.
- 20 *Soil, Water and Plant Analysis by Ion Chromatography*, Dionex, Sunnyvale, CA.

CHROMSYMP. 2278

Carbohydrate analysis with ion chromatography using Eurokat stationary phases

Preparative separation of monosaccharides and their fluorinated derivatives

FRANZ OBERDORFER*

Deutsches Krebsforschungszentrum, Institut für Radiologie und Pathophysiologie, im Neuenheimer Feld 280, D-6900 Heidelberg (Germany)

KATHARINA KEMPER, MICHAEL KALEJA and JOACHIM REUSCH

Knauer Säulentechnik GmbH, Hegauer Weg 38, D-1000 Berlin 37 (Germany)

and

KLAUS GOTTSCHALL

Eurochrom Herstellungsgesellschaft Chromatographischer Produkte Dr. Ing. H. Knauer GmbH, Hegauer Weg 38, D-1000 Berlin 37 (Germany)

ABSTRACT

The interaction of weakly acidic monosaccharides with a polystyrene sulphonate in the H⁺ form resulted in unexpected selectivity for epimeric aldohexoses, deoxyaldohexoses and deoxyfluoroaldohexoses. This led to a new application of high-performance liquid chromatography. The separation is dominated solely by the electrostatic interaction between carbohydrate oxygen atoms and H⁺ of the stationary phase. Column heating was not required. High flow-rates in excess of 7 ml/min were possible, thus allowing preparative separations. Examples include 2-deoxy-2-fluoro-D-glucose, 2-deoxy-2-fluoro-D-mannose and 2-deoxy-2-fluoro-D-galactose.

INTRODUCTION

Synthetic fluorinated carbohydrate analogues (*e.g.*, Fig. 1) offer unique advantages for studies on the carbohydrate biochemical pathways by non-invasive techniques using ¹⁹F NMR spectroscopy or positron emission tomography from ¹⁸F-labelled compounds. For example, the replacement of the hydroxyl group at the C-2 of D-galactose with fluorine permitted studies of the *in vivo* metabolism of 2-deoxy-2-fluoro-D-galactose [1]. It was confirmed by *in vivo* studies that 2-deoxy-2-fluoro-D-galactose has potential as a UTP-depleting chemotherapeutic agent in D-galactose-metabolizing tumours such as hepatocellular carcinoma. The compound also may be used at tracer doses as a diagnostic agent, *in vivo* or *in vitro* pinpointing defects of enzymes in galactosaemia [1].

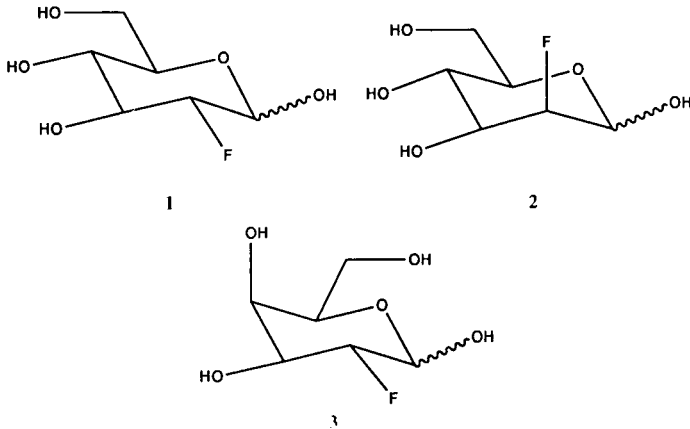


Fig. 1. Fluorination of tri-O-acetyl-D-galactose or -glucose using fluorine diluted to 5% in neon yielded compounds 1, 2 and 3. The reaction is the most straightforward preparation of 2-deoxy-2-fluoro-D-galactose (3), but its isolation and purification was previously tedious.

The chemical and biochemical aspects of these fluorinated carbohydrates and their syntheses by various chemical procedures have been described [2].

It must be noted that particular efforts are necessary in the preparation and purification of fluorinated carbohydrates. These difficulties in synthetic chemistry persisted in chromatography. As fluorinated carbohydrates are used as diagnostic agents in the human body when labelled with the radioactive isotope ^{18}F , it was of crucial importance to provide very pure compounds. Thus a chromatographic procedure was required for the analytical and preparative separation of such mixtures. Consequently, our studies were focused on efficient analytical procedures for the separation of ^{18}F -labelled tracers, on reliable quality control procedures for deoxyfluoroaldohexoses and on practical methods for the isolation of deoxyfluoroaldohexoses on a semi-preparative scale. A high selectivity for epimeric compounds was required, allowing the determination of 2-deoxy-2-fluoro-D-glucose, 2-deoxy-2-fluoro-D-mannose, 2-deoxy-2-fluoro-D-galactose and 2-deoxy-2-fluoro-D-talose in multi-component mixtures. The eluent should preferably be compatible with physiological fluid and high flow-rates should be possible.

EXPERIMENTAL

Fluorinated carbohydrates were prepared routinely by fluorination of unsaturated 3,4,6-tri-O-acetyl derivatives using molecular fluorine diluted in an inert gas [3]. The acidic aqueous solution of products, after hydrolysis with 1 *M* hydrochloric acid, was neutralized using AG1-X8 anion-exchange resin (Bio-Rad Labs.) in the OH^- form. Chromatography was run on a Waters 600 multi-solvent delivery system using manual injection (U6K injector). Detection was usually effected with a Waters 410 differential refractometer at 35°C. The columns used were 30 cm \times 8 mm I.D. and 25 cm \times 32 mm I.D., packed by Eurochrom Knauer (Berlin, Germany) with an improved 9% cross-linked polystyrene sulfonate resin in the H^+ form as stationary

phase. Standard chromatographic conditions employed were 0.8 ml/min with water at room temperature in analytical applications and 7 ml/min with water in preparative applications. Low carbohydrate concentrations were detected by a pulsed amperometric detector (Dionex) with post-column addition of 0.5 M sodium hydroxide solution at 1 ml/min; the detector settings were $E_1 = 0.06$ V, $E_2 = 0.6$ V and $E_3 = 0.8$ V with pulse durations of 300, 120 and 300 ms respectively.

RESULTS

Analytical and preparative chromatography of raw material, which was obtained by fluorination of 3,4,6-tri-O-acetyl-D-galactal is shown in Fig. 2. The preparative run yielded 680 mg of pure 2-deoxy-2-fluoro-D-galactose and 400 mg of pure 2-deoxy-D-galactose (Fig. 2a); the sample load was 2.5 g of raw material in 4 ml of water. The retention time for 2-deoxy-2-fluoro-D-galactose was 27 min. Re-injection of an aliquot under analytical conditions gave the chromatogram in Fig. 2b. A specific identity test by ^1H NMR confirmed that a purity of $\geq 98\%$ was obtained for 2-deoxy-2-fluoro-D-galactose. It was the first time that this compound could be obtained without further purification steps in such quality from the above-mentioned preparation procedure.

Although fluorine is considered in carbohydrates to be an isosteric substitute for hydrogen, the differences in hydrogen bonding and electronegativity make it more like a hydroxyl group. The strong electrostatic interaction of the fluorine substituent at C-2 with the anomeric effect suggested a variety of conformationally clearly different molecules, to which ligand-exchange chromatography with H^+ as counter ion

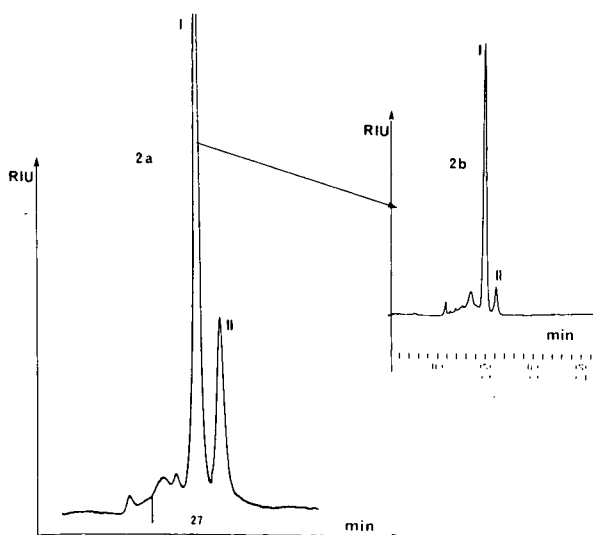


Fig. 2. (a) Preparative and (b) analytical high-performance liquid chromatography of 2-deoxy-2-fluoro-D-galactose, peak I. Peak II is 2-deoxy-D-galactose. As known from previous works [3], 2-deoxy-2-fluoro-D-idose and 2-deoxy-2-fluoro-D-gulose are minor impurities in the reaction mixture. These compounds are not mentioned here. Their enrichment is possible using Eurokat H^+ and peak shaving techniques.

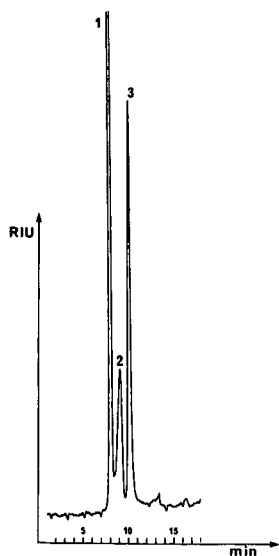


Fig. 3. Ligand-exchange chromatography of a mixture of epimeric 2-deoxy-2-fluoro-D-aldohexoses on a commercial 300×8 mm I.D. Eurokat H^+ column at room elution with water at 0.8 ml/min. Peaks: 1 = 2-deoxy-2-fluoro-D-glucose (capacity factor, $k' = 0.47$); 2 = 2-deoxy-2-fluoro-D-mannose ($k' = 0.69$); 3 = 2-deoxy-2-fluoro-D-galactose ($k' = 0.84$).

may apply. This could be demonstrated in this work. The separation of the epimeric aldohexoses and fluorodeoxyaldohexoses was dominated by hydrogen-bonding interactions between carbohydrate oxygen and carbohydrate fluorine atoms and H^+ of the stationary phase. The contribution of size-exclusion mechanisms to the separation was neglected in this investigation with monosaccharides as the only components. As mutarotation is catalysed by H^+ , and the rates of partitioning between the stationary phase and the mobile phase are fast when only hydrogen bonding is involved, no column heating is required for speeding up the exchange kinetics. An excellent selectivity (Fig. 3) was obtained for the three 2-deoxy-2-fluoroaldohexoses in Fig. 1.

CONCLUSIONS

A convenient resin-based procedure for analytical and preparative carbohydrate separation by high-performance liquid chromatography has been developed. The direction and stereospecificity of interaction with the stationary phase is dominated by hydrogen bonding. The method is characterized by its simplicity despite its broad applicability. Tedious column conditioning does not interfere with routine analytical applications. The column material also allows preparative carbohydrate separations at a high flow-rate. The eluate is compatible with physiological fluid and can be recommended for radiopharmaceutical and pharmaceutical preparations. The application should therefore be in accordance with the EEC Directive on finished product specifications for drug compounds.

Excellent selectivity has been achieved for epimeric 2-deoxy- and 2-deoxy-2-fluorohexoses, but the procedure applies also to other fluorinated derivatives. The k' values are given in Fig. 3.

REFERENCES

- 1 B. R. Grün, U. Berger, F. Oberdorfer, W. E. Hull, H. Ostertag, E. Friedrich, J. Lehmann and D. Keppler, *Eur. J. Biochem.*, 190 (1990) 11.
- 2 N. F. Taylor (Editor), *Fluorinated Carbohydrates. Chemical and Biochemical Aspects (American Chemical Society Symposium Series, No. 374)*, American Chemical Society, Washington, DC, 1988.
- 3 F. Oberdorfer, B.-C. Traving, W. Maier-Borst and W. E. Hull, *J. Labelled Compd. Radiopharm.*, 25 (1988) 465.

CHROMSYMP. 2246

Reversed-phase liquid chromatography coupled on-line with capillary gas chromatography

I. Introduction of large volumes of aqueous mixtures through an on-column interface

E. C. GOOSENS*, D. DE JONG, J. H. M. VAN DEN BERG and G. J. DE JONG

DUPHAR BV, Analytical Development Department, P.O. Box 900, 1380 DA Weesp (The Netherlands)
and

U. A. Th. BRINKMAN

Free University, Department of Analytical Chemistry, de Boelelaan 1083, 1081 HV Amsterdam (The Netherlands)

ABSTRACT

The feasibility of on-line reversed-phase liquid chromatography (LC)–capillary gas chromatography (GC) using an on-column interface was investigated. Large volumes of acetonitrile–water mixtures were introduced into a retention gap which was coated with a very thin film of Carbowax. The retention gap was tested regularly after repeated acetonitrile–water injections; its lifetime was several months. The maximum water content in the eluent must be close to that in the azeotropic mixture, otherwise water which is left in the gap after evaporation of the azeotropic mixture will distort the analysis. An acetonitrile–water mixture allows the introduction of 20–40 μl with an introduction speed of up to 100 $\mu\text{l}/\text{min}$ by using the retention gap technique. This means that 1 mm I.D. LC columns can be used in on-line reversed-phase LC–capillary GC work.

INTRODUCTION

Capillary gas chromatography (GC) is the separation method of choice for the trace-level analysis of complex mixtures because good separation efficiencies can be obtained and sensitive detectors are available. Sample pretreatment techniques are highly important in capillary GC. There are several pretreatment techniques and the difference in volatility and polarity between solutes and solvents generally is the fundamental factor determining the method of choice. Liquid chromatography (LC) is one of these techniques and is a very powerful tool for prepreparing complex samples. Coupled LC–GC is probably the most efficient method for determining trace compounds in a complex mixture, mainly because it involves direct transfer of relevant LC fractions into the GC system. Generally two types of interfaces are used for

LC–GC, *viz.*, an on-column interface for relatively volatile components and a loop-type interface which is mostly applied for less volatile components. Details of these interfaces have been reported elsewhere [1–6].

Many papers have been published on LC–GC applications. Almost all these applications and other LC–GC work have involved normal-phase LC–GC [7]. As about 80% of all LC analyses are performed using reversed-phase systems, there is growing interest in the on-line coupling of reversed-phase LC with GC. The large-volume introduction of polar solvents is more difficult than that of apolar solvents because of the poor wettability of most retention gaps by polar solvents; this is especially true for water, which does not wet surfaces suitably deactivated for GC use. In addition, water forms a very large volume of vapour per unit of liquid and it is a very poor solvent for creating useful solvent effects [8]. Some reversed-phase LC–GC applications have been mainly reported using fully concurrent solvent evaporation, because then there is no need to form a sample film [9–11]. However, the transfer of aqueous eluents using fully concurrent solvent evaporation requires large temperature differences between the transfer step and the elution of the first sharp peak. This means that only very high-boiling solutes can be assayed.

Recently, Grob and Li [12] reported on the wettability of silylated retention gap surfaces by various mixtures of organic solvents and water. They found that deactivation with diphenyltetramethyldisilazane (DPTMDS) produced surfaces with good wettability characteristics. They did not test the wettability of Carbowax-deactivated retention gaps, because they were unable to bind Carbowax to the surface in such a way that it was not removed after a few injections [13]. However, our preliminary results indicated that a Carbowax-deactivated retention gap is appropriate for the introduction of acetonitrile–water mixtures, whereas the DPTMDS-deactivated retention gap did not function satisfactorily either for several model components [14] or for the drug idaverine in an acetonitrile–water mixture [15]. Cortes and co-workers [11,16] investigated the possibility of injections of up to 20 μl of acetonitrile–water mixtures using a non-deactivated fused-silica retention gap, and contrary to our results with raw fused silica [14], this approach worked satisfactorily. This indicates that the selection of an appropriate retention gap for the introduction of aqueous mixtures is still not unambiguous.

In this study, we extended the experiments with the Carbowax-coated retention gap and examined the practicability of large-volume injections (8–40 μl) of acetonitrile–water mixtures into a capillary GC column using the retention gap technique. The influence of the composition of the acetonitrile–water mixture on the peak shape and peak area of solutes and the lifetime of the retention gaps were studied. As it is our final aim to use reversed-phase LC coupled on-line with capillary GC, the eluent introduction speed and introduction volume into the GC system were varied in order to investigate the largest allowable dimensions of the LC column.

EXPERIMENTAL

Equipment

A Phoenix 20 syringe pump (Carlo Erba, Milan, Italy) was used for solvent delivery. A Rheodyne (Cotati, CA, U.S.A.) six-port switching valve was inserted at the outlet of the LC column to lead the eluent either to the UV detector (Jasco,

Tokyo, Japan) or to the gas chromatograph via a fused-silica interface (30 cm \times 75 μm I.D.). Injections on to the LC column can be made by means of a Rheodyne injection valve. In this study, an LC column was not used, so the outlet of the Phoenix pump was connected directly to the Rheodyne switching valve. The GC system consisted of two Carlo Erba gas chromatographs, *viz.*, a 5300 Mega Series gas chromatograph equipped with a cold on-column autosampler (AS550, Carlo Erba) in which the retention gap was installed, and a Vega gas chromatograph equipped with a flame ionization detector for the analytical column. The gas chromatographs were connected with each other by a temperature-controlled interface.

The retention gap used was a fused-silica wide-bore precolumn coated with a very thin film of CPWax 52 CB (2–5 m \times 0.53 mm I.D., film thickness 0.025 μm) from Chrompack (Middelburg, The Netherlands). The analytical column was either a 25 m \times 0.32 mm I.D. CPWax 52 CB fused-silica column with a film thickness of 1.6 μm (Chrompack) or a 30 m \times 0.32 mm I.D. DB-1 fused-silica column with a film thickness of 0.25 μm (J&W, Folsom, CA, U.S.A.).

The two-oven system allows us the temperatures of the retention gap and the analytical column to be programmed independently of each other. This means that solutes that elute only at very high temperatures (*e.g.*, idaverine, which elutes at 325°C) can also be determined in spite of the maximum operating temperature of a Carbowax retention gap being 225°C. The two-oven system can also be used to create a cold trapping effect at the entrance of the separation column.

Chemicals

The Grob test mixture from Alltech (Deerfield, IL, U.S.A.) contained 53.0 mg/l of 2,3-butanediol, 28.3 mg/l of *n*-decane, 35.5 mg/l of 1-octanol, 32.0 mg/l of 2,6-dimethylphenol, 40.0 mg/l of nonanal, 28.7 mg/l of *n*-undecane, 31.3 mg/l of 2,6-dimethylaniline, 38.0 mg/l of 2-ethylhexanecarboxylic acid, 42.3 mg/l of methyl decanecarboxylate, 31.3 mg/l of dicyclohexylamine, 41.9 mg/l of methyl undecanecarboxylate and 41.3 mg/l of methyl dodecanecarboxylate in dichloromethane. Acetonitrile was of high-performance liquid chromatographic grade (Baker, Deventer, The Netherlands). Idaverine was obtained from Duphar (Weesp, The Netherlands). All other chemicals were of analytical-reagent grade.

Variation of eluent composition

Acetonitrile–water mixtures containing 0.02 mg/ml each of naphthalene, biphenyl, phenanthrene and acetanilide were introduced into the GC system by the Phoenix LC pump, which was connected directly with the Rheodyne switching valve. The acetonitrile–water ratio was varied from 84:16 to 50:50. The eluent flow-rate (introduction speed) was 25 $\mu\text{l}/\text{min}$ and the injection time 45 s. The analytical column was the CPWax 52 CB column (25 m \times 0.32 mm I.D., $d_f = 1.6 \mu\text{m}$). The inlet pressure was 100 kPa (helium) and the inlet temperature was 70°C. After 45 s the temperature was raised to 85°C and, after elution of the solvent peak, further to 225°C at 30°C/min. The retention gap (see above) had a length of 2 m.

The above experiment was repeated with the 30 m \times 0.32 mm I.D. DB-1 column ($d_f = 0.25 \mu\text{m}$), now using the two-oven system. The temperature programme of the Mega gas chromatograph (T_1) was 80°C for 4 min, increased to 200°C at 30°C/min, and that of the Vega oven (T_2) was 60°C for 12 min, increased to 200°C at

30°C/min. The temperature of the oven interface was 200°C. The injection time was 10 or 20 s and the eluent flow-rate was 25 $\mu\text{l}/\text{min}$. The retention gap was the same as in the earlier experiments.

Retention gap test

The retention gaps were tested using the Grob test mixture containing compounds which vary widely in polarity and volatility. The test mixture was diluted 10-fold in *n*-hexane and 1 μl was injected on-column onto the retention gap. The analytical column used was the 30 m \times 0.32 mm I.D. DB-1 column ($d_f = 0.25 \mu\text{m}$). Helium was used as the carrier gas with a column pressure of 95 kPa. The temperature was programmed from 40 to 120°C at 1°C/min.

Variation of introduction speed and introduction volume

A solution of 10 $\mu\text{g}/\text{ml}$ of idaverine in acetonitrile–water (90:10) containing 0.1% of triethylamine was introduced into the GC system at speeds varying from 20 to 100 $\mu\text{l}/\text{min}$. The injection volumes were varied from 20 to 40 μl . The inlet pressure was 150 kPa (helium). During the introduction of the idaverine solution, T_1 was 90°C and T_2 220°C. After solvent evaporation, T_1 was immediately raised to 220°C at 30°C/min, but T_2 was kept at 220°C for a further 15 min to await complete reconcentration of idaverine at the inlet of the analytical column; it was then raised to 325°C at 30°C/min. The analytical column was a 30 m \times 0.32 mm I.D. DB-1 column ($d_f = 0.25 \mu\text{m}$). The retention gap had a length of 5 m.

RESULTS AND DISCUSSION

Variation of eluent composition

Acetonitrile and water in the volume-to-volume ratio 84:16 form an azeotropic mixture, which has a boiling point of 76°C at atmospheric pressure. Introduction of water containing solvent mixtures in a retention gap seems to be feasible for azeotropic mixtures and for mixtures containing less water, because with such mixtures no water will remain in the retention gap after evaporation [12].

In a first series of experiments, using a thick-film CPWax 52 CB column and 20- μl injections of the test mixture, we therefore further investigated whether acetonitrile–water mixtures containing over 16% of water can also be used and if so, under what conditions. As an example, two chromatograms are shown in Fig. 1, (A) for the azeotropic mixture, (B) and for acetonitrile–water (50:50) as solvent mixture. Obviously, the solutes in the latter chromatogram still have a good peak shape, but the peaks are very small compared with those in Fig. 1A. Peak areas at different eluent compositions are given in Table I. As can be seen from these data, up to a water content of 20% the peak areas remain virtually the same. At 30% water the peak areas start to decrease and at 40 and 50% water they suddenly collapse. The amount of water that is left behind in the retention gap after evaporation of the azeotropic mixture can be calculated and is given in the last column of Table I. Obviously, if only up to 1 μl of water remains in the gap, there is no significant difference between the peak shapes and areas of the compounds at the various eluent compositions. Peak areas start to decrease if *ca.* 2–3 μl of water remain behind in the retention gap, and higher values cannot be tolerated at all.

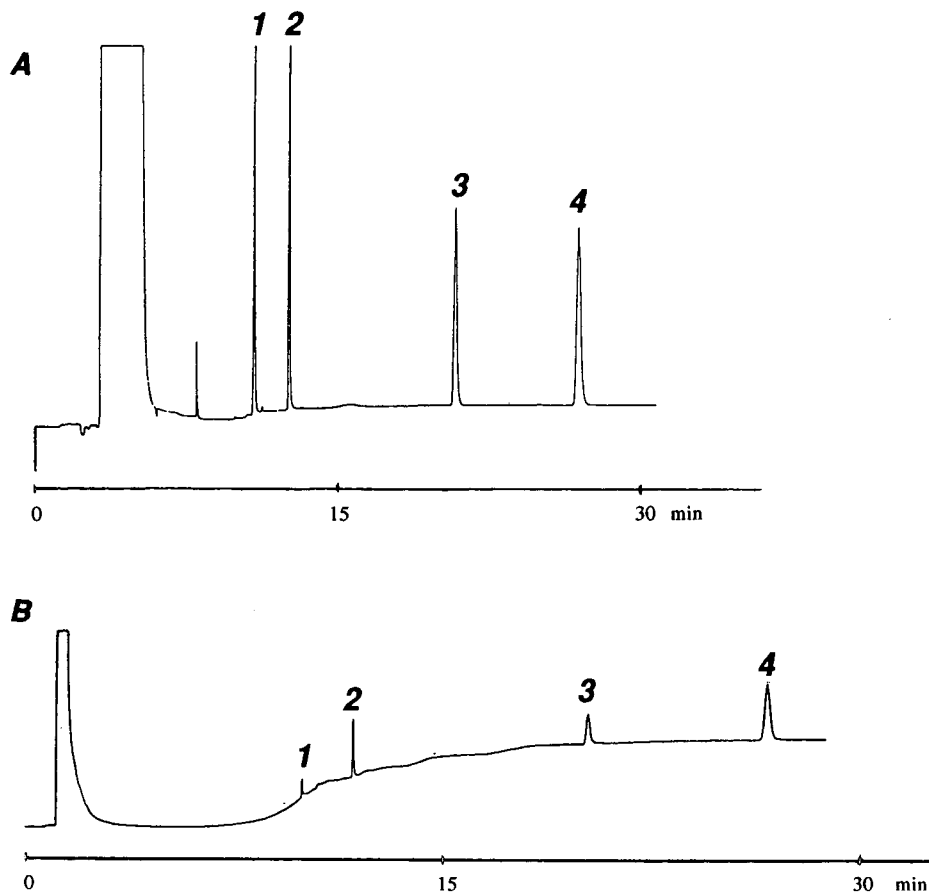


Fig. 1. Gas chromatograms of a 20- μ l injection of 0.02 mg/ml solution each of (1) naphthalene, (2) biphenyl, (3) acetanilide and (4) phenanthrene in (A) acetonitrile-water (84:16) and (B) in acetonitrile-water (50:50) using a 25 m \times 0.32 mm I.D. CPWax 52 CB analytical column ($d_t = 1.6 \mu\text{m}$) and a 2 m \times 0.53 mm I.D. CPWax 52 CB retention gap ($d_t = 0.025 \mu\text{m}$). $T = 70^\circ\text{C}$ (45 s), then increased at $30^\circ\text{C}/\text{min}$ to 220°C .

TABLE I

PEAK AREAS OF VARIOUS COMPOUNDS AFTER 20- μ l INJECTIONS OF TEST MIXTURES WITH DIFFERENT ELUENT COMPOSITIONS INTO THE GC SYSTEM AND THE AMOUNT OF WATER LEFT BEHIND IN THE RETENTION GAP AFTER EVAPORATION OF THE AZEOTROPIC MIXTURE

Conditions: retention gap 2 m \times 0.53 mm I.D. CPWax 52 CB ($d_t = 0.025 \mu\text{m}$); analytical column 25 m \times 0.32 mm I.D. CPWax 52 CB ($d_t = 1.6 \mu\text{m}$).

Acetonitrile: water ratio	Peak areas ($\times 10 \mu\text{V}$) ($n=2$)				Water left in gap (μl)
	Naphthalene	Biphenyl	Acetanilide	Phenanthrene	
84:16	12	10	7	10	-
80:20	13	10	8	10	1
70:30	10	8	6	7	3
60:40	1	1	0.8	0.3	6
50:50	0.06	0.2	0.3	0.5	8

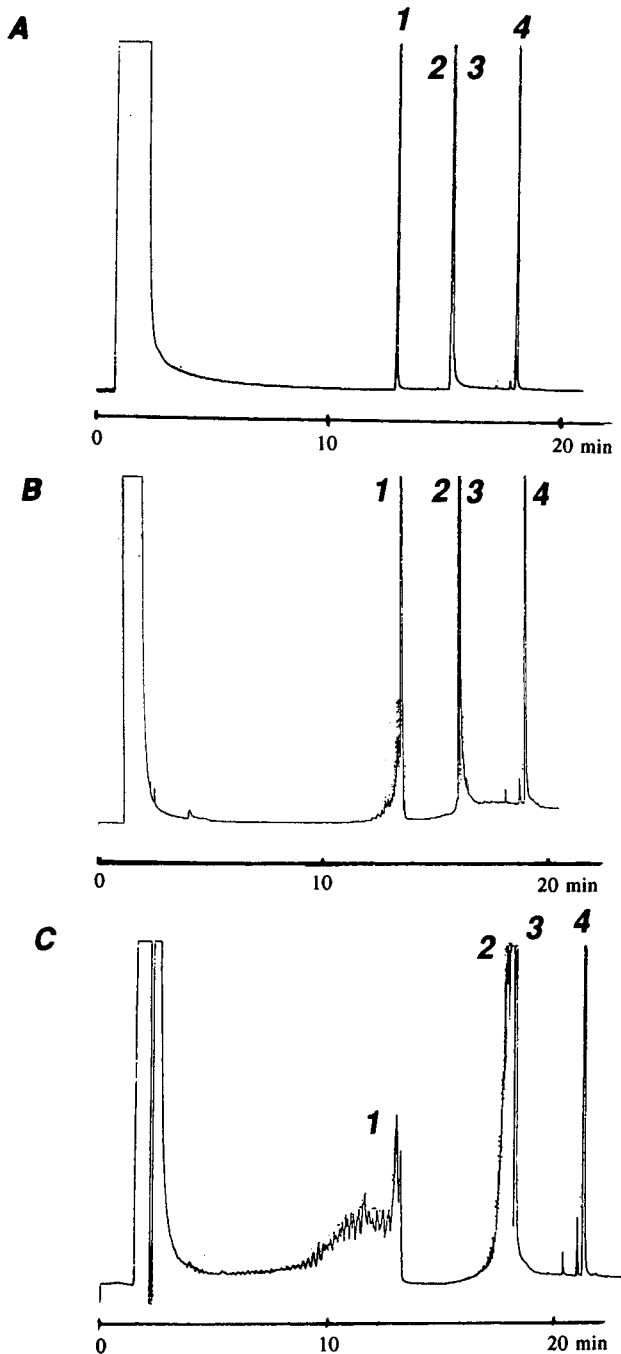


Fig. 2. Gas chromatograms of (A) an 8- μ l injection of a 0.02 mg/ml solution each of (1) naphthalene, (2) biphenyl, (3) acetanilide and (4) phenanthrene in acetonitrile-water (84:16), (B) a 4- μ l injection in acetonitrile-water (60:40) and (C) an 8- μ l injection in acetonitrile-water (60:40) using a 30 m \times 0.32 mm I.D. DB-1 column ($d_f=0.25\ \mu\text{m}$) and 2 m \times 0.53 mm I.D. CPWax 52 CB retention gap ($d_f=0.025\ \mu\text{m}$). $T_1=80^\circ\text{C}$ (4 min), then increased at $30^\circ\text{C}/\text{min}$ to 200°C ; $T_2=65^\circ\text{C}$ (12 min), then increased at $30^\circ\text{C}/\text{min}$ to 200°C .

The above experiment was repeated using another column, *viz.*, a 30 m \times 0.32 mm I.D. DB-1 ($d_f = 0.25 \mu\text{m}$) column using the two-oven system. Fig. 2 shows some relevant data. In this instance a cold trapping effect was created at the entrance of the analytical column by holding the Vega oven at 65°C, while raising the temperature of the Mega oven to 200°C, which was necessary to reconcentrate acetanilide. Using the azeotropic mixture (8 μl), all peaks had a perfect shape, as is shown in Fig. 2A. A 4- μl injection of an eluent containing 40% water led to deformation of the naphthalene peak (see Fig. 2B), while the other peaks were still of good shape. After the evaporation of the azeotrope, about 1 μl of pure water remains in the gap. An 8- μl injection of the same mixture led to deformation of the first three peaks (see Fig. 2C). In this instance, about 2 μl of water remain in the retention gap after evaporation, and this obviously is enough to distort the solvent trapping of the first three peaks completely. Probably owing to the cold trapping effect and the difference in film thickness, the heavier compound (phenanthrene) was reconcentrated after evaporation of the remaining water, giving a peak of perfect shape.

The combined results indicate that if more than *ca.* 1 μl of water is left in the retention gap after the azeotropic solvent mixture has evaporated, the peaks start to distort or areas to collapse. With a thick-film CPWax 52 CB column, the phase soaking effect due to the combination of the polar stationary phase and the polar eluent and also the large difference in retention power between the retention gap and the thick-film column probably contribute to an extra reconcentration of the components [4]. If a few microliters of water are left behind in the retention gap, part of the solute is reconcentrated at the inlet of the column and the remainder is lost during the evaporation of the water, which results in well shaped but too small peaks, whereas with the DB-1 column, where the phase soaking effect is missing and the increase in retention power difference is smaller, complete distortion of the peaks occurs. In this context it is interesting that Cortes and co-workers published two papers on direct large-volume injections of aqueous solutions into a GC system [11,16]. Using a non-deactivated fused-silica gap with a length of 20 m they succeeded in introducing 20 μl of water, still obtaining sharp peaks for the late-eluting components. However, they did not report quantitative results and it is obvious from the published data that the relative peak heights of the components vary considerably between the several chromatograms. However, the major drawback of non-deactivated fused silica is that polar components will be adsorbed by this material so that only apolar and slightly polar components can be analysed.

Grob and Li [12] observed that with a 50- μl on-column injection of water-*n*-propanol (30:70) using an OV-17 deactivated fused-silica retention gap, early-eluting peaks were deformed whereas the later-eluting peaks were of perfect size and shape. One can easily calculate that after the evaporation of the azeotrope water-*n*-propanol (28:72), 1.4 μl of water will remain in the gap and contribute to peak distortion and loss of analytes. On introducing 50 μl of water-*n*-propanol (35:65), which means that 4.8 μl of water will remain in the gap after azeotropic evaporation, they found all peaks to be distorted. Our results essentially agree with their findings. They indicate that the maximum amount of water that can be left behind in the gap after azeotropic evaporation is of the order of 1 μl , the exact amount depending on the retention of the solute and the nature and thickness of the stationary phase of the column.

Lifetime of the Carbowax retention gap

Grob *et al.* [13] stated that water at elevated temperatures (100°C) rapidly deteriorates the deactivation of all kinds of retention gaps, including Carbowax-deactivated gaps. We therefore regularly tested the CPWax 52 CB retention gaps after repeated large-volume injections (8–40 μ l) of acetonitrile–water mixtures with a varying water content. In Fig. 3 several chromatograms are shown for these retention gaps using the Grob test mixture. The peak shape and height of the various solutes give information about the quality of the retention gap [17]. In the chromatogram obtained with a new Carbowax-coated retention gap, no deformation or disappearance of peaks was observed, as is shown in Fig. 3A, except for the dicyclohexylamine

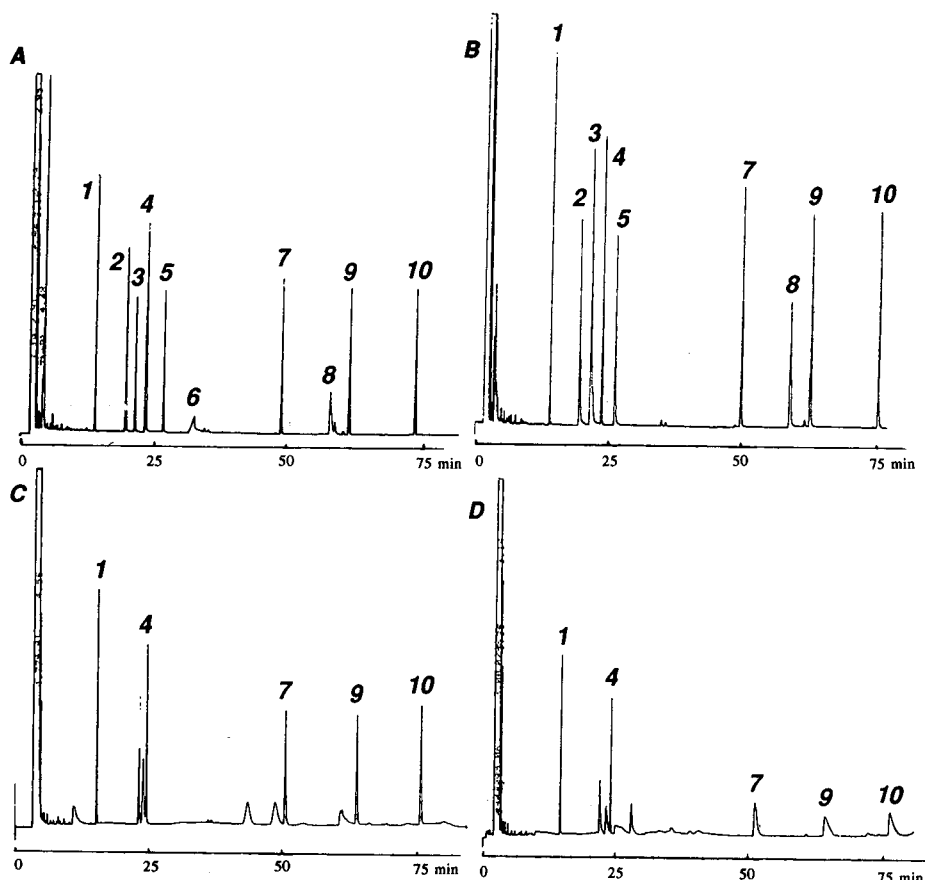


Fig. 3. Test chromatograms of several retention gaps using the Grob test mixture. (A) New, unused 2 m \times 0.53 mm I.D. CPWax 52 CB retention gap ($d_f = 0.025 \mu\text{m}$); (B) retention gap A after about 125 acetonitrile–water large-volume injections; (C) 1 m \times 0.53 mm I.D. CPWax 52 CB retention gap ($d_f = 0.05 \mu\text{m}$) after 1.5 year of use; (D) 1 m \times 0.53 mm I.D. non-deactivated fused silica; analytical column: 30 m \times 0.32 mm I.D. DB-1 ($d_f = 0.25 \mu\text{m}$). Conditions: $T = 40^\circ\text{C}$, then increased at $1^\circ\text{C}/\text{min}$ to 120°C ; carrier gas, helium (100 kPa); injection, 1 μ l on-column. 1 = *n*-Decane; 2 = 1-octanol; 3 = 2,6-dimethylphenol; 4 = *n*-undecane; 5 = 2,6-dimethylaniline; 6 = 2-ethylhexanecarboxylic acid; 7 = methyl decanecarboxylate; 8 = dicyclohexylamine; 9 = methyl undecanecarboxylate; 10 = methyl dodecanecarboxylate.

peak and 2-ethylhexanecarboxylic acid peak. We used this retention gap during the experiments described in the previous section and for other large-volume experiments with acetonitrile–water solutions. After about 125 large-volume injections, this gap was tested again and still no peak deformation was observed, although it is certain that on various occasions pure water had been in contact with the deactivation of the gap. Even the peaks of the polar compounds still were of good shape (See Fig. 3B); the shape of the dicyclohexylamine peak was improved but 2-ethylhexanecarboxylic acid disappeared completely. This might be explained by the fact that the water introduced probably removed the traces of acid from the new, unused Carbowax retention gap, resulting in a less acidic deactivation.

In Fig. 3C, a chromatogram is shown for another CPWax 52 CB gap which was used for more than 1.5 years for several large-volume injections of polar and aqueous solvent mixtures. Most of the polar compounds have disappeared, which means that the deactivation of the retention gap becomes affected, but the apolar compounds still give well shaped peaks. Grob *et al.* [13] found that even after a few water injections the Carbowax was already completely removed from the gaps, leaving a fused silica which was more active than raw fused silica and which adsorbed even the apolar peaks. To verify whether this was also true for our retention gap, for comparison we ran a chromatogram for a raw fused-silica retention gap (see Fig. 3D). Contrary to what is seen in Fig. 3C, the methyl ester peaks are deformed in Fig. 3D. This means that the raw fused-silica column is more active than the Carbowax retention gap which was used for 1.5 years and that even after frequent use the Carbowax deactivation of the gap is not completely lost.

In summary, the experimental data indicate that a very thin-film CPWax 52 CB-coated retention gap can be used for the introduction of aqueous mixtures for several months, without serious determination of the deactivation, even if pure water has remained in the gap.

Introduction speed and introduction volume

Using an on-column interface in on-line LC–GC, the eluent flow-rate of the LC column equals the sample introduction speed in GC. Therefore, the maximum sample

TABLE II

PEAK AREAS OF IDAVERINE AFTER 20- μ l INTRODUCTION OF A 10 μ g/ml IDAVERINE SOLUTION IN ACETONITRILE–WATER (90:10) + 0.1% TRIETHYLAMINE USING VARIOUS INTRODUCTION SPEEDS

Conditions: analytical column 30 m \times 0.32 mm I.D. DB-1 ($d_f = 0.25 \mu$ m); retention gap 5 m \times 0.53 mm I.D. CP Wax 52 CB ($d_f = 0.025 \mu$ m); average area, 4.1×10^6 .

Introduction speed (μ l/min)	Peak area ($\times 10^6$ counts) ^a
20	4.0
40	3.9
60	4.0
80	4.2
100	4.3

^a S.D. = 0.3×10^6 ; R.S.D. = 6.8%.

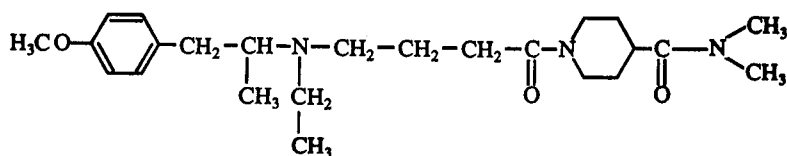
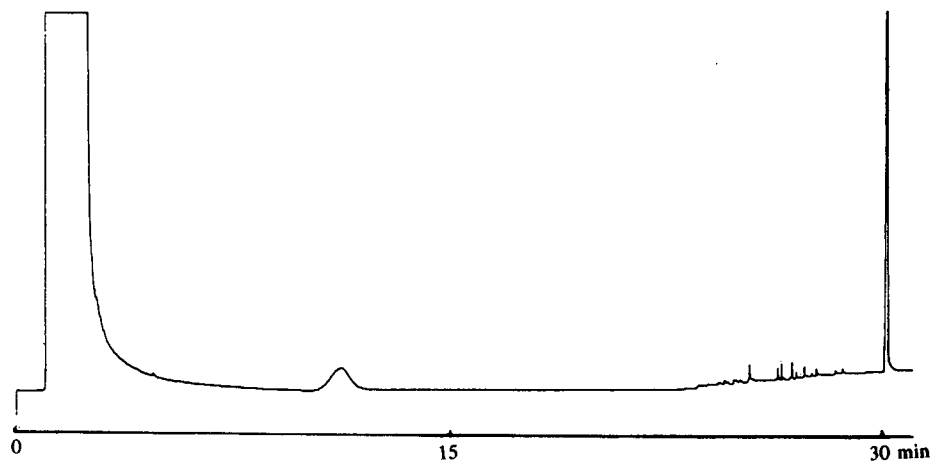
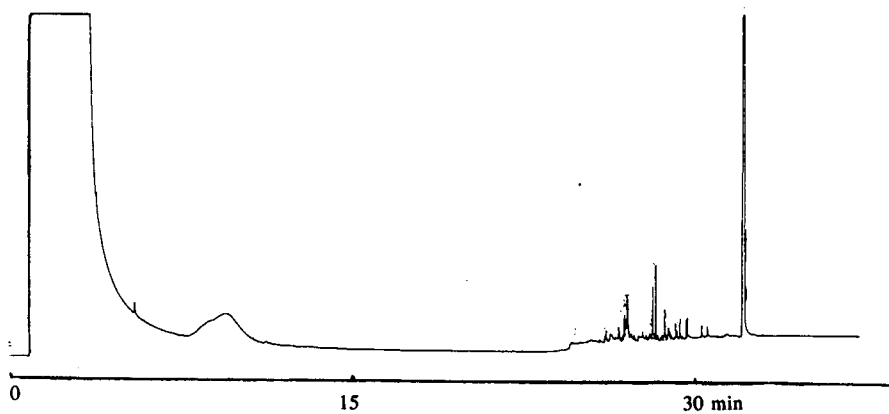
**Idaverine**

Fig. 4. Gas chromatograms of 10 $\mu\text{g/ml}$ idaverine solution in acetonitrile-water (90:10), introduced into a CPWax 52 CB retention gap ($d_f = 0.025 \mu\text{m}$) (A) with a speed of 100 $\mu\text{l/min}$ and an introduction volume of 20 μl and (B) with a speed of 40 $\mu\text{l/min}$ and an introduction volume of 40 μl . Analytical column 30 m \times 0.32 mm I.D. DB-1 ($d_f = 0.25 \mu\text{m}$); retention gap, 5 m \times 0.53 mm I.D. CPWax 52 CB ($d_f = 0.025 \mu\text{m}$); $T_1 = 90^\circ\text{C}$ (during solvent evaporation), then increased at 30°C/min to 220°C ; $T_2 = 220^\circ\text{C}$ (during solvent evaporation + 15 min), then increased at 30°C/min to 325°C ; $T_{\text{interface}} = 220^\circ\text{C}$.

introduction speed into the GC column determines the maximum dimensions of the LC column. In trace analysis low detection limits are required; e.g., drugs often have to be determined in plasma at a level of 0.1–1 $\mu\text{g}/\text{l}$. This means that for on-line LC–GC the LC column must have sufficient sample capacity; a large inside diameter is desirable. We therefore determined the maximum introduction speed of an acetonitrile–water mixture into the GC retention gap, using the drug idaverine as a test component. The results of the experiments are shown in Table II, where the peak areas of a 20- μl injection of a solution of 10 $\mu\text{g}/\text{ml}$ of idaverine in acetonitrile–water (90:10) containing 0.1% triethylamine are given for introduction speeds varying from 20 to 100 $\mu\text{l}/\text{min}$. Triethylamine was added to the solution to prevent adsorption on the LC column. The relative standard deviation (R.S.D.) is small, which means that up to 100 $\mu\text{l}/\text{min}$ no problems are observed. The average peak area of $(4.1 \pm 0.3) \cdot 10^6$ counts is almost equal to the $4.3 \cdot 10^6$ counts obtained on direct on-column injection of 1 μl of a solution of 200 $\mu\text{g}/\text{ml}$ of idaverine in methanol. Obviously, no significant losses of idaverine occur during the large-volume introduction of an acetonitrile–water mixture. During the above work, we observed that, using an inlet pressure of 150 kPa and an introduction temperature of 90°C, sometimes backflow into the injector occurred, which caused long tailing solvent peaks. This problem was solved by increasing the inlet pressure to 200 kPa. A chromatogram of a 20- μl injection of an idaverine solution, introduced at a speed of 100 $\mu\text{l}/\text{min}$, is shown in Fig. 4A. As regards the eluent flow-rate, the above experiments indicate that commercially available 1 mm I.D. microbore columns, which require a flow-rate of about 50 μl , can be used for on-line (reversed-phase) LC–GC using an on-column interface.

However, an increase in the inside diameter of the LC column also results in larger peak volumes and consequently in larger fraction volumes, which have to be transferred to the gas chromatograph (*ca.* 5 μl for a 0.33 mm I.D. LC column *vs.* *ca.* 50 μl for a 1 mm I.D. LC column). Therefore, in Fig. 4B a chromatogram is given for a larger injection volume, *i.e.*, 40 μl , of the 10 $\mu\text{g}/\text{ml}$ idaverine solution using an introduction speed of 40 $\mu\text{l}/\text{min}$. The retention gap used in this instance is a 5 m \times 0.53 mm I.D. CPWax 52 CB ($d_f = 0.025 \mu\text{m}$). Both the idaverine and the solvent peak have a similar shape to that obtained on introduction of 20 μl .

The length of the flooded zone in the retention gap appears to be an indication of the wettability of the gap by the solvent mixture [12]. This length can be calculated from Fig. 4B. As the solvent peak of the 40- μl injection has a width of *ca.* 2 min, the 40 μl must have evaporated at a rate of *ca.* 20 $\mu\text{l}/\text{min}$. This indicates that, using an eluent introduction speed of 40 $\mu\text{l}/\text{min}$, *ca.* 20 μl flooded the retention gap, which means that the flooded zone was *ca.* 25 cm per 1- μl injection. This corresponds well with the flooded zone of 38 cm/ μl found for acetonitrile–water (90:10) using a 0.32 mm I.D. DTMDS retention gap at 25°C [12]. Although in the present instance solvent effects do not play any role because idaverine is a high-boiling compound, it can be concluded that the retention gap has a good wettability for the acetonitrile–water mixture.

CONCLUSIONS

The aim of this study was to investigate the large volume introduction of aqueous solvent mixtures into a retention gap in order to couple reversed-phase LC with

GC using an on-column interface. Retention gaps coated with a very thin film of CPWax 52 CB (0.025 μm) are suitable for this purpose. The lifetime of these retention gaps is several months, in spite of several exposures to acetonitrile–water mixtures of varying compositions. This means that reversed-phase LC can be coupled to capillary GC. The following aspects should, however, be considered. The maximum amount of water in an aqueous–organic LC eluent that can be tolerated is limited. No problem will be encountered if an acetonitrile–water mixture has an azeotropic composition, *i.e.*, 84:16, (v/v), or contain less water. In principle, solvent mixtures containing a higher percentage of water can also be introduced into the retention gap. However, as the performance of the chromatographic system rapidly deteriorates if more than 1 μl of water remains in the retention gap after azeotropic evaporation, the volume that can be introduced into the system will be restricted. The maximum introduction speed into the described GC system of an acetonitrile–water mixture (90:10) is at least 100 $\mu\text{l}/\text{min}$. The maximum introduction volume of such a mixture under the described conditions at a flow-rate of 40 $\mu\text{l}/\text{min}$ is *ca.* 40 μl if a 5 m \times 0.53 mm I.D. CPWax 52 CB retention gap is used. This volume can be increased by lengthening the retention gap or by the use of an early vapour exit [18,19]. These results imply that micro-bore LC columns with inside diameters of up to 1 mm can now be used in reversed-phase LC–GC. Further research in this field will be concentrated on applications of the results obtained here.

REFERENCES

- 1 K. Grob, Jr., B. Schilling, C. Walder, *J. High Resolut. Chromatogr. Chromatogr. Commun.*, 9 (1986) 95.
- 2 K. Grob, Jr., and J. M. Stoll, *J. High Resolut. Chromatogr. Chromatogr. Commun.*, 9 (1986) 518.
- 3 K. Grob, Jr., *On-line coupled LC–GC*, Hüthig, Heidelberg, in press.
- 4 K. Grob, Jr., *On-Column Injection in Capillary GC*, Hüthig, Heidelberg, 1987.
- 5 K. Grob, Jr., *J. Chromatogr.*, 279 (1983) 225.
- 6 K. Grob, Jr., and B. Schilling, *J. Chromatogr.*, 391 (1987) 3.
- 7 I. L. Davies, K. E. Markides, M. L. Lee, M. W. Raynor and K. D. Bartle, *J. High Resolut. Chromatogr.*, 12 (1989) 193.
- 8 K. Grob, Jr., and Z. Li, *J. Chromatogr.*, 473 (1989) 381.
- 9 D. Duquet, C. Dewaele, M. Verzele and S. McKinley, *J. High Resolut. Chromatogr. Chromatogr. Commun.* 11 (1988) 824.
- 10 K. Grob, Jr., and Z. Li, *J. Chromatogr.*, 473 (1989) 423.
- 11 H. J. Cortes, C. D. Pfeiffer, G. L. Jewett and B. E. Richter, *J. Microcolumn Sep.*, 1 (1989) 28.
- 12 K. Grob, Jr., and Z. Li, *J. Chromatogr.*, 473 (1989) 391.
- 13 K. Grob, Jr., H. P. Neukom and Z. Li, *J. Chromatogr.*, 473 (1989) 401.
- 14 A. V. Pouwelse, D. de Jong, and J. H. M. van den Berg, *J. High Resolut. Chromatogr. Chromatogr. Commun.*, 11 (1988) 607.
- 15 A. V. Pouwelse, D. de Jong, N. G. F. M. Lammers and J. H. M. van den Berg, paper presented at the Twelfth International Symposium on Column Liquid Chromatography, HPLC '88, Washington, DC, June 19–24, 1988.
- 16 B. B. Gerhart and H. J. Cortes, *J. Chromatogr.*, 503 (1990) 377.
- 17 K. Grob, Jr., *J. Chromatogr.*, 156 (1978) 1.
- 18 H. G. Schmarr, A. Mosandl and K. Grob, *J. High Resolut. Chromatogr.*, 12 (1989) 721.
- 19 E. Dolecka, J. J. Vreuls, F. A. Maris, G. J. de Jong and U. A. Th. Brinkman, *J. High Resolut. Chromatogr.*, 13 (1990) 405.

CHROMSYMP. 2088

Short Communication

Isolation and quantification of polymers from autoxidized fish oils by high-performance size-exclusion chromatography with an evaporative mass detector

IVAN C. BURKOW*

Institute of Fishery Technology Research, P.O. Box 677, N-9001 Tromsø (Norway)
and

R. JAMES HENDERSON

NERC Unit of Aquatic Biochemistry, University of Stirling, Stirling FK9 4LA (U.K.)

ABSTRACT

Triacylglycerol polymers from autoxidized fish oils were isolated and quantified by size-exclusion chromatography with an evaporative mass detector. Optimum chromatographic conditions were obtained using dichloromethane as the mobile phase and three styrene-divinylbenzene columns coupled in series. The results showed a lack of correlation between polymer content and standard methods for oxidative rancidity assessment. The polymer content was *ca.* 1% in the starting oils, but the value rapidly increased during autoxidation. Depending on the level of oxidation, a mixture of dimer, trimer and higher polymeric triacylglycerols are formed, the dimers predominating when the total polymer content is less than 10%.

INTRODUCTION

Recently there has been increased interest in the polymeric triacylglycerols formed during the autoxidation of highly unsaturated fats and oils and their influence on the quality of marine dietary lipids [1–3]. However, it is not yet known to what extent high-molecular-weight compounds contribute to the possible deleterious effects of oxidized lipids in nutrition. This is partly due to the difficulties encountered during the analysis of these polymers, caused by the complexity of the triacylglycerols present in marine oils.

Among various methods used for the determination of oligomeric and polymeric materials from oxidized lipids, size-exclusion chromatography (SEC) seems to be the most promising. The most successful approach is to use high-performance liquid chromatographic (HPLC) methods with columns packed with macroporous styrene-divinylbenzene copolymers, and such techniques have been used for the sep-

aration of high-molecular-weight compounds from oxidized fatty acids [4-7] and vegetable oils [8-11].

We have previously reported a simple method for the analysis of polymeric triacylglycerols from autoxidized fish oils [12]. The method is based on high-performance SEC with a chromatographic system consisting of a single pump, a 500 Å styrene-divinylbenzene column and an evaporative mass detector. In this study, a more advanced method using SEC columns with styrene-divinylbenzene copolymers of different pore sizes coupled in series was developed. The method is useful for the separation of oligomeric and polymeric triacylglycerols from autoxidized oils and can also be applied to the separation of partial triacylglycerols and non-esterified fatty acids from triacylglycerols.

EXPERIMENTAL

Cod liver oil (CLO) was obtained from Peter Møller (Oslo, Norway), capelin oil (CO) from J. C. Martens (Bergen, Norway) and CPL (chromatographically purified lipid) Fish Oil 30 from Karlshamns (Karlshamn, Sweden). Antioxidants were not added to the oils. All chemicals used were of analytical-reagent grade and were supplied by Fluka (Buchs, Switzerland) or Merck (Darmstadt, Germany), except the solvents, which were of HPLC grade from Rathburn Chemicals (Walkerburn, U.K.). Polystyrene standards (MW 2510, 4080 and 7030) were supplied by Millipore (Milford, MA, U.S.A.).

Analysis of polymers was carried out using an HPLC system consisting of a Waters Model 501 pump with a U6K injector and an Applied Chromatography Systems Model 750/14 evaporative mass (light-scattering) detector. The mass detector was operated with the internal air pressure adjusted to 24 p.s.i. and the evaporator set at 20 (arbitrary figure). The analyses were performed using Waters Ultrastyrigel 500 Å and 1000 Å SEC columns (both 30 cm × 7.8 mm I.D., particle size 10 μm). Dichloromethane (0.8 ml/min) was employed as the mobile phase. The sample concentration was 10-50 mg/ml in the mobile phase and the injection volume was 40 μl. Glycerol was used as an internal standard and peak integration was carried out using a Shimadzu C-R6A integrator.

The method for the analysis of methyl esters of fatty acids has been described previously [12]. Peroxide values (PV) were measured by iodometric titration [13], thiobarbituric acid (TBA) values were determined as described by Ke and Woyewoda [14] and anisidine values (AV) were measured according to IUPAC method 2.504 [15].

The rancification experiments were performed at 35°C with irradiation from an artificial daylight fluorescent tube ($1.1 \times 10^{19} \text{ Q m}^{-2}\text{s}^{-1}$). The oils (40 g) were oxidized in open beakers (4.8 cm I.D.) with stirring.

RESULTS AND DISCUSSION

In order to determine the optimum chromatographic conditions for polymer separation, a number of exploratory experiments were carried out using cod liver oils (CLOs) of different oxidative rancidity as test materials. The separation of polymeric triacylglycerols was hardly affected by replacing the 500 Å (effective molecular weight

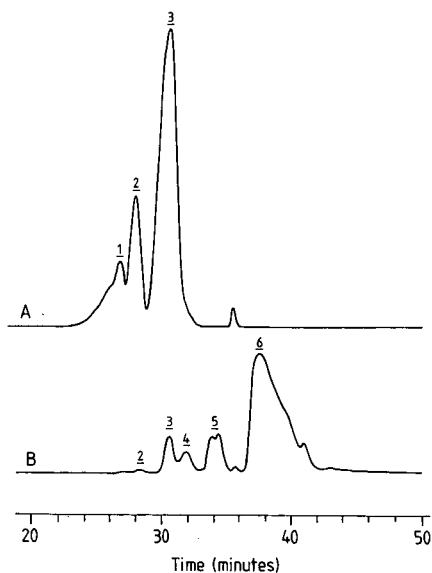


Fig. 1. SEC analyses of cod liver oil using the 500 Å + 500 Å + 1000 Å column system with dichloromethane (0.8 ml/min) as mobile phase. (A) Cod liver oil containing 25% polymers; (B) hydrolysed cod liver oil. Peaks: 1 = trimers and higher polymers; 2 = dimers; 3 = triacylglycerols; 4 = diacylglycerols; 5 = monoacylglycerols; 6 = fatty acids.

range 100–10 000) with the 1000 Å styrene–divinylbenzene column (effective molecular weight range 200–30 000). However, the separation was greatly improved by coupling columns in series, and the results clearly demonstrate that three columns in series (500 Å + 500 Å + 1000 Å) are necessary for baseline separation of oligomeric and polymeric material from triacylglycerols in highly oxidized samples (Fig. 1). The total time of analysis varied from 15 to 45 min depending on the number of columns used.

Although the mobile phase normally affects separation by SEC to only a minor extent, we found that a good separation was dependent on the solvent chosen. Dichloromethane, chloroform, tetrahydrofuran and toluene were tested, all having different solvent polarity indices and solvent strength parameters [16]. Toluene was completely unsuitable as a solvent whereas the others, giving slightly different separations, could be used, indicating the need for a mobile phase of medium polarity (Fig. 2). Dichloromethane was finally chosen as the solvent when the separation between triacylglycerols, diacylglycerols, monoacylglycerols and free fatty acids was also taken into consideration.

Although the most widely used detector in SEC is the refractive index detector, the evaporative mass detector was chosen owing to its slightly superior response for different polymers [17]. In order to achieve reliable results, optimization of the mass detector with respect to aerosol flow and temperature is very critical [12,18,19]. The temperature setting is the most important operating parameter, but unfortunately affects the different compounds to different extents. An increase in the evaporator temperature was followed by an enhanced polymer response whereas the response of

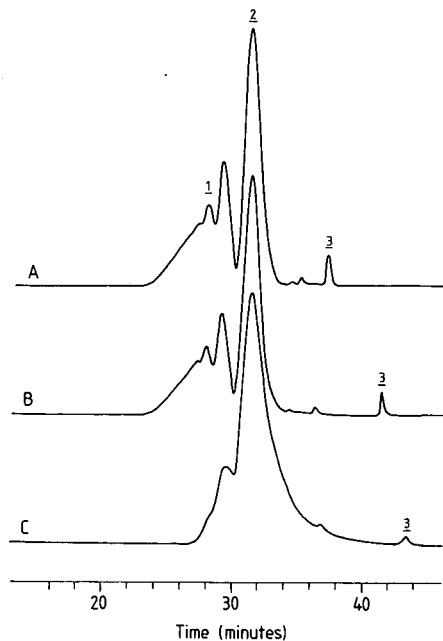


Fig. 2. SEC analysis of cod liver oil containing 18% polymers using the 500 Å + 500 Å + 1000 Å column system and different mobile phases at 0.8 ml/min. (A) Tetrahydrofuran; (B) dichloromethane; (C) toluene. Peak: 1 = polymers; 2 = triacylglycerols; 3 = glycerol.

the internal standard (glycerol) decreased. The triacylglycerol response was not influenced by the temperature setting in the normal working range.

Injection of 2.6–20.8 µg of the polymeric material gave a 20-fold instead of the expected 8-fold area increase. In addition, no linear response relationship between glycerol and polymeric material was observed. Quantification was therefore performed using a constant amount of internal standard added to the samples, and the ratio observed was then corrected according to a curved calibration graph giving the response–weight relationship between the polymers and internal standard [12]. There

TABLE I

CONTENTS OF POLYUNSATURATED FATTY ACIDS (PUFA), PEROXIDE VALUE (PV), ANISIDINE VALUE (AV), THIOBARBITURIC ACID (TBA) VALUE AND THE AMOUNT OF POLYMERS IN STARTING OILS

Oil ^a	PUFA (%)	PV (mequiv./kg)	AV	TBA (µmol/g)	Polymers (%)
CLO	33	4.3	23	0.7	1.3
CO	22	4.1	10	0.4	0.9
CPL	38	3.0	2	0.3	1.0

^a CLO = Cod liver oil; CO = capelin oil; CPL = chromatographically purified fish oil.

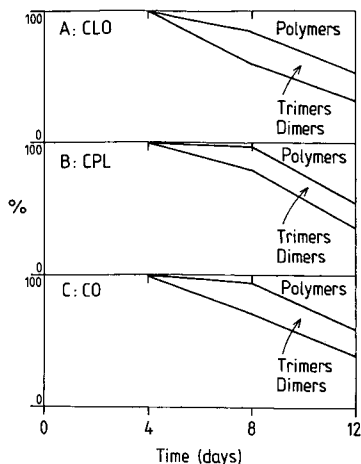


Fig. 3. Distribution of dimers, trimers and higher polymers in autoxidized fish oils. (A) Cod liver oil; (B) chromatographically purified fish oil; (C) capelin oil.

may be several reasons for this non-linear behaviour, including aerosol particle size, refractive index and opacity of the particles [20,21]. A further complication was the finding that different calibration graphs had to be prepared, depending on the number of columns connected in series and the mobile phase used.

The amount of polymers in CLO, capelin oil (CO) and chromatographically purified fish oil (CPL) was found to be *ca.* 1% (Table I). For comparison, the amount of polyunsaturated fatty acids (PUFA) and the standard quality assessment parameters peroxide value (PV), anisidine value (AV) and thiobarbituric acid (TBA) value are also shown. The results show a lack of correlation between polymer content and standard methods for oxidative rancidity assessment. This is an important finding as the polymers seems to be the main oxidation product in autoxidized marine oils [12]. The polymer content increase rapidly during autoxidation, with values as high as 43–48% after 12 days at 35°C. Depending on the level of oxidation, a mixture of dimer, trimer and higher polymeric triacylglycerols is formed (Fig. 3), the dimers predominating when the total polymer content is less than 10%. Peak identification of the triacylglycerols, diacylglycerols, monoacylglycerols and fatty acids was based on authentic samples. The molecular weight determination of the polymers was based on polystyrene standards, and can only be regarded as approximate as the exclusion process is a function of the size and shape of the molecules.

As the past history of the oils was not known, no final conclusions can be drawn regarding the relative stability of the different oils towards autoxidation.

REFERENCES

- 1 W. W. Nawar and H. O. Hultin, *n-3 News*, 3, No. 3 (1988) 1.
- 2 K. Kragballe and V. K. S. Shukla, *Ugeskr. Læger*, 152 (1990) 894.
- 3 Anonymous, *Inform*, 1 (1990) 117.
- 4 S.-Y. Cho, K. Miyashita, T. Miyazawa, K. Fujimoto and T. Kaneda, *J. Am. Oil Chem. Soc.*, 64 (1987) 876.

- 5 S.-Y. Cho, K. Miyashita, T. Miyazawa, K. Fujimoto and T. Kaneda, *Nippon Suisan Gakkaishi*, 53 (1987) 813.
- 6 W. E. Neff, E. N. Frankel and K. Fujimoto, *J. Am. Oil Chem. Soc.*, 65 (1988) 616.
- 7 C. N. Christopoulou and E. G. Perkins, *J. Am. Oil Chem. Soc.*, 66 (1989) 1338.
- 8 D. B. Kupranycz, M. A. Amer and B. E. Baker, *J. Am. Oil Chem. Soc.*, 63 (1986) 332.
- 9 O. N. Jensen and J. Møller, *Fette Seifen Anstrichm.*, 88 (1986) 352.
- 10 N. Sotirhos, C.-T. Ho and S. S. Chang, *Fette Seifen Anstrichm.*, 88 (1986) 45.
- 11 C. Gertz, *Fette Seifen Anstrichm.*, 88 (1986) 475.
- 12 I. C. Burkow and R. J. Henderson, *Lipids*, in press.
- 13 *Official and Tentative Methods of the American Oil Chemists' Society*, 3rd ed., AOCS, Champaign, 1981, AOCS Cd 8.53.
- 14 P. J. Ke and A. D. Woyewoda, *Anal. Chim. Acta*, 106 (1979) 279.
- 15 IUPAC, *Standard Methods for the Analysis of Oils, Fats and Derivatives*, 7th ed., Blackwell, Oxford, 1987, Method 2.5004.
- 16 L. R. Snyder and J. J. Kirkland, *Introduction to Modern Liquid Chromatography*, Wiley, New York, 2nd ed., 1979.
- 17 S. Coulombe, *J. Chromatogr. Sci.*, 26 (1988) 1.
- 18 J. L. Robinson, M. Tsimidou and R. Macrae, *J. Chromatogr.*, 324 (1985) 35.
- 19 G. Guiochon, A. Moysan and C. Holley, *J. Liq. Chromatogr.*, 11 (1988) 2547.
- 20 J. M. Charlesworth, *Anal. Chem.*, 50 (1978) 1414.
- 21 L. E. Oppenheimer and T. H. Mourey, *J. Chromatogr.*, 323 (1985) 297.

Determination of chemical composition of polymers by size-exclusion chromatography with coupled density and refractive index detection

III. Polyethylene oxide and polytetrahydrofuran

B. TRATHNIGG

Institute of Organic Chemistry, Karl-Franzens-Universität Graz, Heinrichstrasse 28, A-8010 Graz (Austria)

ABSTRACT

It is shown that gel permeation chromatography with coupled density and refractive index detection is a useful tool in the analysis of copolymers of ethylene oxide and tetrahydrofuran with respect to their chemical composition as a function of molecular weight.

INTRODUCTION

In the analysis of copolymers or polymer blends it is very important to know the chemical composition along the molecular weight distribution, because non-uniform composition may affect product properties very strongly. Moreover, the chromatogram has to be corrected for chemical composition if the response factors of the detector for both monomer units are considerably different.

Basically, the chemical composition as a function of molecular weight can be obtained by a two-dimensional separation (cross-fractionation [1] or size-exclusion chromatography (SEC) coupled with liquid adsorption chromatography [2–4]) or by SEC with two detectors [5–9].

Because of its simplicity, the second approach is more convenient. However, it is limited by the detectors which can be applied: if one of the monomer units can be detected by a photometer, SEC with coupled refractive index (RI) and UV detection will be the method of choice. In this case, the selective UV detector yields the concentration of one component and the universal RI detector yields the overall concentration (after correction for different response factors). For all other copolymers, one would have to combine two universal detectors. Since the density detector (according to the mechanical oscillator principle) has proven to meet the

demand for an alternative universal detector [10–14], SEC with dual detection can be applied to non-UV-active copolymers.

The working principle of the density detector has been described previously, hence it shall be mentioned only briefly. Density measurement according to the mechanical oscillator method means measurement of the period of an oscillating U-shaped glass tube filled with the sample. Period measurement is performed by comparison with a time base (in the density detector an oven-controlled 10-MHz quartz oscillator). Hence the detector signal is inherently digital (the number of periods of the time base during a fixed number of the measuring cell) and integrated over each measuring interval.

EXPERIMENTAL

The density detection system (A. Paar, Graz, Austria) which was used for these investigations has been described in detail elsewhere [14]. It consisted of a thermostatted box containing the columns and up to two independent measuring cells, which were connected to an intelligent interface. A differential refractometer (Sicon LCD 201) was coupled to one of the measuring cells and connected to the analog input of the interface. In order to maintain the same temperature in both detector cells, the RI detector was arranged in the thermostat circuit behind the column box.

All measurements were performed at a temperature of $25.00 \pm 0.01^\circ\text{C}$. However, during each chromatogram, temperature was constant to approximately $1 \cdot 10^{-4}^\circ\text{C}$, as can be deduced from the baseline value of the density detector, which was very stable after an equilibration period. As we have shown previously [14], it would even be satisfactory to reproduce temperature to $\pm 1^\circ\text{C}$, as long as temperature changes are sufficiently slow. This was achieved by the special design of the column box and the density cell.

All separations were performed using chloroform [high-performance liquid chromatography (HPLC) grade, Merck LiChroSolv 2444] as the mobile phase at a flow-rate of 1.0 ml/min on three different column sets, which could be selected using two Rheodyne 7060 multiposition valves: A: 30×2 cm $\mu\text{Styragel}$, 100–500 Å (Waters); B: 30×2 cm $\mu\text{Styragel}$, 10^3 – 10^4 Å (Waters); C: 30×3 cm Microgel, 10^4 – 10^3 –500 Å (Polymer Labs.). Two Gynkotek 300 C pumps were used in all experiments. Samples were injected using a manual injection valve (Gynkotek) and a Spark SP 125 FIX autosampler, both equipped with 50- μl sample loops. Sample sizes varied from 0.1 to 1 mg, corresponding to concentrations of 2.0–20 g/l, typically 4–8 g/l.

Polymer samples [polyethylene glycols (PEGs) from Merck, polytetrahydrofuran (PTHF) 1300 from Polymer Labs. (Batch No. 20423-1), tetrahydrofuran-ethylene oxide (THF-EO) copolymer from Aldrich] were used as received. Copolymer composition was also determined by ^{13}C nuclear magnetic resonance (NMR) spectroscopy (in chloroform) using a Gemini 200 spectrometer.

Raw data were transferred to an MS-DOS computer and processed using the software CHROMA. Molecular weight tables were written to ASCII files from CHROMA and transferred to a spreadsheet (SYMPHONY and EXCEL).

Principle of dual detection with two universal detectors

If a mass m_i of a copolymer containing the weight fractions w_A and $w_B (= 1 - w_A)$ of the monomer units A and B, respectively, passes the detector cells, it will cause a response x_D of the density detector and x_R of the RI detector:

$$x_D = m_i(f_{D,A}w_A + f_{D,B}w_B) \quad (1)$$

and

$$x_R = m_i(f_{R,A}w_A + f_{R,B}w_B) \quad (2)$$

where $f_{D,A}$, $f_{D,B}$, $f_{R,A}$, and $f_{R,B}$ are the corresponding response factors of the homopolymers of A and B, respectively.

Combination of eqns. 1 and 2 yields:

$$1/w_A = 1 - (f_{D,A}x_R/x_D - f_{R,A})/(f_{D,B}x_R/x_D - f_{R,B}) \quad (3)$$

from which the weight fractions of the monomer units can be calculated. The mass eluted within one measuring interval is given by:

$$m_i = x_D/[f_{D,B} + w_A(f_{D,A} - f_{D,B})] \quad (4)$$

from which the mass distribution is obtained.

$$w_i = m_i / \sum m_i \quad (5)$$

Once w_A and w_B are known, one may correct the chromatogram and the mass distributions using eqns. 4 and 5.

Multiplication of the weight fraction w_i by w_A and w_B , respectively, yields the separated distributions of the monomer units, as will be shown later:

$$w_i(A) = w_i w_A \quad (6)$$

$$w_i(B) = w_i w_B \quad (7)$$

RESULTS AND DISCUSSION

In previous communications [15,16], we have shown that mixtures of PEGs and polypropylene glycols as well as block copolymers of ethylene oxide and propylene oxide can be analyzed using SEC with coupled density and RI detection. We have now applied the new method to mixtures of PTHF and EO-THF copolymers.

As the first step, the validity of the SEC calibration for both homopolymers and the reproducibility of the results had to be checked by repeated injections of samples and calculation of average molecular weights using the calibrations obtained from narrow molecular weight standards of polyethylene oxide (PEO) and PTHF (both from Polymer Labs.). Table I shows the data thus obtained.

The molecular weight averages obtained using the calibrations with PEG and PTHF standards are in good agreement; for the following measurements only the PEG

TABLE I

MOLECULAR WEIGHT AVERAGES OF PEG 1500, PEG 2000 AND PTHF 1300 FROM SEC ON DIFFERENT COLUMN SETS USING CALIBRATIONS WITH PEG AND PTHF STANDARDS

Sample	Column set	Standard	M_w	M_n	M_w/M_n
PEG 1500	B	PEG	1536 ± 5	1460 ± 5	1.052 ± 0.003
	C	PEG	1578 ± 19	1501 ± 24	1.052 ± 0.005
	C	PTHF	1551 ± 21	1454 ± 27	1.066 ± 0.008
PEG 2000	C	PEG	2061 ± 24	1975 ± 32	1.043 ± 0.002
	C	PTHF	2177 ± 13	2032 ± 14	1.072 ± 0.002
PTHF 1300	B	PEG	1272 ± 12	1010 ± 15	1.258 ± 0.012
	B	PTHF	1366 ± 12	1023 ± 12	1.352 ± 0.014
	C	PEG	1352 ± 14	1124 ± 14	1.192 ± 0.007
	C	PTHF	1332 ± 20	1082 ± 13	1.231 ± 0.006

calibration was used. The reproducibility of molecular weight averages is also satisfactory, and so is the accuracy: the values found for PTHF 1300 (Batch No. 20423-1 from Polymer Labs.) agree quite well with the data given by the distributor: weight-average molecular weight, $M_w = 1296$; number-average molecular weight, $M_n = 1163$; $M_w/M_n = 1.13$.

In the second step the accuracy of the response factors was evaluated by analyzing pure homopolymers of EO and THF using the new method.

In Figs. 1 and 2 the weight fractions w_A and w_B of EO and THF units in these

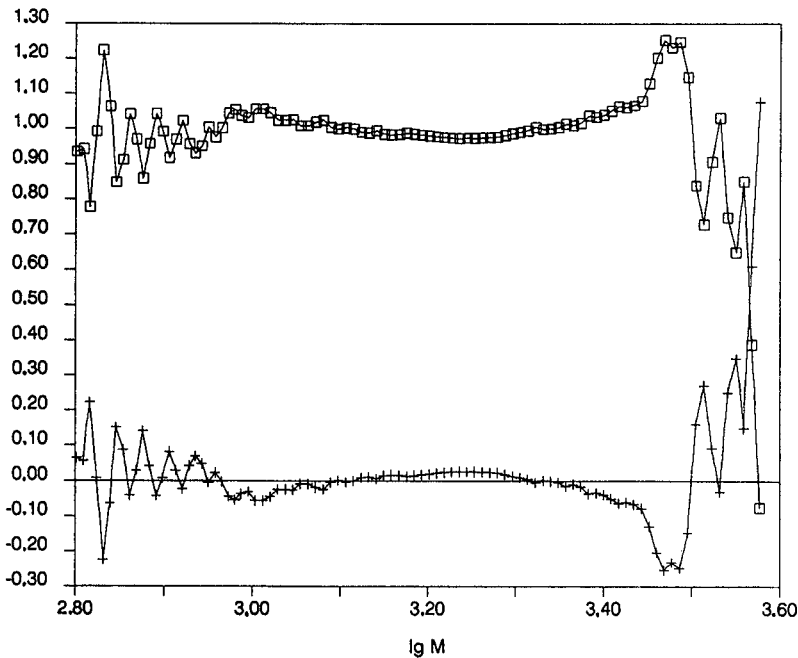


Fig. 1. Weight fractions of the monomer units in PEG 1500 as determined by SEC with density and RI detection. $\square = w_i(\text{EO})$; $+$ = $w_i(\text{THF})$. $\lg = \log$.

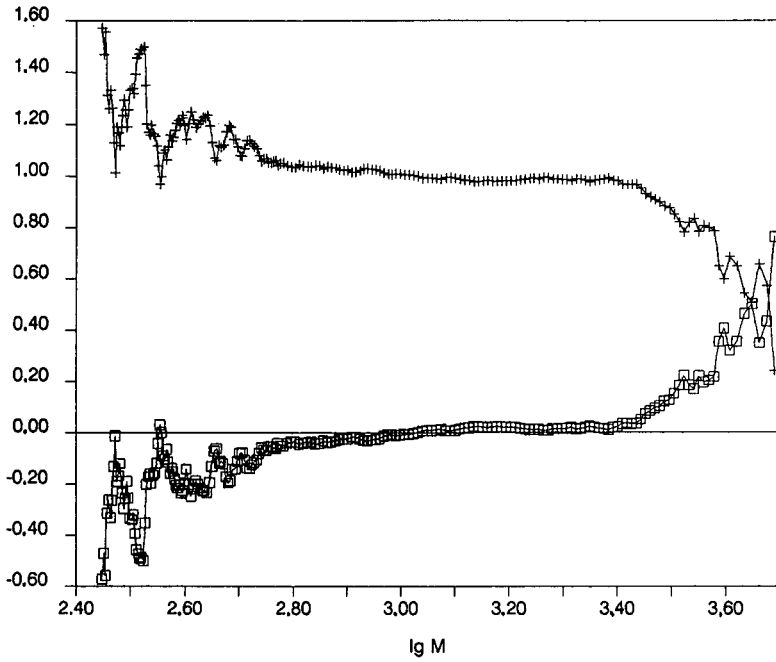


Fig. 2. Weight fractions of the monomer units in PTHF 1300 as determined by SEC with density and RI detection. Symbols as in Fig. 1.

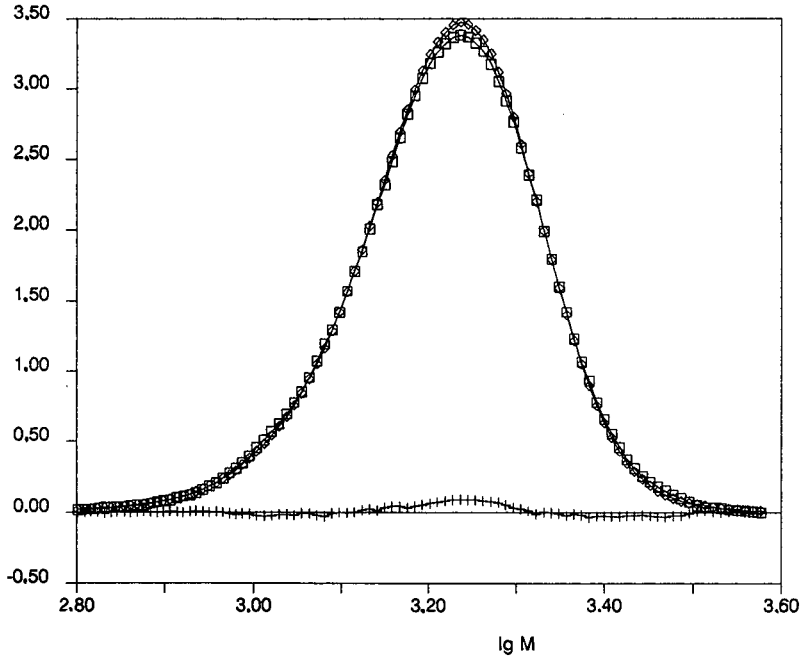


Fig. 3. Molecular weight distribution of PEG 1500 and separated distributions of the monomer units. $\square = w_i(\text{EO})$; $+$ = $w_i(\text{THF})$; $\diamond = w_i(\text{total})$.

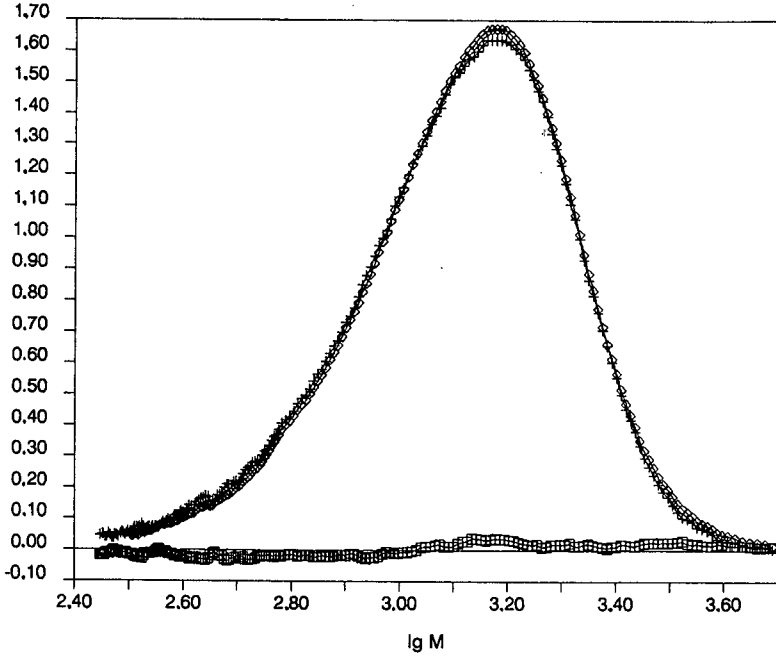


Fig. 4. Molecular weight distribution of PTHF 1300 and separated distributions of the monomer units. Symbols as in Fig. 3.

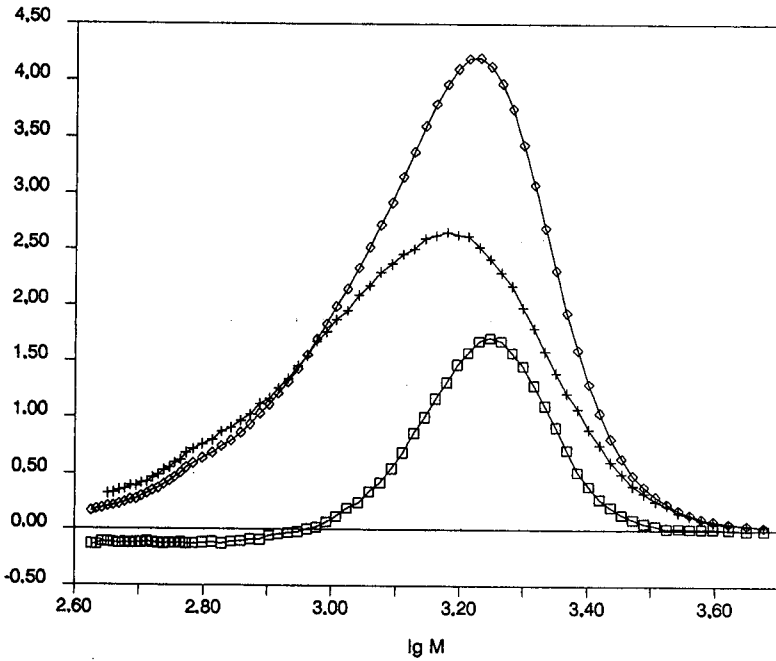


Fig. 5. Molecular weight distribution of a mixture of PEG 2000 with PTHF 1300 and separated distributions of the monomer units. Symbols as in Fig. 3.

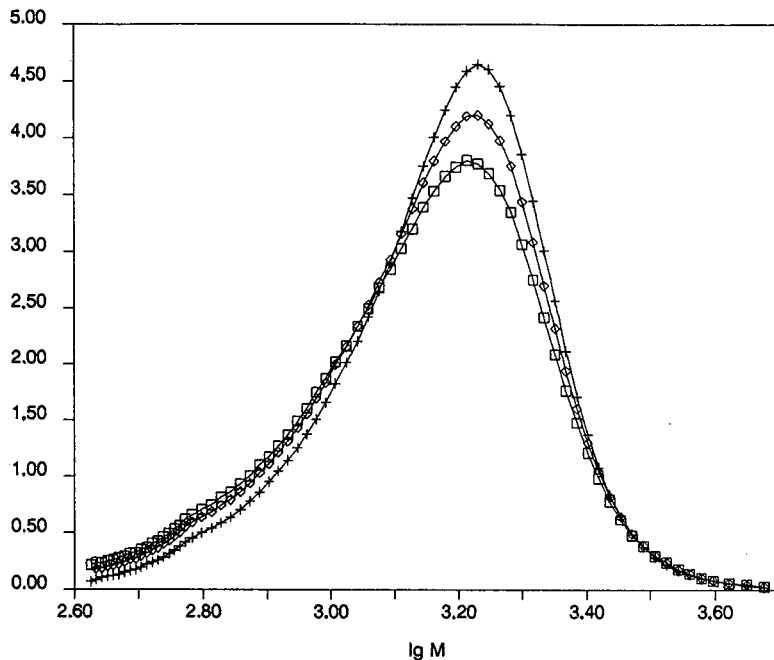


Fig. 6. Molecular weight distribution of a mixture of PEG 2000 with PTHF 1300 from each of the detectors and corrected distribution. \square = w_i (density); $+$ = w_i (RI); \diamond = w_i (corr.).

samples are plotted as a function of molecular weight, and Figs. 3 and 4 show the corrected mass distribution together with the separated distributions of the monomer units. In both cases, the weight fraction of the other monomer is found to be very close to zero over the entire range of the molecular weight distribution, which proves the accuracy of the response factors.

In the third step a mixture of PEG 2000 and PTHF 1300 was analyzed. Fig. 5 shows the overall and the separated mass distributions of the monomer units, which clearly show the non-uniform composition of this sample. In this case, the use of each detector alone would lead to serious errors in the mass distributions and in the molecular weight averages, as is shown in Fig. 6 and Table II.

The fourth step was the application of the new method to a copolymer of EO and

TABLE II

MOLECULAR WEIGHT AVERAGES OF A MIXTURE OF PEG 2000 AND PTHF 1300 DETERMINED BY SEC USING DENSITY AND RI DETECTION

Detection	M_w	M_n
Density	1428	1102
RI	1556	1321
Corrected	1502	1243

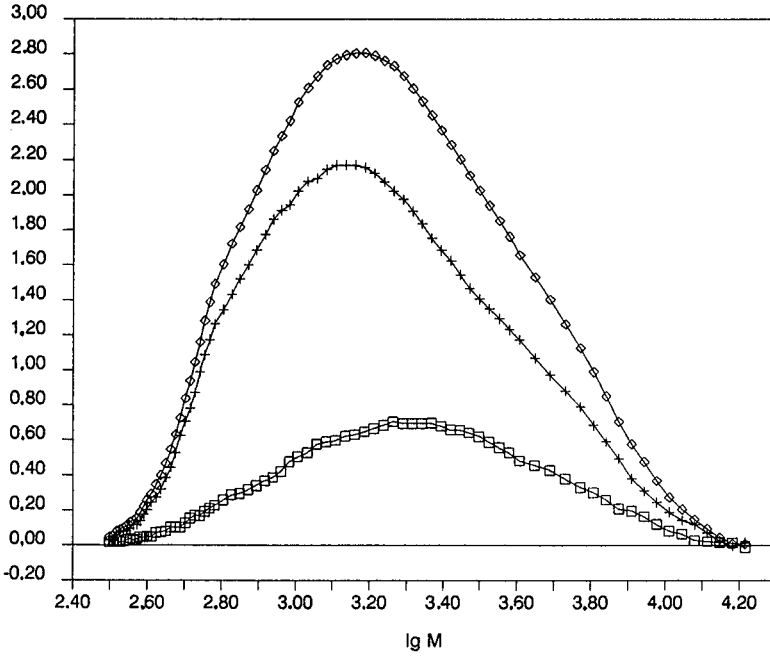


Fig. 7. Molecular weight distribution of EO-THF copolymer and separated distributions of the monomer units. Symbols as in Fig. 3.

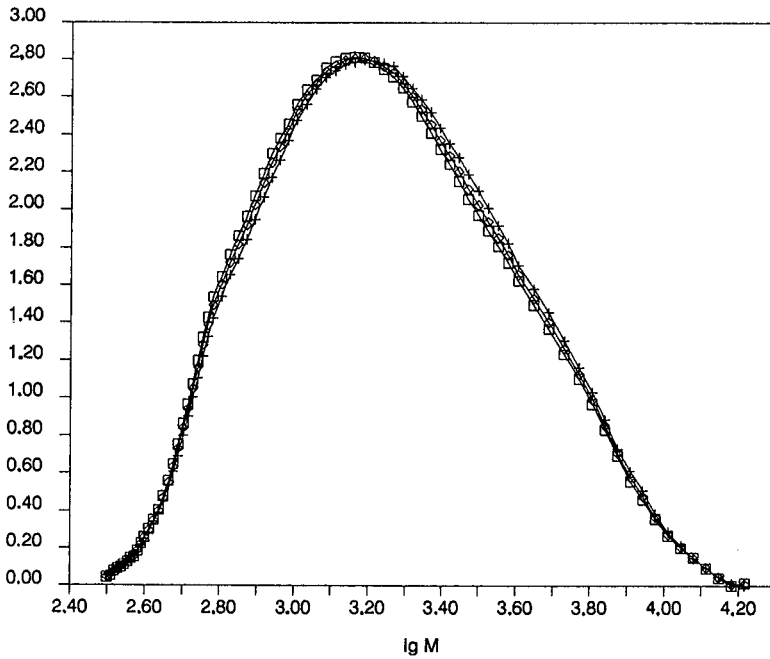


Fig. 8. Molecular weight distribution of EO-THF copolymer from each of the detectors and corrected distribution. Symbols as in Fig. 6.

TABLE III

OVERALL CHEMICAL COMPOSITION OF AN EO-THF COPOLYMER, AS DETERMINED BY ^{13}C NMR SPECTROSCOPY AND SEC WITH DENSITY AND RI DETECTION

	NMR (%)	GPC (%)
EO	23.4	23.5
THF	76.6	76.5

THF, the overall composition of which was also determined by ^{13}C NMR spectroscopy. Figs. 7 and 8 show the molecular weight distribution of this sample in the same representations as in Figs. 5 and 6. Overall this was found to be in very good agreement with the NMR data, as can be seen from Table III. However, the composition is not uniform. Obviously, the EO content increases with molecular weight, which can be seen from Fig. 9.

CONCLUSIONS

SEC with a combination of a density and a RI detector promises to be a very useful tool in the analysis of copolymers of any type with respect to their chemical composition along the molecular weight distribution. Further investigations shall show the scope and limitations of the new method.

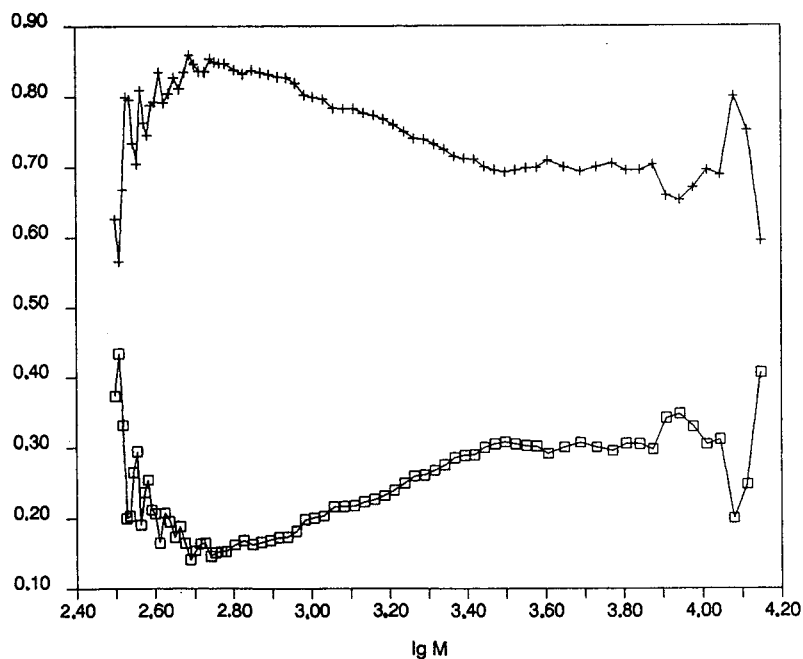


Fig. 9. Weight fractions of the monomer units in EO-THF copolymer as determined by SEC with density and RI detection. Symbols as in Fig. 1.

ACKNOWLEDGEMENT

Financial support from the Austrian "Forschungsförderungs fonds der gewerblichen Wirtschaft" is gratefully acknowledged.

REFERENCES

- 1 M. Hoffmann, H. Krömer and R. Kuhn, *Polymeranalytik I*, Thieme, Stuttgart, 1977, p. 144.
- 2 R. E. Majors, *J. Chromatogr. Sci.*, 18 (1980) 571.
- 3 S. T. Balke and R. D. Patel, in C. D. Craver (Editor), *Polymer Characterization: Spectroscopic, Chromatographic, and Physical Instrumental Methods (Advances in Chemistry Series, No. 203)*, American Chemical Society, Washington, DC, 1983, p. 281.
- 4 G. Glöckner, J. H. M. van den Berg, N. L. J. Meijerink, T. G. Scholte and R. Koningsveld, *J. Chromatogr.*, 317 (1984) 615.
- 5 W. W. Yau, J. J. Kirkland and D. D. Bly, *Modern Size Exclusion Liquid Chromatography*, Wiley, Chichester, New York, 1979, p. 404.
- 6 H. E. Adams, in K. H. Altgelt and L. Segal (Editors), *Gel Permeation Chromatography*, Marcel Dekker, New York, p. 391.
- 7 A. Revillon, *J. Liq. Chromatogr.*, 3 (1980) 1137.
- 8 S. Mori and T. Suzuki, *J. Liq. Chromatogr.*, 4 (1981) 1685.
- 9 T. R. Fang and J. P. Kennedy, *Polym. Bull. (Berlin)*, 10 (1983) 90.
- 10 H. Leopold and B. Trathnigg, *Angew. Makromol. Chem.*, 68 (1978) 185.
- 11 B. Trathnigg and Ch. Jorde, *J. Chromatogr.*, 241 (1982) 147.
- 12 B. Trathnigg and Ch. Jorde, *J. Liq. Chromatogr.*, 7 (1984) 1789.
- 13 B. Trathnigg and Ch. Jorde, *J. Chromatogr.*, 385 (1987) 17.
- 14 B. Trathnigg, Ch. Jorde and B. Maier, *Chromatogr. Anal.*, 5 (1989) 13.
- 15 B. Trathnigg, *J. Liq. Chromatogr.*, 13 (1990) 1731.
- 16 B. Trathnigg, in P. J. Leemstra and L. A. Kleintjens (Editors), *Rolduc Polymer Meetings Proceedings 5, Integration of Fundamental Polymer Science and Technology 5*, Elsevier, Amsterdam, in press.

Miniaturisation of size-exclusion chromatography as a powerful clean-up tool in residue analysis

J. A. VAN RHIJN and L. G. M. Th. TUINSTRAS*

State Institute for Quality Control of Agricultural Products (RIKILT), Bornsesteeg 45, 6708 PD Wageningen (The Netherlands)

ABSTRACT

A miniaturised size-exclusion chromatography (SEC) column with a 2 mm I.D. was developed and compared to a routinely used SEC column with a 10 mm I.D. for the determination of organochlorine pesticides. The flow-rate and sample size were decreased in proportion with the decrease in diameter and the column was tested for recovery of pesticides and for clean-up of animal fat and vegetable samples. Analysis was performed with capillary gas chromatography–electron-capture detection. The miniaturised column proved to be better than the standard SEC column with regard to the removal of the matrix in vegetable samples, while comparable results were obtained with regard to recoveries obtained and results of analysis. Sample size and solvent consumption for the miniaturised SEC column as well as the volume of the collected fraction are dramatically decreased. This facilitates evaporation of solvent which may be necessary to achieve the needed limit of detection.

INTRODUCTION

Since the introduction by Stalling *et al.* [1] of size-exclusion chromatography (SEC) as a versatile and easy to use clean-up method in the area of analysis of organic contaminants, the method has become wide spread. SEC is used to separate the analytes from co-extracted compounds with a higher molecular weight, such as fats and dyes.

Until now a large number of articles have been published dealing with the applicability of SEC in the area of trace analysis of organic contaminants. Several experimental conditions have been used including a number of different column sizes, gel materials, solvents and solvent mixtures [1–4]. Specht and Tillkes [2,3] investigated the elution volume of a large number of organic compounds on a SEC column. Their results indicate very clearly the versatility of SEC as a clean-up method since basically all organic contaminants elute in the same fraction, separated from higher-molecular-weight material. In our laboratory a SEC column (10 mm I.D.) is used on a routine basis for the clean-up of different agricultural products and animal fats in the analysis of pesticides [4]. Other authors use SEC in the determination of animal drugs [5] or polycyclic aromatic hydrocarbons [6].

However, even when using a 10 mm I.D. SEC there are drawbacks, *e.g.* the large solvent consumption and the relatively large volume of the fraction containing the organic contaminants, causing a high degree of dilution of the sample. Dilution of the sample is especially inconvenient when analysis at trace level is to be performed. Evaporation of the solvent, when necessary, is possible but time-consuming and may cause losses of volatile compounds when heating and/or vacuum is used. The results reported by Fernandez *et al.* [6] show clearly the losses due to evaporation; recovery percentages of as low as 52% are reported for some polychlorinated biphenyls, (PCBs) in the analysis of PCBs when using SEC as a clean-up.

In this paper the development of a SEC column of small internal diameter is described and the results are compared to the results obtained with a routinely used SEC system. In general the elution volume of the organic compounds, as well as the flow-rate and the injected sample volume, changes linearly with the square of the column diameter so the same limit of detection (LOD) may be obtained with much lower solvent consumption. Furthermore, concentration of the collected fraction, if necessary, is rapid without the need for heating or applying a vacuum. Evaporation losses are thus reduced to a minimum.

The aim of this work is to miniaturise SEC to such an extent that the resulting small fraction may in future be introduced on-line into a capillary gas chromatographs. In this way a highly automated and very sensitive system for the analysis of pesticides may be obtained.

EXPERIMENTAL

Instrumentation

The 10 mm I.D. SEC column and its operating conditions have already been described by Roos *et al.* [4]. The miniaturised SEC column consisted of a 60 cm \times 2 mm I.D. glass-lined stainless-steel tubing (Techmation, Utrecht, The Netherlands) equipped with column end-fittings and 2- μ m frits. The column was packed with Bio-Beads SX3 gel and eluted with a mixture of ethyl acetate-cyclohexane (1:1) at a flow-rate of 40 μ l/min. All tubing connections were made of 0.18 mm I.D. stainless-steel tubing or 0.3 mm I.D. PTFE tubing and were kept as short as possible to minimise peak broadening. A Gilson 305 high-performance liquid chromatography (HPLC) pump (Meyvis, Bergen op Zoom, The Netherlands) was used together with a Gilson 202 fraction collector. A WISP autosampler (Millipore-Waters, Etten-Leur, The Netherlands) was used to inject 20- μ l aliquots onto the SEC column. SEC chromatograms were recorded using a Merck Hitachi L 4000 UV detector (Merck, Amsterdam, The Netherlands) operated at 280 nm.

The analysis of pesticide-containing fractions was performed by splitless injection of 2- μ l aliquots on a Perkin Elmer 8700 gas chromatograph (Perkin Elmer, Gouda, The Netherlands) equipped with a Perkin Elmer AS 2000 B autosampler, a 25 m \times 0.25 mm I.D. CP SIL 8 CB column with 0.41 μ m film thickness (Chrompack, Middelburg, The Netherlands) and a ^{63}Ni electron-capture detector. Helium was used as carrier gas at a linear velocity of 30 cm/s. After injection, the oven was kept at 90°C for 2 min then the split vent was opened and the oven was heated at a rate of 10°C/min to 250°C. This temperature was maintained for 20 min.

All solvents were purchased from Merck and were distilled in glass prior to use.

For testing purposes a mixture of pesticides was used containing 0.1 $\mu\text{g}/\text{ml}$ HCB (hexachlorobenzene), 0.2 $\mu\text{g}/\text{ml}$ α -HCH (hexachlorocyclohexane), γ -HCH and β -heptachloroepoxide, 0.4 $\mu\text{g}/\text{ml}$ β -HCH, heptachlor, α -chlordane, γ -chlordane, dieldrin, endrin, p,p' -DDE [1,1-dichloro-2,2-bis(*p*-chlorophenyl)ethylene], p,p' -TDE [1,1-dichloro-2,2-bis(*p*-chlorophenyl)ethane] and o,p' -DDT [1,1,1-trichloro-2-(*o*-chlorophenyl)-2-(*p*-chlorophenyl)ethane] and 0.8 $\mu\text{g}/\text{ml}$ p,p' -DDT [1,1,1-trichloro-2,2-bis(*p*-

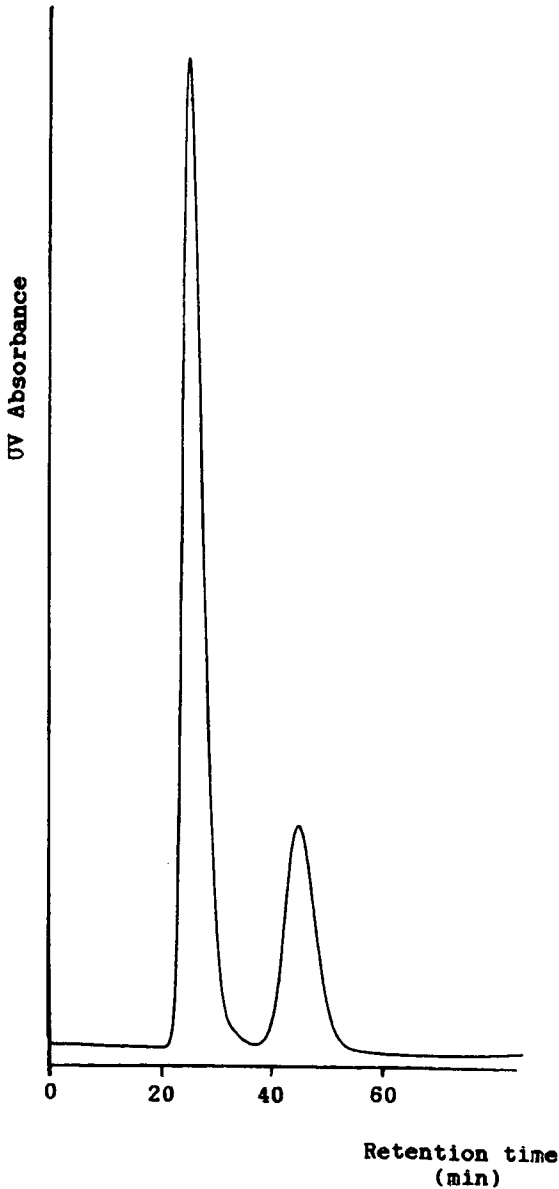


Fig. 1. Typical separation of animal fat and pesticides on a 2 mm I.D. SEC column.

chlorophenyl)ethane]. For the gas chromatographic (GC) determination, this solution was diluted 100-fold to obtain a solution containing 0.001, 0.002, 0.004 and 0.008 $\mu\text{g/ml}$, respectively, of the pesticides mentioned. PCB 138 was added as an internal standard (I.S.) at a final concentration of 0.02 $\mu\text{g/ml}$ in the GC standard solution. For SEC experiments monitored by UV detection, a mixture of the same pesticides was used at concentrations of 10, 20, 40 and 80 $\mu\text{g/ml}$, respectively.

For packing the miniaturised SEC column, the column end-fittings were removed and a reservoir consisting of a piece of 6.4 mm O.D. stainless-steel tubing, length 10 cm, was mounted on top of the column. The reservoir was filled with 10 ml of a slurry of Bio-Beads SX3 in ethyl acetate-cyclohexane (1:1), pre-swollen for 24 h. Trapping of air bubbles in the column packing was avoided by allowing a large part of the thick slurry to flow through the column by gravity. When trapping of air bubbles no longer seemed likely to occur, the column end fitting on the bottom end of the column was replaced and the HPLC pump was connected to the gel reservoir.

The column was then packed over a period of 24 h at a flow-rate of 100 $\mu\text{l/min}$. When packing was completed, the gel reservoir and the surplus of gel slurry were removed and a column end-fitting was mounted. The column was then ready for use.

Procedure

The miniaturised SEC column was connected to a Merck-Hitachi UV detector operated at 280 nm. The flow-rate was set at 40 $\mu\text{l/min}$. A 20- μl aliquot of a solution was injected containing the mentioned fourteen pesticides at concentrations ranging from 10 to 80 $\mu\text{l/ml}$ together with 0.2 g/ml animal fat. The resulting UV chromatogram is shown in Fig. 1. From this chromatogram the elution volume of the pesti-

TABLE I

COMPARISON OF RECOVERY OF PESTICIDES WITH EITHER A 2 MM I.D. SEC COLUMN OR A 10 MM I.D. SEC COLUMN ($n = 10$)

C.V. = Coefficient of variation.

Pesticide	2 mm I.D.		10 mm I.D.	
	Recovery (%)	C.V. (%)	Recovery (%)	C.V. (%)
α -HCH	103	4.2	101	4.2
HCB	89	5.3	102	5.1
β -HCH	85	4.5	101	5.1
γ -HCH	101	4.8	102	4.8
Heptachlor	99	4.7	102	4.1
Heptachloroepoxide	100	3.9	103	3.8
γ -Chlordane	97	2.8	109	3.7
α -Chlordane	98	3.2	106	2.8
p,p' -DDE	94	4.0	110	3.0
p,p' -TDE	92	3.3	107	2.8
o,p' -DDT	96	2.3	108	2.0
p,p' -DDT	99	2.3	109	3.0
Dieldrin	96	3.7	109	3.0
Endrin	96	2.7	105	3.4

TABLE II

RESULTS OF ANALYSIS FOR AN ARTIFICIALLY CONTAMINATED ANIMAL FAT USING EITHER A 2 MM I.D. SEC COLUMN OR A 10 MM I.D. SEC COLUMN ($n = 10$)

Pesticide	Spiking level ($\mu\text{g/g}$)	2 mm I.D. SEC		10 mm I.D. SEC	
		Content ($\mu\text{g/g}$)	C.V. (%)	Content ($\mu\text{g/g}$)	C.V. (%)
α -HCH	0.50	0.50	7.1	0.56	3.8
HCB	0.25	0.24	6.3	0.28	5.6
β -HCH	1.00	0.73	7.7	1.08	3.1
γ -HCH	0.50	0.49	7.3	0.56	3.8
Heptachlor	1.00	1.01	5.4	1.07	3.2
Heptachloroepoxide	0.50	0.49	7.8	0.53	4.3
γ -Chlordane	1.00	0.94	6.7	1.04	4.4
α -Chlordane	1.00	0.97	6.5	1.05	3.7
<i>p,p'</i> -DDE	1.00	1.05	6.7	1.08	4.2
<i>p,p'</i> -TDE	1.00	0.97	7.4	1.04	4.6
<i>o,p</i> -DDT	1.00	1.00	6.2	1.04	3.6
<i>p,p'</i> -DDT	2.00	2.14	8.5	2.10	5.2
Dieldrin	1.00	1.01	5.9	1.08	3.5
Endrin	1.00	0.92	5.7	1.09	3.9

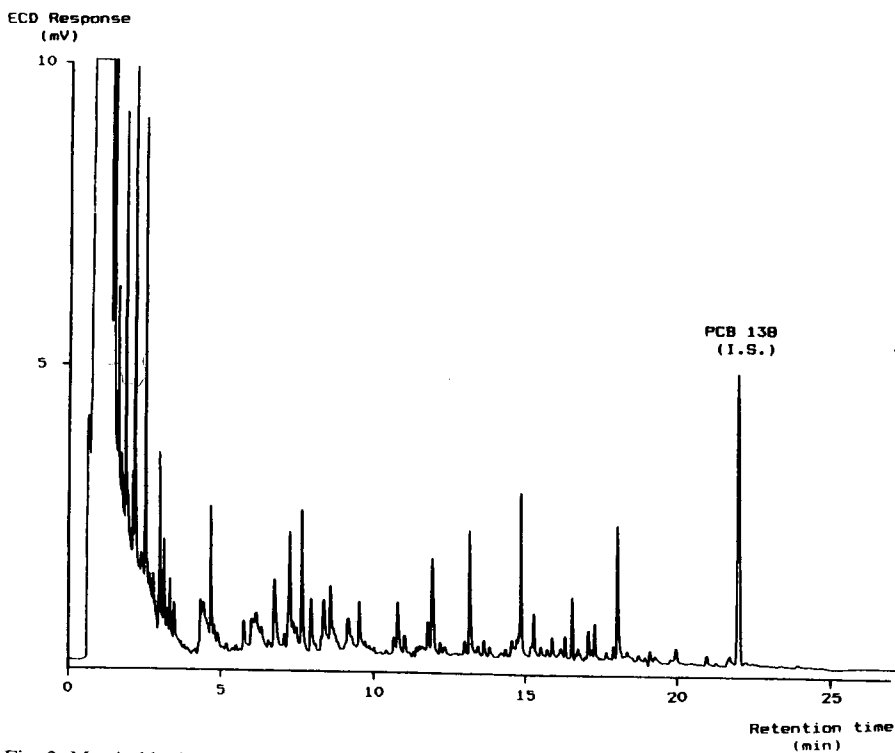


Fig. 2. Matrix blank of pepper obtained with the 10 mm I.D. SEC column. The injected volume corresponds to 0.5 mg of sample.

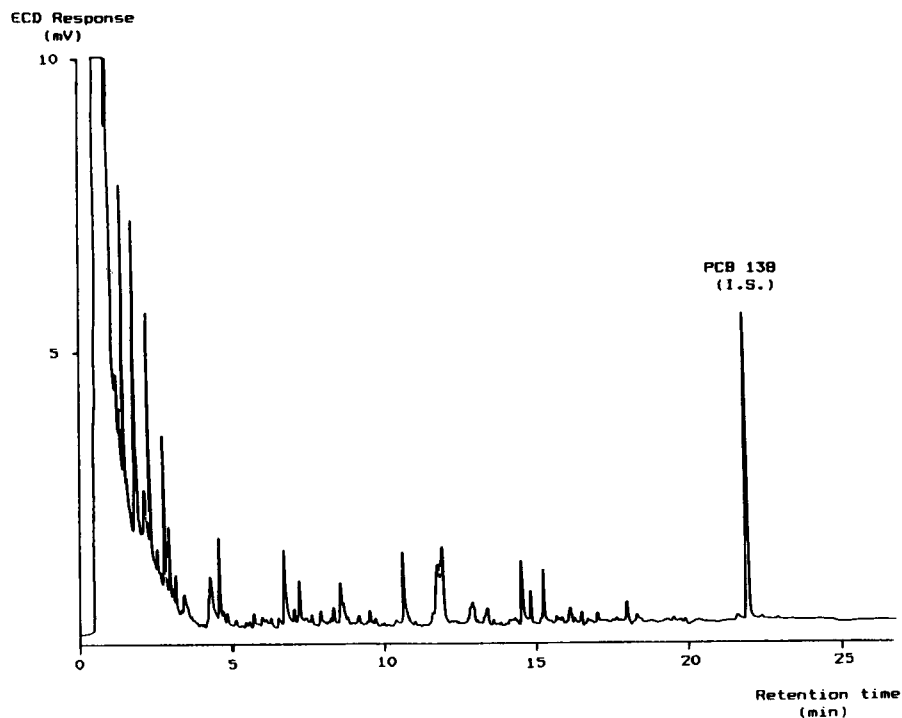


Fig. 3. Matrix blank of pepper obtained with the 2 mm I.D. SEC column. The injected volume corresponds to 0.5 mg of sample.

cides was estimated and the collect and dump times of a fraction collector were adjusted accordingly. Further optimisation was done by injection of a solution of the pesticides over the concentration range 0.1–0.8 $\mu\text{g}/\text{ml}$ and replacing the UV detector by the fraction collector. The pesticides in the fraction collected using the pre-determined collect and dump time were analysed by GC–electron-capture detection (ECD). The collect and dump times were adjusted to obtain a recovery of β -HCH of at least 85% while the recovery of the other pesticides should exceed 90%. These quantitative recoveries of the pesticides could be obtained collecting the eluate between 38.5 and 55 min after injection.

Comparison of the miniaturised SEC column with the 10 mm I.D. SEC column was performed by determining the recovery of fourteen pesticides on each column (Table I). Therefore a 20- μl aliquot of the pesticide solution was injected ten times on each column and the collected fractions were, after addition of PCB 138 as an internal standard, made up to 2 ml, thus yielding the same concentration of pesticides and internal standard in the extract as in the GC standard solution when 100% recovery is obtained.

Artificially contaminated animal fat was also analysed ten times to compare the results of analysis on each column. Pork fat obtained by pentane extraction was used.

The spike levels for the fourteen pesticides and the results of these experiments

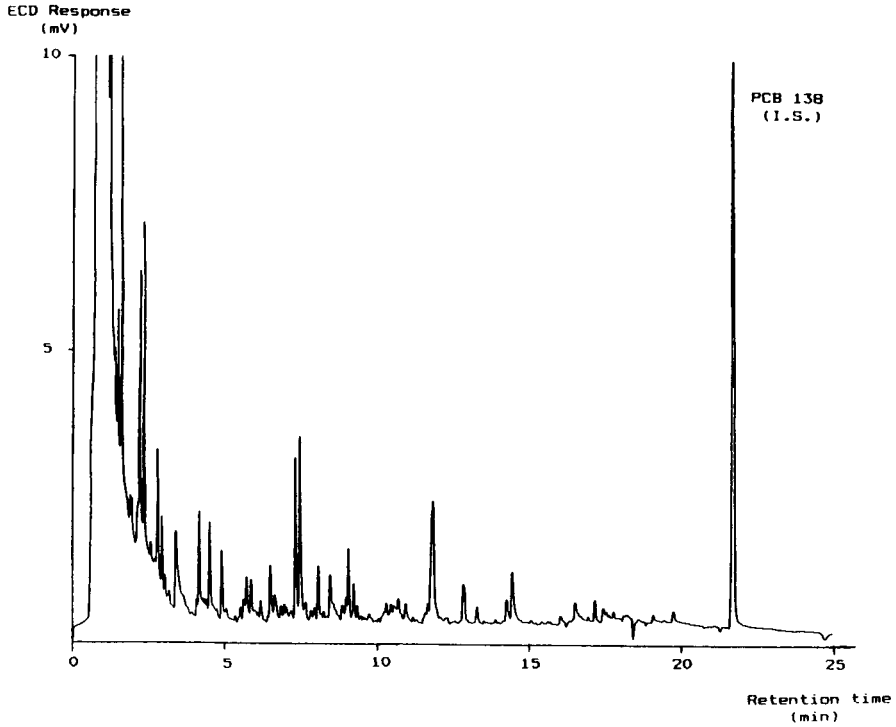


Fig. 4. Matrix blank of pork fat obtained with the 10 mm I.D. SEC column. The injected volume corresponds to 4 mg of sample.

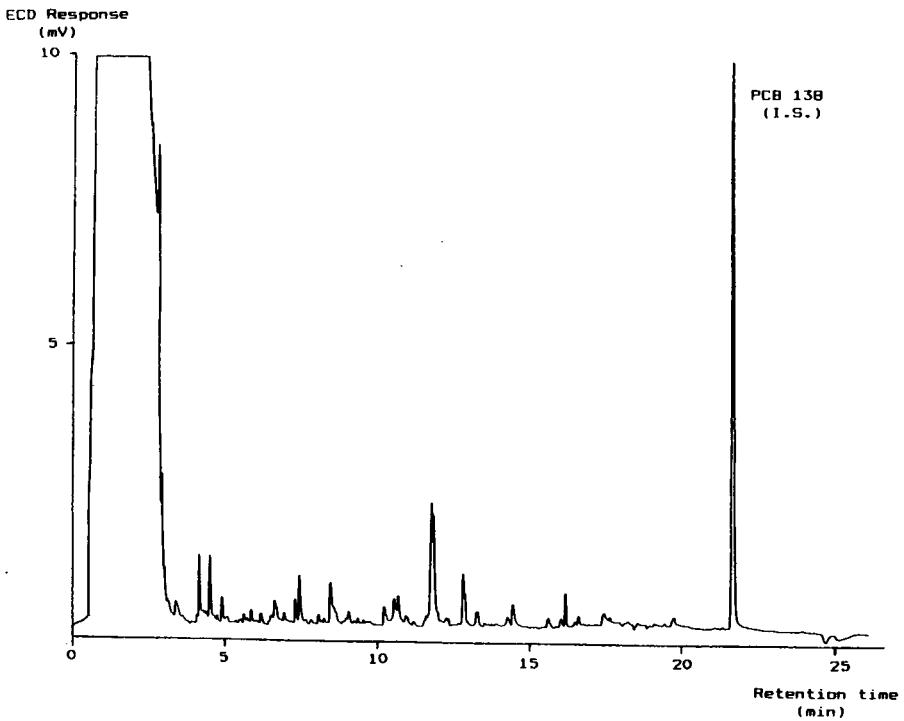


Fig. 5. Matrix blank of pork fat obtained with the 2 mm I.D. SEC column. The injected volume corresponds to 4 mg of sample.

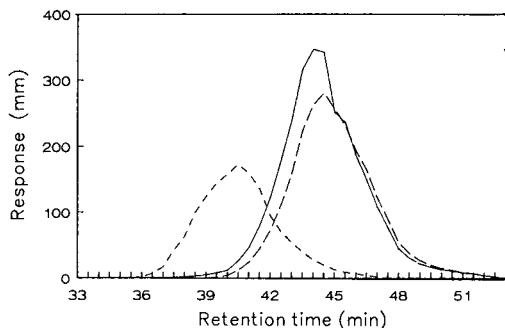


Fig. 6. Elution curves of α -HCH (—), β -HCH (---) and γ -HCH (···) on the 2 mm I.D. SEC column (see text).

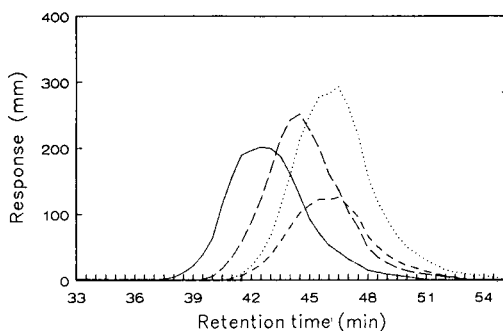


Fig. 7. Elution curves of p,p' -DDE (···), p,p' -TDE (—), o,p' -DDT (---) and p,p' -DDT (-·-·) on the 2 mm I.D. SEC column (see text).

are shown in Table II. The injected aliquot (20 μ l) corresponded to an amount of 4 mg of fat. After addition of PCB 138 as an internal standard, the collected fraction was made up to 1 ml, yielding the same concentration of pesticides and internal standard in the extract as in the GC standard solution when 100% recovery is obtained.

Vegetable extracts were also cleaned on both SEC columns and the chromatograms compared. In Figs. 2, 3, 4 and 5 matrix blanks of a pepper (capsicum) extract and blanks of a pork fat extract are shown as obtained with the 10 mm I.D. columns and the 2 mm I.D. column, respectively.

DISCUSSION

The parameters of the 10 mm I.D. SEC column were decreased in proportion with the square of the column diameter to obtain parameters for the 2 mm I.D. SEC column. Nevertheless, the pesticide-containing fraction on the 2 mm I.D. SEC column appeared larger as compared to the 10 mm I.D. SEC column than expected by calculation. Since the injection volume was reduced in proportion to the decrease of dimensions, this resulted in an even more dilute extract causing an LOD which is,

without evaporation, approximately 20% higher than the LOD obtained with the 10 mm I.D. SEC column.

From the results in Table I the recovery of pesticides appear to be comparable. For β -HCH in general a slightly lower recovery is observed on the miniaturised SEC column (Fig. 6). Increase in the recovery for β -HCH can be obtained by starting the collection of the pesticide fraction earlier, but at the expense of a less thorough clean-up. Since the mean recovery of β -HCH is still 85%, this slightly lower recovery is acceptable. For the other compounds, recoveries on both columns are reasonably good.

The results of analysis of pesticides in an animal fat are comparable on both the miniaturised and the normal SEC column. Again β -HCH gives a lower result on the miniaturised column due to the lower recovery (Table II).

No significant differences in the precision of analysis are observed. From Figs. 2 and 3 a difference in the efficiency of the clean-up becomes clear. The matrix blanks of the pepper extract show some interferences. For the 2 mm I.D. SEC column some interferences are seen but these are significantly smaller than the interferences seen for the 10 mm I.D. SEC column. The greater length of the 2 mm I.D. column probably causes this difference. Also, the difference in residual color was very clear. The same, but to a lesser extent, applies to the clean-up efficiency of samples of animal fat (Figs. 4 and 5). It should be mentioned that when SEC is the sole clean-up technique, only large molecules are removed from the sample extract. Therefore some interferences in the gas chromatogram must be expected.

In Figs. 6 and 7 the elution profile for some pesticides are given. These elution profiles were obtained by fractionating the eluate from the SEC column at 30-s intervals (20 μ l) and determining the pesticide concentration in each collected fraction by GC-ECD. The shown elution profiles were reconstructed from these data. From the difference in elution volume for β -HCH compared to α -HCH and γ -HCH, it is obvious that size exclusion is not the only separating mechanism. These compounds are isomers which differ only in equatorial or axial substitution of chlorine to the cyclohexane ring. When only size exclusion contributes to the separation, all three isomers should have approximately the same elution volume. The same applies to the elution volumes of the DDT-related compounds. In size exclusion the elution volume is influenced by molecular weight as well as molecular shape. The substitution of chlorine on either equatorial or axial positions on the cyclohexane ring of the HCHs may influence molecular shape. However, the observed difference in elution volume is large considering the fact that a low resolution gel is used. Therefore it does not seem likely that size exclusion, including both molecular weight and molecular shape effects, is the only separating mechanism. The difference in elution volume may be caused by adsorption effects. In that case adsorption for all the pesticides differs only slightly, with a sudden adsorption minimum for β -HCH. On the other hand some partitioning may occur, resulting in differences in elution volume. Partitioning may be due to small differences in eluent composition between the stationary and the mobile eluent.

From the data on elution profiles it is clear that β -HCH is the first eluting compound while endrin is the last eluting compound of the pesticides investigated. Using the recovery of these two compounds, the collect and dump times for the collection of a pesticide-containing fraction can be readily optimised.

In the near future, the authors will start experiments to interface a miniaturised SEC column with 2 mm or even smaller I.D., with capillary GC. This interfacing of clean-up method with the method of analysis will make complete automation of clean-up and determination possible.

CONCLUSIONS

Miniaturised SEC is comparable to normal-sized SEC, offers a means of lowering sample and solvent consumption, and facilitates concentration of the collected fraction by evaporation. The LOD is slightly higher for miniaturised SEC due to a less than proportionally larger pesticide fraction.

Both types of columns were compared with respect to the recovery of pesticides, the results of analysis and the precision of analysis. The data presented show that the columns are comparable with respect to these items. The 2 mm I.D. SEC column tested appeared to give better clean-up, probably due to the increased column length. This became most apparent when analyzing vegetable samples containing large amounts of dyes.

ACKNOWLEDGEMENT

The authors wish to thank Professor Dr. A. Ruiter for his important contribution to discussions on the subject.

REFERENCES

- 1 D. L. Stalling, R. C. Tindle and J. L. Johnson, *J. Assoc. Off. Anal. Chem.*, 55 (1972) 32.
- 2 W. Specht and M. Tillkes, *Fresenius Z. Anal. Chem.*, 301 (1980) 300-307.
- 3 W. Specht and M. Tillkes, *Fresenius Z. Anal. Chem.*, 322 (1985) 443-455.
- 4 A. H. Roos, A. J. van Munsteren, F. M. Nab and L. G. M. Th. Tuinstra, *Anal. Chim. Acta*, 196 (1987) 95-102.
- 5 M. Petz and U. Meetschen, *Z. Lebensm. Unters. Forsch.*, 184 (1987) 85-90.
- 6 P. Fernandez, C. Porte, D. Barcelo, J. M. Bayona and J. Albaiges, *J. Chromatogr.*, 456 (1988) 155-164.

CHROMSYMP. 2266

Effects of modifiers in packed and open-tubular supercritical fluid chromatography

HANS-GERD JANSSEN*

Laboratory of Instrumental Analysis, University of Technology, P.O. Box 513, 5600 MB Eindhoven and Philips Research Laboratories, P.O. Box 80 000, 5600 JA Eindhoven (The Netherlands)

PETER J. SCHOENMAKERS

Philips Research Laboratories, P.O. Box 80 000, 5600 JA Eindhoven (The Netherlands)

and

CAREL A. CRAMERS

Laboratory of Instrumental Analysis, University of Technology, P.O. Box 513, 5600 MB Eindhoven (The Netherlands)

ABSTRACT

The applicability of packed and open columns for supercritical fluid chromatography using pure carbon dioxide for the elution of a number of selected test components was investigated. It is shown that the number of solutes that can be eluted as symmetrical peaks is much larger in open-tubular capillary supercritical fluid chromatography. For strong hydrogen donors and acceptors, however, poor peak shapes were observed on both types of columns. In both cases, modifiers are needed. Modifiers may effect retention by increasing the mobile phase polarity and density, and by deactivating active sites. The relative influence of these processes was studied in packed and open columns. The effects of various modifiers in packed and open columns were compared under identical operating conditions. The influence of temperature on retention and peak shape was studied for pure carbon dioxide and carbon dioxide–modifier mixtures. The influence of modifiers on retention was found to be larger at lower operating temperatures. For components with high affinities for silanol groups the influence of polar modifiers on the capacity factor and the peak shape was found to be of comparable magnitude in packed and open columns. Columns packed with alkyl-modified poly(styrene–divinylbenzene) and with porous carbon coated with poly(ethylene glycol) were used to study the influence of modifiers without interference from silanol groups. Polar and non-polar modifiers were used to study the relative influence of the polarity and density effects of the modifiers.

In supercritical fluid chromatography (SFC) both packed and open-tubular columns are routinely used. Packed columns generally offer an increased speed of analysis in comparison with open-tubular columns. However, when high plate numbers are necessary, open columns are preferable [1,2]. Plate numbers in excess of approximately 20 000 are not readily attainable in packed-column SFC, because the maximum length of the column is limited by the maximum allowable pressure drop. With open-tubular columns much higher plate numbers can be obtained. Here the pressure drop is lower owing to the higher permeability of the column.

A distinct disadvantage associated with the use of packed columns in SFC with carbon dioxide is the necessity to add modifiers for the elution of even slightly polar solutes. This largely cancels one of the advantages of SFC over liquid chromatography (LC), *i.e.* the improved detector compatibility. The use of modifiers in packed-column SFC has been more extensive than in open-tubular columns. In packed columns low concentrations of modifiers ($< 1\%$) can drastically reduce retention and drastically improve peak shapes [3–5]. In a recent study we observed a 50-fold reduction in the capacity factor of 2-hydroxyethyl methacrylate on a C_{18} packed column upon adding 0.5% ethanol to the carbon dioxide [6]. In comparison, Fields *et al.* [7] observed an approximately ten-fold reduction of the capacity factor of coronene upon adding 9% 2-propanol to the mobile phase in an open-tubular column coated with a 30% biphenyl methyl polysiloxane stationary phase. The different magnitudes of the effects of modifiers on retention in packed and open columns can be explained by the presence of active sites on the surface of the packing material. The effects of modifiers on retention and peak shape in packed-column SFC have been the subject of a large number of investigations (*e.g.* refs. 3–6 and 8–13). In contrast, few studies on the effects of modifiers in open-tubular SFC have been described [14–18]. A direct comparison of literature data on the effects of modifiers in packed and open columns cannot be made easily, because different solutes and different operating conditions have been used.

We recently identified four different ways in which modifiers might influence retention in packed-column SFC [19]. Mobile phase properties affected by the addition of a modifier include the density and the polarity. Because the mobile phase in packed and open columns is identical, these effects of the modifier are the same. By adsorption onto or partitioning into the stationary phase, modifier molecules can deactivate active sites on the packing material or on the column wall. In addition, increased solvation or swelling of the stationary phase can occur. In previous work we correlated the retention behaviour of solutes with the adsorption isotherms of modifiers in packed-column SFC [6]. The variation in the observed capacity factor with the modifier concentration could be described accurately by a mixed-retention model, in which silanol groups and chemically bonded groups were assumed to contribute independently to overall retention. This suggests that the effects of low concentrations of modifiers in packed-column SFC are primarily the result of stationary phase deactivation.

In this paper we will study the applicability of packed and open-tubular columns using pure carbon dioxide for the elution of a variety of components. The effects of modifiers in packed and open columns will be compared using similar stationary phases under identical operating conditions. The effects of temperature on retention and peak shape will be described. Furthermore, the effects of modifiers in packed and open columns will be investigated at various temperatures. Non-silica-based stationary phases for SFC are used to study the effects of modifiers in a system without interfering silanol groups.

EXPERIMENTAL

All experiments with packed columns were performed on a home-built SFC instrument. The mobile phase delivery system consisted of two reciprocating piston

pumps to allow operation with mixed mobile phases. A detailed description of this system has been published previously [20]. UV detection was used exclusively. The carbon dioxide (Air-liquide, Amsterdam, The Netherlands) had a purity of 99.8%. Ethanol and hexane (both p.a. grade) were used as modifiers and were obtained from Merck (Darmstadt, Germany). Several columns were used during the experimental work. A column packed with polydimethylsiloxane-encapsulated silica (Db-C₁) was obtained from Keystone (Bellefonte, PA, U.S.A.). An alkyl-modified polystyrene-divinylbenzene (PS-DVB) column (ACT-1) was purchased from Bêtron (Rotterdam, The Netherlands). A column packed with porous carbon coated *in situ* with polyethylene glycol, resulting in what we describe as a 'carbonwax' column, was prepared in house [21]. The totally porous carbon was obtained from Professor J. Knox (University of Edinburgh, Edinburgh, U.K.). All packing materials had a nominal particle size of 5 μm. The columns had an inner diameter of 4.6 mm and a length of 150 mm, except the carbonwax column, which had a length of 100 mm.

The experiments with open-tubular columns were carried out on a Carlo Erba 3000 Series SFC system (Carlo Erba, Milan, Italy). The carbon dioxide was obtained from Hoekloos (Schiedam, The Netherlands) and had a purity of 99.8%. Cylinders with carbon dioxide-ethanol mixtures were prepared in house. After filling the pump the composition of the carbon dioxide-modifier mixture in the pump was analyzed. For this analysis, a gaseous sample of the mixed mobile phase was collected in a gas bulb and subsequently analyzed by gas chromatography (GC). In this way uncertainties with regard to the composition of the mixed mobile phase, which might arise from a gradual change in composition of the mixture in a cylinder during usage, were avoided [20]. Several detectors were used during the experiments. A flame ionization detector (FID) and a nitrogen-phosphorous detector (NPD) were obtained from Carlo Erba. A photo ionization detector (PID) was obtained from HNU (Model PI-52-02, HNU, Newton, MA, U.S.A.). All three detectors gave good results with pure carbon dioxide. With mixed mobile phases only the NPD and the PID could be used. Both detectors showed decreasing performance (*i.e.* increased noise and reduced sensitivity and stability) at increasing modifier concentrations. Two open-tubular columns were used. The first one was a DB-1 column (J&W, Folsom, CA, U.S.A.) with a length of 10 m, an inner diameter of 100 μm and a film thickness of 0.4 μm. The second column was a CP-Sil 5 CB column (Chrompack, Middelburg, The Netherlands). This column had a length of 10 m, an inner diameter of 50 μm and a film thickness of 0.2 μm. Both stationary phases are poly(dimethylsiloxane) polymers. The chemical nature of these phases is thus comparable with that of the Db-C₁ packed column.

Solutes were obtained from various sources and were all of the highest purity available. The sample concentrations were approximately 1 mg/ml for aromatic and 10 mg/ml for aliphatic solutes. Dichloromethane, which was assumed to be unretained, was used to measure the dead times.

RESULTS AND DISCUSSION

Retention in SFC is determined by the properties of the solute in relation to those of the mobile and the stationary phase. Because the solvent strength of a supercritical fluid very much depends on the operating pressure and temperature, a direct

comparison of the capacity factors and peak shapes in packed and open columns should be made under identical operating conditions. In that case all differences in the elution behaviour can be ascribed to the stationary phase. If the chemical nature of the stationary phases in the two columns is also identical, then different capacity factors or peak shapes must be the result of either different phase ratios or a more pronounced contribution of active sites to retention in one of the columns.

Table I provides a summary of the peak shapes and the capacity factors observed for 22 solutes on the Db-C₁ packed column and the CP-Sil 5 open column. Both stationary phases are poly(dimethylsiloxanes) and in each case pure carbon dioxide was used as the eluent. The peaks are classified into four categories: sharp, symmetrical peaks (+); broadened, possibly asymmetrical peaks (●); very broad, symmetrical peaks (–); and not eluted (×).

TABLE I

COMPARISON OF THE ELUTION CHARACTERISTICS OF PACKED AND OPEN COLUMNS WITH PURE CARBON DIOXIDE

Conditions: temperature = 50°C; (average) pressure = 105 bar. Packed column: Db-C₁. Open column: CP-Sil 5 CB. The peak shapes are identified as sharp (+), broadened (●) and very broad (–). Components that are not eluted with a capacity factor of 30 or less are identified by ×. Capacity factors were calculated from the peak maxima. Values obtained from distorted peaks are given in parentheses.

Solute	Peak shape		Capacity factor	
	Packed	Open	Packed	Open
Benzene	+	+	0.12	0.045
Toluene	+	+	0.20	0.046
<i>n</i> -Propylbenzene	+	+	0.40	0.094
<i>sec.</i> -Butylbenzene	+	+	0.48	0.12
Phenol	●	●	(1.43)	(0.13)
4-Nitrophenol	×	–	–	(0.98)
2-Nitrophenol	●	+	0.92	0.15
2,4-Dinitrophenol	×	●	–	(0.28)
Bromobenzene	+	+	0.49	0.11
<i>N,N</i> -Dimethylaniline	–	●	(1.27)	(0.14)
2-Nitrotoluene	+	+	0.81	0.15
Benzyl alcohol	–	●	(2.53)	(0.11)
Methyl benzoate	●	+	(0.83)	0.11
Nitrobenzene	+	+	0.78	0.13
Dimethyl phthalate	●	+	(2.79)	0.20
Naphthalene	+	+	0.70	0.21
Biphenyl	+	+	1.40	0.32
2-HEMA ^a	–	●	(3.85)	(0.066)
Diheptyl ether	+	+	0.71	0.31
2-Tridecanone	●	+	(1.68)	0.27
Cyclohexanone	–	+	(1.00)	0.060
Quinoline	×	–	–	(0.31)
Total score:				
+	10	15		
●	5	5		
–	4	2		
×	3	0		

^a 2-HEMA = 2-hydroxyethyl methacrylate.

asymmetrical peaks (–); and components that were not eluted with a capacity factor of 30 or less (\times). All solutes are of fairly low molecular weight and are readily amenable to GC. The selected components, however, represent a wide variety of chemical functionalities and provide an indication of the applicability of packed and open columns with pure carbon dioxide as the mobile phase.

As can be seen in the table, the capacity factors on the packed column are larger than those on the open column. The components that are eluted as symmetrical peaks from both columns have a 2.5–6 times higher capacity factor on the packed column. A constant factor can be attributed to the larger phase ratio of the packed column. It might be possible that, although both phases are (polydimethylsiloxanes), slight differences exist in the chemical properties of the stationary phases in the packed and the open column. Furthermore, the pressure drop over the packed column was significantly greater than that over the open column, which might influence retention measurements. For the solutes that give poor peak shapes on the packed column, the ratio of the capacity factors is much larger than the factors between 2.5 and 6 mentioned above. These solutes are retained to a much larger extent on the packed column, most likely because of a contribution of active sites to retention. As can be seen in the table, the open column gives better peak shapes than the packed column. From the open column 15 out of the 22 solutes are eluted as sharp, symmetrical peaks. On the packed column only ten solutes fall into this category; the remaining twelve solutes are either eluted as (very) broad peaks or are not eluted at all. This indicates that the problems experienced when trying to elute these solutes from the packed column must be caused at least partly by active sites in the column and not only by a poor solubility in the mobile phase. On this column at least seven components require modifiers (categories – and \times in the table). On the open column only the highly polar solutes quinoline and 4-nitrophenol require modified mobile phases.

In Fig. 1 the effects of low modifier concentrations are compared for packed and open columns. Fig. 1A and B shows the effects of the ethanol concentration on the capacity factors of quinoline and 4-nitrophenol, respectively. The capacity factors are normalized to 1 at zero modifier concentration. For quinoline the effect of the modifier is more pronounced in the packed column, although a significant decrease in

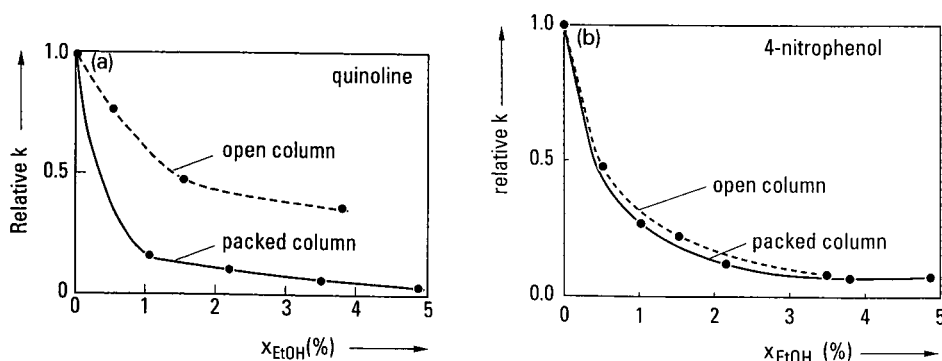


Fig. 1. Variation of normalized capacity factors with modifier concentration in packed and open columns. Open column: DB-1. Packed column: Db-C₁. Conditions: temperature 55°C; (average) pressure, 110 bar. Solutes: A, quinoline; B, 4-nitrophenol. EtOH = Ethanol.

retention also occurs in the open column. As can be seen in Fig. 1B, the effects of modifiers in both columns are very similar for certain solutes when compared on a normalized scale. Fig. 1 clearly illustrates that drastic effects of modifiers on retention are not limited to packed columns but can also occur in open-tubular columns. The fact that very small amounts of modifiers have a dramatic effect on retention in open columns suggests that a significant number of active sites are also present there. Fig. 2 shows the effect of a polar modifier on the peak shape observed for 4-nitrophenol on the open column. A drastic improvement is observed upon the addition of just 0.5% ethanol.

In Table I and Fig. 1 the performance of packed and open columns is compared at identical (average) pressure and temperature. Under these conditions the solvent strengths of the mobile phases are identical and differences in the elution behaviour should be attributed to the stationary phase. In daily practice, however, capillary columns are generally operated at higher temperatures. Two reasons for this can be identified. Firstly, the phase ratio of the open column is much lower than that of the packed column, which implies that a mobile phase with a lower solvent strength must be used to obtain reasonable capacity factors. Operating open columns at higher temperatures is also beneficial with regard to solute diffusivity. Diffusion is enhanced at higher temperatures. This increases the optimum velocity or, at constant velocity, it increases the plate number of the open column. In columns packed with small particles, the interparticle distances are small, so that the speed of diffusion is less critical. Table II gives a summary of the physical properties of carbon dioxide at typical operating temperatures for packed and open columns. The table clearly illustrates the lower solvent strength (or density) and the higher diffusivity under typical conditions for open-tubular SFC.

Because open and packed columns are generally operated at different temperatures, a more detailed study of the effects of temperature on retention and peak shape is required. Fig. 3 illustrates the influence of temperature on retention for the Db-C₁ packed column. In the figure three different zones can be distinguished. The occurrence of these three zones can be understood by carefully evaluating the contri-

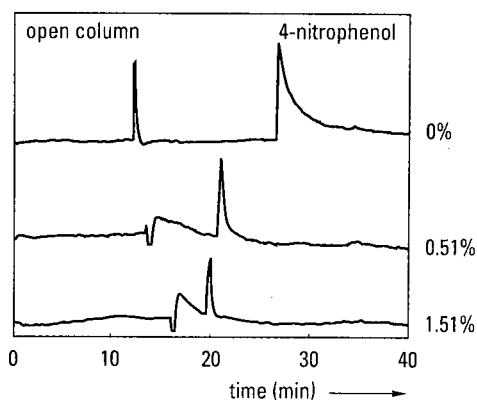


Fig. 2. Effect of modifiers on the peak shape. Open column: DB-1. Solute: 4-nitrophenol. Modifier: ethanol. Further conditions as in Fig. 1.

TABLE II

PHYSICAL PROPERTIES OF CARBON DIOXIDE AT 200 BAR AND DIFFERENT TEMPERATURES

The density values (ρ) were calculated using the IUPAC equation of state [22]. Mobile phase viscosities (η) were obtained from ref. 23. The binary diffusion coefficients (D_m) were estimated for n-C₃₀ using the Wilke-Chang equation [24].

Column	Temperature (°C)	ρ (g/ml)	η (10^{-6} Ns/m ²)	D_m (10^{-5} cm ² /s)
Packed	35	0.866	81.3	3.5
	55	0.755	64.3	5.1
Open	80	0.595	45.8	7.7
	150	0.327	30.3	13.9

butions of the mobile and the stationary phase to retention. The contribution of the stationary phase to retention is relatively straightforward. At a constant solvent strength of the mobile phase, adsorption onto or partitioning into the stationary phase decreases constantly with increasing temperature. The contribution of the mobile phase is more complex. In the LC branch at low temperatures the mobile phase is a liquid with a solvent strength that is only slightly affected by the temperature. In this region retention decreases with increasing temperature because of a reduced interaction of the solute with the stationary phase and, eventually, with active sites. In the SFC part of the curve the decrease in the mobile phase density (thermal expansion) causes retention to increase with temperature. At even higher temperatures solute volatility becomes significant and retention will decrease again with increasing temperature. It can be seen that quinoline may be eluted from this column with the same capacity factors (between 3.8 and 5) under LC, SFC and GC conditions. In Fig. 4 the peak shapes obtained on the packed column at three different temperatures are com-

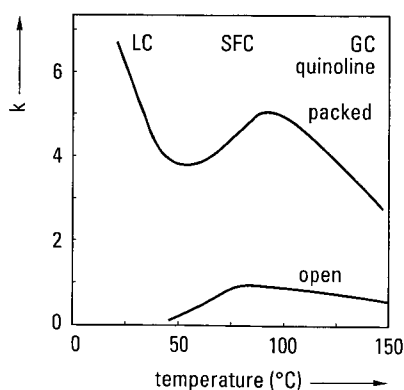


Fig. 3. Effect of temperature on retention in packed and open columns. Solute: quinoline. Open column: CP-Sil 5. Packed column: Db-C₁. The experiments with the open column were performed at a constant pressure of 120 bar. For the packed column constant inlet and outlet pressures of 179 and 162 bar, respectively, were used.

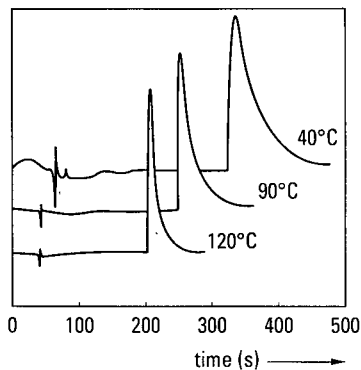


Fig. 4. Effect of temperature on the peak shape. Packed column: Db-C₁. Inlet pressure: 179 bar; Outlet pressure, 162 bar. Solute: quinoline. Mobile phase: pure carbon dioxide.

pared. The figure clearly shows an improved peak shape at higher temperatures, which is an additional reason for performing SFC separations at the maximum temperature allowed by the solute and the stationary phase.

Fig. 5A and B illustrates the influence of ethanol on retention as a function of the temperature. Fig. 5A gives the results on the Db-C₁ packed column. Fig. 5B gives those on the CP-Sil 5 open column. The general trend in the two figures is similar. The effect of the modifier is most pronounced at low temperatures. As an illustration, 4% ethanol gives a sixteen-fold reduction of the capacity factor of quinoline on the packed column at 25°C. At 150°C the same concentration only reduces retention by a factor of 1.7. When 0.5% ethanol was added to the carbon dioxide, the descending branch of the curve in the low-temperature region disappeared. The addition of the

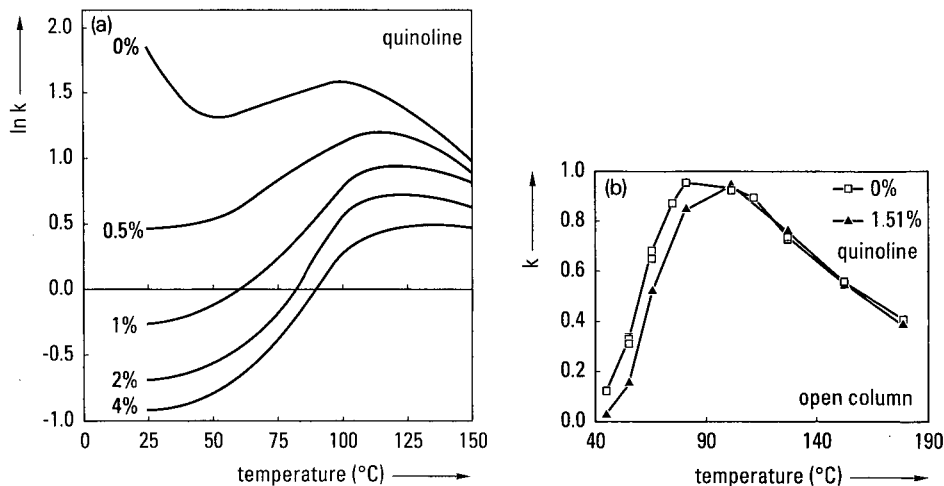


Fig. 5. Effects of ethanol on retention as a function of temperature. Solute: quinoline. (A) Packed column: Db-C₁; inlet pressure: 179 bar; outlet pressure: 162 bar. (B) Open column: CP-Sil 5; pressure: 120 bar.

modifier apparently effectively suppresses the contribution of adsorption to retention. As the contribution of adsorption is largest at low temperatures, the modifier effects are most pronounced in the low-temperature region. This also holds for the open column, as can be seen in Fig. 5B. At temperatures below 90°C, the modifier has a considerable influence on retention. Above 90°C the effect is negligible. The large effects of low modifier concentrations again indicate that adsorption on active sites may also play an important role in open columns.

From the results presented above it can be concluded that packed and open columns may differ in the degree of interaction. The kinds of interaction, however, remain the same. Owing to the interfering effects of silanol groups, no conclusions can be drawn regarding the relative magnitude of mobile and stationary phase effects of the modifier. On both the packed and the open column the mobile phase effects of the modifier are overshadowed by the deactivation effect. To establish the magnitude of the density and the polarity effect of the modifier in the mobile phase, a system free of interfering active sites is necessary. All silica-based stationary phases for packed-column SFC have previously been shown to exhibit some degree of surface activity [19,21]. Non-silica-based phases are necessary to circumvent the contribution of silanol groups to retention. When the stationary phase effects of the modifier can be neglected, the relative magnitude of the polarity and the density effect in the mobile phase can be estimated from a plot of the capacity factor of a test solute *versus* the fluid density. In Fig. 6A and B the effects of the polar modifier ethanol and the non-polar modifier hexane on two columns packed with non-silica-based stationary phases are illustrated. Fig. 6A shows the results obtained on a PS-DVB column, and Fig. 6B those of the carbonwax column. The experiments with modifiers on the PS-DVB column were performed at 55°C and at constant inlet and outlet pressures of 179 and 162 bar, respectively. The experiments on the carbonwax column were performed at 60°C and at inlet and outlet pressures of 179 and 163 bar, respectively. The density of the fluid increased when the modifier was added. Densities of mixed fluids were estimated using the Lee and Kesler method [25], which was previously shown to

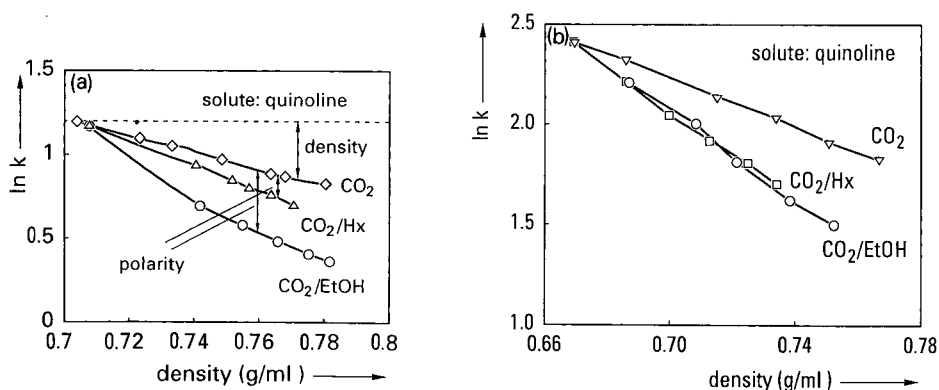


Fig. 6. Effects of polar and non-polar modifiers on retention on non-silica-based materials. Solute: quinoline. Modifiers: EtOH = ethanol; Hx = hexane. (A) Packed column: PS-DVB; temperature: 55°C; inlet pressure: 179 bar; outlet pressure: 162 bar. (B) Packed column: carbonwax; temperature: 60°C; inlet pressure: 179 bar; outlet pressure: 163 bar.

yield accurate estimates [19]. The pseudocritical parameters which are required as input data for the density calculations were estimated from the mixing rules described by Lee and Kesler [25]. The density of pure carbon dioxide was varied by varying the pressure. In the figure the distance between the dashed horizontal line and the line for carbon dioxide represents the effect of density on retention. The differences between the curve of pure carbon dioxide and the curves for the mixed mobile phases represent the effect of the mobile phase polarity on retention. Although hexane is essentially a non-polar solute, it still shows a considerable polarity effect, *i.e.* there appear to be significant molecular interactions between the quinoline molecules and the hexane-containing mobile phase. Significant interactions of solute molecules with a hexane mobile phase were also observed by Phillips and Robey [26] in a comparative study on the properties of liquid hexane and carbon dioxide. The interactions between ethanol as a modifier and the solute molecules are more pronounced, giving rise to a larger polarity effect. The approach to separate the density and polarity effect of the modifier as described above is only valid when interactions between the modifier and the stationary phase can be neglected.

In Fig. 6B a plot similar to that of Fig. 6A is given, but in this case for the carbonwax column. The addition of hexane and ethanol reduces retention when compared with pure carbon dioxide at equal densities. However, in contrast to what is observed in Fig. 6A, the effects of both modifiers are identical. Apparently, modifier interaction with the stationary phase or the support material cannot be neglected. Preferential adsorption of hexane on the surface of the carbonaceous material may possibly occur, as indicated by the results of Engel and Olesik [27], who studied porous glassy carbon (PGC) as a stationary phase in SFC. In their study it was found that PGC tends preferentially to adsorb large molecules. The adsorbed molecules may effectively compete with solutes for the carbon surface, thereby reducing solute retention.

CONCLUSIONS

From open columns more solutes can be eluted with pure carbon dioxide as the mobile phase than from packed columns. However, the elution of highly polar solutes also requires modifiers on open columns. The effects of modifiers in packed and open columns can be of comparable magnitude when compared on a normalized scale under identical operating conditions. This suggests that blocking of active sites by the modifier may also play an important role in open columns. Apparently, a considerable number of active sites is also present on open columns. The contributions of these sites to the chromatographic process increases drastically at lower temperatures, so that modifiers become both more necessary and more effective at low temperatures. By performing a separation at the maximum temperature allowed by the solute and the stationary phase, improved peak shapes can often be obtained without modifiers.

Non-silica-based stationary phases are necessary to study the different effects of modifiers in the mobile phase. By plotting the capacity factor of the test solute as a function of the density of the mobile phase, the density and polarity effects of the modifier can be separated.

REFERENCES

- 1 P. J. Schoenmakers, *J. High Resolut. Chromatogr. Chromatogr. Commun.*, 11 (1988) 278.
- 2 H.-G. Janssen and C. A. Cramers, *J. Chromatogr.*, 505 (1990) 19.
- 3 J. M. Levy and W. M. Ritchey, *J. Chromatogr. Sci.*, 24 (1986) 242.
- 4 A. L. Blilie and T. Greibrokk, *Anal. Chem.*, 57 (1985) 2239.
- 5 P. Mourier, P. Sassiati, M. Caude and R. Rosset, *J. Chromatogr.*, 353 (1986) 61.
- 6 J. G. M. Janssen, P. J. Schoenmakers and C. A. Cramers, *J. High Resolut. Chromatogr.*, 12 (1989) 645.
- 7 S. M. Fields, K. E. Markides and M. L. Lee, *J. High Resolut. Chromatogr. Chromatogr. Commun.*, 11 (1988) 25.
- 8 F. O. Geiser, S. G. Yocklovich, S. M. Lurcott, J. W. Guthrie and E. J. Levy, *J. Chromatogr.*, 459 (1988) 173.
- 9 J. F. Deye, T. A. Berger and A. G. Anderson, *Anal. Chem.*, 62 (1990) 615.
- 10 J. B. Crowther and J. D. Henion, *Anal. Chem.*, 57 (1985) 2711.
- 11 F. P. Schmitz, D. Leyendecker and D. Leyendecker, *J. Chromatogr.*, 389 (1987) 245.
- 12 H. Engelhardt, A. Gross, R. Mertens and M. Petersen, *J. Chromatogr.*, 477 (1989) 169.
- 13 C. H. Lochmüller and L. P. Mink, *J. Chromatogr.*, 471 (1989) 357.
- 14 B. W. Wright, H. T. Kalinoski and R. D. Smith, *Anal. Chem.*, 57 (1985) 2823.
- 15 C. R. Yonker and R. D. Smith, *J. Chromatogr.*, 361 (1986) 25.
- 16 B. W. Wright and R. D. Smith, *J. Chromatogr.*, 355 (1986) 367.
- 17 S. M. Fields, K. E. Markides and M. L. Lee, *J. Chromatogr.*, 406 (1987) 223.
- 18 S. Schmidt, L. G. Blomberg, E. R. Campbell, *Chromatographia* 25 (1988) 775.
- 19 H.-G. Janssen, P. J. Schoenmakers and C. A. Cramers, *Mikrochim. Acta*, in press.
- 20 P. J. Schoenmakers and L. G. M. Uunk, *Adv. Chromatogr.*, 30 (1990) 1.
- 21 P. J. Schoenmakers, L. G. M. Uunk and H.-G. Janssen, *J. Chromatogr.*, 506 (1990) 563.
- 22 S. Angus, B. Armstrong and K. M. de Reuck, *Carbon dioxide. International thermodynamic tables of the fluid state-3*, Pergamon Press, Oxford, 1976.
- 23 K. Stephan and K. Lucas, *Viscosity of dense fluids*, Plenum Press, New York, 1979.
- 24 R. C. Reid, J. M. Prausnitz and T. K. Sherwood, *The properties of gases and liquids*, McGraw-Hill, New York, 3rd ed., 1977, p. 544.
- 25 B. I. Lee and M. G. Kesler, *AIChE J.*, 21 (1975) 510.
- 26 J. H. Phillips and R. J. Robey, *J. Chromatogr.*, 465 (1989) 177.
- 27 T. M. Engel and S. V. Olesik, in P. Sandra (Editor), *Proceedings of the 11th International Symposium on Capillary Chromatography, Monterey, May 1990*, Hüthig, Heidelberg, 1990, p. 736.

CHROMSYMP. 2089

Combination of supercritical fluid chromatography with thin-layer chromatography on a semi-preparative scale

L. WÜNSCHE*, U. KELLER and I. FLAMENT

Research Laboratories, Firmenich SA, B.P. 239, CH-1211 Geneva (Switzerland)

ABSTRACT

Semi-preparative supercritical fluid chromatography (SFC) is a very valuable tool for the separation of unknown complex mixtures, as it may allow the isolation of sufficient amounts of individual constituents for ^1H and ^{13}C NMR spectroscopic identification. Semi-preparative SFC uses large-diameter packed columns and requires an efficient collection system. The performances of 4.6, 10 and 21 mm I.D. columns were compared and three different collection methods were tested for their efficiency: collection in pressurized stainless-steel tubes or in specially shaped glass vials, and condensation of the effluent at the starting line of a semi-preparative thin-layer chromatographic plate. The good yields that characterize the first two techniques could not be achieved with the third. The plate could, however, be developed, leading to a two-dimensional semi-preparative chromatographic separation. The spots must be localized on the plate in a non-destructive way in order to recover the samples. A general method is proposed, using berberine chloride, and also a more specific method, which allows the selective detection of certain classes of compounds.

INTRODUCTION

During the past 30 years, the development of capillary columns, first for gas chromatography (GC) and subsequently for other chromatographic techniques, has increased the efficiency of separations tremendously. This is also true for newer techniques such as supercritical fluid chromatography (SFC), for which efforts have been mainly directed toward capillary open-tubular and capillary packed columns. Thanks to the low flow-rates of mobile phase that they require, such small-bore columns can easily be coupled to mass or IR spectrometers for compound identification. However, mass or IR spectra do not often permit complete structure elucidations of unknown molecules. On the other hand, ^1H and ^{13}C NMR spectroscopy are very valuable identification methods, but they suffer from a lack of sensitivity. The low capacity of capillary columns precludes the use of NMR spectroscopy when encountering unidentified compounds.

There is therefore a real need for powerful semi-preparative separation methods when dealing with complex mixtures of unknown constituents. Large-diameter packed columns possess the high loadability required, but are characterized by higher flow-rates of mobile phase and poorer resolving power than capillary columns. The

large flow of carrier is particularly troublesome in liquid chromatography, owing to safety considerations, disposal problems and tedious work-up to remove the solvent. In addition, the high flow-rate renders difficult the on-line connection of liquid chromatographs in "hyphenated techniques" [1]. This is very detrimental because combinations of different chromatographic methods allow the lower efficiency of large-scale separations to be overcome. In this regard, SFC appears very attractive for preparative work as the volatility of CO₂ allows straightforward solvent elimination for either transfer or collection.

In this work, we used a supercritical instrument that can accommodate packed columns of up to 21 mm I.D. Unlike analytical SFC, the semi-preparative mode implies the collection of the compounds after separation. We therefore also compared three different techniques of collection, namely collection under pressure, collection by decompression and deposition on a thin-layer chromatographic (TLC) plate. As a direct extension, a subsequent part is devoted to the coupling of semi-preparative packed-column SFC with semi-preparative TLC. Coupling of SFC with TLC offers the unique advantage of a two-dimensional semi-preparative separation.

The volatility of CO₂ had been extensively exploited for coupling SFC with SFC [2-4], GC [4], high-performance liquid chromatography (HPLC) [5] and TLC [6,7]. However, these coupled techniques remain on an analytical scale at least in one dimension. On the other hand, coupling of HPLC with TLC has been reported several times, but only a low flow of the liquid solvent could be transferred in order to prevent flooding of the plate [8-10]. We have not found any report in which large-diameter packed-column SFC or semi-preparative TLC were coupled with another semi-preparative or preparative technique.

In order to recover the solutes, semi-preparative SFC-TLC separation requires non-destructive methods for the detection of spots. Two methods, general and specific, have been developed and applied to several examples of two-dimensional separations. All analyses led to the isolation of sufficient pure material for NMR analysis.

In the following sections, the term "semi-preparative" refers to separations of amounts of substances ranging from milligrams to tens of milligrams.

EXPERIMENTAL

The samples used were either commercially available chemicals or came from natural sources. The detailed procedures for their extraction and fractionation are beyond the scope of this paper.

Apparatus

A diaphragm compressor (Nova, Effretikon, Switzerland) is used to fill a stainless-steel buffer tank with highly pressurized CO₂. The CO₂ is then decompressed to the working pressure by a pressure-reducing regulator (Tescom, Elk River, MN, U.S.A.). The CO₂ is mixed with the modifier (methanol) delivered by a syringe pump (MicroGradient System; Brownlee Labs., Applied Biosystems, Santa Clara, CA, U.S.A.), enters the oven and is directed to the six-port injection valve (AC6W; Valco Instruments, Houston, TX, U.S.A.). A direct and accurate determination of the proportion of modifier is not possible as the CO₂-delivery system works on pressure

control whereas the modifier pump works on flow control. However, the proportions of modifier were calculated to be *ca.* 2–3% in all instances. Detection is performed either with a UV detector (UVIS 20; Carlo Erba, Milan, Italy) or with a laser light-scattering detector (Varex, Rockville, MD, U.S.A.), or with both detectors simultaneously. With laser light-scattering detection (LLSD), the flow is split at the outlet of the column and 5–10% is directed to the drift tube of the detector. The remaining part (or the total if the LLSD instrument is not connected) of the flow passes through the high-pressure UV cell, and is directed either to a ten port valve (MCSD10UW; Valco Instruments) fitted with the collection vials or to the TLC interface. These various elements are interconnected with 1/16 in. O.D. and 0.5 mm I.D. stainless-steel tubing. The same tubing is pinched to produce the necessary restrictions in the collection system, the TLC interface and the LLSD instrument. The metallic tubes and glass vials used for collection are shown in Fig. 3 and elsewhere [6]. The TLC interface and plate conveyor have been described previously [7].

The separations were performed on C₁₈ columns [laboratory-filled, 25 cm × 4.6 mm I.D., 10 μm; Supelco, (Bellefonte, PA, U.S.A.), 25 cm × 10 mm I.D., 5 μm; Supelco, 25 cm × 21 mm I.D., 15 μm] and silica gel TLC plates (20 × 20 cm × 2 mm) (No. 5717; Merck, Darmstadt, Germany). The flow-rates were typically 2 ml/min for the 4.6 mm I.D. column, 3.5 ml/min for the 10 mm I.D. column and 14 ml/min for the 21 mm I.D. column. Other chromatographic conditions are given in the legends of the figures.

Detection on TLC plates

General method. A saturated solution of berberine chloride (Fluka, Buchs, Switzerland) in ethanol is sprayed on the plate. The solutes give spots under UV irradiation (254 or 366 nm).

Specific detection. Immediately after elution of the preparative TLC plate, a TLC plastic sheet (20 × 20 cm × 0.2 mm) (No. 5735; Merck) is pressed strongly against the preparative plate for 1–2 min. Alternatively, the preparative plate can be dried and briefly dipped in ethanol before contact. Detection of the spots on the plastic sheet by any method [in this instance with 2,6-dichloroquinonechlorimide (Fluka) for phenol detection] gives the mirror image of the main TLC plate.

RESULTS AND DISCUSSION

Semi-preparative columns

Although the development of high-field Fourier transform (FT) NMR instruments has dramatically increased their sensitivity, NMR analyses still require relatively large amounts of samples, typically in the range 0.5–5 mg for ¹H NMR and 5–50 mg for ¹³C NMR. Such amounts cannot be separated efficiently with the 4.6 mm I.D. columns, but fit well with the sample capacity of 10 and 21 mm I.D. packed columns. Only a few reports of SFC separations with 10 mm I.D. [11,12] and 20 mm I.D. [13,14] column have appeared. Larger-scale SFC separations have been carried out by Perrut and Jusforgues [15]. Both small- and large-scale preparative SFC have recently been reviewed by Berger and Perrut [16].

Fig. 1 compares the separation of tocopherol isomers with 4.6, 10 and 21 mm I.D. columns. Very similar resolutions are obtained, provided that the compression

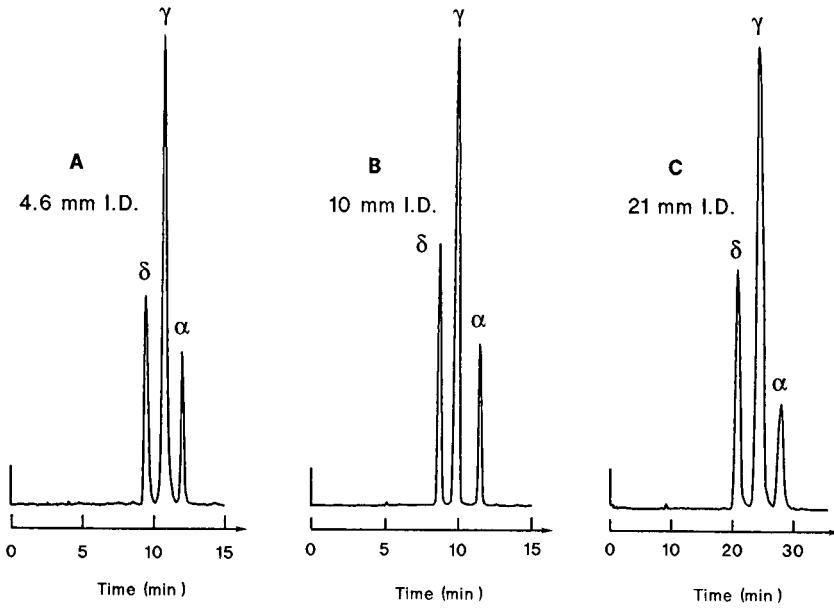


Fig. 1. Separation of a mixture of α -, γ - and δ -tocopherols on C_{18} packed columns. (A) Injection of 0.6 mg on the 4.6 mm I.D. column; (B) injection of 2.5 mg on the 10 mm I.D. column; (C) injection of 10 mg on the 21 mm I.D. column. Eluent: CO_2 + methanol (see Experimental). Temperature, 40°C; pressure, 240 bar, UV detection at 290 nm.

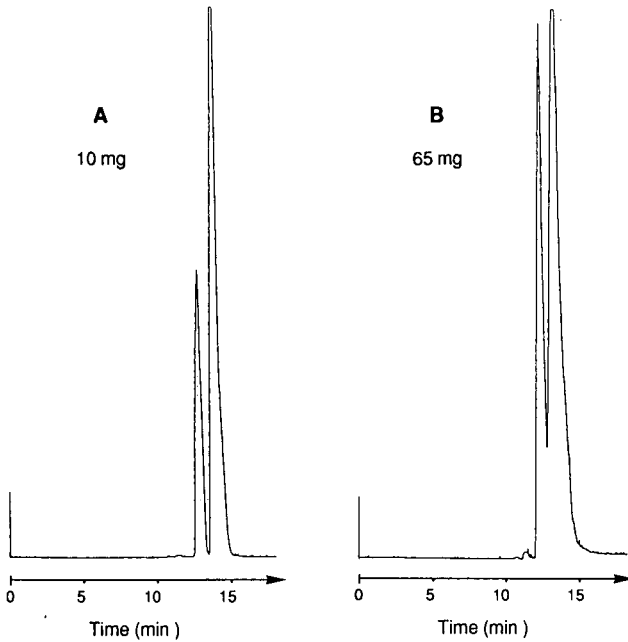


Fig. 2. Separation of phytol isomers with the 21 mm I.D. column. Injection of (A) 10 mg and (B) 65 mg. Eluent: CO_2 + methanol (see Experimental). Temperature, 40°C; pressure, 250 bar; LLS detection.

system can deliver enough mobile phase and that the pressure drop is kept reasonably low by the use of 0.5 mm I.D. tubing. The high capacity of semipreparative columns is demonstrated in Fig. 2. With the 21 mm I.D. column, complete separation of up to 10 mg of *cis-trans*-phytol can be achieved, and the separation of 65 mg of the same mixture without significant loss of resolution is possible. In this example, the amounts of separated compounds are in the range of ^{13}C NMR requirements.

Collection systems

Obviously, semi-preparative separations are performed with the aim of isolating a maximum amount of pure compounds, so the efficiency of the collection step is of prime importance. For SFC with CO_2 , the decompression of the supercritical eluent to atmospheric pressure at the terminal restriction allows its straightforward removal, but also induces a very high flow-rate of gas, which can blow the compounds out of the collection vials. Different systems of collection exist and can be divided in two groups. One involves collection of the solutes before complete decompression, and therefore requires pressure-resistant collection devices [17,18]. Alternatively, the eluent can be decompressed to atmospheric pressure and the solutes trapped from the resulting gas flow [11,12,19,20]. The latter method is usually more convenient but less efficient [11]. Some collectors are also incompatible with the high flow-rates of semi-preparative columns [20].

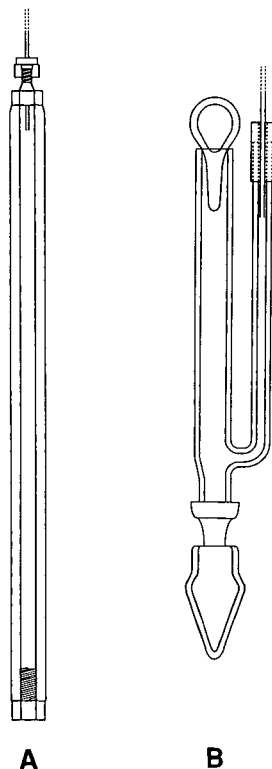


Fig. 3. Collection vials. (A) Stainless-steel tube for collection under pressure; (B) glass vials for collection after decompression.

We used three simple systems of collection and compared their efficiencies. The first is similar to the system described by Campbell and Lee [18]. It consists of closed stainless-steel tubes, into which the fractions are collected under pressure, *i.e.*, in the liquid state (Fig. 3A). The tubes are then very gently decompressed to remove the CO₂. The second type of collector consists of specially shaped glass vials, which trap the dry-ice-modifier droplets produced by the decompression of the mobile phase [6]. (Fig. 3B). A heating system prevents the formation of a blockage of dry ice in the lateral tube. In the third method, the outlet of the restrictor is directed toward a TLC plate, which is slowly moved on a conveyor [7]. After elution, the compounds are recovered by stripping the adsorbent from the plate and washing the silica with a small volume of organic solvent.

Table I compares the recoveries of isophytol and benzyl benzoate after separation and collection with each system. In fact, these values also include losses due to other parts of the chromatographic system, which represent about 10% of the injected amounts. After correction, the efficiencies of the collectors alone are above 90%, except for the TLC system.

Although these results show high efficiencies for both the stainless-steel tube and glass systems, we strongly favour the latter owing to its simplicity and convenience of use. In comparison, the deposition of the eluent on a TLC plate leads to significant losses.

We carried out numerous experiments in order to understand which parameters govern the efficiency of the SFC to TLC transfer. As a result, the yield of deposition was found to be independent of the nature of the solute (functional groups, polarity), its molecular weight (for mol. wt. > 300), and the amount of compound (in the range 1–10 mg). Further, deposition on TLC plates with and without a concentration zone leads to similar results.

On the other hand, the yield of deposition is strongly dependent on the presence of the modifier, the shape of the jet and its temperature, which varies with the flow-rate and the power applied to the restrictor heating block.

Moreover, these parameters interdependently affect the transfer; the best yields are achieved when all the mentioned parameters are set such that the jet of CO₂ leaves a sharp wet line of modifier on the TLC plate. If this condition is not fulfilled, owing to absence of modifier or an unsuitable temperature, poorer transfer occurs, even when the TLC plate is pre-wetted with solvent prior to deposition.

Substrate losses result from the difficulty of retaining on the silica plate the effluent particles expelled at high speed from the restrictor. Obviously, liquid droplets

TABLE I
YIELD OF RECOVERY OF THE COLLECTION SYSTEMS

SFC: 10 mm I.D. column; eluent, CO₂ + methanol (see Experimental). Mean results of three experiments; recovered amounts determined by GC with triplicate on-column injections.

Collection system	Benzyl benzoate (%)	Isophytol (%)
Stainless-steel tube	86	89
Glass vial	85	82
TLC plate	—	36

are held better than solid or gaseous material. Hence, the transfer is enhanced by allowing the solute to be trapped in droplets of modifier and deposited as such on the TLC plate.

On-line coupling of semi-preparative SFC with semi-preparative TLC

Despite its low efficiency, collection of SFC effluents on TLC plates presents obvious advantages. After development, the thin-layer plate can be sprayed with detection reagents, offering a means of detection and a purity check of the SFC fractions [7]. Alternatively, the plate may be used for FT-IR spectroscopy [10,21].

However, the major benefit of this coupling relies on its capability to produce a two-dimensional semi-preparative separation. Semi-preparative TLC is a cheap and widespread method for the separation of non-volatile compounds. One can purchase or prepare TLC plates coated with numerous types of adsorbents; the choice covers normal phases, reversed phases, chiral phases and impregnated supports (*e.g.*, silver nitrate) [22]. However, semi-preparative TLC has a poor resolving power, which often precludes the isolation of pure compounds. Finally, the typical adsorbent thick-

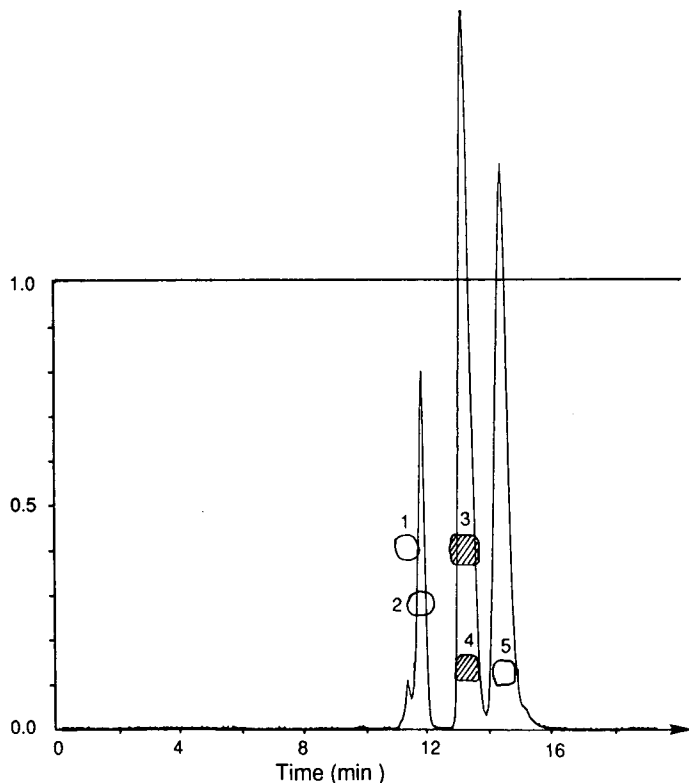


Fig. 4. Two-dimensional SFC-TLC separation. SFC: 21 mm I.D. column; eluent, CO_2 + methanol (see Experimental); temperature, 40°C ; pressure, 210 bar; LSD detection. TLC: solvent, hexane-ethyl acetate (9:1); detection reagent, berberine chloride; UV detection. 1 = Methyl palmitate; 2 = isophytol; 3 = methyl stearate; 4 = *cis*-phytol; 5 = *trans*-phytol. The NMR spectra of the products corresponding to the shaded spots were recorded.

ness (2 mm) allows the deposition of about 7 mg/cm [23], fitting perfectly with the capacity of semi-preparative SFC columns. As a result, semi-preparative TLC emerges as a natural complement to SFC for separations of milligram amounts of complex mixtures.

The two-dimensional separation results in spots of solutes spread all over the TLC plate. For collection, they must be accurately located using a non-destructive method. Two alternatives are possible, depending on whether the detection process should be non-specific or should detect only one class of compounds.

The general detection method takes advantage of berberine chloride. This reagent, when sprayed on the plate, makes organic compounds UV detectable, even fully saturated hydrocarbons. It is insoluble in most of the usual solvents for TLC and remains on normal-phase silica when the compounds are recovered by washing. Surprisingly, we have found only one publication referring to berberine chloride as a detection reagent [24], although it is routinely used in some laboratories [25]. As an example, fig. 4 shows the separation of a mixture of five compounds. Neither SFC nor TLC alone would have led to a complete separation of this sample. In Fig. 5, the same technique was applied to a natural fraction of jasmine extract. In both experiments, the shaded spots were stripped from the plate and the silica was washed with diethyl ether to afford about 1 mg of pure compounds. This was sufficient for both ^1H NMR and mass spectrometry and to identify the compounds isolated from jasmine extract as isophytol, phytol acetate, phytol, squalene epoxide and phytol palmitate.

We developed a second method of detection to be used whenever the berberine chloride method cannot be applied or if a specific class of substances is under in-

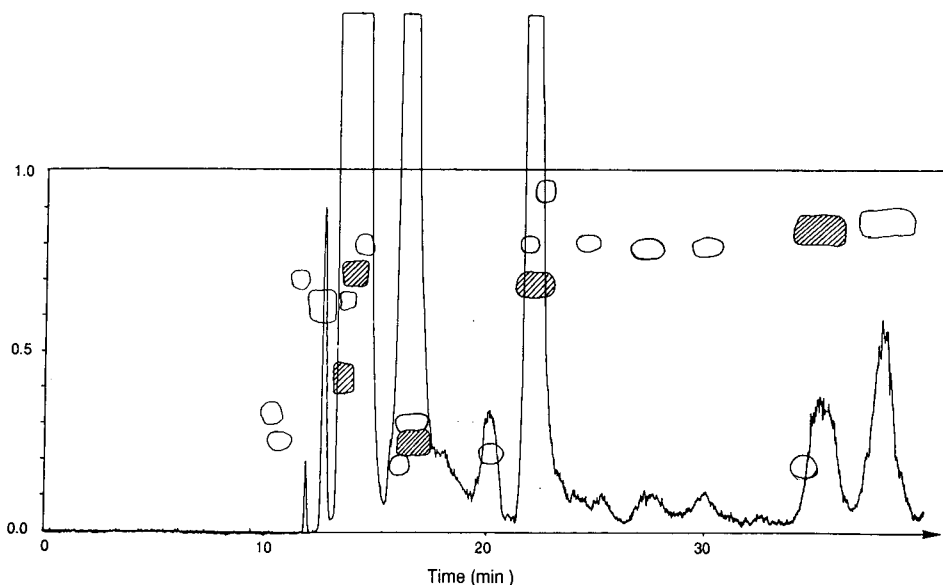


Fig. 5. Two-dimensional SFC-TLC of a fraction of jasmine extract. SFC: 21 mm I.D. column; eluent, CO_2 + methanol (see Experimental); temperature, 40°C ; pressure, 300 bar; LLSD detection. TLC: solvent, hexane-diethyl ether (4:1); detection reagent, berberine chloride; UV detection. The NMR spectra of the products corresponding to the shaded spots were recorded.

vestigation. By firmly pressing a soft (plastic) TLC sheet against the wet, thick plate, tiny fractions of the compounds are transferred. The plastic plate can then be treated by any method, giving the mirror image of the spots of interest. A similar method using filter-paper was mentioned by Mitsryukov [26]. In Fig. 6, we used 2,6-dichloroquinonechlorimide, a specific reagent for phenols. Thus, it was possible to localize selectively tocopherols in a fraction of coffee extract. In this instance, the main plate was also sprayed with berberine chloride, showing that all the compounds in this fraction have similar R_F values on TLC. The mass spectrum of the stripped compound indicates β -tocopherol or γ -tocopherol, but it is not informative enough to distinguish between them. The recovery of sufficient material for NMR analysis permitted the identification of β -tocopherol.

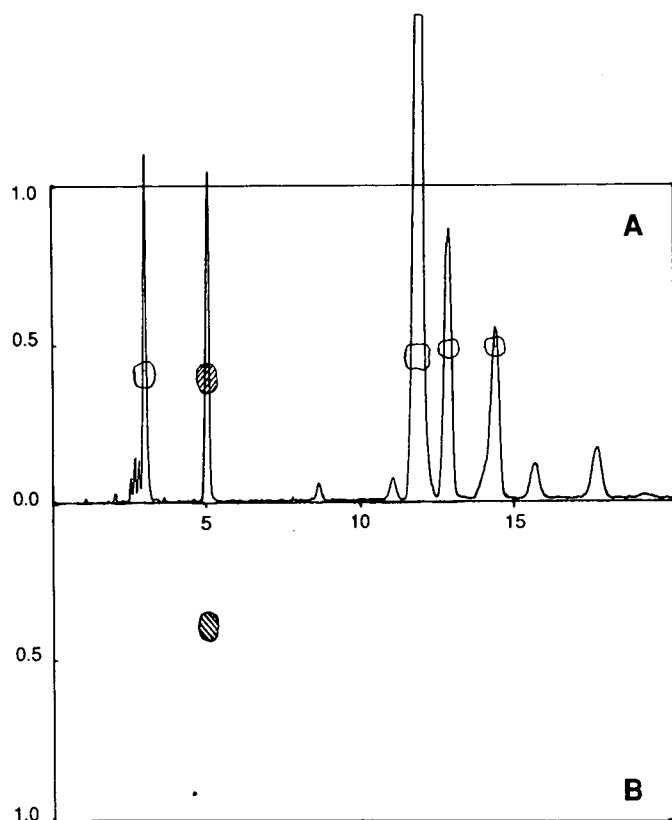


Fig. 6. Two-dimensional SFC-TLC of a fraction of coffee extract. SFC: 10 mm I.D. column; eluent, CO_2 + methanol (see Experimental); temperature, 40°C ; pressure, 250 bar; LLS detection. TLC: solvent, hexane-ethyl acetate (9:1); detection reagent, (A) berberine chloride and (B) 2,6-dichloroquinonechlorimide; UV detection. The NMR spectra of the products corresponding to the shaded spots were recorded.

CONCLUSIONS

Although most of the publications devoted to SFC concern analyses performed with open-tubular or packed capillary columns, SFC also offers very attractive possibilities for larger scale separations. In the semi-preparative mode, the benefits of SFC over GC, *i.e.*, low-temperature separation of the heat-sensitive or non-volatile compounds, are still valid. Further, the benefits of SFC over HPLC, *i.e.*, speed of analysis, non-toxicity and a readily removed mobile phase, are amplified on the semi-preparative scale in comparison with the analytical scale.

Semi-preparative SFC utilizes large-diameter HPLC packed columns filled with very fine and homogeneous silica particles and therefore takes advantage of their unequalled efficiency for separations of relatively large amounts of material. We were able to isolate tens of milligrams of compounds in one injection thanks to the use of such columns and to the development of convenient and efficient collection system.

Alternatively, the effluent can be diverted to a semi-preparative TLC plate for further purification, leading to a unique two-dimensional semi-preparative separation.

However, significant losses occur during the direct transfer from SFC to TLC. If the sample is available in limited amount or if the compounds of interest are minor constituents, fractions should be collected and subsequently deposited on the plate. A non-destructive method must be used to detect the spots. A normal-phase support can be treated with berberine chloride reagent. A second detection method was tested for other adsorbents or for specific detection.

Both high-performance packed columns and TLC plates are available with numerous types of coating. Their combination offers a broad range of selectivity and covers a large field of applications. It turns out to be a particularly useful method when milligram amounts of pure substances have to be isolated from complex mixtures.

REFERENCES

- 1 I. L. Davies, M. W. Raynor, J. P. Kithinji, K. D. Bartle, P. T. Williams and G. E. Andrews, *Anal. Chem.*, 60 (1988) 683A.
- 2 Z. Juvancz, K. M. Payne, K. E. Markides and M. L. Lee, *Anal. Chem.*, 62 (1990) 1384.
- 3 K. M. Payne, I. L. Davies, K. D. Bartle, K. E. Markides and M. L. Lee, *J. Chromatogr.*, 477 (1989) 161.
- 4 J. M. Levy, R. A. Cavalier, T. N. Bosch, A. F. Rynaski and W. E. Huhak, *J. Chromatogr. Sci.*, 27 (1989) 341.
- 5 I. S. Lurie, *LC · GC*, 6 (1988) 1066.
- 6 I. Flament and U. Keller, in M. Perrut (Editor), *Proceedings of the 1st International Symposium on Supercritical Fluids, Nice, October 1988*, Institut National Polytechnique de Lorraine, Nancy, 1988, pp. 465-472.
- 7 U. Keller and I. Flament, *Chromatographia*, 28 (1989) 445.
- 8 J. W. Hofstraat, S. Griffioen, R. J. van de Nesse, U. A. Th. Brinkman, C. Gooijer and N. H. Velthorst, *J. Planar Chromatogr. Mod. TLC*, 1 (1988) 220.
- 9 D. Jänchen, *GIT, Suppl.*, 3 (1988) 78.
- 10 C. Fujimoto, T. Morita and K. Jinno, *J. Chromatogr.*, 438 (1988) 329.
- 11 M. Saito and Y. Yamauchi, *J. Chromatogr.*, 505 (1990) 257.
- 12 M. Saito, T. Hondo and Y. Yamauchi, in R. M. Smith (Editor), *Supercritical Fluid Chromatography*, Royal Society of Chemistry, London, 1988, Ch. 8, p. 203.
- 13 M. Saito, Y. Yamauchi, K. Inomata and W. Kottkamp, *J. Chromatogr. Sci.*, 27 (1989) 79.

- 14 M. Alkio, T. Harvala and V. Komppa, in M. Perrut (Editor), *Proceedings of the 1st International Symposium on Supercritical Fluids, Nice, October 1988*, Institut National Polytechnique de Lorraine, Nancy, 1988, pp. 389–396.
- 15 M. Perrut and P. Jusforgues, *Entropie*, 132 (1986) 3.
- 16 C. Berger and M. Perrut, *J. Chromatogr.*, 505 (1990) 37.
- 17 R. E. Jentoft and T. H. Gouw, *Anal. Chem.*, 44 (1972) 681.
- 18 R. M. Campbell and M. L. Lee, *Anal. Chem.*, 58 (1986) 2247.
- 19 M. E. McNally and J. R. Wheeler, *J. Chromatogr.*, 435 (1988) 63.
- 20 Q. L. Xie, K. E. Markides and M. L. Lee, *J. Chromatogr. Sci.*, 27 (1989) 365.
- 21 C. Fujimoto, T. Morita, K. Jinno and K. H. Shafer, *J. High Resolut. Chromatogr., Chromatogr. Commun.*, 11 (1988) 810.
- 22 H. Halpaap and J. Rippahhn, *Chromatographia*, 10 (1977) 643.
- 23 B. Fried and J. Sherma (Editors), *Thin-Layer Chromatography, Techniques and Applications (Chromatographic Sciences Series, Vol. 35)*, Marcel Dekker, New York, 1986.
- 24 L. Mamluk, *J. Chromatogr. Sci.*, 19 (1981) 53.
- 25 M. L. Cordeiro and C. Djerassi, *J. Org. Chem.*, 55 (1990) 2806.
- 26 E. A. Mistryukov, *J. Chromatogr.*, 9 (1962) 311.

CHROMSYM. 2327

Ion-mobility spectrometry as a detection method for packed-column supercritical fluid chromatography

M. A. MORRISSEY and H. M. WIDMER*

Analytical Research Department, Ciba-Geigy Ltd., CH-4002 Basle (Switzerland)

ABSTRACT

Initial investigations are reported for the use of an ion-mobility spectrometer as a detector for packed-column supercritical fluid chromatography. The spectrometer was coupled to the supercritical fluid chromatography system through a post-column split, and a small portion of the chromatographic flow was introduced directly into the ion-mobility spectrometer using either a frit restrictor or an integral restrictor. The effect of a mobile phase modifier, methanol, on the gas phase ion chemistry of the detector was studied using the reactant ions normally present in the drift tube and the response of the detector to benzoquinone and benzophenone. Separations were performed for a series of Triton X oligomers to demonstrate the various operational modes of the detector. Product ions captured for these compounds had reduced mobilities, a dimensionless measure of mobility, in the range of 1.00 to 0.405, which would make these some of the largest compounds ever introduced, individually, into an ion-mobility spectrometer.

INTRODUCTION

During the last ten years, the use of supercritical fluids has matured from an experimental technique, used mainly in research laboratories, to a useful analytical tool for the extraction and separation of non-polar and moderately polar compounds. As the development has progressed a number of subdisciplines have emerged, such as capillary supercritical fluid chromatography (cSFC), packed column supercritical-fluid chromatography (pSFC), and supercritical fluid extraction (SFE). Each of these techniques has its own strengths and particular applications.

Currently, cSFC is probably the best established and most commonly used. It is a high-resolution technique capable of separating complex samples. An additional advantage of cSFC is the adaptability of the technique to a wide variety of detectors, universal and selective, particularly detectors commonly used for gas chromatography (GC). There are two basic reasons for this advantage: (1) Flow-rates in cSFC are relatively low, less than 10 ml/min of gas. Carbon dioxide, the most common mobile phase, shows no response in flame ionization detection (FID), therefore the chromatography may be accomplished with a mobile phase that neither causes a high background nor extinguishes the flame. Also, the low flow-rate is manageable for direct introduction of the chromatographic effluent into a mass spectrometer. (2) Fused-silica columns are extremely inert, with few active sites. Carbon dioxide is a relatively non-polar solvent. To increase the range of compounds which are amenable to SFC

small amounts of organic solvents, called a modifier, are added to the carbon dioxide. However, it seems that the main effect of the modifiers is to cover up active sites on the column material [1,2]. Since fused-silica capillary columns are already inert, there is little advantage in using a modifier. In most separations organic modifiers, which would show an FID response, are not needed to elute compounds of interest. The disadvantages of cSFC are the long analysis times and the low sample-loading capacity of the columns.

Packed columns are more useful for separations which require high speed or high sample capacity, particularly for samples containing only a few components. In general, the resolution in pSFC is not as high as in cSFC. There are several characteristics of pSFC which make detection more difficult than for cSFC. The mass flow of the mobile phase is much higher. For conventional packed columns, 2–4 mm I.D., the gaseous flow-rate may be several hundred millilitres per minute. If the detector is sensitive to the mobile phase flow, such as a mass spectrometer, it is necessary to split the column effluent after the column, which means that some of the sample is lost. And, while a great deal of progress has been made recently producing inert column packings, in most cases an organic modifier is still necessary to improve separation, so that FID is difficult or impossible.

Previous publications have described a detector based on the principles of ion-mobility spectrometry (IMS), which might be suitable for pSFC [3–5]. IMS is an instrumental technique for the separation of gas phase ions. Organic species are introduced into the spectrometer, by either direct injection or chromatography, ionized through a series of ion–molecule reactions, and separated according to their time of flight through an inert atmosphere. From this drift time the mobility of particular ion may be calculated, which provides information about the ion's size. Chromatographic detection may be accomplished by monitoring the formation of ions in the spectrometer, in a manner analogous to selected ion monitoring in mass spectrometry. Because IMS is rapid and sensitive it has been used in applications as diverse as continuous monitoring, analytical spectrometry and chromatographic detection. IMS has been successfully coupled to GC [5] and cSFC [6], but it has not yet been used with pSFC. IMS combines some of the best features of the other detection systems commonly used for these separation techniques. The sensitivity of the detector is in the picogram range. It is not necessary that analytes contain a chromophore to be detected. Selectivity is based on the size and shape of an analyte molecule, rather than on the presence of a hetero-atom. Qualitative data about analytes may be determined in terms of drift times and mobilities. And finally, IMS shows some promise for being compatible with SFC mobile phases which contain an ionizable organic compound.

There are a number of questions which must be answered concerning IMS as a detection method for pSFC: (1) How much carbon dioxide can the detector tolerate? (2) What are the effects of mobile phase modifiers on the sensitivity of the detector? (3) What types of samples can be detected? This paper is an attempt to answer these questions and evaluate the use of IMS as a detection method for pSFC.

EXPERIMENTAL

A schematic of the combined SFC-IMS instrument is shown in Fig. 1.

Although the pSFC system used for this work has been described in greater detail in a previous publication [7], a brief description is presented here as an aid to the reader. Carbon dioxide, instrument grade, was supplied from a 30-kg tank equipped with a siphon tube. A 2- μm filter was installed in the carbon dioxide line shortly after the tank. The mobile phase was delivered by a pair of piston pumps (Gilson, Model 303), one for carbon dioxide and the other for the modifier. The carbon dioxide pump head was cooled to -10°C with a cooling bath (MGW Lauda, Model RC 6) and special fitting. In addition, the carbon dioxide transfer line was coiled and immersed in the cooling bath prior to the pump, in order to precool the carbon dioxide. Modifier was delivered directly to the second pump. All organic solvents used as modifiers were high-performance liquid chromatograph (HPLC) grade. The two flows were mixed in a three-stage dynamic mixer (Gilson, Model 811). A second particle filter, 0.5 μm (Rheodyne), was placed in the transfer line prior to the injector. Injection was made with an autosampler (Gilson, Model 231) equipped with a four-port, internal loop injector (Rheodyne, Model 7413), 1 μl volume. The column temperature was controlled in a GC oven (Carlo Erba, GC 600 Vega Series). All columns were 100 mm \times 2 mm I.D., packed with 3- μm particles (Stagroma, Switzerland).

The post-column flow was split using a tee with zero dead volume (Valco). The majority of the flow exited the oven, passed first through a heat exchanger, and then passed through a UV-VIS detector (Kratos, Spectraflow 783) equipped with a high-pressure flow cell. The column pressure was controlled after the UV-VIS detector by a pressure valve (HI-TEC, valve Type F-032, controller Type P-532; Bronkhorst Hi Tec, Ruurlo, Netherlands). Pressure programming was accomplished by micropro-

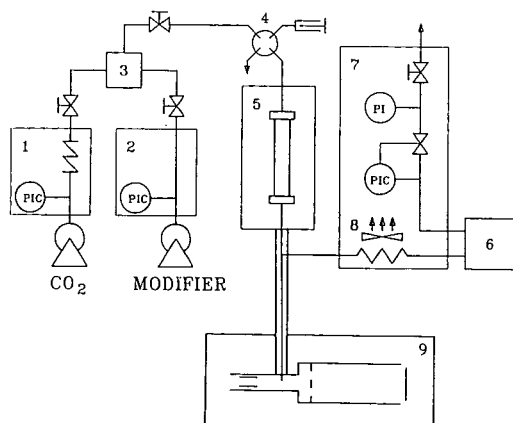


Fig. 1. Schematic diagram of the packed-column SFC system. 1 = Carbon dioxide pump and pump control; 2 = modifier pump and pump control; 3 = dynamic mixing chamber; 4 = autosampler and injection valve; 5 = column oven; 6 = UV detector; 7 = pressure control unit; 8 = heat exchanger; 9 = ion-mobility spectrometer.

cessor control of the pressure control valve. Chromatographic data were collected with a Hewlett-Packard Series 300 computer and software (Xtra Chrom II) from Nelson Analytical.

A small part of the flow was routed to the IMS system. A 1-m \times 60 μ m I.D. fused-silica tube was used as the transfer line. The temperature of the transfer line was maintained using the inlet temperature of the ion-mobility spectrometer. Flow into the detector was controlled by a restrictor at the end of the transfer line. As usual, the choice of restrictor type was important. Frit restrictors (Lee Scientific) were reliable, but did not efficiently transfer high-molecular-weight compounds from the high pressure of the SFC to the atmospheric pressure in the ion-mobility spectrometer. Guthrie, or integral, type restrictors (J&W Scientific) were more successful, but there were problems with plugging and the reproducibility of retention times.

The ion-mobility spectrometer, Model GHT 100, maximum operating temperature 250°C, was purchased from PCP (West Palm Beach, FL, USA). Mobility spectra were collected with a computer (IBM AT) equipped with an analog-to-digital (A/D) board and digital storage oscilloscope emulation software (Graseby Analytics, UK). Nitrogen was used as the drift gas for all experiments; the flow-rates of the drift gas and make-up gas were 400 and 150 ml/min, respectively. A 0- to 5-V output of the ion-mobility spectrometer could be used to collect chromatographic data on the Nelson system.

Qualitative data about the ions in the spectrometer may be gathered from the drift times and mobilities of the ions. Since drift times are dependent on the strength of the electric field, they are usually expressed as a reduced mobility, which is independent of the electric field. The drift time data must then be further corrected for the number density conditions of the drift gas. To compare ion mobilities under equivalent conditions of number density, the mobility must be corrected for temperature and pressure differences, and expressed as a reduced mobility, K_0 . The reduced mobility may be calculated from eqn. 1 [8]:

$$K_0 = (L/t_d E) (273.16/T) (P/760) \quad (1)$$

where T is the temperature of the drift tube in K, P is the atmospheric pressure in mmHg, E is the electric field gradient in V/cm, t_d is the drift time in s and L is length of the drift tube in cm.

An alternative method of computing reduced mobilities using an internal standard has been proposed [9]. Following the suggestion by Karpas [9], 2,4-lutidine was used as the standard and assigned a reduced mobility of 1.95. The mobilities of unknowns could then be calculated from eqn. 2. This method of calculating K_0 eliminates the need to measure the barometric pressure, eliminates errors due to inexact measurement of any of the variables in eqn. 1, and should eliminate some of the disagreement in K_0 values due to design differences in ion-mobility spectrometers:

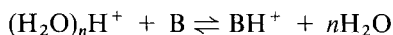
$$K_{0,2} = (1.95) t_{d,1}/t_{d,2} \quad (2)$$

where $K_{0,2}$ is the reduced mobility of the analyte, $t_{d,2}$ is the drift time of the analyte and $t_{d,1}$ is the drift time of the internal standard, 2,4-lutidine.

RESULTS AND DISCUSSION

If carbon dioxide is not efficiently swept from the detector, it may contaminate the drift region and affect the drift times of ions in the detector. It has been shown that drift times are lengthened and sensitivity is lost in a carbon dioxide drift gas [10]. It has also been shown that carbon dioxide can interfere with drift time measurement in a bidirectional flow instrument [11]. It was found that for this particular model up to about 40 ml/min of carbon dioxide did not interfere with the detector. At higher flow-rates the drift times of the reactant ions changed with changes in the carbon dioxide flow, indicating that carbon dioxide contaminated the drift region of the spectrometer, and the intensity of the reactant ions decreased, until finally, at flows over 100 ml/min, the reactant ions completely disappeared. In general the flow of gas into the ion-mobility spectrometer was kept to approximately 20 ml/min. For a 2-mm packed column, the SFC system was operated at a flow of 2 ml/min of liquid carbon dioxide; the split after the column was about 40:1.

Organic analytes which enter the detector are ionized by a series of ion-molecule reactions with background ions, called reactant ions, which exist in the spectrometer. When nitrogen is used as the drift gas these ions have been identified as $(\text{H}_2\text{O})_x\text{NH}_4^+$, $(\text{H}_2\text{O})_y\text{NO}^+$ and $(\text{H}_2\text{O})_z\text{H}^+$, where x , y and z are equal to 0, 1, 2, 3 and depend on the temperature of the drift tube [12-14]. If a neutral analyte entering the ion source has a greater gas-phase basicity than water, the analyte will become protonated through the following general reaction:



The identity and quantity of the reactant ions then determine the sensitivity of the detector. The integrity of the gas phase chemistry in the drift tube can be determined by the ions present, the most obvious clue to identity being the drift time.

Since most pSFC separations require a modifier, it was necessary to determine the effect of the modifier on the identity of the reactant ions. Because methanol is the most commonly used modifier, initial experiments were done with a methanol modifier. The changes in the reactant ions as the amount of methanol in the mobile phase is increased are shown in Fig. 2. Moderate amounts of carbon dioxide by itself had no effect on the mobilities and intensities of the reactant ions. As the concentration of methanol is increased the hydrated water ion is depleted and a new reactant ion, with a longer drift time, is seen in the detector. A summation of reactant ion drift times for different methanol concentrations is given in Table I. This is also true when the pressure of the system is increased for a given concentration of methanol, since the increase in pressure increases the flow through the restrictor.

The effect of a methanol modifier on the IMS sensitivity can be seen in Figs. 3 and 4, the analyses of benzoquinone and benzophenone, respectively. In each case a probe molecule was separated from the solvent by SFC at 80°C, pressure programmed from 125 to 250 bar in 10 min. IMS conditions are given in the figure captions. In Fig. 3 the chromatographic response of the detector to benzoquinone is plotted for conditions of no modifier and 1% methanol as a modifier. Because benzoquinone is a relatively strong base, the modifier has only a small effect on the sensitivity of the detector. Minimum detection limits for both cases are very similar,

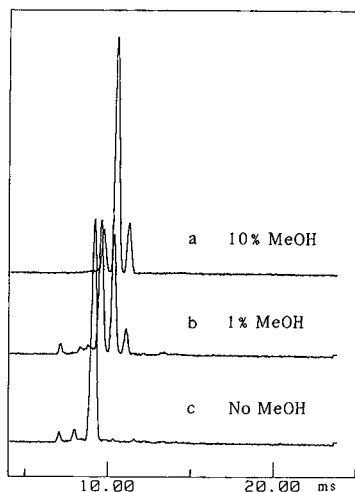


Fig. 2. Reactant ion-mobility spectra. IMS conditions: 225°C, 196.5 V/cm, entrance gate 0.2 ms, total scan time 24 ms, average of 64 scans. Methanol (MeOH) modifier added to mobile phase: (a) 10%; (b) 1%; (c) none.

approximately 0.0020 mg/ml when no methanol is present and approximately 0.0025 mg/ml when 1% methanol is added as a mobile phase modifier. Detection limits were estimated from twice the peak-to-peak noise level.

In Fig. 4 it can be seen that the methanol modifier significantly reduces the IMS response to benzophenone, which is a weaker base, especially at high analyte concentrations of modifier. While the minimum detectable amount of compound is very similar to that found for benzoquinone when only 1% methanol is present, for a 10% concentration of methanol the minimum detectable amount is reduced to approxi-

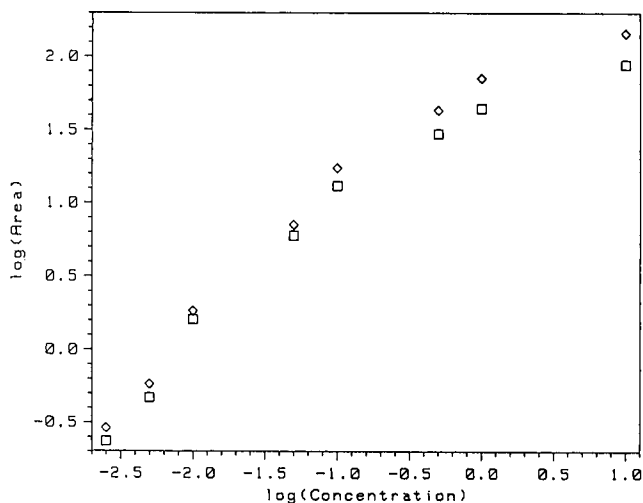


Fig. 3. Effect of methanol modifier on IMS response to benzoquinone. IMS conditions as in Fig. 2; drift times monitored from 12 to 18 ms. \diamond = No methanol; \square = 1% methanol.

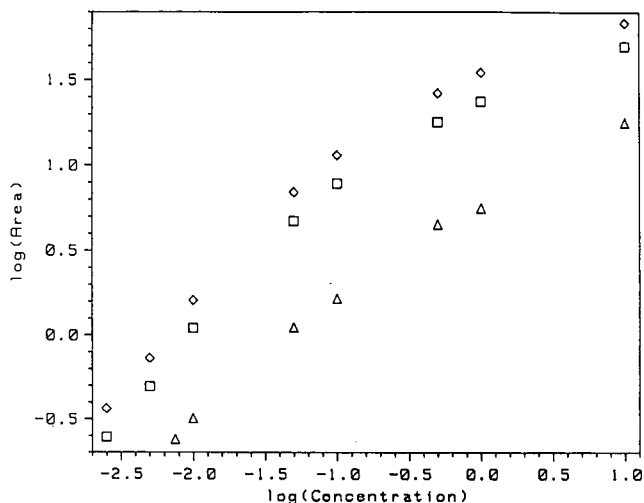


Fig. 4. Effect of methanol modifier on IMS response to benzophenone. IMS conditions as in Fig. 2; drift times monitored from 12 to 18 ms. \diamond = No methanol; \square = 1% methanol; \triangle = 10% methanol.

mately 0.0079 mg/ml. This may be expected from the table of gas phase basicities compiled by Kebarle [15]. The response of the detector then will depend on the amount of methanol entering the ion-mobility spectrometer, which is dependent on the modifier concentration and the column pressure. It should be kept in mind that these figures also reflect the split of the mobile phase. The detection limits reported are for concentrations introduced into the chromatograph. If the entire column effluent was introduced into the spectrometer, there would of course be more sample in the detector, but there would also be more interference from the methanol.

pSFC separation of a Triton X-114, an octyl phenol polyethylene glycol ether non-ionic surfactant (average monomeric subunits, $n = 7-8$), is shown in Fig. 5. Although the concentration of the methanol is relatively high, detection could be accomplished by monitoring drift times outside the range of the reactant ions. The sample, a 2.5% (w/w) solution of Triton X-114 in methanol was separated on a C_{18} column at a temperature of 150°C. The carbon dioxide flow was 2 ml/min and the

TABLE I
REDUCED MOBILITIES OF REACTANT IONS

K_0 ($\text{cm}^2 \text{V}^{-1} \text{s}^{-1}$)

Ion	No methanol	1% Methanol	10% Methanol
1	3.12	3.08	2.28
2	2.74	2.63	2.11
3	2.38	2.49	1.96
4	—	2.29	—
5	—	2.11	—
6	—	1.96	—

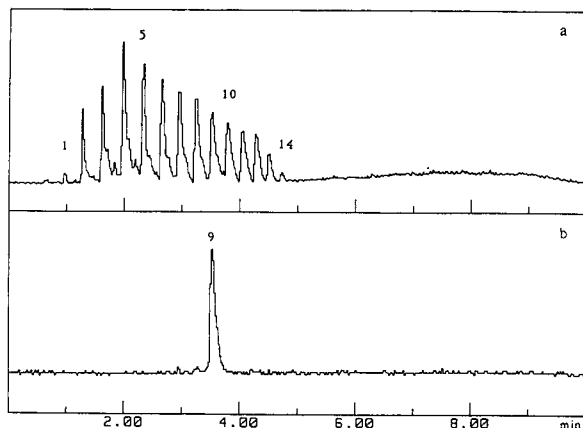


Fig. 5. Chromatograms of Triton X-114. IMS conditions: 150°C, 250 V/cm, 60-ms scan, entrance gate 0.5 ms. (a) Drift times monitored 14–50 ms. (b) Drift times monitored 27.7–28.7 ms.

methanol modifier flow was 0.15 ml/min. The pressure was programmed from 125 to 320 bar in 8 min. IMS conditions are given in the figure caption. Non-selective detection of the polymer mixture is shown in Fig. 5a. It was also possible to demonstrate selective detection of this compound, as shown in Fig. 5b. A list of the reduced mobilities for the ions captured is given in Table II. Reduced mobility values were calculated from an assigned reduced mobility of 1.95 and observed drift time of 10.60 msec for 2,4-lutidine for the IMS conditions given in the figure caption.

A heavier version of the same compound, Triton X-305, average monomeric subunits, $n = 25$, is shown in Fig. 6. In this case the column temperature was 165°C,

TABLE II

REDUCED MOBILITY VALUES FOR TRITON X-114 OLIGOMERS

Peak No.	Retention time t_r (min)	Drift time t_d (ms)	Reduced Mobility ($\text{cm}^2 \text{V}^{-1} \text{s}^{-1}$)
1	0.95	14.8	1.40
2	1.14	14.7	1.41
3	1.61	21.3	0.970
4	1.96	22.4	0.923
5	—	23.5	0.880
6	2.66	24.6	0.840
7	2.94	25.8	0.801
8	3.24	27.0	0.766
9	3.52	28.2	0.733
10	3.79	29.4	0.703
11	4.04	30.5	0.678
12	4.27	31.7	0.652
13	4.51	32.8	0.630
14	—	33.9	0.610
15	—	34.9	0.592
16	—	36.0	0.574

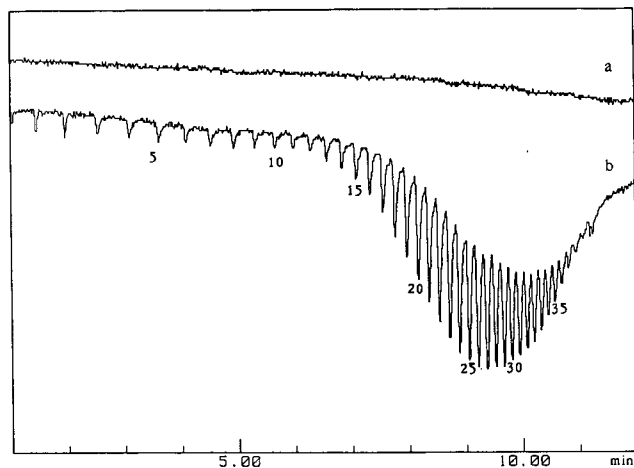


Fig. 6. Chromatograms of Triton X-305. IMS conditions: 100°C, 268 V/cm, 60-ms scan, entrance gate 0.5 ms, drift times monitored 8–12 ms. (a) Methanol injection. (b) Triton X-305 in methanol [10% (w/w)].

the pressure was programmed from 125 to 350 bar in 12 min, and the methanol modifier was programmed from 0.15 to 0.25 ml/min in 10 min. IMS conditions are given in the figure caption. Detection was accomplished by monitoring the depletion of the reactant ions, this is a non-selective method of detection which in this case resulted in better sensitivity, and explains why negative peaks are seen in the chromatogram. Although the reactant ions change, due to the presence of methanol and pressure programming, because the entrance gate was open for a long time, lowering the resolution of the instrument, the reactant ions appeared unchanged as the chromatography progressed. The detector baseline for these conditions is shown in Fig. 6a. This sample was unusual in that the depletion of the reactant ions was associated with the disappearance of any product ion. The drift times and reduced mobilities for some of the product ions captured are shown in Table III. While product ions were captured for all the peaks in the chromatogram, only a few are reported. The peak numbers were assigned, as accurately as possible, by matching the peak retention time with the time elapsed in the chromatographic run. Product ions were observed with

TABLE III

REDUCED MOBILITY VALUES FOR TRITON X-305 OLIGOMERS

Peak No.	Retention time t_r (min)	Drift time t_d (ms)	Reduced Mobility ($\text{cm}^2 \text{V}^{-1} \text{s}^{-1}$)
1	1.51	20.1	1.063
5	3.80	24.5	0.872
10	5.84	30.1	0.710
15	7.22	35.2	0.607
20	8.31	39.9	0.536
25	9.17	44.2	0.484
30	10.08	48.4	0.442
35	10.52	52.8	0.405

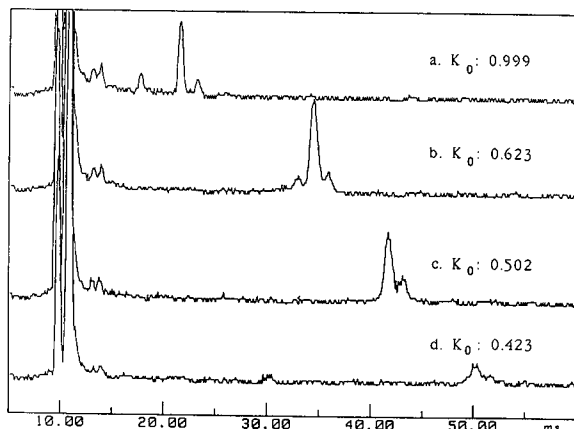


Fig. 7. Ion-mobility spectra of Triton X-305 oligomers. IMS conditions: 100°C, 268 V/cm, 60-ms scan, entrance gate 0.5 ms, average of 32 scans. (a) Peak 2, drift time 21.4 ms, $K_0 = 0.999$. (b) Peak 14, drift time 34.3 ms, $K_0 = 0.623$. (c) Peak 23, drift time 42.6 ms, $K_0 = 0.502$. (d) Peak 32, drift time 50.2 ms, $K_0 = 0.423$.

drift times as long as 52.8 ms and reduced mobilities as low as 0.405. Examples of the product ions captured are shown in Fig. 7.

The introduction to this paper posed three questions concerning detection by IMS after pSFC. The first related to the amount of carbon dioxide which could be introduced into the detector. Our experience showed that the limit appeared to be approximately 40 ml/min of gaseous carbon dioxide. At flow-rates much above this the drift time of the reactant ions began to change and the intensity of the reactant ions decreased, until, at about 100 ml/min, the reactant ions disappeared altogether. It would seem then that the entire flow from capillary columns [16] and micropacked columns may be introduced into the spectrometer, but that for larger columns the mobile phase flow must be split.

The mobile phase modifier was seen to have an effect on the performance of the spectrometer. This is in contrast to earlier work [16]. However, this work was done on capillary columns, where the flow of modifier into the spectrometer is much smaller. A second difference is that the piston pumps used in this work leave no possibility for the modifier to remain in the pump.

Lastly, the types of samples used in this paper showed good response, in some cases superior to UV-VIS detection currently in use. However, a broad study of high-molecular-weight compounds which respond in the ion-mobility spectrometer has not yet been thoroughly performed.

REFERENCES

- 1 A. L. Blilie and T. Greibrokk, *Anal. Chem.*, 57 (1985) 2239.
- 2 A. L. Blilie and T. Greibrokk, *J. Chromatogr.*, 349 (1985) 317.
- 3 F. W. Karasek, *Anal. Chem.*, 46 (1974) 710A.
- 4 F. W. Karasek and R. A. Keller, *J. Chromatogr. Sci.*, 10 (1972) 626.
- 5 M. A. Baim and H. H. Hill, Jr., *Anal. Chem.*, 54 (1982) 38.

- 6 R. L. Eatherton, M. A. Morrissey, W. F. Siems, and H. H. Hill, Jr., *J. High Resolut. Chromatogr. Chromatogr. Commun.*, 9 (1986) 154.
- 7 A. Giorgetti, N. Pericles, H. M. Widmer, K. Anton, and P. Dätwyler, *J. Chromatogr. Sci.*, 27 (1989) 318.
- 8 C. S. Shumate, R. H. St. Louis, and H. H. Hill, Jr., *J. Chromatogr.*, 373 (1986) 141.
- 9 Z. Karpas, *Anal. Chem.*, 61 (1989) 684.
- 10 S. Rokushika, H. Hatano, and H. H. Hill, Jr., *Anal. Chem.*, 59 (1987) 8.
- 11 S. Rokushika, H. Hatano, and H. H. Hill, Jr., *Anal. Chem.*, 58 (1986) 361.
- 12 D. I. Carroll, I. Dzidic, R. N. Stillwell, and E. C. Horning, *Anal. Chem.*, 47 (1975) 393.
- 13 A. Good, D. A. Durden, and P. Kebarle, *J. Chem. Phys.*, 52 (1970) 212.
- 14 F. W. Karasek and D. W. Denney, *Anal. Chem.*, 46 (1974) 633.
- 15 P. Kebarle, *Am. Rev. Phys. Chem.*, 28 (1977) 445.
- 16 M. A. Morrissey, *Ph. D. Dissertation*, Washington State University, Pullman, WA, 1989.

Effects of β -cyclodextrin in the mobile phase on the retention and indirect detection of non-electrolytes in reversed-phase liquid chromatography

I. Study of aliphatic alcohols

MARTINE GOSSELET* and BERNARD SEBILLE

Laboratoire de Physico-Chimie des Biopolymères, Université Paris Val de Marne, Avenue du Général de Gaulle, 94 000 Créteil (France)

ABSTRACT

The influence of β -cyclodextrin-*p*-nitrophenol complexes in a *p*-nitrophenol-containing mobile phase on the chromatographic behaviour of aliphatic alcohols has been investigated. Depending upon the carbon chain length of the alcohol, the injected samples are detected before or after the first "system peak". The sample retention and the slope of the calibration curves depend upon the β -cyclodextrin concentration. The apparent molar absorptivity is maximal when the alcohol retention is close to the system peak. A comparison of these results to those obtained with an eluent devoid of β -cyclodextrin shows poor sensitivity for the indirect detection of alcohols, demonstrating that β -cyclodextrin inclusion complexes have some role in the mobile phase as detection enhancers.

INTRODUCTION

During the past few years several studies have shown that it was possible to detect and quantitate non UV-absorbing ionic compounds by the addition of a UV-absorbing ion in the aqueous mobile phase [1–6]. This method is applicable to both organic and inorganic ions using ion-exchange and reversed-phase chromatography. Recent reports have shown that this method can be extended to uncharged species [7–12]. Gnanasambandan and Freiser have used this method for the indirect UV detection of alcohols [7,8], ketones [7] and monosaccharides [9] with methylene blue in the eluent.

Similarly, Parkin and Lau [10,12] have detected alcohols by addition of UV-absorbing species such as benzamide, *n*-propyl-*p*-aminobenzoate uracil and theobromine in the mobile phase. The alcohols appeared as positive or negative peaks depending upon the chosen UV-detectable species and the respective capacity factors of UV-detectable species and alcohol.

In recent years, there has been considerable interest in the utilization of cyclodextrins (CDs) as stationary or as mobile phase in high-performance liquid

chromatography (HPLC) [13–18]. CDs are toroidal-shaped, cyclic oligosaccharides made up of α -1,4-linked D-glucopyranose units and act as “hosts” to form stable inclusion complexes with a variety of “guest” species. The CD complexes form well defined species and 1:1, 1:2 and 2:1 guest–host inclusion complexes have been reported [19]. On the other hand Fujimura *et al.* [20] have studied the chromatographic properties of solutes (phenols, cresols and aniline derivatives) on reversed-phase RP-8 columns in the presence of β -CD in a water–organic solvent mobile phase.

The purpose of the present work was to examine the effects of the β -CD present in an eluent containing a UV–visible-absorbing compound, *p*-nitrophenol (PNP), in order to show evidence for an indirect detection of non-coloured solutes, such as aliphatic alcohols. We have studied the influence of β -CD concentration on calibration curves and apparent molar absorptivity of the different alcohols and stated the experimental conditions affording the highest detection sensitivity.

EXPERIMENTAL

Chemicals

Methanol, ethanol and propanol were of HPLC grade and were obtained from Prolabo (France). 1-Butanol, 2-butanol, 2-methyl-1-propanol and *p*-nitrophenol were from Aldrich (France). β -CD “Rhodocap” was a gift from Rhône-Poulenc (France).

Apparatus and conditions

The spectra were registered on a UV-visible spectrophotometer (Type 550 SE, Perkin-Elmer, Oakbrook, IL, U.S.A.) connected to a recorder (type R-100, Perkin-Elmer).

The chromatographic equipment consisted of a pump (Model 110A, Beckman Instrument, France), a variable-wavelength detector (LC-3, Pye-Unicam, Cambridge, U.K.) (cell length = 1 cm), monitored at 400 nm, a refractive index detector (Model R 401, Waters Assoc., Milford, MA, U.S.A.) and a 50- μ l loop injector (Rheodyne 7120, Cotati, CA, U.S.A.).

The analytical column was 240 \times 4.6 mm I.D. and the guard column 100 \times 4.6 mm I.D.

Analytical columns were filled with LiChrosorb RP 18 (10 μ m, 100 Å) (Merck, Darmstadt, Germany) by a slurry packing technique. The guard column was packed with LiChrosorb SI 60 (10 μ m) (Merck).

The mobile phases were mixtures of variable composition consisting of 0.01 *M* potassium phosphate buffer (pH 7.85)–methanol (90:10, v/v) containing 10^{−5} *M* PNP and 0–5 \cdot 10^{−3} *M* β -CD. For comparison, buffered water–methanol mobile phases were used. The mobile phase was filtered through a 0.45- μ m Sartorius filter membrane. The flow-rate was 0.95 ml/min.

The experiments were performed at room temperature (20°C), but the column was isolated by a casing to avoid temperature fluctuations.

Procedure

The column was equilibrated with the mobile phase containing PNP and CD, and the breakthrough curve was recorded. The steady-state conditions, corresponding to a constant absorbance at 400 nm, generally required 1 h. All the samples were previously dissolved in the mobile phase.

The capacity factors (k') were calculated from the equation $k' = (V_R - V_m)/V_m$, V_R being the sample retention volume and V_m the mobile phase volume of the column measured from the elution time of sodium nitrate. We have verified that the change of V_m during the experiments was negligible and have measured this value every ten runs. The peak areas were measured by planimetry.

RESULTS

As the mobile phase contains both PNP and β -CD, we first measured the absorbance of buffered water solutions containing different ratios of these compounds. We observed that the absorbance maximum of PNP solution is shifted by the addition of increasing amounts of β -CD ($0-5 \cdot 10^{-3} M$) from 400 to 404 nm. An isobestic point is observed at 381 nm. The apparent molar absorptivity of PNP at 400 nm increases gradually from $15\,600 M^{-1} \text{cm}^{-1}$ ($[\beta\text{-CD}] = 0$) to $17\,870 M^{-1} \text{cm}^{-1}$ ($[\beta\text{-CD}] = 5 \cdot 10^{-3} M$).

The addition of β -CD to a potassium phosphate buffer-methanol (90:10, v/v) solution containing PNP led to the same shift of the absorbance maximum and to the same isobestic point. Moreover the apparent molar absorptivity of PNP increases from $17\,400 M^{-1} \text{cm}^{-1}$ ($[\beta\text{-CD}] = 0$) to $19\,250 M^{-1} \text{cm}^{-1}$ ($[\beta\text{-CD}] = 5 \cdot 10^{-3} M$) at 400 nm.

Chromatographic results

Fig. 1 shows typical chromatograms of alcohols injected separately on the chromatographic system used. 1-Propanol elutes as a positive peak followed by two "system peaks". The former is eluted at the same volume as a PNP sample injected in the same eluting conditions. The latter appears at a retention volume similar to that of β -CD eluted by a mobile phase containing only methanol and buffer (10:90, v/v) (refractive index detection). These two peaks are referred to as "system peaks" since

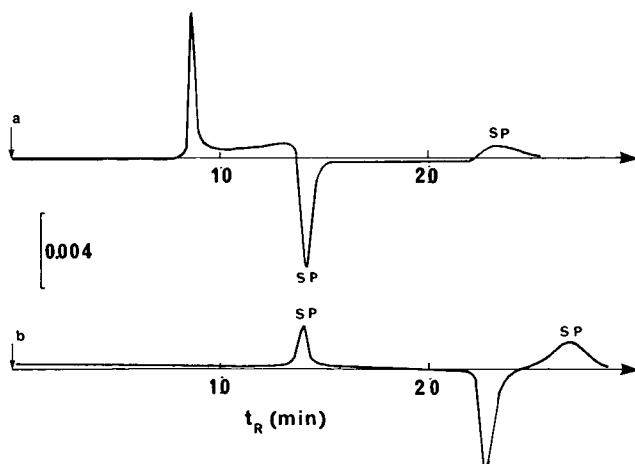


Fig. 1. Indirect detection of 1-propanol (a) and 2-butanol (b). Mobile phase: phosphate buffer-methanol (90:10, v/v), containing $10^{-3} M$ β -CD and $10^{-5} M$ PNP. Injected amounts: $80.34 \mu\text{g}$ for 1-propanol and $20.25 \mu\text{g}$ for 1-butanol. t_R = Retention time.

they correspond to species present in the eluent. The 1-butanol chromatogram shows a positive system peak corresponding to PNP, followed by a negative peak corresponding to the 1-butanol signal and a second positive system peak corresponding to β -CD.

A 15% methanol-containing mobile phase shows system peaks very close to the alcohol peaks in such a way that the detection of some alcohols becomes impossible (e.g. 1-propanol, 2-butanol). This effect of methanol in the eluent limits its effectiveness for these analyses.

In order to apply this system to the detection of a mixture of non visible-absorbing compounds, a sample containing aliphatic primary alcohols was injected (Fig. 2). It can be seen that the resulting peaks eluted at the retention volume of methanol, ethanol, 1-propanol and 2-propanol, before the first system peak, are positive while those eluted at the retention volume of 2-butanol, 2-methyl-1-propanol and 1-butanol, after the first system peak, are negative. Moreover, the sensitivity of the response depends on the alcohol retention time.

Influence of PNP on the capacity factors

A comparison (Fig. 3) of the capacity factors of the alcohols in the absence (k'_0) and the presence (k'_2) of PNP shows that the same sequence of retention is observed. It appears that the presence of PNP in the mobile phase slightly increases the retention of the C_1 – C_3 alcohols but does not modify the retention of the C_4 alcohols. This result can be interpreted as a stronger interaction of C_1 – C_3 alcohols with the stationary phase saturated by the PNP.

Influence of the addition of β -CD to the eluent

Fig. 4 compares the k' values of the C_1 – C_4 alcohols in the presence of β -CD in the eluent to the k'_0 values measured without PNP and β -CD (refractive index detection) in the same eluent. For comparison the k' values of alcohols have been

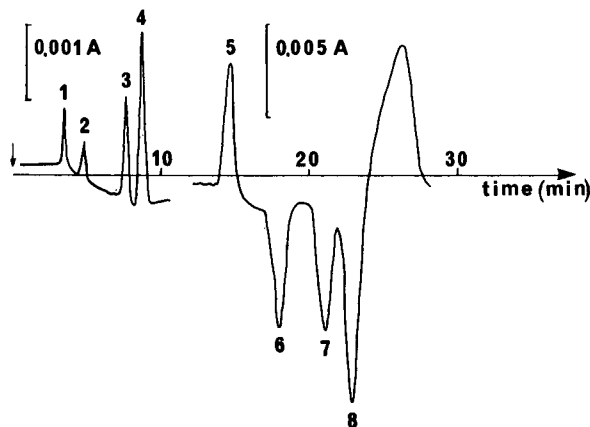


Fig. 2. Indirect detection of a 5% (v/v) aliphatic alcohols mixture. Peaks: 1 = methanol; 2 = ethanol; 3 = 2-propanol; 4 = 1-propanol; 5 = PNP (system peak); 6 = 2-butanol; 7 = 2-methyl-1-propanol; 8 = 1-butanol; 9 = β -CD (system peak). Mobile phase: phosphate buffer–methanol (90:10, v/v), containing 10^{-3} M β -CD and 10^{-5} M PNP. (From ref. 27, with permission).

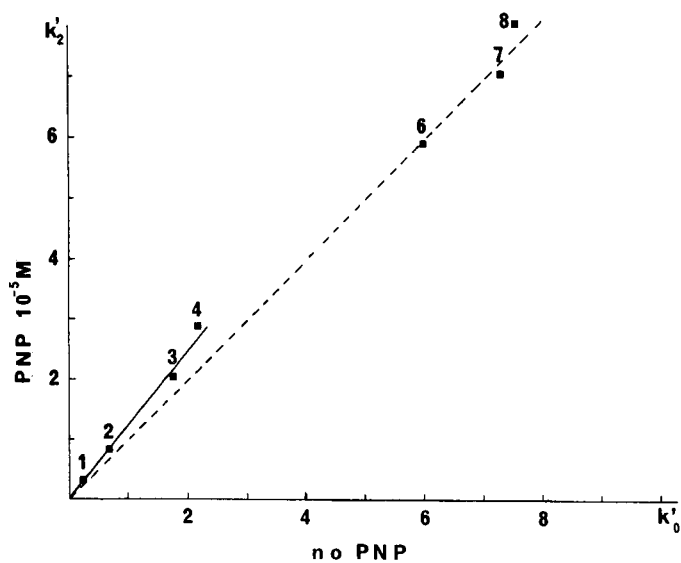


Fig. 3. Comparison of capacity factors of alcohols in the presence or the absence of PNP in the mobile phase. k'_0 values were determined by refractive index detection. The alcohols are referred by the same numbers as in Fig. 2. Mobile phase: phosphate buffer-methanol (90:10, v/v).

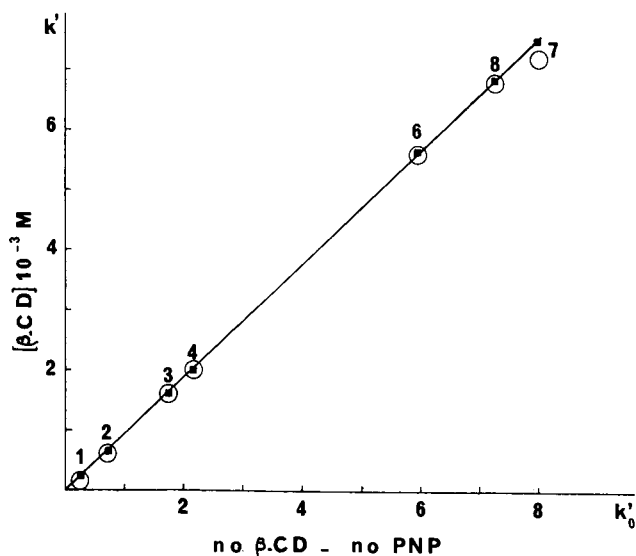


Fig. 4. Comparison of capacity factors of alcohols in different experimental conditions. \blacksquare = $10^{-3} M$ β -CD, no PNP; \circ = $10^{-3} M$ β -CD and $10^{-5} M$ PNP. The alcohols are referred by the same numbers as in Fig. 2. Mobile phase: phosphate buffer-methanol (90:10, v/v).

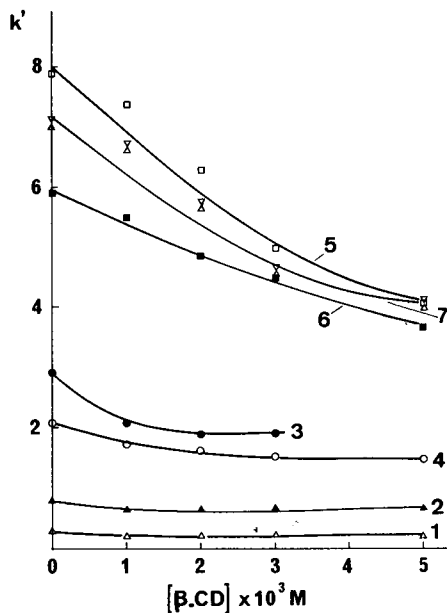


Fig. 5. Variation of capacity factors of aliphatic alcohols on β -CD concentration. 1 = Methanol; 2 = ethanol; 3 = 1-propanol; 4 = 2-propanol; 5 = 1-butanol; 6 = 2-butanol; 7 = 2-methyl-1-propanol. Mobile phase: phosphate buffer-methanol (90:10, v/v), containing 10^{-5} M PNP. The concentration of the alcohol solutions was 5‰ for methanol, 2‰ for ethanol and propanol and 0.5‰ for butanol (v/v).

measured with an indirect detection in the presence of PNP and β -CD in the eluent as a function of k'_0 defined above (Fig. 4). In both cases a linear variation is observed, the slope of which is 0.94, evidencing a slight alcohol- β -CD interaction in the mobile phase. It means that the previously observed short-chain alcohol-PNP interaction disappears.

The effect of β -CD at various concentrations in the mobile phase on the retention of aliphatic alcohols is reported on the Fig. 5. The variation of the capacity factor of all these alcohols with the concentration of β -CD is in agreement with the β -CD inclusion stability constants of these alcohols [24].

Calibration curves

We tested the validity of this indirect detection method in order to develop a quantitative analysis of these aliphatic alcohols. Fig. 6 shows results obtained with 1-propanol (a) and 2-butanol (b), which are eluted just before and after the first system peak, respectively. The detector response was linear and proportional to the amount of alcohol injected (from 10 to 200 μ g). For several alcohols the peak area increases until $[\beta\text{-CD}] = 2 \cdot 10^{-3}$ M and decreases beyond this value.

Similar linear calibration curves were obtained with the other alcohols studied except for the low methanol concentrations for which a deviation was observed. However, the measurement accuracy is low when the sample emerges very near the system peak. For example with 1- and 2-propanol the vicinity of positive and negative peaks lowers the peak area measurement.

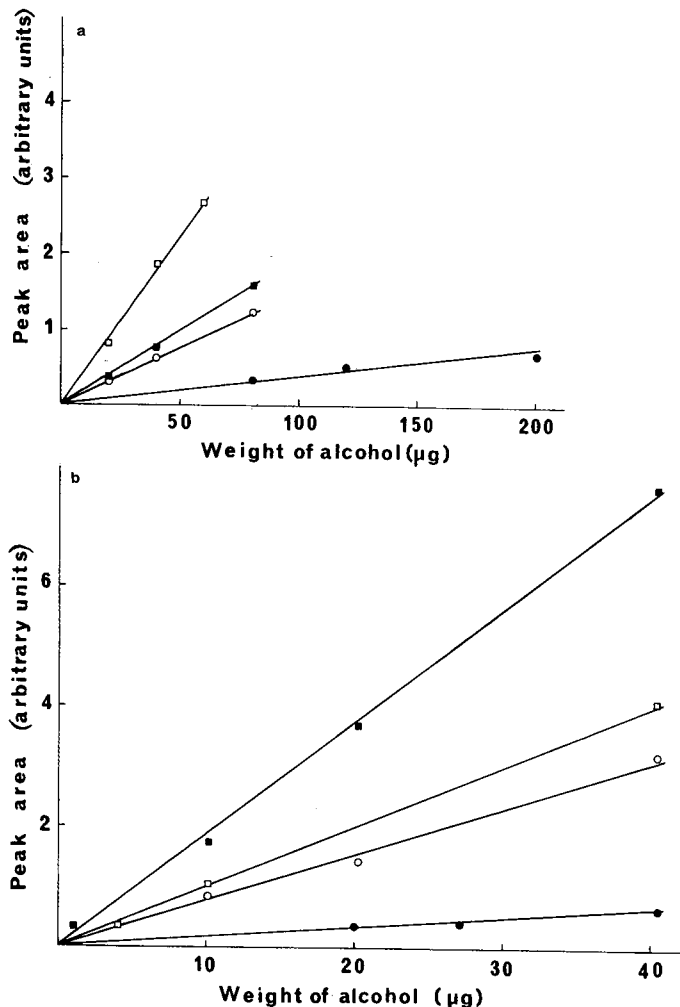


Fig. 6. Calibration curves of 1-propanol (a) and 2-butanol (b) at different β -CD concentrations. ● = $[\beta\text{-CD}] = 0$; ○ = $[\beta\text{-CD}] = 10^{-3} M$; ■ = $[\beta\text{-CD}] = 2 \cdot 10^{-3} M$; □ = $[\beta\text{-CD}] = 3 \cdot 10^{-3} M$. Mobile phase: phosphate buffer-methanol (90:10, v/v), containing $10^{-5} M$ PNP.

Detection sensitivity

We have determined the detection sensitivity obtained with the visible-absorbing PNP probe. The detection sensitivity for a given sample is expressed by the apparent molar absorptivity, ε^* , in the chromatographic systems used. This ε^* coefficient was defined by Hackzell and Schill [4]:

$$\varepsilon^* = Ysu/mbd$$

where Y is the sample peak area, s is the detector setting range, u is the flow-rate, m is the amount of the compound, d is the chart speed and b is the path length in the detector cell.

Fig. 7 shows that the addition of β -CD to an eluent containing 10^{-5} M PNP gives a convenient sample detection. The variation of the conditional molar absorptivity ϵ^* is far more important (for 10^{-3} M and $2 \cdot 10^{-3}$ M β -CD concentrations) than the variation of the absorbance molar coefficient determined from static spectroscopic measurements in the presence of β -CD at the same concentration.

This point was verified from the spectra obtained by adding small amounts of each alcohol studied to a potassium phosphate buffer-methanol (90:10) solution containing 10^{-5} M PNP. No significant variation in absorbance was noticed.

On the other hand, Fig. 7 shows that the detection sensitivity reaches a maximum value when the relative retention of the sample ($k'_{\text{sample}}/k'_{\text{PNP}}$) is close to unity as previously described [3].

It must be emphasized that the addition of β -CD modifies the ratio $k'_{\text{sample}}/k'_{\text{PNP}}$ for a given alcohol. In order to investigate the enhancing effect of β -CD on detection sensitivity we used a potassium phosphate buffer-methanol (85:15) solution containing 10^{-5} M PNP as mobile phase. This percentage was chosen so that the $k'_{\text{sample}}/k'_{\text{PNP}}$ ratio was similar to that obtained in the presence of 10^{-3} M β -CD. In these conditions the ϵ^* values obtained in all cases were from three to twenty times lower than those obtained with 10^{-3} M β -CD in the mobile phase, depending upon the hydrophobic properties of the studied alcohol (Fig. 8).

Fig. 9 shows the variation of the detection sensitivity (response) for each compound with β -CD concentration. For most alcohols studied, the response increases when the β -CD concentration varies from 10^{-3} M to $2 \cdot 10^{-3}$ M. Beyond $2 \cdot 10^{-3}$ M a decrease is observed. However, for the two propanol alcohols, eluted just before the system peak, the response increases continuously with the β -CD concen-

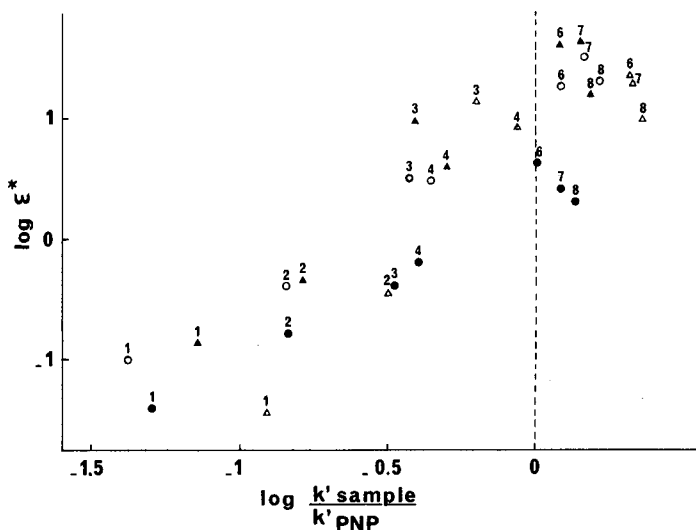


Fig. 7. Influence of relative alcohols retention on the detection sensitivity with different β -CD concentrations in the mobile phase. The alcohols are referred by the same numbers as in Fig. 2. Mobile phase: phosphate buffer-methanol (90:10, v/v) containing 10^{-5} M PNP. ● = $[\beta\text{-CD}] = 0$; ○ = $[\beta\text{-CD}] = 10^{-3}$ M; ▲ = $[\beta\text{-CD}] = 2 \cdot 10^{-3}$ M; △ = $[\beta\text{-CD}] = 3 \cdot 10^{-3}$ M. (From ref. 27, with permission).

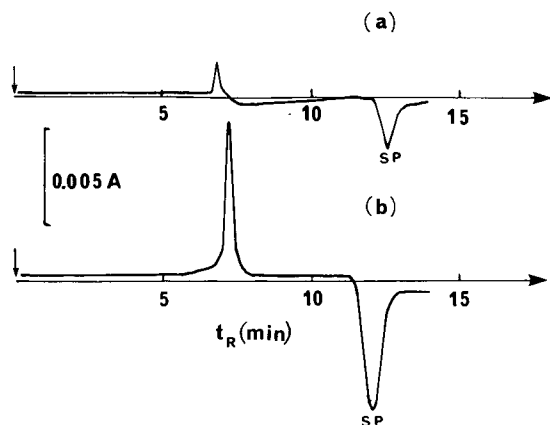


Fig. 8. Indirect detection of 2-propanol without β -CD (a) and with $2 \cdot 10^{-3} M$ β -CD (b). The experimental conditions were: (a): injected 2-propanol solution 5% (v/v), in a mobile phase of phosphate buffer-methanol (85:15, v/v), containing $10^{-5} M$ PNP; (b): injected 2-propanol solution 2% (v/v), in a mobile phase of phosphate buffer-methanol (90:10, v/v), containing $10^{-5} M$ PNP.

tration. The opposite response is obtained with 1-butanol which decreases continuously with increasing β -CD. Thus the $10^{-3} M$ β -CD concentration in the mobile phase is the best compromise between high detection sensitivity and satisfactory separation of the different compounds.

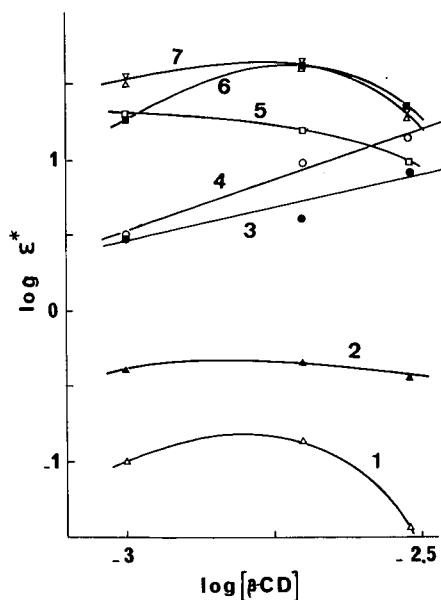


Fig. 9. Dependence of detection sensitivity on β -CD concentration. Mobile phase: phosphate buffer-methanol (90:10, v/v), containing $10^{-5} M$ PNP. 1 = Methanol; 2 = ethanol; 3 = 1-propanol; 4 = 2-propanol; 5 = 1-butanol; 6 = 2-butanol; 7 = 2-methyl-1-propanol.

DISCUSSION

The detection system described here is very complex since the detectable species PNP exists at pH 7.85 mainly in the ionized form PNP^- ($\text{p}K_a = 7.15$) and the ionization equilibrium can be displaced when methanol or β -CD are added to the mobile phase.

The indirect detection principle was given by Parkin [10]. As the eluting peak for all contains a large excess of compound over the UV-detectable species, the author has suggested that the presence of compounds modifies the partitioning characteristics of the UV-absorbing species during its passage through the column.

As a consequence, in all the elution zones the concentration of the eluent constituents, including the detectable species, is slightly different from those of the present eluent. Thus each constituent of the mobile phase of which concentration has been modified can give a "system peak".

Crommen [24] has developed a mathematical analysis in order to explain the sense and the area of the observed peaks. A more complete calculation of the chromatographic profile corresponding to indirect detection was theoretically achieved by Golshan-Shirazi and Guiochon [25].

The present case is different and more complex. Indeed, several species in the eluent can interact with the stationary phase and the alcohols. Different equilibria must be considered:

In the mobile phase:



With the stationary phase:



where A designates the injected alcohol.

Alcohol injection perturbs the partition equilibrium of all the constituents of the mobile phase. The presence of the CD-A complex in the mobile phase modifies the partitioning of CD-PNP and CD which are released in the mobile phase following the two equilibria 5 and 7, displaced to the left, and give rise to two "system peaks". The first peak corresponds to PNP, the second to CD. The intensity of the indirect detection signal essentially depends upon the competition between the reactions 5, 6 and 7.

The increase in β -CD concentration in the mobile phase leads to stronger

complexation of the alcohol and shifts reaction 2 to the right, involving a more important desorption of CD-PNP and CD.

The previously reported properties of the apparent molar absorptivity coefficient are verified in our case in the sense that it is higher when the capacity factors of injected alcohol and PNP are very close to each other. The presence of β -CD in the eluent plays a special role since the release of PNP following the injection of alcohol gives a greater signal than that obtained in the absence of CD, permitting an enhancement of the alcohol detection.

A similar technique applied to steroids has permitted us to increase the efficiency of their indirect detection [26]. A complete analysis of the phenomena involved in the formation of several complexes in the mobile phase is at present underway.

REFERENCES

- 1 N. Parris, *J. Liq. Chromatogr.*, 3 (1980) 1743.
- 2 B. A. Bidlingmeyer, *J. Chromatogr. Sci.*, 18 (1980) 525.
- 3 M. Denkert, L. Hackzell, G. Schill and E. Sjögren, *J. Chromatogr.*, 218 (1981) 31.
- 4 L. Hackzell and G. Schill, *Chromatographia*, 15 (1982) 437.
- 5 A. Herrmann, E. Damawandi and M. Wagmann, *J. Chromatogr.*, 280 (1983) 85.
- 6 L. Hackzell, T. Rydberg and G. Schill, *J. Chromatogr.*, 282 (1983) 179.
- 7 T. Gnanasambandan and H. Freiser, *Anal. Chem.*, 53 (1981) 909.
- 8 T. Gnanasambandan and H. Freiser, *Anal. Chem.*, 54 (1982) 1282.
- 9 T. Gnanasambandan and H. Freiser, *Anal. Chem.*, 54 (1982) 2379.
- 10 J. E. Parkin, *J. Chromatogr.*, 287 (1984) 457.
- 11 S. Banerjee, *Anal. Chem.*, 57 (1985) 2590.
- 12 J. E. Parkin and H. T. Lau, *J. Chromatogr.*, 314 (1984) 488.
- 13 K. Uekama, F. Hirayama and S. Nasu, *J. Chem. Pharm. Bull.*, 26 (1973) 3477.
- 14 W. L. Hinze and D. W. Armstrong, *Anal. Lett.*, 13 (1980) 1093.
- 15 W. L. Hinze, *Sep. Purif. Methods*, 10 (1981) 159.
- 16 D. Sybilska, J. Lipkowski and J. Woycikowski, *J. Chromatogr.*, 253 (1982) 95.
- 17 K. Fujimura and T. Ueda, *Anal. Chem.*, 55 (1983) 446.
- 18 D. Sybilska, J. Debowski, J. Jurczak and J. Zukowski, *J. Chromatogr.*, 286 (1984) 163.
- 19 D. W. Armstrong, F. Nome, L. A. Spino and T. D. Golden, *J. Am. Chem. Soc.*, 108 (1986) 1418, and several references therein.
- 20 K. Fujimura, T. Ueda, M. Kitagama, H. Takayanagi and T. Ando, *Anal. Chem.*, 58 (1986) 2668.
- 21 A. Buvari, J. Szejtli and L. Barcza, *J. Incl. Phenom.*, 1 (1983) 151.
- 22 A. Buvari and L. Barcza, *J. Chem. Soc., Perkin Trans. II*, 4 (1988) 543.
- 23 K. A. Connors and J. M. Lipari, *J. Pharm. Sci.*, 65 (1976) 379.
- 24 J. Crommen, *Thèse d'Agrégation*, Liège University, Liège, (1989).
- 25 S. Golshan-Shirazi and G. Guiochon, *Anal. Chem.*, 62 (1990) 923.
- 26 B. Agnus, M. Gosselet and B. Sebille, *J. Chromatogr.*, 552 (1991) 583.
- 27 M. Gosselet and B. Sebille, *Collection Minutes*, Edition de Santé, Paris, 1990, p. 269.

Column switching for the high-performance liquid chromatographic analysis of polynuclear aromatic hydrocarbons in petroleum products

ANDREW J. PACKHAM*^a and PETER R. FIELDEN

Department of Instrumentation and Analytical Science, University of Manchester, Institute of Science and Technology, P.O. Box 88, Manchester (U.K.)

ABSTRACT

Contact with polynuclear aromatic hydrocarbons which are ubiquitous pollutants can lead to the induction of various cancers. The measurement of these substances is thus of prime importance. However, the complexity of many samples in which they may be found results in a long and difficult analysis. High-performance liquid chromatography, when used in conjunction with column-switching procedures, can realise the separation of specific analytes in complex mixtures such as petroleum products.

The benefits are achieved by concentrating the analytical effort only on compounds of interest, while disregarding the rest. Optimum separations occur when different retention mechanisms are combined within a configuration. However, the incompatibilities that arise due to the range of solvents used can present problems. To overcome these we have investigated the combination of cyclodextrin and reversed-phase bonded phases. The employment of these differing retention mechanisms permits the rapid determination of polynuclear aromatic hydrocarbons with no sample preparation or pretreatment, hence the analysis time is reduced significantly as is the risk of contamination of the laboratory personnel and environment.

INTRODUCTION

Recently, it has become necessary to analyse very complex mixtures such as environmental, biological, food and petroleum samples for low levels of potentially harmful substances. Tighter national and international regulations covering a wide range of consumer products, industrial emissions etc., have increased the need for the accurate analyses of a wide range of multicomponent mixtures.

High-performance liquid chromatography (HPLC) is often the method of choice in many analytical laboratories. However, due to the large number of components in a complex sample, these samples may be difficult to analyse by orthodox liquid chromatographic techniques. The problems associated with analysing complex samples have been shown clearly by Davis and Giddings [1]. In their paper it was estimated that a column efficiency of around 200 000 theoretical plates was required

^a Present address: Technical & Analytical Solutions, Pelham House, 49 Pelham Street, Ashton Under Lyne OL7 0DT, U.K.

to give a 90% probability that a twenty-component mixture would be fully resolved. As a petroleum sample may contain many hundreds, if not thousands of different components, the difficulties that arise can clearly be seen.

The resolving power of HPLC may be enhanced significantly by the introduction of column-switching techniques. These are chromatographic techniques aimed at the determination of the concentration of a specific analyte in a complex matrix. The technique provides the optimum efficiency for separations of the component of interest, whilst simultaneously minimising analysis time by decreasing the time spent in separating the components of a sample that are of no analytical interest. The separation is developed by both chromatographic and mechanical means. This is achieved by using more than one column connected by switching valves so that different parts of the sample may follow different paths through the column configuration. Column switching strategies have been applied to a wide range of analytical problems including polynuclear aromatic hydrocarbons (PNAs) [2-4], pharmaceutical agents [5,6] and biological metabolites [7,8].

PNAs are common environmental pollutants derived from a number of natural and man-made sources, including the combustion of a variety of carbon-based materials. The carcinogenic nature of some of the group members, notably benzo[a]pyrene, has been well documented [9,10], and leads to considerable analytical effort being focused on this group [4]. The determination of these compounds in petroleum products causes significant analytical problems due to the complex nature of the matrix. The analysis of petrochemicals such as crude, processed and synthetic oils present interesting problems to the analyst. There is a wide variety of materials with very different properties present. Additionally, there are important safety considerations due to the flammable nature and toxicity of the matrix. The analytical problem is further complicated by the addition of various performance improvers and additives, notably to fuels and lubricating oils. The presence of a wide range of high-molecular-weight polymers and small, charged additives presents the analyst with a complex problem. By using column-switching techniques, to improve the resolving power of separation techniques, many otherwise difficult analyses may be attempted.

A selective method for the determination of benzo[a]pyrene in aviation fuel, based on a two-column switching procedure, has been published previously by the authors [3]. In this paper an improved method is described that permits the simultaneous analysis of a range of different PNAs. The application of the procedure for the analysis of lubricating oil base stocks of differing complexity is used to illustrate the operation. The use of three-column systems to realise the separation of very complex mixtures is discussed. The method published previously is based on the use of a cyclodextrin column to produce the initial fractionation of the sample. It is interesting to note that while cyclodextrin columns have been used successfully to separate PNAs [11,12], the conditions used here, *i.e.* relatively high organic modifier percentages, would not result in a separation of the group. This is highly advantageous as it simplifies the operation of the system. As the PNAs elute as one unresolved peak only one heart-cut operation is required to transfer the group onto the next column, be it either an analytical or further fractionation column. The mechanism whereby the PNAs are retained is thought to be by inclusion formation, the gamma cyclodextrin, which is the largest of the three cyclodextrin-bonded phases available has a cavity

internal diameter of about 0.95 nm, this compares to benzo[*a*]pyrene which has an estimated size of 0.88 nm across the long axis. Benzo[*a*]pyrene is thus able to enter the cavity of the γ - and β -cyclodextrins, but would be excluded from the α -cyclodextrin (0.57 nm) [13]. Within cavity π - π interactions between the cyclodextrin and the PNA determine the stability of the inclusion complex. The mobile phase modifier has a greater affinity for the cavity than the PNAs and is therefore able to displace them. At concentrations above 25–35% acetonitrile little interaction between the cavity and the PNAs occur.

EXPERIMENTAL

Materials

The PNA standards were obtained from BDH (Poole, U.K.). Chromatographic solvents were also obtained from BDH and were of HiPerSolv grade. The water used in this study was distilled and stored in glass without further purification. The β - and γ -cyclodextrin columns (250 × 4.6 mm I.D.) were packed by Astec (U.S.A.) and supplied through Technicol (Stockport, U.K.). The Vydac C₁₈ 201TP54 (250 × 4.6 mm I.D.) was also obtained from Technicol. Standard PNA solutions were made up in acetonitrile and stored in the dark to avoid photo-induced degradation. As the PNAs used were either confirmed or suspected carcinogens, the appropriate safety precautions were taken when handling the compounds or their solutions. The samples of petroleum products were obtained from commercial sources. Two lubricating oil base stocks were used. The first, sample 1, contains approximately 30% aromatic compounds while the second, sample 2, contains approximately 40%.

Equipment

The chromatography was carried out using the following equipment. A Waters series 6000 HPLC pump was used, the mobile phase being generated by a modified Micromeritic gradient former. All solvents were filtered through a 2- μ m Millipore filter under negative pressure and continuously degassed with helium. To perform on-line dilution, a Kontron Series 420 pump was used. The solvents were mixed using a stainless-steel low dead volume 'T' piece. A Rheodyne Model 7125 syringe loading injection valve with a 20- μ l sample loop was used to introduce the sample. A Perkin-Elmer series 3000 fluorescence detector was used to monitor the eluent. The excitation and emission wavelengths were 254 nm and 420 nm, respectively. The emission and excitation wavelengths were chosen as the best compromise between instrumental noise, limits of detection for PNAs and the greatest discrimination between the analytes and the interferences. Excitation and emission slits were set at 5 nm. A Midas Plus chromatographic data station, Comus Instruments (Hull, U.K.) was used to control the column-switching system and to acquire, process and store the data. A Goerz BBC SE 120 chart recorder was used to record the chromatograms. A schematic diagram of the column configuration has been previously presented [3]. The 'T' piece and second pump required for on-line dilution were placed before the second cyclodextrin fractionation column.

Column switching configuration

The configuration consists of three analytical columns (C2 to C5), typically a

Vydac C₁₈ and two Astec cyclodextrin columns connected in a serial fashion by the use of switching valves, four Rheodyne Model 7000 switching valves with pneumatic actuators (V1 and V3 to V5), a sample injection valve (V2), two pumps and a fluorescence detector.

This very flexible system allows a sample to be analysed on any of the three columns or to allow a sample to be fractionated on either the first or second column with the fraction of interest analysed on the second or third column. In addition pre-concentration is made possible by the inclusion of a guard column (C1) operated in conjunction with the first switching valve (V1).

The valves are all controlled by pneumatic actuators that, in turn, are themselves controlled by the computerised system. Thus, this allows complex column-switching procedures to be performed without operator intervention.

Chromatographic technique

Sample fractionation. The petroleum sample, after filtration, was fractionated using a β -cyclodextrin pre-column (C2), with an isocratic mobile phase of acetonitrile–water (40:60). The timing for the heart cut was determined through the use of a range of standard compounds. For the simple lubricating fuel a 45-s heart cut beginning at 3.75 min was found to be appropriate. If, due to the complexity of the sample, it was found necessary to include a second fractionation step, a γ -cyclodextrin column (C3), was used. This column was equilibrated with acetonitrile–water (10:90). To ensure the analyte was retained strongly at the head of the second column water was mixed, on-line, via a T-piece with the eluent from the first column just prior to the second column. A makeup flow-rate of 1 ml min⁻¹ was found to be sufficient. The sample was then fractionated using the conditions outlined above. In this case however, a heart cut of 65 s beginning at 4.24 min was more appropriate.

Heart-cut analysis. The heart cut was analysed on the 25-cm Vydac C₁₈ column (C4), using a 40-min linear gradient from 30 to 100% acetonitrile at 1 ml min⁻¹. The analytical column was equilibrated at an acetonitrile concentration 10% below that of the fractionation column, to ensure that the heart cut remained as a small plug on the head of the analytical column in order to minimize peak dispersion. The peaks found in the sample were identified by a comparison between the unknown and standard retention times.

RESULTS AND DISCUSSION

The refined products of crude petroleum are complex mixtures that are used either as sources of power, heat, lubrication or building, and more recently, as base stocks for chemicals. Due to the complexity of the product and the inadequacies in analytical techniques, the petroleum industry uses a host of semi-empirical measurements, or customer acceptance tests. While in practice these empirical tests have generally sufficed to ensure the quality of each petroleum product, the use of more selective techniques is required to allow an assessment to be made as to the environmental or health impact of the sample or to allow a particular facet of the product's performance to be studied. The PNAs, in addition to their environmental impact play an important role in the modification of a product's performance characteristics.

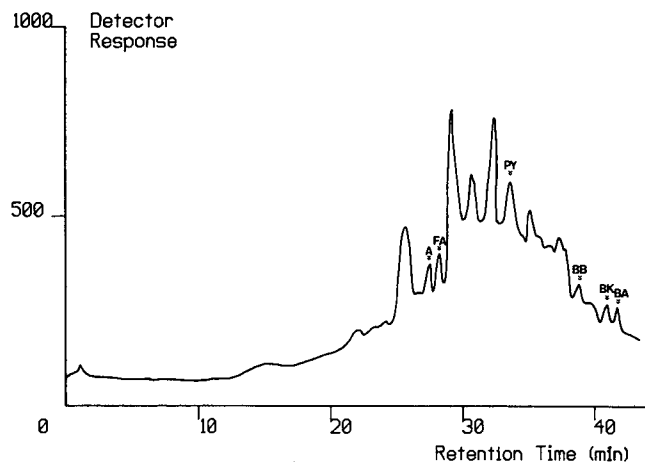


Fig. 1. Separation of sample 1 using a two-column, cyclodextrin- C_{18} column-switching configuration. A = Anthracene; FA = fluoranthene; PY = pyrene; BB = benzo[*b*]pyrene; BK = benzo[*k*]pyrene; BA = benzo[*a*]pyrene.

Fig. 1 shows a separation of the simple base oil sample (30% aromatic) using a two-column technique. The initial fractionation on the cyclodextrin column produces a fraction of considerably lower complexity that can be analysed on the final Vydac C_{18} column. From this chromatogram it is possible to identify specific PNAs.

If, however, the complexity of the sample is further increased, the resolving power of the system fails to separate the sample and a broad peak results. This occurs because even after fractionation the resulting fraction is still too complex. A reduction in the length of the heart-cut window would achieve a fraction of lower complexity but also would exclude a number of the PNAs. The problem may be overcome using one of two approaches. Firstly, it is possible to incorporate an off-line sample pre-treatment step either before or after the fractionation step using a solid-phase extraction column or a further LC separation. Alternatively, it is possible to incorporate a third column within the column-switching configuration. It is preferable to use a third column instead of an off-line technique so as not to negate the advantages of an enclosed analytical system, namely improved safety and analytical performance. The sample would thus undergo two separate fractionation procedures and as two different columns are used the mechanism of fractionation will be different in each case. To maintain the efficiency of the separation it is necessary to ensure that at each fractionation procedure the fraction of interest is reconcentrated at the head of the next column. This is usually achieved by equilibrating the second column with a solvent mixture of lower eluting strength than that which will carry the fraction on to the column. This is, however, difficult to achieve when using the cyclodextrin columns due to the low density of the bonded phase. The amount of organic modifier necessary to elute the fraction suppresses any reconcentration that may occur. Without reconcentration the PNAs pass on to the second column where they begin to undergo separation. The final fraction which would be required to include all the PNAs will also include a large proportion of interfering material. In addition to the

time required for the heart cut on to the analytical column will be such that reconcentration does not occur on this column either.

To achieve the necessary reconcentration it has been found necessary to mix water with the mobile phase immediately before the second column. This has the effect of reducing the percentage of the organic modifier in the solvent stream, thus allowing the necessary reconcentration to occur at the head of the second column. The separation on the second cyclodextrin column results in a fraction of suitable complexity, containing all the PNAs within a tight band, that can be switched rapidly to the analytical column. A separation achieved by this procedure can be seen in Fig. 2.

The mechanism whereby the PNAs are separated from the interferences is unclear. Deviations from the expected retention behaviour of benzo[*a*]pyrene have been reported [14]. At the concentrations of organic modifier used in this study, there will be only minimal retention of PNAs due to inclusion formation. The lack of retention, as compared to the majority of the interferences is advantageous as it allows the rapid elution of the PNAs, as a group and within a small time period.

The quantitation of a component in a complex sample poses many problems. The use of an internal standard may not be appropriate due to either the highly selective nature of the separation or as it may not be fully resolved from either the analytes or the interferences. In this study, to obtain quantitative information, external standards have been used. Each sample was followed by a blank sample and every fifth sample was a calibration blend. It must nonetheless be understood that the information obtained is only of a semi-quantitative nature. When the sample matrix is extremely complex even highly selective column-switching procedures do not result in complete baseline separation and therefore the integration conditions will be different. This leads to inaccuracies in the determination of peak areas and hence analytical concentrations. Table I contains the semi-quantitative data for samples 1 and 2.

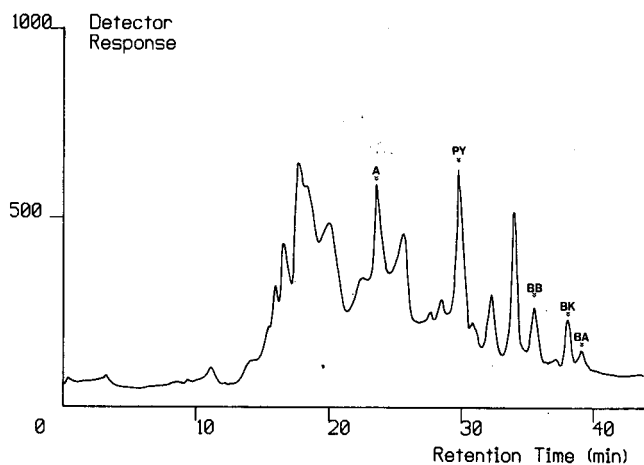


Fig. 2. Separation of sample 2 using a three-column, cyclodextrin-cyclodextrin- C_{18} column-switching configuration with on-line dilution between the first and second cyclodextrin columns. Abbreviations as in Fig. 1.

TABLE I
SEMI-QUANTITATIVE DATA FOR PNAs DETECTED
Mean result, $n = 3$.

Analyte	Sample 1 ($\mu\text{g l}^{-1}$)	Sample 2 ($\mu\text{g l}^{-1}$)
A	40.0	144.0
FA	17.5	Not detected
PY	11.8	35.2
BB	Trace	5.7
BK	Trace	4.2
BA	Trace	Trace

Work is currently in progress to automate the system further by incorporating a degree of 'intelligent processing' to permit the computer program to modify the protocol to obtain the best result with minimal input from the operator. Additionally it is hoped to study the retention and fractionation mechanisms of the cyclodextrin columns more closely.

CONCLUSIONS

Significant advantages over off-line and other on-line techniques are achieved by using a column-switching strategy. In particular, the system increases operator safety due to the reduced environment contamination and sample handling, and sample loss due to the reduced possible adsorption or volatilization of the sample. The removal of any pre-analysis step, such as solid-phase or solvent-solvent extraction significantly reduces the analysis time. The use of a three-column system enables the analysis of very complex mixtures within a closed environment. The use of cyclodextrin columns to fractionate the sample is highly advantageous and results in the rapid production of a greatly simplified matrix. On-line dilution may be successfully used to realise the development of complex column-switched systems in which many different columns are used and to maintain the system efficiency by ensuring that reconcentration, where necessary, does occur.

ACKNOWLEDGEMENTS

The authors gratefully acknowledge the support of A. J. P. who is in receipt of a Science and Engineering Research Council CASE award, co-sponsored by Esso Petroleum Company, Ltd. (Esso Research Centre, Abingdon, U.K.) and for the finance that allowed A. J. P. to attend the 18th *International Symposium on Chromatography*. We are also indebted to Technicol Ltd. (Stockport, U.K.) for the supply of columns used in this study and to Comus Instruments Ltd. (Hull, U.K.) for the Midas Plus data station used.

REFERENCES

- 1 J. M. Davis and J. C. Giddings, *Anal. Chem.*, 55 (1983) 418.
- 2 W. J. Sonnefeld, W. H. Zoller, W. E. May and S. A. Wise, *Anal. Chem.*, 54 (1982) 723.
- 3 P. R. Fielden and A. J. Packham, *J. Chromatogr.*, 479 (1989) 117.
- 4 M. L. Lee, M. V. Novotny and K. D. Bartle, *Analytical Chemistry of Polycyclic Aromatic Compounds*, Academic Press, New York, 1981.
- 5 K. Matsumoto, H. Kikuchi, H. Iri, H. Takahasi and M. Umino, *J. Chromatogr.*, 425 (1988) 323.
- 6 J. A. Apfel, T. V. Alfredson and R. E. Majors, *J. Chromatogr.*, 206 (1981) 43.
- 7 P. Nebinger and M. Koel, *J. Chromatogr.*, 434 (1988) 43.
- 8 A. Niederwiser, W. Staudenmann and E. Wetzel, *J. Chromatogr.*, 290 (1984) 237.
- 9 D. Hoffman and C. E. Wynder, *Chemical Carcinogens (ACS Monograph Series No. 173)*, American Chemical Society, Washington, DC, 1976.
- 10 R. D. Harvey, (Editor), *Polycyclic aromatic hydrocarbons and carcinogenesis (ACS Monograph Series No. 283)*, American Chemical Society, Washington, DC, 1985.
- 11 M. Olsson, L. C. Sander and S. A. Wise, *J. Chromatogr.*, 477 (1989) 277.
- 12 D. W. Armstrong, A. Alak, D. Wade, W. L. Hinze, T. E. Riehl, *J. Liquid Chromatogr.*, 8 (1985) 261.
- 13 R. Woodberry, S. Ransom and C. Fu-Ming, *Anal. Chem.*, 60 (1988) 2621.
- 14 P. R. Fielden and A. J. Packham, *J. Chromatogr.*, 516 (1990) 355.

Effects of β -cyclodextrin in the mobile phase on the retention and indirect detection of non-electrolytes in reversed-phase liquid chromatography

II. Steroids

BENOIT AGNUS*

Laboratoires Besins Iscovesco, 8 Rue Morel, 92120 Montrouge (France)

and

BERNARD SEBILLE and MARTINE GOSSELET

Laboratoire de Physico-Chimie des Biopolymères C.N.R.S.-Université Paris XII, UM 27 2 Rue Henri Duntant, 94320 Thiais (France)

ABSTRACT

The effect of β -cyclodextrin on the chromatographic retention time of two steroids, pregnanolone and progesterone is described. The apparent formation constant of the inclusion complexes has been calculated, and the optimization of indirect photodetection of pregnanolone, in reversed-phase chromatography, has been investigated. The presence of β -cyclodextrin in the mobile phase appears essential to enhance the detection of pregnanolone.

Over the past few years, a great number of papers have been published on the separation, detection and quantitation of steroids. These techniques can be divided into two classes: (a) specific methods, such as colorimetry, fluorimetry, isotopic techniques and immunological assays; these are employed mainly for the quantitation of steroids in physiological fluids [1,2]. (b) Separation techniques that permit quantitation of steroids by UV photometric, fluorimetric or electrochemical detection following high-performance liquid chromatography (HPLC), or flame ionization or mass spectrometric detection following gas chromatography (GC) [3–5].

For the quantitation of steroids in pharmaceutical preparations, two techniques are mainly employed: HPLC with UV detection and GC with flame ionization detection. In the case of pregnanolone, detection is difficult because this steroid has poor UV absorption. Thus we decided to develop a simple method using indirect photodetection following HPLC, and avoiding any derivatization. In this technique, a UV-absorbing probe is included in the mobile phase and distributed on a stationary phase. The injection of non-absorbing species disturbs the equilibrium. This gives a peak at the retention time of the non-UV-absorbing species, followed or preceded by a system peak.

Indirect photodetection has previously been applied to the detection of non-UV-absorbing ionic and non-ionic compounds [6–12]. Furthermore, the inclusion complexation of steroids with β -cyclodextrins (β CD) has been described by many authors [13–16]. Generally, the steroids form complexes with β CD in a 1:1 or 1:2 ratio.

In our previous paper [17], we described the role of β CD in the chromatographic requirements and the indirect photodetection of alcohols. This paper deals with the role of β CD in the chromatographic behaviour of pregnanolone and progesterone and the indirect photodetection of these steroids.

EXPERIMENTAL

Apparatus

The chromatographic equipment included a pump (model 110B, Beckman Instruments, France), a filter wavelength detector (Model 160, Beckman Instruments) with a 10-mm flow-cell length, a 20- μ l loop injector (Altex 210A valve, USA) and an integrator (Model CR5A, Shimadzu, Japan). The columns and guard columns (100 \times 4.6 mm I.D. and 1.5 \times 4.6 mm I.D., respectively) were made of stainless steel equipped with swagelock connectors.

Chemicals and reagents

Methanol of HPLC grade was purchased from Prolabo (France). Pregnanolone, progesterone and β -cyclodextrin were from Sigma (France).

Chromatography

Separations were carried out with columns packed by Interchim (France) with Nucleosil C₄, 5 μ m particle size, porosity 300 Å (Macherey-Nagel, Germany); RP2, 10 μ m particle size, porosity 120 Å (Applied Biosystems, USA).

The room temperature was 20°C \pm 1°C, and the air was conditioned. The flow-rate was 0.8 ml/min. The samples were injected as solutions in the mobile phase. Peak areas were determined with an integrator after conversion of results in square centimetres by planimetry. The void volume was obtained from the front peak of the chromatogram.

RESULTS AND DISCUSSION

Influence of β CD on capacity factor of steroids

The addition of β CD in the eluent decreases the retention time of the injected steroids. Figs. 1 and 2 show, for pregnanolone and progesterone respectively, the variation of the capacity factor with increasing concentrations of β CD in the eluent. The retention times decreased as the concentration of β CD increased. This reveals the formation of inclusion complexes between steroids and β CD. Moreover, this dependence varies with the methanol content of the eluent.

Using the method previously introduced by Love and Aranhyant [18] and

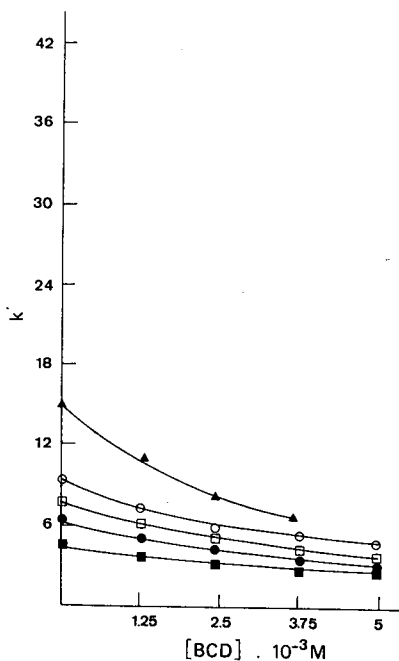
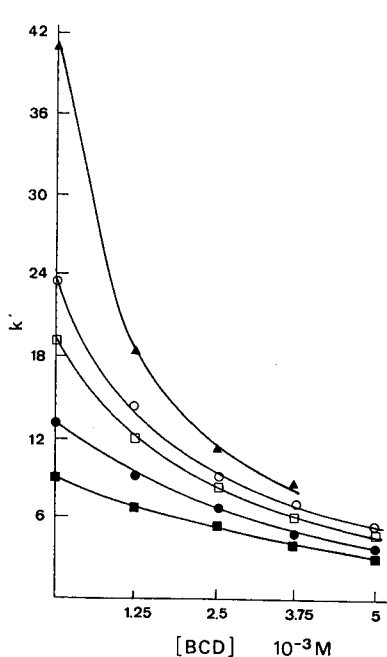


Fig. 1. Variation of pregnanolone capacity factor with increasing concentration of β CD at different proportions of methanol in the mobile phase: (\blacktriangle) [CH₃OH] = 45%; (\circ) [CH₃OH] = 47%; (\square) [CH₃OH] = 50%; (\bullet) [CH₃OH] = 53%; (\blacksquare) [CH₃OH] = 55%. Experimental conditions: column (10 cm \times 4.6 mm I.D.), particle size 5 μ m, 300 \AA ; guard column (1.5 cm \times 4.6 mm I.D.), C₄; particle size 5 μ m, 300 \AA ; flow-rate, 0.8 ml/min; detection wavelength, 280 nm; sample injected, 10 μ g.

Fig. 2. Variation of progesterone capacity factor with increasing concentration of β CD at different proportions of methanol in the mobile phase: (\blacktriangle) [CH₃OH] = 45%; (\circ) [CH₃OH] = 47%; (\square) [CH₃OH] = 50%; (\bullet) [CH₃OH] = 53%; (\blacksquare) [CH₃OH] = 55%. Experimental conditions as in Fig. 1 except detection wavelength, 254 nm.

Fujimura *et al.* [19], we have determined the apparent stability constant of the complexes from the following equation:

$$\frac{1}{k'} = \frac{1}{k'_0} + \frac{[\text{CD}]_T}{K_D k'_0}$$

where k' is the capacity factor in the presence of β CD, K_D the dissociation constant of the complex, k'_0 the capacity factor without β CD and $[\text{CD}]_T$ the total concentration of β CD in mobile phase.

Table I lists the results for different percentages of methanol. These show that the steroid- β CD inclusion complexes have a higher stability when the content of methanol is low. Those results confirm the hydrophobic character of the interaction between steroids and β CD. Furthermore, the β CD-pregnanolone complex is more stable than the β CD-progesterone complex. This was suggested from the higher hydrophobic character of pregnanolone, which was revealed by its higher retention on the reversed-phase column with β CD in the mobile phase.

TABLE I

APPARENT ASSOCIATION CONSTANTS (K_f) OF INCLUSION COMPLEXES β CD-STERIODS FOR VARIOUS PERCENTAGES OF METHANOL IN THE MOBILE PHASE

Proportion of methanol (% v/v)	Pregnanolone K_f (M^{-1})	Progesterone K_f (M^{-1})
45	953	347
47	670	240
50	635	261
53	540	216
55	345	165

Our results can be compared with those from a previous determination of the stability of the progesterone- β CD complex in ethanol-water (15:85, v/v) by Kralova and Mitterhauszerova [20]. In this case, the constant calculated from solubility experiments was $700 M^{-1}$. By the HPLC technique, with methanol-water (45:55, v/v) as the mobile phase, we found a value of $347 M^{-1}$.

Indirect detection

As progesterone has a UV molar absorptivity ($\epsilon_{254} = 12\,700$) much greater than that of pregnanolone ($\epsilon_{\max} = \epsilon_{280} = 150$) we used the first steroid as a marker in the eluent in order to detect the injected second one.

Fig. 3 shows an example of chromatographic profile obtained by using a mobile

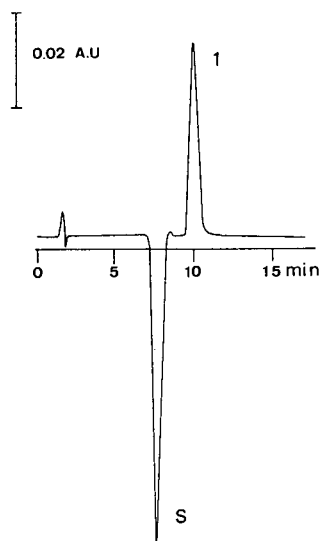


Fig. 3. Chromatographic profile of pregnanolone with progesterone as probe. Mobile phase, methanol-water (47:53, v/v); progesterone concentration, 0.032 mM; β CD concentration 4.9 mM. Peaks: S = system peak; 1 = pregnanolone. Experimental conditions as in Fig. 1, except detection wavelength, 254 nm.

phase containing both β CD (4.9 mM) and progesterone (0.032 mM) and injecting pregnanolone. The first signal (negative) corresponds to the retention time of progesterone obtained in the same eluent without progesterone. The second signal (positive) corresponds to the retention time of pregnanolone in the latter eluent.

We plotted the positive peak area as a function of the injected amount of pregnanolone. Several experiments corresponding to different concentrations of β CD were performed, and gave the calibration curves shown in Fig. 4. It appears that the slope of the calibration lines increases as the β CD concentration increases.

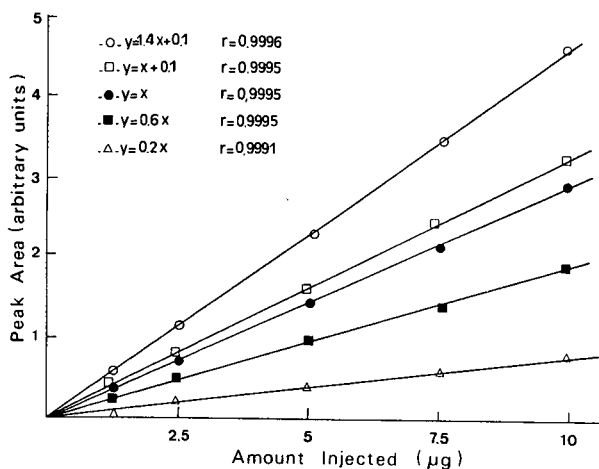


Fig. 4. Calibration curves of pregnanolone at various concentrations of β CD in methanol-water (47:53, v/v) mobile phase with progesterone (0.032 mM) as probe. (Δ) [BCD] = 0 mM; (\blacksquare) [BCD] = 1.23 mM; (\bullet) [BCD] = 2.45 mM; (\square) [BCD] = 3.7 mM; (\circ) [BCD] = 4.9 mM. Experimental conditions as in Fig. 1, except detection wavelength, 254 nm (unless measured at $\lambda_{\max} = 280$ nm). $y = Ax + B$, where A = slope and B = intercept; r = regression coefficient.

The peak area corresponding to the injection of a constant amount of pregnanolone (10 μ g) was measured in the presence of various amounts of β CD in the eluent. The results are shown in Fig. 5. The concentration of β CD is limited by its solubility in the eluent: under the present experimental conditions (methanol-water 47:53 v/v), its maximum solubility is *ca.* 5 mM.

We also studied the influence of methanol content in mobile phase at a constant β CD concentration of 4.9 mM. Fig. 6 shows the results obtained: the slope of calibration curves is greatest for the lowest concentration of methanol. Owing to the limited solubility of progesterone in the eluent, a 47% concentration of methanol is the minimum value for a complete solubilization of this compound.

As previously stated, the indirect detection of a solute gives a maximum response when the capacity factors of the solute and the probe are similar (6–12). In this case, increasing concentrations of β CD in the eluent decrease the separation factor α , defined as the ratio of the capacity factors of pregnanolone and progesterone. The same effect is observed as the methanol concentration in the eluent is decreased. These two effects contribute to an enhancement of pregnanolone detection.

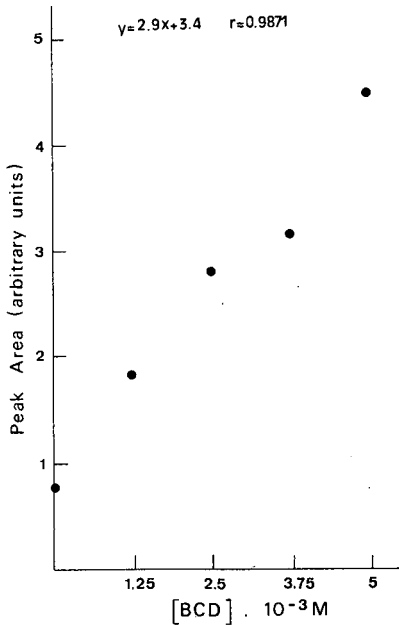


Fig. 5. Peak area of pregnanolone ($10 \mu\text{g}$) plotted versus the concentrations of βCD in methanol-water (47:53, v/v) mobile phase with progesterone (0.032 mM) as probe. Experimental conditions as in Fig. 4.

For example, α varies from 1.47 to 1.37, these values corresponding respectively to 3.7 and 4.9 mM βCD in the mobile phase methanol-water (53:47, v/v). With 3.7 mM βCD , α varies from 1.36 to 1.47 when the proportion of methanol is increased from 47% to 53% (v/v).

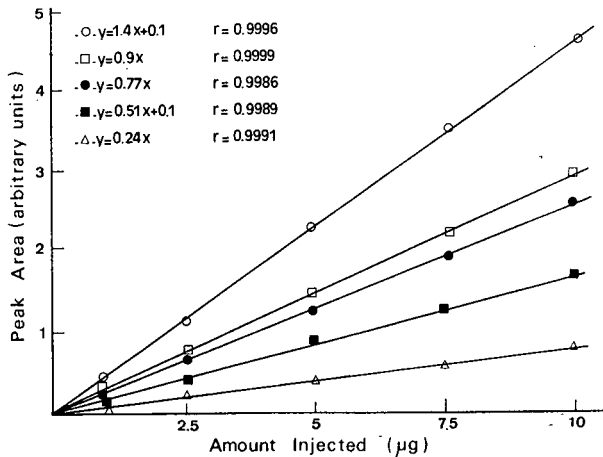


Fig. 6. Calibration curves of pregnanolone at various concentrations of methanol in the mobile phase containing 4.9 mM of βCD : (\triangle) see Fig. 4; (\circ) $[\text{CH}_3\text{OH}] = 47\%$; (\square) $[\text{CH}_3\text{OH}] = 50\%$; (\bullet) $[\text{CH}_3\text{OH}] = 53\%$; (\blacksquare) $[\text{CH}_3\text{OH}] = 55\%$. Experimental conditions as in Fig. 4.

In order to verify this property, we studied the variation of the apparent molar absorptivity as a function of α . The apparent molar absorptivity, ϵ^* , was defined by Hackzell and Schill [6] with the following equation:

$$\epsilon^* = \frac{ysu}{mdb}$$

where y is the sample peak area, s is the detector setting range, u is the flow-rate, m is the amount of compound injected, d is the chart speed and b is the path length of the detector cell. Fig. 7 shows a plot of $\log \epsilon^*$ against $\log \alpha$. The detection response is at a maximum when α is close to the unity.

The eluent composition must be chosen so that the chromatographic resolution of the two steroids is complete, in order to obtain reliable quantitative measurements. Thus, a minimum value of $(\alpha - 1)$ is necessary for indirect detection measurement.

The maximum absorption in the UV spectrum of pregnanolone is at 280 nm in ethanolic solution. We measured the value of ϵ^{**} at this wavelength using an eluent without a probe (progesterone), and found a value of $\epsilon^{**} = 150$. For comparison, at 254 nm the ϵ^{**} value of pregnanolone is 47.

Using indirect detection in the conditions described above, and at a wavelength of 254 nm, the ϵ^* value can reach 915, that is to say a six-fold enhancement for $\epsilon_{254}^*/\epsilon_{280}^{**}$ and a 20-fold enhancement for $\epsilon_{254}^*/\epsilon_{254}^{**}$.

In contrast to other cases of indirect detection of uncharged compounds, in which the system peak appears first as a negative peak, and the solute peak emerges later as a negative peak [7,9,11], we observed a negative system peak followed by a positive sample peak on the C_4 column. This suggests that the injected pregnanolone displaces the progesterone complexed by the β CD in the mobile phase owing to the higher apparent association constant of pregnanolone- β CD mentioned above. So the

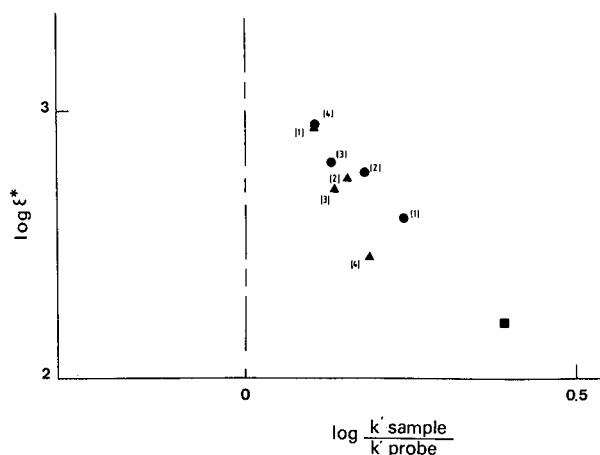


Fig. 7. Influence of the steroid capacity factor ratio on the detection sensitivity: (■) $[\text{CH}_3\text{OH}] = 47\%$; (●) $[\text{CH}_3\text{OH}] = 57\%$ at various concentrations of β CD in the mobile phase: (1) 1.23 mM; (2) 2.45 mM; (3) 3.7 mM; (4) 4.9 mM. (▲) 4.9 mM β CD at various proportions of methanol in the mobile phase: (1) 47%; (2) 50%; (3) 53%; (4) 55%. Experimental conditions as in Fig. 4.

deficit of β CD–progesterone appears as a negative signal, and the positive peak is due to the release of pregnanolone and progesterone.

We compared these results with those obtained in the absence of β CD by selecting a mobile phase composition that gave an α value close to unity. Fig. 8 shows the chromatogram pattern obtained by injecting pregnanolone into the C_4 column and eluted by a mobile phase of methanol–water (72:28, v/v), containing 0.032 mM progesterone. This yielded an α value of 1.5, similar to the best conditions of indirect detection. As in the preceding chromatogram, there is a negative peak at the retention time of progesterone followed by a positive peak corresponding to pregnanolone.

Calculation of the molar apparent absorptivity gives $\epsilon^* = 47$, which is similar to the ϵ^{**} value of pregnanolone at 254 nm measured without progesterone in the eluent. These results are in agreement with the theoretical predictions of Golshan-Shirazi and Guiochon [21] but in this case the indirect detection signal is too weak to permit improved determination of pregnanolone.

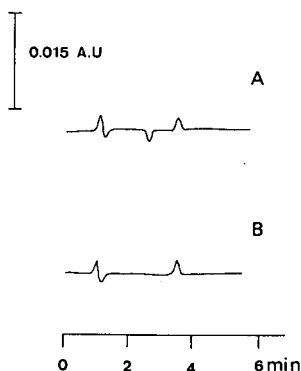


Fig. 8. Chromatographic profiles of pregnanolone without β CD in the mobile phase: (A) methanol–water (72:28, v/v) with progesterone (0.032 mM); (B) methanol–water (72:28, v/v) without progesterone. Experimental conditions as in Fig. 1. Detection wavelength: (A) 254 nm; (B) 280 nm.

Influence of the support on indirect photodetection

We compared the results obtained from the C_4 column with those obtained from a less hydrophobic support, a C_2 column, on which the capacity factors of the two steroids are very similar.

On this type of column, the value of α is 1.18 without β CD and 0.7 with β CD at 4.9 mM. This indicates an inversion of the elution order by β CD. Fig. 9 shows the chromatogram observed following injection of a pregnanolone sample eluted with β CD (4.9 mM) and progesterone (0.032 mM) in the mobile phase. A first signal (positive) appears corresponding to pregnanolone, immediately followed by a second signal (negative) corresponding to the system peak. This procedure permits the detection of pregnanolone with a ten-fold enhancement as compared with simple UV detection at 280 nm. Nevertheless, this is not sufficient (resolution 1.2) to give reliable measurements for quantitation. Several attempts to improve the separation by changing the concentrations of β CD and methanol failed. It must be concluded that the C_2

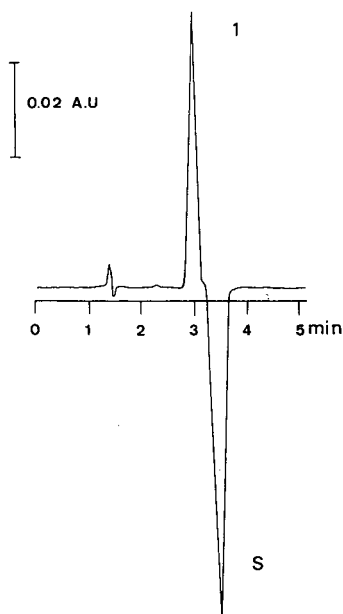


Fig. 9. Chromatographic profile of pregnanolone with progesterone as probe. Mobile phase methanol-water (50:50, v/v) containing 0.032 mM progesterone and 4.9 mM β CD. Peaks: 1 = pregnanolone; S = system peak. Column, C₂ (10 cm \times 4.6 mm I.D.); particle size, 10 μ m, 120 \AA ; flow-rate, 0.8 ml/min; detection wavelength, 254 nm; sample injection, 10 μ g.

column is unable to separate the two steroid compounds with a high enough resolution to achieve a quantitative determination of pregnanolone.

CONCLUSIONS

The formation of inclusion complexes between steroids and β CD modifies their chromatographic properties on reversed-phase column eluted with methanol-water.

Because pregnanolone and progesterone have similar chromatographic properties, the latter was used as a marker in the detection of pregnanolone, which has weak UV absorbance. The detection can be enhanced by the presence of β CD in the eluent. This property, which has previously been observed in the case of alcohols [17], seems to be more general and extends the application of chromatographic indirect detection by the presence in the eluent of an additional compound, such as β CD, that is able to form inclusion complexes with the analyte and probe. Further investigation of this phenomenon is currently being undertaken.

REFERENCES

- 1 C. J. Munro and B. L. Lasley, *Non-Radiometric Assays: Technology and Application in Polypeptide and Steroid Hormone Detection*, Alan R. Liss, New York, 1988, p. 289.
- 2 H. R. Behrman, *Non-Radiometric Assays: Technology and Application in Polypeptide and Steroid Hormone Detection*. Alan R. Liss, New York, 1988, p. 1.

- 3 R. K. Gilpin and L. A. Pachla, *Anal. Chem.*, 61 (1989) 191.
- 4 K. Robards and P. Towers, *Biomed. Chromatogr.*, 4 (1990) 1.
- 5 H. L. J. Makin and E. Heftman, *High Performance Liquid Chromatography of Steroid Hormones*.
- 6 L. Hackzell and G. Schill, *Chromatographia*, 15 (1982) 437.
- 7 P. Herné, M. Renson and J. Crommen, *Chromatographia*, 19 (1984) 274.
- 8 L. Hackzell, T. Rydberg and G. Schill, *J. Chromatogr.*, 282 (1983) 179.
- 9 J. E. Parkin, *J. Chromatogr.*, 287 (1984) 457.
- 10 J. Crommen and P. Herné, *J. Pharm. Biomed. Anal.*, 2 (1984) 241.
- 11 J. E. Parkin and H. T. Lau, *J. Chromatogr.*, 314 (1984) 48.
- 12 J. Crommen, G. Schill, D. Westerlund and L. Hackzell, *Chromatographia*, 24 (1987) 252.
- 13 S. G. Frank and D. R. Kavaliunas, *J. Pharm. Sci.*, 72 (1983) 1215.
- 14 D. W. Armstrong, A. Alak, K. Bui, W. Demond, T. Ward, T. E. Riehl and W. L. Hinze, *J. Inclusion Phenomena*, 2 (1984) 533.
- 15 M. Gazdag, G. Szepesi and L. Huszar, *J. Chromatogr.*, 351 (1986) 128.
- 16 A. Bethod, H. L. Jin, T. E. Beesley, J. D. Duncan and D. W. Armstrong, *J. Pharm. Biomed. Anal.*, 8 (1990) 123.
- 17 M. Gosselet and B. Sebille, *J. Chromatogr.*, 552 (1991) 563–573.
- 18 L. J. Cline Love and M. Arunhyanart, *ACS Symp.*, 297 (1986) 226.
- 19 K. Fujimura, T. Ueda, M. Kitagawa, H. Takayanagi and T. Ando, *Anal. Chem.*, 58 (1986) 2668.
- 20 K. Kralova and L. Mitterhauszerova, *Pharmazie*, 44 (1989) 623.
- 21 S. G. Shirazi and G. Guiochon, *Anal. Chem.*, 62 (1990) 923.

CHROMSYMP. 2345

Use of an evaporative light scattering detector in reversed-phase high-performance liquid chromatography of oligomeric surfactants

Y. MENGERINK, H. C. J. DE MAN and Sj. VAN DER WAL*

DSM Research, P.O. Box 18, 6160 MD Geleen (The Netherlands)

ABSTRACT

The sensitivity of the evaporative light scattering detector was found to be dependent on the analyte concentration and the organic modifier concentration: under reversed-phase gradient conditions calibration is necessary for each analyte. Detection limits for alcohol and carboxylic acid homologues were determined. The advantages of helium over carbon dioxide as a nebulization gas for both volatile and non-volatile or thermolabile analytes are a $>30^{\circ}\text{C}$ lower operating temperature and a five-fold better signal-to-noise ratio. High-resolution separations of polyether alkyl alcohols were effected by reversed-phase gradient high-performance liquid chromatography with ultraviolet transparent mobile phases. Evaporative light scattering detection was compared with refractive index and ultraviolet absorbance detection at 190 nm and found to be superior in signal-to-noise ratio as well as baseline drift. A column-switching system was designed to allow complete compositional analysis of technical samples of ethoxylated alkyl alcohols and their carboxylic acid derivatives.

INTRODUCTION

Sequential evaporation and light scattering detection (ELSD) has been used mainly for triglycerides [1], (phospho)lipids [2], sugars [3] and steroids [4]. Surprisingly little information is available on the use of this technique in the detection of ionogenic oligomeric compounds, although a study of ethoxylated alcohol, alkyl ether sulphate and alkyl sulphonate surfactants has been reported [5].

In chemical manufacturing processes the analysis of oligomeric surfactants could provide very important information in control of the production parameters. For these types of compounds and reaction products reversed-phase high-performance liquid chromatography (HPLC) is the separation method of choice for quantitative analysis. The evaporative light scattering principle would appear ideally suited to these compounds since the essential requirement for this detection technique is a large difference in volatility between solvent and sample.

THEORETICAL

Nebulizer

The mean diameter, D_0 , of the droplets produced by a concentric nebulizer is given by the equation of Nakiyama and Tanasawa (see ref. 6)

$$D_0 = 585 \times \frac{\sqrt{\sigma}}{\Delta u \sqrt{\rho}} + 597 \left(\frac{\eta}{\sqrt{\sigma \cdot \rho}} \right)^{0.45} \left(1000 \frac{F_L}{F_g} \right)^{1.5} \quad (1)$$

where D_0 = mean droplet diameter (μm), σ = surface tension of the eluent (dyne/cm), Δu = linear velocity difference between gas and liquid (m/s), η = viscosity of the eluent (Poise), ρ = density of the eluent (g/ml) and F_L/F_g = eluent/gas flow-rate ratio.

Table I gives some values of D_0 with different eluents. The distribution of the diameter of droplets in the primary aerosol is Gaussian or asymmetrical log-normal [7].

Drift tube

At least three processes take place in the drift tube [8].

- (1) Evaporation of the volatile parts of the aerosol.
- (2) Precipitation on the wall of the tube.
- (3) Coagulation of aerosol droplets.

The time necessary to evaporate the eluent (t_{d_0}) can be calculated using Charlesworth's [6] equation

$$t_d = \frac{2 \Delta H_v \rho D_0^2}{M k_f \Delta T} \quad (2)$$

where t_d = time required for complete evaporation, $\Delta H_v/M$ = molar volatility (proportional to the temperature at which 1 mmHg vapor pressure is reached), ΔT = temperature difference between the nebulization gas and the surface temperature of the droplet and k_f = thermal conductivity of the gas film surrounding the droplets. A decrease in response is expected above a certain temperature since the analyte (x) will evaporate in addition to the eluent (o) and an optimum is obtained at $t_{d_0} < t_d < t_{d_x}$.

The thermal conductivity close to the aerosol droplets is dependent upon the gas used. Each nebulizer gas will have a different set of optimum parameters with respect to the nebulizer, drift tube size, gas flow and temperature for each combination of

TABLE I
MEAN DROPLET DIAMETER IN THE AEROSOL

$\Delta u = 480$ m/s; gas flow nebulizer, 7.1 l/min; eluent flow-rate, 1.0 ml/min.

Eluent	η (cP)	ρ (g/ml)	σ (dyne/cm)	D_0 (μm)
Acetonitrile	0.32	0.78	29	8.6
Methanol	0.52	0.79	22.6	8.1
Water	1.00	1.00	73.0	11.9

sample, eluent and eluent flow. To minimize losses from precipitation on the wall, t_d is chosen to be slightly larger than t_{d_0} .

Coagulation increases with F_L/F_g .

Light scattering cell

Without precipitation and coagulation the average diameter, d , of the aerosol droplets in the light scattering cell is proportional to the analyte concentration, c , in the eluent [7]

$$d \sim D_0 \left(\frac{c}{\rho_a} \right)^{1/3} \quad (3)$$

where ρ_a = density of the analyte. With a concentric nebulizer and an analyte concentration of 1 ppm, the lower limit of Mie scattering ($\lambda/20 < d < 2\lambda$) is reached.

The intensity of scattered light, I , can generally be expressed by [9]

$$I = kN d^2 \left(\frac{d}{\lambda} \right)^y$$

in which k is a constant, N is the number of particles in the scattering volume and y decreases from 4.0 (Rayleigh scattering) to -2.2 with increasing d/λ ratio. Thus at constant λ and N the intensity of scattering increases with d^p ($p < 6$) so, according to eqn. 3 with c^q ($q < 2$):

Decreasing the gas flow-rate increases D_0 and coagulation should enhance the response even further.

An optimum is reached when the minimum gas flow approaches $t_d = t_{d_0}$.

At $d \geq 2\lambda$ refractive index and reflection effects become important [6] and diminish the sensitivity so that the total response curve is sigmoidal.

The effect of the type of eluent on the response is complex and no simple relation has been demonstrated [8].

Calibration curve and detection limit

At lower concentrations the log-log plot of analyte concentration *versus* response is predominantly linear. The detection limit can be determined by

$$m_{\text{LOD}} = \left(\frac{2 x N}{H} \right)^{1/x} m \quad (4)$$

where m_{LOD} = detection limit (g), m = injected mass of analyte (g), N/H = ratio of the noise to the peak height and x = slope of the calibration curve.

EXPERIMENTAL

A Gilson modular gradient pumping system (Villiers-le-Bel, France) was used for HPLC in several configurations.

Gilson 231/401 or Marathon (Spark, Emmen, The Netherlands) autosamplers

were employed to introduce samples onto 250 × 4 mm I.D. or 100 × 4 mm I.D. Nucleosil 120-5C₁₈ reversed-phase columns (Macherey-Nagel, Düren, Germany).

The ELSD tested was the Varex Mark II (Varex, Rockville, MD, U.S.A.). UV absorbance detection was performed with an HP 1040 diode array detector (Hewlett-Packard, Waldbronn, Germany) and refractive index (RI) detection with an HP 79877A refractometer (Hewlett-Packard) thermostatted at 35°C. Water was Milli-Q quality (Millipore, Bedford, MA, U.S.A.) and LiChrosolv acetonitrile was obtained from Merck (Darmstadt, Germany).

The technical surfactant samples were a gift from Chem-Y (Emmerich, Germany) and consisted of mainly (A1) C₁₂H₂₅-O-(C₂H₄O)_n-CH₂-COOH, (A2) C₁₄H₂₉-O-(C₂H₄O)_n-CH₂-COOH, (A3) C₁₂H₂₅-O-(C₂H₄O)_n-H and/or (A4) C₁₄H₂₉-O-(C₂H₄O)_n-H, in which *n* ranges from 0 to approximately 25.

RESULTS AND DISCUSSION

Calibration curves under reversed-phase gradient conditions

From neat organic solvent experiments it is known that the sensitivity of the ELSD can be mobile phase- (ref. 1 *versus* refs. 4 and 8) and concentration- (ref. 5 *versus* refs. 4 and 6) dependent. We investigated the extent to which the dependence of sensitivity during reversed-phase gradients of water to acetonitrile [4] might complicate quantitation.

The temperature and nebulizer gas flow-rate producing maximum response of the ELSD varied with acetonitrile concentration such that at higher acetonitrile concentration an optimum was obtained at lower temperature. However, it was found that under operating conditions this effect was completely obscured by the dependence of the sensitivity on the analyte concentration.

Fig. 1A gives the sensitivity normalized to that for 75% acetonitrile for differing amounts of a non-volatile test compound: glucose. This figure demonstrates that the interdependence of sensitivity, acetonitrile concentration and analyte concentration necessitates the use of calibration curves for analytes under the exact gradient conditions used and that the combined effects could create an illusion of excessive compound dependency [4,10]. At low analyte concentrations the sensitivity difference could be explained by the dependence of the mean particle diameter on the eluent (eqn. 1), water giving larger droplets than acetonitrile (Table I) and thus a larger sensitivity (eqn. 3). The reversal at high analyte concentrations could mean that the temperature and gas flow are suboptimal in this case (see Fig. 1B).

The obligatory use of calibration curves for quantitation of each analyte under the exact analytical conditions is in our opinion a major drawback of this type of detector: quantitation without standards is not possible.

Detection limits for alcohols and carboxylic acids

Detection limits with the ELSD are usually given for long-carbon-chain fatty alcohols and acids, these being economically important classes of compounds, the detection limits of which are less than a microgram. We explored the use of the ELSD in the detection of smaller carboxylic acids and alcohols. Table II shows a clear inverse trend, relating the temperature where the analyte has a vapor pressure of 1 mmHg (or molecular weight) to the detection limit (as defined in eqn. 4). Also the slope of the

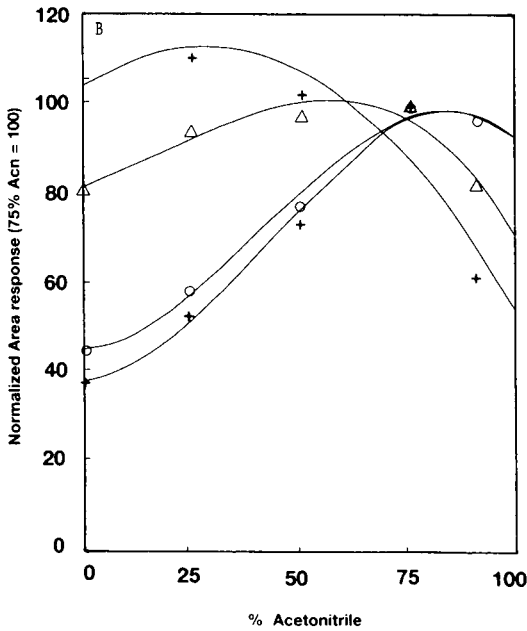
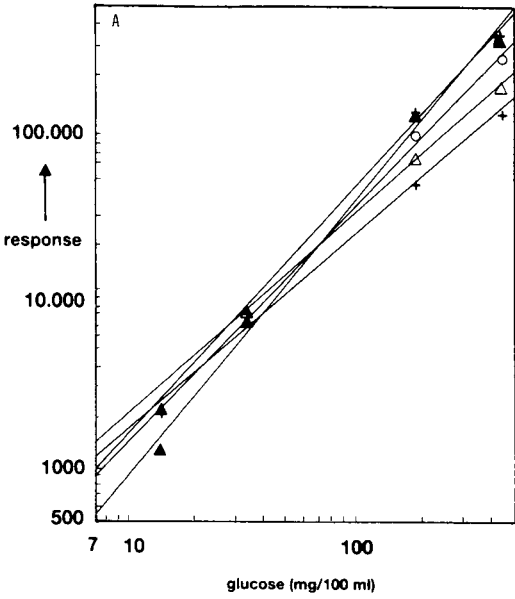


Fig. 1. Dependence of the ELSD response to glucose on the acetonitrile concentration in the eluent. Nebulizer temperature: 125°C. Gas (helium) flow-rate: 7.1 l/min. (A) +, 0%; Δ , 25%; \circ , 50%; +, 75%; Δ , 90% acetonitrile. (B) +, 13.9; Δ , 32.4; \circ , 181; +, 439 mg/ml glucose.

TABLE II
CALIBRATION AND PHYSICAL DATA OF CARBOXYLIC ACIDS AND ALCOHOLS

Compound	Limit of detection (μg)	Slope of calibration curve	Temperature for 1 mmHg vapor pressure ($^{\circ}\text{C}$)	MW
$\text{C}_{17}\text{H}_{35}\text{COOH}$	0.48	1.18	173.7	284.5
$\text{C}_{13}\text{H}_{27}\text{COOH}$	1.20	1.58	142.0	228.4
$\text{C}_{11}\text{H}_{23}\text{COOH}$	1.96	1.73	121.0	200.3
$\text{C}_8\text{H}_{17}\text{COOH}$	8.75	1.94	108.2	158.2
$\text{C}_7\text{H}_{15}\text{COOH}$	19.5	1.94	92.3	144.2
$\text{C}_{18}\text{H}_{37}\text{OH}$	0.90	1.48	150.3	270.5
$\text{C}_{16}\text{H}_{33}\text{OH}$	1.13	1.52	122.7	242.5
$\text{C}_{12}\text{H}_{25}\text{OH}$	3.81	1.62	91.0	186.3
$\text{C}_{10}\text{H}_{21}\text{OH}$	21.1	1.67	69.5	158.3

calibration curve is increased with more volatile compounds. The sensitivity, however, never approached that of the C_{18} analyte. This is all consistent with less prominent evaporation of larger droplets after removal of the solvent.

Helium as a nebulizer gas

In an attempt to improve detection limits for more volatile, polar and thermolabile compounds, helium was studied as a nebulizer gas. At similar gas velocities the five-fold larger thermal conductivity of helium relative to air, nitrogen or carbon dioxide allowed a lower vaporization temperature (at 1 ml/min water *ca.* 25°C lower, see Fig. 2A), thus enabling more volatile analytes like glutaric acid ($T_{1 \text{ mmHg}} = 155.5^{\circ}\text{C}$) to be analysed (see Fig. 3A and B).

Increasing the nebulizer gas flow to a maximum of 20 l/min helium at 10 atm for this brand of instrument decreased the droplet size of the aerosol and therefore the response. However, the lower temperature range limit was extended by a further 15°C .

Depending on the volatility of the analytes, the helium flow-rate on this detector could be adjusted to 20 l/min and the optimum temperature thus determined. Non-volatile analytes had to be measured at the lowest possible nebulizer gas flow ($> t_{d_0}$) at the highest temperature permitted by the analyte. At equal flows helium gives a much larger response for a non-volatile analyte than carbon dioxide (see Fig. 2B).

The optimum for carbon dioxide was found to be at a much lower gas flow-rate than shown in Fig. 2, but not as low as the helium flow, so that the carbon dioxide response never approached the maximum response with helium.

Ethoxylated alkyl alcohols and carboxylic acid derivatives

A comparison of ELSD with UV and RI detection for ethoxylated alkyl alcohols A3 and A4 (see Experimental section) is shown in Fig. 4A, B and C. The signal-to-noise ratio in UV and RI detection was found to be inferior to that with the ELSD. Moreover the larger baseline drift at 190 nm made UV detection difficult so the gradient had to be adapted and sensitive RI detection was rendered impossible, so that Fig. 4C had to be made with an isocratic eluent.

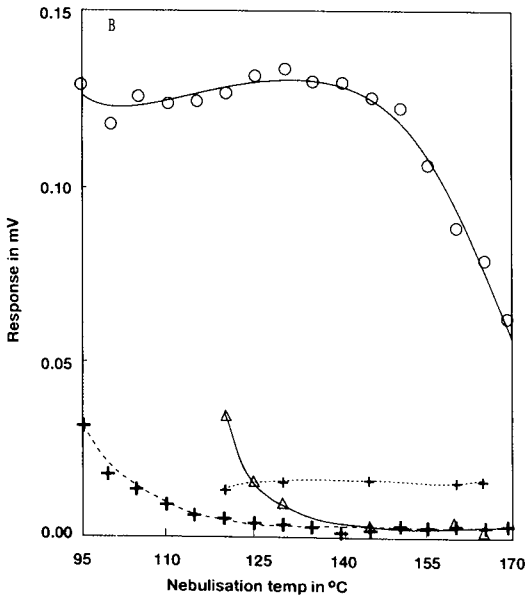
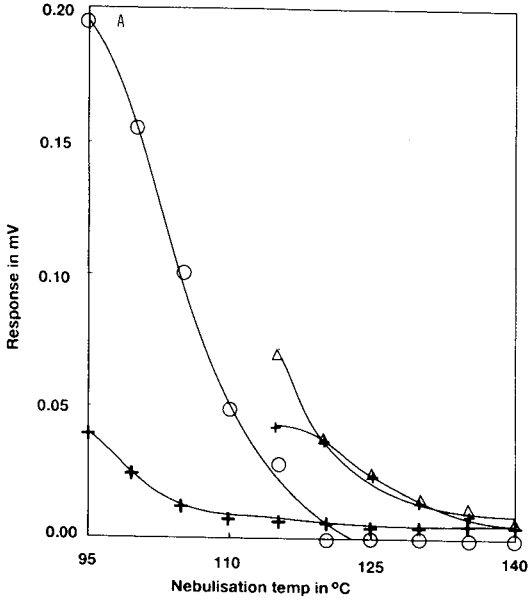


Fig. 2. Variation of the response and noise of the ELSD with temperature for carbon dioxide and helium. Nebulization gas flow-rate: 6.4 l/min. +, Signal carbon dioxide; Δ , noise carbon dioxide; \circ , signal helium; +, noise helium. (A) Glutaric acid. (B) Glucose.

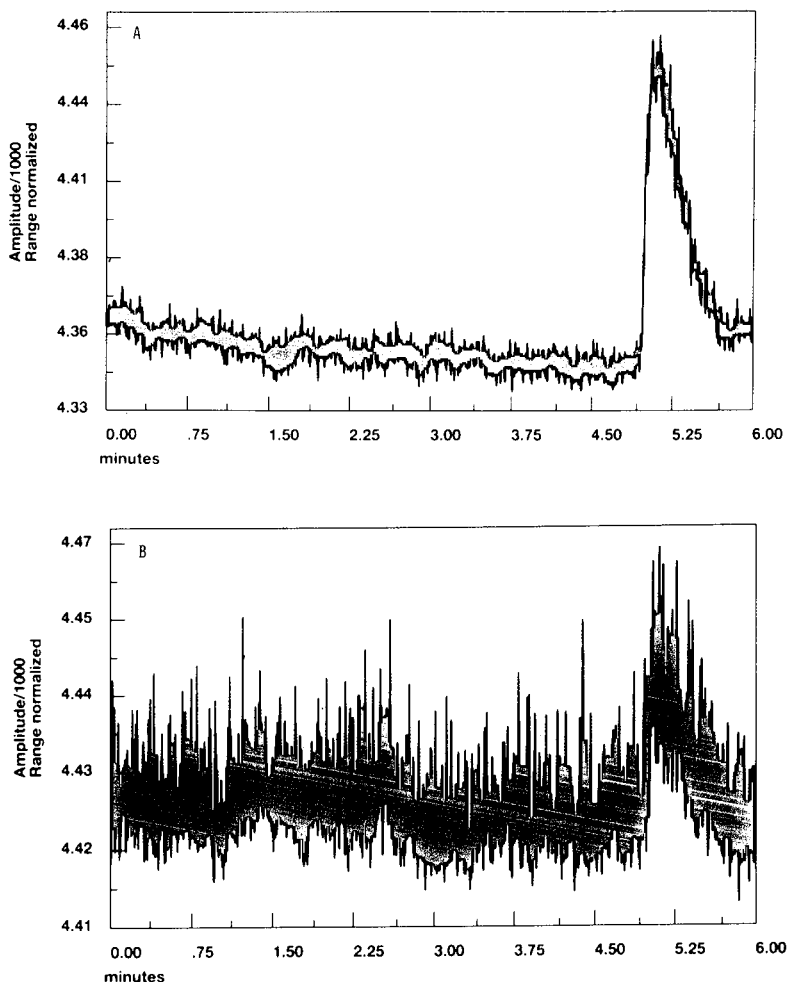


Fig. 3. Comparison of carbon dioxide and helium as a nebulization gas for glutaric acid. Column: 100×4 mm Nucleosil 120-5C₁₈. Mobile phase: 0.1% aqueous acetic acid. Flow-rate: 1.0 ml/min. Injection: 20 μ l containing 90 μ g glutaric acid. (A) $T_{\text{neb}} = 105^\circ\text{C}$, 6.4 l/min helium. (B) $T_{\text{neb}} = 125^\circ\text{C}$, 6.4 l/min carbon dioxide.

The ELSD provided a reasonably predictable but non-equivalent response of a series of oligomers with reversed-phase eluent, in contrast to that found with organic solvents [5].

Fig. 5A and B show the maximum response for the most abundant oligomer to be at $\geq 150^\circ\text{C}$. However, the volatility of the dodecyl triethoxylate oligomer was limited to an operational temperature of 80°C , where accurate compositional analysis [coefficient of variation (C.V.) = 2.8% ($n = 13$), C.V. = 3.6% ($n = 7$)] was afforded. A complete analysis of technical samples containing mixtures of both the ethoxylated alkyl alcohols and their carboxylic acid derivatives would prove useful for detailed reaction modification studies.

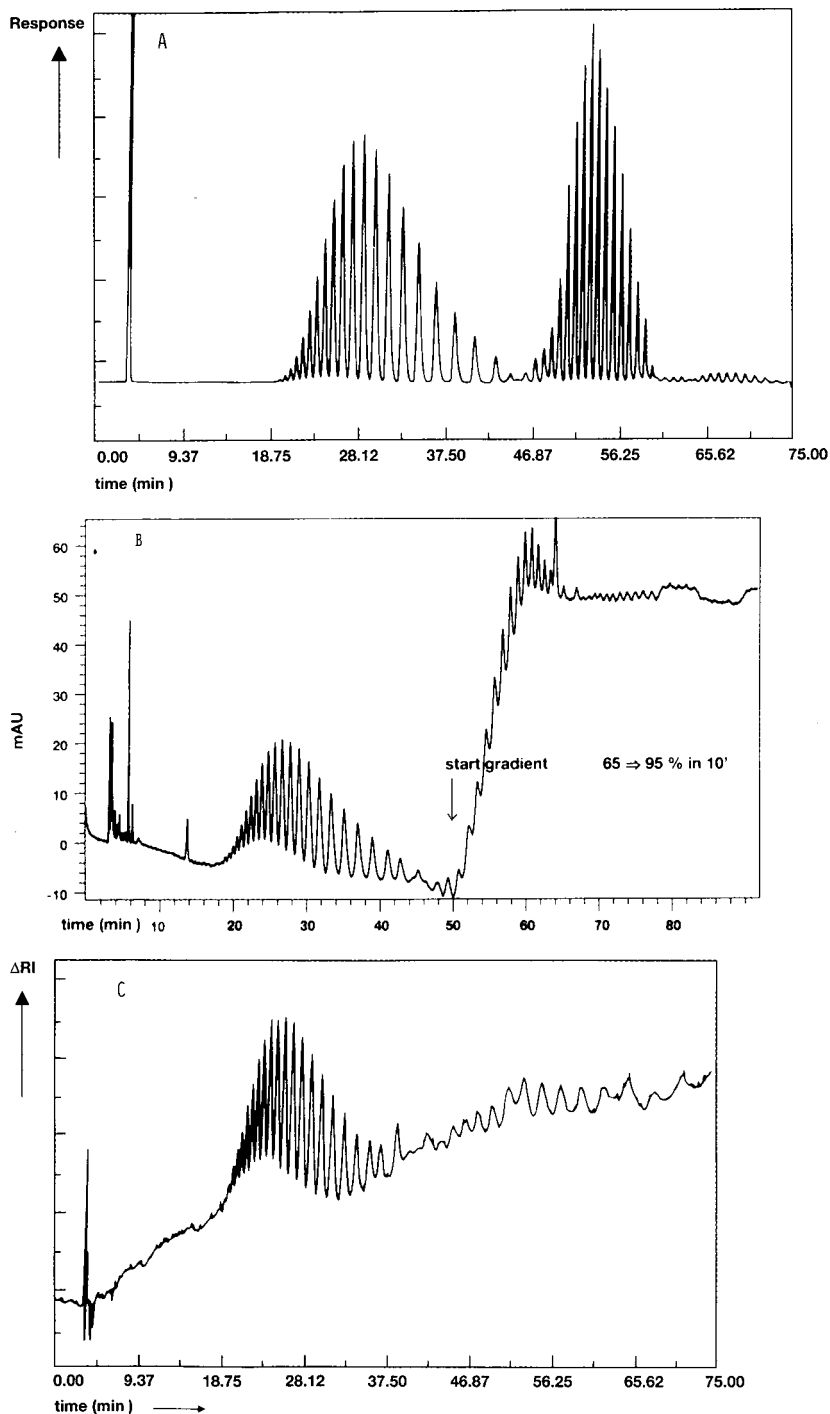


Fig. 4. Comparison of ELSD (A), 190-nm UV (B) and RI (C) detection techniques for alkylethoxylates A3 and A4. Column: $2 \times (250 \times 4 \text{ mm I.D.})$ Nucleosil 120-5C₁₈. Eluent: (A) 0.1% aqueous acetic acid; (B) acetonitrile. Gradient: 65% acetonitrile for 38 min then 90% acetonitrile for 10 min; at 75 min back to 65% acetonitrile for 1 min. Flow-rate: 1.0 ml/min. Injection: 20 μ l containing 1.2 mg sample. (A) $T_{\text{neb}} = 100^\circ\text{C}$, 2.9 l/min carbon dioxide. (B) $\lambda = 190 \text{ nm}$ (4 mm band width), $\lambda_{\text{ref}} = 500 \text{ nm}$ (100 nm, band width). (C) Isocratic separation at 65% acetonitrile, detector sensitivity setting 8.

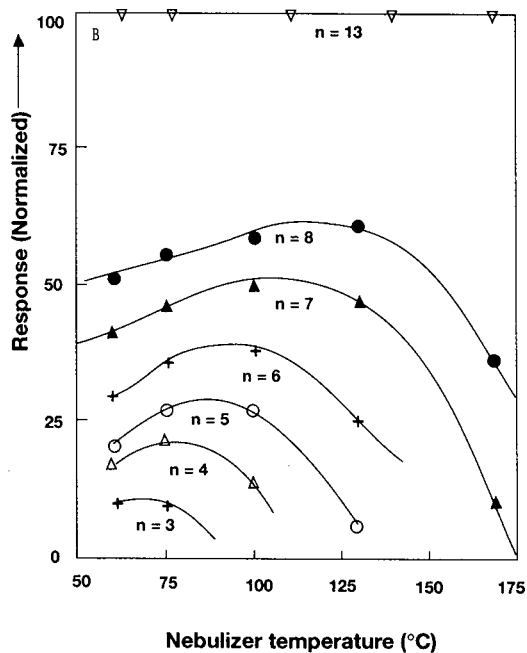
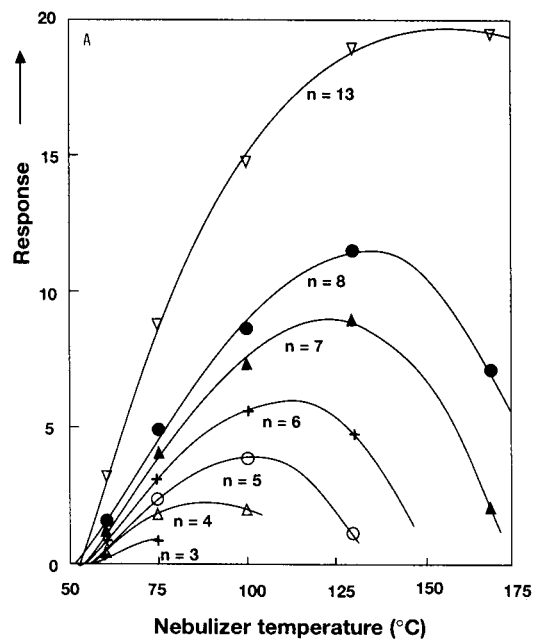


Fig. 5. Response of polyethylene glycol monododecyl ether surfactant homologues (A3) as a function of nebulizer temperature. For chromatographic conditions, see Fig. 4A. Helium flow-rate: optimized. (A) Absolute response. (B) Response normalized to that of tridecaethoxylated dodecanol.

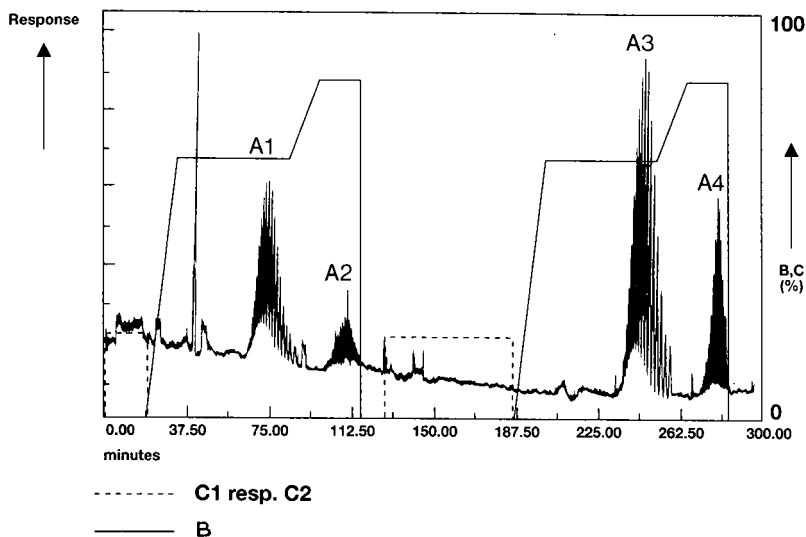


Fig. 6. Separation of the ethoxylated alkyl alcohols (A3 and A4) and their carboxylic acid derivatives (A1 and A2) by automated column-switching HPLC. Sample size: 1.2 mg. Trapping column: 100×4 mm I.D. Nucleosil 120-5C₁₈. Separation columns: one 50×4 mm I.D. plus two (250×4 mm I.D.) Nucleosil 120-5C₁₈. Mobile phases: (A) 1% formic acid in water; (B) acetonitrile; (C1) 65% acetonitrile, 35% 50 mM ammonium bicarbonate; (C2) 82% acetonitrile, 18% 50 mM ammonium bicarbonate. Total mobile phase flow-rate: 1.0 ml/min. The trapping column is only eluted with mobile phase C; mobile phases A and B are introduced between the exit of the trapping column and the 4-ml mixing coil. Detector settings: nebulizer temperature 100°C; nebulizer gas flow 18.4 l/min helium.

Unfortunately, however, these compounds coelute under ion suppression (*e.g.*, pH 2.3) conditions. At neutral pH the alcohols displayed asymmetric peaks. Consequently a decreasing pH and increasing organic modifier gradient would also appear futile.

The desired result was provided by column switching, effectively trapping the alcohol derivatives in a 100×4 mm I.D. first column, at neutral pH and low organic modifier concentration, and allowing the separation of the carboxylic acids on a second column set.

Since the separation of the alcohols was not started before completion of the carboxylic acid separation, a total time of about 5 h was required and was consequently performed automatically (see Fig. 6).

Fig. 6 shows the separation of the ethoxylated alkyl alcohols (A3 and A4) and their carboxylic acid derivatives (A1 and A2). The carboxylic acid derivatives were separated first, the separation being complete in 2 h. After column switching the separation of the ethoxylated alkyl alcohols could be performed and was also completed in 2 h.

Each peak cluster represents a distribution of ethoxylated derivatives of one type of hydrophobic moiety (*e.g.*, C₁₂H₂₅-O-), and each peak within the peak cluster reflects oligomers of differing degrees of ethoxylation.

In order to alleviate the stringent demands of this high-resolution separation on the extra, second column set, peak broadening, the sample fraction eluting from the

first column was further diluted in a 4-ml mixing coil—determined to be the minimum volume— with low-pH acetonitrile-free mobile phase.

This concentration by dilution may only be applied when the increase in capacity factor (k') on the second column set is much larger than the dilution factor—the pH and modifier change for the carboxylic acid derivatives was found to be more effective than just the modifier jump for the alcohols.

ACKNOWLEDGEMENT

The authors thank Mr. R. Green for his invaluable support in the writing of this paper.

REFERENCES

- 1 A. Stolyhwo, H. Colin and G. Guiochon, *Anal. Chem.*, 57 (1985) 1342.
- 2 N. Sotirhos, C. Thörngren and B. Herslöf, *J. Chromatogr.*, 331 (1985) 313.
- 3 R. Macrae and J. Dick, *J. Chromatogr.*, 210 (1981) 138.
- 4 P. A. Asmus and J. B. Landis, *J. Chromatogr.*, 316 (1984) 461.
- 5 G. R. Bear, *J. Chromatogr.*, 459 (1988) 91.
- 6 J. M. Charlesworth, *Anal. Chem.*, 50 (1978) 1414.
- 7 L. E. Oppenheimer and T. H. Mourey, *J. Chromatogr.*, 323 (1985) 297.
- 8 M. Righezza and G. Guiochon, *J. Liq. Chromatogr.*, 11 (1988) 1967.
- 9 S. N. Timasheff, *J. Colloid Sci.*, 21 (1966) 489.
- 10 S. Coulombe, *J. Chromatogr. Sci.*, 26 (1988) 1.

Selection of buffers and of an ion-pairing agent for thermospray liquid chromatographic–mass spectrometric analysis of ionic compounds

A. L. L. DUCHATEAU*, B. H. M. MUNSTERS, G. T. C. KWAKKENBOS and R. G. J. VAN LEUKEN

DSM Research, P.O. Box 18, 6160 MD Geleen (The Netherlands)

ABSTRACT

The applicability of ammonium formate, ammonium acetate and ammonium bicarbonate as volatile electrolytes for thermospray liquid chromatographic–mass spectrometric analysis of three decomposition products of α -aspartame is demonstrated. With these buffers, the pH range of the mobile phases for silica-based reversed-phase columns can be covered. With respect to the buffer capacity and ultraviolet transparency, a buffer salt concentration of 50 mM was used in the mobile phase. The retention times of the compounds studied in the volatile buffers were compared with those obtained in sodium acetate and sodium phosphate buffers and were found to match quite well. For the reversed-phase ion-pair separation of α -aspartame and β -aspartame in combination with thermospray mass spectrometry, a method is described using trifluoroacetate as pairing ion. Liquid chromatographic–mass spectrometric analysis of L-aspartyl-L-phenylalanine shows that the highest signal-to-noise ratio is obtained in ammonium formate. For the compounds studied, no correlation could be found between the signal-to-noise ratio and source temperature, or between signal-to-noise ratio and vaporizer temperature.

INTRODUCTION

Reversed-phase high-performance liquid chromatography (RP-HPLC) is a powerful technique for the separation of both neutral and ionic compounds. Mobile phase additives, such as buffers and ion-pairing agents, are frequently used in the daily practice of this technique.

For thermospray liquid chromatography–mass spectrometry (LC–TSP-MS), however, the non-volatile inorganic buffer salts and ion-pairing agents are detrimental to the MS. By means of post-column suppressor techniques [1,2], it has been shown that certain non-volatile substances may be removed before entering the MS system. Another approach is the replacement of the non-volatile additives in the mobile phase by volatile ones.

Some papers related to the selection of such solvent systems have been presented. Voyksner and Haney [3] evaluated the use of formate, acetate, carbonate and bicarbonate as their ammonium salts for LC–TSP-MS. A comparison between the use

of acetate and formate buffer was also made by Barceló [4]. For the LC-TSP-MS analysis of sulphonated surfactants, ammonium acetate was used both as a volatile buffer and as an ion-pairing agent [5].

Patthy and Gyenge [6] reported the use of trifluoroacetate (TFA) and heptafluorobutyrate as pairing ions for the RP ion-pair separation of monoamine transmitters. In their study, amperometric detection was used. Their conclusion was that short-chain perfluorinated carboxylic acids are a very attractive alternative to alkylsulphonates for the separation of the monoamines studied.

In the above-mentioned studies [3–5], the choice of volatile buffers was mainly related to the MS performance. However, important chromatographic aspects such as buffer capacity and selectivity of volatile buffers in relation to non-volatile buffers were not described.

Another important aspect is the selection of volatile buffers which can be used in combination with both MS and UV detection. In this way chromatographic optimization of the sample compound can be performed by HPLC-UV, meanwhile relieving the MS system. After optimization, HPLC-MS can be applied for identification.

The aim of our work was: (a) to select a set of volatile buffers to cover the entire pH range of silica-based RP material; (b) to investigate the effect on the capacity factor of changeover from a non-volatile buffer to a volatile one; and (c) to select a volatile ion-pairing agent suitable for the LC-TSP-MS analysis of carboxylic compounds.

For this, we chose volatile buffer solutions consisting of formate, acetate and bicarbonate. Ammonia was used as the cationic part of the buffers. The following chromatographic aspects were investigated: concentration of the volatile buffer in relation to UV response and buffer capacity, and comparison of the retention behaviour of ionic compounds in volatile buffers and in non-volatile ones.

With respect to the MS, the effects of the buffer choice on signal-to-noise ratio and spectral characteristics were evaluated. The test compounds used in this study were three decomposition products of the α -dipeptide sweetener aspartame: L-aspartyl-L-phenylalanine (AP), L-phenylalanine (Phe) and 5-benzyl-3,6-dioxo-2-piperazine acetic acid (DKP). For ion-pair LC-TSP-MS, we describe the use of TFA for the separation of α -aspartame (α -APM) and β -aspartame (β -APM).

EXPERIMENTAL

Instrumentation

The chromatographic system consisted of a Gilson (Villiers-le-Bel, France) Model 302 pump, a Rheodyne (Cotati, CA, U.S.A.) Model 7010 injection valve with a 20- μ l loop and a Waters Assoc. (Milford, MA, U.S.A.) Model 481 UV detector for detection at 220 nm. The columns used were Nucleosil 120-C₁₈ (250 \times 4.0 mm I.D., 5 μ m, and 50 \times 4.0 mm I.D., 5 μ m, for the TFA experiment) from Macherey, Nagel (Düren, Germany). The flow-rate was 1 ml/min and the separations were carried out at ambient temperature.

Post-column addition of buffer solution was effected with a Gilson Model 302 pump. The flow-rate was 0.5 ml/min. The solution was added to the column effluent by a Lee (Frankfurt, Germany) visco-jet micromixer. The composition of the solution used for post-column addition was always identical to the composition of the mobile phase.

The MS system consisted of a Finnigan MAT TSQ-70 triple quadrupole mass spectrometer equipped with a thermospray interface (Finnigan MAT, San José, CA, U.S.A.). Trifluoroacetic acid was used for calibration of the mass spectrometer up to 1000 daltons [7]. The ion source temperature and the vaporizer temperature varied, depending on the experiment, and are indicated in the figures. The repeller voltage was kept at 75 V. The electron multiplier was operated at 800 V. Scanning was performed from 110 to 410 daltons with a scan time of 1 s.

Chemicals

α -APM and β -APM were obtained from Tosoh (Nanyo, Japan). AP and DKP were supplied by Bachem (Bubendorf, Switzerland). Phe was obtained from Sigma (St. Louis, MO, U.S.A.). Trifluoroacetic acid was obtained from Janssen (Beerse, Belgium). HPLC-grade acetonitrile was supplied by Merck (Darmstadt, Germany). Water was purified with a Milli-Q system. All other chemicals were of analytical reagent grade.

Buffers

Sodium phosphate buffers (pH 3.0 and 7.0) and the sodium acetate buffer (pH 5.0) were prepared by dissolving the corresponding acids in water and titrating to the required pH with sodium hydroxide solution.

The ammonium bicarbonate buffer was prepared by dissolving the ammonium bicarbonate salt in water and titrating to pH 7.0 with acetic acid. Ammonium formate buffer (pH 3.0) and ammonium acetate buffer (pH 5.0) were prepared by dissolving the corresponding acids in water and titrating to the required pH with ammonia.

The ammonium formate-trifluoroacetate buffer was prepared by dissolving formic acid and trifluoroacetic acid in water and titrating to pH 3.0 with ammonia. The concentration of trifluoroacetic acid was 8 mM.

For all buffers, the final concentration of the acid was 0.05 M. The ammonium bicarbonate buffer consisted of 0.04 M carbonic acid and 0.01 M acetic acid. For chromatography, acetonitrile was added to the buffer solutions. The composition of the mobile phases is indicated in the figures.

RESULTS AND DISCUSSION

Buffer capacity of the volatile buffers

According to the Henderson-Hasselbalch equation, a weak acid and its conjugated base have their maximum buffer capacity at $\text{pH} = \text{p}K_a \pm 1$. For this reason formate ($\text{p}K_a$ 3.75), acetate ($\text{p}K_a$ 4.75) and bicarbonate ($\text{p}K_a$ 6.37) were chosen as volatile buffers for RP-LC-MS. With these three buffers, the pH range of the mobile phases for silica-based RP columns can be covered.

The molar extinction coefficients of formate, acetate and bicarbonate are higher than those of the non-volatile phosphate buffers.

To obtain a comparable UV transparency for the volatile buffers chosen, a decrease in concentration is necessary. Too low a concentration may, however, lead to a situation where the eluent pH varies because of poor buffering. As a consequence, the retention times of the ionizable solutes may vary from one chromatographic run to another. This effect will also depend on the amount of the solute injected.

As we were interested in the low microgram range, the buffer capability at a chosen buffer concentration was experimentally checked. It was found experimentally that an injection of 1 μg of α -APM into a mobile phase consisting of at least 50 mM volatile buffer did not give peak distortion or irreproducible retention times. Therefore a concentration of 50 mM formate, acetate or bicarbonate was chosen in the mobile phase. For this concentration, the capacity (β) of the buffers was calculated according to the following formula [8]

$$\beta = 2.30 \frac{C_A \times C_B}{C_A + C_B} \quad (1)$$

where C_A and C_B are the molar concentrations of the acid chosen and its conjugated base, respectively. By means of the Henderson–Hasselbalch equation, C_A and C_B were calculated for several pH values and substituted into eqn. 1.

The capacity of the ammonium formate, ammonium acetate and ammonium bicarbonate buffers as a function of the pH is shown graphically in Fig. 1. From these curves it can be concluded that, for making a mobile phase with $\text{pH} < 4.2$, ammonium formate is the buffer of choice. For the pH range 4.2–5, both ammonium acetate and ammonium bicarbonate are suitable. For a mobile phase with $\text{pH} > 5$, ammonium bicarbonate is the most appropriate buffer.

Chromatographic selectivity

For the test compounds AP, DKP and Phe, RP separations in combination with UV detection were carried out with the following non-volatile mobile phases: sodium phosphate (pH 3.0)–10% (v/v) acetonitrile, sodium acetate (pH 5.0)–5% (v/v) acetonitrile and sodium phosphate (pH 7.0)–2.5% (v/v) acetonitrile.

To examine the influence on the capacity factor (k') of the test compounds, the non-volatile sodium phosphate buffers (pH 3.0 and 7.0) and sodium acetate buffer were replaced by ammonium formate, ammonium bicarbonate and ammonium acetate. The pH of the volatile mobile phases and the acetonitrile content were kept the same.

The calculated k' values of AP, DKP and Phe in both the non-volatile and volatile solvent systems are given in Table I. From these data it can be seen that the

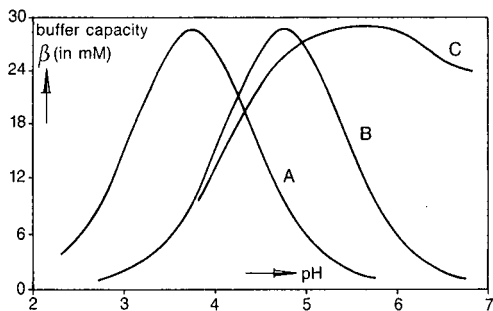


Fig. 1. Buffer capacity (β) as a function of pH. (A) 0.05 M ammonium formate solution; (B) 0.05 M ammonium acetate solution; (C) 0.05 M ammonium bicarbonate solution (pH adjustment with acetic acid).

TABLE I

k' VALUES OF AP, Phe AND DKP AND S/N RATIO OF AP IN VOLATILE AND NON-VOLATILE MOBILE PHASES

Mobile phase ^a	k'			S/N ^b
	Phe	AP	DKP	
I	0.6	1.8	3.2	105
II	0.6	2.0	3.3	11
III	1.1	0.8	2.2	45
IV	1.1	0.8	2.3	45
V	1.9	1.1	2.8	159
VI	1.8	0.9	2.3	120

^a Mobile phases: I = 0.05 M sodium phosphate (pH 3.0)–10% (v/v) acetonitrile; II = 0.05 M ammonium formate (pH 3.0)–10% (v/v) acetonitrile; III = 0.05 M sodium acetate (pH 5.0)–5% (v/v) acetonitrile; IV = 0.05 M ammonium acetate (pH 5.0)–5% (v/v) acetonitrile; V = 0.05 M sodium phosphate (pH 7.0)–2.5% (v/v) acetonitrile; VI = 0.05 M ammonium bicarbonate (pH 7.0)–2.5% (v/v) acetonitrile.

^b S/N ratio of AP at 220 nm (UV detection). The solution injected contains 1.3 μg of AP, 2.3 μg of Phe and 1.9 μg of DKP.

retention times of the compounds match quite well in the non-volatile and the corresponding volatile solvent systems.

For AP, the signal-to-noise (S/N) ratio was calculated in the different mobile phases (Table I). From this table it can be concluded that replacement of the sodium phosphate buffer (pH 7.0) by the ammonium bicarbonate buffer leads to a decrease of the S/N ratio of 25%. On the other hand, changing from sodium acetate to ammonium acetate does not influence the S/N ratio of AP.

The largest decrease of the S/N ratio occurs when replacing the sodium phosphate buffer (pH 3.0) by the ammonium formate buffer. A loss of 90% is observed here.

MS characteristics of the volatile buffers

For Phe and DKP, the quasimolecular ion peaks are the most abundant peaks in the spectra of all three buffer solutions. The most abundant peak in the AP spectrum is the quasimolecular ion for ammonium formate and protonated Phe ($m/z = 166$) for both ammonium acetate and ammonium bicarbonate.

Fragmentation and clustering in the three buffers are alike. However, there are significant differences in relative intensities and in the noise level. The mass spectrum of Phe consists of the peak of the quasimolecular ion $[M + H]^+$ ($m/z = 166$) and the cluster ions $[M + H + \text{CH}_3\text{CN}]^+$ and $[2M + H]^+$ ($m/z = 207$ and $m/z = 331$, respectively). The intensity of the double molecular cluster ion $m/z = 331$ is lower at higher source and vaporizer temperatures.

When source and vaporizer temperatures are increased, more AP molecules thermally decompose into DKP ($m/z = 263$) and Phe ($m/z = 166$). Consequently, the $[M + H]^+$ peak ($m/z = 281$) becomes less abundant.

The mass spectra of DKP give peaks for the ions $[M + H]^+$ and $[M + \text{NH}_4]^+$ ($m/z = 263$ and $m/z = 280$, respectively). Fragmentations were not detected. In the

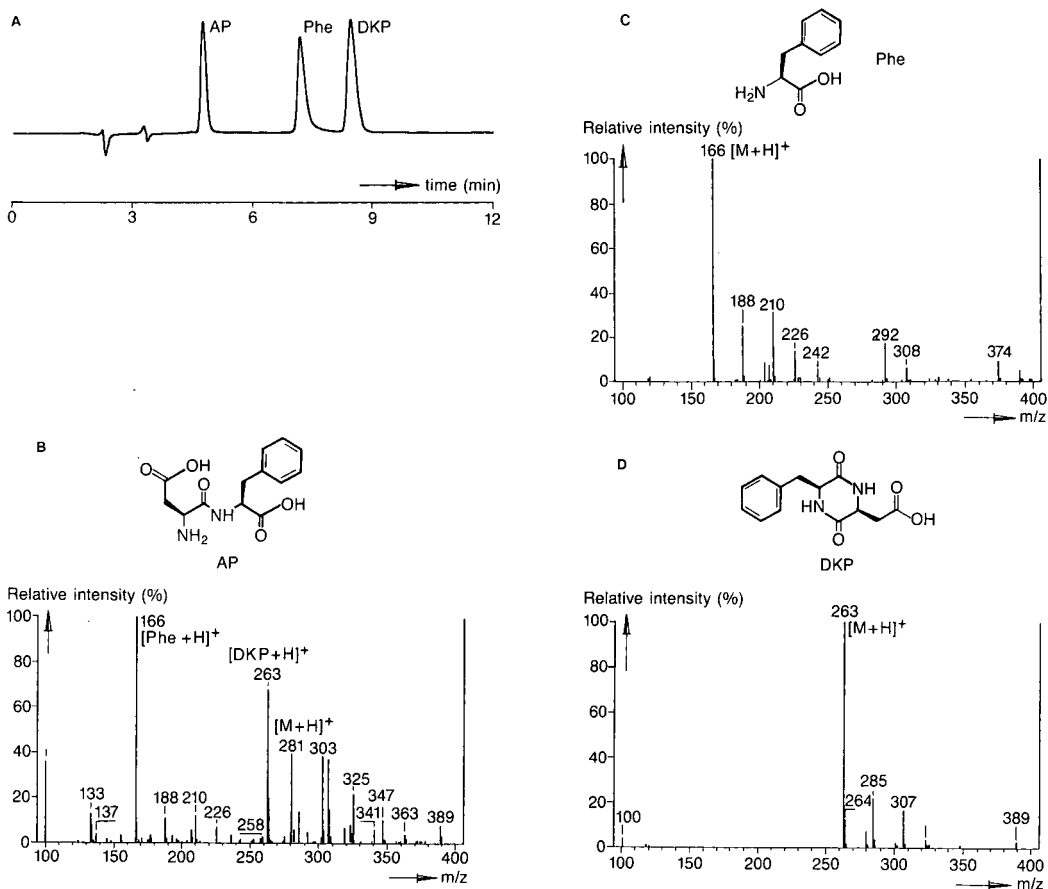


Fig. 2. (A) HPLC profile of a mixture of AP (1.3 μg), Phe (2.3 μg) and DKP (1.9 μg), and (B–D) the corresponding mass spectra. Mobile phase: 0.05 M ammonium bicarbonate (pH 7.0)–2.5% (v/v) acetonitrile.

mass spectra of all three compounds, several sodium and potassium adducts are present, *i.e.*, $[M + 22]^+$, $[M + 38]^+$ and $[M + 60]^+$. Since no sodium or potassium salts of the compounds are used, these ions probably come from the sodium buffer experiments on the HPLC column.

In all spectra, a peak of unknown identity at $[M + 127]^+$ is present.

As an example, the mass spectra of AP, DKP and Phe in ammonium bicarbonate buffer, together with the chromatographic separation, are given in Fig. 2.

For each buffer, maximum sensitivity for AP is obtained at different source and vaporizer temperatures.

The maximum S/N ratio of the quasimolecular ion of AP is found at vaporizer and source temperatures of 110 and 230°C for ammonium formate, 90 and 170°C for ammonium acetate and 110 and 200°C for ammonium bicarbonate, respectively. Ammonium formate gives the highest S/N ratio of the $[M + H]^+$ of AP compared with the other two buffers at their optimum conditions: S/N = 1790 (ammonium formate),

TABLE II

RELATIVE INTENSITIES AND S/N RATIOS OF AP ($m/z = 281$) IN THREE MOBILE PHASES

For mobile phases and concentration of AP, see Table I.

Mobile phase	RI ^a (%)	S/N ^a (%)	S/N
II	100	100	1430
IV	7.3	22	315
VI	1.8	73	1040

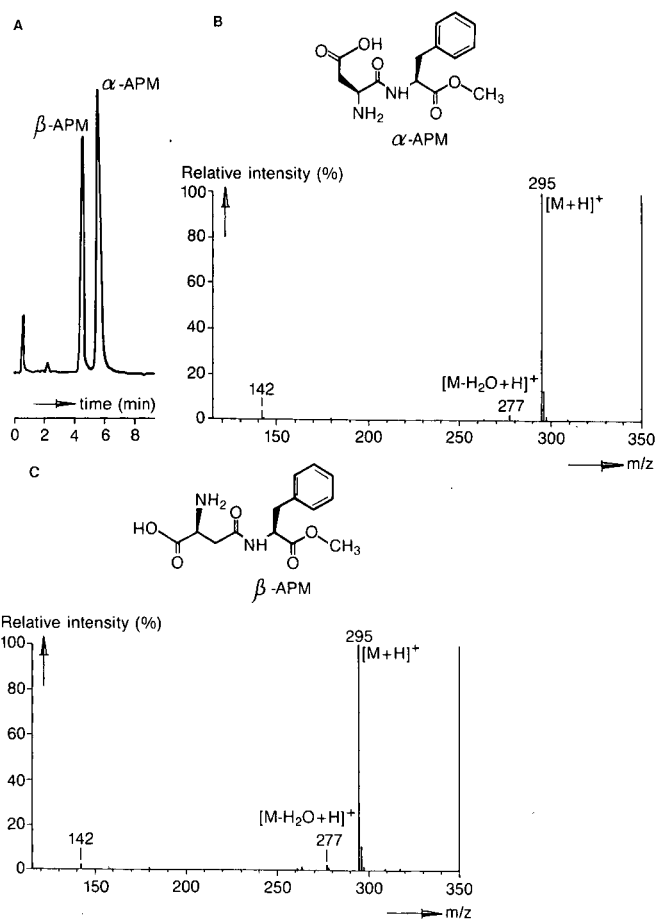
^a Relative to ammonium formate (100%).

Fig. 3. (A) HPLC profile of the separation of α -APM (1.6 μ g) and β -APM (2.2 μ g), and (B and C) the corresponding mass spectra. Mobile phase: 50 mM ammonium formate buffer-8 mM TFA-10% (v/v) acetonitrile.

S/N = 1345 (ammonium acetate) and S/N = 1430 (ammonium bicarbonate) for 1.3 μg of AP.

Table II gives the relative intensity (RI), the S/N ratio and the relative S/N ratio of the quasimolecular ion of AP in the three mobile phases at a vaporizer temperature of 110°C and a source temperature of 200°C. From this table it appears that, depending on the mobile phase used, different values of RI are found. The variation in chemical noise between the various mobile phases is responsible for the difference in S/N ratio.

For the compounds studied, no correlation could be found between the S/N ratio and source temperature, or between S/N ratio and vaporizer temperature.

Choice of an ion-pairing agent for LC-TSP-MS

Several HPLC-UV methods have been described for the separation of α -APM and β -APM. Good resolution and peak shape have been obtained by using alkylsulphonates as ion-pairing agents in the mobile phase [9,10]. For LC-TSP-MS analysis of ionic compounds no volatile ion-pairing agent that can act as a substitute for alkylsulphonates has been reported to our knowledge. We studied the influence of TFA on the separation of α -APM and β -APM. A typical chromatogram is given in Fig. 3. Use of a 50 mM ammonium formate buffer (pH 3.0) and a 50 mM ammonium acetate buffer (pH 5.0), both without the addition of TFA, resulted in a poorer resolution than that obtained in Fig. 3.

The mass spectra of α -APM and β -APM are also shown in Fig. 3. Owing to the low concentration of TFA in the eluent, the background signal of TFA clusters is very low in the mass spectrum, and is in fact eliminated by background subtraction. There are no corresponding mass fragments from TFA and APM, so the detection level of APM is not affected by the addition of TFA.

CONCLUSIONS

With respect to the buffer capacity and chromatographic selectivity, the ammonium salts of formate, acetate and bicarbonate are suitable buffers for the LC-TSP-MS analysis of ionic degradation products of α -APM. For AP as test compound, the largest S/N ratio is obtained with ammonium formate as LC-TSP-MS buffer. Trifluoroacetic acid is a good substitute for alkylsulphonates in the LC-TSP-MS analysis of α -APM and β -APM.

REFERENCES

- 1 R. C. Simpson, C. C. Fenselau, M. R. Hardy, R. R. Townsend, Y. C. Lee and R. J. Cotter, *Anal. Chem.*, 62 (1990) 248.
- 2 J. J. Conboy, J. D. Henion, M. W. Martin and J. A. Zweigenbaum, *Anal. Chem.*, 62 (1990) 800.
- 3 R. D. Voyksner and C. A. Haney, *Anal. Chem.*, 57 (1985) 991.
- 4 D. Barceló, *Org. Mass Spectrom.*, 24 (1989) 219.
- 5 R. E. A. Escott and D. W. Chandler, *J. Chromatogr. Sci.*, 27 (1989) 134.
- 6 M. Patthy and R. Gyenge, *J. Chromatogr.*, 449 (1988) 191.
- 7 S. J. Stout and A. R. daCunha, *Anal. Chem.*, 61 (1989) 2126.
- 8 R. Brodersen, *Z. Vitam. Horm. Fermentforsch.*, 3 (1950) 533.
- 9 J. F. Lawrence and J. R. Iyengar, *J. Chromatogr.*, 404 (1987) 261.
- 10 J. A. Stamp and T. P. Labuza, *J. Food Sci.*, 54 (1989) 1043.

CHROMSYMP. 2268

On-line coupling of liquid chromatography to thin-layer chromatography for the identification of polycyclic aromatic hydrocarbons in marine sediment by fluorescence excitation and emission spectroscopy

R. J. VAN DE NESSE*, G. J. M. HOOGLAND, J. J. M. DE MOEL, C. GOOIJER, U. A. Th. BRINKMAN and N. H. VELTHORST

Department of General and Analytical Chemistry, Free University, De Boelelaan 1083, 1081 HV Amsterdam (The Netherlands)

ABSTRACT

Storage of the effluent from a reversed-phase column liquid chromatography separation on a thin-layer chromatography plate offers two advantages: (1) detection principles that are not applicable on-line with flow systems can be used; (2) the thin-layer chromatography plate itself allows a second separation to be carried out. Both advantages are demonstrated for the separation and identification of polycyclic aromatic hydrocarbons in a marine sediment sample. The effluent from a microbore liquid chromatography column was deposited on a linearly moving thin-layer chromatography plate through a spray jet assembly interface. As with isocratic liquid chromatography, not all polycyclic aromatic hydrocarbons present in the sample could be separated; a second separation of the immobilized chromatogram was applied by means of thin-layer chromatography. The overlapping peaks were then resolved completely. Eleven polycyclic aromatic hydrocarbons were identified by measuring their fluorescence excitation and emission spectra on the thin-layer chromatography plate with a conventional spectrometer.

INTRODUCTION

The on-line coupling of column liquid chromatography (LC) to thin-layer chromatography (TLC), accomplished by depositing the column effluent from an LC column on a TLC plate moving at constant speed, can be used to combine the separation power of LC with the detection potential of TLC. Since the LC chromatogram is stored on the TLC plate as a continuous trace, in principle a broad variety of time-consuming spectroscopic methods capable of yielding structural information from the immobilized analytes can be applied, *e.g.* two-dimensional absorption [1], fluorescence excitation and emission [2], Fourier transform infrared (FT-IR) [3], surface-enhanced Raman (SERS) [4,5] and fluorescence line narrowing (FLN) spectroscopy [2,6].

An important condition for a successful coupling is the conservation of the resolution of the LC chromatogram during the immobilization on the TLC plate. In

previous papers on this subject we have shown that optimization of both the construction and the characteristics of the interface between the LC and TLC system results in a deposition without serious additional band broadening [2,7,8]. the use of fluorescence excitation and emission spectroscopy and of FLN spectroscopy as off-line detection methods has been demonstrated for some model compounds [2].

Until now, in our work the TLC plate served only to store the LC chromatogram for the application of off-line detection methods, while its chromatographic properties were not exploited. Two-dimensional chromatography can be realized by subjecting the immobilized LC chromatogram to a second separation by means of TLC in a direction perpendicular to the deposited trace. In this way, the separation efficiency can be enhanced when different types of chromatographic systems are used in the LC and TLC mode. In 1987, Jänchen [1] described the (on-line) coupling of reversed-phase LC and normal-phase TLC for the separation of 56 pesticides.

In this study the on-line coupling of LC to TLC was directed to the identification of polycyclic aromatic hydrocarbons (PAHs) present in a marine sediment. The same sediment has been analyzed by the Tidal Waters Division (Groningen, The Netherlands) using reversed-phase LC with gradient elution and on-line fluorescence detection; in that case, identification of the PAHs was based only on the retention times of the eluting compounds. In the present study isocratic reversed-phase LC was used, and identification was accomplished by recording fluorescence excitation and emission spectra of the spots in the immobilized chromatogram. The unresolved spots were further separated by developing the stored chromatogram by TLC, thus performing two-dimensional chromatography.

EXPERIMENTAL

Apparatus

Fig. 1 shows a scheme of the LC-TLC coupling set-up. The various aspects are described below.

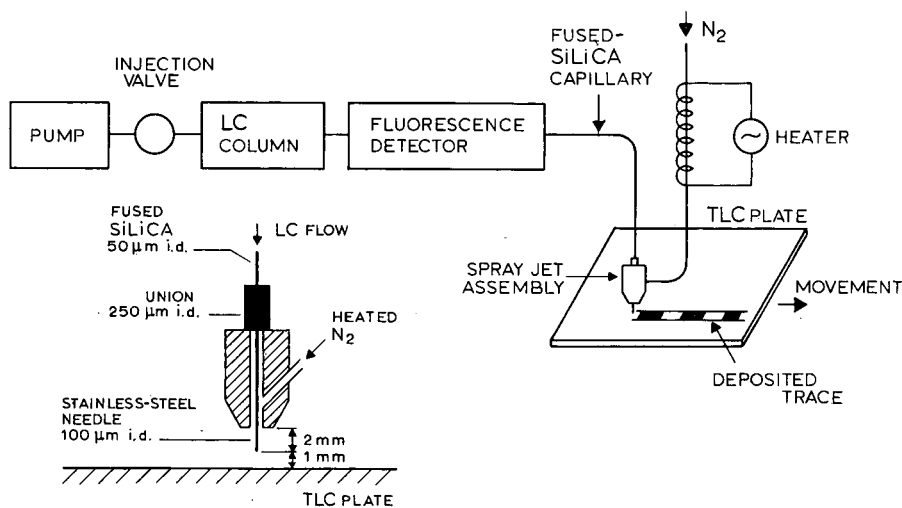


Fig. 1. Schematic of the LC-TLC system and the coupling interface.

Chromatography. A laboratory-made syringe pump and two laboratory-made injection valves were used; one valve had an internal loop of 1.9 μl , the other an external loop of 10 μl . Separations were done by isocratic elution with methanol-water (9:1, v/v) at a flow-rate of 22 $\mu\text{l}/\text{min}$ on a 170 mm \times 1.1 mm I.D. column packed with 5- μm RoSil C₁₈ (Research Separations Labs., Eke, Belgium).

For the two-dimensional chromatography experiments, the TLC plates were developed twice in a direction perpendicular to the deposition trace over a distance of ca. 6 cm with methanol-diethyl ether-water (6:4:1, v/v/v).

On-line (LC) detection. A Varian (Walnut Creek, CA, U.S.A.) Fluorichrom fluorescence detector was used for the on-line monitoring of the LC effluent. To prevent band broadening, the original flow cell and inlet and outlet tubing were replaced by a 40 cm \times 150 μm I.D. fused-silica capillary, the appropriate part of the coating being burned off. Excitation was performed with a deuterium lamp, the light passing through a 10-mm-pathlength cuvette filled with 25% (w/v) nickel sulphate and 40% (w/v) cobalt sulphate in water and a 2-mm UG 11 (Schott, Mainz, Germany) glass band filter. In this way a spectral window ranging from 255 to 368 nm with a maximum transmittance of 32% at 318 nm was obtained. At the emission side a 4-mm Schott GG 13 glass cut-off filter rejected unwanted stray light.

Interface. From the fluorescence detector, the LC effluent was led to the spray jet assembly through a 40 cm \times 50 μm I.D. fused-silica capillary. Basically the present spray jet assembly was the same as that of ref. 7; modifications were made with respect to capillary connections and the means to adjust the position of the needle. The capillary was connected by a 250 μm I.D. (1/16 in. O.D.) union to a 100 μm I.D. (475 μm O.D.) stainless-steel syringe needle with a conically shaped tip. One side of the union was glued to the needle; the other end was attached to the capillary by a fingertight connection. A nitrogen flow around the tip of the needle ensured gentle deposition of the effluent on the TLC plate and provided the partial removal of the mobile phase. For the latter purpose, an electric heater, capable of heating the nitrogen gas up to 100°C, was also used. The distance between the needle tip and the TLC plate was 1 mm; the needle protruded 2 mm from the spray jet.

The TLC plate was moved by placing it on the translation table of a Camag (MuttENZ, Switzerland) Linomat III line applicator; a translation table speed of about 3.3 mm/min was used. For all coupling experiments the translation table was started 8 min after injection of the sample.

Off-line (TLC) detection. The immobilized chromatogram was scanned with a Carl Zeiss (Oberkochen, Germany) densitometer operated in the fluorescence mode. Excitation was done with a 48-W high-pressure mercury arc lamp. After passing an M4Q-III prism monochromator, the light was focused onto the TLC plate as a rectangular spot; the spatial resolution was 0.7 mm in the direction of the scan and 2.1 mm perpendicular to the scan direction. The luminescence of the compounds was distinguished from the excitation light by the use of optical filters and was detected by an RCA (Lancaster, PA, U.S.A.) 1P28 photomultiplier. The response time was 5 s.

Fluorescence emission and excitation spectra were taken *in situ* with a Perkin-Elmer (Norwalk, CT, U.S.A.) MPF-44A fluorescence spectrometer equipped with a special TLC accessory (Hitachi, Tokyo, Japan). A DCSU-2 differential corrected spectra unit was used to subtract blanks. The spectral resolution of the scanning monochromator was 5 nm; for the fixed monochromator it was 10 nm. For all spectra, the response time was 3 s.

Materials

The model compounds anthracene (ANT; Fluka, Buchs, Switzerland), fluoranthene (FLT; Aldrich, Milwaukee, WI, U.S.A.), pyrene (PYR; EGA-Chemie, Steinheim, Germany), benz[*a*]anthracene (B[*a*]A; Rütgerswerke, Castrop, Germany), chrysene (CHR; Materials, Englewood Cliffs, NJ, U.S.A.), perylene (PER; Metron, Allamuchy, NJ, U.S.A.), benzo[*e*]pyrene (B[*e*]P), benzo[*b*]fluoranthene (B[*b*]F), benzo[*k*]fluoranthene (B[*k*]F), benzo[*a*]pyrene (B[*a*]P), indeno [1,2,3-*cd*]pyrene (INDP) and benzo[*ghi*]perylene (BPER; all from Radiant Dyes, Wermelskirchen, Germany) were used as received. Methanol [high-performance liquid chromatography (HPLC) quality] and diethyl ether were obtained from Baker (Deventer, The Netherlands).

Two types of TLC plates were applied: high-performance quality C₁₈ modified silica plates from Merck (Darmstadt, Germany) and 30% acetylated cellulose plates from Macherey–Nagel (Düren, Germany). Both types of plates were cleaned by continuous elution with methanol. The acetylated plates were further purified by elution with diethyl ether.

Sample pretreatment

The marine sediment was collected from the Waddensee (The Netherlands). The cleaned-up sample was received from the Tidal Waters Division as a solution in methanol. A volume of 0.317 ml methanol solution corresponded to 1.00 g of dry sediment. Analysis by the Tidal Waters Division, using reversed-phase LC with methanol–water gradient elution, revealed the presence of the PAHs mentioned as model compounds in the previous section, except for PER. They were all present in concentrations ranging from 120 to 860 ng/ml (*i.e.* $0.7 \cdot 10^{-6}$ to $5 \cdot 10^{-6}$ M); ANT 120 ng/ml, FLT 860 ng/ml, PYR 600 ng/ml, B[*a*] 360 ng/ml, CHR 445 ng/ml, B[*e*]P 450 ng/ml, B[*b*]F 650 ng/ml, B[*k*]F 295 ng/ml, B[*a*]P 375 ng/ml, INDP 555 ng/ml, BPER 475 ng/ml.

RESULTS AND DISCUSSION

The stored LC chromatogram

In this study, two aspects were mainly explored, *viz.* (1) the quality of the stored chromatogram and the information to be derived from it, and (2) the application of the on-line LC–TLC method to real-sample analysis.

A standard mixture of the PAHs known to be present in the marine sediment sample was used to compare the on-line LC chromatogram recorded by conventional fluorescence detection with the stored chromatogram recorded by fluorescence scanning of the deposited trace on the TLC plate with a densitometer. The concentrations in this mixture $3.5 \cdot 10^{-5}$ to $6 \cdot 10^{-7}$ M (the injected amounts range from 16 ng to 290 pg), were chosen to be about fivefold higher than in the sediment sample. In Fig. 2 the on-line chromatogram (a) and the corresponding stored chromatogram (b) are shown for the system C₁₈-modified silica LC–C₁₈-modified silica high-performance thin-layer chromatography (HPTLC). The width of the deposited trace on the TLC was about 1.5 mm.

There are three reasons to prefer the high-performance quality C₁₈-modified silica TLC plate to other types of TLC plates for the immobilization of the LC chromatogram. Firstly, its highly regular surface favours the attainment of low detec-

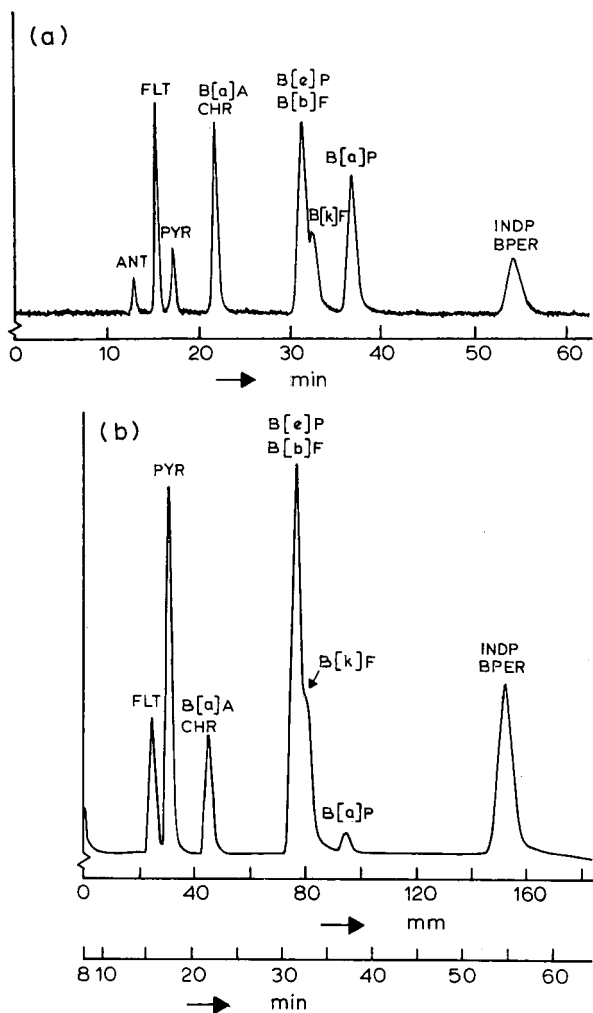


Fig. 2. LC chromatograms of a test mixture of PAHs (concentrations, $3.5 \cdot 10^{-5}$ to $6 \cdot 10^{-7}$ M; the injected amounts range from 16 ng to 290 pg). (a) On-line fluorescence detection. Excitation envelope: 225–368 nm with maximum at 318 nm. Emission wavelength: > 385 nm. (b) Fluorescence detection with densitometry after deposition on a C_{18} -modified silica HPTLC plate. Translation table speed: 3.26 mm/min. Excitation wavelength: 313 nm. Emission wavelength: > 390 nm. Spatial resolution: 0.7×2.3 mm. For abbreviations, see Experimental section.

tion limits in scanning densitometry. As has been pointed out in ref. 2, the detection limits are primarily determined by baseline fluctuations resulting from the surface irregularity of the TLC plate; the level of the statistical noise on the background signal is of minor importance. Secondly, the above HPTLC material has a low background luminescence, which is important when scanning of fluorescence spectra is used for the identification of analytes. As in this case the TLC plate does not move,

surface irregularity now of course plays no role. Thirdly, PAHs adsorbed to C_{18} -modified silica HPTLC plates in comparison with other types hardly suffer from (photo)decomposition [2].

All stored chromatograms were scanned under a nitrogen gas atmosphere. For some analytes this caused an enhanced signal intensity, probably because of a reduction of fluorescence and/or phosphorescence quenching by oxygen. The effect was highest with PYR; the signal increased by a factor of 2. The poor detectability of ANT on the TLC plate is at least partly the result of its relatively high volatility. Furthermore, ANT has a very low molar absorptivity at 313 nm.

Comparison of Fig. 2a and 2b reveals that the LC separation is stored on the TLC plate without substantial loss of resolution (see, for example, B[k]F shoulder). Only solutes with relatively short retention times show some additional band broadening. The resolution in the early part of the stored chromatogram can be improved by increasing the speed of the translation table. In our experiments, the table speed was restricted by the condition that all analytes in the LC chromatogram should be deposited on the 20-cm-long TLC plates. Of course higher translation table speeds also reduce the sensitivity of detection, because the analyte spots of the deposited trace become longer.

Fig. 3 shows a stored chromatogram of the sediment sample, deposited on a C_{18} -modified silica HPTLC plate. The LC separation, LC-TLC interfacing and the detection conditions were the same as in Fig. 2b. As the original LC detector flow cell was replaced by a fused-silica capillary to prevent additional band broadening, on-line fluorescence detection was not sensitive enough in this case to record the on-line chromatogram.

Preliminary assignment of the peaks in Fig. 3 is possible by comparison with the test chromatogram of Fig. 1. Unambiguous identification is achieved by recording

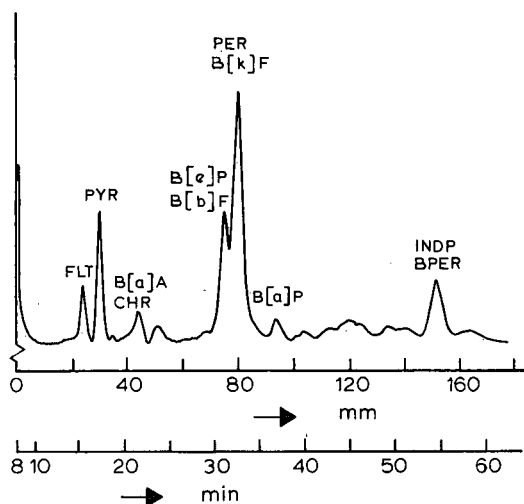


Fig. 3. Densitometer scan of a marine sediment sample (injected amount, $1.9 \mu\text{l}$) after LC separation and deposition of LC effluent on a C_{18} -modified silica HPTLC plate. Translation table speed: 3.27 mm/min . Excitation wavelength: 313 nm . Emission wavelength: $>390 \text{ nm}$. For abbreviations, see Experimental section.

fluorescence excitation and emission spectra *in situ* with a conventional spectrometer equipped with a TLC accessory. Identification of the constituents of the unresolved spots is difficult or even impossible since their spectra are quite similar. However, anticipating further experiments described in the text below, the peaks in Fig. 3 have already been assigned. Fig. 4 shows excitation and emission spectra of FLT, PYR and B[a]P, compounds that are completely resolved by the present LC system. These spectra are identical with those recorded in solution [9], as is shown for B[a]P. The spectra in Fig. 4 were corrected for the background contribution of the TLC plate caused by luminescence and light scattering, which are much more pronounced than

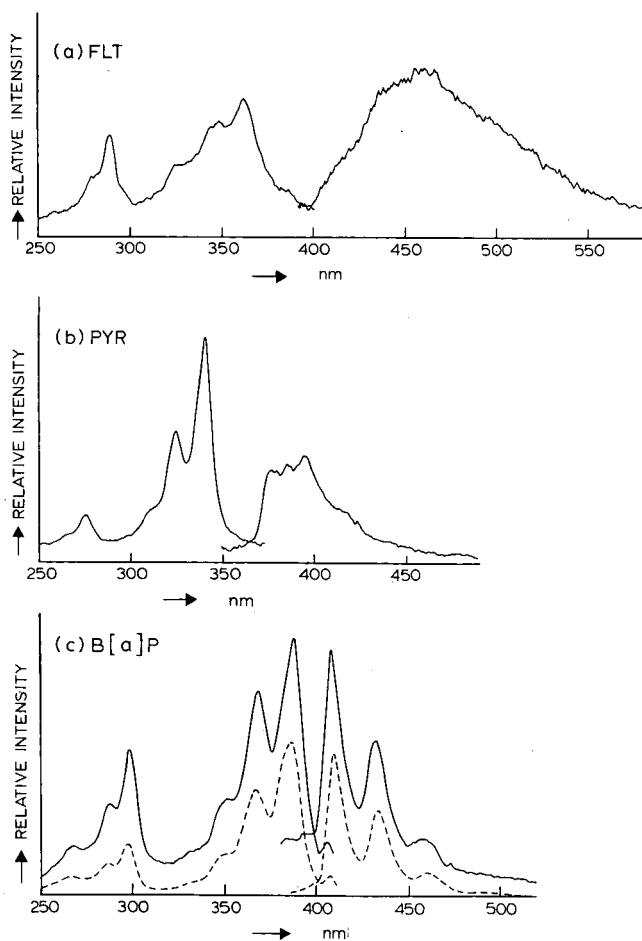


Fig. 4. *In situ* excitation and emission spectra of PAHs from the immobilized LC chromatogram of Fig. 3. (a) FLT. Excitation wavelength: 360 nm. Emission wavelength: 455 nm. (b) PYR. Excitation wavelength: 322 nm. Emission wavelength: 390 nm. (c) B[a]P. Excitation wavelength: 300 nm. Emission wavelength 430 nm. Dashed line: room temperature excitation and emission spectrum of a 10^{-6} M B[a]P solution in methanol. The illuminated area on the TLC plate was 2×2 mm for FLT and PYR, and 6×1 mm for B[a]P.

in solution. It is obvious from this figure that the spectral intensities for PYR and B[a]P are far above the level associated with the identification limit. For the worst case, FLT, identification on the basis of the excitation spectrum can still be done for about 270 pg (corresponding to a 1.9- μ l injection of $7 \cdot 10^{-7}$ M), which is about six times lower than the amount associated with the spectrum in Fig. 4a.

Two-dimensional chromatography

With the present LC system, isocratic elution does not suffice to separate all PAHs in the sediment sample. Therefore a second separation was carried out on the TLC plate. Subsequent to the storage of the LC effluent on a TLC plate, the plate was developed in a direction perpendicular to the deposited LC trace. For this, a 30% acetylated cellulose plate was preferred to a C₁₈-modified silica HPTLC plate, because elution with methanol–diethyl ether–water (6:4:1, v/v/v) allows the complete separation of all unresolved components [10]. When the second (TLC) dimension was used, the injection volume of the LC system was increased from 1.9 to 10 μ l, mainly for two reasons. Firstly, the spots on the TLC plate are more easily located by viewing under UV light; this facilitates the appropriate positioning of the TLC plate in the special accessory needed for the recording of fluorescence spectra. Secondly, densitometric detection of the PAHs on the 30% acetylated cellulose TLC plate was less sensitive than on the C₁₈-modified silica HPTLC plate. The reduced detectability is a result of the more irregular surface of the former type of plate. In addition, the spots deposited on the plate after the LC separation self-evidently become somewhat larger during the TLC separation. Unfortunately, a 30% acetylated cellulose TLC plate offering a high(er) performance quality is not commercially available. The increase of the injection volume had only a minor effect on the resolution in the LC system.

Fig. 5 shows the result of the TLC separation of a sediment sample (after previous on-line LC separation and storage). All PAHs not separated in the isocratic

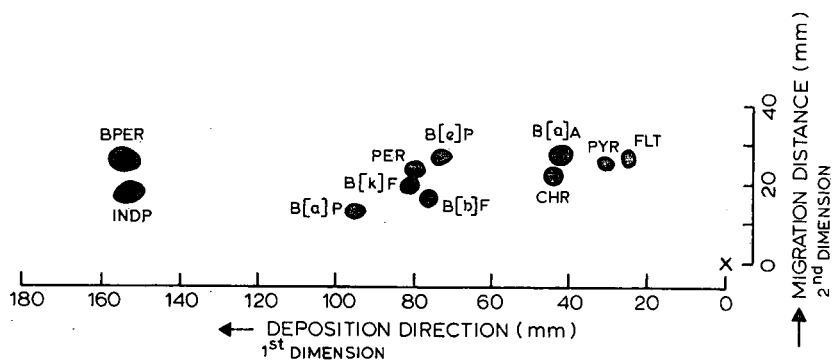


Fig. 5. Two-dimensional LC-TLC of a marine sediment sample. First dimension: isocratic reversed-phase LC separation (methanol–water, 9:1, v/v; injected amount, 10 μ l); LC effluent deposited on a 30% acetylated cellulose TLC plate; translation table speed 3.20 mm/min. Second dimension: TLC perpendicular to the deposition trace with methanol–diethyl ether–water (6:4:1, v/v/v). The cross marks the start of the translation table 8 min after injection. For abbreviations, see Experimental section.

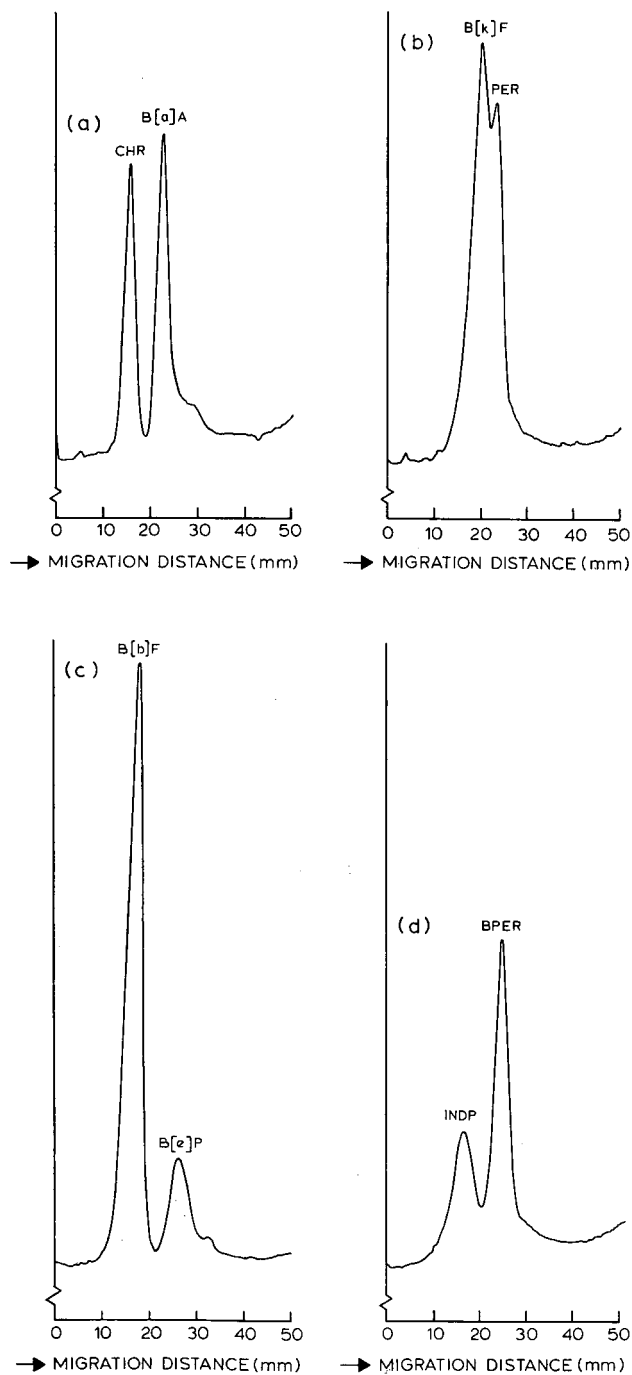


Fig. 6. Densitometer scans of the TLC plate after two-dimensional LC-TLC separation of a marine sediment sample. The scans were taken in the direction of the TLC separation at (a) 44 mm, (b) 75.5 mm, (c) 81 mm and (d) 153 mm from the starting point of the translation table in Fig. 5. (a) CHR and B[a]A. Excitation wavelength: 266 nm. Emission wavelength: >390 nm. Spatial resolution: 0.7×4.1 mm. (b) B[k]F and PER. Excitation wavelength: 254 nm. Emission wavelength: >430 nm. Spatial resolution: 0.7×2.3 mm. (c) B[b]F and B[e]P. Excitation wavelength: 266 nm. Emission wavelength: >390 nm. Spatial resolution: 0.7×2.3 mm. (d) INDP and BPER. Excitation wavelength: 266 nm. Emission wavelength: >390 nm. Spatial resolution: 0.7×4.1 mm.

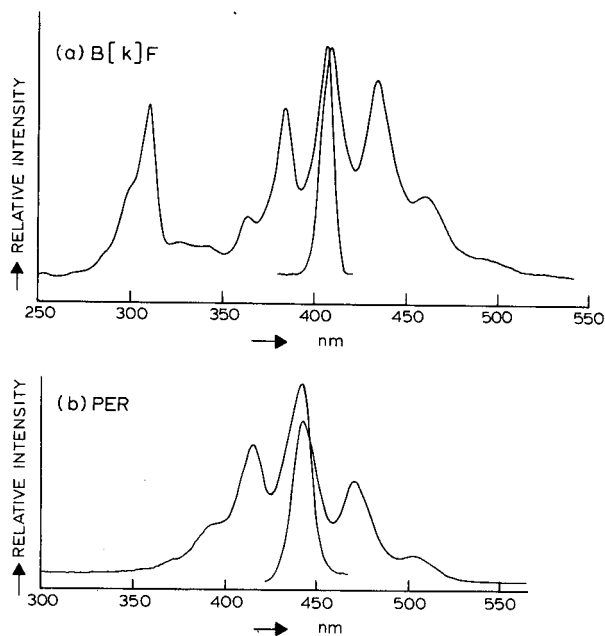


Fig. 7. *In situ* excitation and emission spectra of PAHs after two-dimensional LC-TLC of a marine sediment sample. Illuminated area on the plate: 6×2 mm. (a) B[k]F. Excitation wavelength: 309 nm. Emission wavelength: 430 nm. (b) PER. Excitation wavelength: 400 nm. Emission wavelength: 495 nm.

LC system are completely resolved, as is clear from densitometer scans (see Fig. 6). The analytes were identified by their fluorescence excitation and emission spectra. In Fig. 7 a relevant example is shown; the two-dimensional approach revealed the presence of PER in the sediment. This compound was not detected in the analysis carried out by the Tidal Waters Division; obviously it was obscured by another peak.

CONCLUSIONS

LC-TLC coupling allows the successful separation and identification – by means of fluorescence spectroscopy – of PAHs in marine sediment samples. The use of a second, TLC, separation reduces the demands on the performance of the LC separation and simple isocratic elution is sufficient. Furthermore, in the semi-on-line approach, identification of PAHs is simply accomplished by conventionally recorded fluorescence emission and excitation spectra since time constraints in detection are absent. In the on-line (on-the-fly) mode, identification at trace levels is possible, but it generally requires sophisticated instrumentation such as an intensified linear diode array detector (see, for example, refs. 11–13). Furthermore, on-the-fly excitation spectra are not easily obtainable. In summary, the semi-on-line LC-TLC technique, although obviously more elaborate than on-line (gradient elution) LC, deserves a distinct place in chemical analysis since it offers improved chromatographic separation efficiency as well as a better detection potential.

Future work in our laboratory will focus on the combination of LC with FT-IR spectroscopy following the semi-on-line approach. The present coupling interface will be used for the storage of LC effluents on IR-transparent media such as zinc selenide.

ACKNOWLEDGEMENTS

The authors thank J. W. Hofstraat and F. Smedes from the Tidal Waters Division (Groningen, The Netherlands) for supplying the marine sediment sample and analysis data. The investigation was supported by the Netherlands Foundation for Chemical Research (SON) with financial aid from the Netherlands Organization for the advancement of Scientific Research (NWO), Grant No. 700-344-006.

REFERENCES

- 1 D. E. Jänchen, in H. Traitler, A. Studer and R. E. Kaiser (Editors), *Proceedings of the 4th International Symposium on Instrumental HPTLC*, Institute for Chromatography, Bad Dürkheim, 1987, pp. 185.
- 2 J. W. Hofstraat, M. Engelsma, R. J. van de Nesse, C. Gooijer, U. A. Th. Brinkman and N. H. Velthorst, *Anal. Chim. Acta*, 193 (1987) 193.
- 3 C. Fujimoto, T. Morita and K. Jinno, *J. Chromatogr.*, 438 (1988) 329.
- 4 J.-M. L. Sequareis and E. Koglin, *Anal. Chem.*, 59 (1987) 525.
- 5 S. A. Soper, K. L. Ratzlaff and T. Kuwana, *Anal. Chem.*, 62 (1990) 1438.
- 6 R. S. Cooper, R. Jankowiak, J. M. Hayes, Lu Pei-qi and G. J. Small, *Anal. Chem.*, 60 (1988) 2692.
- 7 J. W. Hofstraat, M. Engelsma, R. J. van de Nesse, C. Gooijer, N. H. Velthorst and U. A. Th. Brinkman, *Anal. Chim. Acta*, 186 (1986) 247.
- 8 J. W. Hofstraat, S. Griffioen, R. J. van de Nesse, U. A. Th. Brinkman, C. Gooijer and N. H. Velthorst, *J. Planar Chromatogr.*, 1 (1988) 220.
- 9 W. Karcher, R. J. Fordham, J. J. Dubois, P. G. J. M. Glaude and J. A. M. Ligthart, *Spectral Atlas of Polycyclic Aromatic Compounds*, Reidel, Dordrecht, 1983.
- 10 J. Kraft, A. Hartung, K. Lies and J. Schulze, in R. E. Kaiser (Editor), *Proceedings of the 2nd International Symposium on Instrumental HPTLC, Interlaken, 1982*, Institute for Chromatography, Bad Dürkheim, 1982, p. 144.
- 11 R. J. van de Nesse, C. Gooijer, G. Ph. Hoornweg, U. A. Th. Brinkman, N. H. Velthorst and S. J. van der Bent, *Anal. Lett.*, 23 (1990) 1235.
- 12 D. B. Skoropinski, J. B. Callis, J. D. S. Danielson and G. D. Christian, *Anal. Chem.*, 58 (1986) 2831.
- 13 J. C. Gluckman, D. C. Shelly and M. V. Novotny, *Anal. Chem.*, 57 (1985) 1546.

Time-resolved luminescence detection of derivatized thiols in column liquid chromatography

M. SCHREURS, L. HELLENDORRN, C. GOOIJER* and N. H. VELTHORST

Department of General and Analytical Chemistry, Free University, De Boelelaan 1083, 1081 HV Amsterdam (The Netherlands)

ABSTRACT

The selectivity of luminescence detection in liquid chromatography is enhanced by applying time-resolved detection with a pulsed xenon lamp and a gated photomultiplier, and by making use of labels with a long luminescence decay time (*i.e.*, longer than 0.1 ms). Sensitized Tb^{3+} luminescence, which needs no solvent deoxygenation, was employed in this study. The derivatization of thiol-containing analytes to sensitizing products was studied in batch experiments; in particular, attention was paid to the reaction conditions for the derivatization of glutathione by 4-maleimidylsalicylic acid. In the chromatographic experiments, derivatization was performed pre-column, a Tb^{3+} solution was added post-column to achieve complexation and sensitized Tb^{3+} luminescence was detected. Compared to direct fluorescence detection, sensitized Tb^{3+} luminescence detection gave better results with respect to sensitivity (the limit of detection of glutathione was $2 \cdot 10^{-8}$ M, 0.3 ng on column) and, particularly, selectivity, as demonstrated for the spiked urine samples.

INTRODUCTION

Fluorescence spectroscopy offers many possibilities for sensitive and selective detection in liquid chromatography. Detection is based on the native fluorescence of the analyte or, if this is absent or only weak, the analyte may be derivatized to a fluorescent product by a chemical reaction [1]. Although fluorescence detection has an inherent sensitivity, there are several processes which contribute to the background signal, *i.e.*, scattering and fluorescence caused by solvent impurities or an excess of derivatization reagent (which is obviously preferred to be non-fluorescent). These phenomena increase the noise and restrict the achievable detection limits. In time-resolved luminescence spectroscopy, the background originating from these short-lived processes can be excluded by introducing a delay time after the start of the excitation pulse during which the photomultiplier is shut so that the detection of the luminescence takes place after the intensity of the pulse has decayed completely. Long-lived luminescence can be detected very sensitively by gating the photomultiplier during a certain interval after the delay time, as shown in Fig. 1. Time-resolved luminescence detection has already been shown to be an interesting method for use in liquid chromatography for a number of applications [2–5].

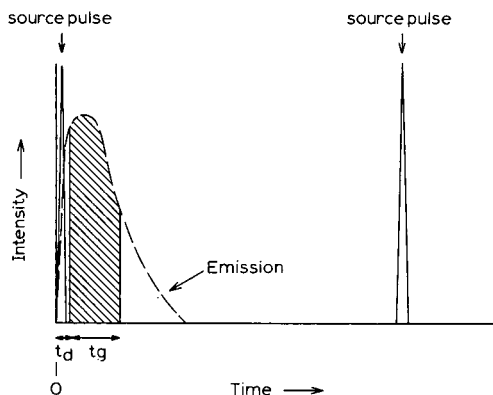


Fig. 1. Emission signal after source excitation flash applying time-resolved luminescence detection: t_d , delay time; t_g , gating time.

Only very few compounds emit long-lived luminescence in liquid solutions. Among these are organic compounds which are phosphorescent in the absence of oxygen and some La^{3+} ions which emit long-lived luminescence ($\tau \geq 0.1$ ms) even in the presence of oxygen [6]. Luminescence of the ions Eu^{3+} and Tb^{3+} , with characteristic decay times of 0.1 and 0.4 ms, respectively, in aqueous solutions, can easily be detected by applying a pulsed xenon lamp. This phenomenon can be utilized for detection purposes in an indirect way, either based on quenching [5,7] or on the sensitizing of lanthanide luminescence, induced by the analytes under consideration. In this paper attention is focused on sensitized luminescence.

Lanthanide ions have low absorptivities (typically smaller than $10 \text{ l mol}^{-1} \text{ cm}^{-1}$), therefore relatively high concentrations are needed to observe their direct luminescence. Intramolecular sensitizing may occur when the ion forms a complex with an absorbing ligand which, after being excited, transfers its energy to an accepting level of the lanthanide ion [8]. Various compounds are known to have sensitizing properties and can be detected very well by sensitized lanthanide luminescence detection. For instance, several tetracyclines sensitize Eu^{3+} luminescence [4,9], salicylate sensitizes Tb^{3+} luminescence [10] and some β -diketonates sensitize Eu^{3+} luminescence, whereas others sensitize Tb^{3+} luminescence [8].

To extend the potential of the time-resolved detection of sensitized lanthanide luminescence as a detection method in liquid chromatography, a derivatization reaction has been developed in which non-sensitizing analytes are converted into sensitizing compounds. This is achieved by coupling chromophoric groups, which are known to have sensitizing properties for lanthanide luminescence, to the analyte. Two commercially available derivatization reagents highly specific for thiol groups, *i.e.*, 4-maleimidylsalicylic acid (4-MSA) and 4-iodoacetamidosalicylic acid (4-ISA), were examined. As a salicylate group sensitizes Tb^{3+} luminescence, this ion is used as a long-lived luminophore. Preliminary experiments have shown that 4-maleimidylsalicylic acid has favourable properties for derivatization and detection [11]. In this paper a detailed spectroscopic and chromatographic study is presented, mainly concentrating on glutathione as a model compound.

EXPERIMENTAL

Chemicals

Terbium(III) chloride hexahydrate (99.9%) was obtained from Aldrich (Milwaukee, WI, U.S.A.), 4-MSA and 4-ISA from Molecular Probes (Eugene, OR, U.S.A.), glutathione (reduced form) from Boehringer (Mannheim, Germany), N-acetylcysteine from Aldrich, L-cysteine, sodium salicylate and Trizma base from Sigma (St. Louis, MO, U.S.A.) and tetrabutylammonium bromide from Kodak (Rochester, NY, U.S.A.). High-performance liquid chromatography (HPLC)-grade acetonitrile was purchased from Baker (Deventer, The Netherlands).

Instrumentation

Batch experiments were performed with a Perkin-Elmer (Beaconsfield, U.K.) MPF-44 fluorescence spectrometer, supplied with a continuous XBO 150 W xenon lamp and Hamamatsu type R777-01-HA photomultipliers.

The HPLC system consisted of a Gilson (Villiers-le-Bel, France) 302 HPLC pump, a Valco six-port injection valve equipped with a 50- μ l injection loop and a stainless-steel column (140 \times 3.1 mm I.D.) packed with RoSil (BioRad-RSL, Eke, Belgium) C₁₈ HL 5- μ m particles. The post-column Tb³⁺ solution was added using a Pye Unicam (Cambridge, U.K.) PU4015 pump. A Perkin-Elmer LS-40 fluorescence detector was used both for fluorescence and for time-resolved Tb³⁺ luminescence detection. Fluorescence detection of the 4-MSA-thiol product was performed at excitation and emission wavelengths of 302 and 408 nm, respectively, whereas the sensitized Tb³⁺ luminescence was detected at excitation and emission wavelengths of 322 and 545 nm, respectively. In the latter mode, the delay and gating times were 0.1 and 2.0 ms, respectively.

Preparation of solutions

Stock solutions of thiols were prepared in doubly distilled water containing $1 \cdot 10^{-4}$ M EDTA, acidified with hydrochloric acid (pH 3.0). Stock solutions of 4-MSA and 4-ISA were prepared in ethanol and aqueous Tris buffer, pH 7.5, respectively.

The mobile phase consisted of acetonitrile-water (25:75, v/v), $5 \cdot 10^{-3}$ M Tris buffer, pH 7.2, and $1 \cdot 10^{-3}$ M tetrabutylammonium bromide; the post-column solution contained $1 \cdot 10^{-3}$ M TbCl₃ in water-acetonitrile (50:50, v/v). The flow-rates of the mobile phase and the post-column solution were both 0.5 ml/min.

The long-term stability of the derivatization products has not been investigated; the derivatized analytes were usually injected within 1 h of preparation.

The clean-up of diluted urine samples was performed using disposable filter holders FP 030/30 2 μ m (Schleicher & Schuell, 's-Hertogenbosch, The Netherlands) and 1-ml octadecyl disposable extraction columns, Bakerbond spe 7020-01 (Baker, Phillipsburg, NJ, U.S.A.).

RESULTS AND DISCUSSION

Batch experiments

When choosing a derivatization label, the following aspects have to be considered: the reaction conditions required; the possible occurrence of competitive reactions

TABLE I

DETECTION WAVELENGTHS AND RELATIVE FLUORESCENCE AND SENSITIZED Tb^{3+} LUMINESCENCE INTENSITIES OF SEVERAL SOLUTION

Solutions were prepared in $5 \cdot 10^{-3} M$ Tris buffer, pH 7.2; the results in the last column were obtained after the addition of EDTA and sodium hydroxide solution.

Solution	Fluorescence	Sensitized Tb^{3+} luminescence (pH 7.2)	Sensitized Tb^{3+} luminescence (pH 12)
Excitation wavelength (nm)	300–305	320–322	320–322
Emission wavelength (nm)	400–410	545	545
Salicylate	+++	++	+++
4-ISA	+	+	++
4-ISA–GSH	+	+	++
4-MSA	0	0	0
4-MSA–GSH	++	++	+ ^a

^a Maximum excitation at 336 nm.

(especially if pre-column derivatization is applied); the difference in spectroscopic properties between the derivatization reagent and its reaction product; and, finally, the linearity, reproducibility and sensitivity of detection of the labelled analytes. Both derivatization reagents studied, 4-ISA and 4-MSA, give fluorescent products on reaction with thiols. The derivatization reaction was first studied in batch experiments by fluorescence spectroscopy using glutathione (GSH) as a model compound. Tb^{3+} was subsequently added and the sensitized lanthanide luminescence was compared with the fluorescence recorded in the absence of Eu^{3+} . The results are discussed below and are summarized in Table I; pure salicylate is included for comparison.

Fluorescence. In a similar manner to other maleimides known from fluorescence derivatization [1,12–18], 4-MSA shows hardly any fluorescence, in contrast with 4-ISA (see Table I). On the addition of GSH to a solution of 4-MSA, the formation of a fluorescent product is observed. In contrast, the presence of a thiol in the 4-ISA solution does not significantly change the fluorescence wavelengths or intensity. The reaction of GSH and 4-MSA was studied in more detail in batch experiments.

Effect of pH on the reaction rate. The reaction rate of the nucleophilic addition of the thiol to the carbon–carbon double bond of the maleimide group is slow in acid solutions and rapid in alkaline solutions as the thiolate ion is a strong nucleophile. As in the following step Tb^{3+} has to be added to the 4-MSA–GSH mixture, the derivatization reaction was studied at pH values where the hydrolysis of Tb^{3+} is relatively slow. In Fig. 2 the increase of fluorescence intensity *versus* time for 4-MSA–GSH at various pH values is shown. It can be concluded that in the buffered solutions the choice of pH is not very critical; at room temperature the reaction is completed within about 10 min. In water (pH 6.0) the reaction proceeds much more slowly, but its rate can be considerably increased by increasing the temperature to 60°C. This is not necessary when the reaction is performed in Tris buffer at pH 7.0–7.5.

Reaction rate at various reagent and thiol concentrations. For a high reaction rate an excess of derivatization reagent is necessary, as shown in Fig. 3. At a 4-MSA concentration of $5 \cdot 10^{-5} M$, a 50-fold excess, the derivatization reaction is completed

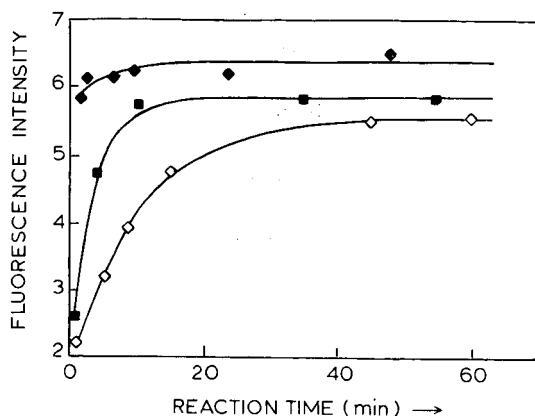


Fig. 2. Reaction rate of 4-MSA and GSH at various pH values: \diamond = water, pH 6; \blacksquare = Tris buffer, pH 7.0; \blacklozenge = Tris buffer, pH 7.5.

in less than 10 min at room temperature. Such an excess is not a serious problem, as the fluorescent 4-MSA-GSH adduct can be readily discriminated from the unreacted, poorly fluorescent 4-MSA. In Fig. 4 the increase of fluorescence intensity is shown for three GSH concentrations at a fixed 4-MSA concentration, indicating the linearity of the fluorescence detection.

Sensitizing of Tb^{3+} luminescence. On the addition of Tb^{3+} to a salicylate, 4-ISA, 4-ISA-GSH, or 4-MSA-GSH solution, the characteristic narrow-banded Tb^{3+} emission becomes clearly visible (see Table I and Fig. 5). Although no time-resolved detection was applied in the batch experiments, the Tb^{3+} luminescence can be easily discriminated from the fluorescence signal as its maximum intensity is at a longer wavelength (545 nm). The appearance of Tb^{3+} luminescence simultaneously involves a decrease in the fluorescence intensity. In 4-ISA and 4-ISA-GSH solutions a rather

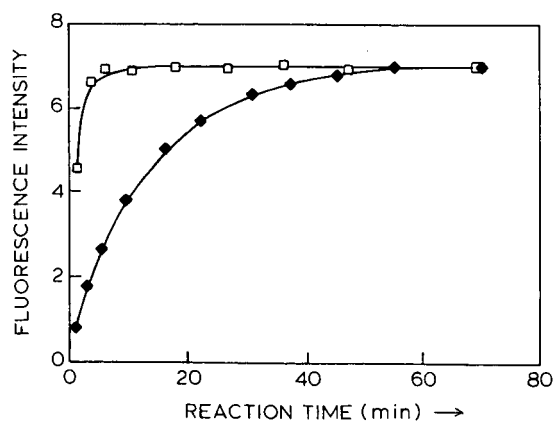


Fig. 3. Reaction rate of 4-MSA and GSH at a five- and fifty-fold excess of 4-MSA. $[GSH] 1 \cdot 10^{-6} M$, reaction in Tris buffer, pH 7.0. \blacklozenge = $[4-MSA] 5 \cdot 10^{-6} M$; \square = $[4-MSA] 5 \cdot 10^{-5} M$.

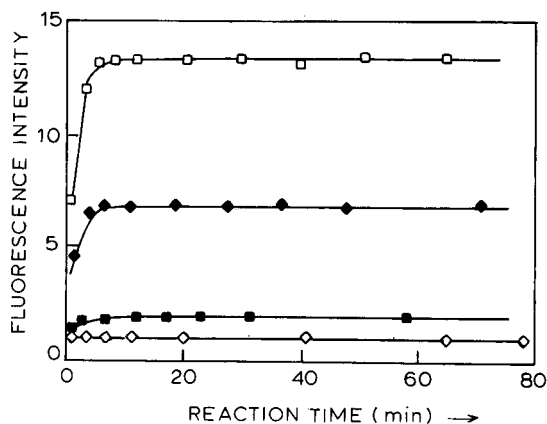


Fig. 4. Reaction rate of 4-MSA and GSH at several GSH concentrations. [4-MSA] $5 \cdot 10^{-5} M$, reaction in Tris buffer, pH 7.0. □ [GSH] $2 \cdot 10^{-6} M$; ◆ = [GSH] $1 \cdot 10^{-6} M$; ■ = [GSH] $2 \cdot 10^{-7} M$; ◇ = blank.

weak sensitized Tb^{3+} luminescence is observed, whereas unreacted 4-MSA does not sensitize the Tb^{3+} luminescence at all.

The intensity of the sensitized lanthanide luminescence as a function of Tb^{3+} concentration (at a fixed concentration of 4-MSA-GSH) is presented in Fig. 6. This figure also shows the decrease of fluorescence noted earlier. More importantly, the direct lanthanide luminescence in the absence of 4-MSA-GSH, which will be present as a background signal and therefore should be as low as possible, is shown. Although around 320 nm the absorptivity of Tb^{3+} is very low [19], at high concentrations some luminescence arising from direct excitation can be observed. A Tb^{3+} concentration of about $5 \cdot 10^{-4} M$ is appropriate.

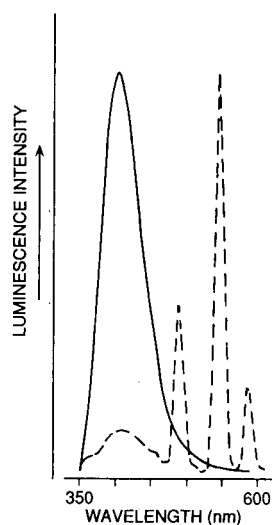


Fig. 5. Fluorescence spectra of 4-MSA-GSH. (—) In the absence of Tb^{3+} , excitation wavelength 302 nm; (---) in the presence of Tb^{3+} , excitation wavelength 322 nm (vertical scale in relative units).

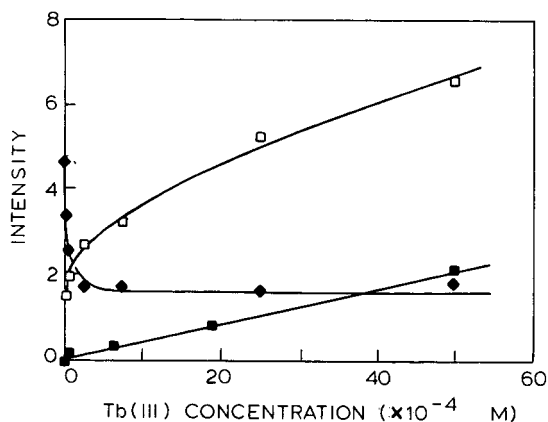


Fig. 6. Luminescence intensities as a function of the Tb^{3+} concentration. □ = Tb^{3+} luminescence intensity sensitized by 4-MSA-GSH, excitation wavelength 322 nm; ◆ = remaining 4-MSA-GSH fluorescence; ■ = direct Tb^{3+} luminescence in the absence of 4-MSA-GSH, excitation wavelength 322 nm.

Tb³⁺ sensitizing at pH \approx 12. For a salicylate ligand, strong alkaline conditions lead to a better complexation of the lanthanide ion and thus more efficient sensitizing [10]. Tb^{3+} was protected from hydrolysis by a two-fold excess of EDTA before the sodium hydroxide solution was added. As shown in Table I, an enhancement of the Tb^{3+} luminescence intensity as observed for salicylate is not seen for 4-MSA-GSH; the sensitized Tb^{3+} luminescence decreased compared to the signal at a pH of about 7 and the maximum excitation wavelength shifted to 336 nm. In 4-ISA and 4-ISA-GSH solutions the Tb^{3+} luminescence is not constant but increases steadily under these alkaline conditions and becomes very intense after several hours (data are not shown; the intensities presented in Table I were measured within a few minutes of the addition of Tb^{3+} to the solutions).

Concluding remarks. 4-MSA was considered to be the most favourable reagent for these purposes; the reaction is fast, is performed under mild conditions, the detection does not require an extreme pH and, most importantly, the excess of derivatizing reagent, which is necessary for a fast reaction does not interfere with the detection. 4-ISA seems less favourable although the high sensitized Tb^{3+} luminescence intensity at pH 12 may have interesting possibilities. Derivatization with 4-ISA was not further investigated in this work.

Chromatographic results

To apply the detection principle for the thiols described in the preceding section to HPLC, the derivatization of the thiol-containing compound with 4-MSA was performed pre-column. Separation was achieved by ion-pair chromatography using a reversed-phase column; the eluent composition was acetonitrile-water (25:75, v/v) containing $5 \cdot 10^{-3}$ M Tris buffer (pH 7.2) and $1 \cdot 10^{-3}$ M tetrabutylammonium bromide. The advantage of this chromatographic system over the system described previously [11] in which the separation was performed under acidic conditions is that, instead of two post-column pumps (*i.e.*, one pump to add a buffer to neutralize the effluent to pH 7 and a second pump to add the Tb^{3+} solution), a single post-column

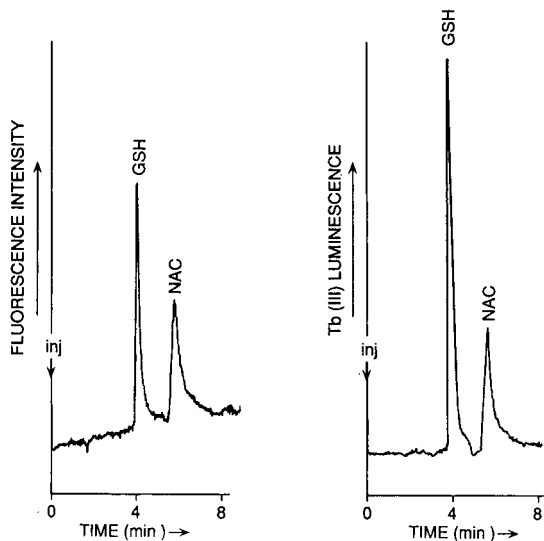


Fig. 7. Mixture of $3.7 \cdot 10^{-7} M$ N-acetylcysteine (NAC) and $4.7 \cdot 10^{-7} M$ glutathione (GSH) derivatized by 4-MSA ($5 \cdot 10^{-5} M$). Left panel, fluorescence detection (vertical scale in relative units); right panel, sensitized Tb^{3+} luminescence detection (vertical scale extended by two times compared with fluorescence detection).

pump to add the Tb^{3+} solution [$1 \cdot 10^{-3} M$ in water–acetonitrile, 50:50 (v/v)] suffices.

The detector used can be operated in a fluorescence mode as well as in a time-resolved (phosphorescence) mode; both methods were applied for the detection of 4-MSA–thiol addition products. In the case of fluorescence detection, no Tb^{3+} solution was added to the effluent as Tb^{3+} quenches the fluorescence. For standard solutions of 4-MSA–GSH it was found that the time-resolved detection mode gave two to three times better signal-to-noise ratios, despite the loss of signal as a result of dilution by the post-column flow. In Fig. 7 chromatograms of a mixture of derivatized N-acetylcysteine and glutathione are shown as obtained by both detection modes.

The detection limit obtained using time-resolved sensitized Tb^{3+} luminescence detection for derivatized glutathione was $2 \cdot 10^{-8} M$, which compares well with the limit of detection for similar thiols obtained by electrochemical methods [20] and by fluorescence detection using other maleimide-based reagents [16,18,21]. However, a few maleimide-based derivatization reagents are reported to give products with considerably lower detection limits [15,17]. It should be noted that these results were obtained for standard solutions. The main advantage of the method reported here is its selectivity. The calibration graph for glutathione was linear from $5 \cdot 10^{-8}$ to $1 \cdot 10^{-6} M$ ($r = 0.998$, $n = 8$). In all solutions the 4-MSA concentration was $5.0 \cdot 10^{-5} M$ and the reaction time was 10–15 min. The repeatability of the peak heights of an reaction mixture (GSH concentration $1 \cdot 10^{-6} M$) injected four times between 10 and 40 min after preparation was 1% (relative standard deviation).

For L-cysteine, the derivatization procedure gave some stability problems. As noted previously [11], reaction mixtures of this analyte and 4-MSA showed a time-

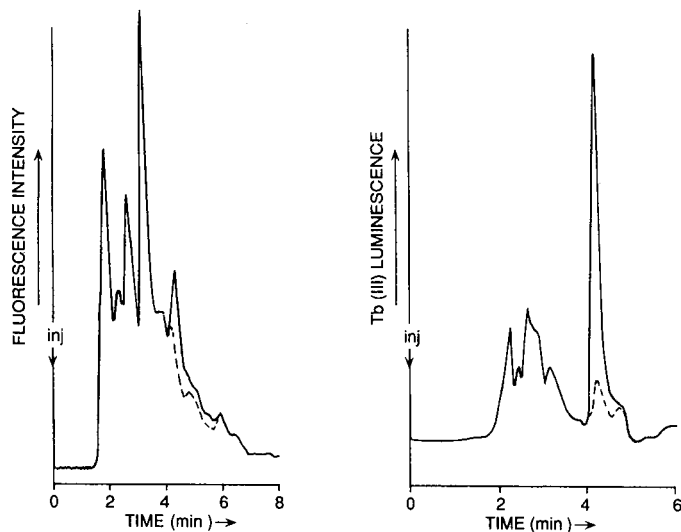


Fig. 8. Chromatograms of a urine sample diluted ten-fold with reaction buffer containing $8 \cdot 10^{-5} M$ EDTA and $1 \cdot 10^{-5} M$ 4-MSA. (---) no GSH added; (—) [GSH] $1 \cdot 10^{-6} M$. Left panel, fluorescence detection; right panel sensitized Tb^{3+} luminescence detection (vertical scales in relative units).

dependent shift in fluorescence wavelengths in batch experiments. These reaction mixtures were also injected in this chromatographic system. On injection of a fresh reaction mixture (10 min), one single peak was observed in the chromatograms. Mixtures injected after standing for more than 1 h at room temperature gave an additional peak at a longer retention time by both fluorescence and sensitized Tb^{3+} luminescence detection. This may be caused by a reaction similar to the thiazane formation described for 1-pyrenemaleimide and cysteine [13].

To illustrate the selectivity of detection by sensitized Tb^{3+} luminescence, the derivatization reaction of GSH was carried out in diluted urine samples as an example of a complex matrix (urine itself does not contain any GSH). To protect the analytical column from contamination, simple clean-up steps were applied before spiking the sample with 4-MSA and GSH. Urine samples, diluted ten-fold with reaction buffer ($5 \cdot 10^{-3} M$ Tris buffer, pH 7.0), were filtered over a membrane filter and an octadecyl disposable extraction column. The chromatograms detected by fluorescence and by sensitized Tb^{3+} luminescence are shown in Fig. 8. As a lot of fluorescent compounds are present in urine, the fluorescence detection of 4-MSA-GSH (at these wavelengths) is not very selective. The number of compounds which cause efficient sensitization of Tb^{3+} luminescence is obviously less, although two small peaks interfere with the 4-MSA-GSH peak in the spiked sample. 4-MSA-GSH can be detected far more selectivity by sensitized Tb^{3+} luminescence than by fluorescence detection.

CONCLUSIONS

The results described in this paper show that for thiol functional groups chemical derivatization with 4-MSA is an appropriate procedure to make use of the tempo-

ral resolution in luminescence detection via the post-column addition of Tb^{3+} . On derivatization a product is generated which is able to form a complex with Tb^{3+} and to sensitize its long-lived luminescence. An excess of reagent does not perturb the detection.

The most interesting aspect of the sensitized Tb^{3+} luminescence detection method is the improvement in selectivity compared to fluorescence detection for the analysis of real samples. This is obvious from the experiment performed with spiked urine samples. Whereas in the fluorescence detection mode the derivatized analyte can hardly be seen as it is not separated from other fluorescent components in the sample, in the time-resolved detection mode the signal-to-noise ratio is much more favourable.

Application of this method to the determination of thiols in biological samples is under current investigation. It would also be interesting to follow a similar approach for other function groups.

REFERENCES

- 1 J. Goto, in H. Lingeman and W. J. M. Underberg (Editors), *Detection-Oriented Derivatization Techniques in Liquid Chromatography*, Marcel Dekker, New York, 1990, p. 323.
- 2 R. A. Baumann, C. Gooijer, N. H. Velthorst and R. W. Frei, *Anal. Chem.*, 57 (1985) 1815.
- 3 R. A. Baumann, M. Schreurs, C. Gooijer, N. H. Velthorst and R. W. Frei, *Can. J. Chem.*, 65 (1987) 965.
- 4 T. J. Wenzel, L. M. Collette, D. T. Dahlen, S. M. Hendrickson and L. W. Yarmaloff, *J. Chromatogr.*, 433 (1988) 149.
- 5 M. Schreurs, G. W. Somsen, C. Gooijer, N. H. Velthorst and R. W. Frei, *J. Chromatogr.*, 482 (1989) 351.
- 6 J. L. Kropp and M. W. Windsor, *J. Chem. Phys.*, 42 (1965) 1599.
- 7 R. A. Baumann, D. A. Kamminga, H. Derlagen, C. Gooijer, N. H. Velthorst and R. W. Frei, *J. Chromatogr.*, 439 (1988) 165.
- 8 W. R. Dawson, J. L. Kropp and M. W. Windsor, *J. Chem. Phys.*, 45 (1966) 2410.
- 9 L. M. Hirschy, E. V. Dose and J. D. Winefordner, *Anal. Chim. Acta*, 147 (1983) 311.
- 10 M. P. Bailey, B. F. Rocks and C. Riley, *Anal. Chim. Acta*, 201 (1987) 335.
- 11 M. Schreurs, C. Gooijer and N. H. Velthorst, *Anal. Chem.*, 62 (1990) 2051.
- 12 Y. Kanaoka, M. Machida, K. Ando and T. Sekine, *Biochim. Biophys. Acta*, 207 (1970) 269.
- 13 C.-W. Wu, L. R. Yarbrough and F. Y.-H. Wu, *Biochemistry*, 15 (1976) 2863.
- 14 H. Takahashi, Y. Nara and K. Tuzimura, *Agric. Biol. Chem.*, 42 (1978) 769.
- 15 B. Kågedal and M. Källberg, *J. Chromatogr.*, 229 (1982) 409.
- 16 J. O. Miners, I. Fearnley, K. J. Smith and D. J. Birkett, *J. Chromatogr.*, 275 (1983) 89.
- 17 K. Nakashima, C. Umekawa, H. Yashida, S. Nakatsiju and S. Akiyama, *J. Chromatogr.*, 414 (1987) 11.
- 18 R. A. G. Garcia, L. L. Hirschberger and M. H. Stipanuk, *Anal. Biochem.*, 170 (1988) 432.
- 19 W. T. Carnall, in K. A. Gschneidner and L. Eyring (Editors), *Handbook on the Chemistry and Physics of Rare Earths*, Vol. 3, North-Holland Publishing Company, Amsterdam, 1979, p. 171.
- 20 A. J. J. Debets, R. van de Straat, W. H. Voogt, H. Vos, N. P. E. Vermeulen and R. W. Frei, *J. Pharm. Biomed. Anal.*, 6 (1988) 329.
- 21 M. Johansson and S. Lenngren, *J. Chromatogr.*, 432 (1988) 65.

CHROMSYMP. 2174

Spray jet assembly interface for the coupling of reversed-phase narrow-bore liquid chromatography and Fourier transform infrared spectrometry

G. W. SOMSEN, R. J. VAN DE NESSE, C. GOOIJER*, U. A. Th. BRINKMAN and N. H. VELT-HORST

Department of General and Analytical Chemistry, Free University, De Boelelaan 1083, 1081 HV Amsterdam (The Netherlands)

and

T. VISSER, P. R. KOOTSTRA and A. P. J. M. DE JONG

National Institute of Public Health and Environmental Protection, Laboratory for Organic-Analytical Chemistry, P.O. Box 1, 3720 BA Bilthoven (The Netherlands)

ABSTRACT

Liquid chromatography was coupled to Fourier transform infrared spectrometry via solvent elimination prior to infrared detection. The method allows the immobilization of analytes separated by reversed-phase liquid chromatography. Using a spray jet assembly, the effluent from a narrow-bore reversed-phase liquid chromatography column was continuously sprayed onto a linearly moving substrate suitable for infrared detection. The deposited compounds were analyzed by Fourier transform infrared microscopy. Transmission measurement using zinc selenide as substrate appears to be preferable to measurement in the reflection mode on an aluminum surface. With polycyclic hydrocarbons and quinones as model compounds, it was shown that the chromatographic separation is hardly affected during the immobilization process. The identification limits for these compounds were 10–20 ng. Aqueous methanol liquid chromatography eluents containing up to about 20% water can be handled.

INTRODUCTION

Hybrid techniques that combine chromatography with mass spectrometry (MS) and Fourier transform infrared spectrometry (FT-IR) have been primarily developed to permit unambiguous identification of sample constituents. Today MS is the most commonly applied technique for characterizing chromatographic peaks. In this respect FT-IR may be a useful alternative and complementary identification method, particularly for the analysis of structural isomers [1]. In gas chromatography (GC) the successful coupling to FT-IR [2] has led to the commercial availability of the equipment concerned. This is not the stage of development for liquid chromatography (LC) [3–5] in which, as in supercritical fluid chromatography (SFC) [6] and thin-layer chromatography (TLC) [7–9], interfacing to FT-IR has not yet reached an advanced state of sophistication.

In the simple LC-FT-IR set-up, the column effluent is led directly through a flow cell, allowing continuous IR analysis [10]. However, this type of detection has several limitations imposed by the mobile phase. Most common LC solvents have intense absorption bands in the mid-IR region, necessitating flow-cell path lengths as short as 100 μm (or even less when the mobile phase is aqueous), which strongly limits the sensitivity of on-line IR detection. Furthermore, because these absorptions take up wide regions of the spectrum, the obtainable spectral information is reduced.

The preferred method to circumvent solvent interferences is the elimination of the solvent prior to the IR measurement of the solute. This involves an interface which evaporates the mobile phase and deposits the analytes onto a substrate suitable for IR detection. The LC chromatogram is stored and the deposited analytes can be examined over a longer period of time. For instance, after a rapid screening of the substrate applying low resolution and only a few scans per spectrum, high-resolution spectra with a high signal-to-noise ratio can be recorded for a few interesting parts of the chromatogram.

Applying normal-phase (NP) LC, the solvent elimination approach has been fairly successful [11,12], because of the high volatility of most organic solvents. Moreover, conventional IR sampling media can be used. In reversed-phase (RP) LC the use of aqueous eluents complicates deposition, because water has a relatively low volatility and it readily dissolves alkali halogenides. Unfortunately, in practice by far the most LC separations are based on RP-LC.

In the literature several solvent elimination interfaces for RP-LC-FT-IR, mostly modifications of NP-LC-FT-IR interfaces, are described. Conroy and co-workers [13,14] reported the on-line extraction of the RP-LC effluent with dichloromethane, which was subsequently deposited onto potassium chloride, kept in a train of sample cups suitable for diffuse reflection infrared detection (DRIFT). Kalasinsky and co-workers [15,16] used the acid-catalyzed reaction of 2,2-dimethoxypropane with water for the conversion of the non-volatile water in the mobile phase to the volatile methanol and acetone, thereby facilitating deposition on potassium chloride and analysis by DRIFT. The buffer memory technique was made appropriate for RP-LC by Fujimoto *et al.* [17], who used a stainless-steel wire net (SSWN) instead of a potassium bromide crystal as sampling medium. The aqueous effluent from a microcolumn is deposited onto the SSWN, from which the solvent is eliminated by a heated nitrogen gas flow. The sample components are partly suspended between the metal meshing, and analysis can be performed in the transmission mode. An impressive method for the coupling of narrow-bore RP-LC to FT-IR applicable for gradients containing up to 55% water in methanol is presented by Gagel and Biemann [18]. The column effluent is nebulized by nitrogen gas in a LC mixing tee and directed to a rotating reflective aluminum disk through a syringe needle which is enveloped by a heated nitrogen gas flow. After deposition, reflection-absorption spectra are recorded. In their paper, the spectrum of a 31-ng injection of phenanthrenequinone is shown, indicating a considerable improvement in sensitivity over the RP-LC-FT-IR systems discussed above, which report detection limits in the (sub)microgram range. The MAGIC (monodisperse aerosol generation) interface, originally developed for MS [19], has been applied by Robertson and co-workers [20,21] for FT-IR. Mobile phases containing between 0 and 100% water at a flow-rate of 0.3 ml/min could be handled without heating the effluent. Buffers can also be applied, although spectral subtrac-

tion remains necessary. This method seems promising, but until now only very few FT-IR chromatograms have been shown, and microgram amounts of compound have to be injected to obtain identifiable spectra.

To accomplish sensitive IR detection of deposited analytes, FT-IR microscopy is the technique of choice, as pointed out by Fraser *et al.* [22]. In the same paper a solvent elimination device for the coupling of NP-LC and FT-IR is described. This device is similar to the spray jet assembly recently used for the coupling of column LC to TLC [23,24]. In the present paper the spray jet assembly is presented as an interface for RP-LC-FT-IR. It allows the continuous deposition of the effluent from a narrow-bore RP-LC column onto the surface of a linearly moving substrate. After deposition, the immobilized chromatogram was analyzed by translating the substrate under an FT-IR microscope while spectra were being collected. The goal of this study was to demonstrate that chromatographic resolution is maintained during immobilization and that identifiable spectra of low amounts (10–20 ng injected) of model compounds can be obtained.

EXPERIMENTAL

A schematic of the LC interface set-up and the construction of the interface is shown in Fig. 1.

Chromatography

A laboratory-made syringe pump or an LDC/Milton Roy (Riviera Beach, FL, U.S.A.) microbore pump were used with a laboratory-made injection valve with an internal loop of 1.9 μ l. During flow-injection experiments a Valco (Houston, TX, U.S.A.) injection valve with a 10- μ l loop was used. Separations were performed on a

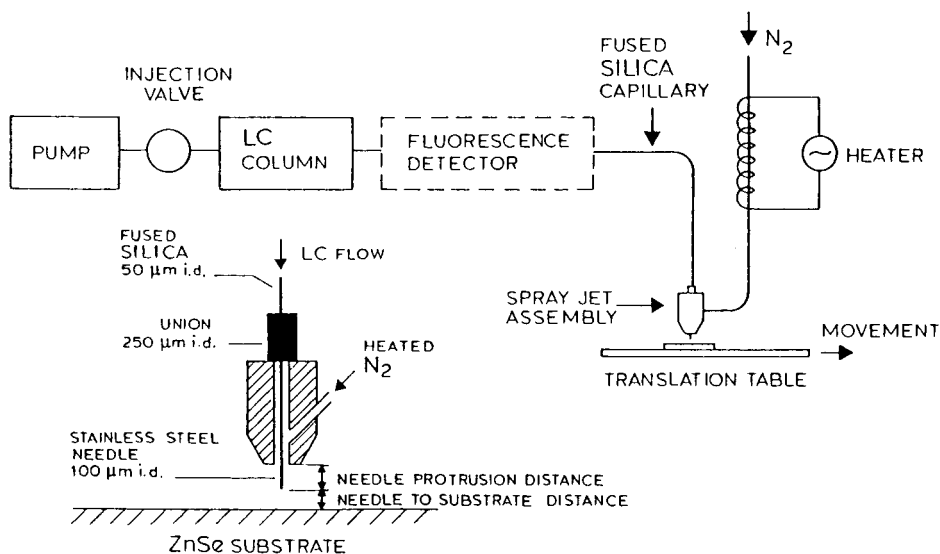


Fig. 1. Schematic of the chromatographic set-up and the interface. The insert shows the construction of the spray jet assembly.

170 mm \times 1.1 mm I.D. column packed with 5- μ m Rosil C₁₈ (Research Separations Labs., Eke, Belgium) or a 250 mm \times 1.0 mm I.D. column packed with 5- μ m Adsorbosphere C₁₈ (Alltech, Zwijndrecht, The Netherlands) at a flow-rate of 20 μ l/min with methanol-water (95:5 or 80:20, v/v) as mobile phase.

Spectroscopy

IR data were obtained by using a Bruker (Karlsruhe, Germany) IFS-85 FT-IR spectrometer equipped with a Bruker A590 FT-IR microscope. The microscope, which contained a 16 \times Cassegrainian lens and a narrow-range mercury-cadmium-telluride (MCT) detector, was used in both the transmission and reflection modes. The aperture was rectangular and of adjustable size. Normally, 128 scans per spectrum were coadded at 8 cm⁻¹ resolution. Background spectra were made using blank spots on the substrate surface in or adjacent to the deposition trace. Spectra were baseline-corrected.

Interface

The LC effluent was led to the spray jet assembly through a *ca.* 40 cm \times 50 μ m I.D. fused-silica capillary, which was connected with a union to a 100 μ m I.D. and 475 μ m O.D. stainless-steel syringe needle with a conically shaped tip. A nitrogen flow around the tip of the needle, which partially protruded from the assembly through a 600 or 900 μ m I.D. nozzle, ensured deposition of the effluent and provided removal of the mobile phase. The evaporation was enhanced by an electric heater capable of heating the nitrogen up to 200°C. The distance between the needle tip and the deposition substrate and the protrusion distance of the needle from the assembly could both be varied. During the immobilization the substrate was moved by the translation table of a Camag (Muttentz, Switzerland) Linomat III applicator or a computer-controlled Bruker microscope X-Y stepper table. The latter was also used for the IR scanning of chromatograms.

Fluorescence detection

For on-line detection of the polycyclic aromatic hydrocarbons (PAHs), a Varian (Walnut Creek, CA, U.S.A.) Fluorichrom fluorescence detector adapted in the laboratory for use in micro LC was applied. Excitation was achieved with a deuterium lamp; the light was passed through a 10-mm path length cuvette filled with 25% (w/v) nickelsulphate and 40% (w/v) cobaltsulphate in water and a 2-mm Schott UG11 glass band filter. In this way a spectral window was obtained ranging from 255 to 368 nm. On the emission side there was a 4-mm Schott GG13 glass cut-off filter. Fluorescence scanning of the immobilized compounds was performed with a Carl Zeiss (Oberkochen, Germany) densitometer operating in the fluorescence mode. Excitation was achieved with a 48-W high-pressure mercury lamp at 313 nm using an M4Q-III prism monochromator. The emitted light of the compounds was passed through an optical filter, which rejected light with a wavelength shorter than 360 nm.

Materials

The model compounds fluoranthene (FLT), acenaphthenequinone, phenanthrenequinone (all from Aldrich, Milwaukee, WI, U.S.A.), pyrene, (PYR) (EGA-Chemie, Steinheim, Germany), benzo[*a*]anthracene (B[*a*]A) (Rütgerswerke, Castrop,

Germany) and benzo[*k*]fluoranthene (B[*k*]F) (Radiant Dyes Wermelskirchen, Germany) were used as received. Methanol (HPLC quality) was obtained from Baker (Deventer, The Netherlands). The water used was either dionized and distilled twice or of Milli-Q quality.

As deposition medium a 50 mm × 10 mm × 3 mm zinc selenide prism (Barnes Analytical, Stamford, CT, U.S.A.) or a 38 mm × 45 mm aluminum-coated mirror (Perkin-Elmer, Norwalk, CT, U.S.A.) was used.

FT-IR analysis

The IR substrate fitted in a rectangular hole in an aluminum plate (10 cm × 10 cm) supported at the edges. The plate fitted in a laboratory-made extension of the microscope table and protruded under a stand holding the spray jet assembly. Next, upon injection of a sample on the RP-LC column, the table started moving at a computer-controlled constant speed and the chromatogram was immobilized. After deposition, the entire aluminum plate, including the substrate with the immobilized chromatogram, was transferred to the microscope beam area and subsequently scanned, under computer control. Scanning parameters and the step width could be selected interactively and the scanning could be interrupted if refocusing or readjustment was required. After the collection of all chromatogram IR data was completed, the spectra were baseline-corrected and if required a three-dimensional stack plot of the chromatogram was produced.

RESULTS AND DISCUSSION

Interface parameters

The spray jet assembly previously developed to couple column LC to TLC [23,24] was used to deposit the RP-LC effluent onto materials suitable for IR analysis. Specific optimization of the device was needed to obtain sensitive IR detection and to ensure a minimum loss of chromatographic resolution during the deposition process. A high IR sensitivity is achieved by concentrating the analytes into an area which is as small as possible. Therefore, interface parameters affecting the deposition spot size were studied. PAHs, which can be very well detected by a densitometer operating in the fluorescence mode, were used as model compounds. Thus, information on depositions could be obtained relatively quickly and easily. Optimization of the interfacing was done by studying the deposition of a single PAH onto an aluminum-coated mirror using a flow-injection (no-column) set-up. The most important optimization aspects are discussed below.

Just before entering the spray jet assembly, the nitrogen gas could be heated by an electric heater. As expected, heating the nitrogen gas clearly enhanced the speed of evaporation of the mobile phase. For a mobile phase of methanol-water (95:5, v/v) efficient solvent removal was obtained at a nitrogen gas temperature of 100°C (range tested, 40–120°C). Sufficient evaporation of more aqueous eluents required higher nitrogen temperatures, e.g. for methanol containing 20% water 140°C was needed. Throughout the investigation no boiling of the effluent was observed, even when using nitrogen temperatures of 100°C or higher. This indicates that the real temperature at the needle tip was below 100°C, the cooling being primarily caused by the evaporation of mobile phase.

The distance which the needle protrudes from the jet influenced the formation of the spray and the efficiency of solvent removal. When the protrusion distance was too large (> 3 mm), the spray appeared as a narrow liquid stream which turned into fast-spreading droplets as soon as it hit the smooth substrate surface. At a small protrusion distance (< 0.5 mm) no well defined spray was formed and the effluent was sprinkled over a large area. Protrusion distances between 0.5 and 1 mm were found to give optimum deposition.

The influence of the distance between the needle tip and the deposition substrate on the peak width across and along the deposition trace is shown in Fig. 2. Upon decreasing the distance, the trace width was strongly reduced, which is favorable to sensitive IR analysis. However, decreasing the needle-to-substrate distance unfortunately caused some broadening of the deposition spot along the trace. Taking the two effects into account, a needle-to-substrate distance of 0.5 mm was chosen in further experiments.

The nitrogen flow causing nebulization of the effluent at the needle tip was controlled by the pressure at the nitrogen cylinder outlet. When the pressure was increased a distinct improvement of the trace width of the deposited spots was obtained, but simultaneously the peak width along the trace increased (Fig. 3). On the basis of the experimental data, 6 bar was selected as the best compromise, applying a mobile phase of methanol-water (95:5, v/v). It should be noted that, with a nitrogen pressure of below 4 bar, solvent removal was not sufficient. In this case too much of the effluent was still fluid when it reached the substrate surface, causing a poor deposition.

The results given so far were obtained with a 900 μm I.D. interface nozzle. Using a nozzle with an I.D. of 600 μm and leaving the other interface parameters unchanged, the width of the spots across the trace could be reduced to 100–300 μm . In further experiments the 600 μm I.D. nozzle was used.

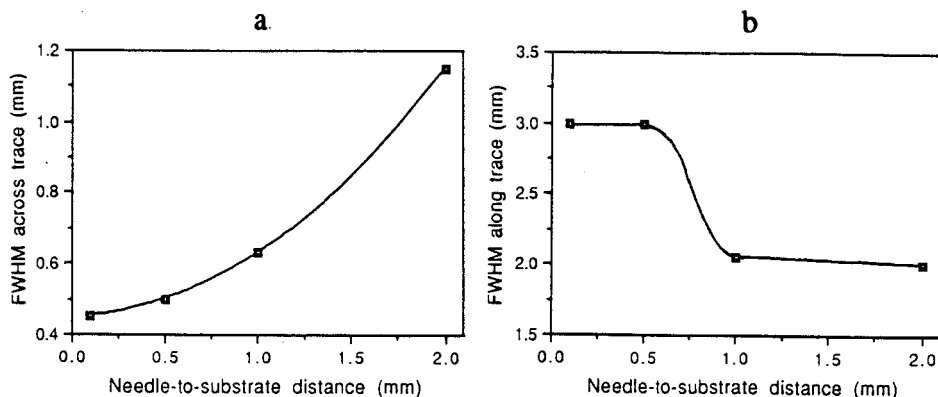


Fig. 2. Influence of the needle end-to-substrate distance on the peak width [(a) Across the trace and (b) along the trace] for the deposition of B[k]F onto an aluminum-coated mirror. FWHM is full width at half-maximum. Conditions: mobile phase, methanol-water (95:5, v/v); flow-rate, 20 $\mu\text{l}/\text{min}$; needle protrusion distance, 0.8 mm; nozzle I.D., 900 μm ; nitrogen pressure, 8 bar; nitrogen temperature, 100°C; table speed, 2 mm/min.

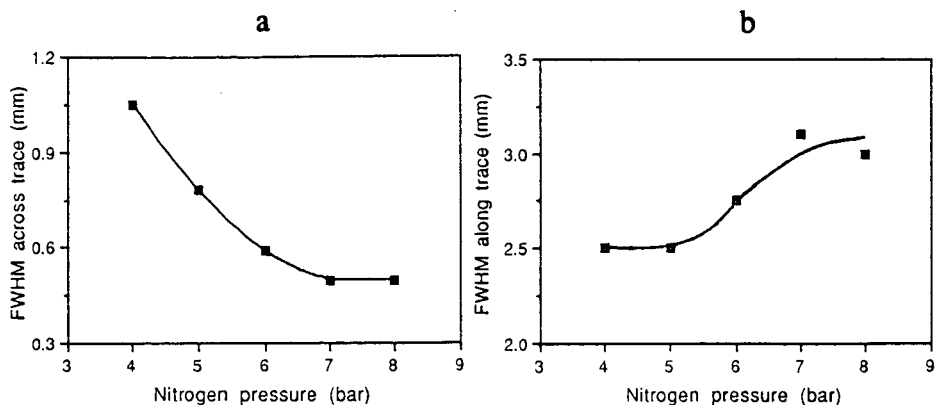


Fig. 3. Influence of the nitrogen gas pressure on the deposition of B[k]F onto an aluminum-coated mirror. (a) Scan across the trace; (b) scan along the trace. Conditions as in Fig. 2 except for needle-to-substrate distance, 0.5 mm.

Deposition substrate

A deposition substrate used in RP-LC-FT-IR should be composed of material which is compatible with aqueous mobile phases and which offers a large wave number area free of absorption bands. In our investigation two types of material were used, *viz.* an aluminum-coated mirror for reflectance-absorbance (R-A) measurements and a zinc selenide window for transmission measurements. Both materials have a hard and smooth surface which complicates deposition. Liquid that hits such a surface easily spreads as a result of the nitrogen flow. To prevent this spreading, solvents should be removed as fast as possible during the deposition. Apparently this requirement is met if the nitrogen gas temperature and pressure are high enough.

As regards deposition, the spots on the aluminum surface were larger than those on zinc selenide, and peaks as observed along the trace on the mirror showed irregularity in shape, which was not seen on zinc selenide. Apparently, the physical properties of the substrate affect the deposition. On the basis of these results zinc selenide is better suited as a deposition substrate than an aluminum-coated mirror. Even more important are the differences from an IR spectroscopic point of view. Transmission spectra of the compounds deposited onto zinc selenide showed better signal-to-noise ratio than the R-A spectra of the same amounts of material deposited onto aluminum. Moreover, zinc selenide allowed comparison with conventionally recorded potassium bromide spectra, whereas some of the R-A spectra were considerably distorted. This phenomenon is attributed to specular reflectance effects, probably the result of the limited film thickness and the very small particle size of the crystalline deposited material. During our study, Fuoco *et al.* [25] published a paper in which six different deposition substrates for SFC-FT-IR were compared. Using an aluminum mirror Fuoco *et al.* [25] also observed distortion of the spectra, depending on film thickness and microcrystalline nature of the deposited analytes. Furthermore, it was reported that best results were obtained with transmission measurements on zinc selenide. Considering this paper and our results, zinc selenide was chosen as the deposition substrate in further experiments.

Immobilization and detection of chromatograms

Fig. 4 shows the chromatogram of an LC separation recorded by fluorescence monitoring both on-line (Fig. 4a) and after immobilization zinc selenide (Fig. 4b); Table I gives the corresponding peak widths along the trace. The results show that the band broadening caused by the interfacing is acceptable. The widths of the spots across the trace of the immobilized analytes, determined visually by microscope, lay in the 100–150 μm range and tended to increase slightly with retention time. These along trace–across trace dimensions of typically (10–15):1 indicate an elongated ellip-

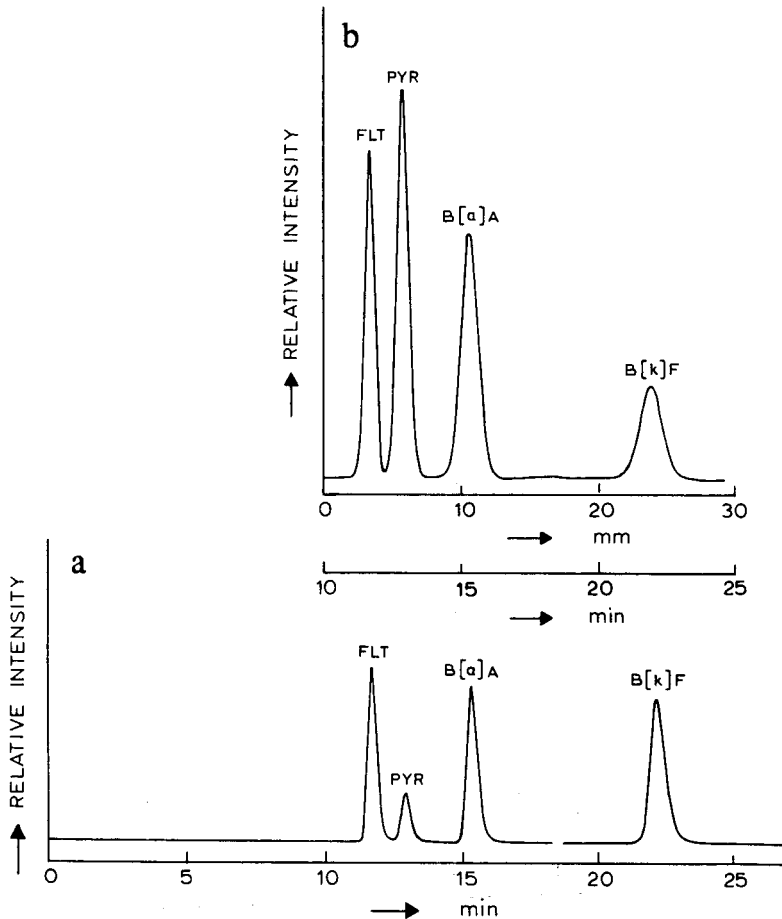


Fig. 4. Chromatogram of a test mixture of FLT, PYR, B[a]A and B[k]F (about 100 ng each; injection volume 1.9 μl). (a) On-line fluorescence detection (detector sensitivity: attenuation 50, except for B[k]F, 500). (b) Off-line fluorescence detection with densitometry after deposition onto zinc selenide. Conditions: column, 170 mm \times 1.1 mm I.D. packed with Rosil C₁₈, 5 μm ; mobile phase, methanol–water (95:5, v/v); flow-rate, 20 $\mu\text{l}/\text{min}$; needle protrusion distance, 0.5 mm; needle-to-substrate distance, 0.5 mm; nozzle I.D., 600 μm ; nitrogen pressure, 6 bar; nitrogen temperature, 100°C; table speed, 2 mm/min. Note that the relative intensities of the two depicted chromatograms cannot be compared because of differences in excitation and emission conditions between on-line and off-line fluorescence detection (see Experimental section).

TABLE I

CHROMATOGRAPHIC BAND WIDTHS BEFORE (ON-LINE) AND AFTER (OFF-LINE) INTERFACING

FWHM is full width at half-maximum. Data taken from Fig. 4.

Compound	FWHM on-line (s)	FWHM off-line (mm)	FWHM off-line (s)
FLT	22	0.82	25
PYR	24	0.98	29
B[a]A	27	1.42	43
B[k]F	37	1.80	54

tical rather than circular spot, making a rectangular microscope aperture more appropriate than a round one for scanning the chromatogram. Fig. 5 shows a three-dimensional RP-LC-FT-IR plot for the separation of the same PAHs as in Fig. 4. The chromatogram was measured by scanning the substrate under the microscope with steps of $200 \mu\text{m}$ using a rectangular aperture. Between 10.4 and 21.4 mm, scans of the trace were produced only every 2 mm. The resulting spectra showed blank baselines. The spectra of individual PAHs are clearly recognizable in the chromatogram. The LC separation is well conserved and allows identification of the analytes by FT-IR. All spectra match well with their corresponding potassium bromide transmission spectra. The signal-to-noise ratio of the spectra is illustrated by Fig. 6A, showing a single spectrum of pyrene taken from the chromatogram. To determine the sensitivity of the method, various amounts of pyrene were injected and deposited.

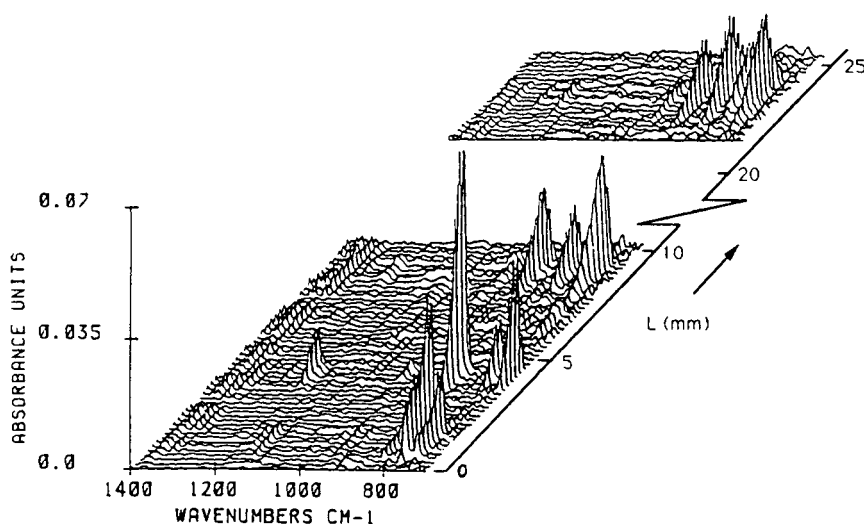


Fig. 5. Chromatogram of a test mixture (see Fig. 4) with IR detection. Conditions as in Fig. 4 except for column, $250 \times 1.0 \text{ mm}$ I.D. packed with Adsorbosphere C_{18} $5 \mu\text{m}$; table speed, 1.8 mm/min . Spectroscopic conditions: distance between spectra, $200 \mu\text{m}$; number of scans per spectrum, 128; resolution, 8 cm^{-1} ; aperture size, $224 \mu\text{m} \times 112 \mu\text{m}$ for FLT and PYR, $224 \mu\text{m} \times 144 \mu\text{m}$ for B[a]A and B[k]F.

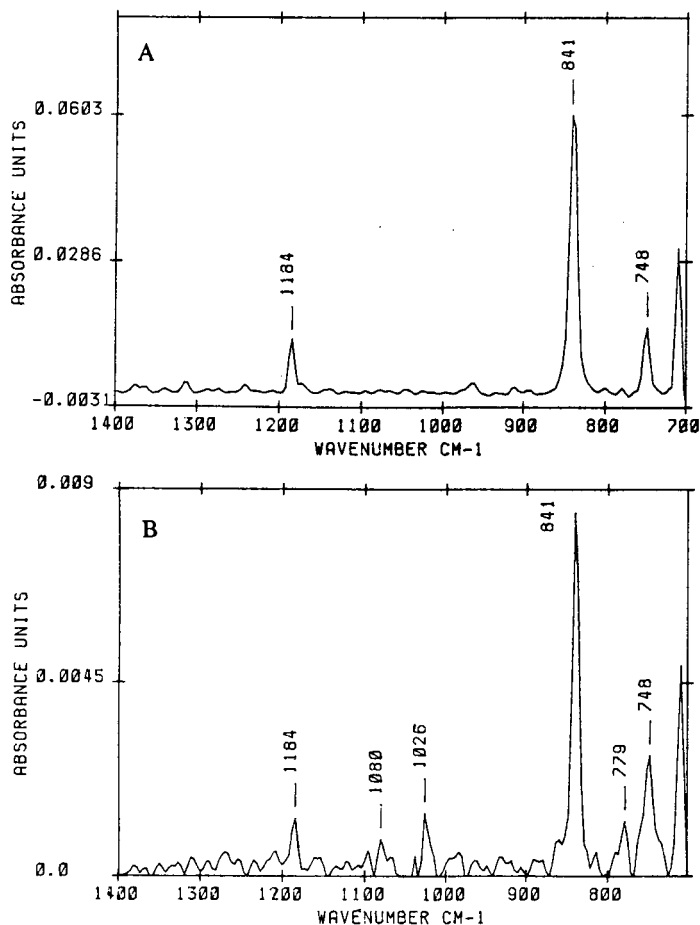


Fig. 6. RP-LC-FT-IR of pyrene. (A) Injection of 92 ng. (B) Injection of 13 ng. Conditions as in Fig. 5, except for aperture size, $200 \mu\text{m} \times 80 \mu\text{m}$, and number of scans, 1024 for (b).

Using 1024 scans, an identifiable spectrum of a 13-ng injection of pyrene was obtained (Fig. 6B).

To explore the potential of the interface, a mixture of acenaphthenequinone (AQ) and phenanthrenequinone (PQ) was separated on a C_{18} column with methanol-water (80:20, v/v) as mobile phase and the resulting chromatogram was immobilized on zinc selenide. AQ and PQ were selected because these quinones have been used as model compounds in several previously published studies on SFC-FT-IR and LC-FT-IR [18,22,25-27]. To obtain sufficient solvent removal the nitrogen gas temperature and pressure were raised to 140°C and 8 bar, respectively. No further optimization of the interface parameters was carried out for this mobile phase composition. The on-line recorded (not shown) baseline separation of AQ ($t_R = 7.9$ min) and PQ ($t_R = 9.9$ min) was retained on zinc selenide and the width of the spots across the trace was about $200 \mu\text{m}$. Fig. 7 shows the spectra of deposited AQ and PQ after injecting

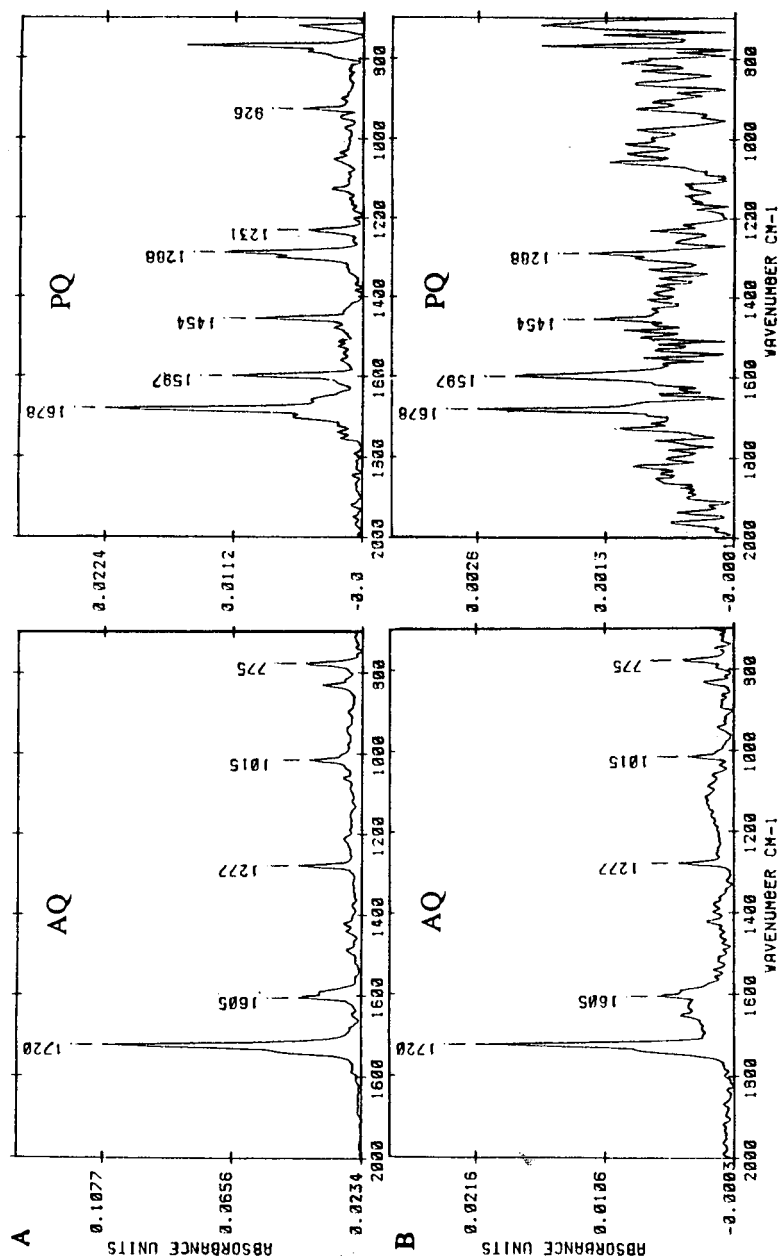


Fig. 7. RP-LC-FT-IR of AQ and PQ. (A) Injection of 154 ng AQ and 166 ng PQ. (B) Injection of 19 ng AQ and 21 ng PQ. Conditions: column, 250 mm \times 1.0 mm I.D. packed with Adsorbosphere C₁₈ 5 μ m; mobile phase, methanol-water (80:20, v/v); flow-rate, 20 μ l/min; needle protrusion distance, 0.5 mm; needle-to-substrate distance, 0.5 mm; nozzle I.D., 600 μ m; nitrogen pressure, 8 bar; nitrogen temperature, 140°C. Spectroscopic conditions: resolution, 8 cm⁻¹. (A) Aperture size, 200 μ m \times 160 μ m; number of scans, 128. (B) Aperture size, 200 μ m \times 65 μ m; number of scans, 1024.

and separating two mixtures containing *ca.* 160 ng and *ca.* 20 ng per compound, respectively. It demonstrates that the interface is able to deposit quinones efficiently from methanol containing 20% water, and 20-ng amounts can still be identified.

CONCLUSION

The usefulness of a spray jet assembly as a relatively simple interface for RP-LC-FT-IR has been demonstrated using PAHs and quinones as model compounds. The chromatographic integrity of the LC separation is essentially maintained during the immobilization, and identifiable IR spectra of analytes can be obtained down to the 10–20 ng range. The main reasons for this good sensitivity are the deposition of the analytes as very narrow spots and the use of an IR microscope for beam condensing. The use of zinc selenide as IR substrate circumvents problems met in R-A FT-IR using aluminum mirrors and allows comparison with conventional potassium bromide transmission spectra.

Future research will concentrate on the handling of more polar compounds using mobile phases with a water content of over 20%. Quick evaporation of these more aqueous eluents will probably demand higher nitrogen gas temperatures. The higher polarity of the analytes could complicate deposition as well, because of the increased solubility of the compounds in an aqueous environment.

ACKNOWLEDGEMENT

The authors thank Dr. J. Gast of Bruker (Karlsruhe, Germany) for the loan of the microscopic X-Y stepper table and the rectangular microscope aperture used in this study.

REFERENCES

- 1 S. A. Borman, *Anal. Chem.*, 54 (1982) 901A.
- 2 P. R. Griffiths, J. A. de Haseth and L. V. Azarraga, *Anal. Chem.*, 55 (1983) 1361A.
- 3 J. W. Hellgeth and L. T. Taylor, *J. Chromatogr. Sci.*, 24 (1986) 519.
- 4 P. R. Griffiths and C. M. Conroy, *Adv. Chromatogr.*, 25 (1986) 105.
- 5 C. Fujimoto and K. Jinno, *Trends Anal. Chem.*, 8 (1989) 90.
- 6 L. T. Taylor and E. M. Calvey, *Chem. Rev.*, 89 (1989) 321.
- 7 G. E. Zuber, R. J. Warren, P. P. Begosh and E. L. O'Donnell, *Anal. Chem.*, 56 (1984) 2935.
- 8 P. R. Brown and B. T. Beauchemin, Jr., *J. Liq. Chromatogr.*, 11 (1988) 1001.
- 9 B. T. Beauchemin, Jr. and P. R. Brown, *Anal. Chem.*, 61 (1989) 615.
- 10 P. R. Griffiths and J. A. de Haseth, *Fourier Transform Infrared Spectroscopy*, Wiley, New York, 1986, p. 611.
- 11 K. Jinno, C. Fujimoto and Y. Hirata, *Appl. Spectrosc.*, 36 (1982) 67.
- 12 C. Fujimoto, K. Jinno and Y. Hirata, *J. Chromatogr.*, 258 (1983) 81.
- 13 C. M. Conroy, P. R. Griffiths, P. J. Duff and L. V. Azarraga, *Anal. Chem.*, 56 (1984) 2636.
- 14 C. M. Conroy, P. R. Griffiths and K. Jinno, *Anal. Chem.*, 57 (1985) 822.
- 15 K. S. Kalasinsky, J. A. S. Smith and V. F. Kalasinsky, *Anal. Chem.*, 57 (1985) 1969.
- 16 V. F. Kalasinsky, K. G. Whitehead, R. C. Kenton, J. A. S. Smith and K. S. Kalasinsky, *J. Chromatogr. Sci.*, 25 (1988) 273.
- 17 C. Fujimoto, T. Oosuka and K. Jinno, *Anal. Chim. Acta*, 178 (1985) 159.
- 18 J. J. Gagel and K. Biemann, *Anal. Chem.*, 59 (1987) 1266.
- 19 R. C. Willoughby and R. F. Browner, *Anal. Chem.*, 56 (1984) 2626.
- 20 R. M. Robertson, J. A. de Haseth, J. D. Kirk and R. F. Browner, *Appl. Spectrosc.*, 42 (1988) 1365.

- 21 R. M. Robertson, J. A. de Haseth and R. F. Browner, *Appl. Spectrosc.*, 44 (1990) 8.
- 22 D. J. J. Fraser, K. L. Norton and P. R. Griffiths, in R. G. Messerschmidt and M. A. Harthcock (Editors), *Infrared Microspectroscopy: Theory and Applications*, Marcel Dekker, New York, 1988, p. 197.
- 23 J. W. Hofstraat, S. Griffioen, R. J. van de Nesse, U. A. Th. Brinkman, C. Gooijer and N. H. Velthorst, *J. Planar Chromatogr.*, 1 (1988) 220.
- 24 R. J. van de Nesse, G. J. M. Hoogland, H. de Moel, C. Gooijer, U. A. Th. Brinkman and N. H. Velthorst, *J. Chromatogr.*, 552 (1991) 613.
- 25 R. Fuoco, S. L. Pentoney, Jr. and P. R. Griffiths, *Anal. Chem.*, 61 (1989) 2212.
- 26 K. H. Shafer, S. L. Pentoney, Jr. and P. R. Griffiths, *Anal. Chem.*, 58 (1986) 58.
- 27 P. R. Griffiths, S. L. Pentoney, Jr., G. L. Pariente and K. L. Norton, *Mikrochim. Acta*, III (1987) 47.

PUBLICATION SCHEDULE FOR 1991

Journal of Chromatography and Journal of Chromatography, Biomedical Applications

MONTH	D 1990– M 1991	J	J	A	S	O	N	D
Journal of Chromatography	Vols. 535–545/1	545/2 546/1 + 2 547/1 + 2	548/1 + 2 549/1 + 2 550/1 + 2	552/1 + 2 553/1 + 2 554/1 + 2 555/1 + 2	556/1 + 2 557/1 + 2 558/1	558/2 559/1 + 2		
Cumulative Indexes. Vols. 501–550				551/1 + 2				
Bibliography Section	560/1	560/2			561/1			561/2
Biomedical Applications	Vols. 562–566	567/1	567/2 568/1	568/2	569/1 + 2 570/1	570/2	571/1 + 2	572/1 + 2

INFORMATION FOR AUTHORS

(Detailed *Instructions to Authors* were published in Vol. 522, pp. 351–354. A free reprint can be obtained by application to the publisher, Elsevier Science Publishers B.V., P.O. Box 330, 1000 AH Amsterdam, The Netherlands.)

Types of Contributions. The following types of papers are published in the *Journal of Chromatography* and the section on *Biomedical Applications*: Regular research papers (Full-length papers), Review articles and Short Communications. Short Communications are usually descriptions of short investigations, or they can report minor technical improvements of previously published procedures; they reflect the same quality of research as Full-length papers, but should preferably not exceed six printed pages. For Review articles, see inside front cover under Submission of Papers.

Submission. Every paper must be accompanied by a letter from the senior author, stating that he/she is submitting the paper for publication in the *Journal of Chromatography*.

Manuscripts. Manuscripts should be typed in double spacing on consecutively numbered pages of uniform size. The manuscript should be preceded by a sheet of manuscript paper carrying the title of the paper and the name and full postal address of the person to whom the proofs are to be sent. As a rule, papers should be divided into sections, headed by a caption (e.g., Abstract, Introduction, Experimental, Results, Discussion, etc.). All illustrations, photographs, tables, etc., should be on separate sheets.

Introduction. Every paper must have a concise introduction mentioning what has been done before on the topic described, and stating clearly what is new in the paper now submitted.

Abstract. All articles should have an abstract of 50–100 words which clearly and briefly indicates what is new, different and significant.

Illustrations. The figures should be submitted in a form suitable for reproduction, drawn in Indian ink on drawing or tracing paper. Each illustration should have a legend, all the legends being typed (with double spacing) together on a separate sheet. If structures are given in the text, the original drawings should be supplied. Coloured illustrations are reproduced at the author's expense, the cost being determined by the number of pages and by the number of colours needed. The written permission of the author and publisher must be obtained for the use of any figure already published. Its source must be indicated in the legend.

References. References should be numbered in the order in which they are cited in the text, and listed in numerical sequence on a separate sheet at the end of the article. Please check a recent issue for the layout of the reference list. Abbreviations for the titles of journals should follow the system used by *Chemical Abstracts*. Articles not yet published should be given as "in press" (journal should be specified), "submitted for publication" (journal should be specified), "in preparation" or "personal communication".

Dispatch. Before sending the manuscript to the Editor please check that the envelope contains four copies of the paper complete with references, legends and figures. One of the sets of figures must be the originals suitable for direct reproduction. Please also ensure that permission to publish has been obtained from your institute.

Proofs. One set of proofs will be sent to the author to be carefully checked for printer's errors. Corrections must be restricted to instances in which the proof is at variance with the manuscript. "Extra corrections" will be inserted at the author's expense.

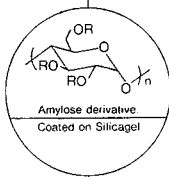
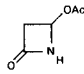
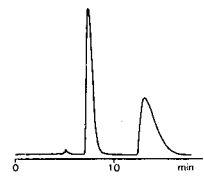
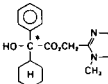
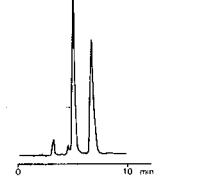
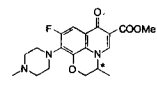
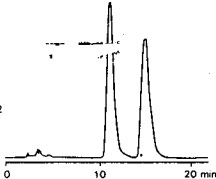
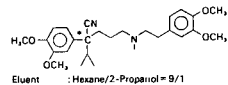
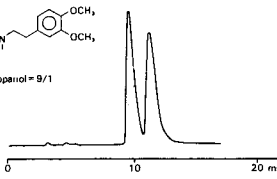
Reprints. Fifty reprints of Full-length papers and Short Communications will be supplied free of charge. Additional reprints can be ordered by the authors. An order form containing price quotations will be sent to the authors together with the proofs of their article.

Advertisements. Advertisement rates are available from the publisher on request. The Editors of the journal accept no responsibility for the contents of the advertisements.

For Superior Chiral Separation From Analytical To Preparative.

The finest from DAICEL.....

Why look beyond DAICEL? We have developed the finest CHIRALCEL, CHIRALPAK and CROWNPAK with up to 17 types of HPLC columns, all providing superior resolution of racemic compounds.

NEW CHIRALPAK AS		NEW CHIRALPAK AD	
<p>● CHIRALPAK AS</p> $R: -C(=O)-N(H)-C(H)(CH_3)-C_6H_5$ <p>for β-Lactam antibiotics</p>	 <p>Amylose derivative Coated on Silicagel</p>	<p>● CHIRALPAK AD</p> $R: -C(=O)-N(H)-C_6H_3(CH_3)_2$	
<p>1-Acetoxy-2-azetidine</p>  <p>Eluent : Hexane/Ethanol = 8/2 Flow rate : 1.0ml/min Temperature : r.t. Detection : UV254 nm</p> 		<p>Oxyphenicyclimine</p>  <p>Eluent : Hexane/2-Propanol = 9/1 Flow rate : 1.0ml/min Temperature : r.t. Detection : UV254 nm</p> 	
<p>Ofloxacin methyl ester</p>  <p>Eluent : Hexane/EtOH = 8/2 Flow rate : 1.2ml/min Temperature : 40°C Detection : UV254 nm</p> 		<p>Verapamil</p>  <p>Eluent : Hexane/2-Propanol = 9/1 Flow rate : 1.0ml/min Temperature : r.t. Detection : UV254 nm</p> 	

Analytical column 0.46cm x 25cm (10 μ m)

CHIRALCEL OA
OB
OC
OD
OJ
OF
OG
OK
CHIRALPAK AS
AD



Normal Phase



Semi-preparative column 2cm x 25cm (10 μ m)

You can have
Pure enantiomer
quickly!!

■ Separation Service

- A pure enantiomer separation in the amount of 100g~10kg is now available.
- Please contact us for additional information regarding the manner of use and application of our chiral columns and how to procure our separation service.



DAICEL CHEMICAL INDUSTRIES, LTD.

chiral chemicals division.

8-1, Kasumigaseki 3-chome, Chiyoda-ku, Tokyo 100, Japan Phone: 03 (507) 3151 FAX: 03 (507) 3193

DAICEL (U.S.A.), INC.

Fort Lee Executive Park
Two Executive Drive, Fort Lee,
New Jersey 07024
Phone: (201) 461-4466
FAX: (201) 461-2776

DAICEL (U.S.A.), INC.

23456 Hawthorne Blvd.
Bldg. 5, Suit 130
Torrance, CA 90505
Phone: (213) 791-2030
FAX: (213) 791-2031

DAICEL (EUROPA) GmbH

Oststr. 22
4000 Düsseldorf 1, F.R. Germany
Phone: (211) 369848
Telex: (41) 8588042 DCEL D
FAX: (211) 364429

DAICEL CHEMICAL (ASIA) PTE. LTD.

65 Chulia Street #40-07
OCBC Centre, Singapore 0104
Phone: 5332511
FAX: 5326454